Modern Control Engineering

Third Edition

Katsuhiko Ogata

University of Minnesota

Prentice Hall, Upper Saddle River, New Jersey 07458

Library of Congress Cataloging-in-Publication Data

Ogata, Katsuhiko.
Modern control engineering / Katsuhiko Ogata. — 3rd ed.
p. cm.
Includes bibliographical references and index.
ISBN: 0-13-227307-1
1. Automatic control. 2. Control theory. I. Title.
TJ213.028 1997
629.8—dc20 96-2345
CIP

Publisher: Tom Robbins
Associate editor: Alice Dworkin
Production editor: Ann Marie Longobardo
Cover designer: Bruce Kenselaar
Manufacturing Buyer: Donna Sullivan

Printed in the United States of America

10 9 8

ISBN: 0-13-227307-1

Prentice-Hall International (UK) Limited, London
Prentice-Hall of Australia Pty. Limited, Sydney
Prentice-Hall Canada Inc., Toronto
Prentice-Hall Hispanoamericana, S.A., Mexico
Prentice-Hall of India Private Limited, New Delhi
Prentice-Hall of Japan, Inc., Tokyo
Simon & Schuster Asia Ltd., Singapore
Editora Prentice-Hall do Brasil, Ltda., Rio de Janeiro

The MathWorks, Inc.
24 Prime Park Way
Natick, MA 01760-1500
Phone: (508) 647-7000
Fax: (508) 647-7001
E-mail: info@mathworks.com
WWW: http://www.mathworks.com

Contents

Preface

This book is written at the level of the senior engineering student and is intended to be used as a text for the first course in control systems. It presents a comprehensive treatment of the analysis and design of continuous-time control systems. It is assumed that the reader has had courses on introductory differential equations, introductory vector-matrix analysis, introductory circuit analysis, and mechanics.

In this third edition, MATLAB® is integrated into the text. All computational problems are solved with MATLAB. Also, design aspects have been strengthened, and new topics, examples and problems are added.

The text is organized into 13 chapters and an appendix. The outline of the book is as follows: Chapter 1 presents introductory materials on control systems. Chapter 2 gives the Laplace transforms of commonly encountered time functions and basic Laplace transform theorems. (If the students have an adequate background on the Laplace transform, this chapter may be skipped.) Chapter 3 treats mathematical modeling of dynamic systems and develops transfer-function models and state-space models. Chapter 4 gives transient-response analysis of first- and second-order systems. This chapter includes a computational analysis of transient response by use of MATLAB. Chapter 5 presents basic control actions in industrial automatic controllers and discusses pneumatic, hydraulic, and electronic controllers. This chapter also discusses the response of higher-order systems and Routh's stability criterion.

Chapter 6 treats the root-locus analysis. The MATLAB approach to plotting root loci is presented in this chapter. Chapter 7 presents the design of lead, lag and lag–lead compensators by the root-locus method. Chapter 8 deals with the frequency-response analysis of control systems. Bode diagrams, polar plots, the Nyquist stability criterion,

and closed-loop frequency response are discussed, including the MATLAB approach to obtain frequency-response plots. Chapter 9 covers the design and compensation techniques using frequency-response methods. Specifically, the Bode diagram approach to the design of lead, lag, and lag–lead compensators is discussed in detail in this chapter. Chapter 10 deals with the basic and modified PID controls. This chapter gives discussions of two-degrees-of-freedom controls and design considerations for robust control.

Chapter 11 presents a basic analysis of control systems in state space. Concepts of controllability and observability are given here. The transformation of system models (from transfer-function model to state-space model, and vice versa) by the use of MATLAB is included in this chapter. Chapter 12 treats the design of control systems in state space. This chapter begins with pole-placement design problems, followed by the design of state observers. A design of a type 1 servo system based on the pole-placement approach is presented, including a computational solution with MATLAB. Chapter 13 begins with Liapunov stability analysis, followed by design of a model-reference control system, where the conditions for Liapunov stability are formulated first and then the system is designed within these limitations. Then quadratic optimal control problems are treated. Here the Liapunov stability equation is used to lead into quadratic optimal control theory. A MATLAB solution to the quadratic optimal control problem is also presented.

No prior knowledge of MATLAB is assumed in this book. If the reader is not yet familiar with MATLAB, it is suggested that he or she read the appendix first and then study MATLAB as presented in the text.

Throughout the book the basic concepts involved are emphasized and highly mathematical arguments are carefully avoided in the presentation of the materials. Mathematical proofs are provided when they contribute to the understanding of the subjects presented. All the material has been organized toward a gradual development of control theory.

Examples are presented at strategic points throughout the book so that the reader will have a better understanding of the subject matter discussed. In addition, a number of solved problems (A-problems) are provided at the end of each chapter. These problems constitute an integral part of the text. It is suggested that the reader study all of these problems carefully to obtain a deeper understanding of the topics discussed. In addition, many unsolved problems (B-problems) are provided for use as homework or quiz problems. An instructor using this text can obtain a complete solutions manual (for B-problems) from the publisher.

Most of the materials presented in this book have been class tested in senior and first-year graduate-level courses on control systems at the University of Minnesota.

If this book is used as a text for a four-hour quarter course (with 40 lecture hours) or a three-hour semester course (with 42 lecture hours), most of the materials in the first 10 chapters may be covered. (The first 10 chapters cover all basic materials of control systems normally required in a first course on control systems.) If this book is used as a text for a four-hour semester course (with 52 lecture hours), a good part of the book may be covered with flexibility in omitting certain subjects. For a two-quarter course sequence (with 60 or more lecture hours), the entire book may be covered. This book can also serve as a self-study book for practicing engineers who wish to study basic materials of control theory.

I would like to express my sincere appreciation to Professor Suhada Jayasuriya of Texas A & M University, who reviewed the final manuscript and made many constructive comments. Appreciation is also due to Linda Ratts Engelman for her enthusiasm in publishing the third edition, to the anonymous reviewers who made valuable suggestions at the early stage of the revision process, and to my former students who solved many of the A-problems and B-problems included in this book.

Katsuhiko Ogata

1

Introduction to Control Systems

1–1 INTRODUCTION

Automatic control has played a vital role in the advance of engineering and science. In addition to its extreme importance in space-vehicle systems, missile-guidance systems, robotic systems, and the like, automatic control has become an important and integral part of modern manufacturing and industrial processes. For example, automatic control is essential in the numerical control of machine tools in the manufacturing industries, in the design of autopilot systems in the aerospace industries, and in the design of cars and trucks in the automobile industries. It is also essential in such industrial operations as controlling pressure, temperature, humidity, viscosity, and flow in the process industries.

Since advances in the theory and practice of automatic control provide the means for attaining optimal performance of dynamic systems, improving productivity, relieving the drudgery of many routine repetitive manual operations, and more, most engineers and scientists must now have a good understanding of this field.

Historical review. The first significant work in automatic control was James Watt's centrifugal governor for the speed control of a steam engine in the eighteenth century. Other significant works in the early stages of development of control theory were due to Minorsky, Hazen, and Nyquist, among many others. In 1922, Minorsky worked on automatic controllers for steering ships and showed how stability could be determined from the differential equations describing the system. In 1932, Nyquist developed a relatively simple procedure for determining the stability of closed-loop systems on the basis of open-loop response to steady-state sinusoidal inputs. In 1934, Hazen, who

introduced the term servomechanisms for position control systems, discussed the design of relay servomechanisms capable of closely following a changing input.

During the decade of the 1940s, frequency-response methods made it possible for engineers to design linear closed-loop control systems that satisfied performance requirements. From the end of the 1940s to early 1950s, the root-locus method due to Evans was fully developed.

The frequency-response and root-locus methods, which are the core of classical control theory, lead to systems that are stable and satisfy a set of more or less arbitrary performance requirements. Such systems are, in general, acceptable but not optimal in any meaningful sense. Since the late 1950s, the emphasis in control design problems has been shifted from the design of one of many systems that work to the design of one optimal system in some meaningful sense.

As modern plants with many inputs and outputs become more and more complex, the description of a modern control system requires a large number of equations. Classical control theory, which deals only with single-input–single-output systems, becomes powerless for multiple-input–multiple-output systems. Since about 1960, because the availability of digital computers made possible time-domain analysis of complex systems, modern control theory, based on time-domain analysis and synthesis using state variables, has been developed to cope with the increased complexity of modern plants and the stringent requirements on accuracy, weight, and cost in military, space, and industrial applications.

During the years from 1960 to 1980, optimal control of both deterministic and stochastic systems, as well as adaptive and learning control of complex systems, were fully investigated. From 1980 to the present, developments in modern control theory centered around robust control, H_∞ control, and associated topics.

Now that digital computers have become cheaper and more compact, they are used as integral parts of control systems. Recent applications of modern control theory include such nonengineering systems as biological, biomedical, economic, and socioeconomic systems.

Definitions. Before we can discuss control systems, some basic terminologies must be defined.

Controlled Variable and Manipulated Variable. The *controlled* variable is the quantity or condition that is measured and controlled. The *manipulated* variable is the quantity or condition that is varied by the controller so as to affect the value of the controlled variable. Normally, the controlled variable is the output of the system. *Control* means measuring the value of the controlled variable of the system and applying the manipulated variable to the system to correct or limit deviation of the measured value from a desired value.

In studying control engineering, we need to define additional terms that are necessary to describe control systems.

Plants. A plant may be a piece of equipment, perhaps just a set of machine parts functioning together, the purpose of which is to perform a particular operation. In this book, we shall call any physical object to be controlled (such as a mechanical device, a heating furnace, a chemical reactor, or a spacecraft) a plant.

Processes. The *Merriam–Webster Dictionary* defines a process to be a natural, progressively continuing operation or development marked by a series of gradual changes that succeed one another in a relatively fixed way and lead toward a particular result or end; or an artifical or voluntary, progressively continuing operation that consists of a series of controlled actions or movements systematically directed toward a particular result or end. In this book we shall call any operation to be controlled a *process.* Examples are chemical, economic, and biological processes.

Systems. A system is a combination of components that act together and perform a certain objective. A system is not limited to physical ones. The concept of the system can be applied to abstract, dynamic phenomena such as those encountered in economics. The word system should, therefore, be interpreted to imply physical, biological, economic, and the like, systems.

Disturbances. A disturbance is a signal that tends to adversely affect the value of the output of a system. If a disturbance is generated within the system, it is called *internal,* while an *external* disturbance is generated outside the system and is an input.

Feedback Control. Feedback control refers to an operation that, in the presence of disturbances, tends to reduce the difference between the output of a system and some reference input and that does so on the basis of this difference. Here only unpredictable disturbances are so specified, since predictable or known disturbances can always be compensated for within the system.

1–2 EXAMPLES OF CONTROL SYSTEMS

In this section we shall present several examples of control systems.

Speed control system. The basic principle of a Watt's speed governor for an engine is illustrated in the schematic diagram of Figure 1–1. The amount of fuel admitted

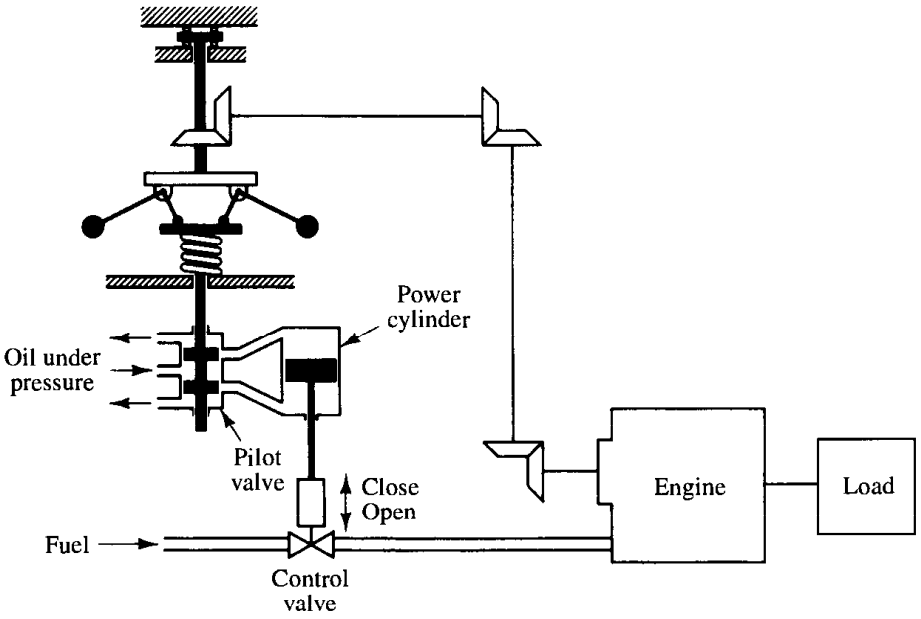

Figure 1–1
Speed control system.

to the engine is adjusted according to the difference between the desired and the actual engine speeds.

The sequence of actions may be stated as follows: The speed governor is adjusted such that, at the desired speed, no pressured oil will flow into either side of the power cylinder. If the actual speed drops below the desired value due to disturbance, then the decrease in the centrifugal force of the speed governor causes the control valve to move downward, supplying more fuel, and the speed of the engine increases until the desired value is reached. On the other hand, if the speed of the engine increases above the desired value, then the increase in the centrifugal force of the governor causes the control valve to move upward. This decreases the supply of fuel, and the speed of the engine decreases until the desired value is reached.

In this speed control system, the plant (controlled system) is the engine and the controlled variable is the speed of the engine. The difference between the desired speed and the actual speed is the error signal. The control signal (the amount of fuel) to be applied to the plant (engine) is the actuating signal. The external input to disturb the controlled variable is the disturbance. An unexpected change in the load is a disturbance.

Robot control system. Industrial robots are frequently used in industry to improve productivity. The robot can handle monotonous jobs as well as complex jobs without errors in operation. The robot can work in an environment intolerable to human operators. For example, it can work in extreme temperatures (both high and low) or in a high- or low-pressure environment or under water or in space. There are special robots for fire fighting, underwater exploration, and space exploration, among many others.

The industrial robot must handle mechanical parts that have particular shapes and weights. Hence, it must have at least an arm, a wrist, and a hand. It must have sufficient power to perform the task and the capability for at least limited mobility. In fact, some robots of today are able to move freely by themselves in a limited space in a factory.

The industrial robot must have some sensory devices. In low-level robots, microswitches are installed in the arms as sensory devices. The robot first touches an object and then, through the microswitches, confirms the existence of the object in space and proceeds in the next step to grasp it.

In a high-level robot, an optical means (such as a television system) is used to scan the background of the object. It recognizes the pattern and determines the presence and orientation of the object. A computer is necessary to process signals in the pattern-recognition process (see Figure 1–2). In some applications, the computerized robot recognizes the presence and orientation of each mechanical part by a pattern-recognition process that consists of reading the code numbers attached to it. Then the robot picks up the part and moves it to an appropriate place for assembling, and there it assembles several parts into a component. A well-programmed digital computer acts as a controller.

Temperature control system. Figure 1–3 shows a schematic diagram of temperature control of an electric furnace. The temperature in the electric furnace is measured by a thermometer, which is an analog device. The analog temperature is converted to a digital temperature by an A/D converter. The digital temperature is fed to a controller through an interface. This digital temperature is compared with the programmed input temperature, and if there is any discrepancy (error), the controller sends out a signal to

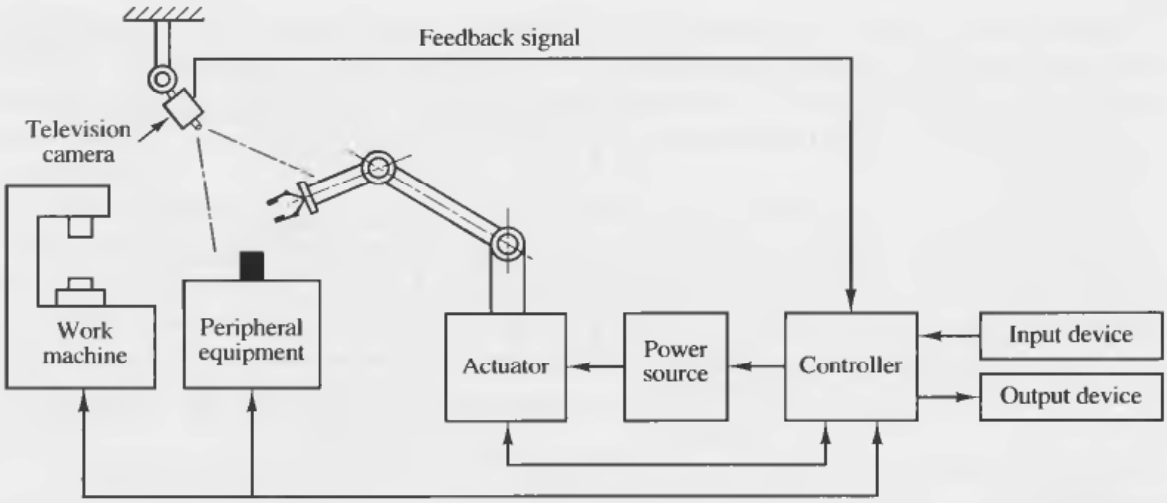

Figure 1–2
Robot using a pattern-recognition process.

the heater, through an interface, amplifier, and relay, to bring the furnace temperature to a desired value.

Temperature control of the passenger compartment of a car. Figure 1–4 shows a functional diagram of temperature control of the passenger compartment of a car. The desired temperature, converted to a voltage, is the input to the controller. The actual temperature of the passenger compartment is converted to a voltage through a sensor and is fed back to the controller for comparison with the input. The ambient temperature and radiation heat transfer from the sun, which are not constant while the car is driven, act as disturbances. This system employs both feedback control and feedforward control. (Feedforward control gives corrective action before the disturbances affect the output.)

The temperature of the passenger car compartment differs considerably depending on the place where it is measured. Instead of using multiple sensors for temperature measurement and averaging the measured values, it is economical to install a small suction blower at the place where passengers normally sense the temperature. The temperature of the air from the suction blower is an indication of the passenger compartment temperature and is considered the output of the system.

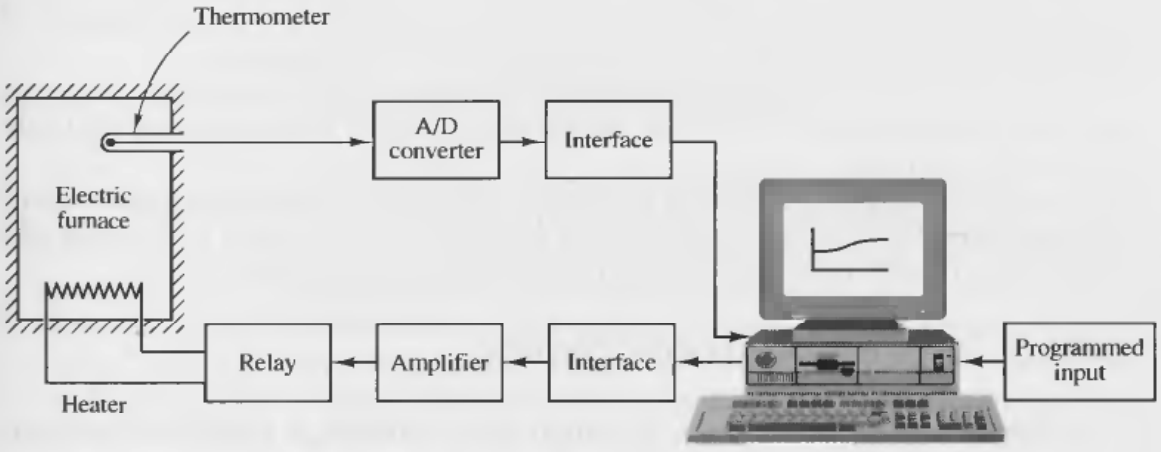

Figure 1–3
Temperature control system.

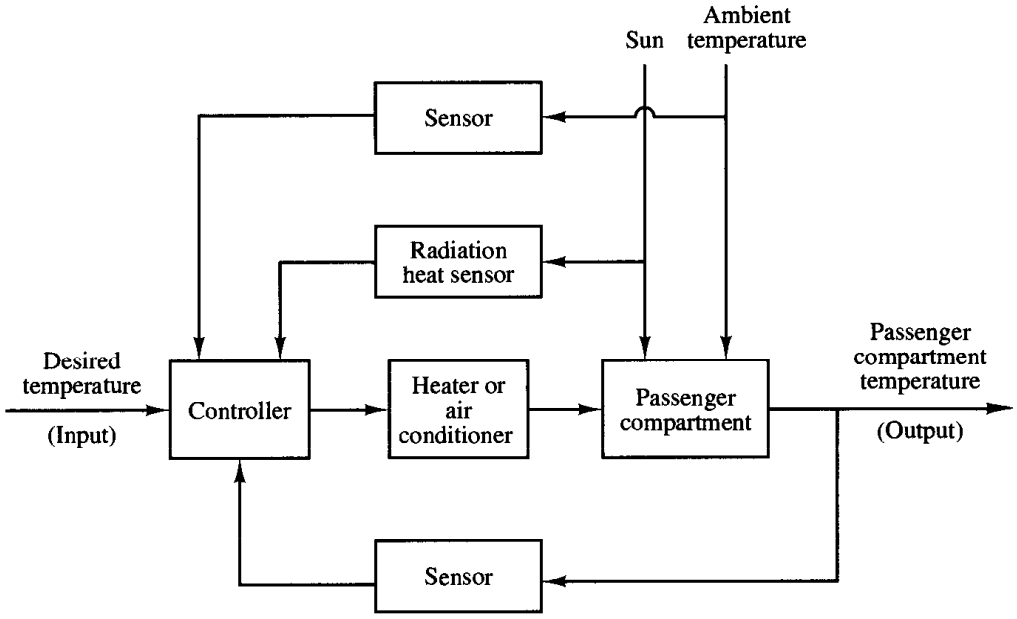

Figure 1–4
Temperature control of passenger compartment of a car.

The controller receives the input signal, output signal, and signals from sensors from disturbance sources. The controller sends out an optimal control signal to the air conditioner or heater to control the amount of cooling air or warm air so that the passenger compartment temperature is about the desired temperature.

Business systems. A business system may consist of many groups. Each task assigned to a group will represent a dynamic element of the system. Feedback methods of reporting the accomplishments of each group must be established in such a system for proper operation. The cross-coupling between functional groups must be made a minimum in order to reduce undesirable delay times in the system. The smaller this cross-coupling, the smoother the flow of work signals and materials will be.

A business system is a closed-loop system. A good design will reduce the managerial control required. Note that disturbances in this system are the lack of personnel or materials, interruption of communication, human errors, and the like.

The establishment of a well-founded estimating system based on statistics is mandatory to proper management. (Note that it is a well-known fact that the performance of such a system can be improved by the use of lead time, or *anticipation.*)

To apply control theory to improve the performance of such a system, we must represent the dynamic characteristic of the component groups of the system by a relatively simple set of equations.

Although it is certainly a difficult problem to derive mathematical representations of the component groups, the application of optimization techniques to business systems significantly improves the performance of the business system.

1–3 CLOSED-LOOP CONTROL VERSUS OPEN-LOOP CONTROL

Feedback control systems. A system that maintains a prescribed relationship between the output and the reference input by comparing them and using the difference as a means of control is called a *feedback control system.* An example would

be a room-temperature control system. By measuring the actual room temperature and comparing it with the reference temperature (desired temperature), the thermostat turns the heating or cooling equipment on or off in such a way as to ensure that the room temperature remains at a comfortable level regardless of outside conditions.

Feedback control systems are not limited to engineering but can be found in various nonengineering fields as well. The human body, for instance, is a highly advanced feedback control system. Both body temperature and blood pressure are kept constant by means of physiological feedback. In fact, feedback performs a vital function: It makes the human body relatively insensitive to external disturbances, thus enabling it to function properly in a changing environment.

Closed-loop control systems. Feedback control systems are often referred to as *closed-loop control systems.* In practice, the terms feedback control and closed-loop control are used interchangeably. In a closed-loop control system the actuating error signal, which is the difference between the input signal and the feedback signal (which may be the output signal itself or a function of the output signal and its derivatives and/or integrals), is fed to the controller so as to reduce the error and bring the output of the system to a desired value. The term closed-loop control always implies the use of feedback control action in order to reduce system error.

Open-loop control systems. Those systems in which the output has no effect on the control action are called *open-loop control systems.* In other words, in an open-loop control system the output is neither measured nor fed back for comparison with the input. One practical example is a washing machine. Soaking, washing, and rinsing in the washer operate on a time basis. The machine does not measure the output signal, that is, the cleanliness of the clothes.

In any open-loop control system the output is not compared with the reference input. Thus, to each reference input there corresponds a fixed operating condition; as a result, the accuracy of the system depends on calibration. In the presence of disturbances, an open-loop control system will not perform the desired task. Open-loop control can be used, in practice, only if the relationship between the input and output is known and if there are neither internal nor external disturbances. Clearly, such systems are not feedback control systems. Note that any control system that operates on a time basis is open loop. For instance, traffic control by means of signals operated on a time basis is another example of open-loop control.

Closed-loop versus open-loop control systems. An advantage of the closed-loop control system is the fact that the use of feedback makes the system response relatively insensitive to external disturbances and internal variations in system parameters. It is thus possible to use relatively inaccurate and inexpensive components to obtain the accurate control of a given plant, whereas doing so is impossible in the open-loop case.

From the point of view of stability, the open-loop control system is easier to build because system stability is not a major problem. On the other hand, stability *is* a major problem in the closed-loop control system, which may tend to overcorrect errors that can cause oscillations of constant or changing amplitude.

It should be emphasized that for systems in which the inputs are known ahead of time and in which there are no disturbances it is advisable to use open-loop control. Closed-loop control systems have advantages only when unpredictable disturbances and/or unpredictable variations in system components are present. Note that the output power rating partially determines the cost, weight, and size of a control system. The number of components used in a closed-loop control system is more than that for a corresponding open-loop control system. Thus, the closed-loop control system is generally higher in cost and power. To decrease the required power of a system, open-loop control may be used where applicable. A proper combination of open-loop and closed-loop controls is usually less expensive and will give satisfactory overall system performance.

1–4 DESIGN OF CONTROL SYSTEMS

Actual control systems are generally nonlinear. However, if they can be approximated by linear mathematical models, we may use one or more of the well-developed design methods. In a practical sense, the performance specifications given to the particular system suggest which method to use. If the performance specifications are given in terms of transient-response characteristics and/or frequency-domain performance measures, then we have no choice but to use a conventional approach based on the root-locus and/or frequency-response methods. (These methods are presented in Chapters 6 through 9.) If the performance specifications are given as performance indexes in terms of state variables, then modern control approaches should be used. (These approaches are presented in Chapters 11 through 13.)

While control system design via the root-locus and frequency-response approaches is an engineering endeavor, system design in the context of modern control theory (state-space methods) employs mathematical formulations of the problem and applies mathematical theory to design problems in which the system can have multiple inputs and multiple outputs and can be time varying. By applying modern control theory, the designer is able to start from a performance index, together with constraints imposed on the system, and to proceed to design a stable system by a completely analytical procedure. The advantage of design based on such modern control theory is that it enables the designer to produce a control system that is optimal with respect to the performance index considered.

The systems that may be designed by a conventional approach are usually limited to single-input–single-output, linear time-invariant systems. The designer seeks to satisfy all performance specifications by means of educated trial-and-error repetition. After a system is designed, the designer checks to see if the designed system satisfies all the performance specifications. If it does not, then he repeats the design process by adjusting parameter settings or by changing the system configuration until the given specifications are met. Although the design is based on a trial-and-error procedure, the ingenuity and know-how of the designer will play an important role in a successful design. An experienced designer may be able to design an acceptable system without using many trials.

It is generally desirable that the designed system should exhibit as small errors as possible in responding to the input signal. In this regard, the damping of the system should be reasonable. The system dynamics should be relatively insensitive to small changes in system parameters. The undesirable disturbances should be well attenuated. [In general, the high-frequency portion should attenuate fast so that high-frequency noises (such as sensor noises) can be attenuated. If the noise or disturbance frequencies are known, notch filters may be used to attenuate these specific frequencies.] If the design of the system is boiled down to a few candidates, an optimal choice among them may be made from such considerations as projected overall performance, cost, space, and weight.

1–5 OUTLINE OF THE BOOK

In what follows we shall briefly present the arrangements and contents of the book.

Chapter 1 has given introductory materials on control systems. Chapter 2 presents basic Laplace transform theory necessary for understanding the control theory presented in this book. Chapter 3 deals with mathematical modeling of dynamic systems in terms of transfer functions and state-space equations. This chapter includes discussions of linearization of nonlinear systems. Chapter 4 treats transient-response analyses of first- and second-order systems. This chapter also gives details of transient-response analysis with MATLAB. Chapter 5 first presents basic control actions and then discusses pneumatic, hydraulic, and electronic controllers. This chapter also discusses Routh's stability criterion.

Chapter 6 gives a root-locus analysis of control systems. General rules for constructing root loci are presented. Detailed discussions for plotting root loci with MATLAB are included. Chapter 7 deals with the design of control systems via the root-locus method. Specifically, root-locus approaches to the design of lead compensators, lag compensators, and lag–lead compensators are discussed in detail. Chapter 8 gives the frequency-response analysis of control systems. Bode diagrams, polar plots, Nyquist stability criterion, and closed-loop frequency response are discussed. Chapter 9 treats control systems design via the frequency-response approach. Here Bode diagrams are used to design lead compensators, lag compensators, and lag–lead compensators. Chapter 10 discusses the basic and modified PID controls. Topics included are tuning rules for PID controllers, modifications of PID control schemes, two-degrees-of-freedom control, and design considerations for robust control.

Chapter 11 presents basic materials for the state-space analysis of control systems. The solution of the time-invariant state equation is derived and concepts of controllability and observability are discussed. Chapter 12 treats the design of control systems in state space. This chapter begins with the pole-placement problems, followed by the design of state observers, and concludes with the design of type 1 servo systems. MATLAB is utilized in solving pole-placement problems, design of state observers, and design of servo systems. Chapter 13, the final chapter, presents the Liapunov stability analysis and the quadratic optimal control. This chapter begins with the Liapunov stability analysis. Then the Liapunov stability approach is used for designing

model-reference control systems. Finally, quadratic optimal control problems are discussed in detail. Here the Liapunov stability approach is utilized to derive the Riccati equation for quadratic optimal control. MATLAB solutions to quadratic optimal control problems are included.

The appendix summarizes background materials necessary for the effective use of MATLAB. This appendix is specifically provided for those readers who are as yet unfamiliar with MATLAB.

EXAMPLE PROBLEMS AND SOLUTIONS

A-1-1. List the major advantages and disadvantages of open-loop control systems.

Solution. The advantages of open-loop control systems are as follows:

1. Simple construction and ease of maintenance.
2. Less expensive than a corresponding closed-loop system.
3. There is no stability problem.
4. Convenient when output is hard to measure or economically not feasible. (For example, in the washer system, it would be quite expensive to provide a device to measure the quality of the output, cleanliness of the clothes, of the washer.)

The disadvantages of open-loop control systems are as follows:

1. Disturbances and changes in calibration cause errors, and the output may be different from what is desired.
2. To maintain the required quality in the output, recalibration is necessary from time to time.

A-1-2. Figure 1–5(a) is a schematic diagram of a liquid-level control system. Here the automatic controller maintains the liquid level by comparing the actual level with a desired level and correcting any error by adjusting the opening of the pneumatic valve. Figure 1–5(b) is a block diagram of the control system. Draw the corresponding block diagram for a human-operated liquid-level control system.

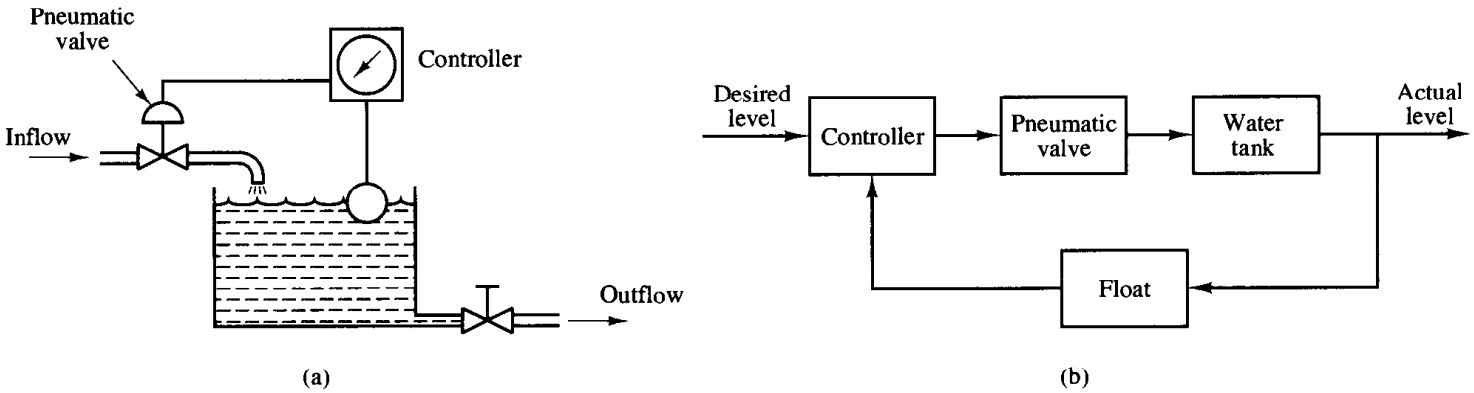

Figure 1–5
(a) Liquid-level control system; (b) block diagram.

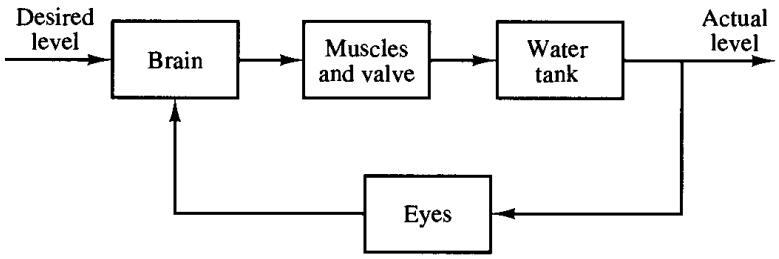

Figure 1–6
Block diagram of human-operated liquid-level control system.

Solution. In the human-operated system, the eyes, brain, and muscles correspond to the sensor, controller, and pneumatic valve, respectively. A block diagram is shown in Figure 1–6.

A-1-3. An engineering organizational system is composed of major groups, such as management, research and development, preliminary design, experiments, product design and drafting, fabrication and assembling, and testing. These groups are interconnected to make up the whole operation.

The system may be analyzed by reducing it to the most elementary set of components necessary that can provide the analytical detail required and by representing the dynamic characteristics of each component by a set of simple equations. (The dynamic performance of such a system may be determined from the relation between progressive accomplishment and time.)

Draw a functional block diagram showing an engineering organizational system.

Solution. A functional block diagram can be drawn by using blocks to represent the functional activities and interconnecting signal lines to represent the information or product output of the system operation. A possible block diagram is shown in Figure 1–7.

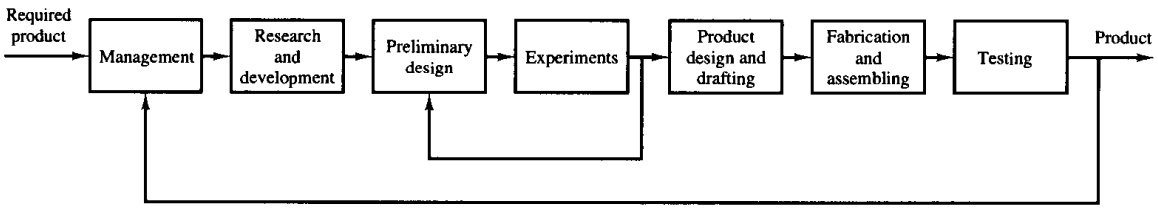

Figure 1–7
Block diagram of an engineering organizational system.

PROBLEMS

B-1-1. Many closed-loop and open-loop control systems may be found in homes. List several examples and describe them.

B-1-2. Give two examples of feedback control systems in which a human acts as a controller.

B-1-3. Figure 1–8 shows a tension control system. Explain the sequence of control actions when the feed speed is suddenly changed for a short time.

B-1-4. Many machines, such as lathes, milling machines, and grinders, are provided with tracers to reproduce the contour of templates. Figure 1–9 shows a schematic diagram of a tracing system in which the tool duplicates the shape of the template on the workpiece. Explain the operation of this system.

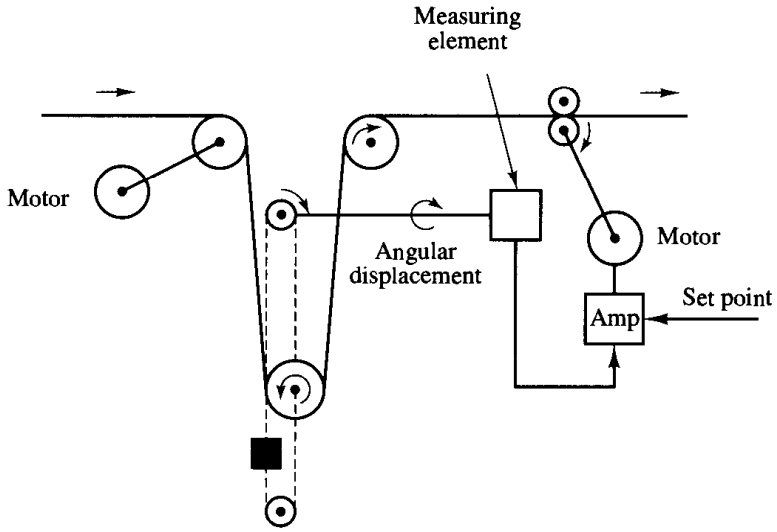

Figure 1–8
Tension control system.

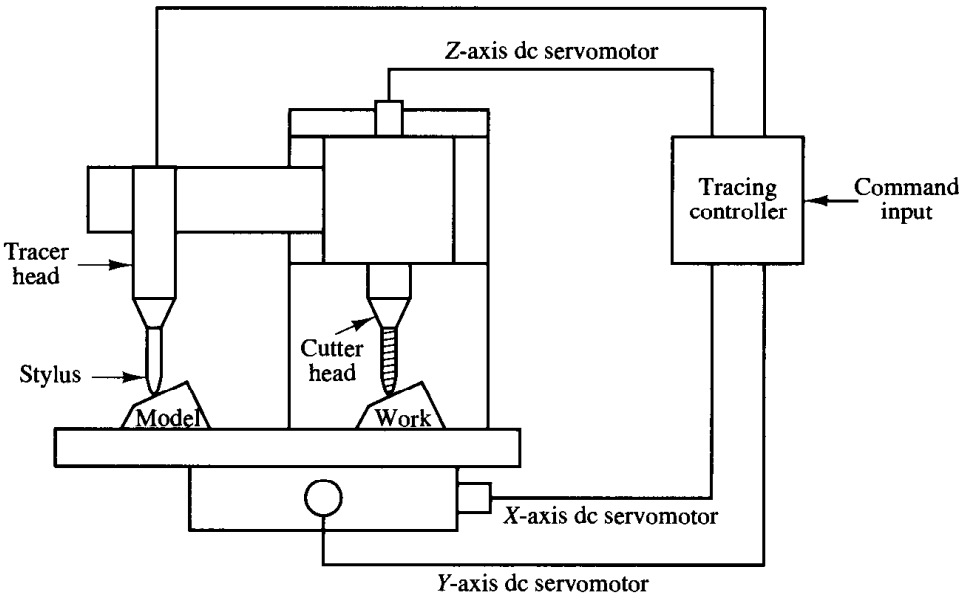

Figure 1–9
Schematic diagram of a tracing system.

2

The Laplace Transform*

2–1 INTRODUCTION

The Laplace transform method is an operational method that can be used advantageously for solving linear differential equations. By use of Laplace transforms, we can convert many common functions, such as sinusoidal functions, damped sinusoidal functions, and exponential functions, into algebraic functions of a complex variable s. Operations such as differentiation and integration can be replaced by algebraic operations in the complex plane. Thus, a linear differential equation can be transformed into an algebraic equation in a complex variable s. If the algebraic equation in s is solved for the dependent variable, then the solution of the differential equation (the inverse Laplace transform of the dependent variable) may be found by use of a Laplace transform table or by use of the partial-fraction expansion technique, which is presented in Section 2–5.

An advantage of the Laplace transform method is that it allows the use of graphical techniques for predicting the system performance without actually solving system differential equations. Another advantage of the Laplace transform method is that, when we solve the differential equation, both the transient component and steady-state component of the solution can be obtained simultaneously.

Outline of the chapter. Section 2–1 presents introductory remarks. Section 2–2 briefly reviews complex variables and complex functions. Section 2–3 derives Laplace

*This chapter may be skipped if the student is already familiar with Laplace transforms.

transforms of time functions that are frequently used in control engineering. Section 2–4 presents useful theorems of Laplace transforms, and Section 2–5 treats the inverse Laplace transformation. Section 2–6 presents the MATLAB approach to obtain partial-fraction expansion of $B(s)/A(s)$, where $A(s)$ and $B(s)$ are polynomials in s. Finally, Section 2–7 deals with solutions of linear time-invariant differential equations by the Laplace transform approach.

2–2 REVIEW OF COMPLEX VARIABLES AND COMPLEX FUNCTIONS

Before we present the Laplace transformation, we shall review the complex variable and complex function. We shall also review Euler's theorem, which relates the sinusoidal functions to exponential functions.

Complex variable. A complex number has a real part and an imaginary part, both of which are constant. If the real part and/or imaginary part are variables, a complex number is called a *complex variable.* In the Laplace transformation we use the notation s as a complex variable; that is,

$$s = \sigma + j\omega$$

where σ is the real part and ω is the imaginary part.

Complex function. A complex function $F(s)$, a function of s, has a real part and an imaginary part or

$$F(s) = F_x + jF_y$$

where F_x and F_y are real quantities. The magnitude of $F(s)$ is $\sqrt{F_x^2 + F_y^2}$, and the angle θ of $F(s)$ is $\tan^{-1}(F_y/F_x)$. The angle is measured counterclockwise from the positive real axis. The complex conjugate of $F(s)$ is $\bar{F}(s) = F_x - jF_y$.

Complex functions commonly encountered in linear control systems analysis are single-valued functions of s and are uniquely determined for a given value of s.

A complex function $G(s)$ is said to be *analytic* in a region if $G(s)$ and all its derivatives exist in that region. The derivative of an analytic function $G(s)$ is given by

$$\frac{d}{ds}G(s) = \lim_{\Delta s \to 0} \frac{G(s + \Delta s) - G(s)}{\Delta s} = \lim_{\Delta s \to 0} \frac{\Delta G}{\Delta s}$$

Since $\Delta s = \Delta\sigma + j\Delta\omega$, Δs can approach zero along an infinite number of different paths. It can be shown, but is stated without a proof here, that if the derivatives taken along two particular paths, that is, $\Delta s = \Delta\sigma$ and $\Delta s = j\Delta\omega$, are equal, then the derivative is unique for any other path $\Delta s = \Delta\sigma + j\Delta\omega$ and so the derivative exists.

For a particular path $\Delta s = \Delta\sigma$ (which means that the path is on the real axis),

$$\frac{d}{ds}G(s) = \lim_{\Delta\sigma \to 0}\left(\frac{\Delta G_x}{\Delta\sigma} + j\frac{\Delta G_y}{\Delta\sigma}\right) = \frac{\partial G_x}{\partial\sigma} + j\frac{\partial G_y}{\partial\sigma}$$

For another particular path $\Delta s = j\Delta\omega$ (which means that the path is on the imaginary axis),

$$\frac{d}{ds}G(s) = \lim_{j\Delta\omega\to 0}\left(\frac{\Delta G_x}{j\Delta\omega} + j\frac{\Delta G_y}{j\Delta\omega}\right) = -j\frac{\partial G_x}{\partial\omega} + \frac{\Delta G_y}{\partial\omega}$$

If these two values of the derivative are equal,

$$\frac{\partial G_x}{\partial\sigma} + j\frac{\partial G_y}{\partial\sigma} = \frac{\partial G_y}{\partial\omega} - j\frac{\partial G_x}{\partial\omega}$$

or if the following two conditions

$$\frac{\partial G_x}{\partial\sigma} = \frac{\partial G_y}{\partial\omega} \qquad \text{and} \qquad \frac{\partial G_y}{\partial\sigma} = -\frac{\partial G_x}{\partial\omega}$$

are satisfied, then the derivative $dG(s)/ds$ is uniquely determined. These two conditions are known as the Cauchy–Riemann conditions. If these conditions are satisfied, the function $G(s)$ is analytic.

As an example, consider the following $G(s)$:

$$G(s) = \frac{1}{s+1}$$

Then

$$G(\sigma + j\omega) = \frac{1}{\sigma + j\omega + 1} = G_x + jG_y$$

where

$$G_x = \frac{\sigma+1}{(\sigma+1)^2 + \omega^2} \qquad \text{and} \qquad G_y = \frac{-\omega}{(\sigma+1)^2 + \omega^2}$$

It can be seen that, except at $s = -1$ (that is, $\sigma = -1, \omega = 0$), $G(s)$ satisfies the Cauchy–Riemann conditions:

$$\frac{\partial G_x}{\partial\sigma} = \frac{\partial G_y}{\partial\omega} = \frac{\omega^2 - (\sigma+1)^2}{[(\sigma+1)^2 + \omega^2]^2}$$

$$\frac{\partial G_y}{\partial\sigma} = -\frac{\partial G_x}{\partial\omega} = \frac{2\omega(\sigma+1)}{[(\sigma+1)^2 + \omega^2]^2}$$

Hence $G(s) = 1/(s+1)$ is analytic in the entire s plane except at $s = -1$. The derivative $dG(s)/ds$, except at $s = 1$, is found to be

$$\frac{d}{ds}G(s) = \frac{\partial G_x}{\partial\sigma} + j\frac{\partial G_y}{\partial\sigma} = \frac{\partial G_y}{\partial\omega} - j\frac{\partial G_x}{\partial\omega}$$

$$= -\frac{1}{(\sigma + j\omega + 1)^2} = -\frac{1}{(s+1)^2}$$

Note that the derivative of an analytic function can be obtained simply by differentiating $G(s)$ with respect to s. In this example,

$$\frac{d}{ds}\left(\frac{1}{s+1}\right) = -\frac{1}{(s+1)^2}$$

Points in the s plane at which the function $G(s)$ is analytic are called *ordinary* points, while points in the s plane at which the function $G(s)$ is not analytic are called *singular* points. Singular points at which the function $G(s)$ or its derivatives approach infinity are called *poles*. In the previous example, $s = -1$ is a singular point and is a pole of the function $G(s)$.

If $G(s)$ approaches infinity as s approaches $-p$ and if the function

$$G(s)(s+p)^n, \qquad \text{for } n = 1, 2, 3, \ldots$$

has a finite, nonzero value at $s = -p$, then $s = -p$ is called a pole of order n. If $n = 1$, the pole is called a simple pole. If $n = 2, 3, \ldots$, the pole is called a second-order pole, a third-order pole, and so on. Points at which the function $G(s)$ equals zero are called *zeros*.

To illustrate, consider the complex function

$$G(s) = \frac{K(s+2)(s+10)}{s(s+1)(s+5)(s+15)^2}$$

$G(s)$ has zeros at $s = -2, s = -10$, simple poles at $s = 0, s = -1, s = -5$, and a double pole (multiple pole of order 2) at $s = -15$. Note that $G(s)$ becomes zero at $s = \infty$. Since for large values of s

$$G(s) \doteq \frac{K}{s^3}$$

$G(s)$ possesses a triple zero (multiple zero of order 3) at $s = \infty$. If points at infinity are included, $G(s)$ has the same number of poles as zeros. To summarize, $G(s)$ has five zeros ($s = -2, s = -10, s = \infty, s = \infty, s = \infty$) and five poles ($s = 0, s = -1, s = -5, s = -15, s = -15$).

Euler's theorem. The power series expansions of $\cos\theta$ and $\sin\theta$ are, respectively,

$$\cos\theta = 1 - \frac{\theta^2}{2!} + \frac{\theta^4}{4!} - \frac{\theta^6}{6!} + \cdots$$

$$\sin\theta = \theta - \frac{\theta^3}{3!} + \frac{\theta^5}{5!} - \frac{\theta^7}{7!} + \cdots$$

And so

$$\cos\theta + j\sin\theta = 1 + (j\theta) + \frac{(j\theta)^2}{2!} + \frac{(j\theta)^3}{3!} + \frac{(j\theta)^4}{4!} + \cdots$$

Since

$$e^x = 1 + x + \frac{x^2}{2!} + \frac{x^3}{3!} + \cdots$$

we see that

$$\cos\theta + j\sin\theta = e^{j\theta} \tag{2–1}$$

This is known as *Euler's theorem.*

By using Euler's theorem, we can express sine and cosine in terms of an exponential function. Noting that $e^{-j\theta}$ is the complex conjugate of $e^{j\theta}$ and that

$$e^{j\theta} = \cos\theta + j\sin\theta$$

$$e^{-j\theta} = \cos\theta - j\sin\theta$$

we find, after adding and subtracting these two equations, that

$$\cos\theta = \frac{1}{2}(e^{j\theta} + e^{-j\theta}) \tag{2–2}$$

$$\sin\theta = \frac{1}{2j}(e^{j\theta} - e^{-j\theta}) \tag{2–3}$$

2–3 LAPLACE TRANSFORMATION

We shall first present a definition of the Laplace transformation and a brief discussion of the condition for the existence of the Laplace transform and then provide examples for illustrating the derivation of Laplace transforms of several common functions.

Let us define

$f(t)$ = a function of time t such that $f(t) = 0$ for $t < 0$

s = a complex variable

$\mathcal{L}$ = an operational symbol indicating that the quantity that it prefixes is to be transformed by the Laplace integral $\int_0^\infty e^{-st}\,dt$

$F(s)$ = Laplace transform of $f(t)$

Then the Laplace transform of $f(t)$ is given by

$$\mathcal{L}[f(t)] = F(s) = \int_0^\infty e^{-st}\,dt[f(t)] = \int_0^\infty f(t)e^{-st}\,dt$$

The reverse process of finding the time function $f(t)$ from the Laplace transform $F(s)$ is called the *inverse Laplace transformation.* The notation for the inverse Laplace transformation is $\mathcal{L}^{-1}$, and the inverse Laplace transform can be found from $F(s)$ by the following inversion integral:

$$\mathcal{L}^{-1}[F(s)] = f(t) = \frac{1}{2\pi j}\int_{c-j\infty}^{c+j\infty} F(s)e^{st}\,ds, \qquad \text{for } t > 0 \tag{2–4}$$

where c, the abscissa of convergence, is a real constant and is chosen larger than the real parts of all singular points of $F(s)$. Thus, the path of integration is parallel to the $j\omega$ axis and is displaced by the amount c from it. This path of integration is to the right of all singular points.

Evaluating the inversion integral appears complicated. In practice, we seldom use this integral for finding $f(t)$. There are simpler methods for finding $f(t)$. We shall discuss such simpler methods in Section 2–5.

It is noted that in this book the time function $f(t)$ is always assumed to be zero for negative time; that is,

$$f(t) = 0, \qquad \text{for } t < 0$$

Existence of Laplace transform. The Laplace transform of a function $f(t)$ exists if the Laplace integral converges. The integral will converge if $f(t)$ is sectionally continuous in every finite interval in the range $t > 0$ and if it is of exponential order as t approaches infinity. A function $f(t)$ is said to be of exponential order if a real, positive constant σ exists such that the function

$$e^{-\sigma t}|f(t)|$$

approaches zero as t approaches infinity. If the limit of the function $e^{-\sigma t}|f(t)|$ approaches zero for σ greater than σ_c and the limit approaches infinity for σ less than σ_c, the value σ_c is called the *abscissa of convergence.*

For the function $f(t) = Ae^{-\alpha t}$

$$\lim_{t\to\infty} e^{-\sigma t}|Ae^{-\alpha t}|$$

approaches zero if $\sigma > -\alpha$. The abscissa of convergence in this case is $\sigma_c = -\alpha$. The integral $\int_0^\infty f(t)e^{-st}\,dt$ converges only if σ, the real part of s, is greater than the abscissa of convergence σ_c. Thus the operator s must be chosen as a constant such that this integral converges.

In terms of the poles of the function $F(s)$, the abscissa of convergence σ_c corresponds to the real part of the pole located farthest to the right in the s plane. For example, for the following function $F(s)$,

$$F(s) = \frac{K(s + 3)}{(s + 1)(s + 2)}$$

the abscissa of convergence σ_c is equal to -1. It can be seen that for such functions as t, $\sin \omega t$, and $t \sin \omega t$ the abscissa of convergence is equal to zero. For functions like e^{-ct}, te^{-ct}, $e^{-ct}\sin \omega t$, and so on, the abscissa of convergence is equal to $-c$. For functions that increase faster than the exponential function, however, it is impossible to find suitable values of the abcissa of convergence. Therefore, such functions as e^{t^2} and te^{t^2} do not possess Laplace transforms.

The reader should be cautioned that although e^{t^2} (for $0 \le t \le \infty$) does not possess a Laplace transform, the time function defined by

$$\begin{aligned} f(t) &= e^{t^2}, \qquad \text{for } 0 \le t \le T < \infty \\ &= 0, \qquad \text{for } t < 0,\ T < t \end{aligned}$$

does possess a Laplace transform since $f(t) = e^{t^2}$ for only a limited time interval $0 \le t \le T$ and not for $0 \le t \le \infty$. Such a signal can be physically generated. Note that the signals that we can physically generate always have corresponding Laplace transforms.

If a function $f(t)$ has a Laplace transform, then the Laplace transform of $Af(t)$, where A is a constant, is given by

$$\mathcal{L}[Af(t)] = A\mathcal{L}[f(t)]$$

This is obvious from the definition of the Laplace transform. Similarly, if functions $f_1(t)$ and $f_2(t)$ have Laplace transforms, then the Laplace transform of the function $f_1(t) + f_2(t)$ is given by

$$\mathcal{L}[f_1(t) + f_2(t)] = \mathcal{L}[f_1(t)] + \mathcal{L}[f_2(t)]$$

Again the proof of this relationship is evident from the definition of the Laplace transform.

In what follows, we derive Laplace transforms of a few commonly encountered functions.

Exponential function. Consider the exponential function

$$\begin{aligned} f(t) &= 0, && \text{for } t < 0 \\ &= Ae^{-\alpha t}, && \text{for } t \geq 0 \end{aligned}$$

where A and α are constants. The Laplace transform of this exponential function can be obtained as follows:

$$\mathcal{L}[Ae^{-\alpha t}] = \int_0^\infty Ae^{-\alpha t}e^{-st}\,dt = A\int_0^\infty e^{-(\alpha+s)t}\,dt = \frac{A}{s+\alpha}$$

It is seen that the exponential function produces a pole in the complex plane.

In deriving the Laplace transform of $f(t) = Ae^{-\alpha t}$, we required that the real part of s be greater than $-\alpha$ (the abscissa of convergence). A question may immediately arise as to whether or not the Laplace transform thus obtained is valid in the range where $\sigma < -\alpha$ in the s plane. To answer this question, we must resort to the theory of complex variables. In the theory of complex variables, there is a theorem known as the analytic extension theorem. It states that, if two analytic functions are equal for a finite length along any arc in a region in which both are analytic, then they are equal everywhere in the region. The arc of equality is usually the real axis or a portion of it. By using this theorem the form of $F(s)$ determined by an integration in which s is allowed to have any real positive value greater than the abscissa of convergence holds for any complex values of s at which $F(s)$ is analytic. Thus, although we require the real part of s to be greater than the abscissa of convergence to make the $\int_0^\infty f(t)e^{-st}\,dt$ absolutely convergent, once the Laplace transform $F(s)$ is obtained, $F(s)$ can be considered valid throughout the entire s plane except at the poles of $F(s)$.

Step function. Consider the step function

$$\begin{aligned} f(t) &= 0, && \text{for } t < 0 \\ &= A, && \text{for } t > 0 \end{aligned}$$

where A is a constant. Note that it is a special case of the exponential function $Ae^{-\alpha t}$, where $\alpha = 0$. The step function is undefined at $t = 0$. Its Laplace transform is given by

$$\mathcal{L}[A] = \int_0^\infty Ae^{-st}\,dt = \frac{A}{s}$$

In performing this integration, we assumed that the real part of s was greater than zero (the abscissa of convergence) and therefore that $\lim_{t\to\infty} e^{-st}$ was zero. As stated

earlier, the Laplace transform thus obtained is valid in the entire s plane except at the pole $s = 0$.

The step function whose height is unity is called *unit-step* function. The unit-step function that occurs at $t = t_0$ is frequently written as $1(t - t_0)$. The step function of height A that occurs at $t = 0$ can then be written as $f(t) = A1(t)$. The Laplace transform of the unit-step function, which is defined by

$$\begin{aligned} 1(t) &= 0, \qquad \text{for } t < 0 \\ &= 1, \qquad \text{for } t > 0 \end{aligned}$$

is $1/s$, or

$$\mathcal{L}[1(t)] = \frac{1}{s}$$

Physically, a step function occurring at $t = 0$ corresponds to a constant signal suddenly applied to the system at time t equals zero.

Ramp function. Consider the ramp function

$$\begin{aligned} f(t) &= 0, \qquad \text{for } t < 0 \\ &= At, \qquad \text{for } t \geq 0 \end{aligned}$$

where A is a constant. The Laplace transform of this ramp function is obtained as

$$\mathcal{L}[At] = \int_0^\infty Ate^{-st}\,dt = At\frac{e^{-st}}{-s}\bigg|_0^\infty - \int_0^\infty \frac{Ae^{-st}}{-s}\,dt$$

$$= \frac{A}{s}\int_0^\infty e^{-st}\,dt = \frac{A}{s^2}$$

Sinusoidal function. The Laplace transform of the sinusoidal function

$$\begin{aligned} f(t) &= 0, \qquad \text{for } t < 0 \\ &= A \sin \omega t, \qquad \text{for } t \geq 0 \end{aligned}$$

where A and ω are constants, is obtained as follows. Referring to Equation (2–3), $\sin \omega t$ can be written

$$\sin \omega t = \frac{1}{2j}(e^{j\omega t} - e^{-j\omega t})$$

Hence

$$\mathcal{L}[A \sin \omega t] = \frac{A}{2j}\int_0^\infty (e^{j\omega t} - e^{-j\omega t})e^{-st}\,dt$$

$$= \frac{A}{2j}\frac{1}{s - j\omega} - \frac{A}{2j}\frac{1}{s + j\omega} = \frac{A\omega}{s^2 + \omega^2}$$

Similarly, the Laplace transform of $A \cos \omega t$ can be derived as follows:

$$\mathcal{L}[A \cos \omega t] = \frac{As}{s^2 + \omega^2}$$

Comments. The Laplace transform of any Laplace transformable function $f(t)$ can be found by multiplying $f(t)$ by e^{-st} and then integrating the product from $t = 0$ to $t = \infty$. Once we know the method of obtaining the Laplace transform, however, it is not necessary to derive the Laplace transform of $f(t)$ each time. Laplace transform tables can conveniently be used to find the transform of a given function $f(t)$. Table 2–1 shows Laplace transforms of time functions that will frequently appear in linear control systems analysis.

In the following discussion we present Laplace transforms of functions as well as theorems on the Laplace transformation that are useful in the study of linear control systems.

Translated function. Let us obtain the Laplace transform of the translated function $f(t - \alpha)1(t - \alpha)$, where $\alpha \geq 0$. This function is zero for $t < \alpha$. The functions $f(t)1(t)$ and $f(t - \alpha)1(t - \alpha)$ are shown in Figure 2–1.

By definition, the Laplace transform of $f(t - \alpha)1(t - \alpha)$ is

$$\mathcal{L}[f(t - \alpha)1(t - \alpha)] = \int_0^\infty f(t - \alpha)1(t - \alpha)e^{-st}\,dt$$

By changing the independent variable from t to τ, where $\tau = t - \alpha$, we obtain

$$\int_0^\infty f(t - \alpha)1(t - \alpha)e^{-st}\,dt = \int_{-\alpha}^\infty f(\tau)1(\tau)e^{-s(\tau+\alpha)}\,d\tau$$

Since in this book we always assume that $f(t) = 0$ for $t < 0$, $f(\tau)1(\tau) = 0$ for $\tau < 0$. Hence we can change the lower limit of integration from $-\alpha$ to 0. Thus

$$\begin{aligned}\int_{-\alpha}^\infty f(\tau)1(\tau)e^{-s(\tau+\alpha)}\,d\tau &= \int_0^\infty f(\tau)1(\tau)e^{-s(\tau+\alpha)}\,d\tau \\ &= \int_0^\infty f(\tau)e^{-s\tau}e^{-\alpha s}\,d\tau \\ &= e^{-\alpha s}\int_0^\infty f(\tau)e^{-s\tau}\,d\tau = e^{-\alpha s}F(s)\end{aligned}$$

where

$$F(s) = \mathcal{L}[f(t)] = \int_0^\infty f(t)e^{-st}\,dt$$

And so

$$\mathcal{L}[f(t - \alpha)1(t - \alpha)] = e^{-\alpha s}F(s), \qquad \text{for } \alpha \geq 0$$

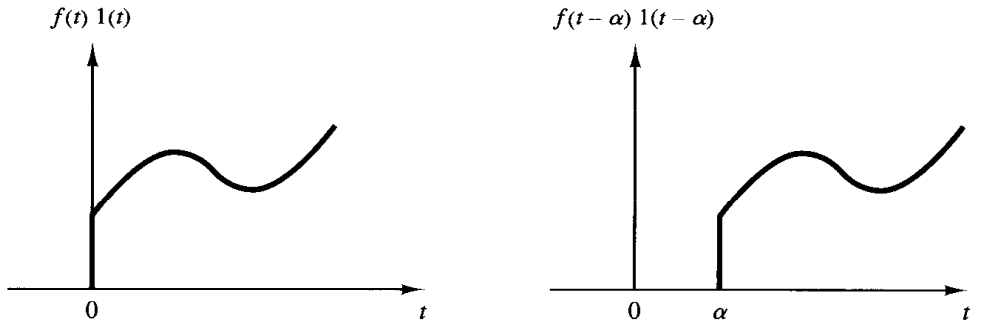

Figure 2–1
Function $f(t)1(t)$ and translated function $f(t - \alpha)1(t - \alpha)$.

Table 2–1 Laplace Transform Pairs

	$f(t)$	$F(s)$
1	Unit impulse $\delta(t)$	1
2	Unit step $1(t)$	$\frac{1}{s}$
3	t	$\frac{1}{s^2}$
4	$\frac{t^{n-1}}{(n-1)!} \quad (n = 1, 2, 3, \ldots)$	$\frac{1}{s^n}$
5	$t^n \quad (n = 1, 2, 3, \ldots)$	$\frac{n!}{s^{n+1}}$
6	e^{-at}	$\frac{1}{s+a}$
7	te^{-at}	$\frac{1}{(s+a)^2}$
8	$\frac{1}{(n-1)!}t^{n-1}e^{-at} \quad (n = 1, 2, 3, \ldots)$	$\frac{1}{(s+a)^n}$
9	$t^n e^{-at} \quad (n = 1, 2, 3, \ldots)$	$\frac{n!}{(s+a)^{n+1}}$
10	$\sin \omega t$	$\frac{\omega}{s^2+\omega^2}$
11	$\cos \omega t$	$\frac{s}{s^2+\omega^2}$
12	$\sinh \omega t$	$\frac{\omega}{s^2-\omega^2}$
13	$\cosh \omega t$	$\frac{s}{s^2-\omega^2}$
14	$\frac{1}{a}(1 - e^{-at})$	$\frac{1}{s(s+a)}$
15	$\frac{1}{b-a}(e^{-at} - e^{-bt})$	$\frac{1}{(s+a)(s+b)}$
16	$\frac{1}{b-a}(be^{-bt} - ae^{-at})$	$\frac{s}{(s+a)(s+b)}$
17	$\frac{1}{ab}\left[1 + \frac{1}{a-b}(be^{-at} - ae^{-bt})\right]$	$\frac{1}{s(s+a)(s+b)}$

Table 2–1 (*Continued*)

18	$\frac{1}{a^2}(1 - e^{-at} - ate^{-at})$	$\frac{1}{s(s+a)^2}$
19	$\frac{1}{a^2}(at - 1 + e^{-at})$	$\frac{1}{s^2(s+a)}$
20	$e^{-at}\sin \omega t$	$\frac{\omega}{(s+a)^2 + \omega^2}$
21	$e^{-at}\cos \omega t$	$\frac{s+a}{(s+a)^2 + \omega^2}$
22	$\frac{\omega_n}{\sqrt{1-\zeta^2}} e^{-\zeta\omega_n t}\sin \omega_n \sqrt{1-\zeta^2}\, t$	$\frac{\omega_n^2}{s^2 + 2\zeta\omega_n s + \omega_n^2}$
23	$-\frac{1}{\sqrt{1-\zeta^2}} e^{-\zeta\omega_n t}\sin(\omega_n \sqrt{1-\zeta^2}\, t - \phi)$ $\phi = \tan^{-1}\frac{\sqrt{1-\zeta^2}}{\zeta}$	$\frac{s}{s^2 + 2\zeta\omega_n s + \omega_n^2}$
24	$1 - \frac{1}{\sqrt{1-\zeta^2}} e^{-\zeta\omega_n t}\sin(\omega_n \sqrt{1-\zeta^2}\, t + \phi)$ $\phi = \tan^{-1}\frac{\sqrt{1-\zeta^2}}{\zeta}$	$\frac{\omega_n^2}{s(s^2 + 2\zeta\omega_n s + \omega_n^2)}$
25	$1 - \cos \omega t$	$\frac{\omega^2}{s(s^2 + \omega^2)}$
26	$\omega t - \sin \omega t$	$\frac{\omega^3}{s^2(s^2 + \omega^2)}$
27	$\sin \omega t - \omega t \cos \omega t$	$\frac{2\omega^3}{(s^2 + \omega^2)^2}$
28	$\frac{1}{2\omega} t \sin \omega t$	$\frac{s}{(s^2 + \omega^2)^2}$
29	$t \cos \omega t$	$\frac{s^2 - \omega^2}{(s^2 + \omega^2)^2}$
30	$\frac{1}{\omega_2^2 - \omega_1^2}(\cos \omega_1 t - \cos \omega_2 t) \qquad (\omega_1^2 \neq \omega_2^2)$	$\frac{s}{(s^2 + \omega_1^2)(s^2 + \omega_2^2)}$
31	$\frac{1}{2\omega}(\sin \omega t + \omega t \cos \omega t)$	$\frac{s^2}{(s^2 + \omega^2)^2}$

This last equation states that the translation of the time function $f(t)1(t)$ by α (where $\alpha \geq 0$) corresponds to the multiplication of the transform $F(s)$ by $e^{-\alpha s}$.

Pulse function. Consider the pulse function

$$\begin{aligned} f(t) &= \frac{A}{t_0}, \qquad \text{for } 0 < t < t_0 \\ &= 0, \qquad \text{for } t < 0, t_0 < t \end{aligned}$$

where A and t_0 are constants.

The pulse function here may be considered a step function of height A/t_0 that begins at $t = 0$ and that is superimposed by a negative step function of height A/t_0 beginning at $t = t_0$; that is,

$$f(t) = \frac{A}{t_0} 1(t) - \frac{A}{t_0} 1(t - t_0)$$

Then the Laplace transform of $f(t)$ is obtained as

$$\begin{aligned} \mathcal{L}[f(t)] &= \mathcal{L}\left[\frac{A}{t_0} 1(t)\right] - \mathcal{L}\left[\frac{A}{t_0} 1(t - t_0)\right] \\ &= \frac{A}{t_0 s} - \frac{A}{t_0 s} e^{-st_0} \\ &= \frac{A}{t_0 s}(1 - e^{-st_0}) \end{aligned} \tag{2–5}$$

Impulse function. The impulse function is a special limiting case of the pulse function. Consider the impulse function

$$\begin{aligned} g(t) &= \lim_{t_0 \to 0} \frac{A}{t_0}, \qquad \text{for } 0 < t < t_0 \\ &= 0, \qquad \text{for } t < 0, t_0 < t \end{aligned}$$

Since the height of the impulse function is A/t_0 and the duration is t_0, the area under the impulse is equal to A. As the duration t_0 approaches zero, the height A/t_0 approaches infinity, but the area under the impulse remains equal to A. Note that the magnitude of the impulse is measured by its area.

Referring to Equation (2–5), the Laplace transform of this impulse function is shown to be

$$\begin{aligned} \mathcal{L}[g(t)] &= \lim_{t_0 \to 0} \left[\frac{A}{t_0 s}(1 - e^{-st_0})\right] \\ &= \lim_{t_0 \to 0} \frac{\dfrac{d}{dt_0}[A(1 - e^{-st_0})]}{\dfrac{d}{dt_0}(t_0 s)} = \frac{As}{s} = A \end{aligned}$$

Thus the Laplace transform of the impulse function is equal to the area under the impulse.

The impulse function whose area is equal to unity is called the *unit-impulse function* or the *Dirac delta function.* The unit-impulse function occurring at $t = t_0$ is usually denoted by $\delta(t - t_0)$. $\delta(t - t_0)$ satisfies the following:

$$\delta(t - t_0) = 0, \qquad \text{for } t \neq t_0$$

$$\delta(t - t_0) = \infty, \qquad \text{for } t = t_0$$

$$\int_{-\infty}^{\infty} \delta(t - t_0)dt = 1$$

It should be mentioned that an impulse that has an infinite magnitude and zero duration is mathematical fiction and does not occur in physical systems. If, however, the magnitude of a pulse input to a system is very large and its duration is very short compared to the system time constants, then we can approximate the pulse input by an impulse function. For instance, if a force or torque input $f(t)$ is applied to a system for a very short time duration, $0 < t < t_0$, where the magnitude of $f(t)$ is sufficiently large so that the integral $\int_0^{t_0} f(t)\,dt$ is not negligible, then this input can be considered an impulse input. (Note that when we describe the impulse input the area or magnitude of the impulse is most important, but the exact shape of the impulse is usually immaterial.) The impulse input supplies energy to the system in an infinitesimal time.

The concept of the impulse function is quite useful in differentiating discontinuous functions. The unit-impulse function $\delta(t - t_0)$ can be considered the derivative of the unit-step function $1(t - t_0)$ at the point of discontinuity $t = t_0$ or

$$\delta(t - t_0) = \frac{d}{dt} 1(t - t_0)$$

Conversely, if the unit-impulse function $\delta(t - t_0)$ is integrated, the result is the unit-step function $1(t - t_0)$. With the concept of the impulse function we can differentiate a function containing discontinuities, giving impulses, the magnitudes of which are equal to the magnitude of each corresponding discontinuity.

Multiplication of $f(t)$ by e^{-at}. If $f(t)$ is Laplace transformable, its Laplace transform being $F(s)$, then the Laplace transform of $e^{-at}f(t)$ is obtained as

$$\mathcal{L}[e^{-at}f(t)] = \int_0^{\infty} e^{-at}f(t)e^{-st}\,dt = F(s + \alpha) \tag{2–6}$$

We see that the multiplication of $f(t)$ by e^{-at} has the effect of replacing s by $(s + \alpha)$ in the Laplace transform. Conversely, changing s to $(s + \alpha)$ is equivalent to multiplying $f(t)$ by e^{-at}. (Note that α may be real or complex.)

The relationship given by Equation (2–6) is useful in finding the Laplace transforms of such functions as $e^{-at} \sin \omega t$ and $e^{-at} \cos \omega t$. For instance, since

$$\mathcal{L}[\sin \omega t] = \frac{\omega}{s^2 + \omega^2} = F(s), \qquad \mathcal{L}[\cos \omega] = \frac{s}{s^2 + \omega^2} = G(s)$$

it follows from Equation (2–6) that the Laplace transforms of $e^{-at} \sin \omega t$ and $e^{-at} \cos \omega t$ are given, respectively, by

$$\mathcal{L}[e^{-\alpha t}\sin \omega t] = F(s+\alpha) = \frac{\omega}{(s+\alpha)^2+\omega^2}$$

$$\mathcal{L}[e^{-\alpha t}\cos \omega t] = G(s+\alpha) = \frac{s+\alpha}{(s+\alpha)^2+\omega^2}$$

Change of time scale. In analyzing physical systems, it is sometimes desirable to change the time scale or normalize a given time function. The result obtained in terms of normalized time is useful because it can be applied directly to different systems having similar mathematical equations.

If t is changed into t/α, where α is a positive constant, then the function $f(t)$ is changed into $f(t/\alpha)$. If we denote the Laplace transform of $f(t)$ by $F(s)$, then the Laplace transform of $f(t/\alpha)$ may be obtained as follows:

$$\mathcal{L}\left[f\left(\frac{t}{\alpha}\right)\right] = \int_0^\infty f\left(\frac{t}{\alpha}\right)e^{-st}\,dt$$

Letting $t/\alpha = t_1$ and $\alpha s = s_1$, we obtain

$$\begin{aligned}\mathcal{L}\left[f\left(\frac{t}{\alpha}\right)\right] &= \int_0^\infty f(t_1)e^{-s_1 t_1}\,d(\alpha t_1)\\ &= \alpha\int_0^\infty f(t_1)e^{-s_1 t_1}\,dt_1\\ &= \alpha F(s_1)\end{aligned}$$

or

$$\mathcal{L}\left[f\left(\frac{t}{\alpha}\right)\right] = \alpha F(\alpha s)$$

As an example, consider $f(t) = e^{-t}$ and $f(t/5) = e^{-0.2t}$. We obtain

$$\mathcal{L}[f(t)] = \mathcal{L}[e^{-t}] = F(s) = \frac{1}{s+1}$$

Hence

$$\mathcal{L}\left[f\left(\frac{t}{5}\right)\right] = \mathcal{L}[e^{-0.2t}] = 5F(5s) = \frac{5}{5s+1}$$

This result can be verified easily by taking the Laplace transform of $e^{-0.2t}$ directly as follows:

$$\mathcal{L}[e^{-0.2t}] = \frac{1}{s+0.2} = \frac{5}{5s+1}$$

Comments on the lower limit of the Laplace integral. In some cases, $f(t)$ possesses an impulse function at $t = 0$. Then the lower limit of the Laplace integral must be clearly specified as to whether it is $0-$ or $0+$, since the Laplace transforms of $f(t)$ differ

for these two lower limits. If such a distinction of the lower limit of the Laplace integral is necessary, we use the notations

$$\mathcal{L}_+[f(t)] = \int_{0+}^{\infty} f(t)e^{-st}\,dt$$

$$\mathcal{L}_-[f(t)] = \int_{0-}^{\infty} f(t)e^{-st}\,dt = \mathcal{L}_+[f(t)] + \int_{0-}^{0+} f(t)e^{-st}\,dt$$

If $f(t)$ involves an impulse function at $t = 0$, then

$$\mathcal{L}_+[f(t)] \neq \mathcal{L}_-[f(t)]$$

since

$$\int_{0-}^{0+} f(t)e^{-st}\,dt \neq 0$$

for such a case. Obviously, if $f(t)$ does not possess an impulse function at $t = 0$ (that is, if the function to be transformed is finite between $t = 0-$ and $t = 0+$), then

$$\mathcal{L}_+[f(t)] = \mathcal{L}_-[f(t)]$$

2–4 LAPLACE TRANSFORM THEOREMS

This section presents several theorems on Laplace transformation that are important in control engineering.

Real differentiation theorem. The Laplace transform of the derivative of a function $f(t)$ is given by

$$\mathcal{L}\left[\frac{d}{dt}f(t)\right] = sF(s) - f(0) \tag{2–7}$$

where $f(0)$ is the initial value of $f(t)$ evaluated at $t = 0$.

For a given function $f(t)$, the values of $f(0+)$ and $f(0-)$ may be the same or different, as illustrated in Figure 2–2. The distinction between $f(0+)$ and $f(0-)$ is important when $f(t)$ has a discontinuity at $t = 0$ because in such a case $df(t)/dt$ will involve an impulse function at $t = 0$. If $f(0+) \neq f(0-)$, Equation (2–7) must be modified to

$$\mathcal{L}_+\left[\frac{d}{dt}f(t)\right] = sF(s) - f(0+)$$

$$\mathcal{L}_-\left[\frac{d}{dt}f(t)\right] = sF(s) - f(0-)$$

To prove the real differentiation theorem, Equation (2–7), we proceed as follows. Integrating the Laplace integral by parts gives

$$\int_0^{\infty} f(t)e^{-st}\,dt = f(t)\frac{e^{-st}}{-s}\bigg|_0^{\infty} - \int_0^{\infty}\left[\frac{d}{dt}f(t)\right]\frac{e^{-st}}{-s}\,dt$$

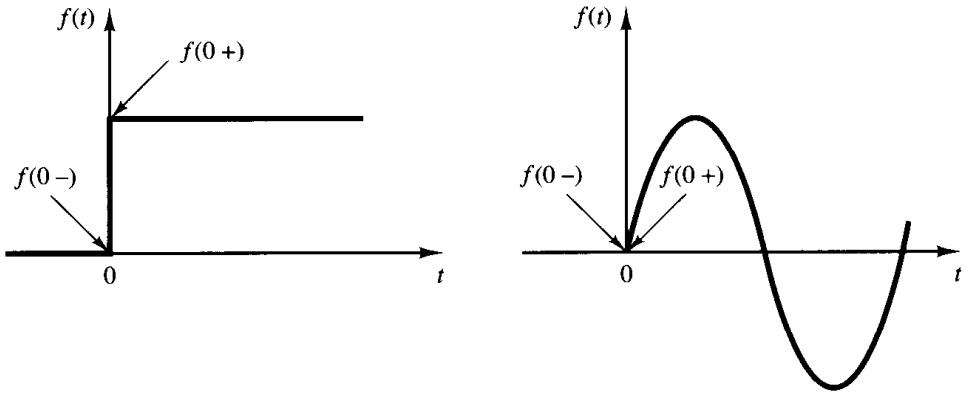

Figure 2–2
Step function and sine function indicating initial values at $t = 0-$ and $t = 0+$.

Hence

$$F(s) = \frac{f(0)}{s} + \frac{1}{s}\mathcal{L}\left[\frac{d}{dt}f(t)\right]$$

It follows that

$$\mathcal{L}\left[\frac{d}{dt}f(t)\right] = sF(s) - f(0)$$

Similarly, we obtain the following relationship for the second derivative of $f(t)$:

$$\mathcal{L}\left[\frac{d^2}{dt^2}f(t)\right] = s^2F(s) - sf(0) - \dot{f}(0)$$

where $\dot{f}(0)$ is the value of $df(t)/dt$ evaluated at $t = 0$. To derive this equation, define

$$\frac{d}{dt}f(t) = g(t)$$

Then

$$\begin{aligned}\mathcal{L}\left[\frac{d^2}{dt^2}f(t)\right] = \mathcal{L}\left[\frac{d}{dt}g(t)\right] &= s\mathcal{L}[g(t)] - g(0)\\ &= s\mathcal{L}\left[\frac{d}{dt}f(t)\right] - \dot{f}(0)\\ &= s^2F(s) - sf(0) - \dot{f}(0)\end{aligned}$$

Similarly, for the nth derivative of $f(t)$, we obtain

$$\mathcal{L}\left[\frac{d^n}{dt^n}f(t)\right] = s^nF(s) - s^{n-1}f(0) - s^{n-2}\dot{f}(0) - \cdots - \overset{(n-2)}{s}f(0) - \overset{(n-1)}{f}(0)$$

where $f(0), \dot{f}(0), \ldots, \overset{(n-1)}{f}(0)$ represent the values of $f(t), df(t)/dt, \ldots, d^{n-1}f(t)/dt^{n-1}$, respectively, evaluated at $t = 0$. If the distinction between $\mathcal{L}_+$ and $\mathcal{L}_-$ is necessary, we substitute $t = 0+$ or $t = 0-$ into $f(t), df(t)/dt, \ldots, d^{n-1}f(t)/dt^{n-1}$, depending on whether we take $\mathcal{L}_+$ or $\mathcal{L}_-$.

Note that, in order for Laplace transforms of derivatives of $f(t)$ to exist, $d^nf(t)/dt^n$ ($n = 1, 2, 3, \ldots$) must be Laplace transformable.

Note also that, if all the initial values of $f(t)$ and its derivatives are equal to zero, then the Laplace transform of the nth derivative of $f(t)$ is given by $s^nF(s)$.

EXAMPLE 2–1 Consider the cosine function.

$$g(t) = 0, \qquad \text{for } t < 0$$
$$= \cos \omega t, \qquad \text{for } t \geq 0$$

The Laplace transform of this cosine function can be obtained directly as in the case of the sinusoidal function considered earlier. The use of the real differentiation theorem, however, will be demonstrated here by deriving the Laplace transform of the cosine function from the Laplace transform of the sine function. If we define

$$f(t) = 0, \qquad \text{for } t < 0$$
$$= \sin \omega t, \qquad \text{for } t \geq 0$$

then

$$\mathcal{L}[\sin \omega t] = F(s) = \frac{\omega}{s^2 + \omega^2}$$

The Laplace transform of the cosine function is obtained as

$$\mathcal{L}[\cos \omega t] = \mathcal{L}\left[\frac{1}{\omega}\left(\frac{d}{dt} \sin \omega t\right)\right] = \frac{1}{\omega}[sF(s) - f(0)]$$
$$= \frac{1}{\omega}\left[\frac{s\omega}{s^2 + \omega^2} - 0\right] = \frac{s}{s^2 + \omega^2}$$

Final-value theorem. The final-value theorem relates the steady-state behavior of $f(t)$ to the behavior of $sF(s)$ in the neighborhood of $s = 0$. This theorem, however, applies if and only if $\lim_{t\to\infty} f(t)$ exists [which means that $f(t)$ settles down to a definite value for $t \to \infty$]. If all poles of $sF(s)$ lie in the left half s plane, $\lim_{t\to\infty} f(t)$ exists. But if $sF(s)$ has poles on the imaginary axis or in the right half s plane, $f(t)$ will contain oscillating or exponentially increasing time functions, respectively, and $\lim_{t\to\infty} f(t)$ will not exist. The final-value theorem does not apply in such cases. For instance, if $f(t)$ is the sinusoidal function $\sin \omega t$, $sF(s)$ has poles at $s = \pm j\omega$ and $\lim_{t\to\infty} f(t)$ does not exist. Therefore, this theorem is not applicable to such a function.

The final-value theorem may be stated as follows. If $f(t)$ and $df(t)/dt$ are Laplace transformable, if $F(s)$ is the Laplace transform of $f(t)$, and if $\lim_{t\to\infty} f(t)$ exists, then

$$\lim_{t\to\infty} f(t) = \lim_{s\to 0} sF(s)$$

To prove the theorem, we let s approach zero in the equation for the Laplace transform of the derivative of $f(t)$ or

$$\lim_{s\to 0} \int_0^\infty \left[\frac{d}{dt} f(t)\right] e^{-st}\, dt = \lim_{s\to 0} [sF(s) - f(0)]$$

Since $\lim_{s\to 0} e^{-st} = 1$, we obtain

$$\int_0^\infty \left[\frac{d}{dt} f(t)\right] dt = f(t)\Big|_0^\infty = f(\infty) - f(0)$$
$$= \lim_{s\to 0} sF(s) - f(0)$$

from which

$$f(\infty) = \lim_{t\to\infty} f(t) = \lim_{s\to 0} sF(s)$$

The final-value theorem states that the steady-state behavior of $f(t)$ is the same as the behavior of $sF(s)$ in the neighborhood of $s = 0$. Thus, it is possible to obtain the value of $f(t)$ at $t = \infty$ directly from $F(s)$.

EXAMPLE 2-2 Given

$$\mathcal{L}[f(t)] = F(s) = \frac{1}{s(s+1)}$$

what is $\lim_{t\to\infty} f(t)$?

Since the pole of $sF(s) = 1/(s+1)$ lies in the left half s plane, $\lim_{t\to\infty} f(t)$ exists. So the final-value theorem is applicable in this case.

$$\lim_{t\to\infty} f(t) = f(\infty) = \lim_{s\to 0} sF(s) = \lim_{s\to 0} \frac{s}{s(s+1)} = \lim_{s\to 0} \frac{1}{s+1} = 1$$

In fact, this result can easily be verified, since

$$f(t) = 1 - e^{-t}, \qquad \text{for } t \geq 0$$

Initial-value theorem. The initial-value theorem is the counterpart of the final-value theorem. By using this theorem, we are able to find the value of $f(t)$ at $t = 0+$ directly from the Laplace transform of $f(t)$. The initial-value theorem does not give the value of $f(t)$ at exactly $t = 0$ but at a time slightly greater than zero.

The initial-value theorem may be stated as follows: If $f(t)$ and $df(t)/dt$ are both Laplace transformable and if $\lim_{s\to\infty} sF(s)$ exists, then

$$f(0+) = \lim_{s\to\infty} sF(s)$$

To prove this theorem, we use the equation for the $\mathcal{L}_+$ transform of $df(t)/dt$:

$$\mathcal{L}_+\left[\frac{d}{dt}f(t)\right] = sF(s) - f(0+)$$

For the time interval $0+ \leq t \leq \infty$, as s approaches infinity, e^{-st} approaches zero. (Note that we must use $\mathcal{L}_+$ rather than $\mathcal{L}_-$ for this condition.) And so

$$\lim_{s\to\infty} \int_{0+}^{\infty} \left[\frac{d}{dt} f(t)\right] e^{-st}\, dt = \lim_{s\to\infty} [sF(s) - f(0+)] = 0$$

or

$$f(0+) = \lim_{s\to\infty} sF(s)$$

In applying the initial-value theorem, we are not limited as to the locations of the poles of $sF(s)$. Thus the initial-value theorem is valid for the sinusoidal function.

It should be noted that the initial-value theorem and the final-value theorem provide a convenient check on the solution, since they enable us to predict the system behavior in the time domain without actually transforming functions in s back to time functions.

Real-integration theorem. If $f(t)$ is of exponential order, then the Laplace transform of $\int f(t)\,dt$ exists and is given by

$$\mathcal{L}\left[\int f(t)\,dt\right] = \frac{F(s)}{s} + \frac{f^{-1}(0)}{s} \tag{2–8}$$

where $F(s) = \mathcal{L}[f(t)]$ and $f^{-1}(0) = \int f(t)\,dt$, evaluated at $t = 0$.

Note that if $f(t)$ involves an impulse function at $t = 0$, then $f^{-1}(0+) \neq f^{-1}(0-)$. So if $f(t)$ involves an impulse function at $t = 0$, we must modify Equation (2–8) as follows:

$$\mathcal{L}_+\left[\int f(t)\,dt\right] = \frac{F(s)}{s} + \frac{f^{-1}(0+)}{s}$$

$$\mathcal{L}_-\left[\int f(t)\,dt\right] = \frac{F(s)}{s} + \frac{f^{-1}(0-)}{s}$$

The real-integration theorem given by Equation (2–8) can be proved in the following way. Integration by parts yields

$$\begin{aligned}\mathcal{L}\left[\int f(t)\,dt\right] &= \int_0^\infty \left[\int f(t)\,dt\right] e^{-st}\,dt \\ &= \left[\int f(t)\,dt\right]\frac{e^{-st}}{-s}\bigg|_0^\infty - \int_0^\infty f(t)\frac{e^{-st}}{-s}\,dt \\ &= \frac{1}{s}\int f(t)\,dt\bigg|_{t=0} + \frac{1}{s}\int_0^\infty f(t)e^{-st}\,dt \\ &= \frac{f^{-1}(0)}{s} + \frac{F(s)}{s}\end{aligned}$$

and the theorem is proved.

We see that integration in the time domain is converted into division in the s domain. If the initial value of the integral is zero, the Laplace transform of the integral of $f(t)$ is given by $F(s)/s$.

The preceding real-integration theorem given by Equation (2–8) can be modified slightly to deal with the definite integral of $f(t)$. If $f(t)$ is of exponential order, the Laplace transform of the definite integral $\int_0^t f(t)\,dt$ is given by

$$\mathcal{L}\left[\int_0^t f(t)\,dt\right] = \frac{F(s)}{s} \tag{2–9}$$

where $F(s) = \mathcal{L}[f(t)]$. This is also referred to as the real-integration theorem. Note that if $f(t)$ involves an impulse function at $t = 0$ then $\int_{0+}^t f(t)\,dt \neq \int_{0-}^t f(t)\,dt$, and the following distinction must be observed:

$$\mathcal{L}_+\left[\int_{0+}^t f(t)\,dt\right] = \frac{\mathcal{L}_+[f(t)]}{s}$$

$$\mathcal{L}_-\left[\int_{0-}^t f(t)\,dt\right] = \frac{\mathcal{L}_-[f(t)]}{s}$$

To prove Equation (2–9), first note that

$$\int_0^t f(t)\,dt = \int f(t)\,dt - f^{-1}(0)$$

where $f^{-1}(0)$ is equal to $\int f(t)\,dt$ evaluated at $t = 0$ and is a constant. Hence

$$\mathcal{L}\left[\int_0^t f(t)\,dt\right] = \mathcal{L}\left[\int f(t)\,dt\right] - \mathcal{L}[f^{-1}(0)]$$

Noting that $f^{-1}(0)$ is a constant so that

$$\mathcal{L}[f^{-1}(0)] = \frac{f^{-1}(0)}{s}$$

we obtain

$$\mathcal{L}\left[\int_0^t f(t)\,dt\right] = \frac{F(s)}{s} + \frac{f^{-1}(0)}{s} - \frac{f^{-1}(0)}{s} = \frac{F(s)}{s}$$

Complex-differentiation theorem. If $f(t)$ is Laplace transformable, then, except at poles of $F(s)$,

$$\mathcal{L}[tf(t)] = -\frac{d}{ds}F(s)$$

where $F(s) = \mathcal{L}[f(t)]$. This is known as the complex-differentiation theorem. Also,

$$\mathcal{L}[t^2 f(t)] = \frac{d^2}{ds^2}F(s)$$

In general,

$$\mathcal{L}[t^n f(t)] = (-1)^n \frac{d^n}{ds^n}F(s), \qquad \text{for } n = 1, 2, 3, \ldots$$

To prove the complex-differentiation theorem, we proceed as follows:

$$\mathcal{L}[tf(t)] = \int_0^\infty tf(t)e^{-st}\,dt = -\int_0^\infty f(t)\frac{d}{ds}(e^{-st})\,dt$$

$$= -\frac{d}{ds}\int_0^\infty f(t)e^{-st}\,dt = -\frac{d}{ds}F(s)$$

Hence the theorem. Similarly, by defining $tf(t) = g(t)$, the result is

$$\mathcal{L}[t^2 f(t)] = \mathcal{L}[tg(t)] = -\frac{d}{ds}G(s) = -\frac{d}{ds}\left[-\frac{d}{ds}F(s)\right]$$

$$= (-1)^2\frac{d^2}{ds^2}F(s) = \frac{d^2}{ds^2}F(s)$$

Repeating the same process, we obtain

$$\mathcal{L}[t^n f(t)] = (-1)^n \frac{d^n}{ds^n} F(s), \qquad \text{for } n = 1, 2, 3, \ldots$$

Convolution integral. Consider the Laplace transform of

$$\int_0^t f_1(t - \tau) f_2(\tau)\, d\tau$$

This integral is often written as

$$f_1(t) * f_2(t)$$

The mathematical operation $f_1(t)*f_2(t)$ is called *convolution.* Note that if we put $t - \tau = \xi$, then

$$\begin{aligned}\int_0^t f_1(t - \tau) f_2(\tau)\, d\tau &= -\int_t^0 f_1(\xi) f_2(t - \xi)\, d\xi \\ &= \int_0^t f_1(\tau) f_2(t - \tau)\, d\tau\end{aligned}$$

Hence

$$\begin{aligned}f_1(t)*f_2(t) &= \int_0^t f_1(t - \tau) f_2(\tau)\, d\tau \\ &= \int_0^t f_1(\tau) f_2(t - \tau)\, d\tau \\ &= f_2(t)*f_1(t)\end{aligned}$$

If $f_1(t)$ and $f_2(t)$ are piecewise continuous and of exponential order, then the Laplace transform of

$$\int_0^t f_1(t - \tau) f_2(\tau)\, d\tau$$

can be obtained as follows:

$$\mathcal{L}\left[\int_0^t f_1(t - \tau) f_2(\tau)\, d\tau\right] = F_1(s)F_2(s) \tag{2–10}$$

where

$$F_1(s) = \int_0^\infty f_1(t) e^{-st}\, dt = \mathcal{L}[f_1(t)]$$

$$F_2(s) = \int_0^\infty f_2(t) e^{-st}\, dt = \mathcal{L}[f_2(t)]$$

To prove Equation (2–10) note that $f_1(t - \tau)1(t - \tau) = 0$ for $\tau > t$. Hence

$$\int_0^t f_1(t - \tau) f_2(\tau)\, d\tau = \int_0^\infty f_1(t - \tau)1(t - \tau) f_2(\tau)\, d\tau$$

Then

$$\mathcal{L}\left[\int_0^t f_1(t-\tau)f_2(\tau)\,d\tau\right] = \mathcal{L}\left[\int_0^\infty f_1(t-\tau)1(t-\tau)f_2(\tau)\,d\tau\right]$$

$$= \int_0^\infty e^{-st}\left[\int_0^\infty f_1(t-\tau)1(t-\tau)f_2(\tau)\,d\tau\right]dt$$

Substituting $t - \tau = \lambda$ in this last equation and changing the order of integration, which is valid in this case because $f_1(t)$ and $f_2(t)$ are Laplace transformable, we obtain

$$\mathcal{L}\left[\int_0^t f_1(t-\tau)f_2(\tau)\,d\tau\right] = \int_0^\infty f_1(t-\tau)1(t-\tau)e^{-st}\,dt\int_0^\infty f_2(\tau)\,d\tau$$

$$= \int_0^\infty f_1(\lambda)e^{-s(\lambda+\tau)}\,d\lambda\int_0^\infty f_2(\tau)\,d\tau$$

$$= \int_0^\infty f_1(\lambda)e^{-s\lambda}\,d\lambda\int_0^\infty f_2(\tau)e^{-s\tau}\,d\tau$$

$$= F_1(s)F_2(s)$$

This last equation gives the Laplace transform of the convolution integral. Conversely, if the Laplace transform of a function is given by a product of two Laplace transform functions, $F_1(s)F_2(s)$, then the corresponding time function (the inverse Laplace transform) is given by the convolution integral $f_1(t)*f_2(t)$.

Laplace transform of product of two time functions. The Laplace transform of the product of two Laplace transformable functions $f(t)$ and $g(t)$ can be given by

$$\mathcal{L}[f(t)g(t)] = \frac{1}{2\pi j}\int_{c-j\infty}^{c+j\infty} F(p)G(s-p)\,dp \tag{2–11}$$

To show this, we may proceed as follows: The Laplace transform of the product of $f(t)$ and $g(t)$ can be written as

$$\mathcal{L}[f(t)g(t)] = \int_0^\infty f(t)g(t)e^{-st}\,dt \tag{2–12}$$

Note that the inversion integral is

$$f(t) = \frac{1}{2\pi j}\int_{c-j\infty}^{c+j\infty} F(s)e^{st}\,ds, \qquad \text{for } t > 0$$

where c is the abscissa of convergence for $F(s)$. Thus,

$$\mathcal{L}[f(t)g(t)] = \frac{1}{2\pi j}\int_0^\infty\int_{c-j\infty}^{c+j\infty} F(p)e^{pt}\,dp\,g(t)e^{-st}\,dt$$

Because of the uniform convergence of the integrals considered, we may invert the order of integration:

$$\mathcal{L}[f(t)g(t)] = \frac{1}{2\pi j}\int_{c-j\infty}^{c+j\infty} F(p)\,dp \int_0^\infty g(t)e^{-(s-p)t}\,dt$$

Noting that

$$\int_0^\infty g(t)e^{-(s-p)t}\,dt = G(s-p)$$

we obtain

$$\mathcal{L}[f(t)g(t)] = \frac{1}{2\pi j}\int_{c-j\infty}^{c+j\infty} F(p)G(s-p)\,dp \tag{2–13}$$

Summary. Table 2–2 summarizes properties and theorems of the Laplace transforms. Most of them have been derived or proved in this section.

2–5 INVERSE LAPLACE TRANSFORMATION

As noted earlier, the inverse Laplace transform can be obtained by use of the inversion integral given by Equation (2–4). However, the inversion integral is complicated and, therefore, its use is not recommended for finding inverse Laplace transforms of commonly encountered functions in control engineering.

A convenient method for obtaining inverse Laplace transforms is to use a table of Laplace transforms. In this case, the Laplace transform must be in a form immediately recognizable in such a table. Quite often the function in question may not appear in tables of Laplace transforms available to the engineer. If a particular transform $F(s)$ cannot be found in a table, then we may expand it into partial fractions and write $F(s)$ in terms of simple functions of s for which the inverse Laplace transforms are already known.

Note that these simpler methods for finding inverse Laplace transforms are based on the fact that the unique correspondence of a time function and its inverse Laplace transform holds for any continuous time function.

Partial-fraction expansion method for finding inverse Laplace transforms. For problems in control systems analysis, $F(s)$, the Laplace transform of $f(t)$, frequently occurs in the form

$$F(s) = \frac{B(s)}{A(s)}$$

where $A(s)$ and $B(s)$ are polynomials in s. In the expansion of $F(s) = B(s)/A(s)$ into a partial-fraction form, it is important that the highest power of s in $A(s)$ be greater than the highest power of s in $B(s)$. If such is not the case, the numerator $B(s)$ must be divided by the denominator $A(s)$ in order to produce a polynomial in s plus a remainder (a ratio of polynomials in s whose numerator is of lower degree than the denominator).

Table 2–2 Properties of Laplace Transforms

1	$\mathcal{L}[Af(t)] = AF(s)$
2	$\mathcal{L}[f_1(t) \pm f_2(t)] = F_1(s) \pm F_2(s)$
3	$\mathcal{L}_{\pm}\left[\frac{d}{dt} f(t)\right] = sF(s) - f(0\pm)$
4	$\mathcal{L}_{\pm}\left[\frac{d^2}{dt^2} f(t)\right] = s^2F(s) - sf(0\pm) - \dot{f}(0\pm)$
5	$\mathcal{L}_{\pm}\left[\frac{d^n}{dt^n} f(t)\right] = s^nF(s) - \sum_{k=1}^{n} s^{n-k} f^{(k-1)}(0\pm)$ where $f^{(k-1)}(t) = \frac{d^{k-1}}{dt^{k-1}} f(t)$
6	$\mathcal{L}_{\pm}\left[\int f(t)\,dt\right] = \frac{F(s)}{s} + \frac{1}{s}\left[\int f(t)\,dt\right]_{t=0\pm}$
7	$\mathcal{L}_{\pm}\left[\int \cdots \int f(t)(dt)^n\right] = \frac{F(s)}{s^n} + \sum_{k=1}^{n} \frac{1}{s^{n-k+1}}\left[\int \cdots \int f(t)(dt)^k\right]_{t=0\pm}$
8	$\mathcal{L}\left[\int_0^t f(t)\,dt\right] = \frac{F(s)}{s}$
9	$\int_0^{\infty} f(t)\,dt = \lim_{s\to 0} F(s)$ if $\int_0^{\infty} f(t)\,dt$ exists
10	$\mathcal{L}[e^{-at} f(t)] = F(s + a)$
11	$\mathcal{L}[f(t - \alpha)1(t - \alpha)] = e^{-\alpha s}F(s) \quad \alpha \geq 0$
12	$\mathcal{L}[tf(t)] = -\frac{dF(s)}{ds}$
13	$\mathcal{L}[t^2 f(t)] = \frac{d^2}{ds^2} F(s)$
14	$\mathcal{L}[t^n f(t)] = (-1)^n \frac{d^n}{ds^n} F(s) \quad n = 1, 2, 3, \ldots$
15	$\mathcal{L}\left[\frac{1}{t} f(t)\right] = \int_s^{\infty} F(s)\,ds$ if $\lim_{t\to 0} \frac{1}{t} f(t)$ exists
16	$\mathcal{L}\left[f\left(\frac{t}{a}\right)\right] = aF(as)$
17	$\mathcal{L}\left[\int_0^t f_1(t - \tau) f_2(\tau)\,d\tau\right] = F_1(s)F_2(s)$
18	$\mathcal{L}[f(t)g(t)] = \frac{1}{2\pi j} \int_{c-j\infty}^{c+j\infty} F(p)G(s - p)\,dp$

If $F(s)$ is broken up into components,

$$F(s) = F_1(s) + F_2(s) + \cdots + F_n(s)$$

and if the inverse Laplace transforms of $F_1(s), F_2(s), \ldots, F_n(s)$ are readily available, then

$$\begin{aligned}\mathcal{L}^{-1}[F(s)] &= \mathcal{L}^{-1}[F_1(s)] + \mathcal{L}^{-1}[F_2(s)] + \cdots + \mathcal{L}^{-1}[F_n(s)] \\ &= f_1(t) + f_2(t) + \cdots + f_n(t)\end{aligned}$$

where $f_1(t), f_2(t), \ldots, f_n(t)$ are the inverse Laplace transforms of $F_1(s), F_2(s), \ldots, F_n(s)$, respectively. The inverse Laplace transform of $F(s)$ thus obtained is unique except possibly at points where the time function is discontinuous. Whenever the time function is continuous, the time function $f(t)$ and its Laplace transform $F(s)$ have a one-to-one correspondence.

The advantage of the partial-fraction expansion approach is that the individual terms of $F(s)$, resulting from the expansion into partial-fraction form, are very simple functions of s; consequently, it is not necessary to refer to a Laplace transform table if we memorize several simple Laplace transform pairs. It should be noted, however, that in applying the partial-fraction expansion technique in the search for the inverse Laplace transform of $F(s) = B(s)/A(s)$ the roots of the denominator polynomial $A(s)$ must be obtained in advance. That is, this method does not apply until the denominator polynomial has been factored.

Partial-fraction expansion when $F(s)$ involves distinct poles only. Consider $F(s)$ written in the factored form

$$F(s) = \frac{B(s)}{A(s)} = \frac{K(s + z_1)(s + z_2)\cdots(s + z_m)}{(s + p_1)(s + p_2)\cdots(s + p_n)}, \qquad \text{for } m < n$$

where $p_1, p_2, \ldots, p_n$ and $z_1, z_2, \ldots, z_m$ are either real or complex quantities, but for each complex p_i or z_i there will occur the complex conjugate of p_i or z_i, respectively. If $F(s)$ involves distinct poles only, then it can be expanded into a sum of simple partial fractions as follows:

$$F(s) = \frac{B(s)}{A(s)} = \frac{a_1}{s + p_1} + \frac{a_2}{s + p_2} + \cdots + \frac{a_n}{s + p_n} \tag{2–14}$$

where a_k $(k = 1, 2, \ldots, n)$ are constants. The coefficient a_k is called the *residue* at the pole at $s = -p_k$. The value of a_k can be found by multiplying both sides of Equation (2–14) by $(s + p_k)$ and letting $s = -p_k$, which gives

$$\begin{aligned}\left[(s + p_k)\frac{B(s)}{A(s)}\right]_{s=-p_k} &= \left[\frac{a_1}{s + p_1}(s + p_k) + \frac{a_2}{s + p_2}(s + p_k)\right. \\ &\qquad \left. + \cdots + \frac{a_k}{s + p_k}(s + p_k) + \cdots + \frac{a_n}{s + p_n}(s + p_k)\right]_{s=-p_k} \\ &= a_k\end{aligned}$$

We see that all the expanded terms drop out with the exception of a_k. Thus the residue a_k is found from

$$a_k = \left[(s + p_k)\frac{B(s)}{A(s)}\right]_{s=-p_k} \tag{2–15}$$

Note that, since $f(t)$ is a real function of time, if p_1 and p_2 are complex conjugates, then the residues a_1 and a_2 are also complex conjugates. Only one of the conjugates, a_1 or a_2, needs to be evaluated because the other is known automatically.

Since

$$\mathcal{L}^{-1}\left[\frac{a_k}{s + p_k}\right] = a_k e^{-p_k t}$$

$f(t)$ is obtained as

$$f(t) = \mathcal{L}^{-1}[F(s)] = a_1 e^{-p_1 t} + a_2 e^{-p_2 t} + \cdots + a_n e^{-p_n t}, \qquad \text{for } t \geq 0$$

EXAMPLE 2–3 Find the inverse Laplace transform of

$$F(s) = \frac{s + 3}{(s + 1)(s + 2)}$$

The partial-fraction expansion of $F(s)$ is

$$F(s) = \frac{s + 3}{(s + 1)(s + 2)} = \frac{a_1}{s + 1} + \frac{a_2}{s + 2}$$

where a_1 and a_2 are found by using Equation (2–15):

$$a_1 = \left[(s + 1)\frac{s + 3}{(s + 1)(s + 2)}\right]_{s=-1} = \left[\frac{s + 3}{s + 2}\right]_{s=-1} = 2$$

$$a_2 = \left[(s + 2)\frac{s + 3}{(s + 1)(s + 2)}\right]_{s=-2} = \left[\frac{s + 3}{s + 1}\right]_{s=-2} = -1$$

Thus

$$\begin{aligned} f(t) &= \mathcal{L}^{-1}[F(s)] \\ &= \mathcal{L}^{-1}\left[\frac{2}{s + 1}\right] + \mathcal{L}^{-1}\left[\frac{-1}{s + 2}\right] \\ &= 2e^{-t} - e^{-2t}, \qquad \text{for } t \geq 0 \end{aligned}$$

EXAMPLE 2–4 Obtain the inverse Laplace transform of

$$G(s) = \frac{s^3 + 5s^2 + 9s + 7}{(s + 1)(s + 2)}$$

Here, since the degree of the numerator polynomial is higher than that of the denominator polynomial, we must divide the numerator by the denominator.

$$G(s) = s + 2 + \frac{s + 3}{(s + 1)(s + 2)}$$

Note that the Laplace transform of the unit-impulse function $\delta(t)$ is 1 and that the Laplace transform of $d\delta(t)/dt$ is s. The third term on the right-hand side of this last equation is $F(s)$ in Example 2–3. So the inverse Laplace transform of $G(s)$ is given as

$$g(t) = \frac{d}{dt}\delta(t) + 2\delta(t) + 2e^{-t} - e^{-2t}, \qquad \text{for } t \geq 0-$$

EXAMPLE 2-5 Find the inverse Laplace transform of

$$F(s) = \frac{2s + 12}{s^2 + 2s + 5}$$

Notice that the denominator polynomial can be factored as

$$s^2 + 2s + 5 = (s + 1 + j2)(s + 1 - j2)$$

If the function $F(s)$ involves a pair of complex-conjugate poles, it is convenient not to expand $F(s)$ into the usual partial fractions but to expand it into the sum of a damped sine and a damped cosine function.

Noting that $s^2 + 2s + 5 = (s + 1)^2 + 2^2$ and referring to the Laplace transforms of $e^{-\alpha t}\sin \omega t$ and $e^{-\alpha t}\cos \omega t$, rewritten thus,

$$\mathcal{L}[e^{-\alpha t}\sin \omega t] = \frac{\omega}{(s + \alpha)^2 + \omega^2}$$

$$\mathcal{L}[e^{-\alpha t}\cos \omega t] = \frac{s + \alpha}{(s + \alpha)^2 + \omega^2}$$

the given $F(s)$ can be written as a sum of a damped sine and a damped cosine function.

$$F(s) = \frac{2s + 12}{s^2 + 2s + 5} = \frac{10 + 2(s + 1)}{(s + 1)^2 + 2^2}$$

$$= 5\frac{2}{(s + 1)^2 + 2^2} + 2\frac{s + 1}{(s + 1)^2 + 2^2}$$

It follows that

$$f(t) = \mathcal{L}^{-1}[F(s)]$$

$$= 5\mathcal{L}^{-1}\left[\frac{2}{(s + 1)^2 + 2^2}\right] + 2\mathcal{L}^{-1}\left[\frac{s + 1}{(s + 1)^2 + 2^2}\right]$$

$$= 5e^{-t}\sin 2t + 2e^{-t}\cos 2t, \qquad \text{for } t \geq 0$$

Partial-fraction expansion when $F(s)$ involves multiple poles. Instead of discussing the general case, we shall use an example to show how to obtain the partial-fraction expansion of $F(s)$. (See also Problem A-2-16.)

Consider the following $F(s)$:

$$F(s) = \frac{s^2 + 2s + 3}{(s + 1)^3}$$

The partial-fraction expansion of this $F(s)$ involves three terms,

$$F(s) = \frac{B(s)}{A(s)} = \frac{b_1}{s + 1} + \frac{b_2}{(s + 1)^2} + \frac{b_3}{(s + 1)^3}$$

where b_3, b_2, and b_1 are determined as follows. By multiplying both sides of this last equation by $(s + 1)^3$, we have

$$(s + 1)^3 \frac{B(s)}{A(s)} = b_1(s + 1)^2 + b_2(s + 1) + b_3 \tag{2–16}$$

Then letting $s = -1$, Equation (2–16) gives

$$\left[(s + 1)^3 \frac{B(s)}{A(s)}\right]_{s=-1} = b_3$$

Also, differentiation of both sides of Equation (2–16) with respect to s yields

$$\frac{d}{ds}\left[(s + 1)^3 \frac{B(s)}{A(s)}\right] = b_2 + 2b_1(s + 1) \tag{2–17}$$

If we let $s = -1$ in equation (2–17), then

$$\frac{d}{ds}\left[(s + 1)^3 \frac{B(s)}{A(s)}\right]_{s=-1} = b_2$$

By differentiating both sides of equation (2–17) with respect to s, the result is

$$\frac{d^2}{ds^2}\left[(s + 1)^3 \frac{B(s)}{A(s)}\right] = 2b_1$$

From the preceding analysis it can be seen that the values of b_3, b_2, and b_1 are found systematically as follows:

$$\begin{aligned}
b_3 &= \left[(s + 1)^3 \frac{B(s)}{A(s)}\right]_{s=-1} \\
&= (s^2 + 2s + 3)_{s=-1} \\
&= 2 \\
b_2 &= \left\{\frac{d}{ds}\left[(s + 1)^3 \frac{B(s)}{A(s)}\right]\right\}_{s=-1} \\
&= \left[\frac{d}{ds}(s^2 + 2s + 3)\right]_{s=-1} \\
&= (2s + 2)_{s=-1} \\
&= 0 \\
b_1 &= \frac{1}{2!}\left\{\frac{d^2}{ds^2}\left[(s + 1)^3 \frac{B(s)}{A(s)}\right]\right\}_{s=-1} \\
&= \frac{1}{2!}\left[\frac{d^2}{ds^2}(s^2 + 2s + 3)\right]_{s=-1} \\
&= \frac{1}{2}(2) = 1
\end{aligned}$$

We thus obtain

$$\begin{aligned} f(t) &= \mathcal{L}^{-1}[F(s)] \\ &= \mathcal{L}^{-1}\left[\frac{1}{s+1}\right] + \mathcal{L}^{-1}\left[\frac{0}{(s+1)^2}\right] + \mathcal{L}^{-1}\left[\frac{2}{(s+1)^3}\right] \\ &= e^{-t} + 0 + t^2e^{-t} \\ &= (1 + t^2)e^{-t}, \qquad \text{for } t \geq 0 \end{aligned}$$

Comments. For complicated functions with denominators involving higher-order polynomials, partial-fraction expansion may be quite time consuming. In such a case, use of MATLAB is recommended. (See Section 2–6.)

2–6 PARTIAL-FRACTION EXPANSION WITH MATLAB

MATLAB has a command to obtain the partial-fraction expansion of $B(s)/A(s)$.

Consider the transfer function

$$\frac{B(s)}{A(s)} = \frac{\text{num}}{\text{den}} = \frac{b_0s^n + b_1s^{n-1} + \cdots + b_n}{s^n + a_1s^{n-1} + \cdots + a_n}$$

where some of a_i and b_j may be zero. In MATLAB row vectors num and den specify the coefficients of the numerator and denominator of the transfer function. That is,

```
num = [b0   b1   ...   bn]
den = [1    a1   ...   an]
```

The command

```
[r,p,k] = residue(num,den)
```

finds the residues, poles, and direct terms of a partial-fraction expansion of the ratio of two polynomials $B(s)$ and $A(s)$.

The partial-fraction expansion of $B(s)/A(s)$ is given by

$$\frac{B(s)}{A(s)} = \frac{r(1)}{s - p(1)} + \frac{r(2)}{s - p(2)} + \cdots + \frac{r(n)}{s - p(n)} + k(s) \tag{2–18}$$

Comparing Equations (2–14) and (2–18), we note that $p(1) = -p_1, p(2) = -p_2, \ldots, p(n) = -p_n; r(1) = a_1, r(2) = a_2, \ldots, r(n) = a_n$. [$k(s)$ is a direct term.]

EXAMPLE 2–6 Consider the following transfer function:

$$\frac{B(s)}{A(s)} = \frac{2s^3 + 5s^2 + 3s + 6}{s^3 + 6s^2 + 11s + 6}$$

For this function.

```
num = [2   5   3   6]
den = [1   6   11   6]
```

The command

```
[r,p,k] = residue(num,den)
```

gives the following result:

```
[r,p,k] = residue(num,den)

r =

    -6.0000
    -4.0000
     3.0000

p =

    -3.0000
    -2.0000
    -1.0000

k =

     2
```

(Note that the residues are returned in column vector r, the pole locations in column vector p, and the direct term in row vector k.) This is the MATLAB representation of the following partial-fraction expansion of $B(s)/A(s)$;

$$\frac{B(s)}{A(s)} = \frac{2s^3 + 5s^2 + 3s + 6}{s^3 + 6s^2 + 11s + 6}$$

$$= \frac{-6}{s+3} + \frac{-4}{s+2} + \frac{3}{s+1} + 2$$

The command

```
[num,den] = residue(r,p,k)
```

where r, p, and k are as given in the previous MATLAB output, converts the partial-fraction expansion back to the polynomial ratio $B(s)/A(s)$, as follows:

```
[num,den] = residue(r,p,k)

num =

    2.0000    5.0000    3.0000    6.0000

den =

    1.0000    6.0000   11.0000    6.0000
```

Note that if $p(j) = p(j+1) = \cdots = p(j+m-1)$ [that is, $p_j = p_{j+1} = \ldots = p_{j+m-1}$], the pole $p(j)$ is a pole of multiplicity m. In such a case, the expansion includes terms of the form

$$\frac{r(j)}{s-p(j)} + \frac{r(j+1)}{[s-p(j)]^2} + \cdots + \frac{r(j+m-1)}{[s-p(j)]^m}$$

For details, see Example 2–7.

EXAMPLE 2–7 Expand the following $B(s)/A(s)$ into partial-fractions with MATLAB.

$$\frac{B(s)}{A(s)} = \frac{s^2+2s+3}{(s+1)^3} = \frac{s^2+2s+3}{s^3+3s^2+3s+1}$$

For this function, we have

```
num = [0  1  2  3]
den = [1  3  3  1]
```

The command

```
[r,p,k] = residue(num,den)
```

gives the result shown on the next page. It is the MATLAB representation of the following partial-fraction expansion of $B(s)/A(s)$:

$$\frac{B(s)}{A(s)} = \frac{1}{s+1} + \frac{0}{(s+1)^2} + \frac{2}{(s+1)^3}$$

Note that the direct term k is zero.

```
num = [0   1   2   3];
den = [1   3   3   1];
[r,p,k] = residue(num,den)


r =


   1.0000
   0.0000
   2.0000


p =


  -1.0000
  -1.0000
  -1.0000


k =


   []
```

2–7 SOLVING LINEAR, TIME-INVARIANT, DIFFERENTIAL EQUATIONS

In this section we are concerned with the use of the Laplace transform method in solving linear, time-invariant, differential equations.

The Laplace transform method yields the complete solution (complementary solution and particular solution) of linear, time-invariant, differential equations. Classical methods for finding the complete solution of a differential equation require the evaluation of the integration constants from the initial conditions. In the case of the Laplace transform method, however, this requirement is unnecessary because the initial conditions are automatically included in the Laplace transform of the differential equation.

If all initial conditions are zero, then the Laplace transform of the differential equation is obtained simply by replacing d/dt with s, d^2/dt^2 with s^2, and so on.

In solving linear, time-invariant, differential equations by the Laplace transform method, two steps are involved.

1. By taking the Laplace transform of each term in the given differential equation, convert the differential equation into an algebraic equation in s and obtain the

expression for the Laplace transform of the dependent variable by rearranging the algebraic equation.

2. The time solution of the differential equation is obtained by finding the inverse Laplace transform of the dependent variable.

In the following discussion, two examples are used to demonstrate the solution of linear, time-invariant, differential equations by the Laplace transform method.

EXAMPLE 2–8 Find the solution $x(t)$ of the differential equation

$$\ddot{x} + 3\dot{x} + 2x = 0, \qquad x(0) = a, \qquad \dot{x}(0) = b$$

where a and b are constants.

By writing the Laplace transform of $x(t)$ as $X(s)$ or

$$\mathcal{L}[x(t)] = X(s)$$

we obtain

$$\mathcal{L}[\dot{x}] = sX(s) - x(0)$$

$$\mathcal{L}[\ddot{x}] = s^2X(s) - sx(0) - \dot{x}(0)$$

And so the given differential equation becomes

$$[s^2X(s) - sx(0) - \dot{x}(0)] + 3[sX(s) - x(0)] + 2X(s) = 0$$

By substituting the given initial conditions into this last equation, we obtain

$$[s^2X(s) - as - b] + 3[sX(s) - a] + 2X(s) = 0$$

or

$$(s^2 + 3s + 2)X(s) = as + b + 3a$$

Solving for $X(s)$, we have

$$X(s) = \frac{as + b + 3a}{s^2 + 3s + 2} = \frac{as + b + 3a}{(s + 1)(s + 2)} = \frac{2a + b}{s + 1} - \frac{a + b}{s + 2}$$

The inverse Laplace transform of $X(s)$ gives

$$x(t) = \mathcal{L}^{-1}[X(s)] = \mathcal{L}^{-1}\left[\frac{2a + b}{s + 1}\right] - \mathcal{L}^{-1}\left[\frac{a + b}{s + 2}\right]$$

$$= (2a + b)e^{-t} - (a + b)e^{-2t}, \qquad \text{for } t \geq 0$$

which is the solution of the given differential equation. Notice that the initial conditions a and b appear in the solution. Thus $x(t)$ has no undetermined constants.

EXAMPLE 2–9 Find the solution $x(t)$ of the differential equation

$$\ddot{x} + 2\dot{x} + 5x = 3, \qquad x(0) = 0, \qquad \dot{x}(0) = 0$$

Noting that $\mathcal{L}[3] = 3/s$, $x(0) = 0$, and $\dot{x}(0) = 0$, the Laplace transform of the differential equation becomes

$$s^2X(s) + 2sX(s) + 5X(s) = \frac{3}{s}$$

Solving for $X(s)$, we find

$$X(s) = \frac{3}{s(s^2 + 2s + 5)} = \frac{3}{5}\frac{1}{s} - \frac{3}{5}\frac{s + 2}{s^2 + 2s + 5}$$

$$= \frac{3}{5}\frac{1}{s} - \frac{3}{10}\frac{2}{(s + 1)^2 + 2^2} - \frac{3}{5}\frac{s + 1}{(s + 1)^2 + 2^2}$$

Hence the inverse Laplace transform becomes

$$x(t) = \mathcal{L}^{-1}[X(s)]$$

$$= \frac{3}{5}\mathcal{L}^{-1}\left[\frac{1}{s}\right] - \frac{3}{10}\mathcal{L}^{-1}\left[\frac{2}{(s + 1)^2 + 2^2}\right] - \frac{3}{5}\mathcal{L}^{-1}\left[\frac{s + 1}{(s + 1)^2 + 2^2}\right]$$

$$= \frac{3}{5} - \frac{3}{10}e^{-t}\sin 2t - \frac{3}{5}e^{-t}\cos 2t, \qquad \text{for } t \geq 0$$

which is the solution of the given differential equation.

EXAMPLE PROBLEMS AND SOLUTIONS

A-2-1. Find the poles of the following $F(s)$:

$$F(s) = \frac{1}{1 - e^{-s}}$$

Solution. The poles are found from

$$e^{-s} = 1$$

or

$$e^{-(\sigma + j\omega)} = e^{-\sigma}(\cos\omega - j\sin\omega) = 1$$

From this it follows that $\sigma = 0, \omega = \pm 2n\pi$ $(n = 0,1,2,\ldots)$. Thus, the poles are located at

$$s = \pm j2n\pi \qquad (n = 0, 1, 2, \ldots)$$

A-2-2. Find the Laplace transform of $f(t)$ defined by

$$f(t) = 0, \qquad \text{for } t < 0$$

$$= te^{-3t}, \qquad \text{for } t \geq 0$$

Solution. Since

$$\mathcal{L}[t] = G(s) = \frac{1}{s^2}$$

referring to Equation (2–6), we obtain

$$F(s) = \mathcal{L}[te^{-3t}] = G(s + 3) = \frac{1}{(s + 3)^2}$$

A-2-3. What is the Laplace transform of

$$f(t) = 0, \qquad \text{for } t < 0$$

$$= \sin(\omega t + \theta), \qquad \text{for } t \geq 0$$

where θ is a constant?

Solution. Noting that

$$\sin(\omega t + \theta) = \sin \omega t \cos \theta + \cos \omega t \sin \theta$$

we have

$$\begin{aligned}\mathcal{L}[\sin(\omega t + \theta)] &= \cos\theta\, \mathcal{L}[\sin \omega t] + \sin\theta\, \mathcal{L}[\cos \omega t] \\ &= \cos\theta \frac{\omega}{s^2 + \omega^2} + \sin\theta \frac{s}{s^2 + \omega^2} \\ &= \frac{\omega \cos\theta + s \sin\theta}{s^2 + \omega^2}\end{aligned}$$

A-2-4. Find the Laplace transform $F(s)$ of the function $f(t)$ shown in Figure 2–3. Also find the limiting value of $F(s)$ as a approaches zero.

Solution. The function $f(t)$ can be written

$$f(t) = \frac{1}{a^2} 1(t) - \frac{2}{a^2} 1(t - a) + \frac{1}{a^2} 1(t - 2a)$$

Then

$$\begin{aligned}F(s) &= \mathcal{L}[f(t)] \\ &= \frac{1}{a^2}\mathcal{L}[1(t)] - \frac{2}{a^2}\mathcal{L}[1(t - a)] + \frac{1}{a^2}\mathcal{L}[1(t - 2a)] \\ &= \frac{1}{a^2}\frac{1}{s} - \frac{2}{a^2}\frac{1}{s}e^{-as} + \frac{1}{a^2}\frac{1}{s}e^{-2as} \\ &= \frac{1}{a^2 s}(1 - 2e^{-as} + e^{-2as})\end{aligned}$$

As a approaches zero, we have

$$\begin{aligned}\lim_{a\to 0} F(s) &= \lim_{a\to 0} \frac{1 - 2e^{-as} + e^{-2as}}{a^2 s} = \lim_{a\to 0} \frac{\dfrac{d}{da}(1 - 2e^{-as} + e^{-2as})}{\dfrac{d}{da}(a^2 s)} \\ &= \lim_{a\to 0} \frac{2se^{-as} - 2se^{-2as}}{2as} = \lim_{a\to 0} \frac{e^{-as} - e^{-2as}}{a} \\ &= \lim_{a\to 0} \frac{\dfrac{d}{da}(e^{-as} - e^{-2as})}{\dfrac{d}{da}(a)} = \lim_{a\to 0} \frac{-se^{-as} + 2se^{-2as}}{1} \\ &= -s + 2s = s\end{aligned}$$

A-2-5. Find the initial value of $df(t)/dt$ when the Laplace transform of $f(t)$ is given by

$$F(s) = \mathcal{L}[f(t)] = \frac{2s + 1}{s^2 + s + 1}$$

Solution. Using the initial-value theorem,

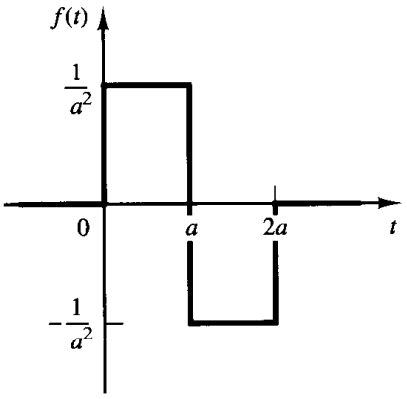

Figure 2–3
Function $f(t)$.

$$\lim_{t\to 0+} f(t) = f(0+) = \lim_{s\to\infty} sF(s) = \lim_{s\to\infty} \frac{s(2s+1)}{s^2+s+1} = 2$$

Since the $\mathcal{L}_+$ transform of $df(t)/dt = g(t)$ is given by

$$\begin{aligned}\mathcal{L}_+[g(t)] &= sF(s) - f(0+) \\ &= \frac{s(2s+1)}{s^2+s+1} - 2 = \frac{-s-2}{s^2+s+1}\end{aligned}$$

the initial value of $df(t)/dt$ is obtained as

$$\begin{aligned}\lim_{t\to 0+} \frac{df(t)}{dt} &= g(0+) = \lim_{s\to\infty} s[sF(s) - f(0+)] \\ &= \lim_{s\to\infty} \frac{-s^2-2s}{s^2+s+1} = -1\end{aligned}$$

A-2-6. The derivative of the unit-impulse function $\delta(t)$ is called a *unit-doublet* function. (Thus, the integral of the unit-doublet function is the unit-impulse function.) Mathematically, an example of the unit-doublet function, which is usually denoted by $u_2(t)$, may be given by

$$u_2(t) = \lim_{t_0\to 0} \frac{1(t) - 2[1(t-t_0)] + 1(t-2t_0)}{t_0^2}$$

Obtain the Laplace transform of $u_2(t)$.

Solution. The Laplace transform of $u_2(t)$ is given by

$$\begin{aligned}\mathcal{L}[u_2(t)] &= \lim_{t_0\to 0} \frac{1}{t_0^2}\left(\frac{1}{s} - \frac{2}{s}e^{-t_0 s} + \frac{1}{s}e^{-2t_0 s}\right) \\ &= \lim_{t_0\to 0} \frac{1}{t_0^2 s}\left[1 - 2\left(1 - t_0 s + \frac{t_0^2 s^2}{2} + \cdots\right) + \left(1 - 2t_0 s + \frac{4t_0^2 s^2}{2} + \cdots\right)\right] \\ &= \lim_{t_0\to 0} \frac{1}{t_0^2 s}[t_0^2 s^2 + (\text{higher-order terms in } t_0 s)] = s\end{aligned}$$

A-2-7. Find the Laplace transform of $f(t)$ defined by

$$\begin{aligned}f(t) &= 0, && \text{for } t < 0 \\ &= t^2 \sin \omega t, && \text{for } t \geq 0\end{aligned}$$

Solution. Since

$$\mathcal{L}[\sin \omega t] = \frac{\omega}{s^2 + \omega^2}$$

applying the complex-differentiation theorem

$$\mathcal{L}[t^2 f(t)] = \frac{d^2}{ds^2} F(s)$$

to this problem, we have

$$\mathcal{L}[f(t)] = \mathcal{L}[t^2 \sin \omega t] = \frac{d^2}{ds^2}\left[\frac{\omega}{s^2 + \omega^2}\right] = \frac{-2\omega^3 + 6\omega s^2}{(s^2 + \omega^2)^3}$$

A-2-8. Prove that if $f(t)$ is of exponential order and if $\int_0^\infty f(t)\,dt$ exists [which means that $\int_0^\infty f(t)\,dt$ assumes a definite value] then

$$\int_0^\infty f(t)\,dt = \lim_{s \to 0} F(s)$$

where $F(s) = \mathcal{L}[f(t)]$.

Solution. Note that

$$\int_0^\infty f(t)\,dt = \lim_{t \to \infty} \int_0^t f(t)\,dt$$

Referring to equation (2–9),

$$\mathcal{L}\left[\int_0^t f(t)\,dt\right] = \frac{F(s)}{s}$$

Since $\int_0^\infty f(t)\,dt$ exists, by applying the final-value theorem to this case,

$$\lim_{t \to \infty} \int_0^t f(t)\,dt = \lim_{s \to 0} s \frac{F(s)}{s}$$

or

$$\int_0^\infty f(t)\,dt = \lim_{s \to 0} F(s)$$

A-2-9. Determine the Laplace transform of the convolution integral

$$f_1(t) * f_2(t) = \int_0^t \tau[1 - e^{-(t-\tau)}]\,d\tau = \int_0^t (t - \tau)(1 - e^{-\tau})\,d\tau$$

where

$$f_1(t) = f_2(t) = 0, \qquad \text{for } t < 0$$
$$f_1(t) = t, \qquad \text{for } t \geq 0$$
$$f_2(t) = 1 - e^{-t}, \qquad \text{for } t \geq 0$$

Solution. Note that

$$\mathcal{L}[t] = F_1(s) = \frac{1}{s^2}$$

$$\mathcal{L}[1 - e^{-t}] = F_2(s) = \frac{1}{s} - \frac{1}{s+1}$$

The Laplace transform of the convolution integral is given by

$$\mathcal{L}[f_1(t)*f_2(t)] = F_1(s)F_2(s) = \frac{1}{s^2}\left(\frac{1}{s} - \frac{1}{s+1}\right)$$

$$= \frac{1}{s^3} - \frac{1}{s^2(s+1)} = \frac{1}{s^3} - \frac{1}{s^2} + \frac{1}{s} - \frac{1}{s+1}$$

To verify that it is indeed the Laplace transform of the convolution integral, let us first perform integration of the convolution integral and then take its Laplace transform.

$$f_1(t)*f_2(t) = \int_0^t \tau[1 - e^{-(t-\tau)}]\,d\tau = \int_0^t (t - \tau)(1 - e^{-\tau})\,d\tau$$

$$= \frac{t^2}{2} - t + 1 - e^{-t}$$

And so

$$\mathcal{L}\left[\frac{t^2}{2} - t + 1 - e^{-t}\right] = \frac{1}{s^3} - \frac{1}{s^2} + \frac{1}{s} - \frac{1}{s+1}$$

A-2-10. Prove that if $f(t)$ is a periodic function with period T then

$$\mathcal{L}[f(t)] = \frac{\int_0^T f(t)e^{-st}\,dt}{1 - e^{-Ts}}$$

Solution.

$$\mathcal{L}[f(t)] = \int_0^\infty f(t)e^{-st}\,dt = \sum_{n=0}^{\infty} \int_{nT}^{(n+1)T} f(t)e^{-st}\,dt$$

By changing the independent variable from t to τ, where $\tau = t - nT$,

$$\mathcal{L}[f(t)] = \sum_{n=0}^{\infty} e^{-nTs} \int_0^T f(\tau)e^{-s\tau}\,d\tau$$

Noting that

$$\sum_{n=0}^{\infty} e^{-nTs} = 1 + e^{-Ts} + e^{-2Ts} + \cdots$$

$$= 1 + e^{-Ts}(1 + e^{-Ts} + e^{-2Ts} + \cdots)$$

$$= 1 + e^{-Ts}\left(\sum_{n=0}^{\infty} e^{-nTs}\right)$$

we obtain

$$\sum_{n=0}^{\infty} e^{-nTs} = \frac{1}{1 - e^{-Ts}}$$

It follows that

$$\mathcal{L}[f(t)] = \frac{\int_0^T f(t)e^{-st}\,dt}{1 - e^{-Ts}}$$

A-2-11. What is the Laplace transform of the periodic function shown in Figure 2–4?

Solution. Note that

$$\begin{aligned}\int_0^T f(t)e^{-st}\,dt &= \int_0^{T/2} e^{-st}\,dt + \int_{T/2}^T (-1)e^{-st}\,dt \\ &= \frac{e^{-st}}{-s}\Big|_0^{T/2} - \frac{e^{-st}}{-s}\Big|_{T/2}^T \\ &= \frac{e^{-(1/2)Ts} - 1}{-s} + \frac{e^{-Ts} - e^{-(1/2)Ts}}{s} \\ &= \frac{1}{s}[e^{-Ts} - 2e^{-(1/2)Ts} + 1] \\ &= \frac{1}{s}[1 - e^{-(1/2)Ts}]^2\end{aligned}$$

Referring to Problem A-2-10, we have

$$\begin{aligned}F(s) &= \frac{\int_0^T f(t)e^{-st}\,dt}{1 - e^{-Ts}} = \frac{(1/s)[1 - e^{-(1/2)Ts}]^2}{1 - e^{-Ts}} \\ &= \frac{1 - e^{-(1/2)Ts}}{s[1 + e^{-(1/2)Ts}]} = \frac{1}{s}\tanh\frac{Ts}{4}\end{aligned}$$

A-2-12. Find the inverse Laplace transform of $F(s)$, where

$$F(s) = \frac{1}{s(s^2 + 2s + 2)}$$

Solution. Since

$$s^2 + 2s + 2 = (s + 1 + j1)(s + 1 - j1)$$

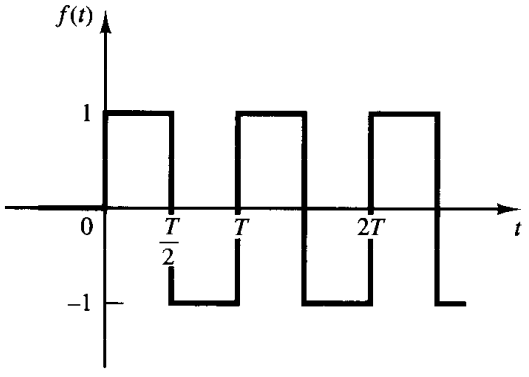

Figure 2–4
Periodic function (square wave).

we notice that $F(s)$ involves a pair of complex-conjugate poles, and so we expand $F(s)$ into the form

$$F(s) = \frac{1}{s(s^2 + 2s + 2)} = \frac{a_1}{s} + \frac{a_2 s + a_3}{s^2 + 2s + 2}$$

where a_1, a_2, and a_3 are determined from

$$1 = a_1(s^2 + 2s + 2) + (a_2 s + a_3)s$$

By comparing coefficients of s^2, s, and s^0 terms on both sides of this last equation, respectively, we obtain

$$a_1 + a_2 = 0, \qquad 2a_1 + a_3 = 0, \qquad 2a_1 = 1$$

from which

$$a_1 = \frac{1}{2}, \qquad a_2 = -\frac{1}{2}, \qquad a_3 = -1$$

Therefore,

$$\begin{aligned} F(s) &= \frac{1}{2}\frac{1}{s} - \frac{1}{2}\frac{s + 2}{s^2 + 2s + 2} \\ &= \frac{1}{2}\frac{1}{s} - \frac{1}{2}\frac{1}{(s + 1)^2 + 1^2} - \frac{1}{2}\frac{s + 1}{(s + 1)^2 + 1^2} \end{aligned}$$

The inverse Laplace transform of $F(s)$ gives

$$f(t) = \frac{1}{2} - \frac{1}{2}e^{-t}\sin t - \frac{1}{2}e^{-t}\cos t, \qquad \text{for } t \geq 0$$

A-2-13. Obtain the inverse Laplace transform of

$$F(s) = \frac{5(s + 2)}{s^2(s + 1)(s + 3)}$$

Solution.

$$F(s) = \frac{5(s + 2)}{s^2(s + 1)(s + 3)} = \frac{b_1}{s} + \frac{b_2}{s^2} + \frac{a_1}{s + 1} + \frac{a_2}{s + 3}$$

where

$$a_1 = \left.\frac{5(s + 2)}{s^2(s + 3)}\right|_{s=-1} = \frac{5}{2}$$

$$a_2 = \left.\frac{5(s + 2)}{s^2(s + 1)}\right|_{s=-3} = \frac{5}{18}$$

$$b_2 = \left.\frac{5(s + 2)}{(s + 1)(s + 3)}\right|_{s=0} = \frac{10}{3}$$

$$\begin{aligned} b_1 &= \frac{d}{ds}\left[\frac{5(s + 2)}{(s + 1)(s + 3)}\right]_{s=0} \\ &= \left.\frac{5(s + 1)(s + 3) - 5(s + 2)(2s + 4)}{(s + 1)^2(s + 3)^2}\right|_{s=0} = -\frac{25}{9} \end{aligned}$$

Thus

$$F(s) = -\frac{25}{9}\frac{1}{s} + \frac{10}{3}\frac{1}{s^2} + \frac{5}{2}\frac{1}{s+1} + \frac{5}{18}\frac{1}{s+3}$$

The inverse Laplace transform of $F(s)$ is

$$f(t) = -\frac{25}{9} + \frac{10}{3}t + \frac{5}{2}e^{-t} + \frac{5}{18}e^{-3t}, \qquad \text{for } t \geq 0$$

A-2-14. Find the inverse Laplace transform of

$$F(s) = \frac{s^4 + 2s^3 + 3s^2 + 4s + 5}{s(s+1)}$$

Solution. Since the numerator polynomial is of higher degree than the denominator polynomial, by dividing the numerator by the denominator until the remainder is a fraction, we obtain

$$F(s) = s^2 + s + 2 + \frac{2s+5}{s(s+1)} = s^2 + s + 2 + \frac{a_1}{s} + \frac{a_2}{s+1}$$

where

$$a_1 = \left.\frac{2s+5}{s+1}\right|_{s=0} = 5$$

$$a_2 = \left.\frac{2s+5}{s}\right|_{s=-1} = -3$$

It follows that

$$F(s) = s^2 + s + 2 + \frac{5}{s} - \frac{3}{s+1}$$

The inverse Laplace transform of $F(s)$ is

$$f(t) = \mathcal{L}^{-1}[F(s)] = \frac{d^2}{dt^2}\delta(t) + \frac{d}{dt}\delta(t) + 2\,\delta(t) + 5 - 3e^{-t}, \qquad \text{for } t \geq 0-$$

A-2-15. Derive the inverse Laplace transform of

$$F(s) = \frac{1}{s(s^2 + \omega^2)}$$

Solution.

$$F(s) = \frac{1}{s(s^2+\omega^2)} = \frac{1}{\omega^2}\frac{1}{s} - \frac{1}{\omega^2}\frac{s}{s^2+\omega^2}$$

Hence the inverse Laplace transform of $F(s)$ is obtained as

$$f(t) = \mathcal{L}^{-1}[F(s)] = \frac{1}{\omega^2}(1 - \cos\omega t), \qquad \text{for } t \geq 0$$

A-2-16. Obtain the inverse Laplace transform of the following $F(s)$:

$$F(s) = \frac{B(s)}{A(s)} = \frac{B(s)}{(s+p_1)^r(s+p_{r+1})(s+p_{r+2})\cdots(s+p_n)}$$

where the degree of polynomial $B(s)$ is lower than that of polynomial $A(s)$.

Solution. The partial-fraction expansion of $F(s)$ is

$$F(s) = \frac{B(s)}{A(s)} = \frac{b_1}{s + p_1} + \frac{b_2}{(s + p_1)^2} + \cdots + \frac{b_{r-1}}{(s + p_1)^{r-1}} + \frac{b_r}{(s + p_1)^r} + \frac{a_{r+1}}{s + p_{r+1}} + \frac{a_{r+2}}{s + p_{r+2}} + \cdots + \frac{a_n}{s + p_n} \tag{2–19}$$

where $b_r, b_{r-1}, \ldots, b_1$ are given by

$$b_r = \left[(s + p_1)^r \frac{B(s)}{A(s)}\right]_{s=-p_1}$$

$$b_{r-1} = \left\{\frac{d}{ds}\left[(s + p_1)^r \frac{B(s)}{A(s)}\right]\right\}_{s=-p_1}$$

$$\vdots$$

$$b_{r-j} = \frac{1}{j!}\left\{\frac{d^j}{ds^j}\left[(s + p_1)^r \frac{B(s)}{A(s)}\right]\right\}_{s=-p_1}$$

$$\vdots$$

$$b_1 = \frac{1}{(r-1)!}\left\{\frac{d^{r-1}}{ds^{r-1}}\left[(s + p_1)^r \frac{B(s)}{A(s)}\right]\right\}_{s=-p_1}$$

The foregoing relationships for the b's may be obtained as follows: By multiplying both sides of Equation (2–19) by $(s + p_1)^r$ and letting s approach $-p_1$, we obtain

$$b_r = \left[(s + p_1)^r \frac{B(s)}{A(s)}\right]_{s=-p_1}$$

If we multiply both sides of Equation (2–19) by $(s + p_1)^r$ and then differentiate with respect to s,

$$\frac{d}{ds}\left[(s + p_1)^r \frac{B(s)}{A(s)}\right] = b_r \frac{d}{ds}\left[\frac{(s + p_1)^r}{(s + p_1)^r}\right] + b_{r-1}\frac{d}{ds}\left[\frac{(s + p_1)^r}{(s + p_1)^{r-1}}\right] + \cdots + b_1 \frac{d}{ds}\left[\frac{(s + p_1)^r}{s + p_1}\right] + a_{r+1}\frac{d}{ds}\left[\frac{(s + p_1)^r}{s + p_{r+1}}\right] + \cdots + a_n \frac{d}{ds}\left[\frac{(s + p_1)^r}{s + p_n}\right]$$

The first term on the right-hand side of this last equation vanishes. The second term becomes b_{r-1}. Each of the other terms contains some power of $(s + p_1)$ as a factor, with the result that, when s is allowed to approach $-p_1$, these terms drop out. Hence

$$b_{r-1} = \lim_{s \to -p_1} \frac{d}{ds}\left[(s + p_1)^r \frac{B(s)}{A(s)}\right] = \left\{\frac{d}{ds}\left[(s + p_1)^r \frac{B(s)}{A(s)}\right]\right\}_{s=-p_1}$$

Similarly, by performing successive differentiations with respect to s and by letting s approach $-p_1$, we obtain equations for the b_{r-j}, where $j = 2, 3, \ldots, r - 1$.

Note that the inverse Laplace transform of $1/(s + p_1)^n$ is given by

$$\mathcal{L}^{-1}\left[\frac{1}{(s + p_1)^n}\right] = \frac{t^{n-1}}{(n-1)!}e^{-p_1 t}$$

The constants $a_{r+1}, a_{r+2}, \ldots, a_n$ in Equation (2–19) are determined from

$$a_k = \left[(s + p_k)\frac{B(s)}{A(s)}\right]_{s=-p_k}, \qquad \text{for } k = r+1, r+2, \ldots, n$$

The inverse Laplace transform of $F(s)$ is then obtained as follows:

$$f(t) = \mathcal{L}^{-1}[F(s)] = \left[b_1 + b_2 t + \cdots + \frac{b_{r-1}}{(r-2)!}t^{r-2} + \frac{b_r}{(r-1)!}t^{r-1}\right]e^{-p_1 t} + a_{r+1}e^{-p_{r+1}t} + a_{r+2}e^{-p_{r+2}t} + \cdots + a_n e^{-p_n t}, \qquad \text{for } t \geq 0$$

A-2-17. Find the Laplace transform of the following differential equation:

$$\ddot{x} + 3\dot{x} + 6x = 0, \qquad x(0) = 0, \qquad \dot{x}(0) = 3$$

Taking the inverse Laplace transform of $X(s)$, obtain the time solution $x(t)$.

Solution. The Laplace transform of the differential equation is

$$s^2X(s) - sx(0) - \dot{x}(0) + 3sX(s) - 3x(0) + 6X(s) = 0$$

Substituting the initial conditions and solving for $X(s)$,

$$X(s) = \frac{3}{s^2 + 3s + 6} = \frac{2\sqrt{3}}{\sqrt{5}} \frac{\frac{\sqrt{15}}{2}}{(s + 1.5)^2 + \left(\frac{\sqrt{15}}{2}\right)^2}$$

The inverse Laplace transform of $X(s)$ is

$$x(t) = \frac{2\sqrt{3}}{\sqrt{5}}e^{-1.5t}\sin\left(\frac{\sqrt{15}}{2}t\right)$$

PROBLEMS

B-2-1. Find the Laplace transforms of the following functions:

(a) $f_1(t) = 0, \qquad \text{for } t < 0$

$= e^{-0.4t}\cos 12t, \qquad \text{for } t \geq 0$

(b) $f_2(t) = 0, \qquad \text{for } t < 0$

$= \sin\left(4t + \frac{\pi}{3}\right), \qquad \text{for } t \geq 0$

B-2-2. Find the Laplace transforms of the following functions:

(a) $f_1(t) = 0, \qquad \text{for } t < 0$

$= 3\sin(5t + 45°) \qquad \text{for } t \geq 0$

(b) $f_2(t) = 0, \qquad \text{for } t < 0$

$= 0.03(1 - \cos 2t) \qquad \text{for } t \geq 0$

B-2-3. Obtain the Laplace transform of the function defined by

$f(t) = 0, \qquad \text{for } t < 0$

$= t^2e^{-at} \qquad \text{for } t \geq 0$

B-2-4. Obtain the Laplace transform of the function defined by

$$f(t) = 0, \qquad \text{for } t < 0$$
$$= \cos 2\omega t \cdot \cos 3\omega t, \qquad \text{for } t \geq 0$$

B-2-5. What is the Laplace transform of the function $f(t)$ shown in Figure 2–5?

B-2-6. Obtain the Laplace transform of the function $f(t)$ shown in Figure 2–6.

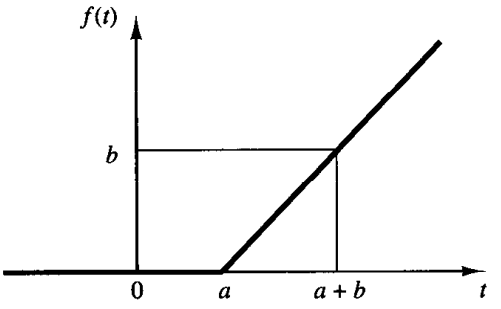

Figure 2–5
Function $f(t)$.

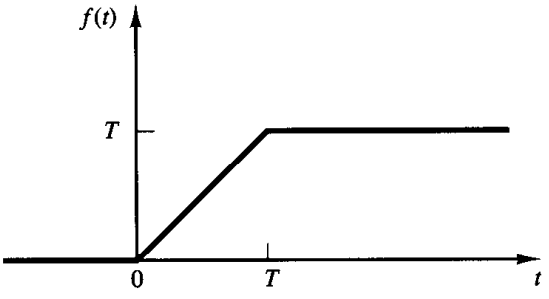

Figure 2–6
Function $f(t)$.

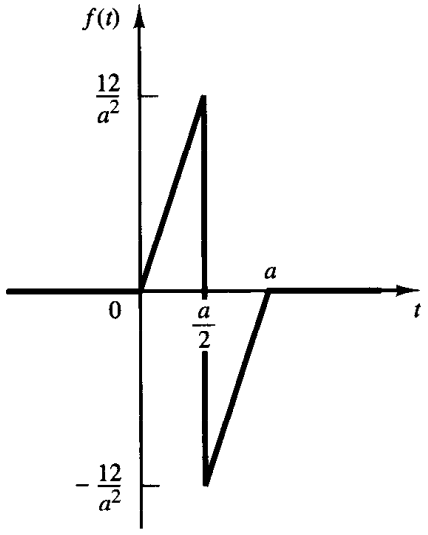

Figure 2–7
Function $f(t)$.

B-2-7. Find the Laplace transform of the function $f(t)$ shown in Figure 2–7. Also, find the limiting value of $\mathcal{L}[f(t)]$ as a approaches zero.

B-2-8. By applying the final-value theorem, find the final value of $f(t)$ whose Laplace transform is given by

$$F(s) = \frac{10}{s(s + 1)}$$

Verify this result by taking the inverse Laplace transform of $F(s)$ and letting $t \to \infty$.

B-2-9. Given

$$F(s) = \frac{1}{(s + 2)^2}$$

determine the values of $f(0+)$ and $\dot{f}(0+)$. (Use the initial-value theorem.)

B-2-10. Find the inverse Laplace transform of

$$F(s) = \frac{s + 1}{s(s^2 + s + 1)}$$

B-2-11. Find the inverse Laplace transforms of the following functions:

(a) $$F_1(s) = \frac{6s + 3}{s^2}$$

(b) $$F_2(s) = \frac{5s + 2}{(s + 1)(s + 2)^2}$$

B-2-12. Find the inverse Laplace transform of

$$F(s) = \frac{1}{s^2(s^2 + \omega^2)}$$

B-2-13. What is the solution of the following differential equation?

$$2\ddot{x} + 7\dot{x} + 3x = 0, \qquad x(0) = 3, \qquad \dot{x}(0) = 0$$

B-2-14. Solve the differential equation

$$\dot{x} + 2x = \delta(t), \qquad x(0-) = 0$$

B-2-15. Solve the following differential equation:

$$\ddot{x} + 2\zeta\omega_n\dot{x} + \omega_n^2 x = 0, \qquad x(0) = a, \qquad \dot{x}(0) = b$$

where a and b are constants.

B-2-16. Obtain the solution of the differential equation

$$\dot{x} + ax = A \sin \omega t, \qquad x(0) = b$$

3

Mathematical Modeling of Dynamic Systems

3–1 INTRODUCTION

In studying control systems the reader must be able to model dynamic systems and analyze dynamic characteristics. A mathematical model of a dynamic system is defined as a set of equations that represents the dynamics of the system accurately or, at least, fairly well. Note that a mathematical model is not unique to a given system. A system may be represented in many different ways and, therefore, may have many mathematical models, depending on one's perspective.

The dynamics of many systems, whether they are mechanical, electrical, thermal, economic, biological, and so on, may be described in terms of differential equations. Such differential equations may be obtained by using physical laws governing a particular system, for example, Newton's laws for mechanical systems and Kirchhoff's laws for electrical systems. We must always keep in mind that deriving a reasonable mathematical model is the most important part of the entire analysis.

Mathematical models. Mathematical models may assume many different forms. Depending on the particular system and the particular circumstances, one mathematical model may be better suited than other models. For example, in optimal control problems, it is advantageous to use state-space representations. On the other hand, for the transient-response or frequency-response analysis of single-input–single-output, linear, time-invariant systems, the transfer function representation may be more convenient than any other. Once a mathematical model of a system is obtained, various analytical and computer tools can be used for analysis and synthesis purposes.

Simplicity versus accuracy. It is possible to improve the accuracy of a mathematical model by increasing its complexity. In some cases, we include hundreds of equations to describe a complete system. In obtaining a mathematical model, however, we must make a compromise between the simplicity of the model and the accuracy of the results of the analysis. If extreme accuracy is not needed, however, it is preferable to obtain only a reasonably simplified model. In fact, we are generally satisfied if we can obtain a mathematical model that is adequate for the problem under consideration. It is important to note, however, that the results obtained from the analysis are valid only to the extent that the model approximates a given dynamic system.

In deriving a reasonably simplified mathematical model, we frequently find it necessary to ignore certain inherent physical properties of the system. In particular, if a linear lumped-parameter mathematical model (that is, one employing ordinary differential equations) is desired, it is always necessary to ignore certain nonlinearities and distributed parameters (that is, ones giving rise to partial differential equations) that may be present in the physical system. If the effects that these ignored properties have on the response are small, good agreement will be obtained between the results of the analysis of a mathematical model and the results of the experimental study of the physical system.

In general, in solving a new problem, we find it desirable first to build a simplified model so that we can get a general feeling for the solution. A more complete mathematical model may then be built and used for a more complete analysis.

We must be well aware of the fact that a linear lumped-parameter model, which may be valid in low-frequency operations, may not be valid at sufficiently high frequencies since the neglected property of distributed parameters may become an important factor in the dynamic behavior of the system. For example, the mass of a spring may be neglected in low-frequency operations, but it becomes an important property of the system at high frequencies.

Linear systems. A system is called linear if the principle of superposition applies. The principle of superposition states that the response produced by the simultaneous application of two different forcing functions is the sum of the two individual responses. Hence, for the linear system, the response to several inputs can be calculated by treating one input at a time and adding the results. It is this principle that allows one to build up complicated solutions to the linear differential equation from simple solutions.

In an experimental investigation of a dynamic system, if cause and effect are proportional, thus implying that the principle of superposition holds, then the system can be considered linear.

Linear time-invariant systems and linear time-varying systems. A differential equation is linear if the coefficients are constants or functions only of the independent variable. Dynamic systems that are composed of linear time-invariant lumped-parameter components may be described by linear time-invariant (constant-coefficient) differential equations. Such systems are called *linear time-invariant* (or *linear constant-coefficient*) systems. Systems that are represented by differential equations whose coefficients are functions of time are called *linear time-varying* systems. An example of a time-varying control system is a spacecraft control system. (The mass of a spacecraft changes due to fuel consumption.)

Nonlinear systems. A system is nonlinear if the principle of superposition does not apply. Thus, for a nonlinear system the response to two inputs cannot be calculated by treating one input at a time and adding the results. Examples of nonlinear differential equations are

$$\frac{d^2x}{dt^2} + \left(\frac{dx}{dt}\right)^2 + x = A \sin \omega t$$

$$\frac{d^2x}{dt^2} + (x^2 - 1)\frac{dx}{dt} + x = 0$$

$$\frac{d^2x}{dt^2} + \frac{dx}{dt} + x + x^3 = 0$$

Although many physical relationships are often represented by linear equations, in most cases actual relationships are not quite linear. In fact, a careful study of physical systems reveals that even so-called "linear systems" are really linear only in limited operating ranges. In practice, many electromechanical systems, hydraulic systems, pneumatic systems, and so on, involve nonlinear relationships among the variables. For example, the output of a component may saturate for large input signals. There may be a dead space that affects small signals. (The dead space of a component is a small range of input variations to which the component is insensitive.) Square-law nonlinearity may occur in some components. For instance, dampers used in physical systems may be linear for low-velocity operations but may become nonlinear at high velocities, and the damping force may become proportional to the square of the operating velocity. Examples of characteristic curves for these nonlinearities are shown in Figure 3–1.

Note that some important control systems are nonlinear for signals of any size. For example, in on–off control systems, the control action is either on or off, and there is no linear relationship between the input and output of the controller.

Procedures for finding the solutions of problems involving such nonlinear systems, in general, are extremely complicated. Because of this mathematical difficulty attached to nonlinear systems, one often finds it necessary to introduce "equivalent" linear systems in place of nonlinear ones. Such equivalent linear systems are valid for only a limited range of operation. Once a nonlinear system is approximated by a linear mathematical model, a number of linear tools may be applied for analysis and design purposes.

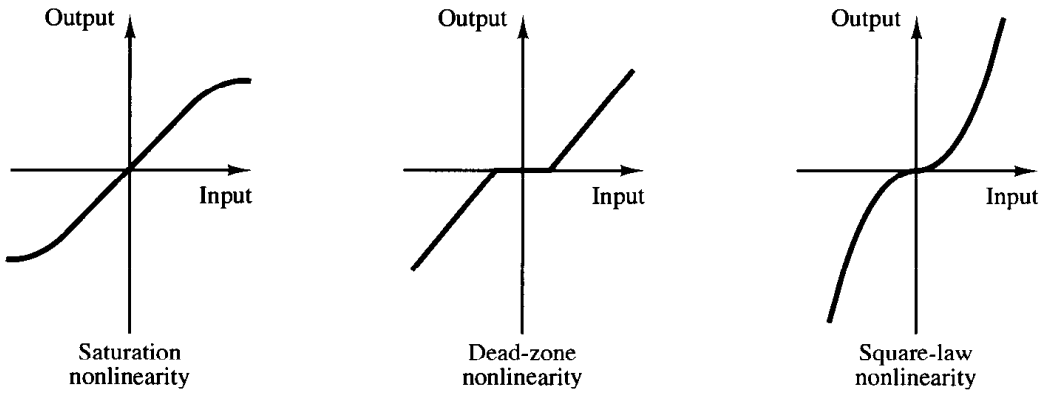

Figure 3–1
Characteristic curves for various nonlinearities.

Linearization of nonlinear systems. In control engineering a normal operation of the system may be around an equilibrium point, and the signals may be considered small signals around the equilibrium. (It should be pointed out that there are many exceptions to such a case.) However, if the system operates around an equilibrium point and if the signals involved are small signals, then it is possible to approximate the nonlinear system by a linear system. Such a linear system is equivalent to the nonlinear system considered within a limited operating range. Such a linearized model (linear, time-invariant model) is very important in control engineering. We shall discuss a linearization technique in Section 3–10.

Outline of the chapter. Section 3–1 has presented an introduction to the mathematical modeling of dynamic systems, including discussions of linear and nonlinear systems. Section 3–2 presents the transfer function and impulse-response function. Section 3–3 introduces block diagrams and Section 3–4 discusses concepts of modeling in state space. Section 3–5 presents state-space representation of dynamic systems. Section 3–6 treats mathematical modeling of mechanical systems. We discuss Newton's approach to modeling mechanical systems. Section 3–7 deals with mathematical modeling of electrical circuits, Section 3–8 treats liquid-level systems, and Section 3–9 presents mathematical modeling of thermal systems. Finally, Section 3–10 discusses the linearization of nonlinear mathematical models. (Mathematical modeling of other types of systems is treated throughout the remaining chapters of the book.)

3–2 TRANSFER FUNCTION AND IMPULSE-RESPONSE FUNCTION

In control theory, functions called transfer functions are commonly used to characterize the input–output relationships of components or systems that can be described by linear, time-invariant, differential equations. We begin by defining the transfer function and follow with a derivation of the transfer function of a mechanical system. Then we discuss the impulse-response function.

Transfer function. The *transfer function* of a linear, time-invariant, differential equation system is defined as the ratio of the Laplace transform of the output (response function) to the Laplace transform of the input (driving function) under the assumption that all initial conditions are zero.

Consider the linear time-invariant system defined by the following differential equation:

$$a_0 y^{(n)} + a_1 y^{(n-1)} + \cdots + a_{n-1}\dot{y} + a_n y = b_0 x^{(m)} + b_1 x^{(m-1)} + \cdots + b_{m-1}\dot{x} + b_m x \qquad (n \geq m) \qquad (3\text{–}1)$$

where y is the output of the system and x is the input. The transfer function of this system is obtained by taking the Laplace transforms of both sides of Equation (3–1), under the assumption that all initial conditions are zero, or

$$\text{Transfer function} = G(s) = \left.\frac{\mathcal{L}[\text{output}]}{\mathcal{L}[\text{input}]}\right|_{\text{zero initial conditions}}$$

$$= \frac{Y(s)}{X(s)} = \frac{b_0 s^m + b_1 s^{m-1} + \cdots + b_{m-1} s + b_m}{a_0 s^n + a_1 s^{n-1} + \cdots + a_{n-1} s + a_n} \tag{3–2}$$

By using the concept of transfer function, it is possible to represent system dynamics by algebraic equations in s. If the highest power of s in the denominator of the transfer function is equal to n, the system is called an *nth-order system.*

Comments on transfer function. The applicability of the concept of the transfer function is limited to linear, time-invariant, differential equation systems. The transfer function approach, however, is extensively used in the analysis and design of such systems. In what follows, we shall list important comments concerning the transfer function. (Note that in the list a system referred to is one described by a linear, time-invariant, differential equation.)

1. The transfer function of a system is a mathematical model in that it is an operational method of expressing the differential equation that relates the output variable to the input variable.
2. The transfer function is a property of a system itself, independent of the magnitude and nature of the input or driving function.
3. The transfer function includes the units necessary to relate the input to the output; however, it does not provide any information concerning the physical structure of the system. (The transfer functions of many physically different systems can be identical.)
4. If the transfer function of a system is known, the output or response can be studied for various forms of inputs with a view toward understanding the nature of the system.
5. If the transfer function of a system is unknown, it may be established experimentally by introducing known inputs and studying the output of the system. Once established, a transfer function gives a full description of the dynamic characteristics of the system, as distinct from its physical description.

Mechanical system. Consider the satellite attitude control system shown in Figure 3–2. The diagram shows the control of only the yaw angle θ. (In the actual system there are controls about three axes.) Small jets apply reaction forces to rotate the satellite body into the desired attitude. The two skew symmetrically placed jets denoted by A or B operate in pairs. Assume that each jet thrust is $F/2$ and a torque $T = Fl$ is applied to the system. The jets are applied for a certain time duration and thus the torque can be written as $T(t)$. The moment of inertia about the axis of rotation at the center of mass is J.

Let us obtain the transfer function of this system by assuming that torque $T(t)$ is the input, and the angular displacement $\theta(t)$ of the satellite is the output. (We consider the motion only in the plane of the page.)

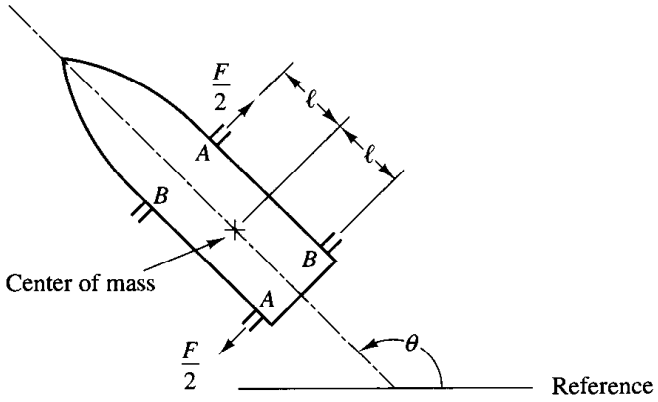

Figure 3–2
Schematic diagram of a satellite attitude control system.

To derive the transfer function, we proceed according to the following steps.

1. Write the differential equation for the system.
2. Take the Laplace transform of the differential equation, assuming all initial conditions are zero.
3. Take the ratio of the output $\Theta(s)$ to the input $T(s)$. This ratio is the transfer function.

Applying Newton's second law to the present system and noting that there is no friction in the environment of the satellite, we have

$$J\frac{d^2\theta}{dt^2} = T$$

Taking the Laplace transform of both sides of this last equation and assuming all initial conditions to be zero yields

$$Js^2\Theta(s) = T(s)$$

where $\Theta(s) = \mathcal{L}[\theta(t)]$ and $T(s) = \mathcal{L}[T(t)]$. The transfer function of the system is thus obtained as

$$\text{Transfer function} = \frac{\Theta(s)}{T(s)} = \frac{1}{Js^2}$$

Convolution integral. For a linear, time-invariant system the transfer function $G(s)$ is

$$G(s) = \frac{Y(s)}{X(s)}$$

where $X(s)$ is the Laplace transform of the input and $Y(s)$ is the Laplace transform of the output, where we assume that all initial conditions involved are zero. It follows that the output $Y(s)$ can be written as the product of $G(s)$ and $X(s)$, or

$$Y(s) = G(s)X(s) \tag{3–3}$$

Note that multiplication in the complex domain is equivalent to convolution in the time domain, so the inverse Laplace transform of Equation (3–3) is given by the following convolution integral:

$$y(t) = \int_0^t x(\tau)g(t - \tau)\, d\tau$$

$$= \int_0^t g(\tau)x(t - \tau)\, d\tau \tag{3–4}$$

where $g(t) = 0$ and $x(t) = 0$ for $t < 0$.

Impulse-response function. Consider the output (response) of a system to a unit-impulse input when the initial conditions are zero. Since the Laplace transform of the unit-impulse function is unity, the Laplace transform of the output of the system is

$$Y(s) = G(s) \tag{3–5}$$

The inverse Laplace transform of the output given by Equation (3–5) gives the impulse response of the system. The inverse Laplace transform of $G(s)$, or

$$\mathcal{L}^{-1}[G(s)] = g(t)$$

is called the impulse-response function. This function $g(t)$ is also called the weighting function of the system.

The impulse-response function $g(t)$ is thus the response of a linear system to a unit-impulse input when the initial conditions are zero. The Laplace transform of this function gives the transfer function. Therefore, the transfer function and impulse-response function of a linear, time-invariant system contain the same information about the system dynamics. It is hence possible to obtain complete information about the dynamic characteristics of the system by exciting it with an impulse input and measuring the response. (In practice, a pulse input with a very short duration compared with the significant time constants of the system can be considered an impulse.)

3–3 BLOCK DIAGRAMS

A control system may consist of a number of components. To show the functions performed by each component, in control engineering, we commonly use a diagram called the *block diagram.* This section explains what a block diagram is, presents a method for obtaining block diagrams for physical systems, and, finally, discusses techniques to simplify such diagrams.

Block diagrams. A *block diagram* of a system is a pictorial representation of the functions performed by each component and of the flow of signals. Such a diagram depicts the interrelationships that exist among the various components. Differing from a purely abstract mathematical representation, a block diagram has the advantage of indicating more realistically the signal flows of the actual system.

In a block diagram all system variables are linked to each other through functional blocks. The *functional block* or simply *block* is a symbol for the mathematical operation on the input signal to the block that produces the output. The transfer functions of the components are usually entered in the corresponding blocks, which are connected by arrows to indicate the direction of the flow of signals. Note that the signal can pass only

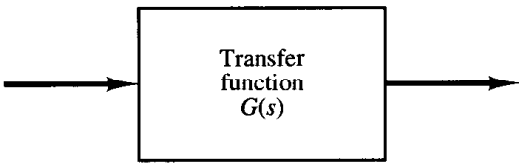

Figure 3–3
Element of a block diagram.

in the direction of the arrows. Thus a block diagram of a control system explicitly shows a unilateral property.

Figure 3–3 shows an element of the block diagram. The arrowhead pointing toward the block indicates the input, and the arrowhead leading away from the block represents the output. Such arrows are referred to as *signals*.

Note that the dimensions of the output signal from the block are the dimensions of the input signal multiplied by the dimensions of the transfer function in the block.

The advantages of the block diagram representation of a system lie in the fact that it is easy to form the overall block diagram for the entire system by merely connecting the blocks of the components according to the signal flow and that it is possible to evaluate the contribution of each component to the overall performance of the system.

In general, the functional operation of the system can be visualized more readily by examining the block diagram than by examining the physical system itself. A block diagram contains information concerning dynamic behavior, but it does not include any information on the physical construction of the system. Consequently, many dissimilar and unrelated systems can be represented by the same block diagram.

It should be noted that in a block diagram the main source of energy is not explicitly shown and that the block diagram of a given system is not unique. A number of different block diagrams can be drawn for a system, depending on the point of view of the analysis.

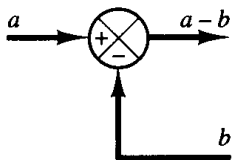

Figure 3–4
Summing point.

Summing Point. Referring to Figure 3–4, a circle with a cross is the symbol that indicates a summing operation. The plus or minus sign at each arrowhead indicates whether that signal is to be added or subtracted. It is important that the quantities being added or subtracted have the same dimensions and the same units.

Branch Point. A *branch point* is a point from which the signal from a block goes concurrently to other blocks or summing points.

Block diagram of a closed-loop system. Figure 3–5 shows an example of a block diagram of a closed-loop system. The output $C(s)$ is fed back to the summing point, where it is compared with the reference input $R(s)$. The closed-loop nature of the system is clearly indicated by the figure. The output of the block, $C(s)$ in this case, is obtained by multiplying the transfer function $G(s)$ by the input to the block, $E(s)$. Any linear control system may be represented by a block diagram consisting of blocks, summing points, and branch points.

When the output is fed back to the summing point for comparison with the input, it is necessary to convert the form of the output signal to that of the input signal. For example, in a temperature-control system, the output signal is usually the controlled temperature. The output signal, which has the dimension of temperature, must be converted

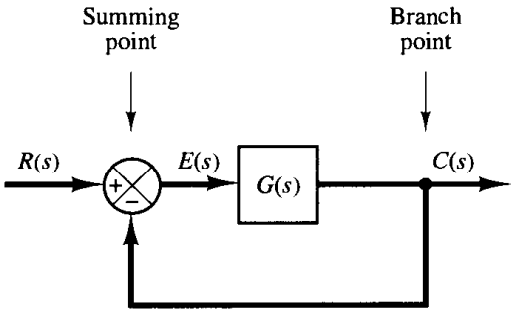

Figure 3–5
Block diagram of a closed-loop system.

to a force or position or voltage before it can be compared with the input signal. This conversion is accomplished by the feedback element whose transfer function is $H(s)$, as shown in Figure 3–6. The role of the feedback element is to modify the output before it is compared with the input. (In most cases the feedback element is a sensor that measures the output of the plant. The output of the sensor is compared with the input, and the actuating error signal is generated.) In the present example, the feedback signal that is fed back to the summing point for comparison with the input is $B(s) = H(s)C(s)$.

Open-loop transfer function and feedforward transfer function. Referring to Figure 3–6, the ratio of the feedback signal $B(s)$ to the actuating error signal $E(s)$ is called the *open-loop transfer function.* That is,

$$\text{Open-loop transfer function} = \frac{B(s)}{E(s)} = G(s)H(s)$$

The ratio of the output $C(s)$ to the actuating error signal $E(s)$ is called the *feedforward transfer function,* so that

$$\text{Feedforward transfer function} = \frac{C(s)}{E(s)} = G(s)$$

If the feedback transfer function $H(s)$ is unity, then the open-loop transfer function and the feedforward transfer function are the same.

Closed-loop transfer function. For the system shown in Figure 3–6, the output $C(s)$ and input $R(s)$ are related as follows:

$$C(s) = G(s)E(s)$$

$$E(s) = R(s) - B(s)$$

$$= R(s) - H(s)C(s)$$

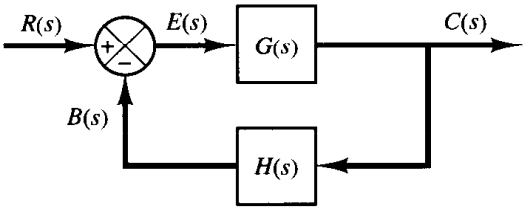

Figure 3–6
Closed-loop system.

Eliminating $E(s)$ from these equations gives

$$C(s) = G(s)[R(s) - H(s)C(s)]$$

or

$$\frac{C(s)}{R(s)} = \frac{G(s)}{1 + G(s)H(s)} \tag{3–6}$$

The transfer function relating $C(s)$ to $R(s)$ is called the *closed-loop transfer function.* This transfer function relates the closed-loop system dynamics to the dynamics of the feedforward elements and feedback elements.

From Equation (3–6), $C(s)$ is given by

$$C(s) = \frac{G(s)}{1 + G(s)H(s)} R(s)$$

Thus the output of the closed-loop system clearly depends on both the closed-loop transfer function and the nature of the input.

Closed-loop system subjected to a disturbance. Figure 3–7 shows a closed-loop system subjected to a disturbance. When two inputs (the reference input and disturbance) are present in a linear system, each input can be treated independently of the other; and the outputs corresponding to each input alone can be added to give the complete output. The way each input is introduced into the system is shown at the summing point by either a plus or minus sign.

Consider the system shown in Figure 3–7. In examining the effect of the disturbance $D(s)$, we may assume that the system is at rest initially with zero error; we may then calculate the response $C_D(s)$ to the disturbance only. This response can be found from

$$\frac{C_D(s)}{D(s)} = \frac{G_2(s)}{1 + G_1(s)G_2(s)H(s)}$$

On the other hand, in considering the response to the reference input $R(s)$, we may assume that the disturbance is zero. Then the response $C_R(s)$ to the reference input $R(s)$ can be obtained from

$$\frac{C_R(s)}{R(s)} = \frac{G_1(s)G_2(s)}{1 + G_1(s)G_2(s)H(s)}$$

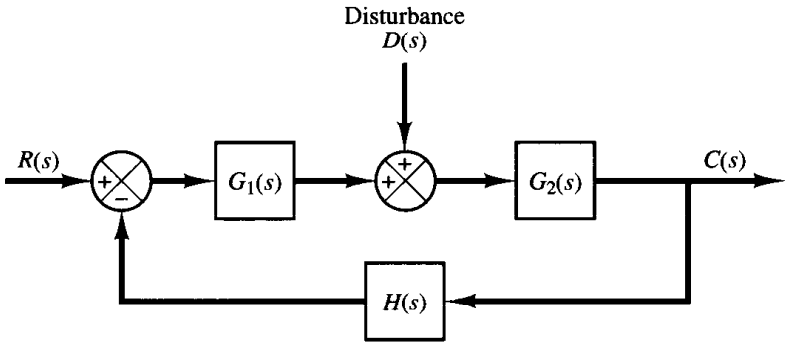

Figure 3–7
Closed-loop system subjected to a disturbance.

The response to the simultaneous application of the reference input and disturbance can be obtained by adding the two individual responses. In other words, the response $C(s)$ due to the simultaneous application of the reference input $R(s)$ and disturbance $D(s)$ is given by

$$C(s) = C_R(s) + C_D(s)$$

$$= \frac{G_2(s)}{1 + G_1(s)G_2(s)H(s)}[G_1(s)R(s) + D(s)]$$

Consider now the case where $|G_1(s)H(s)| \gg 1$ and $|G_1(s)G_2(s)H(s)| \gg 1$. In this case, the closed-loop transfer function $C_D(s)/D(s)$ becomes almost zero, and the effect of the disturbance is suppressed. This is an advantage of the closed-loop system.

On the other hand, the closed-loop transfer function $C_R(s)/R(s)$ approaches $1/H(s)$ as the gain of $G_1(s)G_2(s)H(s)$ increases. This means that if $|G_1(s)G_2(s)H(s)| \gg 1$ then the closed-loop transfer function $C_R(s)/R(s)$ becomes independent of $G_1(s)$ and $G_2(s)$ and becomes inversely proportional to $H(s)$ so that the variations of $G_1(s)$ and $G_2(s)$ do not affect the closed-loop transfer function $C_R(s)/R(s)$. This is another advantage of the closed-loop system. It can easily be seen that any closed-loop system with unity feedback, $H(s) = 1$, tends to equalize the input and output.

Procedures for drawing a block diagram. To draw a block diagram for a system, first write the equations that describe the dynamic behavior of each component. Then take the Laplace transforms of these equations, assuming zero initial conditions, and represent each Laplace-transformed equation individually in block form. Finally, assemble the elements into a complete block diagram.

As an example, consider the RC circuit shown in Figure 3–8(a). The equations for this circuit are

$$i = \frac{e_i - e_o}{R} \tag{3–7}$$

$$e_o = \frac{\int i\,dt}{C} \tag{3–8}$$

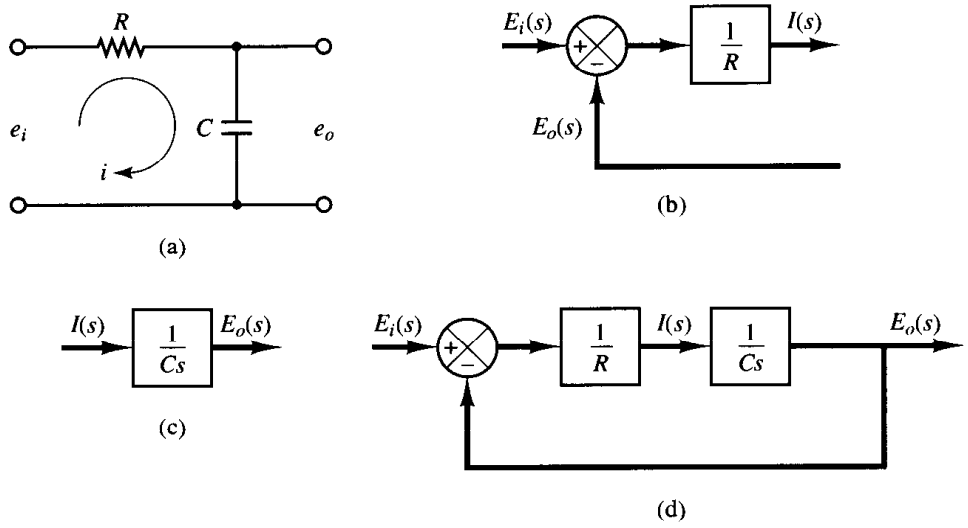

Figure 3–8
(a) RC circuit; (b) block diagram representing Equation (3–9); (c) block diagram representing Equation (3–10); (d) block diagram of the RC circuit.

The Laplace transforms of Equations (3–7) and (3–8), with zero initial condition, become

$$I(s) = \frac{E_i(s) - E_o(s)}{R} \tag{3–9}$$

$$E_o(s) = \frac{I(s)}{Cs} \tag{3–10}$$

Equation (3–9) represents a summing operation, and the corresponding diagram is shown in Figure 3–8(b). Equation (3–10) represents the block as shown in Figure 3–8(c). Assembling these two elements, we obtain the overall block diagram for the system as shown in Figure 3–8(d).

Block diagram reduction. It is important to note that blocks can be connected in series only if the output of one block is not affected by the next following block. If there are any loading effects between the components, it is necessary to combine these components into a single block.

Any number of cascaded blocks representing nonloading components can be replaced by a single block, the transfer function of which is simply the product of the individual transfer functions.

A complicated block diagram involving many feedback loops can be simplified by a step-by-step rearrangement, using rules of block diagram algebra. Some of these important rules are given in Table 3–1. They are obtained by writing the same equation in

Table 3–1 Rules of Block Diagram Algebra

	Original Block Diagrams	Equivalent Block Diagrams
1	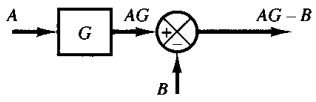	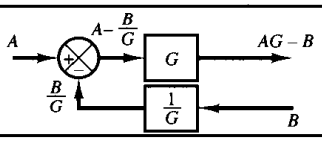
2	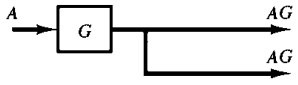	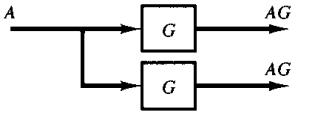
3	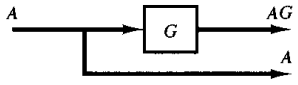	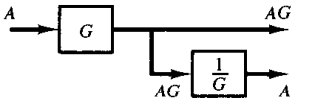
4	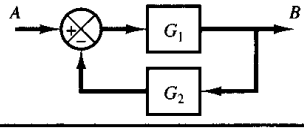	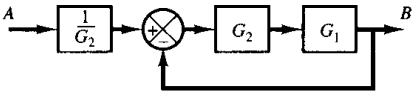
5	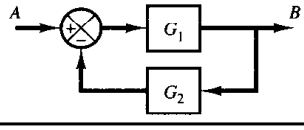	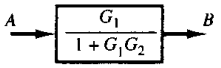

a different way. Simplification of the block diagram by rearrangements and substitutions considerably reduces the labor needed for subsequent mathematical analysis. It should be noted, however, that as the block diagram is simplified the transfer functions in new blocks become more complex because new poles and new zeros are generated.

In simplifying a block diagram, remember the following.

1. The product of the transfer functions in the feedforward direction must remain the same.
2. The product of the transfer functions around the loop must remain the same.

EXAMPLE 3–1 Consider the system shown in Figure 3–9(a). Simplify this diagram.

By moving the summing point of the negative feedback loop containing H_2 outside the positive feedback loop containing H_1, we obtain Figure 3–9(b). Eliminating the positive feedback

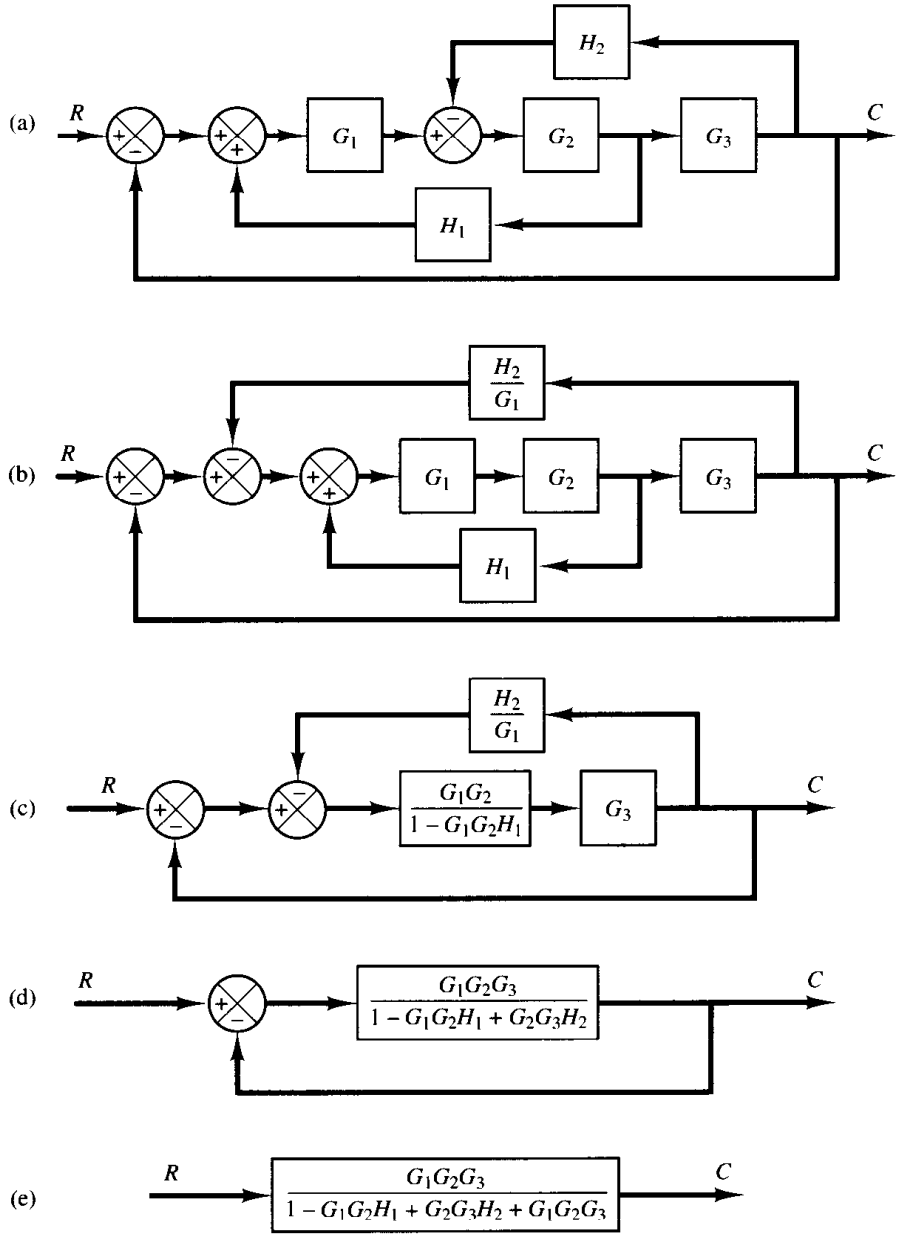

Figure 3–9
(a) Multiple-loop system; (b)–(e) successive reductions of the block diagram shown in (a).

loop, we have Figure 3–9(c). The elimination of the loop containing H_2/G_1 gives Figure 3–9(d). Finally, eliminating the feedback loop results in Figure 3–9(e).

Notice that the numerator of the closed-loop transfer function $C(s)/R(s)$ is the product of the transfer functions of the feedforward path. The denominator of $C(s)/R(s)$ is equal to

$$1 - \sum (\text{product of the transfer functions around each loop})$$

$$= 1 - (G_1G_2H_1 - G_2G_3H_2 - G_1G_2G_3)$$

$$= 1 - G_1G_2H_1 + G_2G_3H_2 + G_1G_2G_3$$

(The positive feedback loop yields a negative term in the denominator.)

3–4 MODELING IN STATE SPACE

In this section we shall present introductory material on state-space analysis of control systems.

Modern control theory. The modern trend in engineering systems is toward greater complexity, due mainly to the requirements of complex tasks and good accuracy. Complex systems may have multiple inputs and multiple outputs and may be time varying. Because of the necessity of meeting increasingly stringent requirements on the performance of control systems, the increase in system complexity, and easy access to large-scale computers, modern control theory, which is a new approach to the analysis and design of complex control systems, has been developed since around 1960. This new approach is based on the concept of state. The concept of state by itself is not new since it has been in existence for a long time in the field of classical dynamics and other fields.

Modern control theory versus conventional control theory. Modern control theory is contrasted with conventional control theory in that the former is applicable to multiple-input–multiple-output systems, which may be linear or nonlinear, time invariant or time varying, while the latter is applicable only to linear time-invariant single-input–single-output systems. Also, modern control theory is essentially a time-domain approach, while conventional control theory is a complex frequency-domain approach. Before we proceed further, we must define state, state variables, state vector, and state space.

State. The state of a dynamic system is the smallest set of variables (called *state variables*) such that the knowledge of these variables at $t = t_0$, together with the knowledge of the input for $t \geq t_0$, completely determines the behavior of the system for any time $t \geq t_0$.

Note that the concept of state is by no means limited to physical systems. It is applicable to biological systems, economic systems, social systems, and others.

State variables. The state variables of a dynamic system are the variables making up the smallest set of variables that determine the state of the dynamic system. If at least n variables $x_1, x_2, \ldots, x_n$ are needed to completely describe the behavior of a dy-

namic system (so that once the input is given for $t \geq t_0$ and the initial state at $t = t_0$ is specified, the future state of the system is completely determined), then such n variables are a set of state variables.

Note that state variables need not be physically measurable or observable quantities. Variables that do not represent physical quantities and those that are neither measurable nor observable can be chosen as state variables. Such freedom in choosing state variables is an advantage of the state-space methods. Practically, however, it is convenient to choose easily measurable quantities for the state variables, if this is possible at all, because optimal control laws will require the feedback of all state variables with suitable weighting.

State vector. If n state variables are needed to completely describe the behavior of a given system, then these n state variables can be considered the n components of a vector $\mathbf{x}$. Such a vector is called a *state vector*. A state vector is thus a vector that determines uniquely the system state $\mathbf{x}(t)$ for any time $t \geq t_0$, once the state at $t = t_0$ is given and the input $\mathbf{u}(t)$ for $t \geq t_0$ is specified.

State space. The n-dimensional space whose coordinate axes consist of the x_1 axis, x_2 axis, . . . , x_n axis is called a *state space*. Any state can be represented by a point in the state space.

State-space equations. In state-space analysis we are concerned with three types of variables that are involved in the modeling of dynamic systems: input variables, output variables, and state variables. As we shall see in Section 3–5, the state-space representation for a given system is not unique, except that the number of state variables is the same for any of the different state-space representations of the same system.

The dynamic system must involve elements that memorize the values of the input for $t \geq t_1$. Since integrators in a continuous-time control system serve as memory devices, the outputs of such integrators can be considered as the variables that define the internal state of the dynamic system. Thus the outputs of integrators serve as state variables. The number of state variables to completely define the dynamics of the system is equal to the number of integrators involved in the system.

Assume that a multiple-input–multiple-output system involves n integrators. Assume also that there are r inputs $u_1, u_2(t), \ldots, u_r(t)$ and m outputs $y_1(t), y_2(t), \ldots, y_m(t)$. Define n outputs of the integrators as state variables: $x_1(t), x_2(t), \ldots, x_n(t)$. Then the system may be described by

$$\begin{aligned}
\dot{x}_1(t) &= f_1(x_1, x_2, \ldots, x_n; u_1, u_2, \ldots, u_r; t) \\
\dot{x}_2(t) &= f_2(x_1, x_2, \ldots, x_n; u_1, u_2, \ldots, u_r; t) \\
&\vdots \\
\dot{x}_n(t) &= f_n(x_1, x_2, \ldots, x_n; u_1, u_2, \ldots, u_r; t)
\end{aligned} \tag{3–11}$$

The outputs $y_1(t), y_2(t), \ldots, y_m(t)$ of the system may be given by

$$\begin{aligned} y_1(t) &= g_1(x_1, x_2, \ldots, x_n; u_1, u_2, \ldots, u_r; t) \\ y_2(t) &= g_2(x_1, x_2, \ldots, x_n; u_1, u_2, \ldots, u_r; t) \\ &\cdot \\ &\cdot \\ &\cdot \\ y_m(t) &= g_m(x_1, x_2, \ldots, x_n; u_1, u_2, \ldots, u_r; t) \end{aligned} \tag{3–12}$$

If we define

$$\mathbf{x}(t) = \begin{bmatrix} x_1(t) \\ x_2(t) \\ \cdot \\ \cdot \\ \cdot \\ x_n(t) \end{bmatrix}, \qquad \mathbf{f}(\mathbf{x}, \mathbf{u}, t) = \begin{bmatrix} f_1(x_1, x_2, \ldots, x_n; u_1, u_2, \ldots, u_r; t) \\ f_2(x_1, x_2, \ldots, x_n; u_1, u_2, \ldots, u_r; t) \\ \cdot \\ \cdot \\ \cdot \\ f_n(x_1, x_2, \ldots, x_n; u_1, u_2, \ldots, u_r; t) \end{bmatrix}$$

$$\mathbf{y}(t) = \begin{bmatrix} y_1(t) \\ y_2(t) \\ \cdot \\ \cdot \\ \cdot \\ y_m(t) \end{bmatrix}, \qquad \mathbf{g}(\mathbf{x}, \mathbf{u}, t) = \begin{bmatrix} g_1(x_1, x_2, \ldots, x_n; u_1, u_2, \ldots, u_r; t) \\ g_2(x_1, x_2, \ldots, x_n; u_1, u_2, \ldots, u_r; t) \\ \cdot \\ \cdot \\ \cdot \\ g_m(x_1, x_2, \ldots, x_n; u_1, u_2, \ldots, u_r; t) \end{bmatrix}, \qquad \mathbf{u}(t) = \begin{bmatrix} u_1(t) \\ u_2(t) \\ \cdot \\ \cdot \\ \cdot \\ u_r(t) \end{bmatrix}$$

then Equations (3–11) and (3–12) become

$$\dot{\mathbf{x}}(t) = \mathbf{f}(\mathbf{x}, \mathbf{u}, t) \tag{3–13}$$

$$\mathbf{y}(t) = \mathbf{g}(\mathbf{x}, \mathbf{u}, t) \tag{3–14}$$

where Equation (3–13) is the state equation and Equation (3–14) is the output equation. If vector functions **f** and/or **g** involve time t explicitly, then the system is called a time-varying system.

If Equations (3–13) and (3–14) are linearized about the operating state, then we have the following linearized state equation and output equation:

$$\dot{\mathbf{x}}(t) = \mathbf{A}(t)\mathbf{x}(t) + \mathbf{B}(t)\mathbf{u}(t) \tag{3–15}$$

$$\mathbf{y}(t) = \mathbf{C}(t)\mathbf{x}(t) + \mathbf{D}(t)\mathbf{u}(t) \tag{3–16}$$

where $\mathbf{A}(t)$ is called the state matrix, $\mathbf{B}(t)$ the input matrix, $\mathbf{C}(t)$ the output matrix, and $\mathbf{D}(t)$ the direct transmission matrix. (Details of linearization of nonlinear systems about the operating state are discussed in Section 3–10.) A block diagram representation of Equations (3–15) and (3–16) is shown in Figure 3–10.

If vector functions **f** and **g** do not involve time t explicitly then the system is called a time-invariant system. In this case, Equations (3–15) and (3–16) can be simplified to

$$\dot{\mathbf{x}}(t) = \mathbf{A}\mathbf{x}(t) + \mathbf{B}\mathbf{u}(t) \tag{3–17}$$

$$\mathbf{y}(t) = \mathbf{C}\mathbf{x}(t) + \mathbf{D}\mathbf{u}(t) \tag{3–18}$$

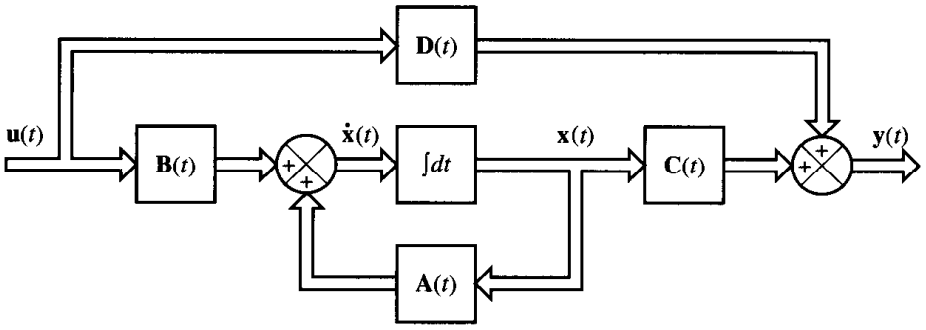

Figure 3–10
Block diagram of the linear continuous-time control system represented in state space.

Equation (3–17) is the state equation of the linear, time-invariant system. Equation (3–18) is the output equation for the same system. In this book we shall be concerned mostly with systems described by Equations (3–17) and (3–18).

In what follows we shall present an example for deriving a state equation and output equation.

EXAMPLE 3–2

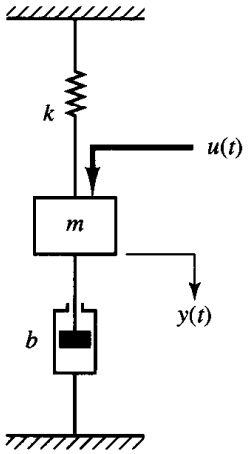

Figure 3–11
Mechanical system.

Consider the mechanical system shown in Figure 3–11. We assume that the system is linear. The external force $u(t)$ is the input to the system, and the displacement $y(t)$ of the mass is the output. The displacement $y(t)$ is measured from the equilibrium position in the absence of the external force. This system is a single-input–single-output system.

From the diagram, the system equation is

$$m\ddot{y} + b\dot{y} + ky = u \tag{3–19}$$

This system is of second order. This means that the system involves two integrators. Let us define state variables $x_1(t)$ and $x_2(t)$ as

$$x_1(t) = y(t)$$
$$x_2(t) = \dot{y}(t)$$

Then we obtain

$$\dot{x}_1 = x_2$$
$$\dot{x}_2 = \frac{1}{m}(-ky - b\dot{y}) + \frac{1}{m}u$$

or

$$\dot{x}_1 = x_2 \tag{3–20}$$
$$\dot{x}_2 = -\frac{k}{m}x_1 - \frac{b}{m}x_2 + \frac{1}{m}u \tag{3–21}$$

The output equation is

$$y = x_1 \tag{3–22}$$

In a vector-matrix form, Equations (3–20) and (3–21) can be written as

$$\begin{bmatrix} \dot{x}_1 \\ \dot{x}_2 \end{bmatrix} = \begin{bmatrix} 0 & 1 \\ -\frac{k}{m} & -\frac{b}{m} \end{bmatrix} \begin{bmatrix} x_1 \\ x_2 \end{bmatrix} + \begin{bmatrix} 0 \\ \frac{1}{m} \end{bmatrix} u \tag{3–23}$$

The output equation, Equation (3–22), can be written as

$$y = [1 \quad 0]\begin{bmatrix} x_1 \\ x_2 \end{bmatrix} \tag{3–24}$$

Equation (3–23) is a state equation and Equation (3–24) is an output equation for the system. Equations (3–23) and (3–24) are in the standard form:

$$\dot{\mathbf{x}} = \mathbf{A}\mathbf{x} + \mathbf{B}u$$

$$y = \mathbf{C}\mathbf{x} + Du$$

where

$$\mathbf{A} = \begin{bmatrix} 0 & 1 \\ -\dfrac{k}{m} & -\dfrac{b}{m} \end{bmatrix}, \qquad \mathbf{B} = \begin{bmatrix} 0 \\ \dfrac{1}{m} \end{bmatrix}, \qquad \mathbf{C} = [1 \quad 0], \qquad D = 0$$

Figure 3–12 is a block diagram for the system. Notice that the outputs of the integrators are state variables.

Correlation between transfer functions and state-space equations. In what follows we shall show how to derive the transfer function of a single-input–single-output system from the state-space equations.

Let us consider the system whose transfer function is given by

$$\frac{Y(s)}{U(s)} = G(s) \tag{3–25}$$

This system may be represented in state space by the following equations:

$$\dot{\mathbf{x}} = \mathbf{A}\mathbf{x} + \mathbf{B}u \tag{3–26}$$

$$y = \mathbf{C}\mathbf{x} + Du \tag{3–27}$$

where $\mathbf{x}$ is the state vector, u is the input, and y is the output. The Laplace transforms of Equations (3–26) and (3–27) are given by

$$s\mathbf{X}(s) - \mathbf{x}(0) = \mathbf{A}\mathbf{X}(s) + \mathbf{B}U(s) \tag{3–28}$$

$$Y(s) = \mathbf{C}\mathbf{X}(s) + DU(s) \tag{3–29}$$

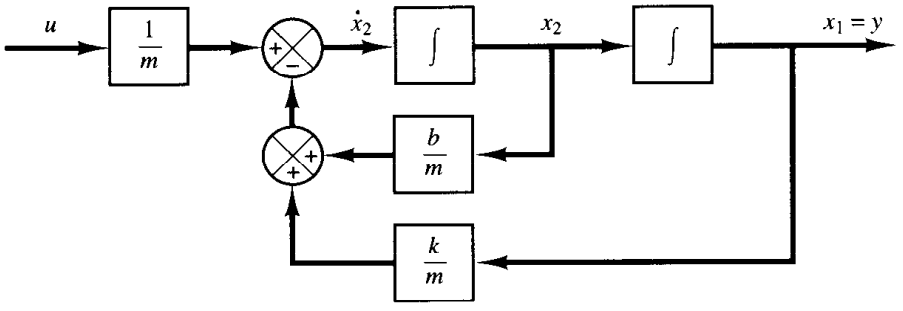

Figure 3–12
Block diagram of the mechanical system shown in Figure 3–11.

Since the transfer function was previously defined as the ratio of the Laplace transform of the output to the Laplace transform of the input when the initial conditions were zero, we assume that $\mathbf{x}(0)$ in Equation (3–28) is zero. Then we have

$$s\mathbf{X}(s) - \mathbf{A}\mathbf{X}(s) = \mathbf{B}U(s)$$

or

$$(s\mathbf{I} - \mathbf{A})\mathbf{X}(s) = \mathbf{B}U(s)$$

By premultiplying $(s\mathbf{I} - \mathbf{A})^{-1}$ to both sides of this last equation, we obtain

$$\mathbf{X}(s) = (s\mathbf{I} - \mathbf{A})^{-1}\mathbf{B}U(s) \tag{3–30}$$

By substituting Equation (3–30) into Equation (3–29), we get

$$Y(s) = [\mathbf{C}(s\mathbf{I} - \mathbf{A})^{-1}\mathbf{B} + D]U(s) \tag{3–31}$$

Upon comparing Equation (3–31) with Equation (3–25), we see that

$$G(s) = \mathbf{C}(s\mathbf{I} - \mathbf{A})^{-1}\mathbf{B} + D \tag{3–32}$$

This is the transfer-function expression in terms of $\mathbf{A}$, $\mathbf{B}$, $\mathbf{C}$, and D.

Note that the right-hand side of equation (3–32) involves $(s\mathbf{I} - \mathbf{A})^{-1}$. Hence $G(s)$ can be written as

$$G(s) = \frac{Q(s)}{|s\mathbf{I} - \mathbf{A}|}$$

where $Q(s)$ is a polynomial in s. Therefore, $|s\mathbf{I} - \mathbf{A}|$ is equal to the characteristic polynomial of $G(s)$. In other words, the eigenvalues of $\mathbf{A}$ are identical to the poles of $G(s)$.

EXAMPLE 3–3 Consider again the mechanical system shown in Figure 3–11. State-space equations for the system are given by Equations (3–23) and (3–24). We shall obtain the transfer function for the system from the state-space equations.

By substituting $\mathbf{A}$, $\mathbf{B}$, $\mathbf{C}$, and D into Equation (3–32), we obtain

$$\begin{aligned} G(s) &= \mathbf{C}(s\mathbf{I} - \mathbf{A})^{-1}\mathbf{B} + D \\ &= [1 \quad 0]\left\{\begin{bmatrix} s & 0 \\ 0 & s \end{bmatrix} - \begin{bmatrix} 0 & 1 \\ -\dfrac{k}{m} & -\dfrac{b}{m} \end{bmatrix}\right\}^{-1}\begin{bmatrix} 0 \\ \dfrac{1}{m} \end{bmatrix} + 0 \\ &= [1 \quad 0]\begin{bmatrix} s & -1 \\ \dfrac{k}{m} & s + \dfrac{b}{m} \end{bmatrix}^{-1}\begin{bmatrix} 0 \\ \dfrac{1}{m} \end{bmatrix} \end{aligned}$$

Since

$$\begin{bmatrix} s & -1 \\ \dfrac{k}{m} & s + \dfrac{b}{m} \end{bmatrix}^{-1} = \frac{1}{s^2 + \dfrac{b}{m}s + \dfrac{k}{m}}\begin{bmatrix} s + \dfrac{b}{m} & 1 \\ -\dfrac{k}{m} & s \end{bmatrix}$$

we have

$$G(s) = [1 \quad 0] \frac{1}{s^2 + \frac{b}{m}s + \frac{k}{m}} \begin{bmatrix} s + \frac{b}{m} & 1 \\ -\frac{k}{m} & s \end{bmatrix} \begin{bmatrix} 0 \\ \frac{1}{m} \end{bmatrix}$$

$$= \frac{1}{ms^2 + bs + k}$$

which is the transfer function of the system. The same transfer function can be obtained from Equation (3–19).

Transfer matrix. Next, consider a multiple-input–multiple-output system. Assume that there are r inputs $u_1, u_2, \ldots, u_r$ and m outputs $y_1, y_2, \ldots, y_m$. Define

$$\mathbf{y} = \begin{bmatrix} y_1 \\ y_2 \\ \cdot \\ \cdot \\ \cdot \\ y_m \end{bmatrix}, \qquad \mathbf{u} = \begin{bmatrix} u_1 \\ u_2 \\ \cdot \\ \cdot \\ \cdot \\ u_r \end{bmatrix}$$

The transfer matrix $\mathbf{G}(s)$ relates the output $\mathbf{Y}(s)$ to the input $\mathbf{U}(s)$, or

$$\mathbf{Y}(s) = \mathbf{G}(s)\mathbf{U}(s) \tag{3–33}$$

Since the input vector $\mathbf{u}$ is r dimensional and the output vector $\mathbf{y}$ is m dimensional, the transfer matrix is an $m \times r$ matrix.

3–5 STATE-SPACE REPRESENTATION OF DYNAMIC SYSTEMS

A dynamic system consisting of a finite number of lumped elements may be described by ordinary differential equations in which time is the independent variable. By use of vector-matrix notation, an nth-order differential equation may be expressed by a first-order vector-matrix differential equation. If n elements of the vector are a set of state variables, then the vector-matrix differential equation is a *state* equation. In this section we shall present methods for obtaining state-space representations of continuous-time systems.

State-space representation of nth-order systems of linear differential equations in which the forcing function does not involve derivative terms. Consider the following nth-order system:

$$\overset{(n)}{y} + a_1 \overset{(n-1)}{y} + \cdots + a_{n-1}\dot{y} + a_n y = u \tag{3–34}$$

Noting that the knowledge of $y(0), \dot{y}(0), \ldots \overset{(n-1)}{y}(0)$, together with the input $u(t)$ for $t \geq 0$, determines completely the future behavior of the system, we may take $y(t)$, $\dot{y}(t), \ldots, \overset{(n-1)}{y}(t)$ as a set of n state variables. (Mathematically, such a choice of state vari-

ables is quite convenient. Practically, however, because higher-order derivative terms are inaccurate, due to the noise effects inherent in any practical situations, such a choice of the state variables may not be desirable.)

Let us define

$$\begin{aligned} x_1 &= y \\ x_2 &= \dot{y} \\ &\vdots \\ x_n &= y^{(n-1)} \end{aligned}$$

Then Equation (3–34) can be written as

$$\begin{aligned} \dot{x}_1 &= x_2 \\ \dot{x}_2 &= x_3 \\ &\vdots \\ \dot{x}_{n-1} &= x_n \\ \dot{x}_n &= -a_n x_1 - \cdots - a_1 x_n + u \end{aligned}$$

or

$$\dot{\mathbf{x}} = \mathbf{A}\mathbf{x} + \mathbf{B}u \tag{3–35}$$

where

$$\mathbf{x} = \begin{bmatrix} x_1 \\ x_2 \\ \vdots \\ x_n \end{bmatrix}, \quad \mathbf{A} = \begin{bmatrix} 0 & 1 & 0 & \cdots & 0 \\ 0 & 0 & 1 & \cdots & 0 \\ \vdots & \vdots & \vdots & & \vdots \\ 0 & 0 & 0 & \cdots & 1 \\ -a_n & -a_{n-1} & -a_{n-2} & \cdots & -a_1 \end{bmatrix}, \quad \mathbf{B} = \begin{bmatrix} 0 \\ 0 \\ \vdots \\ 0 \\ 1 \end{bmatrix}$$

The output can be given by

$$y = [1 \quad 0 \quad \cdots \quad 0] \begin{bmatrix} x_1 \\ x_2 \\ \vdots \\ x_n \end{bmatrix}$$

or

$$y = \mathbf{C}\mathbf{x} \tag{3–36}$$

where

$$\mathbf{C} = [1 \quad 0 \quad \cdots \quad 0]$$

[Note that D in Equation (3–27) is zero.] The first-order differential equation, Equation (3–35), is the state equation, and the algebraic equation, Equation (3–36), is the output equation. A block diagram realization of the state equation and output equation given by Equations (3–35) and (3–36), respectively, is shown in Figure 3–13.

Note that the state-space representation for the transfer function system

$$\frac{Y(s)}{U(s)} = \frac{1}{s^n + a_1 s^{n-1} + \cdots + a_{n-1}s + a_n}$$

is given also by Equations (3–35) and (3–36).

State-space representation of *n*th-order systems of linear differential equations in which the forcing function involves derivative terms. If the differential equation of the system involves derivatives of the forcing function, such as

$$\overset{(n)}{y} + a_1 \overset{(n-1)}{y} + \cdots + a_{n-1}\dot{y} + a_n y = b_0 \overset{(n)}{u} + b_1 \overset{(n-1)}{u} + \ldots + b_{n-1}\dot{u} + b_n u \qquad (3\text{–}37)$$

then the set of n variables $y, \dot{y}, \ddot{y}, \ldots, \overset{(n-1)}{y}$ does not qualify as a set of state variables, and the straightforward method previously employed cannot be used. This is because n first-order differential equations

$$\begin{aligned}
\dot{x}_1 &= x_2 \\
\dot{x}_2 &= x_3 \\
&\vdots \\
\dot{x}_n &= -a_n x_1 - a_{n-1}x_2 - \cdots - a_1 x_n + b_0 \overset{(n)}{u} + b_1 \overset{(n-1)}{u} + \cdots + b_n u
\end{aligned}$$

where $x_1 = y$, may not yield a unique solution.

The main problem in defining the state variables for this case lies in the derivative terms on the right-hand side of the last of the preceding n equations. The state variables must be such that they will eliminate the derivatives of u in the state equation.

One way to obtain a state equation and output equation is to define the following n variables as a set of n state variables:

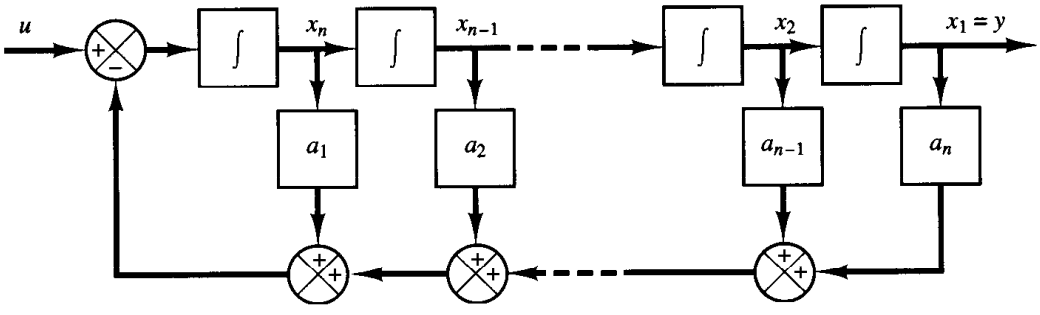

Figure 3–13
Block diagram realization of state equation and output equation given by Equations (3–35) and (3–36), respectively.

$$
\begin{aligned}
x_1 &= y - \beta_0 u \\
x_2 &= \dot{y} - \beta_0 \dot{u} - \beta_1 u = \dot{x}_1 - \beta_1 u \\
x_3 &= \ddot{y} - \beta_0 \ddot{u} - \beta_1 \dot{u} - \beta_2 u = \dot{x}_2 - \beta_2 u \\
&\vdots \\
x_n &= y^{(n-1)} - \beta_0 u^{(n-1)} - \beta_1 u^{(n-2)} - \cdots - \beta_{n-2}\dot{u} - \beta_{n-1} u = \dot{x}_{n-1} - \beta_{n-1} u
\end{aligned} \tag{3-38}
$$

where $\beta_0, \beta_1, \beta_2, \ldots, \beta_n$ are determined from

$$
\begin{aligned}
\beta_0 &= b_0 \\
\beta_1 &= b_1 - a_1\beta_0 \\
\beta_2 &= b_2 - a_1\beta_1 - a_2\beta_0 \\
\beta_3 &= b_3 - a_1\beta_2 - a_2\beta_1 - a_3\beta_0 \\
&\vdots \\
\beta_n &= b_n - a_1\beta_{n-1} - \cdots - a_{n-1}\beta_1 - a_n\beta_0
\end{aligned} \tag{3-39}
$$

With this choice of state variables the existence and uniqueness of the solution of the state equation is guaranteed. (Note that this is not the only choice of a set of state variables.) With the present choice of state variables, we obtain

$$
\begin{aligned}
\dot{x}_1 &= x_2 + \beta_1 u \\
\dot{x}_2 &= x_3 + \beta_2 u \\
&\vdots \\
\dot{x}_{n-1} &= x_n + \beta_{n-1} u \\
\dot{x}_n &= -a_n x_1 - a_{n-1} x_2 - \cdots - a_1 x_n + \beta_n u
\end{aligned} \tag{3-40}
$$

[To derive Equation (3–40), see Problem A-3-3.] In terms of vector-matrix equations, Equation (3–40) and the output equation can be written as

$$
\begin{bmatrix} \dot{x}_1 \\ \dot{x}_2 \\ \vdots \\ \dot{x}_{n-1} \\ \dot{x}_n \end{bmatrix} = \begin{bmatrix} 0 & 1 & 0 & \cdots & 0 \\ 0 & 0 & 1 & \cdots & 0 \\ \vdots & \vdots & \vdots & & \vdots \\ 0 & 0 & 0 & \cdots & 1 \\ -a_n & -a_{n-1} & -a_{n-2} & \cdots & -a_1 \end{bmatrix} \begin{bmatrix} x_1 \\ x_2 \\ \vdots \\ x_{n-1} \\ x_n \end{bmatrix} + \begin{bmatrix} \beta_1 \\ \beta_2 \\ \vdots \\ \beta_{n-1} \\ \beta_n \end{bmatrix} u
$$

$$
y = \begin{bmatrix} 1 & 0 & \cdots & 0 \end{bmatrix} \begin{bmatrix} x_1 \\ x_2 \\ \vdots \\ x_n \end{bmatrix} + \beta_0 u
$$

or

$$\dot{\mathbf{x}} = \mathbf{A}\mathbf{x} + \mathbf{B}u \tag{3–41}$$

$$y = \mathbf{C}\mathbf{x} + Du \tag{3–42}$$

where

$$\mathbf{x} = \begin{bmatrix} x_1 \\ x_2 \\ . \\ . \\ . \\ x_{n-1} \\ x_n \end{bmatrix}, \qquad \mathbf{A} = \begin{bmatrix} 0 & 1 & 0 & \cdots & 0 \\ 0 & 0 & 1 & \cdots & 0 \\ . & . & . & & . \\ . & . & . & & . \\ . & . & . & & . \\ 0 & 0 & 0 & \cdots & 1 \\ -a_n & -a_{n-1} & -a_{n-2} & \cdots & -a_1 \end{bmatrix}$$

$$\mathbf{B} = \begin{bmatrix} \beta_1 \\ \beta_2 \\ . \\ . \\ . \\ \beta_{n-1} \\ \beta_n \end{bmatrix}, \qquad \mathbf{C} = [1 \quad 0 \quad \cdots \quad 0], \qquad D = \beta_0 = b_0$$

The initial condition $\mathbf{x}(0)$ may be determined by use of Equation (3–38).

In this state-space representation, matrices **A** and **C** are exactly the same as those for the system of Equation (3–34). The derivatives on the right-hand side of Equation (3–37) affect only the elements of the **B** matrix.

Note that the state-space representation for the transfer function

$$\frac{Y(s)}{U(s)} = \frac{b_0 s^n + b_1 s^{n-1} + \cdots + b_{n-1}s + b_n}{s^n + a_1 s^{n-1} + \cdots + a_{n-1}s + a_n} \tag{3–43}$$

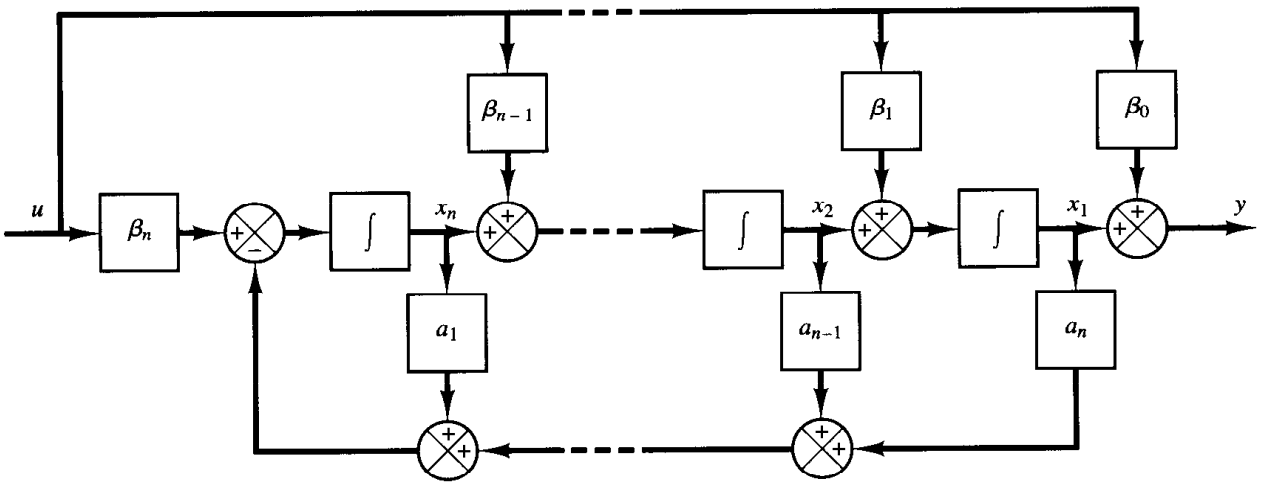

Figure 3–14
Block diagram realization of state equation and output equation given by Equations (3–41) and (3–42), respectively.

is given also by Equations (3–41) and (3–42). Figure 3–14 is a block diagram realization of the state equation and output equation given by Equations (3–41) and (3–42), respectively.

There are many ways to obtain state-space representations of systems. Some of them are presented in Problems A-3-4 through A-3-7. Methods for obtaining canonical representations of systems in state space (such as controllable canonical form, observable canonical form, diagonal canonical form, and Jordan canonical form) are presented in Chapter 11.

3–6 MECHANICAL SYSTEMS

In this section we shall discuss mathematical modeling of mechanical systems. The fundamental law governing mechanical systems is Newton's second law. It can be applied to any mechanical system. In this section we shall derive mathematical models of two mechanical systems. (Mathematical models of additional mechanical systems will be derived and analyzed throughout the remaining chapters.) Before we discuss mechanical systems, let us review definitions of mass, force, and unit systems.

Mass. The *mass* of a body is the quantity of matter in it, which is assumed to be constant. Physically, mass is the property of a body that gives it inertia, that is, resistance to starting and stopping. A body is attracted by Earth, and the magnitude of the force that Earth exerts on it is called its *weight.*

In practical situations, we know the weight w of a body but not the mass m. We calculate mass m from

$$m = \frac{w}{g}$$

where g is the gravitational acceleration constant. The value of g varies slightly from point to point on Earth's surface. As a result, the weight of a body varies slightly at different points on Earth's surface, but its mass remains constant. For engineering purposes, g is taken as

$$g = 9.81 \text{ m/s}^2 = 981 \text{ cm/s}^2 = 32.2 \text{ ft/s}^2 = 386 \text{ in./s}^2$$

Far out in space, a body becomes weightless. Yet its mass remains constant and so the body possesses inertia.

The units of mass are kg, g, lb, $\text{kg}_f\text{-s}^2/\text{m}$, and slug, as shown in Table 3–2. If mass is expressed in units of kilogram (or pound), we call it kilogram mass (or pound mass) to distinguish it from the unit of force, which is termed kilogram force (or pound force). In this book kg is used to denote a kilogram mass and kg_f a kilogram force. Similarly, lb denotes a pound mass and lb_f a pound force.

A slug is a unit of mass such that, when acted on by 1-pound force, a 1-slug mass accelerates at 1 ft/s^2 (slug = $\text{lb}_f\text{-s}^2/\text{ft}$). In other words, if a mass of 1 slug is acted on by 32.2 pounds force, it accelerates at 32.2 ft/s^2 ($= g$). Hence the mass of a body weighing 32.2 lb_f at the earth's surface is 1 slug or

$$m = \frac{w}{g} = \frac{32.2 \text{ lb}_f}{32.2 \text{ ft/s}^2} = 1 \text{ slug}$$

Table 3–2 Systems of Units

Quantity \ Systems of units	Absolute systems			Gravitational systems	
	Metric			Metric engineering	British engineering
	SI	mks	cgs		
Length	m	m	cm	m	ft
Mass	kg	kg	g	$\frac{kg_f\text{-}s^2}{m}$	$\text{slug} = \frac{lb_f\text{-}s^2}{ft}$
Time	s	s	s	s	s
Force	$N = \frac{kg\text{-}m}{s^2}$	$N = \frac{kg\text{-}m}{s^2}$	$dyn = \frac{g\text{-}cm}{s^2}$	kg_f	lb_f
Energy	J = N-m	J = N-m	erg = dyn-cm	kg_f-m	ft-lb_f or Btu
Power	$W = \frac{N\text{-}m}{s}$	$W = \frac{N\text{-}m}{s}$	$\frac{dyn\text{-}cm}{s}$	$\frac{kg_f\text{-}m}{s}$	$\frac{ft\text{-}lb_f}{s}$ or hp

Force. *Force* can be defined as the cause that tends to produce a change in motion of a body on which it acts. To move a body, force must be applied to it. Two types of forces are capable of acting on a body: *contact* forces and *field* forces. Contact forces are those that come into direct contact with a body, whereas field forces, such as gravitational force and magnetic force, act on a body but do not come into contact with it.

The units of force are newton (N), dyne (dyn), kg_f, and lb_f. In SI units and the mks system (a metric absolute system) of units the force unit is the newton. The newton is the force that will give a 1-kilogram mass an acceleration of 1 m/s^2 or

$$1 \text{ N} = 1 \text{ kg-m/s}^2$$

This means that 9.81 newtons will give a kilogram mass an acceleration of 9.81 m/s^2. Since the gravitational acceleration is $g = 9.81$ m/s^2 (as stated earlier, for engineering calculations, the value of g may be taken as 9.81 m/s^2 or 32.2 ft/s^2), a mass of 1 kilogram will produce a force on its support of 9.81 newtons.

The force unit in the cgs system (a metric absolute system) is the dyne, which will give a gram mass an acceleration of 1 cm/s^2 or

$$1 \text{ dyn} = 1 \text{ g-cm/s}^2$$

The force unit in the metric engineering (gravitational) system is kg_f, which is a primary dimension in the system. Similarly, in the British engineering system the force unit is lb_f. It is also a primary dimension in this system of units.

Comments. SI units for force, mass, and length are the newton (N), kilogram mass (kg), and meter (m). The mks units for force, mass, and length are the same as the SI units. Similarly, the cgs units for force, mass, and length are the dyne (dyn), gram (g), and centimeter (cm), and those for BES units are pound force (lb_f), slug, and foot (ft). Each of the unit systems is consistent in that the unit of force accelerates the unit of mass 1 unit of length per second per second.

In the systems of units shown in Table 3–2, "s" is used for the second. In engineering papers and books, however, "sec" is commonly used. Therefore, in this book we use "sec", rather than "s", for the second.

Mechanical system. Consider the spring–mass–dashpot system mounted on a massless cart as shown in Figure 3–15. A dashpot is a device that provides viscous friction, or damping. It consists of a piston and oil-filled cylinder. Any relative motion between the piston rod and the cylinder is resisted by the oil because the oil must flow around the piston (or through orifices provided in the piston) from one side of the piston to the other. The dashpot essentially absorbs energy. This absorbed energy is dissipated as heat, and the dashpot does not store any kinetic or potential energy. The dashpot is also called a *damper*.

Let us obtain a mathematical model of this spring–mass–dashpot system mounted on a cart by assuming that the cart is standing still for $t < 0$. In this system, $u(t)$ is the displacement of the cart and is the input to the system. At $t = 0$, the cart is moved at a constant speed, or $\dot{u} =$ constant. The displacement $y(t)$ of the mass is the output. (The displacement is relative to the ground.) In this system, m denotes the mass, b denotes the viscous friction coefficient, and k denotes the spring constant. We assume that the friction force of the dashpot is proportional to $\dot{y} - \dot{u}$ and that the spring is a linear spring; that is, the spring force is proportional to $y - u$.

For translational systems, Newton's second law states that

$$ma = \sum F$$

where m is a mass, a is the acceleration of the mass, and ΣF is the sum of the forces acting on the mass. Applying Newton's second law to the present system and noting that the cart is massless, we obtain

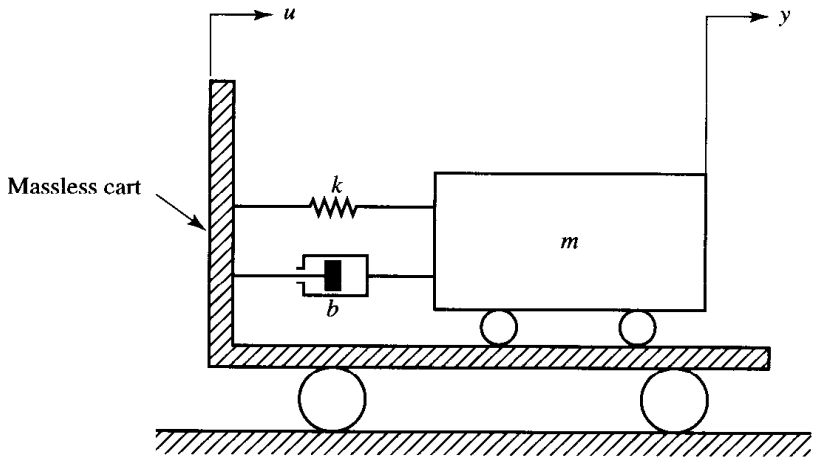

Figure 3–15
Spring–mass–dashpot system mounted on a cart.

$$m\frac{d^2y}{dt^2} = -b\left(\frac{dy}{dt} - \frac{du}{dt}\right) - k(y - u)$$

or

$$m\frac{d^2y}{dt^2} + b\frac{dy}{dt} + ky = b\frac{du}{dt} + ku \tag{3-44}$$

Equation (3–44) gives a mathematical model of the system considered.

A transfer function model is another way of representing a mathematical model of a linear, time-invariant system. For the present mechanical system, the transfer function model can be obtained as follows: Taking the Laplace transform of each term of Equation (3–44) gives

$$\mathcal{L}\left[m\frac{d^2y}{dt^2}\right] = m[s^2Y(s) - sy(0) - \dot{y}(0)]$$

$$\mathcal{L}\left[b\frac{dy}{dt}\right] = b[sY(s) - y(0)]$$

$$\mathcal{L}[ky] = kY(s)$$

$$\mathcal{L}\left[b\frac{du}{dt}\right] = b[sU(s) - u(0)]$$

$$\mathcal{L}[ku] = kU(s)$$

If we set the initial conditions equal to zero, or set $y(0) = 0, \dot{y}(0) = 0$, and $u(0) = 0$, the Laplace transform of Equation (3–44) can be written as

$$(ms^2 + bs + k)Y(s) = (bs + k)U(s)$$

Taking the ratio of $Y(s)$ to $U(s)$, we find the transfer function of the system to be

$$\text{Transfer function} = G(s) = \frac{Y(s)}{U(s)} = \frac{bs + k}{ms^2 + bs + k}$$

Such a transfer-function representation of a mathematical model is used very frequently in control engineering. It should be noted, however, that transfer-function models apply only to linear, time-invariant systems, since the transfer functions are defined only for such systems.

Next we shall obtain a state-space model of this system. We shall first compare the differential equation for this system

$$\ddot{y} + \frac{b}{m}\dot{y} + \frac{k}{m}y = \frac{b}{m}\dot{u} + \frac{k}{m}u$$

with the standard form

$$\ddot{y} + a_1\dot{y} + a_2y = b_0\ddot{u} + b_1\dot{u} + b_2u$$

and identify a_1, a_2, b_0, b_1, and b_2 as follows:

$$a_1 = \frac{b}{m}, \qquad a_2 = \frac{k}{m}, \qquad b_0 = 0, \qquad b_1 = \frac{b}{m}, \qquad b_2 = \frac{k}{m}$$

Referring to Equation (3–39), we have

$$\beta_0 = b_0 = 0$$

$$\beta_1 = b_1 - a_1\beta_0 = \frac{b}{m}$$

$$\beta_2 = b_2 - a_1\beta_1 - a_2\beta_0 = \frac{k}{m} - \left(\frac{b}{m}\right)^2$$

Then, referring to Equation (3–38), define

$$x_1 = y - \beta_0 u = y$$

$$x_2 = \dot{x}_1 - \beta_1 u = \dot{x}_1 - \frac{b}{m}u$$

From Equation (3–40) we have

$$\dot{x}_1 = x_2 + \beta_1 u = x_2 + \frac{b}{m}u$$

$$\dot{x}_2 = -a_2 x_1 - a_1 x_2 + \beta_2 u = -\frac{k}{m}x_1 - \frac{b}{m}x_2 + \left[\frac{k}{m} - \left(\frac{b}{m}\right)^2\right]u$$

and the output equation becomes

$$y = x_1$$

or

$$\begin{bmatrix} \dot{x}_1 \\ \dot{x}_2 \end{bmatrix} = \begin{bmatrix} 0 & 1 \\ -\frac{k}{m} & -\frac{b}{m} \end{bmatrix} \begin{bmatrix} x_1 \\ x_2 \end{bmatrix} + \begin{bmatrix} \frac{b}{m} \\ \frac{k}{m} - \left(\frac{b}{m}\right)^2 \end{bmatrix} u \tag{3–45}$$

and

$$y = \begin{bmatrix} 1 & 0 \end{bmatrix} \begin{bmatrix} x_1 \\ x_2 \end{bmatrix} \tag{3–46}$$

Equations (3–45) and (3–46) give a state-space representation of the system. (Note that this is not the only state-space representation. There are infinitely many state-space representations for the system.)

EXAMPLE 3–4 An inverted pendulum mounted on a motor-driven cart is shown in Figure 3–16(a). This is a model of the attitude control of a space booster on takeoff. (The objective of the attitude control problem is to keep the space booster in a vertical position.) The inverted pendulum is unstable in that it may fall over any time in any direction unless a suitable control force is applied. Here we consider only a two-dimensional problem in which the pendulum moves only in the plane of the page. The control force u is applied to the cart. Assume that the center of gravity of the pendulum rod is at its geometric center. Obtain a mathematical model for the system. Assume that the mass m of the pendulum rod is 0.1 kg, the mass M of the cart is 2 kg, and the length $2l$ of the pendulum rod is 1 m, or

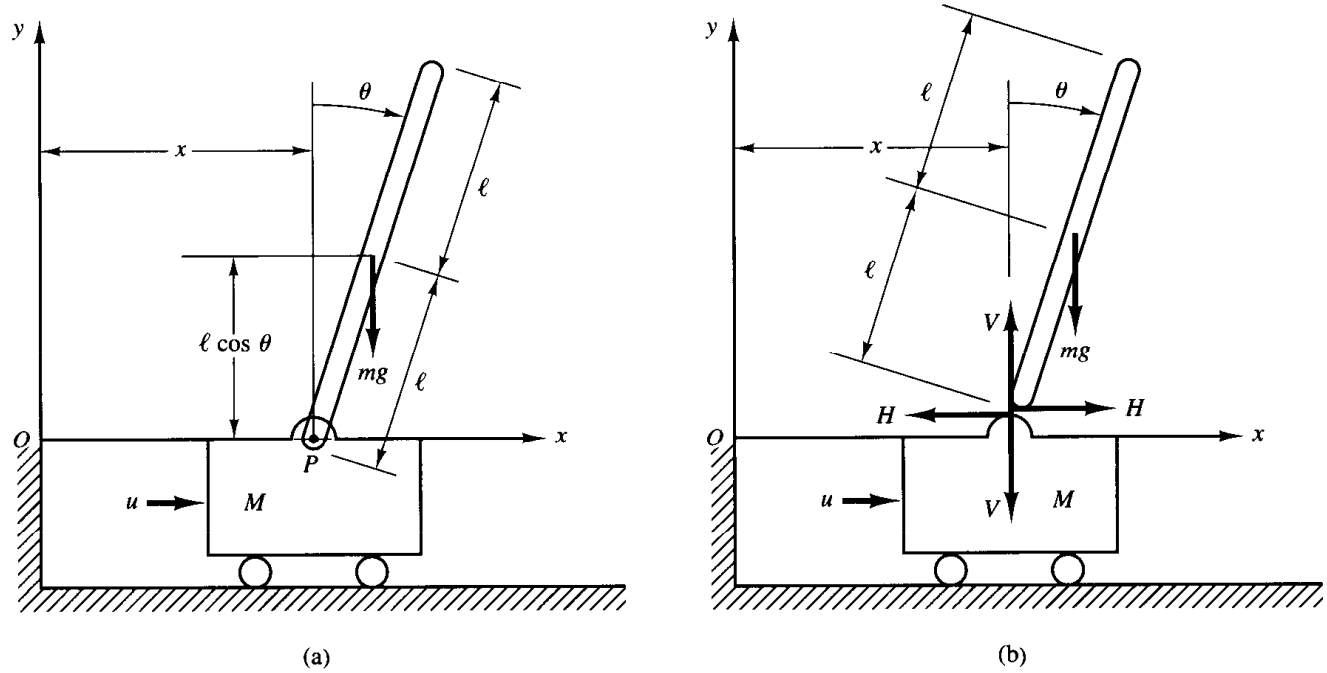

Figure 3–16
(a) Inverted pendulum system; (b) free-body diagram.

$$m = 0.1 \text{ kg}, \qquad M = 2 \text{ kg}, \qquad 2l = 1 \text{ m}$$

Define the angle of the rod from the vertical line as θ. Define also the (x, y) coordinates of the center of gravity of the pendulum rod as (x_G, y_G). Then

$$x_G = x + l \sin \theta$$

$$y_G = l \cos \theta$$

To derive the equations of motion for the system, consider the free-body diagram shown in Figure 3–16(b). The rotational motion of the pendulum rod about its center of gravity can be described by

$$I\ddot{\theta} = Vl \sin \theta - Hl \cos \theta \tag{3–47}$$

where I is the moment of inertia of the rod about its center of gravity.

The horizontal motion of center of gravity of pendulum rod is given by

$$m \frac{d^2}{dt^2}(x + l \sin \theta) = H \tag{3–48}$$

The vertical motion of center of gravity of pendulum rod is

$$m \frac{d^2}{dt^2}(l \cos \theta) = V - mg \tag{3–49}$$

The horizontal motion of cart is described by

$$M \frac{d^2x}{dt^2} = u - H \tag{3–50}$$

Equations (3–47) through (3–50) describe the motion of the inverted-pendulum-on-the-cart system. Because these equations involve $\sin\theta$ and $\cos\theta$, they are nonlinear equations.

If we assume angle θ to be small, Equations (3–47) through (3–50) may be linearized as follows:

$$I\ddot{\theta} = Vl\theta - Hl \tag{3–51}$$

$$m(\ddot{x} + l\ddot{\theta}) = H \tag{3–52}$$

$$0 = V - mg \tag{3–53}$$

$$M\ddot{x} = u - H \tag{3–54}$$

From Equations (3–52) and (3–54), we obtain

$$(M + m)\ddot{x} + ml\ddot{\theta} = u \tag{3–55}$$

From Equations (3–51) and (3–53), we have

$$\begin{aligned} I\ddot{\theta} &= mgl\theta - Hl \\ &= mgl\theta - l(m\ddot{x} + ml\ddot{\theta}) \end{aligned}$$

or

$$(I + ml^2)\ddot{\theta} + ml\ddot{x} = mgl\theta \tag{3–56}$$

Equations (3–55) and (3–56) describe the motion of the inverted-pendulum-on-the-cart system. They constitute a mathematical model of the system. (Later in Chapters 12 and 13, we design controllers to keep the pendulum upright in the presence of disturbances.)

3–7 ELECTRICAL SYSTEMS

In this section we shall deal with electrical circuits involving resistors, capacitors, and inductors.

Basic laws governing electrical circuits are Kirchhoff's current law and voltage law. Kirchhoff's current law (node law) states that the algebraic sum of all currents entering and leaving a node is zero. (This law can also be stated as follows: The sum of currents entering a node is equal to the sum of currents leaving the same node.) Kirchhoff's voltage law (loop law) states that at any given instant the algebraic sum of the voltages around any loop in an electrical circuit is zero. (This law can also be stated as follows: The sum of the voltage drops is equal to the sum of the voltage rises around a loop.) A mathematical model of an electrical circuit can be obtained by applying one or both of Kirchhoff's laws to it.

This section deals with simple electrical circuits. Mathematical modeling of operational amplifier systems is presented in Chapter 5.

***LRC* circuit.** Consider the electrical circuit shown in Figure 3–17. The circuit consists of an inductance L (henry), a resistance R (ohm), and a capacitance C (farad). Applying Kirchhoff's voltage law to the system, we obtain the following equations:

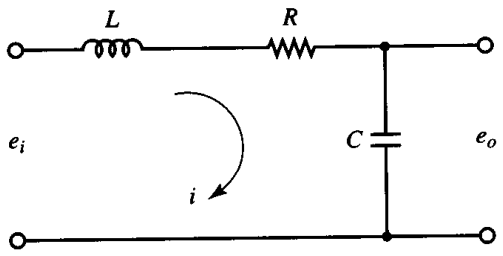

Figure 3–17
Electrical circuit.

$$L\frac{di}{dt} + Ri + \frac{1}{C}\int i\,dt = e_i \tag{3–57}$$

$$\frac{1}{C}\int i\,dt = e_o \tag{3–58}$$

Equations (3–57) and (3–58) give a mathematical model of the circuit.

A transfer function model of the circuit can also be obtained as follows: Taking the Laplace transforms of Equations (3–57) and (3–58), assuming zero initial conditions, we obtain

$$LsI(s) + RI(s) + \frac{1}{C}\frac{1}{s}I(s) = E_i(s)$$

$$\frac{1}{C}\frac{1}{s}I(s) = E_o(s)$$

If e_i is assumed to be the input and e_o the output, then the transfer function of this system is found to be

$$\frac{E_o(s)}{E_i(s)} = \frac{1}{LCs^2 + RCs + 1} \tag{3–59}$$

Complex impedances. In driving transfer functions for electrical circuits, we frequently find it convenient to write the Laplace-transformed equations directly, without writing the differential equations. Consider the system shown in Figure 3–18(a). In this system, Z_1 and Z_2 represent complex impedances. The complex impedance $Z(s)$ of a two-terminal circuit is the ratio of $E(s)$, the Laplace transform of the voltage across the terminals, to $I(s)$, the Laplace transform of the current through the element, under the assumption that the initial conditions are zero, so that $Z(s) = E(s)/I(s)$. If the two-terminal elements is a resistance R, capacitance C, or inductance L, then the complex impedance is given by R, $1/Cs$, or Ls, respectively. If complex impedances are connected in series, the total impedance is the sum of the individual complex impedances.

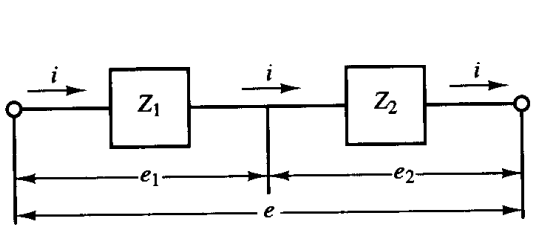

(a)

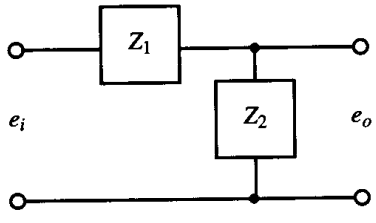

(b)

Figure 3–18
Electrical circuits.

Remember that the impedance approach is valid only if the initial conditions involved are all zeros. Since the transfer function requires zero initial conditions, the impedance approach can be applied to obtain the transfer function of the electrical circuit. This approach greatly simplifies the derivation of transfer functions of electrical circuits.

Consider the circuit shown in Figure 3–18(b). Assume that the voltages e_i and e_o are the input and output of the circuit, respectively. Then the transfer function of this circuit is

$$\frac{E_o(s)}{E_i(s)} = \frac{Z_2(s)}{Z_1(s) + Z_2(s)}$$

For the system shown in Figure 3–17,

$$Z_1 = Ls + R, \qquad Z_2 = \frac{1}{Cs}$$

Hence the transfer function $E_o(s)/E_i(s)$ can be found as follows:

$$\frac{E_o(s)}{E_i(s)} = \frac{\dfrac{1}{Cs}}{Ls + R + \dfrac{1}{Cs}} = \frac{1}{LCs^2 + RCs + 1}$$

which is, of course, identical to Equation (3–59).

State-space representation. A state-space model of the system shown in Figure 3–17 may be obtained as follows: First, note that the differential equation for the system can be obtained from Equation (3–59) as

$$\ddot{e}_o + \frac{R}{L}\dot{e}_o + \frac{1}{LC}e_o = \frac{1}{LC}e_i$$

Then by defining state variables by

$$x_1 = e_o$$
$$x_2 = \dot{e}_o$$

and the input and output variables by

$$u = e_i$$
$$y = e_o = x_1$$

we obtain

$$\begin{bmatrix} \dot{x}_1 \\ \dot{x}_2 \end{bmatrix} = \begin{bmatrix} 0 & 1 \\ -\dfrac{1}{LC} & -\dfrac{R}{L} \end{bmatrix} \begin{bmatrix} x_1 \\ x_2 \end{bmatrix} + \begin{bmatrix} 0 \\ \dfrac{1}{LC} \end{bmatrix} u$$

and

$$y = [1 \quad 0] \begin{bmatrix} x_1 \\ x_2 \end{bmatrix}$$

These two equations give a mathematical model of the system in state space.

Transfer functions of cascaded elements. Many feedback systems have components that load each other. Consider the system shown in Figure 3–19. Assume that e_i is the input and e_o is the output. In this system the second stage of the circuit (R_2C_2 portion) produces a loading effect on the first stage (R_1C_1 portion). The equations for this system are

$$\frac{1}{C_1}\int (i_1 - i_2)\,dt + R_1 i_1 = e_i \tag{3–60}$$

and

$$\frac{1}{C_1}\int (i_2 - i_1)\,dt + R_2 i_2 + \frac{1}{C_2}\int i_2\,dt = 0 \tag{3–61}$$

$$\frac{1}{C_2}\int i_2\,dt = e_o \tag{3–62}$$

Taking the Laplace transforms of Equations (3–60) through (3–62), respectively, assuming zero initial conditions, we obtain

$$\frac{1}{C_1 s}[I_1(s) - I_2(s)] + R_1 I_1(s) = E_i(s) \tag{3–63}$$

$$\frac{1}{C_1 s}[I_2(s) - I_1(s)] + R_2 I_2(s) + \frac{1}{C_2 s} I_2(s) = 0 \tag{3–64}$$

$$\frac{1}{C_2 s} I_2(s) = E_o(s) \tag{3–65}$$

Eliminating $I_1(s)$ from Equations (3–63) and (3–64) and writing $E_i(s)$ in terms of $I_2(s)$, we find the transfer function between $E_o(s)$ and $E_i(s)$ to be

$$\frac{E_o(s)}{E_i(s)} = \frac{1}{(R_1C_1 s + 1)(R_2C_2 s + 1) + R_1C_2 s}$$

$$= \frac{1}{R_1C_1R_2C_2 s^2 + (R_1C_1 + R_2C_2 + R_1C_2)s + 1} \tag{3–66}$$

The term $R_1C_2 s$ in the denominator of the transfer function represents the interaction of two simple RC circuits. Since $(R_1C_1 + R_2C_2 + R_1C_2)^2 > 4R_1C_1R_2C_2$, the two roots of the denominator of Equation (3–66) are real.

The present analysis shows that, if two RC circuits are connected in cascade so that the output from the first circuit is the input to the second, the overall transfer function

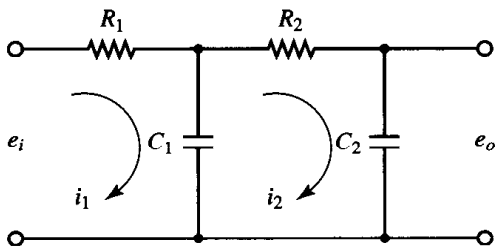

Figure 3–19
Electrical system.

is not the product of $1/(R_1C_1s + 1)$ and $1/(R_2C_2s + 1)$. The reason for this is that, when we derive the transfer function for an isolated circuit, we implicitly assume that the output is unloaded. In other words, the load impedance is assumed to be infinite, which means that no power is being withdrawn at the output. When the second circuit is connected to the output of the first, however, a certain amount of power is withdrawn, and thus the assumption of no loading is violated. Therefore, if the transfer function of this system is obtained under the assumption of no loading, then it is not valid. The degree of the loading effect determines the amount of modification of the transfer function.

Transfer functions of nonloading cascaded elements. The transfer function of a system consisting of two nonloading cascaded elements can be obtained by eliminating the intermediate input and output. For example, consider the system shown in Figure 3–20(a). The transfer functions of the elements are

$$G_1(s) = \frac{X_2(s)}{X_1(s)} \quad \text{and} \quad G_2(s) = \frac{X_3(s)}{X_2(s)}$$

If the input impedance of the second element is infinite, the output of the first element is not affected by connecting it to the second element. Then the transfer function of the whole system becomes

$$G(s) = \frac{X_3(s)}{X_1(s)} = \frac{X_2(s)X_3(s)}{X_1(s)X_2(s)} = G_1(s)G_2(s)$$

The transfer function of the whole system is thus the product of the transfer functions of the individual elements. This is shown in Figure 3–20(b).

As an example, consider the system shown in Figure 3–21. The insertion of an isolating amplifier between the circuits to obtain nonloading characteristics is frequently used in combining circuits. Since amplifiers have very high input impedances, an isolation amplifier inserted between the two circuits justifies the nonloading assumption.

The two simple RC circuits, isolated by an amplifier as shown in Figure 3–21, have negligible loading effects, and the transfer function of the entire circuit equals the product of the individual transfer functions. Thus, in this case,

$$\frac{E_o(s)}{E_i(s)} = \left(\frac{1}{R_1C_1s + 1}\right)(K)\left(\frac{1}{R_2C_2s + 1}\right)$$
$$= \frac{K}{(R_1C_1s + 1)(R_2C_2s + 1)}$$

Figure 3–20
(a) System consisting of two nonloading cascaded elements; (b) an equivalent system.

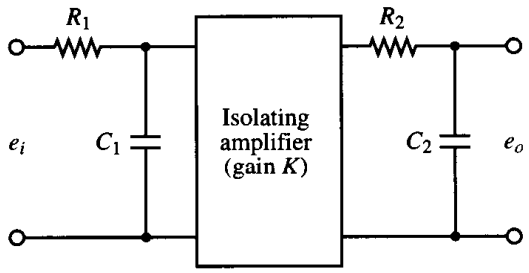

Figure 3–21
Electrical system.

3–8 LIQUID-LEVEL SYSTEMS

In analyzing systems involving fluid flow, we find it necessary to divide flow regimes into laminar flow and turbulent flow, according to the magnitude of the Reynolds number. If the Reynolds number is greater than about 3000 to 4000, then the flow is turbulent. The flow is laminar if the Reynolds number is less than about 2000. In the laminar case, fluid flow occurs in streamlines with no turbulence. Systems involving turbulent flow often have to be represented by nonlinear differential equations, while systems involving laminar flow may be represented by linear differential equations. (Industrial processes often involve flow of liquids through connecting pipes and tanks. The flow in such processes is often turbulent and not laminar.)

In this section we shall derive mathematical models of liquid-level systems. By introducing the concept of resistance and capacitance for such liquid-level systems, it is possible to describe the dynamic characteristics of such systems in simple forms.

Resistance and capacitance of liquid-level systems. Consider the flow through a short pipe connecting two tanks. The resistance R for liquid flow in such a pipe or restriction is defined as the change in the level difference (the difference of the liquid levels of the two tanks) necessary to cause a unit change in flow rate; that is,

$$R = \frac{\text{change in level difference, m}}{\text{change in flow rate, m}^3/\text{sec}}$$

Since the relationship between the flow rate and level difference differs for the laminar flow and turbulent flow, we shall consider both cases in the following.

Consider the liquid-level system shown in Figure 3–22(a). In this system the liquid spouts through the load valve in the side of the tank. If the flow through this restriction is laminar, the relationship between the steady-state flow rate and steady-state head at the level of the restriction is given by

$$Q = KH$$

where Q = steady-state liquid flow rate, m^3/sec
K = coefficient, m^2/sec
H = steady-state head, m

Notice that the law governing laminar flow is analogous to Coulomb's law, which states that the current is directly proportional to the potential difference.

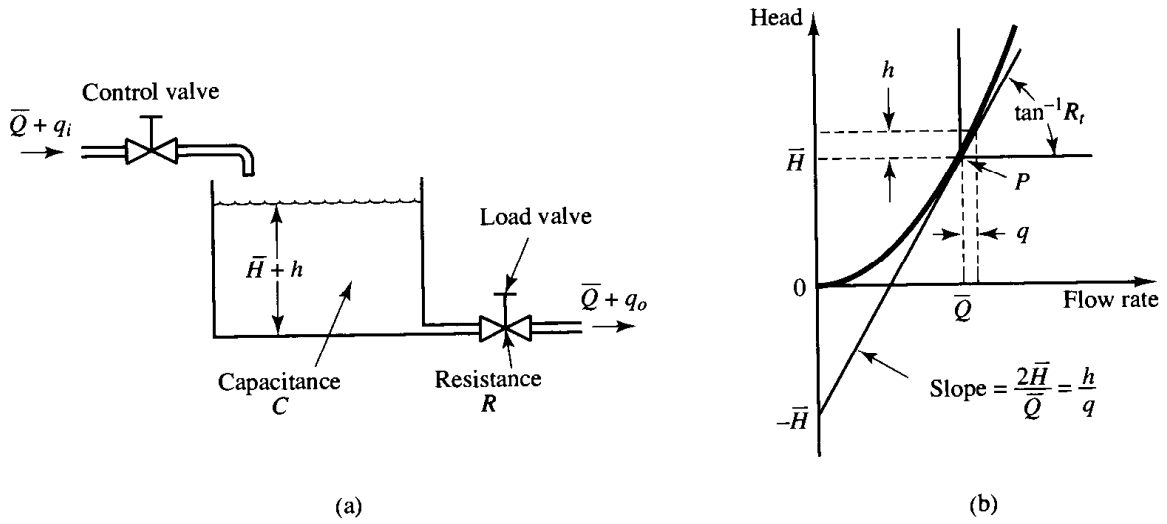

Figure 3–22
(a) Liquid-level system; (b) head versus flow rate curve.

For laminar flow, the resistance R_l is obtained as

$$R_l = \frac{dH}{dQ} = \frac{H}{Q}$$

The laminar-flow resistance is constant and is analogous to the electrical resistance.

If the flow through the restriction is turbulent, the steady-state flow rate is given by

$$Q = K\sqrt{H} \tag{3–67}$$

where Q = steady-state liquid flow rate, m^3/sec
K = coefficient, $m^{2.5}/sec$
H = steady-state head, m

The resistance R_t for turbulent flow is obtained from

$$R_t = \frac{dH}{dQ}$$

Since from Equation (3–67) we obtain

$$dQ = \frac{K}{2\sqrt{H}}\,dH$$

we have

$$\frac{dH}{dQ} = \frac{2\sqrt{H}}{K} = \frac{2\sqrt{H}\sqrt{H}}{Q} = \frac{2H}{Q}$$

Thus,

$$R_t = \frac{2H}{Q} \tag{3–68}$$

The value of the turbulent-flow resistance R_t depends on the flow rate and the head. The value of R_t, however, may be considered constant if the changes in head and flow rate are small.

By use of the turbulent-flow resistance, the relationship between Q and H can be given by

$$Q = \frac{2H}{R_t}$$

Such linearization is valid, provided that changes in the head and flow rate from their respective steady-state values are small.

In many practical cases, the value of the coefficient K in Equation (3–67), which depends on the flow coefficient and the area of restriction, is not known. Then the resistance may be determined by plotting the head versus flow rate curve based on experimental data and measuring the slope of the curve at the operating condition. An example of such a plot is shown in Figure 3–22(b). In the figure, point P is the steady-state operating point. The tangent line to the curve at point P intersects the ordinate at point $(-\bar{H}, 0)$. Thus, the slope of this tangent line is $2\bar{H}/\bar{Q}$. Since the resistance R_t at the operating point P is given by $2\bar{H}/\bar{Q}$, the resistance R_t is the slope of the curve at the operating point.

Consider the operating condition in the neighborhood of point P. Define a small deviation of the head from the steady-state value as h and the corresponding small change of the flow rate as q. Then the slope of the curve at point P can be given by

$$\text{Slope of curve at point } P = \frac{h}{q} = \frac{2\bar{H}}{\bar{Q}} = R_t$$

The linear approximation is based on the fact that the actual curve does not differ much from its tangent line if the operating condition does not vary too much.

The capacitance C of a tank is defined to be the change in quantity of stored liquid necessary to cause a unit change in the potential (head). (The potential is the quantity that indicates the energy level of the system.)

$$C = \frac{\text{change in liquid stored, m}^3}{\text{change in head, m}}$$

It should be noted that the capacity (m^3) and the capacitance (m^2) are different. The capacitance of the tank is equal to its cross-sectional area. If this is constant, the capacitance is constant for any head.

Liquid-level systems. Consider the system shown in Figure 3–22(a). The variables are defined as follows:

$\bar{Q}$ = steady-state flow rate (before any change has occurred), m^3/sec

q_i = small deviation of inflow rate from its steady-state value, m^3/sec

q_o = small deviation of outflow rate from its steady-state value, m^3/sec

$\bar{H}$ = steady-state head (before any change has occurred), m

h = small deviation of head from its steady-state value, m

As stated previously, a system can be considered linear if the flow is laminar. Even if the flow is turbulent, the system can be linearized if changes in the variables are kept small. Based on the assumption that the system is either linear or linearized, the differential

equation of this system can be obtained as follows: Since the inflow minus outflow during the small time interval dt is equal to the additional amount stored in the tank, we see that

$$C\,dh = (q_i - q_o)\,dt$$

From the definition of resistance, the relationship between q_o and h is given by

$$q_o = \frac{h}{R}$$

The differential equation for this system for a constant value of R becomes

$$RC\frac{dh}{dt} + h = Rq_i \tag{3–69}$$

Note that RC is the time constant of the system. Taking the Laplace transforms of both sides of Equation (3–69), assuming the zero initial condition, we obtain

$$(RCs + 1)H(s) = RQ_i(s)$$

where

$$H(s) = \mathcal{L}[h] \qquad \text{and} \qquad Q_i(s) = \mathcal{L}[q_i]$$

If q_i is considered the input and h the output, the transfer function of the system is

$$\frac{H(s)}{Q_i(s)} = \frac{R}{RCs + 1}$$

If, however, q_o is taken as the output, the input being the same, then the transfer function is

$$\frac{Q_o(s)}{Q_i(s)} = \frac{1}{RCs + 1}$$

where we have used the relationship

$$Q_o(s) = \frac{1}{R}H(s)$$

Liquid-level systems with interaction. Consider the system shown in Figure 3–23. In this system, the two tanks interact. Thus the transfer function of the system is not the product of two first-order transfer functions.

In the following, we shall assume only small variations of the variables from the steady-state values. Using the symbols as defined in Figure 3–23, we can obtain the following equations for this system:

$$\frac{h_1 - h_2}{R_1} = q_1 \tag{3–70}$$

$$C_1\frac{dh_1}{dt} = q - q_1 \tag{3–71}$$

$$\frac{h_2}{R_2} = q_2 \tag{3–72}$$

$$C_2\frac{dh_2}{dt} = q_1 - q_2 \tag{3–73}$$

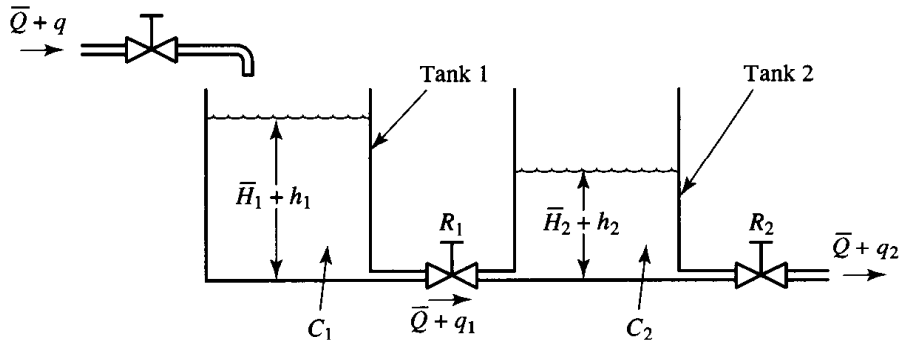

Figure 3–23
Liquid-level system with interaction.

$\bar{Q}$: Steady-state flow rate
$\bar{H}_1$: Steady-state liquid level of tank 1
$\bar{H}_2$: Steady-state liquid level of tank 2

If q is considered the input and q_2 the output, the transfer function of the system is

$$\frac{Q_2(s)}{Q(s)} = \frac{1}{R_1C_1R_2C_2s^2 + (R_1C_1 + R_2C_2 + R_2C_1)s + 1} \tag{3–74}$$

It is instructive to obtain Equation (3–74), the transfer function of the interacted system, by block diagram reduction. From Equations (3–70) through (3–73), we obtain the elements of the block diagram, as shown in Figure 3–24(a). By connecting signals properly, we can construct a block diagram, as shown in Figure 3–24(b). This block diagram can be simplified, as shown in Figure 3–24(c). Further simplifications result in Figures 3–24(d) and (e). Figure 3–24(e) is equivalent to Equation (3–74).

Notice the similarity and difference between the transfer function given by Equation (3–74) and that given by Equation (3–66). The term R_2C_1s that appears in the denominator of Equation (3–74) exemplifies the interaction between the two tanks. Similarly, the term R_1C_2s in the denominator of Equation (3–66) represents the interaction between the two RC circuits shown in Figure 3–19.

3–9 THERMAL SYSTEMS

Thermal systems are those that involve the transfer of heat from one substance to another. Thermal systems may be analyzed in terms of resistance and capacitance, although the thermal capacitance and thermal resistance may not be represented accurately as lumped parameters since they are usually distributed throughout the substance. For precise analysis, distributed-parameter models must be used. Here, however, to simplify the analysis we shall assume that a thermal system can be represented by a lumped-parameter model, that substances that are characterized by resistance to heat flow have negligible heat capacitance, and that substances that are characterized by heat capacitance have negligible resistance to heat flow.

There are three different ways heat can flow from one substance to another: conduction, convection, and radiation. Here we consider only conduction and convection. (Radiation heat transfer is appreciable only if the temperature of the emitter is very high compared to that of the receiver. Most thermal processes in process control systems do not involve radiation heat transfer.)

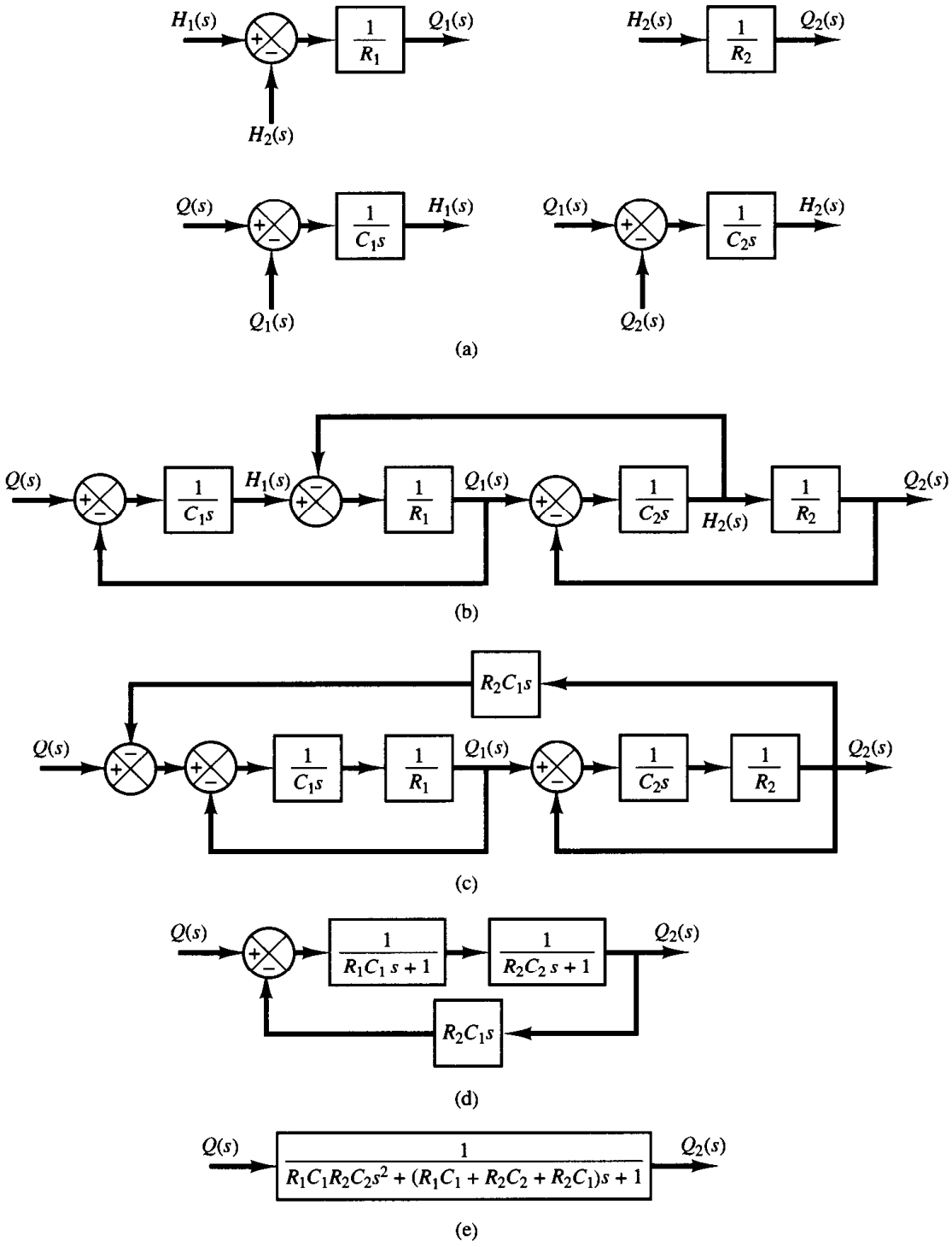

Figure 3–24
(a) Elements of the block diagram of the system shown in Figure 3–23; (b) block diagram of the system; (c)–(e) successive reductions of the block diagram.

For conduction or convection heat transfer,

$$q = K\,\Delta\theta$$

where q = heat flow rate, kcal/sec
$\Delta\theta$ = temperature difference, °C
K = coefficient, kcal/sec °C

The coefficient K is given by

$$K = \frac{kA}{\Delta X}, \qquad \text{for conduction}$$

$$= HA, \qquad \text{for convection}$$

where k = thermal conductivity, kcal/m sec °C
A = area normal to heat flow, m^2
ΔX = thickness of conductor, m
H = convection coefficient, kcal/m^2 sec °C

Thermal resistance and thermal capacitance. The thermal resistance R for heat transfer between two substances may be defined as follows:

$$R = \frac{\text{change in temperature difference, °C}}{\text{change in heat flow rate, kcal/sec}}$$

The thermal resistance for conduction or convection heat transfer is given by

$$R = \frac{d(\Delta\theta)}{dq} = \frac{1}{K}$$

Since the thermal conductivity and convection coefficients are almost constant, the thermal resistance for either conduction or convection is constant.

The thermal capacitance C is defined by

$$C = \frac{\text{change in heat stored, kcal}}{\text{change in temperature, °C}}$$

or

$$C = mc$$

where m = mass of substance considered, kg
c = specific heat of substance, kcal/kg °C

Thermal systems. Consider the system shown in Figure 3–25(a). It is assumed that the tank is insulated to eliminate heat loss to the surrounding air. It is also assumed that there is no heat storage in the insulation and that the liquid in the tank is perfectly mixed so that it is at a uniform temperature. Thus, a single temperature is used to describe the temperature of the liquid in the tank and of the outflowing liquid.

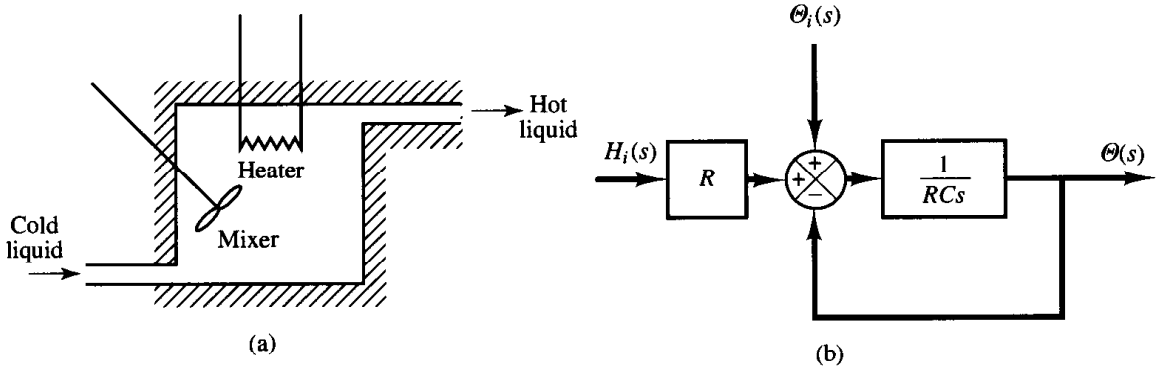

Figure 3–25
(a) Thermal system; (b) block diagram of the system.

Let us define

$\bar{\Theta}_i$ = steady-state temperature of inflowing liquid, °C

$\bar{\Theta}_o$ = steady-state temperature of outflowing liquid, °C

G = steady-state liquid flow rate, kg/sec

M = mass of liquid in tank, kg

c = specific heat of liquid, kcal/kg °C

R = thermal resistance, °C sec/kcal

C = thermal capacitance, kcal/°C

$\bar{H}$ = steady-state heat input rate, kcal/sec

Assume that the temperature of the inflowing liquid is kept constant and that the heat input rate to the system (heat supplied by the heater) is suddenly changed from $\bar{H}$ to $\bar{H} + h_i$, where h_i represents a small change in the heat input rate. The heat outflow rate will then change gradually from $\bar{H}$ to $\bar{H} + h_o$. The temperature of the outflowing liquid will also be changed from $\bar{\Theta}_o$ to $\bar{\Theta}_o + \theta$. For this case, h_o, C, and R are obtained, respectively, as

$$h_o = Gc\theta$$

$$C = Mc$$

$$R = \frac{\theta}{h_o} = \frac{1}{Gc}$$

The differential equation for this system is

$$C\frac{d\theta}{dt} = h_i - h_o$$

which may be rewritten as

$$RC\frac{d\theta}{dt} + \theta = Rh_i$$

Note that the time constant of the system is equal to RC or M/G seconds. The transfer function relating θ and h_i is given by

$$\frac{\Theta(s)}{H_i(s)} = \frac{R}{RCs + 1}$$

where $\Theta(s) = \mathcal{L}[\theta(t)]$ and $H_i(s) = \mathcal{L}[h_i(t)]$.

In practice, the temperature of the inflowing liquid may fluctuate and may act as a load disturbance. (If a constant outflow temperature is desired, an automatic controller may be installed to adjust the heat inflow rate to compensate for the fluctuations in the temperature of the inflowing liquid.) If the temperature of the inflowing liquid is suddenly changed from $\bar{\Theta}_i$ to $\bar{\Theta}_i + \theta_i$ while the heat input rate H and the liquid flow rate G are kept constant, then the heat outflow rate will be changed from $\bar{H}$ to $\bar{H} + h_o$, and the temperature of the outflowing liquid will be changed from $\bar{\Theta}_o$ to $\bar{\Theta}_o + \theta$. The differential equation for this case is

$$C\frac{d\theta}{dt} = Gc\theta_i - h_o$$

which may be rewritten

$$RC\frac{d\theta}{dt} + \theta = \theta_i$$

The transfer function relating θ and θ_i is given by

$$\frac{\Theta(s)}{\Theta_i(s)} = \frac{1}{RCs + 1}$$

where $\Theta(s) = \mathcal{L}[\theta(t)]$ and $\Theta_i(s) = \mathcal{L}[\theta_i(t)]$.

If the present thermal system is subjected to changes in both the temperature of the inflowing liquid and the heat input rate, while the liquid flow rate is kept constant, the change θ in the temperature of the outflowing liquid can be given by the following equation:

$$RC\frac{d\theta}{dt} + \theta = \theta_i + Rh_i$$

A block diagram corresponding to this case is shown in Figure 3–25(b). Notice that the system involves two inputs.

3–10 LINEARIZATION OF NONLINEAR MATHEMATICAL MODELS

In this section we present a linearization technique that is applicable to many nonlinear systems. The process of linearizing nonlinear systems is important, for by linearizing nonlinear equations, it is possible to apply numerous linear analysis methods that will produce information on the behavior of nonlinear systems. The linearization procedure presented here is based on the expansion of the nonlinear function into a

Taylor series about the operating point and the retention of only the linear term. Because we neglect higher-order terms of Taylor series expansion, these neglected terms must be small enough; that is, the variables deviate only slightly from the operating condition.

In what follows we shall first present mathematical aspects of the linearization technique and then apply the technique to a hydraulic servo system to obtain a linear model for the system.

Linear approximation of nonlinear mathematical models. To obtain a linear mathematical model for a nonlinear system, we assume that the variables deviate only slightly from some operating condition. Consider a system whose input is $x(t)$ and output is $y(t)$. The relationship between $y(t)$ and $x(t)$ is given by

$$y = f(x) \tag{3–75}$$

If the normal operating condition corresponds to $\bar{x}, \bar{y}$, then Equation (3–75) may be expanded into a Taylor series about this point as follows:

$$\begin{aligned} y &= f(x) \\ &= f(\bar{x}) + \frac{df}{dx}(x - \bar{x}) + \frac{1}{2!}\frac{d^2f}{dx^2}(x - \bar{x})^2 + \cdots \end{aligned} \tag{3–76}$$

where the derivatives df/dx, d^2f/dx^2, . . . are evaluated at $x = \bar{x}$. If the variation $x - \bar{x}$ is small, we may neglect the higher-order terms in $x - \bar{x}$. Then Equation (3–76) may be written as

$$y = \bar{y} + K(x - \bar{x}) \tag{3–77}$$

where

$$\bar{y} = f(\bar{x})$$

$$K = \left.\frac{df}{dx}\right|_{x=\bar{x}}$$

Equation (3–77) may be rewritten as

$$y - \bar{y} = K(x - \bar{x}) \tag{3–78}$$

which indicates that $y - \bar{y}$ is proportional to $x - \bar{x}$. Equation (3–78) gives a linear mathematical model for the nonlinear system given by Equation (3–75) near the operating point $x = \bar{x}, y = \bar{y}$.

Next, consider a nonlinear system whose output y is a function of two inputs x_1 and x_2, so that

$$y = f(x_1, x_2) \tag{3–79}$$

To obtain a linear approximation to this nonlinear system, we may expand Equation (3–79) into a Taylor series about the normal operating point $\bar{x}_1, \bar{x}_2$. Then Equation (3–79) becomes

$$y = f(\bar{x}_1, \bar{x}_2) + \left[\frac{\partial f}{\partial x_1}(x_1 - \bar{x}_1) + \frac{\partial f}{\partial x_2}(x_2 - \bar{x}_2)\right] + \frac{1}{2!}\left[\frac{\partial^2 f}{\partial x_1^2}(x_1 - \bar{x}_1)^2 + 2\frac{\partial^2 f}{\partial x_1 \partial x_2}(x_1 - \bar{x}_1)(x_2 - \bar{x}_2) + \frac{\partial^2 f}{\partial x_2^2}(x_2 - \bar{x}_2)^2\right] + \cdots$$

where the partial derivatives are evaluated at $x_1 = \bar{x}_1, x_2 = \bar{x}_2$. Near the normal operating point, the higher-order terms may be neglected. The linear mathematical model of this nonlinear system in the neighborhood of the normal operating condition is then given by

$$y - \bar{y} = K_1(x_1 - \bar{x}_1) + K_2(x_2 - \bar{x}_2)$$

where

$$\bar{y} = f(\bar{x}_1, \bar{x}_2)$$

$$K_1 = \left.\frac{\partial f}{\partial x_1}\right|_{x_1=\bar{x}_1, x_2=\bar{x}_2}$$

$$K_2 = \left.\frac{\partial f}{\partial x_2}\right|_{x_1=\bar{x}_1, x_2=\bar{x}_2}$$

The linearization technique presented here is valid in the vicinity of the operating condition. If the operating conditions vary widely, however, such linearized equations are not adequate, and nonlinear equations must be dealt with. It is important to remember that a particular mathematical model used in analysis and design may accurately represent the dynamics of an actual system for certain operating conditions, but may not be accurate for other operating conditions.

Linearization of a hydraulic servo system. Figure 3–26(a) shows a hydraulic servomotor. It is essentially a pilot-valve-controlled hydraulic power amplifier and actuator. The pilot valve is a balanced valve, in the sense that the pressure forces acting on it are all balanced. A very large power output can be controlled by a pilot valve, which can be positioned with very little power.

In practice, the ports shown in Figure 3–26(a) are often made wider than the corresponding valves. In such a case, there is always leakage through the valves. Such leakage improves both the sensitivity and the linearity of the hydraulic servomotor. In the following analysis we shall make the assumption that the ports are made wider than the valves, that is, the valves are underlapped. [Note that sometimes a dither signal, a high-frequency signal of very small amplitude (with respect to the maximum displacement of the valve), is superimposed on the motion of the pilot valve. This also improves the sensitivity and linearity. In this case also there is leakage through the valve.]

We shall apply the linearization technique just presented to obtain a linearized mathematical model of the hydraulic servomotor. We assume that the valve is underlapped and symmetrical and admits hydraulic fluid under high pressure into a power cylinder that contains a large piston, so that a large hydraulic force is established to

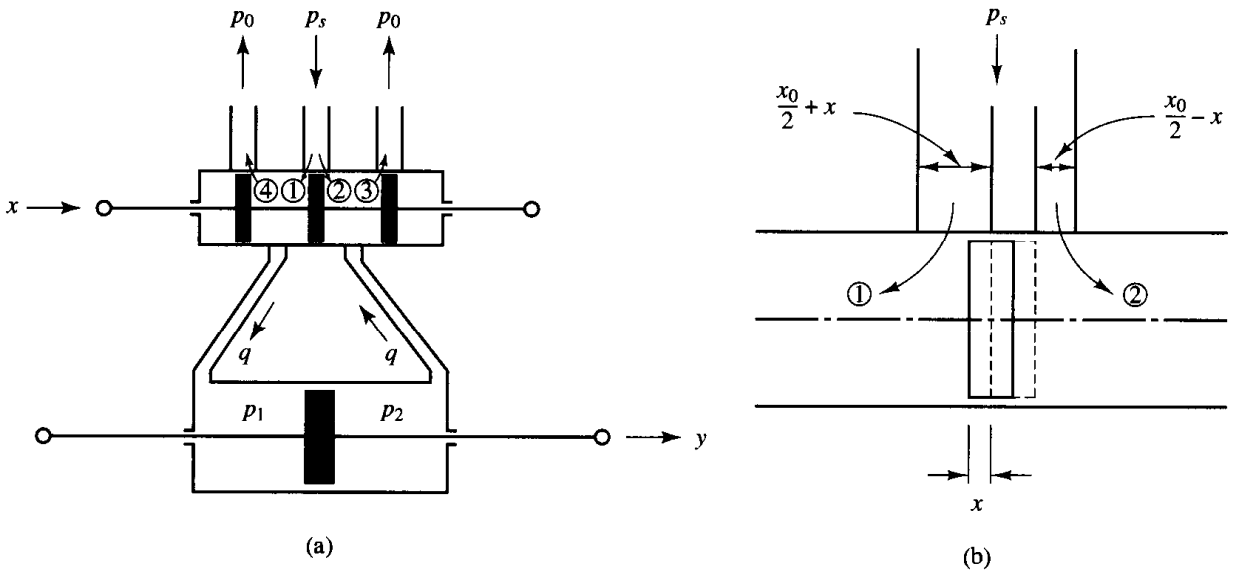

Figure 3–26
(a) Hydraulic servo system; (b) enlarged diagram of the valve orifice area.

move a load. We assume that the load inertia and friction are small compared to the large hydraulic force. In the present analysis, the hydraulic fluid is assumed to be incompressible and the inertia force of the power piston negligible. We also assume that, as is usually the case, the orifice area (the width of the slot in the valve sleeve) at each port is proportional to the valve displacement x.

In Figure 3–26(b) we have an enlarged diagram of the valve orifice area. Let us define the valve orifice areas of ports 1, 2, 3, 4 as A_1, A_2, A_3, A_4, respectively. Also, define the flow rates through ports 1, 2, 3, 4 as q_1, q_2, q_3, q_4, respectively. Note that, since the valve is symmetrical, $A_1 = A_3$ and $A_2 = A_4$. Assuming the displacement x to be small, we obtain

$$A_1 = A_3 = k\left(\frac{x_0}{2} + x\right)$$

$$A_2 = A_4 = k\left(\frac{x_0}{2} - x\right)$$

where k is a constant.

Furthermore, we shall assume that the return pressure p_0 in the return line is small and thus can be neglected. Then, referring to Figure 3–26(a), flow rates through valve orifices are

$$q_1 = c_1 A_1 \sqrt{\frac{2g}{\gamma}(p_s - p_1)} = C_1 \sqrt{p_s - p_1}\left(\frac{x_0}{2} + x\right)$$

$$q_2 = c_2 A_2 \sqrt{\frac{2g}{\gamma}(p_s - p_2)} = C_2 \sqrt{p_s - p_2}\left(\frac{x_0}{2} - x\right)$$

$$q_3 = c_1 A_3 \sqrt{\frac{2g}{\gamma}(p_2 - p_0)} = C_1 \sqrt{p_2 - p_0}\left(\frac{x_0}{2} + x\right) = C_1 \sqrt{p_2}\left(\frac{x_0}{2} + x\right)$$

$$q_4 = c_2 A_4 \sqrt{\frac{2g}{\gamma}(p_1 - p_0)} = C_2 \sqrt{p_1 - p_0}\left(\frac{x_0}{2} - x\right) = C_2 \sqrt{p_1}\left(\frac{x_0}{2} - x\right)$$

where $C_1 = c_1 k\sqrt{2g/\gamma}$ and $C_2 = c_2 k\sqrt{2g/\gamma}$, and γ is the specific weight and is given by $\gamma = \varrho g$, where ϱ is mass density and g is the acceleration of gravity. The flow rate q to the left-hand side of the power piston is

$$q = q_1 - q_4 = C_1\sqrt{p_s - p_1}\left(\frac{x_0}{2} + x\right) - C_2\sqrt{p_1}\left(\frac{x_0}{2} - x\right) \tag{3–80}$$

The flow rate from the right-hand side of the power piston to the drain is the same as this q and is given by

$$q = q_3 - q_2 = C_1\sqrt{p_2}\left(\frac{x_0}{2} + x\right) - C_2\sqrt{p_s - p_2}\left(\frac{x_0}{2} - x\right)$$

Note that the fluid is incompressible and that the valve is symmetrical. So we have $q_1 = q_3$ and $q_2 = q_4$. By equating q_1 and q_3, we obtain

$$p_s - p_1 = p_2$$

or

$$p_s = p_1 + p_2$$

If we define the pressure difference across the power piston as Δp or

$$\Delta p = p_1 - p_2$$

then

$$p_1 = \frac{p_s + \Delta p}{2}, \qquad p_2 = \frac{p_s - \Delta p}{2}$$

For the symmetrical valve shown in Figure 3–26(a), the pressure in each side of the power piston is $\frac{1}{2}p_s$ when no load is applied, or $\Delta p = 0$. As the spool valve is displaced, the pressure in one line increases as the pressure in the other line decreases by the same amount.

In terms of p_s and Δp, we can rewrite the flow rate q given by Equation (3–80) as

$$q = q_1 - q_4 = C_1\sqrt{\frac{p_s - \Delta p}{2}}\left(\frac{x_0}{2} + x\right) - C_2\sqrt{\frac{p_s + \Delta p}{2}}\left(\frac{x_0}{2} - x\right)$$

Noting that the supply pressure p_s is constant, the flow rate q can be written as a function of the valve displacement x and pressure difference Δp, or

$$q = C_1\sqrt{\frac{p_s - \Delta p}{2}}\left(\frac{x_0}{2} + x\right) - C_2\sqrt{\frac{p_s + \Delta p}{2}}\left(\frac{x_0}{2} - x\right) = f(x, \Delta p)$$

By applying the linearization technique presented earlier in this section to this case, the linearized equation about point $x = \bar{x}$, $\Delta p = \Delta\bar{p}$, $q = \bar{q}$ is

$$q - \bar{q} = a(x - \bar{x}) + b(\Delta p - \Delta\bar{p}) \tag{3–81}$$

where

$$\bar{q} = f(\bar{x}, \Delta\bar{p})$$

$$a = \left.\frac{\partial f}{\partial x}\right|_{x=\bar{x},\Delta p=\Delta\bar{p}} = C_1\sqrt{\frac{p_s - \Delta\bar{p}}{2}} + C_2\sqrt{\frac{p_s + \Delta\bar{p}}{2}}$$

$$b = \frac{\partial f}{\partial \Delta p}\bigg|_{x=\bar{x},\Delta p=\Delta\bar{p}} = -\left[\frac{C_1}{2\sqrt{2}\sqrt{p_s - \Delta\bar{p}}}\left(\frac{x_0}{2} + \bar{x}\right)\right.$$
$$\left. + \frac{C_2}{2\sqrt{2}\sqrt{p_s + \Delta\bar{p}}}\left(\frac{x_0}{2} - \bar{x}\right)\right] < 0$$

Coefficients a and b here are called *valve coefficients*. Equation (3–81) is a linearized mathematical model of the spool valve near an operating point $x = \bar{x}, \Delta p = \Delta\bar{p}, q = \bar{q}$. The values of valve coefficients a and b vary with the operating point. Note that $\partial f/\partial \Delta p$ is negative and so b is negative.

Since the normal operating point is the point where $\bar{x} = 0, \Delta\bar{p} = 0, \bar{q} = 0$, near the normal operating point, Equation (3–81) becomes

$$q = K_1 x - K_2 \Delta p \tag{3–82}$$

where

$$K_1 = (C_1 + C_2)\sqrt{\frac{p_s}{2}} > 0$$

$$K_2 = (C_1 + C_2)\frac{x_0}{4\sqrt{2}\sqrt{p_s}} > 0$$

Equation (3–82) is a linearized mathematical model of the spool valve near the origin ($\bar{x} = 0, \Delta\bar{p} = 0, \bar{q} = 0$). Note that the region near the origin is most important in this kind of system, because the system operation usually occurs near this point. (For a derivation of a mathematical model of a hydraulic servo system when the load reactive forces are not negligible, see Problem A-3-20.)

EXAMPLE PROBLEMS AND SOLUTIONS

A-3-1. Simplify the block diagram shown in Figure 3–27.

Solution. First, move the branch point of the path involving H_1 outside the loop involving H_2, as shown in Figure 3–28(a). Then eliminating two loops results in Figure 3–28(b). Combining two blocks into one gives Figure 3–28(c).

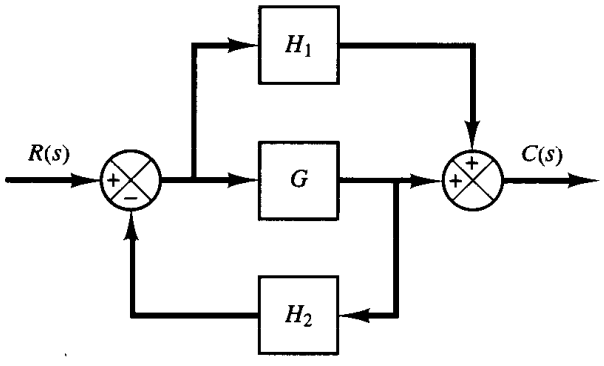

Figure 3–27
Block diagram of a system.

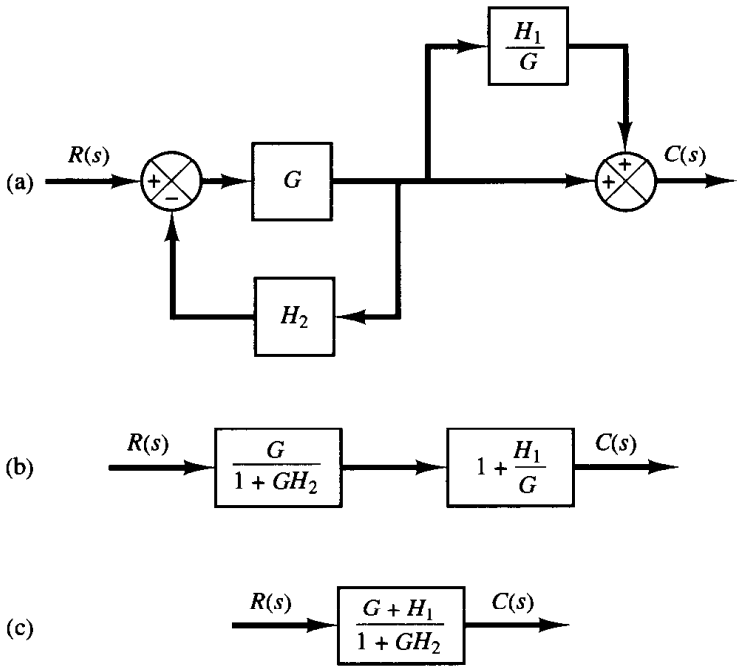

Figure 3–28
Simplified block diagrams for the system shown in Figure 3–27.

A-3-2. Simplify the block diagram shown in Figure 3–29. Obtain the transfer function relating $C(s)$ and $R(s)$.

Solution. The block diagram of Figure 3–29 can be modified to that shown in Figure 3–30(a). Eliminating the minor feedforward path, we obtain Figure 3–30(b), which can be simplified to that shown in Figure 3–30(c). The transfer function $C(s)/R(s)$ is thus given by

$$\frac{C(s)}{R(s)} = G_1G_2 + G_2 + 1$$

The same result can also be obtained by proceeding as follows: Since signal $X(s)$ is the sum of two signals $G_1R(s)$ and $R(s)$, we have

$$X(s) = G_1R(s) + R(s)$$

The output signal $C(s)$ is the sum of $G_2X(s)$ and $R(s)$. Hence

$$C(s) = G_2X(s) + R(s) = G_2[G_1R(s) + R(s)] + R(s)$$

And so we have the same result as before:

$$\frac{C(s)}{R(s)} = G_1G_2 + G_2 + 1$$

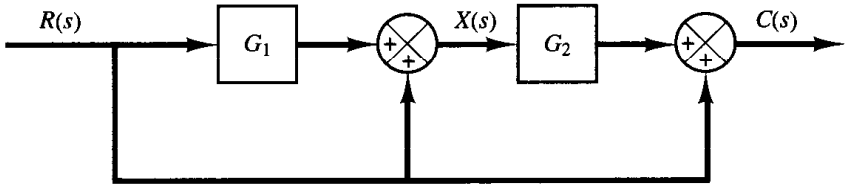

Figure 3–29
Block diagram of a system.

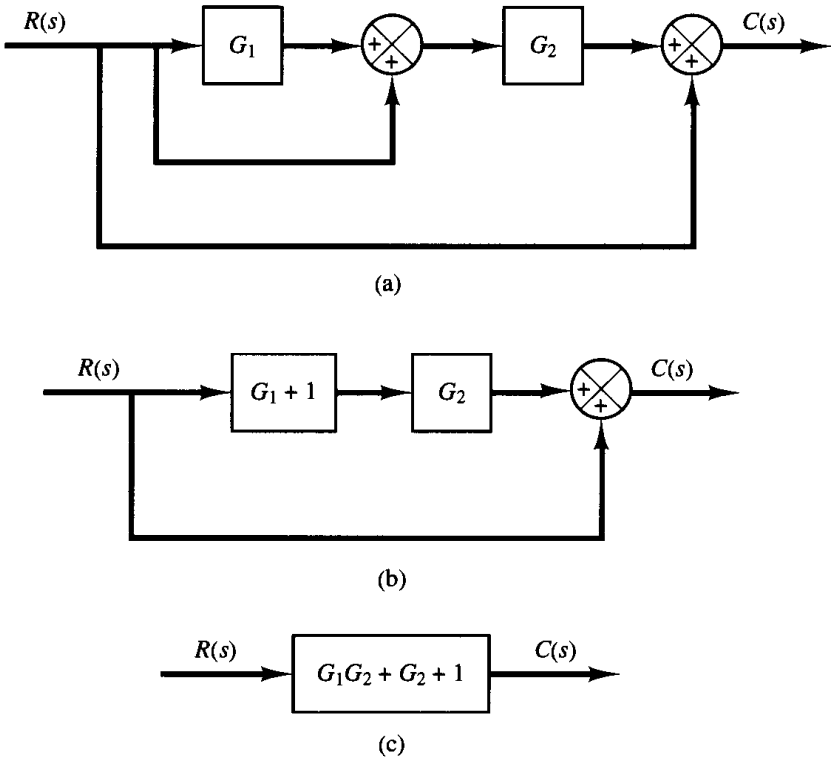

Figure 3–30
Reduction of the block diagram shown in Figure 3–29.

A-3-3. Show that for the differential equation system

$$\dddot{y} + a_1\ddot{y} + a_2\dot{y} + a_3 y = b_0\dddot{u} + b_1\ddot{u} + b_2\dot{u} + b_3 u \tag{3–83}$$

state and output equations can be given, respectively, by

$$\begin{bmatrix} \dot{x}_1 \\ \dot{x}_2 \\ \dot{x}_3 \end{bmatrix} = \begin{bmatrix} 0 & 1 & 0 \\ 0 & 0 & 1 \\ -a_3 & -a_2 & -a_1 \end{bmatrix} \begin{bmatrix} x_1 \\ x_2 \\ x_3 \end{bmatrix} + \begin{bmatrix} \beta_1 \\ \beta_2 \\ \beta_3 \end{bmatrix} u \tag{3–84}$$

and

$$y = [1 \quad 0 \quad 0] \begin{bmatrix} x_1 \\ x_2 \\ x_3 \end{bmatrix} + \beta_0 u \tag{3–85}$$

where state variables are defined by

$$x_1 = y - \beta_0 u$$
$$x_2 = \dot{y} - \beta_0\dot{u} - \beta_1 u = \dot{x}_1 - \beta_1 u$$
$$x_3 = \ddot{y} - \beta_0\ddot{u} - \beta_1\dot{u} - \beta_2 u = \dot{x}_2 - \beta_2 u$$

and

$$\beta_0 = b_0$$
$$\beta_1 = b_1 - a_1\beta_0$$
$$\beta_2 = b_2 - a_1\beta_1 - a_2\beta_0$$
$$\beta_3 = b_3 - a_1\beta_2 - a_2\beta_1 - a_3\beta_0$$

Solution. From the definition of state variables x_2 and x_3, we have

$$\dot{x}_1 = x_2 + \beta_1 u \tag{3–86}$$

$$\dot{x}_2 = x_3 + \beta_2 u \tag{3–87}$$

To derive the equation for $\dot{x}_3$, we first note from Equation (3–83) that

$$\dddot{y} = -a_1\ddot{y} - a_2\dot{y} - a_3 y + b_0\dddot{u} + b_1\ddot{u} + b_2\dot{u} + b_3 u$$

Since

$$x_3 = \ddot{y} - \beta_0\ddot{u} - \beta_1\dot{u} - \beta_2 u$$

we have

$$\begin{aligned}
\dot{x}_3 &= \dddot{y} - \beta_0\dddot{u} - \beta_1\ddot{u} - \beta_2\dot{u} \\
&= (-a_1\ddot{y} - a_2\dot{y} - a_3 y) + b_0\dddot{u} + b_1\ddot{u} + b_2\dot{u} + b_3 u - \beta_0\dddot{u} - \beta_1\ddot{u} - \beta_2\dot{u} \\
&= -a_1(\ddot{y} - \beta_0\ddot{u} - \beta_1\dot{u} - \beta_2 u) - a_1\beta_0\ddot{u} - a_1\beta_1\dot{u} - a_1\beta_2 u \\
&\quad -a_2(\dot{y} - \beta_0\dot{u} - \beta_1 u) - a_2\beta_0\dot{u} - a_2\beta_1 u - a_3(y - \beta_0 u) - a_3\beta_0 u \\
&\quad + b_0\dddot{u} + b_1\ddot{u} + b_2\dot{u} + b_3 u - \beta_0\dddot{u} - \beta_1\ddot{u} - \beta_2\dot{u} \\
&= -a_1 x_3 - a_2 x_2 - a_3 x_1 + (b_0 - \beta_0)\dddot{u} + (b_1 - \beta_1 - a_1\beta_0)\ddot{u} \\
&\quad + (b_2 - \beta_2 - a_1\beta_1 - a_2\beta_0)\dot{u} + (b_3 - a_1\beta_2 - a_2\beta_1 - a_3\beta_0)u \\
&= -a_1 x_3 - a_2 x_2 - a_3 x_1 + (b_3 - a_1\beta_2 - a_2\beta_1 - a_3\beta_0)u \\
&= -a_1 x_3 - a_2 x_2 - a_3 x_1 + \beta_3 u
\end{aligned}$$

Hence, we get

$$\dot{x}_3 = -a_3 x_1 - a_2 x_2 - a_1 x_3 + \beta_3 u \tag{3–88}$$

Combining Equations (3–86), (3–87), and (3–88) into a vector-matrix differential equation, we obtain Equation (3–84). Also, from the definition of state variable x_1, we get the output equation given by Equation (3–85).

A-3-4 Obtain a state-space model of the system shown in Figure 3–31.

Solution. The system involves one integrator and two delayed integrators. The output of each integrator or delayed integrator can be a state variable. Let us define the output of the plant as x_1, the output of the controller as x_2, and the output of the sensor as x_3. Then we obtain

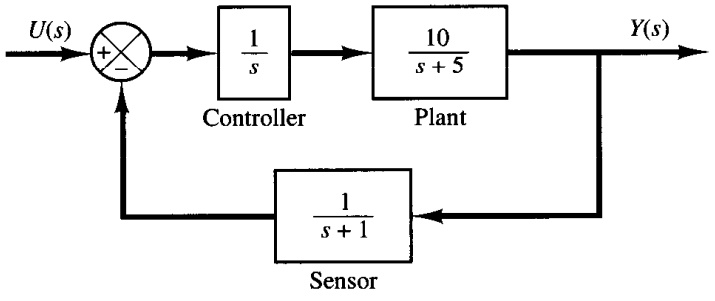

Figure 3–31
Control system.

$$\frac{X_1(s)}{X_2(s)} = \frac{10}{s+5}$$

$$\frac{X_2(s)}{U(s) - X_3(s)} = \frac{1}{s}$$

$$\frac{X_3(s)}{X_1(s)} = \frac{1}{s+1}$$

$$Y(s) = X_1(s)$$

which can be rewritten as

$$sX_1(s) = -5X_1(s) + 10X_2(s)$$

$$sX_2(s) = -X_3(s) + U(s)$$

$$sX_3(s) = X_1(s) - X_3(s)$$

$$Y(s) = X_1(s)$$

By taking the inverse Laplace transforms of the preceding four equations, we obtain

$$\dot{x}_1 = -5x_1 + 10x_2$$

$$\dot{x}_2 = -x_3 + u$$

$$\dot{x}_3 = x_1 - x_3$$

$$y = x_1$$

Thus, a state-space model of the system in the standard form is given by

$$\begin{bmatrix} \dot{x}_1 \\ \dot{x}_2 \\ \dot{x}_3 \end{bmatrix} = \begin{bmatrix} -5 & 10 & 0 \\ 0 & 0 & -1 \\ 1 & 0 & -1 \end{bmatrix} \begin{bmatrix} x_1 \\ x_2 \\ x_3 \end{bmatrix} + \begin{bmatrix} 0 \\ 1 \\ 0 \end{bmatrix} u$$

$$y = \begin{bmatrix} 1 & 0 & 0 \end{bmatrix} \begin{bmatrix} x_1 \\ x_2 \\ x_3 \end{bmatrix}$$

It is important to note that this is not the only state-space representation of the system. Many other state-space representations are possible. However, the number of state variables is the same in any state-space representation of the same system. In the present system, the number of state variables is three, regardless of what variables are chosen as state variables.

A-3-5. Obtain a state-space model for the system shown in Figure 3–32(a).

Solution. First, notice that $(as + b)/s^2$ involves a derivative term. Such a derivative term may be avoided if we modify $(as + b)/s^2$ as

$$\frac{as + b}{s^2} = \left(a + \frac{b}{s}\right)\frac{1}{s}$$

Using this modification, the block diagram of Figure 3–32(a) can be modified to that shown in Figure 3–32(b).

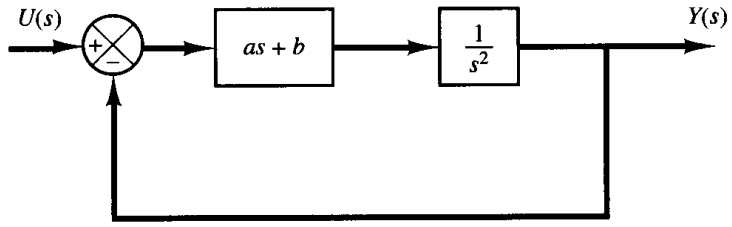

(a)

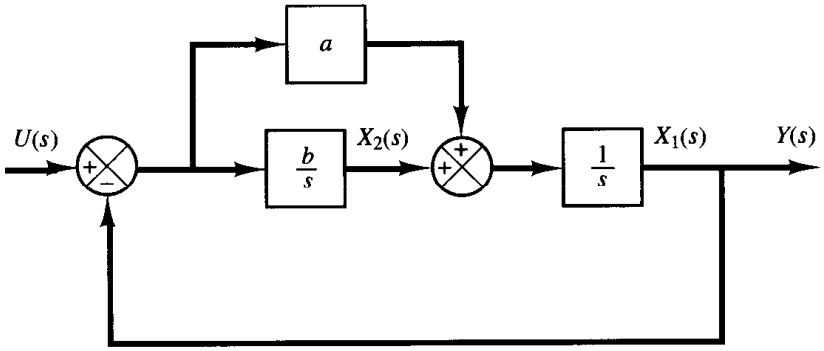

(b)

Figure 3–32
(a) Control system; (b) modified block diagram.

Define the outputs of the integrators as state variables, as shown in Figure 3–32(b). Then from Figure 3–32(b) we obtain

$$\frac{X_1(s)}{X_2(s) + a[U(s) - X_1(s)]} = \frac{1}{s}$$

$$\frac{X_2(s)}{U(s) - X_1(s)} = \frac{b}{s}$$

$$Y(s) = X_1(s)$$

which may be modified to

$$sX_1(s) = X_2(s) + a[U(s) - X_1(s)]$$

$$sX_2(s) = -bX_1(s) + bU(s)$$

$$Y(s) = X_1(s)$$

Taking the inverse Laplace transforms of the preceding three equations, we obtain

$$\dot{x}_1 = -ax_1 + x_2 + au$$

$$\dot{x}_2 = -bx_1 + bu$$

$$y = x_1$$

Rewriting the state and output equations in the standard vector-matrix form, we obtain

$$\begin{bmatrix} \dot{x}_1 \\ \dot{x}_2 \end{bmatrix} = \begin{bmatrix} -a & 1 \\ -b & 0 \end{bmatrix} \begin{bmatrix} x_1 \\ x_2 \end{bmatrix} + \begin{bmatrix} a \\ b \end{bmatrix} u$$

$$y = \begin{bmatrix} 1 & 0 \end{bmatrix} \begin{bmatrix} x_1 \\ x_2 \end{bmatrix}$$

A-3-6. Obtain a state-space representation of the system shown in Figure 3–33(a).

Solution. In this problem, first expand $(s + z)/(s + p)$ into partial fractions.

$$\frac{s+z}{s+p} = 1 + \frac{z-p}{s+p}$$

Next covert $K/[s(s + a)]$ into the product of K/s and $1/(s + a)$. Then redraw the block diagram, as shown in Figure 3–33(b). Defining a set of state variables, as shown in Figure 3–33(b), we obtain the following equations:

$$\dot{x}_1 = -ax_1 + x_2$$
$$\dot{x}_2 = -Kx_1 + Kx_3 + Ku$$
$$\dot{x}_3 = -(z-p)x_1 - px_3 + (z-p)u$$
$$y = x_1$$

Rewriting gives

$$\begin{bmatrix} \dot{x}_1 \\ \dot{x}_2 \\ \dot{x}_3 \end{bmatrix} = \begin{bmatrix} -a & 1 & 0 \\ -K & 0 & K \\ -(z-p) & 0 & -p \end{bmatrix} \begin{bmatrix} x_1 \\ x_2 \\ x_3 \end{bmatrix} + \begin{bmatrix} 0 \\ K \\ z-p \end{bmatrix} u$$

$$y = [1 \quad 0 \quad 0] \begin{bmatrix} x_1 \\ x_2 \\ x_3 \end{bmatrix}$$

Notice that the output of the integrator and the outputs of the first-order delayed integrators $[1/(s + a)$ and $(z - p)/(s + p)]$ are chosen as state variables. It is important to remember that the output of the block $(s + z)/(s + p)$ in Figure 3–33(a) cannot be a state variable, because this block involves a derivative term, $s + z$.

A-3-7. Gyros for sensing angular motion are commonly used in inertial guidance systems, autopilot systems, and the like. Figure 3–34(a) shows a single-degree-of-freedom gyro. The spinning wheel is

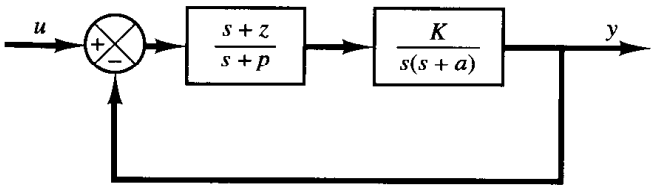

(a)

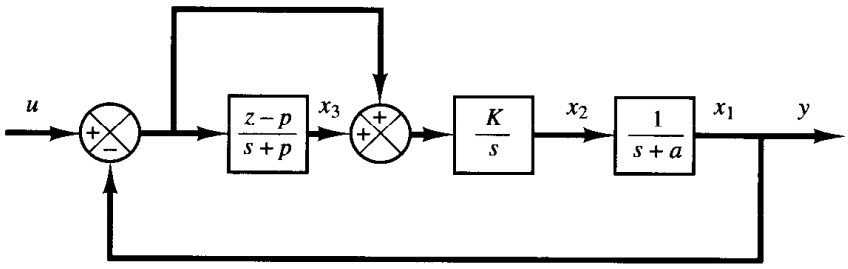

(b)

Figure 3–33
(a) Control system; (b) block diagram defining state variables for the system.

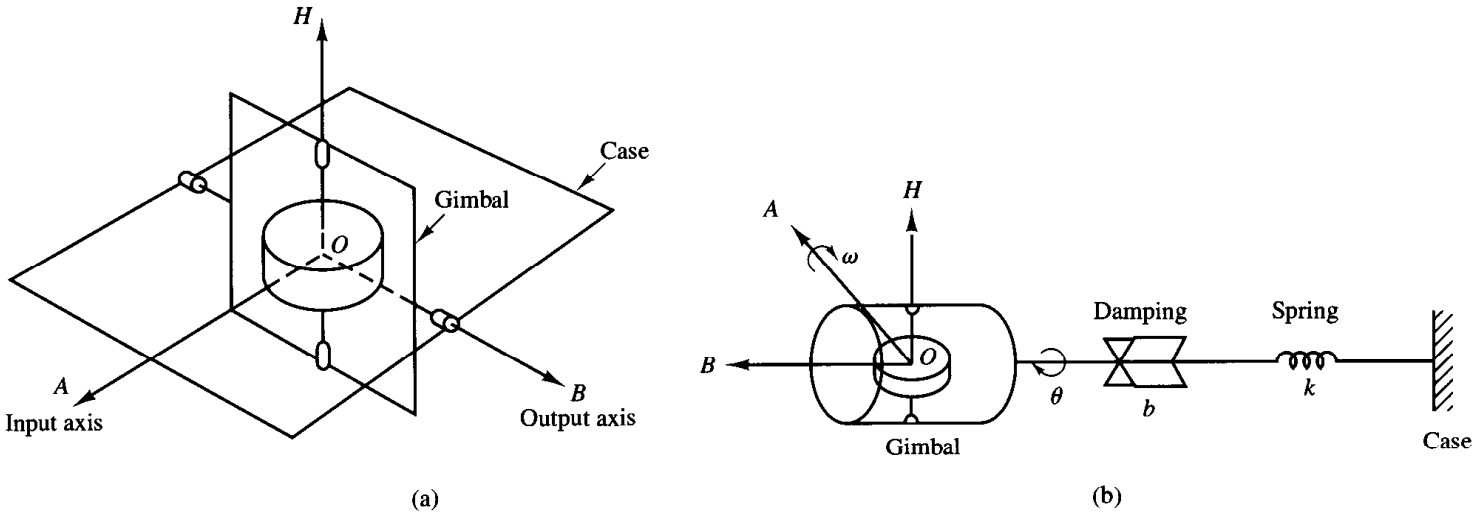

Figure 3–34
(a) Schematic diagram of a single-degree-of-freedom gyro; (b) functional diagram of the gyro shown in part (a).

mounted in a movable gimbal, which is, in turn, mounted in a gyro case. The gimbal is free to move relative to the case about the output axis OB. Note that the output axis is perpendicular to the wheel spin axis. The input axis around which a turning rate, or angle, is measured is perpendicular to both the output and spin axes. Information on the input signal (the turning rate or angle around the input axis) is obtained from the resulting motion of the gimbal about the output axis, relative to the case.

Figure 3–34(b) shows a functional diagram of the gyro system. The equation of motion about the output axis can be obtained by equating the rate of change of angular momentum to the sum of the external torques.

The change in angular momentum about axis OB consists of two parts: $I\ddot{\theta}$, the change due to acceleration of the gimbal around axis OB, and $-H\omega \cos\theta$, the change due to the turning of the wheel angular-momentum vector around axis OA. The external torques consist of $-b\dot{\theta}$, the damping torque, and $-k\theta$, the spring torque. Thus the equation of the gyro system is

$$I\ddot{\theta} - H\omega \cos\theta = -b\dot{\theta} - k\theta$$

or

$$I\ddot{\theta} + b\dot{\theta} + k\theta = H\omega \cos\theta \tag{3–89}$$

In practice, θ is a very small angle, usually not more than $\pm 2.5°$.

Obtain a state-space representation of the gyro system.

Solution. In this system, θ and $\dot{\theta}$ may be chosen as state variables. The input variable is ω and the output variable is θ. Let us define

$$\mathbf{x} = \begin{bmatrix} x_1 \\ x_2 \end{bmatrix} = \begin{bmatrix} \theta \\ \dot{\theta} \end{bmatrix}, \qquad u = \omega, \qquad y = \theta$$

Then Equation (3–89) can be written as follows:

$$\dot{x}_1 = x_2$$

$$\dot{x}_2 = -\frac{k}{I}x_1 - \frac{b}{I}x_2 + \frac{H}{I}u \cos x_1$$

or

$$\dot{\mathbf{x}} = \mathbf{f}(\mathbf{x}, u)$$

where

$$\mathbf{x} = \begin{bmatrix} x_1 \\ x_2 \end{bmatrix}, \qquad \mathbf{f}(\mathbf{x}, u) = \begin{bmatrix} f_1(\mathbf{x}, u) \\ f_2(\mathbf{x}, u) \end{bmatrix} = \begin{bmatrix} x_2 \\ -\frac{k}{I}x_1 - \frac{b}{I}x_2 + \frac{H}{I}u\cos x_1 \end{bmatrix}$$

Clearly, $f_2(\mathbf{x}, u)$ involves a nonlinear term in x_1 and u. By expanding $\cos x_1$ into its series representation,

$$\cos x_1 = 1 - \frac{1}{2}x_1^2 + \cdots$$

and noting that x_1 is a very small angle, we may approximate $\cos x_1$ by unity to obtain the following linearized state equation:

$$\begin{bmatrix} \dot{x}_1 \\ \dot{x}_2 \end{bmatrix} = \begin{bmatrix} 0 & 1 \\ -\frac{k}{I} & -\frac{b}{I} \end{bmatrix}\begin{bmatrix} x_1 \\ x_2 \end{bmatrix} + \begin{bmatrix} 0 \\ \frac{H}{I} \end{bmatrix}u$$

The output equation is

$$y = [1 \quad 0]\begin{bmatrix} x_1 \\ x_2 \end{bmatrix}$$

A-3-8. Consider a system defined by the following state-space equations:

$$\begin{bmatrix} \dot{x}_1 \\ \dot{x}_2 \end{bmatrix} = \begin{bmatrix} -5 & -1 \\ 3 & -1 \end{bmatrix}\begin{bmatrix} x_1 \\ x_2 \end{bmatrix} + \begin{bmatrix} 2 \\ 5 \end{bmatrix}u$$

$$y = [1 \quad 2]\begin{bmatrix} x_1 \\ x_2 \end{bmatrix}$$

Obtain the transfer function $G(s)$ of the system.

Solution. Referring to Equation (3–32), the transfer function of the system can be obtained as follows (note that $D = 0$ in this case):

$$\begin{aligned} G(s) &= \mathbf{C}(s\mathbf{I} - \mathbf{A})^{-1}\mathbf{B} \\ &= [1 \quad 2]\begin{bmatrix} s+5 & 1 \\ -3 & s+1 \end{bmatrix}^{-1}\begin{bmatrix} 2 \\ 5 \end{bmatrix} \\ &= [1 \quad 2]\begin{bmatrix} \frac{s+1}{(s+2)(s+4)} & \frac{-1}{(s+2)(s+4)} \\ \frac{3}{(s+2)(s+4)} & \frac{s+5}{(s+2)(s+4)} \end{bmatrix}\begin{bmatrix} 2 \\ 5 \end{bmatrix} \\ &= \frac{12s + 59}{(s+2)(s+4)} \end{aligned}$$

A-3-9. Figure 3–35(a) shows a schematic diagram of an automobile suspension system. As the car moves along the road, the vertical displacements at the tires act as the motion excitation to the automobile suspension system. The motion of this system consists of a translational motion of the center of mass and a rotational motion about the center of mass. Mathematical modeling of the complete system is quite complicated.

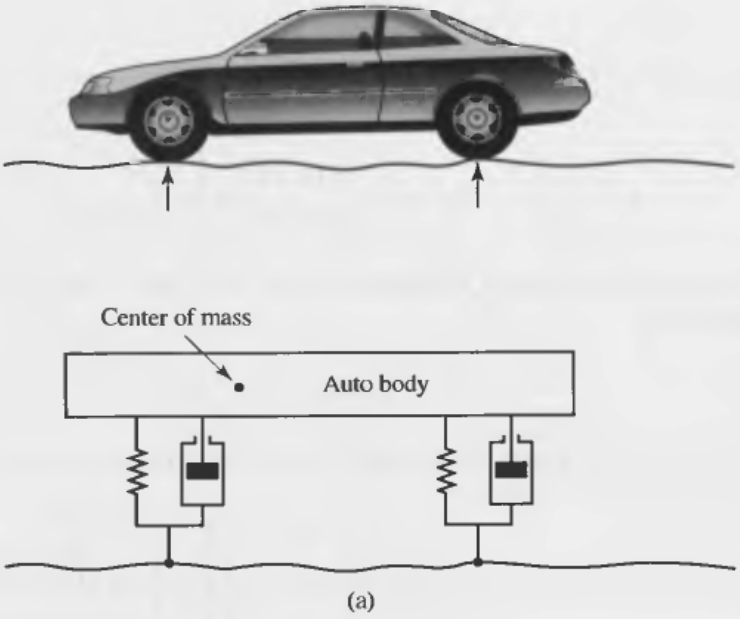

Figure 3–35
(a) Automobile suspension system; (b) simplified suspension system.

A very simplified version of the suspension system is shown in Figure 3–35(b). Assuming that the motion x_i at point P is the input to the system and the vertical motion x_o of the body is the output, obtain the transfer function $X_o(s)/X_i(s)$. (Consider the motion of the body only in the vertical direction.) Displacement x_o is measured from the equilibrium position in the absence of input x_i.

Solution. The equation of motion for the system shown in Figure 3–35(b) is

$$m\ddot{x}_o + b(\dot{x}_o - \dot{x}_i) + k(x_o - x_i) = 0$$

or

$$m\ddot{x}_o + b\dot{x}_o + kx_o = b\dot{x}_i + kx_i$$

Taking the Laplace transform of this last equation, assuming zero initial conditions, we obtain

$$(ms^2 + bs + k)X_o(s) = (bs + k)X_i(s)$$

Hence the transfer function $X_o(s)/X_i(s)$ is given by

$$\frac{X_o(s)}{X_i(s)} = \frac{bs + k}{ms^2 + bs + k}$$

A-3-10. Obtain the transfer function $Y(s)/U(s)$ of the system shown in Figure 3–36. (Similar to the system of Problem A-3-9, this is also a simplified version of an automobile or motorcycle suspension system.)

Solution. Applying the Newton's second law to the system, we obtain

$$m_1\ddot{x} = k_2(y - x) + b(\dot{y} - \dot{x}) + k_1(u - x)$$

$$m_2\ddot{y} = -k_2(y - x) - b(\dot{y} - \dot{x})$$

Hence, we have

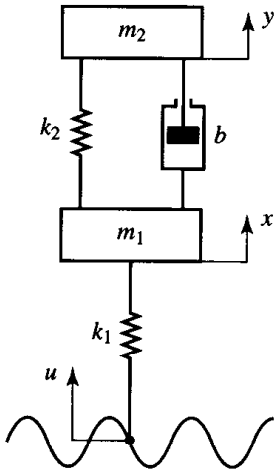

Figure 3–36
Suspension system.

$$m_1\ddot{x} + b\dot{x} + (k_1 + k_2)x = b\dot{y} + k_2y + k_1u$$

$$m_2\ddot{y} + b\dot{y} + k_2y = b\dot{x} + k_2x$$

Taking Laplace transforms of these two equations, assuming zero initial conditions, we obtain

$$[m_1s^2 + bs + (k_1 + k_2)]X(s) = (bs + k_2)Y(s) + k_1U(s)$$

$$[m_2s^2 + bs + k_2]Y(s) = (bs + k_2)X(s)$$

Eliminating $X(s)$ from the last two equations, we have

$$(m_1s^2 + bs + k_1 + k_2)\frac{m_2s^2 + bs + k_2}{bs + k_2}Y(s) = (bs + k_2)Y(s) + k_1U(s)$$

which yields

$$\frac{Y(s)}{U(s)} = \frac{k_1(bs + k_2)}{m_1m_2s^4 + (m_1 + m_2)bs^3 + [k_1m_2 + (m_1 + m_2)k_2]s^2 + k_1bs + k_1k_2}$$

A-3-11. Consider the electrical circuit shown in Figure 3–37. Obtain the transfer function $E_o(s)/E_i(s)$ by use of the block diagram approach.

Solution. Equations for the circuits are

$$\frac{1}{C_1}\int (i_1 - i_2)\,dt + R_1i_1 = e_i \tag{3–90}$$

$$\frac{1}{C_1}\int (i_2 - i_1)\,dt + R_2i_2 + \frac{1}{C_2}\int i_2\,dt = 0 \tag{3–91}$$

$$\frac{1}{C_2}\int i_2\,dt = e_o \tag{3–92}$$

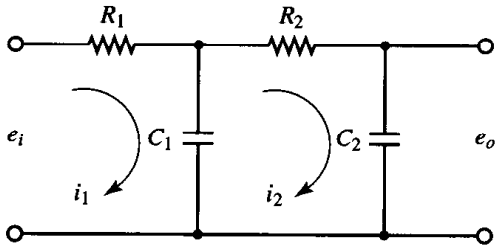

Figure 3–37
Electrical circuit.

The Laplace transforms of Equations (3–90), (3–91), and (3–92), with zero initial conditions, give

$$\frac{1}{C_1 s}[I_1(s) - I_2(s)] + R_1 I_1(s) = E_i(s) \tag{3–93}$$

$$\frac{1}{C_1 s}[I_2(s) - I_1(s)] + R_2 I_2(s) + \frac{1}{C_2 s} I_2(s) = 0 \tag{3–94}$$

$$\frac{1}{C_2 s} I_2(s) = E_o(s) \tag{3–95}$$

Equation (3–93) can be rewritten as

$$C_1 s[E_i(s) - R_1 I_1(s)] = I_1(s) - I_2(s) \tag{3–96}$$

Equation (3–96) gives the block diagram shown in Figure 3–38(a). Equation (3–94) can be modified to

$$I_2(s) = \frac{C_2 s}{R_2 C_2 s + 1} \frac{1}{C_1 s}[I_1(s) - I_2(s)] \tag{3–97}$$

Equation (3–97) yields the block diagram shown in Figure 3–38(b). Also, Equation (3–95) gives the block diagram shown in Figure 3–38(c). Combining the block diagrams of Figures 3–38(a), (b), and (c), we obtain Figure 3–39(a). This block diagram can be successively modified as shown in Figures 3–39(b) through (e). Thus we obtained the transfer function $E_o(s)/E_i(s)$ of the system. [This is the same as that we derived earlier for the same electrical circuit. See Equation (3–66).]

A-3-12. Obtain the transfer function of the mechanical system shown in Figure 3–40(a). Also obtain the transfer function of the electrical system shown in Figure 3–40(b). Show that the transfer functions of the two systems are of identical form and thus they are analogous systems.

Solution. The equations of motion for the mechanical system shown in Figure 3–40(a) are

$$b_1(\dot{x}_i - \dot{x}_o) + k_1(x_i - x_o) = b_2(\dot{x}_o - \dot{y})$$

$$b_2(\dot{x}_o - \dot{y}) = k_2 y$$

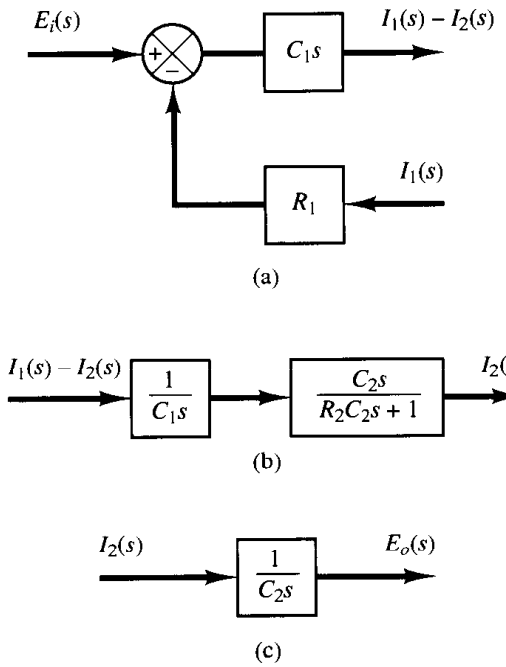

Figure 3–38
Block diagrams: (a) corresponding to Equation (3–96); (b) corresponding to Equation (3–97); (c) corresponding to Equation (3–95).

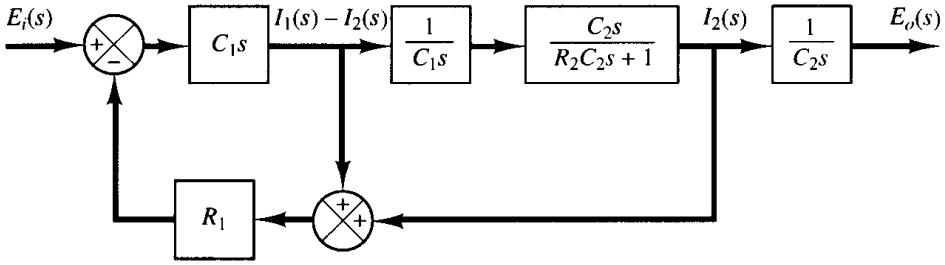

(a)

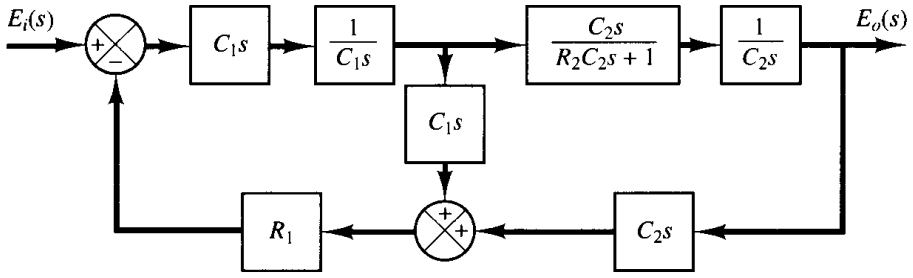

(b)

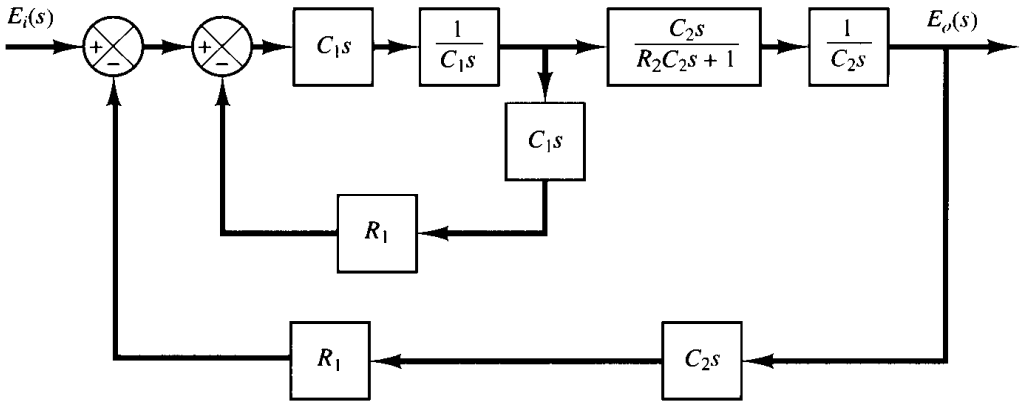

(c)

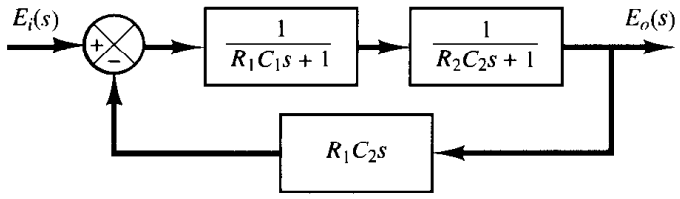

(d)

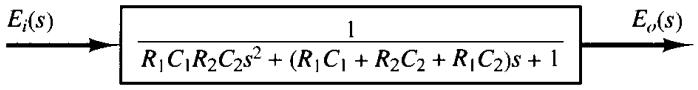

(e)

Figure 3–39
Block diagrams for the system shown in Figure 3–37. (a) through (e) show successive simplifications of block diagrams.

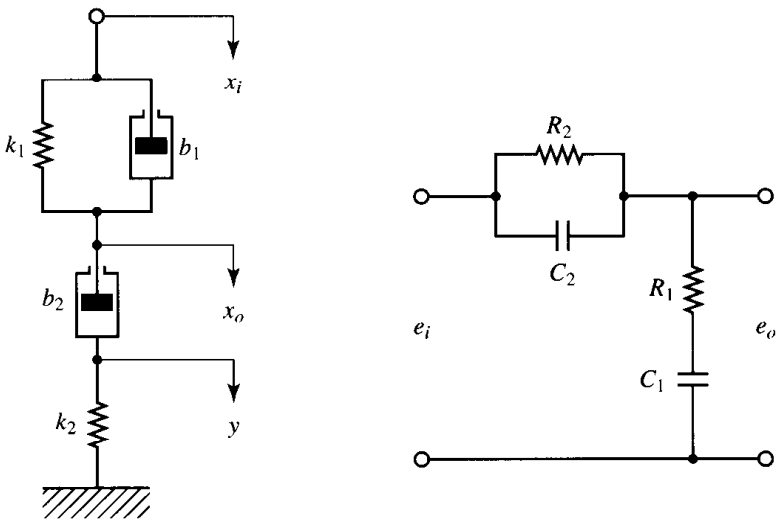

Figure 3–40
(a) Mechanical system; (b) analogous electrical system.

By taking the Laplace transforms of these two equations, assuming zero initial conditions, we have

$$b_1[sX_i(s) - sX_o(s)] + k_1[X_i(s) - X_o(s)] = b_2[sX_o(s) - sY(s)]$$
$$b_2[sX_o(s) - sY(s)] = k_2Y(s)$$

If we eliminate $Y(s)$ from the last two equations, then we obtain

$$b_1[sX_i(s) - sX_o(s)] + k_1[X_i(s) - X_o(s)] = b_2sX_o(s) - b_2s\frac{b_2sX_o(s)}{b_2s + k_2}$$

or

$$(b_1s + k_1)X_i(s) = \left(b_1s + k_1 + b_2s - b_2s\frac{b_2s}{b_2s + k_2}\right)X_o(s)$$

Hence the transfer function $X_o(s)/X_i(s)$ can be obtained as

$$\frac{X_o(s)}{X_i(s)} = \frac{\left(\frac{b_1}{k_1}s + 1\right)\left(\frac{b_2}{k_2}s + 1\right)}{\left(\frac{b_1}{k_1}s + 1\right)\left(\frac{b_2}{k_2}s + 1\right) + \frac{b_2}{k_1}s}$$

For the electrical system shown in Figure 3–40(b), the transfer function $E_o(s)/E_i(s)$ is found to be

$$\frac{E_o(s)}{E_i(s)} = \frac{R_1 + \frac{1}{C_1s}}{\frac{1}{(1/R_2) + C_2s} + R_1 + \frac{1}{C_1s}}$$
$$= \frac{(R_1C_1s + 1)(R_2C_2s + 1)}{(R_1C_1s + 1)(R_2C_2s + 1) + R_2C_1s}$$

A comparison of the transfer functions shows that the systems shown in Figures 3–40(a) and (b) are analogous.

A-3-13. In the liquid-level system of Figure 3–41, assume that the outflow rate Q m^3/sec through the outflow valve is related to the head H m by

$$Q = K\sqrt{H} = 0.01\sqrt{H}$$

Assume also that when the inflow rate Q_i is 0.015 m^3/sec the head stays constant. At $t = 0$ the inflow valve is closed and so there is no inflow for $t \geq 0$. Find the time necessary to empty the tank to half the original head. The capacitance C of the tank is 2 m^2.

Solution. When the head is stationary, the inflow rate equals the outflow rate. Thus head H_o at $t = 0$ is obtained from

$$0.015 = 0.01\sqrt{H_o}$$

or

$$H_o = 2.25 \text{ m}$$

The equation for the system for $t > 0$ is

$$-C\,dH = Q\,dt$$

or

$$\frac{dH}{dt} = -\frac{Q}{C} = \frac{-0.01\sqrt{H}}{2}$$

Hence

$$\frac{dH}{\sqrt{H}} = -0.005\,dt$$

Assume that, at $t = t_1$, $H = 1.125$ m. Integrating both sides of this last equation, we obtain

$$\int_{2.25}^{1.125} \frac{dH}{\sqrt{H}} = \int_0^{t_1} (-0.005)\,dt = -0.005t_1$$

It follows that

$$2\sqrt{H}\Big|_{2.25}^{1.125} = 2\sqrt{1.125} - 2\sqrt{2.25} = -0.005t_1$$

or

$$t_1 = 175.7$$

Thus, the head becomes half the original value (2.25 m) in 175.7 sec.

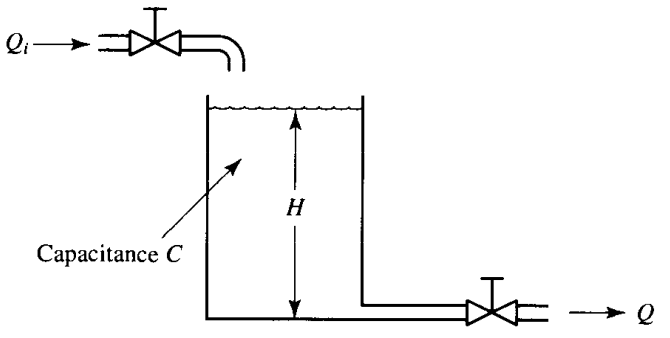

Figure 3–41
Liquid-level system.

A-3-14. Consider the liquid-level system shown in Figure 3–42. At steady state, the inflow rate and outflow rate are both $\bar{Q}$ and the flow rate between the tanks is zero. The heads of tanks 1 and 2 are both $\bar{H}$. At $t = 0$, the inflow rate is changed from $\bar{Q}$ to $\bar{Q} + q$, where q is a small change in the inflow rate. The resulting changes in the heads (h_1 and h_2) and flow rates (q_1 and q_2) are assumed to be small. The capacitances of tanks 1 and 2 are C_1 and C_2, respectively. The resistance of the valve between the tanks is R_1 and that of the outflow valve is R_2.

Derive mathematical models for the system when (a) q is the input and h_2 the output, (b) q is the input and q_2 the output, and (c) q is the input and h_1 the output.

Solution. (a) For tank 1, we have

$$C_1\,dh_1 = q_1\,dt$$

where

$$q_1 = \frac{h_2 - h_1}{R_1}$$

Consequently,

$$R_1C_1\frac{dh_1}{dt} + h_1 = h_2 \tag{3–98}$$

For tank 2, we get

$$C_2\,dh_2 = (q - q_1 - q_2)\,dt$$

where

$$q_1 = \frac{h_2 - h_1}{R_1}, \qquad q_2 = \frac{h_2}{R_2}$$

It follows that

$$R_2C_2\frac{dh_2}{dt} + \frac{R_2}{R_1}h_2 + h_2 = R_2q + \frac{R_2}{R_1}h_1 \tag{3–99}$$

By eliminating h_1 from Equations (3–98) and (3–99), we have

$$R_1C_1R_2C_2\frac{d^2h_2}{dt^2} + (R_1C_1 + R_2C_2 + R_2C_1)\frac{dh_2}{dt} + h_2 = R_1R_2C_1\frac{dq}{dt} + R_2q \tag{3–100}$$

In terms of the transfer function, we have

$$\frac{H_2(s)}{Q(s)} = \frac{R_2(R_1C_1s + 1)}{R_1C_1R_2C_2s^2 + (R_1C_1 + R_2C_2 + R_2C_1)s + 1}$$

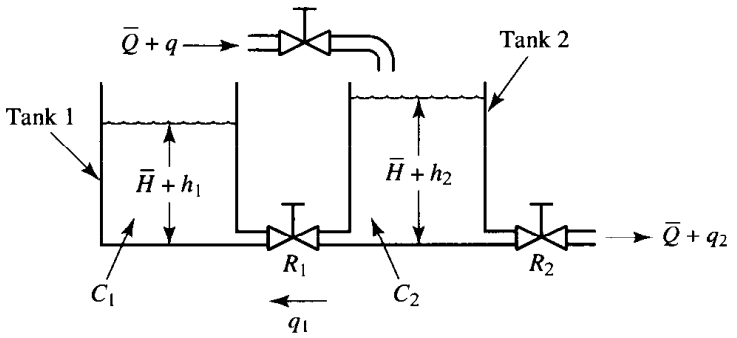

Figure 3–42
Liquid-level system.

This is the desired mathematical model in which q is considered the input and h_2 is the output.
(b) Substitution of $h_2 = R_2 q_2$ into Equation (3–100) gives

$$R_1C_1R_2C_2\frac{d^2q_2}{dt^2} + (R_1C_1 + R_2C_2 + R_2C_1)\frac{dq_2}{dt} + q_2 = R_1C_1\frac{dq}{dt} + q$$

This equation is a mathematical model of the system when q is considered the input and q_2 is the output. In terms of the transfer function, we obtain

$$\frac{Q_2(s)}{Q(s)} = \frac{R_1C_1s + 1}{R_1C_1R_2C_2s^2 + (R_1C_1 + R_2C_2 + R_2C_1)s + 1}$$

(c) Elimination of h_2 from Equations (3–98) and (3–99) yields

$$R_1C_1R_2C_2\frac{d^2h_1}{dt^2} + (R_1C_1 + R_2C_2 + R_2C_1)\frac{dh_1}{dt} + h_1 = R_2q$$

which is a mathematical model of the system in which q is considered the input and h_1 is the output. In terms of the transfer function, we get

$$\frac{H_1(s)}{Q(s)} = \frac{R_2}{R_1C_1R_2C_2s^2 + (R_1C_1 + R_2C_2 + R_2C_1)s + 1}$$

A-3-15. Consider the liquid-level system shown in Figure 3–43. In the system, $\bar{Q}_1$ and $\bar{Q}_2$ are steady-state inflow rates and $\bar{H}_1$ and $\bar{H}_2$ are steady-state heads. The quantities $q_{i1}, q_{i2}, h_1, h_2, q_1$, and q_o are considered small. Obtain a state-space representation for the system when h_1 and h_2 are the outputs and q_{i1} and q_{i2} are the inputs.

Solution. The equations for the system are

$$C_1dh_1 = (q_{i1} - q_1)\,dt \tag{3–101}$$

$$\frac{h_1 - h_2}{R_1} = q_1 \tag{3–102}$$

$$C_2dh_2 = (q_1 + q_{i2} - q_o)\,dt \tag{3–103}$$

$$\frac{h_2}{R_2} = q_o \tag{3–104}$$

Elimination of q_1 from Equation (3–101) using Equation (3–102) results in

$$\frac{dh_1}{dt} = \frac{1}{C_1}\left(q_{i1} - \frac{h_1 - h_2}{R_1}\right) \tag{3–105}$$

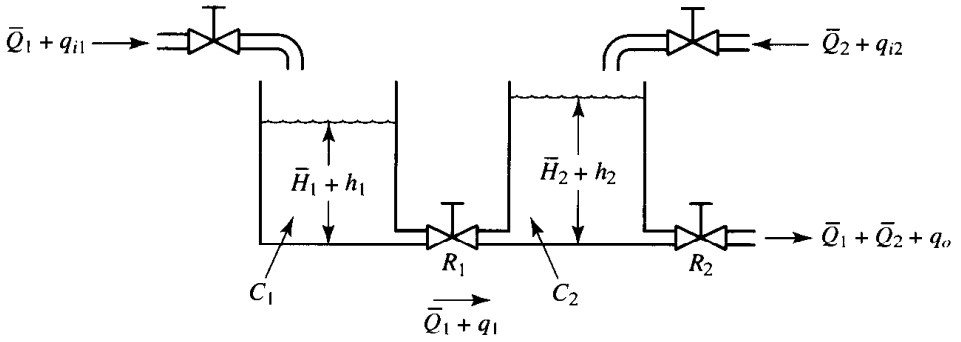

Figure 3–43
Liquid-level system.

Eliminating q_1 and q_o from Equation (3–103) by using Equations (3–102) and (3–104) gives

$$\frac{dh_2}{dt} = \frac{1}{C_2}\left(\frac{h_1 - h_2}{R_1} + q_{i2} - \frac{h_2}{R_2}\right) \tag{3–106}$$

Define state variables x_1 and x_2 by

$$x_1 = h_1$$
$$x_2 = h_2$$

the input variables u_1 and u_2 by

$$u_1 = q_{i1}$$
$$u_2 = q_{i2}$$

and the output variables y_1 and y_2 by

$$y_1 = h_1 = x_1$$
$$y_2 = h_2 = x_2$$

Then Equations (3–105) and (3–106) can be written as

$$\dot{x}_1 = -\frac{1}{R_1C_1}x_1 + \frac{1}{R_1C_1}x_2 + \frac{1}{C_1}u_1$$
$$\dot{x}_2 = \frac{1}{R_1C_2}x_1 - \left(\frac{1}{R_1C_2} + \frac{1}{R_2C_2}\right)x_2 + \frac{1}{C_2}u_2$$

In the form of the standard vector-matrix representation, we have

$$\begin{bmatrix}\dot{x}_1\\ \dot{x}_2\end{bmatrix} = \begin{bmatrix}-\dfrac{1}{R_1C_1} & \dfrac{1}{R_1C_1}\\ \dfrac{1}{R_1C_2} & -\left(\dfrac{1}{R_1C_2} + \dfrac{1}{R_2C_2}\right)\end{bmatrix}\begin{bmatrix}x_1\\ x_2\end{bmatrix} + \begin{bmatrix}\dfrac{1}{C_1} & 0\\ 0 & \dfrac{1}{C_2}\end{bmatrix}\begin{bmatrix}u_1\\ u_2\end{bmatrix}$$

which is the state equation, and

$$\begin{bmatrix}y_1\\ y_2\end{bmatrix} = \begin{bmatrix}1 & 0\\ 0 & 1\end{bmatrix}\begin{bmatrix}x_1\\ x_2\end{bmatrix}$$

which is the output equation.

A-3-16. Considering small deviations from steady-state operation, draw a block diagram of the air heating system shown in Figure 3–44. Assume that the heat loss to the surroundings and the heat capacitance of the metal parts of the heater are negligible.

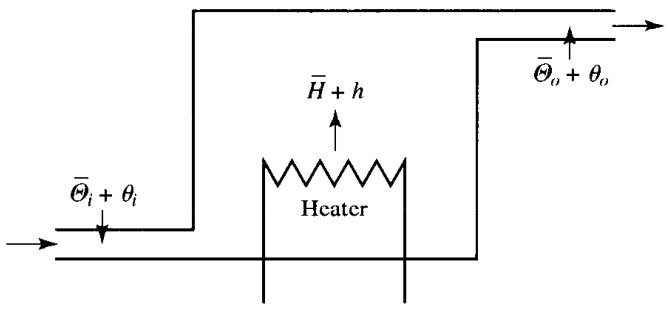

Figure 3–44
Air heating system.

Solution. Let us define

$\bar{\Theta}_i$ = steady-state temperature of inlet air, °C

$\bar{\Theta}_o$ = steady-state temperature of outlet air, °C

G = mass flow rate of air through the heating chamber, kg/sec

M = mass of air contained in the heating chamber, kg

c = specific heat of air, kcal/kg °C

R = thermal resistance, °C sec/kcal

C = thermal capacitance of air contained in the heating chamber = Mc, kcal/°C

$\bar{H}$ = steady-state heat input, kcal/sec

Let us assume that the heat input is suddenly changed from $\bar{H}$ to $\bar{H} + h$ and the inlet air temperature is suddenly changed from $\bar{\Theta}_i$ to $\bar{\Theta}_i + \theta_i$. Then the outlet air temperature will be changed from $\bar{\Theta}_o$ to $\bar{\Theta}_o + \theta_o$.

The equation describing the system behavior is

$$C\,d\theta_o = [h + Gc(\theta_i - \theta_o)]\,dt$$

or

$$C\frac{d\theta_o}{dt} = h + Gc(\theta_i - \theta_o)$$

Noting that

$$Gc = \frac{1}{R}$$

we obtain

$$C\frac{d\theta_o}{dt} = h + \frac{1}{R}(\theta_i - \theta_o)$$

or

$$RC\frac{d\theta_o}{dt} + \theta_o = Rh + \theta_i$$

Taking the Laplace transforms of both sides of this last equation and substituting the initial condition that $\theta_o(0) = 0$, we obtain

$$\Theta_o(s) = \frac{R}{RCs + 1}H(s) + \frac{1}{RCs + 1}\Theta_i(s)$$

The block diagram of the system corresponding to this equation is shown in Figure 3–45.

A-3-17. Consider the thin, glass-wall, mercury thermometer system shown in Figure 3–46. Assume that the thermometer is at a uniform temperature $\bar{\Theta}$ °C (ambient temperature) and that at $t = 0$ it is immersed in a bath of temperature $\bar{\Theta} + \theta_b$°C, where θ_b is the bath temperature (which may be constant or changing) measured from the ambient temperature $\bar{\Theta}$. Define the instantaneous thermometer temperature by $\bar{\Theta} + \theta$°C so that θ is the change in the thermometer temperature satisfying the condition that $\theta(0) = 0$. Obtain a mathematical model for the system. Also obtain an electrical analog of the thermometer system.

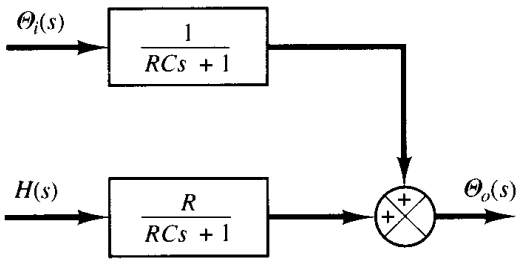

Figure 3–45
Block diagram of the air heating system shown in Figure 3–44.

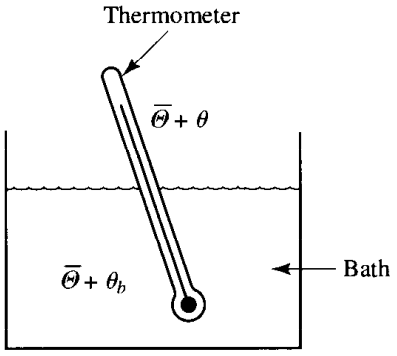

Figure 3–46
Thin, glass-wall, mercury thermometer system.

Solution. A mathematical model for the system can be derived by considering heat balance as follows: The heat entering the thermometer during dt sec is $q\,dt$, where q is the heat flow rate to the thermometer. This heat is stored in the thermal capacitance C of the thermometer, thereby raising its temperature by $d\theta$. Thus the heat-balance equation is

$$C\,d\theta = q\,dt \tag{3–107}$$

Since thermal resistance R may be written as

$$R = \frac{d(\Delta\theta)}{dq} = \frac{\Delta\theta}{q}$$

heat flow rate q may be given, in terms of thermal resistance R, as

$$q = \frac{(\bar{\Theta} + \theta_b) - (\bar{\Theta} + \theta)}{R} = \frac{\theta_b - \theta}{R}$$

where $\bar{\Theta} + \theta_b$ is the bath temperature and $\bar{\Theta} + \theta$ is the thermometer temperature. Hence, we can rewrite Equation (3–107) as

$$C\frac{d\theta}{dt} = \frac{\theta_b - \theta}{R}$$

or

$$RC\frac{d\theta}{dt} + \theta = \theta_b \tag{3–108}$$

Equation (3–108) is a mathematical model of the thermometer system.

Referring to Equation (3–108), an electrical analog for the thermometer system can be written as

$$RC\frac{de_o}{dt} + e_o = e_i$$

An electrical circuit represented by this last equation is shown in Figure 3–47.

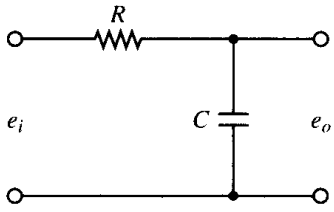

Figure 3–47
Electrical analog of the thermometer system shown in Figure 3–46.

A-3-18. Linearize the nonlinear equation

$$z = xy$$

in the region $5 \leq x \leq 7, 10 \leq y \leq 12$. Find the error if the linearized equation is used to calculate the value of z when $x = 5, y = 10$.

Solution. Since the region considered is given by $5 \leq x \leq 7, 10 \leq y \leq 12$, choose $\bar{x} = 6, \bar{y} = 11$. Then $\bar{z} = \bar{x}\bar{y} = 66$. Let us obtain a linearized equation for the nonlinear equation near a point $\bar{x} = 6, \bar{y} = 11$.

Expanding the nonlinear equation into a Taylor series about point $x = \bar{x}, y = \bar{y}$ and neglecting the higher-order terms, we have

$$z - \bar{z} = a(x - \bar{x}) + b(y - \bar{y})$$

where

$$a = \left.\frac{\partial(xy)}{\partial x}\right|_{x=\bar{x}, y=\bar{y}} = \bar{y} = 11$$

$$b = \left.\frac{\partial(xy)}{\partial y}\right|_{x=\bar{x}, y=\bar{y}} = \bar{x} = 6$$

Hence the linearized equation is

$$z - 66 = 11(x - 6) + 6(y - 11)$$

or

$$z = 11x + 6y - 66$$

When $x = 5, y = 10$, the value of z given by the linearized equation is

$$z = 11x + 6y - 66 = 55 + 60 - 66 = 49$$

The exact value of z is $z = xy = 50$. The error is thus $50 - 49 = 1$. In terms of percentage, the error is 2%.

A-3-19. Consider the liquid-level system shown in Figure 3–48. At steady state the inflow rate is $Q_i = \bar{Q}$, the outflow rate is $Q_o = \bar{Q}$, and head is $H = \bar{H}$. If the flow is turbulent, then we have

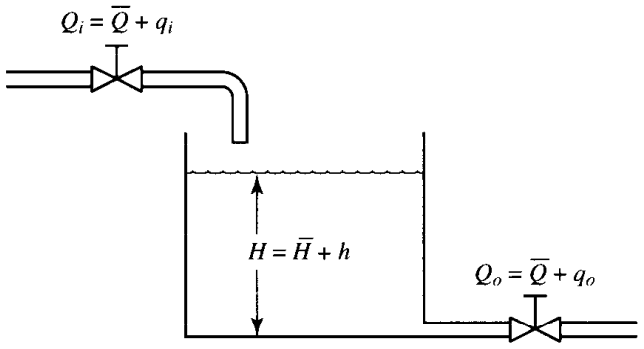

Figure 3–48
Liquid-level system.

$$\bar{Q} = K\sqrt{\bar{H}}$$

Assume that at $t = 0$ the inflow rate is changed from $Q_i = \bar{Q}$ to $Q_i = \bar{Q} + q_i$. This change causes the head to change from $H = \bar{H}$ to $H = \bar{H} + h$, which, in turn, causes the outflow rate to change from $Q_o = \bar{Q}$ to $Q_o = \bar{Q} + q_o$. For this system we have

$$C\frac{dH}{dt} = Q_i - Q_o = Q_i - K\sqrt{H}$$

where C is the capacitance of the tank. Let us define

$$\frac{dH}{dt} = f(H, Q_i) = \frac{1}{C}Q_i - \frac{K\sqrt{H}}{C} \tag{3–109}$$

Note that the steady-state operating condition is $(\bar{H}, \bar{Q})$ and $H = \bar{H} + h$, $Q_i = \bar{Q} + q_i$. Since at steady-state operation $dH/dt = 0$, we have $f(\bar{H}, \bar{Q}) = 0$.

Linearize Equation (3–109) near the operating point $(\bar{H}, \bar{Q})$.

Solution. Using the linearization technique presented in Section 3–10, a linearized equation for Equation (3–109) can be obtained as follows:

$$\frac{dH}{dt} - f(\bar{H}, \bar{Q}) = \frac{\partial f}{\partial H}(H - \bar{H}) + \frac{\partial f}{\partial Q_i}(Q_i - \bar{Q}) \tag{3–110}$$

where

$$f(\bar{H}, \bar{Q}) = 0$$

$$\left.\frac{\partial f}{\partial H}\right|_{H=\bar{H},\, Q_i=\bar{Q}} = -\frac{K}{2C\sqrt{\bar{H}}} = -\frac{\bar{Q}}{\sqrt{\bar{H}}}\frac{1}{2C\sqrt{\bar{H}}} = -\frac{\bar{Q}}{2C\bar{H}} = -\frac{1}{RC}$$

where we used the resistance R defined by

$$R = \frac{2\bar{H}}{\bar{Q}}$$

Also,

$$\left.\frac{\partial f}{\partial Q_i}\right|_{H=\bar{H},\, Q_i=\bar{Q}} = \frac{1}{C}$$

Then Equation (3–110) can be written as

$$\frac{dH}{dt} = -\frac{1}{RC}(H - \bar{H}) + \frac{1}{C}(Q_i - \bar{Q}) \tag{3–111}$$

Since $H - \bar{H} = h$ and $Q_i - \bar{Q} = q_i$, Equation (3–111) can be written as

$$\frac{dh}{dt} = -\frac{1}{RC}h + \frac{1}{C}q_i$$

or

$$RC\frac{dh}{dt} + h = Rq_i$$

which is the linearized equation for the liquid-level system and is the same as Equation (3–69) that we obtained in Section 3–8.

A-3-20. Consider the hydraulic servo system shown in Figure 3–49. Assuming that the load reaction forces are not negligible, derive a mathematical model of the system. Assume also that the mass of the power piston is included in the load mass m.

Solution. In deriving a mathematical model of the system when the load reactive forces are not negligible, such effects as the pressure drop across the orifice, the leakage of oil around the valve and around the piston, and the compressibility of the oil must be considered.

The pressure drop across the orifice is a function of the supply pressure p_s and the pressure difference $\Delta p = p_1 - p_2$. Thus the flow rate q is a nonlinear function of valve displacement x and pressure difference Δp or

$$q = f(x, \Delta p)$$

Linearizing this nonlinear equation about the origin ($x = 0, \Delta p = 0, q = 0$), we obtain, referring to Equation (3–82),

$$q = K_1 x - K_2 \Delta p \tag{3–112}$$

The flow rate q can be considered as consisting of three parts

$$q = q_0 + q_L + q_C \tag{3–113}$$

where q_0 = useful flow rate to the power cylinder causing power piston to move, kg/sec
q_L = leakage flow rate, kg/sec
q_C = equivalent compressibility flow rate, kg/sec

Let us obtain specific expressions for q_0, q_L, and q_C. The flow $q_0\,dt$ to the left-hand side of the power piston causes the piston to move to the right by dy. So we have

$$A\varrho\,dy = q_0\,dt$$

where A (m^2) is the power piston area, ϱ (kg/m^3) the density of oil, and dy (m) the displacement of the power piston. Then

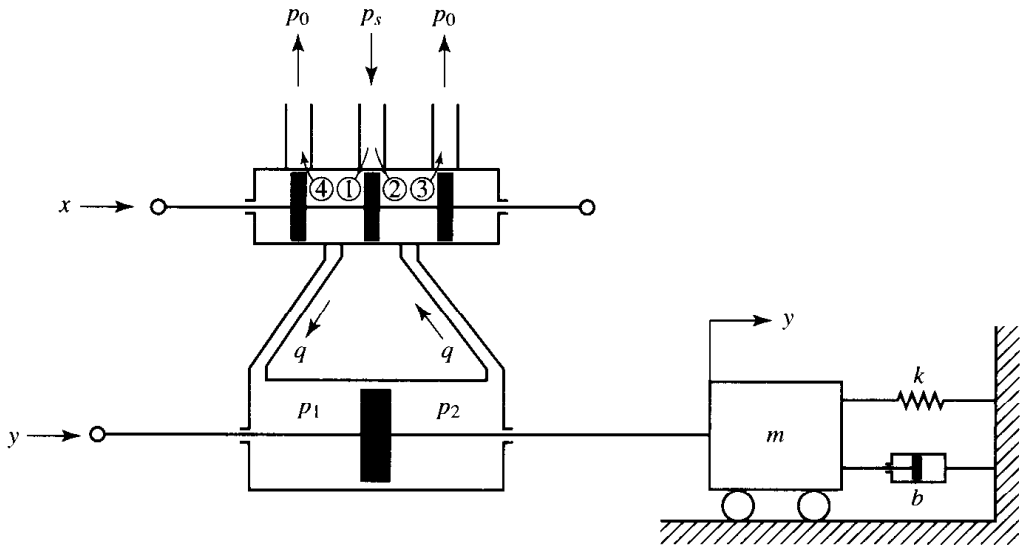

Figure 3–49
Hydraulic servo system.

$$q_0 = A\varrho \frac{dy}{dt} \tag{3–114}$$

The leakage component q_L can be written

$$q_L = L\,\Delta p \tag{3–115}$$

where L is the leakage coefficient of the system.

The equivalent compressibility flow rate q_C can be expressed in terms of the effective bulk modulus K of oil (including the effects of entrapped air, expansion of pipes, etc.), where

$$K = \frac{d\,\Delta p}{-dV/V}$$

(Here dV is negative and so $-dV$ is positive.) Rewriting this last equation gives

$$-dV = \frac{V}{K} d\,\Delta p$$

or

$$\varrho \frac{-dV}{dt} = \frac{\varrho V}{K} \frac{d\,\Delta p}{dt}$$

Noting that $q_C = \varrho(-dV)/dt$, we find

$$q_C = \frac{\varrho V}{K} \frac{d\,\Delta p}{dt} \tag{3–116}$$

where V is the effective volume of oil under compression (that is, approximately half the total power cylinder volume).

Using Equations (3–112) through (3–116),

$$q = K_1 x - K_2\,\Delta p = A\varrho \frac{dy}{dt} + L\,\Delta p + \frac{\varrho V}{K} \frac{d\,\Delta p}{dt}$$

or

$$A\varrho \frac{dy}{dt} + \frac{\varrho V}{K} \frac{d\Delta p}{dt} + (L + K_2)\,\Delta p = K_1 x \tag{3–117}$$

The force developed by the power piston is $A\,\Delta p$, and this force is applied to the load elements. Thus

$$m \frac{d^2y}{dt^2} + b \frac{dy}{dt} + ky = A\,\Delta p \tag{3–118}$$

Eliminating Δp from Equations (3–117) and (3–118) results in

$$\frac{\varrho Vm}{KA} \frac{d^3y}{dt^3} + \left[\frac{\varrho Vb}{KA} + \frac{(L + K_2)m}{A}\right] \frac{d^2y}{dt^2} + \left[A\varrho + \frac{\varrho Vk}{KA} + \frac{(L + K_2)b}{A}\right] \frac{dy}{dt} + \frac{(L + K_2)k}{A}\, y = K_1 x$$

This is a mathematical model of the system relating the valve spool displacement x and the power piston displacement y when the load reactive forces are not negligible.

PROBLEMS

B-3-1. Simplify the block diagram shown in Figure 3–50 and obtain the closed-loop transfer function $C(s)/R(s)$.

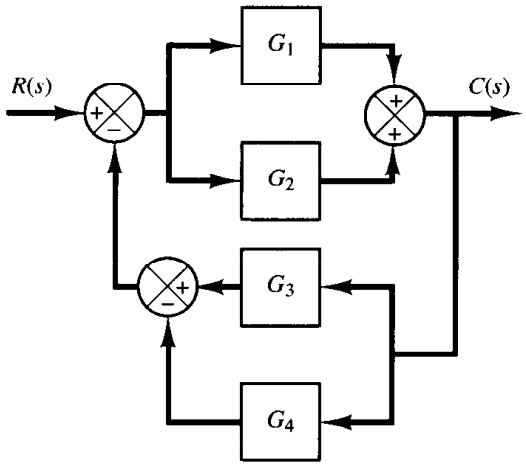

Figure 3–50 Block diagram of a system.

B-3-2. Simplify the block diagram shown in Figure 3–51 and obtain the transfer function $C(s)/R(s)$.

B-3-3. Simplify the block diagram shown in Figure 3–52 and obtain the closed-loop transfer function $C(s)/R(s)$.

B-3-4. Obtain a state-space representation of the system shown in Figure 3–53.

B-3-5. Consider the system described by

$$\dddot{y} + 3\ddot{y} + 2\dot{y} = u$$

Derive a state-space representation of the system.

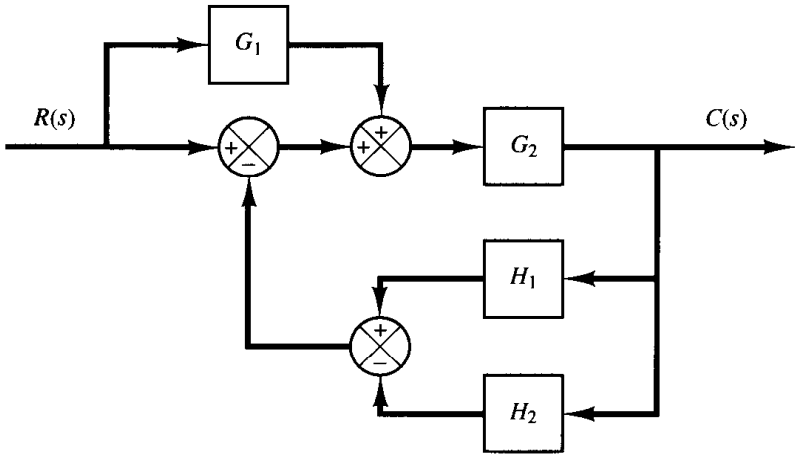

Figure 3–51 Block diagram of a system.

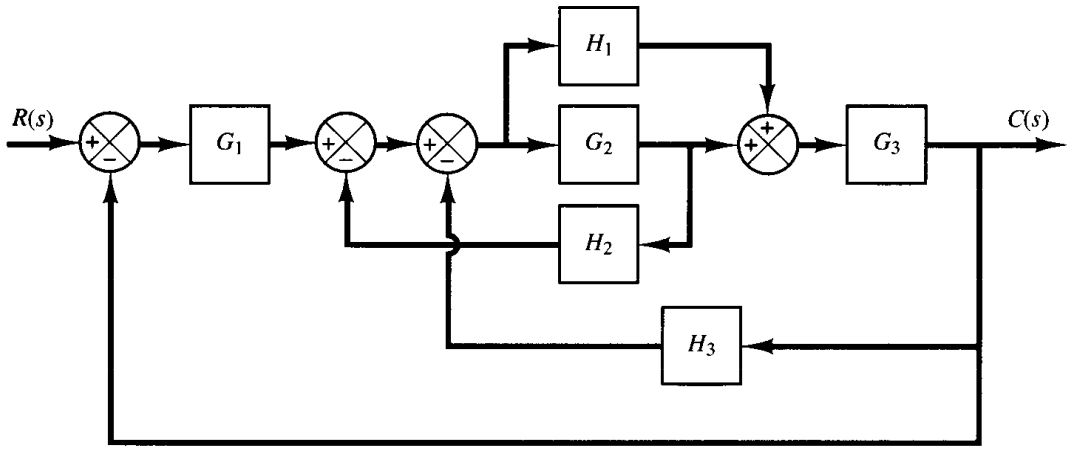

Figure 3–52 Block diagram of a system.

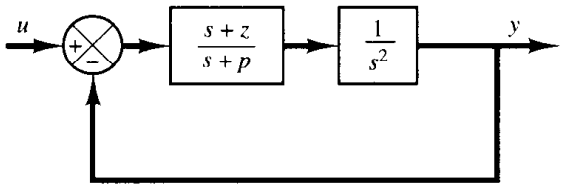

Figure 3–53 Control system.

B-3-6. Consider the system described by

$$\begin{bmatrix} \dot{x}_1 \\ \dot{x}_2 \end{bmatrix} = \begin{bmatrix} -4 & -1 \\ 3 & -1 \end{bmatrix} \begin{bmatrix} x_1 \\ x_2 \end{bmatrix} + \begin{bmatrix} 1 \\ 1 \end{bmatrix} u$$

$$y = [1 \quad 0] \begin{bmatrix} x_1 \\ x_2 \end{bmatrix}$$

Obtain the transfer function of the system.

B-3-7. Obtain the transfer function $X_o(s)/X_i(s)$ of each of the three mechanical systems shown in Figure 3–54. In the diagrams, x_i denotes the input displacement and x_o denotes the output displacement. (Each displacement is measured from its equilibrium position.)

B-3-8. Obtain mathematical models of the mechanical systems shown in Figures 3–55(a) and (b).

B-3-9. Obtain a state-space representation of the mechanical system shown in Figure 3–56, where u_1 and u_2 are the inputs and y_1 and y_2 are the outputs.

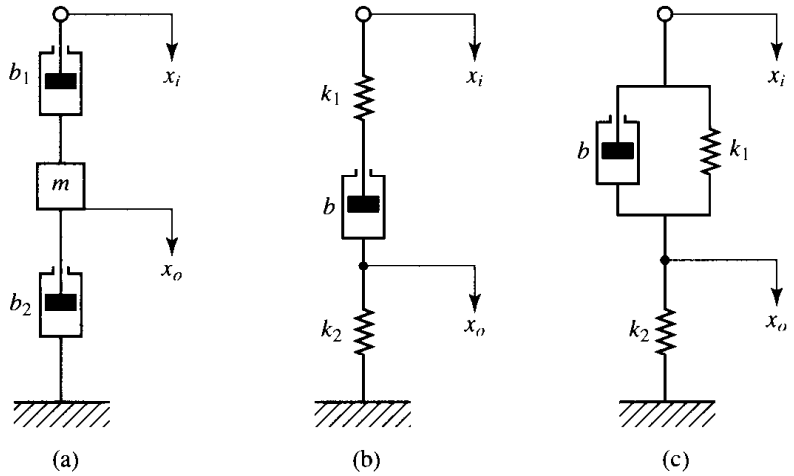

Figure 3–54 Mechanical systems.

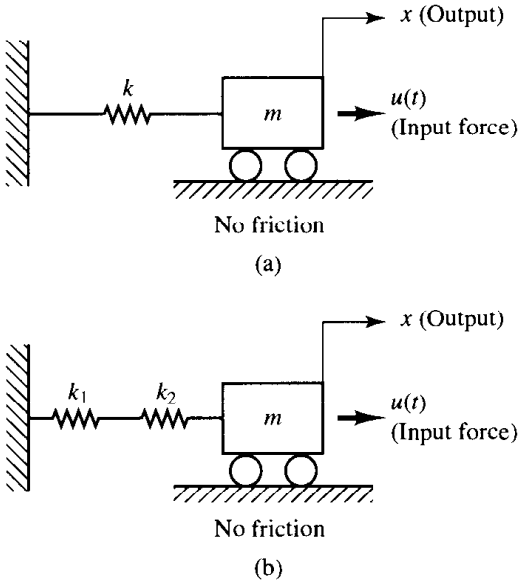

Figure 3–55 Mechanical systems.

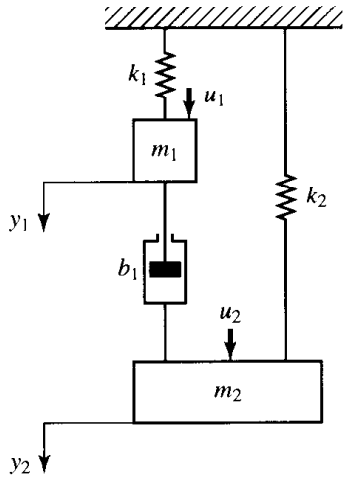

Figure 3–56
Mechanical system.

B-3-10. Consider the spring-loaded pendulum system shown in Figure 3–57. Assume that the spring force acting on the pendulum is zero when the pendulum is vertical, or $\theta = 0$. Assume also that the friction involved is negligible and the angle of oscillation θ is small. Obtain a mathematical model of the system.

B-3-11. Referring to Example 3–4, consider the inverted pendulum system shown in Figure 3–58. Assume that the mass of the inverted pendulum is m and is evenly distributed along the length of the rod. (The center of gravity of the pendulum is located at the center of the rod.) Assuming that θ is small, derive mathematical models for the system in the forms of differential equations, transfer functions, and state-space equations.

B-3-12. Derive the transfer function of the electrical system shown in Figure 3–59. Draw a schematic diagram of an analogous mechanical system.

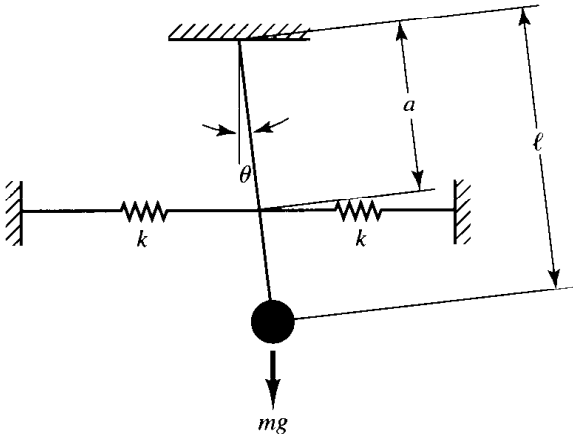

Figure 3–57 Spring-loaded pendulum system.

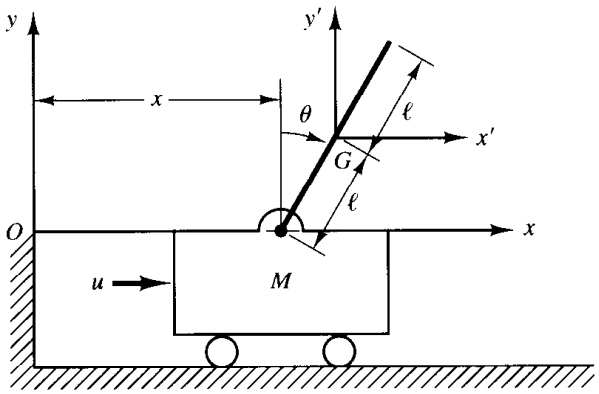

Figure 3–58 Inverted pendulum system.

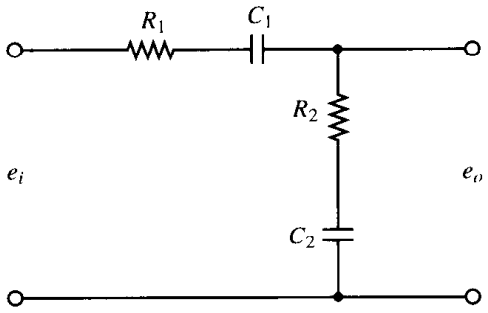

Figure 3–59 Electrical system.

B-3-13. Consider the liquid-level system shown in Figure 3–60. Assuming that $\bar{H} = 3$ m, $\bar{Q} = 0.02$ m³/sec, and the cross-sectional area of the tank is equal to 5 m², obtain the time constant of the system at the operating point $(\bar{H}, \bar{Q})$. Assume that the flow through the valve is turbulent.

B-3-14. Consider the conical water tank system shown in Figure 3–61. The flow through the valve is turbulent and is related to the head H by

$$Q = 0.005\sqrt{H}$$

where Q is the flow rate measured in m³/sec and H is in meters.

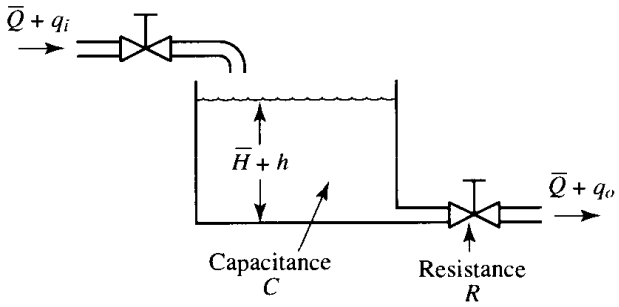

Figure 3–60 Liquid-level system.

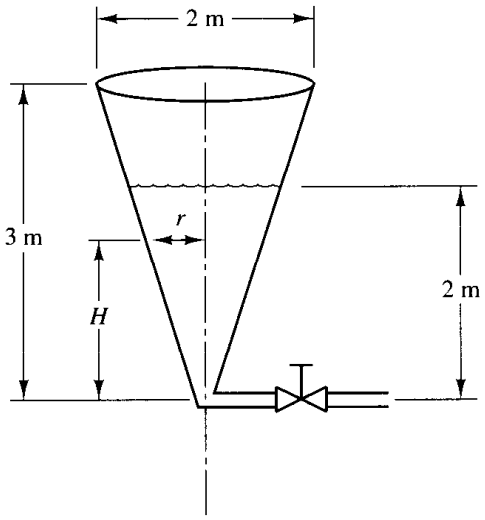

Figure 3–61 Conical water tank system.

Suppose that the head is 2 m at $t = 0$. What will be the head at $t = 60$ sec?

B-3-15. Consider the liquid-level system shown in Figure 3–62. At steady state the inflow rate is $\bar{Q}$ and the outflow rate is also $\bar{Q}$. Assume that at $t = 0$ the inflow rate is changed from $\bar{Q}$ to $\bar{Q} + q_i$, where q_i is a small quantity. The disturbance input is q_d, which is also a small quantity. Draw a block diagram of the system and simplify it to obtain $H_2(s)$ as a function of $Q_i(s)$ and $Q_d(s)$, where $H_2(s) = \mathcal{L}[h_2(t)]$, $Q_i(s) = \mathcal{L}[q_i(t)]$, and $Q_d(s) = \mathcal{L}[q_d(t)]$. The capacitances of tanks 1 and 2 are C_1 and C_2, respectively.

B-3-16. A thermocouple has a time constant of 2 sec. A thermal well has a time constant of 30 sec. When the thermocouple is inserted into the well, this temperature-measuring device can be considered a two-capacitance system.

Determine the time constants of the combined thermocouple–thermal well system. Assume that the weight of the thermocouple is 8 g and the weight of the thermal well is 40 g. Assume also that the specific heats of the thermocouple and thermal well are the same.

B-3-17. Suppose that the flow rate Q and head H in a liquid-level system are related by

$$Q = 0.002\sqrt{H}$$

Obtain a linearized mathematical model relating the flow rate and head near the steady-state operating point $(\bar{H}, \bar{Q})$, where $\bar{H} = 2.25$ m and $\bar{Q} = 0.003$ m³/sec.

B-3-18. Find a linearized equation for

$$y = 0.2x^3$$

about a point $\bar{x} = 2$.

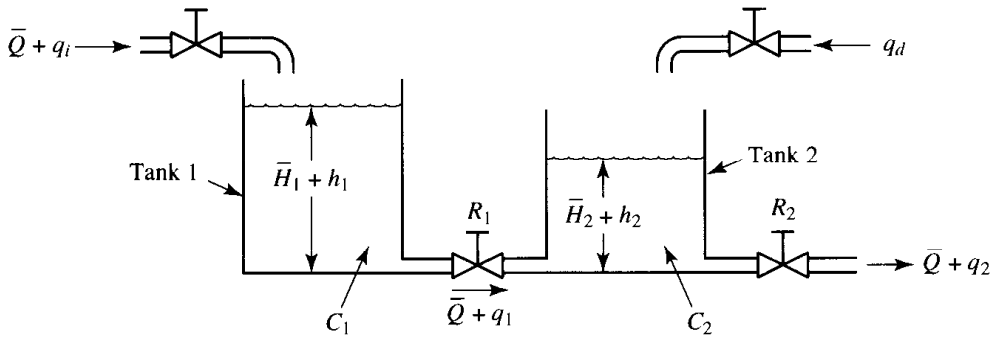

Figure 3–62 Liquid-level system.

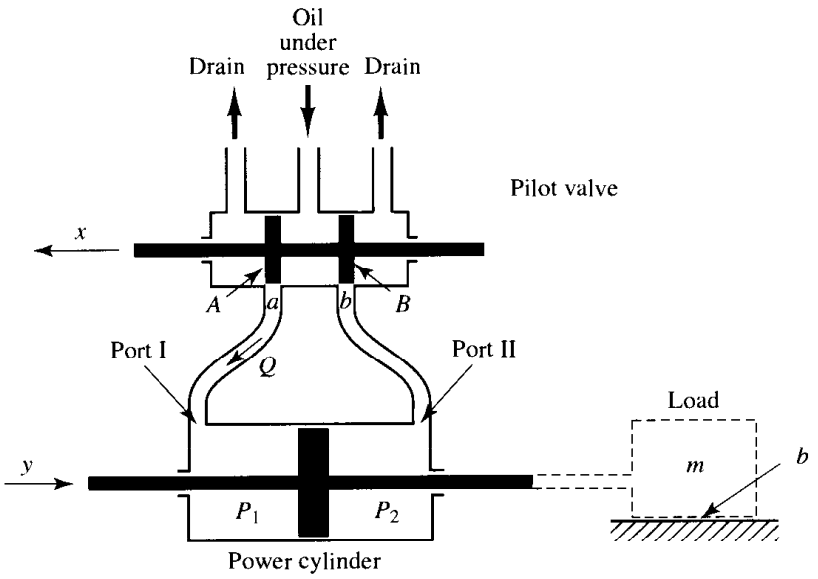

Figure 3–63 Schematic diagram of a hydraulic servomotor.

B-3-19. Linearize the nonlinear equation

$$z = x^2 + 4xy + 6y^2$$

in the region defined by $8 \leq x \leq 10, 2 \leq y \leq 4$.

B-3-20. Consider the hydraulic servomotor shown in Figure 3–63. Derive the transfer function $Y(s)/X(s)$. Assume that the inertia force due to the mass of power piston and shaft is negligible compared with the inertia force due to the load mass m and viscous friction force $b\dot{y}$.

4

Transient-Response Analysis

4–1 INTRODUCTION

It was stated in Chapter 3 that the first step in analyzing a control system was to derive a mathematical model of the system. Once such a model is obtained, various methods are available for the analysis of system performance.

In practice, the input signal to a control system is not known ahead of time but is random in nature, and the instantaneous input cannot be expressed analytically. Only in some special cases is the input signal known in advance and expressible analytically or by curves, such as in the case of the automatic control of cutting tools.

In analyzing and designing control systems, we must have a basis of comparison of performance of various control systems. This basis may be set up by specifying particular test input signals and by comparing the responses of various systems to these input signals.

Many design criteria are based on such signals or on the response of systems to changes in initial conditions (without any test signals). The use of test signals can be justified because of a correlation existing between the response characteristics of a system to a typical test input signal and the capability of the system to cope with actual input signals.

Typical test signals. The commonly used test input signals are those of step functions, ramp functions, acceleration functions, impulse functions, sinusoidal functions, and the like. With these test signals, mathematical and experimental analyses of control systems can be carried out easily since the signals are very simple functions of time.

Which of these typical input signals to use for analyzing system characteristics may be determined by the form of the input that the system will be subjected to most frequently under normal operation. If the inputs to a control system are gradually changing functions of time, then a ramp function of time may be a good test signal. Similarly, if a system is subjected to sudden disturbances, a step function of time may be a good test signal; and for a system subjected to shock inputs, an impulse function may be best. Once a control system is designed on the basis of test signals, the performance of the system in response to actual inputs is generally satisfactory. The use of such test signals enables one to compare the performance of all systems on the same basis.

Transient response and steady-state response. The time response of a control system consists of two parts: the transient and the steady-state response. By transient response, we mean that which goes from the initial state to the final state. By steady-state response, we mean the manner in which the system output behaves as t approaches infinity.

Absolute stability, relative stability, and steady-state error. In designing a control system, we must be able to predict the dynamic behavior of the system from a knowledge of the components. The most important characteristic of the dynamic behavior of a control system is absolute stability, that is, whether the system is stable or unstable. A control system is in equilibrium if, in the absence of any disturbance or input, the output stays in the same state. A linear time-invariant control system is stable if the output eventually comes back to its equilibrium state when the system is subjected to an initial condition. A linear time-invariant control system is critically stable if oscillations of the output continue forever. It is unstable if the output diverges without bound from its equilibrium state when the system is subjected to an initial condition. Actually, the output of a physical system may increase to a certain extent but may be limited by mechanical "stops," or the system may break down or become nonlinear after the output exceeds a certain magnitude so that the linear differential equations no longer apply.

Important system behavior (other than absolute stability) to which we must give careful consideration includes relative stability and steady-state error. Since a physical control system involves energy storage, the output of the system, when subjected to an input, cannot follow the input immediately but exhibits a transient response before a steady state can be reached. The transient response of a practical control system often exhibits damped oscillations before reaching a steady state. If the output of a system at steady state does not exactly agree with the input, the system is said to have steady-state error. This error is indicative of the accuracy of the system. In analyzing a control system, we must examine transient-response behavior and steady-state behavior.

Outline of the chapter. This chapter is concerned with system responses to aperiodic signals (such as step, ramp, acceleration, and impulse functions of time). The outline of the chapter is as follows: Section 4–1 has presented introductory material for the chapter. Section 4–2 treats the response of first-order systems to aperiodic inputs. Section 4–3 deals with the transient response of the second-order systems. Detailed analyses of the step response, ramp response, and impulse response of the second-order systems are presented. (The transient response analysis of higher-order systems is discussed in Chapter 5.) Section 4–4 gives an introduction to the MATLAB approach

to the solution of transient response. Section 4–5 presents an example of a transient-response problem solved with MATLAB.

4–2 FIRST-ORDER SYSTEMS

Consider the first-order system shown in Figure 4–1(a). Physically, this system may represent an RC circuit, thermal system, or the like. A simplified block diagram is shown in Figure 4–1(b). The input–output relationship is given by

$$\frac{C(s)}{R(s)} = \frac{1}{Ts + 1} \tag{4–1}$$

In the following, we shall analyze the system responses to such inputs as the unit-step, unit-ramp, and unit-impulse functions. The initial conditions are assumed to be zero.

Note that all systems having the same transfer function will exhibit the same output in response to the same input. For any given physical system, the mathematical response can be given a physical interpretation.

Unit-step response of first-order systems. Since the Laplace transform of the unit-step function is $1/s$, substituting $R(s) = 1/s$ into Equation (4–1), we obtain

$$C(s) = \frac{1}{Ts + 1}\frac{1}{s}$$

Expanding $C(s)$ into partial fractions gives

$$C(s) = \frac{1}{s} - \frac{T}{Ts + 1} = \frac{1}{s} - \frac{1}{s + (1/T)} \tag{4–2}$$

Taking the inverse Laplace transform of Equation (4–2), we obtain

$$c(t) = 1 - e^{-t/T}, \qquad \text{for } t \geq 0 \tag{4–3}$$

Equation (4–3) states that initially the output $c(t)$ is zero and finally it becomes unity. One important characteristic of such an exponential response curve $c(t)$ is that at $t = T$ the value of $c(t)$ is 0.632, or the response $c(t)$ has reached 63.2% of its total change. This may be easily seen by substituting $t = T$ in $c(t)$. That is,

$$c(T) = 1 - e^{-1} = 0.632$$

Note that the smaller the time constant T, the faster the system response. Another important characteristic of the exponential response curve is that the slope of the tangent line at $t = 0$ is $1/T$, since

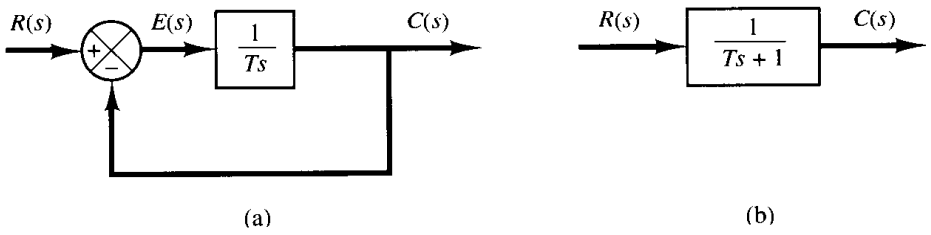

Figure 4–1
(a) Block diagram of a first-order system; (b) simplified block diagram.

$$\frac{dc}{dt} = \frac{1}{T} e^{-t/T} \bigg|_{t=0} = \frac{1}{T} \tag{4-4}$$

The output would reach the final value at $t = T$ if it maintained its initial speed of response. From Equation (4–4) we see that the slope of the response curve $c(t)$ decreases monotonically from $1/T$ at $t = 0$ to zero at $t = \infty$.

The exponential response curve $c(t)$ given by Equation (4–3) is shown in Figure 4–2. In one time constant, the exponential response curve has gone from 0 to 63.2% of the final value. In two time constants, the response reaches 86.5% of the final value. At $t = 3T$, $4T$, and $5T$, the response reaches 95%, 98.2%, and 99.3%, respectively, of the final value. Thus, for $t \geq 4T$, the response remains within 2% of the final value. As seen from Equation (4–3), the steady state is reached mathematically only after an infinite time. In practice, however, a reasonable estimate of the response time is the length of time the response curve needs to reach the 2% line of the final value, or four time constants.

Consider the system shown in Figure 4–3. To determine experimentally whether or not the system is of first order, plot the curve $\log |c(t) - c(\infty)|$, where $c(t)$ is the system output, as a function of t. If the curve turns out to be a straight line, the system is of first order. The time constant T can be read from the graph as the time T that satisfies the following equation:

$$c(T) - c(\infty) = 0.368\,[c(0) - c(\infty)]$$

Note that instead of plotting $\log |c(t) - c(\infty)|$ versus t it is convenient to plot $|c(t) - c(\infty)|/|c(0) - c(\infty)|$ versus t on semilog paper, as shown in Figure 4–4.

Unit-ramp response of first-order systems. Since the Laplace transform of the unit-ramp function is $1/s^2$, we obtain the output of the system of Figure 4–1(a) as

$$C(s) = \frac{1}{Ts + 1} \frac{1}{s^2}$$

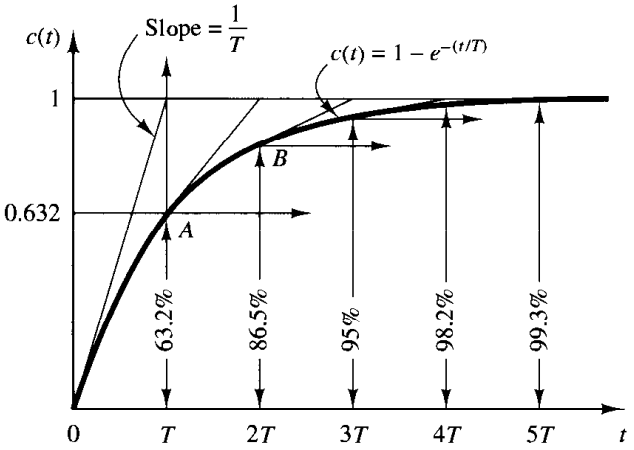

Figure 4–2
Exponential response curve.

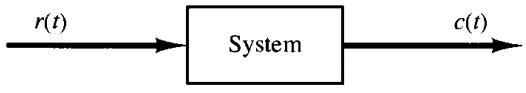

Figure 4–3
A general system.

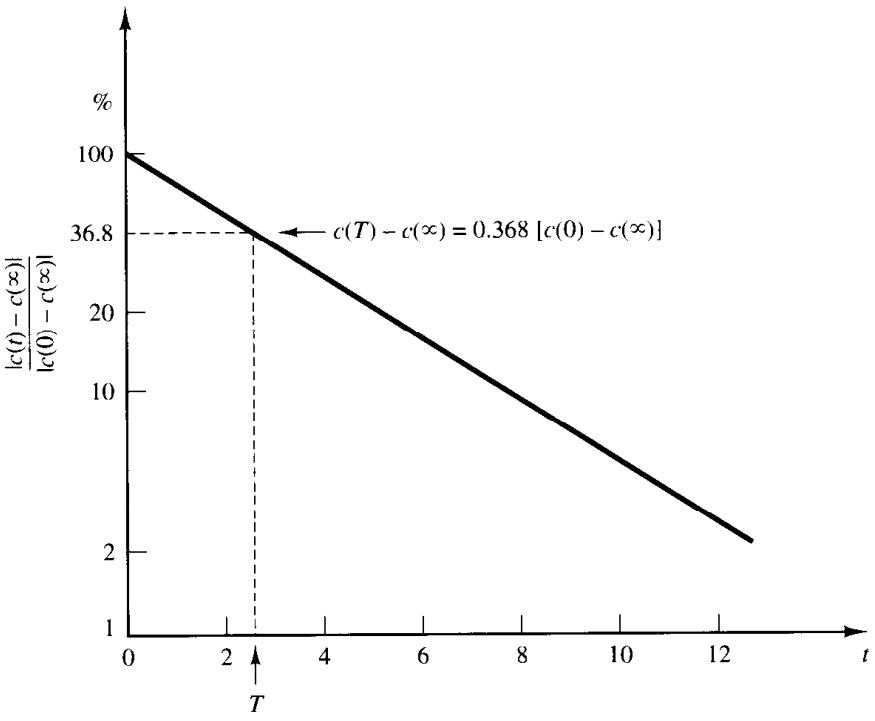

Figure 4–4
Plot of $|c(t) - c(\infty)| / |c(0) - c(\infty)|$ versus t on semilog paper.

Expanding $C(s)$ into partial fractions gives

$$C(s) = \frac{1}{s^2} - \frac{T}{s} + \frac{T^2}{Ts + 1} \tag{4–5}$$

Taking the inverse Laplace transform of Equation (4–5), we obtain

$$c(t) = t - T + Te^{-t/T}, \qquad \text{for } t \geq 0$$

The error signal $e(t)$ is then

$$\begin{aligned} e(t) &= r(t) - c(t) \\ &= T(1 - e^{-t/T}) \end{aligned}$$

As t approaches infinity, $e^{-t/T}$ approaches zero, and thus the error signal $e(t)$ approaches T or

$$e(\infty) = T$$

The unit-ramp input and the system output are shown in Figure 4–5. The error in following the unit-ramp input is equal to T for sufficiently large t. The smaller the time constant T, the smaller the steady-state error in following the ramp input.

Unit-impulse response of first-order systems. For the unit-impulse input, $R(s) = 1$ and the output of the system of Figure 4–1(a) can be obtained as

$$C(s) = \frac{1}{Ts + 1}$$

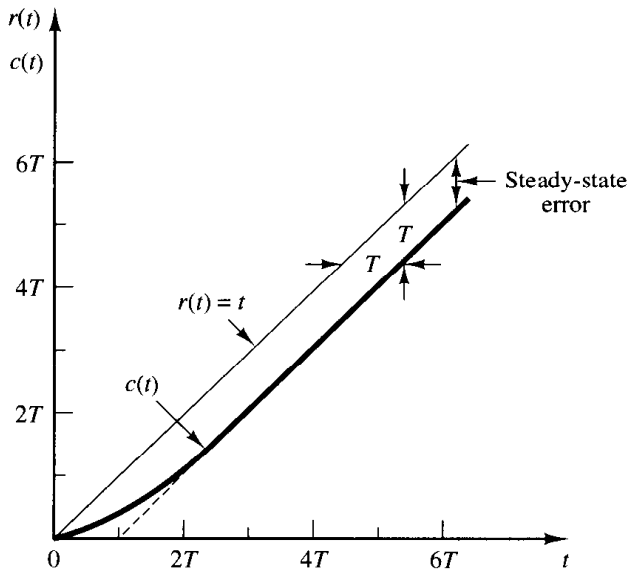

Figure 4–5
Unit-ramp response of the system shown in Figure 4–1(a).

or

$$c(t) = \frac{1}{T} e^{-t/T}, \qquad \text{for } t \geq 0 \tag{4–6}$$

The response curve given by Equation (4–6) is shown in Figure 4–6.

An important property of linear time-invariant systems. In the analysis above, it has been shown that for the unit-ramp input the output $c(t)$ is

$$c(t) = t - T + Te^{-t/T}, \qquad \text{for } t \geq 0$$

For the unit-step input, which is the derivative of unit-ramp input, the output $c(t)$ is

$$c(t) = 1 - e^{-t/T}, \qquad \text{for } t \geq 0$$

Finally, for the unit-impulse input, which is the derivative of unit-step input, the output $c(t)$ is

$$c(t) = \frac{1}{T} e^{-t/T}, \qquad \text{for } t \geq 0$$

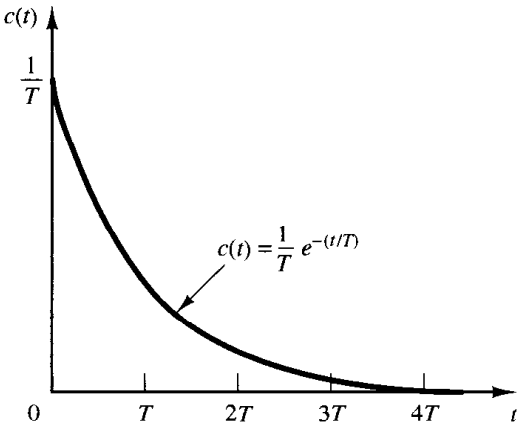

Figure 4–6
Unit-impulse response of the system shown in Figure 4–1(a).

Comparison of the system responses to these three inputs clearly indicates that the response to the derivative of an input signal can be obtained by differentiating the response of the system to the original signal. It can also be seen that the response to the integral of the original signal can be obtained by integrating the response of the system to the original signal and by determining the integration constants from the zero output initial condition. This is a property of linear time-invariant systems. Linear time-varying systems and nonlinear systems do not possess this property.

EXAMPLE 4–1 Consider the liquid-level control system shown in Figure 4–7(a). (The controller is assumed to be a proportional controller; that is, the output of the controller is proportional to the input of the controller.) We assume that all the variables, r, q_i, h, and q_o are measured from their respective steady-state values $\bar{R}$, $\bar{Q}$, $\bar{H}$, and $\bar{Q}$. We also assume that the magnitudes of the variables r, q_i, h, and q_o are sufficiently small so that the system can be approximated by a linear mathematical model.

Referring to Section 3–8, we can obtain the transfer function of the liquid-level system as

$$\frac{H(s)}{Q_i(s)} = \frac{R}{RCs + 1}$$

Since the controller is a proportional controller, the change in inflow q_i is proportional to the actuating error e so that $q_i = K_p K_v e$, where K_p is the gain of the controller and K_v is the gain of the control valve. In terms of Laplace-transformed quantities,

$$Q_i(s) = K_p K_v E(s)$$

A block diagram of this system is shown in Figure 4–7(b). A simplified block diagram is given in Figure 4–7(c), where $X(s) = (1/K_b)R(s)$, $K = K_p K_v R K_b$, and $T = RC$.

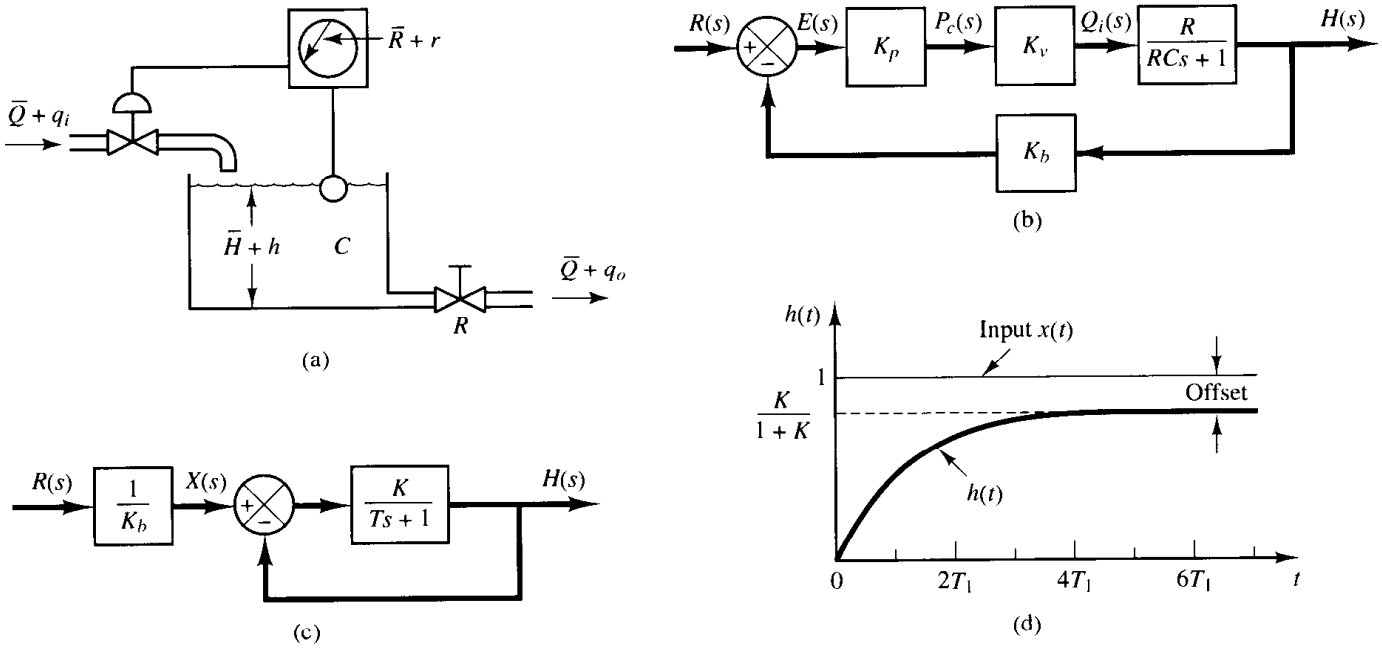

Figure 4–7
(a) Liquid-level control system; (b) block diagram; (c) simplified block diagram; (d) curve $h(t)$ versus t.

In what follows we shall investigate the response $h(t)$ to a change in the reference input. We shall assume a unit-step change in $x(t)$, where $x(t) = (1/K_b)r(t)$. The closed-loop transfer function between $H(s)$ and $X(s)$ is given by

$$\frac{H(s)}{X(s)} = \frac{K}{Ts + 1 + K} \tag{4-7}$$

Since the Laplace transform of the unit-step function is $1/s$, substituting $X(s) = 1/s$ into Equation (4–7) gives

$$H(s) = \frac{K}{Ts + 1 + K}\frac{1}{s}$$

Expanding $H(s)$ into partial fractions gives

$$H(s) = \frac{K}{1 + K}\frac{1}{s} - \frac{K}{1 + K}\frac{1}{s + (1 + K)/T}$$

Taking the inverse Laplace transforms of both sides of this last equation, we obtain the following time solution $h(t)$:

$$h(t) = \frac{K}{1 + K}(1 - e^{-t/T_1}), \qquad \text{for } t \geq 0 \tag{4-8}$$

where

$$T_1 = \frac{T}{1 + K}$$

The response curve $h(t)$ is plotted in Figure 4–7(d). From Equation (4–8), notice that the time constant T_1 of the closed-loop system is different from the time constant T of the feedforward block.

From Equation (4–8), we see that as t approaches infinity the value of $h(t)$ approaches $K/(1 + K)$, or

$$h(\infty) = \frac{K}{1 + K}$$

Since $x(\infty) = 1$, there is a steady-state error of $1/(1 + K)$. Such an error is called *offset*. The value of the offset becomes smaller as the gain K becomes larger.

Offset is a characteristic of the proportional control of a plant whose transfer function does not possess an integrating element. (In such a case we need a nonzero error to provide a nonzero output.) To eliminate such offset, we must add integral control action. (Refer to Section 5–3.)

4–3 SECOND-ORDER SYSTEMS

In this section, we shall obtain the response of a typical second-order control system to a step input, ramp input, and impulse input. Here we consider a dc servomotor as an example of a second-order system. Conventional dc motors use mechanical brushes and commutators that require regular maintenance. Due to improvements that have been made in the brushes and commutators, however, many dc motors used in servo systems can be operated almost maintenance free. Some dc motors use electronic commutation. They are called brushless dc motors.

DC servomotors. There are many types of dc motors in use in industries. DC motors that are used in servo systems are called dc servomotors. In dc servomotors, the rotor inertias have been made very small, with the result that motors with very high torque-to-inertia ratios are commercially available. Some dc servomotors have extremely small time constants. DC servomotors with relatively small power ratings are used in instruments and computer-related equipment such as disk drives, tape drives, printers, and word processors. DC servomotors with medium and large power ratings are used in robot systems, numerically controlled milling machines, and so on.

In dc servomotors, the field windings may be connected in series with the armature or the field windings may be separate from the armature. (That is, the magnetic field is produced by a separate circuit.) In the latter case, where the field is excited separately, the magnetic flux is independent of the armature current. In some dc servomotors, the magnetic field is produced by a permanent magnet and, therefore, the magnetic flux is constant. Such dc servomotors are called permanent magnet dc servomotors. DC servomotors with separately excited fields, as well as permanent magnet dc servomotors, can be controlled by the armature current. Such a scheme to control the output of the dc servomotor by the armature current is called armature control of dc servomotors.

In the case where the armature current is maintained constant and the speed is controlled by the field voltage, the dc motor is called a field-controlled dc motor. (Some speed control systems use field-controlled dc motors.) The requirement of constant armature current, however, is a serious disadvantage. (Providing a constant current source is much more difficult than providing a constant voltage source.) The time constants of the field-controlled dc motor are generally large compared with the time constants of a comparable armature-controlled dc motor.

A dc servomotor may also be driven by an electronic motion controller, frequently called a servodriver, as a motor–driver combination. The servodriver controls the motion of a dc servomotor and operates in various modes. Some of the features are point-to-point positioning, velocity profiling, and programmable acceleration. The use of an electronic motion controller using a pulse-width-modulated driver to control a dc servomotor is frequently seen in robot control systems, numerical control systems, and other position and/or speed control systems.

In what follows we shall discuss armature control of dc servomotors.

A servo system. Consider the servo system shown in Figure 4–8(a). The objective of this system is to control the position of the mechanical load in accordance with the reference position. The operation of this system is as follows: A pair of potentiometers acts as an error-measuring device. They convert the input and output positions into proportional electric signals. The command input signal determines the angular position r of the wiper arm of the input potentiometer. The angular position r is the reference input to the system, and the electric potential of the arm is proportional to the angular position of the arm. The output shaft position determines the angular position c of the wiper arm of the output potentiometer. The difference between the input angular position r and the output angular position c is the error signal e, or

$$e = r - c$$

The potential difference $e_r - e_c = e_v$ is the error voltage, where e_r is proportional to r and e_c is proportional to c; that is, $e_r = K_0 r$ and $e_c = K_0 c$, where K_0 is a proportionality

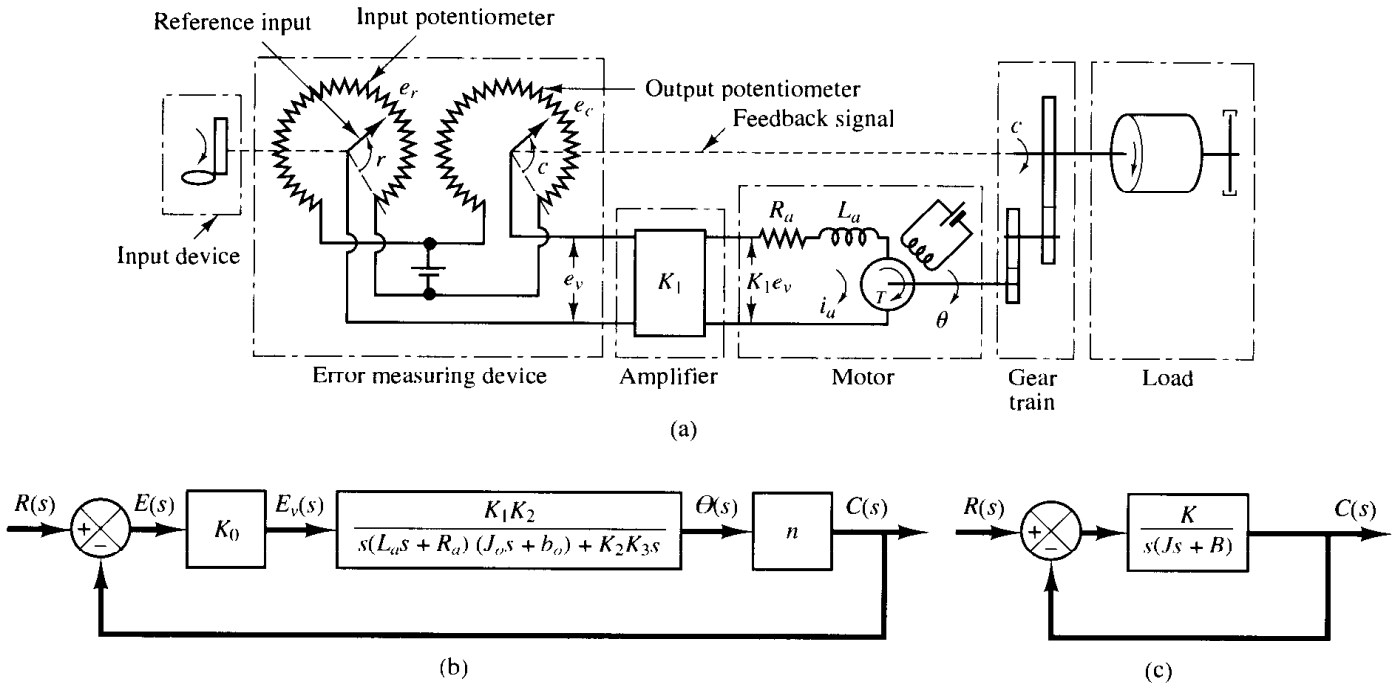

Figure 4–8
(a) Schematic diagram of servo system; (b) block diagram for the system; (c) simplified block diagram.

constant. The error voltage that appears at the potentiometer terminals is amplified by the amplifier whose gain constant is K_1. The output voltage of this amplifier is applied to the armature circuit of the dc motor. (The amplifier must have very high input impedance because the potentiometers are essentially high impedance circuits and do not tolerate current drain. At the same time, the amplifier must have low output impedance since it feeds into the armature circuit of the motor.) A fixed voltage is applied to the field winding. If an error exists, the motor develops a torque to rotate the output load in such a way as to reduce the error to zero. For constant field current, the torque developed by the motor is

$$T = K_2 i_a$$

where K_2 is the motor torque constant and i_a is the armature current.

Notice that if the sign of the current i_a is reversed the sign of the torque T will be reversed, which will result in the reversion of the direction of rotor rotation.

When the armature is rotating, a voltage proportional to the product of the flux and angular velocity is induced in the armature. For a constant flux, the induced voltage e_b is directly proportional to the angular velocity $d\theta/dt$, or

$$e_b = K_3 \frac{d\theta}{dt} \tag{4–9}$$

where e_b is the back emf, K_3 is the back emf constant of the motor, and θ is the angular displacement of the motor shaft.

The speed of an armature-controlled dc servomotor is controlled by the armature voltage e_a. (The armature voltage $e_a = K_1 e_v$ is the output of the amplifier.) The differential equation for the armature circuit is

$$L_a \frac{di_a}{dt} + R_a i_a + e_b = e_a$$

or

$$L_a \frac{di_a}{dt} + R_a i_a + K_3 \frac{d\theta}{dt} = K_1 e_v \tag{4–10}$$

The equation for torque equilibrium is

$$J_0 \frac{d^2\theta}{dt^2} + b_0 \frac{d\theta}{dt} = T = K_2 i_a \tag{4–11}$$

where J_0 is the inertia of the combination of the motor, load, and gear train referred to the motor shaft and b_0 is the viscous-friction coefficient of the combination of the motor, load, and gear train referred to the motor shaft. The transfer function between the motor shaft displacement and the error voltage is obtained from Equations (4–10) and (4–11) as follows:

$$\frac{\Theta(s)}{E_v(s)} = \frac{K_1 K_2}{s(L_a s + R_a)(J_0 s + b_0) + K_2 K_3 s} \tag{4–12}$$

where $\Theta(s) = \mathcal{L}[\theta(t)]$ and $E_v(s) = \mathcal{L}[e_v(t)]$. We assume that the gear ratio of the gear train is such that the output shaft rotates n times for each revolution of the motor shaft. Thus,

$$C(s) = n\Theta(s) \tag{4–13}$$

where $C(s) = \mathcal{L}[c(t)]$ and $c(t)$ is the angular displacement of the output shaft. The relationship among $E_v(s)$, $R(s)$, and $C(s)$ is

$$E_v(s) = K_0[R(s) - C(s)] = K_0 E(s) \tag{4–14}$$

where $R(s) = \mathcal{L}[r(t)]$. The block diagram of this system can be constructed from Equations (4–12), (4–13), and (4–14), as shown in Figure 4–8(b). The transfer function in the feedforward path of this system is

$$G(s) = \frac{C(s)}{\Theta(s)} \frac{\Theta(s)}{E_v(s)} \frac{E_v(s)}{E(s)} = \frac{K_0 K_1 K_2 n}{s[(L_a s + R_a)(J_0 s + b_0) + K_2 K_3]}$$

Since L_a is usually small, it can be neglected, and the transfer function $G(s)$ in the feedforward path becomes

$$\begin{aligned} G(s) &= \frac{K_0 K_1 K_2 n}{s[R_a(J_0 s + b_0) + K_2 K_3]} \\ &= \frac{K_0 K_1 K_2 n / R_a}{J_0 s^2 + \left(b_0 + \dfrac{K_2 K_3}{R_a}\right) s} \end{aligned} \tag{4–15}$$

The term $[b_0 + (K_2K_3/R_a)]s$ indicates that the back emf of the motor effectively increases the viscous friction of the system. The inertia J_0 and viscous friction coefficient $b_0 + (K_2K_3/R_a)$ are referred to the motor shaft. When J_0 and $b_0 + (K_2K_3/R_a)$ are multiplied by $1/n^2$, the inertia and viscous-friction coefficient are expressed in terms of the output shaft. Introducing new parameters defined by

$J = J_0/n^2$ = moment of inertia referred to the output shaft

$B = [b_0 + (K_2K_3/R_a)]/n^2$ = viscous-friction coefficient referred to the output shaft

$K = K_0K_1K_2/nR_a$

the transfer function $G(s)$ given by Equation (4–15) can be simplified, yielding

$$G(s) = \frac{K}{Js^2 + Bs}$$

or

$$G(s) = \frac{K_m}{s(T_m s + 1)} \tag{4–16}$$

where

$$K_m = \frac{K}{B}, \qquad T_m = \frac{J}{B} = \frac{R_a J_0}{R_a b_0 + K_2 K_3}$$

The block diagram of the system shown in Figure 4–8(b) can thus be simplified as shown in Figure 4–8(c).

In the following, we shall investigate the dynamic responses of this system to unit-step, unit-ramp, and unit-impulse inputs.

From Equations (4–15) and (4–16), it can be seen that the transfer functions involve the term $1/s$. Thus, this system possesses an integrating property. In Equation (4–16), notice that the time constant of the motor is smaller for a smaller R_a and smaller J_0. With small J_0, as the resistance R_a is reduced, the motor time constant approaches zero, and the motor acts as an ideal integrator.

Effect of load on servomotor dynamics. Most important among the characteristics of the servomotor is the maximum acceleration obtainable. For a given available torque, the rotor moment of inertia must be a minimum. Since the servomotor operates under continuously varying conditions, acceleration and deceleration of the rotor occur from time to time. The servomotor must be able to absorb mechanical energy as well as to generate it. The performance of the servomotor when used as a brake should be satisfactory.

Let J_m and b_m be, respectively, the moment of inertia and viscous-friction coefficient of the rotor, and let J_L and b_L be, respectively, the moment of inertia and viscous-friction coefficient of the load on the output shaft. Assume that the moment of inertia and viscous-friction coefficient of the gear train are either negligible or included in J_L and b_L, respectively. Then, the equivalent moment of inertia J_{eq} referred to the motor shaft and equivalent viscous-friction coefficient b_{eq} referred to the motor shaft can be written as (for details, refer to Problem A-4-4)

$$J_{eq} = J_m + n^2 J_L$$
$$b_{eq} = b_m + n^2 f_L$$

where $n(n < 1)$ is the gear ratio between the motor and load. If the gear ratio n is small and $J_m \gg n^2 J_L$, then the moment of inertia of the load referred to the motor shaft is negligible with respect to the rotor moment of inertia. A similar argument applies to the load friction. In general, when the gear ratio n is small, the transfer function of the electric servomotor may be obtained without taking into account the load moment of inertia and friction. If neither J_m nor $n^2 J_L$ is negligibly small compared with the other, however, then the equivalent moment of inertia J_{eq} must be used for evaluating the transfer function of the motor–load combination.

Step response of second-order systems. The closed-loop transfer function of the system shown in Figure 4–8(c) is

$$\frac{C(s)}{R(s)} = \frac{K}{Js^2 + Bs + K} \tag{4–17}$$

which can be rewritten as

$$\frac{C(s)}{R(s)} = \frac{\dfrac{K}{J}}{\left[s + \dfrac{B}{2J} + \sqrt{\left(\dfrac{B}{2J}\right)^2 - \dfrac{K}{J}}\right]\left[s + \dfrac{B}{2J} - \sqrt{\left(\dfrac{B}{2J}\right)^2 - \dfrac{K}{J}}\right]} \tag{4–18}$$

The closed-loop poles are complex if $B^2 - 4JK < 0$, and they are real if $B^2 - 4JK \geq 0$. In transient-response analysis, it is convenient to write

$$\frac{K}{J} = \omega_n^2, \qquad \frac{B}{J} = 2\zeta\omega_n = 2\sigma$$

where σ is called the *attenuation;* ω_n, the *undamped natural frequency;* and ζ, the *damping ratio* of the system. The damping ratio ζ is the ratio of the actual damping B to the critical damping $B_c = 2\sqrt{JK}$ or

$$\zeta = \frac{B}{B_c} = \frac{B}{2\sqrt{JK}}$$

In terms of ζ and ω_n, the system shown in Figure 4–8(c) can be modified to that shown in Figure 4–9, and the closed-loop transfer function $C(s)/R(s)$ given by Equation (4–18) can be written

$$\frac{C(s)}{R(s)} = \frac{\omega_n^2}{s^2 + 2\zeta\omega_n s + \omega_n^2} \tag{4–19}$$

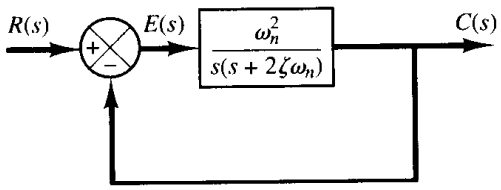

Figure 4–9
Second-order system.

The dynamic behavior of the second-order system can then be described in terms of two parameters ζ and ω_n. If $0 < \zeta < 1$, the closed-loop poles are complex conjugates and lie in the left-half s plane. The system is then called underdamped, and the transient response is oscillatory. If $\zeta = 1$, the system is called critically damped. Overdamped systems correspond to $\zeta > 1$. The transient response of critically damped and overdamped systems do not oscillate. If $\zeta = 0$, the transient response does not die out.

We shall now solve for the response of the system shown in Figure 4–9 to a unit-step input. We shall consider three different cases: the underdamped ($0 < \zeta < 1$), critically damped ($\zeta = 1$), and overdamped ($\zeta > 1$) cases.

(1) Underdamped case ($0 < \zeta < 1$): In this case, $C(s)/R(s)$ can be written

$$\frac{C(s)}{R(s)} = \frac{\omega_n^2}{(s + \zeta\omega_n + j\omega_d)(s + \zeta\omega_n - j\omega_d)}$$

where $\omega_d = \omega_n\sqrt{1 - \zeta^2}$. The frequency ω_d is called the *damped natural frequency*. For a unit-step input, $C(s)$ can be written

$$C(s) = \frac{\omega_n^2}{(s^2 + 2\zeta\omega_n s + \omega_n^2)s} \tag{4–20}$$

The inverse Laplace transform of Equation (4–20) can be obtained easily if $C(s)$ is written in the following form:

$$\begin{aligned} C(s) &= \frac{1}{s} - \frac{s + 2\zeta\omega_n}{s^2 + 2\zeta\omega_n s + \omega_n^2} \\ &= \frac{1}{s} - \frac{s + \zeta\omega_n}{(s + \zeta\omega_n)^2 + \omega_d^2} - \frac{\zeta\omega_n}{(s + \zeta\omega_n)^2 + \omega_d^2} \end{aligned}$$

In Chapter 2 it was shown that

$$\mathcal{L}^{-1}\left[\frac{s + \zeta\omega_n}{(s + \zeta\omega_n)^2 + \omega_d^2}\right] = e^{-\zeta\omega_n t}\cos\omega_d t$$

$$\mathcal{L}^{-1}\left[\frac{\omega_d}{(s + \zeta\omega_n)^2 + \omega_d^2}\right] = e^{-\zeta\omega_n t}\sin\omega_d t$$

Hence the inverse Laplace transform of Equation (4–20) is obtained as

$$\begin{aligned} \mathcal{L}^{-1}[C(s)] &= c(t) \\ &= 1 - e^{-\zeta\omega_n t}\left(\cos\omega_d t + \frac{\zeta}{\sqrt{1 - \zeta^2}}\sin\omega_d t\right) \\ &= 1 - \frac{e^{-\zeta\omega_n t}}{\sqrt{1 - \zeta^2}}\sin\left(\omega_d t + \tan^{-1}\frac{\sqrt{1 - \zeta^2}}{\zeta}\right), \qquad \text{for } t \geq 0 \end{aligned} \tag{4–21}$$

This result can be obtained directly by using a table of Laplace transforms. From Equation (4–21), it can be seen that the frequency of transient oscillation is the damped natural frequency ω_d and thus varies with the damping ratio ζ. The error signal for this system is the difference between the input and output and is

$$e(t) = r(t) - c(t)$$
$$= e^{-\zeta\omega_n t}\left(\cos \omega_d t + \frac{\zeta}{\sqrt{1-\zeta^2}} \sin \omega_d t\right) \qquad \text{for } t \geq 0$$

This error signal exhibits a damped sinusoidal oscillation. At steady state, or at $t = \infty$, no error exists between the input and output.

If the damping ratio ζ is equal to zero, the response becomes undamped and oscillations continue indefinitely. The response $c(t)$ for the zero damping case may be obtained by substituting $\zeta = 0$ in Equation (4–21), yielding

$$c(t) = 1 - \cos \omega_n t, \qquad \text{for } t \geq 0 \tag{4–22}$$

Thus, from Equation (4–22), we see that ω_n represents the undamped natural frequency of the system. That is, ω_n is that frequency at which the system would oscillate if the damping were decreased to zero. If the linear system has any amount of damping, the undamped natural frequency cannot be observed experimentally. The frequency that may be observed is the damped natural frequency ω_d, which is equal to $\omega_n\sqrt{1-\zeta^2}$. This frequency is always lower than the undamped natural frequency. An increase in ζ would reduce the damped natural frequency ω_d. If ζ is increased beyond unity, the response becomes overdamped and will not oscillate.

(2) Critically damped case ($\zeta = 1$): If the two poles of $C(s)/R(s)$ are nearly equal, the system may be approximated by a critically damped one.

For a unit-step input, $R(s) = 1/s$ and $C(s)$ can be written

$$C(s) = \frac{\omega_n^2}{(s + \omega_n)^2 s} \tag{4–23}$$

The inverse Laplace transform of Equation (4–23) may be found as

$$c(t) = 1 - e^{-\omega_n t}(1 + \omega_n t), \qquad \text{for } t \geq 0 \tag{4–24}$$

This result can be obtained by letting ζ approach unity in Equation (4–21) and by using the following limit:

$$\lim_{\zeta \to 1} \frac{\sin \omega_d t}{\sqrt{1-\zeta^2}} = \lim_{\zeta \to 1} \frac{\sin \omega_n\sqrt{1-\zeta^2}\, t}{\sqrt{1-\zeta^2}} = \omega_n t$$

(3) Overdamped case ($\zeta > 1$): In this case, the two poles of $C(s)/R(s)$ are negative real and unequal. For a unit-step input, $R(s) = 1/s$ and $C(s)$ can be written

$$C(s) = \frac{\omega_n^2}{(s + \zeta\omega_n + \omega_n\sqrt{\zeta^2-1})(s + \zeta\omega_n - \omega_n\sqrt{\zeta^2-1})s} \tag{4–25}$$

The inverse Laplace transform of Equation (4–25) is

$$c(t) = 1 + \frac{1}{2\sqrt{\zeta^2-1}(\zeta + \sqrt{\zeta^2-1})} e^{-(\zeta + \sqrt{\zeta^2-1})\omega_n t}$$
$$- \frac{1}{2\sqrt{\zeta^2-1}(\zeta - \sqrt{\zeta^2-1})} e^{-(\zeta - \sqrt{\zeta^2-1})\omega_n t}$$

$$= 1 + \frac{\omega_n}{2\sqrt{\zeta^2 - 1}}\left(\frac{e^{-s_1 t}}{s_1} - \frac{e^{-s_2 t}}{s_2}\right), \qquad \text{for } t \geq 0 \tag{4-26}$$

where $s_1 = (\zeta + \sqrt{\zeta^2 - 1})\omega_n$ and $s_2 = (\zeta - \sqrt{\zeta^2 - 1})\omega_n$. Thus, the response $c(t)$ includes two decaying exponential terms.

When ζ is appreciably greater than unity, one of the two decaying exponentials decreases much faster than the other, so the faster decaying exponential term (which corresponds to a smaller time constant) may be neglected. That is, if $-s_2$ is located very much closer to the $j\omega$ axis than $-s_1$ (which means $|s_2| \ll |s_1|$), then for an approximate solution we may neglect $-s_1$. This is permissible because the effect of $-s_1$ on the response is much smaller than that of $-s_2$, since the term involving s_1 in Equation (4–26) decays much faster than the term involving s_2. Once the faster decaying exponential term has disappeared, the response is similar to that of a first-order system, and $C(s)/R(s)$ may be approximated by

$$\frac{C(s)}{R(s)} = \frac{\zeta\omega_n - \omega_n\sqrt{\zeta^2 - 1}}{s + \zeta\omega_n - \omega_n\sqrt{\zeta^2 - 1}} = \frac{s_2}{s + s_2}$$

This approximate form is a direct consequence of the fact that the initial values and final values of both the original $C(s)/R(s)$ and the approximate one agree with each other.

With the approximate transfer function $C(s)/R(s)$, the unit-step response can be obtained as

$$C(s) = \frac{\zeta\omega_n - \omega_n\sqrt{\zeta^2 - 1}}{(s + \zeta\omega_n - \omega_n\sqrt{\zeta^2 - 1})s}$$

The time response $c(t)$ is then

$$c(t) = 1 - e^{-(\zeta - \sqrt{\zeta^2 - 1})\omega_n t}, \qquad \text{for } t \geq 0$$

This gives an approximate unit-step response when one of the poles of $C(s)/R(s)$ can be neglected.

A family of curves $c(t)$ with various values of ζ is shown in Figure 4–10, where the abscissa is the dimensionless variable $\omega_n t$. The curves are functions only of ζ. These

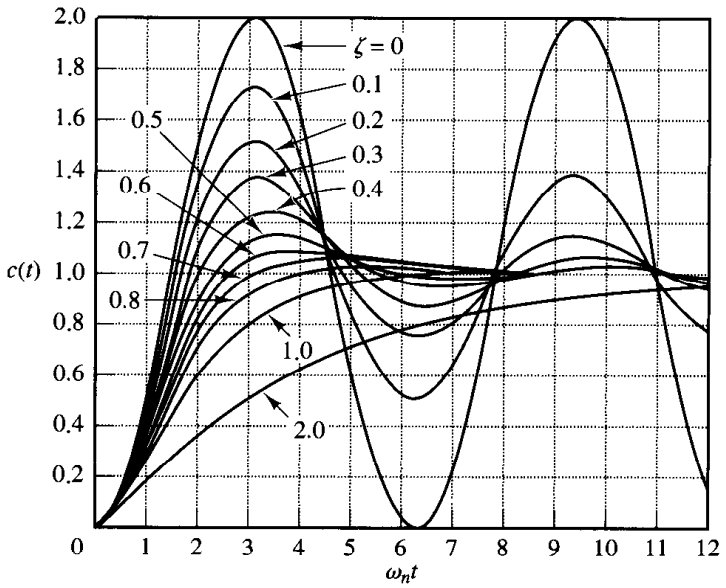

Figure 4–10
Unit-step response curves of the system shown in Figure 4–9.

curves are obtained from Equations (4–21), (4–24), and (4–26). The system described by these equations was initially at rest.

Note that two second-order systems having the same ζ but different ω_n will exhibit the same overshoot and the same oscillatory pattern. Such systems are said to have the same relative stability.

It is important to note that, for second-order systems whose closed-loop transfer functions are different from that given by Equation (4–19), the step-response curves may look quite different from those shown in Figure 4–10.

From Figure 4–10, we see that an underdamped system with ζ between 0.5 and 0.8 gets close to the final value more rapidly than a critically damped or overdamped system. Among the systems responding without oscillation, a critically damped system exhibits the fastest response. An overdamped system is always sluggish in responding to any inputs.

Definitions of transient-response specifications. In many practical cases, the desired performance characteristics of control systems are specified in terms of time-domain quantities. Systems with energy storage cannot respond instantaneously and will exhibit transient responses whenever they are subjected to inputs or disturbances.

Frequently, the performance characteristics of a control system are specified in terms of the transient response to a unit-step input since it is easy to generate and is sufficiently drastic. (If the response to a step input is known, it is mathematically possible to compute the response to any input.)

The transient response of a system to a unit-step input depends on the initial conditions. For convenience in comparing transient responses of various systems, it is a common practice to use the standard initial condition that the system is at rest initially with output and all time derivatives thereof zero. Then the response characteristics can be easily compared.

The transient response of a practical control system often exhibits damped oscillations before reaching steady state. In specifying the transient-response characteristics of a control system to a unit-step input, it is common to specify the following:

1. Delay time, t_d
2. Rise time, t_r
3. Peak time, t_p
4. Maximum overshoot, M_p
5. Settling time, t_s

These specifications are defined in what follows and are shown graphically in Figure 4–11.

1. Delay time, t_d: The delay time is the time required for the response to reach half the final value the very first time.
2. Rise time, t_r: The rise time is the time required for the response to rise from 10% to 90%, 5% to 95%, or 0% to 100% of its final value. For underdamped second-order systems, the 0% to 100% rise time is normally used. For overdamped systems, the 10% to 90% rise time is commonly used.

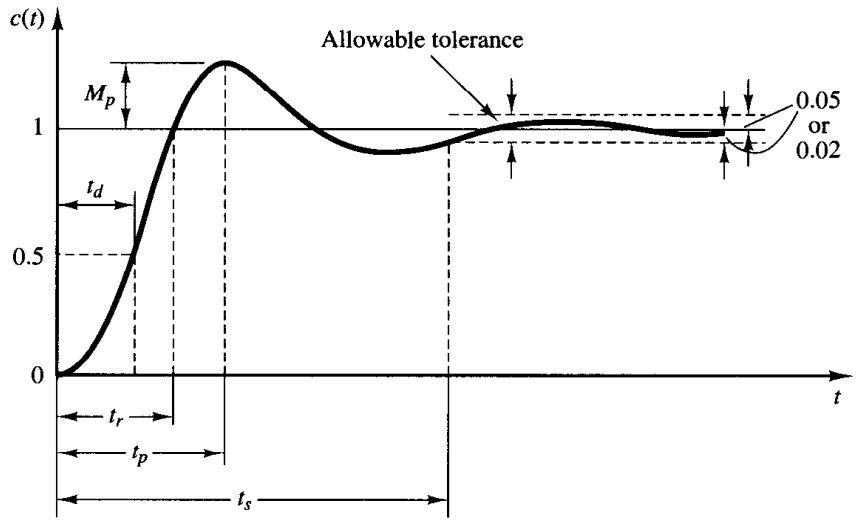

Figure 4–11
Unit-step response curve showing t_d, t_r, t_p, M_p, and t_s.

3. Peak time, t_p: The peak time is the time required for the response to reach the first peak of the overshoot.
4. Maximum (percent) overshoot, M_p: The maximum overshoot is the maximum peak value of the response curve measured from unity. If the final steady-state value of the response differs from unity, then it is common to use the maximum percent overshoot. It is defined by

$$\text{Maximum percent overshoot} = \frac{c(t_p) - c(\infty)}{c(\infty)} \times 100\%$$

The amount of the maximum (percent) overshoot directly indicates the relative stability of the system.

5. Settling time, t_s: The settling time is the time required for the response curve to reach and stay within a range about the final value of size specified by absolute percentage of the final value (usually 2% or 5%). The settling time is related to the largest time constant of the control system. Which percentage error criterion to use may be determined from the objectives of the system design in question.

The time-domain specifications just given are quite important since most control systems are time-domain systems; that is, they must exhibit acceptable time responses. (This means that the control system must be modified until the transient response is satisfactory.) Note that if we specify the values of t_d, t_r, t_p, t_s, and M_p, then the shape of the response curve is virtually determined. This may be seen clearly from Figure 4–12.

Note that not all these specifications necessarily apply to any given case. For example, for an overdamped system, the terms peak time and maximum overshoot do not apply. (For systems that yield steady-state errors for step inputs, this error must be kept within a specified percentage level. Detailed discussions of steady-state errors are postponed until Section 5–10.)

A few comments on transient-response specifications. Except for certain applications where oscillations cannot be tolerated, it is desirable that the transient

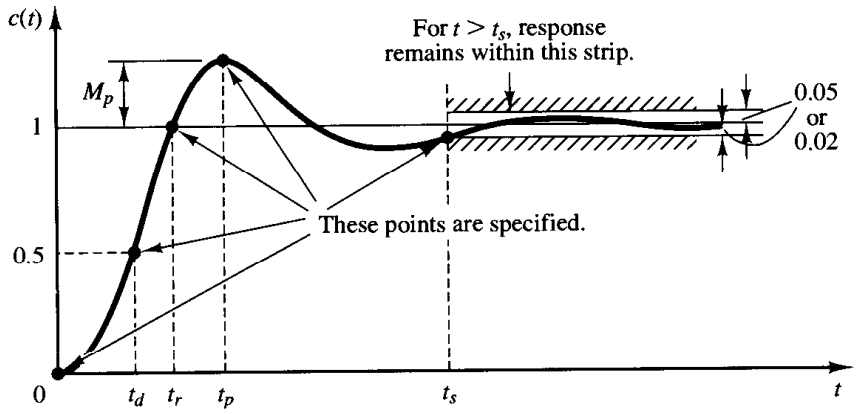

Figure 4–12
Transient-response specifications.

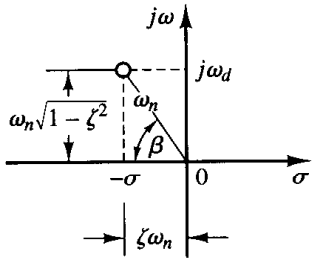

Figure 4–13
Definition of the angle β.

response be sufficiently fast and be sufficiently damped. Thus, for a desirable transient response of a second-order system, the damping ratio must be between 0.4 and 0.8. Small values of ζ ($\zeta < 0.4$) yield excessive overshoot in the transient response, and a system with a large value of ζ ($\zeta > 0.8$) responds sluggishly.

We shall see later that the maximum overshoot and the rise time conflict with each other. In other words, both the maximum overshoot and the rise time cannot be made smaller simultaneously. If one of them is made smaller, the other necessarily becomes larger.

Second-order systems and transient-response specifications. In the following, we shall obtain the rise time, peak time, maximum overshoot, and settling time of the second-order system given by Equation (4–19). These values will be obtained in terms of ζ and ω_n. The system is assumed to be underdamped.

Rise time t_r: Referring to Equation (4–21), we obtain the rise time t_r by letting $c(t_r) = 1$ or

$$c(t_r) = 1 = 1 - e^{-\zeta\omega_n t_r}\left(\cos \omega_d t_r + \frac{\zeta}{\sqrt{1-\zeta^2}} \sin \omega_d t_r\right) \tag{4–27}$$

Since $e^{-\zeta\omega_n t_r} \neq 0$, we obtain from Equation (4–27) the following equation:

$$\cos \omega_d t_r + \frac{\zeta}{\sqrt{1-\zeta^2}} \sin \omega_d t_r = 0$$

or

$$\tan \omega_d t_r = -\frac{\sqrt{1-\zeta^2}}{\zeta} = -\frac{\omega_d}{\sigma}$$

Thus, the rise time t_r is

$$t_r = \frac{1}{\omega_d} \tan^{-1}\left(\frac{\omega_d}{-\sigma}\right) = \frac{\pi - \beta}{\omega_d} \tag{4–28}$$

where β is defined in Figure 4–13. Clearly, for a small value of t_r, ω_d must be large.

Peak time t_p: Referring to Equation (4–21), we may obtain the peak time by differentiating $c(t)$ with respect to time and letting this derivative equal zero. Since

$$\frac{dc}{dt} = \zeta\omega_n e^{-\zeta\omega_n t}\left(\cos\omega_d t + \frac{\zeta}{\sqrt{1-\zeta^2}}\sin\omega_d t\right) + e^{-\zeta\omega_n t}\left(\omega_d \sin\omega_d t - \frac{\zeta\omega_d}{\sqrt{1-\zeta^2}}\cos\omega_d t\right)$$

and the cosine terms in this last equation cancel each other, dc/dt, evaluated at $t = t_p$, can be simplified to

$$\left.\frac{dc}{dt}\right|_{t=t_p} = (\sin\omega_d t_p)\frac{\omega_n}{\sqrt{1-\zeta^2}}e^{-\zeta\omega_n t_p} = 0$$

This last equation yields the following equation:

$$\sin\omega_d t_p = 0$$

or

$$\omega_d t_p = 0, \pi, 2\pi, 3\pi, \ldots$$

Since the peak time corresponds to the first peak overshoot, $\omega_d t_p = \pi$. Hence

$$t_p = \frac{\pi}{\omega_d} \tag{4–29}$$

The peak time t_p corresponds to one-half cycle of the frequency of damped oscillation.

Maximum overshoot M_p: The maximum overshoot occurs at the peak time or at $t = t_p = \pi/\omega_d$. Thus, from Equation (4–21), M_p is obtained as

$$\begin{aligned} M_p &= c(t_p) - 1 \\ &= -e^{-\zeta\omega_n(\pi/\omega_d)}\left(\cos\pi + \frac{\zeta}{\sqrt{1-\zeta^2}}\sin\pi\right) \\ &= e^{-(\sigma/\omega_d)\pi} = e^{-(\zeta/\sqrt{1-\zeta^2})\pi} \end{aligned} \tag{4–30}$$

The maximum percent overshoot is $e^{-(\sigma/\omega_d)\pi} \times 100\%$.

Settling time t_s: For an underdamped second-order system, the transient response is obtained from Equation (4–21) as

$$c(t) = 1 - \frac{e^{-\zeta\omega_n t}}{\sqrt{1-\zeta^2}}\sin\left(\omega_d t + \tan^{-1}\frac{\sqrt{1-\zeta^2}}{\zeta}\right), \qquad \text{for } t \geq 0$$

The curves $1 \pm (e^{-\zeta\omega_n t}/\sqrt{1-\zeta^2})$ are the envelope curves of the transient response for a unit-step input. The response curve $c(t)$ always remains within a pair of the envelope curves, as shown in Figure 4–14. The time constant of these envelope curves is $1/\zeta\omega_n$.

The speed of decay of the transient response depends on the value of the time constant $1/\zeta\omega_n$. For a given ω_n, the settling time t_s is a function of the damping ratio ζ. From Figure 4–10, we see that for the same ω_n and for a range of ζ between 0 and 1 the settling time t_s for a very lightly damped system is larger than that for a properly damped system. For an overdamped system, the settling time t_s becomes large because of the sluggish start of the response.

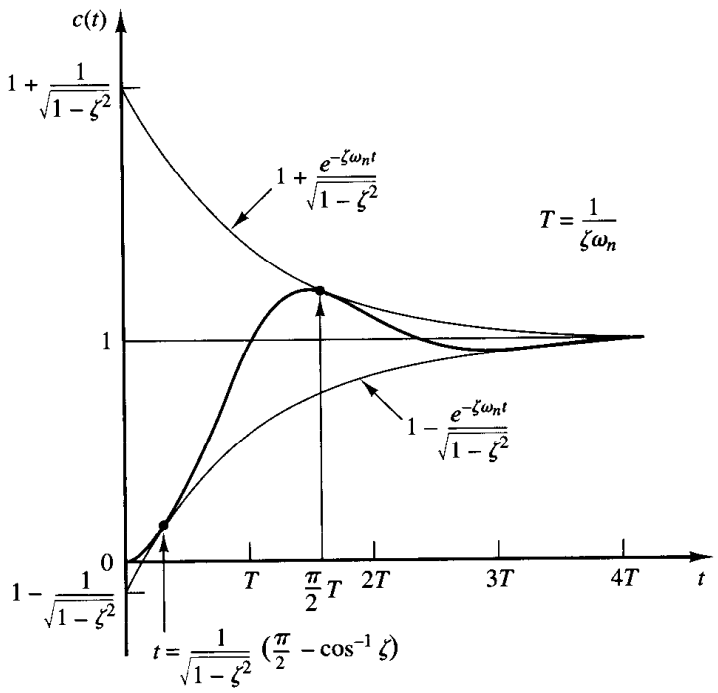

Figure 4–14
Pair of envelope curves for the unit-step response curve of the system shown in Figure 4–9.

The settling time corresponding to a ±2% or ±5% tolerance band may be measured in terms of the time constant $T = 1/\zeta\omega_n$ from the curves of Figure 4–10 for different values of ζ. The results are shown in Figure 4–15. For $0 < \zeta < 0.9$, if the 2% criterion is used t_s is approximately four times the time constant of the system. If the 5% criterion is used, then t_s is approximately three times the time constant. Note that the settling time reaches a minimum value around $\zeta = 0.76$ (for the 2% criterion) or $\zeta = 0.68$ (for the 5% criterion) and then increases almost linearly for large values of ζ. The discontinuities in the curves of Figure 4–15 arise because an infinitesimal change in the value of ζ can cause a finite change in the settling time.

For convenience in comparing the responses of systems, we commonly define the settling time t_s to be

$$t_s = 4T = \frac{4}{\sigma} = \frac{4}{\zeta\omega_n} \qquad \text{(2\% criterion)} \tag{4–31}$$

or

$$t_s = 3T = \frac{3}{\sigma} = \frac{3}{\zeta\omega_n} \qquad \text{(5\% criterion)} \tag{4–32}$$

Note that the settling time is inversely proportional to the product of the damping ratio and the undamped natural frequency of the system. Since the value of ζ is usually determined from the requirement of permissible maximum overshoot, the settling time is determined primarily by the undamped natural frequency ω_n. This means that the duration of the transient period may be varied, without changing the maximum overshoot, by adjusting the undamped natural frequency ω_n.

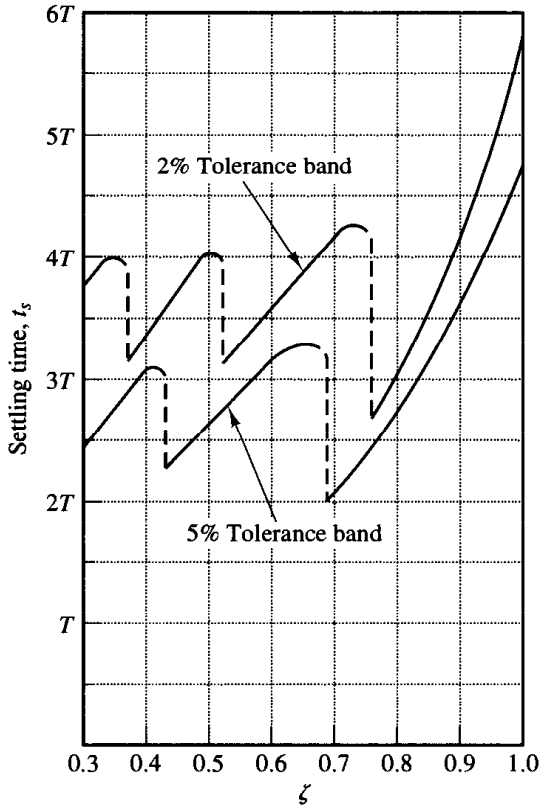

Figure 4–15
Settling time t_s versus ζ curves.

From the preceding analysis, it is evident that for rapid response ω_n must be large. To limit the maximum overshoot M_p and to make the settling time small, the damping ratio ζ should not be too small. The relationship between the maximum percent overshoot M_p and the damping ratio ζ is presented in Figure 4–16. Note that if the damping ratio is between 0.4 and 0.8 then the maximum percent overshoot for step response is between 25% and 2.5%.

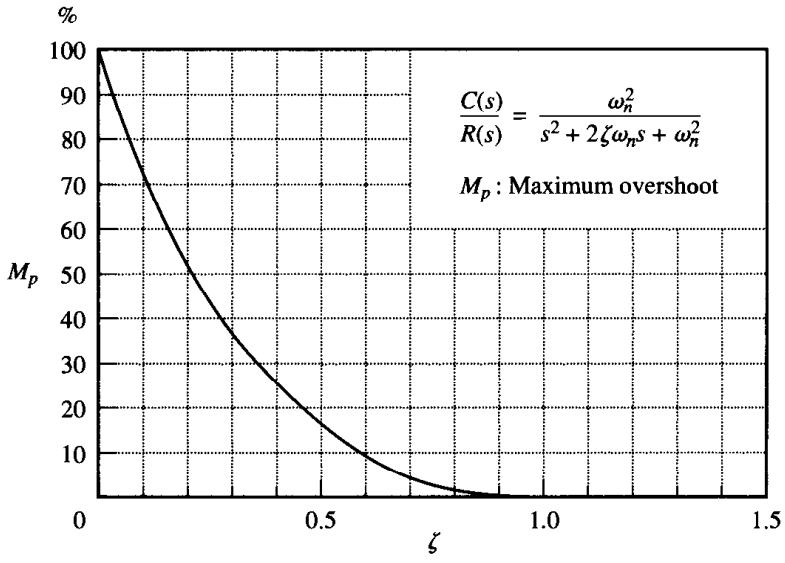

Figure 4–16
M_p versus ζ curve.

EXAMPLE 4–2 Consider the system shown in Figure 4–9, where $\zeta = 0.6$ and $\omega_n = 5$ rad/sec. Let us obtain the rise time t_r, peak time t_p, maximum overshoot M_p, and settling time t_s when the system is subjected to a unit-step input.

From the given values of ζ and ω_n, we obtain $\omega_d = \omega_n\sqrt{1 - \zeta^2} = 4$ and $\sigma = \zeta\omega_n = 3$.

Rise time t_r: The rise time is

$$t_r = \frac{\pi - \beta}{\omega_d} = \frac{3.14 - \beta}{4}$$

where β is given by

$$\beta = \tan^{-1}\frac{\omega_d}{\sigma} = \tan^{-1}\frac{4}{3} = 0.93 \text{ rad}$$

The rise time t_r is thus

$$t_r = \frac{3.14 - 0.93}{4} = 0.55 \text{ sec}$$

Peak time t_p: The peak time is

$$t_p = \frac{\pi}{\omega_d} = \frac{3.14}{4} = 0.785 \text{ sec}$$

Maximum overshoot M_p: The maximum overshoot is

$$M_p = e^{-(\sigma/\omega_d)\pi} = e^{-(3/4)\times 3.14} = 0.095$$

The maximum percent overshoot is thus 9.5%

Settling time t_s: For the 2% criterion, the settling time is

$$t_s = \frac{4}{\sigma} = \frac{4}{3} = 1.33 \text{ sec}$$

For the 5% criterion,

$$t_s = \frac{3}{\sigma} = \frac{3}{3} = 1 \text{ sec}$$

Servo system with velocity feedback. The derivative of the output signal can be used to improve system performance. In obtaining the derivative of the output position signal, it is desirable to use a tachometer instead of physically differentiating the output signal. (Note that the differentiation amplifies noise effects. In fact, if discontinuous noises are present, differentiation amplifies the discontinuous noises more than the useful signal. For example, the output of a potentiometer is a discontinuous voltage signal because, as the potentiometer brush is moving on the windings, voltages are induced in the switchover turns and thus generate transients. The output of the potentiometer therefore should not be followed by a differentiating element.)

Consider the servo system shown in Figure 4–17(a). In this device, the velocity signal, together with the positional signal, is fed back to the input to produce the actuating error signal. In any servo system, such a velocity signal can be easily generated by a

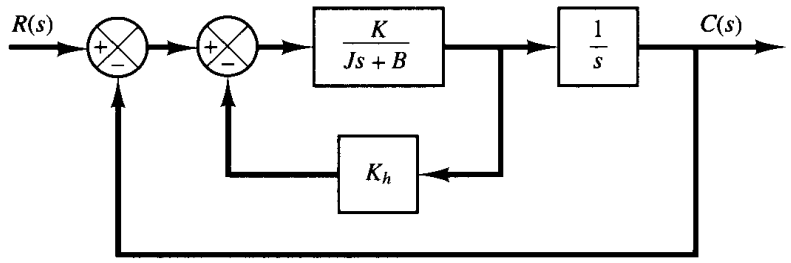

(a)

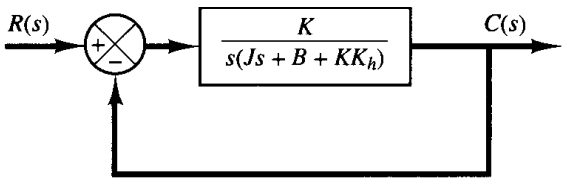

(b)

Figure 4–17
(a) Block diagram of a servo system; (b) simplified block diagram.

tachometer. The block diagram shown in Figure 4–17(a) can be simplified, as shown in Figure 4–17(b), giving

$$\frac{C(s)}{R(s)} = \frac{K}{Js^2 + (B + KK_h)s + K} \tag{4–33}$$

Comparing Equation (4–33) with Equation (4–17), notice that the velocity feedback has the effect of increasing damping. The damping ratio ζ becomes

$$\zeta = \frac{B + KK_h}{2\sqrt{KJ}} \tag{4–34}$$

The undamped natural frequency $\omega_n = \sqrt{K/J}$ is not affected by velocity feedback. Noting that the maximum overshoot for a unit-step input can be controlled by controlling the value of the damping ratio ζ, we can reduce the maximum overshoot by adjusting the velocity feedback constant K_h so that ζ is between 0.4 and 0.7.

Remember that velocity feedback has the effect of increasing the damping ratio without affecting the undamped natural frequency of the system.

EXAMPLE 4–3 For the system shown in Figure 4–17(a), determine the values of gain K and velocity feedback constant K_h so that the maximum overshoot in the unit-step response is 0.2 and the peak time is 1 sec. With these values of K and K_h, obtain the rise time and settling time. Assume that $J = 1$ kg-m^2 and $B = 1$ N-m/rad/sec.

Determination of the values of K and K_h: The maximum overshoot M_p is given by Equation (4–30) as

$$M_p = e^{-(\zeta/\sqrt{1-\zeta^2})\pi}$$

This value must be 0.2. Thus,

$$e^{-(\zeta/\sqrt{1-\zeta^2})\pi} = 0.2$$

or

$$\frac{\zeta\pi}{\sqrt{1-\zeta^2}} = 1.61$$

which yields

$$\zeta = 0.456$$

The peak time t_p is specified as 1 sec; therefore, from Equation (4–29),

$$t_p = \frac{\pi}{\omega_d} = 1$$

or

$$\omega_d = 3.14$$

Since ζ is 0.456, ω_n is

$$\omega_n = \frac{\omega_d}{\sqrt{1-\zeta^2}} = 3.53$$

Since the natural frequency ω_n is equal to $\sqrt{K/J}$,

$$K = J\omega_n^2 = \omega_n^2 = 12.5 \text{ N-m}$$

Then, K_h is, from Equation (4–34),

$$K_h = \frac{2\sqrt{KJ}\zeta - B}{K} = \frac{2\sqrt{K}\zeta - 1}{K} = 0.178 \text{ sec}$$

Rise time t_r: From Equation (4–28), the rise time t_r is

$$t_r = \frac{\pi - \beta}{\omega_d}$$

where

$$\beta = \tan^{-1}\frac{\omega_d}{\sigma} = \tan^{-1} 1.95 = 1.10$$

Thus, t_r is

$$t_r = 0.65 \text{ sec}$$

Settling time t_s: For the 2% criterion,

$$t_s = \frac{4}{\sigma} = 2.48 \text{ sec}$$

For the 5% criterion,

$$t_s = \frac{3}{\sigma} = 1.86 \text{ sec}$$

Impulse response of second-order systems. For a unit-impulse input $r(t)$, the corresponding Laplace transform is unity, or $R(s) = 1$. The unit-impulse response $C(s)$ of the second-order system shown in Figure 4–9 is

$$C(s) = \frac{\omega_n^2}{s^2 + 2\zeta\omega_n s + \omega_n^2}$$

The inverse Laplace transform of this equation yields the time solution for the response $c(t)$ as follows:

For $0 \leq \zeta < 1$,

$$c(t) = \frac{\omega_n}{\sqrt{1-\zeta^2}} e^{-\zeta\omega_n t} \sin \omega_n \sqrt{1-\zeta^2}\, t, \qquad \text{for } t \geq 0 \tag{4-35}$$

For $\zeta = 1$,

$$c(t) = \omega_n^2 t e^{-\omega_n t}, \qquad \text{for } t \geq 0 \tag{4-36}$$

For $\zeta > 1$,

$$c(t) = \frac{\omega_n}{2\sqrt{\zeta^2-1}} e^{-(\zeta-\sqrt{\zeta^2-1})\omega_n t} - \frac{\omega_n}{2\sqrt{\zeta^2-1}} e^{-(\zeta+\sqrt{\zeta^2-1})\omega_n t}, \qquad \text{for } t \geq 0 \tag{4-37}$$

Note that without taking the inverse Laplace transform of $C(s)$ we can also obtain the time response $c(t)$ by differentiating the corresponding unit-step response since the unit-impulse function is the time derivative of the unit-step function. A family of unit-impulse response curves given by Equations (4–35) and (4–36) with various values of ζ is shown in Figure 4–18. The curves $c(t)/\omega_n$ are plotted against the dimensionless variable $\omega_n t$, and thus they are functions only of ζ. For the critically damped and overdamped cases, the unit-impulse response is always positive or zero; that is, $c(t) \geq 0$. This can be seen from Equations (4–36) and (4–37). For the underdamped case, the unit-impulse response $c(t)$ oscillates about zero and takes both positive and negative values.

From the foregoing analysis, we may conclude that if the impulse response $c(t)$ does not change sign, the system is either critically damped or overdamped, in which case the

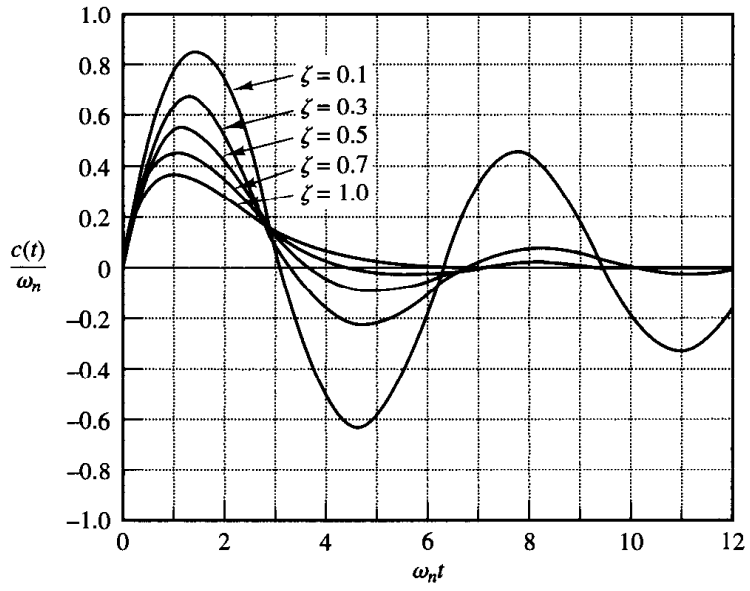

Figure 4–18
Unit-impulse response curves of the system shown in Figure 4–9.

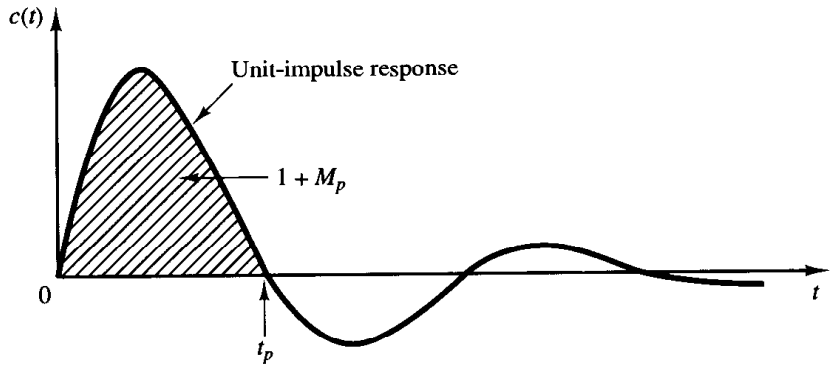

Figure 4–19
Unit-impulse response curve of the system shown in Figure 4–9.

corresponding step response does not overshoot but increases or decreases monotonically and approaches a constant value.

The maximum overshoot for the unit-impulse response of the underdamped system occurs at

$$t = \frac{\tan^{-1}\dfrac{\sqrt{1-\zeta^2}}{\zeta}}{\omega_n\sqrt{1-\zeta^2}}, \qquad \text{where } 0 < \zeta < 1$$

and the maximum overshoot is

$$c(t)_{\max} = \omega_n \exp\left(-\frac{\zeta}{\sqrt{1-\zeta^2}}\tan^{-1}\frac{\sqrt{1-\zeta^2}}{\zeta}\right), \qquad \text{where } 0 < \zeta < 1$$

Since the unit-impulse response function is the time derivative of the unit-step response function, the maximum overshoot M_p for the unit-step response can be found from the corresponding unit-impulse response. That is, the area under the unit-impulse response curve from $t = 0$ to the time of the first zero, as shown in Figure 4–19, is $1 + M_p$, where M_p is the maximum overshoot (for the unit-step response) given by Equation (4–30). The peak time t_p (for the unit-step response) given by Equation (4–29) corresponds to the time that the unit-impulse response first crosses the time axis.

4–4 TRANSIENT-RESPONSE ANALYSIS WITH MATLAB

Introduction. In this section we present the computational approach to the transient-response analysis with MATLAB. Those readers who are as yet unfamiliar with MATLAB may wish to read Appendix before studying this section.

As stated earlier in this chapter, transient responses (such as the step response, impulse response, and ramp response) are used frequently to investigate the time-domain characteristics of control systems.

MATLAB representation of linear systems. The transfer function of a system is represented by two arrays of numbers. Consider the system

$$\frac{C(s)}{R(s)} = \frac{25}{s^2 + 4s + 25} \tag{4–38}$$

This system is represented as two arrays each containing the coefficients of the polynomials in decreasing powers of s as follows:

```
num = [0   0   25]
den = [1   4   25]
```

Note that zeros are padded where necessary.

If num and den (the numerator and denominator of the closed-loop transfer function) are known, commands such as

```
step(num,den),        step(num,den,t)
```

will generate plots of unit-step responses. (t in the step command is the user-specified time.)

For a control system defined in a state-space form, where state matrix **A**, control matrix **B**, output matrix **C**, and direct transmission matrix **D** of state-space equations are known, the command

```
step(A,B,C,D)
```

will generate plots of unit-step responses. The time vector is automatically determined when t is not explicitly included in the step commands.

Note that when step commands have left-hand arguments such as

```
[y,x,t] = step(num,den,t)
[y,x,t] = step(A,B,C,D,iu)
[y,x,t] = step(A,B,C,D,iu,t)                    (4–39)
```

no plot is shown on the screen. Hence it is necessary to use a *plot* command to see the response curves. The matrices y and x contain the output and state response of the system, respectively, evaluated at the computation time points t. (y has as many columns as outputs and one row for each element in t. x has as many columns as states and one row for each element in t.)

Note in Equation (4–39) that the scalar iu is an index into the inputs of the system and specifies which input is to be used for the response, and t is the user-specified time. If the system involves multiple inputs and multiple outputs, the step command, such as given by Equation (4–39), produces a series of step response plots, one for each input and output combination of

$$\dot{\mathbf{x}} = \mathbf{Ax} + \mathbf{Bu}$$

$$\mathbf{y} = \mathbf{Cx} + \mathbf{Du}$$

(For details, see Example 4–4.)

Obtaining the unit-step response of the transfer-function system. Let us consider the unit-step response of the system given by Equation (4–38). MATLAB Program 4–1 will yield a plot of the unit-step response of this system. A plot of the unit-step response curve is shown in Figure 4–20.

MATLAB Program 4–1

```
% ---------Unit-step response---------

% ***** Enter the numerator and denominator of the transfer
% function *****

num = [0    0    25];
den = [1    4    25];

% ***** Enter the following step-response command *****

step(num,den)

% ***** Enter grid and title of the plot *****

grid
title ('Unit-Step Response of G(s) = 25/(s^2 + 4s + 25)')
```

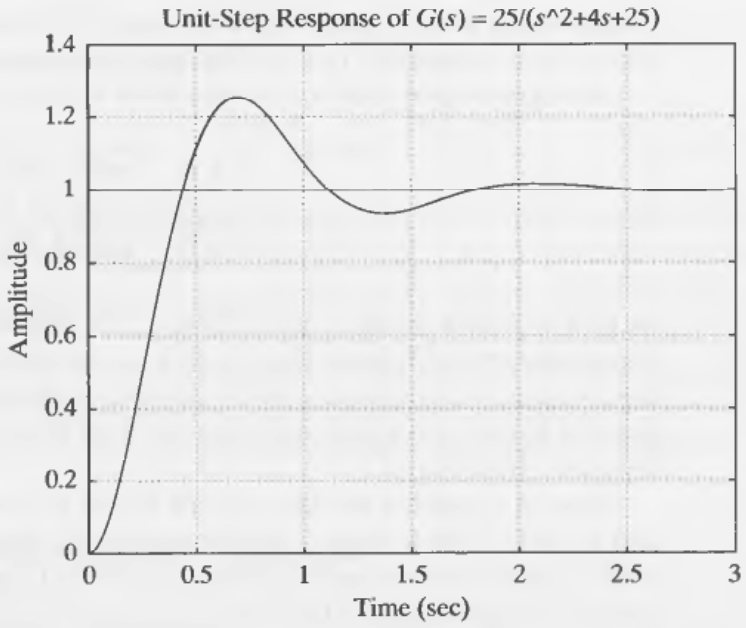

Figure 4–20
Unit-step response curve.

EXAMPLE 4–4 Consider the following system:

$$\begin{bmatrix} \dot{x}_1 \\ \dot{x}_2 \end{bmatrix} = \begin{bmatrix} -1 & -1 \\ 6.5 & 0 \end{bmatrix} \begin{bmatrix} x_1 \\ x_2 \end{bmatrix} + \begin{bmatrix} 1 & 1 \\ 1 & 0 \end{bmatrix} \begin{bmatrix} u_1 \\ u_2 \end{bmatrix}$$

$$\begin{bmatrix} y_1 \\ y_2 \end{bmatrix} = \begin{bmatrix} 1 & 0 \\ 0 & 1 \end{bmatrix} \begin{bmatrix} x_1 \\ x_2 \end{bmatrix} + \begin{bmatrix} 0 & 0 \\ 0 & 0 \end{bmatrix} \begin{bmatrix} u_1 \\ u_2 \end{bmatrix}$$

Obtain the unit-step response curves.

Although it is not necessary to obtain the transfer function expression for the system to obtain the unit-step response curves with MATLAB, we shall derive such an expression for reference. For the system defined by

$$\dot{\mathbf{x}} = \mathbf{Ax} + \mathbf{Bu}$$

$$\mathbf{y} = \mathbf{Cx} + \mathbf{Du}$$

the transfer matrix $\mathbf{G}(s)$ is a matrix that relates $\mathbf{Y}(s)$ and $\mathbf{U}(s)$ as follows:

$$\mathbf{Y}(s) = \mathbf{G}(s)\mathbf{U}(s)$$

Taking Laplace transforms of the state-space equations, we obtain

$$s\mathbf{X}(s) - \mathbf{x}(0) = \mathbf{AX}(s) + \mathbf{BU}(s) \tag{4-40}$$

$$\mathbf{Y}(s) = \mathbf{CX}(s) + \mathbf{DU}(s) \tag{4-41}$$

In deriving the transfer matrix, we assume that $\mathbf{x}(0) = \mathbf{0}$. Then, from Equation (4–40), we get

$$\mathbf{X}(s) = (s\mathbf{I} - \mathbf{A})^{-1}\mathbf{BU}(s) \tag{4-42}$$

Substituting Equation (4–42) into Equation (4–41), we obtain

$$\mathbf{Y}(s) = [\mathbf{C}(s\mathbf{I} - \mathbf{A})^{-1}\mathbf{B} + \mathbf{D}]\mathbf{U}(s)$$

Thus the transfer matrix $\mathbf{G}(s)$ is given by

$$\mathbf{G}(s) = \mathbf{C}(s\mathbf{I} - \mathbf{A})^{-1}\mathbf{B} + \mathbf{D}$$

The transfer matrix $\mathbf{G}(s)$ for the given system becomes

$$\begin{aligned}
\mathbf{G}(s) &= \mathbf{C}(s\mathbf{I} - \mathbf{A})^{-1}\mathbf{B} \\
&= \begin{bmatrix} 1 & 0 \\ 0 & 1 \end{bmatrix} \begin{bmatrix} s+1 & 1 \\ -6.5 & s \end{bmatrix}^{-1} \begin{bmatrix} 1 & 1 \\ 1 & 0 \end{bmatrix} \\
&= \frac{1}{s^2 + s + 6.5} \begin{bmatrix} s & -1 \\ 6.5 & s+1 \end{bmatrix} \begin{bmatrix} 1 & 1 \\ 1 & 0 \end{bmatrix} \\
&= \frac{1}{s^2 + s + 6.5} \begin{bmatrix} s-1 & s \\ s+7.5 & 6.5 \end{bmatrix}
\end{aligned}$$

Hence

$$\begin{bmatrix} Y_1(s) \\ Y_2(s) \end{bmatrix} = \begin{bmatrix} \dfrac{s-1}{s^2 + s + 6.5} & \dfrac{s}{s^2 + s + 6.5} \\ \dfrac{s+7.5}{s^2 + s + 6.5} & \dfrac{6.5}{s^2 + s + 6.5} \end{bmatrix} \begin{bmatrix} U_1(s) \\ U_2(s) \end{bmatrix}$$

Since this system involves two inputs and two outputs, four transfer functions may be defined depending on which signals are considered as input and output. Note that, when considering the signal u_1 as the input, we assume that signal u_2 is zero, and vice versa. The four transfer functions are

$$\frac{Y_1(s)}{U_1(s)} = \frac{s-1}{s^2 + s + 6.5}, \qquad \frac{Y_2(s)}{U_1(s)} = \frac{s+7.5}{s^2 + s + 6.5}$$

$$\frac{Y_1(s)}{U_2(s)} = \frac{s}{s^2 + s + 6.5}, \qquad \frac{Y_2(s)}{U_2(s)} = \frac{6.5}{s^2 + s + 6.5}$$

The four individual step-response curves can be plotted by use of the command

```
step(A,B,C,D)
```

MATLAB Program 4–2 produces four such step-response curves. The curves are shown in Figure 4–21.

```
MATLAB Program 4–2

A = [−1   −1;6.5   0];
B = [1    1;1    0];
C = [1    0;0    1];
D = [0    0;0    0];
step(A,B,C,D)
```

To plot two step-response curves for the input u_1 in one diagram and two step-response curves for the input u_2 in another diagram, we may use the commands

```
step(A,B,C,D,1)
```

and

```
step(A,B,C,D,2)
```

respectively. MATLAB Program 4–3 is a program to plot two step-response curves for the input u_1 in one diagram and two step-response curves for the input u_2 in another diagram. Figure 4–22 shows the two diagrams, each consisting of two step-response curves.

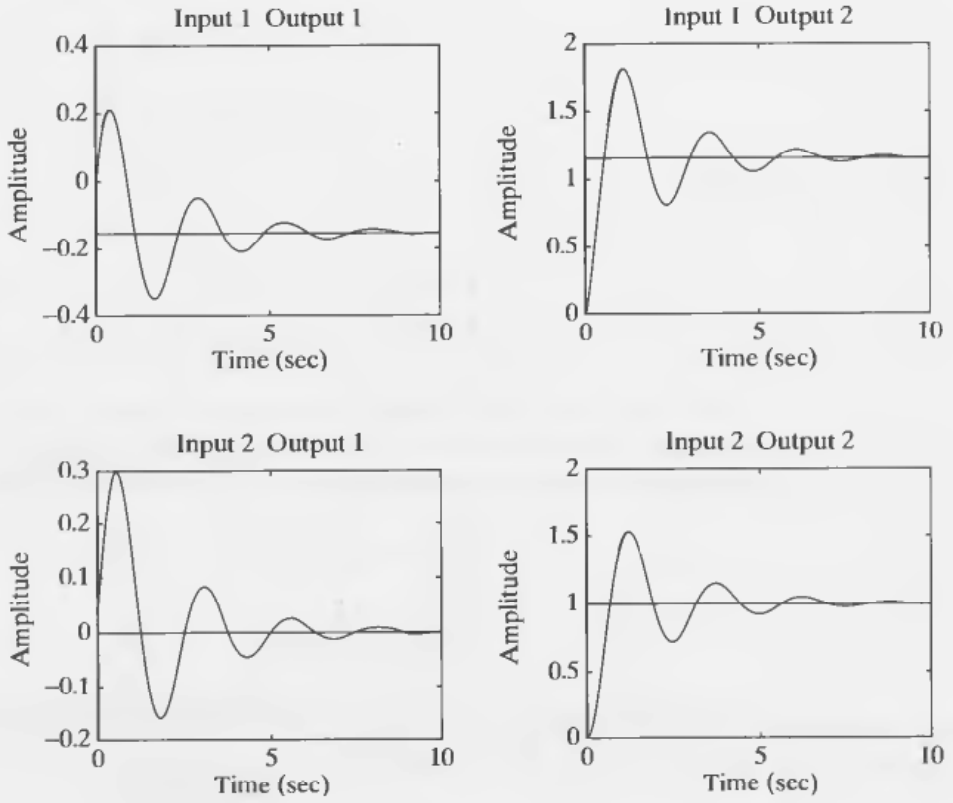

Figure 4–21
Unit-step response curves.

MATLAB Program 4–3

```
% ---------- Step-response curves for system defined in state
% space ----------

% ***** In this program we plot step-response curves of a system
% having two inputs (u1 and u2) and two outputs (y1 and y2) *****

% ***** We shall first plot step-response curves when the input is
% u1. Then we shall plot step-response curves when the input is
% u2 *****

% ***** Enter matrices A, B, C, and D *****

A = [-1   -1;6.5   0];
B = [1   1;1   0];
C = [1   0;0   1];
D = [0   0;0   0];

% ***** To plot step-response curves when the input is u1, enter
% the command 'step(A,B,C,D,1)' *****

step(A,B,C,D,1)
grid
title ('Step-Response Plots: Input = u1 (u2 = 0)')
text(3.4,-0.06,'Y1')
text(3.4,1.4,'Y2')

% ***** Next, we shall plot step-response curves when the input
% is u2. Enter the command 'step(A,B,C,D,2)' *****

step(A,B,C,D,2);
grid
title('Step-Response Plots: Input = u2 (u1 = 0)')
text(3,0.14,'Y1')
text(2.8,1.1,'Y2')
```

Writing text on the graphics screen. To write text on the graphics screen, enter, for example, the following statements:

```
text(3.4,-0.06,'Y1')
```

and

```
text(3.4,1.4,'Y2')
```

The first statement tells the computer to write 'Y1' beginning at the coordinates $x = 3.4$, $y = -0.06$. Similarly, the second statement tells the computer to write 'Y2' beginning at the coordinates $x = 3.4$, $y = 1.4$. [See MATLAB Program 4–3 and Figure 4–22(a).]

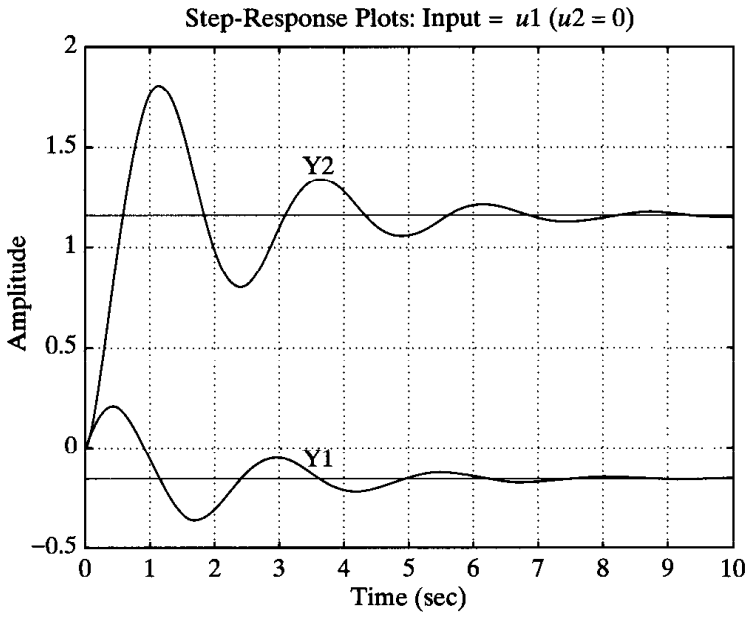

(a)

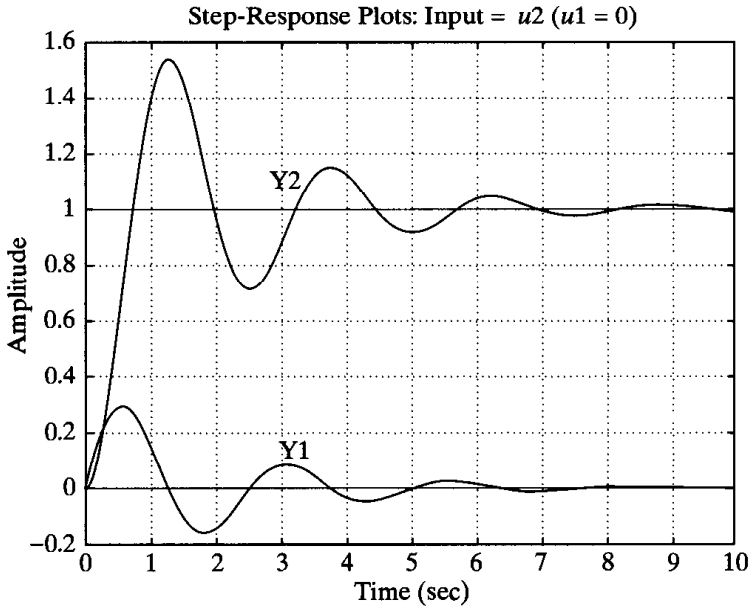

(b)

Figure 4–22
Unit-step response curves. (a) u_1 is the input ($u_2 = 0$); (b) u_2 is the input ($u_1 = 0$).

Impulse response. The unit-impulse response of a control system may be obtained by use of one of the following MATLAB commands:

```
impulse(num,den)
impulse(A,B,C,D)
[y,x,t] = impulse (num,den)
[y,x,t] = impulse(num,den,t)                    (4–43)
```

```
[y,x,t] = impulse(A,B,C,D)
[y,x,t] = impulse(A,B,C,D,iu)                    (4–44)
[y,x,t] = impulse (A,B,C,D,iu,t)                 (4–45)
```

The command "impulse(num,den)" plots the unit-impulse response on the screen. The command "impulse(A,B,C,D)" produces a series of unit-impulse-response plots, one for each input and output combination of the system

$$\dot{\mathbf{x}} = \mathbf{Ax} + \mathbf{Bu}$$

$$\mathbf{y} = \mathbf{Cx} + \mathbf{Du}$$

with the time vector automatically determined. Note that in Equations (4–44) and (4–45) the scalar iu is an index into the inputs of the system and specifies which input to be used for the impulse response.

Note also that in Equations (4–43) and (4–45) t is the user-supplied time vector. The vector t specifies the times at which the impulse response is to be computed.

If MATLAB is invoked with the left-hand argument [y,x,t], such as in the case of [y,x,t] = impulse(A,B,C,D), the command returns the output and state responses of the system and the time vector t. No plot is drawn on the screen. The matrices y and x contain the output and state responses of the system evaluated at the time points t. (y has as many columns as outputs and one row for each element in t. x has as many columns as state variables and one row for each element in t.)

EXAMPLE 4–5 Obtain the unit-impulse response of the following system:

$$\begin{bmatrix} \dot{x}_1 \\ \dot{x}_2 \end{bmatrix} = \begin{bmatrix} 0 & 1 \\ -1 & -1 \end{bmatrix} \begin{bmatrix} x_1 \\ x_2 \end{bmatrix} + \begin{bmatrix} 0 \\ 1 \end{bmatrix} u$$

$$y = \begin{bmatrix} 1 & 0 \end{bmatrix} \begin{bmatrix} x_1 \\ x_2 \end{bmatrix} + [0]u$$

A possible MATLAB program is shown in MATLAB Program 4–4. The resulting response curve is shown in Figure 4–23.

MATLAB Program 4–4

```
A = [0   1;−1   −1];
B = [0;1];
C = [1   0];
D = [0];
impulse(A,B,C,D);
grid;
title('Unit-Impulse Response')
```

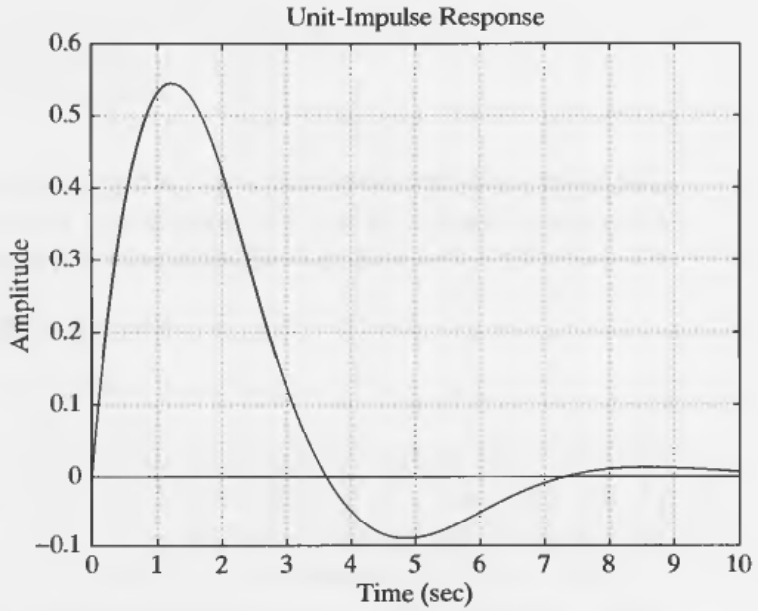

Figure 4–23
Unit-impulse response curve.

EXAMPLE 4–6 Obtain the unit-impulse response of the following system:

$$\frac{C(s)}{R(s)} = G(s) = \frac{1}{s^2 + 0.2s + 1}$$

MATLAB Program 4–5 will produce the unit-impulse response. The resulting plot is shown in Figure 4–24.

MATLAB Program 4–5

```
num = [0   0   1];
den = [1   0.2   1];
impulse(num,den);
grid
title('Unit-Impulse Response of G(s) = 1/(s^2 + 0.2s + 1)')
```

Alternative approach to obtain impulse response. Note that when the initial conditions are zero the unit-impulse response of $G(s)$ is the same as the unit-step response of $sG(s)$.

Consider the unit-impulse response of the system considered in Example 4–6. Since $R(s) = 1$ for the unit-impulse input, we have

$$\frac{C(s)}{R(s)} = C(s) = G(s) = \frac{1}{s^2 + 0.2s + 1}$$

$$= \frac{s}{s^2 + 0.2s + 1}\frac{1}{s}$$

We can thus convert the unit-impulse response of $G(s)$ to the unit-step response of $sG(s)$.

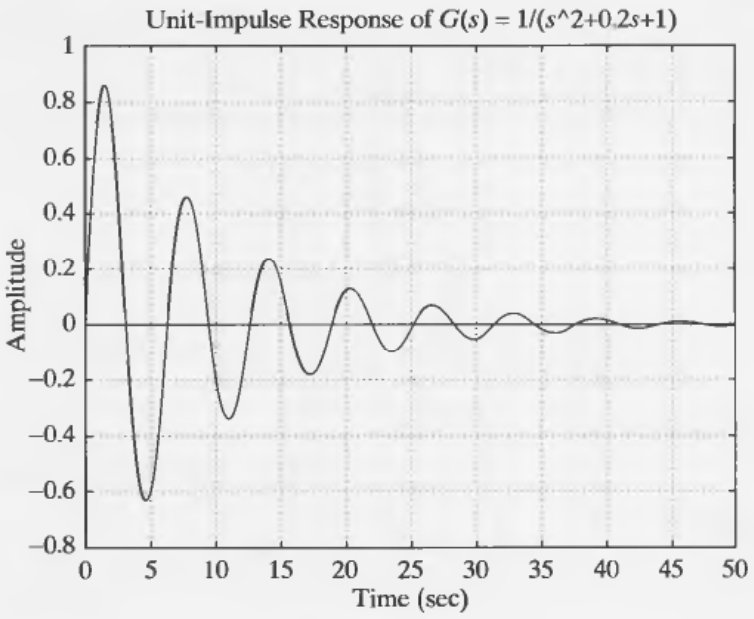

Figure 4–24
Unit-impulse response curve.

If we enter the following num and den into MATLAB,

```
num = [0   1   0]
den = [1   0.2   1]
```

and use the step-response command, as given in MATLAB Program 4–6, we obtain a plot of the unit-impulse response of the system as shown in Figure 4–25.

MATLAB Program 4–6

```
num = [0   1   0];
den = [1   0.2   1];
step(num,den);
grid;
title('Unit-Step Response of sG(s) = s/(s^2 + 0.2s + 1)')
```

Notice in Figure 4–25 (and many others) that the x axis and y axis labels are automatically determined. If it is desired to label the x axis and y axis differently, we need to modify the step command. For example, if it is desired to label the x axis as 't Sec' and the y axis as 'Input and Output,' then use step-response commands with left-hand arguments, such as

```
c = step(num,den,t)
```

or, more generally,

```
[y,x,t] = step(num,den,t)
```

See MATLAB Program 4–7.

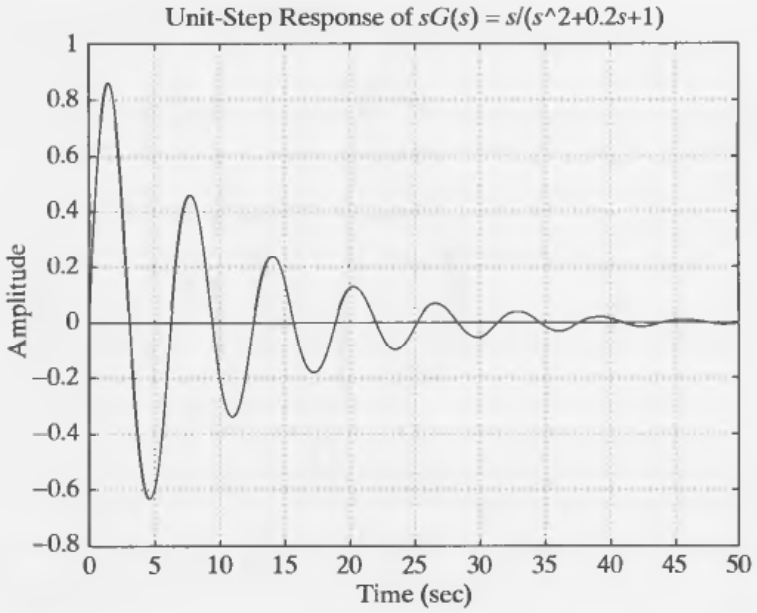

Figure 4–25
Unit-impulse response curve obtained as the unit-step response of $sG(s) = s/(s^2 + 0.2s + 1)$.

MATLAB Program 4–7

```
% --------- Unit-ramp response ---------

% ***** The unit-ramp response is obtained as the unit-step
% response of G(s)/s *****

% ***** Enter the numerator and denominator of G(s)/s *****

num = [0   0   0   1];
den = [1   1   1   0];

% ***** Specify the computing time points (such as t = 0:0.1:7)
% and then enter step-response command: c = step(num,den,t) *****

t = 0:0.1:7;
c = step(num,den,t);

% ***** In plotting the ramp-response curve, add the reference
% input to the plot. The reference input is t. Add to the
% argument of the plot command with the following: t,t,'-'. Thus
% the plot command becomes as follows: plot(t,c,'o',t,t,'-') *****

plot(t,c,'o',t,t,'-')

% ***** Add grid, title, xlabel, and ylabel *****

grid
title('Unit-Ramp Response Curve for System G(s) = 1/(s^2 + s + 1)')
xlabel('t Sec')
ylabel('Input and Output')
```

Ramp response. There is no ramp command in MATLAB. Therefore, we need to use the step command to obtain the ramp response. Specifically, to obtain the ramp response of the transfer-function system $G(s)$, divide $G(s)$ by s and use the step-response command. For example, consider the closed-loop system

$$\frac{C(s)}{R(s)} = \frac{1}{s^2 + s + 1}$$

For a unit-ramp input, $R(s) = 1/(s^2)$. Hence

$$C(s) = \frac{1}{s^2 + s + 1}\frac{1}{s^2} = \frac{1}{(s^2 + s + 1)s}\frac{1}{s}$$

To obtain the unit-ramp response of this system, enter the following numerator and denominator into the MATLAB program,

```
num = [0  0  0  1];
den = [1  1  1  0];
```

and use the step-response command. See MATLAB Program 4–7. The plot obtained by using this program is shown in Figure 4–26.

Unit-ramp response of a system defined in state space. Next, we shall treat the unit-ramp response of the system in state-space form. Consider the system described by

$$\dot{\mathbf{x}} = \mathbf{A}\mathbf{x} + \mathbf{B}u$$

$$y = \mathbf{C}\mathbf{x} + Du$$

In what follows, we shall consider a simple example to explain the method. Let us assume that

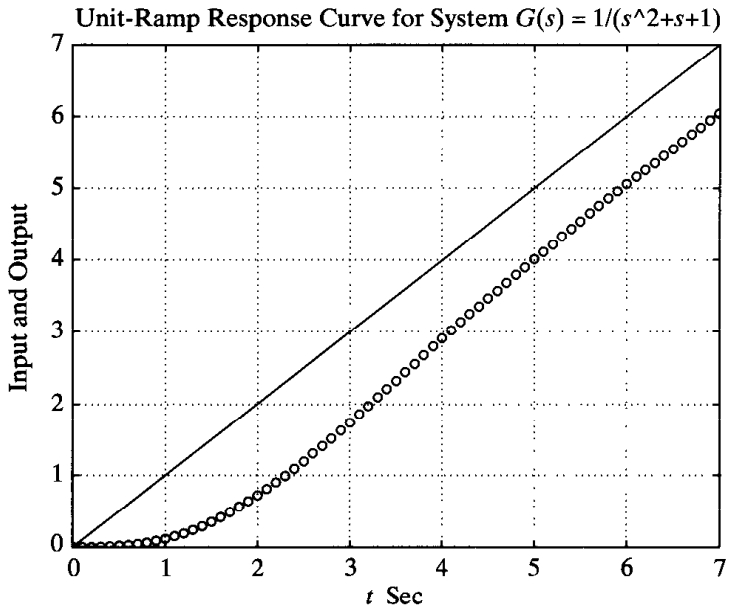

Figure 4–26
Unit-ramp response curve.

$$\mathbf{A} = \begin{bmatrix} 0 & 1 \\ -1 & -1 \end{bmatrix}, \qquad \mathbf{B} = \begin{bmatrix} 0 \\ 1 \end{bmatrix}, \qquad \mathbf{x}(0) = \mathbf{0}$$
$$\mathbf{C} = [1 \quad 0], \qquad D = [0]$$

When the initial conditions are zeros, the unit-ramp response is the integral of the unit-step response. Hence the unit-ramp response can be given by

$$z = \int_0^t y\, dt \tag{4-46}$$

From Equation (4–46), we obtain

$$\dot{z} = y = x_1 \tag{4-47}$$

Let us define

$$z = x_3$$

Then Equation (4–47) becomes

$$\dot{x}_3 = x_1 \tag{4-48}$$

Combining Equation (4–48) with the original state-space equation, we obtain

$$\begin{bmatrix} \dot{x}_1 \\ \dot{x}_2 \\ \dot{x}_3 \end{bmatrix} = \begin{bmatrix} 0 & 1 & 0 \\ -1 & -1 & 0 \\ 1 & 0 & 0 \end{bmatrix} \begin{bmatrix} x_1 \\ x_2 \\ x_3 \end{bmatrix} + \begin{bmatrix} 0 \\ 1 \\ 0 \end{bmatrix} u$$
$$z = [0 \quad 0 \quad 1] \begin{bmatrix} x_1 \\ x_2 \\ x_3 \end{bmatrix}$$

which can be written as

$$\dot{\mathbf{x}} = \mathbf{AA}\mathbf{x} + \mathbf{BB}u$$
$$z = \mathbf{CC}\mathbf{x} + DDu$$

where

$$\mathbf{AA} = \begin{bmatrix} 0 & 1 & 0 \\ -1 & -1 & 0 \\ 1 & 0 & 0 \end{bmatrix} = \left[\begin{array}{cc:c} & & 0 \\ \multicolumn{2}{c:}{\mathbf{A}} & 0 \\ \hdashline \multicolumn{2}{c:}{\mathbf{C}} & 0 \end{array}\right]$$
$$\mathbf{BB} = \begin{bmatrix} 0 \\ 1 \\ 0 \end{bmatrix} = \left[\begin{array}{c} \mathbf{B} \\ \hdashline 0 \end{array}\right], \qquad \mathbf{CC} = [0 \quad 0 \quad 1], \qquad DD = [0]$$

Note that x_3 is the third element of $\mathbf{x}$. A plot of the unit-ramp response curve $z(t)$ can be obtained by entering MATLAB Program 4–8 into the computer. A plot of

MATLAB Program 4–8

```
% ---------- Unit-ramp response ----------

% ***** The unit-ramp response is obtained by adding a new
% state variable x3. The dimension of the state equation
% is enlarged by one *****

% ***** Enter matrices A, B, C, and D of the original state
% equation and output equation *****

A = [0   1;-1   -1];
B = [0;1];
C = [1   0];
D = [0];

% ***** Enter matrices AA, BB, CC, and DD of the new,
% enlarged state equation and output equation *****

AA = [A   zeros(2,1);C   0];
BB = [B;0];
CC = [0   0   1];
DD = [0];

% ***** Enter step-response command: [z,x,t] = step(AA,BB,CC,DD) *****

[z,x,t] = step(AA,BB,CC,DD);

% ***** In plotting x3 add the unit-ramp input t in the plot
% by entering the following command: plot(t,x3,'o',t,t,'-') *****

x3 = [0   0   1]*x'; plot(t,x3,'o',t,t,'-')
grid
title('Unit-Ramp Response')
xlabel('t Sec')
ylabel('Input and Output')
```

the unit-ramp response curve obtained from this MATLAB program is shown in Figure 4–27.

Response to initial condition (transfer-function approach). In what follows we shall present a method for obtaining the response to an initial condition by use of an example.

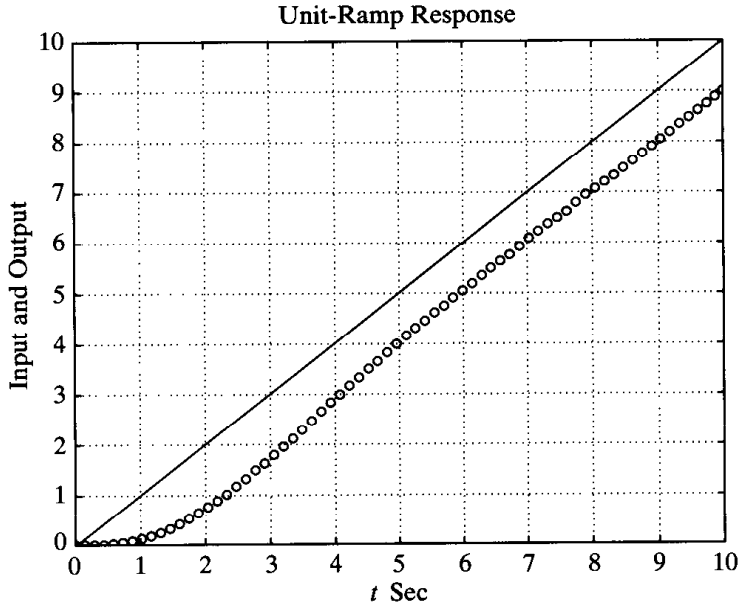

Figure 4–27
Unit-ramp response curve.

EXAMPLE 4–7

In this example, we shall consider a system subjected only to an initial condition.

Consider the mechanical system shown in Figure 4–28, where $m = 1$ kg, $b = 3$ N-sec/m, and $k = 2$ N/m. Assume that at $t = 0$ the mass m is pulled downward such that $x(0) = 0.1$ m and $\dot{x}(0) = 0.05$ m/sec. Obtain the motion of the mass subjected to the initial condition. (Assume no external forcing function.)

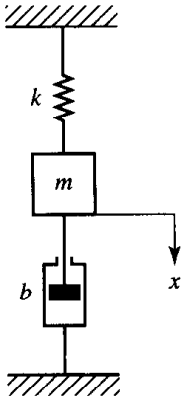

Figure 4–28
Mechanical system.

The system equation is

$$m\ddot{x} + b\dot{x} + kx = 0$$

with the initial conditions $x(0) = 0.1$ m and $\dot{x}(0) = 0.05$ m/sec. The Laplace transform of the system equation gives

$$m[s^2X(s) - sx(0) - \dot{x}(0)] + b[sX(s) - x(0)] + kX(s) = 0$$

or

$$(ms^2 + bs + k)X(s) = mx(0)s + m\dot{x}(0) + bx(0)$$

Solving this last equation for $X(s)$ and substituting the given numerical values, we obtain

$$X(s) = \frac{mx(0)s + m\dot{x}(0) + bx(0)}{ms^2 + bs + k}$$

$$= \frac{0.1s + 0.35}{s^2 + 3s + 2}$$

This equation can be written as

$$X(s) = \frac{0.1s^2 + 0.35s}{s^2 + 3s + 2}\frac{1}{s}$$

Hence the motion of the mass m may be obtained as the unit-step response of the following system:

$$G(s) = \frac{0.1s^2 + 0.35s}{s^2 + 3s + 2}$$

MATLAB Program 4–9 will give a plot of the motion of the mass. The plot is shown in Figure 4–29.

MATLAB Program 4–9

```
% ---------- Response to initial conditions ----------

% ***** System response to initial conditions is converted to
% a unit-step response by modifying the numerator polynomial *****

% ***** Enter the numerator and denominator of the transfer
% function G(s) *****

num = [0.1   0.35   0];
den = [1   3   2];

% ***** Enter the following step-response command *****

step(num,den)

% ***** Enter grid and title of the plot *****

grid
title('Response of Spring-Mass-Damper System to Initial Conditions')
```

Response to initial condition (state-space approach, case 1). Consider the system defined by

$$\dot{\mathbf{x}} = \mathbf{A}\mathbf{x}, \qquad \mathbf{x}(0) = \mathbf{x}_0 \tag{4–49}$$

Let us obtain the response $\mathbf{x}(t)$ when the initial condition $\mathbf{x}(0)$ is specified. (There is no external input function acting on this system.) Assume that $\mathbf{x}$ is an n-vector.

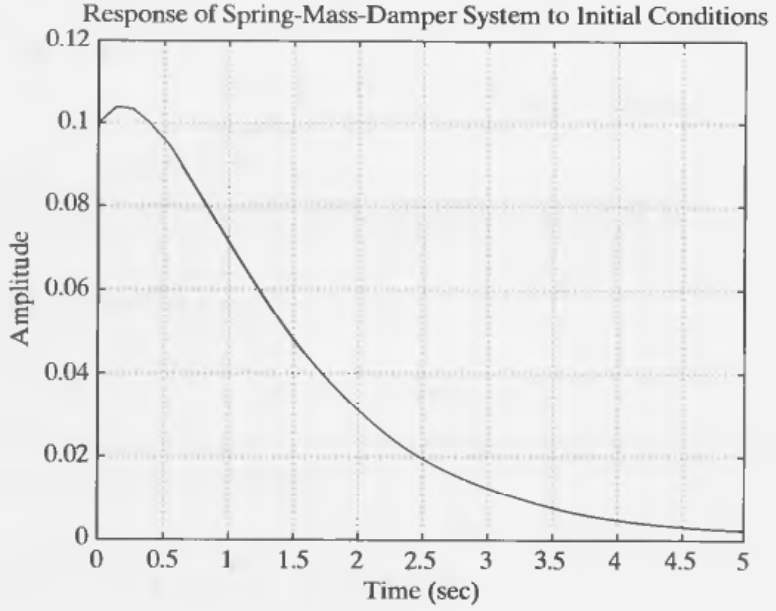

Figure 4–29
Response of the mechanical system considered in Example 4–7.

First, take Laplace transforms of both sides of Equation (4–49).

$$s\mathbf{X}(s) - \mathbf{x}(0) = \mathbf{A}\mathbf{X}(s)$$

This equation can be rewritten as

$$s\mathbf{X}(s) = \mathbf{A}\mathbf{X}(s) + \mathbf{x}(0) \tag{4–50}$$

Taking the inverse Laplace transform of Equation (4–50), we obtain

$$\dot{\mathbf{x}} = \mathbf{A}\mathbf{x} + \mathbf{x}(0)\,\delta(t) \tag{4–51}$$

(Notice that by taking the Laplace transform of a differential equation and then by taking the inverse Laplace transform of the Laplace-transformed equation we generate a differential equation that involves the initial condition.)

Now define

$$\dot{\mathbf{z}} = \mathbf{x} \tag{4–52}$$

Then Equation (4–51) can be written as

$$\ddot{\mathbf{z}} = \mathbf{A}\dot{\mathbf{z}} + \mathbf{x}(0)\,\delta(t) \tag{4–53}$$

By integrating Equation (4–53) with respect to t, we obtain

$$\dot{\mathbf{z}} = \mathbf{A}\mathbf{z} + \mathbf{x}(0)1(t) = \mathbf{A}\mathbf{z} + \mathbf{B}u \tag{4–54}$$

where

$$\mathbf{B} = \mathbf{x}(0), \qquad u = 1(t)$$

Referring to Equation (4–52), the state $\mathbf{x}(t)$ is given by $\dot{\mathbf{z}}(t)$. Thus,

$$\mathbf{x} = \dot{\mathbf{z}} = \mathbf{A}\mathbf{z} + \mathbf{B}u \tag{4–55}$$

Equation (4–55) gives the response to the initial condition.

Summarizing, the response of Equation (4–49) to the initial condition $\mathbf{x}(0)$ is obtained by solving the following state-space equations:

$$\dot{\mathbf{z}} = \mathbf{A}\mathbf{z} + \mathbf{B}u$$

$$\mathbf{x} = \mathbf{A}\mathbf{z} + \mathbf{B}u$$

where

$$\mathbf{B} = \mathbf{x}(0), \qquad u = 1(t)$$

MATLAB commands to obtain the response curves in one diagram are given next.

```
[x,z,t] = step(A,B,A,B);
x1 = [1   0   0 . . . 0]*x';
x2 = [0   1   0 . . . 0]*x';
   .
   .
   .

xn = [0   0   0 . . . 1]*x';
plot(t,xl,t,x2, . . . ,t,xn)
```

Response to initial condition (state-space approach, case 2). Consider the system defined by

$$\dot{\mathbf{x}} = \mathbf{A}\mathbf{x}, \qquad \mathbf{x}(0) = \mathbf{x}_0 \tag{4–56}$$

$$\mathbf{y} = \mathbf{C}\mathbf{x} \tag{4–57}$$

(Assume that $\mathbf{x}$ is an n-vector and $\mathbf{y}$ is an m-vector.)

Similar to case 1, by defining

$$\dot{\mathbf{z}} = \mathbf{x}$$

we can obtain the following equation:

$$\ddot{\mathbf{z}} = \mathbf{A}\dot{\mathbf{z}} + \mathbf{x}(0)1(t) = \mathbf{A}\dot{\mathbf{z}} + \mathbf{B}u \tag{4–58}$$

where

$$\mathbf{B} = \mathbf{x}(0), \qquad u = 1(t)$$

Noting that $\mathbf{x} = \dot{\mathbf{z}}$, Equation (4–57) can be written as

$$\mathbf{y} = \mathbf{C}\dot{\mathbf{z}} \tag{4–59}$$

By substituting Equation (4–58) into Equation (4–59), we obtain

$$\mathbf{y} = \mathbf{C}(\mathbf{A}\dot{\mathbf{z}} + \mathbf{B}u) = \mathbf{C}\mathbf{A}\dot{\mathbf{z}} + \mathbf{C}\mathbf{B}u \tag{4–60}$$

The solution of Equations (4–58) and (4–60) gives the response of the system to a given initial condition. MATLAB commands to obtain the response curves (output curves y1 versus t, y2 versus t, . . . , ym versus t) are shown next.

```
[y,z,t] = step(A,B,C*A,C*B)
y1 = [1   0   0 . . . 0]*y';
y2 = [0   1   0 . . . 0]*y';
      .
      .
      .

ym = [0   0   0 . . . 1]*y';
plot(t,y1,t,y2 . . . ,t,ym)
```

EXAMPLE 4–8 Obtain the response of the system subjected to the given initial condition.

$$\begin{bmatrix} \dot{x}_1 \\ \dot{x}_2 \end{bmatrix} = \begin{bmatrix} 0 & 1 \\ -10 & -5 \end{bmatrix} \begin{bmatrix} x_1 \\ x_2 \end{bmatrix}, \qquad \begin{bmatrix} x_1(0) \\ x_2(0) \end{bmatrix} = \begin{bmatrix} 2 \\ 1 \end{bmatrix}$$

or

$$\dot{\mathbf{x}} = \mathbf{A}\mathbf{x}, \qquad \mathbf{x}(0) = \mathbf{x}_0$$

Obtaining the response of the system to the given initial condition becomes that of solving the unit-step response of the following system:

$$\ddot{\mathbf{z}} = \mathbf{A}\dot{\mathbf{z}} + \mathbf{B}u$$

$$\mathbf{x} = \mathbf{A}\dot{\mathbf{z}} + \mathbf{B}u$$

where

$$\mathbf{B} = \mathbf{x}(0), \qquad u = 1(t)$$

Hence a possible MATLAB program for obtaining the response may be given as shown in MATLAB Program 4–10. The resulting response curves are shown in Figure 4–30.

MATLAB Program 4–10

```
A = [0   1;−10   −5];
B = [2;1];
[x,z,t] = step(A,B,A,B);
x1 = [1   0]*x';
x2 = [0   1]*x';
plot(t,x1,'o',t,x2,'-')
grid
title('Response to Initial Condition')
xlabel('t Sec')
ylabel('x1   x2')
```

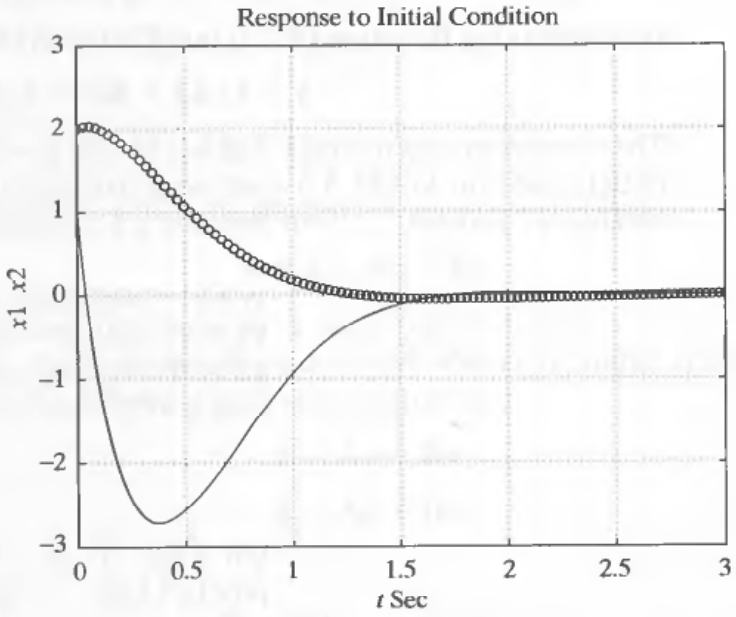

Figure 4–30
Response of system in Example 4–8 to initial condition.

4–5 AN EXAMPLE PROBLEM SOLVED WITH MATLAB

The purpose of this section is to present a MATLAB solution of the response of a mechanical vibratory system. The mathematical model of the system is first developed, then the system is simulated using MATLAB for a continuous-time and a discrete-time approach, and response curves are generated for each approach.

Mechanical vibratory system. Consider the mechanical vibratory system shown in Figure 4–31(a). A wheel has a spring–mass–damper system hanging from it. The wheel is in a track that contains a flat (horizontal) portion, a slanted (downward at 45°)

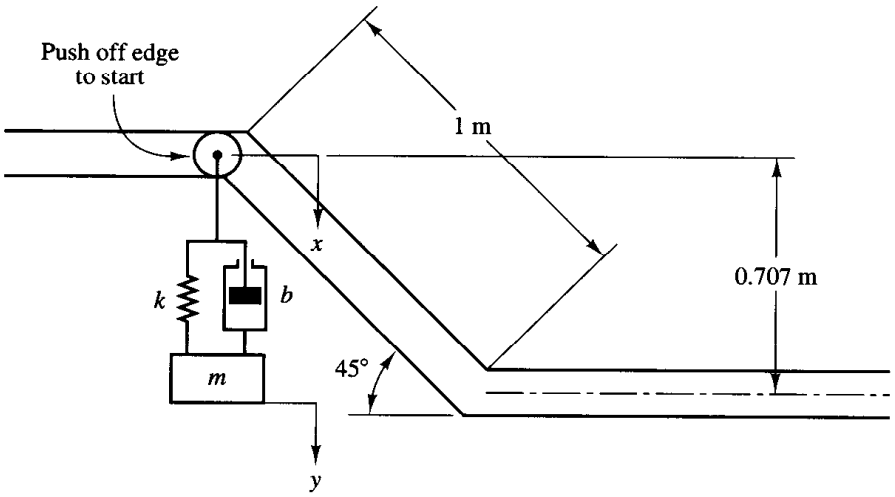

(a)

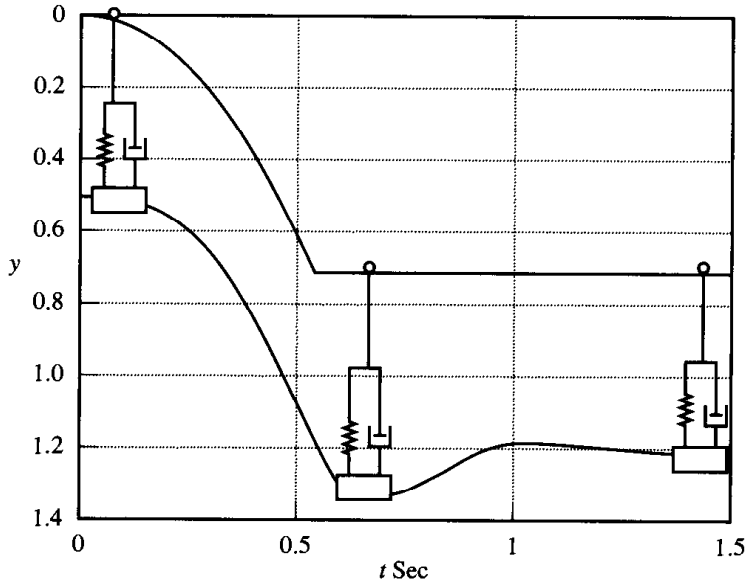

(b)

Figure 4–31
(a) Wheel with hanging mass-damper system; (b) dynamic response of the system.

portion, and another flat (horizontal) portion. We start the motion of the system by nudging the wheel over the edge of the ramp. As the wheel drops down the ramp for a total of 0.707 m (vertically measured), the mass m hanging from the spring and damper drops with it, and the mass gains momentum that dissipates gradually. In this problem the wheel is assumed to slide on the slanted portion of the track without friction. On the second flat portion of the track, the wheel slides and rolls. The wheel continues to move on the flat portion of the track until it is stopped by an external means.

Assume the following numerical values for m, b, and k:

$$m = 4 \text{ kg}, \qquad b = 40 \text{ N-sec/m}, \qquad k = 400 \text{ N/m}$$

Assume also that the mass m_p of the wheel is negligible compared with the mass m. Obtain $x(t)$, the vertical motion of the wheel. Then obtain $Y(s)$, the Laplace transform of $y(t)$, which represents the up and down motion of mass m. The coordinate y is attached to the spring–mass–damper system as shown in Figure 4–31 and is measured from the

equilibrium position of the system. The initial conditions are that $y(0) = 0$ and $\dot{y}(0) = 0$. Note that in this problem we are interested only in the vertical motions of the spring–mass–damper system. Note also that the system is frictionless with the exception of the damper, which relies on viscosity for its operation.

As the spring–mass–damper component travels down the ramp, it will undergo an acceleration produced as a result of the gravity force. When the spring–mass–damper reaches the level region at the bottom of the ramp, a shock will immediately be imposed on the spring–mass–damper component. It will, however, eventually come to a state of equilibrium following the impact due to the settling effects of the damper and spring. The dynamic response of this system is shown in Figure 4–31(b).

Determination of x(t). The system starts with zero initial velocity and follows the track. The input to the system is the vertical position x along the track, and the output is the vertical position y of the mass. Since we assume no sliding friction, referring to Figure 4–32(a) we have in the z direction the following equation:

$$m\ddot{z} = mg \sin 45^\circ$$

or

$$\ddot{z} = 9.81 \times 0.707 = 6.9357$$

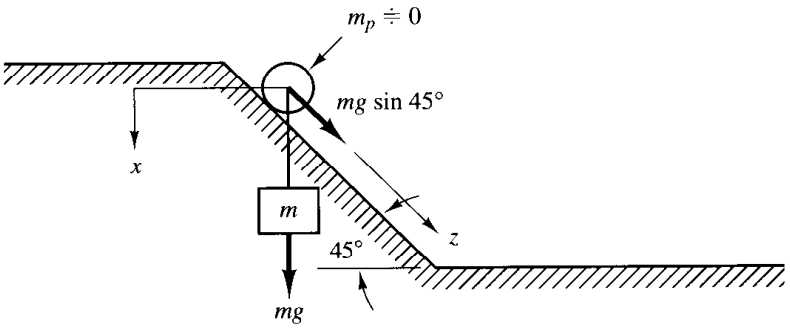

(a)

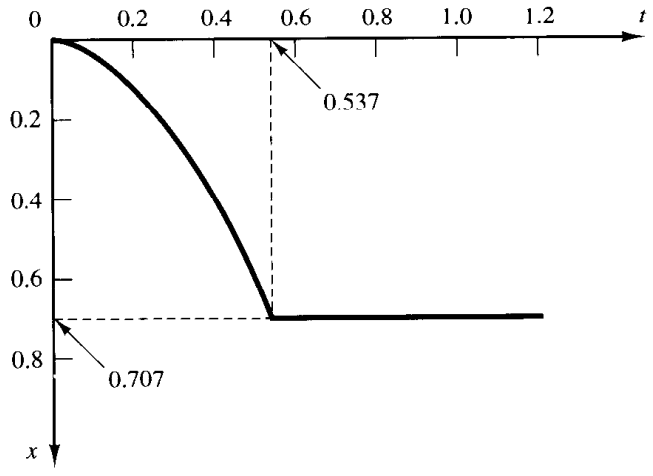

(b)

Figure 4–32
(a) Wheel with mass m slides on inclined plane; (b) curve $x(t)$ versus t.

Let us define the time it takes for the wheel to move from $z = 0$ to $z = 1$ m as t_1. Then

$$z = 6.9357 \frac{t_1^2}{2} = 1$$

which yields

$$t_1 = 0.537 \text{ sec}$$

Thus $x(t)$ can be given as follows:

$$\begin{aligned} x(t) = 0.707z = 0.707 \times 3.4678t^2 &= 2.452t^2, \qquad \text{for } 0 \le t \le 0.537 \\ &= 0.707, \qquad \text{for } 0.537 < t \end{aligned}$$

It follows that from $t = 0.537$ sec to $t = \infty$ we have an input defined by a constant of 0.707. The position x at the end of the ramp is 0.707 and it takes approximately 0.537 sec to get there. A curve $x(t)$ versus t is shown in Figure 4–32(b). Note that the positive direction of $x(t)$ is vertically downward.

To get a better picture of the events taking place in the system, we need to look at the input, shown in Figure 4–32(b). The effects of gravity do not allow us to model the behavior of the system with an ordinary ramp, but rather a parabolic function, which is followed by a constant input.

Determination of Transfer Function $Y(s)/X(s)$. Next, we shall first obtain the equation of motion for the system and then the transfer function $Y(s)/X(s)$. Since y is measured from the equilibrium position, the system equation becomes

$$m\ddot{y} + b(\dot{y} - \dot{x}) + k(y - x) = 0$$

or

$$m\ddot{y} + b\dot{y} + ky = b\dot{x} + kx$$

where x is the input to the system and y is the output. By substituting the given numerical values for m, b, and k, we obtain

$$4\ddot{y} + 40\dot{y} + 400y = 40\dot{x} + 400x$$

or

$$\ddot{y} + 10\dot{y} + 100y = 10\dot{x} + 100x \tag{4–61}$$

The transfer function for the system can now be given by

$$\frac{Y(s)}{X(s)} = \frac{10s + 100}{s^2 + 10s + 100} \tag{4–62}$$

where the input $x(t)$ is given by

$$\begin{aligned} x(t) &= 2.452t^2, \qquad 0 \le t \le 0.537 \\ &= 0.707, \qquad 0.537 < t \end{aligned} \tag{4–63}$$

Our problem here is to use MATLAB to find the inverse Laplace transform of $Y(s)$ given by Equation (4–62). In what follows we consider two approaches. One is to work in the continuous-time domain using the step command. The other is to work in the discrete-time domain using the filter command. We shall first present the continuous-time approach and then the discrete-time approach.

Computer simulation (continuous-time approach). In the continuous-time approach we separate the time region into two parts; $0 \le t \le 0.537$ and $0.537 < t$.

For $0 \le t \le 0.537$:

$$x_1(t) = 2.452t^2$$

Hence

$$X_1(s) = \frac{2.452 \times 2}{s^3} = \frac{4.904}{s^3}$$

The output $Y(s)$ can then be given by

$$\begin{aligned} Y(s) &= \frac{10s + 100}{s^2 + 10s + 100}\frac{4.904}{s^3} \\ &= \frac{49.04s + 490.4}{s^4 + 10s^3 + 100s^2}\frac{1}{s} \end{aligned} \tag{4–64}$$

For $0.537 < t$:

$$x_2(t) = 0.707$$

Since

$$\frac{Y_2(s)}{X_2(s)} = \frac{10s + 100}{s^2 + 10s + 100}$$

the corresponding differential equation becomes

$$\ddot{y}_2 + 10\dot{y}_2 + 100y_2 = 10\dot{x}_2 + 100x_2$$

The Laplace transform of this last equation becomes

$$\begin{aligned} [s^2Y_2(s) - sy_2(0) - \dot{y}_2(0)] + 10[sY_2(s) - y_2(0)] + 100Y_2(s) \\ = 10[sX_2(s) - x_2(0)] + 100X_2(s) \end{aligned}$$

or

$$\begin{aligned} (s^2 + 10s + 100)Y_2(s) = (10s + 100)X_2(s) + sy_2(0) \\ + \dot{y}_2(0) + 10y_2(0) - 10x_2(0) \end{aligned}$$

Hence

$$Y_2(s) = \frac{10s + 100}{s^2 + 10s + 100} X_2(s) + \frac{sy_2(0) + \dot{y}_2(0) + 10y_2(0) - 10x_2(0)}{s^2 + 10s + 100}$$

The initial conditions are found from $y_2(0) = y_1(0.537)$ and $\dot{y}_2(0) = \dot{y}_1(0.537)$. Therefore,

$$Y_2(s) = \frac{10s + 100}{s^2 + 10s + 100} \frac{0.707}{s} + \frac{s^2[y_1(0.537)] + [\dot{y}_1(0.537) + 10y_1(0.537) - 10(0.707)]s}{s^2 + 10s + 100} \frac{1}{s}$$

or

$$Y_2(s) = \frac{10s + 100}{s^2 + 10s + 100} \frac{0.707}{s} + \frac{s^2[y1(537)] + [y1dot(537) + 10y1(537) - 7.07]s}{s^2 + 10s + 100} \frac{1}{s} \qquad (4\text{–}65)$$

where

$$y1(537) = y_1(0.537), \qquad y1dot(537) = \dot{y}_1(0.537)$$

A MATLAB program to obtain the response $y(t)$ based on the continuous-time approach is given in MATLAB Program 4–11. The resulting response curve $y(t)$ versus t, as well as the input $x(t)$ versus t, is shown in Figure 4–33.

MATLAB Program 4–11

```
% --------- Continuous-time approach ---------
% ***** Obtain y1 and y1dot *****
num1 = [0   0   0   49.04   490.4];
den1 = [1   10   100   0   0];
t1 = 0:0.001:0.537;
y1 = step(num1,den1,t1);
num2 = [0   0   49.04   490.4];
den2 = [1   10   100   0];
y1dot = step(num2,den2,t1);
% ***** Determine the initial values of y1(537) and y1dot(537)
% for the second part. The initial values for the second
% part are output y2_ini = y1(537) and y2dot_ini = y1dot(537) *****
```

```
y2_ini = y1(537);
y2dot_ini = y1dot(537);
t2 = 0.538:0.001:1.5;
num3 = [0    7.07    70.7];
den3 = [1    10    100];
num4 = [y1(537)    y1dot(537)+10*y1(537)−7.07    0];
y2o = step(num3,den3,t2);
y2i = step(num4,den3,t2);
y2 = y2o + y2i;
y = [y1'    y2'];
t = [t1    t2];
plot(t,−y,'.')

hold

Current plot held

x1 = 2.452*t1.^2;
x2 = 0.707*ones(size(t2));
x = [x1    x2];
plot(t,−x,'-')
grid
title('Response of System (Continuous-Time Approach)')
xlabel('t Sec')
ylabel('Input x and Output y')
text(0.2,−0.54,'Input x')
text(0.47,−0.25,'Output y')
```

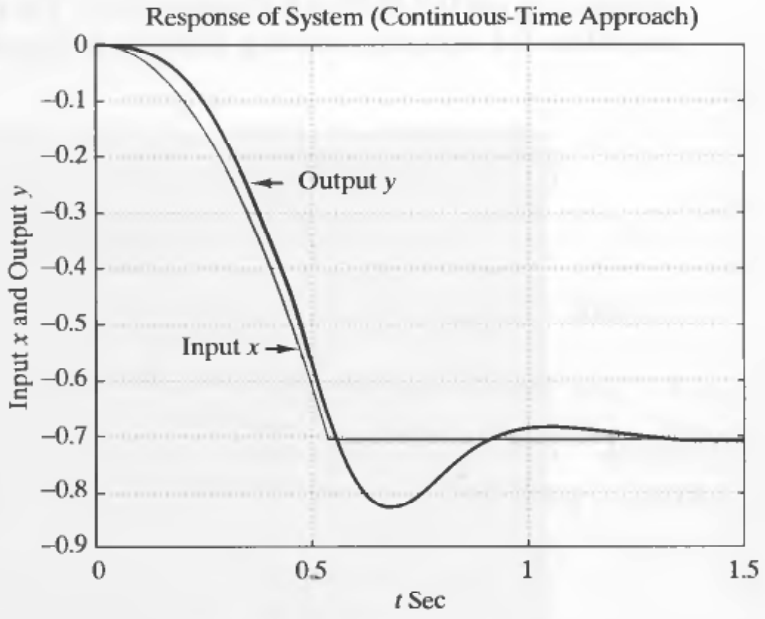

Figure 4–33
Input $x(t)$ and output $y(t)$ obtained by the continuous-time approach.

It is noted that when plotting multiple curves on one diagram we may use the "hold" command. If we enter the command "hold" in the computer, the screen will show

```
hold

Current plot held
```

To release the held plot, enter the command "hold" again. Then the current plot will be released as shown next.

```
hold

Current plot held

hold

Current plot released
```

Computer simulation (discrete-time approach). The continuous-time transfer function may be converted to a pulse transfer function (discrete-time transfer function) using general formulas. The simpler method is to convert the continuous-time transfer function to a pulse transfer function using MATLAB commands. The first step is to convert the continuous-time transfer function to a continuous-time set of state-space equations using the MATLAB command [A,B,C,D] = tf2ss(num,den). The state-space equations can then be converted from continuous-time to discrete-time using the command [G,H] = c2d(A,B,Ts), where Ts is the desired time step (sampling period). The discrete-time state-space equations are converted to a pulse transfer function with the command [numz,denz] = ss2tf(G,H,C,D).

In the present case we choose $T = 0.001$ sec. The input function $x(t)$ must first be discretized. The continuous-time input function was determined to be

$$x(t) = 2.452t^2, \qquad \text{for } 0 \leq t \leq 0.537$$
$$x(t) = 0.707, \qquad \text{for } 0.537 < t$$

Note that we define x as an array of points in MATLAB. This array initially follows $x(t) = 2.452t^2$ and, after $t = 0.537$ sec, follows $x(t) = 0.707$. We assume that the time region is $0 \leq t \leq 1.5$.

The acceleration input in the first part can be written as

```
k1 = 0:537;
x1 = [2.452*(0.001*k1).^2]
```

where k1 represents a time count and x1 is the first part of the complete input function. (There are 538 calculation points from the initial position until the input reaches

0.707 m.) For the second part of the input, we need a step function with magnitude 0.707. After time 0.537 sec,

```
k2 = 538:1500;
x2 = [0.707*ones(size(k2))]
```

(There are 963 points from 0.538 sec through 1.5 sec, inclusive.) The next step is to transform both inputs to one complete input:

```
x = [x1   x2];
```

(The two input equations are transformed into a single vector in order to appear as a single entry in the filter command argument.)

Now we can use the filter command, assigning a variable y,

```
y = filter(numz,denz,x);
```

and plot the response y(t), as well as the original input itself, x(t), taking care with the time intervals using t:

```
t = 0:1500;
plot(t/1000,-y,'.',t/1000,-x,'-')
```

(We divide t by 1000 because the time step is 0.001 sec.) Note also that the plotted input and output functions are negated. (Otherwise, we would have a positive acceleration input and response, which would be incorrect.)

A possible MATLAB program using the discrete-time approach is shown in MATLAB Program 4–12. The resulting response curves $x(t)$ versus t and $y(t)$ versus t are shown in Figure 4–34.

MATLAB Program 4–12

```
% ---------- Discrete-time approach ----------

% ***** Convert continuous-time transfer function to discrete-time
% transfer function (pulse transfer function) by choosing the time
% step (sampling period) to be 0.001 sec *****

num = [0   10   100];
den = [1   10   100];
[A,B,C,D] = tf2ss(num,den);
[G,H] = c2d(A,B,0.001);
[numz,denz] = ss2tf(G,H,C,D);

% ***** Enter the inputs x1 and x2 *****
```

```
k1 = 0:537;
x1 = [2.452*(0.001*k1).^2];
k2 = 538:1500;
x2 = [0.707*ones(size(k2))];
x = [x1   x2];

% ***** Using the filter command, obtain the response y *****

y = filter(numz,denz,x);
t = 0:1500;
plot(t/1000,-y,'.',t/1000,-x,'-')
grid
title('Response of System (Discrete-Time Approach)')
xlabel('t Sec')
ylabel('Input x  and  Output y')
text(0.2,-0.54,'Input x')
text(0.47,-0.25, 'Output y')
```

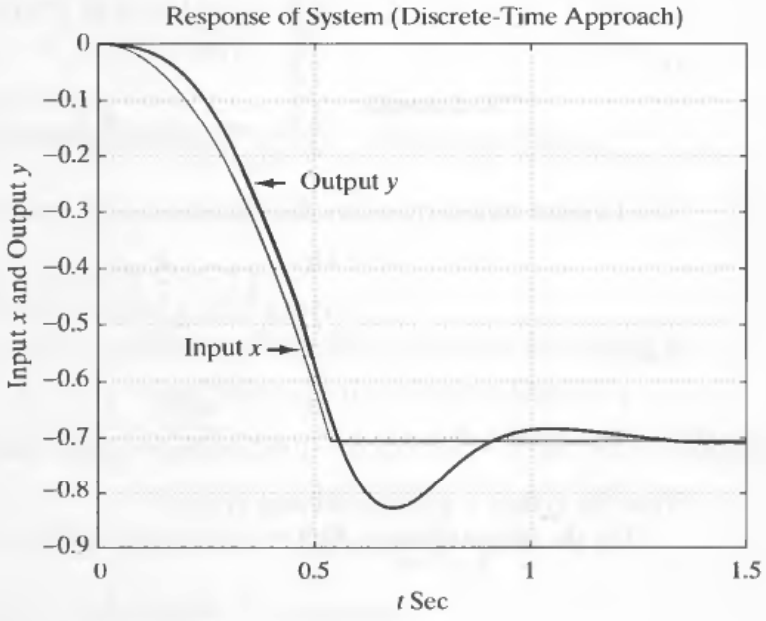

Figure 4–34
Input $x(t)$ and output $y(t)$ obtained by the discrete-time approach.

EXAMPLE PROBLEMS AND SOLUTIONS

A-4-1. In the system of Figure 4–35, $x(t)$ is the input displacement and $\theta(t)$ is the output angular displacement. Assume that the masses involved are negligibly small and that all motions are restricted to be small; therefore, the system can be considered linear. The initial conditions for x and θ are zeros, or $x(0-) = 0$ and $\theta(0-) = 0$. Show that this system is a differentiating element. Then obtain the response $\theta(t)$ when $x(t)$ is a unit-step input.

Solution. The equation for the system is

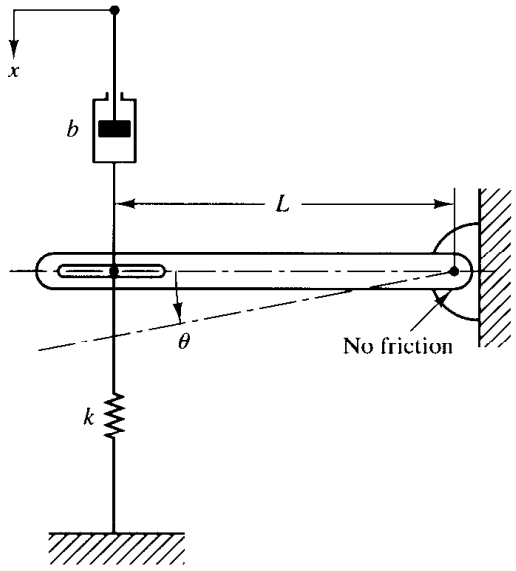

Figure 4–35
Mechanical system.

$$b(\dot{x} - L\dot{\theta}) = kL\theta$$

or

$$L\dot{\theta} + \frac{k}{b}L\theta = \dot{x}$$

The Laplace transform of this last equation, using zero initial conditions, gives

$$\left(Ls + \frac{k}{b}L\right)\Theta(s) = sX(s)$$

And so

$$\frac{\Theta(s)}{X(s)} = \frac{1}{L}\frac{s}{s + (k/b)}$$

Thus the system is a differentiating system.

For the unit-step input $X(s) = 1/s$, the output $\Theta(s)$ becomes

$$\Theta(s) = \frac{1}{L}\frac{1}{s + (k/b)}$$

The inverse Laplace transform of $\Theta(s)$ gives

$$\theta(t) = \frac{1}{L}e^{-(k/b)t}$$

Note that if the value of k/b is large the response $\theta(t)$ approaches a pulse signal as shown in Figure 4–36.

A-4-2. Consider the mechanical system shown in Figure 4–37. Suppose that the system is at rest initially $[x(0) = 0, \dot{x}(0) = 0]$, and at $t = 0$ it is set into motion by a unit-impulse force. Obtain a mathematical model for the system. Then find the motion of the system.

Solution. The system is excited by a unit-impulse input. Hence

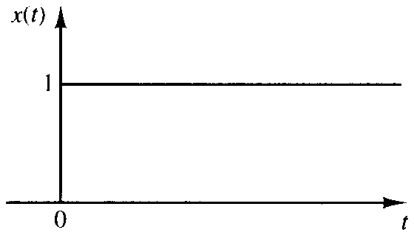

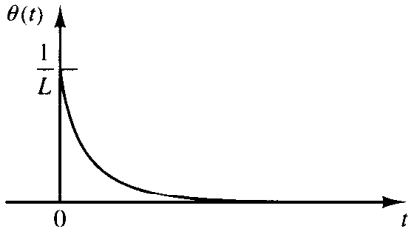

Figure 4–36
Unit-step input and the response of the mechanical system shown in Figure 4–35.

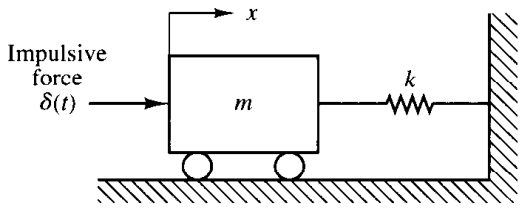

Figure 4–37
Mechanical system.

$$m\ddot{x} + kx = \delta(t)$$

This is a mathematical model for the system.

Taking the Laplace transform of both sides of this last equation gives

$$m[s^2X(s) - sx(0) - \dot{x}(0)] + kX(s) = 1$$

By substituting the initial conditions $x(0) = 0$ and $\dot{x}(0) = 0$ into this last equation and solving for $X(s)$, we obtain

$$X(s) = \frac{1}{ms^2 + k}$$

The inverse Laplace transform of $X(s)$ becomes

$$X(t) = \frac{1}{\sqrt{mk}} \sin \sqrt{\frac{k}{m}}\, t$$

The oscillation is a simple harmonic motion. The amplitude of the oscillation is $1/\sqrt{mk}$.

A-4-3. Obtain the closed-loop transfer function for the positional servo system shown in Figure 4–38. Assume that the input and output of the system are the input shaft position and the output shaft position, respectively. Assume the following numerical values for system constants:

r = angular displacement of the reference input shaft, radians
c = angular displacement of the output shaft, radians
θ = angular displacement of the motor shaft, radians
K_0 = gain of the potentiometric error detector = $24/\pi$ V/rad

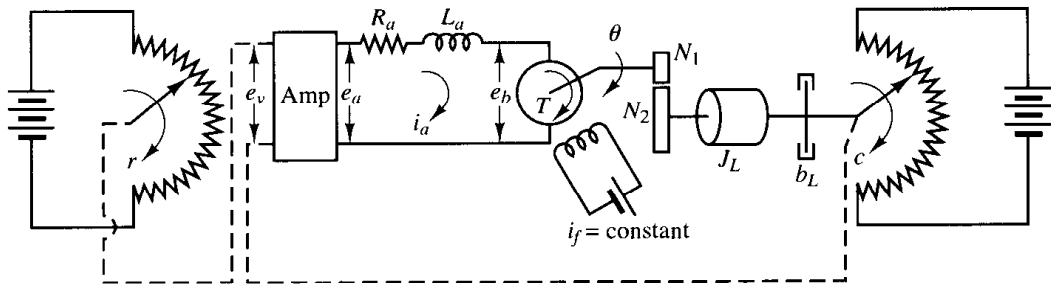

Figure 4–38
Positional servo system.

K_1 = amplifier gain = 10 V/V
e_a = armature voltage, V
e_b = back emf, V
R_a = armature-winding resistance = 0.2 Ω
L_a = armature-winding inductance = negligible
i_a = armature-winding current, A
K_3 = back emf constant = 5.5×10^{-2} V-sec/rad
K_2 = motor torque constant = 6×10^{-5} N-m/A
J_m = moment of inertia of the motor referred to the motor shaft = 1×10^{-5} kg-m^2
b_m = viscous-friction coefficient of the motor referred to the motor shaft = negligible
J_L = moment of inertia of the load referred to the output shaft = 4.4×10^{-3} kg-m^2
b_L = viscous-friction coefficient of the load referred to the output shaft = 4×10^{-2}N-m/rad/sec
n = gear ratio $N_1/N_2 = \frac{1}{10}$

Solutiou. The equivalent moment of inertia J_0 and equivalent viscous friction coefficient b_0 referred to the motor shaft are, respectively,

$$\begin{aligned} J_0 &= J_m + n^2 J_L \\ &= 1 \times 10^{-5} + 4.4 \times 10^{-5} = 5.4 \times 10^{-5} \end{aligned}$$

$$\begin{aligned} b_0 &= b_m + n^2 b_L \\ &= 4 \times 10^{-4} \end{aligned}$$

Referring to Equation (4–16), we obtain

$$\frac{C(s)}{E(s)} = \frac{K_m}{s(T_m s + 1)}$$

where

$$K_m = \frac{K_0 K_1 K_2 n}{R_a b_0 + K_2 K_3} = \frac{7.64 \times 10 \times 6 \times 10^{-5} \times 0.1}{(0.2)(4 \times 10^{-4}) + (6 \times 10^{-5})(5.5 \times 10^{-2})} = 5.5$$

$$T_m = \frac{R_a J_0}{R_a b_0 + K_2 K_3} = \frac{(0.2)(5.4 \times 10^{-5})}{(0.2)(4 \times 10^{-4}) + (6 \times 10^{-5})(5.5 \times 10^{-2})} = 0.13$$

Thus,

$$\frac{C(s)}{E(s)} = \frac{5.5}{s(0.13s + 1)} \tag{4–66}$$

Using Equation (4–66), we can draw the block diagram of the system as shown in Figure 4–39. The closed-loop transfer function of the system is

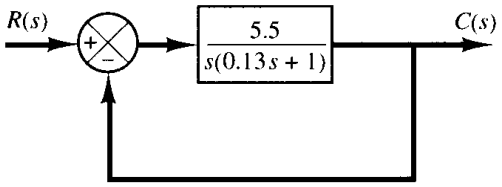

Figure 4–39
Block diagram of the system shown in Figure 4–38.

$$\frac{C(s)}{R(s)} = \frac{5.5}{0.13s^2 + s + 5.5} = \frac{42.3}{s^2 + 7.69s + 42.3}$$

A-4-4. Gear trains are often used in servo systems to reduce speed, to magnify torque, or to obtain the most efficient power transfer by matching the driving member to the given load.

Consider the gear train system shown in Figure 4–40. In this system, a load is driven by a motor through the gear train. Assuming that the stiffness of the shafts of the gear train is infinite (there is neither backlash nor elastic deformation) and that the number of teeth on each gear is proportional to the radius of the gear, obtain the equivalent moment of inertia and equivalent viscous-friction coefficient referred to the motor shaft and referred to the load shaft.

In Figure 4–40 the numbers of teeth on gears 1, 2, 3, and 4 are N_1, N_2, N_3, and N_4, respectively. The angular displacements of shafts, 1, 2, and 3 are θ_1, θ_2, and θ_3, respectively. Thus, $\theta_2/\theta_1 = N_1/N_2$ and $\theta_3/\theta_2 = N_3/N_4$. The moment of inertia and viscous-friction coefficient of each gear train component are denoted by J_1, b_1; J_2, b_2; and J_3, b_3; respectively. (J_3 and b_3 include the moment of inertia and friction of the load.)

Solution. For this gear train system, we can obtain the following three equations: For shaft 1,

$$J_1\ddot{\theta}_1 + b_1\dot{\theta}_1 + T_1 = T_m \tag{4–67}$$

where T_m is the torque developed by the motor and T_1 is the load torque on gear 1 due to the rest of the gear train. For shaft 2,

$$J_2\ddot{\theta}_2 + b_2\dot{\theta}_2 + T_3 = T_2 \tag{4–68}$$

where T_2 is the torque transmitted to gear 2 and T_3 is the load torque on gear 3 due to the rest of the gear train. Since the work done by gear 1 is equal to that of gear 2,

$$T_1\theta_1 = T_2\theta_2 \qquad \text{or} \qquad T_2 = T_1\frac{N_2}{N_1}$$

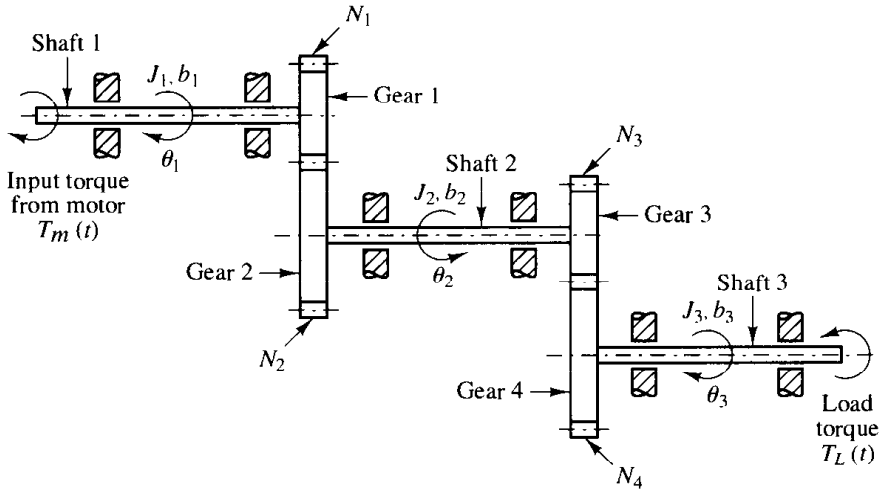

Figure 4–40
Gear train system.

If $N_1/N_2 < 1$, the gear ratio reduces the speed as well as magnifies the torque. For the third shaft,

$$J_3\ddot{\theta}_3 + b_3\dot{\theta}_3 + T_L = T_4 \tag{4-69}$$

where T_L is the load torque and T_4 is the torque transmitted to gear 4. T_3 and T_4 are related by

$$T_4 = T_3 \frac{N_4}{N_3}$$

and θ_3 and θ_1 are related by

$$\theta_3 = \theta_2 \frac{N_3}{N_4} = \theta_1 \frac{N_1}{N_2} \frac{N_3}{N_4}$$

Elimination of T_1, T_2, T_3, and T_4 from Equations (4–67), (4–68), and (4–69) yields

$$J_1\ddot{\theta}_1 + b_1\dot{\theta}_1 + \frac{N_1}{N_2}(J_2\ddot{\theta}_2 + b_2\dot{\theta}_2) + \frac{N_1N_3}{N_2N_4}(J_3\ddot{\theta}_3 + b_3\dot{\theta}_3 + T_L) = T_m$$

Eliminating θ_2 and θ_3 from this last equation and writing the resulting equation in terms of θ_1 and its time derivatives, we obtain

$$\left[J_1 + \left(\frac{N_1}{N_2}\right)^2 J_2 + \left(\frac{N_1}{N_2}\right)^2\left(\frac{N_3}{N_4}\right)^2 J_3\right]\ddot{\theta}_1 + \left[b_1 + \left(\frac{N_1}{N_2}\right)^2 b_2 + \left(\frac{N_1}{N_2}\right)^2\left(\frac{N_3}{N_4}\right)^2 b_3\right]\dot{\theta}_1 + \left(\frac{N_1}{N_2}\right)\left(\frac{N_3}{N_4}\right)T_L = T_m \tag{4-70}$$

Thus, the equivalent moment of inertia and viscous-friction coefficient of the gear train referred to shaft 1 are given, respectively, by

$$J_{1\text{eq}} = J_1 + \left(\frac{N_1}{N_2}\right)^2 J_2 + \left(\frac{N_1}{N_2}\right)^2\left(\frac{N_3}{N_4}\right)^2 J_3$$

$$b_{1\text{eq}} = b_1 + \left(\frac{N_1}{N_2}\right)^2 b_2 + \left(\frac{N_1}{N_2}\right)^2\left(\frac{N_3}{N_4}\right)^2 b_3$$

Similarly, the equivalent moment of inertia and viscous-friction coefficient of the gear train referred to the load shaft (shaft 3) are given, respectively, by

$$J_{3\text{eq}} = J_3 + \left(\frac{N_4}{N_3}\right)^2 J_2 + \left(\frac{N_2}{N_1}\right)^2\left(\frac{N_4}{N_3}\right)^2 J_1$$

$$b_{3\text{eq}} = b_3 + \left(\frac{N_4}{N_3}\right)^2 b_2 + \left(\frac{N_2}{N_1}\right)^2\left(\frac{N_4}{N_3}\right)^2 b_1$$

The relationship between $J_{1\text{eq}}$ and $J_{3\text{eq}}$ is thus

$$J_{1\text{eq}} = \left(\frac{N_1}{N_2}\right)^2\left(\frac{N_3}{N_4}\right)^2 J_{3\text{eq}}$$

and that between $b_{1\text{eq}}$ and $b_{3\text{eq}}$ is

$$b_{1\text{eq}} = \left(\frac{N_1}{N_2}\right)^2\left(\frac{N_3}{N_4}\right)^2 b_{3\text{eq}}$$

The effect of J_2 and J_3 on an equivalent moment of inertia is determined by the gear ratios N_1/N_2 and N_3/N_4. For speed-reducing gear trains, the ratios N_1/N_2 and N_3/N_4 are usually less than unity.

If $N_1/N_2 \ll 1$ and $N_3/N_4 \ll 1$, then the effect of J_2 and J_3 on the equivalent moment of inertia J_{1eq} is negligible. Similar comments apply to the equivalent viscous-friction coefficient b_{1eq} of the gear train. In terms of the equivalent moment of inertia J_{1eq} and equivalent viscous-friction coefficient b_{1eq}, Equation (4–70) can be simplified to give

$$J_{1eq}\ddot{\theta}_1 + b_{1eq}\dot{\theta}_1 + nT_L = T_m$$

where

$$n = \frac{N_1}{N_2}\frac{N_3}{N_4}$$

A-4-5. Show that the torque-to-inertia ratios referred to the motor shaft and to the load shaft differ from each other by a factor of n. Show also that the torque squared-to-inertia ratios referred to the motor shaft and to the load shaft are the same.

Solution. Suppose that T_{max} is the maximum torque that can be produced on the motor shaft. Then the torque-to-inertia ratio referred to the motor shaft is

$$\frac{T_{max}}{J_m + n^2 J_L}$$

where J_m = moment of inertia of the rotor
J_L = moment of inertia of the load
n = gear ratio

The torque-to-inertia ratio referred to the load shaft is

$$\frac{\dfrac{T_{max}}{n}}{J_L + \dfrac{J_m}{n^2}} = \frac{nT_{max}}{J_m + n^2 J_L}$$

Clearly, they differ from each other by a factor of n. Hence, in comparing torque-to-inertia ratios of motors, we find it necessary to specify which shaft is the reference.

Note that the ratio of torque squared to inertia referred to the motor shaft is

$$\frac{T_{max}^2}{J_m + n^2 J_L}$$

and that referred to the load shaft is

$$\frac{\dfrac{T_{max}^2}{n^2}}{J_L + \dfrac{J_m}{n^2}} = \frac{T_{max}^2}{J_m + n^2 J_L}$$

These two ratios are clearly the same.

A-4-6. When the system shown in Figure 4–41(a) is subjected to a unit-step input, the system output responds as shown in Figure 4–41(b). Determine the values of K and T from the response curve.

Solution. The maximum overshoot of 25.4% corresponds to $\zeta = 0.4$. From the response curve we have

$$t_p = 3$$

Consequently,

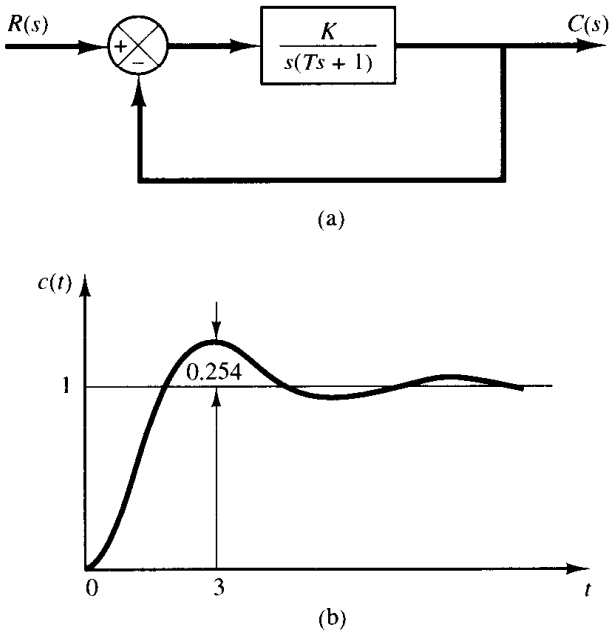

Figure 4–41
(a) Closed-loop system; (b) unit-step response curve.

$$t_p = \frac{\pi}{\omega_d} = \frac{\pi}{\omega_n\sqrt{1-\zeta^2}} = \frac{\pi}{\omega_n\sqrt{1-0.4^2}} = 3$$

It follows that

$$\omega_n = 1.14$$

From the block diagram we have

$$\frac{C(s)}{R(s)} = \frac{K}{Ts^2 + s + K}$$

from which

$$\omega_n = \sqrt{\frac{K}{T}}, \qquad 2\zeta\omega_n = \frac{1}{T}$$

Therefore, the values of T and K are determined as

$$T = \frac{1}{2\zeta\omega_n} = \frac{1}{2 \times 0.4 \times 1.14} = 1.09$$

$$K = \omega_n^2 T = 1.14^2 \times 1.09 = 1.42$$

A-4-7. Determine the values of K and k of the closed-loop system shown in Figure 4–42 so that the maximum overshoot in unit-step response is 25% and the peak time is 2 sec. Assume that $J = 1$ kg-m^2.

Solution. The closed-loop transfer function is

$$\frac{C(s)}{R(s)} = \frac{K}{Js^2 + Kks + K}$$

By substituting $J = 1$ kg-m^2 into this last equation, we have

$$\frac{C(s)}{R(s)} = \frac{K}{s^2 + Kks + K}$$

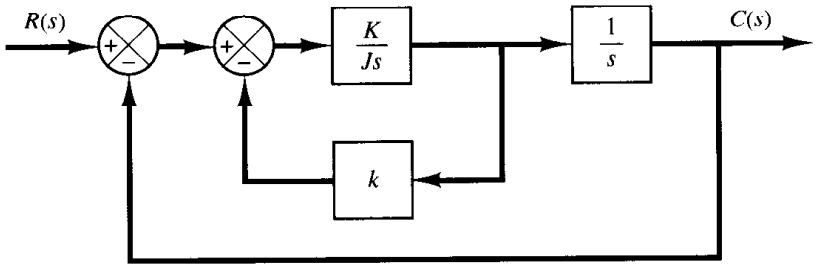

Figure 4–42
Closed-loop system.

Note that

$$\omega_n = \sqrt{K}, \qquad 2\zeta\omega_n = Kk$$

The maximum overshoot M_p is

$$M_p = e^{-\zeta\pi/\sqrt{1-\zeta^2}}$$

which is specified as 25%. Hence

$$e^{-\zeta\pi/\sqrt{1-\zeta^2}} = 0.25$$

from which

$$\frac{\zeta\pi}{\sqrt{1-\zeta^2}} = 1.386$$

or

$$\zeta = 0.404$$

The peak time t_p is specified as 2 sec. And so

$$t_p = \frac{\pi}{\omega_d} = 2$$

or

$$\omega_d = 1.57$$

Then the undamped natural frequency ω_n is

$$\omega_n = \frac{\omega_d}{\sqrt{1-\zeta^2}} = \frac{1.57}{\sqrt{1-0.404^2}} = 1.72$$

Therefore, we obtain

$$K = \omega_n^2 = 1.72^2 = 2.95 \text{ N-m}$$

$$k = \frac{2\zeta\omega_n}{K} = \frac{2 \times 0.404 \times 1.72}{2.95} = 0.471 \text{ sec}$$

A-4-8. What is the unit-step response of the system shown in Figure 4–43?

Solution. The closed-loop transfer function is

$$\frac{C(s)}{R(s)} = \frac{10s + 10}{s^2 + 10s + 10}$$

For the unit-step input $[R(s) = 1/s]$, we have

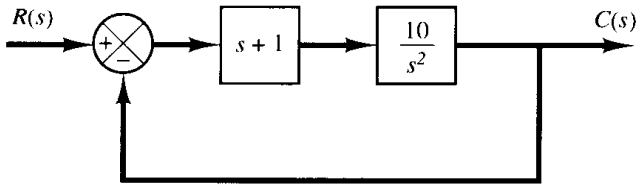

Figure 4–43
Closed-loop system.

$$C(s) = \frac{10s + 10}{s^2 + 10s + 10}\frac{1}{s}$$

$$= \frac{10s + 10}{(s + 5 + \sqrt{15})(s + 5 - \sqrt{15})s}$$

$$= \frac{-4 - \sqrt{15}}{3 + \sqrt{15}}\frac{1}{s + 5 + \sqrt{15}} + \frac{-4 + \sqrt{15}}{3 - \sqrt{15}}\frac{1}{s + 5 - \sqrt{15}} + \frac{1}{s}$$

The inverse Laplace transform of $C(s)$ gives

$$c(t) = -\frac{4 + \sqrt{15}}{3 + \sqrt{15}}e^{-(5+\sqrt{15})t} + \frac{4 - \sqrt{15}}{-3 + \sqrt{15}}e^{-(5-\sqrt{15})t} + 1$$

$$= -1.1455e^{-8.87t} + 0.1455e^{-1.13t} + 1$$

Clearly, the output will not exhibit any oscillation. The response curve exponentially approaches the final value $c(\infty) = 1$.

A-4-9. Figure 4–44(a) shows a mechanical vibratory system. When 2 lb of force (step input) is applied to the system, the mass oscillates, as shown in Figure 4–44(b). Determine m, b, and k of the system from this response curve. The displacement x is measured from the equilibrium position.

Solution. The transfer function of this system is

$$\frac{X(s)}{P(s)} = \frac{1}{ms^2 + bs + k}$$

Since

$$P(s) = \frac{2}{s}$$

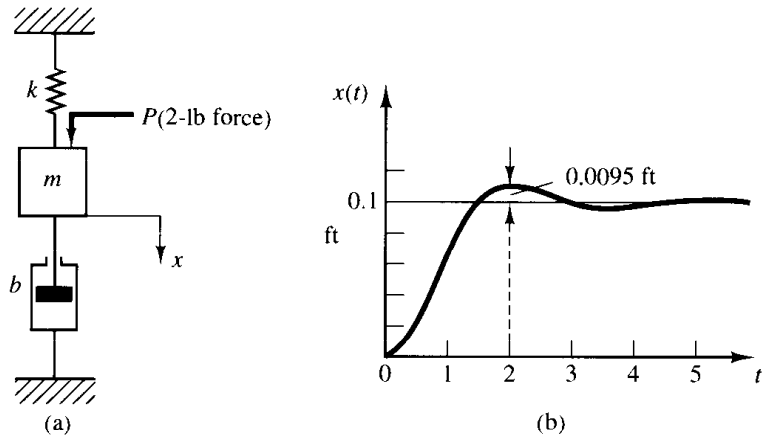

Figure 4–44
(a) Mechanical vibratory system; (b) step-response curve.

we obtain

$$X(s) = \frac{2}{s(ms^2 + bs + k)}$$

It follows that the steady-state value of x is

$$x(\infty) = \lim_{s \to 0} sX(s) = \frac{2}{k} = 0.1 \text{ ft}$$

Hence

$$k = 20 \text{ lb}_\text{f}/\text{ft}$$

Note that $M_p = 9.5\%$ corresponds to $\zeta = 0.6$. The peak time t_p is given by

$$t_p = \frac{\pi}{\omega_d} = \frac{\pi}{\omega_n\sqrt{1 - \zeta^2}} = \frac{\pi}{0.8\omega_n}$$

The experimental curve shows that $t_p = 2$ sec. Therefore,

$$\omega_n = \frac{3.14}{2 \times 0.8} = 1.96 \text{ rad/sec}$$

Since $\omega_n^2 = k/m = 20/m$, we obtain

$$m = \frac{20}{\omega_n^2} = \frac{20}{1.96^2} = 5.2 \text{ slugs} = 166 \text{ lb}$$

(Note that 1 slug = 1 lb_f-sec^2/ft.) Then b is determined from

$$2\zeta\omega_n = \frac{b}{m}$$

or

$$b = 2\zeta\omega_n m = 2 \times 0.6 \times 1.96 \times 5.2 = 12.2 \text{ lb}_\text{f}/\text{ft/sec}$$

A-4-10. Assuming that the mechanical system shown in Figure 4–45 is at rest before excitation force $P \sin \omega t$ is given, derive the complete solution $x(t)$ and the steady-state solution $x_{ss}(t)$. The displacement x is measured from the equilibrium position. Assume that the system is underdamped.

Solution. The equation of motion for the system is

$$m\ddot{x} + b\dot{x} + kx = P \sin \omega t$$

Noting that $x(0) = 0$ and $\dot{x}(0) = 0$, the Laplace transform of this equation is

$$(ms^2 + bs + k)X(s) = P\frac{\omega}{s^2 + \omega^2}$$

or

$$X(s) = \frac{P\omega}{(s^2 + \omega^2)(ms^2 + bs + k)}$$

Since the system is underdamped, $X(s)$ can be written as follows:

$$X(s) = \frac{P\omega}{m} \frac{1}{s^2 + \omega^2} \frac{1}{s^2 + 2\zeta\omega_n s + \omega_n^2}, \qquad \text{where } 0 < \zeta < 1$$

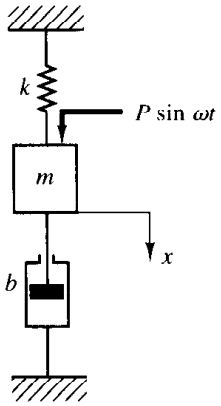

Figure 4–45
Mechanical system.

where $\omega_n = \sqrt{k/m}$ and $\zeta = b/(2\sqrt{mk})$. $X(s)$ can be expanded as

$$X(s) = \frac{P\omega}{m}\left(\frac{as + c}{s^2 + \omega^2} + \frac{-as + d}{s^2 + 2\zeta\omega_n s + \omega_n^2}\right)$$

By simple calculations it can be found that

$$a = \frac{-2\zeta\omega_n}{(\omega_n^2 - \omega^2)^2 + 4\zeta^2\omega_n^2\omega^2}, \qquad c = \frac{(\omega_n^2 - \omega^2)}{(\omega_n^2 - \omega^2)^2 + 4\zeta^2\omega_n^2\omega^2}, \qquad d = \frac{4\zeta^2\omega_n^2 - (\omega_n^2 - \omega^2)}{(\omega_n^2 - \omega^2)^2 + 4\zeta^2\omega_n^2\omega^2}$$

Hence

$$X(s) = \frac{P\omega}{m}\frac{1}{(\omega_n^2 - \omega^2)^2 + 4\zeta^2\omega_n^2\omega^2}\left[\frac{-2\zeta\omega_n s + (\omega_n^2 - \omega^2)}{s^2 + \omega^2} + \frac{2\zeta\omega_n(s + \zeta\omega_n) + 2\zeta^2\omega_n^2 - (\omega_n^2 - \omega^2)}{s^2 + 2\zeta\omega_n s + \omega_n^2}\right]$$

The inverse Laplace transform of $X(s)$ gives

$$x(t) = \frac{P\omega}{m[(\omega_n^2 - \omega^2)^2 + 4\zeta^2\omega_n^2\omega^2]}\left[-2\zeta\omega_n\cos\omega t + \frac{(\omega_n^2 - \omega^2)}{\omega}\sin\omega t + 2\zeta\omega_n e^{\zeta\omega_n t}\cos\omega_n\sqrt{1-\zeta^2}\,t + \frac{2\zeta^2\omega_n^2 - (\omega_n^2 - \omega^2)}{\omega_n\sqrt{1-\zeta^2}}e^{-\zeta\omega_n t}\sin\omega_n\sqrt{1-\zeta^2}\,t\right]$$

At steady state ($t \to \infty$) the terms involving $e^{-\zeta\omega_n t}$ approach zero. Thus at steady state

$$\begin{aligned} x_{ss}(t) &= \frac{P\omega}{m[(\omega_n^2 - \omega^2)^2 + 4\zeta^2\omega_n^2\omega^2]}\left(-2\zeta\omega_n\cos\omega t + \frac{\omega_n^2 - \omega^2}{\omega}\sin\omega t\right) \\ &= \frac{P\omega}{(k - m\omega^2)^2 + b^2\omega^2}\left(-b\cos\omega t + \frac{k - m\omega^2}{\omega}\sin\omega t\right) \\ &= \frac{P}{\sqrt{(k - m\omega^2)^2 + b^2\omega^2}}\sin\left(\omega t - \tan^{-1}\frac{b\omega}{k - m\omega^2}\right) \end{aligned}$$

A-4-11. Consider the unit-step response of the second-order system

$$\frac{C(s)}{R(s)} = \frac{\omega_n^2}{s^2 + 2\zeta\omega_n s + \omega_n^2}$$

The amplitude of the exponentially damped sinusoid changes as a geometric series. At time $t = t_p = \pi/\omega_d$, the amplitude is equal to $e^{-(\sigma/\omega_d)\pi}$. After one oscillation, or at $t = t_p + 2\pi/\omega_d = 3\pi/\omega_d$, the amplitude is equal to $e^{-(\sigma/\omega_d)3\pi}$; after another cycle of oscillation, the amplitude is $e^{-(\sigma/\omega_d)5\pi}$. The logarithm of the ratio of successive amplitudes is called the *logarithmic decrement.* Determine the logarithmic decrement for this second-order system. Describe a method for experimental determination of the damping ratio from the rate of decay of the oscillation.

Solution. Let us define the amplitude of the output oscillation at $t = t_i$ to be x_i, where $t_i = t_p + (i - 1)T$ (T = period of oscillation). The amplitude ratio per one period of damped oscillation is

$$\frac{x_1}{x_2} = \frac{e^{-(\sigma/\omega_d)\pi}}{e^{-(\sigma/\omega_d)3\pi}} = e^{2(\sigma/\omega_d)\pi} = e^{2\zeta\pi/\sqrt{1-\zeta^2}}$$

Thus, the logarithmic decrement δ is

$$\delta = \ln \frac{x_1}{x_2} = \frac{2\zeta\pi}{\sqrt{1-\zeta^2}}$$

It is a function only of the damping ratio ζ. Thus, the damping ratio ζ can be determined by use of the logarithmic decrement.

In the experimental determination of the damping ratio ζ from the rate of decay of the oscillation, we measure the amplitude x_1 at $t = t_p$ and amplitude x_n at $t = t_p + (n-1)T$. Note that it is necessary to choose n large enough so that the ratio x_1/x_n is not near unity. Then

$$\frac{x_1}{x_n} = e^{(n-1)2\zeta\pi/\sqrt{1-\zeta^2}}$$

or

$$\ln \frac{x_1}{x_n} = (n-1)\frac{2\zeta\pi}{\sqrt{1-\zeta^2}}$$

Hence

$$\zeta = \frac{\frac{1}{n-1}\left(\ln \frac{x_1}{x_n}\right)}{\sqrt{4\pi^2 + \left[\frac{1}{n-1}\left(\ln \frac{x_1}{x_n}\right)\right]^2}}$$

A-4-12. In the system shown in Figure 4–46, the numerical values of m, b, and k are given as $m = 1$ kg, $b = 2$ N-sec/m, and $k = 100$ N/m. The mass is displaced 0.05 m and released without initial velocity. Find the frequency observed in the vibration. In addition, find the amplitude four cycles later. The displacement x is measured from the equilibrium position.

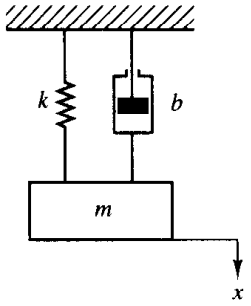

Figure 4–46
Spring–mass–damper system.

Solution. The equation of motion for the system is

$$m\ddot{x} + b\dot{x} + kx = 0$$

Substituting the numerical values for m, b, and k into this equation gives

$$\ddot{x} + 2\dot{x} + 100x = 0$$

where the initial conditions are $x(0) = 0.05$ and $\dot{x}(0) = 0$. From this last equation the undamped natural frequency ω_n and the damping ratio ζ are found to be

$$\omega_n = 10, \qquad \zeta = 0.1$$

The frequency actually observed in the vibration is the damped natural frequency ω_d.

$$\omega_d = \omega_n\sqrt{1-\zeta^2} = 10\sqrt{1-0.01} = 9.95 \text{ rad/sec}$$

In the present analysis, $\dot{x}(0)$ is given as zero. Thus, solution $x(t)$ can be written as

$$x(t) = x(0)e^{-\zeta\omega_n t}\left(\cos \omega_d t + \frac{\zeta}{\sqrt{1-\zeta^2}} \sin \omega_d t\right)$$

It follows that at $t = nT$, where $T = 2\pi/\omega_d$,

$$x(nT) = x(0)e^{-\zeta\omega_n nT}$$

Consequently, the amplitude four cycles later becomes

$$x(4T) = x(0)e^{-\zeta\omega_n 4T} = x(0)e^{-(0.1)(10)(4)(0.6315)}$$
$$= 0.05e^{-2.526} = 0.05 \times 0.07998 = 0.004 \text{ m}$$

A-4-13. Consider a system whose closed-loop poles and closed-loop zero are located in the s plane on a line parallel to the $j\omega$ axis, as shown in Figure 4–47. Show that the impulse response of such a system is a damped cosine function.

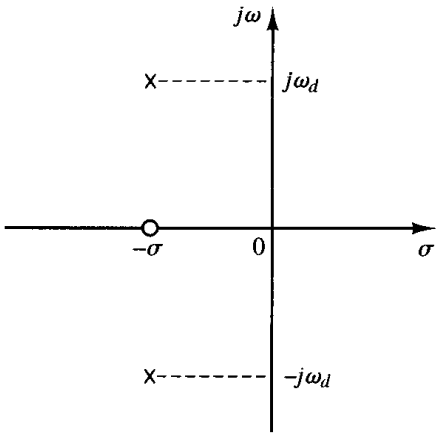

Figure 4–47
Closed-loop pole–zero configuration of system whose impulse response is a damped cosine function.

Solution. The closed-loop transfer function is

$$\frac{C(s)}{R(s)} = \frac{K(s + \sigma)}{(s + \sigma + j\omega_d)(s + \sigma - j\omega_d)}$$

For a unit-impulse input, $R(s) = 1$ and

$$C(s) = \frac{K(s + \sigma)}{(s + \sigma)^2 + \omega_d^2}$$

The inverse Laplace transform of $C(s)$ is

$$c(t) = Ke^{-\sigma t}\cos \omega_d t, \qquad \text{for } t \geq 0$$

which is a damped cosine function.

A-4-14. Consider the liquid-level control system shown in Figure 4–48. The controller is of the proportional type. The set point of the controller is fixed.

Draw a block diagram of the system, assuming that changes in the variables are small. Obtain the transfer function between the level of the second tank and the disturbance input q_d. Obtain the steady-state error when the disturbance q_d is a unit-step function.

Solution. Figure 4–49(a) is a block diagram of this system when changes in the variables are small. Since the set point of the controller is fixed, $r = 0$. (Note that r is the change in set point.)

To investigate the response of the level of the second tank subjected to a unit-step disturbance q_d, we find it convenient to modify the block diagram of Figure 4–49(a) to the one shown in Figure 4–49(b).

The transfer function between $H_2(s)$ and $Q_d(s)$ can be obtained as

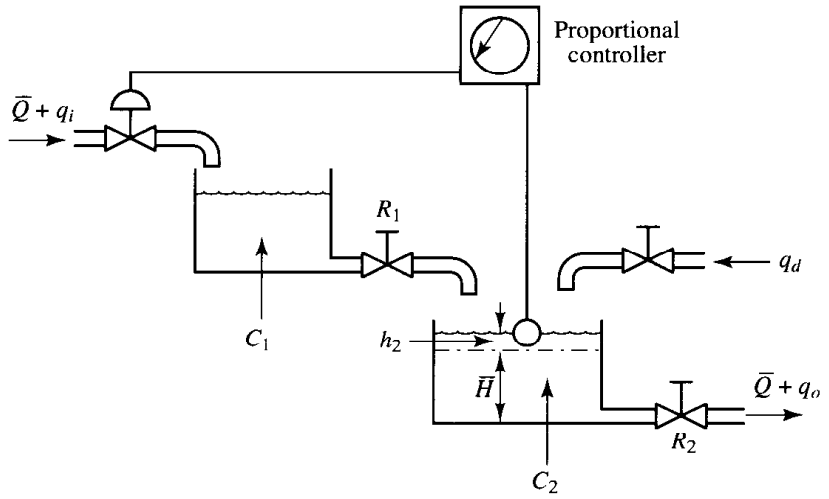

Figure 4–48
Liquid-level control system.

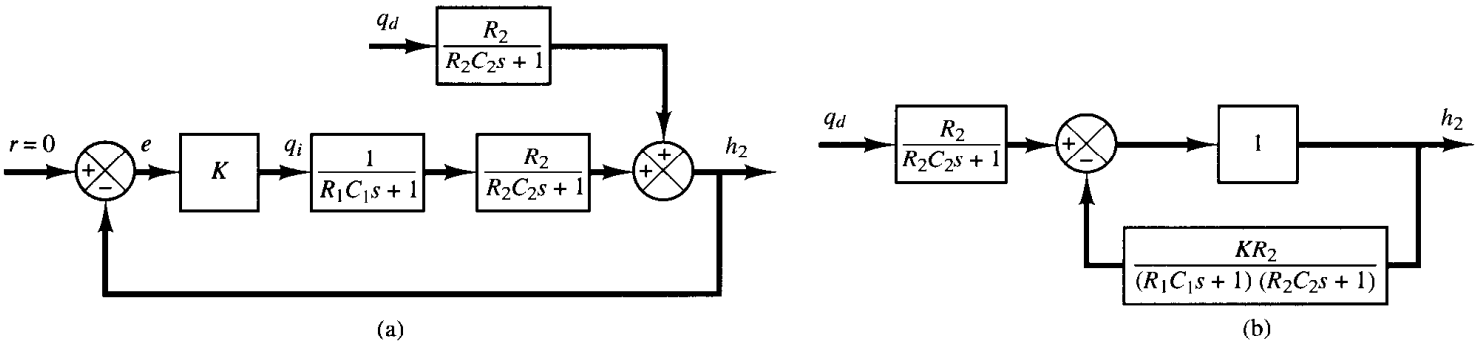

Figure 4–49
(a) Block diagram of the system shown in Figure 4–48; (b) modified block diagram.

$$\frac{H_2(s)}{Q_d(s)} = \frac{R_2(R_1C_1s + 1)}{(R_1C_1s + 1)(R_2C_2s + 1) + KR_2}$$

From this equation, the response $H_2(s)$ to the disturbance $Q_d(s)$ can be found. The effect of the controller is seen by the presence of K in the denominator of this last equation.

For the unit-step disturbance $Q_d(s)$, we obtain

$$h_2(\infty) = \frac{R_2}{1 + KR_2}$$

or

$$\text{Steady-state error} = -\frac{R_2}{1 + KR_2}$$

The system exhibits offset in the response to a unit-step disturbance.

Note that the characteristic equation for the disturbance input and that for the reference input are the same. The characteristic equation for this system is

$$(R_1C_1s + 1)(R_2C_2s + 1) + KR_2 = 0$$

which can be modified to

$$s^2 + \left(\frac{R_1C_1 + R_2C_2}{R_1C_1R_2C_2}\right)s + \frac{1 + KR_2}{R_1C_1R_2C_2} = 0$$

The undamped natural frequency ω_n and the damping ratio ζ are given by

$$\omega_n = \sqrt{\frac{1 + KR_2}{R_1C_1R_2C_2}}, \qquad \zeta = \frac{R_1C_1 + R_2C_2}{2\sqrt{R_1C_1R_2C_2}\sqrt{1 + KR_2}}$$

Both the undamped natural frequency and the damping ratio depend on the value of the gain K. This gain must be adjusted so that the transient responses to both the reference input and disturbance input show reasonable damping and reasonable speed.

A-4-15. Consider the liquid-level control system shown in Figure 4–50. The inlet valve is controlled by a hydraulic integral controller. Assume that the steady-state inflow rate is $\bar{Q}$ and steady-state outflow rate is also $\bar{Q}$, the steady-state head is $\bar{H}$, steady-state pilot valve displacement is $\bar{X} = 0$, and steady-state valve position is $\bar{Y}$. We assume that the set point $\bar{R}$ corresponds to the steady-state head $\bar{H}$. The set point is fixed. Assume also that the disturbance inflow rate q_d, which is a small quantity, is applied to the water tank at $t = 0$. This disturbance causes the head to change from $\bar{H}$ to $\bar{H} + h$. This change results in a change in the outflow rate by q_o. Through the hydraulic controller, the change in head causes a change in the inflow rate from $\bar{Q}$ to $\bar{Q} + q_i$. (The integral controller tends to keep the head constant as much as possible in the presence of disturbances.) We assume that all changes are of small quantities.

Assuming the following numerical values for the system,

$$C = 2\ \text{m}^2, \qquad R = 0.5\ \text{sec/m}^2, \qquad K_v = 1\ \text{m}^2/\text{sec}$$
$$a = 0.25\ \text{m}, \qquad b = 0.75\ \text{m}, \qquad K_1 = 4\ \text{sec}^{-1}$$

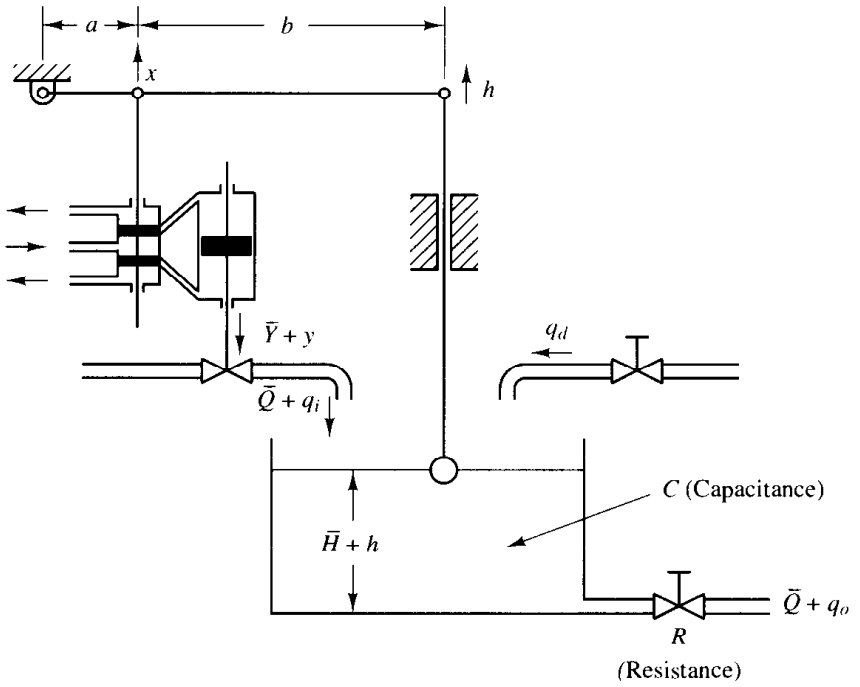

Figure 4–50
Liquid-level control system.

obtain the response $h(t)$ when the disturbance input q_d is a unit-step function. Also obtain this response $h(t)$ with MATLAB.

Solution. Since the increase of water in the tank during dt seconds is equal to the net inflow to the tank during the same dt seconds, we have

$$C\,dh = (q_i - q_o + q_d)\,dt \tag{4–71}$$

where

$$q_o = \frac{h}{R} \tag{4–72}$$

For the feedback lever mechanism, we have

$$x = \frac{a}{a + b}h \tag{4–73}$$

We assume that the velocity of the power piston (valve) is proportional to pilot valve displacement x, or

$$\frac{dy}{dt} = K_1 x \tag{4–74}$$

where K_1 is a positive constant. We also assume that the change in the inflow rate q_i is negatively proportional to the change in the valve opening y, or

$$q_i = -K_v y \tag{4–75}$$

where K_v is a positive constant.

Now we obtain the equations for the system as follows: From Equations (4–71), (4–72), and (4–75), we get

$$C\frac{dh}{dt} = -K_v y - \frac{h}{R} + q_d \tag{4–76}$$

From Equations (4–73) and (4–74), we have

$$\frac{dy}{dt} = \frac{K_1 a}{a + b}h \tag{4–77}$$

By substituting the given numerical values into Equations (4–76) and (4–77), we obtain

$$2\frac{dh}{dt} = -y - 2h + q_d$$

$$\frac{dy}{dt} = h$$

Taking the Laplace transforms of the preceding two equations, assuming zero initial conditions, we obtain

$$2sH(s) = -Y(s) - 2H(s) + Q_d(s)$$

$$sY(s) = H(s)$$

By eliminating $Y(s)$ from the last two equations and noting that the disturbance input is a unit-step function, or $Q_d(s) = 1/s$, we get

$$H(s) = \frac{s}{2s^2 + 2s + 1}\frac{1}{s} = \frac{0.5}{(s + 0.5)^2 + 0.5^2}$$

The inverse Laplace transform of $H(s)$ gives the time response $h(t)$.

$$h(t) = e^{-0.5t} \sin 0.5t$$

Notice that the unit-step disturbance input q_d caused a transient error in the head which becomes zero at steady state. The integral controller thus eliminated the error caused by the disturbance input q_d.

Plotting the response curve $h(t)$ with MATLAB. Since the response $H(s)$ is given by

$$H(s) = \frac{s}{2s^2 + 2s + 1}\frac{1}{s}$$

MATLAB Program 4–13 may be used to obtain the response to the unit-step disturbance input. The resulting response curve is shown in Figure 4–51.

MATLAB Program 4–13

```
% ---------- Unit-step response ----------

% ***** Enter numerator and denominator of the transfer
% function *****

num = [0   1   0];
den = [2   2   1];

% ***** Enter step command *****

step(num,den)
grid
title('Unit-Step Response')
```

A-4-16. Consider the impulse response of the standard second-order system defined by

$$\frac{C(s)}{R(s)} = \frac{\omega_n^2}{s^2 + 2\zeta\omega_n s + \omega_n^2}$$

For a unit-impulse input, $R(s) = 1$. Thus

$$C(s) = \frac{\omega_n^2}{s^2 + 2\zeta\omega_n s + \omega_n^2} = \frac{\omega_n^2 s}{s^2 + 2\zeta\omega_n s + \omega_n^2}\frac{1}{s}$$

Consider the normalized system where $\omega_n = 1$. Then

$$C(s) = \frac{s}{s^2 + 2\zeta s + 1}\frac{1}{s}$$

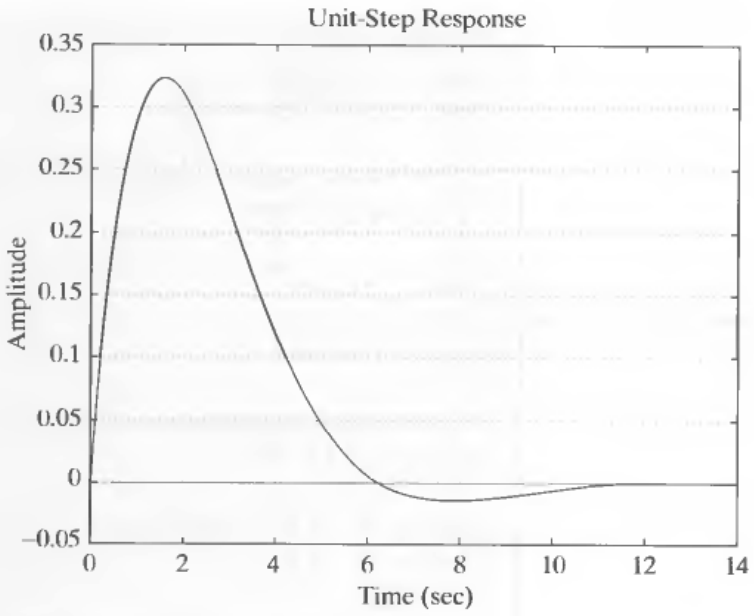

Figure 4–51
Response to unit-step disturbance input.

Consider five different values of zeta: $\zeta = 0.1, 0.3, 0.5, 0.7$, and 1.0. Obtain the unit-impulse response curves for each zeta with MATLAB.

Solution. A MATLAB program for plotting the five unit-impulse response curves in one diagram is given in MATLAB Program 4–14. The resulting diagram is shown in Figure 4–52.

MATLAB Program 4–14

```
% ---------- Unit-impulse response ----------

% ***** Unit-impulse response curves for the normalized
% second-order system G(s) = 1/[s^2 + 2(zeta)s + 1] *****

% ***** The unit-impulse response is obtained as the
% unit-step response of sG(s) *****

% ***** The values of zeta considered here are 0.1, 0.3,
% 0.5, 0.7, and 1.0 *****

% ***** Enter the numerator and denominator of sG(s) for
% zeta = 0.1 *****

num = [0   1   0];
den1 = [1   0.2   1];

% ***** Specify the computing time points (such as t = 0:0.1:10).
% Then enter the step-response command step(num,den,t) and text
% command text(, ,' ') *****
```

```
t = 0:0.1:10;
step(num,den1,t);
text(2.2,0.88,'Zeta = 0.1')

% ***** Hold this plot and add other unit-impulse response
% curves to it *****

hold

Current plot held

% ***** Enter denominators of sG(s) for zeta = 0.3, 0.5,
% 0.7, and 1.0 *****

den2 = [1   0.6   1]; den3 = [1   1   1]; den4 = [1   1.4   1];
den5 = [1   2   1];

% ***** Superimpose on the held plot the unit-impulse response
% curves for zeta = 0.3, 0.5, 0.7, and 1.0 by entering
% successively the step-response command step(num,den,t)
% and text command text(, ,' ') *****

step(num,den2,t);
text(1.33,0.72,'0.3')
step(num,den3,t);
text(1.15,0.58,'0.5')
step(num,den4,t);
text(1.1,0.46,'0.7')
step(num,den5,t);
text(0.8,0.28,'1.0')

% ***** Enter grid and title of the plot *****

grid
title(Impulse-Response Curves for G(s) = 1/]s^2 + 2(zeta)s + 1]')

% ***** Clear hold on graphics *****

hold

Current plot released
```

From the unit-impulse response curves for different values of zeta, we may conclude that if the impulse response $c(t)$ does not change sign the system is either critically damped or overdamped, in which case the corresponding step response does not overshoot, but increases or decreases monotonically and approaches a constant value.

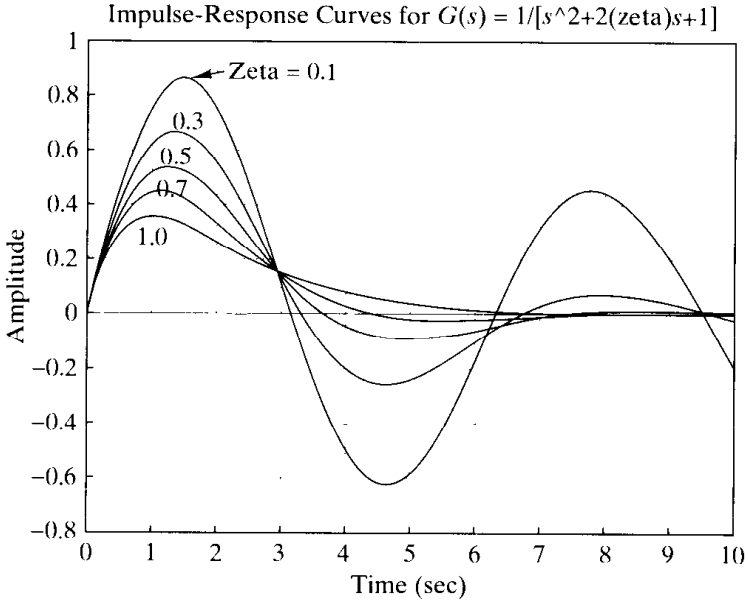

Figure 4–52
Unit-impulse response curves.

PROBLEMS

B-4-1. A thermometer requires 1 min to indicate 98% of the response to a step input. Assuming the thermometer to be a first-order system, find the time constant.

If the thermometer is placed in a bath, the temperature of which is changing linearly at a rate of 10°/min, how much error does the thermometer show?

B-4-2. Consider the system shown in Figure 4–53. An armature-controlled dc servomotor drives a load consisting of the moment of inertia J_L. The torque developed by the motor is T. The angular displacements of the motor rotor and the load element are θ_m and θ, respectively. The gear ratio is $n = \theta/\theta_m$. Obtain the transfer function $\Theta(s)/E_i(s)$.

B-4-3. Consider the system shown in Figure 4–54(a). The damping ratio of this system is 0.158 and the undamped natural frequency is 3.16 rad/sec. To improve the relative stability, we employ tachometer feedback. Figure 4–54(b) shows such a tachometer-feedback system.

Determine the value of K_h so that the damping ratio of the system is 0.5. Draw unit-step response curves of both the original and tachometer-feedback systems. Also draw the error-versus-time curves for the unit-ramp response of both systems.

B-4-4. Obtain the unit-step response of a unity-feedback system whose open-loop transfer function is

$$G(s) = \frac{4}{s(s + 5)}$$

B-4-5. Consider the unit-step response of a unity-feedback control system whose open-loop transfer function is

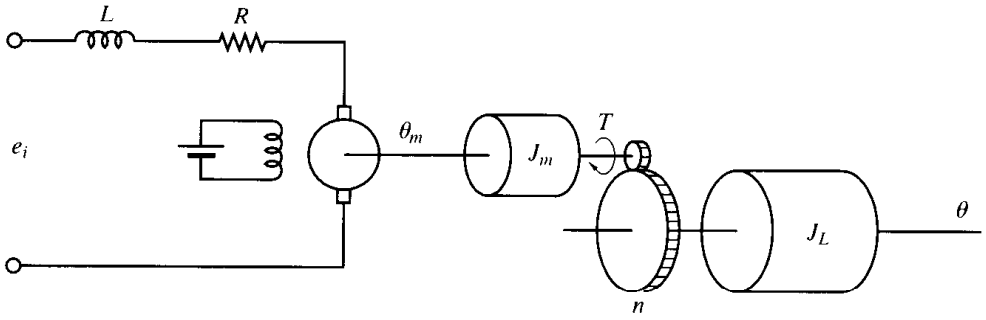

Figure 4–53
Armature-controlled dc servomotor system.

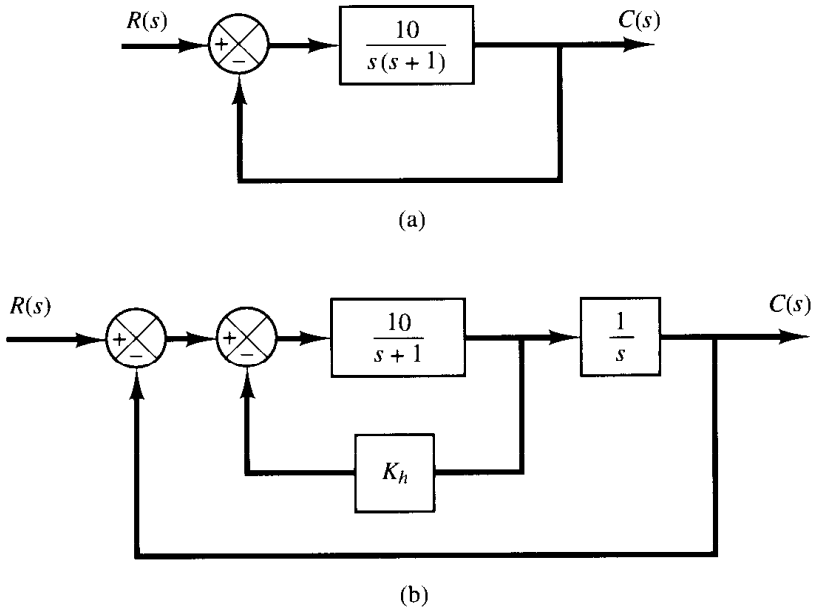

Figure 4–54
(a) Control system; (b) control system with tachometer feedback.

$$G(s) = \frac{1}{s(s + 1)}$$

Obtain the rise time, peak time, maximum overshoot, and settling time.

B-4-6. Consider the closed-loop system given by

$$\frac{C(s)}{R(s)} = \frac{\omega_n^2}{s^2 + 2\zeta\omega_n s + \omega_n^2}$$

Determine the values of ζ and ω_n so that the system responds to a step input with approximately 5% overshoot and with a settling time of 2 sec. (Use the 2% criterion.)

B-4-7. Figure 4–55 is a block diagram of a space-vehicle attitude-control system. Assuming the time constant T of the controller to be 3 sec and the ratio of torque to inertia K/J to be $\frac{2}{9}$ rad^2/sec^2, find the damping ratio of the system.

B-4-8. Consider the system shown in Figure 4–56. The system is initially at rest. Suppose that the cart is set into motion by an impulsive force whose strength is unity. Can it be stopped by another such impulsive force?

B-4-9. Obtain the unit-impulse response and the unit-step response of a unity-feedback system whose open-loop transfer function is

$$G(s) = \frac{2s + 1}{s^2}$$

B-4-10. Consider the system shown in Figure 4–57. Show that the transfer function $Y(s)/X(s)$ has a zero in the right-

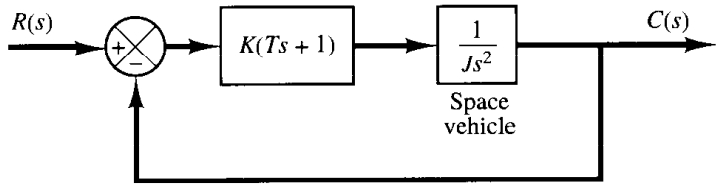

Figure 4–55
Space-vehicle attitude-control system.

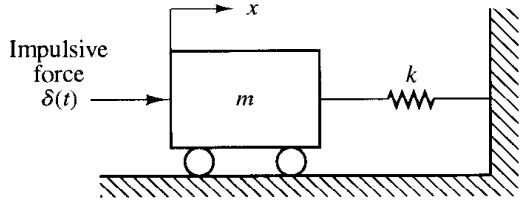

Figure 4–56
Mechanical system.

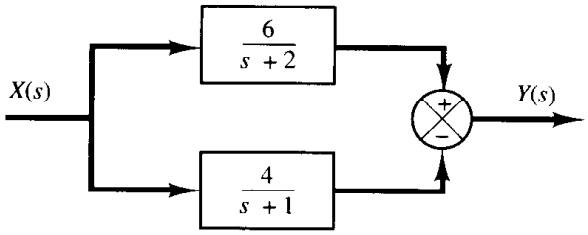

Figure 4–57
System with zero in the right-half s plane.

half s plane. Then obtain $y(t)$ when $x(t)$ is a unit step. Plot $y(t)$ versus t.

B-4-11. An oscillatory system is known to have a transfer function of the following form:

$$G(s) = \frac{\omega_n^2}{s^2 + 2\zeta\omega_n s + \omega_n^2}$$

Assume that a record of a damped oscillation is available as shown in Figure 4–58. Determine the damping ratio ζ of the system from the graph.

B-4-12. Referring to the system shown in Figure 4–59, determine the values of K and k such that the system has a damping ratio ζ of 0.7 and an undamped natural frequency ω_n of 4 rad/sec.

B-4-13. Consider the system shown in Figure 4–60. Determine the value of k such that the damping ratio ζ is 0.5. Then obtain the rise time t_r, peak time t_p, maximum overshoot M_p, and settling time t_s in the unit-step response.

B-4-14. Using MATLAB, obtain the unit-step response, unit-ramp response, and unit-impulse response of the following system:

$$\frac{C(s)}{R(s)} = \frac{10}{s^2 + 2s + 10}$$

where $R(s)$ and $C(s)$ are Laplace transforms of the input $r(t)$ and output $c(t)$, respectively.

B-4-15. Using MATLAB, obtain the unit-step response, unit-ramp response, and unit-impulse response of the

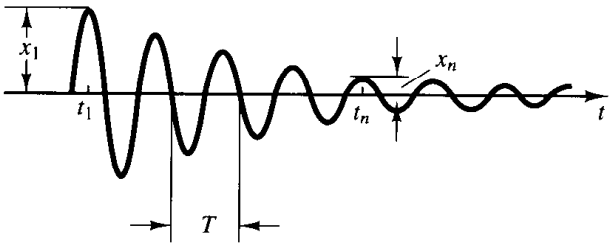

Figure 4–58
Decaying oscillation.

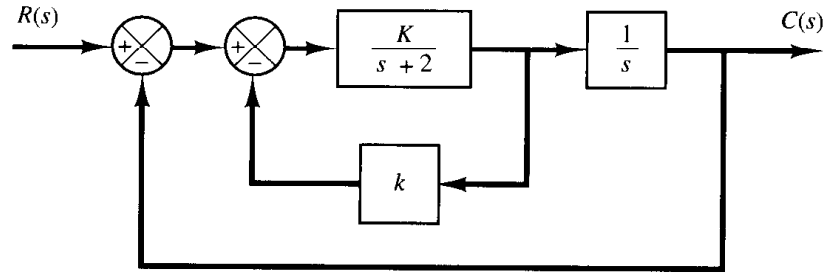

Figure 4–59
Closed-loop system.

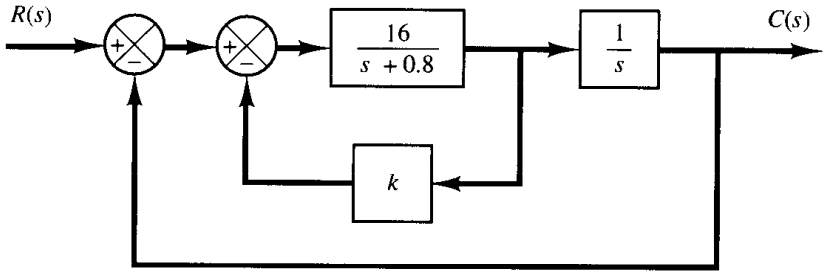

Figure 4–60
Block diagram of a system.

following system:

$$\begin{bmatrix} \dot{x}_1 \\ \dot{x}_2 \end{bmatrix} = \begin{bmatrix} -1 & -0.5 \\ 1 & 0 \end{bmatrix} \begin{bmatrix} x_1 \\ x_2 \end{bmatrix} + \begin{bmatrix} 0.5 \\ 0 \end{bmatrix} u$$

$$y = [1 \quad 0] \begin{bmatrix} x_1 \\ x_2 \end{bmatrix}$$

where u is the input and y is the output.

B-4-16. Consider the same problem as discussed in Problem A-4-16. It is desired to use different marks for different curves (such as 'o', '×', '--', '-', ':'). Modify MATLAB Program 4–14 for this purpose.

5

Basic Control Actions and Response of Control Systems

5–1 INTRODUCTION

An automatic controller compares the actual value of the plant output with the reference input (desired value), determines the deviation, and produces a control signal that will reduce the deviation to zero or to a small value. The manner in which the automatic controller produces the control signal is called the *control action.*

In this chapter we shall first discuss the basic control actions used in industrial control systems. Then we shall discuss the effects of integral and derivative control actions on the system response. We shall next consider the response of higher-order systems. Any physical system will become unstable if any of the closed-loop poles lies in the right-half s plane. To check the existence or nonexistence of such right-half plane poles, the Routh stability criterion is useful. We shall include discussions of this stability criterion in this chapter.

Many industrial automatic controllers are electronic, hydraulic, pneumatic, or their combinations. In this chapter we present principles of pneumatic controllers, hydraulic controllers, and electronic controllers.

The outline of this chapter follows: Section 5–1 has presented introductory material. Section 5–2 gives the basic control actions commonly used in industrial automatic controllers. Section 5–3 discusses the effects of integral and derivative control actions on system performance. Section 5–4 deals with higher-order systems, and Section 5–5 treats Routh's stability criterion. Sections 5–6 and 5–7 discuss pneumatic controllers and hydraulic controllers, respectively. Here we introduce the principle of operation of pneumatic and hydraulic controllers and methods for generating various control actions.

Section 5–8 treats electronic controllers using operational amplifiers. Section 5–9 discusses phase lead and phase lag in sinusoidal response. We derive the sinusoidal transfer function and show phase lead and phase lag that may occur in the sinusoidal response. Finally, in Section 5–10 we treat steady-state errors in system responses.

5-2 BASIC CONTROL ACTIONS

In this section we shall discuss the details of basic control actions used in industrial analog controllers. We shall begin with classifications of industrial analog controllers.

Classifications of industrial controllers. Industrial controllers may be classified according to their control actions as:

1. Two-position or on–off controllers
2. Proportional controllers
3. Integral controllers
4. Proportional-plus-integral controllers
5. Proportional-plus-derivative controllers
6. Proportional-plus-integral-plus-derivative controllers

Most industrial controllers use electricity or pressurized fluid such as oil or air as power sources. Controllers may also be classified according to the kind of power employed in the operation, such as pneumatic controllers, hydraulic controllers, or electronic controllers. What kind of controller to use must be decided based on the nature of the plant and the operating conditions, including such considerations as safety, cost, availability, reliability, accuracy, weight, and size.

Automatic controller, actuator, and sensor (measuring element). Figure 5–1 is a block diagram of an industrial control system, which consists of an automatic controller, an actuator, a plant, and a sensor (measuring element). The controller detects the actuating error signal, which is usually at a very low power level, and amplifies it to a sufficiently high level. The output of an automatic controller is fed to an actuator, such as a pneumatic motor or valve, a hydraulic motor, or an electric motor. (The actuator is

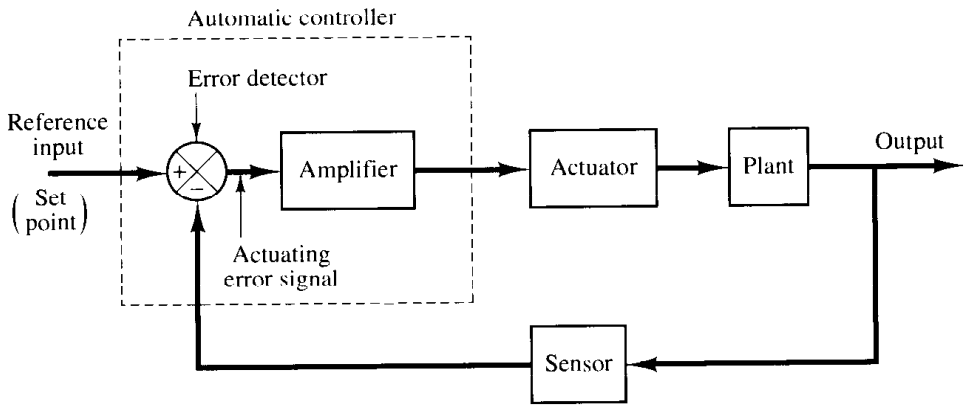

Figure 5–1
Block diagram of an industrial control system, which consists of an automatic controller, an actuator, a plant, and a sensor (measuring element).

a power device that produces the input to the plant according to the control signal so that the output signal will approach the reference input signal.)

The sensor or measuring element is a device that converts the output variable into another suitable variable, such as a displacement, pressure, or voltage, that can be used to compare the output to the reference input signal. This element is in the feedback path of the closed-loop system. The set point of the controller must be converted to a reference input with the same units as the feedback signal from the sensor or measuring element.

Self-operated controllers. In most industrial automatic controllers, separate units are used for the measuring element and for the actuator. In a very simple one, however, such as a self-operated controller, these elements are assembled in one unit. Self-operated controllers utilize power developed by the measuring element and are very simple and inexpensive. An example of such a self-operated controller is shown in Figure 5–2. The set point is determined by the adjustment of the spring force. The controlled pressure is measured by the diaphragm. The actuating error signal is the net force acting on the diaphragm. Its position determines the valve opening.

The operation of the self-operated controller is as follows: Suppose that the output pressure is lower than the reference pressure, as determined by the set point. Then the downward spring force is greater than the upward pressure force, resulting in a downward movement of the diaphragm. This increases the flow rate and raises the output pressure. When the upward pressure force equals the downward spring force, the valve plug stays stationary and the flow rate is constant. Conversely, if the output pressure is higher than the reference pressure, the valve opening becomes small and reduces the flow rate through the valve opening. Such a self-operated controller is widely used for water and gas pressure control.

Two-position or on–off control action. In a two-position control system, the actuating element has only two fixed positions, which are, in many cases, simply on and off. Two-position or on-off control is relatively simple and inexpensive and, for this reason, is very widely used in both industrial and domestic control systems.

Let the output signal from the controller be $u(t)$ and the actuating error signal be $e(t)$. In two-position control, the signal $u(t)$ remains at either a maximum or minimum value, depending on whether the actuating error signal is positive or negative, so that

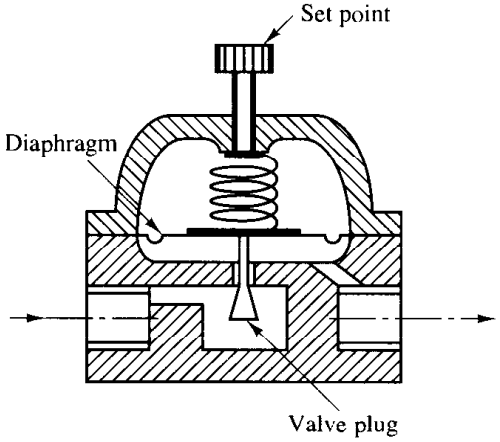

Figure 5–2
Self-operated controller.

$$u(t) = U_1, \quad \text{for } e(t) > 0$$
$$= U_2, \quad \text{for } e(t) < 0$$

where U_1 and U_2 are constants. The minimum value U_2 is usually either zero or $-U_1$. Two-position controllers are generally electrical devices, and an electric solenoid-operated valve is widely used in such controllers. Pneumatic proportional controllers with very high gains act as two-position controllers and are sometimes called pneumatic two-position controllers.

Figures 5–3 (a) and (b) show the block diagrams for two-position controllers. The range through which the actuating error signal must move before the switching occurs is called the *differential gap*. A differential gap is indicated in Figure 5–3(b). Such a differential gap causes the controller output $u(t)$ to maintain its present value until the actuating error signal has moved slightly beyond the zero value. In some cases, the differential gap is a result of unintentional friction and lost motion; however, quite often it is intentionally provided in order to prevent too frequent operation of the one–off mechanism.

Consider the liquid-level control system shown in Figure 5–4(a), where the electromagnetic valve shown in Figure 5–4(b) is used for controlling the inflow rate. This valve is either open or closed. With this two-position control, the water inflow rate is either a positive constant or zero. As shown in Figure 5–5, the output signal continuously moves between the two limits required to cause the actuating element to move from one fixed

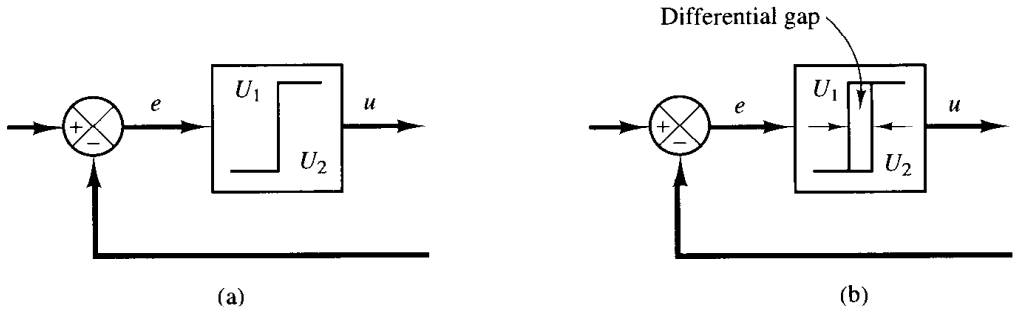

Figure 5–3
(a) Block diagram of an on-off controller; (b) block diagram of an on-off controller with differential gap.

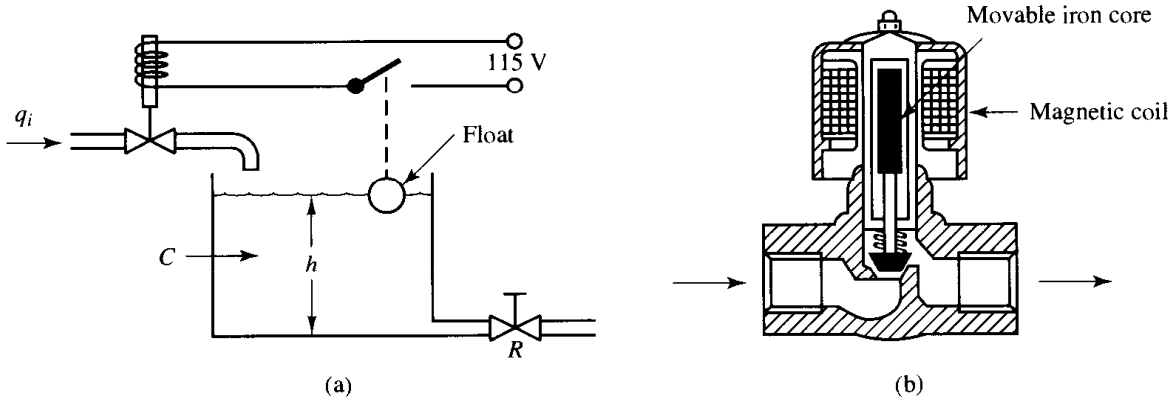

Figure 5–4
(a) Liquid-level control system; (b) electromagnetic valve.

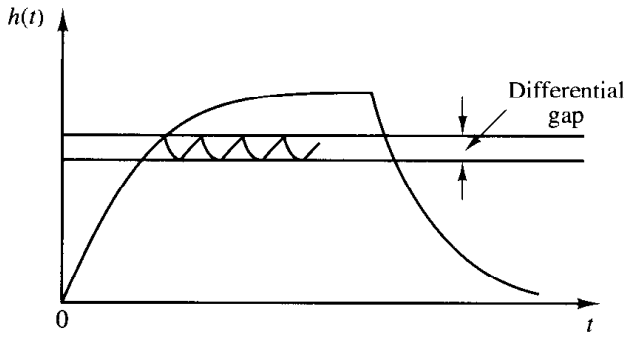

Figure 5–5
Level $h(t)$ versus t curve for the system shown in Figure 5–4(a).

position to the other. Notice that the output curve follows one of two exponential curves, one corresponding to the filling curve and the other to the emptying curve. Such output oscillation between two limits is a typical response characteristic of a system under two-position control.

From Figure 5–5, we notice that the amplitude of the output oscillation can be reduced by decreasing the differential gap. The decrease in the differential gap, however, increases the number of on–off switchings per minute and reduces the useful life of the component. The magnitude of the differential gap must be determined from such considerations as the accuracy required and the life of the component.

Proportional control action. For a controller with proportional control action, the relationship between the output of the controller $u(t)$ and the actuating error signal $e(t)$ is

$$u(t) = K_p e(t)$$

or, in Laplace-transformed quantities,

$$\frac{U(s)}{E(s)} = K_p$$

where K_p is termed the proportional gain.

Whatever the actual mechanism may be and whatever the form of the operating power, the proportional controller is essentially an amplifier with an adjustable gain. A block diagram of such a controller is shown in Figure 5–6.

Integral control action. In a controller with integral control action, the value of the controller output $u(t)$ is changed at a rate proportional to the actuating error signal $e(t)$. That is,

$$\frac{du(t)}{dt} = K_i e(t)$$

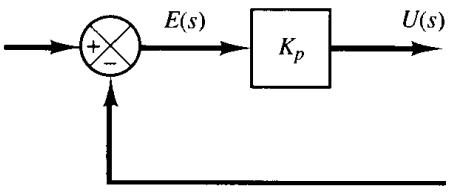

Figure 5–6
Block diagram of a proportional controller.

or

$$u(t) = K_i \int_0^t e(t)\, dt$$

where K_i is an adjustable constant. The transfer function of the integral controller is

$$\frac{U(s)}{E(s)} = \frac{K_i}{s}$$

If the value of $e(t)$ is doubled, then the value of $u(t)$ varies twice as fast. For zero actuating error, the value of $u(t)$ remains stationary. The integral control action is sometimes called reset control. Figure 5–7 shows a block diagram of such a controller.

Proportional-plus-integral control action. The control action of a proportional-plus-integral controller is defined by

$$u(t) = K_p e(t) + \frac{K_p}{T_i} \int_0^t e(t)\, dt$$

or the transfer function of the controller is

$$\frac{U(s)}{E(s)} = K_p\left(1 + \frac{1}{T_i s}\right)$$

where K_p is the proportional gain, and T_i is called the *integral time*. Both K_p and T_i are adjustable. The integral time adjusts the integral control action, while a change in the value of K_p affects both the proportional and integral parts of the control action. The inverse of the integral time T_i is called the *reset rate*. The reset rate is the number of times per minute that the proportional part of the control action is duplicated. Reset rate is measured in terms of repeats per minute. Figure 5–8 (a) shows a block diagram of a proportional-plus-integral controller. If the actuating error signal $e(t)$ is a unit-step function as shown in Figure 5–8(b), then the controller output $u(t)$ becomes as shown in Figure 5–8(c).

Proportional-plus-derivative control action. The control action of a proportional-plus-derivative controller is defined by

$$u(t) = K_p e(t) + K_p T_d \frac{de(t)}{dt}$$

and the transfer function is

$$\frac{U(s)}{E(s)} = K_p(1 + T_d s)$$

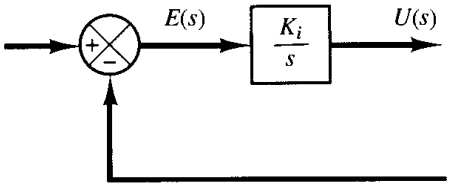

Figure 5–7
Block diagram of an integral controller.

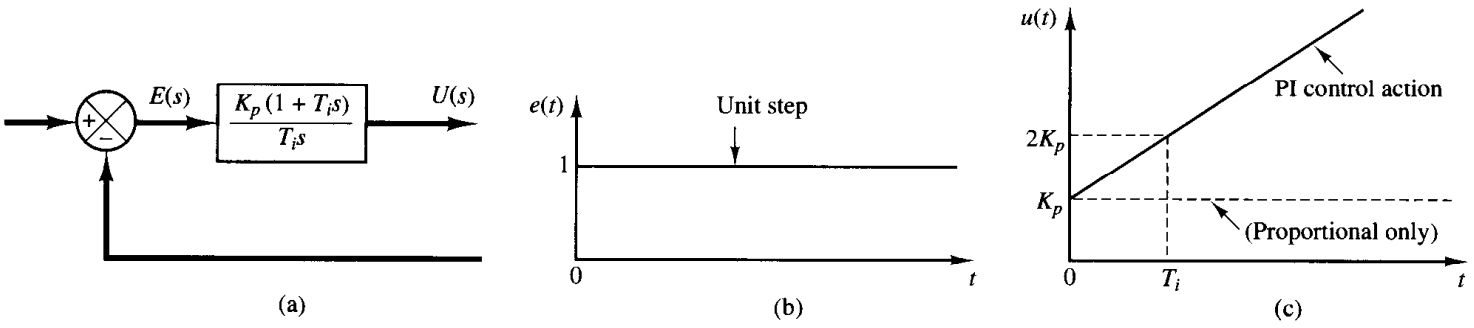

Figure 5–8
(a) Block diagram of a proportional-plus-integral controller; (b) and (c) diagrams depicting a unit-step input and the controller output.

where K_p is the proportional gain and T_d is a constant called the *derivative time*. Both K_p and T_d are adjustable. The derivative control action, sometimes called *rate control,* is where the magnitude of the controller output is proportional to the rate of change of the actuating error signal. The derivative time T_d is the time interval by which the rate action advances the effect of the proportional control action. Figure 5–9(a) shows a block diagram of a proportional-plus-derivative controller. If the actuating error signal $e(t)$ is a unit-ramp function as shown in Figure 5–9(b), then the controller output $u(t)$ becomes as shown in Figure 5–9(c). As may be seen from Figure 5–9(c), the derivative control action has an anticipatory character. As a matter of course, however, derivative control action can never anticipate any action that has not yet taken place.

While derivative control action has the advantage of being anticipatory, it has the disadvantages that it amplifies noise signals and may cause a saturation effect in the actuator.

Note that derivative control action can never be used alone because this control action is effective only during transient periods.

Proportional-plus-integral-plus-derivative control action. The combination of proportional control action, integral control action, and derivative control action is termed proportional-plus-integral-plus-derivative control action. This combined action

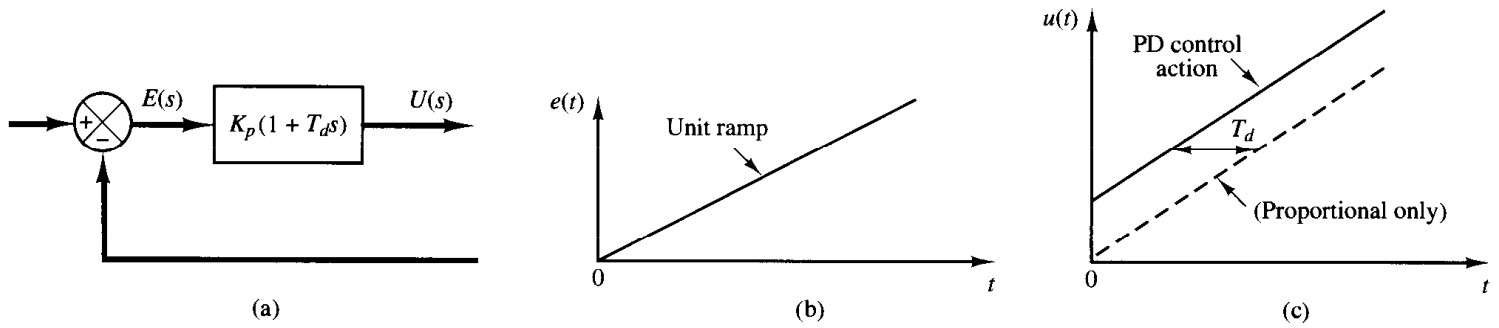

Figure 5–9
(a) Block diagram of a proportional-plus-derivative controller; (b) and (c) diagrams depicting a unit-ramp input and the controller output.

has the advantages of each of the three individual control actions. The equation of a controller with this combined action is given by

$$u(t) = K_p e(t) + \frac{K_p}{T_i}\int_0^t e(t)\,dt + K_p T_d \frac{de(t)}{dt}$$

or the transfer function is

$$\frac{U(s)}{E(s)} = K_p\left(1 + \frac{1}{T_i s} + T_d s\right)$$

where K_p is the proportional gain, T_i is the integral time, and T_d is the derivative time. The block diagram of a proportional-plus-integral-plus-derivative controller is shown in Figure 5–10(a). If $e(t)$ is a unit-ramp function as shown in Figure 5–10(b), then the controller output $u(t)$ becomes as shown in Figure 5–10(c).

Effects of the sensor (measuring element) on system performance. Since the dynamic and static characteristics of the sensor or measuring element affect the indication of the actual value of the output variable, the sensor plays an important role in determining the overall performance of the control system. The sensor usually determines the transfer function in the feedback path. If the time constants of a sensor are negligibly small compared with other time constants of the control system, the transfer function of the sensor simply becomes a constant. Figures 5–11(a), (b), and (c) show block diagrams of automatic controllers having a first-order sensor, an overdamped second-order sensor, and an underdamped second-order sensor, respectively. The response of a thermal sensor is often of the overdamped second-order type.

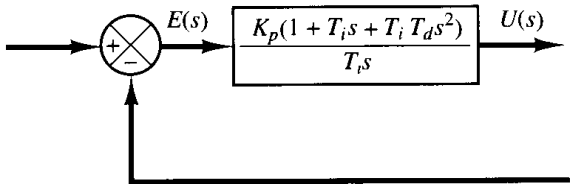

(a)

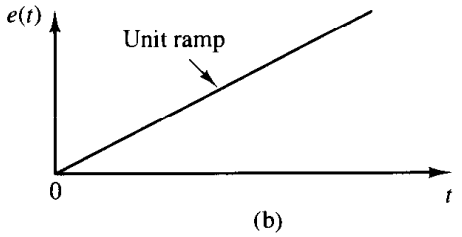

(b)

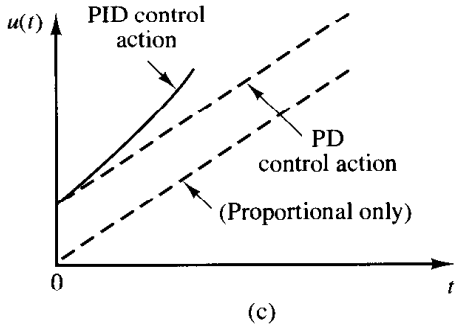

(c)

Figure 5–10
(a) Block diagram of a proportional-plus-integral-plus-derivative controller; (b) and (c) diagrams depicting a unit-ramp input and the controller output.

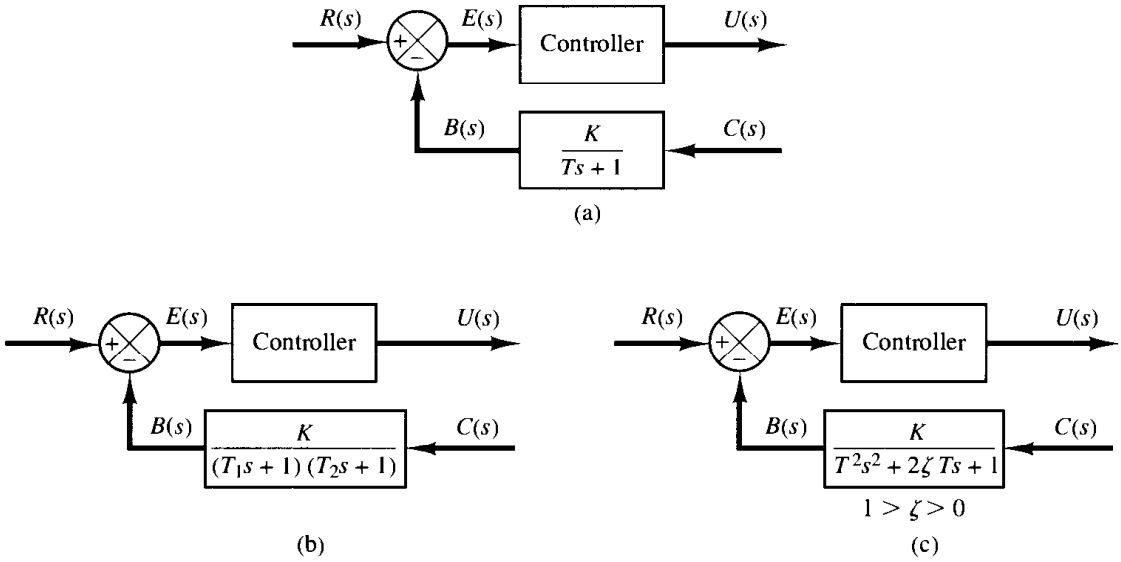

Figure 5–11
Block diagrams of automatic controllers with (a) first-order sensor; (b) overdamped second-order sensor; (c) underdamped second-order sensor.

5–3 EFFECTS OF INTEGRAL AND DERIVATIVE CONTROL ACTIONS ON SYSTEM PERFORMANCE

In this section, we shall investigate the effects of integral and derivative control actions on the system performance. Here we shall consider only simple systems so that the effects of integral and derivative control actions on system performance can be clearly seen.

Integral control action. In the proportional control of a plant whose transfer function does not possess an integrator $1/s$, there is a steady-state error, or offset, in the response to a step input. Such an offset can be eliminated if the integral control action is included in the controller.

In the integral control of a plant, the control signal, the output signal from the controller, at any instant is the area under the actuating error signal curve up to that instant. The control signal $u(t)$ can have a nonzero value when the actuating error signal $e(t)$ is zero, as shown in Figure 5–12(a). This is impossible in the case of the proportional controller since a nonzero control signal requires a nonzero actuating error signal. (A nonzero actuating error signal at steady state means that there is an offset.) Figure 5–12(b) shows the curve $e(t)$ versus t and the corresponding curve $u(t)$ versus t when the controller is of the proportional type.

Note that integral control action, while removing offset or steady-state error, may lead to oscillatory response of slowly decreasing amplitude or even increasing amplitude, both of which are usually undesirable.

Integral control of liquid-level control systems. In Section 4–2, we found that the proportional control of a liquid-level system will result in a steady-state error with a step input. We shall now show that such an error can be eliminated if integral control action is included in the controller.

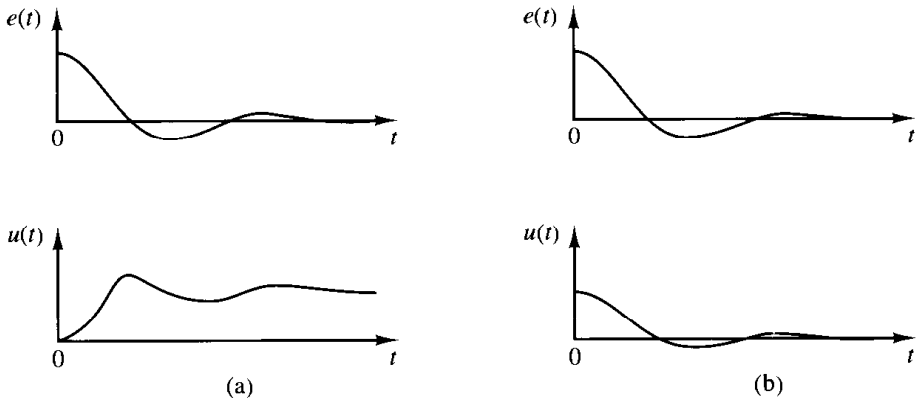

Figure 5–12
(a) Plots of $e(t)$ and $u(t)$ curves showing nonzero control signal when the actuating error signal is zero (integral control); (b) plots of $e(t)$ and $u(t)$ curves showing zero control signal when the actuating error signal is zero (proportional control).

Figure 5–13(a) shows a liquid-level control system. We assume that the controller is an integral controller. We also assume that the variables x, q_i, h, and q_o, which are measured from their respective steady-state values $\bar{X}$, $\bar{Q}$, $\bar{H}$, and $\bar{Q}$, are small quantities so that the system can be considered linear. Under these assumptions, the block diagram of the system can be obtained as shown in Figure 5–13(b). From Figure 5–13(b), the closed-loop transfer function between $H(s)$ and $X(s)$ is

$$\frac{H(s)}{X(s)} = \frac{KR}{RCs^2 + s + KR}$$

Hence

$$\frac{E(s)}{X(s)} = \frac{X(s) - H(s)}{X(s)}$$

$$= \frac{RCs^2 + s}{RCs^2 + s + KR}$$

Since the system is stable, the steady-state error for the unit-step response is obtained by applying the final-value theorem, as follows:

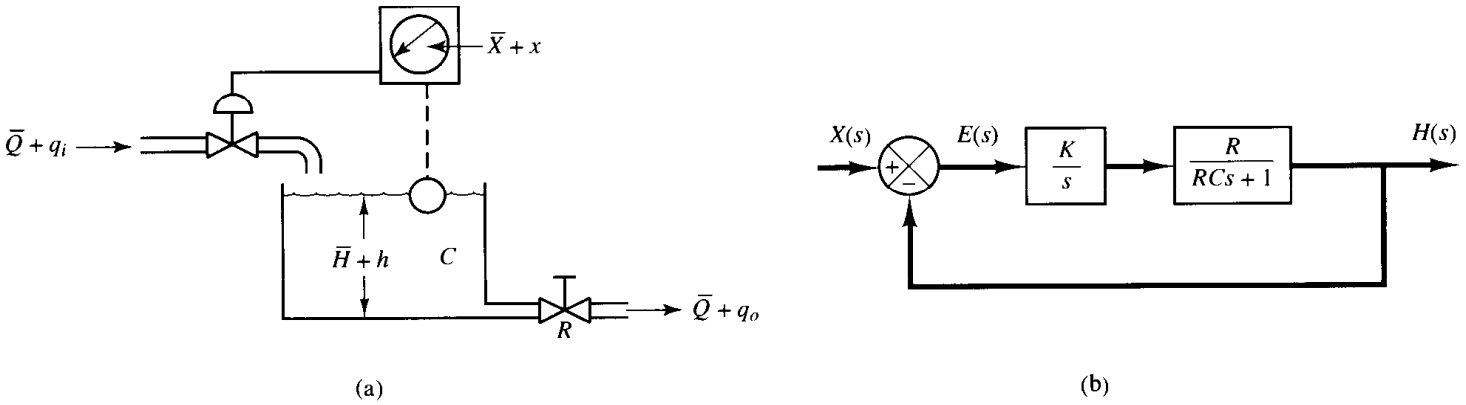

Figure 5–13
(a) Liquid-level control system; (b) block diagram of the system.

$$
\begin{aligned}
e_{ss} &= \lim_{s \to 0} sE(s) \\
&= \lim_{s \to 0} \frac{s(RCs^2 + s)}{RCs^2 + s + KR} \frac{1}{s} \\
&= 0
\end{aligned}
$$

Integral control of the liquid-level system thus eliminates the steady-state error in the response to the step input. This is an important improvement over the proportional control alone, which gives offset.

Response to torque disturbances (proportional control). Let us investigate the effect of a torque disturbance occurring at the load element. Consider the system shown in Figure 5–14. The proportional controller delivers torque T to position the load element, which consists of moment of inertia and viscous friction. Torque disturbance is denoted by D.

Assuming that the reference input is zero or $R(s) = 0$, the transfer function between $C(s)$ and $D(s)$ is given by

$$
\frac{C(s)}{D(s)} = \frac{1}{Js^2 + bs + K_p}
$$

Hence

$$
\frac{E(s)}{D(s)} = -\frac{C(s)}{D(s)} = -\frac{1}{Js^2 + bs + K_p}
$$

The steady-state error due to a step disturbance torque of magnitude T_d is given by

$$
\begin{aligned}
e_{ss} &= \lim_{s \to 0} sE(s) \\
&= \lim_{s \to 0} \frac{-s}{Js^2 + bs + K_p} \frac{T_d}{s} \\
&= -\frac{T_d}{K_p}
\end{aligned}
$$

At steady state, the proportional controller provides the torque $-T_d$, which is equal in magnitude but opposite in sign to the disturbance torque T_d. The steady-state output due to the step disturbance torque is

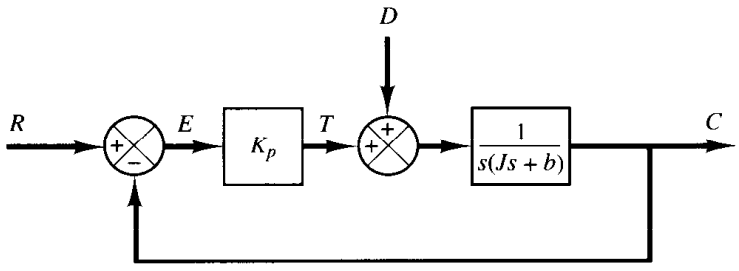

Figure 5–14
Control system with a torque disturbance.

$$c_{ss} = -e_{ss} = \frac{T_d}{K_p}$$

The steady-state error can be reduced by increasing the value of the gain K_p. Increasing this value, however, will cause the system response to be more oscillatory.

Obtaining responses with MATLAB. In what follows, we shall obtain the response curves of the system shown in Figure 5–14 when it is subjected to a unit-step disturbance. Specifically, we shall obtain step-response curves for a small value of K_p and a large value of K_p.

Consider two cases:

Case 1: $J = 1, b = 0.5, K_p = 1$ (system 1):

$$\frac{C(s)}{D(s)} = \frac{1}{s^2 + 0.5s + 1}$$

Case 2: $J = 1, b = 0.5, K_p = 4$ (system 2):

$$\frac{C(s)}{D(s)} = \frac{1}{s^2 + 0.5s + 4}$$

Note that for system 1

```
num1 = [0   0   1]
den1 = [1   0.5   1]
```

For system 2

```
num2 = [0   0   1]
den2 = [1   0.5   4]
```

In MATLAB Program 5–1 we have used notations y1 and y2 for the response. y1 is the response $c(t)$ of system 1, and y2 is the response $c(t)$ of system 2.

In MATLAB Program 5–1, note that we have used the plot command with multiple arguments, rather than using the *hold* command. (We get the same result either way.) To use the *plot* command with multiple arguments, the sizes of the y1 and y2 vectors need not be the same. However, it is convenient if the two vectors are of the same length. Hence, we specify the same number of computing points by specifying the computing time points (such as t = 0:0.1:20). The *step* command must include this user-specified time t. Thus, in MATLAB Program 5–1 we have used the following *step* command:

```
[y, x, t] = step(num, den,t)
```

The unit-step response curves obtained by use of MATLAB Program 5–1 are shown in Figure 5–15.

MATLAB Program 5–1

```
% ---------- Plotting two step-response curves on one
% diagram ----------

% *****Enter numerators and denominators of two
% transfer functions*****

num1 = [0   0   1];
den1 = [1   0.5   1];
num2 = [0   0   1];
den2 = [1   0.5   4];

% ***** To plot two step-response curves y1 versus t
% and y2 versus t on one diagram and write texts
% 'System 1' and 'System 2' to distinguish two curves,
% enter the following commands *****

t = 0:0.1:20;
[y1,x1,t] = step(num1,den1,t);
[y2,x2,t] = step(num2,den2,t);
plot(t,y1,t,y2)
grid
text(11,0.75,'System 1'), text(11.2,0.16,'System 2')

% ***** Add title of the plot, xlabel, and ylabel *****

title('Step Responses of Two Systems')
xlabel('t Sec')
ylabel('Outputs y1 and y2')
```

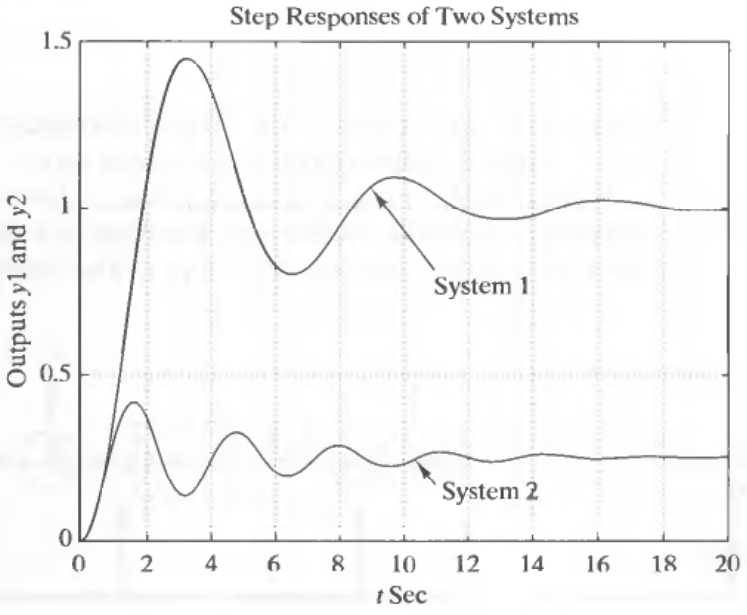

Figure 5–15
Unit-step response curves.

Response to torque disturbances (proportional-plus-integral control). To eliminate offset due to torque disturbance, the proportional controller may be replaced by a proportional-plus-integral controller.

If integral control action is added to the controller, then, as long as there is an error signal, a torque is developed by the controller to reduce this error, provided the control system is a stable one.

Figure 5–16 shows the proportional-plus-integral control of the load element, consisting of moment of inertia and viscous friction.

The closed-loop transfer function between $C(s)$ and $D(s)$ is

$$\frac{C(s)}{D(s)} = \frac{s}{Js^3 + bs^2 + K_p s + \dfrac{K_p}{T_i}}$$

In the absence of the reference input, or $r(t) = 0$, the error signal is obtained from

$$E(s) = -\frac{s}{Js^3 + bs^2 + K_p s + \dfrac{K_p}{T_i}} D(s)$$

If this control system is stable, that is, if the roots of the characteristic equation

$$Js^3 + bs^2 + K_p s + \frac{K_p}{T_i} = 0$$

have negative real parts, then the steady-state error in the response to a unit-step disturbance torque can be obtained by applying the final-value theorem as follows:

$$\begin{aligned} e_{ss} &= \lim_{s \to 0} sE(s) \\ &= \lim_{s \to 0} \frac{-s^2}{Js^3 + bs^2 + K_p s + \dfrac{K_p}{T_i}} \frac{1}{s} \\ &= 0 \end{aligned}$$

Thus steady-state error to the step disturbance torque can be eliminated if the controller is of the proportional-plus-integral type.

Note that the integral control action added to the proportional controller has converted the originally second-order system to a third-order one. Hence the control system may become unstable for a large value of K_p since the roots of the characteristic

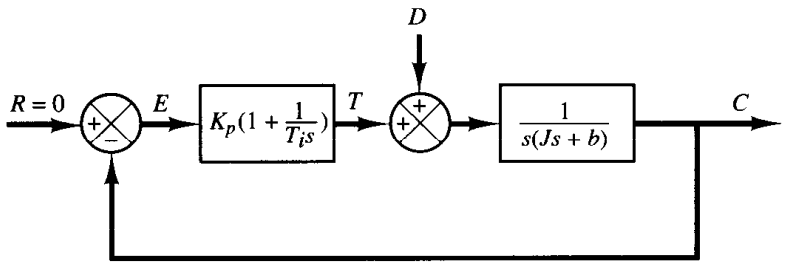

Figure 5–16
Proportional-plus-integral control of a load element consisting of moment of inertia and viscous friction.

equation may have positive real parts. (The second-order system is always stable if the coefficients in the system differential equation are all positive.)

It is important to point out that if the controller were an integral controller, as in Figure 5–17, then the system always becomes unstable because the characteristic equation

$$Js^3 + bs^2 + K = 0$$

will have roots with positive real parts. Such an unstable system cannot be used in practice.

Note that in the system of Figure 5–16 the proportional control action tends to stabilize the system, while the integral control action tends to eliminate or reduce steady-state error in response to various inputs.

Derivative control action. Derivative control action, when added to a proportional controller, provides a means of obtaining a controller with high sensitivity. An advantage of using derivative control action is that it responds to the rate of change of the actuating error and can produce a significant correction before the magnitude of the actuating error becomes too large. Derivative control thus anticipates the actuating error, initiates an early corrective action, and tends to increase the stability of the system.

Although derivative control does not affect the steady-state error directly, it adds damping to the system and thus permits the use of a larger value of the gain K, which will result in an improvement in the steady-state accuracy.

Because derivative control operates on the rate of change of the actuating error and not the actuating error itself, this mode is never used alone. It is always used in combination with proportional or proportional-plus-integral control action.

Proportional control of systems with inertia load. Before we discuss the effect of derivative control action on system performance, we shall consider the proportional control of an inertia load.

Consider the system shown in Figure 5–18(a). The closed-loop transfer function is obtained as

$$\frac{C(s)}{R(s)} = \frac{K_p}{Js^2 + K_p}$$

Since the roots of the characteristic equation

$$Js^2 + K_p = 0$$

are imaginary, the response to a unit-step input continues to oscillate indefinitely, as shown in Figure 5–18(b).

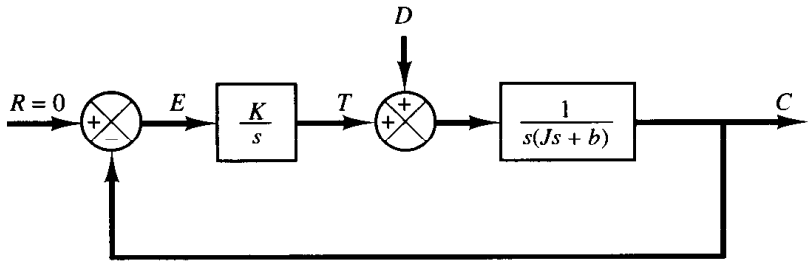

Figure 5–17
Integral control of a load element consisting of moment of inertia and viscous friction.

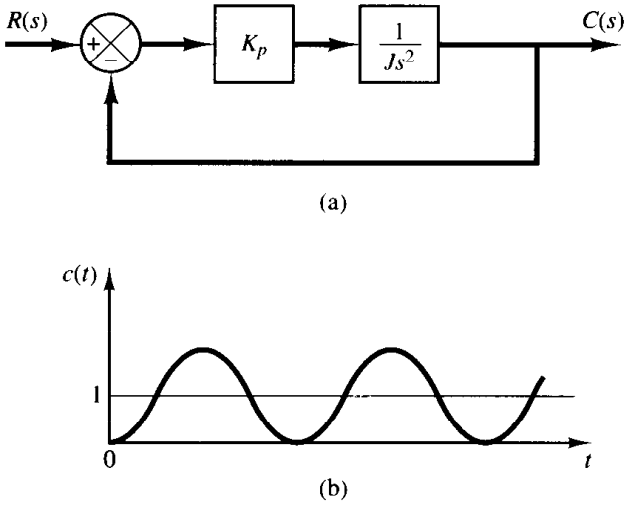

Figure 5–18
(a) Proportional control of a system with inertia load; (b) response to a unit-step input.

Control systems exhibiting such response characteristics are not desirable. We shall see that the addition of derivative control will stabilize the system.

Proportional-plus-derivative control of a system with inertia load. Let us modify the proportional controller to a proportional-plus-derivative controller whose transfer function is $K_p(1 + T_d s)$. The torque developed by the controller is proportional to $K_p(e + T_d \dot{e})$. Derivative control is essentially anticipatory, measures the instantaneous error velocity, and predicts the large overshoot ahead of time and produces an appropriate counteraction before too large an overshoot occurs.

Consider the system shown in Figure 5–19(a). The closed-loop transfer function is given by

$$\frac{C(s)}{R(s)} = \frac{K_p(1 + T_d s)}{Js^2 + K_p T_d s + K_p}$$

The characteristic equation

$$Js^2 + K_p T_d s + K_p = 0$$

now has two roots with negative real parts for positive values of J, K_p, and T_d. Thus derivative control introduces a damping effect. A typical response curve $c(t)$ to a unit-step input is shown in Figure 5–19(b). Clearly, the response curve shows a marked improvement over the original response curve shown in Figure 5–18(b).

Proportional-plus-derivative control of second-order systems. A compromise between acceptable transient-response behavior and acceptable steady-state behavior may be achieved by use of proportional-plus-derivative control action.

Consider the system shown in Figure 5–20. The closed-loop transfer function is

$$\frac{C(s)}{R(s)} = \frac{K_p + K_d s}{Js^2 + (B + K_d)s + K_p}$$

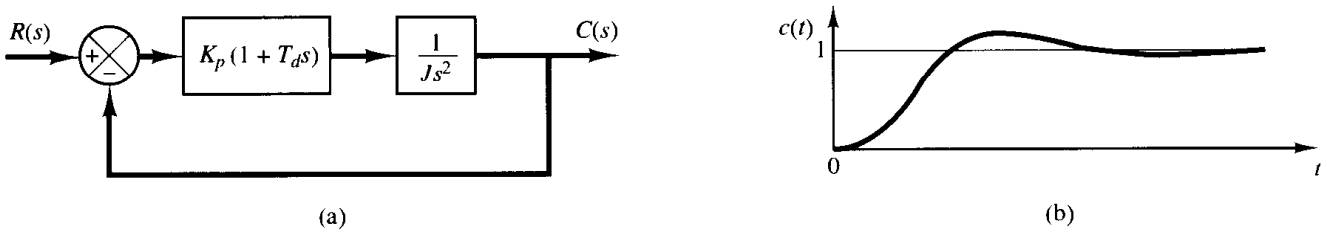

(a) (b)

Figure 5–19
(a) Proportional-plus-derivative control of a system with inertia load; (b) response to a unit-step input.

The steady-state error for a unit-ramp input is

$$e_{ss} = \frac{B}{K_p}$$

The characteristic equation is

$$Js^2 + (B + K_d)s + K_p = 0$$

The effective damping coefficient of this system is thus $B + K_d$ rather than B. Since the damping ratio ζ of this system is

$$\zeta = \frac{B + K_d}{2\sqrt{K_p J}}$$

it is possible to make both the steady-state error e_{ss} for a ramp input and the maximum overshoot for a step input small by making B small, K_p large, and K_d large enough so that ζ is between 0.4 and 0.7.

In the following, we shall examine the unit-step response of the system shown in Figure 5–20. Let us define

$$\omega_n = \sqrt{\frac{K_p}{J}}, \qquad z = \frac{K_p}{K_d}$$

The closed-loop transfer function can then be written

$$\frac{C(s)}{R(s)} = \frac{\omega_n^2}{z} \frac{s + z}{s^2 + 2\zeta\omega_n s + \omega_n^2}$$

When a second-order system has a zero near the closed-loop poles, the transient-response behavior becomes considerably different from that of a second-order system without a zero.

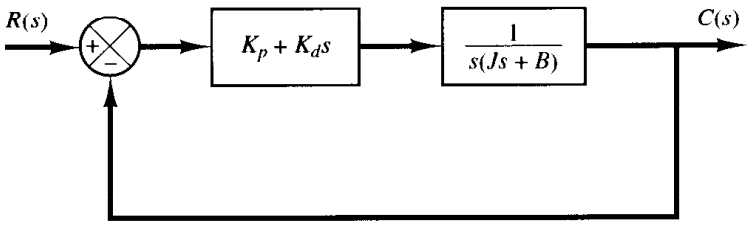

Figure 5–20
Control system.

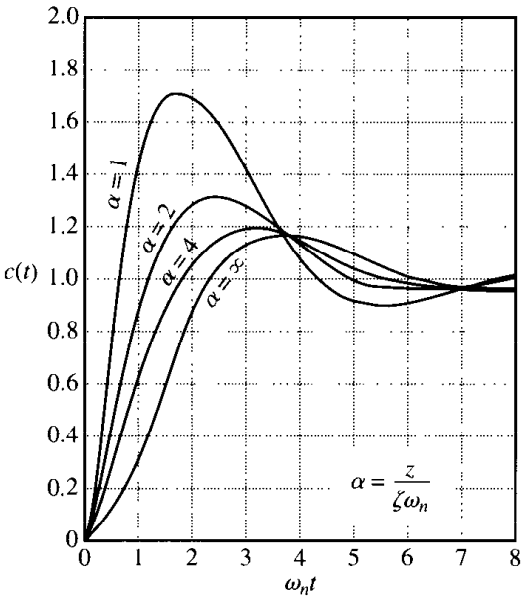

Figure 5–21
Unit-step response curves of the second-order system

$$\frac{C(s)}{R(s)} = \frac{\omega_n^2}{z}\,\frac{s + z}{s^2 + 2\zeta\omega_n s + \omega_n^2}$$

$\zeta = 0.5$

If the zero at $s = -z$ is located close to the $j\omega$ axis, the effect of the zero on the unit-step response is quite significant. Typical step-response curves of this system with $\zeta = 0.5$ and various values of $z/(\zeta\omega_n)$ are shown in Figure 5–21.

5–4 HIGHER-ORDER SYSTEMS

In this section, we shall first discuss the unit-step response of a particular type of higher-order system. We shall then present a transient response analysis of higher-order systems in general terms. Finally, we shall present a discussion of stability analysis in the complex plane.

Transient response of higher-order systems. Consider the system shown in Figure 5–22. The closed loop transfer function is

$$\frac{C(s)}{R(s)} = \frac{G(s)}{1 + G(s)H(s)} \tag{5–1}$$

In general, $G(s)$ and $H(s)$ are given as ratios of polynomials in s, or

$$G(s) = \frac{p(s)}{q(s)} \qquad \text{and} \qquad H(s) = \frac{n(s)}{d(s)}$$

where $p(s)$, $q(s)$, $n(s)$, and $d(s)$ are polynomials in s. The closed-loop transfer function given by Equation (5–1) may then be written

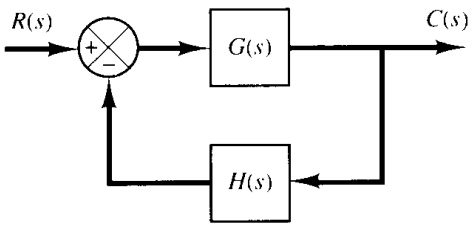

Figure 5–22
Control system.

$$\frac{C(s)}{R(s)} = \frac{p(s)d(s)}{q(s)d(s) + p(s)n(s)}$$

$$= \frac{b_0 s^m + b_1 s^{m-1} + \cdots + b_{m-1}s + b_m}{a_0 s^n + a_1 s^{n-1} + \cdots + a_{n-1}s + a_n} \qquad (m \leq n)$$

The transient response of this system to any given input can be obtained by a computer simulation (see Section 4–4). If an analytical expression for the transient response is desired, then it is necessary to factor the denominator polynomial. [MATLAB may be used for finding the roots of the denominator polynomial. Use the command roots(den).] Once the numerator and the denominator have been factored, $C(s)/R(s)$ can be written as

$$\frac{C(s)}{R(s)} = \frac{K(s + z_1)(s + z_2)\cdots(s + z_m)}{(s + p_1)(s + p_2)\cdots(s + p_n)} \tag{5–2}$$

Let us examine the response behavior of this system to a unit-step input. Consider first the case where the closed-loop poles are all real and distinct. For a unit-step input, Equation (5–2) can be written

$$C(s) = \frac{a}{s} + \sum_{i=1}^{n} \frac{a_i}{s + p_i} \tag{5–3}$$

where a_i is the residue of the pole at $s = -p_i$.

If all closed-loop poles lie in the left-half s plane, the relative magnitudes of the residues determine the relative importance of the components in the expanded form of $C(s)$. If there is a closed-loop zero close to a closed-loop pole, then the residue at this pole is small and the coefficient of the transient-response term corresponding to this pole becomes small. A pair of closely located poles and zeros will effectively cancel each other. If a pole is located very far from the origin, the residue at this pole may be small. The transients corresponding to such a remote pole are small and last a short time. Terms in the expanded form of $C(s)$ having very small residues contribute little to the transient response, and these terms may be neglected. If this is done, the higher-order system may be approximated by a lower-order one. (Such an approximation often enables us to estimate the response characteristics of a higher-order system from those of a simplified one.)

Next, consider the case where the poles of $C(s)$ consist of real poles and pairs of complex-conjugate poles. A pair of complex-conjugate poles yields a second-order term in s. Since the factored form of the higher-order characteristic equation consists of first- and second-order terms, Equation (5–3) can be rewritten

$$C(s) = \frac{K\prod_{i=1}^{m}(s + z_i)}{s\prod_{j=1}^{q}(s + p_j)\prod_{k=1}^{r}(s^2 + 2\zeta_k\omega_k s + \omega_k^2)} \tag{5–4}$$

where $q + 2r = n$. If the closed-loop poles are distinct, Equation (5–4) can be expanded into partial fractions as follows:

$$C(s) = \frac{a}{s} + \sum_{j=1}^{q}\frac{a_j}{s + p_j} + \sum_{k=1}^{r}\frac{b_k(s + \zeta_k\omega_k) + c_k\omega_k\sqrt{1 - \zeta_k^2}}{s^2 + 2\zeta_k\omega_k s + \omega_k^2}$$

From this last equation, we see that the response of a higher-order system is composed of a number of terms involving the simple functions found in the responses of first- and second-order systems. The unit-step response $c(t)$, the inverse Laplace transform of $C(s)$, is then

$$c(t) = a + \sum_{j=1}^{q} a_j e^{-p_j t} + \sum_{k=1}^{r} b_k e^{-\zeta_k\omega_k t}\cos\omega_k\sqrt{1 - \zeta_k^2}\,t + \sum_{k=1}^{r} c_k e^{-\zeta_k\omega_k t}\sin\omega_k\sqrt{1 - \zeta_k^2}\,t, \qquad \text{for } t \geq 0 \tag{5–5}$$

Thus the response curve of a stable higher-order system is the sum of a number of exponential curves and damped sinusoidal curves.

If all closed-loop poles lie in the left-half s plane, then the exponential terms and the damped exponential terms in Equation (5–5) will approach zero as time t increases. The steady-state output is then $c(\infty) = a$.

Let us assume that the system considered is a stable one. Then the closed-loop poles that are located far from the $j\omega$ axis have large negative real parts. The exponential terms that correspond to these poles decay very rapidly to zero. (Note that the horizontal distance from a closed-loop pole to the $j\omega$ axis determines the settling time of transients due to that pole. The smaller the distance is, the longer the settling time.)

Remember that the type of transient response is determined by the closed-loop poles, while the shape of the transient response is primarily determined by the closed-loop zeros. As we have seen earlier, the poles of the input $R(s)$ yield the steady-state response terms in the solution, while the poles of $C(s)/R(s)$ enter into the exponential transient-response terms and/or damped sinusoidal transient-response terms. The zeros of $C(s)/R(s)$ do not affect the exponents in the exponential terms, but they do affect the magnitudes and signs of the residues.

Dominant closed-loop poles. The relative dominance of closed-loop poles is determined by the ratio of the real parts of the closed-loop poles, as well as by the relative magnitudes of the residues evaluated at the closed-loop poles. The magnitudes of the residues depend on both the closed-loop poles and zeros.

If the ratios of the real parts exceed 5 and there are no zeros nearby, then the closed-loop poles nearest the $j\omega$ axis will dominate in the transient-response behavior because

these poles correspond to transient-response terms that decay slowly. Those closed-loop poles that have dominant effects on the transient-response behavior are called *dominant closed-loop* poles. Quite often the dominant closed-loop poles occur in the form of a complex-conjugate pair. The dominant closed-loop poles are most important among all closed-loop poles.

The gain of a higher-order system is often adjusted so that there will exist a pair of dominant complex-conjugate closed-loop poles. The presence of such poles in a stable system reduces the effect of such nonlinearities as dead zone, backlash, and coulomb friction.

Remember that, although the concept of dominant closed-loop poles is useful for estimating the dynamic behavior of a closed-loop system, we must be careful to see that the underlying assumptions are met before using it.

Stability analysis in the complex plane. The stability of a linear closed-loop system can be determined from the location of the closed-loop poles in the s plane. If any of these poles lie in the right-half s plane, then with increasing time they give rise to the dominant mode, and the transient response increases monotonically or oscillates with increasing amplitude. This represents an unstable system. For such a system, as soon as the power is turned on, the output may increase with time. If no saturation takes place in the system and no mechanical stop is provided, then the system may eventually be subjected to damage and fail since the response of a real physical system cannot increase indefinitely. Therefore, closed-loop poles in the right-half s plane are not permissible in the usual linear control system. If all closed-loop poles lie to the left of the $j\omega$ axis, any transient response eventually reaches equilibrium. This represents a stable system.

Whether a linear system is stable or unstable is a property of the system itself and does not depend on the input or driving function of the system. The poles of the input, or driving function, do not affect the property of stability of the system, but they contribute only to steady-state response terms in the solution. Thus, the problem of absolute stability can be solved readily by choosing no closed-loop poles in the right-half s plane, including the $j\omega$ axis. (Mathematically, closed-loop poles on the $j\omega$ axis will yield oscillations, the amplitude of which is neither decaying nor growing with time. In practical cases, where noise is present, however, the amplitude of oscillations may increase at a rate determined by the noise power level. Therefore, a control system should not have closed-loop poles on the $j\omega$ axis.)

Note that the mere fact that all closed-loop poles lie in the left-half s plane does not guarantee satisfactory transient-response characteristics. If dominant complex-conjugate closed-loop poles lie close to the $j\omega$ axis, the transient response may exhibit excessive oscillations or may be very slow. Therefore, to guarantee fast, yet well-damped, transient-response characteristics, it is necessary that the closed-loop poles of the system lie in a particular region in the complex plane, such as the region bounded by the shaded area in Figure 5–23.

Since the relative stability and transient performance of a closed-loop control system are directly related to the closed-loop pole–zero configuration in the s plane, it is frequently necessary to adjust one or more system parameters in order to obtain suitable configurations. The effects of varying system parameters on the closed-loop poles will be discussed in detail in Chapter 6.

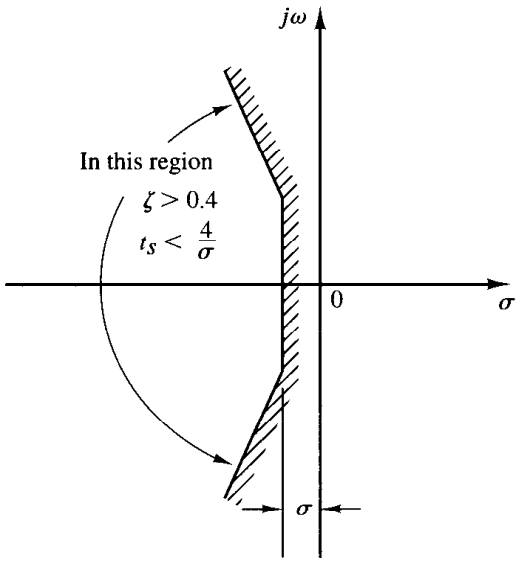

Figure 5–23
Region in the complex plane satisfying the conditions $\zeta > 0.4$ and $t_s < 4/\sigma$.

5–5 ROUTH'S STABILITY CRITERION

The most important problem in linear control systems concerns stability. That is, under what conditions will a system become unstable? If it is unstable, how should we stabilize the system? In Section 5–4 it was stated that a control system is stable if and only if all closed-loop poles lie in the left-half s plane. Since most linear closed-loop systems have closed-loop transfer functions of the form

$$\frac{C(s)}{R(s)} = \frac{b_0 s^m + b_1 s^{m-1} + \cdots + b_{m-1}s + b_m}{a_0 s^n + a_1 s^{n-1} + \cdots + a_{n-1}s + a_n} = \frac{B(s)}{A(s)}$$

where the a's and b's are constants and $m \leq n$, we must first factor the polynomial $A(s)$ in order to find the closed-loop poles. A simple criterion, known as Routh's stability criterion, enables us to determine the number of closed-loop poles that lie in the right-half s plane without having to factor the polynomial.

Routh's stability criterion. Routh's stability criterion tells us whether or not there are unstable roots in a polynomial equation without actually solving for them. This stability criterion applies to polynomials with only a finite number of terms. When the criterion is applied to a control system, information about absolute stability can be obtained directly from the coefficients of the characteristic equation.

The procedure in Routh's stability criterion is as follows:

1. Write the polynomial in s in the following form:

$$a_0 s^n + a_1 s^{n-1} + \cdots + a_{n-1}s + a_n = 0 \tag{5–6}$$

where the coefficients are real quantities. We assume that $a_n \neq 0$; that is, any zero root has been removed.

2. If any of the coefficients are zero or negative in the presence of at least one positive coefficient, there is a root or roots that are imaginary or that have positive real parts.

Therefore, in such a case, the system is not stable. If we are interested in only the absolute stability, there is no need to follow the procedure further. Note that all the coefficients must be positive. This is a necessary condition, as may be seen from the following argument: A polynomial in s having real coefficients can always be factored into linear and quadratic factors, such as $(s + a)$ and $(s^2 + bs + c)$, where a, b, and c are real. The linear factors yield real roots and the quadratic factors yield complex roots of the polynomial. The factor $(s^2 + bs + c)$ yields roots having negative real parts only if b and c are both positive. For all roots to have negative real parts, the constants a, b, c, and so on, in all factors must be positive. The product of any number of linear and quadratic factors containing only positive coefficients always yields a polynomial with positive coefficients. It is important to note that the condition that all the coefficients be positive is not sufficient to assure stability. The necessary but not sufficient condition for stability is that the coefficients of Equation (5–6) all be present and all have a positive sign. (If all a's are negative, they can be made positive by multiplying both sides of the equation by -1.)

3. If all coefficients are positive, arrange the coefficients of the polynomial in rows and columns according to the following pattern:

s^n	a_0	a_2	a_4	a_6	.	.	.
s^{n-1}	a_1	a_3	a_5	a_7	.	.	.
s^{n-2}	b_1	b_2	b_3	b_4	.	.	.
s^{n-3}	c_1	c_2	c_3	c_4	.	.	.
s^{n-4}	d_1	d_2	d_3	d_4	.	.	.
.	.	.					
.	.	.					
.	.	.					
s^2	e_1	e_2					
s^1	f_1						
s^0	g_1						

The coefficients b_1, b_2, b_3, and so on, are evaluated as follows:

$$b_1 = \frac{a_1 a_2 - a_0 a_3}{a_1}$$

$$b_2 = \frac{a_1 a_4 - a_0 a_5}{a_1}$$

$$b_3 = \frac{a_1 a_6 - a_0 a_7}{a_1}$$

.
.
.

The evaluation of the b's is continued until the remaining ones are all zero. The same pattern of cross-multiplying the coefficients of the two previous rows is followed in evaluating the c's, d's, e's, and so on. That is,

$$c_1 = \frac{b_1 a_3 - a_1 b_2}{b_1}$$

$$c_2 = \frac{b_1 a_5 - a_1 b_3}{b_1}$$

$$c_3 = \frac{b_1 a_7 - a_1 b_4}{b_1}$$

.
.
.

and

$$d_1 = \frac{c_1 b_2 - b_1 c_2}{c_1}$$

$$d_2 = \frac{c_1 b_3 - b_1 c_3}{c_1}$$

.
.
.

This process is continued until the nth row has been completed. The complete array of coefficients is triangular. Note that in developing the array an entire row may be divided or multiplied by a positive number in order to simplify the subsequent numerical calculation without altering the stability conclusion.

Routh's stability criterion states that the number of roots of Equation (5–6) with positive real parts is equal to the number of changes in sign of the coefficients of the first column of the array. It should be noted that the exact values of the terms in the first column need not be known; instead, only the signs are needed. The necessary and sufficient condition that all roots of Equation (5–6) lie in the left-half s plane is that all the coefficients of Equation (5–6) be positive and all terms in the first column of the array have positive signs.

EXAMPLE 5–1 Let us apply Routh's stability criterion to the following third-order polynomial:

$$a_0 s^3 + a_1 s^2 + a_2 s + a_3 = 0$$

where all the coefficients are positive numbers. The array of coefficients becomes

s^3	a_0	a_2
s^2	a_1	a_3
s^1	$\dfrac{a_1 a_2 - a_0 a_3}{a_1}$	
s^0	a_3	

The condition that all roots have negative real parts is given by

$$a_1 a_2 > a_0 a_3$$

EXAMPLE 5–2 Consider the following polynomial:

$$s^4 + 2s^3 + 3s^2 + 4s + 5 = 0$$

Let us follow the procedure just presented and construct the array of coefficients. (The first two rows can be obtained directly from the given polynomial. The remaining terms are obtained from these. If any coefficients are missing, they may be replaced by zeros in the array.)

s^4	1	3	5	s^4	1	3	5	
s^3	2	4	0	s^3	2	4	0	The second row is divided by 2.
					1	2	0	
s^2	1	5		s^2	1	5		
s^1	−6			s^1	−3			
s_0	5			s^0	5			

In this example, the number of changes in sign of the coefficients in the first column is 2. This means that there are two roots with positive real parts. Note that the result is unchanged when the coefficients of any row are multiplied or divided by a positive number in order to simplify the computation.

Special cases. If a first-column term in any row is zero, but the remaining terms are not zero or there is no remaining term, then the zero term is replaced by a very small positive number ϵ and the rest of the array is evaluated. For example, consider the following equation:

$$s^3 + 2s^2 + s + 2 = 0 \tag{5–7}$$

The array of coefficients is

s^3	1	1
s^2	2	2
s^1	$0 \approx \epsilon$	
s^0	2	

If the sign of the coefficient above the zero (ϵ) is the same as that below it, it indicates that there are a pair of imaginary roots. Actually, Equation (5–7) has two roots at $s = \pm j$.

If, however, the sign of the coefficient above the zero (ϵ) is opposite that below it, it indicates that there is one sign change. For example, for the equation

$$s^3 - 3s + 2 = (s - 1)^2(s + 2) = 0$$

the array of coefficients is

	s^3	1	−3
One sign change:	s^2	$0 \approx \epsilon$	2
One sign change:	s^1	$-3 - \frac{2}{\epsilon}$	
	s^0	2	

There are two sign changes of the coefficients in the first column. This agrees with the correct result indicated by the factored form of the polynomial equation.

If all the coefficients in any derived row are zero, it indicates that there are roots of equal magnitude lying radially opposite in the s plane, that is, two real roots with equal magnitudes and opposite signs and/or two conjugate imaginary roots. In such a case, the evaluation of the rest of the array can be continued by forming an auxiliary polynomial

with the coefficients of the last row and by using the coefficients of the derivative of this polynomial in the next row. Such roots with equal magnitudes and lying radially opposite in the s plane can be found by solving the auxiliary polynomial, which is always even. For a $2n$-degree auxiliary polynomial, there are n pairs of equal and opposite roots. For example, consider the following equation:

$$s^5 + 2s^4 + 24s^3 + 48s^2 - 25s - 50 = 0$$

The array of coefficients is

s^5	1	24	−25	
s^4	2	48	−50	←Auxiliary polynomial $P(s)$
s^3	0	0		

The terms in the s^3 row are all zero. The auxiliary polynomial is then formed from the coefficients of the s^4 row. The auxiliary polynomial $P(s)$ is

$$P(s) = 2s^4 + 48s^2 - 50$$

which indicates that there are two pairs of roots of equal magnitude and opposite sign. These pairs are obtained by solving the auxiliary polynomial equation $P(s) = 0$. The derivative of $P(s)$ with respect to s is

$$\frac{dP(s)}{ds} = 8s^3 + 96s$$

The terms in the s^3 row are replaced by the coefficients of the last equation, that is, 8 and 96. The array of coefficients then becomes

s^5	1	24	−25	
s^4	2	48	−50	
s^3	8	96		←Coefficients of $dP(s)/ds$
s^2	24	−50		
s^1	112.7	0		
s^0	−50			

We see that there is one change in sign in the first column of the new array. Thus, the original equation has one root with a positive real part. By solving for roots of the auxiliary polynomial equation,

$$2s^4 + 48s^2 - 50 = 0$$

we obtain

$$s^2 = 1, \qquad s^2 = -25$$

or

$$s = \pm 1, \qquad s = \pm j5$$

These two pairs of roots are a part of the roots of the original equation. As a matter of fact, the original equation can be written in factored form as follows:

$$(s + 1)(s - 1)(s + j5)(s - j5)(s + 2) = 0$$

Clearly, the original equation has one root with a positive real part.

Relative stability analysis. Routh's stability criterion provides the answer to the question of absolute stability. This, in many practical cases, is not sufficient. We usually require information about the relative stability of the system. A useful approach for examining relative stability is to shift the s-plane axis and apply Routh's stability criterion. That is, we substitute

$$s = \hat{s} - \sigma \qquad (\sigma = \text{constant})$$

into the characteristic equation of the system, write the polynomial in terms of $\hat{s}$, and apply Routh's stability criterion to the new polynomial in $\hat{s}$. The number of changes of sign in the first column of the array developed for the polynomial in $\hat{s}$ is equal to the number of roots that are located to the right of the vertical line $s = -\sigma$. Thus, this test reveals the number of roots that lie to the right of the vertical line $s = -\sigma$.

Application of Routh's stability criterion to control system analysis. Routh's stability criterion is of limited usefulness in linear control system analysis mainly because it does not suggest how to improve relative stability or how to stabilize an unstable system. It is possible, however, to determine the effects of changing one or two parameters of a system by examining the values that cause instability. In the following, we shall consider the problem of determining the stability range of a parameter value.

Consider the system shown in Figure 5–24. Let us determine the range of K for stability. The closed-loop transfer function is

$$\frac{C(s)}{R(s)} = \frac{K}{s(s^2 + s + 1)(s + 2) + K}$$

The characteristic equation is

$$s^4 + 3s^3 + 3s^2 + 2s + K = 0$$

The array of coefficients becomes

s^4	1	3	K
s^3	3	2	0
s^2	$\frac{7}{3}$	K	
s^1	$2 - \frac{9}{7}K$		
s^0	K		

For stability, K must be positive, and all coefficients in the first column must be positive. Therefore,

$$\tfrac{14}{9} > K > 0$$

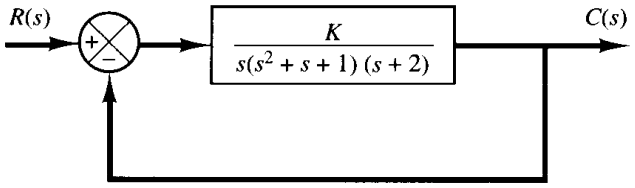

Figure 5–24
Control system.

When $K = \frac{14}{9}$, the system becomes oscillatory and, mathematically, the oscillation is sustained at constant amplitude.

5–6 PNEUMATIC CONTROLLERS

As the most versatile medium for transmitting signals and power, fluids, either as liquids or gases, have wide usage in industry. Liquids and gases can be distinguished basically by their relative incompressibilities and the fact that a liquid may have a free surface, whereas a gas expands to fill its vessel. In the engineering field the term *pneumatic* describes fluid systems that use air or gases and *hydraulic* applies to those using oil.

Pneumatic systems are extensively used in the automation of production machinery and in the field of automatic controllers. For instance, pneumatic circuits that convert the energy of compressed air into mechanical energy enjoy wide usage, and various types of pneumatic controllers are found in industry.

Since pneumatic systems and hydraulic systems are often compared, in what follows we shall give a brief comparison of these two kinds of systems.

Comparison between pneumatic systems and hydraulic systems. The fluid generally found in pneumatic systems is air; in hydraulic systems it is oil. And it is primarily the different properties of the fluids involved that characterize the differences between the two systems. These differences can be listed as follows:

1. Air and gases are compressible, whereas oil is incompressible.
2. Air lacks lubricating property and always contains water vapor. Oil functions as a hydraulic fluid as well as a lubricator.
3. The normal operating pressure of pneumatic systems is very much lower than that of hydraulic systems.
4. Output powers of pneumatic systems are considerably less than those of hydraulic systems.
5. Accuracy of pneumatic actuators is poor at low velocities, whereas accuracy of hydraulic actuators may be made satisfactory at all velocities.
6. In pneumatic systems, external leakage is permissible to a certain extent, but internal leakage must be avoided because the effective pressure difference is rather small. In hydraulic systems internal leakage is permissible to a certain extent, but external leakage must be avoided.
7. No return pipes are required in pneumatic systems when air is used, whereas they are always needed in hydraulic systems.
8. Normal operating temperature for pneumatic systems is 5° to 60°C (41° to 140°F). The pneumatic system, however, can be operated in the 0° to 200°C (32° to 392°F) range. Pneumatic systems are insensitive to temperature changes, in contrast to hydraulic systems, in which fluid friction due to viscosity depends greatly on temperature. Normal operating temperature for hydraulic systems is 20° to 70°C(68° to 158°F).
9. Pneumatic systems are fire- and explosion-proof, whereas hydraulic systems are not.

In what follows we begin with a mathematical modeling of pneumatic systems. Then we shall present pneumatic proportional controllers. We shall illustrate the fact that

proportional controllers utilize the principle of negative feedback in themselves. We shall give a detailed discussion of the principle by which proportional controllers operate. Finally, we shall treat methods for obtaining derivative and integral control actions. Throughout the discussions, we shall place emphasis on the fundamental principles, rather than on the details of the operation of the actual mechanisms.

Pneumatic systems. The past decades have seen a great development in low-pressure pneumatic controllers for industrial control systems, and today they are used extensively in industrial processes. Reasons for their broad appeal include an explosion-proof character, simplicity, and ease of maintenance.

Resistance and capacitance of pressure systems. Many industrial processes and pneumatic controllers involve the flow of a gas or air through connected pipelines and pressure vessels.

Consider the pressure system shown in Figure 5–25(a). The gas flow through the restriction is a function of the gas pressure difference $p_i - p_o$. Such a pressure system may be characterized in terms of a resistance and a capacitance.

The gas flow resistance R may be defined as follows:

$$R = \frac{\text{change in gas pressure difference, lb}_f/\text{ft}^2}{\text{change in gas flow rate, lb/sec}}$$

or

$$R = \frac{d(\Delta P)}{dq} \tag{5–8}$$

where $d(\Delta P)$ is a small change in the gas pressure difference and dq is a small change in the gas flow rate. Computation of the value of the gas flow resistance R may be quite time consuming. Experimentally, however, it can be easily determined from a plot of the pressure difference versus flow rate by calculating the slope of the curve at a given operating condition, as shown in Figure 5–25(b).

The capacitance of the pressure vessel may be defined by

$$C = \frac{\text{change in gas stored, lb}}{\text{change in gas pressure, lb}_f/\text{ft}^2}$$

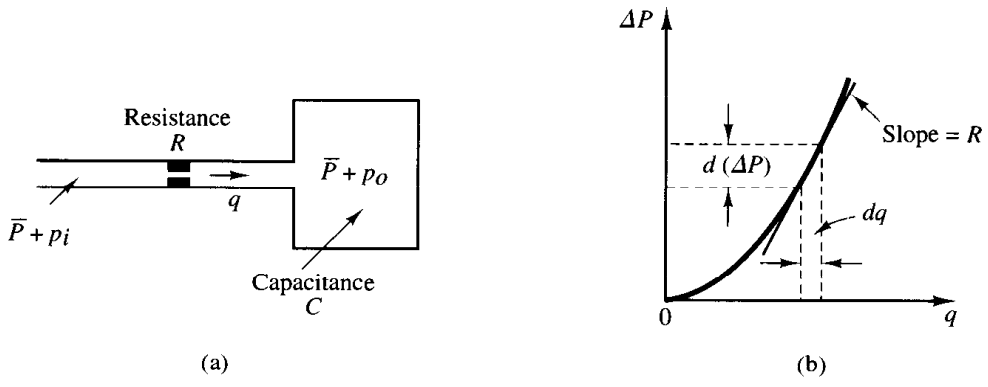

Figure 5–25
(a) Schematic diagram of a pressure system; (b) pressure difference versus flow rate curve.

or

$$C = \frac{dm}{dp} = V\frac{d\rho}{dp} \tag{5–9}$$

where C = capacitance, lb-ft^2/lb$_f$
m = mass of gas in vessel, lb
p = gas pressure, lb$_f$/ft^2
V = volume of vessel, ft^3
ρ = density, lb/ft^3

The capacitance of the pressure system depends on the type of expansion process involved. The capacitance can be calculated by use of the ideal gas law. If the gas expansion process is polytropic and the change of state of the gas is between isothermal and adiabatic, then

$$p\left(\frac{V}{m}\right)^n = \frac{p}{\rho^n} = \text{constant} \tag{5–10}$$

where n = polytropic exponent.

For ideal gases,

$$p\bar{v} = \bar{R}T \qquad \text{or} \qquad pv = \frac{\bar{R}}{M}T$$

where p = absolute pressure, lb$_f$/ft^2
$\bar{v}$ = volume occupied by 1 mole of a gas, ft^3/lb-mole
$\bar{R}$ = universal gas constant, ft-lb$_f$/lb-mole °R
T = absolute temperature, °R
v = specific volume of gas, ft^3/lb
M = molecular weight of gas per mole, lb/lb-mole

Thus

$$pv = \frac{p}{\rho} = \frac{\bar{R}}{M}T = R_{\text{gas}}T \tag{5–11}$$

where R_{gas} = gas constant, ft-lb$_f$/lb °R.

The polytropic exponent n is unity for isothermal expansion. For adiabatic expansion, n is equal to the ratio of specific heats c_p/c_v, where c_p is the specific heat at constant pressure and c_v is the specific heat at constant volume. In many practical cases, the value of n is approximately constant, and thus the capacitance may be considered constant. The value of $d\rho/dp$ is obtained from Equations (5–10) and (5–11) as

$$\frac{d\rho}{dp} = \frac{1}{nR_{\text{gas}}T}$$

The capacitance is then obtained as

$$C = \frac{V}{nR_{\text{gas}}T} \tag{5–12}$$

The capacitance of a given vessel is constant if the temperature stays constant. (In many practical cases, the polytropic exponent n is approximately $1.0 \sim 1.2$ for gases in uninsulated metal vessels.)

Pressure systems. Consider the system shown in Figure 5–25(a). If we assume only small deviations in the variables from their respective steady-state values, then this system may be considered linear.

Let us define

$\bar{P}$ = gas pressure in the vessel at steady state (before changes in pressure have occurred), lb_f/ft^2

p_i = small change in inflow gas pressure, lb_f/ft^2

p_o = small change in gas pressure in the vessel, lb_f/ft^2

V = volume of the vessel, ft^3

m = mass of gas in vessel, lb

q = gas flow rate, lb/sec

ρ = density of gas, lb/ft^3

For small values of p_i and p_o, the resistance R given by Equation (5–8) becomes constant and may be written as

$$R = \frac{p_i - p_o}{q}$$

The capacitance C is given by Equation (5–9), or

$$C = \frac{dm}{dp}$$

Since the pressure change dp_o times the capacitance C is equal to the gas added to the vessel during dt seconds, we obtain

$$C\,dp_o = q\,dt$$

or

$$C\frac{dp_o}{dt} = \frac{p_i - p_o}{R}$$

which can be written as

$$RC\frac{dp_o}{dt} + p_o = p_i$$

If p_i and p_o are considered the input and output, respectively, then the transfer function of the system is

$$\frac{P_o(s)}{P_i(s)} = \frac{1}{RCs + 1}$$

where RC has the dimension of time and is the time constant of the system.

Pneumatic nozzle–flapper amplifiers. A schematic diagram of a pneumatic nozzle–flapper amplifier is shown in Figure 5–26(a). The power source for this amplifier is a supply of air at constant pressure. The nozzle–flapper amplifier converts small changes in the position of the flapper into large changes in the back pressure in the nozzle. Thus a large power output can be controlled by the very little power that is needed to position the flapper.

In Figure 5–26(a), pressurized air is fed through the orifice, and the air is ejected from the nozzle toward the flapper. Generally, the supply pressure P_s for such a controller is 20 psig (1.4 kg_f/cm^2 gage). The diameter of the orifice is on the order of 0.01 in. (0.25 mm) and that of the nozzle is on the order of 0.016 in. (0.4 mm). To ensure proper functioning of the amplifier, the nozzle diameter must be larger than the orifice diameter.

In operating this system, the flapper is positioned against the nozzle opening. The nozzle back pressure P_b is controlled by the nozzle–flapper distance X. As the flapper approaches the nozzle, the opposition to the flow of air through the nozzle increases, with the result that the nozzle back pressure P_b increases. If the nozzle is completely closed by the flapper, the nozzle back pressure P_b becomes equal to the supply pressure P_s. If the flapper is moved away from the nozzle, so that the nozzle–flapper distance is wide (on the order of 0.01 in.), then there is practically no restriction to flow, and the nozzle back pressure P_b takes on a minimum value that depends on the nozzle–flapper device. (The lowest possible pressure will be the ambient pressure P_a.)

Note that, because the air jet puts a force against the flapper, it is necessary to make the nozzle diameter as small as possible.

A typical curve relating the nozzle back pressure P_b to the nozzle–flapper distance X is shown in Figure 5–26(b). The steep and almost linear part of the curve is utilized in the actual operation of the nozzle–flapper amplifier. Because the range of flapper displacements is restricted to a small value, the change in output pressure is also small, unless the curve is very steep.

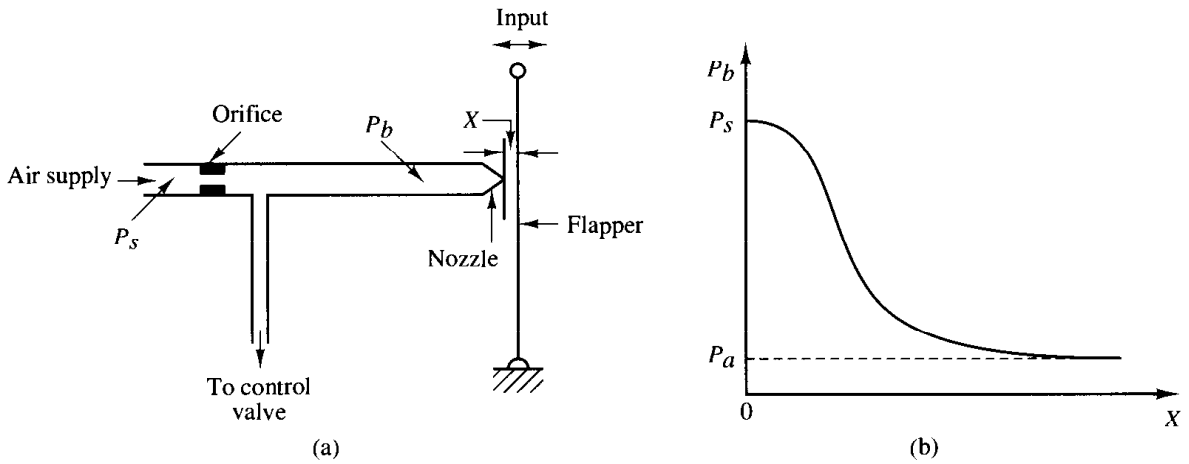

Figure 5–26
(a) Schematic diagram of a pneumatic nozzle–flapper amplifier; (b) characteristic curve relating nozzle back pressure and nozzle–flapper distance.

The nozzle–flapper amplifier converts displacement into a pressure signal. Since industrial process control systems require large output power to operate large pneumatic actuating valves, the power amplification of the nozzle–flapper amplifier is usually insufficient. Consequently, a pneumatic relay often serves as a power amplifier in connection with the nozzle–flapper amplifier.

Pneumatic relays. In practice, in a pneumatic controller, a nozzle–flapper amplifier acts as the first-stage amplifier and a pneumatic relay as the second-stage amplifier. The pneumatic relay is capable of handling a large quantity of airflow.

A schematic diagram of a pneumatic relay is shown in Figure 5–27(a). As the nozzle back pressure P_b increases, the diaphragm valve moves downward. The opening to the atmosphere decreases and the opening to the pneumatic valve increases, thereby increasing the control pressure P_c. When the diaphragm valve closes the opening to the atmosphere, the control pressure P_c becomes equal to the supply pressure P_s. When the nozzle back pressure P_b decreases and the diaphragm valve moves upward and shuts off the air supply, the control pressure P_c drops to the ambient pressure P_a. The control pressure P_c can thus be made to vary from 0 psig to full supply pressure, usually 20 psig.

The total movement of the diaphragm valve is very small. In all positions of the valve, except at the position to shut off the air supply, air continues to bleed into the atmosphere, even after the equilibrium condition is attained between the nozzle back pressure and the control pressure. Thus the relay shown in Figure 5–27(a) is called a bleed-type relay.

There is another type of relay, the nonbleed type. In this one the air bleed stops when the equilibrium condition is obtained and, therefore, there is no loss of pressurized air at steady-state operation. Note, however, that the nonbleed-type relay must have an atmospheric relief to release the control pressure P_c from the pneumatic actuating valve. A schematic diagram of a nonbleed-type relay is shown in Figure 5–27(b).

In either type of relay, the air supply is controlled by a valve, which is in turn controlled by the nozzle back pressure. Thus, the nozzle back pressure is converted into the control pressure with power amplification.

Since the control pressure P_c changes almost instantaneously with changes in the nozzle back pressure P_b, the time constant of the pneumatic relay is negligible compared with the other larger time constants of the pneumatic controller and the plant.

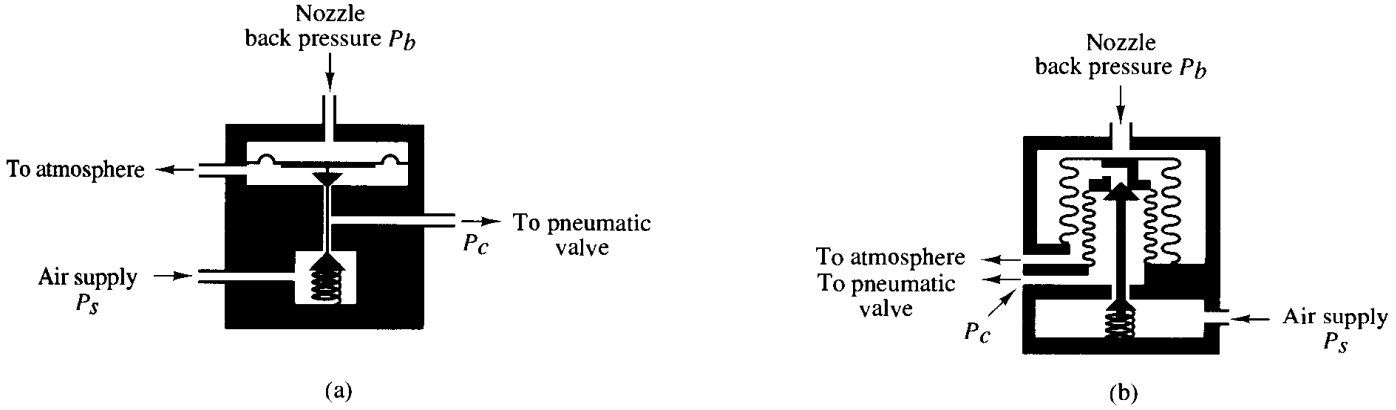

Figure 5–27
(a) Schematic diagram of a bleed-type relay; (b) schematic diagram of a nonbleed-type relay.

It is noted that some pneumatic relays are reverse acting. For example, the relay shown in Figure 5–28 is a reverse-acting relay. Here, as the nozzle back pressure P_b increases, the ball valve is forced toward the lower seat, thereby decreasing the control pressure P_c. Thus, this relay is a reverse-acting relay.

Pneumatic proportional controllers (force–distance type). Two types of pneumatic controllers, one called the force–distance type and the other the force–balance type, are used extensively in industry. Regardless of how differently industrial pneumatic controllers may appear, careful study will show the close similarity in the functions of the pneumatic circuit. Here we shall consider the force–distance type of pneumatic controllers.

Figure 5–29(a) shows a schematic diagram of such a proportional controller. The nozzle–flapper amplifier constitutes the first-stage amplifier, and the nozzle back pressure is controlled by the nozzle–flapper distance. The relay-type amplifier constitutes the second-stage amplifier. The nozzle back pressure determines the position of the diaphragm valve for the second-stage amplifier, which is capable of handling a large quantity of airflow.

In most pneumatic controllers, some type of pneumatic feedback is employed. Feedback of the pneumatic output reduces the amount of actual movement of the flapper. Instead of mounting the flapper on a fixed point, as shown in Figure 5–29(b), it is often pivoted on the feedback bellows, as shown in Figure 5–29(c). The amount of feedback can be regulated by introducing a variable linkage between the feedback bellows and the flapper connecting point. The flapper then becomes a floating link. It can be moved by both the error signal and the feedback signal.

The operation of the controller shown in Figure 5–29(a) is as follows. The input signal to the two-stage pneumatic amplifier is the actuating error signal. Increasing the actuating error signal moves the flapper to the left. This move will, in turn, increase the nozzle back pressure, and the diaphragm valve moves downward. This results in an increase of the control pressure. This increase will cause bellows F to expand and move the flapper to the right, thus opening the nozzle. Because of this feedback, the nozzle–flapper displacement is very small, but the change in the control pressure can be large.

It should be noted that proper operation of the controller requires that the feedback bellows move the flapper less than that movement caused by the error signal alone. (If these two movements were equal, no control action would result.)

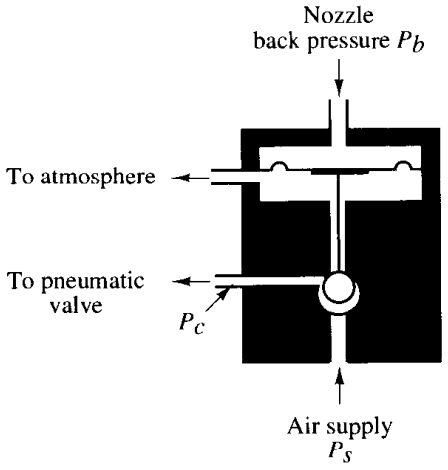

Figure 5–28
Reverse-acting relay.

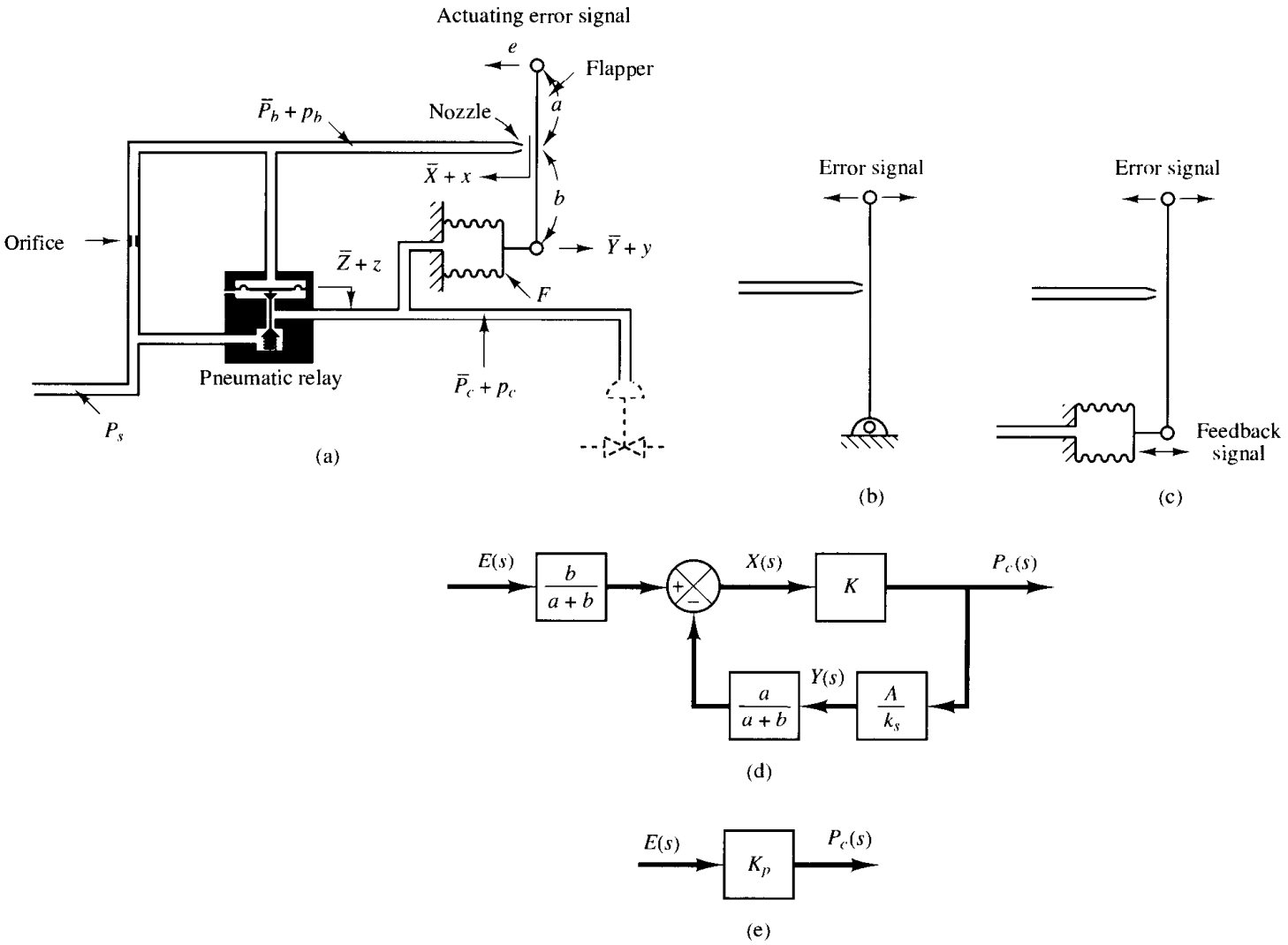

Figure 5–29
(a) Schematic diagram of a force–distance type of pneumatic proportional controller; (b) flapper mounted on a fixed point; (c) flapper mounted on a feedback bellows; (d) block diagram for the controller; (e) simplified block diagram for the controller.

Equations for this controller can be derived as follows. When the actuating error is zero, or $e = 0$, an equilibrium state exists with the nozzle–flapper distance equal to $\bar{X}$, the displacement of bellows equal to $\bar{Y}$, the displacement of the diaphragm equal to $\bar{Z}$, the nozzle back pressure equal to $\bar{P}_b$, and the control pressure equal to $\bar{P}_c$. When an actuating error exists, the nozzle–flapper distance, the displacement of the bellows, the displacement of the diaphragm, the nozzle back pressure, and the control pressure deviate from their respective equilibrium values. Let these deviations be x, y, z, p_b, and p_c, respectively. (The positive direction for each displacement variable is indicated by an arrowhead in the diagram.)

Assuming that the relationship between the variation in the nozzle back pressure and the variation in the nozzle–flapper distance is linear, we have

$$p_b = K_1 x \tag{5–13}$$

where K_1 is a positive constant. For the diaphragm valve,

$$p_b = K_2 z \tag{5–14}$$

where K_2 is a positive constant. The position of the diaphragm valve determines the control pressure. If the diaphragm valve is such that the relationship between p_c and z is linear, then

$$p_c = K_3 z \tag{5–15}$$

where K_3 is a positive constant. From Equations (5–13), (5–14), and (5–15), we obtain

$$p_c = \frac{K_3}{K_2} p_b = Kx \tag{5–16}$$

where $K = K_1 K_3 / K_2$ is a positive constant. For the flapper movement, we have

$$x = \frac{b}{a + b} e - \frac{a}{a + b} y \tag{5–17}$$

The bellows acts like a spring, and the following equation holds true:

$$A p_c = k_s y \tag{5–18}$$

where A is the effective area of the bellows and k_s is the equivalent spring constant, that is, the stiffness due to the action of the corrugated side of the bellows.

Assuming that all variations in the variables are within a linear range, we can obtain a block diagram for this system from Equations (5–16), (5–17), and (5–18) as shown in Figure 5–29(d). From Figure 5–29(d), it can be clearly seen that the pneumatic controller shown in Figure 5–29(a) itself is a feedback system. The transfer function between p_c and e is given by

$$\frac{P_c(s)}{E(s)} = \frac{\dfrac{b}{a + b} K}{1 + K \dfrac{a}{a + b} \dfrac{A}{k_s}} = K_p \tag{5–19}$$

A simplified block diagram is shown in Figure 5–29(e). Since p_c and e are proportional, the pneumatic controller shown in Figure 5–29(a) is called a *pneumatic proportional controller*. As seen from Equation (5–19), the gain of the pneumatic proportional controller can be widely varied by adjusting the flapper connecting linkage. [The flapper connecting linkage is not shown in Figure 5–29(a).] In most commercial proportional controllers an adjusting knob or other mechanism is provided for varying the gain by adjusting this linkage.

As noted earlier, the actuating error signal moved the flapper in one direction, and the feedback bellows moved the flapper in the opposite direction, but to a smaller degree. The effect of the feedback bellows is thus to reduce the sensitivity of the controller. The principle of feedback is commonly used to obtain wide proportional-band controllers.

Pneumatic controllers that do not have feedback mechanisms [which means that one end of the flapper is fixed, as shown in Figure 5–30(a)] have high sensitivity and are called *pneumatic two-position controllers* or *pneumatic on–off controllers*. In such a controller, only a small motion between the nozzle and the flapper is required to give a com-

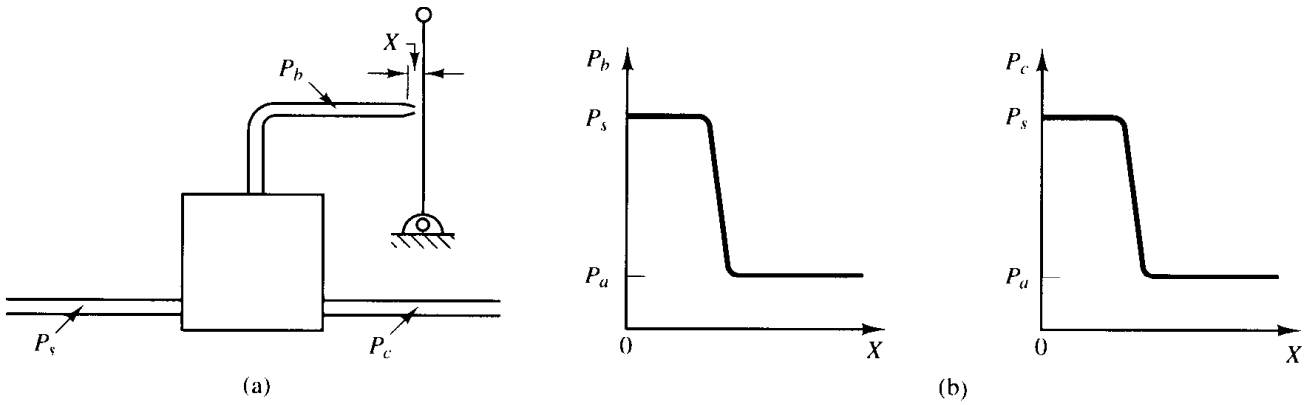

Figure 5–30
(a) Pneumatic controller without a feedback mechanism; (b) curves P_b versus X and P_c versus X.

plete change from the maximum to the minimum control pressure. The curves relating P_b to X and P_c to X are shown in Figure 5–30(b). Notice that a small change in X can cause a large change in P_b, which causes the diaphragm valve to be completely open or completely closed.

Pneumatic proportional controllers (force–balance type). Figure 5–31 shows a schematic diagram of a force–balance pneumatic proportional controller. Force–balance controllers are in extensive use in industry. Such controllers are called stack controllers. The basic principle of operation does not differ from that of the force–distance controller. The main advantage of the force–balance controller is that it eliminates many mechanical linkages and pivot joints, thereby reducing the effects of friction.

In what follows, we shall consider the principle of the force–balance controller. In the controller shown in Figure 5–31, the reference input pressure P_r and the output pressure P_o are fed to large diaphragm chambers. Note that a force-balance pneumatic controller operates only on pressure signals. Therefore, it is necessary to convert the reference input and system output to corresponding pressure signals.

As in the case of the force–distance controller, this controller employs a flapper, nozzle, and orifices. In Figure 5–31, the drilled opening in the bottom chamber is the nozzle. The diaphragm just above the nozzle acts as a flapper.

The operation of the force–balance controller shown in Figure 5–31 may be summarized as follows: 20-psig air from an air supply flows through an orifice, causing a reduced

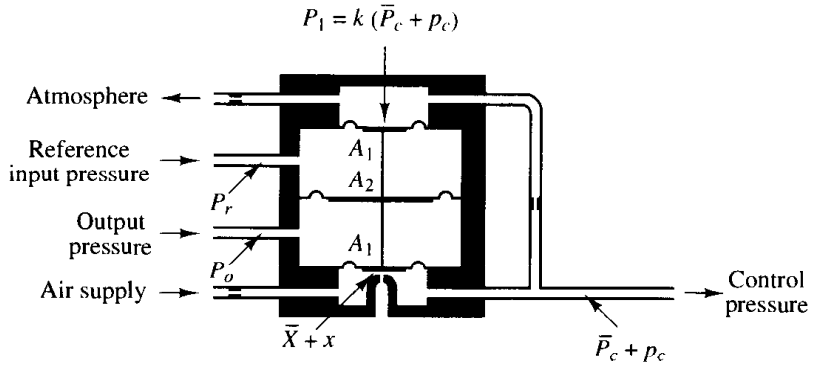

Figure 5–31
Schematic diagram of a force–balance type of pneumatic proportional controller.

pressure in the bottom chamber. Air in this chamber escapes to the atmosphere through the nozzle. The flow through the nozzle depends on the gap and the pressure drop across it. An increase in the reference input pressure P_r, while the output pressure P_o remains the same, causes the valve stem to move down, decreasing the gap between the nozzle and the flapper diaphragm. This causes the control pressure P_c to increase. Let

$$p_e = P_r - P_o \tag{5–20}$$

If $p_c = 0$, there is an equilibrium state with the nozzle–flapper distance equal to $\bar{X}$ and the control pressure equal to $\bar{P}_c$. At this equilibrium state, $P_1 = \bar{P}_c k$ (where $k < 1$) and

$$\bar{X} = \alpha(\bar{P}_c A_1 - \bar{P}_c k A_1) \tag{5–21}$$

where α is a constant.

Let us assume that $p_e \neq 0$ and define small variations in the nozzle–flapper distance and control pressure as x and p_c, respectively. Then we obtain the following equation:

$$\bar{X} + x = \alpha[(\bar{P}_c + p_c)A_1 - (\bar{P}_c + p_c)kA_1 - p_e(A_2 - A_1)] \tag{5–22}$$

From Equations (5–21) and (5–22), we obtain

$$x = \alpha[p_c(1 - k)A_1 - p_e(A_2 - A_1)] \tag{5–23}$$

At this point, we must examine the quantity x. In the design of pneumatic controllers, the nozzle–flapper distance is made quite small. In view of the fact that x/α is a higher-order term than $p_c(1 - k)A_1$ or $p_e(A_2 - A_1)$, that is, for $p_c \neq 0$,

$$\frac{x}{\alpha} \ll p_c(1 - k)A_1$$

$$\frac{x}{\alpha} \ll p_e(A_2 - A_1)$$

we may neglect the term x in our analysis. Equation (5–23) can then be rewritten to reflect this assumption as follows:

$$p_c(1 - k)A_1 = p_e(A_2 - A_1)$$

and the transfer function between p_c and p_e becomes

$$\frac{P_c(s)}{P_e(s)} = \frac{A_2 - A_1}{A_1}\frac{1}{1 - k} = K_p$$

where p_e is defined by Equation (5–20). The controller shown in Figure 5–31 is a proportional controller. The value of gain K_p increases as k approaches unity. Note that the value of k depends on the diameters of the orifices in the inlet and outlet pipes of the feedback chamber. (The value of k approaches unity as the resistance to flow in the orifice of the inlet pipe is made smaller.)

Pneumatic actuating valves. One characteristic of pneumatic controls is that they almost exclusively employ pneumatic actuating valves. A pneumatic actuating valve can provide a large power output. (Since a pneumatic actuator requires a large power input to produce a large power output, it is necessary that a sufficient quantity of pressurized air be available.) In practical pneumatic actuating valves, the valve char-

acteristics may not be linear; that is, the flow may not be directly proportional to the valve stem position, and also there may be other nonlinear effects, such as hysteresis.

Consider the schematic diagram of a pneumatic actuating valve shown in Figure 5–32. Assume that the area of the diaphragm is A. Assume also that when the actuating error is zero the control pressure is equal to $\bar{P}_c$ and the valve displacement is equal to $\bar{X}$.

In the following analysis, we shall consider small variations in the variables and linearize the pneumatic actuating valve. Let us define the small variation in the control pressure and the corresponding valve displacement to be p_c and x, respectively. Since a small change in the pneumatic pressure force applied to the diaphragm repositions the load, consisting of the spring, viscous friction, and mass, the force balance equation becomes

$$Ap_c = m\ddot{x} + b\dot{x} + kx \tag{5–24}$$

where m = mass of the valve and valve stem
b = viscous-friction coefficient
k = spring constant

If the force due to the mass and viscous friction are negligibly small, then Equation (5–24) can be simplified to:

$$Ap_c = kx$$

The transfer function between x and p_c thus becomes

$$\frac{X(s)}{P_c(s)} = \frac{A}{k} = K_c$$

where $X(s) = \mathcal{L}[x]$ and $P_c(s) = \mathcal{L}[p_c]$. If q_i, the change in flow through the pneumatic actuating valve, is proportional to x, the change in the valve-stem displacement, then

$$\frac{Q_i(s)}{X(s)} = K_q$$

where $Q_i(s) = \mathcal{L}[q_i]$ and K_q is a constant. The transfer function between q_i and p_c becomes

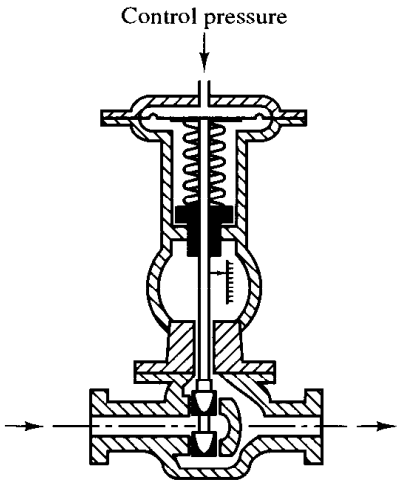

Figure 5–32
Schematic diagram of a pneumatic actuating valve.

$$\frac{Q_i(s)}{P_c(s)} = K_c K_q = K_v$$

where K_v is a constant.

The standard control pressure for this kind of a pneumatic actuating valve is between 3 and 15 psig. The valve-stem displacement is limited by the allowable stroke of the diaphragm and is only a few inches. If a longer stroke is needed, a piston–spring combination may be employed.

In pneumatic actuating valves, the static-friction force must be limited to a low value so that excessive hysteresis does not result. Because of the compressibility of air, the control action may not be positive; that is, an error may exist in the valve-stem position. The use of a valve positioner results in improvements in the performance of a pneumatic actuating valve.

Basic principle for obtaining derivative control action. We shall now present methods for obtaining derivative control action. We shall again place the emphasis on the principle and not on the details of the actual mechanisms.

The basic principle for generating a desired control action is to insert the inverse of the desired transfer function in the feedback path. For the system shown in Figure 5–33, the closed-loop transfer function is

$$\frac{C(s)}{R(s)} = \frac{G(s)}{1 + G(s)H(s)}$$

If $|G(s)H(s)| \gg 1$, then $C(s)/R(s)$ can be modified to

$$\frac{C(s)}{R(s)} = \frac{1}{H(s)}$$

Thus, if proportional-plus-derivative control action is desired, we insert an element having the transfer function $1/(Ts + 1)$ in the feedback path.

Consider the pneumatic controller shown in Figure 5–34(a). Considering small changes in the variables, we can draw a block diagram of this controller as shown in Figure 5–34(b). From the block diagram we see that the controller is of proportional type.

We shall now show that the addition of a restriction in the negative feedback path will modify the proportional controller to a proportional-plus-derivative controller, commonly called a PD controller.

Consider the pneumatic controller shown in Figure 5–35(a). Assuming again small changes in the actuating error, nozzle–flapper distance, and control pressure, we can

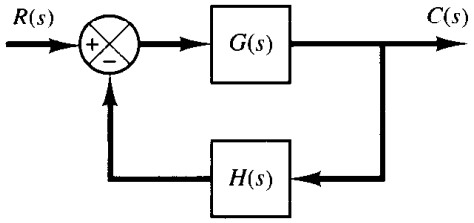

Figure 5–33
Control system.

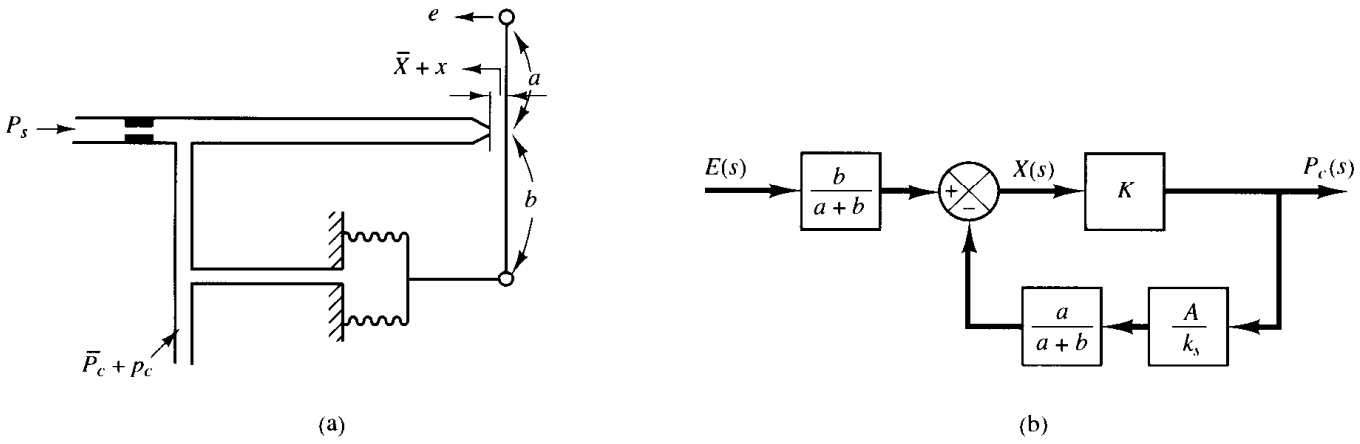

Figure 5–34
(a) Pneumatic proportional controller; (b) block diagram of the controller.

summarize the operation of this controller as follows: Let us first assume a small step change in e. Then the change in the control pressure p_c will be instantaneous. The restriction R will momentarily prevent the feedback bellows from sensing the pressure change p_c. Thus the feedback bellows will not respond momentarily, and the pneumatic actuating valve will feel the full effect of the movement of the flapper. As time goes on, the feedback bellows will expand or contract. The change in the nozzle-flapper distance x and the change in the control pressure p_c can be plotted against time t, as shown in Figure 5–35(b). At steady state, the feedback bellows acts like an ordinary feedback

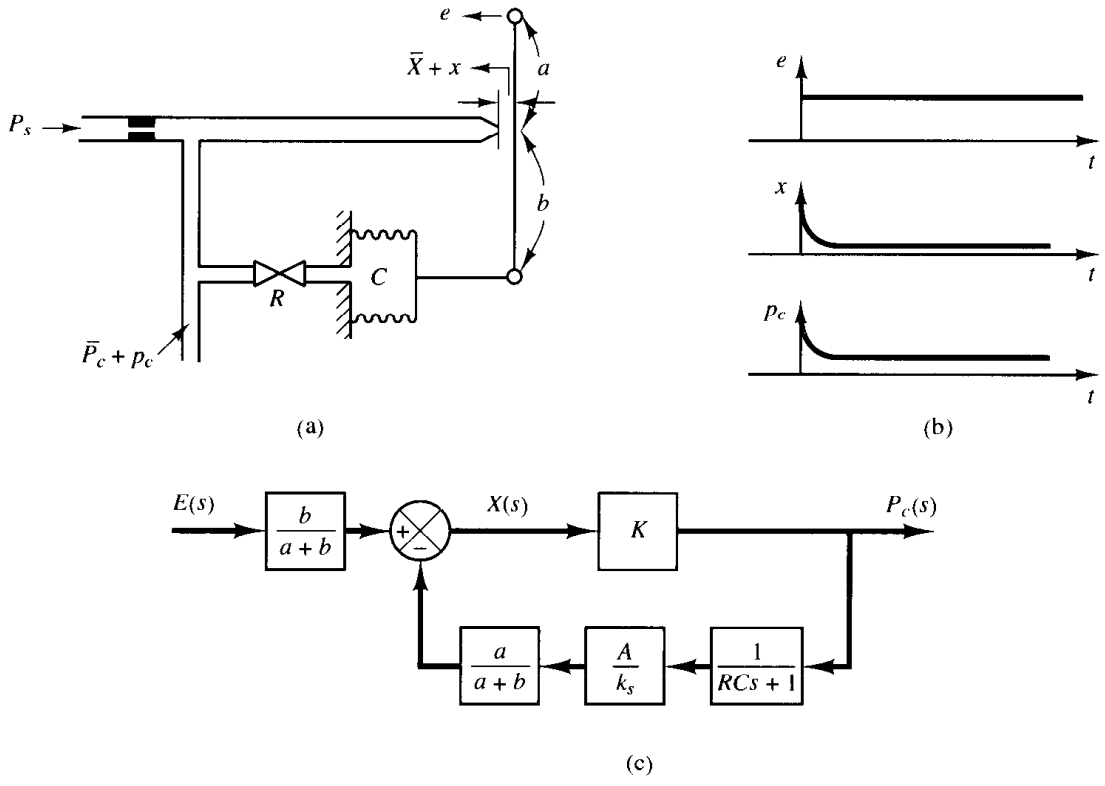

Figure 5–35
(a) Pneumatic proportional-plus-derivative controller; (b) step change in e and the corresponding changes in x and p_c plotted versus t; (c) block diagram of the controller.

mechanism. The curve p_c versus t clearly shows that this controller is of the proportional-plus-derivative type.

A block diagram corresponding to this pneumatic controller is shown in Figure 5–35(c). In the block diagram, K is a constant, A is the area of the bellows, and k_s is the equivalent spring constant of the bellows. The transfer function between p_c and e can be obtained from the block diagram as follows:

$$\frac{P_c(s)}{E(s)} = \frac{\dfrac{b}{a+b}K}{1 + \dfrac{Ka}{a+b}\dfrac{A}{k_s}\dfrac{1}{RCs+1}}$$

In such a controller the loop gain $|KaA/[(a + b)k_s(RCs + 1)]|$ is normally very much greater than unity. Thus the transfer function $P_c(s)/E(s)$ can be simplified to give

$$\frac{P_c(s)}{E(s)} = K_p(1 + T_d s)$$

where

$$K_p = \frac{bk_s}{aA}, \qquad T_d = RC$$

Thus, delayed negative feedback, or the transfer function $1/(RCs + 1)$ in the feedback path, modifies the proportional controller to a proportional-plus-derivative controller.

Note that if the feedback valve is fully opened the control action becomes proportional. If the feedback valve is fully closed, the control action becomes narrow-band proportional (on–off).

Obtaining pneumatic proportional-plus-integral control action. Consider the proportional controller shown in Figure 5–34(a). Considering small changes in the variables, we can show that the addition of delayed positive feedback will modify this proportional controller to a proportional-plus-integral controller, commonly called a PI controller.

Consider the pneumatic controller shown in Figure 5–36(a). The operation of this controller is as follows: The bellows denoted by I is connected to the control pressure source without any restriction. The bellows denoted by II is connected to the control pressure source through a restriction. Let us assume a small step change in the actuating error. This will cause the back pressure in the nozzle to change instantaneously. Thus a change in the control pressure p_c also occurs instantaneously. Due to the restriction of the valve in the path to bellows II, there will be a pressure drop across the valve. As time goes on, air will flow across the valve in such a way that the change in pressure in bellows II attains the value p_c. Thus bellows II will expand or contract as time elapses in such a way as to move the flapper an additional amount in the direction of the original

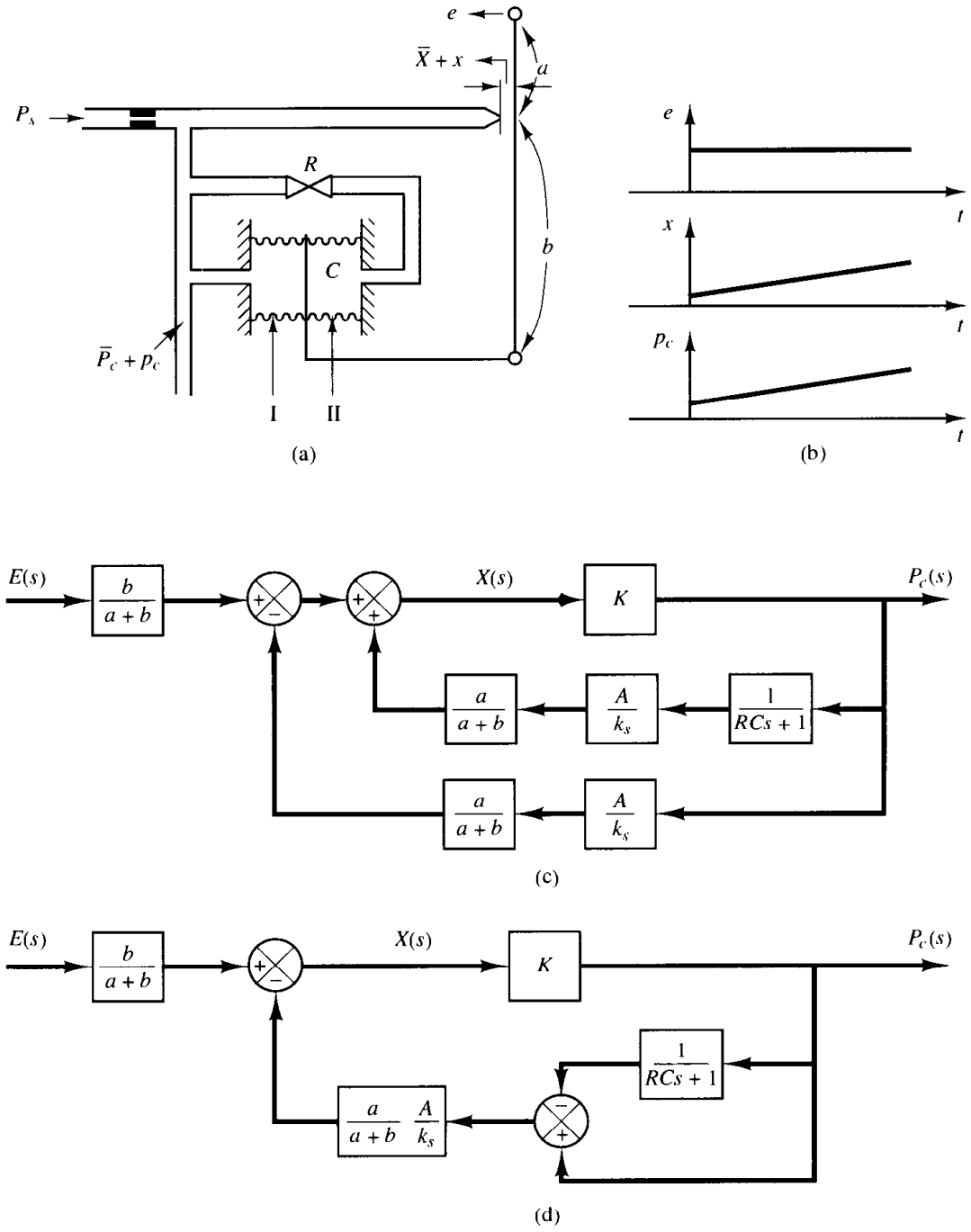

Figure 5–36
(a) Pneumatic proportional-plus-integral controller; (b) step change in e and the corresponding changes in x and p_c plotted versus t; (c) block diagram of the controller; (d) simplified block diagram.

displacement e. This will cause the back pressure p_c in the nozzle to change continuously, as shown in Figure 5–36(b).

Note that the integral control action in the controller takes the form of slowly canceling the feedback that the proportional control originally provided.

A block diagram of this controller under the assumption of small variations in the variables is shown in Figure 5–36(c). A simplification of this block diagram yields Figure 5–36(d). The transfer function of this controller is

$$\frac{P_c(s)}{E(s)} = \frac{\dfrac{b}{a+b}K}{1 + \dfrac{Ka}{a+b}\dfrac{A}{k_s}\left(1 - \dfrac{1}{RCs+1}\right)}$$

where K is a constant, A is the area of the bellows, and k_s is the equivalent spring constant of the combined bellows. If $\left|KaARCs/[(a+b)k_s(RCs+1)]\right| \gg 1$, which is usually the case, the transfer function can be simplified to

$$\frac{P_c(s)}{E(s)} = K_p\left(1 + \frac{1}{T_i s}\right)$$

where

$$K_p = \frac{bk_s}{aA}, \qquad T_i = RC$$

Obtaining pneumatic proportional-plus-integral-plus-derivative control action. A combination of the pneumatic controllers shown in Figures 5–35(a) and 5–36(a) yields a proportional-plus-integral-plus-derivative controller, commonly called a PID controller. Figure 5–37(a) shows a schematic diagram of such a controller. Figure 5–37(b) shows a block diagram of this controller under the assumption of small variations in the variables.

The transfer function of this controller is

$$\frac{P_c(s)}{E(s)} = \frac{\dfrac{bK}{a+b}}{1 + \dfrac{Ka}{a+b}\dfrac{A}{k_s}\dfrac{(R_iC - R_dC)s}{(R_dCs+1)(R_iCs+1)}}$$

By defining

$$T_i = R_iC, \qquad T_d = R_dC$$

and noting that under normal operation $\left|KaA(T_i - T_d)s/[(a+b)k_s(T_ds+1)(T_is+1)]\right| \gg 1$ and $T_i \gg T_d$, we obtain

$$\begin{aligned}\frac{P_c(s)}{E(s)} &\doteqdot \frac{bk_s}{aA}\frac{(T_ds+1)(T_is+1)}{(T_i - T_d)s} \\ &\doteqdot \frac{bk_s}{aA}\frac{T_dT_is^2 + T_is + 1}{T_is} \\ &= K_p\left(1 + \frac{1}{T_is} + T_ds\right)\end{aligned} \tag{5–25}$$

where

$$K_p = \frac{bk_s}{aA}$$

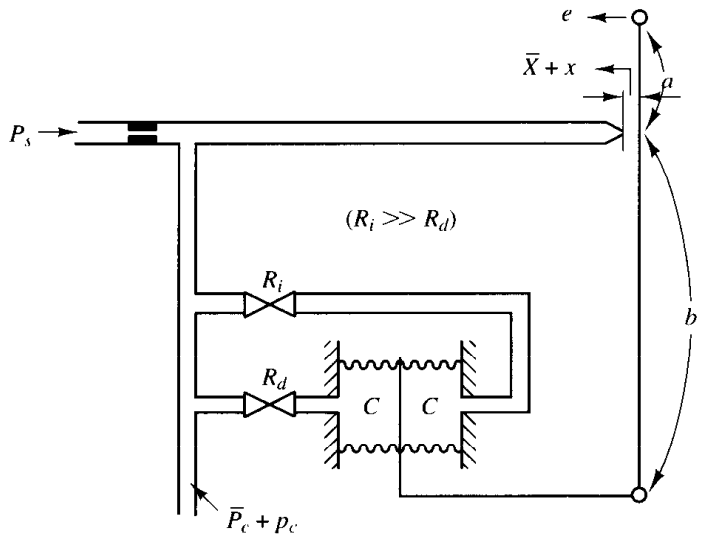

(a)

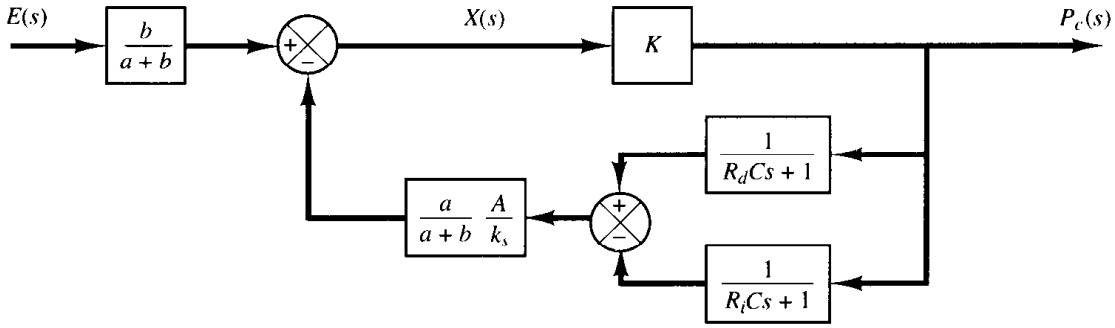

(b)

Figure 5–37
(a) Pneumatic proportional-plus-integral-plus-derivative controller; (b) block diagram of the controller.

Equation (5–25) indicates that the controller shown in Figure 5–37(a) is a proportional-plus-integral-plus-derivative controller (a PID controller).

5–7 HYDRAULIC CONTROLLERS

Except for low-pressure pneumatic controllers, compressed air has seldom been used for the continuous control of the motion of devices having significant mass under external load forces. For such a case, hydraulic controllers are generally preferred.

Hydraulic systems. The widespread use of hydraulic circuitry in machine tool applications, aircraft control systems, and similar operations occurs because of such factors as positiveness, accuracy, flexibility, high horsepower-to-weight ratio, fast starting, stopping, and reversal with smoothness and precision, and simplicity of operations.

The operating pressure in hydraulic systems is somewhere between 145 and 5000 $lb_f/in.^2$ (between 1 and 35 MPa). In some special applications, the operating pressure may go up to 10,000 $lb_f/in.^2$ (70 MPa). For the same power requirement, the weight and size of the hydraulic unit can be made smaller by increasing the supply pressure. With

high-pressure hydraulic systems, very large force can be obtained. Rapid-acting, accurate positioning of heavy loads is possible with hydraulic systems. A combination of electronic and hydraulic systems is widely used because it combines the advantages of both electronic control and hydraulic power.

Advantages and disadvantages of hydraulic systems. There are certain advantages and disadvantages in using hydraulic systems rather than other systems. Some of the advantages are the following:

1. Hydraulic fluid acts as a lubricant, in addition to carrying away heat generated in the system to a convenient heat exchanger.
2. Comparatively small sized hydraulic actuators can develop large forces or torques.
3. Hydraulic actuators have a higher speed of response with fast starts, stops, and speed reversals.
4. Hydraulic actuators can be operated under continuous, intermittent, reversing, and stalled conditions without damage.
5. Availability of both linear and rotary actuators gives flexibility in design.
6. Because of low leakages in hydraulic actuators, speed drop when loads are applied is small.

On the other hand, several disadvantages tend to limit their use.

1. Hydraulic power is not readily available compared to electric power.
2. Cost of a hydraulic system may be higher than a comparable electrical system performing a similar function.
3. Fire and explosion hazards exist unless fire-resistant fluids are used.
4. Because it is difficult to maintain a hydraulic system that is free from leaks, the system tends to be messy.
5. Contaminated oil may cause failure in the proper functioning of a hydraulic system.
6. As a result of the nonlinear and other complex characteristics involved, the design of sophisticated hydraulic systems is quite involved.
7. Hydraulic circuits have generally poor damping characteristics. If a hydraulic circuit is not designed properly, some unstable phenomena may occur or disappear, depending on the operating condition.

Comments. Particular attention is necessary to ensure that the hydraulic system is stable and satisfactory under all operating conditions. Since the viscosity of hydraulic fluid can greatly affect damping and friction effects of the hydraulic circuits, stability tests must be carried out at the highest possible operating temperature.

Note that most hydraulic systems are nonlinear. Sometimes, however, it is possible to linearize nonlinear systems so as to reduce their complexity and permit solutions that are sufficiently accurate for most purposes. A useful linearization technique for dealing with nonlinear systems was presented in Section 3–10.

Hydraulic integral controllers. The hydraulic servomotor shown in Figure 5–38 is essentially a pilot-valve-controlled hydraulic power amplifier and actuator. The pilot valve is a balanced valve in the sense that the pressure forces acting on it are all bal-

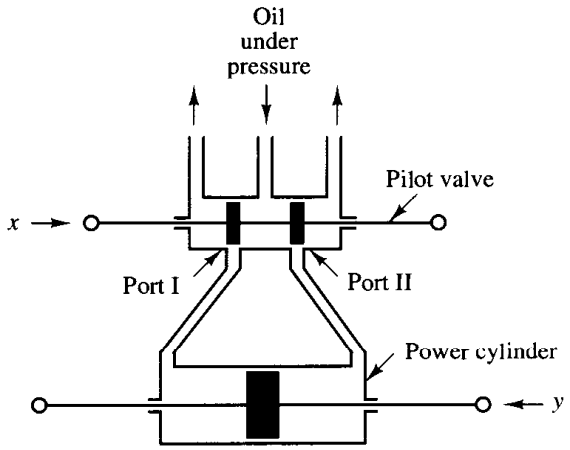

Figure 5–38
Hydraulic servomotor.

anced. A very large power output can be controlled by a pilot valve, which can be positioned with very little power.

It will be shown in the following that for negligibly small load mass the servomotor shown in Figure 5–38 acts as an integrator or an integral controller. Such a servomotor constitutes the basis of the hydraulic control circuit.

In the hydraulic servomotor shown in Figure 5–38, the pilot valve (a four-way valve) has two lands on the spool. If the width of the land is smaller than the port in the valve sleeve, the valve is said to be *underlapped. Overlapped* valves have a land width greater than the port width. A *zero-lapped* valve has a land width that is identical to the port width. (If the pilot valve is not a zero-lapped valve, analyses of hydraulic servomotors become very complicated.)

In the present analysis, we assume that hydraulic fluid is incompressible and that the inertia force of the power piston and load is negligible compared to the hydraulic force at the power piston. We also assume that the pilot valve is a zero-lapped valve, and the oil flow rate is proportional to the pilot valve displacement.

Operation of this hydraulic servomotor is as follows. If input x moves the pilot valve to the right, port II is uncovered, and so high-pressure oil enters the right side of the power piston. Since port I is connected to the drain port, the oil in the left side of the power piston is returned to the drain. The oil flowing into the power cylinder is at high pressure; the oil flowing out from the power cylinder into the drain is at low pressure. The resulting difference in pressure on both sides of the power piston will cause it to move to the left.

Note that the rate of flow of oil q (kg/sec) times dt (sec) is equal to the power piston displacement dy(m) times the piston area A(m^2) times the density of oil ρ (kg/m^3). Therefore,

$$A\rho\, dy = q\, dt \tag{5–26}$$

Because of the assumption that the oil flow rate q is proportional to the pilot valve displacement x, we have

$$q = K_1 x \tag{5–27}$$

where K_1 is a positive constant. From Equations (5–26) and (5–27) we obtain

$$A\rho \frac{dy}{dt} = K_1 x$$

The Laplace transform of this last equation, assuming a zero initial condition, gives

$$A\rho s Y(s) = K_1 X(s)$$

or

$$\frac{Y(s)}{X(s)} = \frac{K_1}{A\rho s} = \frac{K}{s}$$

where $K = K_1/(A\rho)$. Thus the hydraulic servomotor shown in Figure 5–38 acts as an integral controller.

Hydraulic proportional controllers. It has been shown that the servomotor in Figure 5–38 acts as an integral controller. This servomotor can be modified to a proportional controller by means of a feedback link. Consider the hydraulic controller shown in Figure 5–39(a). The left side of the pilot valve is joined to the left side of the power piston by a link ABC. This link is a floating link rather than one moving about a fixed pivot.

The controller here operates in the following way. If input e moves the pilot valve to the right, port II will be uncovered and high-pressure oil will flow through port II into the right side of the power piston and force this piston to the left. The power piston, in moving to the left, will carry the feedback link ABC with it, thereby moving the pilot valve to the left. This action continues until the pilot piston again covers ports I and II. A block diagram of the system can be drawn as in Figure 5–39(b). The transfer function between $Y(s)$ and $E(s)$ is given by

$$\frac{Y(s)}{E(s)} = \frac{\dfrac{b}{a+b}\dfrac{K}{s}}{1 + \dfrac{K}{s}\dfrac{a}{a+b}}$$

$$= \frac{bK}{s(a+b) + Ka}$$

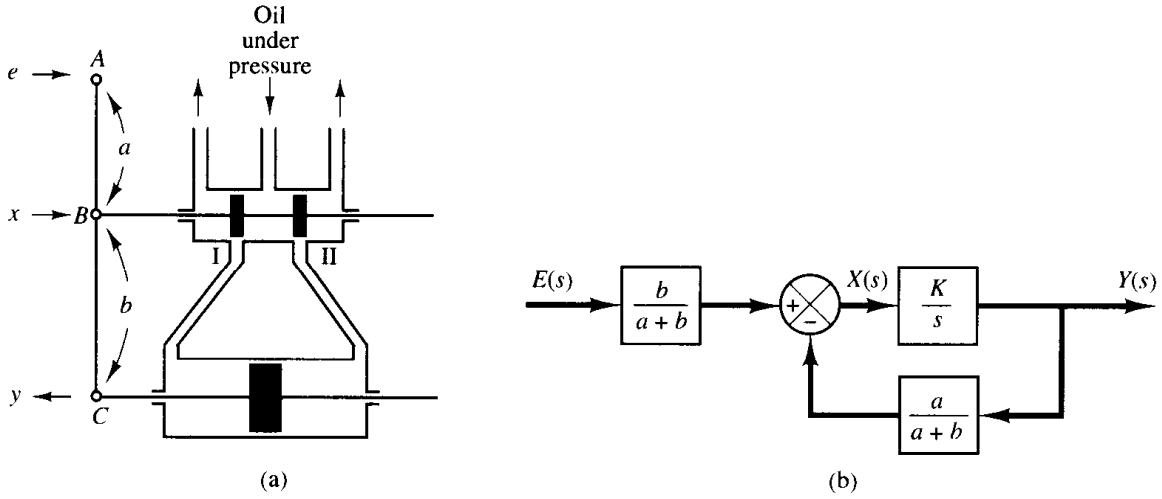

Figure 5–39
(a) Servomotor that acts as a proportional controller; (b) block diagram of the servomotor.

Noting that under the normal operating conditions we have $|Ka/[s(a + b)]| \gg 1$, this last equation can be simplified to

$$\frac{Y(s)}{E(s)} = \frac{b}{a} = K_p$$

The transfer function between y and e becomes a constant. Thus, the hydraulic controller shown in Figure 5–39(a) acts as a proportional controller, the gain of which is K_p. This gain can be adjusted by effectively changing the lever ratio b/a. (The adjusting mechanism is not shown in the diagram.)

We have thus seen that the addition of a feedback link will cause the hydraulic servomotor to act as a proportional controller.

Dashpots. The dashpot (also called a damper) shown in Figure 5–40(a) acts as a differentiating element. Suppose that we introduce a step displacement to the piston position x. Then the displacement y becomes equal to x momentarily. Because of the spring force, however, the oil will flow through the resistance R and the cylinder will come back to the original position. The curves x versus t and y versus t are shown in Figure 5–40(b).

Let us derive the transfer function between the displacement y and displacement x. Define the pressures existing on the right and left sides of the piston as P_1 (lb/in.^{2}) and P_2 (lb/in.^{2}), respectively. Suppose that the inertia force involved is negligible. Then the force acting on the piston must balance the spring force. Thus

$$A(P_1 - P_2) = ky$$

where A = piston area, in.^{2}
k = spring constant, lb$_f$/in.

The flow rate q is given by

$$q = \frac{P_1 - P_2}{R}$$

where q = flow rate through the restriction, lb/sec
R = resistance to flow at the restriction, lb$_f$-sec/in.^{2}-lb

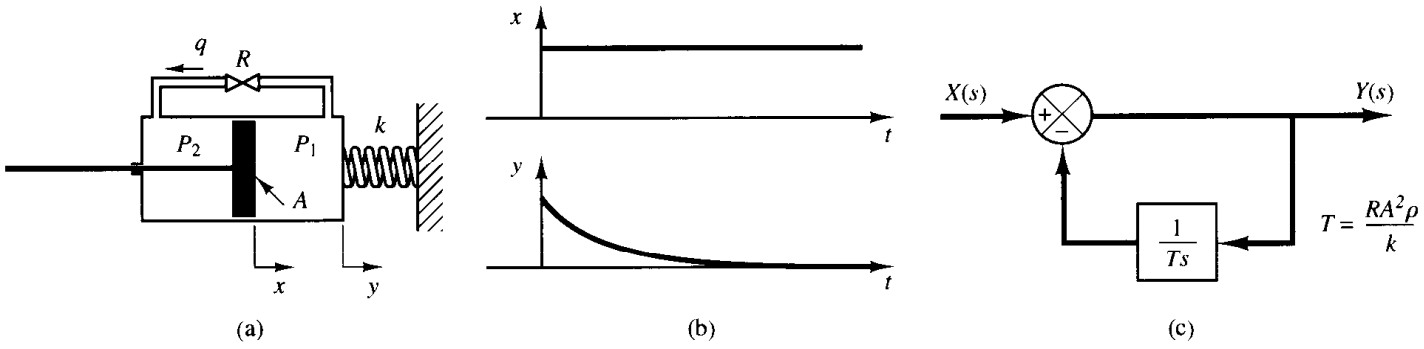

Figure 5–40
(a) Dashpot; (b) step change in x and the corresponding change in y plotted versus t; (c) block diagram of the dashpot.

Since the flow through the restriction during dt seconds must equal the change in the mass of oil to the left of the piston during the same dt seconds, we obtain

$$q\,dt = A\rho(dx - dy)$$

where ρ = density, lb/in.^{3}. (We assume that the fluid is incompressible or ρ = constant.) This last equation can be rewritten as

$$\frac{dx}{dt} - \frac{dy}{dt} = \frac{q}{A\rho} = \frac{P_1 - P_2}{RA\rho} = \frac{ky}{RA^2\rho}$$

or

$$\frac{dx}{dt} = \frac{dy}{dt} + \frac{ky}{RA^2\rho}$$

Taking the Laplace transforms of both sides of this last equation, assuming zero initial conditions, we obtain

$$sX(s) = sY(s) + \frac{k}{RA^2\rho}Y(s)$$

The transfer function of this system thus becomes

$$\frac{Y(s)}{X(s)} = \frac{s}{s + \dfrac{k}{RA^2\rho}}$$

Let us define $RA^2\rho/k = T$. Then

$$\frac{Y(s)}{X(s)} = \frac{Ts}{Ts + 1} = \frac{1}{1 + \dfrac{1}{Ts}}$$

Figure 5–40(c) shows a block diagram representation for this system.

Obtaining hydraulic proportional-plus-integral control action. Figure 5–41(a) shows a schematic diagram of a hydraulic proportional-plus-integral controller. A block diagram of this controller is shown in Figure 5–41(b). The transfer function $Y(s)/E(s)$ is given by

$$\frac{Y(s)}{E(s)} = \frac{\dfrac{b}{a+b}\dfrac{K}{s}}{1 + \dfrac{Ka}{a+b}\dfrac{T}{Ts+1}}$$

In such a controller, under normal operation $|KaT/[(a + b)(Ts + 1)]| \gg 1$, with the result that

$$\frac{Y(s)}{E(s)} = K_p\left(1 + \frac{1}{T_i s}\right)$$

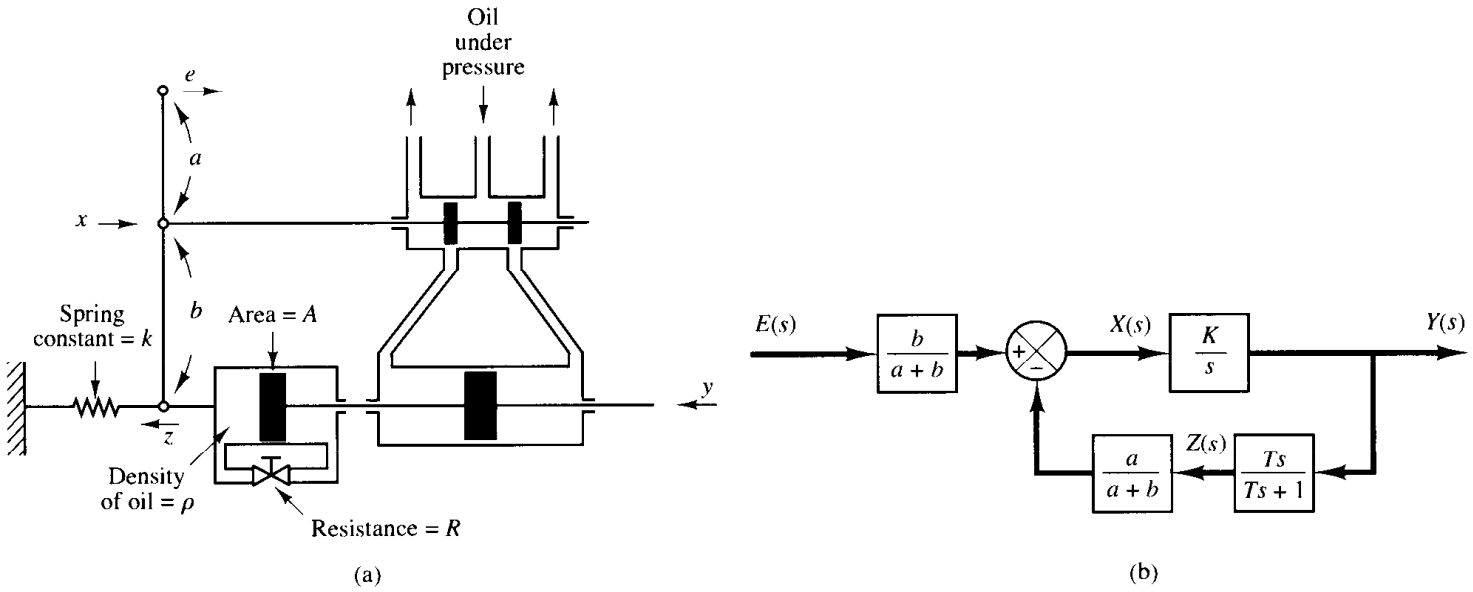

Figure 5–41
(a) Schematic diagram of a hydraulic proportional-plus-integral controller; (b) block diagram of the controller.

where

$$K_p = \frac{b}{a}, \qquad T_i = T = \frac{RA^2\rho}{k}$$

Thus the controller shown in Figure 5–52(a) is a proportional-plus-integral controller (a PI controller.)

Obtaining hydraulic proportional-plus-derivative control action. Figure 5–42(a) shows a schematic diagram of a hydraulic proportional-plus-derivative

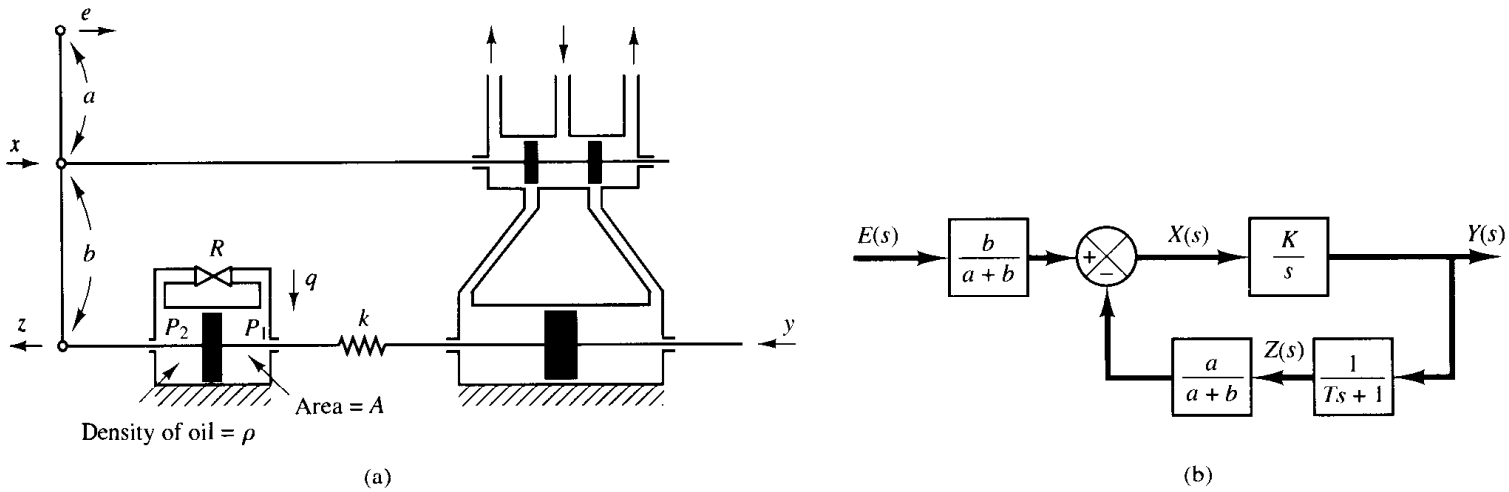

Figure 5–42
(a) Schematic diagram of a hydraulic proportional-plus-derivative controller; (b) block diagram of the controller.

controller. The cylinders are fixed in space and the pistons can move. For this system, notice that

$$k(y - z) = A(P_2 - P_1)$$

$$q = \frac{P_2 - P_1}{R}$$

$$q\,dt = \rho A\,dz$$

Hence

$$y = z + \frac{A}{k}qR = z + \frac{RA^2\rho}{k}\frac{dz}{dt}$$

or

$$\frac{Z(s)}{Y(s)} = \frac{1}{Ts + 1}$$

where

$$T = \frac{RA^2\rho}{k}$$

A block diagram for this system is shown in Figure 5–42(b). From the block diagram the transfer function $Y(s)/E(s)$ can be obtained as

$$\frac{Y(s)}{E(s)} = \frac{\dfrac{b}{a+b}\dfrac{K}{s}}{1 + \dfrac{a}{a+b}\dfrac{K}{s}\dfrac{1}{Ts+1}}$$

Under normal operation we have $\left|aK/[(a + b)s(Ts + 1)]\right| \gg 1$. Hence

$$\frac{Y(s)}{E(s)} = K_p(1 + Ts)$$

where

$$K_p = \frac{b}{a}, \qquad T = \frac{RA^2\rho}{k}$$

Thus the controller shown in Figure 5–42(a) is a proportional-plus-derivative controller (a PD controller).

5–8 ELECTRONIC CONTROLLERS

This section discusses electronic controllers using operational amplifiers. We begin by deriving the transfer functions of simple operational-amplifier circuits. Then we derive the transfer functions of some of the operational-amplifier controllers. Finally, we give operational-amplifier controllers and their transfer functions in the form of a table.

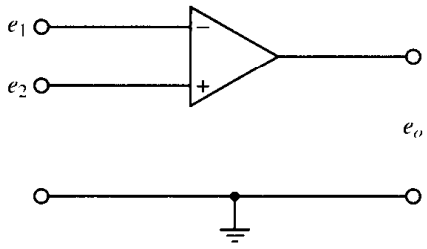

Figure 5–43
Operational amplifier.

Operational amplifiers. Operational amplifiers, often called op amps, are frequently used to amplify signals in sensor circuits. Op amps are also frequently used in filters used for compensation purposes. Figure 5–43 shows an op amp. It is a common practice to choose the ground as 0 volt and measure the input voltages e_1 and e_2 relative to the ground. The input e_1 to the minus terminal of the amplifier is inverted, and the input e_2 to the plus terminal is not inverted. The total input to the amplifier thus becomes $e_2 - e_1$. Hence, for the circuit shown in Figure 5–54, we have

$$e_o = K(e_2 - e_1) = -K(e_1 - e_2)$$

where the inputs e_1 and e_2 may be dc or ac signals and K is the differential gain or voltage gain. The magnitude of K is approximately $10^5 \sim 10^6$ for dc signals and ac signals with frequencies less than approximately 10 Hz. (The differential gain K decreases with the signal frequency and becomes about unity for frequencies of 1 MHz ~ 50 MHz.) Note that the op amp amplifies the difference in voltages e_1 and e_2. Such an amplifier is commonly called a differential amplifier. Since the gain of the op amp is very high, it is necessary to have a negative feedback from the output to the input to make the amplifier stable. (The feedback is made from the output to the inverted input so that the feedback is a negative feedback.)

In the ideal op amp, no current flows into the input terminals, and the output voltage is not affected by the load connected to the output terminal. In other words, the input impedance is infinity and the output impedance is zero. In an actual op amp, a very small (almost negligible) current flows into an input terminal and the output cannot be loaded too much. In our analysis here, we make the assumption that the op amps are ideal.

Inverting amplifier. Consider the operational amplifier circuit shown in Figure 5–44. Let us obtain the output voltage e_o.

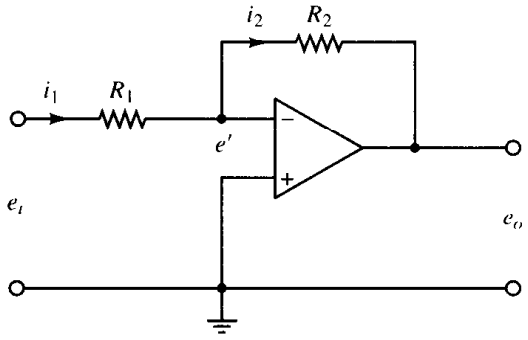

Figure 5–44
Inverting amplifier.

The equation for this circuit can be obtained as follows: Define

$$i_1 = \frac{e_i - e'}{R_1}, \qquad i_2 = \frac{e' - e_o}{R_2}$$

Since only a negligible current flows into the amplifier, the current i_1 must be equal to current i_2. Thus

$$\frac{e_i - e'}{R_1} = \frac{e' - e_o}{R_2}$$

Since $K(0 - e') = e_0$ and $K \gg 1$, e' must be almost zero, or $e' \doteq 0$. Hence we have

$$\frac{e_i}{R_1} = \frac{-e_o}{R_2}$$

or

$$e_o = -\frac{R_2}{R_1} e_i$$

Thus the circuit shown is an inverting amplifier. If $R_1 = R_2$, then the op-amp circuit shown acts as a sign inverter.

Noninverting amplifier. Figure 5–45(a) shows a noninverting amplifier. A circuit equivalent to this one is shown in Figure 5–45(b). For the circuit of Figure 5–45(b), we have

$$e_o = K\left(e_i - \frac{R_1}{R_1 + R_2} e_o\right)$$

where K is the differential gain of the amplifier. From this last equation, we get

$$e_i = \left(\frac{R_1}{R_1 + R_2} + \frac{1}{K}\right) e_o$$

Since $K \gg 1$, if $R_1/(R_1 + R_2) \gg 1/K$, then

$$e_o = \left(1 + \frac{R_2}{R_1}\right) e_i$$

This equation gives the output voltage e_o. Since e_o and e_i have the same signs, the op-amp circuit shown in Figure 5–45(a) is noninverting.

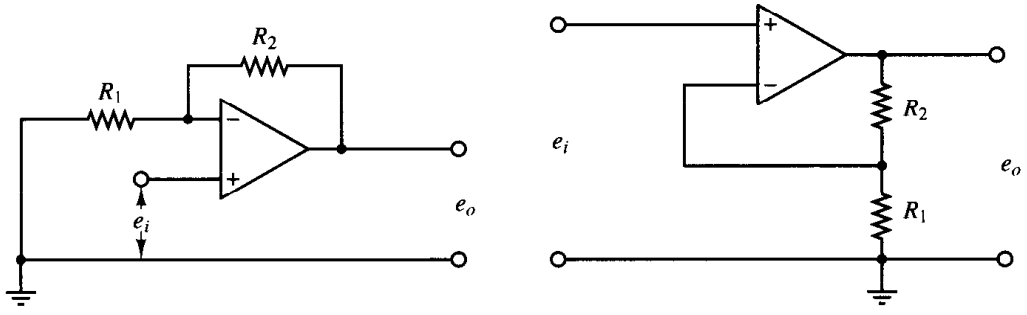

Figure 5–45
(a) Noninverting operational amplifier; (b) equivalent circuit.

EXAMPLE 5–3 Figure 5–46 shows an electrical circuit involving an operational amplifier. Obtain the output e_o.

Let us define

$$i_1 = \frac{e_i - e'}{R_1}, \qquad i_2 = C\frac{d(e' - e_o)}{dt}, \qquad i_3 = \frac{e' - e_o}{R_2}$$

Noting that the current flowing into the amplifier is negligible, we have

$$i_1 = i_2 + i_3$$

Hence

$$\frac{e_i - e'}{R_1} = C\frac{d(e' - e_o)}{dt} + \frac{e' - e_o}{R_2}$$

Since $e' \doteq 0$, we have

$$\frac{e_i}{R_1} = -C\frac{de_o}{dt} - \frac{e_o}{R_2}$$

Taking the Laplace transform of this last equation, assuming the zero initial condition, we have

$$\frac{E_i(s)}{R_1} = -\frac{R_2Cs + 1}{R_2}E_o(s)$$

which can be written as

$$\frac{E_o(s)}{E_i(s)} = -\frac{R_2}{R_1}\frac{1}{R_2Cs + 1}$$

The op-amp circuit shown in Figure 5–46 is a first-order lag circuit. (Several other circuits involving op amps are shown in Table 5–1 together with their transfer functions.)

Impedance approach for obtaining transfer functions. Consider the op-amp circuit shown in Figure 5–47. Similar to the case of electrical circuits we discussed earlier, the impedance approach can be applied to op-amp circuits to obtain their transfer functions. For the circuit shown in Figure 5–47, we have

$$E_i(s) = Z_1(s)I(s), \qquad E_o(s) = -Z_2(s)I(s)$$

Hence, the transfer function for the circuit is obtained as

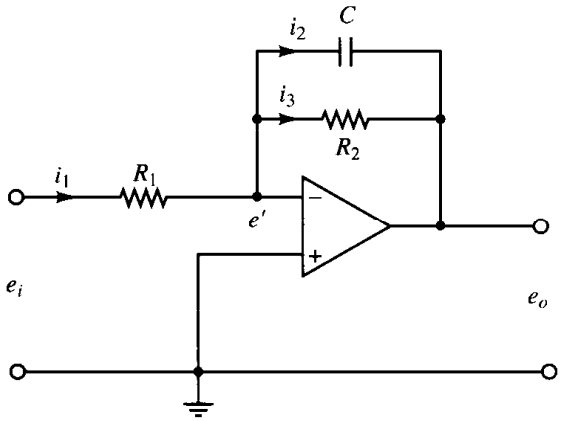

Figure 5–46
First-order lag circuit using operational amplifier.

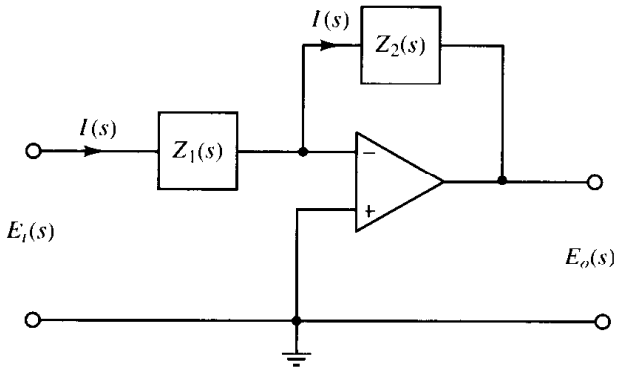

Figure 5–47
Operational amplifier circuit.

$$\frac{E_o(s)}{E_i(s)} = -\frac{Z_2(s)}{Z_1(s)}$$

EXAMPLE 5–4 Referring to the op-amp circuit shown in Figure 5–46, obtain the transfer function $E_o(s)/E_i(s)$ by use of the impedance approach.

The complex impedances $Z_1(s)$ and $Z_2(s)$ for this circuit are

$$Z_1(s) = R_1 \qquad \text{and} \qquad Z_2(s) = \frac{1}{Cs + \dfrac{1}{R_2}} = \frac{R_2}{R_2Cs + 1}$$

Hence, $E_i(s)$ and $E_o(s)$ are obtained as

$$E_i(s) = R_1 I(s), \qquad E_o(s) = -\frac{R_2}{R_2Cs + 1} I(s)$$

The transfer function $E_o(s)/E_i(s)$ is, therefore, obtained as

$$\frac{E_o(s)}{E_i(s)} = -\frac{R_2}{R_1} \frac{1}{R_2Cs + 1}$$

which is, of course, the same as that obtained in Example 5–3.

Lead or lag networks using operational amplifiers. Figure 5–48(a) shows an electronic circuit using an operational amplifier. The transfer function for this circuit

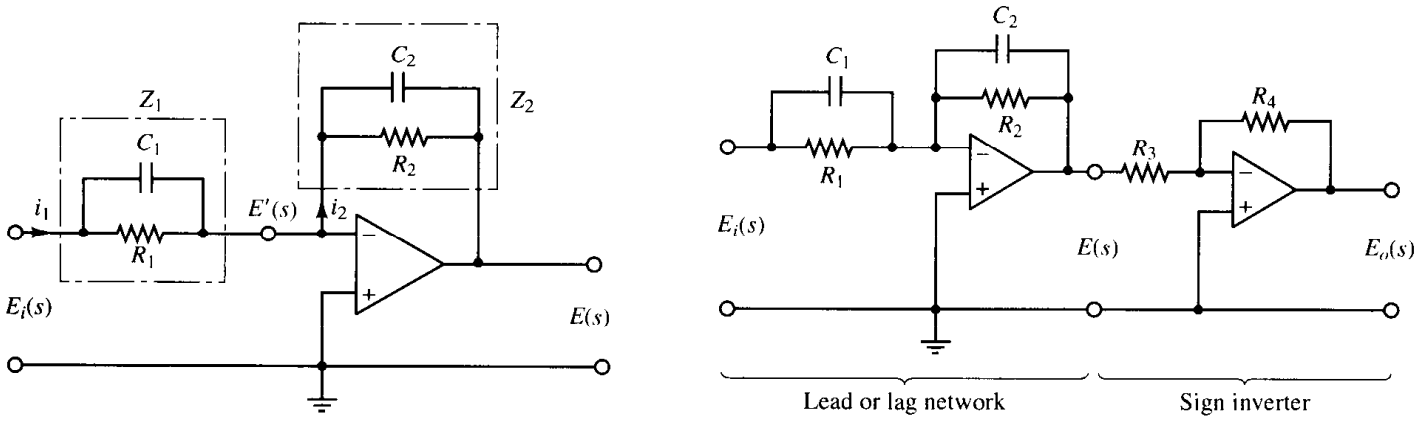

Figure 5–48
(a) Operational-amplifier circuit; (b) operational-amplifier circuit used as a lead or lag compensator.

can be obtained as follows: Define the input impedance and feedback impedance as Z_1 and Z_2, respectively. Then

$$Z_1 = \frac{R_1}{R_1C_1s + 1}, \qquad Z_2 = \frac{R_2}{R_2C_2s + 1}$$

Since the current flowing into the amplifier is negligible, current i_1 is equal to current i_2. Thus $i_1 = i_2$, or

$$\frac{E_i(s) - E'(s)}{Z_1} = \frac{E'(s) - E(s)}{Z_2}$$

Since $E'(s) \doteqdot 0$, we have

$$\frac{E(s)}{E_i(s)} = -\frac{Z_2}{Z_1} = -\frac{R_2}{R_1}\frac{R_1C_1s + 1}{R_2C_2s + 1} = -\frac{C_1}{C_2}\frac{s + \dfrac{1}{R_1C_1}}{s + \dfrac{1}{R_2C_2}} \tag{5–28}$$

Notice that the transfer function in Equation (5–28) contains a minus sign. Thus, this circuit is sign inverting. If such a sign inversion is not convenient in the actual application, a sign inverter may be connected to either the input or the output of the circuit of Figure 5–48(a). An example is shown in Figure 5–48(b). The sign inverter has the transfer function of

$$\frac{E_o(s)}{E(s)} = -\frac{R_4}{R_3}$$

The sign inverter has the gain of $-R_4/R_3$. Hence the network shown in Figure 5–48(b) has the following transfer function:

$$\frac{E_o(s)}{E_i(s)} = \frac{R_2R_4}{R_1R_3}\frac{R_1C_1s + 1}{R_2C_2s + 1} = \frac{R_4C_1}{R_3C_2}\frac{s + \dfrac{1}{R_1C_1}}{s + \dfrac{1}{R_2C_2}}$$

$$= K_c\alpha\frac{Ts + 1}{\alpha Ts + 1} = K_c\frac{s + \dfrac{1}{T}}{s + \dfrac{1}{\alpha T}} \tag{5–29}$$

where

$$T = R_1C_1, \qquad \alpha T = R_2C_2, \qquad K_c = \frac{R_4C_1}{R_3C_2}$$

Notice that

$$K_c\alpha = \frac{R_4C_1}{R_3C_2}\frac{R_2C_2}{R_1C_1} = \frac{R_2R_4}{R_1R_3}, \qquad \alpha = \frac{R_2C_2}{R_1C_1}$$

This network has a dc gain of $K_c\alpha = R_2R_4/(R_1R_3)$.

Referring to Equation (5–29), this network is a lead network if $R_1C_1 > R_2C_2$, or $\alpha < 1$. It is a lag network if $R_1C_1 < R_2C_2$. (For the definitions of lead and lag networks, refer to Section 5–9.)

PID controller using operational amplifiers. Figure 5–49 shows an electronic proportional-plus-integral-plus-derivative controller (a PID controller) using operational amplifiers. The transfer function $E(s)/E_i(s)$ is given by

$$\frac{E(s)}{E_i(s)} = -\frac{Z_2}{Z_1}$$

where

$$Z_1 = \frac{R_1}{R_1C_1s + 1}, \qquad Z_2 = \frac{R_2C_2s + 1}{C_2s}$$

Thus

$$\frac{E(s)}{E_i(s)} = -\left(\frac{R_2C_2s + 1}{C_2s}\right)\left(\frac{R_1C_1s + 1}{R_1}\right)$$

Noting that

$$\frac{E_o(s)}{E(s)} = -\frac{R_4}{R_3}$$

we have

$$\begin{aligned}\frac{E_o(s)}{E_i(s)} &= \frac{E_o(s)}{E(s)}\frac{E(s)}{E_i(s)} = \frac{R_4R_2}{R_3R_1}\frac{(R_1C_1s + 1)(R_2C_2s + 1)}{R_2C_2s} \\ &= \frac{R_4R_2}{R_3R_1}\left(\frac{R_1C_1 + R_2C_2}{R_2C_2} + \frac{1}{R_2C_2s} + R_1C_1s\right) \\ &= \frac{R_4(R_1C_1 + R_2C_2)}{R_3R_1C_2}\left[1 + \frac{1}{(R_1C_1 + R_2C_2)s} + \frac{R_1C_1R_2C_2}{R_1C_1 + R_2C_2}s\right] \end{aligned} \tag{5–30}$$

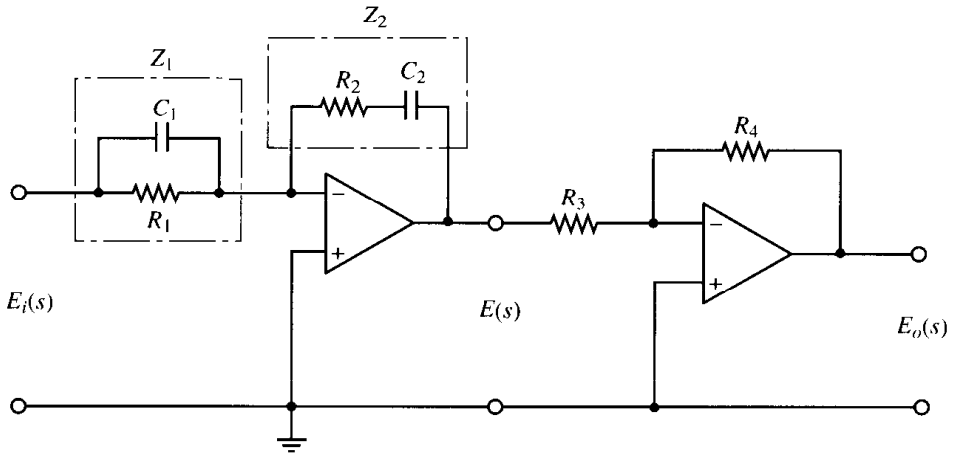

Figure 5–49
Electronic PID controller.

Thus

$$K_p = \frac{R_4(R_1C_1 + R_2C_2)}{R_3R_1C_2}$$

$$T_i = R_1C_1 + R_2C_2$$

$$T_d = \frac{R_1C_1R_2C_2}{R_1C_1 + R_2C_2}$$

In terms of the proportional gain, integral gain, and derivative gain, we have

$$K_p = \frac{R_4(R_1C_1 + R_2C_2)}{R_3R_1C_2}$$

$$K_i = \frac{R_4}{R_3R_1C_2}$$

$$K_d = \frac{R_4R_2C_1}{R_3}$$

Notice that the second operational-amplifier circuit acts as a sign inverter as well as a gain adjuster.

Table 5–1 shows a list of operational-amplifier circuits that may be used as controllers or compensators.

5–9 PHASE LEAD AND PHASE LAG IN SINUSOIDAL RESPONSE

For a sinusoidal input, the steady-state output of a linear time-invariant system is sinusoidal with a phase shift that is a function of the input frequency. This phase angle varies as the frequency is increased from zero to infinity. If the steady-state sinusoidal output of a network leads (lags) the input sinusoid, it is called a lead (lag) network. We shall first derive the steady-state output of a linear, time-invariant network to a sinusoidal input.

Obtaining steady-state outputs to sinusoidal inputs. We shall show that the steady-state output of a transfer function system can be obtained directly from the sinusoidal transfer function, that is, the transfer function in which s is replaced by $j\omega$, where ω is frequency.

Consider the stable, linear, time-invariant system shown in Figure 5–50. The input and output of the system, whose transfer function is $G(s)$, are denoted by $x(t)$ and $y(t)$, respectively. If the input $x(t)$ is a sinusoidal signal, the steady-state output will also be a sinusoidal signal of the same frequency but with possibly different magnitude and phase angle.

Let us assume that the input signal is given by

$$x(t) = X \sin \omega t$$

Suppose that the transfer function $G(s)$ can be written as a ratio of two polynomials in s; that is,

Table 5–1 Operational-Amplifier Circuits That May Be Used as Compensators

	Control Action	$G(s) = \frac{E_o(s)}{E_i(s)}$	Operational Amplifier Circuits
1	P	$\frac{R_4}{R_3}\frac{R_2}{R_1}$	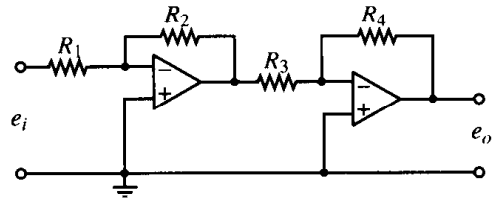
2	I	$\frac{R_4}{R_3}\frac{1}{R_1C_2s}$	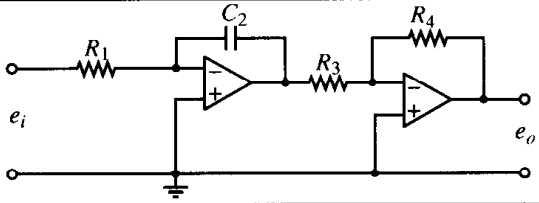
3	PD	$\frac{R_4}{R_3}\frac{R_2}{R_1}(R_1C_1s+1)$	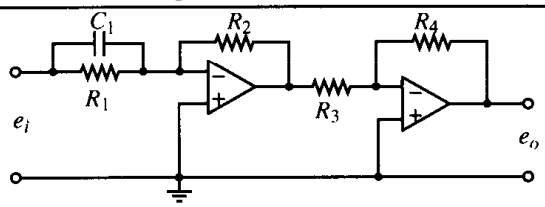
4	PI	$\frac{R_4}{R_3}\frac{R_2}{R_1}\frac{R_2C_2s+1}{R_2C_2s}$	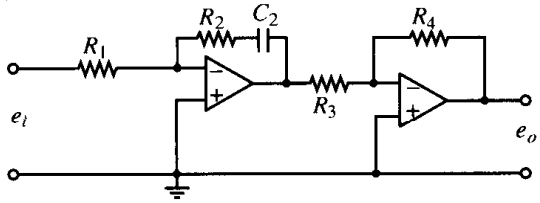
5	PID	$\frac{R_4}{R_3}\frac{R_2}{R_1}\frac{(R_1C_1s+1)(R_2C_2s+1)}{R_2C_2s}$	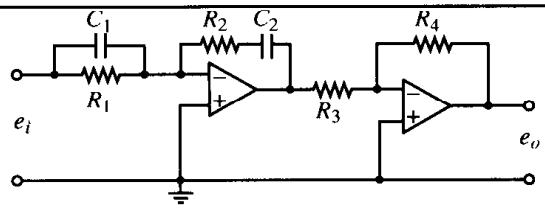
6	Lead or lag	$\frac{R_4}{R_3}\frac{R_2}{R_1}\frac{R_1C_1s+1}{R_2C_2s+1}$	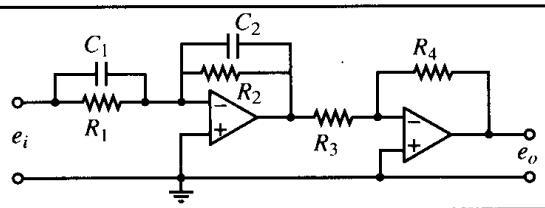
7	Lag–lead	$\frac{R_6}{R_5}\frac{R_4}{R_3}\frac{[(R_1+R_3)C_1s+1](R_2C_2s+1)}{(R_1C_1s+1)[(R_2+R_4)C_2s+1]}$	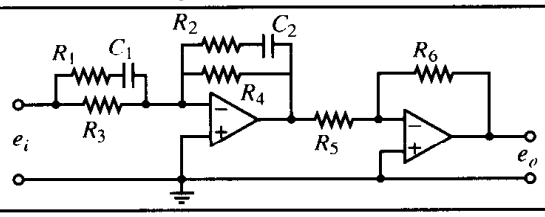

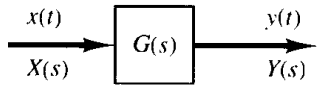

Figure 5–50
Stable, linear, time-invariant system.

$$G(s) = \frac{p(s)}{q(s)} = \frac{p(s)}{(s + s_1)(s + s_2)\cdots(s + s_n)}$$

The Laplace-transformed output $Y(s)$ is then

$$Y(s) = G(s)X(s) = \frac{p(s)}{q(s)}X(s) \tag{5–31}$$

where $X(s)$ is the Laplace transform of the input $x(t)$.

It will be shown that after waiting until steady-state conditions are reached the frequency response can be calculated by replacing s in the transfer function by $j\omega$. It will also be shown that the steady-state response can be given by

$$G(j\omega) = Me^{j\phi} = M\angle\phi$$

where M is the amplitude ratio of the output and input sinusoids and ϕ is the phase shift between the input sinusoid and the output sinusoid. In the frequency-response test, the input frequency ω is varied until the entire frequency range of interest is covered.

The steady-state response of a stable, linear, time-invariant system to a sinusoidal input does not depend on the initial conditions. (Thus, we can assume the zero initial condition.) If $Y(s)$ has only distinct poles, then the partial fraction expansion of Equation (5–31) yields

$$\begin{aligned} Y(s) = G(s)X(s) &= G(s)\frac{\omega X}{s^2 + \omega^2} \\ &= \frac{a}{s + j\omega} + \frac{\bar{a}}{s - j\omega} + \frac{b_1}{s + s_1} + \frac{b_2}{s + s_2} + \cdots + \frac{b_n}{s + s_n} \end{aligned} \tag{5–32}$$

where a and the b_i (where $i = 1, 2, \ldots, n$) are constants and $\bar{a}$ is the complex conjugate of a. The inverse Laplace transform of Equation (5–32) gives

$$y(t) = ae^{-j\omega t} + \bar{a}e^{j\omega t} + b_1e^{-s_1t} + b_2e^{-s_2t} + \cdots + b_ne^{-s_nt} \qquad (t \geq 0) \tag{5–33}$$

For a stable system, $-s_1, -s_2, \ldots, -s_n$ have negative real parts. Therefore, as t approaches infinity, the terms $e^{-s_1t}, e^{-s_2t}, \ldots$, and e^{-s_nt} approach zero. Thus, all the terms on the right-hand side of Equation (5–33), except the first two, drop out at steady state.

If $Y(s)$ involves multiple poles s_j of multiplicity m_j, then $y(t)$ will involve terms such as $t^{h_j}e^{-s_jt}$ ($h_j = 0, 1, 2, \ldots, m_j - 1$). For a stable system, the terms $t^{h_j}e^{-s_jt}$ approach zero as t approaches infinity.

Thus, regardless of whether the system is of the distinct-pole type, the steady-state response becomes

$$y_{ss}(t) = ae^{-j\omega t} + \bar{a}e^{j\omega t} \tag{5–34}$$

where the constant a can be evaluated from Equation (5–32) as follows:

$$a = G(s)\frac{\omega X}{s^2 + \omega^2}(s + j\omega)\bigg|_{s=-j\omega} = -\frac{XG(-j\omega)}{2j}$$

Note that

$$\bar{a} = G(s)\frac{\omega X}{s^2 + \omega^2}(s - j\omega)\bigg|_{s=j\omega} = \frac{XG(j\omega)}{2j}$$

Since $G(j\omega)$ is a complex quantity, it can be written in the following form:

$$G(j\omega) = |G(j\omega)|e^{j\phi}$$

where $|(Gj\omega)|$ represents the magnitude and ϕ represents the angle of $G(j\omega)$; that is,

$$\phi = \underline{/G(j\omega)} = \tan^{-1}\left[\frac{\text{imaginary part of } G(j\omega)}{\text{real part of } G(j\omega)}\right]$$

The angle ϕ may be negative, positive, or zero. Similarly, we obtain the following expression for $G(-j\omega)$:

$$G(-j\omega) = |G(-j\omega)|e^{-j\phi} = |G(j\omega)|e^{-j\phi}$$

Then, noting that

$$a = -\frac{X|G(j\omega)|e^{-j\phi}}{2j}, \qquad \bar{a} = \frac{X|G(j\omega)|e^{j\phi}}{2j}$$

Equation (5–34) can be written

$$\begin{aligned} y_{ss}(t) &= X|G(j\omega)|\frac{e^{j(\omega t+\phi)} - e^{-j(\omega t+\phi)}}{2j} \\ &= X|G(j\omega)|\sin(\omega t + \phi) \\ &= Y\sin(\omega t + \phi) \end{aligned} \tag{5–35}$$

where $Y = X|G(j\omega)|$. We see that a stable, linear, time-invariant system subjected to a sinusoidal input will, at steady state, have a sinusoidal output of the same frequency as the input. But the amplitude and phase of the output will, in general, be different from those of the input. In fact, the amplitude of the output is given by the product of that of the input and $|G(j\omega)|$, while the phase angle differs from that of the input by the amount $\phi = \underline{/G(j\omega)}$. An example of input and output sinusoidal signals is shown in Figure 5–51.

On the basis of this, we obtain this important result: For sinusoidal inputs,

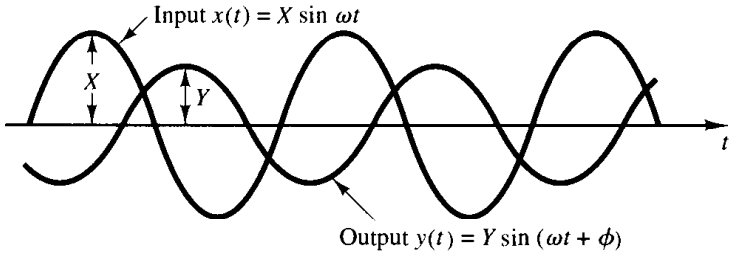

Figure 5–51
Input and output sinusoidal signals.

$$|G(j\omega)| = \left|\frac{Y(j\omega)}{X(j\omega)}\right| = \text{amplitude ratio of the output sinuisoid to the input sinusoid}$$

$$\angle G(j\omega) = \angle\frac{Y(j\omega)}{X(j\omega)} = \text{phase shift of the output sinusoid with respect to the input sinusoid}$$

Hence, the response characteristics of a system to a sinusoidal input can be obtained directly from

$$\frac{Y(j\omega)}{X(j\omega)} = G(j\omega)$$

The function $G(j\omega)$ is called the *sinusoidal transfer function.* It is the ratio of $Y(j\omega)$ to $X(j\omega)$, is a complex quantity, and can be represented by the magnitude and phase angle with frequency as a parameter. (A negative phase angle is called *phase lag*, and a positive phase angle is called *phase lead.*) The sinusoidal transfer function of any linear system is obtained by substituting $j\omega$ for s in the transfer function of the system.

A network that has phase-lead characteristics is commonly called a lead network. Similarly, a network that has phase-lag characteristics is called a lag network.

EXAMPLE 5–5 Consider the system shown in Figure 5–52. The transfer function $G(s)$ is

$$G(s) = \frac{K}{Ts + 1}$$

For the sinusoidal input $x(t) = X \sin \omega t$, the steady-state output $y_{ss}(t)$ can be found as follows: Substituting $j\omega$ for s in $G(s)$ yields

$$G(j\omega) = \frac{K}{jT\omega + 1}$$

The amplitude ratio of the output to input is

$$|G(j\omega)| = \frac{K}{\sqrt{1 + T^2\omega^2}}$$

while the phase angle ϕ is

$$\phi = \angle G(j\omega) = -\tan^{-1} T\omega$$

Thus, for the input $x(t) = X \sin \omega t$, the steady-state output $y_{ss}(t)$ can be obtained from Equation (5–35) as follows:

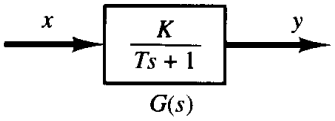

Figure 5–52
First-order system.

$$y_{ss}(t) = \frac{XK}{\sqrt{1 + T^2\omega^2}} \sin(\omega t - \tan^{-1} T\omega) \tag{5-36}$$

From Equation (5–36) it can be seen that for small ω the amplitude of the steady-state output $y_{ss}(t)$ is almost equal to K times the amplitude of the input. The phase shift of the output is small for small ω. For large ω, the amplitude of the output is small and almost inversely proportional to ω. The phase shift approaches $-90°$ as ω approaches infinity. This is a phase-lag network.

EXAMPLE 5–6 Consider the network given by

$$G(s) = \frac{s + \dfrac{1}{T_1}}{s + \dfrac{1}{T_2}}$$

Find if this network is a lead network or lag network.

For the sinusoidal input $x(t) = X \sin \omega t$, the steady-state output $y_{ss}(t)$ can be found as follows: Since

$$G(j\omega) = \frac{j\omega + \dfrac{1}{T_1}}{j\omega + \dfrac{1}{T_2}} = \frac{T_2(1 + T_1 j\omega)}{T_1(1 + T_2 j\omega)}$$

we have

$$|G(j\omega)| = \frac{T_2\sqrt{1 + T_1^2\omega^2}}{T_1\sqrt{1 + T_2^2\omega^2}}$$

and

$$\phi = \underline{/G(j\omega)} = \tan^{-1} T_1\omega - \tan^{-1} T_2\omega$$

Thus the steady-state output is

$$y_{ss}(t) = \frac{XT_2\sqrt{1 + T_1^2\omega^2}}{T_1\sqrt{1 + T_2^2\omega^2}} \sin(\omega t + \tan^{-1} T_1\omega - \tan^{-1} T_2\omega)$$

From this expression, we find that if $T_1 > T_2$ then $\tan^{-1} T_1\omega - \tan^{-1} T_2\omega > 0$. Thus, if $T_1 > T_2$, then the network is a lead network. If $T_1 < T_2$, then the network is a lag network.

5–10 STEADY-STATE ERRORS IN UNITY-FEEDBACK CONTROL SYSTEMS

Errors in a control system can be attributed to many factors. Changes in the reference input will cause unavoidable errors during transient periods and may also cause steady-state errors. Imperfections in the system components, such as static friction, backlash, and amplifier drift, as well as aging or deterioration, will cause errors at steady state. In this section, however, we shall not discuss errors due to imperfections in the system components. Rather, we shall investigate a type of steady-state error that is caused by the incapability of a system to follow particular types of inputs.

Any physical control system inherently suffers steady-state error in response to certain types of inputs. A system may have no steady-state error to a step input, but the same system may exhibit nonzero steady-state error to a ramp input. (The only way we may be able to eliminate this error is to modify the system structure.) Whether a given system will exhibit steady-state error for a given type of input depends on the type of open-loop transfer function of the system, to be discussed in what follows.

Classification of control systems. Control systems may be classified according to their ability to follow step inputs, ramp inputs, parabolic inputs, and so on. This is a reasonable classification scheme because actual inputs may frequently be considered combinations of such inputs. The magnitudes of the steady-state errors due to these individual inputs are indicative of the goodness of the system.

Consider the unity-feedback control system with the following open-loop transfer function $G(s)$:

$$G(s) = \frac{K(T_a s + 1)(T_b s + 1)\cdots(T_m s + 1)}{s^N(T_1 s + 1)(T_2 s + 1)\cdots(T_p s + 1)}$$

It involves the term s^N in the denominator, representing a pole of multiplicity N at the origin. The present classification scheme is based on the number of integrations indicated by the open-loop transfer function. A system is called type 0, type 1, type 2, . . . , if $N = 0, N = 1, N = 2, \ldots$, respectively. Note that this classification is different from that of the order of a system. As the type number is increased, accuracy is improved; however, increasing the type number aggravates the stability problem. A compromise between steady-state accuracy and relative stability is always necessary. In practice, it is rather exceptional to have type 3 or higher systems because we find it generally difficult to design stable systems having more than two integrations in the feedforward path.

We shall see later that, if $G(s)$ is written so that each term in the numerator and denominator, except the term s^N, approaches unity as s approaches zero, then the open-loop gain K is directly related to the steady-state error.

Steady-state errors. Consider the system shown in Figure 5–53. The closed-loop transfer function is

$$\frac{C(s)}{R(s)} = \frac{G(s)}{1 + G(s)}$$

The transfer function between the error signal $e(t)$ and the input signal $r(t)$ is

$$\frac{E(s)}{R(s)} = 1 - \frac{C(s)}{R(s)} = \frac{1}{1 + G(s)}$$

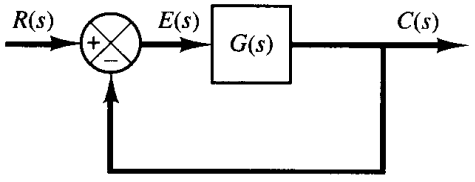

Figure 5–53
Control system.

where the error $e(t)$ is the difference between the input signal and the output signal.

The final-value theorem provides a convenient way to find the steady-state performance of a stable system. Since $E(s)$ is

$$E(s) = \frac{1}{1 + G(s)} R(s)$$

the steady-state error is

$$e_{ss} = \lim_{t \to \infty} e(t) = \lim_{s \to 0} sE(s) = \lim_{s \to 0} \frac{sR(s)}{1 + G(s)}$$

The static error constants defined in the following are figures of merit of control systems. The higher the constants, the smaller the steady-state error. In a given system, the output may be the position, velocity, pressure, temperature, or the like. The physical form of the output, however, is immaterial to the present analysis. Therefore, in what follows, we shall call the output "position," the rate of change of the output "velocity," and so on. This means that in a temperature control system "position" represents the output temperature, "velocity" represents the rate of change of the output temperature, and so on.

Static position error constant K_p. The steady-state error of the system for a unit-step input is

$$e_{ss} = \lim_{s \to 0} \frac{s}{1 + G(s)} \frac{1}{s}$$

$$= \frac{1}{1 + G(0)}$$

The static position error constant K_p is defined by

$$K_p = \lim_{s \to 0} G(s) = G(0)$$

Thus, the steady-state error in terms of the static position error constant K_p is given by

$$e_{ss} = \frac{1}{1 + K_p}$$

For a type 0 system,

$$K_p = \lim_{s \to 0} \frac{K(T_a s + 1)(T_b s + 1) \cdots}{(T_1 s + 1)(T_2 s + 1) \cdots} = K$$

For a type 1 or higher system,

$$K_p = \lim_{s \to 0} \frac{K(T_a s + 1)(T_b s + 1) \cdots}{s^N (T_1 s + 1)(T_2 s + 1) \cdots} = \infty, \qquad \text{for } N \geq 1$$

Hence, for a type 0 system, the static position error constant K_p is finite, while for a type 1 or higher system, K_p is infinite.

For a unit-step input, the steady-state error e_{ss} may be summarized as follows:

$$e_{ss} = \frac{1}{1 + K}, \qquad \text{for type 0 systems}$$

$$e_{ss} = 0, \qquad \text{for type 1 or higher systems}$$

From the foregoing analysis, it is seen that the response of a feedback control system to a step input involves a steady-state error if there is no integration in the feedforward path. (If small errors for step inputs can be tolerated, then a type 0 system may be permissible, provided that the gain K is sufficiently large. If the gain K is too large, however, it is difficult to obtain reasonable relative stability.) If zero steady-state error for a step input is desired, the type of the system must be one or higher.

Static velocity error constant K_v. The steady-state error of the system with a unit-ramp input is given by

$$e_{ss} = \lim_{s \to 0} \frac{s}{1 + G(s)} \frac{1}{s^2}$$

$$= \lim_{s \to 0} \frac{1}{sG(s)}$$

The static velocity error constant K_v is defined by

$$K_v = \lim_{s \to 0} sG(s)$$

Thus, the steady-state error in terms of the static velocity error constant K_v is given by

$$e_{ss} = \frac{1}{K_v}$$

The term *velocity error* is used here to express the steady-state error for a ramp input. The dimension of the velocity error is the same as the system error. That is, velocity error is not an error in velocity, but it is an error in position due to a ramp input.

For a type 0 system,

$$K_v = \lim_{s \to 0} \frac{sK(T_a s + 1)(T_b s + 1) \cdots}{(T_1 s + 1)(T_2 s + 1) \cdots} = 0$$

For a type 1 system,

$$K_v = \lim_{s \to 0} \frac{sK(T_a s + 1)(T_b s + 1) \cdots}{s(T_1 s + 1)(T_2 s + 1) \cdots} = K$$

For a type 2 or higher system,

$$K_v = \lim_{s \to 0} \frac{sK(T_a s + 1)(T_b s + 1) \cdots}{s^N(T_1 s + 1)(T_2 s + 1) \cdots} = \infty, \qquad \text{for } N \geq 2$$

The steady-state error e_{ss} for the unit-ramp input can be summarized as follows:

$$e_{ss} = \frac{1}{K_v} = \infty, \qquad \text{for type 0 systems}$$

$$e_{ss} = \frac{1}{K_v} = \frac{1}{K}, \qquad \text{for type 1 systems}$$

$$e_{ss} = \frac{1}{K_v} = 0, \qquad \text{for type 2 or higher systems}$$

The foregoing analysis indicates that a type 0 system is incapable of following a ramp input in the steady state. The type 1 system with unity feedback can follow the ramp input with a finite error. In steady-state operation, the output velocity is exactly the same as the input velocity, but there is a positional error. This error is proportional to the velocity of the input and is inversely proportional to the gain K. Figure 5–54 shows an example of the response of a type 1 system with unity feedback to a ramp input. The type 2 or higher system can follow a ramp input with zero error at steady state.

Static acceleration error constant K_a. The steady-state error of the system with a unit-parabolic input (acceleration input), which is defined by

$$r(t) = \frac{t^2}{2}, \qquad \text{for } t \geq 0$$

$$= 0, \qquad \text{for } t < 0$$

is given by

$$e_{ss} = \lim_{s \to 0} \frac{s}{1 + G(s)} \frac{1}{s^3}$$

$$= \frac{1}{\lim_{s \to 0} s^2 G(s)}$$

The static acceleration error constant K_a is defined by the equation

$$K_a = \lim_{s \to 0} s^2 G(s)$$

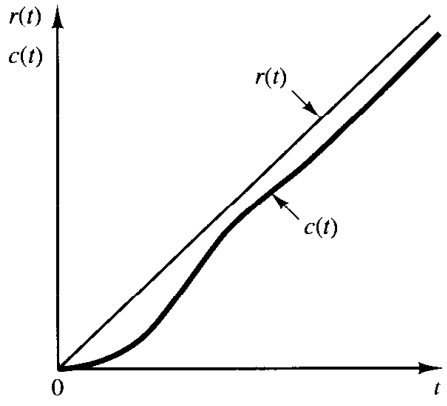

Figure 5–54
Response of a type 1 unity-feedback system to a ramp input.

The steady-state error is then

$$e_{ss} = \frac{1}{K_a}$$

Note that the acceleration error, the steady-state error due to a parabolic input, is an error in position.

The values of K_a are obtained as follows:

For a type 0 system,

$$K_a = \lim_{s \to 0} \frac{s^2 K(T_a s + 1)(T_b s + 1) \cdots}{(T_1 s + 1)(T_2 s + 1) \cdots} = 0$$

For a type 1 system,

$$K_a = \lim_{s \to 0} \frac{s^2 K(T_a s + 1)(T_b s + 1) \cdots}{s(T_1 s + 1)(T_2 s + 1) \cdots} = 0$$

For a type 2 system,

$$K_a = \lim_{s \to 0} \frac{s^2 K(T_a s + 1)(T_b s + 1) \cdots}{s^2(T_1 s + 1)(T_2 s + 1) \cdots} = K$$

For a type 3 or higher system,

$$K_a = \lim_{s \to 0} \frac{s^2 K(T_a s + 1)(T_b s + 1) \cdots}{s^N(T_1 s + 1)(T_2 s + 1) \cdots} = \infty, \qquad \text{for } N \geq 3$$

Thus, the steady-state error for the unit parabolic input is

$$e_{ss} = \infty, \qquad \text{for type 0 and type 1 systems}$$

$$e_{ss} = \frac{1}{K}, \qquad \text{for type 2 systems}$$

$$e_{ss} = 0, \qquad \text{for type 3 or higher systems}$$

Note that both type 0 and type 1 systems are incapable of following a parabolic input in the steady state. The type 2 system with unity feedback can follow a parabolic input with a finite error signal. Figure 5–55 shows an example of the response of a type 2 system with unity feedback to a parabolic input. The type 3 or higher system with unity feedback follows a parabolic input with zero error at steady state.

Summary. Table 5–2 summarizes the steady-state errors for type 0, type 1, and type 2 systems when they are subjected to various inputs. The finite values for steady-state errors appear on the diagonal line. Above the diagonal, the steady-state errors are infinity; below the diagonal, they are zero.

Remember that the terms *position error*, *velocity error*, and *acceleration error* mean steady-state deviations in the output position. A finite velocity error implies that after transients have died out the input and output move at the same velocity but have a finite position difference.

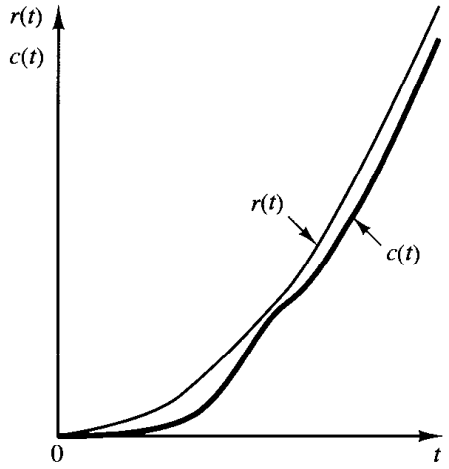

Figure 5–55
Response of a type 2 unity-feedback system to a parabolic input.

The error constants K_p, K_v, and K_a describe the ability of a unity-feedback system to reduce or eliminate steady-state error. Therefore, they are indicative of the steady-state performance. It is generally desirable to increase the error constants, while maintaining the transient response within an acceptable range. If there is any conflict between the static velocity error constant and the static acceleration error constant, then the latter may be considered less important than the former. It is noted that to improve the steady-state performance we can increase the type of the system by adding an integrator or integrators to the feedforward path. This, however, introduces an additional stability problem. The design of a satisfactory system with more than two integrators in series in the feedforward path is generally difficult.

Comparison of steady-state errors in open-loop control system and closed-loop control system. Consider the open-loop control system and closed-loop control system shown in Figure 5–56. In the open loop one, gain K_c is calibrated so that $K_c = 1/K$. Thus, the transfer function of the open-loop control system is

$$G_0(s) = \frac{1}{K}\frac{K}{Ts + 1} = \frac{1}{Ts + 1}$$

In the closed-loop control system, gain K_p of the controller is set so that $K_pK \gg 1$.

Table 5–2 Steady-State Error in Terms of Gain K

	Step Input $r(t) = 1$	Ramp Input $r(t) = t$	Acceleration Input $r(t) = \frac{1}{2}t^2$
Type 0 system	$\frac{1}{1 + K}$	∞	∞
Type 1 system	0	$\frac{1}{K}$	∞
Type 2 system	0	0	$\frac{1}{K}$

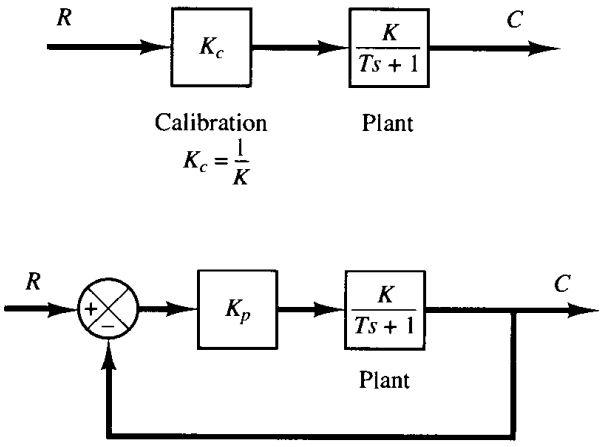

Figure 5–56
Block diagrams of an open-loop control system and a closed-loop control system.

Assuming a unit-step input, let us compare the steady-state errors for these control systems. For the open-loop control system, the error signal is

$$e(t) = r(t) - c(t)$$

or

$$\begin{aligned} E(s) &= R(s) - C(s) \\ &= [1 - G_0(s)]R(s) \end{aligned}$$

The steady-state error in the unit-step response is

$$\begin{aligned} e_{ss} &= \lim_{s \to 0} sE(s) \\ &= \lim_{s \to 0} s[1 - G_0(s)]\frac{1}{s} \\ &= 1 - G_0(0) \end{aligned}$$

If $G_o(0)$, the dc gain of the open-loop control system, is equal to unity, then the steady-state error is zero. Due to environmental changes and aging of components, however, the dc gain $G_o(0)$ will drift from unity as time elapses, and the steady-state error will no longer be equal to zero. Such steady-state error in an open-loop control system will remain until the system is recalibrated.

For the closed-loop control system, the error signal is

$$\begin{aligned} E(s) &= R(s) - C(s) \\ &= \frac{1}{1 + G(s)} R(s) \end{aligned}$$

where

$$G(s) = \frac{K_p K}{Ts + 1}$$

The steady-state error in the unit-step response is

$$e_{ss} = \lim_{s \to 0} s\left[\frac{1}{1 + G(s)}\right]\frac{1}{s}$$

$$= \frac{1}{1 + G(0)}$$

$$= \frac{1}{1 + K_p K}$$

In the closed-loop control system, gain K_p is set at a large value compared with $1/K$. Thus the steady-state error can be made small, although not exactly zero.

Let us assume the following variation in the transfer function of the plant, assuming K_c and K_p constant:

$$\frac{K + \Delta K}{Ts + 1}$$

For simplicity, let us assume that $K = 10, \Delta K = 1$, or $\Delta K/K = 0.1$. Then the steady-state error in the unit-step response for the open-loop control system becomes

$$e_{ss} = 1 - \frac{1}{K}(K + \Delta K)$$

$$= 1 - 1.1 = -0.1$$

For the closed-loop control system, if K_p is set at $100/K$, then the steady-state error in the unit-step response becomes

$$e_{ss} = \frac{1}{1 + G(0)}$$

$$= \frac{1}{1 + \dfrac{100}{K}(K + \Delta K)}$$

$$= \frac{1}{1 + 110} = 0.009$$

Thus, the closed-loop control system is superior to the open-loop control system in the presence of environmental changes, aging of components, and the like, which definitely affect the steady-state performance.

EXAMPLE PROBLEMS AND SOLUTIONS

A-5-1. Explain why the proportional control of a plant that does not possess an integrating property (which means that the plant transfer function does not include the factor $1/s$) suffers offset in response to step inputs.

Solution. Consider, for example, the system shown in Figure 5–57. At steady state, if c were equal to a nonzero constant r, then $e = 0$ and $u = Ke = 0$, resulting in $c = 0$, which contradicts the assumption that $c = r =$ nonzero constant.

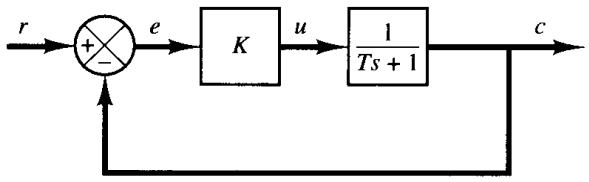

Figure 5–57
Control system.

A nonzero offset must exist for proper operation of such a control system. In other words, at steady state, if e were equal to $r/(1 + K)$, then $u = Kr/(1 + K)$ and $c = Kr/(1 + K)$, which results in the assumed error signal $e = r/(1 + K)$. Thus the offset of $r/(1 + K)$ must exist in such a system.

A-5-2. Consider the system shown in Figure 5–58. Show that the steady-state error in following the unit-ramp input is B/K. This error can be made smaller by choosing B small and/or K large. However, making B small and/or K large would have the effect of making the damping ratio small, which is normally not desirable. Describe a method or methods to make B/K small and yet make the damping ratio have reasonable value ($0.5 < \zeta < 0.7$).

Solution. From Figure 5–58 we obtain

$$E(s) = R(s) - C(s) = \frac{Js^2 + Bs}{Js^2 + Bs + K} R(s)$$

The steady-state error for the unit-ramp response can be obtained as follows: For the unit-ramp input, the steady-state error e_{ss} is

$$\begin{aligned} e_{ss} &= \lim_{s \to 0} sE(s) \\ &= \lim_{s \to 0} s \frac{Js^2 + Bs}{Js^2 + Bs + K} \frac{1}{s^2} \\ &= \frac{B}{K} \\ &= \frac{2\zeta}{\omega_n} \end{aligned}$$

where

$$\zeta = \frac{B}{2\sqrt{KJ}}, \qquad \omega_n = \sqrt{\frac{K}{J}}$$

To assure acceptable transient response and acceptable steady-state error in following a ramp input, ζ must not be too small and ω_n must be sufficiently large. It is possible to make the steady-state error e_{ss} small by making the value of the gain K large. (A large value of K has an additional advantage of suppressing undesirable effects caused by dead zone, backlash, coulomb friction,

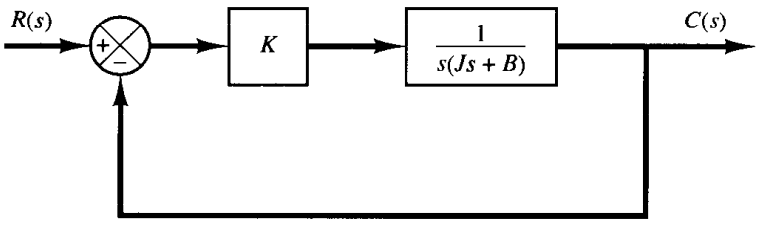

Figure 5–58
Control system.

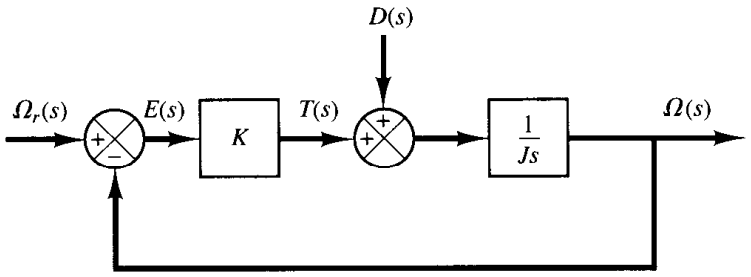

Figure 5–59
Block diagram of a speed control system.

and the like.) A large value of K would, however, make the value of ζ small and increase the maximum overshoot, which is undesirable.

It is therefore necessary to compromise between the magnitude of the steady-state error to a ramp input and the maximum overshoot to a unit-step input. In the system shown in Figure 5–58, a reasonable compromise may not be reached easily. It is then desirable to consider other types of control action that may improve both the transient-response and steady-state behavior. Two schemes to improve both the transient-response and steady-state behavior are available. One scheme is to use a proportional-plus-derivative controller and the other is to use tachometer feedback.

A-5-3. The block diagram of Figure 5–59 shows a speed control system in which the output member of the system is subject to a torque disturbance. In the diagram, $\Omega_r(s)$, $\Omega(s)$, $T(s)$, and $D(s)$ are the Laplace transforms of the reference speed, output speed, driving torque, and disturbance torque, respectively. In the absence of a disturbance torque, the output speed is equal to the reference speed.

Investigate the response of this system to a unit-step disturbance torque. Assume that the reference input is zero, or $\Omega_r(s) = 0$.

Solution. Figure 5–60 is a modified block diagram convenient for the present analysis. The closed-loop transfer function is

$$\frac{\Omega_D(s)}{D(s)} = \frac{1}{Js + K}$$

where $\Omega_D(s)$ is the Laplace transform of the output speed due to the disturbance torque. For a unit-step disturbance torque, the steady-state output velocity is

$$\begin{aligned}\omega_D(\infty) &= \lim_{s\to 0} s\Omega_D(s) \\ &= \lim_{s\to 0} \frac{s}{Js + K}\frac{1}{s} \\ &= \frac{1}{K}\end{aligned}$$

From this analysis, we conclude that, if a step disturbance torque is applied to the output member of the system, an error speed will result so that the ensuing motor torque will exactly

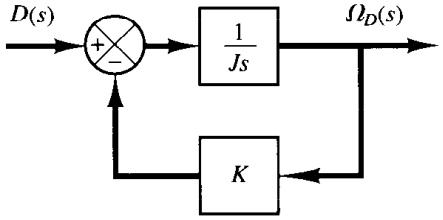

Figure 5–60
Block diagram of the speed control system of Figure 5–59 when $\Omega_r(s) = 0$.

cancel the disturbance torque. To develop this motor torque, it is necessary that there be an error in speed so that nonzero torque will result.

A-5-4. In the system considered in Problem A-5-3, it is desired to eliminate as much as possible the speed errors due to torque disturbances.

Is it possible to cancel the effect of a disturbance torque at steady state so that a constant disturbance torque applied to the output member will cause no speed change at steady state?

Solution. Suppose that we choose a suitable controller whose transfer function is $G_c(s)$, as shown in Figure 5–61. Then in the absence of the reference input the closed-loop transfer function between the output velocity $\Omega_D(s)$ and the disturbance torque $D(s)$ is

$$\frac{\Omega_D(s)}{D(s)} = \frac{\dfrac{1}{Js}}{1 + \dfrac{1}{Js} G_c(s)}$$

$$= \frac{1}{Js + G_c(s)}$$

The steady-state output speed due to a unit-step disturbance torque is

$$\omega_D(\infty) = \lim_{s \to 0} s\Omega_D(s)$$

$$= \lim_{s \to 0} \frac{s}{Js + G_c(s)} \frac{1}{s}$$

$$= \frac{1}{G_c(0)}$$

To satisfy the requirement that

$$\omega_D(\infty) = 0$$

we must choose $G_c(0) = \infty$. This can be realized if we choose

$$G_c(s) = \frac{K}{s}$$

Integral control action will continue to correct until the error is zero. This controller, however, presents a stability problem because the characteristic equation will have two imaginary roots.

One method of stabilizing such a system is to add a proportional mode to the controller or choose

$$G_c(s) = K_p + \frac{K}{s}$$

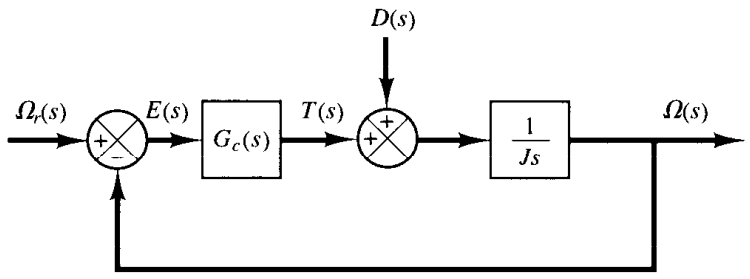

Figure 5–61
Block diagram of a speed control system.

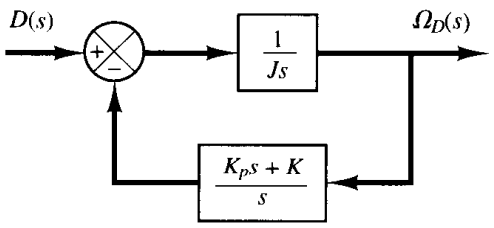

Figure 5–62
Block diagram of the speed control system of Figure 5–61 when $G_c(s) = K_p + (K/s)$ and $\Omega_r(s) = 0$.

With this controller, the block diagram of Figure 5–61 in the absence of the reference input can be modified to that of Figure 5–62. The closed-loop transfer function $\Omega_D(s)/D(s)$ becomes

$$\frac{\Omega_D(s)}{D(s)} = \frac{s}{Js^2 + K_p s + K}$$

For a unit-step disturbance torque, the steady-state output speed is

$$\omega_D(\infty) = \lim_{s\to 0} s\Omega_D(s) = \lim_{s\to 0} \frac{s^2}{Js^2 + K_p s + K}\frac{1}{s} = 0$$

Thus, we see that the proportional-plus-integral controller eliminates speed error at steady state.

The use of integral control action has increased the order of the system by 1. (This tends to produce an oscillatory response.)

In the present system, a step disturbance torque will cause a transient error in the output speed, but the error will become zero at steady state. The integrator provides a nonzero output with zero error. (The nonzero output of the integrator produces a motor torque that exactly cancels the disturbance torque.)

Note that the integrator in the transfer function of the plant does not eliminate the steady-state error due to a step disturbance torque. To eliminate this, we must have an integrator before the point where the disturbance torque enters.

A-5-5. Consider the system shown in Figure 5–63(a). The steady-state error to a unit-ramp input is $e_{ss} = 2\zeta/\omega_n$. Show that the steady-state error for following a ramp input may be eliminated if the input is introduced to the system through a proportional-plus-derivative filter, as shown in Figure 5–63(b), and the value of k is properly set. Note that the error $e(t)$ is given by $r(t) - c(t)$.

Solution. The closed-loop transfer function of the system shown in Figure 5–63(b) is

$$\frac{C(s)}{R(s)} = \frac{(1 + ks)\omega_n^2}{s^2 + 2\zeta\omega_n s + \omega_n^2}$$

Then

$$R(s) - C(s) = \left(\frac{s^2 + 2\zeta\omega_n s - \omega_n^2 ks}{s^2 + 2\zeta\omega_n s + \omega_n^2}\right) R(s)$$

If the input is a unit ramp, then the steady-state error is

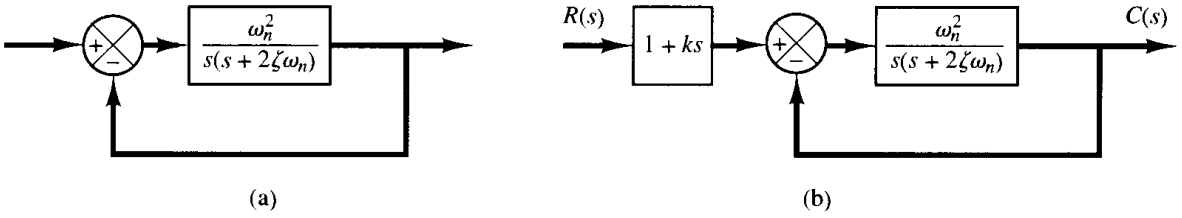

Figure 5–63
(a) Control system; (b) control system with input filter.

$$
\begin{aligned}
e(\infty) &= r(\infty) - c(\infty) \\
&= \lim_{s \to 0} s\left(\frac{s^2 + 2\zeta\omega_n s - \omega_n^2 k s}{s^2 + 2\zeta\omega_n s + \omega_n^2}\right)\frac{1}{s^2} \\
&= \frac{2\zeta\omega_n - \omega_n^2 k}{\omega_n^2}
\end{aligned}
$$

Therefore, if k is chosen as

$$
k = \frac{2\zeta}{\omega_n}
$$

then the steady-state error for following a ramp input can be made equal to zero. Note that, if there are any variations in the values of ζ and/or ω_n due to environmental changes or aging, then a nonzero steady-state error for a ramp response may result.

A-5-6. Consider the liquid-level control system shown in Figure 5–64. Assume that the set point of the controller is fixed. Assuming a step disturbance of magnitude D_0, determine the error. Assume that D_0 is small and the variations in the variables from their respective steady-state values are also small. The controller is proportional.

If the controller is not proportional, but integral, what is the steady-state error?

Solution. Figure 5–65 is a block diagram of the system when the controller is proportional with gain K_p. (We assume the transfer function of the pneumatic valve to be unity.) Since the set point is fixed, the variation in the set point is zero, or $X(s) = 0$. The Laplace transform of $h(t)$ is

$$
H(s) = \frac{K_p R}{RCs + 1}E(s) + \frac{R}{RCs + 1}D(s)
$$

Then

$$
E(s) = -H(s) = -\frac{K_p R}{RCs + 1}E(s) - \frac{R}{RCs + 1}D(s)
$$

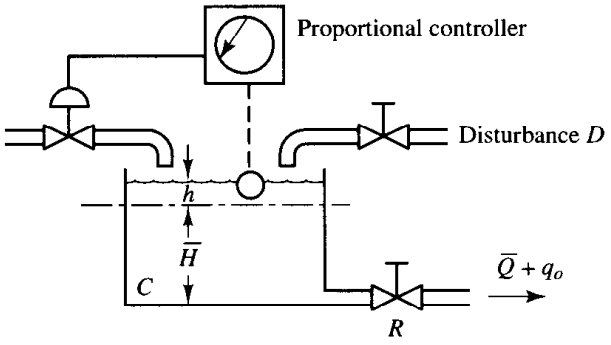

Figure 5–64
Liquid-level control system.

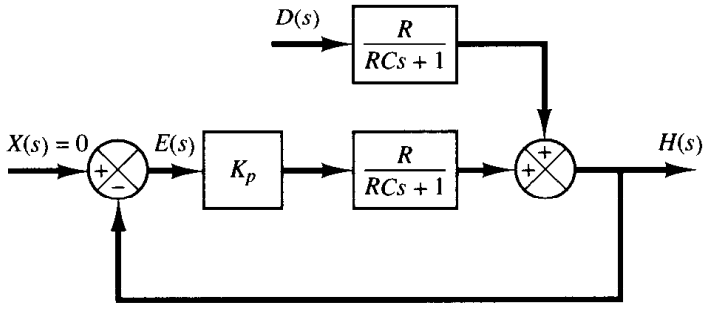

Figure 5–65
Block diagram of the liquid-level control system shown in Figure 5–64.

Hence

$$E(s) = -\frac{R}{RCs + 1 + K_pR} D(s)$$

Since

$$D(s) = \frac{D_0}{s}$$

we obtain

$$E(s) = -\frac{R}{RCs + 1 + K_pR} \frac{D_0}{s}$$

$$= \frac{RD_0}{1 + K_pR} \left(\frac{1}{s + \dfrac{1 + K_pR}{RC}} \right) - \frac{RD_0}{1 + K_pR} \frac{1}{s}$$

The time solution for $t > 0$ is

$$e(t) = \frac{RD_0}{1 + K_pR} \left[\exp\left(-\frac{1 + K_pR}{RC} t \right) - 1 \right]$$

Thus, the time constant is $RC/(1 + K_pR)$. (In the absence of the controller, the time constant is equal to RC.) As the gain of the controller is increased, the time constant is decreased. The steady-state error is

$$e(\infty) = -\frac{RD_0}{1 + K_pR}$$

As the gain K_p of the controller is increased, the steady-state error, or offset, is reduced. Thus, mathematically, the larger the gain K_p is, the smaller the offset and time constant are. In practical systems, however, if the gain K_p of the proportional controller is increased to a very large value, oscillation may result in the output since in our analysis all the small lags and small time constants that may exist in the actual control system are neglected. (If these small lags and time constants are included in the analysis, the transfer function becomes higher order, and for very large values of K_p the possibility of oscillation or even instability may occur.)

If the controller is integral, then assuming the transfer function of the controller to be

$$G_c = \frac{K}{s}$$

we obtain

$$E(s) = -\frac{Rs}{RCs^2 + s + KR} D(s)$$

The steady-state error for a step disturbance $D(s) = D_0/(s)$ is

$$e(\infty) = \lim_{s \to 0} sE(s)$$

$$= \lim_{s \to 0} \frac{-Rs^2}{RCs^2 + s + KR} \frac{D_0}{s}$$

$$= 0$$

Thus, an integral controller eliminates steady-state error or offset due to the step disturbance. (The value of K must be chosen so that the transient response due to the command input and/or disturbance damps out with a reasonable speed.)

A-5-7. Obtain both analytical and computational solutions of the unit-step response of a unity-feedback system whose open-loop transfer function is

$$G(s) = \frac{5(s + 20)}{s(s + 4.59)(s^2 + 3.41s + 16.35)}$$

Solution. The closed-loop transfer function is

$$\frac{C(s)}{R(s)} = \frac{5(s + 20)}{s(s + 4.59)(s^2 + 3.41s + 16.35) + 5(s + 20)}$$

$$= \frac{5s + 100}{s^4 + 8s^3 + 32s^2 + 80s + 100}$$

$$= \frac{5(s + 20)}{(s^2 + 2s + 10)(s^2 + 6s + 10)}$$

The unit-step response of this system is then

$$C(s) = \frac{5(s + 20)}{s(s^2 + 2s + 10)(s^2 + 6s + 10)}$$

$$= \frac{1}{s} + \frac{\frac{3}{8}(s + 1) - \frac{17}{8}}{(s + 1)^2 + 3^2} + \frac{\frac{-11}{8}(s + 3) - \frac{13}{8}}{(s + 3)^2 + 1^2}$$

The time response $c(t)$ can be found by taking the inverse Laplace transform of $C(s)$ as follows:

$$c(t) = 1 + \tfrac{3}{8}e^{-t}\cos 3t - \tfrac{17}{24}e^{-t}\sin 3t - \tfrac{11}{8}e^{-3t}\cos t - \tfrac{13}{8}e^{-3t}\sin t, \qquad \text{for } t \geq 0$$

A MATLAB program to obtain the unit-step response of this system is shown in MATLAB Program 5–2. The resulting unit-step response curve is shown in Figure 5–66.

MATLAB Program 5–2

```
% --------- Unit-step-response ----------

num = [0   0   0   5   100];
den = [1   8   32   80   100];
step(num,den)
grid
title('Unit-Step Response of C(s)/R(s) = (5s + 100)/(s^4 + 8s^3 + 32s^2 + 80s + 100)')
```

A-5-8. Consider the following characteristic equation:

$$s^4 + Ks^3 + s^2 + s + 1 = 0$$

Determine the range of K for stability.

Solution. The Routh array of coefficients is

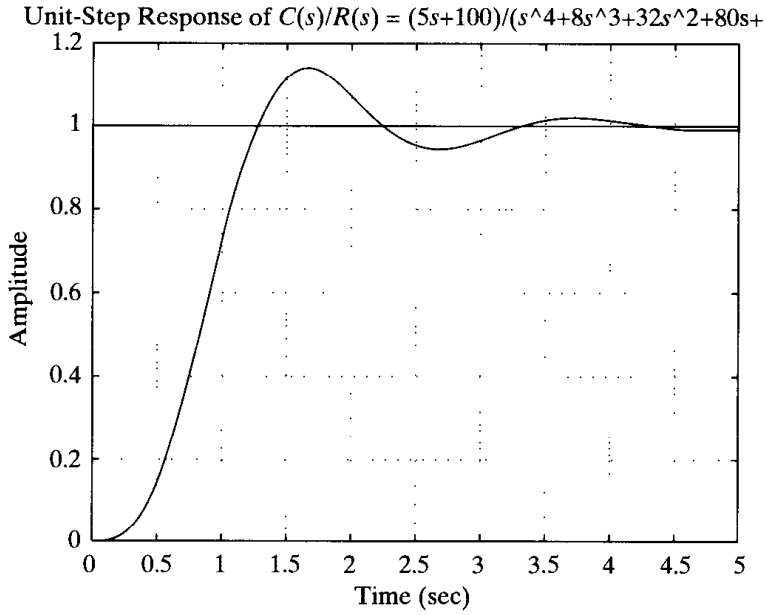

Figure 5–66
Unit-step response curve.

$$\begin{array}{lll} s^4 & 1 & 1 \quad 1 \\ s^3 & K & 1 \quad 0 \\ s^2 & \dfrac{K-1}{K} & 1 \quad 0 \\ s^1 & 1 - \dfrac{K^2}{K-1} & 0 \\ s^0 & 1 & \end{array}$$

For stability, we require that

$$K > 0$$

$$\frac{K-1}{K} > 0$$

$$1 - \frac{K^2}{K-1} > 0$$

From the first and second conditions, K must be greater than 1. For $K > 1$, notice that the term $1 - [K^2/(K-1)]$ is always negative, since

$$\frac{K-1-K^2}{K-1} = \frac{-1+K(1-K)}{K-1} < 0$$

Thus, the three conditions cannot be fulfilled simultaneously. Therefore, there is no value of K that allows stability of the system.

A-5-9. Consider the characteristic equation given by

$$a_0 s^n + a_1 s^{n-1} + a_2 s^{n-2} + \cdots + a_{n-1} s + a_n = 0 \qquad (5\text{–}37)$$

The Hurwitz stability criterion, given next, gives conditions for all the roots to have negative real parts in terms of the coefficients of the polynomial. As stated in the discussions of Routh's stability criterion in Section 5–5, for all the roots to have negative real parts, all the coefficients a's

must be positive. This is a necessary condition but not a sufficient condition. If this condition is not satisfied, it indicates that some of the roots have positive real parts or are imaginary or zero. A sufficient condition for all the roots to have negative real parts is given in the following Hurwitz stability criterion: If all the coefficients of the polynomial are positive, arrange these coefficients in the following determinant:

$$\Delta_n = \begin{vmatrix} a_1 & a_3 & a_5 & \cdots & 0 & 0 & 0 \\ a_0 & a_2 & a_4 & \cdots & \cdot & \cdot & \cdot \\ 0 & a_1 & a_3 & \cdots & a_n & 0 & 0 \\ 0 & a_0 & a_2 & \cdots & a_{n-1} & 0 & 0 \\ \cdot & \cdot & \cdot & & a_{n-2} & a_n & 0 \\ \cdot & \cdot & \cdot & & a_{n-3} & a_{n-1} & 0 \\ 0 & 0 & 0 & \cdots & a_{n-4} & a_{n-2} & a_n \end{vmatrix}$$

where we substituted zero for a_s if $s > n$. For all the roots to have negative real parts, it is necessary and sufficient that successive principal minors of Δ_n be positive. The successive principal minors are the following determinants:

$$\Delta_i = \begin{vmatrix} a_1 & a_3 & \cdots & a_{2i-1} \\ a_0 & a_2 & \cdots & a_{2i-2} \\ 0 & a_1 & \cdots & a_{2i-3} \\ \cdot & \cdot & & \cdot \\ 0 & 0 & \cdots & a_i \end{vmatrix} \qquad (i = 1, 2, \ldots, n-1)$$

where $a_s = 0$ if $s > n$. (It is noted that some of the conditions for the lower-order determinants are included in the conditions for the higher-order determinants.) If all these determinants are positive, and $a_0 > 0$ as already assumed, the equilibrium state of the system whose characteristic equation is given by Equation (5–37) is asymptotically stable. Note that exact values of determinants are not needed; instead, only signs of these determinants are needed for the stability criterion.

Now consider the following characteristic equation:

$$a_0 s^4 + a_1 s^3 + a_2 s^2 + a_3 s + a_4 = 0$$

Obtain the condition for stability using the Hurwitz stability criterion.

Solution. The conditions for stability are that all the a's be positive and that

$$\Delta_2 = \begin{vmatrix} a_1 & a_3 \\ a_0 & a_2 \end{vmatrix} = a_1 a_2 - a_0 a_3 > 0$$

$$\Delta_3 = \begin{vmatrix} a_1 & a_3 & 0 \\ a_0 & a_2 & a_4 \\ 0 & a_1 & a_3 \end{vmatrix}$$

$$= a_1(a_2 a_3 - a_1 a_4) - a_0 a_3^2$$

$$= a_3(a_1 a_2 - a_0 a_3) - a_1^2 a_4 > 0$$

It is clear that, if all the a's are positive and if the condition $\Delta_3 > 0$ is satisfied, the condition $\Delta_2 > 0$ is also satisfied. Therefore, for all the roots of the given characteristic equation to have negative real parts, it is necessary and sufficient that all the coefficients a's are positive and $\Delta_3 > 0$.

A-5-10. Show that the Routh's stability criterion and Hurwitz stability criterion are equivalent.

Solution. If we write Hurwitz determinants in the triangular form

$$\Delta_i = \begin{vmatrix} a_{11} & & & * \\ & a_{22} & & \\ & & \ddots & \\ 0 & & & a_{ii} \end{vmatrix} \qquad (i = 1, 2, \ldots, n)$$

where the elements below the diagonal line are all zeros and the elements above the diagonal line any numbers, then the Hurwitz conditions for asymptotic stability become

$$\Delta_i = a_{11}a_{22} \cdots a_{ii} > 0 \qquad (i = 1, 2, \ldots, n)$$

which are equivalent to the conditions

$$a_{11} > 0, \qquad a_{22} > 0, \qquad \ldots, \qquad a_{nn} > 0$$

We shall show that these conditions are equivalent to

$$a_1 > 0, \qquad b_1 > 0, \qquad c_1 > 0, \qquad \ldots$$

where $a_1, b_1, c_1, \ldots$ are the elements of the first column in the Routh array.

Consider, for example, the following Hurwitz determinant, which corresponds to $n = 4$:

$$\Delta_4 = \begin{vmatrix} a_1 & a_3 & a_5 & a_7 \\ a_0 & a_2 & a_4 & a_6 \\ 0 & a_1 & a_3 & a_5 \\ 0 & a_0 & a_2 & a_4 \end{vmatrix}$$

The determinant is unchanged if we subtract from the ith row k times the jth row. By subtracting from the second row a_0/a_1 times the first row, we obtain

$$\Delta_4 = \begin{vmatrix} a_{11} & a_3 & a_5 & a_7 \\ 0 & a_{22} & a_{23} & a_{24} \\ 0 & a_1 & a_3 & a_5 \\ 0 & a_0 & a_2 & a_4 \end{vmatrix}$$

where

$$a_{11} = a_1$$

$$a_{22} = a_2 - \frac{a_0}{a_1} a_3$$

$$a_{23} = a_4 - \frac{a_0}{a_1} a_5$$

$$a_{24} = a_6 - \frac{a_0}{a_1} a_7$$

Similarly, subtracting from the fourth row a_0/a_1 times the third row yields

$$\Delta_4 = \begin{vmatrix} a_{11} & a_3 & a_5 & a_7 \\ 0 & a_{22} & a_{23} & a_{24} \\ 0 & a_1 & a_3 & a_5 \\ 0 & 0 & \hat{a}_{43} & \hat{a}_{44} \end{vmatrix}$$

where

$$\hat{a}_{43} = a_2 - \frac{a_0}{a_1} a_3$$

$$\hat{a}_{44} = a_4 - \frac{a_0}{a_1} a_5$$

Next, subtracting from the third row a_1/a_{22} times the second row yields

$$\Delta_4 = \begin{vmatrix} a_{11} & a_3 & a_5 & a_7 \\ 0 & a_{22} & a_{23} & a_{24} \\ 0 & 0 & a_{33} & a_{34} \\ 0 & 0 & \hat{a}_{43} & \hat{a}_{44} \end{vmatrix}$$

where

$$a_{33} = a_3 - \frac{a_1}{a_{22}} a_{23}$$

$$a_{34} = a_5 - \frac{a_1}{a_{22}} a_{24}$$

Finally, subtracting from the last row $\hat{a}_{43}/a_{33}$ times the third row yields

$$\Delta_4 = \begin{vmatrix} a_{11} & a_3 & a_5 & a_7 \\ 0 & a_{22} & a_{23} & a_{24} \\ 0 & 0 & a_{33} & a_{34} \\ 0 & 0 & 0 & a_{44} \end{vmatrix}$$

where

$$a_{44} = \hat{a}_{44} - \frac{\hat{a}_{43}}{a_{33}} a_{34}$$

From this analysis, we see that

$$\Delta_4 = a_{11}a_{22}a_{33}a_{44}$$

$$\Delta_3 = a_{11}a_{22}a_{33}$$

$$\Delta_2 = a_{11}a_{22}$$

$$\Delta_1 = a_{11}$$

The Hurwitz conditions for asymptotic stability

$$\Delta_1 > 0, \qquad \Delta_2 > 0, \qquad \Delta_3 > 0, \qquad \Delta_4 > 0, \qquad \ldots$$

reduce to the conditions

$$a_{11} > 0, \qquad a_{22} > 0, \qquad a_{33} > 0, \qquad a_{44} > 0, \qquad \ldots$$

The Routh array for the polynomial

$$a_0 s^4 + a_1 s^3 + a_2 s^2 + a_3 s + a_4 = 0$$

where $a_0 > 0$, is given by

$$\begin{array}{llll} a_0 & a_2 & a_4 \\ a_1 & a_3 \\ b_1 & b_2 \\ c_1 \\ d_1 \end{array}$$

From this Routh array, we see that

$$a_{11} = a_1$$

$$a_{22} = a_2 - \frac{a_0}{a_1} a_3 = b_1$$

$$a_{33} = a_3 - \frac{a_1}{a_{22}} a_{23} = \frac{a_3 b_1 - a_1 b_2}{b_1} = c_1$$

$$a_{44} = \hat{a}_{44} - \frac{\hat{a}_{43}}{a_{33}} a_{34} = \frac{b_2 c_1 - b_1 c_2}{c_1} = d_1$$

Hence the Hurwitz conditions for asymptotic stability become

$$a_1 > 0, \qquad b_1 > 0, \qquad c_1 > 0, \qquad d_1 > 0, \qquad \ldots$$

Thus we have demonstrated that Hurwitz conditions for asymptotic stability can be reduced to Routh's conditions for asymptotic stability. The same argument can be extended to Hurwitz determinants of any order, and the equivalence of Routh's stability criterion and Hurwitz stability criterion can be established.

A-5-11. Show that the first column of the Routh array of

$$s^n + a_1 s^{n-1} + a_2 s^{n-2} + \cdots + a_{n-1} s + a_n = 0$$

is given by

$$1, \qquad \Delta_1, \qquad \frac{\Delta_2}{\Delta_1}, \qquad \frac{\Delta_3}{\Delta_2}, \qquad \ldots, \qquad \frac{\Delta_n}{\Delta_{n-1}}$$

where

$$\Delta_r = \begin{vmatrix} a_1 & 1 & 0 & 0 & \cdots & 0 \\ a_3 & a_2 & a_1 & 1 & \cdots & 0 \\ a_5 & a_4 & a_3 & a_2 & \cdots & 0 \\ \cdot & \cdot & \cdot & \cdot & & \cdot \\ \cdot & \cdot & \cdot & \cdot & & \cdot \\ \cdot & \cdot & \cdot & \cdot & & \cdot \\ a_{2r-1} & \cdot & \cdot & \cdot & \cdots & a_r \end{vmatrix}$$

$$a_k = 0 \qquad \text{if } k > n$$

Solution. The Routh array of coefficients has the form

$$
\begin{array}{ccccccc}
1 & a_2 & a_4 & a_6 & \cdots & a_n \\
a_1 & a_3 & a_5 & \cdots & & \\
b_1 & b_2 & b_3 & \cdots & & \\
c_1 & c_2 & . & & & \\
. & . & . & & & \\
. & . & . & & & \\
. & . & . & & &
\end{array}
$$

The first term in the first column of the Routh array is 1. The next term in the first column is a_1, which is equal to Δ_1. The next term is b_1, which is equal to

$$\frac{a_1a_2 - a_3}{a_1} = \frac{\Delta_2}{\Delta_1}$$

The next term in the first column is c_1, which is equal to

$$\frac{b_1a_3 - a_1b_2}{b_1} = \frac{\left[\frac{a_1a_2 - a_3}{a_1}\right]a_3 - a_1\left[\frac{a_1a_4 - a_5}{a_1}\right]}{\left[\frac{a_1a_2 - a_3}{a_1}\right]}$$

$$= \frac{a_1a_2a_3 - a_3^2 - a_1^2a_4 + a_1a_5}{a_1a_2 - a_3}$$

$$= \frac{\Delta_3}{\Delta_2}$$

In a similar manner the remaining terms in the first column of the Routh array can be found.

The Routh array has the property that the last nonzero terms of any columns are the same; that is, if the array is given by

$$
\begin{array}{cccc}
a_0 & a_2 & a_4 & a_6 \\
a_1 & a_3 & a_5 & a_7 \\
b_1 & b_2 & b_3 & \\
c_1 & c_2 & c_3 & \\
d_1 & d_2 & & \\
e_1 & e_2 & & \\
f_1 & & & \\
g_1 & & &
\end{array}
$$

then

$$a_7 = c_3 = e_2 = g_1$$

and if the array is given by

$$
\begin{array}{cccc}
a_0 & a_2 & a_4 & a_6 \\
a_1 & a_3 & a_5 & 0 \\
b_1 & b_2 & b_3 & \\
c_1 & c_2 & 0 & \\
d_1 & d_2 & & \\
e_1 & 0 & & \\
f_1 & & &
\end{array}
$$

then

$$a_6 = b_3 = d_2 = f_1$$

In any case, the last term of the first column is equal to a_n, or

$$a_n = \frac{\Delta_{n-1} a_n}{\Delta_{n-1}} = \frac{\Delta_n}{\Delta_{n-1}}$$

For example, if $n = 4$, then

$$\Delta_4 = \begin{vmatrix} a_1 & 1 & 0 & 0 \\ a_3 & a_2 & a_1 & 1 \\ a_5 & a_4 & a_3 & a_2 \\ a_7 & a_6 & a_5 & a_4 \end{vmatrix} = \begin{vmatrix} a_1 & 1 & 0 & 0 \\ a_3 & a_2 & a_1 & 1 \\ 0 & a_4 & a_3 & a_2 \\ 0 & 0 & 0 & a_4 \end{vmatrix} = \Delta_3 a_4$$

Thus it has been shown that the first column of the Routh array is given by

$$1, \quad \Delta_1, \quad \frac{\Delta_2}{\Delta_1}, \quad \frac{\Delta_3}{\Delta_2}, \quad \ldots, \quad \frac{\Delta_n}{\Delta_{n-1}}$$

A-5-12. The value of the gas constant for any gas may be determined from accurate experimental observations of simultaneous values of p, v, and T.

Obtain the gas constant R_{air} for air. Note that at 32°F and 14.7 psia the specific volume of air is 12.39 ft³/lb. Then obtain the capacitance of a 20-ft³ pressure vessel that contains air at 160°F. Assume that the expansion process is isothermal.

Solntion.

$$R_{air} = \frac{pv}{T} = \frac{14.7 \times 144 \times 12.39}{460 + 32} = 53.3 \text{ ft-lb}_f/\text{lb °R}$$

Referring to Equation (5–12), the capacitance of a 20-ft³ pressure vessel is

$$C = \frac{V}{nR_{air}T} = \frac{20}{1 \times 53.3 \times 620} = 6.05 \times 10^{-4} \frac{\text{lb}}{\text{lb}_f/\text{ft}^2}$$

Note that in terms of SI units, R_{air} is given by

$$R_{air} = 287 \text{ N-m/kg K}$$

A-5-13. Figure 5–67 is a schematic diagram of a pneumatic diaphragm valve. At steady state the control pressure from a controller is $\bar{P}_c$, the pressure in the valve is also $\bar{P}_c$, and the valve-stem displacement is $\bar{X}$. Assume that at $t = 0$ the control pressure is changed from $\bar{P}_c$ to $\bar{P}_c + p_c$. Then the valve pressure will be changed from $\bar{P}_c$ to $\bar{P}_c + p_v$. The change in valve pressure p_v will cause the valve-stem displacement to change from $\bar{X}$ to $\bar{X} + x$. Find the transfer function between the change in valve-stem displacement x and the change in control pressure p_c.

Solntion. Let us define the airflow rate to the diaphragm valve through resistance R as q. Then

$$q = \frac{p_c - p_v}{R}$$

For the air chamber in the diaphragm valve, we have

$$C\, dp_v = q\, dt$$

Consequently,

$$C \frac{dp_v}{dt} = q = \frac{p_c - p_v}{R}$$

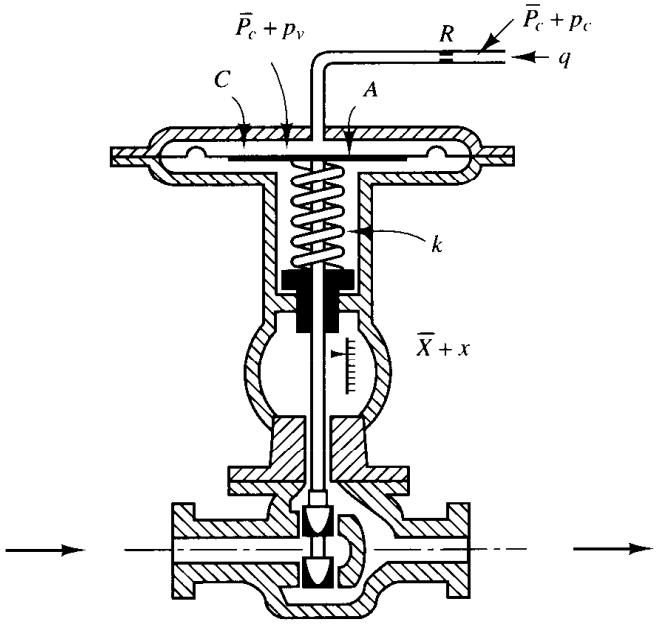

Figure 5–67
Pneumatic diaphragm valve.

from which

$$RC\frac{dp_v}{dt} + p_v = p_c$$

Noting that

$$Ap_v = kx$$

we have

$$\frac{k}{A}\left(RC\frac{dx}{dt} + x\right) = p_c$$

The transfer function between x and p_c is

$$\frac{X(s)}{P_c(s)} = \frac{A/k}{RCs + 1}$$

A-5-14. In the pneumatic pressure system of Figure 5–68(a), assume that, for $t < 0$, the system is at steady state and that the pressure of the entire system is $\bar{P}$. Also, assume that the two bellows are identical. At $t = 0$, the input pressure is changed from $\bar{P}$ to $\bar{P} + p_i$. Then the pressures in bellows 1 and 2 will change from $\bar{P}$ to $\bar{P} + p_1$ and from $\bar{P}$ to $\bar{P} + p_2$, respectively. The capacity (volume) of each bellows is 5×10^{-4} m^3, and the operating pressure difference Δp (difference between p_i and p_1 or difference between p_i and p_2) is between -0.5×10^5 N/m^2 and 0.5×10^5 N/m^2. The corresponding mass flow rates (kg/sec) through the valves are shown in Figure 5–68(b). Assume that the bellows expand or contract linearly with the air pressures applied to them, that the equivalent spring constant of the bellows system is $k = 1 \times 10^5$ N/m, and that each bellows has area $A = 15 \times 10^{-4}$ m^2.

Defining the displacement of the midpoint of the rod that connects two bellows as x, find the transfer function $X(s)/P_i(s)$. Assume that the expansion process is isothermal and that the temperature of the entire system stays at 30°C.

Solution. Referring to Section 5–6, transfer function $P_1(s)/P_i(s)$ can be obtained as

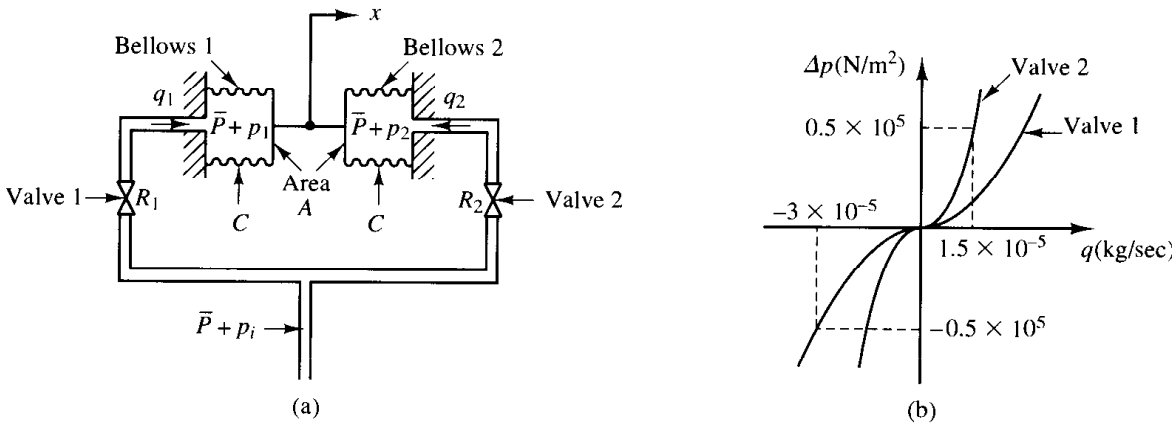

Figure 5–68
(a) Pneumatic pressure system; (b) pressure difference versus mass flow rate curve.

$$\frac{P_1(s)}{P_i(s)} = \frac{1}{R_1Cs + 1} \tag{5–38}$$

Similarly, transfer function $P_2(s)/P_i(s)$ is

$$\frac{P_2(s)}{P_i(s)} = \frac{1}{R_2Cs + 1} \tag{5–39}$$

The force acting on bellows 1 in the x direction is $A(\bar{P} + p_1)$, and the force acting on bellows 2 in the negative x direction is $A(\bar{P} + p_2)$. The resultant force balances with kx, the equivalent spring force of the corrugated side of the bellows.

$$A(p_1 - p_2) = kx$$

or

$$A[P_1(s) - P_2(s)] = kX(s) \tag{5–40}$$

Referring to Equations (5–38) and (5–39), we see that

$$P_1(s) - P_2(s) = \left(\frac{1}{R_1Cs + 1} - \frac{1}{R_2Cs + 1}\right) P_i(s)$$

$$= \frac{R_2Cs - R_1Cs}{(R_1Cs + 1)(R_2Cs + 1)} P_i(s)$$

By substituting this last equation into Equation (5–40) and rewriting, the transfer function $X(s)/P_i(s)$ is obtained as

$$\frac{X(s)}{P_i(s)} = \frac{A}{k} \frac{(R_2C - R_1C)s}{(R_1Cs + 1)(R_2Cs + 1)} \tag{5–41}$$

The numerical values of average resistances R_1 and R_2 are

$$R_1 = \frac{d\,\Delta p}{dq_1} = \frac{0.5 \times 10^5}{3 \times 10^{-5}} = 0.167 \times 10^{10} \frac{\text{N/m}^2}{\text{kg/sec}}$$

$$R_2 = \frac{d\,\Delta p}{dq_2} = \frac{0.5 \times 10^5}{1.5 \times 10^{-5}} = 0.333 \times 10^{10} \frac{\text{N/m}^2}{\text{kg/sec}}$$

The numerical value of capacitance C of each bellows is

$$C = \frac{V}{nR_{\text{air}}T} = \frac{5 \times 10^{-4}}{1 \times 287 \times (273 + 30)} = 5.75 \times 10^{-9} \frac{\text{kg}}{\text{N/m}^2}$$

where R_{air} = 287 N-m/kg K. (See Problem A-5-12.) Consequently,

$$R_1C = 0.167 \times 10^{10} \times 5.75 \times 10^{-9} = 9.60 \text{ sec}$$

$$R_2C = 0.333 \times 10^{10} \times 5.75 \times 10^{-9} = 19.2 \text{ sec}$$

By substituting the numerical values for A, k, R_1C, and R_2C into Equation (5–41), we obtain

$$\frac{X(s)}{P_i(s)} = \frac{1.44 \times 10^{-7} s}{(9.6s + 1)(19.2s + 1)}$$

A-5-15. Draw a block diagram of the pneumatic controller shown in Figure 5–69. Then derive the transfer function of this controller.

If the resistance R_d is removed (replaced by the line-sized tubing), what control action do we get? If the resistance R_i is removed (replaced by the line-sized tubing), what control action do we get?

Solution. Let us assume that when $e = 0$ the nozzle–flapper distance is equal to $\bar{X}$ and the control pressure is equal to $\bar{P}_c$. In the present analysis, we shall assume small deviations from the respective reference values as follows:

e = small error signal

x = small change in the nozzle-flapper distance

p_c = small change in the control pressure

p_I = small pressure change in bellows I due to small change in the control pressure

p_{II} = small pressure change in bellows II due to small change in the control pressure

y = small displacement at the lower end of the flapper

In this controller, p_c is transmitted to bellows I through the resistance R_d. Similarly, p_c is transmitted to bellows II through the series of resistances R_d and R_i. An approximate relationship between p_I and p_c is

$$\frac{P_I(s)}{P_c(s)} = \frac{1}{R_dCs + 1} = \frac{1}{T_ds + 1}$$

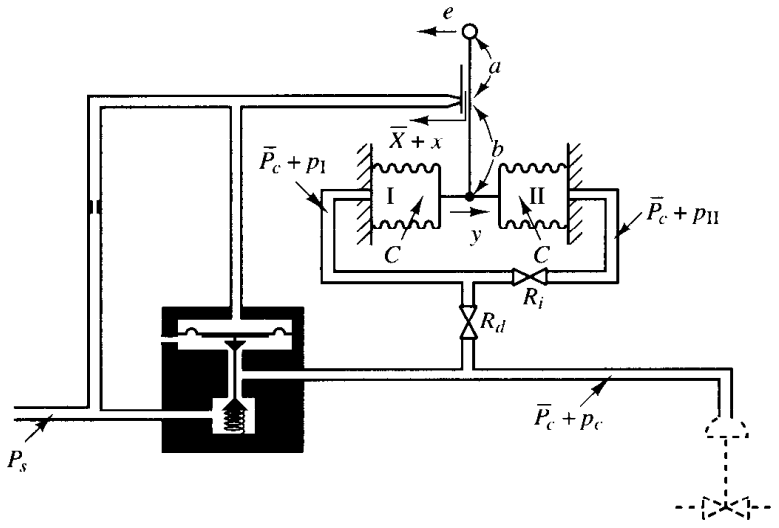

Figure 5–69
Schematic diagram of a pneumatic controller.

where $T_d = R_dC$ = derivative time. Similarly, p_{II} and p_I are related by the transfer function

$$\frac{P_{II}(s)}{P_I(s)} = \frac{1}{R_iCs + 1} = \frac{1}{T_is + 1}$$

where $T_i = R_iC$ = integral time. The force–balance equation for the two bellows is

$$(p_I - p_{II})A = k_s y$$

where k_s is the stiffness of the two connected bellows and A is the cross-sectional area of the bellows. The relationship among the variables e, x, and y is

$$x = \frac{b}{a + b}e - \frac{a}{a + b}y$$

The relationship between p_c and x is

$$p_c = Kx \qquad (K > 0)$$

From the equations just derived, a block diagram of the controller can be drawn, as shown in Figure 5–70(a). Simplification of this block diagram results in Figure 5–70(b).

The transfer function between $P_c(s)$ and $E(s)$ is

$$\frac{P_c(s)}{E(s)} = \frac{\dfrac{b}{a + b}K}{1 + K\dfrac{a}{a + b}\dfrac{A}{k_s}\left(\dfrac{T_is}{T_is + 1}\right)\left(\dfrac{1}{T_ds + 1}\right)}$$

For a practical controller, under normal operation $KaAT_is/[(a + b)k_s(T_is + 1)(T_ds + 1)]$ is very much greater than unity and $T_i \gg T_d$. Therefore, the transfer function can be simplified as follows:

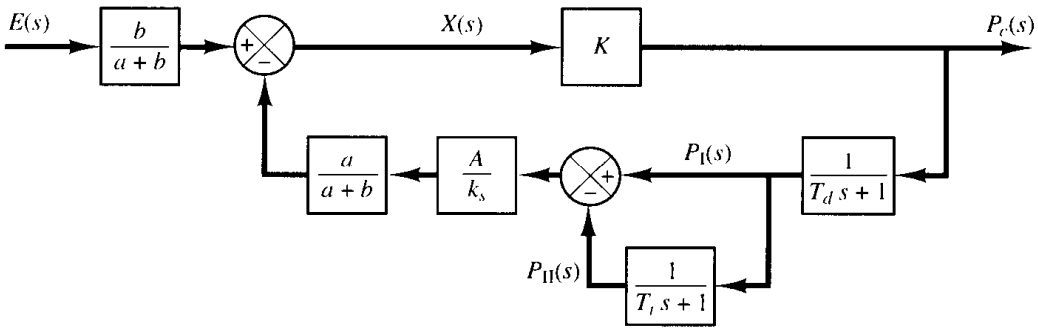

(a)

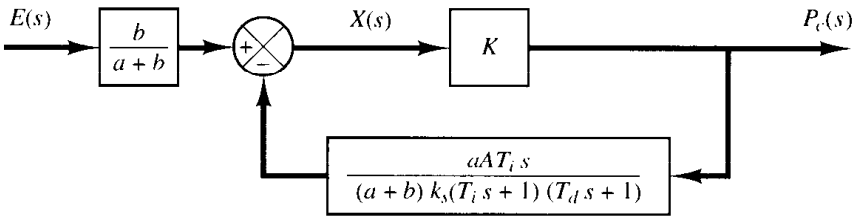

(b)

Figure 5–70
(a) Block diagram of the pneumatic controller shown in Figure 5–69; (b) simplified block diagram.

$$\frac{P_c(s)}{E(s)} \doteqdot \frac{bk_s(T_i s + 1)(T_d s + 1)}{aAT_i s}$$

$$= \frac{bk_s}{aA}\left(\frac{T_i + T_d}{T_i} + \frac{1}{T_i s} + T_d s\right)$$

$$\doteqdot K_p\left(1 + \frac{1}{T_i s} + T_d s\right)$$

where

$$K_p = \frac{bk_s}{aA}$$

Thus the controller shown in Figure 5–69 is a proportional-plus-integral-plus-derivative one.

If the resistance R_d is removed, or $R_d = 0$, the action becomes that of a proportional-plus-integral controller.

If the resistance R_i is removed, or $R_i = 0$, the action becomes that of a narrow-band proportional, or two-position, controller. (Note that the actions of two feedback bellows cancel each other, and there is no feedback.)

A-5-16. Actual spool valves are either overlapped or underlapped because of manufacturing tolerances. Consider the overlapped and underlapped spool valves shown in Figure 5–71(a) and (b). Sketch curves relating the uncovered port area A versus displacement x.

Solution. For the overlapped valve, a dead zone exists between $-\frac{1}{2}x_0$ and $\frac{1}{2}x_0$, or $-\frac{1}{2}x_0 < x < \frac{1}{2}x_0$. The uncovered port area A versus displacement x curve is shown in Figure 5–72(a). Such an overlapped valve is unfit as a control valve.

For the underlapped valve, the port area A versus displacement x curve is shown in Figure 5–72(b). The effective curve for the underlapped region has a higher slope, meaning a higher sensitivity. Valves used for controls are usually underlapped.

A-5-17. Figure 5–73 shows a hydraulic jet-pipe controller. Hydraulic fluid is ejected from the jet pipe. If the jet pipe is shifted to the right from the neutral position, the power piston moves to the left, and vice versa. The jet pipe valve is not used as much as the flapper valve because of large null flow, slower response, and rather unpredictable characteristics. Its main advantage lies in its insensitivity to dirty fluids.

Suppose that the power piston is connected to a light load so that the inertia force of the load element is negligible compared to the hydraulic force developed by the power piston. What type of control action does this controller produce?

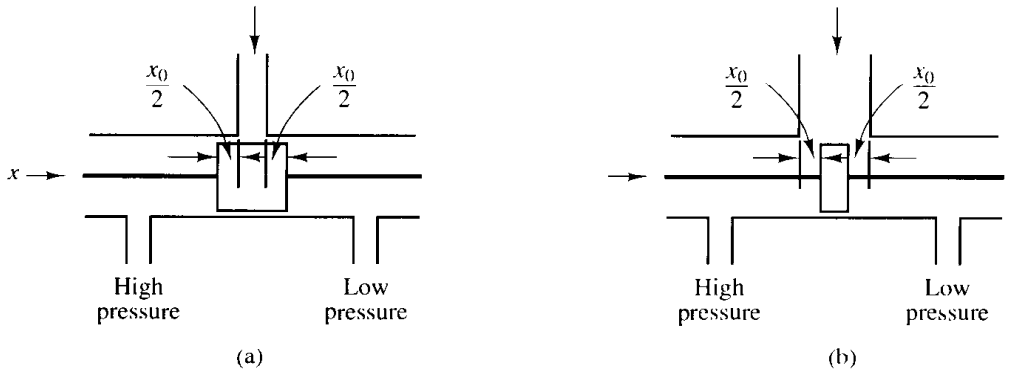

Figure 5–71
(a) Overlapped spool valve; (b) underlapped spool valve.

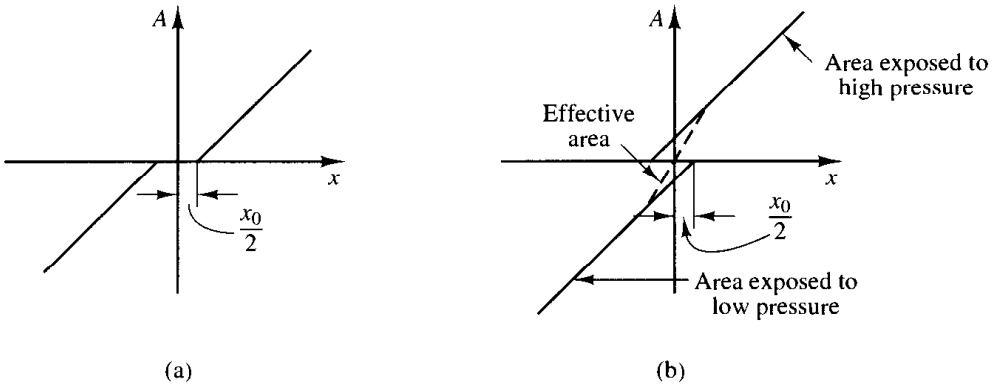

Figure 5–72
(a) Uncovered port area A versus displacement x curve for the overlapped valve; (b) uncovered port area A versus displacement x curve for the underlapped valve.

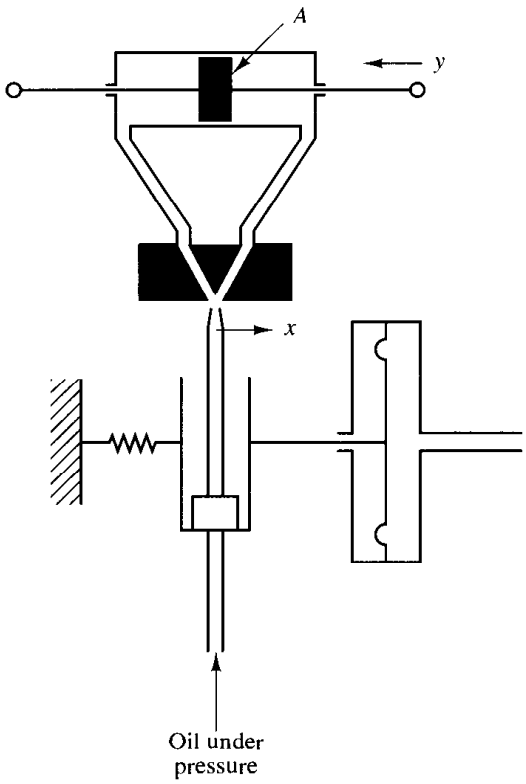

Figure 5–73
Hydraulic jet-pipe controller.

Solution. Define the displacement of the jet nozzle from the neutral position as x and the displacement of the power piston as y. If the jet nozzle is moved to the right by a small displacement x, the oil flows to the right side of the power piston, and the oil in the left side of the power piston is returned to the drain. The oil flowing into the power cylinder is at high pressure; the oil flowing out from the power cylinder into the drain is at low pressure. The resulting pressure difference causes the power piston to move to the left.

For a small jet nozzle displacement x, the flow rate q to the power cylinder is proportional to x; that is,

$$q = K_1 x$$

For the power cylinder,

$$A\rho\, dy = q\, dt$$

where A is the power piston area and ρ is the density of oil. Hence

$$\frac{dy}{dt} = \frac{q}{A\rho} = \frac{K_1}{A\rho}x = Kx$$

where $K = K_1/(A\rho)$ = constant. The transfer function $Y(s)/X(s)$ is thus

$$\frac{Y(s)}{X(s)} = \frac{K}{s}$$

The controller produces the integral control action.

A-5-18. Figure 5–74 shows a hydraulic jet-pipe applied to a flow control system. The jet-pipe controller governs the position of the butterfly valve. Discuss the operation of this system. Plot a possible curve relating the displacement x of the nozzle to the total force F acting on the power piston.

Solution. The operation of this system is as follows: The flow rate is measured by the orifice, and the pressure difference produced by this orifice is transmitted to the diaphragm of the pressure-measuring device. The diaphragm is connected to the free swinging nozzle, or jet pipe, through a linkage. High-pressure oil ejects from the nozzle all the time. When the nozzle is at a neutral position, no oil flows through either of the pipes to move the power piston. If the nozzle is displaced by the motion of the balance arm to one side, the high-pressure oil flows through the corresponding pipe, and the oil in the power cylinder flows back to the sump through the other pipe.

Assume that the system is initially at rest. If the reference input is changed suddenly to a higher flow rate, then the nozzle is moved in such a direction as to move the power piston and open the butterfly valve. Then the flow rate will increase, the pressure difference across the orifice becomes larger, and the nozzle will move back to the neutral position. The movement of the power piston stops when x, the displacement of the nozzle, comes back to and stays at the neutral position. (The jet pipe controller thus possesses an integrating property.)

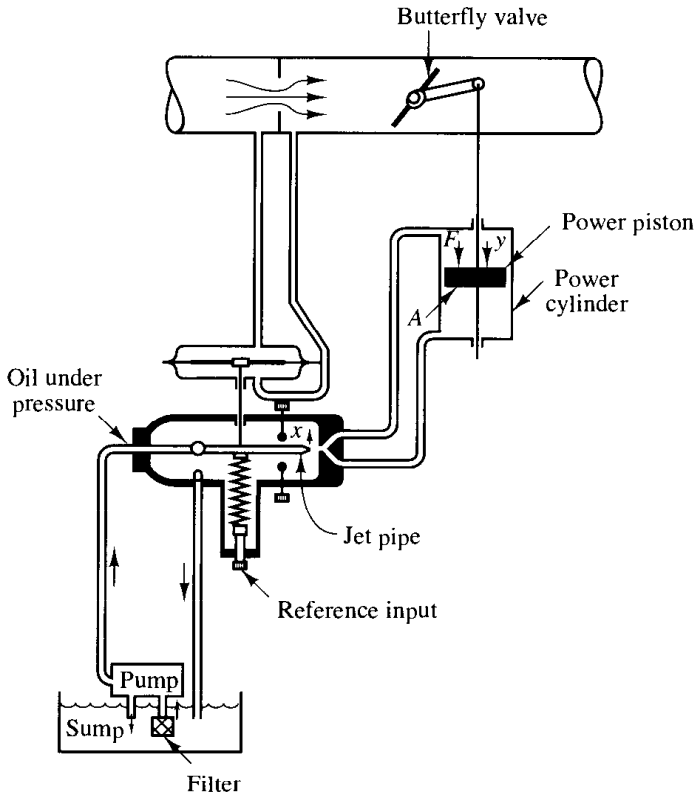

Figure 5–74
Schematic diagram of a flow control system using a hydraulic jet-pipe controller.

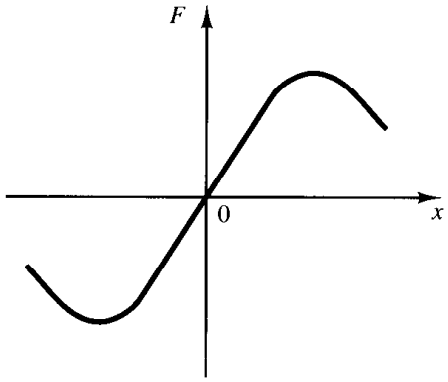

Figure 5–75
Force versus diplacement curve.

The relationship between the total force F acting on the power piston and the displacement x of the nozzle is shown in Figure 5–75. The total force is equal to the pressure difference ΔP across the piston times the area A of the power piston. For a small displacement x of the nozzle, the total force F and displacement x may be considered proportional.

A-5-19. Explain the operation of the speed control system shown in Figure 5–76.

Solution. If the engine speed increases, the sleeve of the fly-ball governor moves upward. This movement acts as the input to the hydraulic controller. A positive error signal (upward motion of the sleeve) causes the power piston to move downward, reduces the fuel-valve opening, and decreases the engine speed. A block diagram for the system is shown in Figure 5–77.

From the block diagram the transfer function $Y(s)/E(s)$ can be obtained as

$$\frac{Y(s)}{E(s)} = \frac{a_2}{a_1 + a_2} \frac{\dfrac{K}{s}}{1 + \dfrac{a_1}{a_1 + a_2} \dfrac{bs}{bs + k} \dfrac{K}{s}}$$

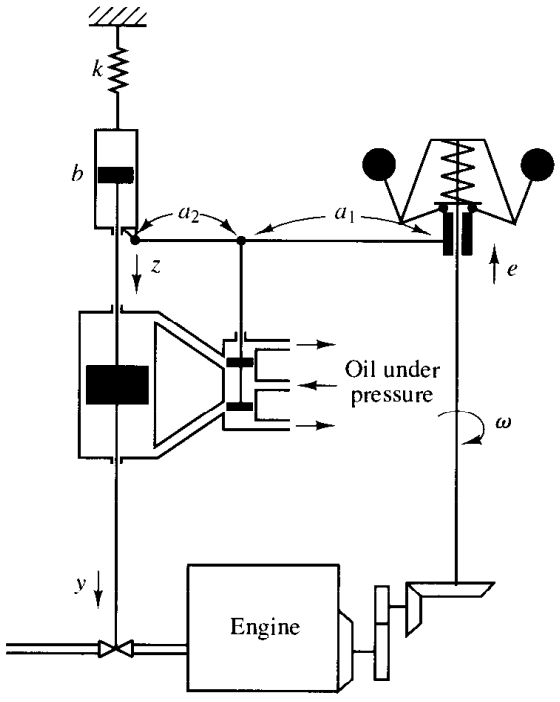

Figure 5–76
Speed control system.

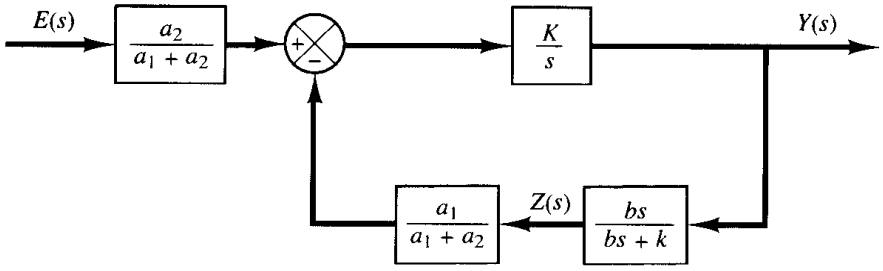

Figure 5–77
Block diagram for the speed control system shown in Figure 5–76.

If the following condition applies,

$$\left| \frac{a_1}{a_1 + a_2} \frac{bs}{bs + k} \frac{K}{s} \right| \gg 1$$

the transfer function $Y(s)/E(s)$ becomes

$$\frac{Y(s)}{E(s)} \doteq \frac{a_2}{a_1 + a_2} \frac{a_1 + a_2}{a_1} \frac{bs + k}{bs} = \frac{a_2}{a_1}\left(1 + \frac{k}{bs}\right)$$

The speed controller has proportional-plus-integral control action.

A-5-20. Consider the hydraulic servo system shown in Figure 5–78. Assuming that signal $e(t)$ is the input and power piston displacement $y(t)$ the output, find the transfer function $Y(s)/E(s)$.

Solution. A block diagram for the system can be drawn as shown in Figure 5–79. Assuming that $|K_1a_1/[s(a_1 + a_2)]| \gg 1$ and $|K_2b_1/[s(b_1 + b_2)]| \gg 1$, we obtain

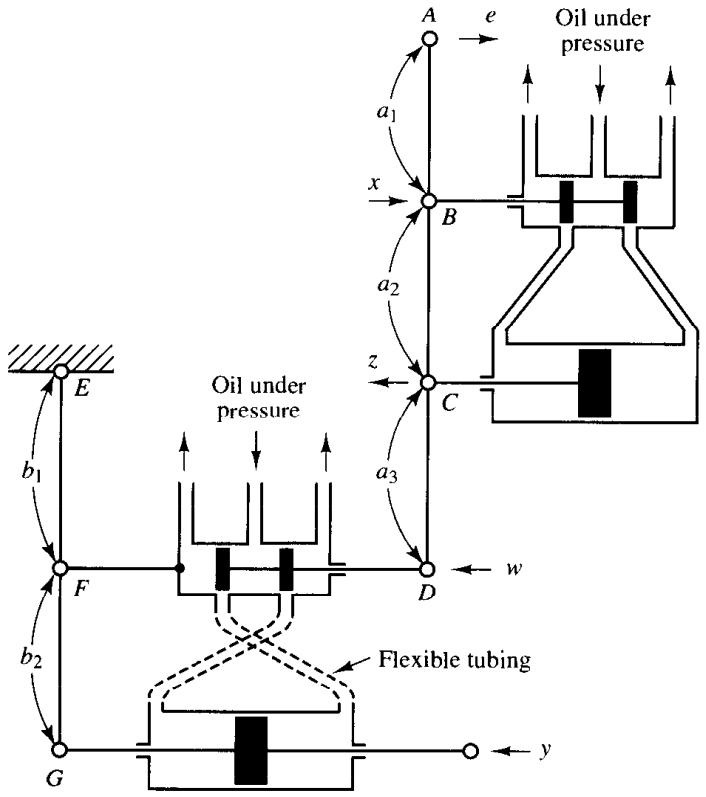

Figure 5–78
Hydraulic servo system.

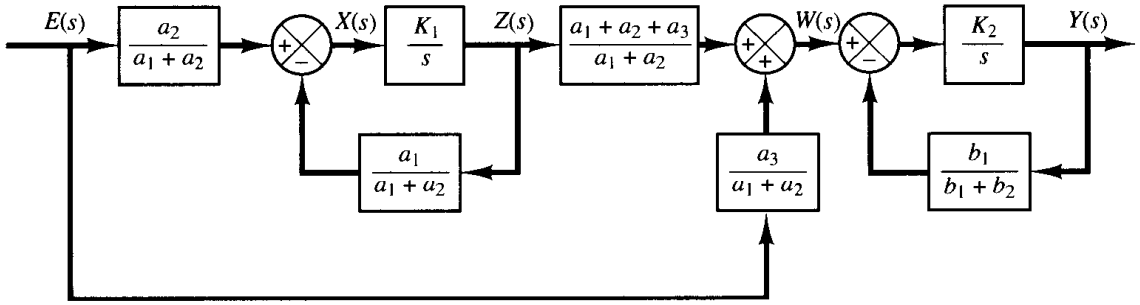

Figure 5–79
Block diagram for the system shown in Figure 5–78.

$$\frac{Z(s)}{E(s)} = \frac{\dfrac{a_2}{a_1 + a_2} \cdot \dfrac{K_1}{s}}{1 + \dfrac{K_1}{s} \cdot \dfrac{a_1}{a_1 + a_2}} \doteq \frac{a_2}{a_1 + a_2} \cdot \frac{a_1 + a_2}{a_1} = \frac{a_2}{a_1}$$

$$\frac{W(s)}{E(s)} = \frac{a_1 + a_2 + a_3}{a_1 + a_2} \cdot \frac{Z(s)}{E(s)} + \frac{a_3}{a_1 + a_2} = \frac{a_2 + a_3}{a_1}$$

$$\frac{Y(s)}{W(s)} = \frac{\dfrac{K_2}{s}}{1 + \dfrac{b_1}{b_1 + b_2} \dfrac{K_2}{s}} \doteq \frac{b_1 + b_2}{b_1}$$

Hence

$$\frac{Y(s)}{E(s)} = \frac{Y(s)}{W(s)} \cdot \frac{W(s)}{E(s)} = \frac{(a_2 + a_3)(b_1 + b_2)}{a_1 b_1}$$

This servo system is a proportional controller.

A-5-21. Obtain the transfer function $E_o(s)/E_i(s)$ of the op-amp circuit shown in Figure 5–80.

Solution. Define the voltage at point A as e_A. Then

$$\frac{E_A(s)}{E_i(s)} = \frac{R_1}{\dfrac{1}{Cs} + R_1} = \frac{R_1 Cs}{R_1 Cs + 1}$$

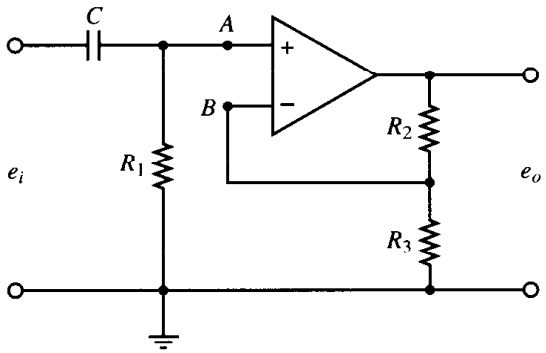

Figure 5–80
Operational-amplifier circuit.

Define the voltage at point B as e_B. Then

$$E_B(s) = \frac{R_3}{R_2 + R_3} E_o(s)$$

Noting that

$$[E_A(s) - E_B(s)]K = E_o(s)$$

and $K \gg 1$, we must have

$$E_A(s) = E_B(s)$$

Hence

$$E_A(s) = \frac{R_1 Cs}{R_1 Cs + 1} E_i(s) = E_B(s) = \frac{R_3}{R_2 + R_3} E_o(s)$$

from which we obtain

$$\frac{E_o(s)}{E_i(s)} = \frac{R_2 + R_3}{R_3} \frac{R_1 Cs}{R_1 Cs + 1} = \frac{\left(1 + \dfrac{R_2}{R_3}\right)s}{s + \dfrac{1}{R_1 C}}$$

A-5-22. Obtain the transfer function $E_o(s)/E_i(s)$ of the op-amp circuit shown in Figure 5–81.

Solution. The voltage at point A is

$$e_A = \frac{1}{2}(e_i - e_o) + e_o$$

The Laplace-transformed version of this last equation is

$$E_A(s) = \frac{1}{2}[E_i(s) + E_o(s)]$$

The voltage at point B is

$$E_B(s) = \frac{\dfrac{1}{Cs}}{R_2 + \dfrac{1}{Cs}} E_i(s) = \frac{1}{R_2 Cs + 1} E_i(s)$$

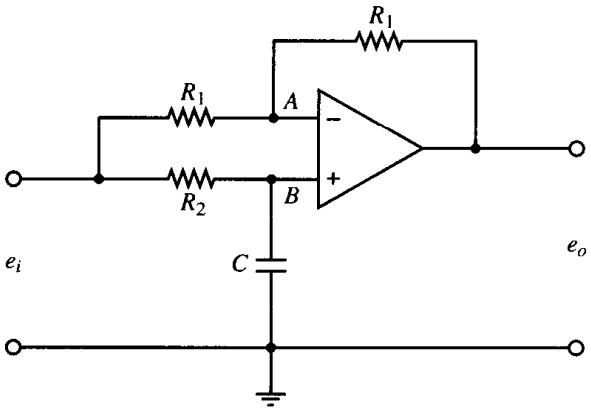

Figure 5–81
Operational-amplifier circuit.

Since $[E_B(s) - E_A(s)]K = E_o(s)$ and $K \gg 1$, we must have $E_A(s) = E_B(s)$. Thus

$$\frac{1}{2}[E_i(s) + E_o(s)] = \frac{1}{R_2Cs + 1}E_i(s)$$

Hence

$$\frac{E_o(s)}{E_i(s)} = -\frac{R_2Cs - 1}{R_2Cs + 1} = -\frac{s - \dfrac{1}{R_2C}}{s + \dfrac{1}{R_2C}}$$

A-5-23. Consider the stable unity-feedback control system with feedforward transfer function $G(s)$. Suppose that the closed-loop transfer function can be written

$$\frac{C(s)}{R(s)} = \frac{G(s)}{1 + G(s)} = \frac{(T_as + 1)(T_bs + 1)\cdots(T_ms + 1)}{(T_1s + 1)(T_2s + 1)\cdots(T_ns + 1)} \qquad (m \leq n)$$

Show that

$$\int_0^\infty e(t)\,dt = (T_1 + T_2 + \cdots + T_n) - (T_a + T_b + \cdots + T_m)$$

where $e(t)$ is the error in the unit-step response. Show also that

$$\frac{1}{\lim\limits_{s\to 0} sG(s)} = (T_1 + T_2 + \cdots + T_n) - (T_a + T_b + \cdots + T_m)$$

Solution. Let us define

$$(T_as + 1)(T_bs + 1)\cdots(T_ms + 1) = P(s)$$

and

$$(T_1s + 1)(T_2s + 1)\cdots(T_ns + 1) = Q(s)$$

Then

$$\frac{C(s)}{R(s)} = \frac{P(s)}{Q(s)}$$

and

$$E(s) = \frac{Q(s) - P(s)}{Q(s)}R(s)$$

For a unit-step input, $R(s) = 1/s$ and

$$E(s) = \frac{Q(s) - P(s)}{sQ(s)}$$

Since the system is stable, $\int_0^\infty e(t)\,dt$ converges to a constant value. Referring to Table 2–2 (item 9), we have

$$\int_0^\infty e(t)\,dt = \lim_{s\to 0} s\frac{E(s)}{s} = \lim_{s\to 0} E(s)$$

Hence

$$\int_0^\infty e(t)\,dt = \lim_{s\to 0} \frac{Q(s) - P(s)}{sQ(s)}$$

$$= \lim_{s\to 0} \frac{Q'(s) - P'(s)}{Q(s) + sQ'(s)}$$

$$= \lim_{s\to 0} [Q'(s) - P'(s)]$$

Since

$$\lim_{s\to 0} P'(s) = T_a + T_b + \cdots + T_m$$

$$\lim_{s\to 0} Q'(s) = T_1 + T_2 + \cdots + T_n$$

we have

$$\int_0^\infty e(t)\,dt = (T_1 + T_2 + \cdots + T_n) - (T_a + T_b + \cdots + T_m)$$

For a unit-step input $r(t)$, since

$$\int_0^\infty e(t)\,dt = \lim_{s\to 0} E(s) = \lim_{s\to 0} \frac{1}{1 + G(s)} R(s) = \lim_{s\to 0} \frac{1}{1 + G(s)} \frac{1}{s} = \frac{1}{\lim_{s\to 0} sG(s)} = \frac{1}{K_v}$$

we have

$$\frac{1}{\lim_{s\to 0} sG(s)} = (T_1 + T_2 + \cdots + T_n) - (T_a + T_b + \cdots + T_m)$$

Note that zeros in the left half-plane (that is, positive $T_a, T_b, \ldots, T_m$) will improve K_v. Poles close to the origin cause low velocity-error constants unless there are zeros nearby.

PROBLEMS

B-5-1. If the feedforward path of a control system contains at least one integrating element, then the output continues to change as long as an error is present. The output stops when the error is precisely zero. If an external disturbance enters the system, it is desirable to have an integrating element between the error-measuring element and the point where the disturbance enters so that the effect of the external disturbance may be made zero at steady state.

Show that, if the disturbance is a ramp function, then the steady-state error due to this ramp disturbance may be eliminated only if two integrators precede the point where the disturbance enters.

B-5-2. Consider industrial automatic controllers whose control actions are proportional, integral, proportional-plus-integral, proportional-plus-derivative, and proportional-plus-integral-plus-derivative. The transfer functions of these controllers can be given, respectively, by

$$\frac{U(s)}{E(s)} = K_p$$

$$\frac{U(s)}{E(s)} = \frac{K_i}{s}$$

$$\frac{U(s)}{E(s)} = K_p\left(1 + \frac{1}{T_i s}\right)$$

$$\frac{U(s)}{E(s)} = K_p(1 + T_d s)$$

$$\frac{U(s)}{E(s)} = K_p\left(1 + \frac{1}{T_i s} + T_d s\right)$$

where $U(s)$ is the Laplace transform of $u(t)$, the controller output, and $E(s)$ the Laplace transform of $e(t)$, the actuating error signal. Sketch $u(t)$ versus t curves for each of the five types of controllers when the actuating error signal is

(a) $e(t)$ = unit-step function

(b) $e(t)$ = unit-ramp function

In sketching curves, assume that the numerical values of K_p, K_i, T_i, and T_d are given as

K_p = proportional gain = 4

K_i = integral gain = 2

T_i = integral time = 2 sec

T_d = derivative time = 0.8 sec

B-5-3. Consider a unity-feedback control system whose open-loop transfer function is

$$G(s) = \frac{K}{s(Js + B)}$$

Discuss the effects that varying the values of K and B has on the steady-state error in unit-ramp response. Sketch typical unit-ramp response curves for a small value, medium value, and large value of K.

B-5-4. Figure 5–82 shows three systems. System I is a positional servo system. System II is a positional servo system with PD control action. System III is a positional servo system with velocity feedback. Compare the unit-step, unit-impulse, and unit-ramp responses of the three systems. Which system is best with respect to the speed of response and maximum overshoot in the step response?

B-5-5. Consider the position control system shown in Figure 5–83. Write a MATLAB program to obtain a unit-step response and a unit-ramp response of the system. Plot curves $x_1(t)$ versus t, $x_2(t)$ versus t, $x_3(t)$ versus t, and $e(t)$ versus t [where $e(t) = r(t) - x_1(t)$] for both the unit-step response and the unit-ramp response.

B-5-6. Determine the range of K for stability of a unity-feedback control system whose open-loop transfer function is

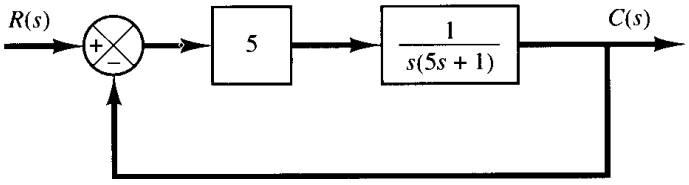

System I

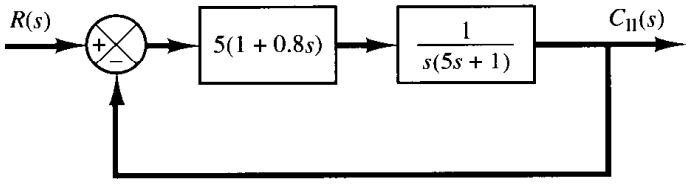

System II

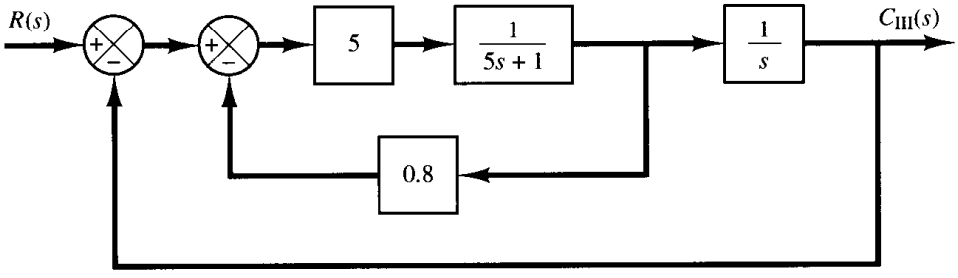

System III

Figure 5–82
(a) Positional servo system; (b) positional servo system with PD control action; (c) positional servo system with velocity feedback.

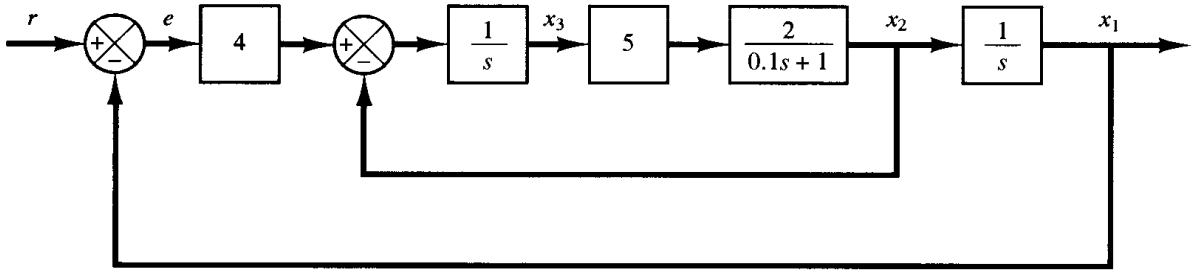

Figure 5–83
Position control system.

$$G(s) = \frac{K}{s(s + 1)(s + 2)}$$

B-5-7. Consider the unity-feedback control system with the following open-loop transfer function:

$$G(s) = \frac{10}{s(s - 1)(2s + 3)}$$

Is this system stable?

B-5-8. Consider the system

$$\dot{\mathbf{x}} = \mathbf{A}\mathbf{x}$$

where matrix **A** is given by

$$\mathbf{A} = \begin{bmatrix} 0 & 1 & 0 \\ -b_3 & 0 & 1 \\ 0 & -b_2 & -b_1 \end{bmatrix}$$

(**A** is called Schwarz matrix.) Show that the first column of the Routh's array of the characteristic equation $|s\mathbf{I} - \mathbf{A}| = 0$ consists of $1, b_1, b_2$, and $b_1 b_3$.

B-5-9. Consider the pneumatic system shown in Figure 5–84. Obtain the transfer function $X(s)/P_i(s)$.

B-5-10. Figure 5–85 shows a pneumatic controller. What kind of control action does this controller produce? Derive the transfer function $P_c(s)/E(s)$.

B-5-11. Consider the pneumatic controller shown in Figure 5–86. Assuming that the pneumatic relay has the characteristics that $p_c = Kp_b$ (where $K > 0$), determine the control action of this controller. The input to the controller is e and the output is p_c.

B-5-12. Figure 5–87 shows a pneumatic controller. The signal e is the input and the change in the control pressure p_c is the output. Obtain the transfer function $P_c(s)/E(s)$. Assume that the pneumatic relay has the characteristics that $p_c = Kp_b$, where $K > 0$.

B-5-13. Consider the pneumatic controller shown in Figure 5–88. What control action does this controller produce? Assume that the pneumatic relay has the characteristics that $p_c = Kp_b$, where $K > 0$.

B-5-14. Figure 5–89 shows an electric-pneumatic transducer. Show that the change in the output pressure is proportional to the change in the input current.

B-5-15. Figure 5–90 shows a flapper valve. It is placed between two opposing nozzles. If the flapper is moved slightly to the right, the pressure unbalance occurs in the nozzles and the power piston moves to the left, and vice versa. Such a device is frequently used in hydraulic servos as the first-stage valve in two-stage servovalves. This usage occurs because considerable force may be needed to stroke larger spool valves that result from the steady-state flow force. To reduce or compensate this force, two-stage valve configuration is often employed; a flapper valve or jet pipe is used as the first-stage valve to provide a necessary force to stroke the second-stage spool valve.

Figure 5–91 shows a schematic diagram of a hydraulic servomotor in which the error signal is amplified in two stages using a jet pipe and a pilot valve. Draw a block diagram of the system of Figure 5–91 and then find the trans-

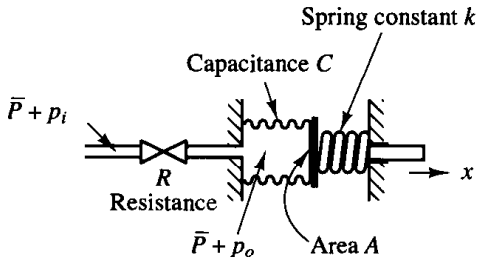

Figure 5–84
Pneumatic system.

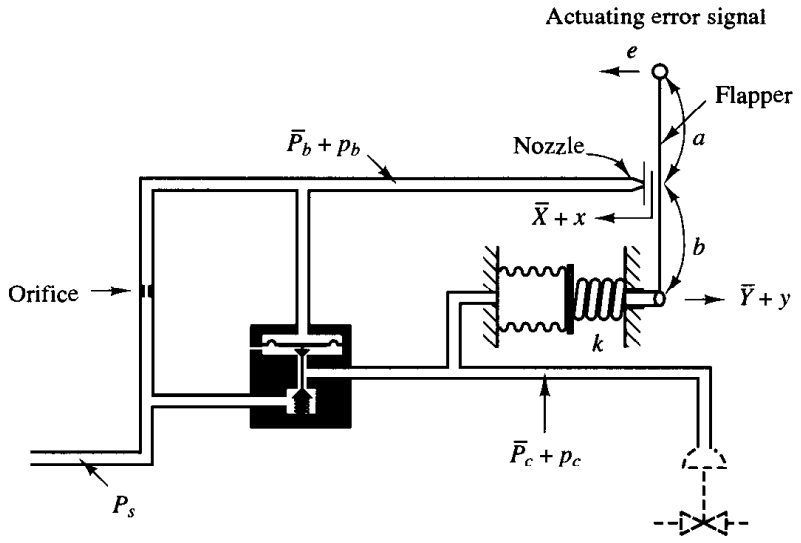

Figure 5–85
Pneumatic controller.

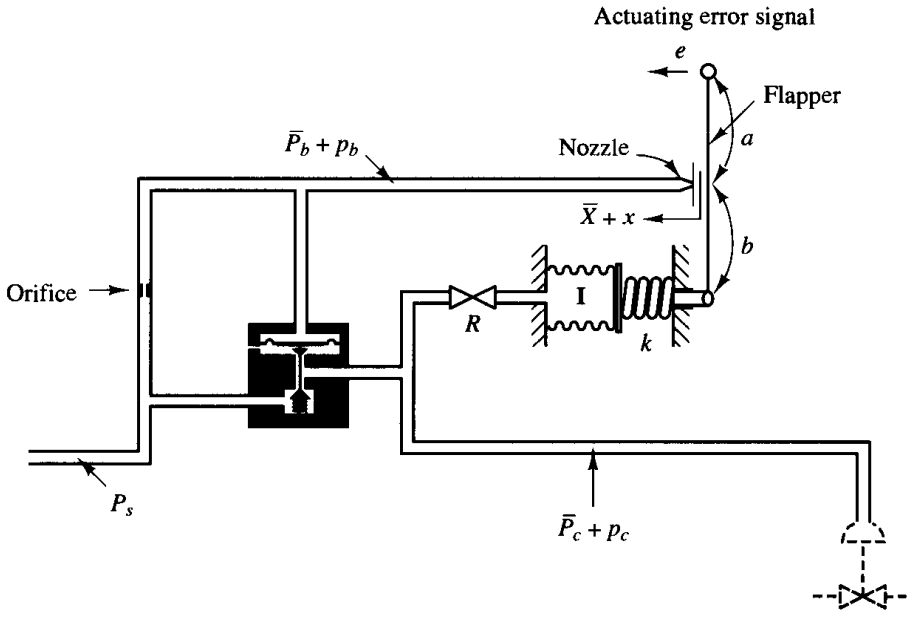

Figure 5–86
Pneumatic controller.

fer function between y and x, where x is the air pressure and y is the displacement of the power piston.

B-5-16. Figure 5–92 is a schematic diagram of an aircraft elevator control system. The input to the system is the deflection angle θ of the control lever, and the output is the elevator angle ϕ. Assume that angles θ and ϕ are relatively small. Show that for each angle θ of the control lever there is a corresponding (steady-state) elevator angle ϕ.

B-5-17. Consider the controller shown in Figure 5–93. The input is the air pressure p_i and the output is the displacement y of the power piston. Obtain the transfer function $Y(s)/P_i(s)$.

B-5-18. Obtain the transfer function $E_o(s)/E_i(s)$ of the op-amp circuit shown in Figure 5–94.

B-5-19. Obtain the transfer function $E_o(s)/E_i(s)$ of the op-amp circuit shown in Figure 5–95.

B-5-20. Consider a unity-feedback control system with the closed-loop transfer function

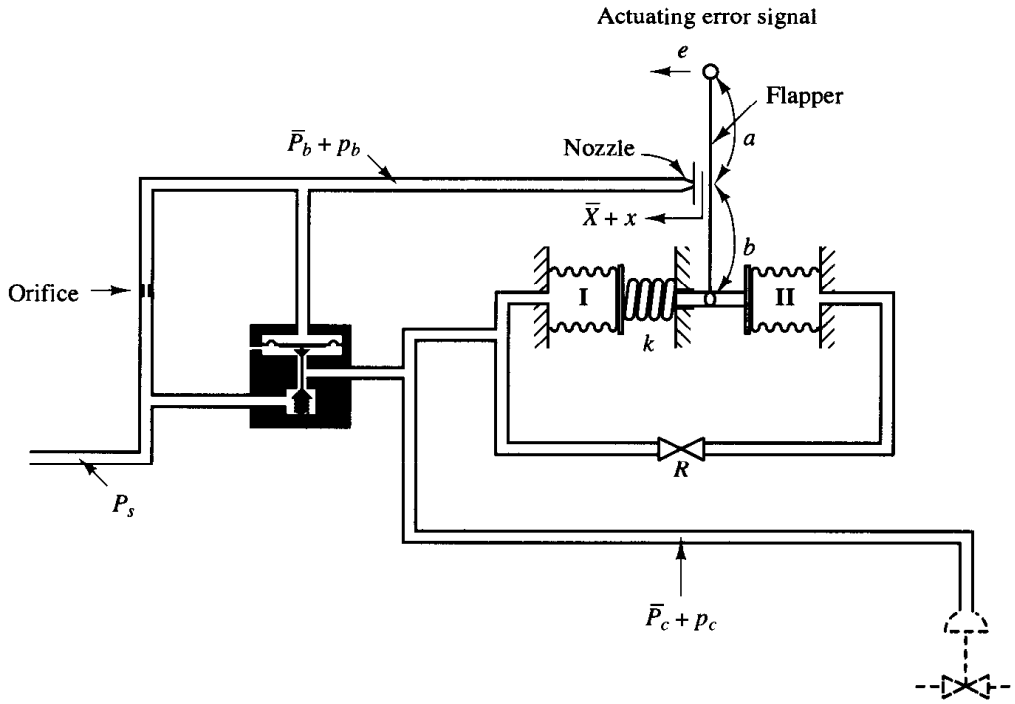

Figure 5–87
Pneumatic controller.

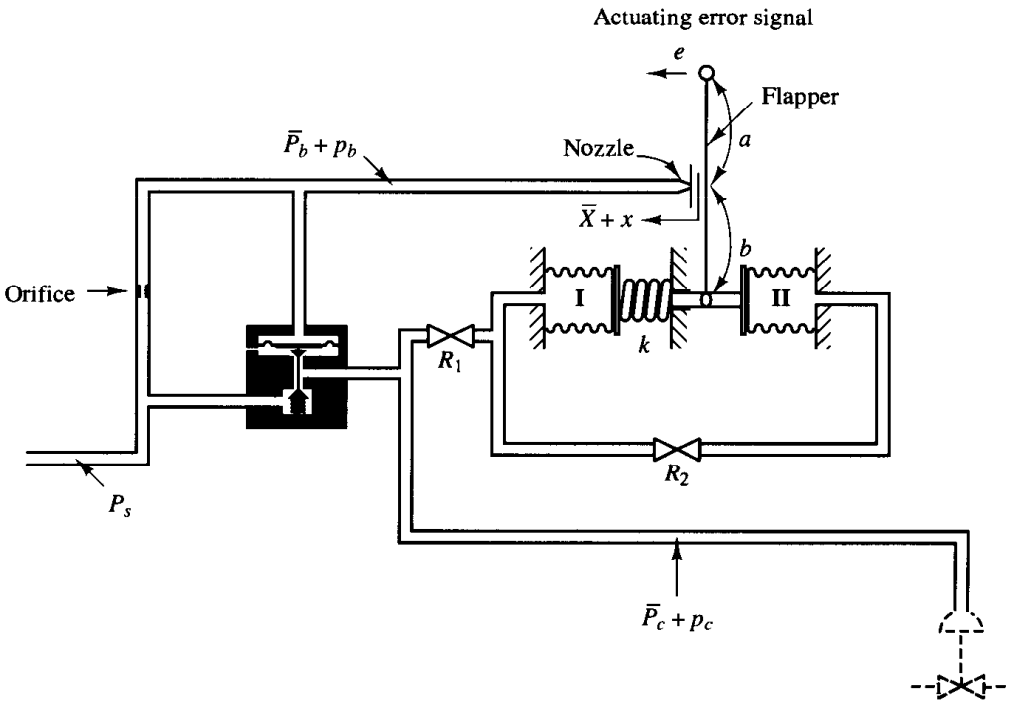

Figure 5–88
Pneumatic controller.

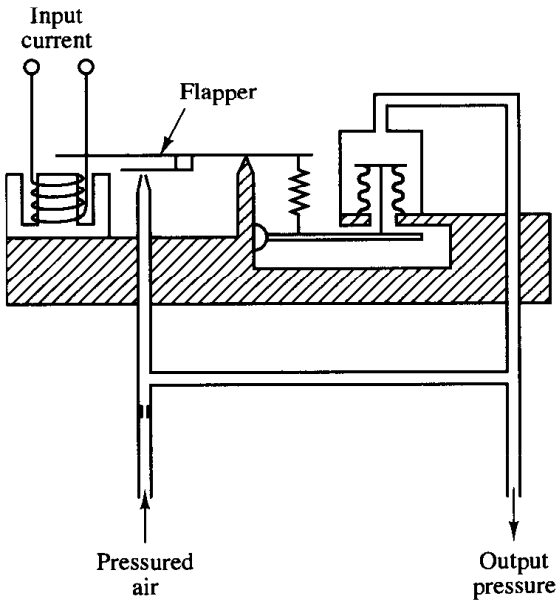

Figure 5–89
Electric-pneumatic transducer.

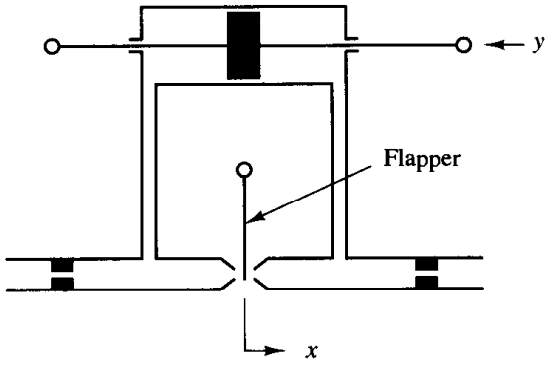

Figure 5–90
Flapper valve.

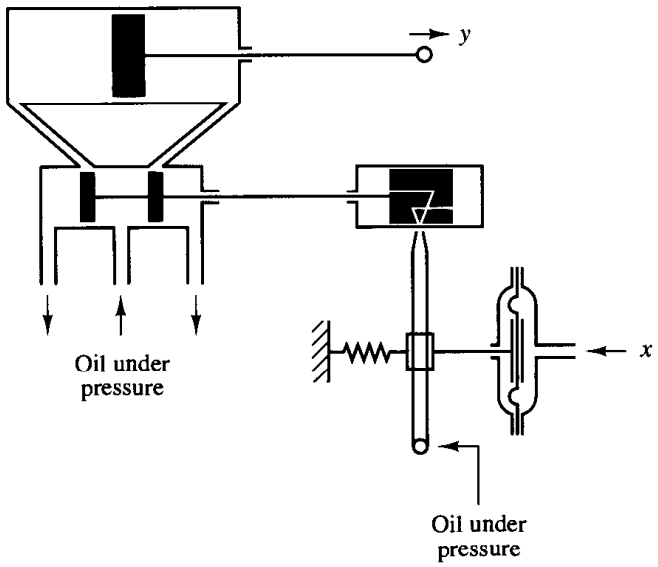

Figure 5–91
Schematic diagram of a hydraulic servomotor.

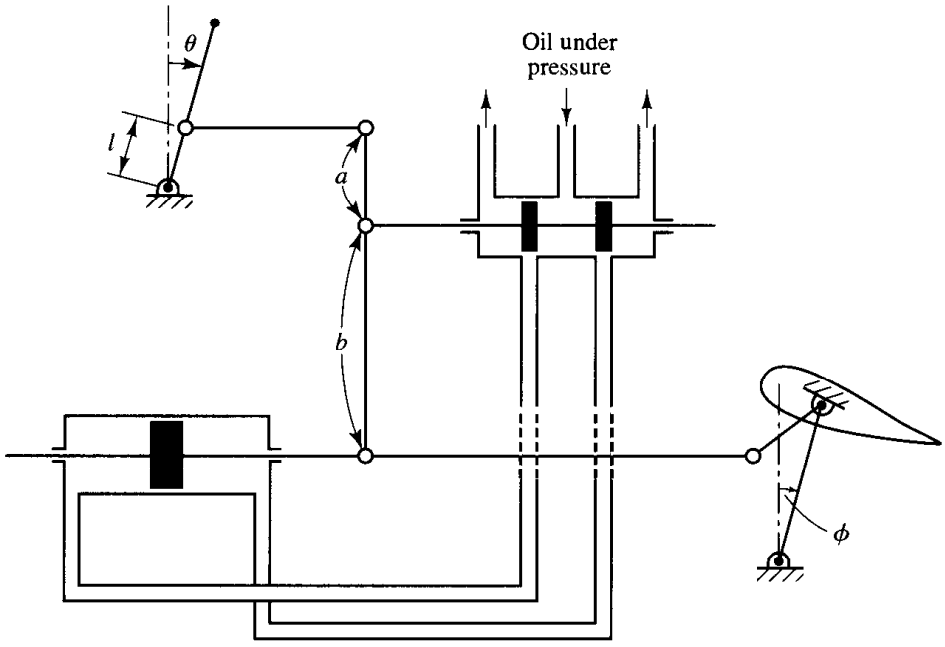

Figure 5–92
Aircraft elevator control system.

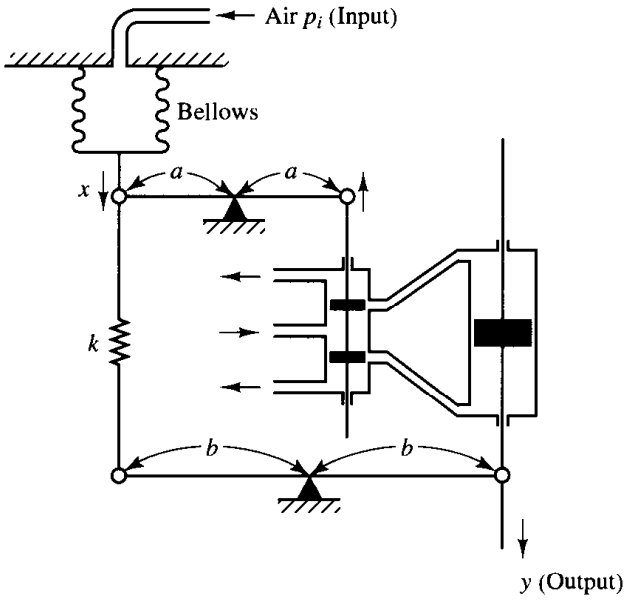

Figure 5–93
Controller.

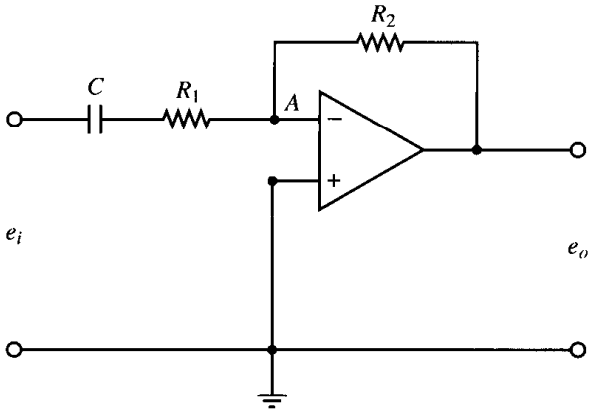

Figure 5–94
Operational-amplifier circuit.

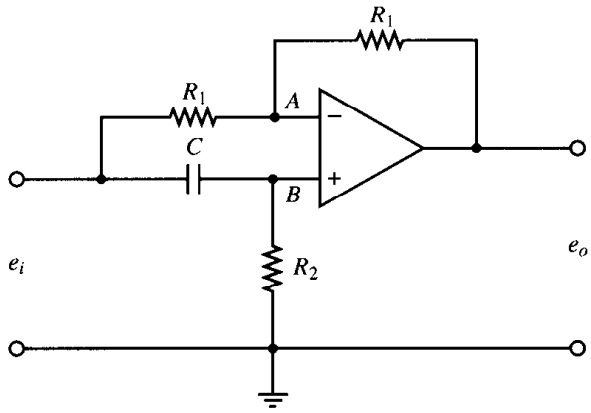

Figure 5–95
Operational amplifier circuit.

$$\frac{C(s)}{R(s)} = \frac{Ks + b}{s^2 + as + b}$$

Determine the open-loop transfer function $G(s)$.

Show that the steady-state error in the unit-ramp response is given by

$$e_{ss} = \frac{1}{K_v} = \frac{a - K}{b}$$

B-5-21. Show that the steady-state error in the response to ramp inputs can be made zero if the closed-loop transfer function is given by

$$\frac{C(s)}{R(s)} = \frac{a_{n-1}s + a_n}{s^n + a_1 s^{n-1} + \cdots + a_{n-1}s + a_n}$$

6

Root-Locus Analysis

6-1 INTRODUCTION

The basic characteristic of the transient response of a closed-loop system is closely related to the location of the closed-loop poles. If the system has a variable loop gain, then the location of the closed-loop poles depends on the value of the loop gain chosen. It is important, therefore, that the designer know how the closed-loop poles move in the s plane as the loop gain is varied.

From the design viewpoint, in some systems simple gain adjustment may move the closed-loop poles to desired locations. Then the design problem may become the selection of an appropriate gain value. If the gain adjustment alone does not yield a desired result, addition of a compensator to the system will become necessary. (This subject is discussed in detail in Chapter 7.)

The closed-loop poles are the roots of the characteristic equation. Finding the roots of the characteristic equation of degree higher than 3 is laborious and will need computer solution. (MATLAB provides a simple solution to this problem.) However, just finding the roots of the characteristic equation may be of limited value, because as the gain of the open-loop transfer function varies the characteristic equation changes and the computations must be repeated.

A simple method for finding the roots of the characteristic equation has been developed by W. R. Evans and used extensively in control engineering. This method, called the *root-locus method,* is one in which the roots of the characteristic equation are plotted for all values of a system parameter. The roots corresponding to a particular value of this parameter can then be located on the resulting graph. Note that the parameter

is usually the gain, but any other variable of the open-loop transfer function may be used. Unless otherwise stated, we shall assume that the gain of the open-loop transfer function is the parameter to be varied through all values, from zero to infinity.

By using the root-locus method the designer can predict the effects on the location of the closed-loop poles of varying the gain value or adding open-loop poles and/or open-loop zeros. Therefore, it is desired that the designer have a good understanding of the method for generating the root loci of the closed-loop system, both by hand and by use of a computer software like MATLAB.

Root-locus method. The basic idea behind the root-locus method is that the values of s that make the transfer function around the loop equal -1 must satisfy the characteristic equation of the system.

The locus of roots of the characteristic equation of the closed-loop system as the gain is varied from zero to infinity gives the method its name. Such a plot clearly shows the contributions of each open-loop pole or zero to the locations of the closed-loop poles.

In designing a linear control system, we find that the root-locus method proves quite useful since it indicates the manner in which the open-loop poles and zeros should be modified so that the response meets system performance specifications. This method is particularly suited to obtaining approximate results very quickly.

Some control systems may involve more than one parameter to be adjusted. The root-locus diagram for a system having multiple parameters may be constructed by varying one parameter at a time. In this chapter we include the discussion of the root loci for a system having two parameters. The root loci for such a case is called the *root contour.*

The root-locus method is a very powerful graphical technique for investigating the effects of the variation of a system parameter on the location of the closed-loop poles. In most cases, the system parameter is the loop gain K, although the parameter can be any other variable of the system. If the designer follows the general rules for constructing the root loci, sketching the root loci of a given system may become a simple matter.

Because generating the root loci by use of MATLAB is a very simple matter, one may think sketching the root loci by hand is a waste of time and effort. However, experience in sketching the root loci by hand is invaluable for interpreting computer-generated root loci, as well as for getting a rough idea of the root loci very quickly.

By using the root-locus method, it is possible to determine the value of the loop gain K that will make the damping ratio of the dominant closed-loop poles as prescribed. If the location of an open-loop pole or zero is a system variable, then the root-locus method suggests the way to choose the location of an open-loop pole or zero. (See Example 6–8 and Problems A-6-12 through A-6-14.) More on the control system design based on the root-locus method will be given in Chapter 7.

Outline of the chapter. This chapter introduces the basic concept of the root-locus method and presents useful rules for graphically constructing the root loci, as well as the generation of root loci with MATLAB.

The outline of the chapter is as follows: Section 6–1 has presented an introduction to the root-locus method. Section 6–2 details the concepts underlying the root-locus method and presents the general procedure for sketching root loci using illustrative

examples. Section 6–3 summarizes general rules for constructing root loci, and Section 6–4 discusses generating root-locus plots with MATLAB. Section 6–5 treats special cases: the first case occurs when the variable K does not appear as a multiplicative factor and the second case when the closed-loop system has positive feedback. Section 6–6 analyzes closed-loop systems by use of the root-locus method. Section 6–7 extends the root-locus method to treat closed-loop systems with transport lag. Finally, Section 6–8 discusses root-contour plots.

6-2 ROOT-LOCUS PLOTS

Angle and magnitude conditions. Consider the system shown in Figure 6–1. The closed-loop transfer function is

$$\frac{C(s)}{R(s)} = \frac{G(s)}{1 + G(s)H(s)} \tag{6–1}$$

The characteristic equation for this closed-loop system is obtained by setting the denominator of the right-hand side of Equation (6–1) equal to zero. That is,

$$1 + G(s)H(s) = 0$$

or

$$G(s)H(s) = -1 \tag{6–2}$$

Here we assume that $G(s)H(s)$ is a ratio of polynomials in s. [Later in Section 6–7 we extend the analysis to the case when $G(s)H(s)$ involves the transport lag e^{-Ts}.] Since $G(s)H(s)$ is a complex quantity, Equation (6–2) can be split into two equations by equating the angles and magnitudes of both sides, respectively, to obtain the following:

Angle condition:

$$\underline{/G(s)H(s)} = \pm 180°(2k + 1) \qquad (k = 0, 1, 2, \ldots) \tag{6–3}$$

Magnitude condition:

$$|G(s)H(s)| = 1 \tag{6–4}$$

The values of s that fulfill both the angle and magnitude conditions are the roots of the characteristic equation, or the closed-loop poles. A plot of the points in the complex plane satisfying the angle condition alone is the root locus. The roots of the characteristic equation (the closed-loop poles) corresponding to a given value of the gain can be determined from the magnitude condition. The details of applying the angle and magnitude conditions to obtain the closed-loop poles are presented later in this section.

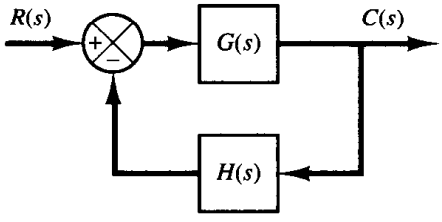

Figure 6–1
Control system.

In many cases, $G(s)H(s)$ involves a gain parameter K, and the characteristic equation may be written as

$$1 + \frac{K(s + z_1)(s + z_2) \cdots (s + z_m)}{(s + p_1)(s + p_2) \cdots (s + p_n)} = 0 \tag{6–5}$$

Then the root loci for the system are the loci of the closed-loop poles as the gain K is varied from zero to infinity.

Note that to begin sketching the root loci of a system by the root-locus method we must know the location of the poles and zeros of $G(s)H(s)$. Remember that the angles of the complex quantities originating from the open-loop poles and open-loop zeros to the test point s are measured in the counterclockwise direction. For example, if $G(s)H(s)$ is given by

$$G(s)H(s) = \frac{K(s + z_1)}{(s + p_1)(s + p_2)(s + p_3)(s + p_4)}$$

where $-p_2$ and $-p_3$ are complex-conjugate poles, then the angle of $G(s)H(s)$ is

$$\underline{/G(s)H(s)} = \phi_1 - \theta_1 - \theta_2 - \theta_3 - \theta_4$$

where ϕ_1, θ_1, θ_2, θ_3, and θ_4 are measured counterclockwise as shown in Figures 6–2(a) and (b). The magnitude of $G(s)H(s)$ for this system is

$$|G(s)H(s)| = \frac{KB_1}{A_1A_2A_3A_4}$$

where A_1, A_2, A_3, A_4, and B_1 are the magnitudes of the complex quantities $s + p_1, s + p_2$, $s + p_3, s + p_4$, and $s + z_1$, respectively, as shown in Figure 6–2(a).

Note that, because the open-loop complex-conjugate poles and complex-conjugate zeros, if any, are always located symmetrically about the real axis, the root loci are always

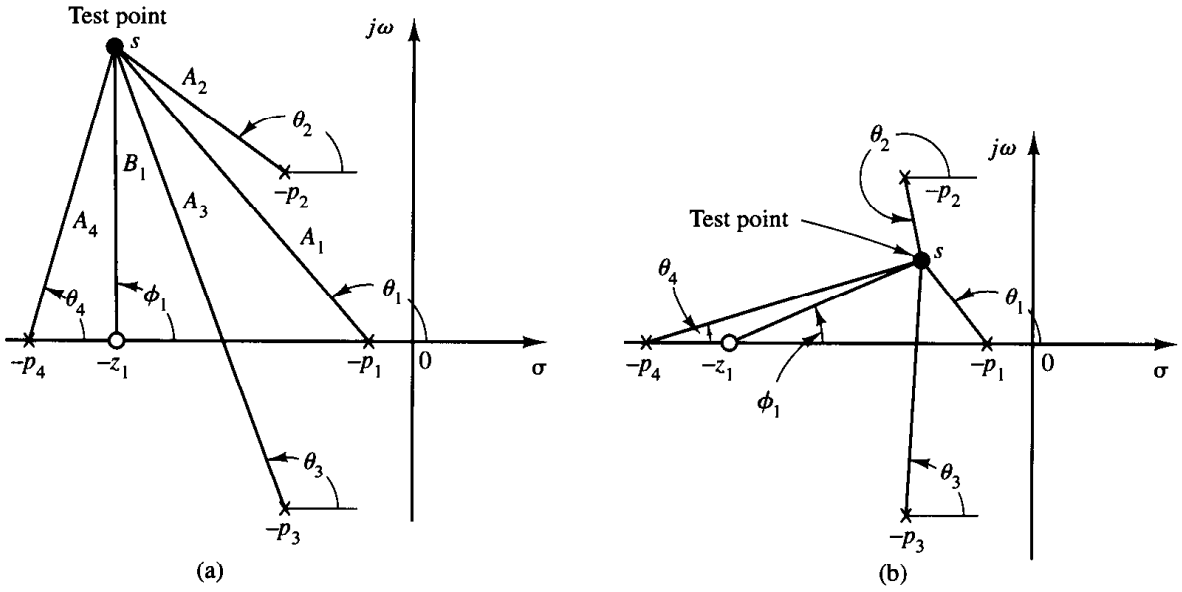

Figure 6–2
(a) and (b) Diagrams showing angle measurements from open-loop poles and open-loop zero to test point s.

symmetrical with respect to this axis. Therefore, we only need to construct the upper half of the root loci and draw the mirror image of the upper half in the lower-half s plane.

Illustrative examples. In what follows, two illustrative examples for constructing root-locus plots will be presented. Although computer approaches to the construction of the root loci are easily available, here we shall use graphical computation, combined with inspection, to determine the root loci upon which the roots of the characteristic equation of the closed-loop system must lie. Such a graphical approach will enhance understanding of how the closed-loop poles move in the complex plane as the open-loop poles and zeros are moved. Although we employ only simple systems for illustrative purposes, the procedure for finding the root loci is no more complicated for higher-order systems.

The first step in the procedure for constructing a root-locus plot is to seek out the loci of possible roots using the angle condition. Then, if necessary, the loci can be scaled, or graduated, in gain using the magnitude condition.

Because graphical measurements of angles and magnitudes are involved in the analysis, we find it necessary to use the same divisions on the abscissa as on the ordinate axis when sketching the root locus on graph paper.

EXAMPLE 6–1 Consider the system shown in Figure 6–3. (We assume that the value of gain K is nonnegative.) For this system,

$$G(s) = \frac{K}{s(s+1)(s+2)}, \qquad H(s) = 1$$

Let us sketch the root-locus plot and then determine the value of K such that the damping ratio ζ of a pair of dominant complex-conjugate closed-loop poles is 0.5.

For the given system, the angle condition becomes

$$\begin{aligned} \angle G(s) &= \angle \frac{K}{s(s+1)(s+2)} \\ &= -\angle s - \angle s+1 - \angle s+2 \\ &= \pm 180°(2k+1) \qquad (k = 0, 1, 2, \ldots) \end{aligned}$$

The magnitude condition is

$$|G(s)| = \left| \frac{K}{s(s+1)(s+2)} \right| = 1$$

A typical procedure for sketching the root-locus plot is as follows:

1. *Determine the root loci on the real axis.* The first step in constructing a root-locus plot is to locate the open-loop poles, $s = 0$, $s = -1$, and $s = -2$, in the complex plane. (There are no

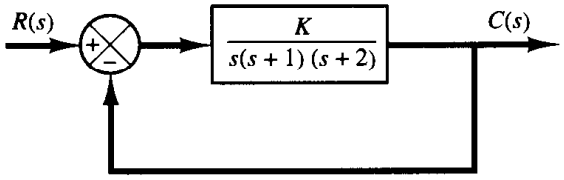

Figure 6–3
Control system.

open-loop zeros in this system.) The locations of the open-loop poles are indicated by crosses. (The locations of the open-loop zeros in this book will be indicated by small circles.) Note that the starting points of the root loci (the points corresponding to $K = 0$) are open-loop poles. The number of individual root loci for this system is three, which is the same as the number of open-loop poles.

To determine the root loci on the real axis, we select a test point, s. If the test point is on the positive real axis, then

$$\underline{/s} = \underline{/s + 1} = \underline{/s + 2} = 0°$$

This shows that the angle condition cannot be satisfied. Hence, there is no root locus on the positive real axis. Next, select a test point on the negative real axis between 0 and -1. Then

$$\underline{/s} = 180°, \qquad \underline{/s + 1} = \underline{/s + 2} = 0°$$

Thus

$$-\underline{/s} - \underline{/s + 1} - \underline{/s + 2} = -180°$$

and the angle condition is satisfied. Therefore, the portion of the negative real axis between 0 and -1 forms a portion of the root locus. If a test point is selected between -1 and -2, then

$$\underline{/s} = \underline{/s + 1} = 180°, \qquad \underline{/s + 2} = 0°$$

and

$$-\underline{/s} - \underline{/s + 1} - \underline{/s + 2} = -360°$$

It can be seen that the angle condition is not satisfied. Therefore, the negative real axis from -1 to -2 is not a part of the root locus. Similarly, if a test point is located on the negative real axis from -2 to $-\infty$, the angle condition is satisfied. Thus, root loci exist on the negative real axis between 0 and -1 and between -2 and $-\infty$.

2. *Determine the asymptotes of the root loci.* The asymptotes of the root loci as s approaches infinity can be determined as follows: If a test point s is selected very far from the origin, then

$$\lim_{s\to\infty} G(s) = \lim_{s\to\infty} \frac{K}{s(s + 1)(s + 2)} = \lim_{s\to\infty} \frac{K}{s^3}$$

and the angle condition becomes

$$-3\underline{/s} = \pm 180°(2k + 1) \qquad (k = 0, 1, 2, \ldots)$$

or

$$\text{Angles of asymptotes} = \frac{\pm 180°(2k + 1)}{3} \qquad (k = 0, 1, 2, \ldots)$$

Since the angle repeats itself as k is varied, the distinct angles for the asymptotes are determined as 60°, $-60°$, and 180°. Thus, there are three asymptotes. The one having the angle of 180° is the negative real axis.

Before we can draw these asymptotes in the complex plane, we must find the point where they intersect the real axis. Since

$$G(s) = \frac{K}{s(s + 1)(s + 2)} \tag{6-6}$$

if a test point is located very far from the origin, then $G(s)$ may be written as

$$G(s) = \frac{K}{s^3 + 3s^2 + \cdots} \tag{6-7}$$

Since the characteristic equation is

$$G(s) = -1$$

referring to Equation (6–7) the characteristic equation may be written as

$$s^3 + 3s^2 + \cdots = -K$$

For a large value of s, this last equation may be approximated by

$$(s + 1)^3 = 0$$

If the abscissa of the intersection of the asymptotes and the real axis is denoted by $s = -\sigma_a$, then

$$\sigma_a = -1$$

and the point of origin of the asymptotes is $(-1, 0)$. The asymptotes are almost part of the root loci in regions very far from the origin.

3. *Determine the breakaway point.* To plot root loci accurately, we must find the breakaway point, where the root-locus branches originating from the poles at 0 and -1 break away (as K is increased) from the real axis and move into the complex plane. The breakaway point corresponds to a point in the s plane where multiple roots of the characteristic equation occur.

A simple method for finding the breakaway point is available. We shall present this method in the following: Let us write the characteristic equation as

$$f(s) = B(s) + KA(s) = 0 \tag{6-8}$$

where $A(s)$ and $B(s)$ do not contain K. Note that $f(s) = 0$ has multiple roots at points where

$$\frac{df(s)}{ds} = 0$$

This can be seen as follows: Suppose that $f(s)$ has multiple roots of order r. Then $f(s)$ may be written as

$$f(s) = (s - s_1)^r(s - s_2) \cdots (s - s_n)$$

If we differentiate this equation with respect to s and set $s = s_1$, then we get

$$\left.\frac{df(s)}{ds}\right|_{s=s_1} = 0 \tag{6-9}$$

This means that multiple roots of $f(s)$ will satisfy Equation (6–9). From Equation (6–8), we obtain

$$\frac{df(s)}{ds} = B'(s) + KA'(s) = 0 \tag{6-10}$$

where

$$A'(s) = \frac{dA(s)}{ds}, \qquad B'(s) = \frac{dB(s)}{ds}$$

The particular value of K that will yield multiple roots of the characteristic equation is obtained from Equation (6–10) as

$$K = -\frac{B'(s)}{A'(s)}$$

If we substitute this value of K into Equation (6–8), we get

$$f(s) = B(s) - \frac{B'(s)}{A'(s)} A(s) = 0$$

or

$$B(s)A'(s) - B'(s)A(s) = 0 \tag{6–11}$$

If Equation (6–11) is solved for s, the points where multiple roots occur can be obtained. On the other hand, from Equation (6–8) we obtain

$$K = -\frac{B(s)}{A(s)}$$

and

$$\frac{dK}{ds} = -\frac{B'(s)A(s) - B(s)A'(s)}{A^2(s)}$$

If dK/ds is set equal to zero, we get the same equation as Equation (6–11). Therefore, the breakaway points can be simply determined from the roots of

$$\frac{dK}{ds} = 0$$

It should be noted that not all the solutions of Equation (6–11) or of $dK/ds = 0$ correspond to actual breakaway points. If a point at which $df(s)/ds = 0$ is on a root locus, it is an actual breakaway or break-in point. Stated differently, if at a point at which $df(s)/ds = 0$ the value of K takes a real positive value then that point is an actual breakaway or break-in point.

For the present example, the characteristic equation $G(s) + 1 = 0$ is given by

$$\frac{K}{s(s + 1)(s + 2)} + 1 = 0$$

or

$$K = -(s^3 + 3s^2 + 2s)$$

By setting $dK/ds = 0$, we obtain

$$\frac{dK}{ds} = -(3s^2 + 6s + 2) = 0$$

or

$$s = -0.4226, \qquad s = -1.5774$$

Since the breakaway point must lie on a root locus between 0 and -1, it is clear that $s = -0.4226$ corresponds to the actual breakaway point. Point $s = -1.5774$ is not on the root locus. Hence, this point is not an actual breakaway or break-in point. In fact, evaluation of the values of K corresponding to $s = -0.4226$ and $s = -1.5774$ yields

$$K = 0.3849, \qquad \text{for } s = -0.4226$$

$$K = -0.3849, \qquad \text{for } s = -1.5774$$

4. *Determine the points where the root loci cross the imaginary axis.* These points can be found by use of Routh's stability criterion as follows: Since the characteristic equation for the present system is

$$s^3 + 3s^2 + 2s + K = 0$$

the Routh array becomes

$$\begin{array}{lll} s^3 & 1 & 2 \\ s^2 & 3 & K \\ s^1 & \dfrac{6-K}{3} & \\ s^0 & K & \end{array}$$

The value of K that makes the s^1 term in the first column equal zero is $K = 6$. The crossing points on the imaginary axis can then be found by solving the auxiliary equation obtained from the s^2 row; that is,

$$3s^2 + K = 3s^2 + 6 = 0$$

which yields

$$s = \pm j\sqrt{2}$$

The frequencies at the crossing points on the imaginary axis are thus $\omega = \pm\sqrt{2}$. The gain value corresponding to the crossing points is $K = 6$.

An alternative approach is to let $s = j\omega$ in the characteristic equation, equate both the real part and the imaginary part to zero, and then solve for ω and K. For the present system, the characteristic equation, with $s = j\omega$, is

$$(j\omega)^3 + 3(j\omega)^2 + 2(j\omega) + K = 0$$

or

$$(K - 3\omega^2) + j(2\omega - \omega^3) = 0$$

Equating both the real and imaginary parts of this last equation to zero, we obtain

$$K - 3\omega^2 = 0, \qquad 2\omega - \omega^3 = 0$$

from which

$$\omega = \pm\sqrt{2}, \qquad K = 6 \qquad \text{or} \qquad \omega = 0, \qquad K = 0$$

Thus, root loci cross the imaginary axis at $\omega = \pm\sqrt{2}$, and the value of K at the crossing points is 6. Also, a root-locus branch on the real axis touches the imaginary axis at $\omega = 0$.

5. *Choose a test point in the broad neighborhood of the jω axis and the origin,* as shown in Figure 6–4, and apply the angle condition. If a test point is on the root loci, then the sum of the

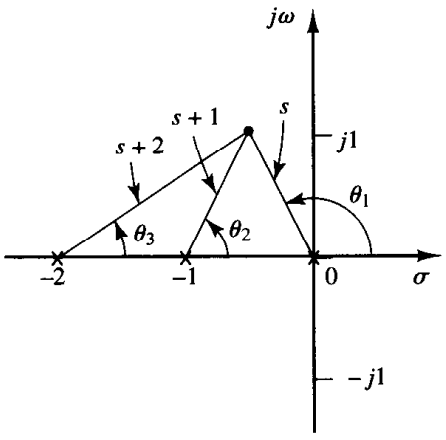

Figure 6–4
Construction of root locus.

three angles, $\theta_1 + \theta_2 + \theta_3$, must be 180°. If the test point does not satisfy the angle condition, select another test point until it satisfies the condition. (The sum of the angles at the test point will indicate which direction the test point should be moved.) Continue this process and locate a sufficient number of points satisfying the angle condition.

6. *Draw the root loci,* based on the information obtained in the foregoing steps, as shown in Figure 6–5.

7. *Determine a pair of dominant complex-conjugate closed-loop poles such that the damping ratio ζ is 0.5.* Closed-loop poles with $\zeta = 0.5$ lie on lines passing through the origin and making the angles $\pm\cos^{-1}\zeta = \pm\cos^{-1}0.5 = \pm 60°$ with the negative real axis. From Figure 6–5, such closed-loop poles having $\zeta = 0.5$ are obtained as follows:

$$s_1 = -0.3337 + j0.5780, \qquad s_2 = -0.3337 - j0.5780$$

The value of K that yields such poles is found from the magnitude condition as follows:

$$K = |s(s+1)(s+2)|_{s=-0.3337+j0.5780}$$
$$= 1.0383$$

Using this value of K, the third pole is found at $s = -2.3326$.

Note that, from step 4, it can be seen that for $K = 6$ the dominant closed-loop poles lie on the imaginary axis at $s = \pm j\sqrt{2}$. With this value of K, the system will exhibit sustained oscillations. For $K > 6$, the dominant closed-loop poles lie in the right-half s plane, resulting in an unstable system.

Finally, note that, if necessary, the root loci can be easily graduated in terms of K by use of the magnitude condition. We simply pick out a point on a root locus, measure the magnitudes of the three complex quantities s, $s + 1$, and $s + 2$, and multiply these magnitudes; the product is equal to the gain value K at that point, or

$$|s| \cdot |s+1| \cdot |s+2| = K$$

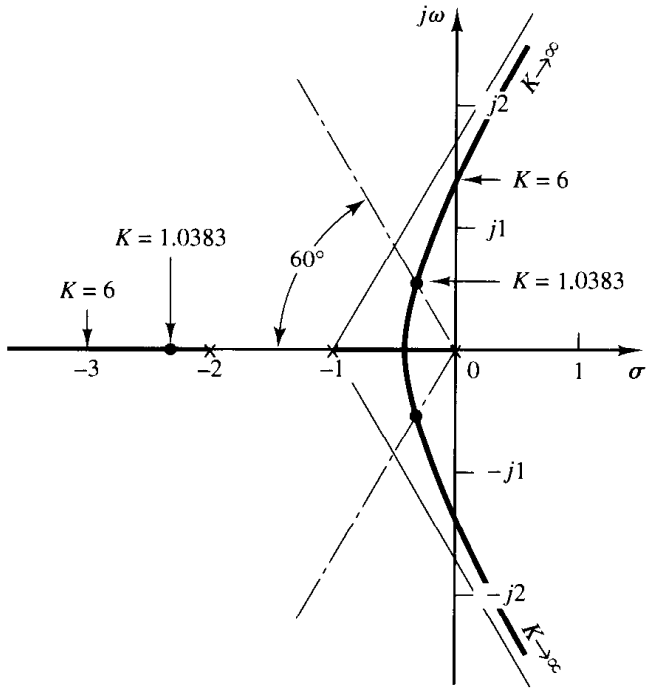

Figure 6–5
Root-locus plot.

EXAMPLE 6–2 In this example, we shall sketch the root-locus plot of a system with complex-conjugate open-loop poles. Consider the system shown in Figure 6–6. For this system,

$$G(s) = \frac{K(s + 2)}{s^2 + 2s + 3}, \qquad H(s) = 1$$

It is seen that $G(s)$ has a pair of complex-conjugate poles at

$$s = -1 + j\sqrt{2}, \qquad s = -1 - j\sqrt{2}$$

A typical procedure for sketching the root-locus plot is as follows:

1. *Determine the root loci on the real axis.* For any test point s on the real axis, the sum of the angular contributions of the complex-conjugate poles is 360°, as shown in Figure 6–7. Thus the net effect of the complex-conjugate poles is zero on the real axis. The location of the root locus on the real axis is determined from the open-loop zero on the negative real axis. A simple test reveals that a section of the negative real axis, that between -2 and $-\infty$, is a part of the root locus. It is noted that, since this locus lies between two zeros (at $s = -2$ and $s = -\infty$), it is actually a part of two root loci, each of which starts from one of the two complex-conjugate poles. In other words, two root loci break in the part of the negative real axis between -2 and $-\infty$.

Since there are two open-loop poles and one zero, there is one asymptote, which coincides with the negative real axis.

2. *Determine the angle of departure from the complex-conjugate open-loop poles.* The presence of a pair of complex-conjugate open-loop poles requires determination of the angle of departure from these poles. Knowledge of this angle is important since the root locus near a complex pole yields information as to whether the locus originating from the complex pole migrates toward the real axis or extends toward the asymptote.

Referring to Figure 6–8, if we choose a test point and move it in the very vicinity of the complex open-loop pole at $s = -p_1$, we find that the sum of the angular contributions from the pole at $s = -p_2$ and zero at $s = -z_1$ to the test point can be considered remaining the same. If the test

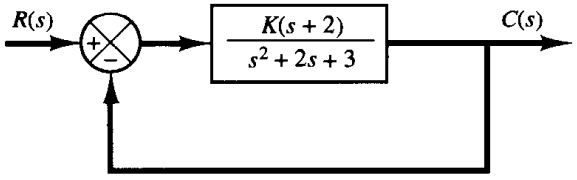

Figure 6–6
Control system.

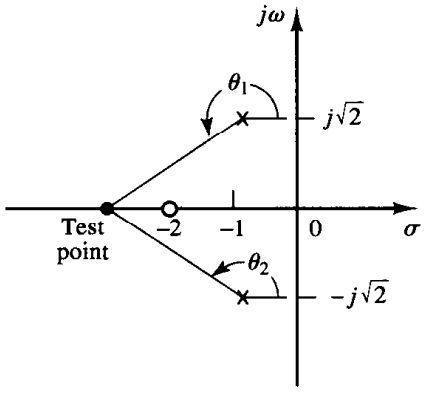

Figure 6–7
Determination of the root locus on the real axis.

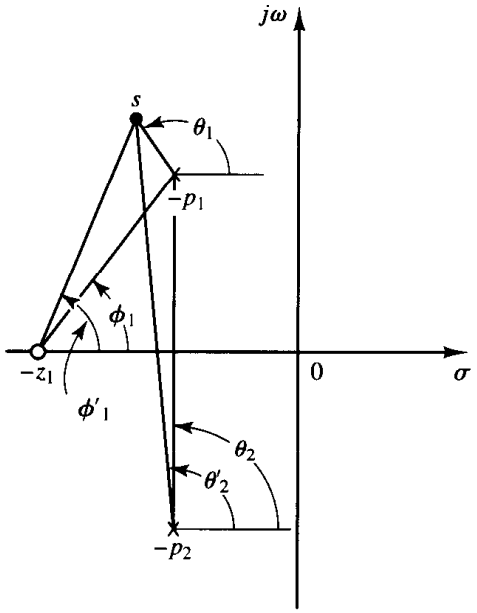

Figure 6–8
Determination of the angle of departure.

point is to be on the root locus, then the sum of ϕ_1', $-\theta_1$, and $-\theta_2'$ must be $\pm 180°(2k + 1)$, where $k = 0, 1, 2, \ldots$. Thus, in the example,

$$\phi_1' - (\theta_1 + \theta_2') = \pm 180°(2k + 1)$$

or

$$\theta_1 = 180° - \theta_2' + \phi_1' = 180° - \theta_2 + \phi_1$$

The angle of departure is then

$$\theta_1 = 180° - \theta_2 + \phi_1 = 180° - 90° + 55° = 145°$$

Since the root locus is symmetric about the real axis, the angle of departure from the pole at $s = -p_2$ is $-145°$.

3. *Determine the break-in point.* A break-in point exists where a pair of root-locus branches coalesce as K is increased. For this problem, the break-in point can be found as follows: Since

$$K = -\frac{s^2 + 2s + 3}{s + 2}$$

we have

$$\frac{dK}{ds} = -\frac{(2s + 2)(s + 2) - (s^2 + 2s + 3)}{(s + 2)^2} = 0$$

which gives

$$s^2 + 4s + 1 = 0$$

or

$$s = -3.7320 \quad \text{or} \quad s = -0.2680$$

Notice that point $s = -3.7320$ is on the root locus. Hence this point is an actual break-in point. (Note that at point $s = -3.7320$ the corresponding gain value is $K = 5.4641$.) Since point $s = -0.2680$ is not on the root locus, it cannot be a break-in point. (For point $s = -0.2680$, the corresponding gain value is $K = -1.4641$.)

4. *Sketch a root-locus plot,* based on the information obtained in the foregoing steps. To determine accurate root loci, several points must be found by trial and error between the break-in point and the complex open-loop poles. (To facilitate sketching the root-locus plot, we should find the direction in which the test point should be moved by mentally summing up the changes on the angles of the poles and zeros.) Figure 6–9 shows a complete root-locus plot for the system considered.

The value of the gain K at any point on root locus can be found by applying the magnitude condition. For example, the value of K at which the complex-conjugate closed-loop poles have the damping ratio $\zeta = 0.7$ can be found by locating the roots, as shown in Figure 6–9, and computing the value of K as follows:

$$K = \left| \frac{(s + 1 - j\sqrt{2})(s + 1 + j\sqrt{2})}{s + 2} \right|_{s=-1.67+j1.70} = 1.34$$

It is noted that in this system the root locus in the complex plane is a part of a circle. Such a circular root locus will not occur in most systems. Circular root loci may occur in systems that involve two poles and one zero, two poles and two zeros, or one pole and two zeros. Even in such systems, whether circular root loci occur depends on the locations of poles and zeros involved.

To show the occurrence of a circular root locus in the present system, we need to derive the equation for the root locus. For the present system, the angle condition is

$$\underline{/s + 2} - \underline{/s + 1 - j\sqrt{2}} - \underline{/s + 1 + j\sqrt{2}} = \pm 180°(2k + 1)$$

If $s = \sigma + j\omega$ is substituted into this last equation, we obtain

$$\underline{/\sigma + 2 + j\omega} - \underline{/\sigma + 1 + j\omega - j\sqrt{2}} - \underline{/\sigma + 1 + j\omega + j\sqrt{2}} = \pm 180°(2k + 1)$$

which can be written as

$$\tan^{-1}\left(\frac{\omega}{\sigma + 2}\right) - \tan^{-1}\left(\frac{\omega - \sqrt{2}}{\sigma + 1}\right) - \tan^{-1}\left(\frac{\omega + \sqrt{2}}{\sigma + 1}\right) = \pm 180°(2k + 1)$$

or

$$\tan^{-1}\left(\frac{\omega - \sqrt{2}}{\sigma + 1}\right) + \tan^{-1}\left(\frac{\omega + \sqrt{2}}{\sigma + 1}\right) = \tan^{-1}\left(\frac{\omega}{\sigma + 2}\right) \pm 180°(2k + 1)$$

Taking tangents of both sides of this last equation using the relationship

$$\tan(x \pm y) = \frac{\tan x \pm \tan y}{1 \mp \tan x \tan y} \tag{6–12}$$

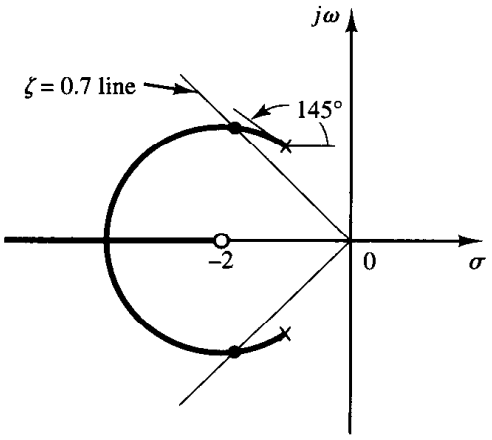

Figure 6–9
Root-locus plot.

we obtain

$$\tan\left[\tan^{-1}\left(\frac{\omega-\sqrt{2}}{\sigma+1}\right)+\tan^{-1}\left(\frac{\omega+\sqrt{2}}{\sigma+1}\right)\right]=\tan\left[\tan^{-1}\left(\frac{\omega}{\sigma+2}\right)\pm 180°(2k+1)\right]$$

or

$$\frac{\dfrac{\omega-\sqrt{2}}{\sigma+1}+\dfrac{\omega+\sqrt{2}}{\sigma+1}}{1-\left(\dfrac{\omega-\sqrt{2}}{\sigma+1}\right)\left(\dfrac{\omega+\sqrt{2}}{\sigma+1}\right)}=\frac{\dfrac{\omega}{\sigma+2}\pm 0}{1\mp\dfrac{\omega}{\sigma+2}\times 0}$$

which can be simplified to

$$\frac{2\omega(\sigma+1)}{(\sigma+1)^2-(\omega^2-2)}=\frac{\omega}{\sigma+2}$$

or

$$\omega[(\sigma+2)^2+\omega^2-3]=0$$

This last equation is equivalent to

$$\omega=0 \qquad \text{or} \qquad (\sigma+2)^2+\omega^2=(\sqrt{3})^2$$

These two equations are the equations for the root loci for the present system. Notice that the first equation, $\omega = 0$, is the equation for the real axis. The real axis from $s = -2$ to $s = -\infty$ corresponds to a root locus for $K \geq 0$. The remaining part of the real axis corresponds to a root locus when K is negative. (In the present system, K is nonnegative.) The second equation for the root locus is an equation of a circle with center at $\sigma = -2, \omega = 0$ and the radius equal to $\sqrt{3}$. That part of the circle to the left of the complex-conjugate poles corresponds to a root locus for $K \geq 0$. The remaining part of the circle corresponds to a root locus when K is negative.

It is important to note that easily interpretable equations for the root locus can be derived for simple systems only. For complicated systems having many poles and zeros, any attempt to derive equations for the root loci is discouraged. Such derived equations are very complicated and their configuration in the complex plane is difficult to visualize.

6–3 SUMMARY OF GENERAL RULES FOR CONSTRUCTING ROOT LOCI

For a complicated system with many open-loop poles and zeros, constructing a root-locus plot may seem complicated, but actually it is not difficult if the rules for constructing the root loci are applied. By locating particular points and asymptotes and by computing angles of departure from complex poles and angles of arrival at complex zeros, we can construct the general form of the root loci without difficulty.

Some of the rules for constructing root loci were given in Section 6–2. The purpose of this section is to summarize the general rules for constructing root loci of the system shown in Figure 6–10. While the root-locus method is essentially based on a trial-and-error technique, the number of trials required can be greatly reduced if we use these rules.

General rules for constructing root loci. We shall now summarize the general rules and procedure for constructing the root loci of the system shown in Figure 6–10.

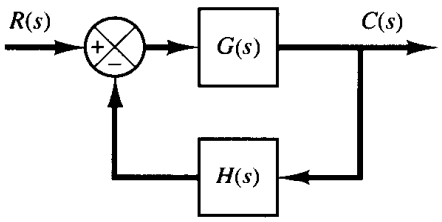

Figure 6–10
Control system.

First, obtain the characteristic equation

$$1 + G(s)H(s) = 0$$

Then rearrange this equation so that the parameter of interest appears as the multiplying factor in the form

$$1 + \frac{K(s + z_1)(s + z_2) \cdots (s + z_m)}{(s + p_1)(s + p_2) \cdots (s + p_n)} = 0 \tag{6–13}$$

In the present discussions, we assume that the parameter of interest is the gain K, where $K > 0$. (If $K < 0$, which corresponds to the positive-feedback case, the angle condition must be modified. See Section 6–5.) Note, however, that the method is still applicable to systems with parameters of interest other than gain.

1. *Locate the poles and zeros of $G(s)H(s)$ on the s plane. The root-locus branches start from open-loop poles and terminate at zeros (finite zeros or zeros at infinity).* From the factored form of the open-loop transfer function, locate the open-loop poles and zeros in the s plane. [Note that the open-loop zeros are the zeros of $G(s)H(s)$, while the closed-loop zeros consist of the zeros of $G(s)$ and the poles of $H(s)$.]

Note that the root loci are symmetrical about the real axis of the s plane, because the complex poles and complex zeros occur only in conjugate pairs.

Find the starting points and terminating points of the root loci and find also the number of separate root loci. The points on the root loci corresponding to $K = 0$ are open-loop poles. This can be seen from the magnitude condition by letting K approach zero, or

$$\lim_{K \to 0} \left| \frac{(s + z_1)(s + z_2) \cdots (s + z_m)}{(s + p_1)(s + p_2) \cdots (s + p_n)} \right| = \lim_{K \to 0} \frac{1}{K} = \infty$$

This last equation implies that as K is decreased the value of s must approach one of the open-loop poles. Each root locus thus originates at a pole of the open-loop transfer function $G(s)H(s)$. As K is increased to infinity, each root-locus approaches either a zero of the open-loop transfer function or infinity in the complex plane. This can be seen as follows: If we let K approach infinity in the magnitude condition, then

$$\lim_{K \to \infty} \left| \frac{(s + z_1)(s + z_2) \cdots (s + z_m)}{(s + p_1)(s + p_2) \cdots (s + p_n)} \right| = \lim_{K \to \infty} \frac{1}{K} = 0$$

Hence the value of s must approach one of the finite open-loop zeros or an open-loop zero at infinity. [If the zeros at infinity are included in the count, $G(s)H(s)$ has the same number of zeros as poles.]

A root-locus plot will have just as many branches as there are roots of the characteristic equation. Since the number of open-loop poles generally exceeds that of zeros,

the number of branches equals that of poles. If the number of closed-loop poles is the same as the number of open-loop poles, then the number of individual root-locus branches terminating at finite open-loop zeros is equal to the number m of the open-loop zeros. The remaining $n - m$ branches terminate at infinity ($n - m$ implicit zeros at infinity) along asymptotes.

If we include poles and zeros at infinity, the number of open-loop poles is equal to that of open-loop zeros. Hence we can always state that the root loci start at the poles of $G(s)H(s)$ and end at the zeros of $G(s)H(s)$, as K increases from zero to infinity, where the poles and zeros include both those in the finite s plane and those at infinity.

2. *Determine the root loci on the real axis.* Root loci on the real axis are determined by open-loop poles and zeros lying on it. The complex-conjugate poles and zeros of the open-loop transfer function have no effect on the location of the root loci on the real axis because the angle contribution of a pair of complex-conjugate poles or zeros is 360° on the real axis. Each portion of the root locus on the real axis extends over a range from a pole or zero to another pole or zero. In constructing the root loci on the real axis, choose a test point on it. If the total number of real poles and real zeros to the right of this test point is odd, then this point lies on a root locus. The root locus and its complement form alternate segments along the real axis.

3. *Determine the asymptotes of root loci.* If the test point s is located far from the origin, then the angle of each complex quantity may be considered the same. One open-loop zero and one open-loop pole then cancel the effects of the other. Therefore, the root loci for very large values of s must be asymptotic to straight lines whose angles (slopes) are given by

$$\text{Angles of asymptotes} = \frac{\pm 180°(2k + 1)}{n - m} \qquad (k = 0, 1, 2, \ldots)$$

where n = number of finite poles of $G(s)H(s)$
m = number of finite zeros of $G(s)H(s)$

Here, $k = 0$ corresponds to the asymptotes with the smallest angle with the real axis. Although k assumes an infinite number of values, as k is increased, the angle repeats itself, and the number of distinct asymptotes is $n - m$.

All the asymptotes intersect on the real axis. The point at which they do so is obtained as follows: If both the numerator and denominator of the open-loop transfer function are expanded, the result is

$$G(s)H(s) = \frac{K[s^m + (z_1 + z_2 + \cdots + z_m)s^{m-1} + \cdots + z_1 z_2 \cdots z_m]}{s^n + (p_1 + p_2 + \cdots + p_n)s^{n-1} + \cdots + p_1 p_2 \cdots p_n}$$

If a test point is located very far from the origin, then by dividing the denominator by the numerator $G(s)H(s)$ may be written as

$$G(s)H(s) = \frac{K}{s^{n-m} + [(p_1 + p_2 + \cdots + p_n) - (z_1 + z_2 + \cdots + z_m)]s^{n-m-1} + \cdots}$$

Since the characteristic equation is

$$G(s)H(s) = -1$$

it may be written

$$s^{n-m} + [(p_1 + p_2 + \cdots + p_n) - (z_1 + z_2 + \cdots + z_m)]s^{n-m-1} + \cdots = -K \qquad (6\text{–}14)$$

For a large value of s, Equation (6–14) may be approximated by

$$\left[s + \frac{(p_1 + p_2 + \cdots + p_n) - (z_1 + z_2 + \cdots + z_m)}{n - m}\right]^{n-m} = 0$$

If the abscissa of the intersection of the asymptotes and the real axis is denoted by $s = \sigma_a$, then

$$\sigma_a = -\frac{(p_1 + p_2 + \cdots + p_n) - (z_1 + z_2 + \cdots + z_m)}{n - m} \qquad (6\text{–}15)$$

or

$$\sigma_a = \frac{\text{(sum of poles)} - \text{(sum of zeros)}}{n - m} \qquad (6\text{–}16)$$

Because all the complex poles and zeros occur in conjugate pairs, σ_a is always a real quantity. Once the intersection of the asymptotes and the real axis is found, the asymptotes can be readily drawn in the complex plane.

It is important to note that the asymptotes show the behavior of the root loci for $|s| \gg 1$. A root locus branch may lie on one side of the corresponding asymptote or may cross the corresponding asymptote from one side to the other side.

4. *Find the breakaway and break-in points.* Because of the conjugate symmetry of the root loci, the breakaway points and break-in points either lie on the real axis or occur in complex-conjugate pairs.

If a root locus lies between two adjacent open-loop poles on the real axis, then there exists at least one breakaway point between the two poles. Similarly, if the root locus lies between two adjacent zeros (one zero may be located at $-\infty$) on the real axis, then there always exists at least one break-in point between the two zeros. If the root locus lies between an open-loop pole and a zero (finite or infinite) on the real axis, then there may exist no breakaway or break-in points or there may exist both breakaway and break-in points.

Suppose that the characteristic equation is given by

$$B(s) + KA(s) = 0$$

The breakaway points and break-in points correspond to multiple roots of the characteristic equation. Hence, the breakaway and break-in points can be determined from the roots of

$$\frac{dK}{ds} = -\frac{B'(s)A(s) - B(s)A'(s)}{A^2(s)} = 0 \qquad (6\text{–}17)$$

where the prime indicates differentiation with respect to s. It is important to note that the breakaway points and break-in points must be the roots of Equation (6–17), but not all roots of Equation (6–17) are breakaway or break-in points. If a real root of Equation (6–17) lies on the root locus portion of the real axis, then it is an actual breakaway or break-in point. If a real root of Equation (6–17) is not on the root locus portion of the real axis, then this root corresponds to neither a breakaway point nor a break-in point. If two roots $s = s_1$ and $s = -s_1$ of Equation (6–17) are a complex-conjugate pair

and if it is not certain whether they are on root loci, then it is necessary to check the corresponding K value. If the value of K corresponding to a root $s = s_1$ of $dK/ds = 0$ is positive, point $s = s_1$ is an actual breakaway or break-in point. (Since K is assumed to be nonnegative, if the value of K thus obtained is negative, then point $s = s_1$ is neither a breakaway nor break-in point.)

5. *Determine the angle of departure (angle of arrival) of the root locus from a complex pole (at a complex zero).* To sketch the root loci with reasonable accuracy, we must find the directions of the root loci near the complex poles and zeros. If a test point is chosen and moved in the very vicinity of a complex pole (or complex zero), the sum of the angular contributions from all other poles and zeros can be considered remaining the same. Therefore, the angle of departure (or angle of arrival) of the root locus from a complex pole (or at a complex zero) can be found by subtracting from 180° the sum of all the angles of vectors from all other poles and zeros to the complex pole (or complex zero) in question, with appropriate signs included.

Angle of departure from a complex pole = 180°
− (sum of the angles of vectors to a complex pole in question from other poles)
+ (sum of the angles of vectors to a complex pole in question from zeros)

Angle of arrival at a complex zero = 180°
− (sum of the angles of vectors to a complex zero in question from other zeros)
+ (sum of the angles of vectors to a complex zero in question from poles)

The angle of departure is shown in Figure 6–11.

6. *Find the points where the root loci may cross the imaginary axis.* The points where the root loci intersect the $j\omega$ axis can be found easily by (a) use of Routh's stability criterion or (b) letting $s = j\omega$ in the characteristic equation, equating both the real part and the imaginary part to zero, and solving for ω and K. The values of ω thus found give the frequencies at which root loci cross the imaginary axis. The K value corresponding to each crossing frequency gives the gain at the crossing point.

7. *Taking a series of test points in the broad neighborhood of the origin of the s plane, sketch the root loci.* Determine the root loci in the broad neighborhood of the $j\omega$ axis and the origin. The most important part of the root loci is on neither the real axis nor the asymptotes but the part in the broad neighborhood of the $j\omega$ axis and the origin. The

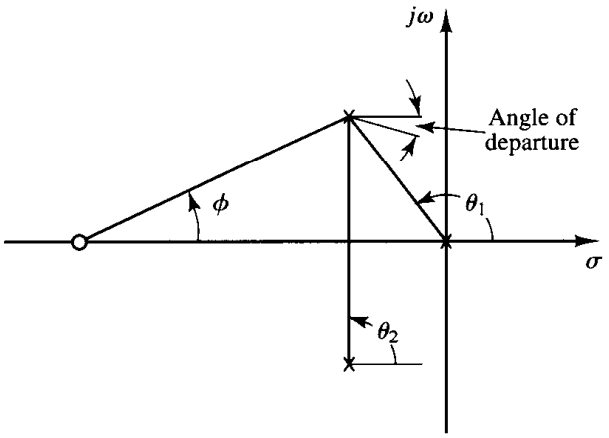

Figure 6–11
Construction of the root locus. [Angle of departure = 180° − $(\theta_1 + \theta_2) + \phi$.]

shape of the root loci in this important region in the s plane must be obtained with sufficient accuracy.

8. *Determine closed-loop poles.* A particular point on each root-locus branch will be a closed-loop pole if the value of K at that point satisfies the magnitude condition. Conversely, the magnitude condition enables us to determine the value of the gain K at any specific root location on the locus. (If necessary, the root loci may be graduated in terms of K. The root loci are continuous with K.)

The value of K corresponding to any point s on a root locus can be obtained using the magnitude condition, or

$$K = \frac{\text{product of lengths between point } s \text{ to poles}}{\text{product of lengths between point } s \text{ to zeros}}$$

This value can be evaluated either graphically or analytically.

If the gain K of the open-loop transfer function is given in the problem, then by applying the magnitude condition we can find the correct locations of the closed-loop poles for a given K on each branch of the root loci by a trial-and-error approach or by use of MATLAB, which will be presented in Section 6–4.

Comments on the root-locus plots. It is noted that the characteristic equation of the system whose open-loop transfer function is

$$G(s)H(s) = \frac{K(s^m + b_1 s^{m-1} + \cdots + b_m)}{s^n + a_1 s^{n-1} + \cdots + a_n} \qquad (n \geq m)$$

is an nth-degree algebraic equation in s. If the order of the numerator of $G(s)H(s)$ is lower than that of the denominator by two or more (which means that there are two or more zeros at infinity), then the coefficient a_1 is the negative sum of the roots of the equation and is independent of K. In such a case, if some of the roots move on the locus toward the left as K is increased, then the other roots must move toward the right as K is increased. This information is helpful in finding the general shape of the root loci.

It is also noted that a slight change in the pole–zero configuration may cause significant changes in the root-locus configurations. Figure 6–12 demonstrates the fact that a slight change in the location of a zero or pole will make the root-locus configuration look quite different.

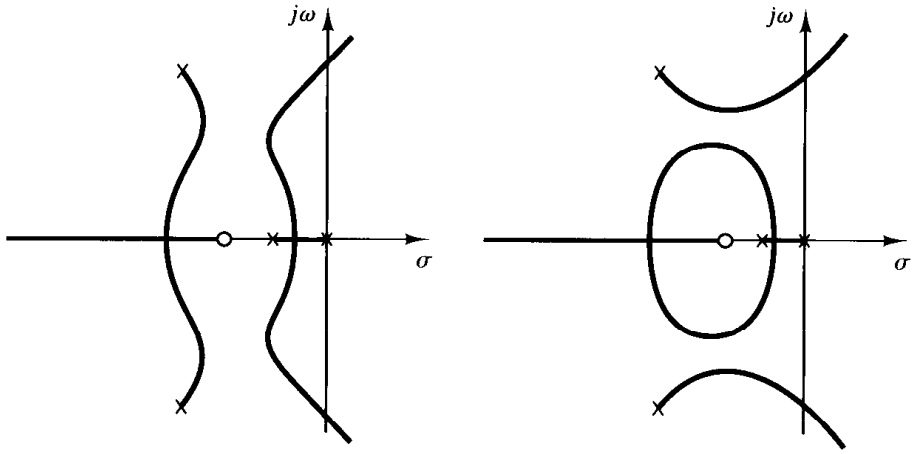

Figure 6–12
Root-locus plot.

Cancellation of poles $G(s)$ with zeros of $H(s)$. It is important to note that if the denominator of $G(s)$ and the numerator of $H(s)$ involve common factors then the corresponding open-loop poles and zeros will cancel each other, reducing the degree of the characteristic equation by one or more. For example, consider the system shown in Figure 6–13(a). (This system has velocity feedback.) By modifying the block diagram of Figure 6–13(a) to that shown in Figure 6–13(b), it is clearly seen that $G(s)$ and $H(s)$ have a common factor $s + 1$. The closed-loop transfer function $C(s)/R(s)$ is

$$\frac{C(s)}{R(s)} = \frac{K}{s(s + 1)(s + 2) + K(s + 1)}$$

The characteristic equation is

$$[s(s + 2) + K](s + 1) = 0$$

Because of the cancellation of the terms $(s + 1)$ appearing in $G(s)$ and $H(s)$, however, we have

$$1 + G(s)H(s) = 1 + \frac{K(s + 1)}{s(s + 1)(s + 2)}$$

$$= \frac{s(s + 2) + K}{s(s + 2)}$$

The reduced characteristic equation is

$$s(s + 2) + K = 0$$

The root-locus plot of $G(s)H(s)$ does not show all the roots of the characteristic equation, only the roots of the reduced equation.

To obtain the complete set of closed-loop poles, we must add the canceled pole of $G(s)H(s)$ to those closed-loop poles obtained from the root-locus plot of $G(s)H(s)$. The

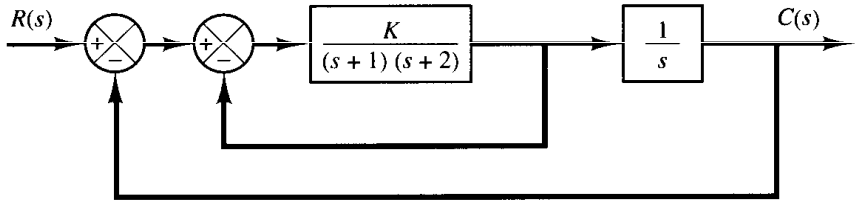

(a)

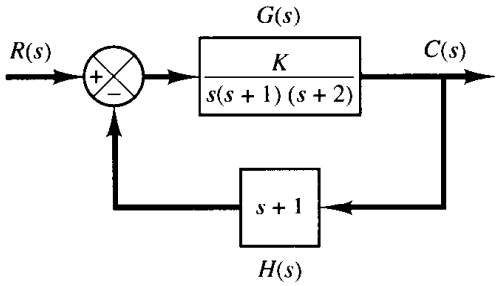

(b)

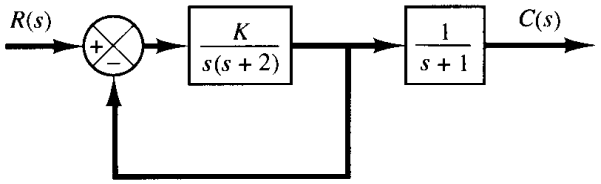

(c)

Figure 6–13
(a) Control system with velocity feedback; (b) and (c) modified block diagrams.

important thing to remember is that the canceled pole of $G(s)H(s)$ is a closed-loop pole of the system, as seen from Figure 6–13(c).

Typical pole–zero configurations and corresponding root loci. In concluding this section, we show several open-loop pole–zero configurations and their corresponding root loci in Table 6–1. The pattern of the root loci depends only on the relative separation of the open-loop poles and zeros. If the number of open-loop poles

Table 6–1 Open-Loop Pole–Zero Configurations and the Corresponding Root Loci

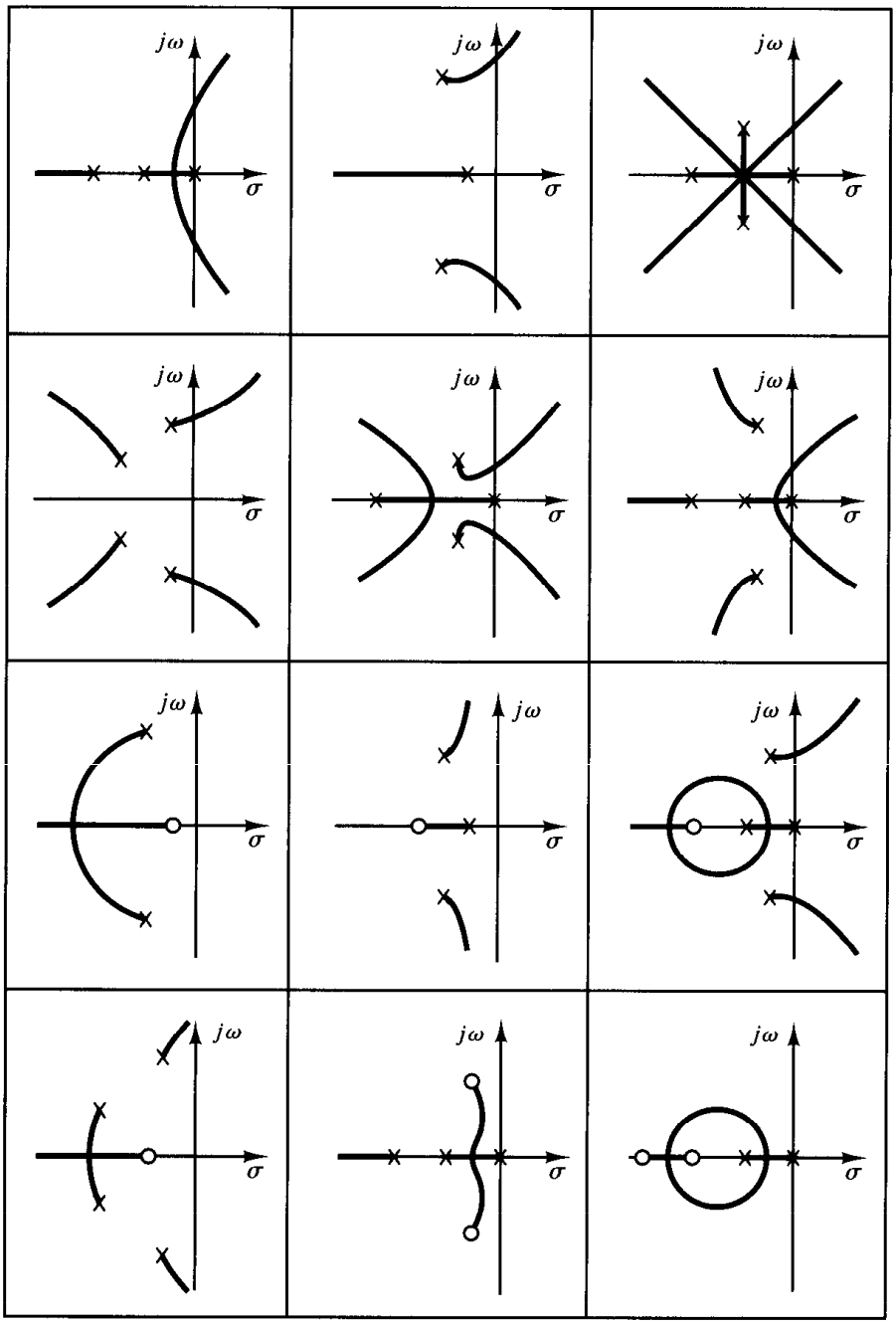

exceeds the number of finite zeros by three or more, there is a value of the gain K beyond which root loci enter the right-half s plane, and thus the system can become unstable. A stable system must have all its closed-loop poles in the left-half s plane.

Note that once we have some experience with the method we can easily evaluate the changes in the root loci due to the changes in the number and location of the open-loop poles and zeros by visualizing the root-locus plots resulting from various pole–zero configurations.

Summary. From the preceding discussions, it should be clear that it is possible to sketch a reasonably accurate root-locus diagram for a given system by following simple rules. (The reader is suggested to study various root-locus diagrams shown in the solved problems at the end of the chapter.) At preliminary design stages, we may not need the precise locations of the closed-loop poles. Often their approximate locations are all that is needed to make an estimate of system performance. Thus, it is important that the designer have the capability of quickly sketching the root loci for a given system.

6-4 ROOT-LOCUS PLOTS WITH MATLAB

In this section we present the MATLAB approach to the generation of root-locus plots.

Plotting root loci with MATLAB. In plotting root loci with MATLAB we deal with the system equation given in the form of Equation (6–13), which may be written as

$$1 + K\frac{\text{num}}{\text{den}} = 0$$

where num is the numerator polynomial and den is the denominator polynomial. That is,

$$\begin{aligned}\text{num} &= (s + z_1)(s + z_2)\cdots(s + z_m)\\ &= s^m + (z_1 + z_2 + \cdots + z_m)s^{m-1} + \cdots + z_1 z_2 \cdots z_m\\ \text{den} &= (s + p_1)(s + p_2)\cdots(s + p_n)\\ &= s^n + (p_1 + p_2 + \cdots + p_n)s^{n-1} + \cdots + p_1 p_2 \cdots p_n\end{aligned}$$

Note that both vectors num and den must be written in descending powers of s.

A MATLAB command commonly used for plotting root loci is

```
rlocus(num,den)
```

Using this command, the root-locus plot is drawn on the screen. The gain vector K is automatically determined. The command rlocus works for both continuous- and discrete-time systems.

For the systems defined in state space, rlocus(A,B,C,D) plots the root locus of the system with the gain vector automatically determined.

Note that commands

```
rlocus(num,den,K)      and      rlocus(A,B,C,D,K)
```

use the user-supplied gain vector K. (The vector K contains all the gain values for which the closed-loop poles are to be computed.)

If invoked with left-hand arguments

```
[r,K] = rlocus(num,den)
[r,K] = rlocus(num,den,K)
[r,K] = rlocus(A,B,C,D)
[r,K] = rlocus(A,B,C,D,K)
```

the screen will show the matrix r and gain vector K. (r has length K rows and length den − 1 columns containing the complex root locations. Each row of the matrix corresponds to a gain from vector K.) The plot command

```
plot(r,' ')
```

plots the root loci.

If it is desired to plot the root loci with marks 'o' or 'x', it is necessary to use the following command:

```
r = rlocus(num,den)
plot(r,'o')      or      plot(r,'x')
```

Plotting root loci using marks 'o' or 'x' is instructive, since each calculated closed-loop pole is graphically shown; in some portion of the root loci those marks are densely placed and in another portion of the root loci they are sparsely placed. MATLAB supplies its own set of gain values used to calculate a root-locus plot. It does so by an internal adaptive step-size routine. Also, MATLAB uses the automatic axis-scaling feature of the *plot* command.

Finally, note that, since the gain vector is automatically determined, root-locus plots of

$$G(s)H(s) = \frac{K(s + 1)}{s(s + 2)(s + 3)}$$

$$G(s)H(s) = \frac{10K(s + 1)}{s(s + 2)(s + 3)}$$

$$G(s)H(s) = \frac{200K(s + 1)}{s(s + 2)(s + 3)}$$

are all the same. The num and den set of the system is the same for all three systems. The num and den are

```
num = [0   0   1   1]
den = [1   5   6   0]
```

EXAMPLE 6–3 Consider the control system shown in Figure 6–14. To plot the root-locus diagram with MATLAB, it is necessary to find the numerator and denominator polynomials of the open loop.

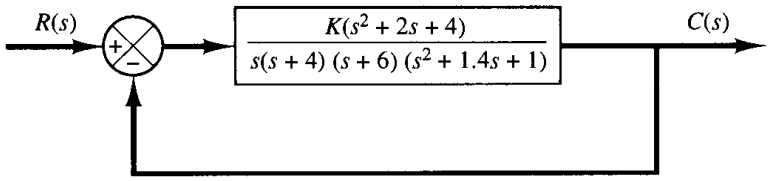

Figure 6–14
Control system.

For this problem, the numerator is already given as a polynomial in s. However, the denominator is given as a product of first- and second-order terms, with the result that we must multiply these terms to get a polynomial in s. The multiplication of these terms can be done easily by use of the *convolution command,* as shown next.

Define

$$a = s(s + 4) = s^2 + 4s \quad : \quad \text{a = [1 4 0]}$$
$$b = s + 6 \quad : \quad \text{b = [1 6]}$$
$$c = s^2 + 1.4s + 1 \quad : \quad \text{c = [1 1.4 1]}$$

Then use the following command:

```
d = conv(a,b);      e = conv(c,d)
```

[Note that conv(a,b) gives the product of two polynomials a and b.] See the following computer output:

```
a = [1   4   0];
b = [1   6];
c = [1   1.4   1];
d = conv(a,b)

d =

     1   10   24   0

e = conv(c,d)

e =

     1.0000   11.4000   39.0000   43.6000   24.0000   0
```

The denominator polynomial is thus found to be

```
den = [1   11.4   39   43.6   24   0]
```

To find the open-loop zeros of the given transfer function, we may use the following roots command:

```
p = [1   2   4]
r = roots(p)
```

The command and the computer output are shown next.

```
p = [1   2   4];
r = roots(p)

r =

  -1.0000 + 1.7321i
  -1.0000 - 1.7321i
```

Similarly, to find the complex-conjugate open-loop poles (the roots of $s^2 + 1.4s + 1 = 0$), we may enter the roots commands as follows:

```
q = roots(c)

q =

    -0.7000 + 0.7141i
    -0.7000 - 0.7141i
```

Thus the system has the following open-loop zeros and open-loop poles;

$$\begin{aligned} &\text{Open-loop zeros:} && s = -1 + j1.7321, && s = -1 - j1.7321 \\ &\text{Open-loop poles:} && s = -0.7 + j0.7141, && s = -0.7 - j0.7141 \\ & && s = 0, \quad s = -4, && s = -6 \end{aligned}$$

MATLAB Program 6–1 will plot the root-locus diagram for this system. The plot is shown in Figure 6–15.

MATLAB Program 6–1

```
% ---------- Root-locus plot ----------

num = [0   0   0   1   2   4];
den = [1   11.4   39   43.6   24   0];
rlocus(num,den)

Warning: Divide by zero
v = [-10   10   -10   10]; axis(v)
grid
title('Root-Locus Plot of G(s) = K(s^2 + 2s + 4)/[s(s + 4)(s + 6)(s^2 + 1.4s + 1)]')
```

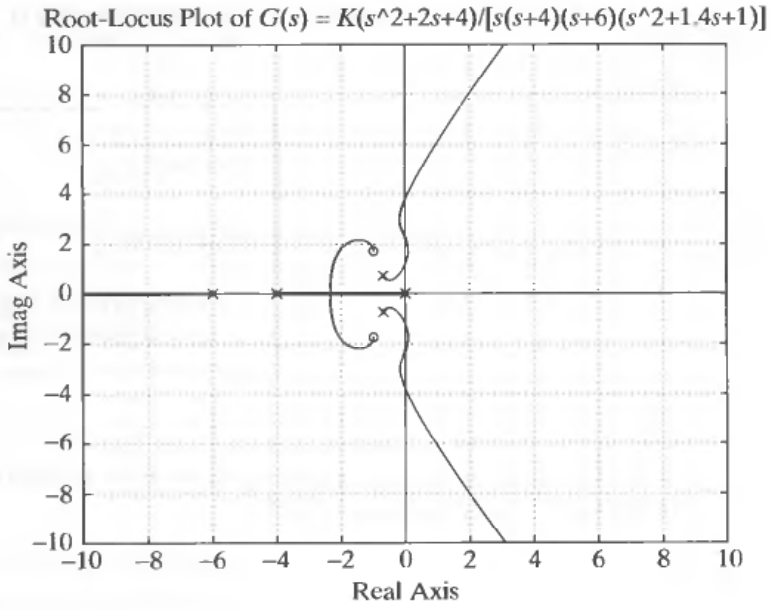

Figure 6–15
Root-locus plot.

EXAMPLE 6–4 Consider the system shown in Figure 6–16, where the open-loop transfer function $G(s)H(s)$ is

$$G(s)H(s) = \frac{K(s + 0.2)}{s^2(s + 3.6)}$$

The open-loop zero is at $s = -0.2$, and open-loop poles are at $s = 0, s = 0$, and $s = -3.6$.

MATLAB Program 6–2 generates a root-locus plot. The resulting root-locus plot is shown in Figure 6–17.

MATLAB Program 6–2

```
% --------- Root-locus plot ----------

num = [0   0   1   0.2];
den = [1   3.6   0   0];
rlocus(num,den)
v = [−4   2   −4   4]; axis(v)
grid
title('Root-Locus Plot of G(s) = K(s + 0.2)/[s^2(s + 3.6)]')
```

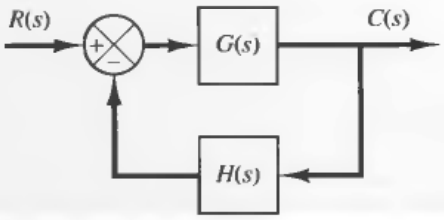

Figure 6–16
Control system.

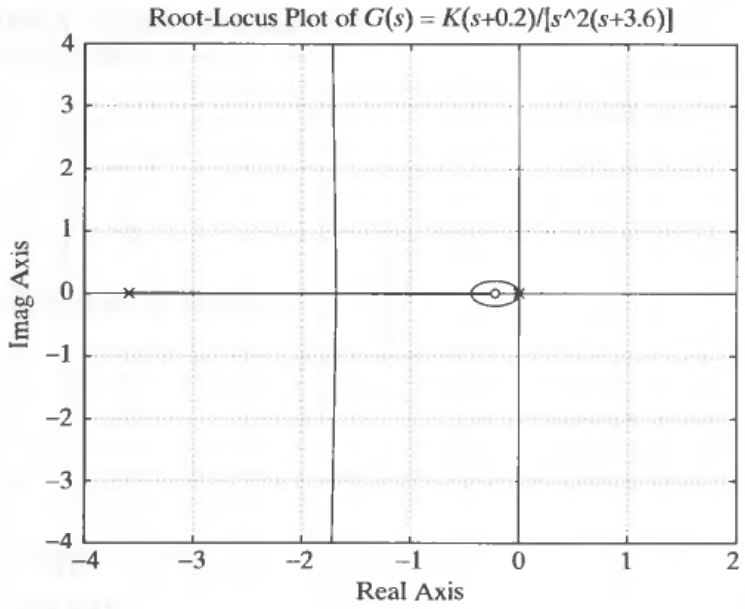

Figure 6–17
Root-locus plot.

EXAMPLE 6–5 Consider the system shown in Figure 6–18. Plot root loci with a square aspect ratio so that a line with slope 1 is a true 45° line.

To set the plot region on the screen to be square, enter the command axis('square'). With this command, a line with slope 1 is at a true 45°, not skewed by the irregular shape of the screen. (It is important to note that a hard-copy plot may or may not be of a square region depending on a printer.)

MATLAB Program 6–3 produces a root-locus plot in a square region. The resulting plot is shown in Figure 6–19.

MATLAB Program 6–3

```
% ---------- Root-locus plot ----------

num = [0   0   0   1   1];
den = [1   3   12   −16   0];
rlocus(num,den)
v = [−6   6   −6   6]; axis(v);axis('square')
grid
title('Root-Locus Plot of G(s) = K(s + 1)/[s(s − 1)(s^2 + 4s + 16)]')
```

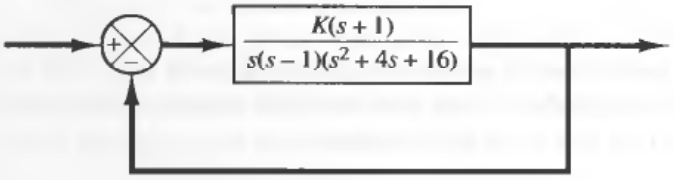

Figure 6–18
Control system.

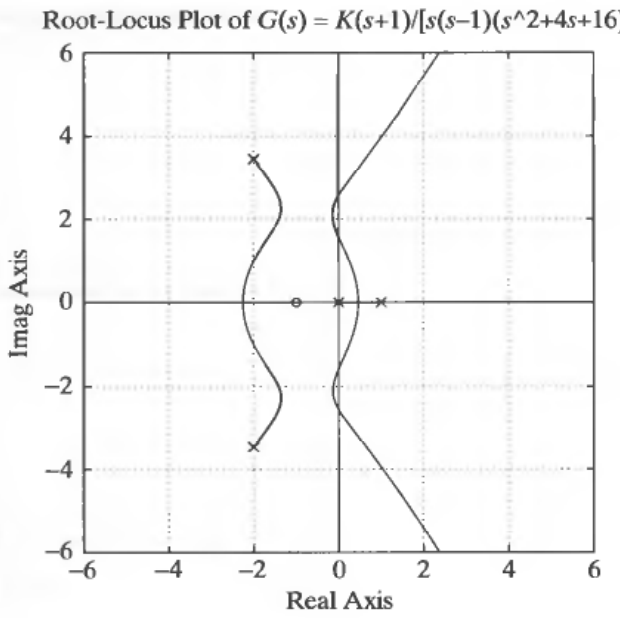

Figure 6–19
Root-locus plot.

EXAMPLE 6–6 Consider the system whose open-loop transfer function $G(s)H(s)$ is

$$G(s)H(s) = \frac{K}{s(s + 0.5)(s^2 + 0.6s + 10)}$$

$$= \frac{K}{s^4 + 1.1s^3 + 10.3s^2 + 5s}$$

There are no open-loop zeros. Open-loop poles are located at $s = -0.3 + j3.1480$, $s = -0.3 - j3.1480$, $s = -0.5$, and $s = 0$.

Entering MATLAB Program 6–4 into the computer, we obtain the root-locus plot shown in Figure 6–20.

MATLAB Program 6–4

```
% ---------- Root-locus plot ---------

num = [0   0   0   0   1];
den = [1   1.1   10.3   5   0];
rlocus(num,den)
grid
title('Root-Locus Plot of G(s) = K/[s(s + 0.5)(s^2 + 0.6s + 10)]')
```

Notice that in the regions near $x = -0.3$, $y = 2.3$ and $x = -0.3$, $y = -2.3$ two loci approach each other. We may wonder if these two branches should touch or not. To explore this situation, we may plot the root loci using the command

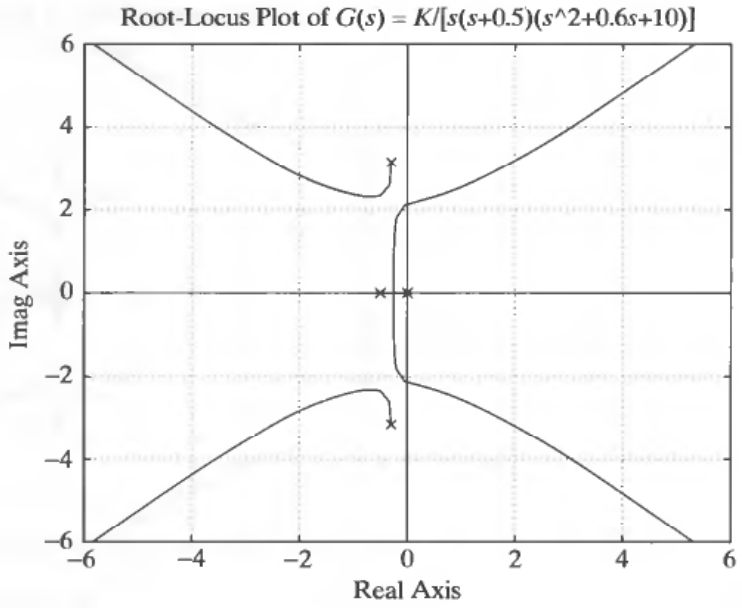

Figure 6–20
Root-locus plot.

```
r = rlocus(num,den)
plot(r,'o')
```

as shown in MATLAB Program 6–5. Figure 6–21 shows the resulting plot.

MATLAB Program 6–5

```
% --------- Root-locus plot ---------

num = [0   0   0   0   1];
den = [1   1.1   10.3   5   0];
r = rlocus(num,den);
plot(r,'or')
v = [−6   6   −6   6]; axis(v)
grid
title('Root-Locus Plot of G(s) = K/[s(s + 0.5)(s^2 + 0.6s + 10)]')
xlabel('Real Axis')
ylabel('Imag Axis')

% ***** Note that the command 'plot(r,'or')' gives small circles
% in the screen plot in red color *****
```

Since there are no computed points near $(-0.3, 2.3)$ and $(-0.3, -2.3)$, it is necessary to adjust steps in gain K. By a trial and error approach, we find the particular region of interest to be $20 \leq K \leq 30$. By entering MATLAB Program 6–6, we obtain the root-locus plot shown in Figure 6–22. From this plot, it is clear that the two branches that approach in the upper half-plane (or in the lower half-plane) do not touch.

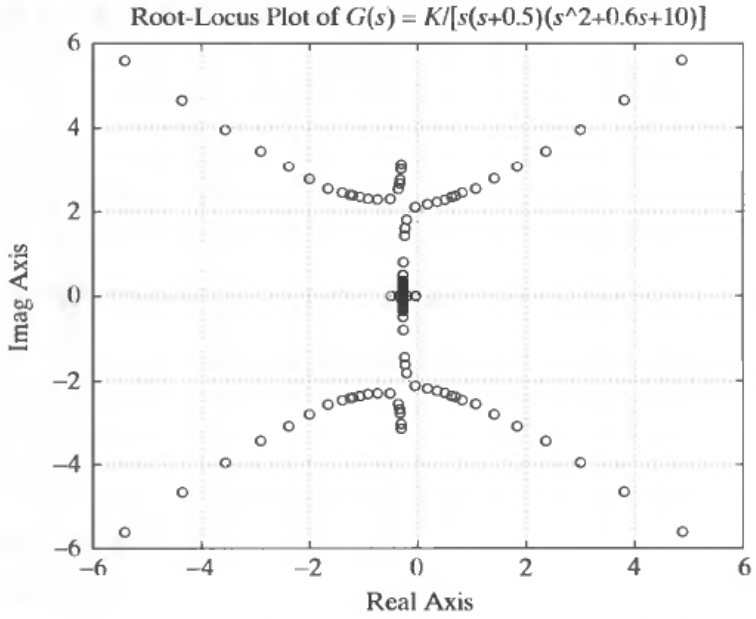

Figure 6–21
Root-locus plot.

MATLAB Program 6–6

```
% ---------- Root-locus plot ----------

num = [0   0   0   0   1];
den = [1   1.1   10.3   5   0];
K1 = 0:0.2:20;
K2 = 20:0.1:30;
K3 = 30:5:1000;
K = [K1   K2   K3];
r = rlocus(num,den,K);
plot(r,'ob')
v = [−4   4   −4   4]; axis(v)
grid
title('Root-Locus Plot of G(s) = K/[s(s + 0.5)(s^2 + 0.6s + 10)]')
xlabel('Real Axis')
ylabel('Imag Axis')

% ***** Note that the command 'plot(r,'ob')' gives small circles
% in the screen plot in blue color *****
```

EXAMPLE 6–7 Consider the system shown in Figure 6–23. The system equations are

$$\dot{\mathbf{x}} = \mathbf{A}\mathbf{x} + \mathbf{B}u$$

$$y = \mathbf{C}\mathbf{x} + Du$$

$$u = r - y$$

In this example problem we shall obtain the root-locus diagram of the system defined in state space. Let us assume, for example, that matrices **A**, **B**, **C**, and D are given by

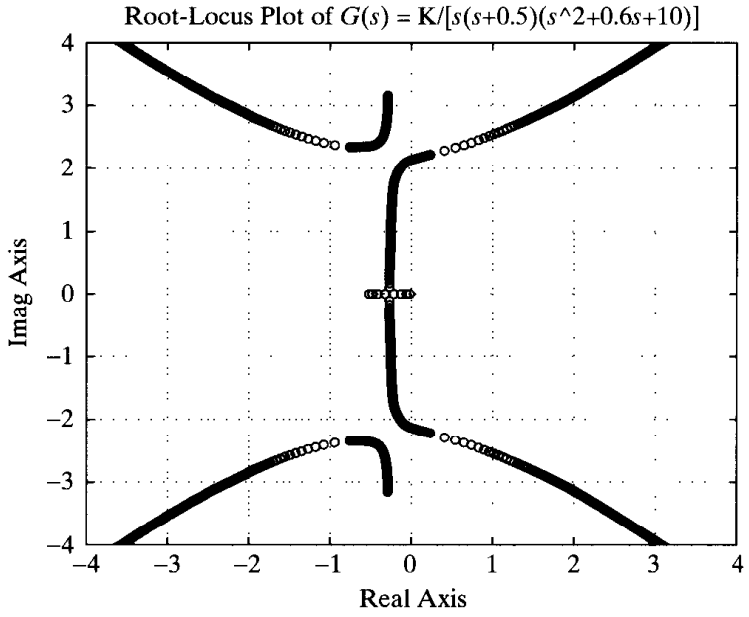

Figure 6–22
Root-locus plot.

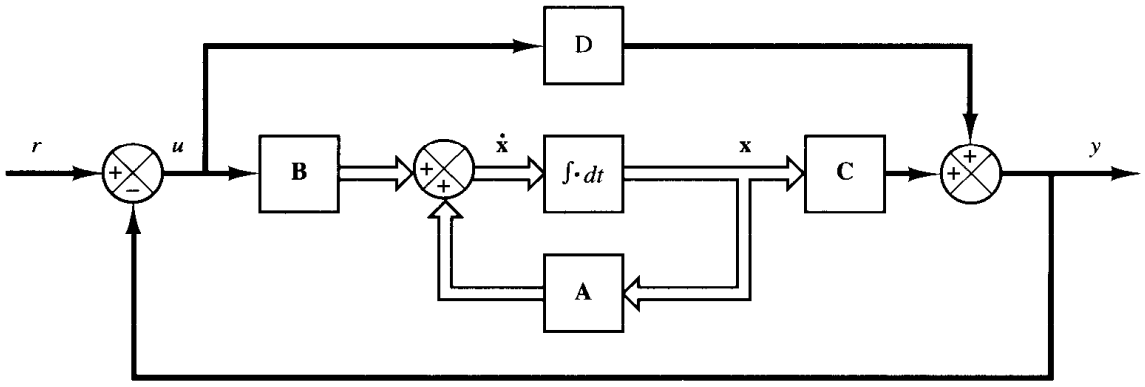

Figure 6–23
Closed-loop control system.

$$\mathbf{A} = \begin{bmatrix} 0 & 1 & 0 \\ 0 & 0 & 1 \\ -160 & -56 & -14 \end{bmatrix}, \quad \mathbf{B} = \begin{bmatrix} 0 \\ 1 \\ -14 \end{bmatrix} \tag{6–18}$$

$$\mathbf{C} = [1 \quad 0 \quad 0], \qquad D = [0]$$

The root-locus plot for this system can be obtained with MATLAB by use of the following command:

```
rlocus(A,B,C,D)
```

This command will produce the same root-locus plot as can be obtained by use of the rlocus (num,den) command, where num and den are obtained from

```
[num,den] = ss2tf(A,B,C,D)
```

as follows:

```
num = [0   0   1   0]
den = [1   14   56   160]
```

MATLAB Program 6–7 gives a program that will generate the root-locus plot as shown in Figure 6–24.

MATLAB Program 6–7

```
% ---------- Root-locus plot ----------

% ***** Root-locus plot of system defined in state space *****

% ***** Enter matrices A, B, C, and D *****

A = [0   1   0;0   0   1;−160   −56   −14];
B = [0;1;−14];
C = [1   0   0];
D = [0];

% ***** Enter rlocus(A,B,C,D) command in the computer *****

rlocus(A,B,C,D)
grid
title('Root-Locus Plot of System defined in State Space')
```

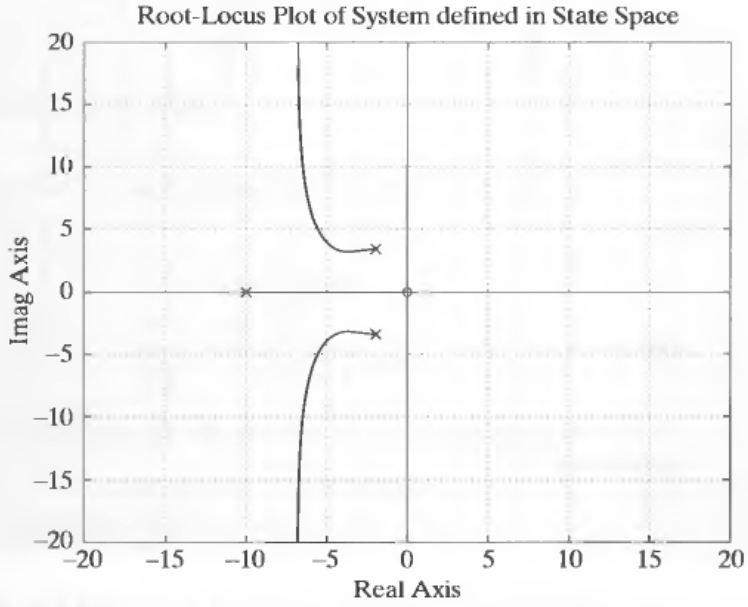

Figure 6–24
Root-locus plot of system defined in state space, where **A**, **B**, **C**, and D are as given by Equation (6–18).

6–5 SPECIAL CASES

In this section we shall consider two special cases. One is the case in which the gain K does not appear as a multiplicative factor, and in the other the closed-loop system is a positive-feedback system, rather than a negative-feedback system.

Constructing root loci when a variable parameter does not appear as a multiplying factor. In some cases the variable parameter K may not appear as a multiplying factor of $G(s)H(s)$. In such cases it may be possible to rewrite the characteristic equation such that the variable parameter K appears as a multiplying factor of $G(s)H(s)$. Example 6–8 illustrates how to proceed in such a case.

EXAMPLE 6–8 Consider the system in Figure 6–25. Draw a root-locus diagram. Then determine the value of k such that the damping ratio of the dominant closed-loop poles is 0.4.

Here the system involves velocity feedback. The open-loop transfer function is

$$\text{Open-loop transfer function} = \frac{20}{s(s+1)(s+4)+20ks}$$

Notice that the adjustable variable k does not appear as a multiplying factor. The characteristic equation for the system is

$$s^3 + 5s^2 + 4s + 20 + 20ks = 0 \tag{6–19}$$

Define

$$20k = K$$

Then Equation (6–19) becomes

$$s^3 + 5s^2 + 4s + Ks + 20 = 0 \tag{6–20}$$

Dividing both sides of Equation (6–20) by the sum of the terms that do not contain K, we get

$$1 + \frac{Ks}{s^3 + 5s^2 + 4s + 20} = 0$$

or

$$1 + \frac{Ks}{(s+j2)(s-j2)(s+5)} = 0 \tag{6–21}$$

Equation (6–21) is now of the form of Equation (6–5).

We shall now sketch the root loci of the system given by Equation (6–21). Notice that the open-loop poles are located at $s = j2, s = -j2, s = -5$, and the open-loop zero is located at $s = 0$. The root locus exists on the real axis between 0 and -5. Since

$$\lim_{s\to\infty} \frac{Ks}{(s+j2)(s-j2)(s+5)} = \lim_{s\to\infty} \frac{K}{s^2}$$

we have

$$\text{Angle of asymptote} = \frac{\pm 180°(2k+1)}{2} = \pm 90°$$

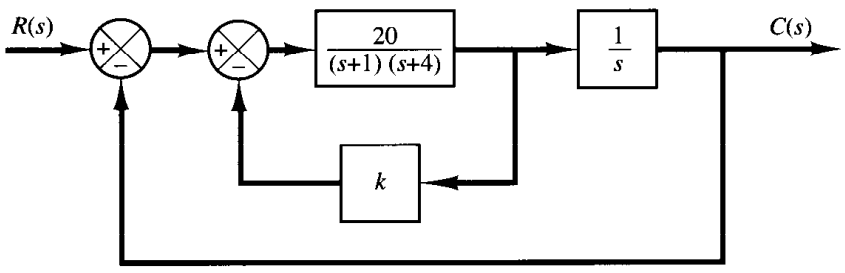

Figure 6–25
Control system.

The intersection of the asymptotes with the real axis can be found from

$$\lim_{s\to\infty} \frac{Ks}{s^3 + 5s^2 + 4s + 20} = \lim_{s\to\infty} \frac{K}{s^2 + 5s + \cdots} = \lim_{s\to\infty} \frac{K}{(s + 2.5)^2}$$

as

$$\sigma_a = -2.5$$

The angle of departure (angle θ) from the pole at $s = j2$ is obtained as follows:

$$\theta = 180° - 90° - 21.8° + 90° = 158.2°$$

Thus, the angle of departure from the pole $s = j2$ is 158.2°. Figure 6–26 shows a root-locus plot for the system.

Note that the closed-loop poles with $\zeta = 0.4$ must lie on straight lines passing through the origin and making the angles $\pm 66.42°$ with the negative real axis. In the present case, there are two intersections of the root-locus branch in the upper half s plane and the straight line of angle 66.42°. Thus, two values of K will give the damping ratio ζ of the closed-loop poles equal to 0.4. At point P, the value of K is

$$K = \left| \frac{(s + j2)(s - j2)(s + 5)}{s} \right|_{s=-1.0490+j2.4065} = 8.9801$$

Hence

$$k = \frac{K}{20} = 0.4490 \qquad \text{at point } P$$

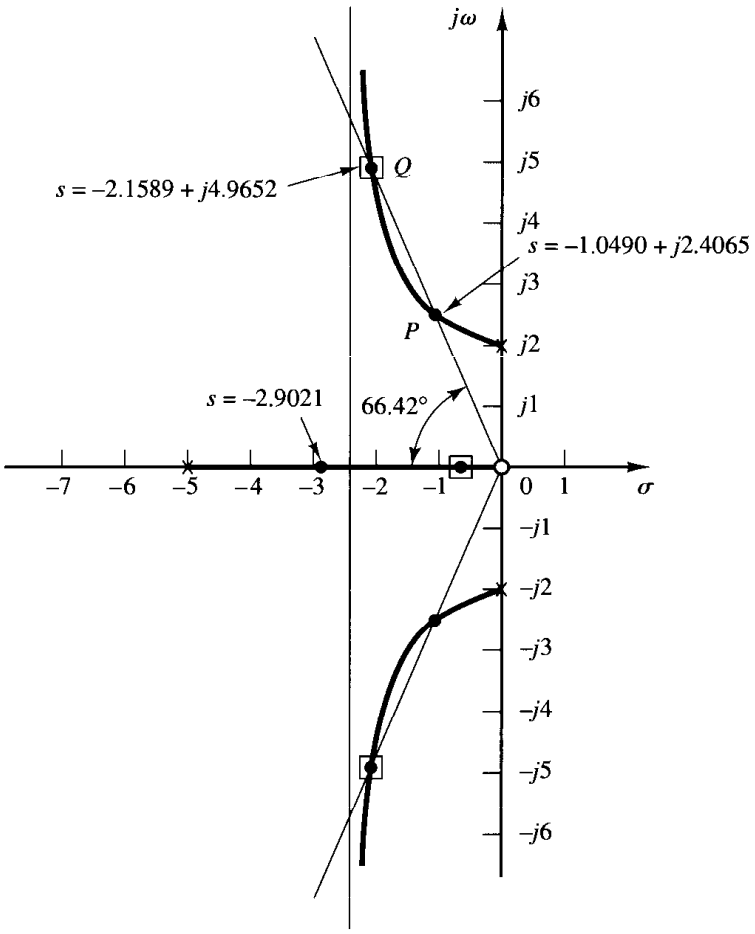

Figure 6–26
Root-locus plot for the system shown in Figure 6–25.

At point Q, the value of K is

$$K = \left| \frac{(s + j2)(s - j2)(s + 5)}{s} \right|_{s=-2.1589+j4.9652} = 28.260$$

Hence

$$k = \frac{K}{20} = 1.4130 \qquad \text{at point } Q$$

Thus, we have two solutions for this problem. For $k = 0.4490$, the three closed-loop poles are located at

$$s = -1.0490 + j2.4065, \qquad s = -1.0490 - j2.4065, \qquad s = -2.9021$$

For $k = 1.4130$, the three closed-loop poles are located at

$$s = -2.1589 + j4.9652, \qquad s = -2.1589 - j4.9652, \qquad s = -0.6823$$

It is important to point out that the zero at the origin is the open-loop zero, but not the closed-loop zero. This is evident, because the original system shown in Figure 6–25 does not have a closed-loop zero, since

$$\frac{C(s)}{R(s)} = \frac{20}{s(s + 1)(s + 4) + 20(1 + ks)}$$

The open-loop zero at $s = 0$ was introduced in the process of modifying the characteristic equation such that the adjustable variable $K = 20k$ was to appear as a multiplying factor.

We have obtained two different values of k to satisfy the requirement that the damping ratio of the dominant closed-loop poles be equal to 0.4. The closed-loop transfer function with $k = 0.4490$ is given by

$$\frac{C(s)}{R(s)} = \frac{20}{s^3 + 5s^2 + 12.98s + 20}$$

$$= \frac{20}{(s + 1.0490 + j2.4065)(s + 1.0490 - j2.4065)(s + 2.9021)}$$

The closed-loop transfer function with $k = 1.4130$ is given by

$$\frac{C(s)}{R(s)} = \frac{20}{s^3 + 5s^2 + 32.26s + 20}$$

$$= \frac{20}{(s + 2.1589 + j4.9652)(s + 2.1589 - j4.9652)(s + 0.6823)}$$

Notice that the system with $k = 0.4490$ has a pair of dominant complex-conjugate closed-loop poles, while in the system with $k = 1.4130$ the real closed-loop pole at $s = -0.6823$ is dominant, and the complex-conjugate closed-loop poles are not dominant. In this case, the response characteristic is primarily determined by the real closed-loop pole.

Let us compare the unit-step responses of both systems. MATLAB Program 6–8 may be used for plotting the unit-step response curves in one diagram. The resulting unit-step response curves [$c_1(t)$ for $k = 0.4490$ and $c_2(t)$ for $k = 1.4130$] are shown in Figure 6–27.

From Figure 6–27 we notice that the response of the system with $k = 0.4490$ is oscillatory. (The effect of the closed-loop pole at $s = -2.9021$ on the unit-step response is small.) For the system with $k = 1.4130$, the oscillations due to the closed-loop poles at $s = -2.1589 \pm j4.9652$ damp out much faster than purely exponential response due to the closed-loop pole at $s = -0.6823$.

MATLAB Program 6–8

```
% ---------- Unit-step response ----------

% ***** Enter numerators and denominators of system with
% k = 0.4490 and k = 1.4130, respectively. *****

num1 = [0   0   0   20];
den1 = [1   5   12.98   20];
num2 = [0   0   0   20];
den2 = [1   5   32.26   20];
t = 0:0.1:10;
[c1,x1,t] = step(num1,den1,t);
[c2,x2,t] = step(num2,den2,t);
plot(t,c1,t,c2)
text(2.5,1.12,'k = 0.4490')
text(3.7,0.85,'k = 1.4130')
grid
title('Unit-Step Responses of Two Systems')
xlabel('t Sec')
ylabel('Outputs c1 and c2')
```

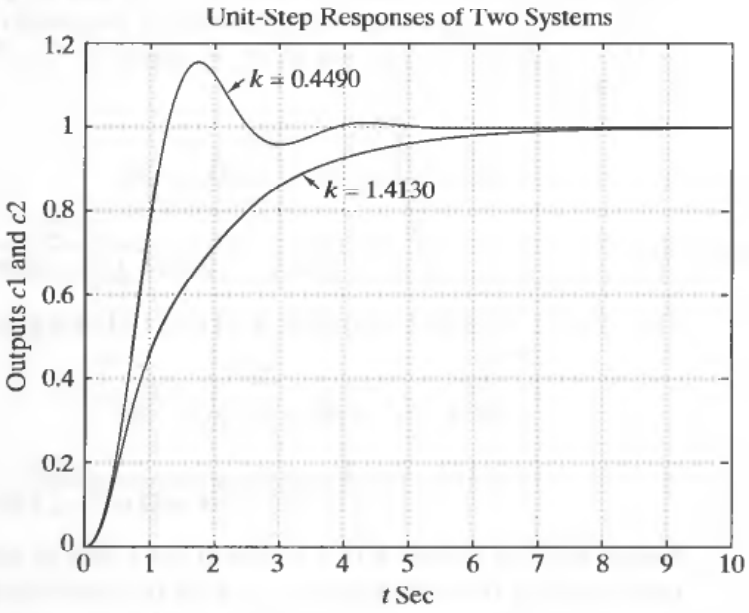

Figure 6–27
Unit-step response curves for the system shown in Figure 6–25 when the damping ratio ζ of the dominant closed-loop poles is set equal to 0.4. (Two possible values of k give the damping ratio ζ equal to 0.4.)

The system with $k = 0.4490$ (which exhibits a faster response with relatively small overshoot) has a much better response characteristic than the system with $k = 1.4130$ (which exhibits a slow overdamped response). Therefore, we should choose $k = 0.4490$ for the present system.

Root loci for positive-feedback systems.* In a complex control system, there may be a positive-feedback inner loop as shown in Figure 6–28. Such a loop is usu-

* Reference W–5.

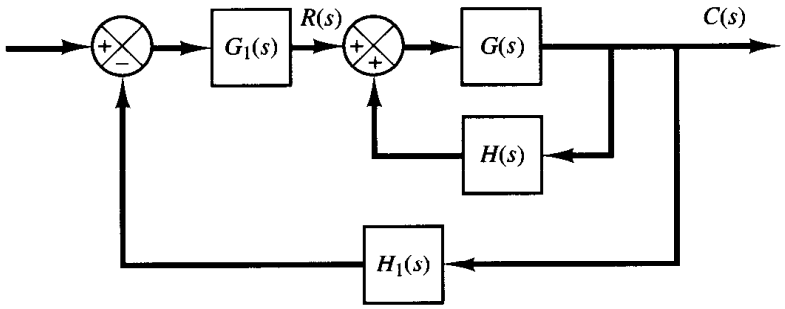

Figure 6–28
Control system.

ally stabilized by the outer loop. In what follows, we shall be concerned only with the positive-feedback inner loop. The closed-loop transfer function of the inner loop is

$$\frac{C(s)}{R(s)} = \frac{G(s)}{1 - G(s)H(s)}$$

The characteristic equation is

$$1 - G(s)H(s) = 0 \tag{6–22}$$

This equation can be solved in a manner similar to the development of the root-locus method in Section 6–2. The angle condition, however, must be altered.

Equation (6–22) can be rewritten as

$$G(s)H(s) = 1$$

which is equivalent to the following two equations:

$$\underline{/G(s)H(s)} = 0° \pm k360° \qquad (k = 0, 1, 2, \ldots)$$

$$|G(s)H(s)| = 1$$

The total sum of all angles from the open-loop poles and zeros must be equal to $0° \pm k360°$. Thus the root locus follows a 0° locus in contrast to the 180° locus considered previously. The magnitude condition remains unaltered.

To illustrate the root-locus plot for the positive feedback system, we shall use the following transfer functions $G(s)$ and $H(s)$ as an example.

$$G(s) = \frac{K(s + 2)}{(s + 3)(s^2 + 2s + 2)}, \qquad H(s) = 1$$

The gain K is assumed to be positive.

The general rules for constructing root loci given in Section 6–3 must be modified in the following way:

Rule 2 is modified as follows: If the total number of real poles and real zeros to the right of a test point on the real axis is even, then this test point lies on the root locus.

Rule 3 is modified as follows:

$$\text{Angles of asymptotes} = \frac{\pm k360^\circ}{n - m} \qquad (k = 0, 1, 2, \ldots)$$

where n = number of finite poles of $G(s)H(s)$
m = number of finite zeros of $G(s)H(s)$

Rule 5 is modified as follows: When calculating the angle of departure (or angle of arrival) from a complex open-loop pole (or at a complex zero), subtract from 0° the sum of all angles of the vectors from all the other poles and zeros to the complex pole (or complex zero) in question, with appropriate signs included.

Other rules for constructing the root-locus plot remain the same. We shall now apply the modified rules to construct the root-locus plot.

1. Plot the open-loop poles ($s = -1 + j$, $s = -1 - j$, $s = -3$) and zero ($s = -2$) in the complex plane. As K is increased from 0 to ∞, the closed-loop poles start at the open-loop poles and terminate at the open-loop zeros (finite or infinite), just as in the case of negative-feedback systems.
2. Determine the root loci on the real axis. Root loci exist on the real axis between -2 and $+\infty$ and between -3 and $-\infty$.
3. Determine the asymptotes of the root loci. For the present system,

$$\text{Angle of asymptote} = \frac{\pm k360^\circ}{3 - 1} = \pm 180^\circ$$

This simply means that asymptotes are on the real axis.

4. Determine the breakaway and break-in points. Since the characteristic equation is

$$(s + 3)(s^2 + 2s + 2) - K(s + 2) = 0$$

we obtain

$$K = \frac{(s + 3)(s^2 + 2s + 2)}{s + 2}$$

By differentiating K with respect to s, we obtain

$$\frac{dK}{ds} = \frac{2s^3 + 11s^2 + 20s + 10}{(s + 2)^2}$$

Note that

$$\begin{aligned} 2s^3 + 11s^2 + 20s + 10 &= 2(s + 0.8)(s^2 + 4.7s + 6.24) \\ &= 2(s + 0.8)(s + 2.35 + j0.77)(s + 2.35 - j0.77) \end{aligned}$$

Point $s = -0.8$ is on the root locus. Since this point lies between two zeros (a finite zero and an infinite zero), it is an actual break-in point. Points $s = -2.35 \pm j0.77$ do not satisfy the angle condition and, therefore, they are neither breakaway nor break-in points.

5. Find the angle of departure of the root locus from a complex pole. For the complex pole at $s = -1 + j$, the angle of departure θ is

$$\theta = 0^\circ - 27^\circ - 90^\circ + 45^\circ$$

or

$$\theta = -72°$$

(The angle of departure from the complex pole at $s = -1 - j$ is 72°.)

6. Choose a test point in the broad neighborhood of the $j\omega$ axis and the origin and apply the angle condition. Locate a sufficient number of points that satisfy the angle condition.

Figure 6–29 shows the root loci for the given positive-feedback system. The root loci are shown with dashed lines and curve.

Note that if

$$K > \left.\frac{(s+3)(s^2+2s+2)}{s+2}\right|_{s=0} = 3$$

one real root enters the right-half s plane. Hence, for values of K greater than 3, the system becomes unstable. (For $K > 3$, the system must be stabilized with an outer loop.)

Note that the closed-loop transfer function for the positive-feedback system is given by

$$\frac{C(s)}{R(s)} = \frac{G(s)}{1 - G(s)H(s)} = \frac{K(s+2)}{(s+3)(s^2+2s+2) - K(s+2)}$$

To compare this root-locus plot with that of the corresponding negative-feedback system, we show in Figure 6–30 the root loci for the negative-feedback system whose closed-loop transfer function is

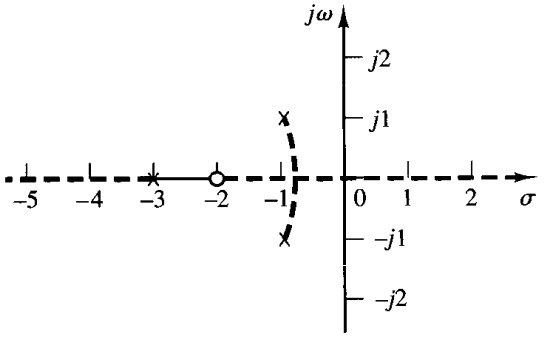

Figure 6–29
Root-locus plot for the positive-feedback system with $G(s) = K(s+2)/[(s+3)(s^2+2s+2)]$, $H(s) = 1$.

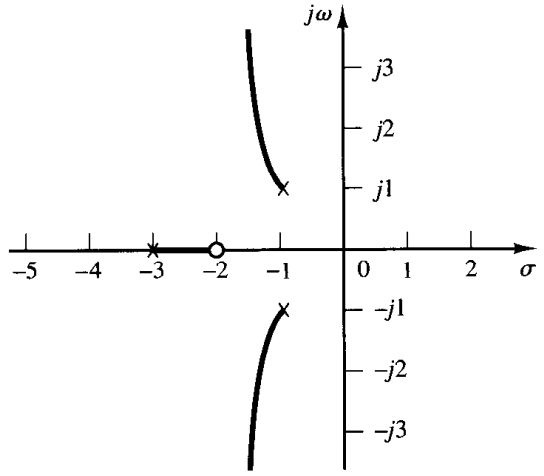

Figure 6–30
Root-locus plot for the negative-feedback system with $G(s) = K(s+2)/[(s+3)(s^2+2s+2)]$, $H(s) = 1$.

$$\frac{C(s)}{R(s)} = \frac{K(s + 2)}{(s + 3)(s^2 + 2s + 2) + K(s + 2)}$$

Table 6–2 shows various root-locus plots of negative-feedback and positive-feedback systems. The closed-loop transfer functions are given by

Table 6–2 Root-Locus Plots of Negative-Feedback and Positive-Feedback Systems

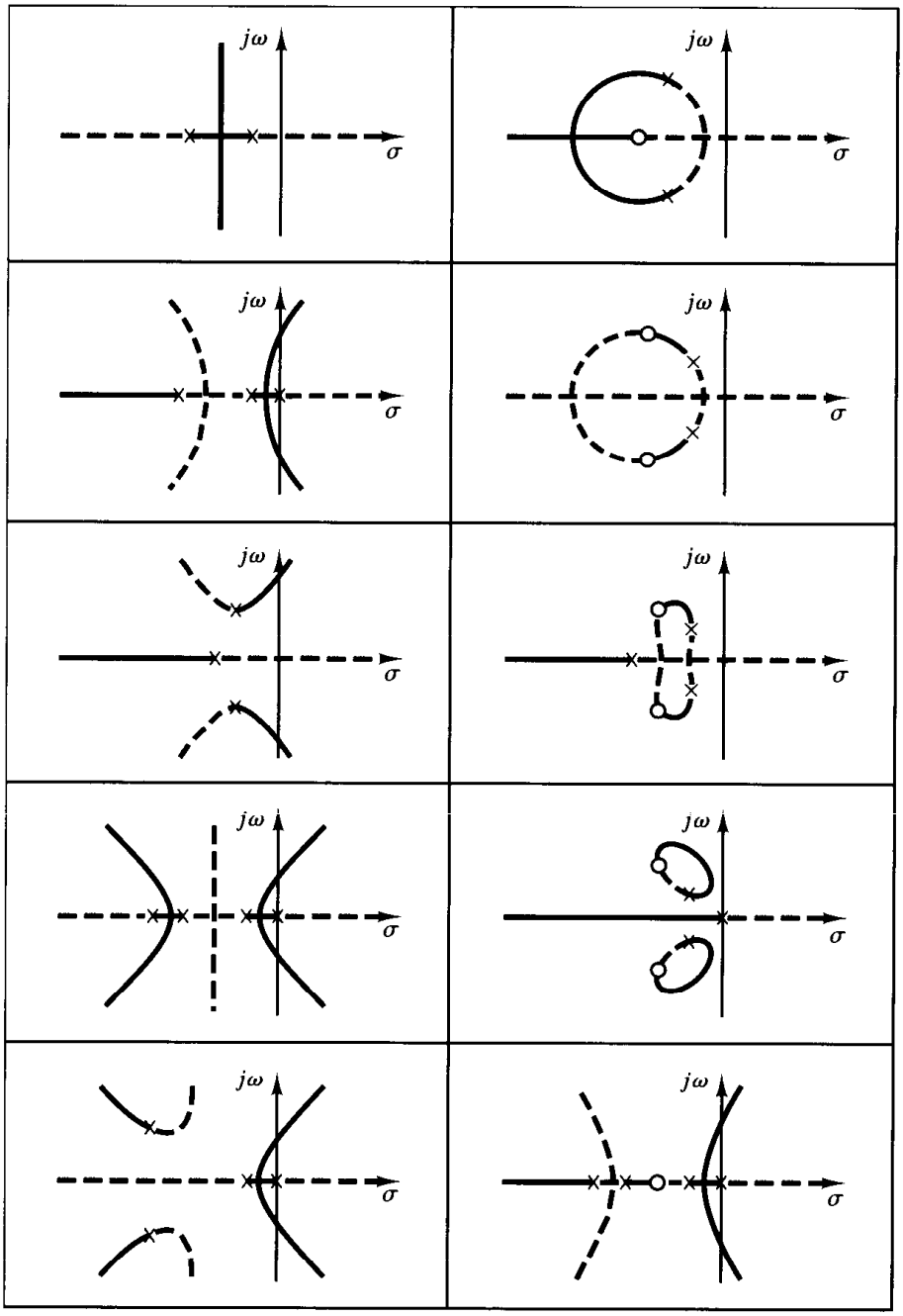

Heavy lines and curves correspond to negative-feedback systems; dashed lines and curves correspond to positive-feedback systems.

$$\frac{C}{R} = \frac{G}{1 + GH}, \qquad \text{for negative-feedback systems}$$

$$\frac{C}{R} = \frac{G}{1 - GH}, \qquad \text{for positive-feedback systems}$$

where GH is the open-loop transfer function. In Table 6–2, the root loci for negative-feedback systems are drawn with heavy lines and curves and those for positive-feedback systems are drawn with dashed lines and curves.

6–6 ROOT-LOCUS ANALYSIS OF CONTROL SYSTEMS

In this section we shall first discuss orthogonality of the root loci and constant-gain loci for the closed-loop systems. Next, we discuss conditionally stable systems. Finally, we analyze nonminimum-phase systems.

Orthogonality of root loci and constant-gain loci. Consider the system whose open-loop transfer function is $G(s)H(s)$. In the $G(s)H(s)$ plane, the loci of $|G(s)H(s)|$ = constant are circles centered at the origin, and the loci corresponding to $\underline{/G(s)H(s)} = \pm 180°(2k + 1)$ $(k = 0, 1, 2, \ldots)$ lie on the negative real axis of the $G(s)H(s)$ plane, as shown in Figure 6–31. [Note that the complex plane employed here is not the s plane, but the $G(s)H(s)$ plane.]

The root loci and constant-gain loci in the s plane are conformal mappings of the loci of $\underline{/G(s)H(s)} = \pm 180°(2k + 1)$ and of $|G(s)H(s)|$ = constant in the $G(s)H(s)$ plane.

Since the constant-phase and constant-gain loci in the $G(s)H(s)$ plane are orthogonal, the root loci and constant-gain loci in the s plane are orthogonal. Figure 6–32(a) shows the root loci and constant-gain loci for the following system:

$$G(s) = \frac{K(s + 2)}{s^2 + 2s + 3}, \qquad H(s) = 1$$

Notice that since the pole–zero configuration is symmetrical about the real axis the constant-gain loci are also symmetrical about the real axis.

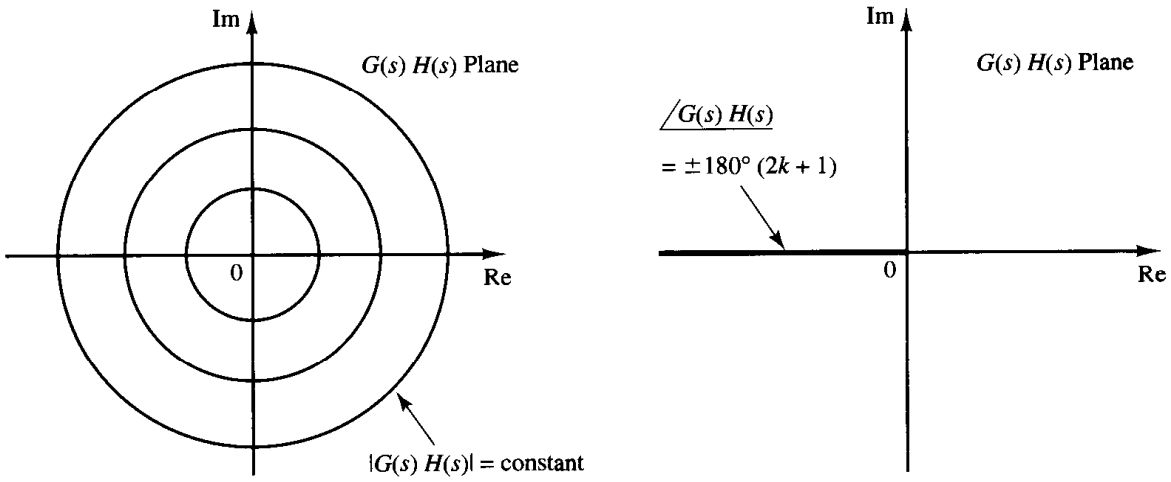

Figure 6–31
Plots of constant-gain and constant-phase loci in the $G(s)H(s)$ plane.

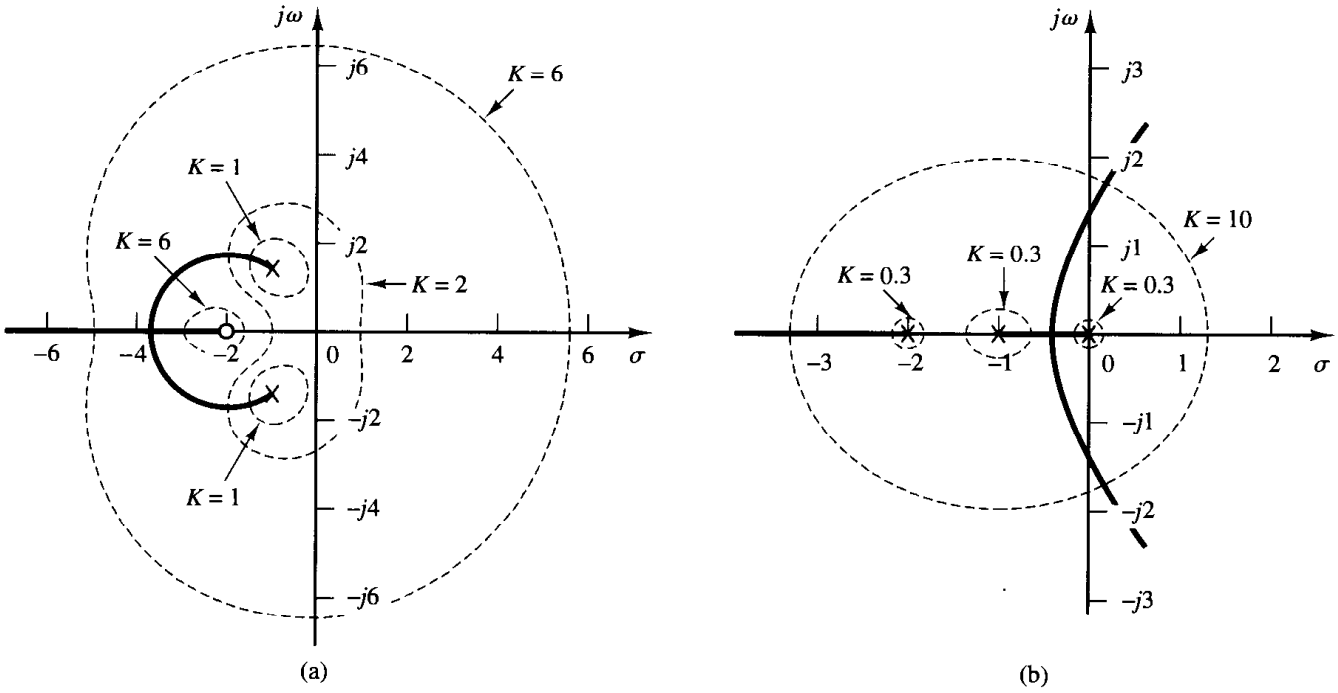

Figure 6–32
Plots of root loci and constant-gain loci. (a) System with $G(s) = K(s + 2)/(s^2 + 2s + 3)$, $H(s) = 1$; (b) system with $G(s) = K/[s(s + 1)(s + 2)]$, $H(s) = 1$.

Figure 6–32(b) shows the root loci and constant-gain loci for the system:

$$G(s) = \frac{K}{s(s + 1)(s + 2)}, \qquad H(s) = 1$$

Notice that since the configuration of the poles in the s plane is symmetrical about the real axis and the line parallel to the imaginary axis passing through point $(\sigma = -1, \omega = 0)$, the constant-gain loci are symmetrical about the $\omega = 0$ line (real axis) and the $\sigma = -1$ line.

Conditionally stable systems. Consider the system shown in Figure 6–33(a). The root loci for this system can be plotted by applying the general rules and procedure for constructing root loci. A root-locus plot for this system is shown in Figure 6–33(b). It can be seen that this system is stable only for limited ranges of the value of K; that is, $0 < K < 14$ and $64 < K < 195$. The system becomes unstable for $14 < K < 64$ and $195 < K$. If K assumes a value corresponding to unstable operation, the system may break down or may become nonlinear due to a saturation nonlinearity that may exist. Such a system is called *conditionally stable.*

In practice, conditionally stable systems are not desirable. Conditional stability is dangerous but does occur in certain systems, in particular, a system that has an unstable feedforward path. Such a feedforward path may occur if the system has a minor loop. It is advisable to avoid such conditional stability since, if the gain drops beyond the critical value for some reason, the system becomes unstable. Note that the addition of a proper compensating network will eliminate conditional stability. [An addition of a zero will cause the root loci to bend to the left. (See Section 7–2). Hence conditional stability may be eliminated by adding proper compensation.]

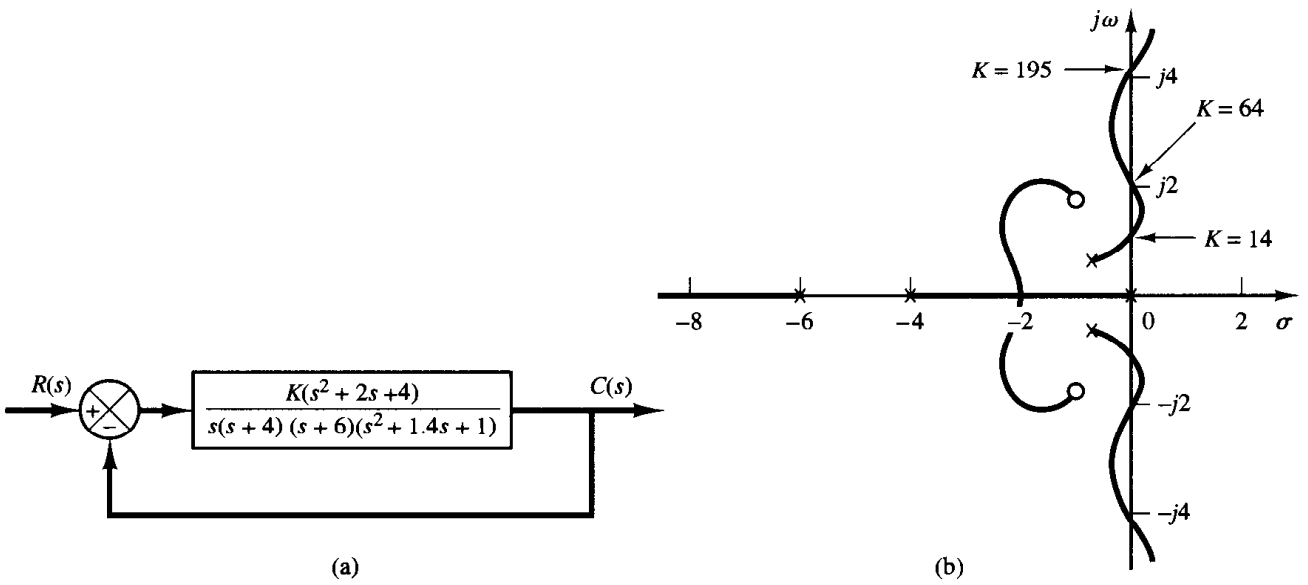

Figure 6–33
(a) Conditionally stable system; (b) root-locus plot.

Nonminimum-phase systems. If all the poles and zeros of a system lie in the left-half s plane, then the system is called *minimum phase.* If a system has at least one pole or zero in the right-half s plane, then the system is called *nonminimum phase.* The term nonminimum phase comes from the phase shift characteristics of such a system when subjected to sinusoidal inputs.

Consider the system shown in Figure 6–34(a). For this system

$$G(s) = \frac{K(1 - T_a s)}{s(Ts + 1)} \qquad (T_a > 0), \qquad H(s) = 1$$

This is a nonminimum-phase system since there is one zero in the right-half s plane. For this system, the angle condition becomes

$$\angle G(s) = \left| -\frac{K(T_a s - 1)}{s(Ts + 1)} \right.$$

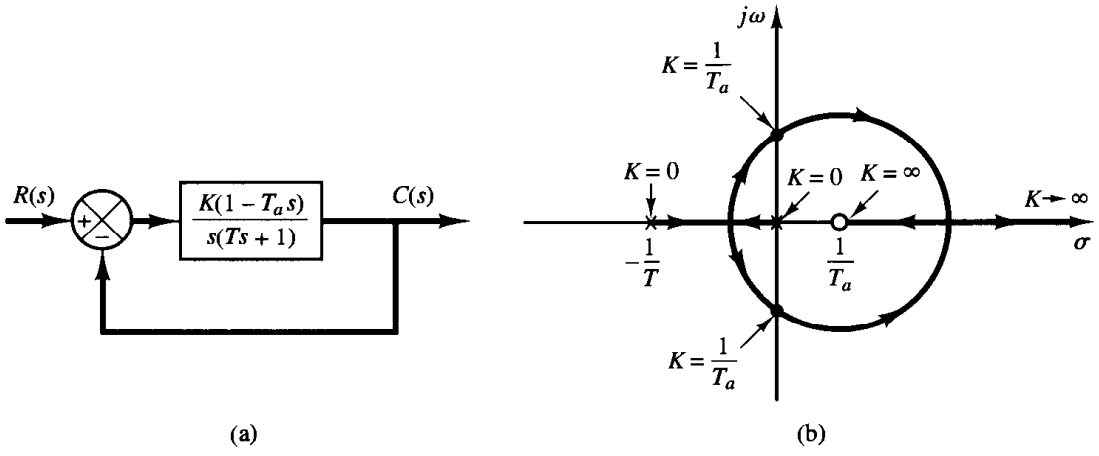

Figure 6–34
(a) Nonminimum phase system; (b) root-locus plot.

$$= \angle \frac{K(T_a s - 1)}{s(Ts + 1)} + 180°$$

$$= \pm 180°(2k + 1) \qquad (k = 0, 1, 2, \ldots)$$

or

$$\angle \frac{K(T_a s - 1)}{s(Ts + 1)} = 0° \tag{6-23}$$

The root loci can be obtained from Equation (6–23). Figure 6–34(b) shows a root-locus plot for this system. From the diagram, we see that the system is stable if the gain K is less than $1/T_a$.

6-7 ROOT LOCI FOR SYSTEMS WITH TRANSPORT LAG

Figure 6–35 shows a thermal system in which hot air is circulated to keep the temperature of a chamber constant. In this system, the measuring element is placed downstream a distance L ft from the furnace, the air velocity is v ft/sec, and $T = L/v$ sec would elapse before any change in the furnace temperature is sensed by the thermometer. Such a delay in measuring, delay in controller action, or delay in actuator operation, and the like, is called *transport lag* or *dead time*. Dead time is present in most process control systems.

The input $x(t)$ and the output $y(t)$ of a transport lag or dead time element are related by

$$y(t) = x(t - T)$$

where T is dead time. The transfer function of transport lag or dead time is given by

$$\text{Transfer function of transport lag or dead time} = \frac{\mathcal{L}[x(t - T)1(t - T)]}{\mathcal{L}[x(t)1(t)]}$$

$$= \frac{X(s)e^{-Ts}}{X(s)} = e^{-Ts}$$

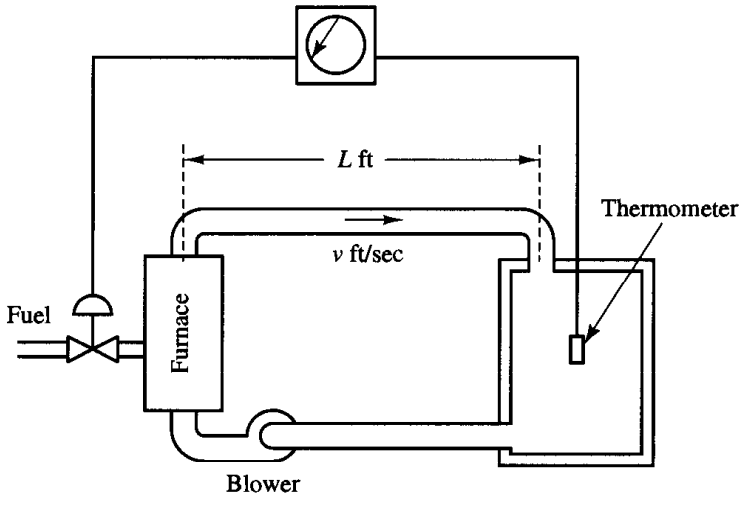

Figure 6–35
Thermal system.

Suppose that the feedforward transfer function of this thermal system can be approximated by

$$G(s) = \frac{Ke^{-Ts}}{s + 1}$$

as shown in Figure 6–36. Let us construct a root-locus plot for this system. The characteristic equation for this closed-loop system is

$$1 + \frac{Ke^{-Ts}}{s + 1} = 0 \tag{6–24}$$

It is noted that for systems with transport lag the rules of construction presented earlier need to be modified. For example, the number of the root-locus branches is infinite, since the characteristic equation has an infinite number of roots. The number of asymptotes is infinite. They are all parallel to the real axis of the s plane.

From Equation (6–24), we obtain

$$\frac{Ke^{-Ts}}{s + 1} = -1$$

Thus, the angle condition becomes

$$\underline{\left/\frac{Ke^{-Ts}}{s + 1}\right.} = \underline{/e^{-Ts}} - \underline{/s + 1} = \pm 180°(2k + 1) \qquad (k = 0, 1, 2, \ldots) \tag{6–25}$$

To find the angle of e^{-Ts}, substitute $s = \sigma + j\omega$. Then we obtain

$$e^{-Ts} = e^{-T\sigma - j\omega T}$$

Since $e^{-T\sigma}$ is a real quantity, the angle of $e^{-T\sigma}$ is zero. Hence

$$\begin{aligned} \underline{/e^{-Ts}} &= \underline{/e^{-j\omega T}} = \underline{/\cos \omega T - j \sin \omega T} \\ &= -\omega T \qquad \text{(radians)} \\ &= -57.3\omega T \qquad \text{(degrees)} \end{aligned}$$

The angle condition, Equation (6–25), then becomes

$$-57.3\omega T - \underline{/s + 1} = \pm 180°(2k + 1)$$

Since T is a given constant, the angle of e^{-Ts} is a function of ω only.

We shall next determine the angle contribution due to e^{-Ts}. For $k = 0$, the angle condition may be written

$$\underline{/s + 1} = \pm 180° - 57.3°\omega T \tag{6–26}$$

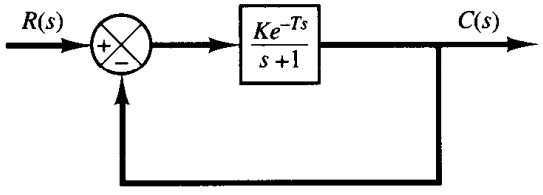

Figure 6–36
Block diagram of the system shown in Figure 6–35.

Since the angle contribution of e^{-Ts} is zero for $\omega = 0$, the real axis from -1 to $-\infty$ forms a part of the root loci. Now assume a value ω_1 for ω and compute $57.3°\omega_1 T$. At point -1 on the negative real axis, draw a line that makes an angle of $180° - 57.3°\omega_1 T$ with the real axis. Find the intersection of this line and the horizontal line $\omega = \omega_1$. This intersection, point P in Figure 6–37(a), is a point satisfying Equation (6–26) and hence is on a root locus. Continuing the same process, we obtain the root-locus plot as shown in Figure 6–37(b).

Note that as s approaches minus infinity, the open-loop transfer function

$$\frac{Ke^{-Ts}}{s+1}$$

approaches minus infinity since

$$\lim_{s=-\infty} \frac{Ke^{-Ts}}{s+1} = \left.\frac{\frac{d}{ds}(Ke^{-Ts})}{\frac{d}{ds}(s+1)}\right|_{s=-\infty}$$
$$= -KTe^{-Ts}\big|_{s=-\infty}$$
$$= -\infty$$

Therefore, $s = -\infty$ is a pole of the open-loop transfer function. Thus, root loci start from $s = -1$ or $s = -\infty$ and terminate at $s = \infty$, as K increases from zero to infinity. Since the right-hand side of the angle condition given by Equation (6–25) has an infinite number of values, there are an infinite number of root loci, as the value of k ($k = 0, 1, 2, \ldots$) goes from zero to infinity. For example, if $k = 1$, the angle condition becomes

$$\angle s + 1 = \pm 540° - 57.3°\omega T \quad \text{(degrees)}$$
$$= \pm 3\pi - \omega T \quad \text{(radians)}$$

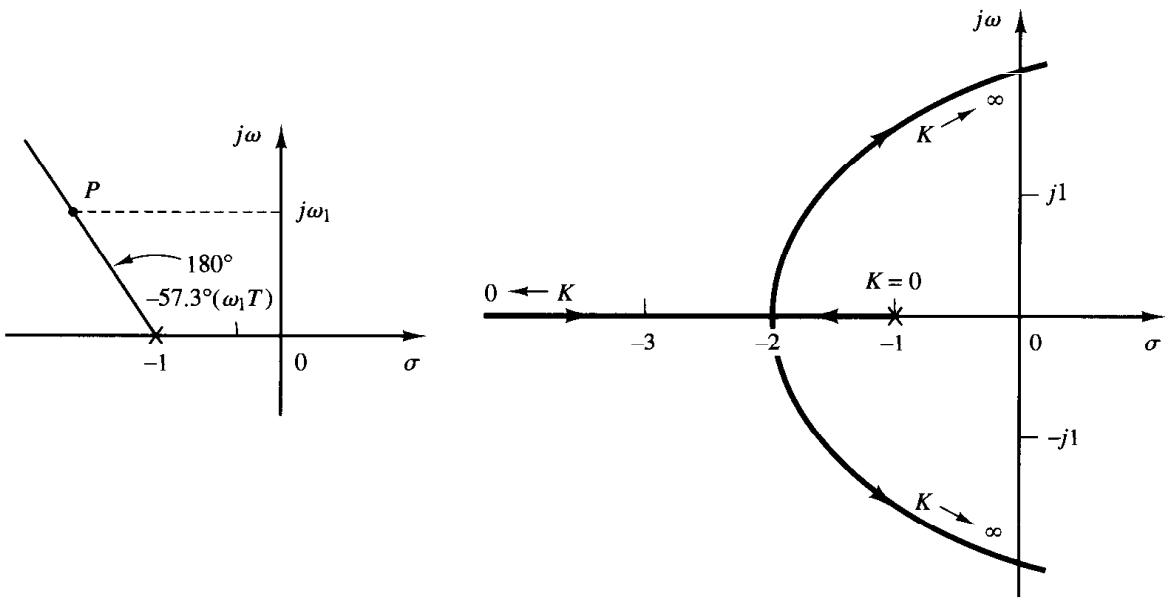

Figure 6–37
(a) Construction of the root locus; (b) root-locus plot.

The construction of the root loci for $k = 1$ is the same as that for $k = 0$. A plot of root loci for $k = 0, 1$, and 2 when $T = 1$ sec is shown in Figure 6–38.

The magnitude condition states that

$$\left|\frac{Ke^{-Ts}}{s+1}\right| = 1$$

Since the magnitude of e^{-Ts} is equal to that of $e^{-T\sigma}$ or

$$|e^{-Ts}| = |e^{-T\sigma}| \cdot |e^{-j\omega T}| = e^{-T\sigma}$$

the magnitude condition becomes

$$|s+1| = Ke^{-T\sigma}$$

The root loci shown in Figure 6–38 are graduated in terms of K when $T = 1$ sec.

Although there are an infinite number of root-locus branches, the primary branch that lies between $-j\pi$ and $j\pi$ is most important. Referring to Figure 6–38, the critical value of K at the primary branch is equal to 2, while the critical values of K at other branches are much higher (8, 14, . . .). Therefore, the critical value $K = 2$ on the primary branch is most significant from the stability viewpoint. The transient response of the system is determined by the roots located closest to the $j\omega$ axis and lie on the primary branch. In summary, the root-locus branch corresponding to $k = 0$ is the dominant one; other branches corresponding to $k = 1, 2, 3, \ldots$ are not so important and may be neglected.

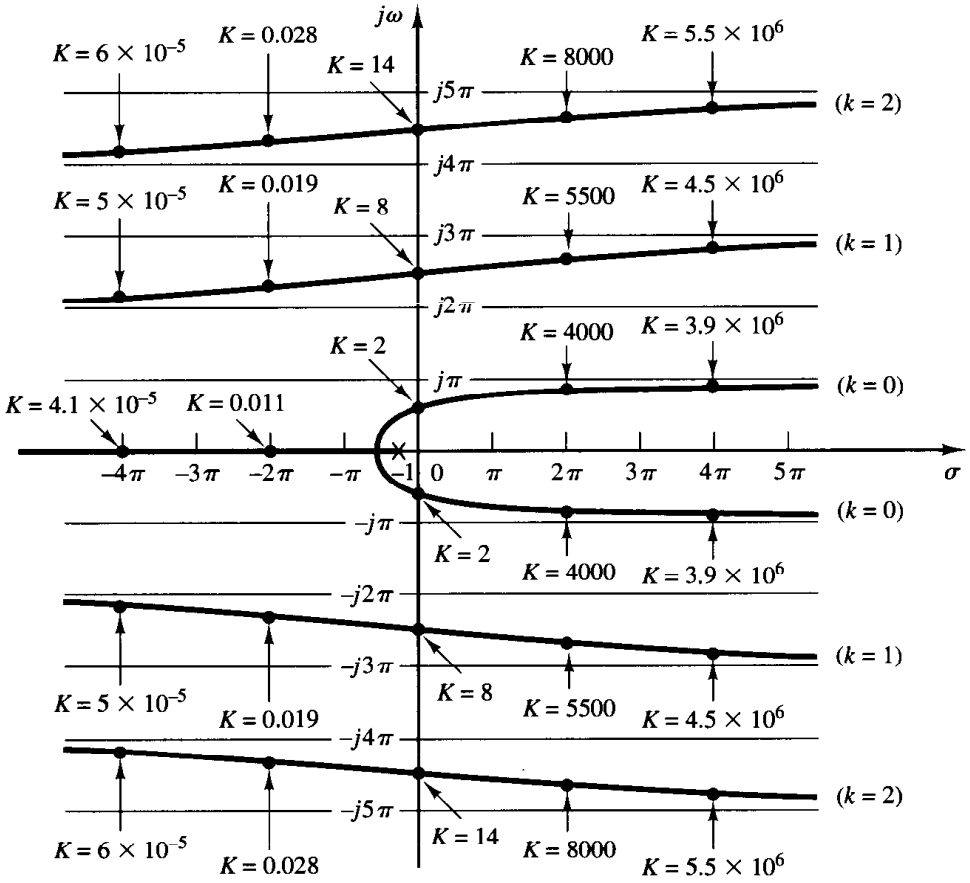

Figure 6–38
Root-locus plot for the system shown in Figure 6–36 ($T = 1$ sec).

This example illustrates the fact that dead time can cause instability even in the first-order system because the root loci enter the right-half s plane for large values of K. Therefore, although the gain K of the first-order system can be set at a high value in the absence of dead time, it cannot be set too high if dead time is present. (For the system considered here, the value of gain K must be considerably less than 2 for a satisfactory operation.)

Approximation of transport lag or dead time. If the dead time T is very small, then e^{-Ts} is frequently approximated by

$$e^{-Ts} \doteqdot 1 - Ts$$

or

$$e^{-Ts} \doteqdot \frac{1}{Ts + 1}$$

Such approximations are good if the dead time is very small and, in addition, the input time function $f(t)$ to the dead-time element is smooth and continuous. [This means that the second- and higher-order derivatives of $f(t)$ are small.]

A more elaborate expression to approximate e^{-Ts} is available and is

$$e^{-Ts} = \frac{1 - \frac{Ts}{2} + \frac{(Ts)^2}{8} - \frac{(Ts)^3}{48} + \cdots}{1 + \frac{Ts}{2} + \frac{(Ts)^2}{8} + \frac{(Ts)^3}{48} + \cdots}$$

If only the first two terms in the numerator and denominator are taken, then

$$e^{-Ts} \doteqdot \frac{1 - \frac{Ts}{2}}{1 + \frac{Ts}{2}} = \frac{2 - Ts}{2 + Ts}$$

This approximation is also used frequently.

6-8 ROOT-CONTOUR PLOTS

Effects of parameter variations on closed-loop poles. In many design problems, the effects on the closed-loop poles of the variations of parameters other than the gain K need to be investigated. Such effects can be easily investigated by the root-locus method. When two (or more) parameters are varied, the corresponding root loci are called *root contours.*

We shall use an example to illustrate the construction of the root contours when two parameters are varied, respectively, from zero to infinity.

Consider a servo system having tachometer feedback as shown in Figure 6–39(a). By eliminating the minor loop, the block diagram can be simplified [Figure 6–39(b)]. By defining

$$a = b + KK_h$$

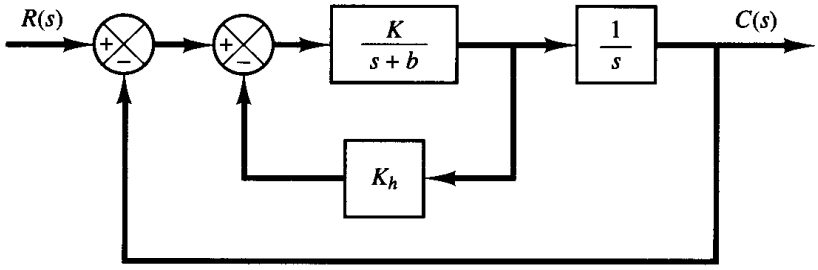

(a)

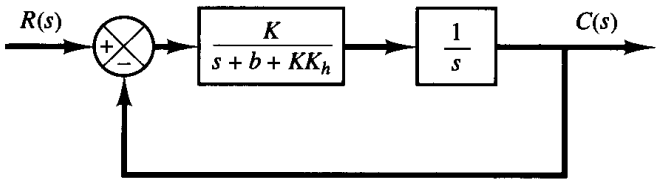

(b)

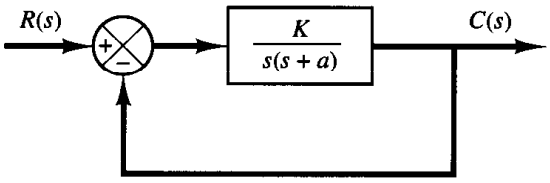

(c)

Figure 6–39
(a) Servo system with tachometer feedback; (b), (c) simplified block diagrams ($a = b + KK_h$).

this block diagram can be modified to that shown in Figure 6–39(c). This system involves two variables, parameter a and gain K.

In what follows we shall investigate the effect of varying the parameter a as well as the gain K. The closed-loop transfer function of this system becomes

$$\frac{C(s)}{R(s)} = \frac{K}{s^2 + as + K}$$

The characteristic equation is

$$s^2 + as + K = 0 \tag{6–27}$$

which may be rewritten

$$1 + \frac{as}{s^2 + K} = 0.$$

or

$$\frac{as}{s^2 + K} = -1 \tag{6–28}$$

In Equation (6–28), the parameter a is written as a multiplying factor. For a given value of K, the effect of a on the closed-loop poles can be investigated from Equation (6–28). The root contours for this system can be constructed by following the usual procedure for constructing root loci.

We shall now construct the root contours as K and a vary, respectively, from zero to infinity. The root contours start from the poles (at $s = \pm j\sqrt{K}$) and terminate at the zeros (at $s = 0$ and infinity).

We shall first construct the locus of roots when $a = 0$. This can be done easily as follows: Substitute $a = 0$ into Equation (6–27). Then

$$s^2 + K = 0$$

or

$$\frac{K}{s^2} = -1 \tag{6–29}$$

The open-loop poles are thus a double pole at the origin. The root-locus plot of Equation (6–29) is shown in Figure 6–40(a).

To construct the root contours, let us assume that K is a constant; for example, $K = 4$. Then Equation (6–28) becomes

$$\frac{as}{s^2 + 4} = -1 \tag{6–30}$$

The open-loop poles are $s = \pm j2$. The finite open-loop zero is at the origin. The root-locus plot corresponding to Equation (6–30) is shown in Figure 6–40(b). For different values of K, Equation (6–30) yields similar root loci.

The root contour, the diagram showing the root loci corresponding to $0 \leq K \leq \infty$, $0 \leq a \leq \infty$, can be plotted as in Figure 6–40(c). Clearly, the root contours start at the

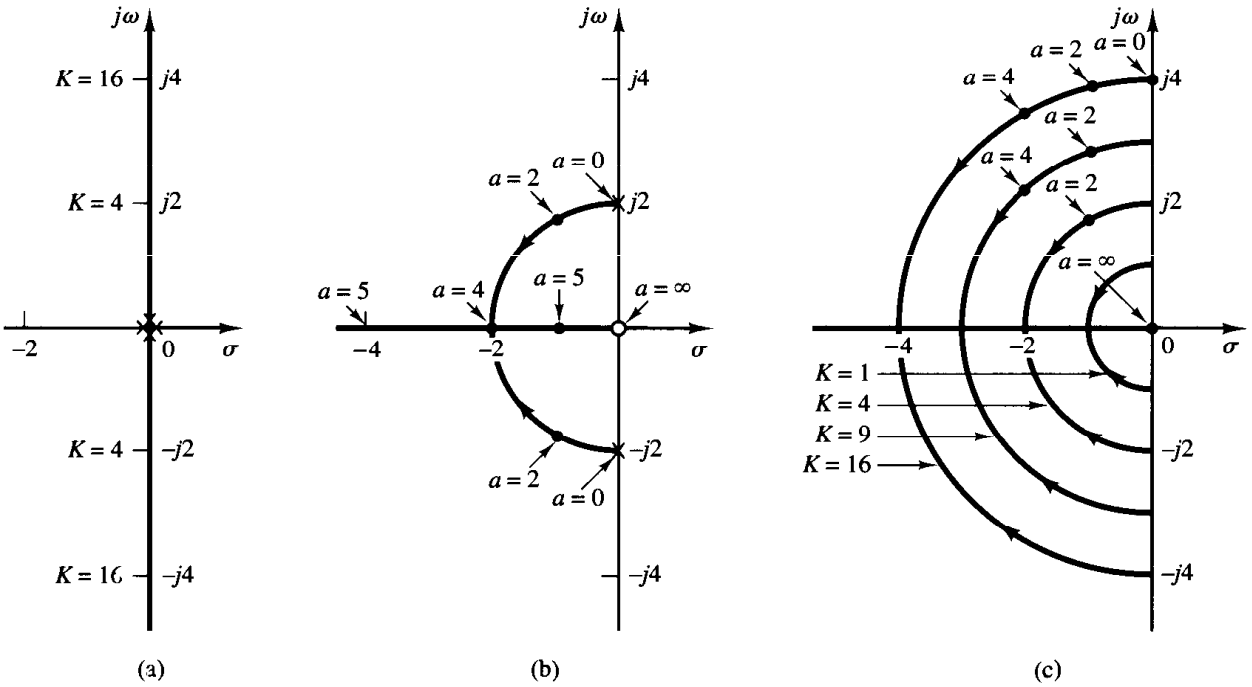

Figure 6–40
(a) Root-locus plot for the system shown in Figure 6–39(c) ($a = 0, 0 \leq K \leq \infty$); (b) root locus plot ($0 \leq a \leq \infty, K = 4$); (c) root-contour plot.

poles of and end at the zeros of the transfer function $as/(s^2 + K)$. The arrowheads on the root contours indicate the direction of increase in the value of a.

The root contours show the effects of the variations of system parameters on the closed-loop poles. From the root-contour plot shown in Figure 6–40(c), we see that, for $0 < K < \infty$, $0 < a < \infty$, the closed-loop poles lie in the left-half s plane and the system is stable.

Note that if the value of K is fixed, say $K = 4$, then the root contours become simply the root loci, as shown in Figure 6–40(b).

We have illustrated a method for constructing root contours when the gain K and parameter a are varied, respectively, from zero to infinity. Basically, we assign one parameter a constant value at a time and vary the other parameter from 0 to ∞ and sketch the root loci. Then we change the value of the first parameter and repeat sketching the root loci. By repeating this process we can sketch the root contour.

A MATLAB program to generate the root-contour plot is given in MATLAB Program 6–9. The resulting plot is shown in Figure 6–41.

MATLAB Program 6–9

```
% --------- Root-contour plot ---------

% ***** Plot root contour of the system shown in Figure 6-39(c),
% where a and K are variables *****

% ***** In Equation (6-28), as/(s^2 + K) = -1, assume K = 1, 4, 9,
% 16, . . . and plot root loci as a varies from zero to infinity *****

% ***** Enter the numerator and denominators *****

num = [0   1   0];
den1 = [1   0   1];
den2 = [1   0   4];
den3 = [1   0   9];
den4 = [1   0   16];

% ***** Enter rlocus(num,den) command *****

rlocus(num,den1)
hold
Current plot held
rlocus(num,den2)
rlocus(num,den3)
rlocus(num,den4)
v = [-5   2   -5   5]; axis(v); axis('square');
grid
title('Root-Contour Plot')

% ***** Remove hold on graphics *****

hold
Current plot released
```

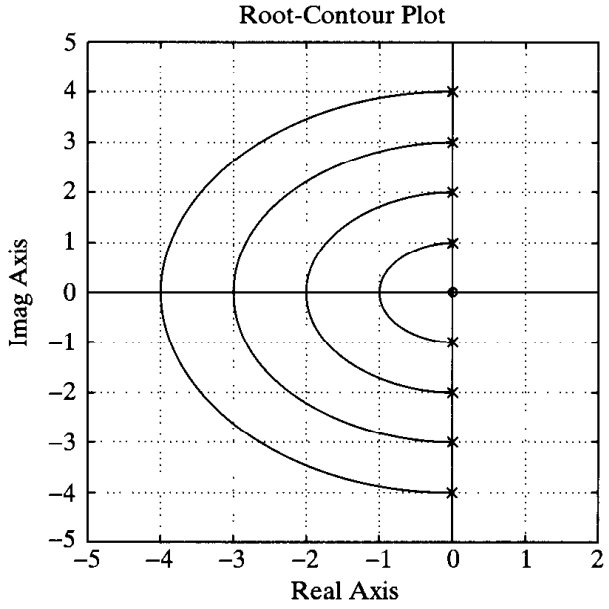

Figure 6–41
Root-contour plot generated with MATLAB.

EXAMPLE PROBLEMS AND SOLUTIONS

A-6-1. Sketch the root loci for the system shown in Figure 6–42(a). (The gain K is assumed to be positive.) Observe that for small or large values of K the system is overdamped and for medium values of K it is underdamped.

Solution. The procedure for plotting the root loci is as follows:

1. Locate the open-loop poles and zeros on the complex plane. Root loci exist on the negative real axis between 0 and -1 and between -2 and -3.

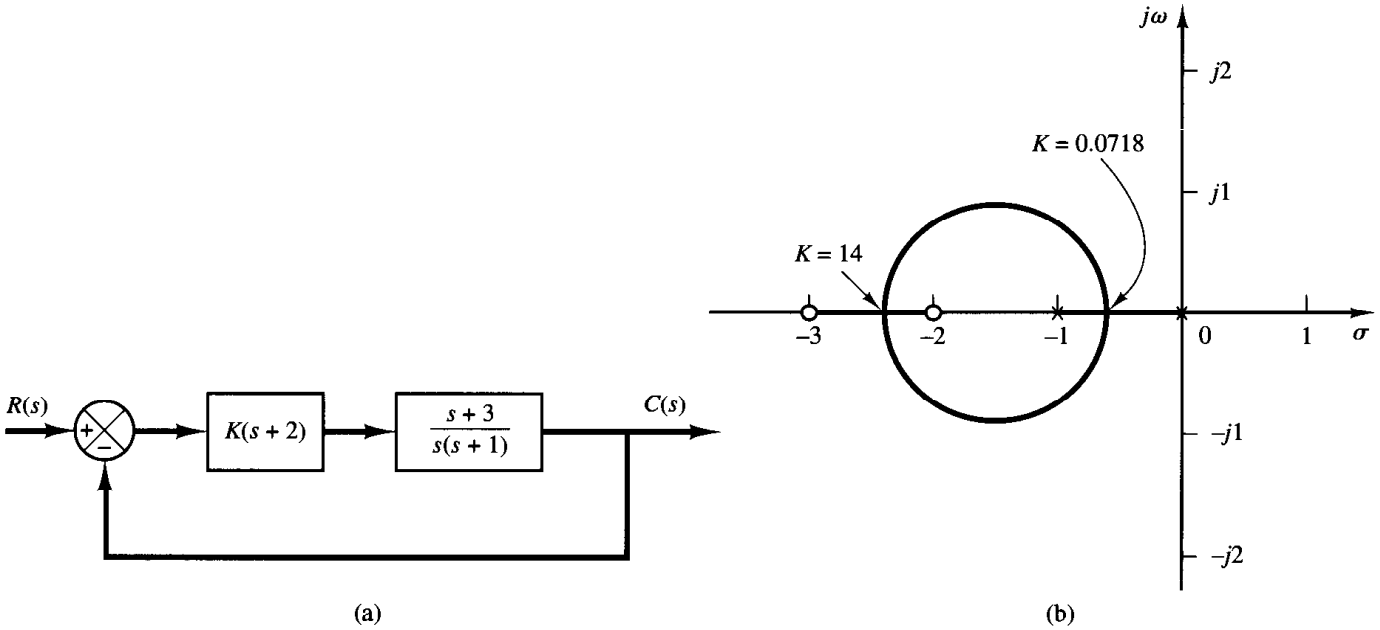

Figure 6–42
(a) Control system; (b) root-locus plot.

2. The number of open-loop poles and that of finite zeros are the same. This means that there are no asymptotes in the complex region of the s plane.

3. Determine the breakaway and break-in points. The characteristic equation for the system is

$$1 + \frac{K(s+2)(s+3)}{s(s+1)} = 0$$

or

$$K = -\frac{s(s+1)}{(s+2)(s+3)}$$

The breakaway and break-in points are determined from

$$\frac{dK}{ds} = -\frac{(2s+1)(s+2)(s+3) - s(s+1)(2s+5)}{[(s+2)(s+3)]^2}$$

$$= -\frac{4(s+0.634)(s+2.366)}{[(s+2)(s+3)]^2}$$

$$= 0$$

as follows:

$$s = -0.634, \qquad s = -2.366$$

Notice that both points are on root loci. Therefore, they are actual breakaway or break-in points. At point $s = -0.634$, the value of K is

$$K = -\frac{(-0.634)(0.366)}{(1.366)(2.366)} = 0.0718$$

Similarly, at $s = -2.366$,

$$K = -\frac{(-2.366)(-1.366)}{(-0.366)(0.634)} = 14$$

(Because point $s = -0.634$ lies between two poles, it is a breakaway point and because point $s = -2.366$ lies between two zeros, it is a break-in point.)

4. Determine a sufficient number of points that satisfy the angle condition. (It can be found that the root locus is a circle with center at -1.5 that passes through the breakaway and break-in points.) The root-locus plot for this system is shown in Figure 6–42(b).

Note that this system is stable for any positive value of K since all the root loci lie in the left-half s plane.

Small values of K ($0 < K < 0.0718$) correspond to an overdamped system. Medium values of K ($0.0718 < K < 14$) correspond to an underdamped system. Finally, large values of K ($14 < K$) correspond to an overdamped system. With a large value of K, the steady state can be reached in much shorter time than with a small value of K.

The value of K should be adjusted so that system performance is optimum according to a given performance index.

A-6-2. A simplified form of the open-loop transfer function of an airplane with an autopilot in the longitudinal mode is

$$G(s)H(s) = \frac{K(s+a)}{s(s-b)(s^2 + 2\zeta\omega_n s + \omega_n^2)}, \qquad a > 0, \qquad b > 0$$

Such a system involving an open-loop pole in the right-half s plane may be conditionally stable. Sketch the root loci when $a = b = 1$, $\zeta = 0.5$, and $\omega_n = 4$. Find the range of gain K for stability.

Solution. The open-loop transfer function for the system is

$$G(s)H(s) = \frac{K(s + 1)}{s(s - 1)(s^2 + 4s + 16)}$$

To sketch the root loci, we follow this procedure:

1. Locate the open-loop poles and zero in the complex plane. Root loci exist on the real axis between 1 and 0 and between -1 and $-\infty$.

2. Determine the asymptotes of the root loci. There are three asymptotes whose angles can be determined as

$$\text{Angles of asymptotes} = \frac{180°(2k + 1)}{4 - 1} = 60°, -60°, 180°$$

Referring to Equation (6–15), the abscissa of the intersection of the asymptotes and the real axis is

$$\sigma_a = -\frac{(0 - 1 + 2 + j2\sqrt{3} + 2 - j2\sqrt{3}) - 1}{4 - 1} = -\frac{2}{3}$$

3. Determine the breakaway and break-in points. Since the characteristic equation is

$$1 + \frac{K(s + 1)}{s(s - 1)(s^2 + 4s + 16)} = 0$$

we obtain

$$K = -\frac{s(s - 1)(s^2 + 4s + 16)}{s + 1}$$

By differentiating K with respect to s, we get

$$\frac{dK}{ds} = -\frac{3s^4 + 10s^3 + 21s^2 + 24s - 16}{(s + 1)^2}$$

The numerator can be factored as follows:

$$3s^4 + 10s^3 + 21s^2 + 24s - 16$$
$$= 3(s + 0.76 + j2.16)(s + 0.76 - j2.16)(s + 2.26)(s - 0.45)$$

Points $s = 0.45$ and $s = -2.26$ are on root loci on the real axis. Hence, these points are actual breakaway and break-in points, respectively. Points $s = -0.76 \pm j2.16$ do not satisfy the angle condition. Hence, they are neither breakaway nor break-in points.

4. Using Routh's stability criterion, determine the value of K at which the root loci cross the imaginary axis. Since the characteristic equation is

$$s^4 + 3s^3 + 12s^2 + (K - 16)s + K = 0$$

the Routh array becomes

$$
\begin{array}{lcc}
s^4 & 1 & 12 \quad K \\
s^3 & 3 & K - 16 \quad 0 \\
s^2 & \dfrac{52 - K}{3} & K \quad 0 \\
s^1 & \dfrac{-K^2 + 59K - 832}{52 - K} & 0 \\
s^0 & K &
\end{array}
$$

The values of K that make the s^1 term in the first column equal zero are $K = 35.7$ and $K = 23.3$.

The crossing points on the imaginary axis can be found by solving the auxiliary equation obtained from the s^2 row, that is, by solving the following equation for s:

$$\frac{52 - K}{3} s^2 + K = 0$$

The results are

$$s = \pm j2.56, \qquad \text{for } K = 35.7$$

$$s = \pm j1.56, \qquad \text{for } K = 23.3$$

The crossing points on the imaginary axis are thus $s = \pm j2.56$ and $s = \pm j1.56$.

5. Find the angles of departure of the root loci from the complex poles. For the open-loop pole at $s = -2 + j2\sqrt{3}$, the angle of departure θ is

$$\theta = 180° - 120° - 130.5° - 90° + 106°$$

or

$$\theta = -54.5°$$

(The angle of departure from the open-loop pole at $s = -2 - j2\sqrt{3}$ is 54.5°.)

6. Choose a test point in the broad neighborhood of the $j\omega$ axis and the origin and apply the angle condition. If the test point does not satisfy the angle condition, select another test point until it does. Continue the same process and locate a sufficient number of points that satisfy the angle condition.

Figure 6–43 shows the root loci for this system. From step 4 the system is stable for $23.3 < K < 35.7$. Otherwise, it is unstable.

A-6-3. Sketch the root loci of the control system shown in Figure 6–44(a).

Solution. The open-loop poles are located at $s = 0$, $s = -3 + j4$, and $s = -3 - j4$. A root locus branch exists on the real axis between the origin and $-\infty$. There are three asymptotes for the root loci. The angles of asymptotes are

$$\text{Angles of asymptotes} = \frac{\pm 180°(2k + 1)}{3} = 60°, -60°, 180°$$

Referring to Equation (6–15), the intersection of the asymptotes and the real axis is obtained as

$$\sigma_a = -\frac{0 + 3 + 3}{3} = -2$$

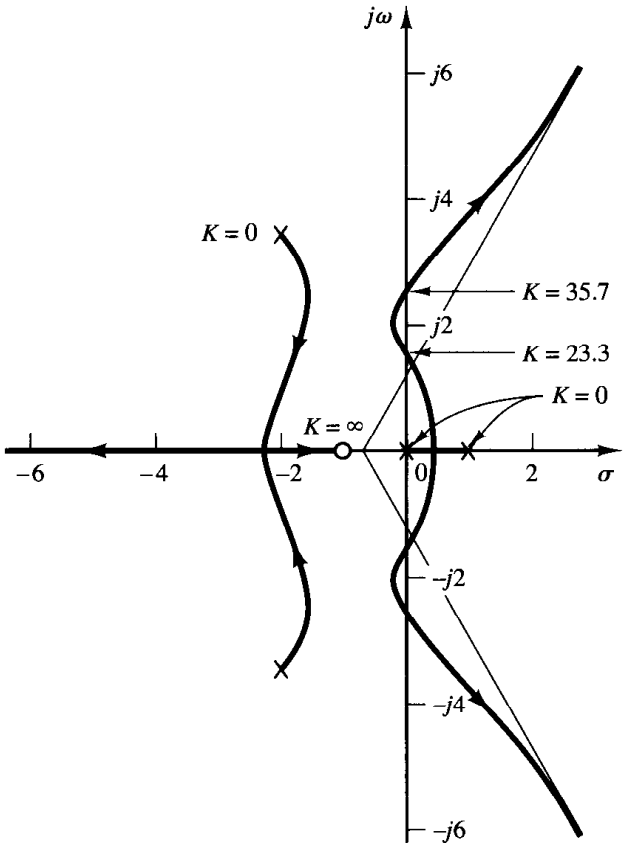

Figure 6–43
Root-locus plot.

Next we check the breakaway and break-in points. For this system we have

$$K = -s(s^2 + 6s + 25)$$

Now we set

$$\frac{dK}{ds} = -(3s^2 + 12s + 25) = 0$$

which yields

$$s = -2 + j2.0817, \qquad s = -2 - j2.0817$$

Notice that at points $s = -2 \pm j2.0817$ the angle condition is not satisfied. Hence, they are neither breakaway nor break-in points. In fact, if we calculate the value of K, we obtain

$$K = -s(s^2 + 6s + 25)\Big|_{s=-2\pm j2.0817} = 34 \pm j18.04$$

(To be an actual breakaway or break-in point, the corresponding value of K must be real and positive.)

The angle of departure from the complex pole in the upper half s plane is

$$\theta = 180° - 126.87° - 90°$$

or

$$\theta = -36.87°$$

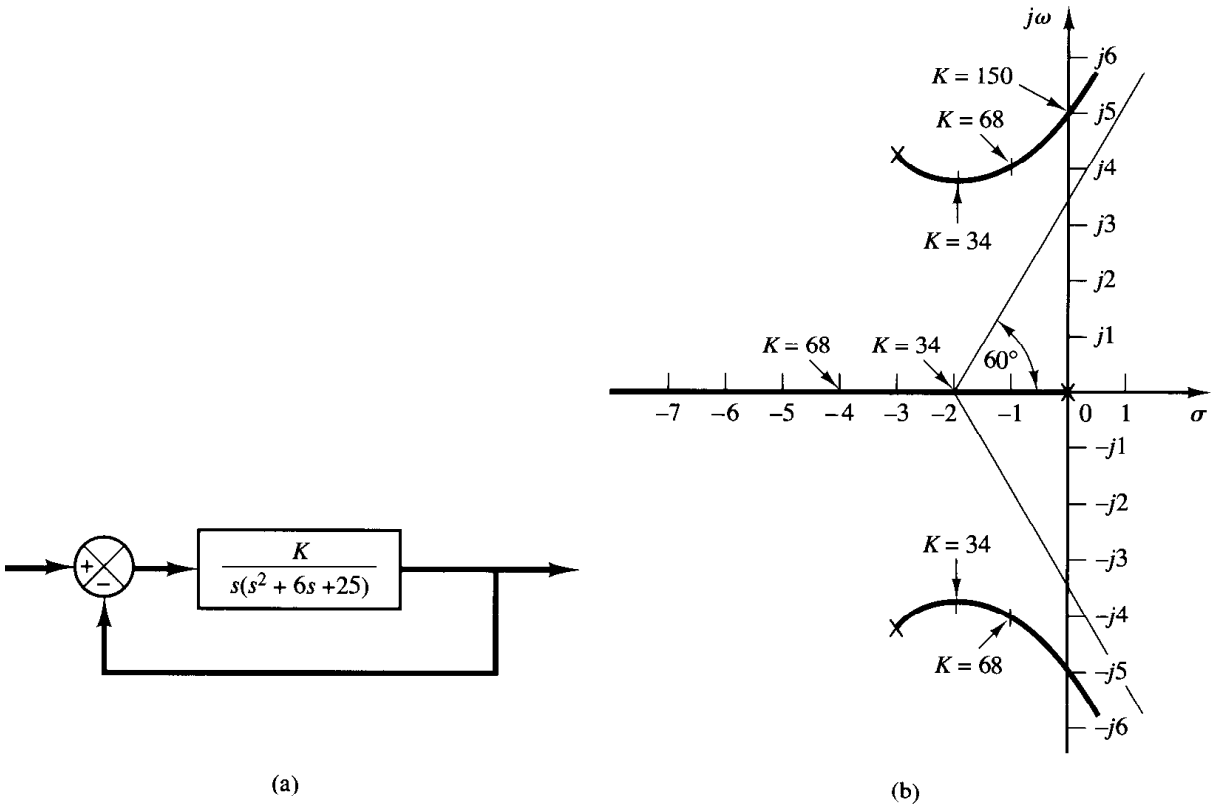

Figure 6–44
(a) Control system; (b) root-locus plot.

The points where root-locus branches cross the imaginary axis may be found by substituting $s = j\omega$ into the characteristic equation and solving the equation for ω and K as follows: Noting that the characteristic equation is

$$s^3 + 6s^2 + 25s + K = 0$$

we have

$$(j\omega)^3 + 6(j\omega)^2 + 25(j\omega) + K = (-6\omega^2 + K) + j\omega(25 - \omega^2) = 0$$

which yields

$$\omega = \pm 5, \qquad K = 150 \qquad \text{or} \qquad \omega = 0, \qquad K = 0$$

Root-locus branches cross the imaginary axis at $\omega = 5$ and $\omega = -5$. The value of gain K at the crossing points is 150. Also, the root-locus branch on the real axis touches the imaginary axis at $\omega = 0$. Figure 6–44(b) shows a root-locus plot for the system.

It is noted that if the order of the numerator of $G(s)H(s)$ is lower than that of the denominator by two or more, and if some of the closed-loop poles move on the root locus toward the right as gain K is increased, then other closed-loop poles must move toward the left as gain K is increased. This fact can be seen clearly in this problem. If the gain K is increased from $K = 34$ to $K = 68$, the complex-conjugate closed-loop poles are moved from $s = -2 + j3.65$ to $s = -1 + j4$; the third pole is moved from $s = -2$ (which corresponds to $K = 34$) to $s = -4$ (which corresponds to $K = 68$). Thus, the movements of two complex-conjugate closed-loop poles to the right by one unit cause the remaining closed-loop pole (real pole in this case) to move to the left by two units.

A-6-4. Consider the system shown in Figure 6–45(a). Sketch the root loci for the system. Observe that for small or large values of K the system is underdamped and for medium values of K it is overdamped.

Solution. A root locus exists on the real axis between the origin and $-\infty$. The angles of asymptotes of the root-locus branches are obtained as

$$\text{Angles of asymptotes} = \frac{\pm 180°(2k + 1)}{3} = 60°, -60°, -180°$$

The intersection of the asymptotes and the real axis is located on the real axis at

$$\sigma_a = -\frac{0 + 2 + 2}{3} = -1.3333$$

The breakaway and break-in points are found from $dK/ds = 0$. Since the characteristic equation is

$$s^3 + 4s^2 + 5s + K = 0$$

we have

$$K = -(s^3 + 4s^2 + 5s)$$

Now we set

$$\frac{dK}{ds} = -(3s^2 + 8s + 5) = 0$$

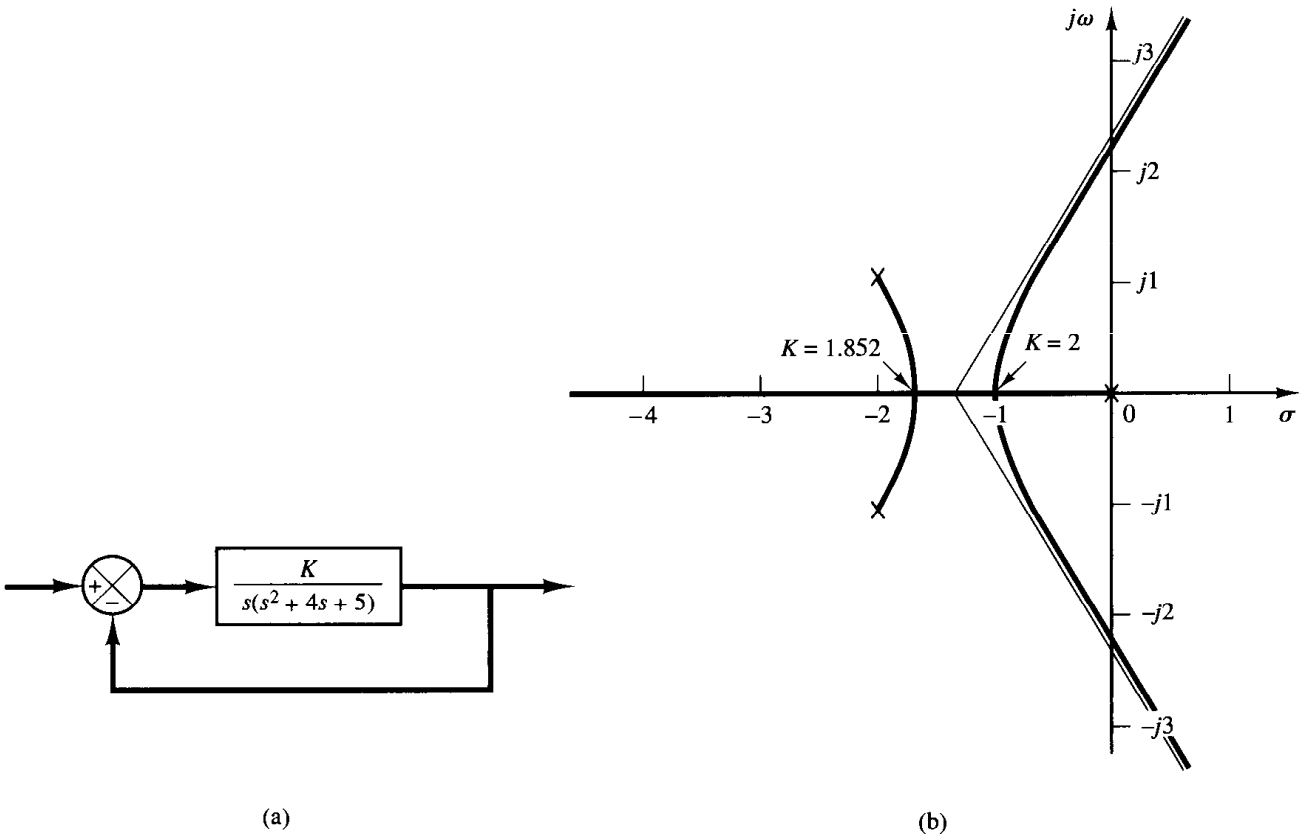

Figure 6–45
(a) Control system; (b) root-locus plot.

which yields

$$s = -1, \qquad s = -1.6667$$

Since these points are on root loci, they are actual breakaway or break-in points. (At point $s = -1$, the value of K is 2, and at point $s = -1.6667$, the value of K is 1.852.)

The angle of departure from a complex pole in the upper half s plane is obtained from

$$\theta = 180° - 153.43° - 90°$$

or

$$\theta = -63.43°$$

The root-locus branch from the complex pole in the upper half s plane breaks into the real axis at $s = -1.6667$.

Next we determine the points where root-locus branches cross the imaginary axis. By substituting $s = j\omega$ into the characteristic equation, we have

$$(j\omega)^3 + 4(j\omega)^2 + 5(j\omega) + K = 0$$

or

$$(K - 4\omega^2) + j\omega(5 - \omega^2) = 0$$

from which we obtain

$$\omega = \pm\sqrt{5}, \qquad K = 20 \quad \text{or} \quad \omega = 0, \qquad K = 0$$

Root-locus branches cross the imaginary axis at $\omega = \sqrt{5}$ and $\omega = -\sqrt{5}$. The root-locus branch on the real axis touches the $j\omega$ axis at $\omega = 0$. A sketch of the root loci for the system is shown in Figure 6–45(b).

Note that since this system is of third order there are three closed-loop poles. The nature of the system response to a given input depends on the locations of the closed-loop poles.

For $0 < K < 1.852$, there are a set of complex-conjugate closed-loop poles and a real closed-loop pole. For $1.852 \leq K \leq 2$, there are three real closed-loop poles. For example, the closed-loop poles are located at

$$s = -1.667, \qquad s = -1.667, \qquad s = -0.667, \qquad \text{for } K = 1.852$$

$$s = -1, \qquad s = -1, \qquad s = -2, \qquad \text{for } K = 2$$

For $2 < K$, there are a set of complex-conjugate closed-loop poles and a real closed-loop pole. Thus, small values of K ($0 < K < 1.852$) correspond to an underdamped system. (Since the real closed-loop pole dominates, only a small ripple may show up in the transient response.) Medium values of K ($1.852 \leq K \leq 2$) correspond to an overdamped system. Large values of K ($2 < K$) correspond to an underdamped system. With a large value of K, the system responds much faster than with a smaller value of K.

A-6-5. Sketch the root loci for the system shown in Figure 6–46(a).

Solution. The open-loop poles are located at $s = 0$, $s = -1$, $s = -2 + j3$, and $s = -2 - j3$. A root locus exists on the real axis between points $s = 0$ and $s = -1$. The asymptotes are found as follows:

$$\text{Angles of asymptotes} = \frac{\pm 180°(2k + 1)}{4} = 45°, -45°, 135°, -135°$$

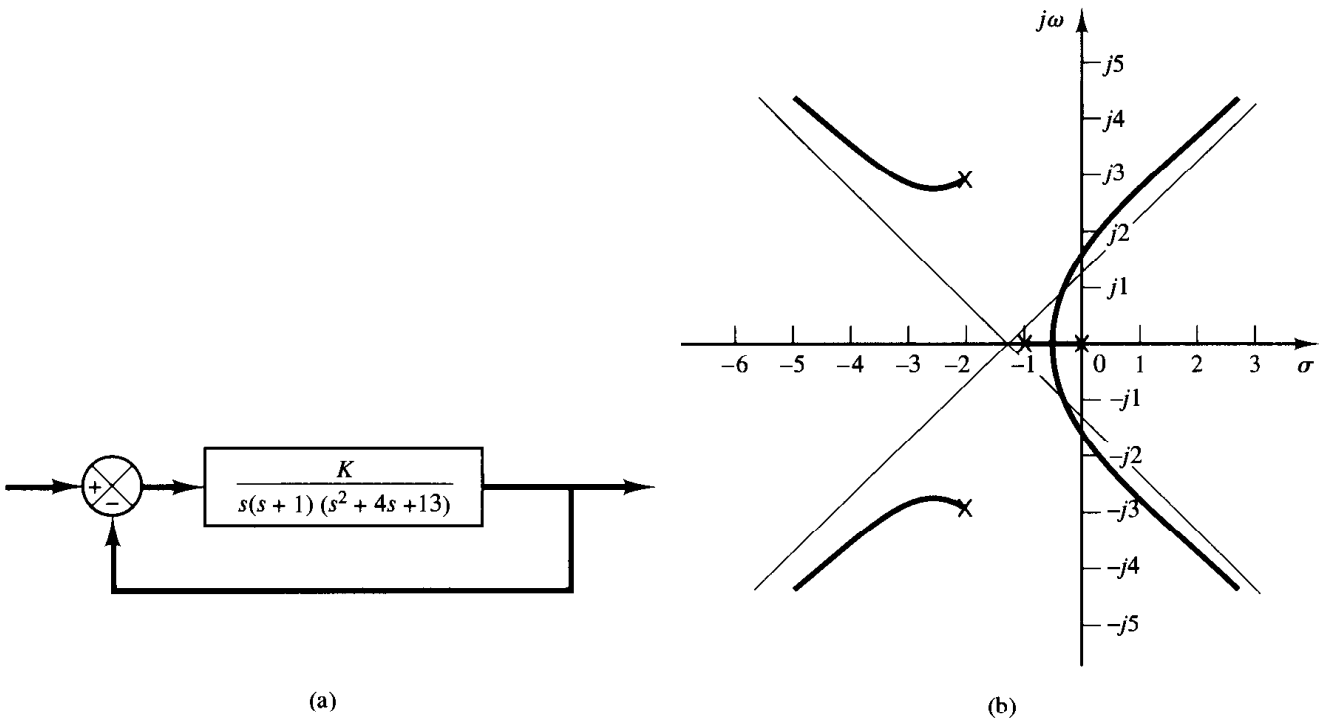

Figure 6–46
(a) Control system; (b) root-locus plot.

The intersection of the asymptotes and the real axis is found from

$$\sigma_a = -\frac{0 + 1 + 2 + 2}{4} = -1.25$$

The breakaway and break-in points are found from $dK/ds = 0$. Noting that

$$K = -s(s + 1)(s^2 + 4s + 13) = -(s^4 + 5s^3 + 17s^2 + 13s)$$

we have

$$\frac{dK}{ds} = -(4s^3 + 15s^2 + 34s + 13) = 0$$

from which we get

$$s = -0.467, \qquad s = -1.642 + j2.067, \qquad s = -1.642 - j2.067$$

The point $s = -0.467$ is on a root locus. Therefore, it is an actual breakaway point. The gain values K corresponding to points $s = -1.642 \pm j2.067$ are complex quantities. Since the gain values are not real positive, these points are neither breakaway nor break-in points.

The angle of departure from the complex pole in the upper half s plane is

$$\theta = 180° - 123.69° - 108.44° - 90°$$

or

$$\theta = -142.13°$$

Next we shall find the points where root loci may cross the $j\omega$ axis. Since the characteristic equation is

$$s^4 + 5s^3 + 17s^2 + 13s + K = 0$$

by substituting $s = j\omega$ into it we obtain

$$(j\omega)^4 + 5(j\omega)^3 + 17(j\omega)^2 + 13(j\omega) + K = 0$$

or

$$(K + \omega^4 - 17\omega^2) + j\omega(13 - 5\omega^2) = 0$$

from which we obtain

$$\omega = \pm 1.6125, \quad K = 37.44 \quad \text{or} \quad \omega = 0, \quad K = 0$$

The root-locus branches that extend to the right-half s plane cross the imaginary axis at $\omega = \pm 1.6125$. Also, the root-locus branch on the real axis touches the imaginary axis at $\omega = 0$. Figure 6–46(b) shows a sketch of the root loci for the system. Notice that each root-locus branch that extends to the right half s plane crosses its own asymptote.

A-6-6. Sketch the root loci for the system shown in Figure 6–47(a).

Solution. A root locus exists on the real axis between points $s = -1$ and $s = -3.6$. The asymptotes can be determined as follows:

$$\text{Angles of asymptotes} = \frac{\pm 180°(2k + 1)}{3 - 1} = 90°, -90°$$

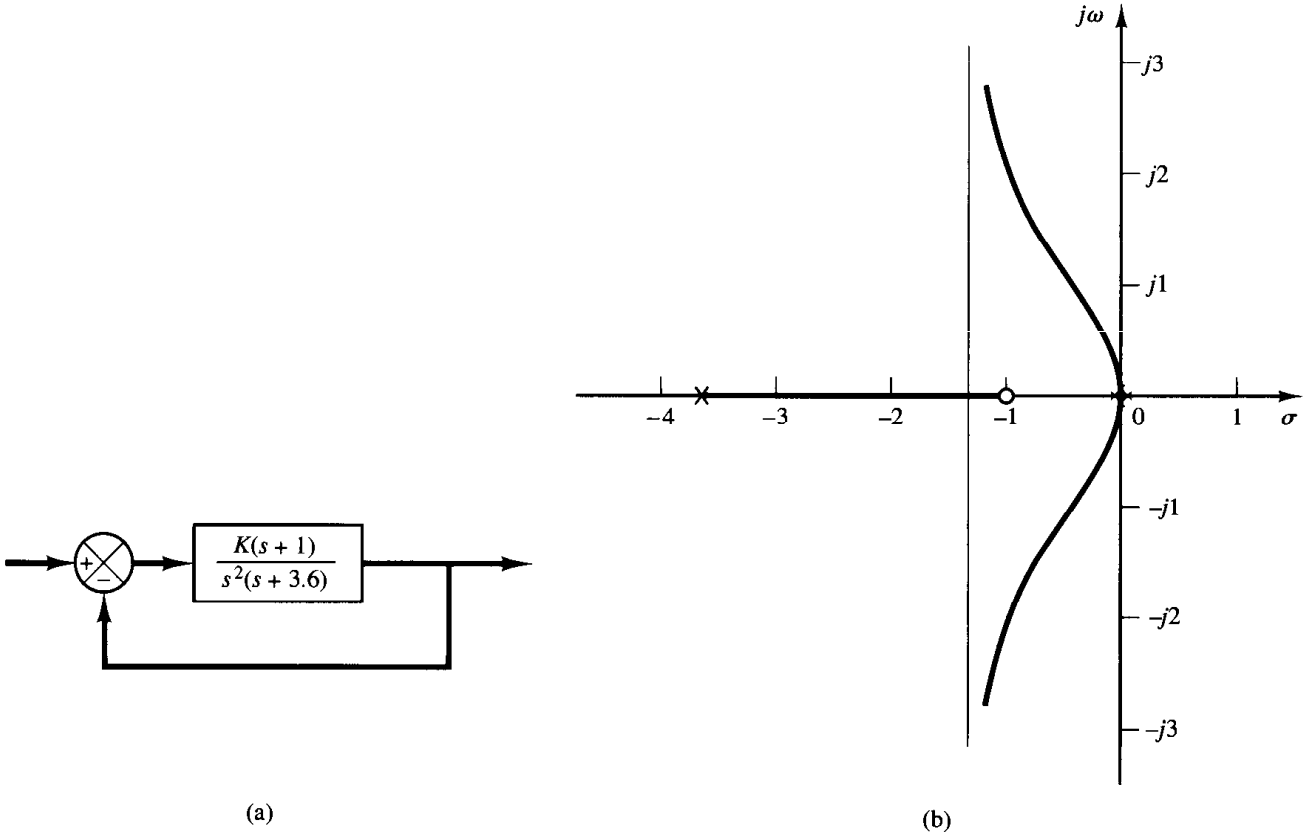

Figure 6–47
(a) Control system; (b) root-locus plot.

The intersection of the asymptotes and the real axis is found from

$$\sigma_a = -\frac{0 + 0 + 3.6 - 1}{3 - 1} = -1.3$$

Since the characteristic equation is

$$s^3 + 3.6s^2 + K(s + 1) = 0$$

we have

$$K = -\frac{s^3 + 3.6s^2}{s + 1}$$

The breakaway and break-in points are found from

$$\frac{dK}{ds} = -\frac{(3s^2 + 7.2s)(s + 1) - (s^3 + 3.6s^2)}{(s + 1)^2} = 0$$

or

$$s^3 + 3.3s^2 + 3.6s = 0$$

from which we get

$$s = 0, \qquad s = -1.65 + j0.9367, \qquad s = -1.65 - j0.9367$$

Point $s = 0$ corresponds to the actual breakaway point. But points $s = -1.65 \pm j0.9367$ are neither breakaway nor break-in points, because the corresponding gain values K become complex quantities.

To check the points where root-locus branches may cross the imaginary axis, substitute $s = j\omega$ into the characteristic equation.

$$(j\omega)^3 + 3.6(j\omega)^2 + Kj\omega + K = 0$$

or

$$(K - 3.6\omega^2) + j\omega(K - \omega^2) = 0$$

Notice that this equation can be satisfied only if $\omega = 0$, $K = 0$. Because of the presence of a double pole at the origin, the root locus is tangent to the $j\omega$ axis at $\omega = 0$. The root-locus branches do not cross the $j\omega$ axis. Figure 6–47(b) is a sketch of the root loci for this system.

A-6-7. Sketch the root loci for the system shown in Figure 6–48(a).

Solution. A root locus exists on the real axis between point $s = -0.4$ and $s = -3.6$. The asymptotes can be found as follows:

$$\text{Angles of asymptotes} = \frac{\pm 180°(2k + 1)}{3 - 1} = 90°, -90°$$

The intersection of the asymptotes and the real axis is obtained from

$$\sigma_a = -\frac{0 + 0 + 3.6 - 0.4}{3 - 1} = -1.6$$

Next we shall find the breakaway points. Since the characteristic equation is

$$s^3 + 3.6s^2 + Ks + 0.4K = 0$$

we have

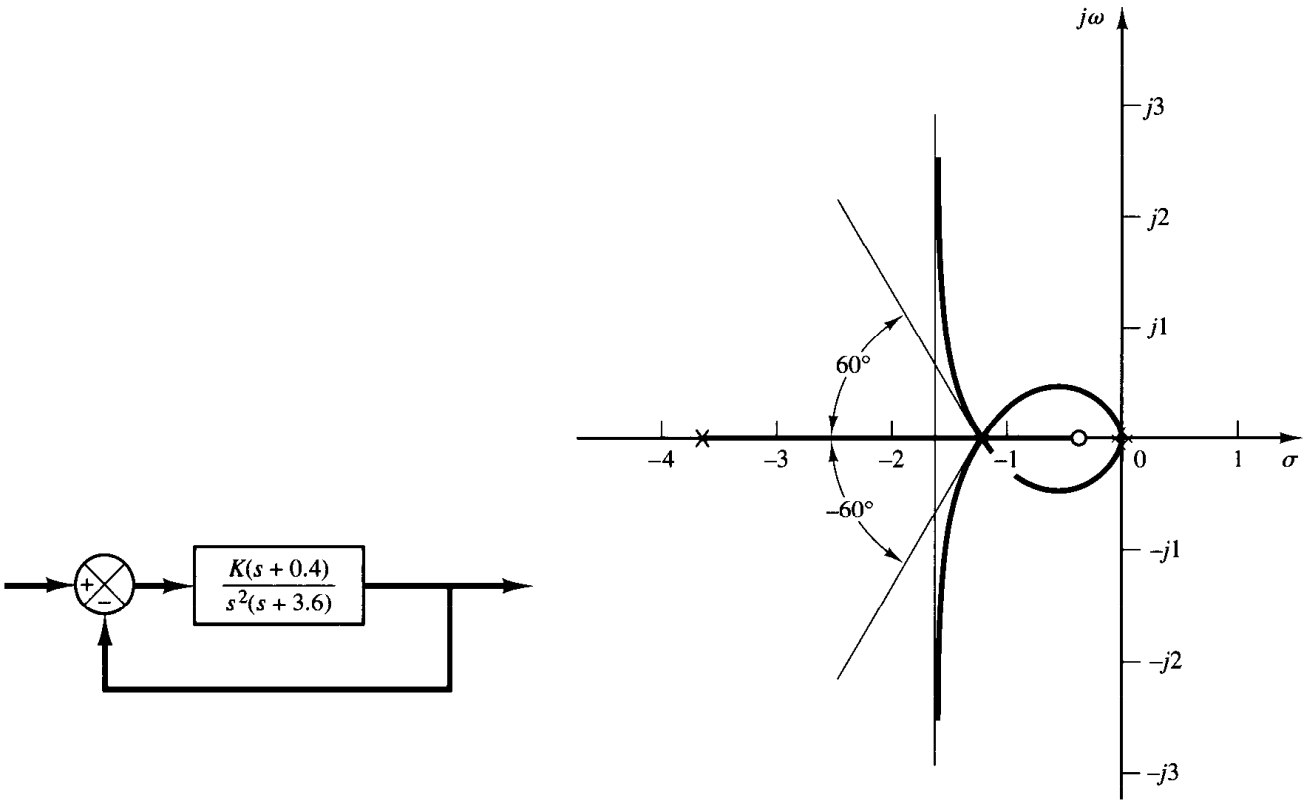

Figure 6–48
(a) Control system; (b) root-locus plot.

$$K = -\frac{s^3 + 3.6s^2}{s + 0.4}$$

The breakaway and break-in points are found from

$$\frac{dK}{ds} = -\frac{(3s^2 + 7.2s)(s + 0.4) - (s^3 + 3.6s^2)}{(s + 0.4)^2} = 0$$

from which we get

$$s^3 + 2.4s^2 + 1.44s = 0$$

or

$$s(s + 1.2)^2 = 0$$

Thus, the breakaway or break-in points are at $s = 0$ and $s = -1.2$. Note that $s = -1.2$ is a double root. When a double root occurs in $dK/ds = 0$ at point $s = -1.2$, $d^2K/(ds^2) = 0$ at this point. The value of gain K at point $s = -1.2$ is

$$K = -\frac{s^3 + 3.6s^2}{s + 0.4}\bigg|_{s=-1.2} = 4.32$$

This means that with $K = 4.32$ the characteristic equation has a triple root at point $s = -1.2$. This can be easily verified as follows:

$$s^3 + 3.6s^2 + 4.32s + 1.728 = (s + 1.2)^3 = 0$$

Hence, three root-locus branches meet at point $s = -1.2$. The angles of departures at point $s = -1.2$ of the root locus branches that approach the asymptotes are $\pm 180°/3$, that is, 60° and −60°. (See Problem A-6-8.)

Finally, we shall examine if root-locus branches cross the imaginary axis. By substituting $s = j\omega$ into the characteristic equation, we have

$$(j\omega)^3 + 3.6(j\omega)^2 + K(j\omega) + 0.4K = 0$$

or

$$(0.4K - 3.6\omega^2) + j\omega(K - \omega^2) = 0$$

This equation can be satisfied only if $\omega = 0, K = 0$. At point $\omega = 0$, the root locus is tangent to the $j\omega$ axis because of the presence of a double pole at the origin. There are no points that root-locus branches cross the imaginary axis.

A sketch of the root loci for this system is shown in Figure 6–48(b).

A-6-8. Referring to Problem A-6-7, obtain the equations for the root-locus branches for the system shown in Figure 6–48(a). Show that the root-locus branches cross the real axis at the breakaway point at angles ±60°.

Solution. The equations for the root-locus branches can be obtained from the angle condition

$$\underline{/\frac{K(s + 0.4)}{s^2(s + 3.6)}} = \pm 180°(2k + 1)$$

which can be rewritten as

$$\underline{/s + 0.4} - 2\underline{/s} - \underline{/s + 3.6} = \pm 180°(2k + 1)$$

By substituting $s = \sigma + j\omega$, we obtain

$$\underline{/\sigma + j\omega + 0.4} - 2\underline{/\sigma + j\omega} - \underline{/\sigma + j\omega + 3.6} = \pm 180°(2k + 1)$$

or

$$\tan^{-1}\left(\frac{\omega}{\sigma + 0.4}\right) - 2\tan^{-1}\left(\frac{\omega}{\sigma}\right) - \tan^{-1}\left(\frac{\omega}{\sigma + 3.6}\right) = \pm 180°(2k + 1)$$

By rearranging, we have

$$\tan^{-1}\left(\frac{\omega}{\sigma + 0.4}\right) - \tan^{-1}\left(\frac{\omega}{\sigma}\right) = \tan^{-1}\left(\frac{\omega}{\sigma}\right) + \tan^{-1}\left(\frac{\omega}{\sigma + 3.6}\right) \pm 180°(2k + 1)$$

Taking tangents of both sides of this last equation, and noting that

$$\tan\left[\tan^{-1}\left(\frac{\omega}{\sigma + 3.6}\right) \pm 180°(2k + 1)\right] = \frac{\omega}{\sigma + 3.6}$$

we obtain

$$\frac{\dfrac{\omega}{\sigma + 0.4} - \dfrac{\omega}{\sigma}}{1 + \dfrac{\omega}{\sigma + 0.4}\dfrac{\omega}{\sigma}} = \frac{\dfrac{\omega}{\sigma} + \dfrac{\omega}{\sigma + 3.6}}{1 - \dfrac{\omega}{\sigma}\dfrac{\omega}{\sigma + 3.6}}$$

which can be simplified to

$$\frac{\omega\sigma - \omega(\sigma + 0.4)}{(\sigma + 0.4)\sigma + \omega^2} = \frac{\omega(\sigma + 3.6) + \omega\sigma}{\sigma(\sigma + 3.6) - \omega^2}$$

or

$$\omega(\sigma^3 + 2.4\sigma^2 + 1.44\sigma + 1.6\omega^2 + \sigma\omega^2) = 0$$

which can be further simplified to

$$\omega[\sigma(\sigma + 1.2)^2 + (\sigma + 1.6)\omega^2] = 0$$

For $\sigma \neq -1.6$, we may write this last equation as

$$\omega\left[\omega - (\sigma + 1.2)\sqrt{\frac{-\sigma}{\sigma + 1.6}}\right]\left[\omega + (\sigma + 1.2)\sqrt{\frac{-\sigma}{\sigma + 1.6}}\right] = 0$$

which gives the equations for the root-locus as follows:

$$\omega = 0$$

$$\omega = (\sigma + 1.2)\sqrt{\frac{-\sigma}{\sigma + 1.6}}$$

$$\omega = -(\sigma + 1.2)\sqrt{\frac{-\sigma}{\sigma + 1.6}}$$

The equation $\omega = 0$ represents the real axis. The root locus for $0 \leq K \leq \infty$ is between points $s = -0.4$ and $s = -3.6$. (The real axis other than this line segment and the origin $s = 0$ corresponds to the root locus for $-\infty \leq K < 0$.)

The equations

$$\omega = \pm(\sigma + 1.2)\sqrt{\frac{-\sigma}{\sigma + 1.6}} \tag{6-31}$$

represent the complex branches for $0 \leq K \leq \infty$. These two branches lie between $\sigma = -1.6$ and $\sigma = 0$. [See Figure 6–48(b).] The slopes of the complex root-locus branches at the breakaway point ($\sigma = -1.2$) can be found by evaluating $d\omega/d\sigma$ of Equation (6–31) at point $\sigma = -1.2$.

$$\left.\frac{d\omega}{d\sigma}\right|_{\sigma=-1.2} = \left.\pm\sqrt{\frac{-\sigma}{\sigma + 1.6}}\right|_{\sigma=-1.2} = \pm\sqrt{\frac{1.2}{0.4}} = \pm\sqrt{3}$$

Since $\tan^{-1}\sqrt{3} = 60°$, the root-locus branches intersect the real axis with angles $\pm 60°$.

A-6-9. Consider the system shown in Figure 6–49, which has an unstable feedforward transfer function. Sketch the root-locus plot and locate the closed-loop poles. Show that, although the closed-loop poles lie on the negative real axis and the system is not oscillatory, the unit-step response curve will exhibit overshoot.

Solution. The root-locus plot for this system is shown in Figure 6–50. The closed-loop poles are located at $s = -2$ and $s = -5$.

The closed-loop transfer function becomes

$$\frac{C(s)}{R(s)} = \frac{10(s + 1)}{s^2 + 7s + 10}$$

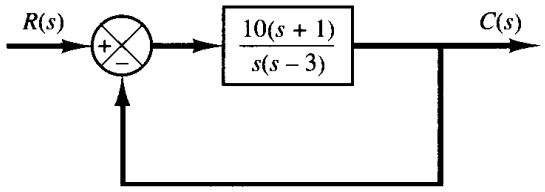

Figure 6–49
Control system.

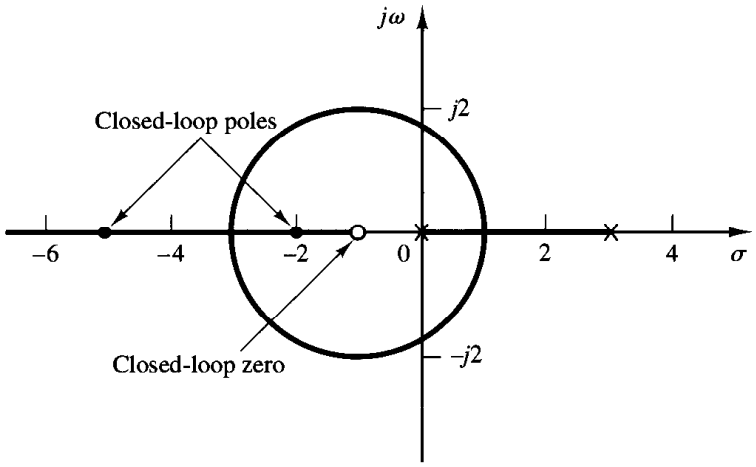

Figure 6–50
Root-locus plot for the system shown in Figure 6–49.

The unit-step response of this system is

$$C(s) = \frac{10(s + 1)}{s(s + 2)(s + 5)}$$

The inverse Laplace transform of $C(s)$ gives

$$c(t) = 1 + 1.666e^{-2t} - 2.666e^{-5t}, \qquad \text{for } t \geq 0$$

The unit-step response curve is shown in Figure 6–51. Although the system is not oscillatory, the unit-step response curve exhibits overshoot. (This is due to the presence of a zero at $s = -1$.)

A-6-10. Sketch the root loci of the control system shown in Figure 6–52(a). Determine the range of gain K for stability.

Solution. Open-loop poles are located at $s = 1, s = -2 + j\sqrt{3}$, and $s = -2 - j\sqrt{3}$. A root locus exists on the real axis between points $s = 1$ and $s = -\infty$. The asymptotes of the root-locus branches are found as follows:

$$\text{Angles of asymptotes} = \frac{\pm 180°(2k + 1)}{3} = 60°, -60°, 180°$$

The intersection of the asymptotes and the real axis is obtained as

$$\sigma_a = -\frac{-1 + 2 + 2}{3} = -1$$

The breakaway and break-in points can be located from $dK/ds = 0$. Since

$$K = -(s - 1)(s^2 + 4s + 7) = -(s^3 + 3s^2 + 3s - 7)$$

we have

$$\frac{dK}{ds} = -(3s^2 + 6s + 3) = 0$$

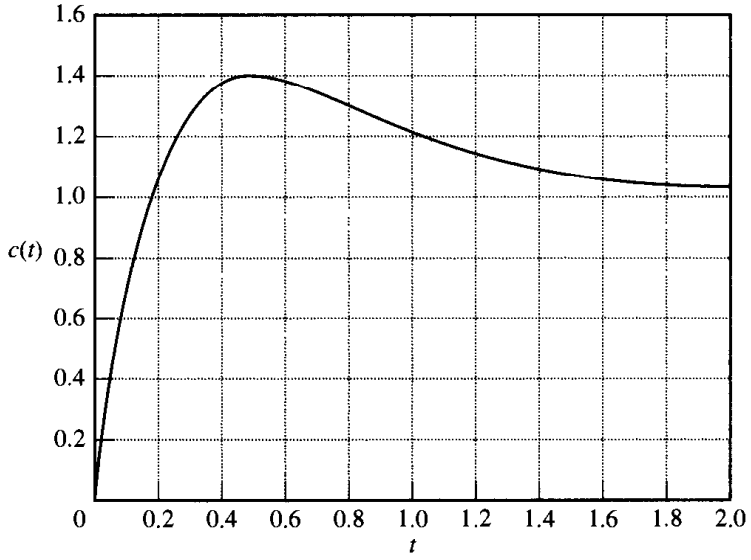

Figure 6–51
Unit-step response curve for the system shown in Figure 6–49.

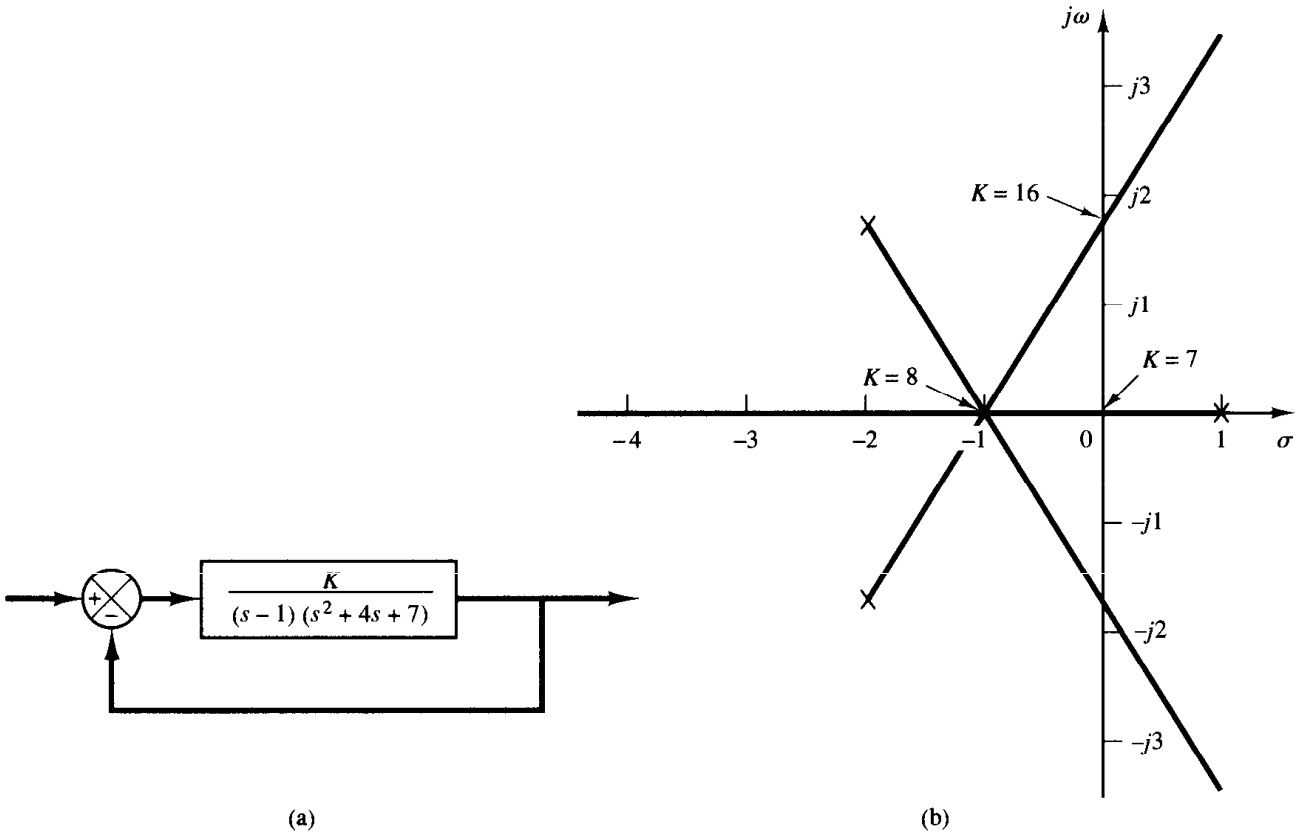

Figure 6–52
(a) Control system; (b) root-locus plot.

which yields

$$(s + 1)^2 = 0$$

Thus the equation $dK/ds = 0$ has a double root at $s = -1$. The breakaway point is located at $s = -1$. Three root locus branches meet at this breakaway point. The angles of departure of the branches at the breakaway point are $\pm 180°/3$, that is, 60° and −60°.

We shall next determine the points where root-locus branches may cross the imaginary axis. Noting that the characteristic equation is

$$(s - 1)(s^2 + 4s + 7) + K = 0$$

or

$$s^3 + 3s^2 + 3s - 7 + K = 0$$

we substitute $s = j\omega$ into it and obtain

$$(j\omega)^3 + 3(j\omega)^2 + 3(j\omega) - 7 + K = 0$$

By rewriting this last equation, we have

$$(K - 7 - 3\omega^2) + j\omega(3 - \omega^2) = 0$$

This equation is satisfied when

$$\omega = \pm\sqrt{3}, \qquad K = 7 + 3\omega^2 = 16 \qquad \text{or} \qquad \omega = 0, \qquad K = 7$$

The root-locus branches cross the imaginary axis at $\omega = \pm\sqrt{3}$ (where $K = 16$) and $\omega = 0$ (where $K = 7$). Since the value of gain K at the origin is 7, the range of gain value K for stability is

$$7 < K < 16$$

Figure 6–52(b) shows a sketch of the root loci for the system. Notice that all branches consist of parts of straight lines.

The fact that the root-locus branches consist of straight lines can be verified as follows: Since the angle condition is

$$\underline{/\ \frac{K}{(s - 1)(s + 2 + j\sqrt{3})(s + 2 - j\sqrt{3})}} = \pm 180°(2k + 1)$$

we have

$$-\underline{/\ s - 1} - \underline{/\ s + 2 + j\sqrt{3}} - \underline{/\ s + 2 - j\sqrt{3}} = \pm 180°(2k + 1)$$

By substituting $s = \sigma + j\omega$ into this last equation,

$$\underline{/\ \sigma - 1 + j\omega} + \underline{/\ \sigma + 2 + j\omega + j\sqrt{3}} + \underline{/\ \sigma + 2 + j\omega - j\sqrt{3}} = \pm 180°(2k + 1)$$

or

$$\underline{/\ \sigma + 2 + j(\omega + \sqrt{3})} + \underline{/\ \sigma + 2 + j(\omega - \sqrt{3})} = -\underline{/\ \sigma - 1 + j\omega} \pm 180°(2k + 1)$$

which can be rewritten as

$$\tan^{-1}\left(\frac{\omega + \sqrt{3}}{\sigma + 2}\right) + \tan^{-1}\left(\frac{\omega - \sqrt{3}}{\sigma + 2}\right) = -\tan^{-1}\left(\frac{\omega}{\sigma - 1}\right) \pm 180°(2k + 1)$$

Taking tangents of both sides of this last equation, we obtain

$$\frac{\dfrac{\omega + \sqrt{3}}{\sigma + 2} + \dfrac{\omega - \sqrt{3}}{\sigma + 2}}{1 - \left(\dfrac{\omega + \sqrt{3}}{\sigma + 2}\right)\left(\dfrac{\omega - \sqrt{3}}{\sigma + 2}\right)} = -\frac{\omega}{\sigma - 1}$$

or

$$\frac{2\omega(\sigma + 2)}{\sigma^2 + 4\sigma + 4 - \omega^2 + 3} = -\frac{\omega}{\sigma - 1}$$

which can be simplified to

$$2\omega(\sigma + 2)(\sigma - 1) = -\omega(\sigma^2 + 4\sigma + 7 - \omega^2)$$

or

$$\omega(3\sigma^2 + 6\sigma + 3 - \omega^2) = 0$$

Further simplification of this last equation yields

$$\omega\left(\sigma + 1 + \frac{1}{\sqrt{3}}\omega\right)\left(\sigma + 1 - \frac{1}{\sqrt{3}}\right) = 0$$

which defines three lines:

$$\omega = 0, \qquad \sigma + 1 + \frac{1}{\sqrt{3}}\omega = 0, \qquad \sigma + 1 - \frac{1}{\sqrt{3}}\omega = 0$$

Thus the root-locus branches consist of three lines. Note that the root loci for $K > 0$ consist of portions of the straight lines as shown in Figure 6–52(b). (Note that each straight line starts from an open-loop pole and extends to infinity in the direction of 180°, 60°, or −60° measured from the real axis.) The remaining portion of each straight line corresponds to $K < 0$.

A-6-11. Consider the system shown in Figure 6–53(a). Sketch the root loci.

Solution. The open-loop zeros of the system are located at $s = \pm j$. The open-loop poles are located at $s = 0$ and $s = -2$. This system involves two poles and two zeros. Hence, there is a possibility that a circular root-locus branch exists. In fact, such a circular root locus exists in this case, as shown in the following. The angle condition is

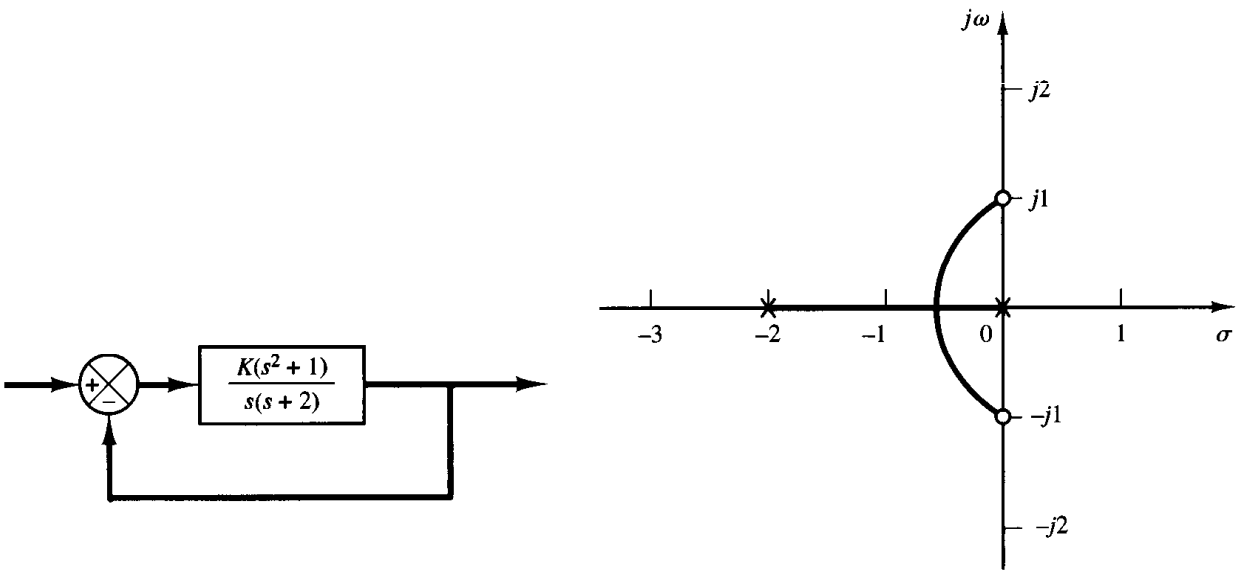

Figure 6–53
(a) Control system; (b) root-locus plot.

$$\angle \frac{K(s+j)(s-j)}{s(s+2)} = \pm 180°(2k+1)$$

or

$$\angle s+j + \angle s-j - \angle s - \angle s+2 = \pm 180°(2k+1)$$

By substituting $s = \sigma + j\omega$ into this last equation, we obtain

$$\angle \sigma + j\omega + j + \angle \sigma + j\omega - j = \angle \sigma + j\omega + \angle \sigma + 2 + j\omega \pm 180°(2k+1)$$

or

$$\tan^{-1}\left(\frac{\omega+1}{\sigma}\right) + \tan^{-1}\left(\frac{\omega-1}{\sigma}\right) = \tan^{-1}\left(\frac{\omega}{\sigma}\right) + \tan^{-1}\left(\frac{\omega}{\sigma+2}\right) \pm 180°(2k+1)$$

Taking tangents of both sides of this equation and noting that

$$\tan\left[\tan^{-1}\left(\frac{\omega}{\sigma+2}\right) \pm 180°\right] = \frac{\omega}{\sigma+2}$$

we obtain

$$\frac{\dfrac{\omega+1}{\sigma} + \dfrac{\omega-1}{\sigma}}{1 - \dfrac{\omega+1}{\sigma}\dfrac{\omega-1}{\sigma}} = \frac{\dfrac{\omega}{\sigma} + \dfrac{\omega}{\sigma+2}}{1 - \dfrac{\omega}{\sigma}\dfrac{\omega}{\sigma+2}}$$

or

$$\omega\left[\left(\sigma - \frac{1}{2}\right)^2 + \omega^2 - \frac{5}{4}\right] = 0$$

which is equivalent to

$$\omega = 0 \quad \text{or} \quad \left(\sigma - \frac{1}{2}\right)^2 + \omega^2 = \frac{5}{4}$$

These two equations are equations for the root loci. The first equation corresponds to the root locus on the real axis. (The segment between $s = 0$ and $s = -2$ corresponds to the root locus for $0 \le K < \infty$. The remaining parts of the real axis correspond to the root locus for $K < 0$.) The second equation is an equation for a circle. Thus, there exists a circular root locus with center at $\sigma = \frac{1}{2}$, $\omega = 0$ and the radius equal to $\sqrt{5/2}$. The root loci are sketched in Figure 6–53(b). [That part of the circular locus to the left of the imaginary zeros corresponds to $K > 0$. The portion of the circular locus not shown in Figure 6–53(b) corresponds to $K < 0$.]

A-6-12. Consider the system shown in Figure 6–54. Determine the value of α such that the damping ratio ζ of the dominant closed-loop poles is 0.5.

Solution. In this system the characteristic equation is

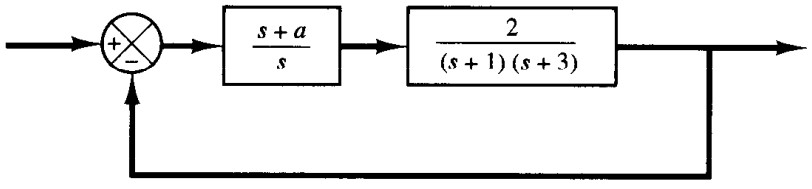

Figure 6–54
Control system.

$$1 + \frac{2(s + a)}{s(s + 1)(s + 3)} = 0$$

Notice that the variable a is not a multiplying factor. Hence, we need to rewrite the characteristic equation

$$s(s + 1)(s + 3) + 2s + 2a = 0$$

as follows:

$$1 + \frac{2a}{s^3 + 4s^2 + 5s} = 0$$

Define

$$2a = K$$

Then we get the characteristic equation in the form

$$1 + \frac{K}{s(s^2 + 4s + 5)} = 0 \tag{6–32}$$

In Problem A-6-4 we constructed the root-locus diagram for the system defined by Equation (6–32). Hence, the solution to this problem is available in Problem A-6-4. Referring to Figure 6–45(b), the closed-loop poles having the damping ratio $\zeta = 0.5$ can be located at $s = -0.63 \pm j1.09$. The value of K at point $s = -0.63 + j1.09$ may be found as 4.32. Hence, the value of a in this problem is obtained as follows:

$$a = \frac{K}{2} = 2.16$$

A-6-13. Consider the system shown in Figure 6–55(a). Determine the value of a such that the damping ratio ζ of the dominant closed poles is 0.5.

Solution. The characteristic equation is

$$1 + \frac{10(s + a)}{s(s + 1)(s + 8)} = 0$$

The variable a is not a multiplying factor. Hence, we need to modify the characteristic equation. Since the characteristic equation can be written as

$$s^3 + 9s^2 + 18s + 10a = 0$$

we rewrite this equation such that a appears as a multiplying factor as follows:

$$1 + \frac{10a}{s(s^2 + 9s + 18)} = 0$$

Define

$$10a = K$$

Then the characteristic equation becomes

$$1 + \frac{K}{s(s^2 + 9s + 18)} = 0$$

Notice that the characteristic equation is in a suitable form for the construction of the root loci.

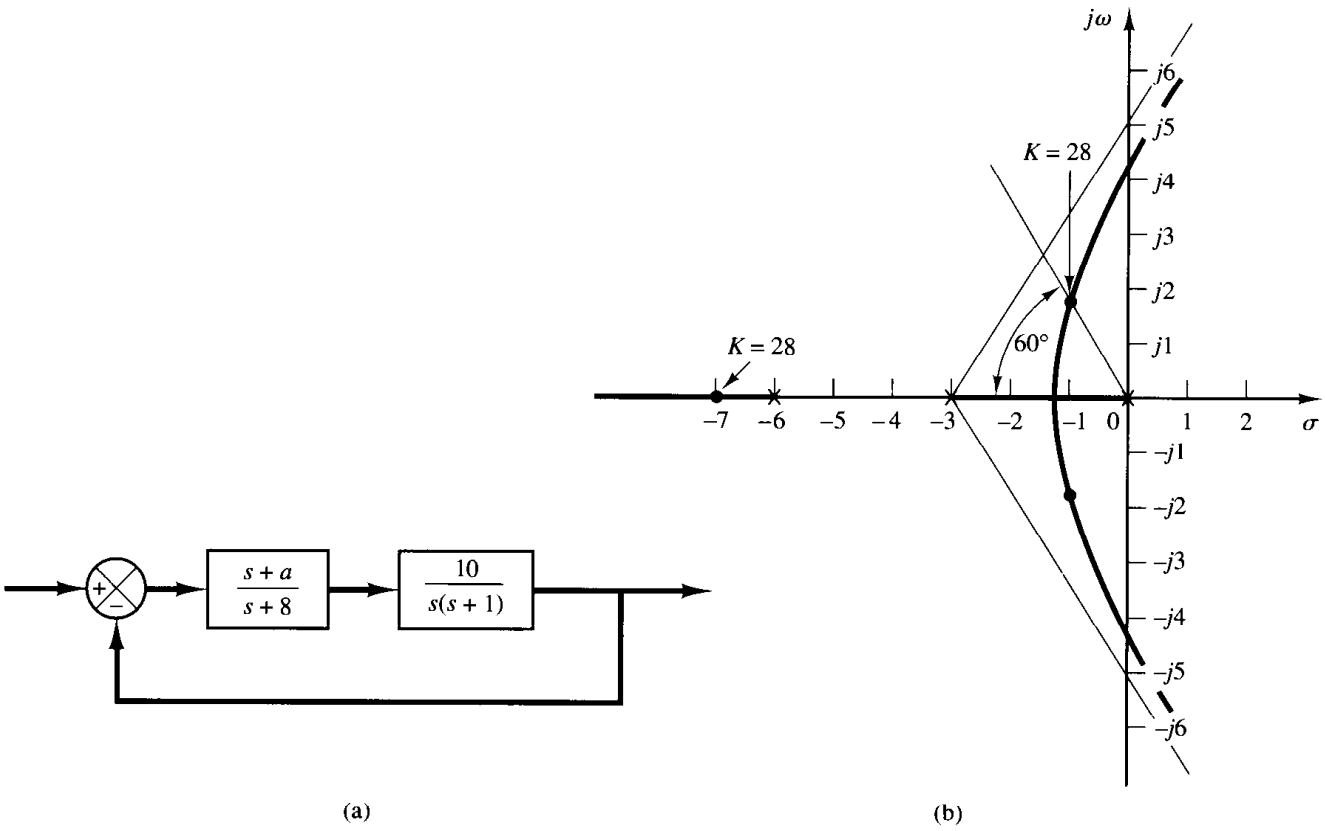

Figure 6–55
(a) Control system; (b) root-locus plot, where $K = 10a$.

This system involves three poles and no zero. The three poles are at $s = 0, s = -3$, and $s = -6$. A root-locus branch exists on the real axis between points $s = 0$ and $s = -3$. Also, another branch exists between points $s = -6$ and $s = -\infty$.

The asymptotes for the root loci are found as follows:

$$\text{Angles of asymptotes} = \frac{\pm 180°(2k + 1)}{3} = 60°, -60°, 180°$$

The intersection of the asymptotes and the real axis is obtained from

$$\sigma_a = -\frac{0 + 3 + 6}{3} = -3$$

The breakaway and break-in points can be determined from $dK/ds = 0$, where

$$K = -(s^3 + 9s^2 + 18s)$$

Now we set

$$\frac{dK}{ds} = -(3s^2 + 18s + 18) = 0$$

which yields

$$s^2 + 6s + 6 = 0$$

or

$$s = -1.268, \qquad s = -4.732$$

Point $s = -1.268$ is on a root-locus branch. Hence, point $s = -1.268$ is an actual breakaway point. But point $s = -4.732$ is not on the root locus and therefore is neither a breakaway nor break-in point.

Next we shall find points where root-locus branches cross the imaginary axis. We substitute $s = j\omega$ in the characteristic equation, which is

$$s^3 + 9s^2 + 18s + K = 0$$

as follows:

$$(j\omega)^3 + 9(j\omega)^2 + 18(j\omega) + K = 0$$

or

$$(K - 9\omega^2) + j\omega(18 - \omega^2) = 0$$

from which we get

$$\omega = \pm 3\sqrt{2}, \qquad K = 9\omega^2 = 162 \qquad \text{or} \qquad \omega = 0, \qquad K = 0$$

The crossing points are at $\omega = \pm 3\sqrt{2}$ and the corresponding value of gain K is 162. Also, a root-locus branch touches the imaginary axis at $\omega = 0$. Figure 6–55(b) shows a sketch of the root loci for the system.

Since the damping ratio of the dominant closed-loop poles is specified as 0.5, the desired closed-loop pole in the upper-half s plane is located at the intersection of the root-locus branch in the upper-half s plane and a straight line having an angle of 60° with the negative real axis. The desired dominant closed-loop poles are located at

$$s = -1 + j1.732, \qquad s = -1 - j1.732$$

At these points, the value of gain K is 28. Hence,

$$a = \frac{K}{10} = 2.8$$

Since the system involves two or more poles than zeros (in fact, three poles and no zero), the third pole can be located on the negative real axis from the fact that the sum of the three closed-loop poles is -9. Hence, the third pole is found to be at

$$s = -9 - (-1 + j1.732) - (-1 - j1.732)$$

or

$$s = -7$$

A-6-14. Consider the system shown in Figure 6–56(a). Sketch the root loci of the system as the velocity feedback gain k varies from zero to infinity. Determine the value of k such that the closed-loop poles have the damping ratio ζ of 0.7.

Solution. The open-loop transfer function is

$$\text{Open-loop transfer function} = \frac{10}{(s + 1 + 10k)s + 10}$$

Since k is not a multiplying factor, we modify the equation such that k appears as a multiplying factor. Since the characteristic equation is

$$s^2 + s + 10ks + 10 = 0$$

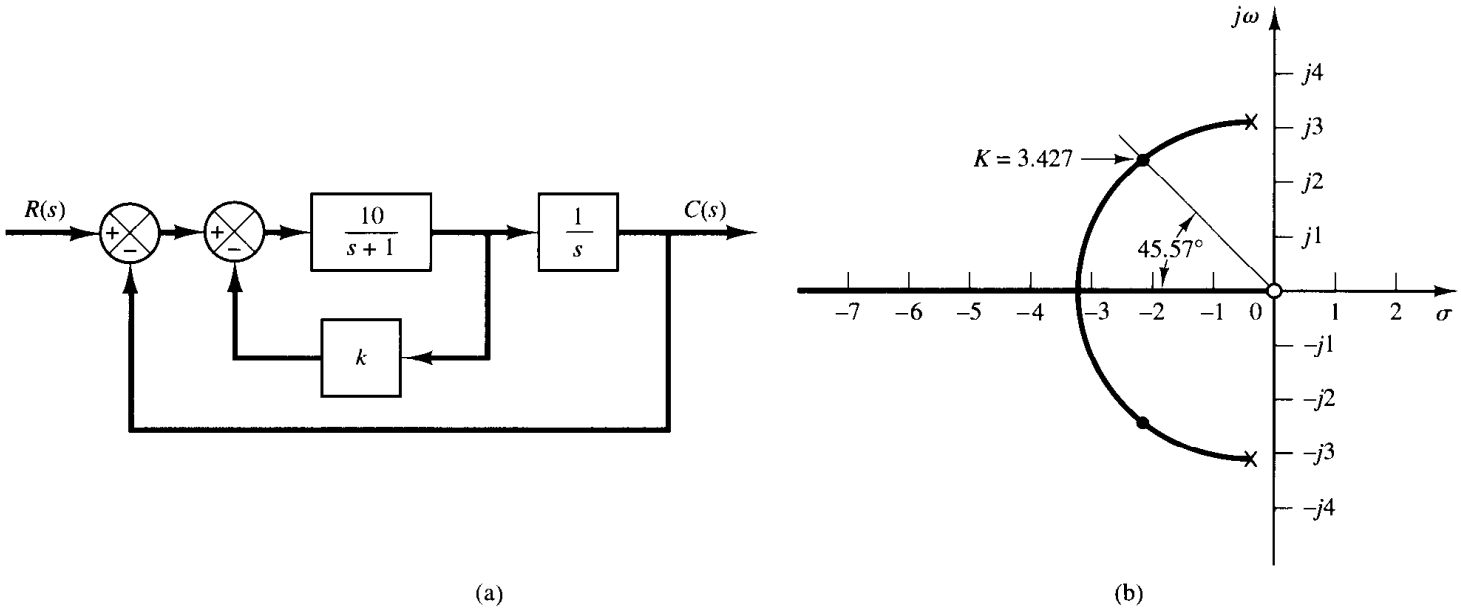

Figure 6–56
(a) Control system; (b) root-locus plot, where $K = 10k$.

we rewrite this equation as follows:

$$1 + \frac{10ks}{s^2 + s + 10} = 0 \tag{6–33}$$

Define

$$10k = K$$

Then Equation (6–33) becomes

$$1 + \frac{Ks}{s^2 + s + 10} = 0$$

Notice that the system has a zero at $s = 0$ and two poles at $s = -0.5 \pm j3.1225$. Since this system involves two poles and one zero, there is a possibility that a circular root locus exists. In fact, this system has a circular root locus, as will be shown. Since the angle condition is

$$\underline{/\ \frac{Ks}{s^2 + s + 10}} = \pm 180°(2k + 1)$$

we have

$$\underline{/\ s} - \underline{/\ s + 0.5 + j3.1225} - \underline{/\ s + 0.5 - j3.1225} = \pm 180°(2k + 1)$$

By substituting $s = \sigma + j\omega$ into this last equation and rearranging, we obtain

$$\underline{/\ \sigma + 0.5 + j(\omega + 3.1225)} + \underline{/\ \sigma + 0.5 + j(\omega - 3.1225)} = \underline{/\ \sigma + j\omega} \pm 180°(2k + 1)$$

which can be rewritten as

$$\tan^{-1}\left(\frac{\omega + 3.1225}{\sigma + 0.5}\right) + \tan^{-1}\left(\frac{\omega - 3.1225}{\sigma + 0.5}\right) = \tan^{-1}\left(\frac{\omega}{\sigma}\right) \pm 180°(2k + 1)$$

Taking tangents of both sides of this last equation, we obtain

$$\frac{\dfrac{\omega + 3.1225}{\sigma + 0.5} + \dfrac{\omega - 3.1225}{\sigma + 0.5}}{1 - \left(\dfrac{\omega + 3.1225}{\sigma + 0.5}\right)\left(\dfrac{\omega - 3.1225}{\sigma + 0.5}\right)} = \frac{\omega}{\sigma}$$

which can be simplified to

$$\frac{2\omega(\sigma + 0.5)}{(\sigma + 0.5)^2 - (\omega^2 - 3.1225^2)} = \frac{\omega}{\sigma}$$

or

$$\omega(\sigma^2 - 10 + \omega^2) = 0$$

which yields

$$\omega = 0 \qquad \text{or} \qquad \sigma^2 + \omega^2 = 10$$

Notice that $\omega = 0$ corresponds to the real axis. The negative real axis (between $s = 0$ and $s = -\infty$) corresponds to $K \geq 0$, and the positive real axis corresponds to $K < 0$. The equation

$$\sigma^2 + \omega^2 = 10$$

is an equation of a circle with center at $\sigma = 0, \omega = 0$ with the radius equal to $\sqrt{10}$. A portion of this circle that lies to the left of the complex poles corresponds to the root locus for $K > 0$. The portion of the circle which lies to the right of the complex poles corresponds to the root locus for $K < 0$. Hence, this portion is not a root locus for the present system, where $K > 0$. Figure 6–56(b) shows a sketch of the root loci.

Since we require $\zeta = 0.7$ for the closed-loop poles, we find the intersection of the circular root locus and a line having an angle of 45.57° (note that $\cos 45.57° = 0.7$) with the negative real axis. The intersection is at $s = -2.214 + j2.258$. The gain K corresponding to this point is 3.427. Hence, the desired value of the velocity feedback gain k is

$$k = \frac{K}{10} = 0.3427$$

A-6-15. Consider the control system shown in Figure 6–57. Plot root loci with MATLAB.

Solution. MATLAB Program 6–10 generates a root-locus plot as shown in Figure 6–58. The root loci must be symmetric about the real axis. However, Figure 6–58 shows otherwise.

MATLAB supplies its own set of gain values that are used to calculate a root-locus plot. It does so by an internal adaptive step-size routine. However, in certain systems, very small changes in the gain cause drastic changes in root locations within a certain range of gains. Thus, MATLAB takes too big a jump in its gain values when calculating the roots, and root locations change by a relatively large amount. When plotting, MATLAB connects these points and causes a strange looking graph at the location of sensitive gains. Such erroneous root-locus plots typically occur when the loci approach a double pole (or triple or higher pole), since the locus is very sensitive to small gain changes.

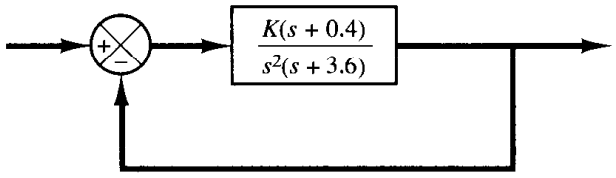

Figure 6–57
Control system.

```
MATLAB Program 6–10

% --------- Root-locus plot ---------

num = [0   0   1   0.4];
den = [1   3.6   0   0];
rlocus(num,den);
v = [−5   1   −3   3]; axis(v)
grid
title('Root-Locus Plot of G(s) = K(s + 0.4)/[s^2(s + 3.6)]')
```

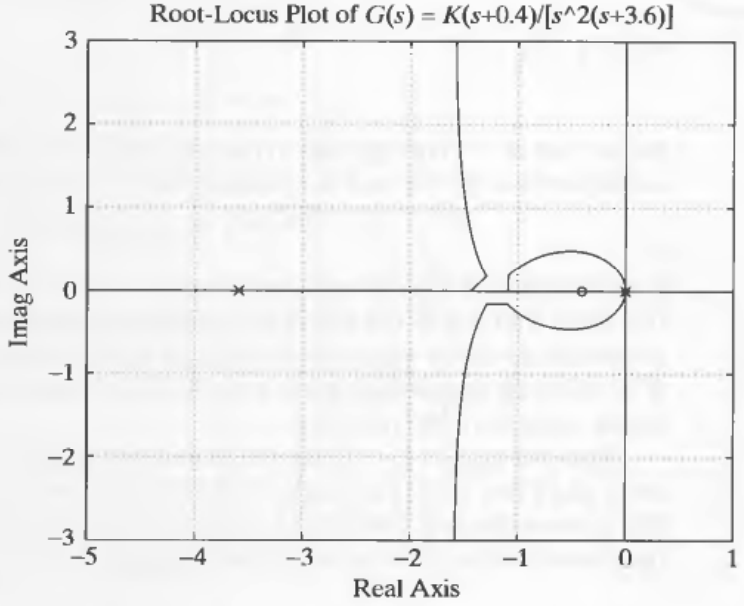

Figure 6–58
Root-locus plot.

In the problem considered here, the critical region of gain K is between 4.2 and 4.4. Thus we need to set the step size small enough in this region. We may divide the region for K as follows:

```
K1 = [0:0.2:4.2];
K2 = [4.2:0.002:4.4];
K3 = [4.4:0.2:10];
K4 = [10:5:200];
K = [K1   K2   K3   K4];
```

Entering MATLAB Program 6–11 into the computer, we obtain the plot as shown in Figure 6–59. If we change the plot command plot(r,'o') in MATLAB Program 6–11 to plot(r,'-'), we obtain Figure 6–60. Figures 6–59 and 6–60 respectively show satisfactory root-locus plots.

A-6-16. Consider the system whose open-loop transfer function $G(s)H(s)$ is given by

$$G(s)H(s) = \frac{K}{s(s+1)(s+2)}$$

Using MATLAB, plot root loci and their asymptotes.

MATLAB Program 6–11

```
% --------- Root-locus plot ---------

num = [0   0   1   0.4];
den = [1   3.6   0   0];
K1 = [0:0.2:4.2];
K2 = [4.2:0.002:4.4];
K3 = [4.4:0.02:10];
K4 = [10:5:200];
K = [K1   K2   K3   K4];
r = rlocus(num,den,K);
plot(r,'o')
v = [−5   1   −5   5]; axis(v)
grid
title('Root-Locus Plot of G(s) = K(s + 0.4)/[s^2(s + 3.6)]')
xlabel('Real Axis')
ylabel('Imag Axis')
```

Solution. We shall plot the root loci and asymptotes on one diagram. Since the open-loop transfer function is given by

$$G(s)H(s) = \frac{K}{s(s+1)(s+2)}$$

$$= \frac{K}{s^3 + 3s^2 + 2s}$$

the equation for the asymptotes may be obtained as follows: Noting that

$$\lim_{s\to\infty} \frac{K}{s^3 + 3s^2 + 2s} \doteq \lim_{s\to\infty} \frac{K}{s^3 + 3s^2 + 3s + 1} = \frac{K}{(s+1)^3}$$

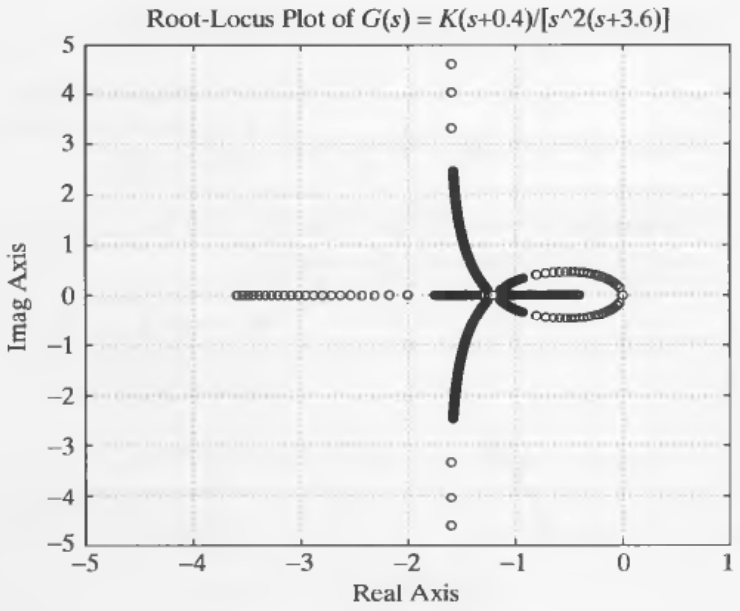

Figure 6–59
Root-locus plot.

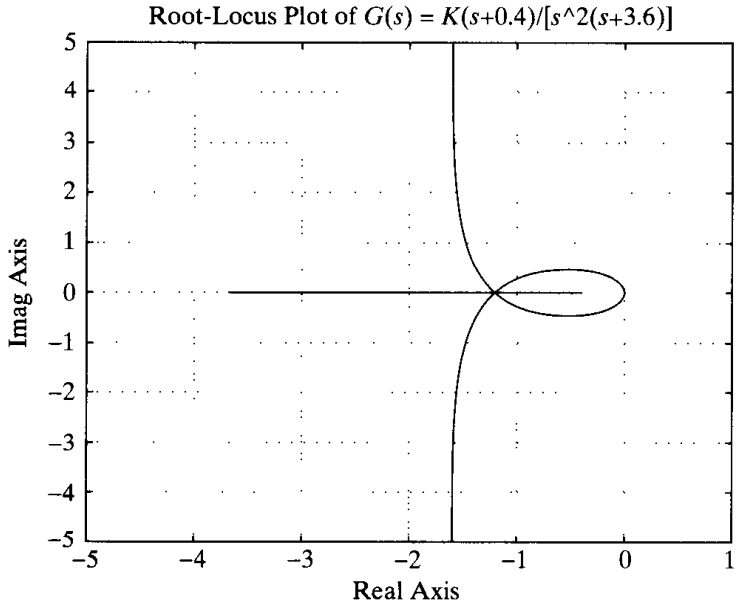

Figure 6–60
Root-locus plot.

the equation for the asymptotes may be given by

$$G_a(s)H_a(s) = \frac{K}{(s+1)^3}$$

Hence, for the system we have

```
num = [0  0  0  1]
den = [1  3  2  0]
```

and for the asymptotes,

```
numa = [0  0  0  1]
dena = [1  3  3  1]
```

In using the following root-locus and plot commands

```
r = rlocus(num,den)
a = rlocus(numa,dena)
plot([r  a])
```

the number of rows of r and that of a must be the same. To ensure this, we include the gain constant K in the commands. For example,

```
K1 = 0:0.1:0.3;
K2 = 0.3:0.005:0.5:
K3 = 0.5:0.5:10;
K4 = 10:5:100;
K = [K1  K2  K3  K4]
r = rlocus(num,den,K)
a = rlocus(numa,dena,K)
y = [r     a]
plot(y,' ')
```

Including gain K in rlocus command ensures that the r matrix and a matrix have the same number of rows. MATLAB Program 6–12 will generate a plot of root loci and their asymptotes. See Figure 6–61.

MATLAB Program 6–12

```
% --------- Root-Locus Plots ----------

num = [0   0   0   1];
den = [1   3   2   0];
numa = [0   0   0   1];
dena = [1   3   3   1];
K1 = 0:0.1:0.3;
K2 = 0.3:0.005:0.5;
K3 = 0.5:0.5:10;
K4 = 10:5:100;
K = [K1   K2   K3   K4];
r = rlocus(num,den,K);
a = rlocus(numa,dena,K);
y = [r   a];
plot(y,'-')
v = [−4   4   −4   4]; axis(v)
grid
title('Root-Locus Plot of G(s) = K/[s(s + 1)(s + 2)] and Asymptotes')
xlabel('Real Axis')
ylabel('Imag Axis')

% ***** Manually draw open-loop poles in the hard copy *****
```

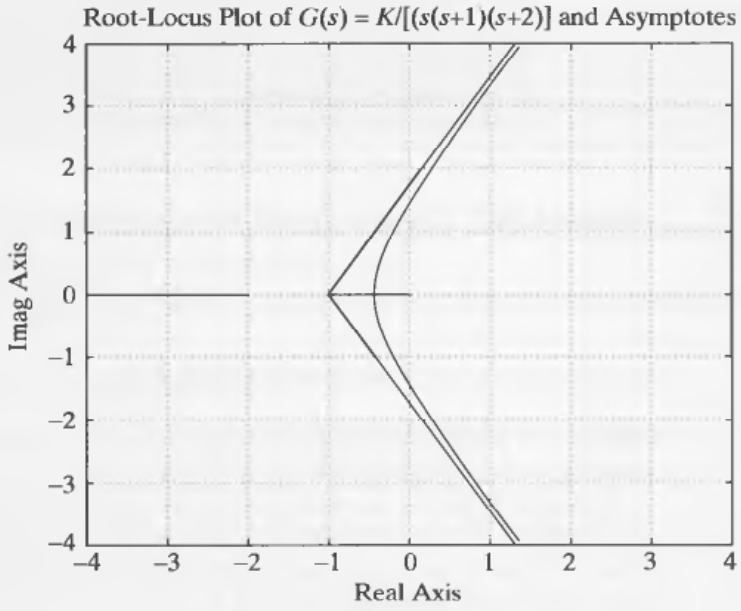

Figure 6–61
Root-locus plot.

Drawing two or more plots in one diagram can be accomplished by using the hold command. MATLAB Program 6–13 uses the hold command. The resulting root-locus plot is shown in Figure 6–62.

MATLAB Program 6–13

```
% ---------- Root-Locus Plots ----------

num = [0   0   0   1];
den = [1   3   2   0];
numa = [0   0   0   1];
dena = [1   3   3   1];
K1 = 0:0.1:0.3;
K2 = 0.3:0.005:0.5;
K3 = 0.5:0.5:10;
K4 = 10:5:100;
K = [K1   K2   K3   K4];
r = rlocus(num,den,K);
a = rlocus(numa,dena,K);
plot(r,'o')
hold
Current plot held
plot(a,'-')
v = [−4   4   −4   4]; axis(v)
grid
title('Root-Locus Plot of G(s) = K/[s(s + 1)(s + 2)] and Asymptotes')
xlabel('Real Axis')
ylabel('Imag Axis')

% ***** Manually draw open-loop poles in the hard copy *****

% ***** Remove hold on graphics *****

hold
Current plot released
```

A-6-17. Consider a unity-feedback system with the following feedforward transfer function $G(s)$:

$$G(s) = \frac{K(s + 2)^2}{(s^2 + 4)(s + 5)^2}$$

Plot root loci for the system with MATLAB.

Solution. A MATLAB program to plot the root loci is given as MATLAB Program 6–14. The resulting root-locus plot is shown in Figure 6–63.

Notice that this is a special case where no root locus exists on the real axis. This means that for any value of $K > 0$ the closed-loop poles of the system are two sets of complex-conjugate poles. (No real closed-loop poles exist.) Since no closed-loop poles exist in the right-half s plane, the system is stable for all values of $K > 0$.

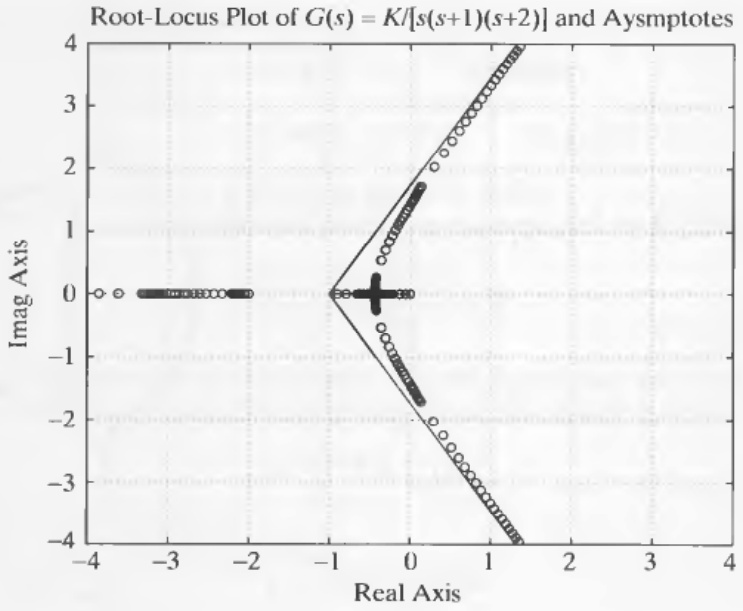

Figure 6–62
Root-locus plot.

MATLAB Program 6–14

```
% ---------- Root-Locus Plot ----------

num = [0   0   1   4   4];
den = [1   10   29   40   100];
r = rlocus(num,den);
plot(r,'o')
hold
Current plot held
plot(r,'-')
v = [−8   4   −6   6]; axis(v); axis('square')
grid
title('Root-Locus Plot of G(s) = (s + 2)^2/[(s^2 + 4)(s + 5)^2]')
xlabel('Real Axis')
ylabel('Imag Axis')
```

A-6-18. Consider the system with transport lag shown in Figure 6–64(a). Sketch the root loci and find the two pairs of closed-loop poles nearest the $j\omega$ axis.

Using only the dominant closed-loop poles, obtain the unit-step response and sketch the response curve.

Solution. The characteristic equation is

$$\frac{2e^{-0.3s}}{s+1} + 1 = 0$$

which is equivalent to the following angle and magnitude conditions:

$$\angle \frac{2e^{-0.3s}}{s+1} = \pm 180^\circ(2k+1)$$

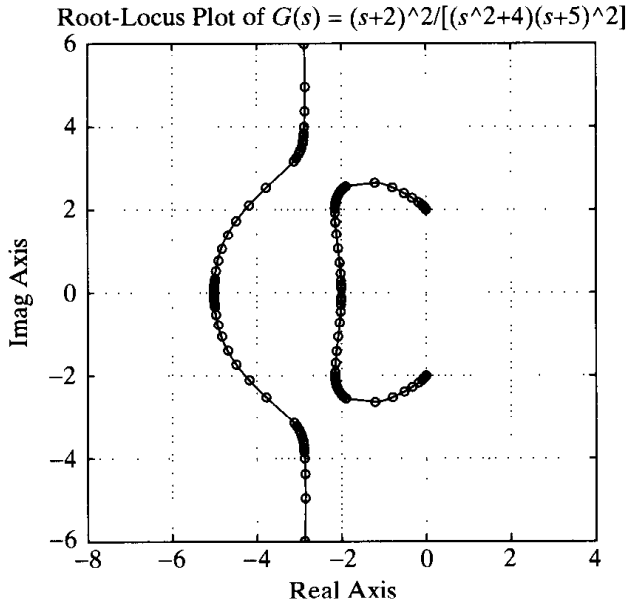

Figure 6–63
Root-locus plot.

$$\left|\frac{2e^{-0.3s}}{s+1}\right| = 1$$

The angle condition reduces to

$$\underline{/s+1} = \pm\pi(2k+1) - 0.3\omega \qquad \text{(radians)}$$

For $k = 0$,

$$\underline{/s+1} = \pm\pi - 0.3\omega \qquad \text{(radians)}$$

$$= \pm 180° - 17.2°\omega \qquad \text{(degrees)}$$

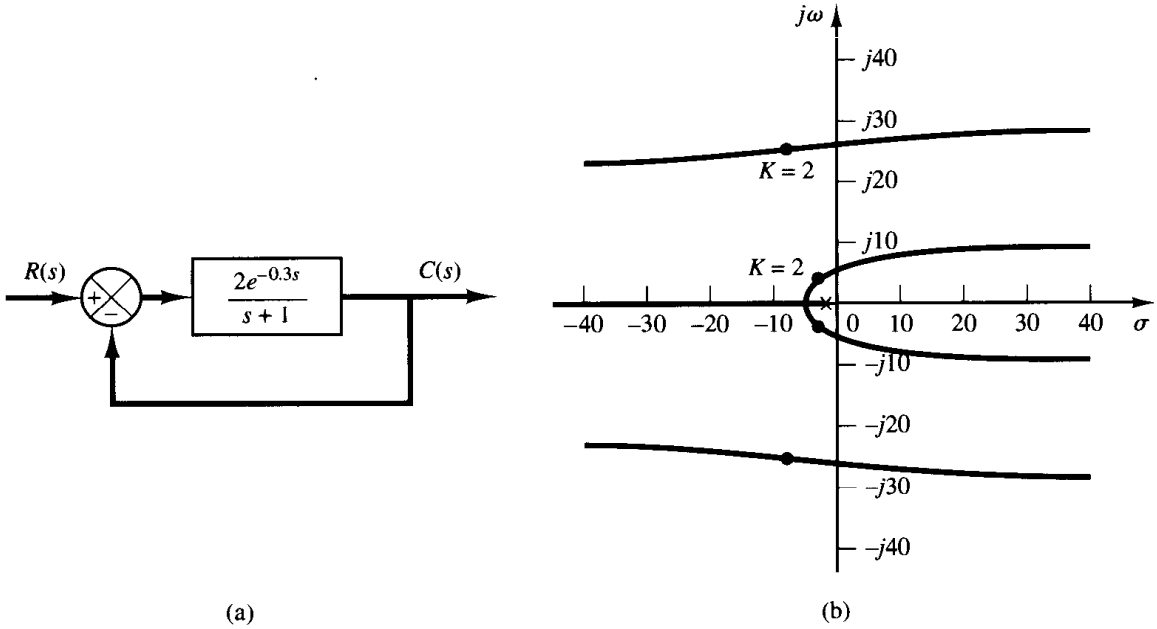

Figure 6–64
(a) Control system with transport lag; (b) root-locus plot.

For $k = 1$,

$$\underline{/s + 1} = \pm 3\pi - 0.3\omega \qquad \text{(radians)}$$

$$= \pm 540° - 17.2°\omega \qquad \text{(degrees)}$$

The root-locus plot for this system is shown in Figure 6–64(b).

Let us set $s = \sigma + j\omega$ in the magnitude condition and replace 2 by K. Then we obtain

$$\frac{\sqrt{(1 + \sigma)^2 + \omega^2}}{e^{-0.3\sigma}} = K$$

By evaluating K at different points on the root loci, the points may be found for which $K = 2$. These points are closed-loop poles. The dominant pair of closed-loop poles is

$$s = -2.5 \pm j3.9$$

The next pair of closed-loop poles is

$$s = -8.6 \pm j25.1$$

Using only the pair of dominant closed-loop poles, the closed-loop transfer function may be approximated as follows: Noting that

$$\frac{C(s)}{R(s)} = \frac{2e^{-0.3s}}{1 + s + 2e^{-0.3s}}$$

$$= \frac{2e^{-0.3s}}{1 + s + 2\left(1 - 0.3s + \dfrac{0.09s^2}{2} + \cdots\right)}$$

$$= \frac{2e^{-0.3s}}{3 + 0.4s + 0.09s^2 + \cdots}$$

and

$$(s + 2.5 + j3.9)(s + 2.5 - j3.9) = s^2 + 5s + 21.46$$

we may approximate $C(s)/R(s)$ by

$$\frac{C(s)}{R(s)} = \frac{\frac{2}{3}(21.46)e^{-0.3s}}{s^2 + 5s + 21.46}$$

or

$$\frac{C(s)}{R(s)} = \frac{14.31e^{-0.3s}}{(s + 2.5)^2 + 3.9^2}$$

For a unit-step input,

$$C(s) = \frac{14.31e^{-0.3s}}{[(s + 2.5)^2 + 3.9^2]s}$$

Note that

$$\frac{14.31}{[(s + 2.5)^2 + 3.9^2]s} = \frac{\frac{2}{3}}{s} + \frac{-\frac{2}{3}s - \frac{10}{3}}{(s + 2.5)^2 + 3.9^2}$$

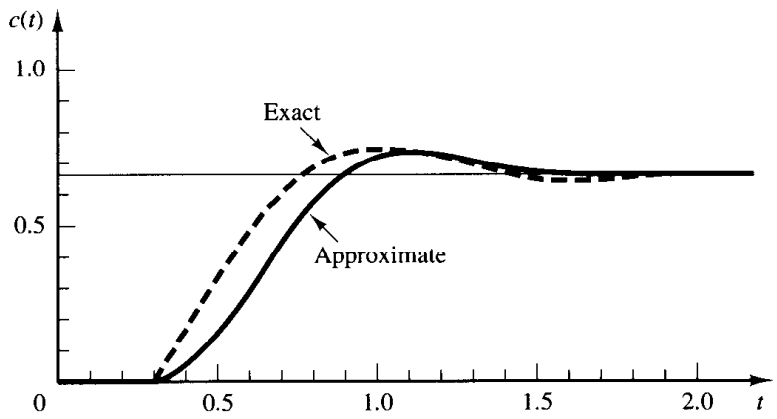

Figure 6–65
Unit-step response curves for the system shown in Figure 6–64(a).

Hence,

$$C(s) = \left(\frac{\frac{2}{3}}{s}\right)e^{-0.3s} + \left[\frac{-\frac{2}{3}s - \frac{10}{3}}{(s + 2.5)^2 + 3.9^2}\right]e^{-0.3s}$$

The inverse Laplace transform of $C(s)$ gives

$$c(t) = \tfrac{2}{3}[1 - e^{-2.5(t-0.3)} \cos 3.9(t - 0.3) - 0.641e^{-2.5(t-0.3)} \sin 3.9(t - 0.3)]1(t - 0.3)$$

where $1(t - 0.3)$ is the unit-step function occurring at $t = 0.3$.

Figure 6–65 shows the approximate response curve thus obtained, together with the exact unit-step response curve obtained by a computer simulation. Note that in this system a fairly good approximation can be obtained by use of only the dominant closed-loop poles.

PROBLEMS

B-6-1. Plot the root loci for the closed-loop control system with

$$G(s) = \frac{K}{s(s + 1)(s^2 + 4s + 5)}, \qquad H(s) = 1$$

B-6-2. Plot the root loci for a closed-loop control system with

$$G(s) = \frac{K(s + 9)}{s(s^2 + 4s + 11)}, \qquad H(s) = 1$$

Locate the closed-loop poles on the root loci such that the dominant closed-loop poles have a damping ratio equal to 0.5. Determine the corresponding value of gain K.

B-6-3. Plot the root loci for the system with

$$G(s) = \frac{K}{s(s + 0.5)(s^2 + 0.6s + 10)}, \qquad H(s) = 1$$

B-6-4. Plot the root loci for a system with

$$G(s) = \frac{K}{(s^2 + 2s + 2)(s^2 + 2s + 5)}, \qquad H(s) = 1$$

Determine the exact points where the root loci cross the $j\omega$ axis.

B-6-5. Show that the root loci for a control system with

$$G(s) = \frac{K(s^2 + 6s + 10)}{s^2 + 2s + 10}, \qquad H(s) = 1$$

are arcs of the circle centered at the origin with radius equal to $\sqrt{10}$.

B-6-6. Plot the root loci for a closed-loop control system with

$$G(s) = \frac{K(s + 0.2)}{s^2(s + 3.6)}, \qquad H(s) = 1$$

B-6-7. Plot the root loci for a closed-loop control system with

$$G(s) = \frac{K(s + 0.5)}{s^3 + s^2 + 1}, \qquad H(s) = 1$$

B-6-8. Plot the root loci for the system shown in Figure 6–66. Determine the range of gain K for stability.

B-6-9. Consider a unity-feedback control system with the following feedforward transfer function:

$$G(s) = \frac{K}{s(s^2 + 4s + 8)}$$

Plot the root loci for the system. If the value of gain K is set equal to 2, where are the closed-loop poles located?

B-6-10. Consider the system shown in Figure 6–67. Determine the values of the gain K and the velocity feedback coefficient K_h so that the closed-loop poles are at $s = -1 \pm j\sqrt{3}$. Then, using the determined value of K_h, plot the root loci.

B-6-11. Consider the system shown in Figure 6–68. The system involves velocity feedback. Determine the value of gain K such that the dominant closed-loop poles have a damping ratio of 0.5. Using the gain K thus determined, obtain the unit-step response of the system.

B-6-12. Consider the system whose open-loop transfer function $G(s)H(s)$ is given by

$$G(s)H(s) = \frac{K}{(s^2 + 2s + 2)(s^2 + 2s + 5)} = \frac{K}{s^4 + 4s^3 + 11s^2 + 14s + 10}$$

Plot a root-locus diagram with MATLAB.

B-6-13. Consider the system whose open-loop transfer function is given by

$$G(s)H(s) = \frac{K(s - 0.6667)}{s^4 + 3.3401s^3 + 7.0325s^2}$$

Show that the equation for the asymptotes is given by

$$G_a(s)H_a(s) = \frac{K}{s^3 + 4.0068s^2 + 5.3515s + 2.3825}$$

Using MATLAB, plot the root loci and asymptotes for the system.

B-6-14. Consider the unity-feedback system whose feedforward transfer function is

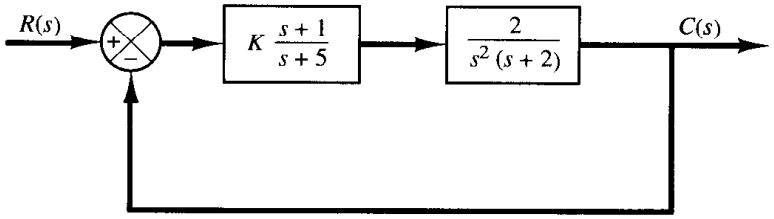

Figure 6–66
Control system.

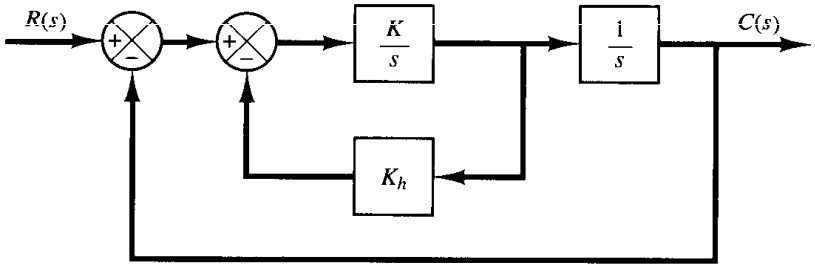

Figure 6–67
Control system.

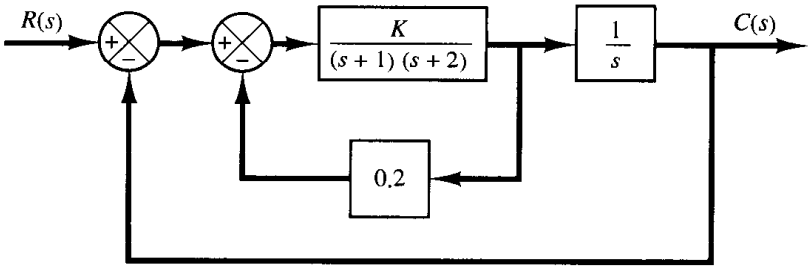

Figure 6–68
Control system.

$$G(s) = \frac{K}{s(s + 1)}$$

The constant-gain locus for the system for a given value of K is defined by the following equation:

$$\left|\frac{K}{s(s + 1)}\right| = 1$$

Show that the constant-gain loci for $0 \leq K \leq \infty$ may be given by

$$[\sigma(\sigma + 1) + \omega^2]^2 + \omega^2 = K^2$$

Sketch the constant-gain loci for $K = 1, 2, 5, 10$, and 20 on the s plane.

B-6-15. Consider the system shown in Figure 6–69. Plot the root loci. Locate the closed-loop poles when the gain K is set equal to 2.

B-6-16. Consider the system shown in Figure 6–70. Plot the root loci as a varies from 0 to ∞. Determine the value of a such that the damping ratio of the dominant closed-loop poles is 0.5.

B-6-17. Consider the system shown in Figure 6–71. Plot the root loci as the value of k varies from 0 to ∞. What value of k will give the damping ratio of the dominant closed-loop poles equal to 0.5? Find the static velocity error constant with this value of k.

B-6-18. Plot the root loci for the system shown in Figure 6–72. Show that the system may become unstable for large values of K.

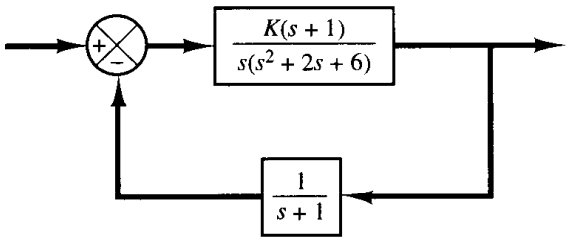

Figure 6–69
Control system.

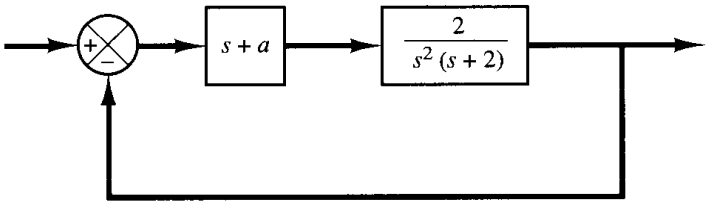

Figure 6–70
Control system.

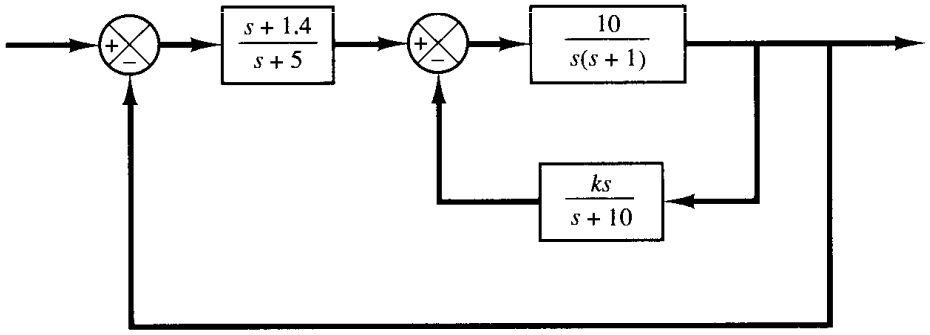

Figure 6–71
Control system.

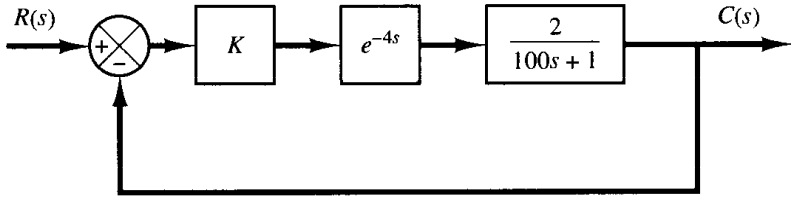

Figure 6–72
Control system.

B-6-19. Plot the root contours for the system shown in Figure 6–73 when the gain K and parameter a vary, respectively, from zero to infinity.

B-6-20. Consider the system shown in Figure 6–74. Assuming that the value of gain K varies from 0 to ∞, plot the root loci when $K_h = 0.5$. Then sketch the root contours for $0 \leq K < \infty$ and $0 \leq K_h < \infty$. Locate the closed-loop poles on the root contour when $K = 10$ and $K_h = 0.5$.

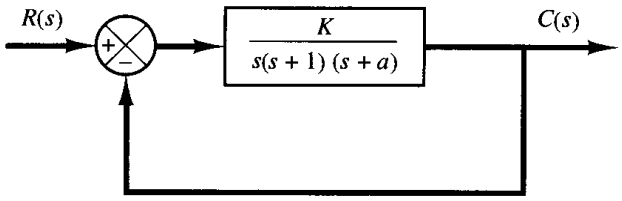

Figure 6–73
Control system.

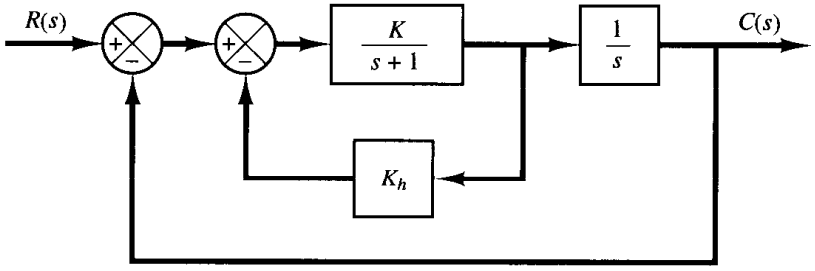

Figure 6–74
Control system.

7

Control Systems Design by the Root-Locus Method

7–1 INTRODUCTION

The primary objective of this chapter is to present procedures for the design and compensation of single-input–single-output linear time-invariant control systems. Compensation is the modification of the system dynamics to satisfy the given specifications. The approach to the control system design and compensation used in this chapter is the root-locus approach. (The frequency-response approach and the state-space approach to the control systems design and compensation will be presented in Chapter 9 and Chapter 11, respectively.)

Performance specifications. Control systems are designed to perform specific tasks. The requirements imposed on the control system are usually spelled out as performance specifications. They generally relate to accuracy, relative stability, and speed of response.

For routine design problems, the performance specifications may be given in terms of precise numerical values. In other cases, they may be given partially in terms of precise numerical values and partially in terms of qualitative statements. In the latter case, the specifications may have to be modified during the course of design since the given specifications may never be satisfied (because of conflicting requirements) or may lead to a very expensive system.

Generally, the performance specifications should not be more stringent than necessary to perform the given task. If the accuracy at steady-state operation is of prime importance in a given control system, then we should not require unnecessarily rigid performance specifications on the transient response since such specifications will re-

quire expensive components. Remember that the most important part of control system design is to state the performance specifications precisely so that they will yield an optimal control system for the given purpose.

System compensation. Setting the gain is the first step in adjusting the system for satisfactory performance. In many practical cases, however, the adjustment of the gain alone may not provide sufficient alteration of the system behavior to meet the given specifications. As is frequently the case, increasing the gain value will improve the steady-state behavior but will result in poor stability or even instability. It is then necessary to redesign the system (by modifying the structure or by incorporating additional devices or components) to alter the overall behavior so that the system will behave as desired. Such a redesign or addition of a suitable device is called *compensation*. A device inserted into the system for the purpose of satisfying the specifications is called a *compensator*. The compensator compensates for deficit performance of the original system.

Series compensation and feedback (or parallel) compensation. Figures 7–1 (a) and (b) show compensation schemes commonly used for feedback control systems. Figure 7–1(a) shows the configuration where the compensator $G_c(s)$ is placed in series with the plant. This scheme is called *series compensation*.

An alternative to series compensation is to feed back the signal(s) from some element(s) and place a compensator in the resulting inner feedback path, as shown in Figure 7–1(b). Such compensation is called *feedback compensation* or *parallel compensation*.

In compensating control systems, we see that the problem usually boils down to a suitable design of a series or feedback compensator. The choice between series compensation and feedback compensation depends on the nature of the signals in the

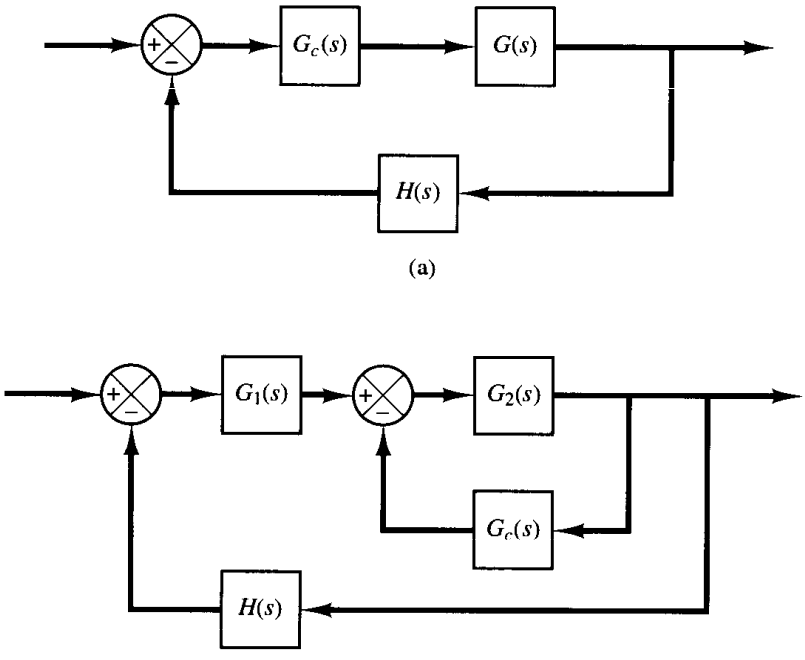

Figure 7–1
(a) Series compensation; (b) feedback or parallel compensation.

system, the power levels at various points, available components, the designer's experience, economic considerations, and so on.

In general, series compensation may be simpler than feedback compensation; however, series compensation frequently requires additional amplifiers to increase the gain and/or to provide isolation. (To avoid power dissipation, the series compensator is inserted at the lowest energy point in the feedforward path.) Note that, in general, the number of components required in feedback compensation will be less than the number of components in series compensation, provided a suitable signal is available, because the energy transfer is from a higher power level to a lower level. (This means that additional amplifiers may not be necessary.)

In discussing compensators, we frequently use such terminologies as *lead network, lag network,* and *lag–lead network.* As stated in Section 5–9, if a sinusoidal input e_i is applied to the input of a network and the steady-state output e_o (which is also sinusoidal) has a phase lead, then the network is called a lead network. (The amount of phase lead angle is a function of the input frequency.) If the steady-state output e_o has a phase lag, then the network is called a lag network. In a lag–lead network, both phase lag and phase lead occur in the output but in different frequency regions; phase lag occurs in the low-frequency region and phase lead occurs in the high-frequency region. A compensator having a characteristic of a lead network, lag network, or lag–lead network is called a lead compensator, lag compensator, or lag–lead compensator.

Compensators. If a compensator is needed to meet the performance specifications, the designer must realize a physical device that has the prescribed transfer function of the compensator.

Numerous physical devices have been used for such purposes. In fact, many noble and useful ideas for physically constructing compensators may be found in the literature.

Among the many kinds of compensators, widely employed compensators are the lead compensators, lag compensators, lag–lead compensators, and velocity-feedback (tachometer) compensators. In this chapter we shall limit our discussions mostly to these types. Lead, lag, and lag–lead compensators may be electronic devices (such as circuits using operational amplifiers) or *RC* networks (electrical, mechanical, pneumatic, hydraulic, or combinations thereof) and amplifiers.

In the actual design of a control system, whether to use an electronic, pneumatic, or hydraulic compensator is a matter that must be decided partially based on the nature of the controlled plant. For example, if the controlled plant involves flammable fluid, then we have to choose pneumatic components (both a compensator and an actuator) to avoid the possibility of sparks. If, however, no fire hazard exists, then electronic compensators are most commonly used. (In fact, we often transform nonelectrical signals into electrical signals because of the simplicity of transmission, increased accuracy, increased reliability, ease of compensation, and the like.)

Design procedures. In the trial-and-error approach to system design, we set up a mathematical model of the control system and adjust the parameters of a compensator. The most time-consuming part of such work is the checking of the system performance by analysis with each adjustment of the parameters. The designer should make use of a digital computer to avoid much of the numerical drudgery necessary for this checking.

Once a satisfactory mathematical model has been obtained, the designer must construct a prototype and test the open-loop system. If absolute stability of the closed loop is assured, the designer closes the loop and tests the performance of the resulting closed-loop system. Because of the neglected loading effects among the components, nonlinearities, distributed parameters, and so on, which were not taken into consideration in the original design work, the actual performance of the prototype system will probably differ from the theoretical predictions. Thus the first design may not satisfy all the requirements on performance. By trial and error, the designer must make changes in the prototype until the system meets the specifications. In doing this, he or she must analyze each trial, and the results of the analysis must be incorporated into the next trial. The designer must see that the final system meets the performance specifications and, at the same time, is reliable and economical.

It is noted that in designing control systems by the root-locus or frequency-response methods the final result is not unique, because the best or optimal solution may not be precisely defined if the time-domain specifications or frequency-domain specifications are given.

Outline of the chapter. Section 7–1 has presented an introduction to the compensation of control systems. Section 7–2 discusses preliminary considerations for the root-locus approach to the control systems design. Section 7–3 treats details of the lead compensation techniques based on the root-locus method. Section 7–4 deals with the lag compensation techniques by the root-locus method. Section 7–5 presents lag–lead compensation techniques. Detailed discussions of the design of lag–lead compensators are presented.

7–2 PRELIMINARY DESIGN CONSIDERATIONS

In building a control system, we know that proper modification of the plant dynamics may be a simple way to meet the performance specifications. This, however, may not be possible in many practical situations because the plant may be fixed and may not be modified. Then we must adjust parameters other than those in the fixed plant. In this book, we assume that the plant is given and unalterable.

The design problems, therefore, become those of improving system performance by insertion of a compensator. Compensation of a control system is reduced to the design of a filter whose characteristics tend to compensate for the undesirable and unalterable characteristics of the plant. Our discussions are limited to continuous-time compensators.

In Section 7–3 through 7–5, we shall specifically consider the design of lead compensators, lag compensators, and lag–lead compensators. In such design problems, we place a compensator in series with the unalterable transfer function $G(s)$ to obtain desirable behavior. The main problem then involves the judicious choice of the pole(s) and zero(s) of the compensator $G_c(s)$ to alter the root locus (or frequency response) so that the performance specifications will be met.

Root–locus approach to control system design. The root-locus method is a graphical method for determining the locations of all closed-loop poles from knowledge

of the locations of the open-loop poles and zeros as some parameter (usually the gain) is varied from zero to infinity. The method yields a clear indication of the effects of parameter adjustment.

In practice, the root-locus plot of a system may indicate that the desired performance cannot be achieved just by the adjustment of gain. In fact, in some cases, the system may not be stable for all values of gain. Then it is necessary to reshape the root loci to meet the performance specifications.

In designing a control system, if other than a gain adjustment is required, we must modify the original root loci by inserting a suitable compensator. Once the effects on the root locus of the addition of poles and/or zeros are fully understood, we can readily determine the locations of the pole(s) and zero(s) of the compensator that will reshape the root locus as desired. In essence, in the design by the root-locus method, the root loci of the system are reshaped through the use of a compensator so that a pair of dominant closed-loop poles can be placed at the desired location. (Often, the damping ratio and undamped natural frequency of a pair of dominant closed-loop poles are specified.)

Effects of the addition of poles. The addition of a pole to the open-loop transfer function has the effect of pulling the root locus to the right, tending to lower the system's relative stability and to slow down the settling of the response. (Remember that the addition of integral control adds a pole at the origin, thus making the system less stable.) Figure 7–2 shows examples of root loci illustrating the effects of the addition of a pole to a single-pole system and the addition of two poles to a single-pole system.

Effects of the addition of zeros. The addition of a zero to the open-loop transfer function has the effect of pulling the root locus to the left, tending to make the system more stable and to speed up the settling of the response. (Physically, the addition of a zero in the feedforward transfer function means the addition of derivative control to the system. The effect of such control is to introduce a degree of anticipation into the system and speed up the transient response.) Figure 7–3(a) shows the root loci for a system that is stable for small gain but unstable for large gain. Figures 7–3(b), (c), and (d) show root-locus plots for the system when a zero is added to the open-loop transfer

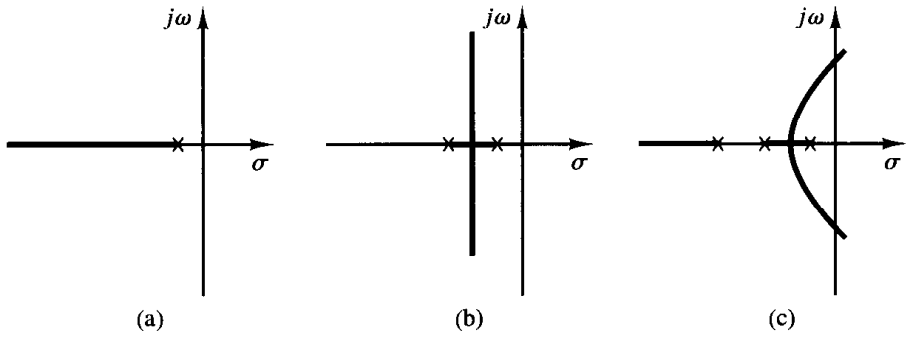

Figure 7–2
(a) Root-locus plot of a single-pole system; (b) root-locus plot of a two-pole system; (c) root-locus plot of a three-pole system.

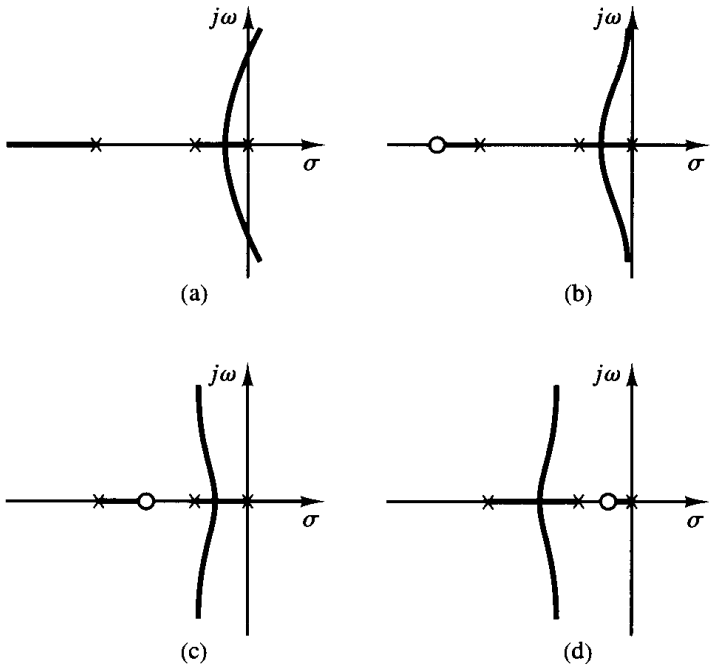

Figure 7–3
(a) Root-locus plot of a three-pole system; (b), (c), and (d) root-locus plots showing effects of addition of a zero to the three-pole system.

function. Notice that when a zero is added to the system of Figure 7–3(a) it becomes stable for all values of gain.

7–3 LEAD COMPENSATION

Lead compensators. There are many ways to realize continuous-time (or analog) lead compensators, such as electronic networks using operational amplifiers, electrical *RC* networks, and mechanical spring–dashpot systems. Compensators using operational amplifiers are frequently used in practice. (Refer to Chapter 5 for networks using operational amplifiers.)

Figure 7–4 shows an electronic circuit using operational amplifiers. The transfer function for this circuit was obtained in Chapter 5 as follows:

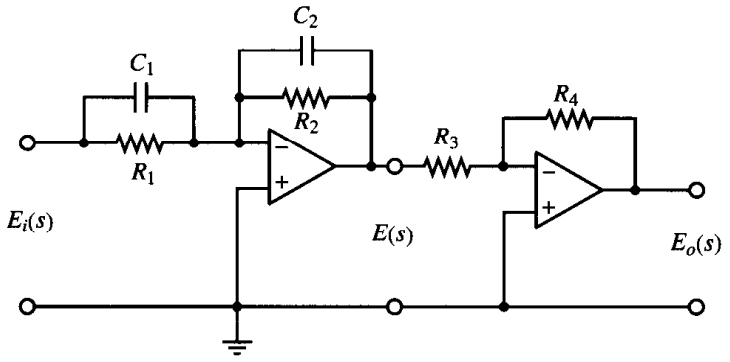

Figure 7–4
Electronic circuit that is a lead network if $R_1C_1 > R_2C_2$ and a lag network if $R_1C_1 < R_2C_2$.

$$\frac{E_o(s)}{E_i(s)} = \frac{R_2R_4}{R_1R_3}\frac{R_1C_1s + 1}{R_2C_2s + 1} = \frac{R_4C_1}{R_3C_2}\frac{s + \dfrac{1}{R_1C_1}}{s + \dfrac{1}{R_2C_2}}$$

$$= K_c\alpha\frac{Ts + 1}{\alpha Ts + 1} = K_c\frac{s + \dfrac{1}{T}}{s + \dfrac{1}{\alpha T}} \tag{7-1}$$

where

$$T = R_1C_1, \qquad \alpha T = R_2C_2, \qquad K_c = \frac{R_4C_1}{R_3C_2}$$

Notice that

$$K_c\alpha = \frac{R_4C_1}{R_3C_2}\frac{R_2C_2}{R_1C_1} = \frac{R_2R_4}{R_1R_3}, \qquad \alpha = \frac{R_2C_2}{R_1C_1}$$

This network has a dc gain of $K_c\alpha = R_2R_4/(R_1R_3)$.

From Equation (7–1), we see that this network is a lead network if $R_1C_1 > R_2C_2$, or $\alpha < 1$. It is a lag network if $R_1C_1 < R_2C_2$. The pole–zero configurations of this network when $R_1C_1 > R_2C_2$ and $R_1C_1 < R_2C_2$ are shown in Figure 7–5(a) and (b), respectively.

Lead compensation techniques based on the root-locus approach. The root-locus approach to design is very powerful when the specifications are given in terms of time-domain quantities, such as the damping ratio and undamped natural frequency of the desired dominant closed-loop poles, maximum overshoot, rise time, and settling time.

Consider a design problem in which the original system either is unstable for all values of gain or is stable but has undesirable transient-response characteristics. In such a

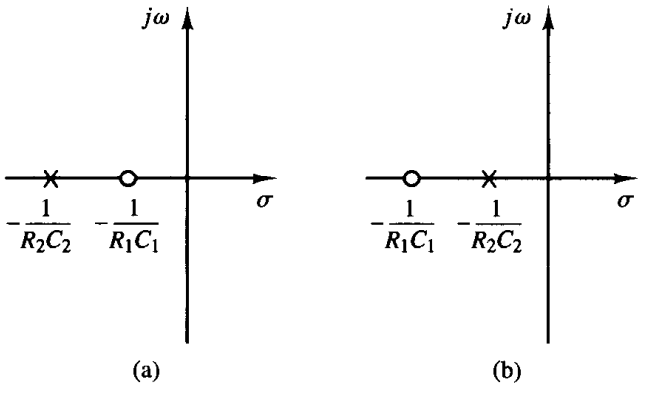

Figure 7–5
Pole–zero configurations: (a) lead network; (b) lag network.

case, the reshaping of the root locus is necessary in the broad neighborhood of the $j\omega$ axis and the origin in order that the dominant closed-loop poles be at desired locations in the complex plane. This problem may be solved by inserting an appropriate lead compensator in cascade with the feedforward transfer function.

The procedures for designing a lead compensator for the system shown in Figure 7–6 by the root-locus method may be stated as follows:

1. From the performance specifications, determine the desired location for the dominant closed-loop poles.

2. By drawing the root-locus plot, ascertain whether or not the gain adjustment alone can yield the desired closed-loop poles. If not, calculate the angle deficiency ϕ. This angle must be contributed by the lead compensator if the new root locus is to pass through the desired locations for the dominant closed-loop poles.

3. Assume the lead compensator $G_c(s)$ to be

$$G_c(s) = K_c\alpha\frac{Ts + 1}{\alpha Ts + 1} = K_c\frac{s + \dfrac{1}{T}}{s + \dfrac{1}{\alpha T}}, \qquad (0 < \alpha < 1)$$

where α and T are determined from the angle deficiency. K_c is determined from the requirement of the open-loop gain.

4. If static error constants are not specified, determine the location of the pole and zero of the lead compensator so that the lead compensator will contribute the necessary angle ϕ. If no other requirements are imposed on the system, try to make the value of α as large as possible. A larger value of α generally results in a larger value of K_v, which is desirable. (If a particular static error constant is specified, it is generally simpler to use the frequency-response approach.)

5. Determine the open-loop gain of the compensated system from the magnitude condition.

Once a compensator has been designed, check to see whether all performance specifications have been met. If the compensated system does not meet the performance specifications, then repeat the design procedure by adjusting the compensator pole and zero until all such specifications are met. If a large static error constant is required, cascade a lag network or alter the lead compensator to a lag–lead compensator.

Note that if the selected dominant closed-loop poles are not really dominant, it will be necessary to modify the location of the pair of such selected dominant closed-loop

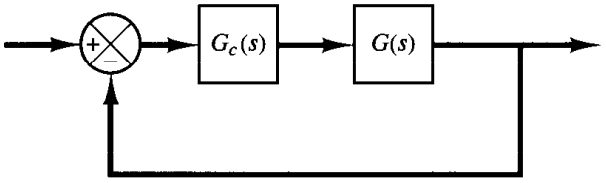

Figure 7–6
Control system.

poles. (The closed-loop poles other than dominant ones modify the response obtained from the dominant closed-loop poles alone. The amount of modification depends on the location of these remaining closed-loop poles.) Also, the closed-loop zeros affect the response if they are located near the origin.

EXAMPLE 7–1 Consider the system shown in Figure 7–7(a). The feedforward transfer function is

$$G(s) = \frac{4}{s(s + 2)}$$

The root-locus plot for this system is shown in Figure 7–7(b). The closed-loop transfer function becomes

$$\frac{C(s)}{R(s)} = \frac{4}{s^2 + 2s + 4}$$

$$= \frac{4}{(s + 1 + j\sqrt{3})(s + 1 - j\sqrt{3})}$$

The closed-loop poles are located at

$$s = -1 \pm j\sqrt{3}$$

The damping ratio of the closed-loop poles is 0.5. The undamped natural frequency of the closed-loop poles is 2 rad/sec. The static velocity error constant is 2 $\sec^{-1}$.

It is desired to modify the closed-loop poles so that an undamped natural frequency $\omega_n = 4$ rad/sec is obtained, without changing the value of the damping ratio, $\zeta = 0.5$.

Recall that in the complex plane the damping ratio ζ of a pair of complex conjugate poles can be expressed in terms of the angle θ, which is measured from the $j\omega$ axis, as shown in Figure 7–8(a), with

$$\zeta = \sin \theta$$

In other words, lines of constant damping ratio ζ are radial lines passing through the origin as shown in Figure 7–8(b). For example, a damping ratio of 0.5 requires that the complex poles lie on the lines drawn through the origin making angles of $\pm 60°$ with the negative real axis. (If the real part of a pair of complex poles is positive, which means that the system is unstable, the cor-

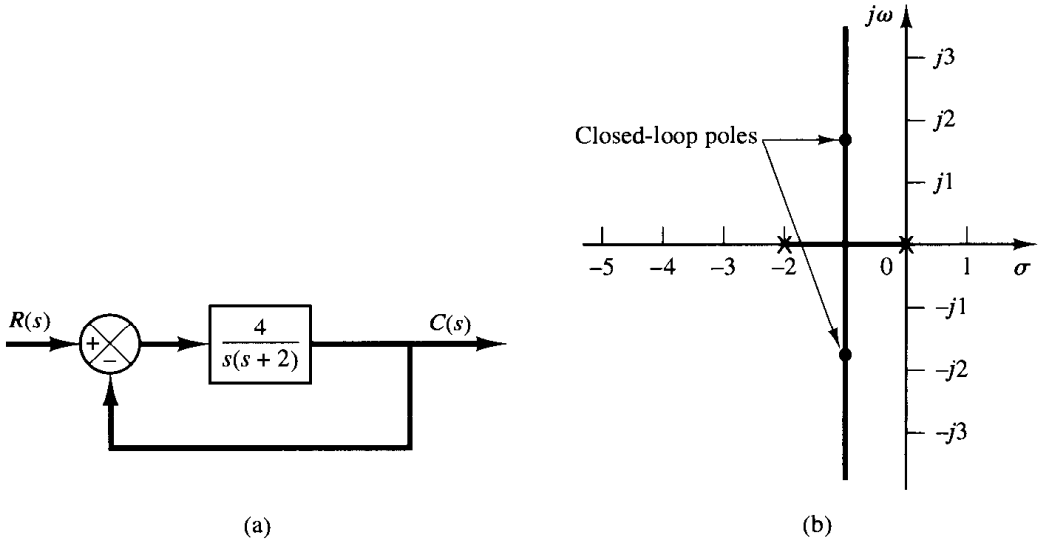

Figure 7–7
(a) Control system;
(b) root-locus plot.

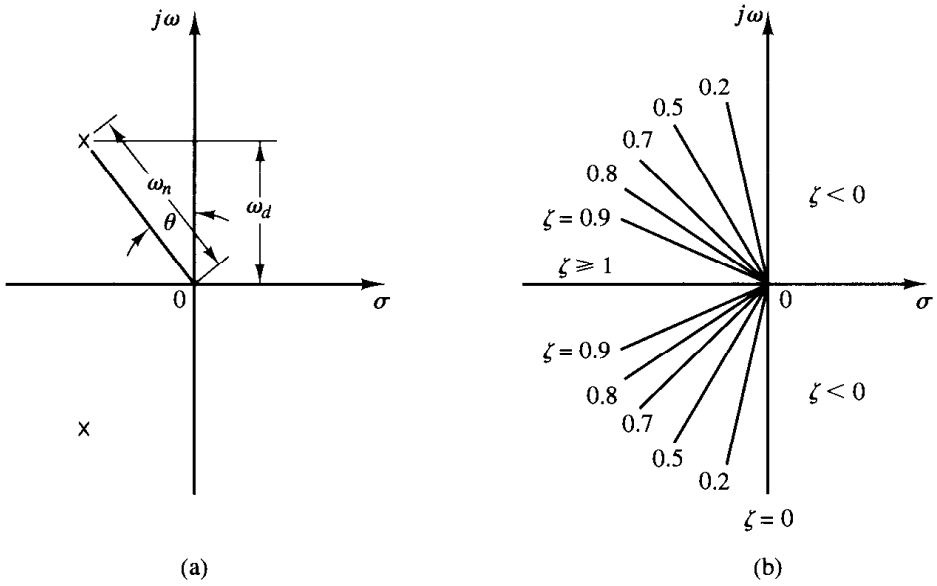

(a) (b)

Figure 7–8
(a) Complex poles; (b) lines of constant damping ratio ζ.

responding ζ is negative.) The damping ratio determines the angular location of the poles, while the distance of the pole from the origin is determined by the undamped natural frequency ω_n.

In the present example, the desired locations of the closed-loop poles are

$$s = -2 \pm j2\sqrt{3}$$

In some cases, after the root loci of the original system have been obtained, the dominant closed-loop poles may be moved to the desired location by simple gain adjustment. This is, however, not the case for the present system. Therefore, we shall insert a lead compensator in the feedforward path.

A general procedure for determining the lead compensator is as follows: First, find the sum of the angles at the desired location of one of the dominant closed-loop poles with the open-loop poles and zeros of the original system, and determine the necessary angle ϕ to be added so that the total sum of the angles is equal to $\pm 180°(2k + 1)$. The lead compensator must contribute this angle ϕ. (If the angle ϕ is quite large, then two or more lead networks may be needed rather than a single one.)

If the original system has the open-loop transfer function $G(s)$, then the compensated system will have the open-loop transfer function

$$G_c(s)G(s) = \left(K_c \frac{s + \dfrac{1}{T}}{s + \dfrac{1}{\alpha T}} \right) G(s)$$

where

$$G_c(s) = K_c \alpha \frac{Ts + 1}{\alpha Ts + 1} = K_c \frac{s + \dfrac{1}{T}}{s + \dfrac{1}{\alpha T}}, \qquad (0 < \alpha < 1)$$

Notice that there are many possible values for T and α that will yield the necessary angle contribution at the desired closed-loop poles.

The next step is to determine the locations of the zero and pole of the lead compensator. There are many possibilities for the choice of such locations. (See the comments at the end of this example problem.) In what follows, we shall introduce a procedure to obtain the largest possible value for α. (Note that a larger value of α will produce a larger value of K_v. In most cases, the larger the K_v is, the better the system performance.) First, draw a horizontal line passing through point P, the desired location for one of the dominant closed-loop poles. This is shown as line PA in Figure 7–9. Draw also a line connecting point P and the origin. Bisect the angle between the lines PA and PO, as shown in Figure 7–9. Draw two lines PC and PD that make angles $\pm\phi/2$ with the bisector PB. The intersections of PC and PD with the negative real axis give the necessary location for the pole and zero of the lead network. The compensator thus designed will make point P a point on the root locus of the compensated system. The open-loop gain is determined by use of the magnitude condition.

In the present system, the angle of $G(s)$ at the desired closed-loop pole is

$$\left/ \frac{4}{s(s+2)} \right|_{s=-2+j2\sqrt{3}} = -210^\circ$$

Thus, if we need to force the root locus to go through the desired closed-loop pole, the lead compensator must contribute $\phi = 30^\circ$ at this point. By following the foregoing design procedure, we determine the zero and pole of the lead compensator, as shown in Figure 7–10, to be

$$\text{Zero at } s = -2.9, \qquad \text{Pole at } s = -5.4$$

or

$$T = \frac{1}{2.9} = 0.345, \qquad \alpha T = \frac{1}{5.4} = 0.185$$

Thus $\alpha = 0.537$. The open-loop transfer function of the compensated system becomes

$$G_c(s)G(s) = K_c \frac{s+2.9}{s+5.4} \frac{4}{s(s+2)} = \frac{K(s+2.9)}{s(s+2)(s+5.4)}$$

where $K = 4K_c$. The root-locus plot for the compensated system is shown in Figure 7–10. The gain K is evaluated from the magnitude condition as follows: Referring to the root-locus plot for the compensated system shown in Figure 7–10, the gain K is evaluated from the magnitude condition as

$$\left| \frac{K(s+2.9)}{s(s+2)(s+5.4)} \right|_{s=-2+j2\sqrt{3}} = 1$$

or

$$K = 18.7$$

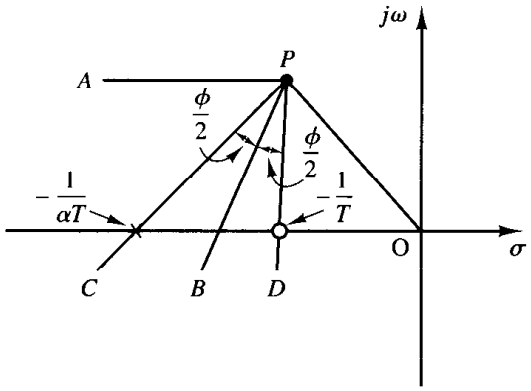

Figure 7–9
Determination of the pole and zero of a lead network.

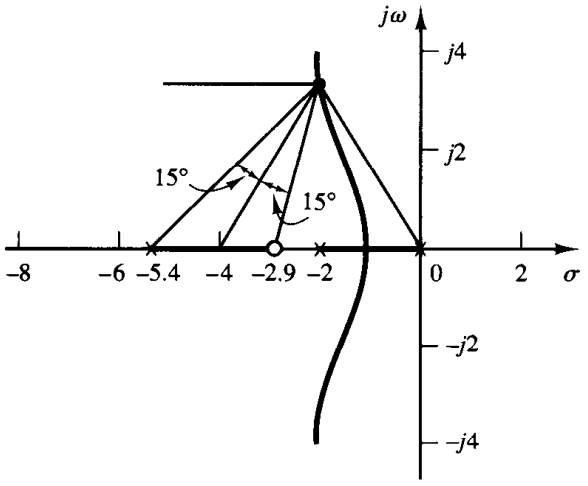

Figure 7–10
Root-locus plot of the compensated system.

It follows that

$$G_c(s)G(s) = \frac{18.7(s + 2.9)}{s(s + 2)(s + 5.4)}$$

The constant K_c of the lead compensator is

$$K_c = \frac{18.7}{4} = 4.68$$

Hence, $K_c\alpha = 2.51$. The lead compensator, therefore, has the transfer function

$$G_s(s) = 2.51\,\frac{0.345s + 1}{0.185s + 1} = 4.68\,\frac{s + 2.9}{s + 5.4}$$

If the electronic circuit using operational amplifiers as shown in Figure 7–4 is used as the lead compensator just designed, then the parameter values of the lead compensator are determined from

$$\frac{E_o(s)}{E_i(s)} = \frac{R_2R_4}{R_1R_3}\,\frac{R_1C_1s + 1}{R_2C_2s + 1} = 2.51\,\frac{0.345s + 1}{0.185s + 1}$$

as shown in Figure 7–11, where we have arbitrarily chosen $C_1 = C_2 = 10\,\mu$F and $R_3 = 10$ kΩ.

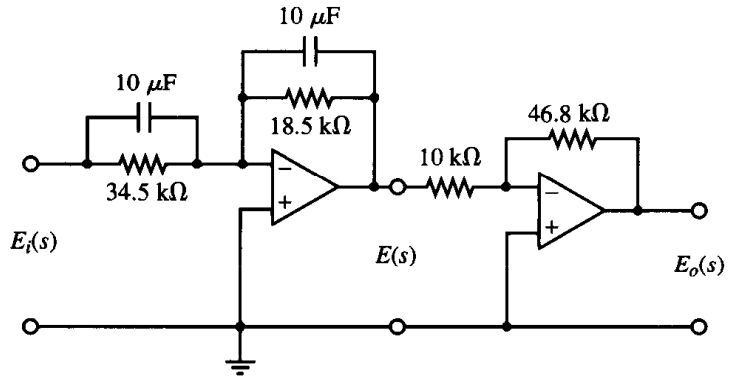

Figure 7–11
Lead compensator.

The static velocity error constant K_v is obtained from the expression

$$K_v = \lim_{s \to 0} sG_c(s)G(s)$$

$$= \lim_{s \to 0} \frac{s18.7(s + 2.9)}{s(s + 2)(s + 5.4)}$$

$$= 5.02 \text{ sec}^{-1}$$

Note that the third closed-loop pole of the designed system is found by dividing the characteristic equation by the known factors as follows:

$$s(s + 2)(s + 5.4) + 18.7(s + 2.9) = (s + 2 + j2\sqrt{3})(s + 2 - j2\sqrt{3})(s + 3.4)$$

The foregoing compensation method enables us to place the dominant closed-loop poles at the desired points in the complex plane. The third pole at $s = 3.4$ is close to the added zero at $s = -2.9$. Therefore, the effect of this pole on the transient response is relatively small. Since no restriction has been imposed on the nondominant pole and no specification has been given concerning the value of the static velocity error coefficient, we conclude that the present design is satisfactory.

Comments. We may place the zero of the compensator at $s = -2$ and pole at $s = -4$ so that the angle contribution of the lead compensator is 30°. (In this case the zero of the lead compensator will cancel a pole of the plant, resulting in the second-order system, rather than the third-order system as we designed.) It can be seen that the K_v value in this case is 4 sec^{-1}. Other combinations can be selected that will yield 30° phase lead. (For different combinations of a zero and pole of the compensator that contribute 30°, the value of α will be different and the value of K_v will also be different.) Although a certain change in the value of K_v can be made by altering the pole–zero location of the lead compensator, if a large increase in the value of K_v is desired, then we must alter the lead compensator to a lag–lead compensator. (See Section 7–5 for lag–lead compensation.)

Comparison of step responses of the compensated and uncompensated systems. In what follows we shall examine the unit-step responses of the compensated and uncompensated systems with MATLAB.

The closed-loop transfer function of the compensated system is

$$\frac{C(s)}{R(s)} = \frac{18.7(s + 2.9)}{s(s + 2)(s + 5.4) + 18.7(s + 2.9)}$$

$$= \frac{18.7s + 54.23}{s^3 + 7.4s^2 + 29.5s + 54.23}$$

Hence,

```
numc = [0   0    18.7   54.23]
denc = [1   7.4  29.5   54.23]
```

For the uncompensated system, the closed-loop transfer function is

$$\frac{C(s)}{R(s)} = \frac{4}{s^2 + 2s + 4}$$

Hence,

```
num = [0   0   4]
den = [1   2   4]
```

MATLAB Program 7–1 produces the unit-step response curves for the two systems. The resulting plot is shown in Figure 7–12.

MATLAB Program 7–1

```
% ---------- Unit-step response ----------

% ***** Unit-step responses of compensated and uncompensated
% systems *****

numc = [0   0   18.7   54.23];
denc = [1   7.4   29.5   54.23];
num = [0   0   4];
den = [1   2   4];
t = 0:0.05:5;
[c1,x1,t] = step(numc,denc,t);
[c2,x2,t] = step(num,den,t);
plot(t,c1,t,c1,'o',t,c2,t,c2,'x')
grid
title('Unit-Step Responses of Compensated and Uncompensated Systems')
xlabel('t Sec')
ylabel('Outputs c1 and c2')
text(0.6,1.32,'Compensated system')
text(1.3,0.68,'Uncompensated system')
```

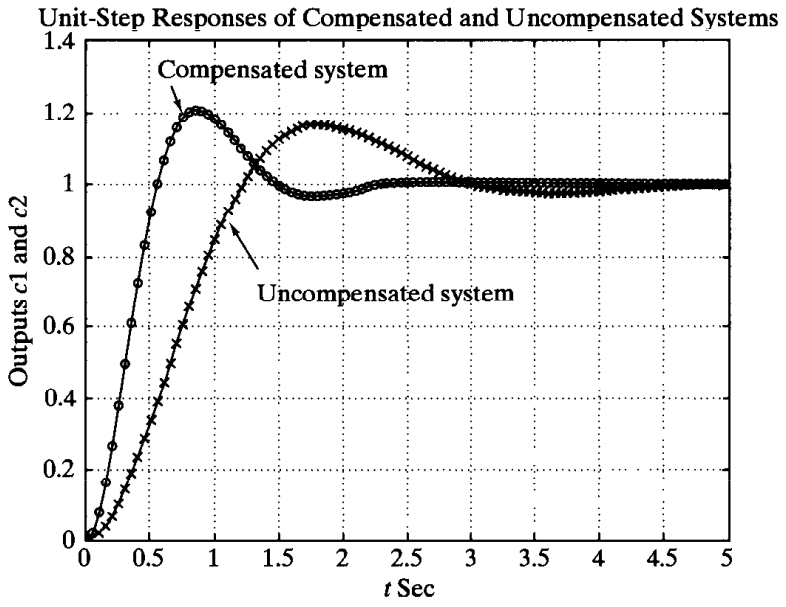

Figure 7–12
Unit-step responses of compensated and uncompensated systems.

7–4 LAG COMPENSATION

Electronic lag compensator using operational amplifiers. The configuration of the electronic lag compensator using operational amplifiers is the same as that for the lead compensator shown in Figure 7–4. If we choose $R_2C_2 > R_1C_1$ in the circuit shown in Figure 7–4, it becomes a lag compensator. Referring to Figure 7–4, the transfer function of the lag compensator is given by

$$\frac{E_o(s)}{E_i(s)} = \hat{K}_c\beta\frac{Ts + 1}{\beta Ts + 1} = \hat{K}_c\frac{s + \dfrac{1}{T}}{s + \dfrac{1}{\beta T}}$$

where

$$T = R_1C_1, \qquad \beta T = R_2C_2, \qquad \beta = \frac{R_2C_2}{R_1C_1} > 1, \qquad \hat{K}_c = \frac{R_4C_1}{R_3C_2}$$

Note that we use β instead of α in the above expressions. [In the lead compensator we used α to indicate the ratio $R_2C_2/(R_1C_1)$, which was less than 1, or $0 < \alpha < 1$.] In this chapter we always assume that $0 < \alpha < 1$ and $\beta > 1$.

Lag compensation techniques based on the root-locus approach. Consider the problem of finding a suitable compensation network for the case where the system exhibits satisfactory transient-response characteristics but unsatisfactory steady-state characteristics. Compensation in this case essentially consists of increasing the open-loop gain without appreciably changing the transient-response characteristics. This means that the root locus in the neighborhood of the dominant closed-loop poles should not be changed appreciably, but the open-loop gain should be increased as much as needed. This can be accomplished if a lag compensator is put in cascade with the given feedforward transfer function.

To avoid an appreciable change in the root loci, the angle contribution of the lag network should be limited to a small amount, say 5°. To assure this, we place the pole and zero of the lag network relatively close together and near the origin of the s plane. Then the closed-loop poles of the compensated system will be shifted only slightly from their original locations. Hence, the transient-response characteristics will be changed only slightly.

Consider a lag compensator $G_c(s)$, where

$$G_c(s) = \hat{K}_c\beta\frac{Ts + 1}{\beta Ts + 1} = \hat{K}_c\frac{s + \dfrac{1}{T}}{s + \dfrac{1}{\beta T}} \tag{7–2}$$

If we place the zero and pole of the lag compensator very close to each other, then at $s = s_1$, where s_1 is one of the dominant closed-loop poles, the magnitudes $s_1 + (1/T)$ and $s_1 + [1/(\beta T)]$ are almost equal, or

$$|G_c(s_1)| = \left| \hat{K}_c \frac{s_1 + \dfrac{1}{T}}{s_1 + \dfrac{1}{\beta T}} \right| \doteq \hat{K}_c$$

This implies that if gain $\hat{K}_c$ of the lag compensator is set equal to 1 then the transient-response characteristics will not be altered. (This means that the overall gain of the open-loop transfer function can be increased by a factor of β where $\beta > 1$.) If the pole and zero are placed very close to the origin, then the value of β can be made large. (A large value of β may be used, provided physical realization of the lag compensator is possible.) It is noted that the value of T must be large, but its exact value is not critical. However, it should not be too large in order to avoid difficulties in realizing the phase lag compensator by physical components.

An increase in the gain means an increase in the static error constants. If the open-loop transfer function of the uncompensated system is $G(s)$, then the static velocity error constant K_v of the uncompensated system is

$$K_v = \lim_{s \to 0} sG(s)$$

If the compensator is chosen as given by Equation (7–2), then for the compensated system with the open-loop transfer function $G_c(s)G(s)$ the static velocity error constant $\hat{K}_v$ becomes

$$\begin{aligned} \hat{K}_v &= \lim_{s \to 0} sG_c(s)G(s) \\ &= \lim_{s \to 0} G_c(s)K_v \\ &= \hat{K}_c \beta K_v \end{aligned}$$

Thus if the compensator is given by Equation (7–2), then the static velocity error constant is increased by a factor of $\hat{K}_c\beta$, where $\hat{K}_c$ is approximately unity.

Design procedures for lag compensation by the root-locus method. The procedure for designing lag compensators for the system shown in Figure 7–13 by the root-locus method may be stated as follows (we assume that the uncompensated system meets the transient-response specifications by simple gain adjustment; if this is not the case, refer to Section 7–5):

1. Draw the root-locus plot for the uncompensated system whose open-loop transfer function is $G(s)$. Based on the transient-response specifications, locate the dominant closed-loop poles on the root locus.

2. Assume the transfer function of the lag compensator to be

$$G_c(s) = \hat{K}_c \beta \frac{Ts + 1}{\beta Ts + 1} = \hat{K}_c \frac{s + \dfrac{1}{T}}{s + \dfrac{1}{\beta T}}$$

Then the open-loop transfer function of the compensated system becomes $G_c(s)G(s)$.

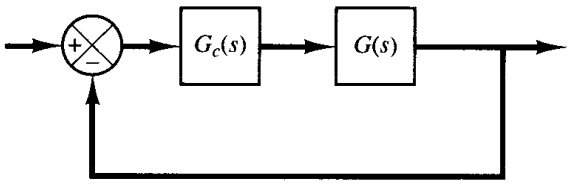

Figure 7–13
Control system.

3. Evaluate the particular static error constant specified in the problem.

4. Determine the amount of increase in the static error constant necessary to satisfy the specifications.

5. Determine the pole and zero of the lag compensator that produce the necessary increase in the particular static error constant without appreciably altering the original root loci. (Note that the ratio of the value of gain required in the specifications and the gain found in the uncompensated system is the required ratio between the distance of the zero from the origin and that of the pole from the origin.)

6. Draw a new root-locus plot for the compensated system. Locate the desired dominant closed-loop poles on the root locus. (If the angle contribution of the lag network is very small, that is, a few degrees, then the original and new root loci are almost identical. Otherwise, there will be a slight discrepancy between them. Then locate, on the new root locus, the desired dominant closed-loop poles based on the transient-response specifications.)

7. Adjust gain $\hat{K}_c$ of the compensator from the magnitude condition so that the dominant closed-loop poles lie at the desired location.

EXAMPLE 7–2 Consider the system shown in Figure 7–14(a). The feedforward transfer function is

$$G(s) = \frac{1.06}{s(s + 1)(s + 2)}$$

The root-locus plot for the system is shown in Figure 7–14(b). The closed-loop transfer function becomes

$$\frac{C(s)}{R(s)} = \frac{1.06}{s(s + 1)(s + 2) + 1.06}$$

$$= \frac{1.06}{(s + 0.3307 - j0.5864)(s + 0.3307 + j0.5864)(s + 2.3386)}$$

The dominant closed-loop poles are

$$s = -0.3307 \pm j0.5864$$

The damping ratio of the dominant closed-loop poles is $\zeta = 0.491$. The undamped natural frequency of the dominant closed-loop poles is 0.673 rad/sec. The static velocity error constant is 0.53 sec^{-1}.

It is desired to increase the static velocity error constant K_v to about 5 sec^{-1} without appreciably changing the location of the dominant closed-loop poles.

To meet this specification, let us insert a lag compensator as given by Equation (7–2) in cascade with the given feedforward transfer function. To increase the static velocity error constant

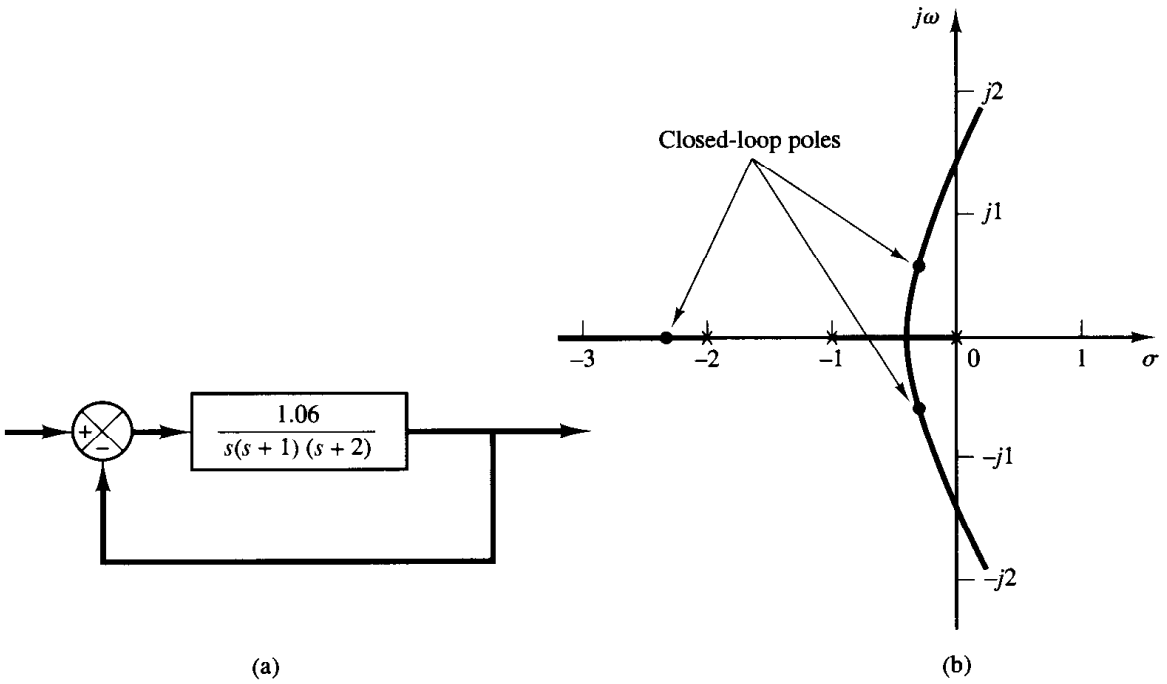

Figure 7–14
(a) Control system; (b) root-locus plot.

by a factor of about 10, let us choose $\beta = 10$ and place the zero and pole of the lag compensator at $s = -0.05$ and $s = -0.005$, respectively. The transfer function of the lag compensator becomes

$$G_c(s) = \hat{K}_c \frac{s + 0.05}{s + 0.005}$$

The angle contribution of this lag network near a dominant closed-loop pole is about 4°. Because this angle contribution is not very small, there is a small change in the new root locus near the desired dominant closed-loop poles.

The open-loop transfer function of the compensated system then becomes

$$G_c(s)G(s) = \hat{K}_c \frac{s + 0.05}{s + 0.005} \frac{1.06}{s(s + 1)(s + 2)}$$

$$= \frac{K(s + 0.05)}{s(s + 0.005)(s + 1)(s + 2)}$$

where

$$K = 1.06\hat{K}_c$$

The block diagram of the compensated system is shown in Figure 7–15(a). The root-locus plot for the compensated system near the dominant closed-loop poles is shown in Figure 7–15(b), together with the original root-locus plot. Figure 7–15(c) shows the root-locus plot of the compensated system near the origin. The MATLAB program to generate the root-locus plots shown in Figures 7–15(b) and (c) is given in MATLAB Program 7–2.

If the damping ratio of the new dominant closed-loop poles is kept the same, then the poles are obtained from the new root-locus plot as follows:

$$s_1 = -0.31 + j0.55, \qquad s_2 = -0.31 - j0.55$$

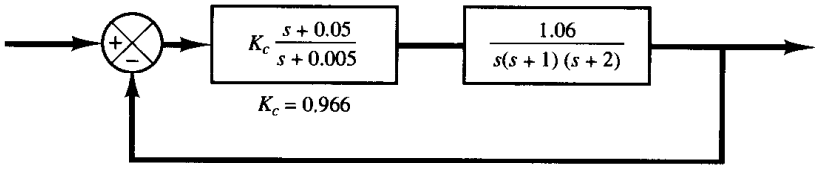

(a)

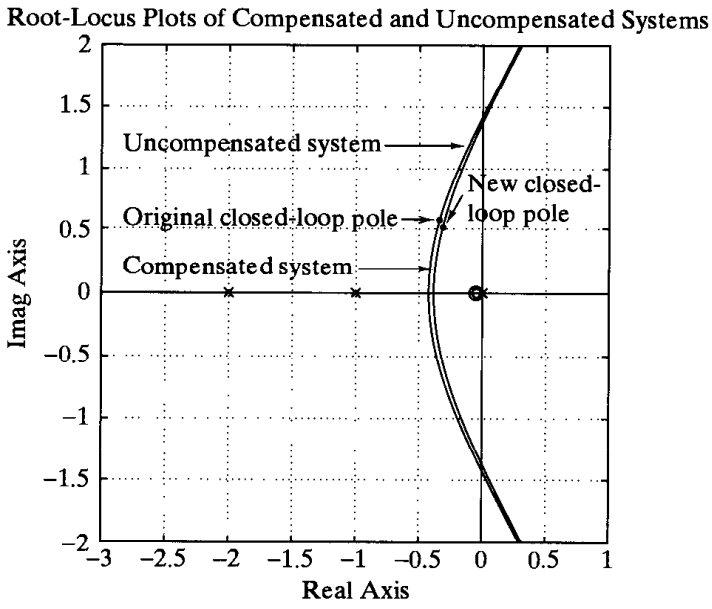

(b)

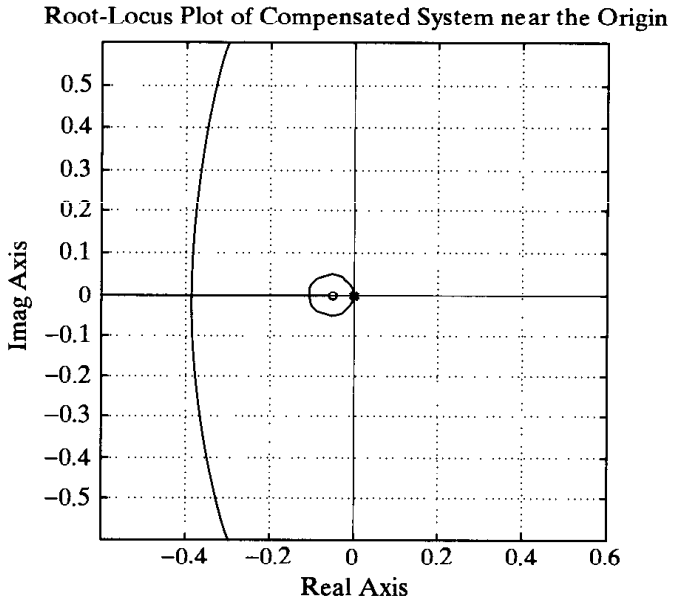

(c)

Figure 7–15
(a) Compensated system; (b) root-locus plots of the compensated system and the uncompensated system; (c) root-locus plot of compensated system near the origin.

MATLAB Program 7–2

```
% ---------- Root Locus Plot ---------

% ***** Root locus plots of the compensated system and
% uncompensated system *****

% ***** Enter the numerators and denominators of the
% compensated and uncompensated systems *****

numc = [0   0   0   1   0.05];
denc = [1   3.005   2.015   0.01   0];
num = [0   0   0   1.06];
den = [1   3   2   0];

% ***** Enter rlocus command. Plot the root loci of both
% systems *****

rlocus(numc,denc)
hold
Current plot held
rlocus(num,den)
v = [-3   1   -2   2]; axis(v); axis('square')
grid
text(-2,8,0.2,'Compensated system')
text(-2.8,1.2,'Uncompensated system')
text(-2.8,0.58,'Original closed-loop pole')
text(-0.1,0.85,'New closed-')
text(-0.1,0.62,'loop pole')
title('Root-Locus Plots of Compensated and Uncompensated Systems')

hold
Current plot released

% ***** Plot root loci of the compensated system near the origin *****

rlocus(numc,denc)
v = [-0.6   0.6   -0.6   0.6]; axis(v); axis('square')
grid
title('Root-Locus Plot of Compensated System near the Origin')
```

The open-loop gain K is

$$K = \left| \frac{s(s + 0.005)(s + 1)(s + 2)}{s + 0.05} \right|_{s = -0.31 + j0.55}$$

$$= 1.0235$$

Then the lag compensator gain $\hat{K}_c$ is determined as

$$\hat{K}_c = \frac{K}{1.06} = \frac{1.0235}{1.06} = 0.9656$$

Thus the transfer function of the lag compensator designed is

$$G_c(s) = 0.9656\frac{s + 0.05}{s + 0.005} = 9.656\frac{20s + 1}{200s + 1}$$

Then the compensated system has the following open-loop transfer function:

$$G_1(s) = \frac{1.0235(s + 0.05)}{s(s + 0.005)(s + 1)(s + 2)}$$
$$= \frac{5.12(20s + 1)}{s(200s + 1)(s + 1)(0.5s + 1)}$$

The static velocity error constant K_v is

$$K_v = \lim_{s\to 0} sG_1(s) = 5.12\ \text{sec}^{-1}$$

In the compensated system, the static velocity error constant has increased to 5.12 sec^{-1}, or 5.12/0.53 = 9.66 times the original value. (The steady-state error with ramp inputs has decreased to about 10% of that of the original system.) We have essentially accomplished the design objective of increasing the static velocity error constant to about 5 sec^{-1}.

Note that, since the pole and zero of the lag compensator are placed close together and are located very near the origin, their effect on the shape of the original root loci has been small. Except for the presence of a small closed root locus near the origin, the root loci of the compensated and the uncompensated systems are very similar to each other. However, the value of the static velocity error constant of the compensated system is 9.66 times greater than that of the uncompensated system.

The two other closed-loop poles for the compensated system are found as follows:

$$s_3 = -2.326, \qquad s_4 = -0.0549$$

The addition of the lag compensator increases the order of the system from 3 to 4, adding one additional closed-loop pole close to the zero of the lag compensator. (The added closed-loop pole at $s = -0.0549$ is close to the zero at $s = -0.05$.) Such a pair of a zero and pole creates a long tail of small amplitude in the transient response, as we will see later in the unit-step response. Since the pole at $s = -2.326$ is very far from the $j\omega$ axis compared with the dominant closed-loop poles, the effect of this pole on the transient response is also small. Therefore, we may consider the closed-loop poles at $s = -0.31 \pm j0.55$ to be the dominant closed-loop poles.

The undamped natural frequency of the dominant closed-loop poles of the compensated system is 0.631 rad/sec. This value is about 6% less than the original value, 0.673 rad/sec. This implies that the transient response of the compensated system is slower than that of the original system. The response will take a longer time to settle down. The maximum overshoot in the step response will increase in the compensated system. If such adverse effects can be tolerated, the lag compensation as discussed here presents a satisfactory solution to the given design problem.

Next, we shall compare the unit-ramp responses of the compensated system against the uncompensated system and verify that the steady-state performance is much better in the compensated system than the uncompensated system.

To obtain the unit-ramp response with MATLAB, we use the step command for the system $C(s)/[sR(s)]$. Since $C(s)/[sR(s)]$ for the compensated system is

$$\frac{C(s)}{sR(s)} = \frac{1.0235(s + 0.05)}{s[s(s + 0.005)(s + 1)(s + 2) + 1.0235(s + 0.05)]}$$
$$= \frac{1.0235s + 0.0512}{s^5 + 3.005s^4 + 2.015s^3 + 1.0335s^2 + 0.0512s}$$

we have

```
numc = [0   0   0   0   1.0235   0.0512]
denc = [1   3.005   2.015   1.0335   0.0512   0]
```

Also, $C(s)/[sR(s)]$ for the uncompensated system is

$$\frac{C(s)}{sR(s)} = \frac{1.06}{s[s(s+1)(s+2)+1.06]}$$

$$= \frac{1.06}{s^4 + 3s^3 + 2s^2 + 1.06s}$$

Hence,

```
num = [0   0   0   0   1.06]
den = [1   3   2   1.06   0]
```

MATLAB Program 7–3 produces the plot of the unit-ramp response curves. Figure 7–16 shows the result. Clearly, the compensated system shows much smaller steady-state error (one-tenth of the original steady-state error) in following the unit-ramp input.

MATLAB Program 7–4 gives the unit-step response curves of the compensated and uncompensated systems. The unit-step response curves are shown in Figure 7–17. Notice that the

MATLAB Program 7–3

```
% ---------- Unit ramp response ----------

% ***** Unit-ramp responses of compensated system and
% uncompensated system *****

% ***** Unit-ramp response will be obtained as the unit-step
% response of C(s)/[sR(s)] *****

% ***** Enter the numerators and denominators of C1(s)/[sR(s)]
% and C2(s)/[sR(s)], where C1(s) and C2(s) are Laplace
% transforms of the outputs of the compensated and un-
% compensated systems, respectively. *****

numc = [0   0   0   0   1.0235   0.0512];
denc = [1   3.005   2.015   1.0335   0.0512   0];
num = [0   0   0   0   1.06];
den = [1   3   2   1.06   0];

% ***** Specify the time range (such as t = 0:0.1:50) and enter
% step command and plot command. *****

t = 0:0.1:50;
[c1,x1,t] = step(numc,denc,t);
[c2,x2,t] = step(num,den,t);
plot(t,c1,'-',t,c2,'.',t,t,'- -')
grid
text(2.2,27,'Compensated system');
text(26,21.3,'Uncompensated system')
title('Unit-Ramp Responses of Compensated and Uncompensated Systems')
xlabel('t Sec');
ylabel('Outputs c1 and c2')
```

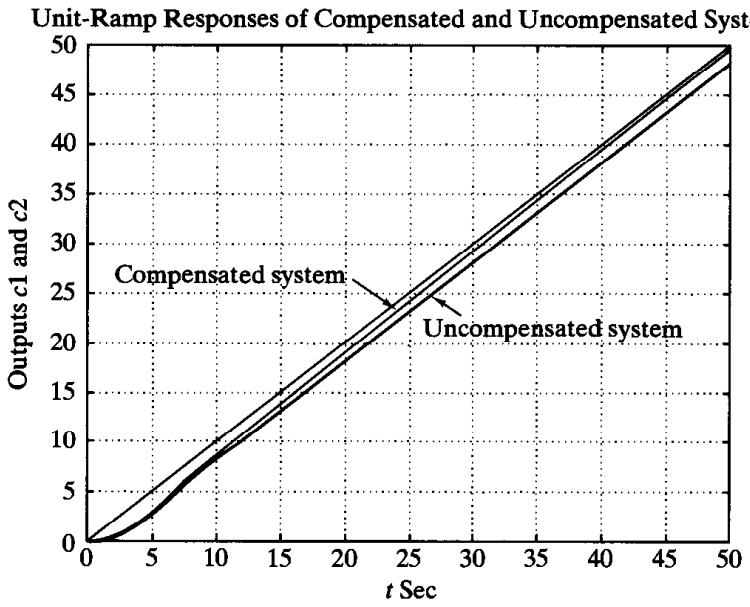

Figure 7–16
Unit-ramp responses of compensated and uncompensated systems.

MATLAB Program 7–4

```
% ---------- Unit-step response ----------

% ***** Unit-step responses of compensated system and
% uncompensated system *****

% ***** Enter the numerators and denominators of the
% compensated and uncompensated systems *****

numc = [0   0   0   1.0235   0.0512];
denc = [1   3.005   2.015   1.0335   0.0512];
num = [0   0   0   1.06];
den = [1   3   2   1.06];

% ***** Specify the time range (such as t = 0:0.1:40) and enter
% step command and plot command. *****

t = 0:0.1:40;
[c1,x1,t] = step(numc,denc,t);
[c2,x2,t] = step(num,den,t);
plot(t,c1,'-',t,c2,'.')
grid
text(13,1.12,'Compensated system')
text(13.6,0.88,'Uncompensated system')
title('Unit-Step Responses of Compensated and Uncompensated Systems')
xlabel('t Sec')
ylabel('Outputs c1 and c2')
```

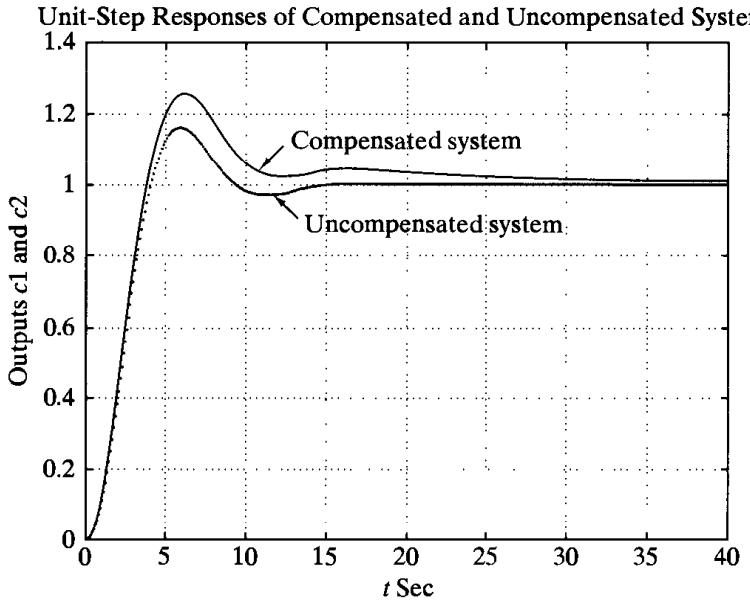

Figure 7–17
Unit-step responses of compensated and uncompensated systems.

lag-compensated system exhibits a larger maximum overshoot and slower response than the original uncompensated system. Notice that a pair of the pole at $s = -0.0549$ and zero at $s = -0.05$ generates a long tail of small amplitude in the transient response. If a larger maximum overshoot and a slower response are not desired, we need to use a lag–lead compensator as presented in Section 7–5.

7–5 LAG–LEAD COMPENSATION

Lead compensation basically speeds up the response and increases the stability of the system. Lag compensation improves the steady-state accuracy of the system, but reduces the speed of the response.

If improvements in both transient response and steady-state response are desired, then both a lead compensator and a lag compensator may be used simultaneously. Rather than introducing both a lead compensator and a lag compensator as separate elements, however, it is economical to use a single lag–lead compensator.

Lag-lead compensation combines the advantages of lag and lead compensations. Since the lag–lead compensator possesses two poles and two zeros, such a compensation increases the order of the system by 2, unless cancellation of pole(s) and zero(s) occurs in the compensated system.

Electronic lag–lead compensator using operational amplifiers. Figure 7–18 shows an electronic lag–lead compensator using operational amplifiers. The transfer function for this compensator may be obtained as follows: The complex impedance Z_1 is given by

$$\frac{1}{Z_1} = \frac{1}{R_1 + \dfrac{1}{C_1 s}} + \frac{1}{R_3}$$

or

$$Z_1 = \frac{(R_1C_1s + 1)R_3}{(R_1 + R_3)C_1s + 1}$$

Similarly, complex impedance Z_2 is given by

$$Z_2 = \frac{(R_2C_2s + 1)R_4}{(R_2 + R_4)C_2s + 1}$$

Hence, we have

$$\frac{E(s)}{E_i(s)} = -\frac{Z_2}{Z_1} = -\frac{R_4}{R_3}\frac{(R_1 + R_3)C_1s + 1}{R_1C_1s + 1} \cdot \frac{R_2C_2s + 1}{(R_2 + R_4)C_2s + 1}$$

The sign inverter has the transfer function

$$\frac{E_o(s)}{E(s)} = -\frac{R_6}{R_5}$$

Thus the transfer function of the compensator shown in Figure 7–18 is

$$\frac{E_o(s)}{E_i(s)} = \frac{E_o(s)}{E(s)}\frac{E(s)}{E_i(s)} = \frac{R_4R_6}{R_3R_5}\left[\frac{(R_1 + R_3)C_1s + 1}{R_1C_1s + 1}\right]\left[\frac{R_2C_2s + 1}{(R_2 + R_4)C_2s + 1}\right] \tag{7–3}$$

Let us define

$$T_1 = (R_1 + R_3)C_1, \qquad \frac{T_1}{\gamma} = R_1C_1, \qquad T_2 = R_2C_2, \qquad \beta T_2 = (R_2 + R_4)C_2$$

Then Equation (7–3) becomes

$$\frac{E_o(s)}{E_i(s)} = K_c\frac{\beta}{\gamma}\left(\frac{T_1s + 1}{\frac{T_1}{\gamma}s + 1}\right)\left(\frac{T_2s + 1}{\beta T_2s + 1}\right) = K_c\frac{\left(s + \frac{1}{T_1}\right)\left(s + \frac{1}{T_2}\right)}{\left(s + \frac{\gamma}{T_1}\right)\left(s + \frac{1}{\beta T_2}\right)} \tag{7–4}$$

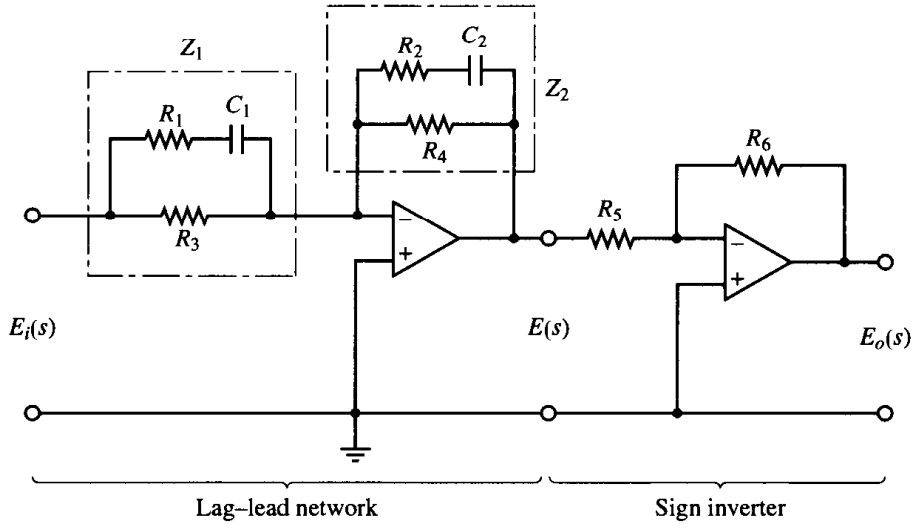

Figure 7–18
Lag-lead compensator.

where

$$\gamma = \frac{R_1 + R_3}{R_1} > 1, \qquad \beta = \frac{R_2 + R_4}{R_2} > 1, \qquad K_c = \frac{R_2R_4R_6}{R_1R_3R_5}\frac{R_1 + R_3}{R_2 + R_4}$$

Note that β is often chosen to be equal to γ.

Lag–lead compensation techniques based on the root-locus approach. Consider the system shown in Figure 7–19. Assume that we use the lag–lead compensator:

$$G_c(s) = K_c\frac{\beta}{\gamma}\frac{(T_1s + 1)(T_2s + 1)}{\left(\frac{T_1}{\gamma}s + 1\right)(\beta T_2 s + 1)} = K_c\left(\frac{s + \frac{1}{T_1}}{s + \frac{\gamma}{T_1}}\right)\left(\frac{s + \frac{1}{T_2}}{s + \frac{1}{\beta T_2}}\right) \tag{7–5}$$

where $\beta > 1$ and $\gamma > 1$. (Consider K_c to belong to the lead portion of the lag–lead compensator.)

In designing lag–lead compensators, we consider two cases where $\gamma \neq \beta$ and $\gamma = \beta$.

Case 1. $\gamma \neq \beta$. In this case, the design process is a combination of the design of the lead compensator and that of the lag compensator. The design procedure for the lag–lead compensator follows:

1. From the given performance specifications, determine the desired location for the dominant closed-loop poles.

2. Using the uncompensated open-loop transfer function $G(s)$, determine the angle deficiency ϕ if the dominant closed-loop poles are to be at the desired location. The phase-lead portion of the lag–lead compensator must contribute this angle ϕ.

3. Assuming that we later choose T_2 sufficiently large so that the magnitude of the lag portion

$$\left|\frac{s_1 + \frac{1}{T_2}}{s_1 + \frac{1}{\beta T_2}}\right|$$

is approximately unity, where $s = s_1$ is one of the dominant closed-loop poles, choose the values of T_1 and γ from the requirement that

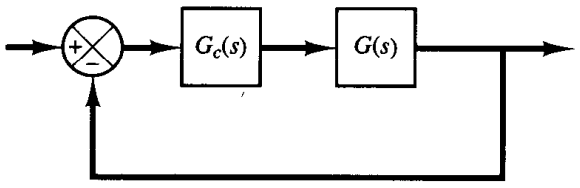

Figure 7–19
Control system.

$$\angle \frac{s_1 + \frac{1}{T_1}}{s_1 + \frac{\gamma}{T_1}} = \phi$$

The choice of T_1 and γ is not unique. (Infinitely many sets of T_1 and γ are possible.) Then determine the value of K_c from the magnitude condition:

$$\left| K_c \frac{s_1 + \frac{1}{T_1}}{s_1 + \frac{\gamma}{T_1}} G(s_1) \right| = 1$$

4. If the static velocity error constant K_v is specified, determine the value of β to satisfy the requirement for K_v. The static velocity error constant K_v is given by

$$\begin{aligned} K_v &= \lim_{s \to 0} sG_c(s)G(s) \\ &= \lim_{s \to 0} sK_c \left(\frac{s + \frac{1}{T_1}}{s + \frac{\gamma}{T_1}} \right) \left(\frac{s + \frac{1}{T_2}}{s + \frac{1}{\beta T_2}} \right) G(s) \\ &= \lim_{s \to 0} sK_c \frac{\beta}{\gamma} G(s) \end{aligned}$$

where K_c and γ are aleady determined in step 3. Hence, given the value of K_v, the value of β can be determined from this last equation. Then, using the value of β thus determined, choose the value of T_2 such that

$$\left| \frac{s_1 + \frac{1}{T_2}}{s_1 + \frac{1}{\beta T_2}} \right| \doteqdot 1$$

$$-5° < \angle \frac{s_1 + \frac{1}{T_2}}{s_1 + \frac{1}{\beta T_2}} < 0°$$

(The preceding design procedure is illustrated in Example 7–3.)

Case 2. $\gamma = \beta$. If $\gamma = \beta$ is required in Equation (7–5), then the preceeding design procedure for the lag–lead compensator may be modified as follows:

1. From the given performance specifications, determine the desired location for the dominant closed-loop poles.

2. The lag–lead compensator given by Equation (7–5) is modified to

$$G_c(s) = K_c \frac{(T_1 s + 1)(T_2 s + 1)}{\left(\frac{T_1}{\beta} s + 1\right)(\beta T_2 s + 1)} = K_c \frac{\left(s + \frac{1}{T_1}\right)\left(s + \frac{1}{T_2}\right)}{\left(s + \frac{\beta}{T_1}\right)\left(s + \frac{1}{\beta T_2}\right)} \tag{7–6}$$

where $\beta > 1$. The open-loop transfer function of the compensated system is $G_c(s)G(s)$. If the static velocity error constant K_v is specified, determine the value of constant K_c from the following equation:

$$K_v = \lim_{s \to 0} sG_c(s)G(s)$$
$$= \lim_{s \to 0} sK_cG(s)$$

3. To have the dominant closed-loop poles at the desired location, calculate the angle contribution ϕ needed from the phase lead portion of the lag–lead compensator.

4. For the lag–lead compensator, we later choose T_2 sufficiently large so that

$$\left| \frac{s_1 + \frac{1}{T_2}}{s_1 + \frac{1}{\beta T_2}} \right|$$

is approximately unity, where $s = s_1$ is one of the dominant closed-loop poles. Determine the values of T_1 and β from the magnitude and angle conditions:

$$\left| K_c \left(\frac{s_1 + \frac{1}{T_1}}{s_1 + \frac{\beta}{T_1}} \right) G(s_1) \right| = 1$$

$$\angle \frac{s_1 + \frac{1}{T_1}}{s_1 + \frac{\beta}{T_1}} = \phi$$

5. Using the value of β just determined, choose T_2 so that

$$\left| \frac{s_1 + \frac{1}{T_2}}{s_1 + \frac{1}{\beta T_2}} \right| \doteq 1$$

$$-5° < \angle \frac{s_1 + \frac{1}{T_2}}{S_1 + \frac{1}{\beta T_2}} < 0°$$

The value of βT_2, the largest time constant of the lag–lead compensator, should not be too large to be physically realized. (An example of the design of the lag–lead compensator when $\gamma = \beta$ is given in Example 7–4).

EXAMPLE 7–3 Consider the control system shown in Figure 7–20. The feedforward transfer function is

$$G(s) = \frac{4}{s(s + 0.5)}$$

This system has closed-loop poles at

$$s = -0.2500 \pm j1.9843$$

The damping ratio is 0.125, the undamped natural frequency is 2 rad/sec, and the static velocity error constant is 8 $\sec^{-1}$.

It is desired to make the damping ratio of the dominant closed-loop poles equal to 0.5 and to increase the undamped natural frequency to 5 rad/sec and the static velocity error constant to 80 $\sec^{-1}$. Design an appropriate compensator to meet all the performance specifications.

Let us assume that we use a lag–lead compensator having the transfer function

$$G_c(s) = K_c\left(\frac{s + \frac{1}{T_1}}{s + \frac{\gamma}{T_1}}\right)\left(\frac{s + \frac{1}{T_2}}{s + \frac{1}{\beta T_2}}\right) \qquad (\gamma > 1, \beta > 1)$$

where γ is not equal to β. Then the compensated system will have the transfer function

$$G_c(s)G(s) = K_c\left(\frac{s + \frac{1}{T_1}}{s + \frac{\gamma}{T_1}}\right)\left(\frac{s + \frac{1}{T_2}}{s + \frac{1}{\beta T_2}}\right)G(s)$$

From the performance specifications, the dominant closed-loop poles must be at

$$s = -2.50 \pm j4.33$$

Since

$$\left/\frac{4}{s(s + 0.5)}\right|_{s=-2.50+j4.33} = -235°$$

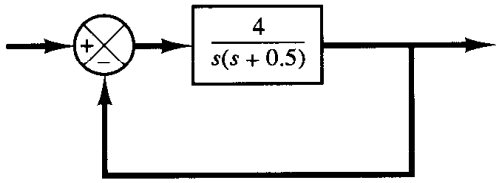

Figure 7–20
Control system.

the phase lead portion of the lag–lead compensator must contribute 55° so that the root locus passes through the desired location of the dominant closed-loop poles.

To design the phase lead portion of the compensator, we first determine the location of the zero and pole that will give 55° contribution. There are many possible choices, but we shall here choose the zero at $s = -0.5$ so that this zero will cancel the pole at $s = -0.5$ of the plant. Once the zero is chosen, the pole can be located such that the angle contribution is 55°. By simple calculation or graphical analysis, the pole must be located at $s = -5.021$. Thus, the phase lead portion of the lag–lead compensator becomes

$$K_c \frac{s + \dfrac{1}{T_1}}{s + \dfrac{\gamma}{T_1}} = K_c \frac{s + 0.5}{s + 5.021}$$

Thus

$$T_1 = 2, \qquad \gamma = \frac{5.021}{0.5} = 10.04$$

Next we determine the value of K_c from the magnitude condition:

$$\left| K_c \frac{s + 0.5}{s + 5.021} \frac{4}{s(s + 0.5)} \right|_{s=-2.5+j4.33} = 1$$

Hence,

$$K_c = \left| \frac{(s + 5.021)s}{4} \right|_{s=-2.5+j4.33} = 6.26$$

The phase lag portion of the compensator can be designed as follows: First the value of β is determined to satisfy the requirement on the static velocity error constant:

$$K_v = \lim_{s \to 0} sG_c(s)G(s) = \lim_{s \to 0} sK_c \frac{\beta}{\gamma} G(s)$$

$$= \lim_{s \to 0} s(6.26) \frac{\beta}{10.04} \frac{4}{s(s + 0.5)} = 4.988\beta = 80$$

Hence, β is determined as

$$\beta = 16.04$$

Finally, we choose the value of T_2 large enough so that

$$\left| \frac{s + \dfrac{1}{T_2}}{s + \dfrac{1}{16.04T_2}} \right|_{s=-2.5+j4.33} \doteq 1$$

and

$$-5° < \angle \left| \frac{s + \dfrac{1}{T_2}}{s + \dfrac{1}{16.04T_2}} \right|_{s=-2.5+j4.33} < 0°$$

Since $T_2 \doteqdot 5$ (or any number greater than 5) satisfies the above two requirements, we may choose

$$T_2 = 5$$

Now the transfer function of the designed lag–lead compensator is given by

$$\begin{aligned} G_c(s) &= (6.26)\left(\frac{s + \frac{1}{2}}{s + \frac{10.04}{2}}\right)\left(\frac{s + \frac{1}{5}}{s + \frac{1}{16.04 \times 5}}\right) \\ &= 6.26\left(\frac{s + 0.5}{s + 5.02}\right)\left(\frac{s + 0.2}{s + 0.01247}\right) \\ &= \frac{10(2s + 1)(5s + 1)}{(0.1992s + 1)(80.19s + 1)} \end{aligned}$$

The compensated system will have the open-loop transfer function

$$G_c(s)G(s) = \frac{25.04(s + 0.2)}{s(s + 5.02)(s + 0.01247)}$$

Because of the cancellation of the $(s + 0.5)$ terms, the compensated system is a third-order system. (Mathematically, this cancellation is exact, but practically such cancellation will not be exact because some approximations are usually involved in deriving the mathematical model of the system and, as a result, the time constants are not precise.) The root-locus plot of the compensated system is shown in Figure 7–21(a). An enlarged view of the root-locus plot near the origin is shown in Figure 7–21(b). Because the angle contribution of the phase lag portion of the lag–lead compensator is quite small, there is only a small change in the location of the dominant closed-loop poles from the desired location, $s = -2.5 \pm j4.33$. In fact, the new closed-loop poles are located

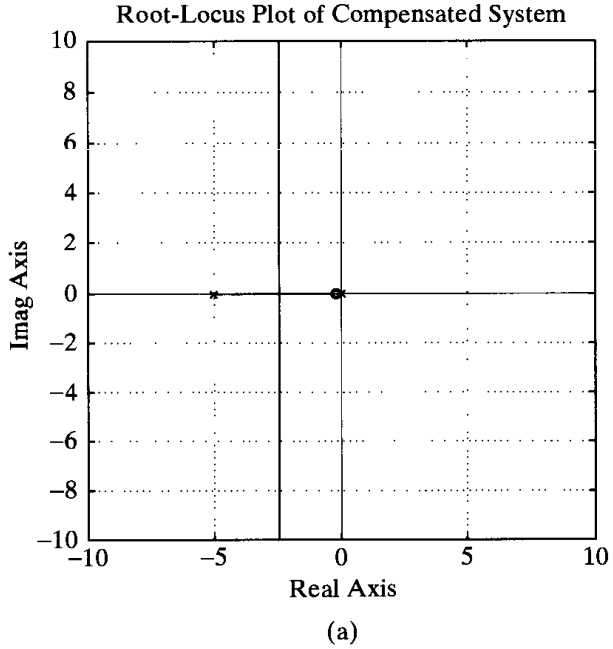

Figure 7–21
(a) Root-locus plot of the compensated system; (b) root-locus plot near the origin.

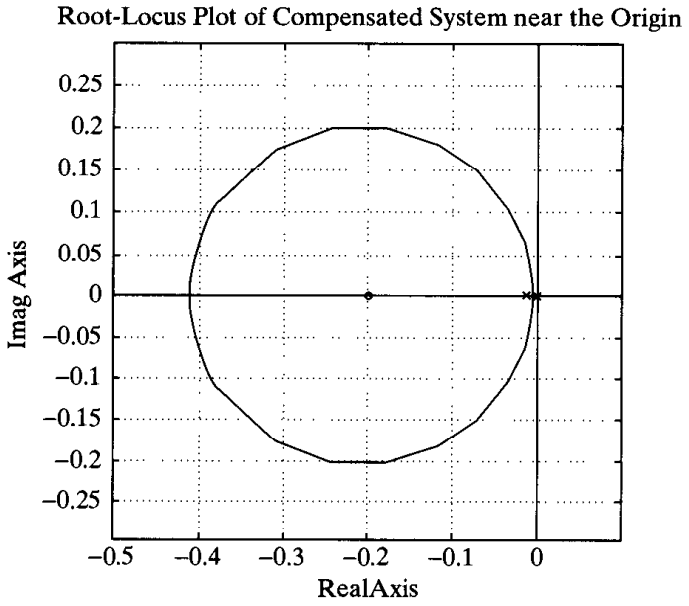

(b)

Figure 7–21
(Continued)

at $s = -2.4123 \pm j4.2756$. (The new damping ratio is $\zeta = 0.491$.) Therefore, the compensated system meets all the required performance specifications. The third closed-loop pole of the compensated system is located at $s = -0.2078$. Since this closed-loop pole is very close to the zero at $s = -0.2$, the effect of this pole on the response is small. (Note that, in general, if a pole and a zero lie close to each other on the negative real axis near the origin, then such a pole-zero combination will yield a long tail of small amplitude in the transient response.)

The unit-step response curves and unit-ramp response curves before and after compensation are shown in Figure 7–22.

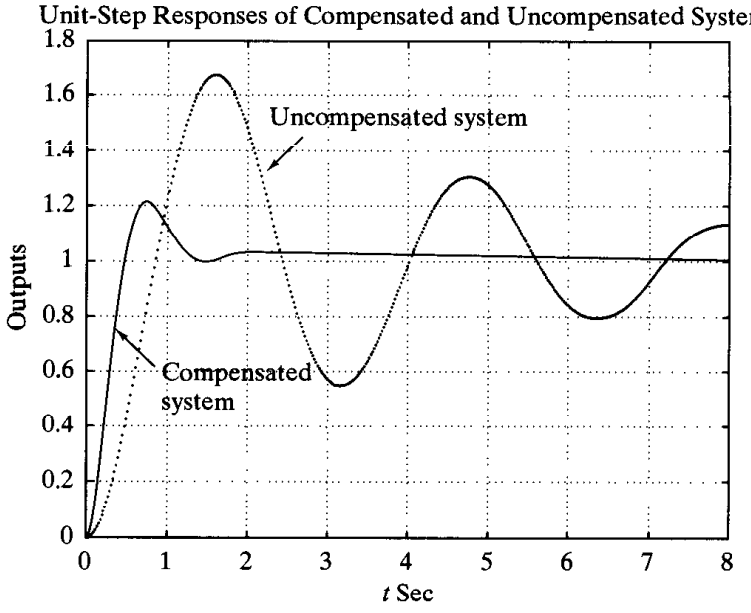

(a)

Figure 7–22
Transient response curves for the compensated system and the uncompensated system. (a) Unit-step response curves; (b) unit-ramp response curves.

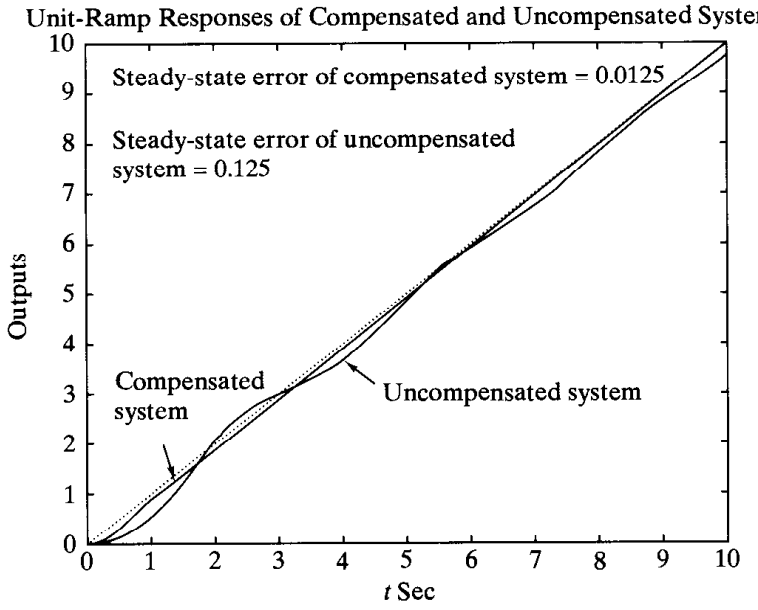

(b)

Figure 7–22
(Continued)

EXAMPLE 7–4 Consider the control system of Example 7–3. Suppose that we use a lag–lead compensator of the form given by Equation (7–6), or

$$G_c(s) = K_c \frac{\left(s + \frac{1}{T_1}\right)\left(s + \frac{1}{T_2}\right)}{\left(s + \frac{\beta}{T_1}\right)\left(s + \frac{1}{\beta T_2}\right)} \qquad (\beta > 1)$$

Assuming the specifications are the same as those given in Example 7–3, design a compensator $G_c(s)$.

The desired locations for the dominant closed-loop poles are at

$$s = -2.50 \pm j4.33$$

The open-loop transfer function of the compensated system is

$$G_c(s)G(s) = K_c \frac{\left(s + \frac{1}{T_1}\right)\left(s + \frac{1}{T_2}\right)}{\left(s + \frac{\beta}{T_1}\right)\left(s + \frac{1}{\beta T_2}\right)} \cdot \frac{4}{s(s + 0.5)}$$

Since the requirement on the static velocity error constant K_v is 80 $\sec^{-1}$, we have

$$K_v = \lim_{s \to 0} sG_c(s)G(s) = \lim_{s \to 0} K_c \frac{4}{0.5} = 8K_c = 80$$

Thus

$$K_c = 10$$

The time constant T_1 and the value of β are determined from

$$\left|\frac{s + \frac{1}{T_1}}{s + \frac{\beta}{T_1}}\right| \left|\frac{40}{s(s + 0.5)}\right|_{s=-2.5+j4.33} = \left|\frac{s + \frac{1}{T_1}}{s + \frac{\beta}{T_1}}\right| \frac{8}{4.77} = 1$$

$$\left/ \frac{s + \frac{1}{T_1}}{s + \frac{\beta}{T_1}} \right|_{s=-2.5+j4.33} = 55°$$

Referring to Figure 7–23, we can easily locate points A and B such that

$$\angle APB = 55°, \qquad \frac{\overline{PA}}{\overline{PB}} = \frac{4.77}{8}$$

(Use a graphical approach or a trigonometric approach.) The result is

$$\overline{AO} = 2.38, \qquad \overline{BO} = 8.34$$

or

$$T_1 = \frac{1}{2.38} = 0.420, \qquad \beta = 8.34T_1 = 3.503$$

The phase lead portion of the lag–lead network thus becomes

$$10\left(\frac{s + 2.38}{s + 8.34}\right)$$

For the phase lag portion, we may choose

$$T_2 = 10$$

Then

$$\frac{1}{\beta T_2} = \frac{1}{3.503 \times 10} = 0.0285$$

Thus, the lag–lead compensator becomes

$$G_c(s) = (10)\left(\frac{s + 2.38}{s + 8.34}\right)\left(\frac{s + 0.1}{s + 0.0285}\right)$$

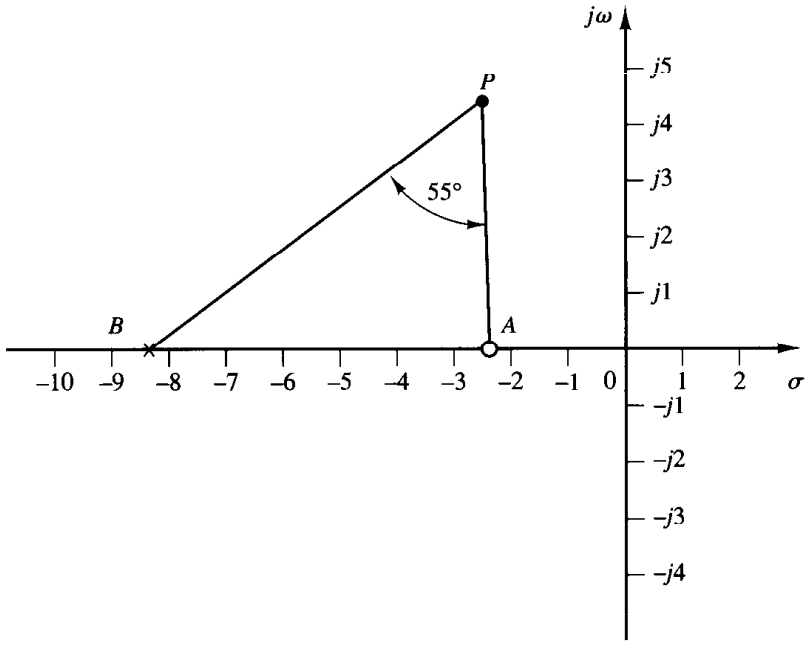

Figure 7–23
Determination of the desired pole-zero location.

The compensated system will have the open-loop transfer function

$$G_c(s)G(s) = \frac{40(s + 2.38)(s + 0.1)}{(s + 8.34)(s + 0.0285)s(s + 0.5)}$$

No cancellation occurs in this case, and the compensated system is of fourth order. Because the angle contribution of the phase lag portion of the lag–lead network is quite small, the dominant closed-loop poles are located very near the desired location. In fact, the dominant closed-loop poles are located at $s = -2.4539 \pm j4.3099$. The two other closed-loop poles are located at

$$s = -0.1003, \qquad s = -3.8604$$

Since the closed-loop pole at $s = -0.1003$ is very close to a zero at $s = -0.1$, they almost cancel each other. Thus, the effect of this closed-loop pole is very small. The remaining closed-loop pole

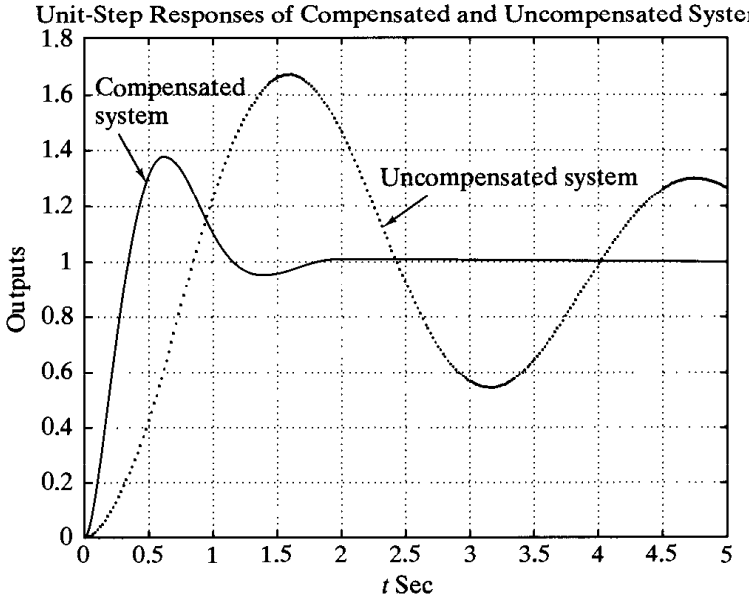

(a)

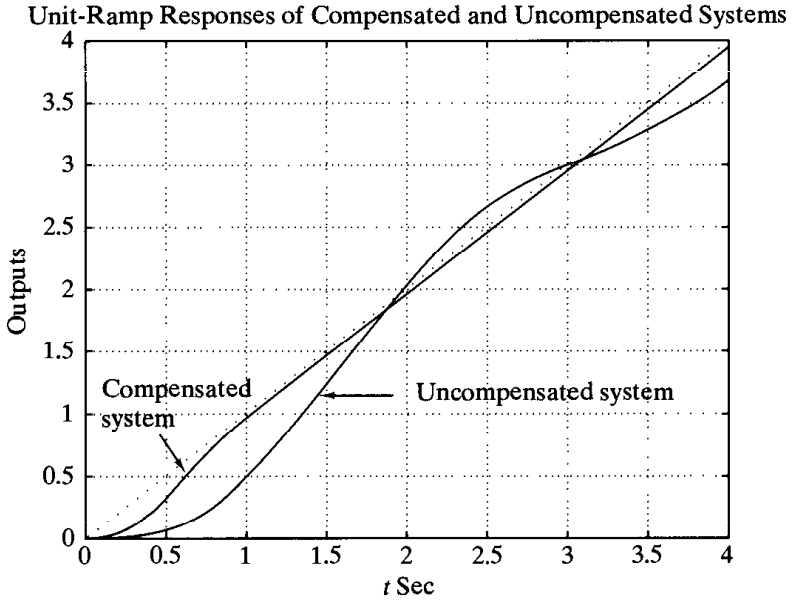

(a)

Figure 7–24
(a) Unit-step response curves for the compensated and uncompensated systems; (b) unit-ramp response curves for both systems.

($s = -3.8604$) does not quite cancel the zero at $s = -2.4$. The effect of this zero is to cause a larger overshoot in the step response than a similar system without such a zero. The unit-step response curves of the compensated and uncompensated systems are shown in Figure 7–24(a). The unit-ramp response curves for both systems are depicted in Figure 7–24(b).

EXAMPLE PROBLEMS AND SOLUTIONS

A-7-1. Obtain the transfer function of the mechanical system shown in Figure 7–25. Assume that the displacement x_i is the input and displacement x_o is the output of the system.

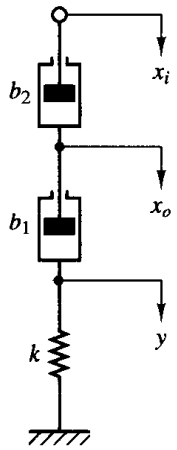

Figure 7–25
Mechanical system.

Solution. From the diagram we obtain the following equations of motion:

$$b_2(\dot{x}_i - \dot{x}_o) = b_1(\dot{x}_o - \dot{y})$$
$$b_1(\dot{x}_o - \dot{y}) = ky$$

Taking the Laplace transforms of these two equations, assuming zero initial conditions, and then eliminating $Y(s)$, we obtain

$$\frac{X_o(s)}{X_i(s)} = \frac{b_2}{b_1 + b_2} \frac{\frac{b_1}{k}s + 1}{\frac{b_2}{b_1 + b_2}\frac{b_1}{k}s + 1}$$

This is the transfer function between $X_o(s)$ and $X_i(s)$. By defining

$$\frac{b_1}{k} = T, \qquad \frac{b_2}{b_1 + b_2} = \alpha < 1$$

we obtain

$$\frac{X_o(s)}{X_i(s)} = \alpha \frac{Ts + 1}{\alpha Ts + 1} = \frac{s + \frac{1}{T}}{s + \frac{1}{\alpha T}}$$

This mechanical system is a mechanical lead network.

A-7-2. Obtain the transfer function of the mechanical system shown in Figure 7–26. Assume that the displacement x_i is the input and displacement x_o is the output.

Solution. The equations of motion for this system are

$$b_2(\dot{x}_i - \dot{x}_o) + k_2(x_i - x_o) = b_1(\dot{x}_o - \dot{y})$$
$$b_1(\dot{x}_o - \dot{y}) = ky$$

By taking the Laplace transforms of these two equations, assuming zero initial conditions, we obtain

$$b_2[sX_i(s) - sX_o(s)] + k_2[X_i(s) - X_o(s)] = b_1[sX_o(s) - sY(s)]$$
$$b_1[sX_o(s) - sY(s)] = k_1Y(s)$$

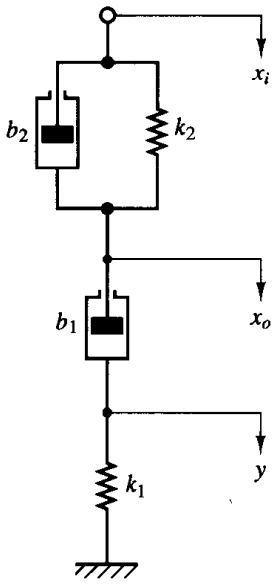

Figure 7–26
Mechanical system.

If we eliminate $Y(s)$ from the last two equations, the transfer function $X_o(s)/X_i(s)$ can be obtained as

$$\frac{X_o(s)}{X_i(s)} = \frac{\left(\frac{b_1}{k_1}s + 1\right)\left(\frac{b_2}{k_2}s + 1\right)}{\left(\frac{b_1}{k_1}s + 1\right)\left(\frac{b_2}{k_2}s + 1\right) + \frac{b_1}{k_2}s}$$

Define

$$T_1 = \frac{b_1}{k_1}, \qquad T_2 = \frac{b_2}{k_2}, \qquad \frac{b_1}{k_1} + \frac{b_2}{k_2} + \frac{b_1}{k_2} = \frac{T_1}{\beta} + \beta T_2 \qquad (\beta > 1)$$

Then $X_o(s)/X_i(s)$ can be simplified as

$$\frac{X_o(s)}{X_i(s)} = \frac{(T_1 s + 1)(T_2 s + 1)}{\left(\frac{T_1}{\beta}s + 1\right)(\beta T_2 s + 1)} = \frac{\left(s + \frac{1}{T_1}\right)\left(s + \frac{1}{T_2}\right)}{\left(s + \frac{\beta}{T_1}\right)\left(s + \frac{1}{\beta T_2}\right)}$$

From this transfer function we see that this mechanical system is a mechanical lag–lead network.

A-7-3. Consider the electrical network shown in Figure 7–27. Derive the transfer function of the network. (As usual in the derivation of the transfer function of any four-terminal network, we

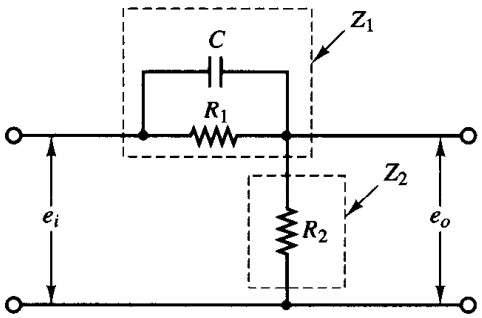

Figure 7–27
Electrical network.

assume that the source impedance that the network sees is zero and that the output load impedance is infinite.)

Solution. Using the symbols defined in Figure 7–27, we find that the complex impedances Z_1 and Z_2 are

$$Z_1 = \frac{R_1}{R_1Cs + 1}, \qquad Z_2 = R_2$$

The transfer function between the output $E_o(s)$ and the input $E_i(s)$ is

$$\frac{E_o(s)}{E_i(s)} = \frac{Z_2}{Z_1 + Z_2} = \frac{R_2}{R_1 + R_2} \frac{R_1Cs + 1}{\frac{R_1R_2}{R_1 + R_2}Cs + 1}$$

Define

$$R_1C = T, \qquad \frac{R_2}{R_1 + R_2} = \alpha < 1$$

Then the transfer function becomes

$$\frac{E_o(s)}{E_i(s)} = \alpha \frac{Ts + 1}{\alpha Ts + 1} = \frac{s + \frac{1}{T}}{s + \frac{1}{\alpha T}}$$

Since α is less than 1, this network is a lead network.

A-7-4. Obtain the transfer function of the network shown in Figure 7–28.

Solution. The complex impedances Z_1 and Z_2 are

$$Z_1 = \frac{R_1}{R_1C_1s + 1}, \qquad Z_2 = R_2 + \frac{1}{C_2s}$$

The transfer function between $E_o(s)$ and $E_i(s)$ is

$$\frac{E_o(s)}{E_i(s)} = \frac{Z_2}{Z_1 + Z_2} = \frac{(R_1C_1s + 1)(R_2C_2s + 1)}{(R_1C_1s + 1)(R_2C_2s + 1) + R_1C_2s}$$

The denominator of this transfer function can be factored into two real terms. Let us define

$$R_1C_1 = T_1, \qquad R_2C_2 = T_2, \qquad R_1C_1 + R_2C_2 + R_1C_2 = \frac{T_1}{\beta} + \beta T_2 \qquad (\beta > 1)$$

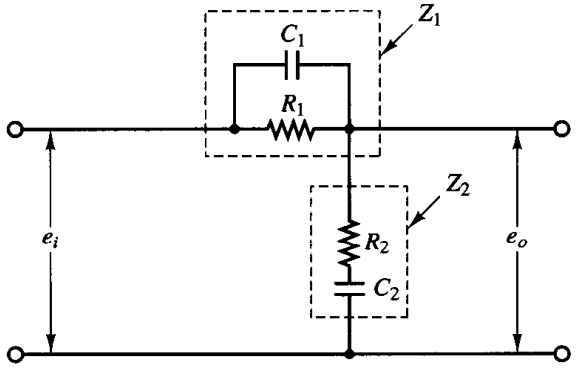

Figure 7–28
Electrical network.

Then $E_o(s)/E_i(s)$ can be simplified to

$$\frac{E_o(s)}{E_i(s)} = \frac{(T_1 s + 1)(T_2 s + 1)}{\left(\frac{T_1}{\beta} s + 1\right)(\beta T_2 s + 1)} = \frac{\left(s + \frac{1}{T_1}\right)\left(s + \frac{1}{T_2}\right)}{\left(s + \frac{\beta}{T_1}\right)\left(s + \frac{1}{\beta T_2}\right)}$$

This is a lag–lead network.

A-7-5. A control system with

$$G(s) = \frac{K}{s^2(s + 1)}, \qquad H(s) = 1$$

is unstable for all positive values of gain K.

Plot the root loci of the system. By using this plot, show that this system can be stabilized by adding a zero on the negative real axis or by modifying $G(s)$ to $G_1(s)$, where

$$G_1(s) = \frac{K(s + \alpha)}{s^2(s + 1)} \qquad (0 \leq \alpha < 1)$$

Solution. A root-locus plot for the system with

$$G(s) = \frac{K}{s^2(s + 1)}, \qquad H(s) = 1$$

is shown in Figure 7–29(a). Since two branches lie in the right half-plane, the system is unstable for any value of $K > 0$.

Addition of a zero to the transfer function $G(s)$ bends the right half-plane branches to the left and brings all root-locus branches to the left half-plane, as shown in the root-locus plot in Figure 7–29(b). Thus, the system with

$$G_1 = \frac{K(s + a)}{s^2(s + 1)}, \qquad H(s) = 1 \qquad (0 \leq a < 1)$$

is stable for all $K > 0$.

A-7-6. Consider a system with an unstable plant as shown in Figure 7–30a. Using the root-locus approach, design a proportional-plus-derivative controller (that is, determine the values of K_p and T_d) such that the damping ratio ζ of the closed-loop system is 0.7 and the undamped natural frequency ω_n is 0.5 rad/sec.

Solntion. Note that the open-loop transfer function involves two poles at $s = 1.085$ and $s = -1.085$ and one zero at $s = -1/T_d$, which is unknown at this point.

Since the desired closed-loop poles must have $\omega_n = 0.5$ rad/sec and $\zeta = 0.7$, they must be located at

$$s = 0.5 \angle 180° \pm 45.573°$$

($\zeta = 0.7$ corresponds to a line having an angle of 45.573° with the negative real axis.) Hence, the desired closed-loop poles are at

$$s = -0.35 \pm j0.357$$

The open-loop poles and the desired closed-loop pole in the upper half-plane are located in the diagram shown in Figure 7–30b. The angle deficiency at point $s = -0.35 + j0.357$ is

$$-166.026° - 25.913° + 180° = -11.938°$$

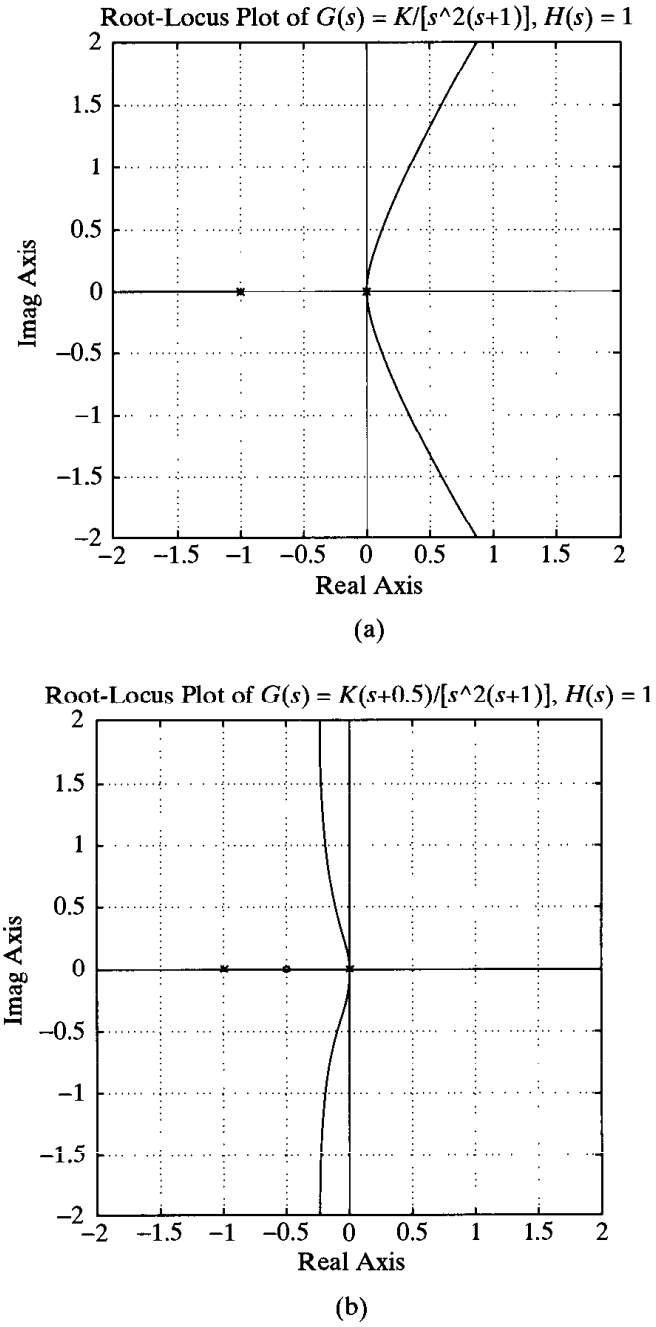

Figure 7–29
(a) Root-locus plot of the system with $G(s) = K/[s^2(s + 1)]$ and $H(s) = 1$; (b) root-locus plot of the system with $G_1(s) = K(s + a)/[s^2(s + 1)]$ and $H(s) = 1$, where $a = 0.5$.

This means that the zero at $s = -1/T_d$ must contribute 11.938°, which, in turn, determines the location of the zero as follows:

$$s = -\frac{1}{T_d} = -2.039$$

Hence, we have

$$K_p(1 + T_d s) = K_p T_d\left(\frac{1}{T_d} + s\right) = K_p T_d(s + 2.039) \tag{7–7}$$

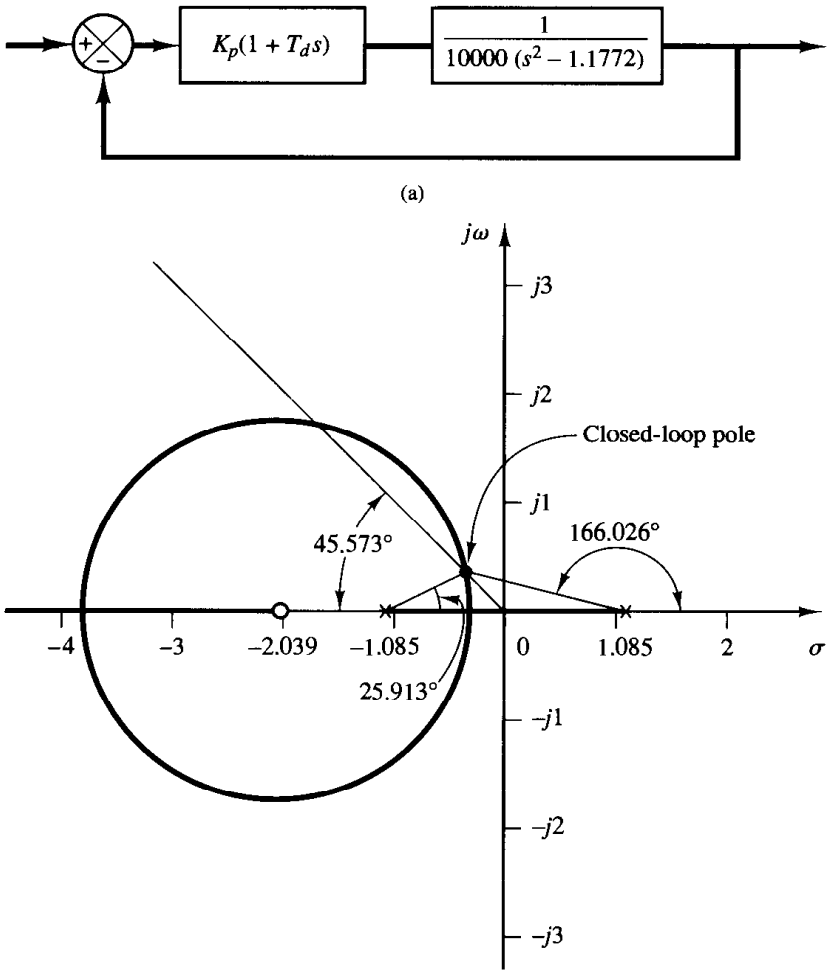

Figure 7–30
(a) PD control of an unstable plant; (b) root-locus diagram for the system.

The value of T_d is

$$T_d = \frac{1}{2.039} = 0.4904$$

The value of gain K_p can be determined from the magnitude condition as follows:

$$\left| K_p T_d \frac{s + 2.039}{10000(s^2 - 1.1772)} \right|_{s=-0.35+j0.357} = 1$$

or

$$K_p T_d = 6999.5$$

Hence,

$$K_p = \frac{6999.5}{0.4904} = 14{,}273$$

By substituting the numerical values of T_d and K_p into Equation (7–7), we obtain

$$K_p(1 + T_d s) = 14{,}273(1 + 0.4904s) = 6999.5(s + 2.039)$$

which gives the transfer function of the desired proportional-plus-derivative controller.

A-7-7. Consider the control system shown in Figure 7–31. Design a lag compensator $G_c(s)$ such that the static velocity error constant K_v is 50 $\sec^{-1}$ without appreciably changing the location of the original closed-loop poles, which are at $s = -2 \pm j\sqrt{6}$.

Solution. Assume that the transfer function of the lag compensator is

$$G_c(s) = \hat{K}_c \frac{s + \dfrac{1}{T}}{s + \dfrac{1}{\beta T}} \qquad (\beta > 1)$$

Since K_v is specified as 50 $\sec^{-1}$, we have

$$K_v = \lim_{s \to 0} sG_c(s) \frac{10}{s(s + 4)} = \hat{K}_c \beta 2.5 = 50$$

Thus

$$\hat{K}_c \beta = 20$$

Now choose $\hat{K}_c = 1$. Then

$$\beta = 20$$

Choose $T = 10$. Then the lag compensator can be given by

$$G_c(s) = \frac{s + 0.1}{s + 0.005}$$

The angle contribution of the lag compensator at the closed-loop pole $s = -2 + j\sqrt{6}$ is

$$\angle G_c(s)\Big|_{s=-2+j\sqrt{6}} = \tan^{-1}\frac{\sqrt{6}}{-1.9} - \tan^{-1}\frac{\sqrt{6}}{-1.995}$$
$$= -1.3616°$$

which is small. Thus the change in the location of the dominant closed-loop poles is very small.

The open-loop transfer function of the system becomes

$$G_c(s)G(s) = \frac{s + 0.1}{s + 0.005} \frac{10}{s(s + 4)}$$

The closed-loop transfer function is

$$\frac{C(s)}{R(s)} = \frac{10s + 1}{s^3 + 4.005s^2 + 10.02s + 1}$$

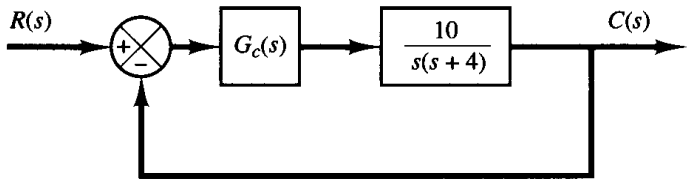

Figure 7–31
Control system.

To compare the transient-response characteristics before and after the compensation, the unit-step and unit-ramp responses of the compensated and uncompensated systems are shown in Figures 7–32(a) and (b), respectively. The steady-state error in the unit-ramp response is shown in Figure 7–32(c).

A-7-8. Consider a unity-feedback control system whose feedforward transfer function is given by

$$G(s) = \frac{10}{s(s + 2)(s + 8)}$$

Design a compensator such that the dominant closed-loop poles are located at $s = -2 \pm j2\sqrt{3}$ and the static velocity error constant K_v is equal to 80 sec^{-1}.

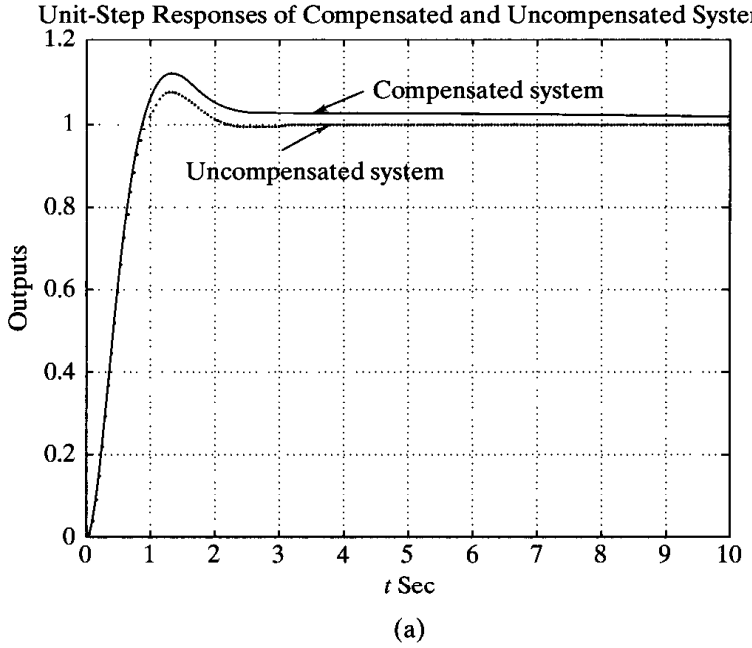

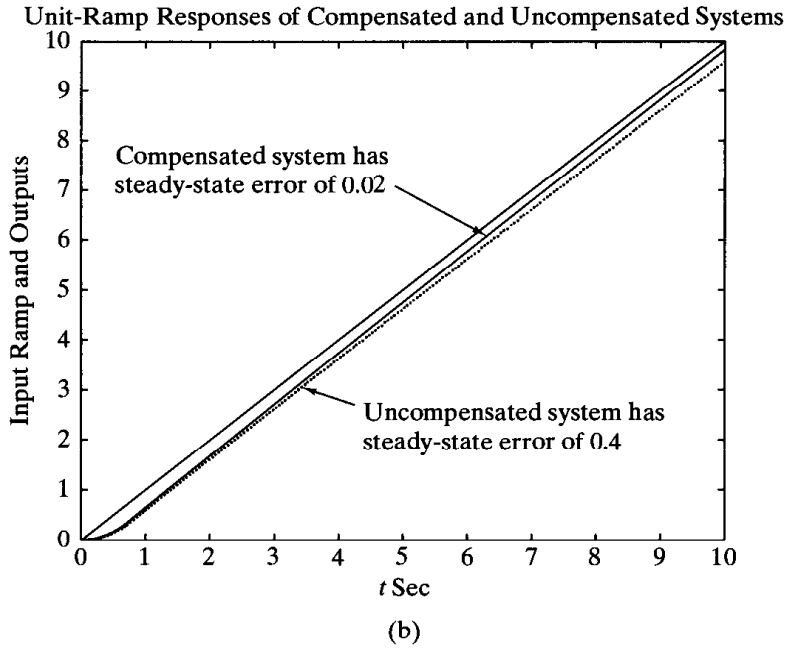

Figure 7–32
(a) Unit-step responses of the compensated and uncompensated systems; (b) unit-ramp responses of both systems; (c) unit-ramp responses showing steady-state errors.

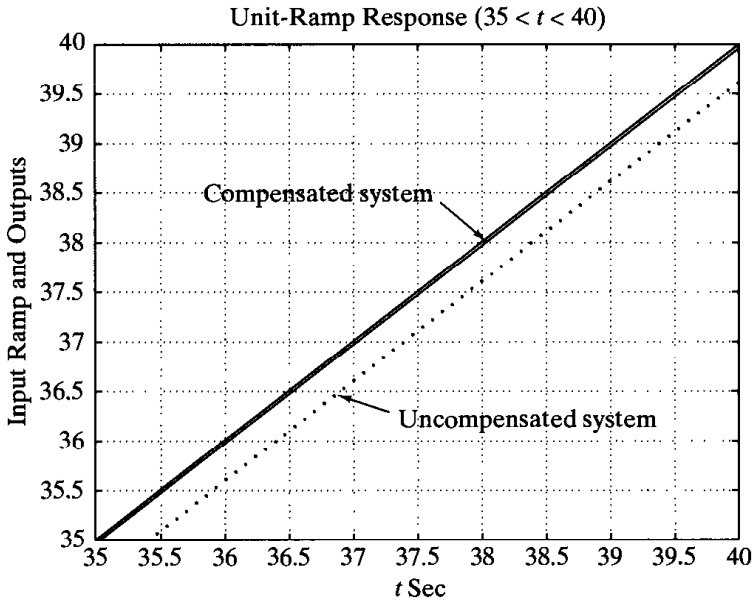

(c)

Figure 7–32
(Continued)

Solution. The static velocity error constant of the uncompensated system is $K_v = \frac{10}{16} = 0.625$. Since $K_v = 80$ is required, we need to increase the open-loop gain by 128. (This implies that we need a lag compensator.) The root-locus plot of the uncompensated system reveals that it is not possible to bring the dominant closed-loop poles to $-2 \pm j2\sqrt{3}$ by just a gain adjustment alone. See Figure 7–33. (This means that we also need a lead compensator.) Therefore, we shall employ a lag–lead compensator.

Let us assume that the transfer function of the lag–lead compensator to be

$$G_c(s) = K_c\left(\frac{s + \frac{1}{T_1}}{s + \frac{\beta}{T_1}}\right)\left(\frac{s + \frac{1}{T_2}}{s + \frac{1}{\beta T_2}}\right) \qquad (\alpha = \beta)$$

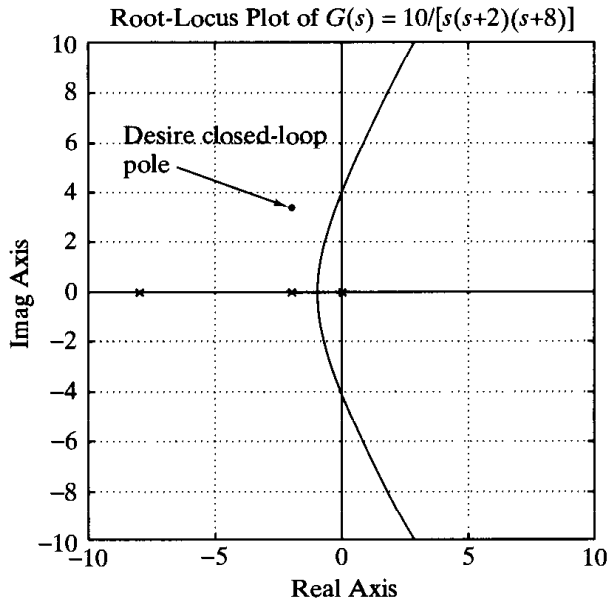

Figure 7–33
Root-locus plot of $G(s) = 10/[s(s + 2)(s + 8)]$.

where $K_c = 128$. This is because

$$K_v = \lim_{s\to 0} sG_c(s)G(s) = \lim_{s\to 0} sK_cG(s) = K_c\frac{10}{16} = 80$$

and we obtain $K_c = 128$. The angle deficiency at the desired closed-loop pole $s = -2 + j2\sqrt{3}$ is

$$\text{Angle deficiency} = 120° + 90° + 30° - 180° = 60°$$

The lead portion of the lag–lead compensator must contribute this angle. To choose T_1 we may use the graphical method presented in Section 7–5.

The lead portion must satisfy the following conditions:

$$\left| 128\left(\frac{s_1 + \frac{1}{T_1}}{s_1 + \frac{\beta}{T_1}}\right)G(s_1)\right|_{s_1=-2+j2\sqrt{3}} = 1$$

and

$$\left/\frac{s_1 + \frac{1}{T_1}}{s_1 + \frac{\beta}{T_1}}\right|_{s_1=-2+j2\sqrt{3}} = 60°$$

The first condition can be simplified as

$$\left|\frac{s_1 + \frac{1}{T_1}}{s_1 + \frac{\beta}{T_1}}\right|_{s_1=-2+j2\sqrt{3}} = \frac{1}{13.3333}$$

By using the same approach as used in Section 7–5, the zero ($s = 1/T_1$) and pole ($s = \beta/T_1$) can be determined as follows:

$$\frac{1}{T_1} = 3.70, \qquad \frac{\beta}{T_1} = 53.35$$

See Figure 7–34. The value of β is thus determined as

$$\beta = 14.419$$

For the lag portion of the compensator, we may choose

$$\frac{1}{\beta T_2} = 0.01$$

Then

$$\frac{1}{T_2} = 0.1442$$

Noting that

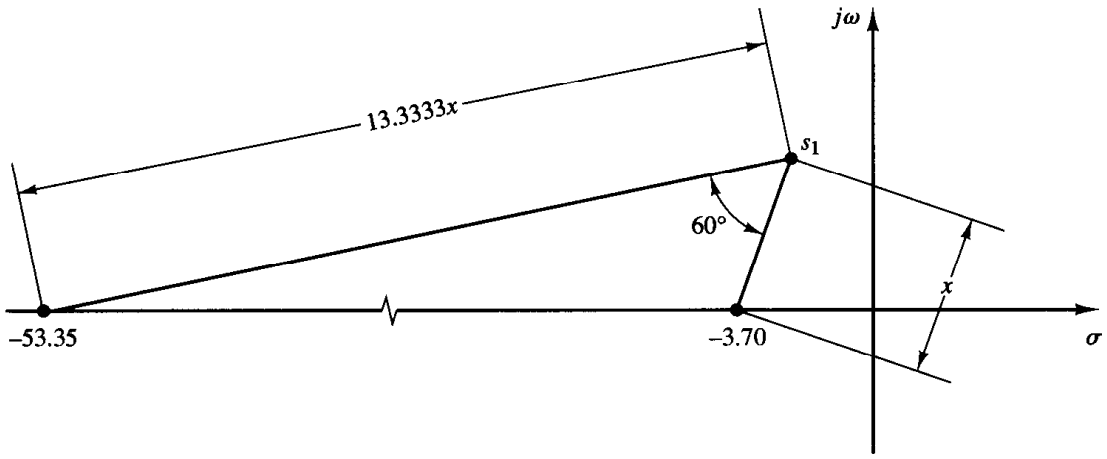

Figure 7–34
Graphical determination of the zero and pole of the lead portion of the compensator.

$$\left|\frac{s_1 + 0.1442}{s_1 + 0.01}\right|_{s_1=-2+j2\sqrt{3}} = 0.9837$$

$$\left/\frac{s_1 + 0.1442}{s_1 + 0.01}\right|_{s_1=-2+j2\sqrt{3}} = -1.697°$$

the angle contribution of the lag portion is $-1.697°$ and the magnitude contribution is 0.9837. This means that the dominant closed-loop poles lie close to the desired location $s = -2 \pm j2\sqrt{3}$. Thus the compensator designed,

$$G_c(s) = 128\left(\frac{s + 3.70}{s + 53.35}\right)\left(\frac{s + 0.1442}{s + 0.01}\right)$$

is acceptable. The feedforward transfer function of the compensated system becomes

$$G_c(s)G(s) = \frac{1280(s + 3.7)(s + 0.1442)}{s(s + 53.35)(s + 0.01)(s + 2)(s + 8)}$$

A root-locus plot of the compensated system is shown in Figure 7–35(a). An enlarged root-locus plot near the origin is shown in Figure 7–35(b).

To verify the improved system performance of the compensated system, see the unit-step responses and unit-ramp responses of the compensated and uncompensated systems shown in Figures 7–36 (a) and (b), respectively.

A-7-9. Consider the system shown in Figure 7–37. Design a lag–lead compensator such that the static velocity error constant K_v is 50 $\sec^{-1}$ and the damping ratio ζ of the dominant closed-loop poles is 0.5. (Choose the zero of the lead portion of the lag–lead compensator to cancel the pole at $s = -1$ of the plant.) Determine all closed-loop poles of the compensated system.

Solution. Let us employ the lag–lead compensator given by

$$G_c(s) = K_c\left(\frac{s + \frac{1}{T_1}}{s + \frac{\beta}{T_1}}\right)\left(\frac{s + \frac{1}{T_2}}{s + \frac{1}{\beta T_2}}\right) = K_c\frac{(T_1 s + 1)(T_2 s + 1)}{\left(\frac{T_1}{\beta}s + 1\right)(\beta T_2 s + 1)}$$

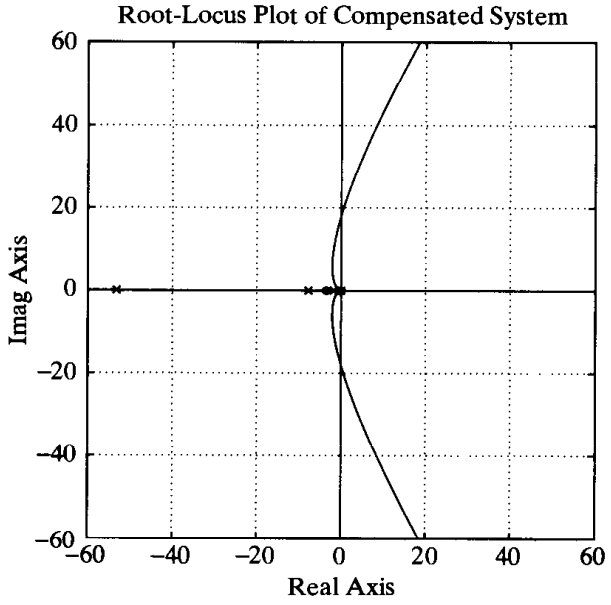

(a)

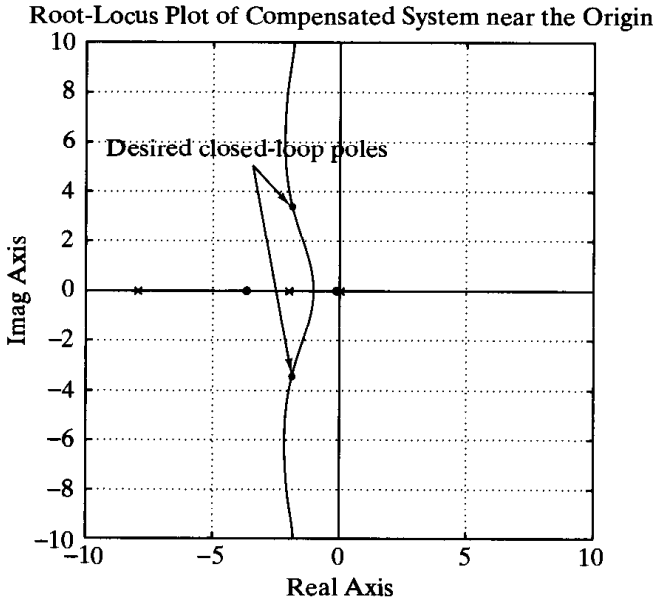

(b)

Figure 7–35
(a) Root-locus plot of compensated system; (b) root-locus plot near the origin.

where $\beta > 1$. Then

$$K_v = \lim_{s \to 0} sG_c(s)G(s)$$

$$= \lim_{s \to 0} s \frac{K_c(T_1 s + 1)(T_2 s + 1)}{\left(\frac{T_1}{\beta} s + 1\right)\left(\beta T_2 s + 1\right)} \frac{1}{s(s + 1)(s + 5)}$$

$$= \frac{K_c}{5}$$

The specification that $K_v = 50\ \text{sec}^{-1}$ determines the value of K_c, or

$$K_c = 250$$

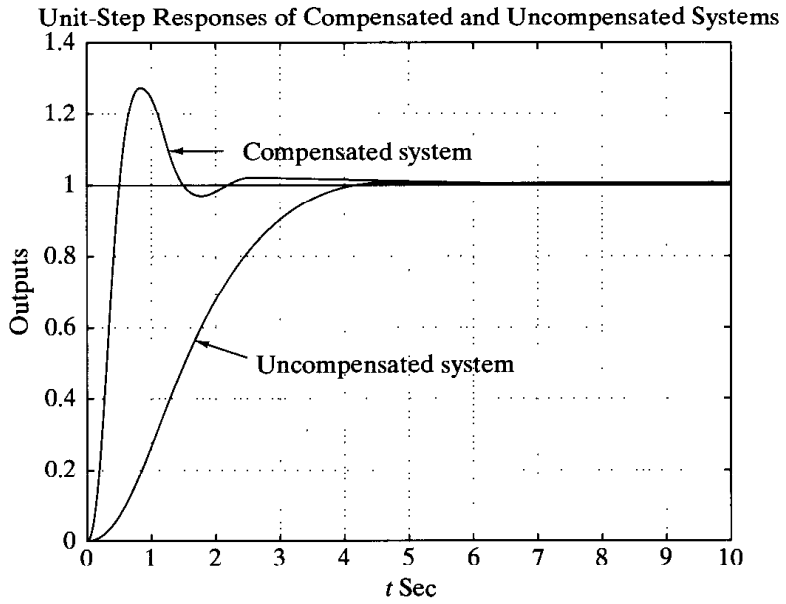

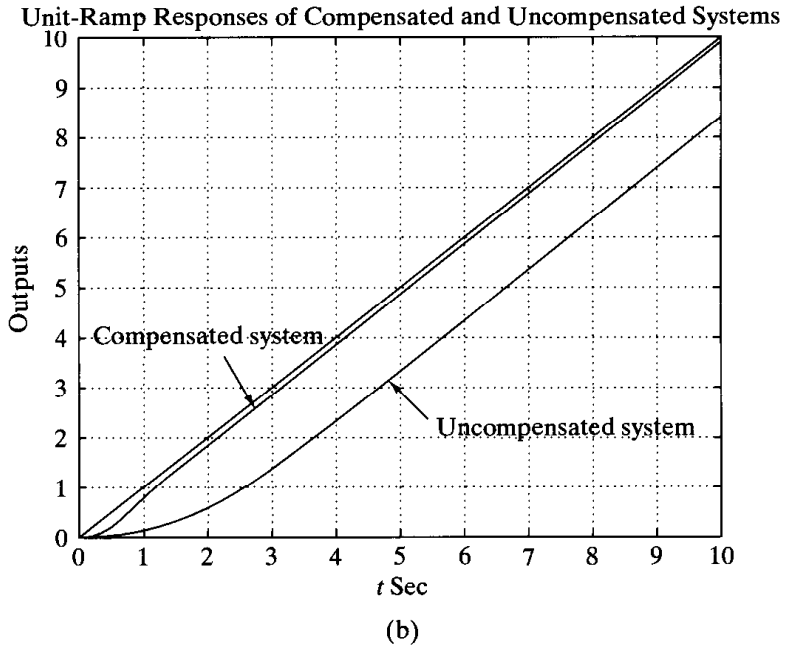

Figure 7–36
(a) Unit-step responses of compensated and uncompensated systems; (b) unit-ramp responses of both systems.

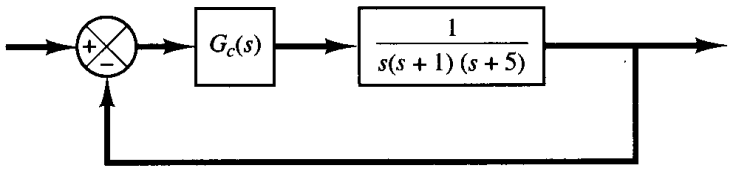

Figure 7–37
Control system.

We now choose $T_1 = 1$ so that $s + (1/T_1)$ will cancel the $(s + 1)$ term of the plant. The lead portion then becomes

$$\frac{s + 1}{s + \beta}$$

For the lag portion of the lag–lead compensator we require

$$\left| \frac{s_1 + \frac{1}{T_2}}{s_1 + \frac{1}{\beta T_2}} \right| \doteq 1, \qquad -5° < \underline{/\ \frac{s_1 + \frac{1}{T_2}}{s_1 + \frac{1}{\beta T_2}}} < 0°$$

where $s = s_1$ is one of the dominant closed-loop poles. For $s = s_1$, the open-loop transfer function becomes

$$G_c(s_1)G(s_1) \doteq K_c \left(\frac{s_1 + 1}{s_1 + \beta} \right) \frac{1}{s_1(s_1 + 1)(s_1 + 5)} = K_c \frac{1}{(s_1 + \beta)s_1(s_1 + 5)}$$

Noting that at $s = s_1$ the magnitude and angle conditions are satisfied, we have

$$\left| K_c \frac{1}{s_1(s_1 + \beta)(s_1 + 5)} \right| = 1 \tag{7–8}$$

$$\underline{/\ K_c \frac{1}{s_1(s + \beta)(s_1 + 5)}} = \pm 180°(2k + 1) \tag{7–9}$$

where $k = 0,1,2,\ldots$. In Equations (7–8) and (7–9), β and s_1 are unknowns. Since the damping ratio ζ of the dominant closed-loop poles is specified as 0.5, the closed-loop pole $s = s_1$ can be written as

$$s_1 = -x + j\sqrt{3}\,x$$

where x is as yet undetermined.

Notice that the magnitude condition, Equation (7–8), can be rewritten as

$$\left| \frac{K_c}{(-x + j\sqrt{3}\,x)(-x + \beta + j\sqrt{3}\,x)(-x + 5 + j\sqrt{3}\,x)} \right| = 1$$

Noting that $K_c = 250$, we have

$$x\sqrt{(\beta - x)^2 + 3x^2}\,\sqrt{(5 - x)^2 + 3x^2} = 125 \tag{7–10}$$

The angle condition, Equation (7–9), can be rewritten as

$$\underline{/\ K_c \frac{1}{(-x + j\sqrt{3}\,x)(-x + \beta + j\sqrt{3}\,x)(-x + 5 + j\sqrt{3}\,x)}}$$

$$= -120° - \tan^{-1}\left(\frac{\sqrt{3}\,x}{-x + \beta} \right) - \tan^{-1}\left(\frac{\sqrt{3}\,x}{-x + 5} \right) = -180°$$

or

$$\tan^{-1}\left(\frac{\sqrt{3}\,x}{-x + \beta} \right) + \tan^{-1}\left(\frac{\sqrt{3}\,x}{-x + 5} \right) = 60° \tag{7–11}$$

We need to solve Equations (7–10) and (7–11) for β and x. By several trial-and-error calculations, it can be found that

$$\beta = 16.025, \qquad x = 1.9054$$

Thus

$$s_1 = -1.9054 + j\sqrt{3}\,(1.9054) = -1.9054 + j3.3002$$

The lag portion of the lag–lead compensator can be determined as follows: Noting that the pole and zero of the lag portion of the compensator must be located near the origin, we may choose

$$\frac{1}{\beta T_2} = 0.01$$

That is,

$$\frac{1}{T_2} = 0.16025 \qquad \text{or} \qquad T_2 = 6.25$$

With the choice of $T_2 = 6.25$, we find

$$\left|\frac{s_1 + \dfrac{1}{T_2}}{s_1 + \dfrac{1}{\beta T_2}}\right| = \left|\frac{-1.9054 + j3.3002 + 0.16025}{-1.9054 + j3.3002 + 0.01}\right|$$

$$= \left|\frac{-1.74515 + j3.3002}{-1.89054 + j3.3002}\right| = 0.98 \doteq 1 \tag{7–12}$$

and

$$\angle\frac{s_1 + \dfrac{1}{T_2}}{s_1 + \dfrac{\gamma}{\beta T_2}} = \angle\frac{-1.9054 + j3.3002 + 0.16025}{-1.9054 + j3.3002 + 0.01}$$

$$= \tan^{-1}\left(\frac{3.3002}{-1.74515}\right) - \tan^{-1}\left(\frac{3.3002}{-1.89054}\right) = -1.937^\circ \tag{7–13}$$

Since

$$-5^\circ < -1.937^\circ < 0^\circ$$

our choice of $T_2 = 6.25$ is acceptable. Then the lag–lead compensator just designed can be written as

$$G_c(s) = 250\left(\frac{s + 1}{s + 16.025}\right)\left(\frac{s + 0.16025}{s + 0.01}\right)$$

Therefore, the compensated system has the following open-loop transfer function:

$$G_c(s)G(s) = \frac{250(s + 0.16025)}{s(s + 0.01)(s + 5)(s + 16.025)}$$

A root-locus plot of the compensated system is shown in Figure 7–38(a). An enlarged root-locus plot near the origin is shown in Figure 7–38(b).

The closed loop transfer function becomes

$$\frac{C(s)}{R(s)} = \frac{250(s + 0.16025)}{s(s + 0.01)(s + 5)(s + 16.025) + 250(s + 0.16025)}$$

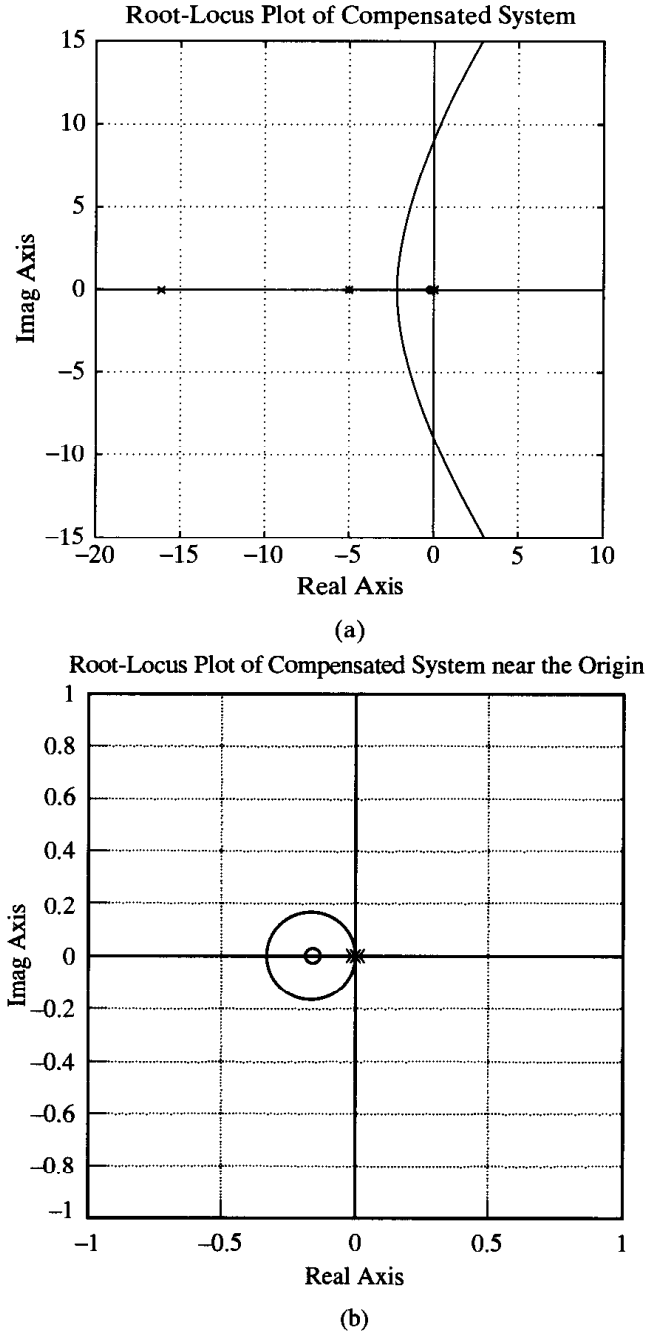

Figure 7–38
(a) Root-locus plot of compensated system; (b) root-locus plot near the origin.

The closed-loop poles are located at

$$s = -1.8308 \pm j3.2359$$

$$s = -0.1684$$

$$s = -17.205$$

Notice that the dominant closed-loop poles $s = -1.8308 \pm j3.2359$ differ from the dominant closed-loop poles $s = \pm s_1$ assumed in the computation of β and T_2. Small deviations of the dominant closed-loop poles $s = -1.8308 \pm j3.2359$ from $s = \pm s_1 = -1.9054 \pm j3.3002$ are due to the approximations involved in determining the lag portion of the compensator [See Equations (7–12) and (7–13)].

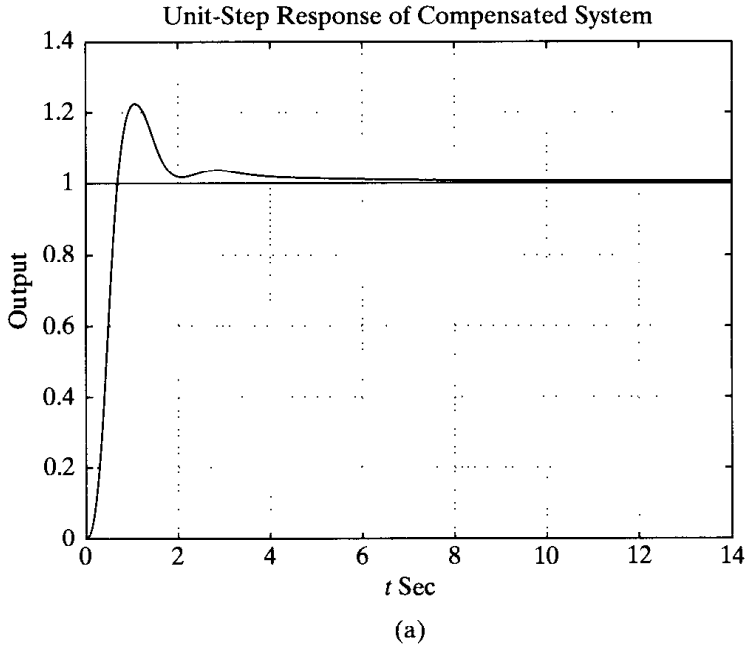

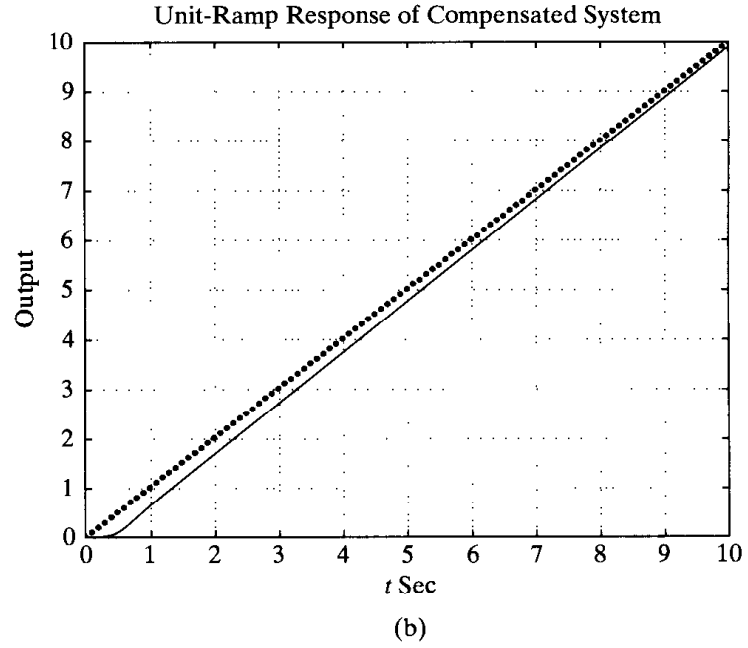

Figure 7–39
(a) Unit-step response of the compensated system; (b) unit-ramp response of the compensated system.

Figures 7–39(a) and (b) show the unit-step response and unit-ramp response of the designed system, respectively. Note that the closed-loop pole at $s = -0.1684$ almost cancels the zero at $s = -0.16025$. However, this pair of closed-loop pole and zero located near the origin produces a long tail of small amplitude. Since the closed-loop pole at $s = -17.205$ is located very much farther to the left compared to the closed-loop poles at $s = -1.8308 \pm j3.2359$, the effect of this real pole on the system response is also very small. Therefore, the closed-loop poles at $s = -1.8308 \pm j3.2359$ are indeed dominant closed-loop poles that determine the response characteristics of the closed-loop system. In the unit-ramp response, the steady-state error in following the unit-ramp input eventually becomes $1/K_v = \frac{1}{50} = 0.02$.

A-7-10. Consider the system shown in Figure 7–40. It is desired to design a PID controller $G_c(s)$ such that the dominant closed-loop poles are located at $s = -1 \pm j\sqrt{3}$. For the PID controller,

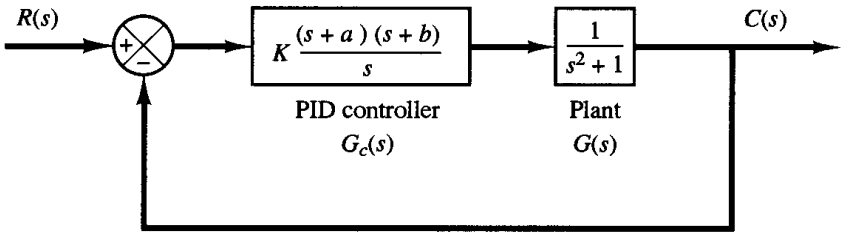

Figure 7–40
PID-controlled system.

choose $a = 1$ and then determine the values of K and b. Sketch the root-locus diagram for the designed system.

Solution. Since

$$G_c(s)G(s) = K\frac{(s+1)(s+b)}{s}\frac{1}{s^2+1}$$

the sum of the angles at $s = -1 + j\sqrt{3}$, one of the desired closed-loop poles, from the zero at $s = -1$ and poles at $s = 0, s = j$, and $s = -j$ is

$$90° - 143.794° - 120° - 110.104° = -283.898°$$

Hence the zero at $s = -b$ must contribute 103.898°. This requires that the zero be located at

$$b = 0.5714$$

The gain constant K can be determined from the magnitude condition.

$$\left|K\frac{(s+1)(s+0.5714)}{s}\frac{1}{s^2+1}\right|_{s=-1+j\sqrt{3}} = 1$$

or

$$K = 2.3333$$

Then the compensator can be written as follows:

$$G_c(s) = 2.3333\frac{(s+1)(s+0.5714)}{s}$$

The open-loop transfer function becomes

$$G_c(s)G(s) = \frac{2.3333(s+1)(s+0.5714)}{s}\frac{1}{s^2+1}$$

From this equation a root-locus plot for the compensated system can be drawn. Figure 7–41 is a root-locus plot.

The closed-loop transfer function is given by

$$\frac{C(s)}{R(s)} = \frac{2.3333(s+1)(s+0.5714)}{s^3 + s + 2.3333(s+1)(s+0.5714)}$$

The closed-loop poles are located at $s = -1 \pm j\sqrt{3}$ and $s = -0.3333$. A unit-step response curve is shown in Figure 7–42. The closed-loop pole at $s = -0.3333$ and a zero at $s = -0.5714$ produces a long tail of small amplitude.

A-7-11. Figure 7–43(a) is a block diagram of a model for an attitude-rate control system. The closed-loop transfer function for this system is

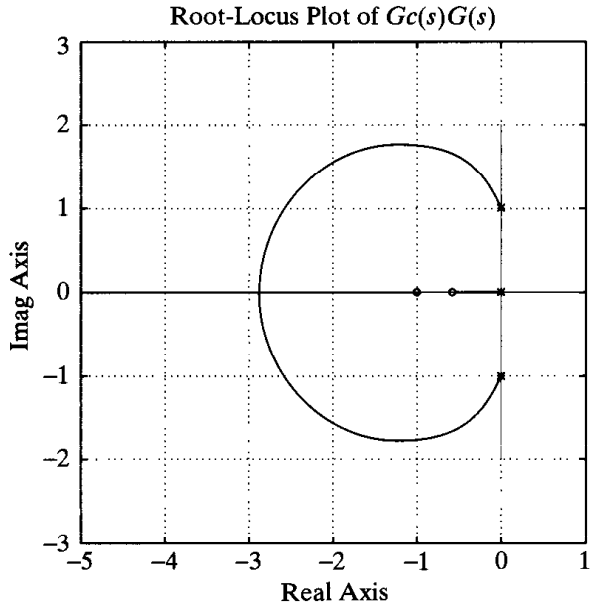

Figure 7–41
Root-locus plot of the compensated system (Problem A-7-10).

$$\frac{C(s)}{R(s)} = \frac{2s + 0.1}{s^3 + 0.1s^2 + 6s + 0.1}$$

$$= \frac{2(s + 0.05)}{(s + 0.0417 + j2.4489)(s + 0.0417 - j2.4489)(s + 0.0167)}$$

The unit-step response of this system is shown in Figure 7–43(b). The response shows high-frequency oscillations at the beginning of the response due to the poles at $s = -0.0417 \pm j2.4489$. The response is dominated by the pole at $s = -0.0167$. The settling time is approximately 240 sec.

It is desired to speed up the response and also eliminate the oscillatory mode at the beginning of the response. Design a suitable compensator such that the dominant closed-loop poles are at $s = -2 \pm j2\sqrt{3}$.

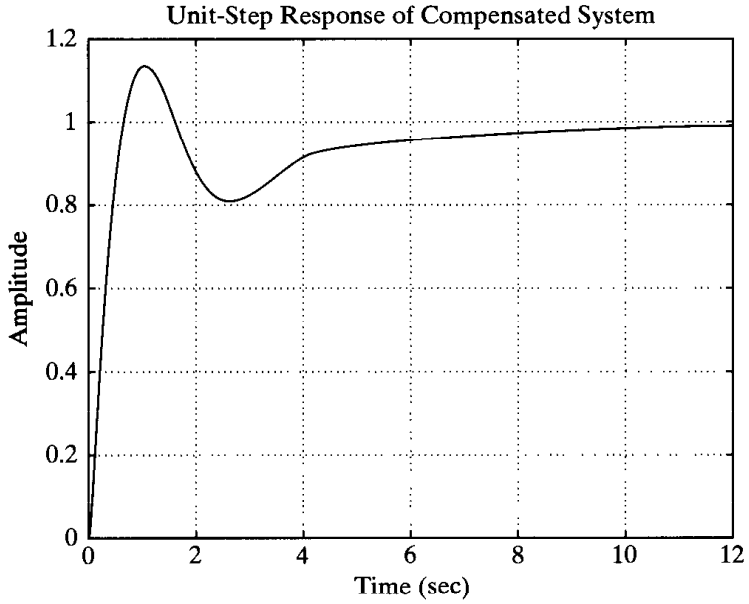

Figure 7–42
Unit-step response of the compensated system (Problem A-7-10).

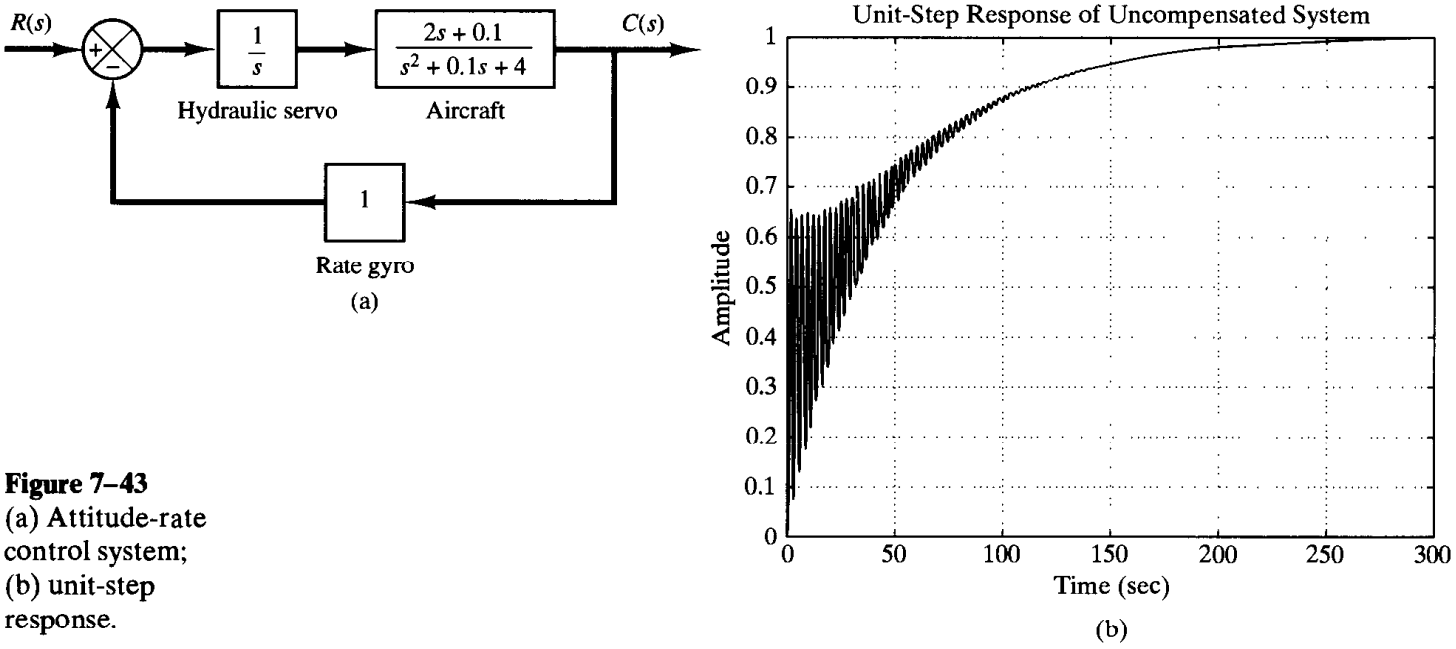

Figure 7–43
(a) Attitude-rate control system; (b) unit-step response.

Solution. Figure 7–44 shows a block diagram for the compensated system. Note that the open-loop zero at $s = -0.05$ and the open-loop pole at $s = 0$ generate a closed-loop pole between $s = 0$ and $s = -0.05$. Such a closed-loop pole becomes a dominant closed-loop pole and make the response quite slow. Hence, it is necessary to replace this zero by a zero that is located far away from the $j\omega$ axis, for example, a zero at $s = -4$.

We now choose the compensator in the following form:

$$G_c(s) = \hat{G}_c(s)\frac{s + 4}{2s + 0.1}$$

Then the open-loop transfer function of the compensated system becomes

$$G_c(s)G(s) = \hat{G}_c(s)\frac{s + 4}{2s + 0.1}\frac{1}{s}\frac{2s + 0.1}{s^2 + 0.1s + 4}$$

$$= \hat{G}_c(s)\frac{s + 4}{s(s^2 + 0.1s + 4)}$$

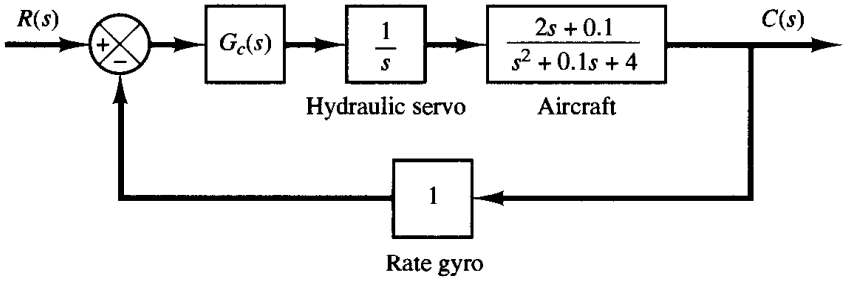

Figure 7–44
Compensated attitude-rate control system.

To determine $\hat{G}_c(s)$ by the root-locus method, we need to find the angle deficiency at the desired closed-loop pole $s = -2 + j2\sqrt{3}$. The angle deficiency can be found as follows:

$$\begin{aligned}\text{Angle deficiency} &= -143.088° - 120° - 109.642° + 60° + 180° \\ &= -132.73°\end{aligned}$$

Hence, the lead compensator $\hat{G}_c(s)$ must provide 132.73°. Since the angle deficiency is 132.73°, we need two lead compensators, each providing 66.365°. Thus $G_c(s)$ will have the following form:

$$G_c(s) = K_c\left(\frac{s + s_z}{s + s_p}\right)^2$$

Suppose that we choose two zeros at $s = -2$. Then the two poles of the lead compensators can be obtained from

$$\frac{3.4641}{s_p - 2} = \tan(90° - 66.365°) = 0.4376169$$

or

$$\begin{aligned}s_p &= 2 + \frac{3.4641}{0.4376169} \\ &= 9.9158\end{aligned}$$

Hence,

$$\hat{G}_c(s) = K_c\left(\frac{s + 2}{s + 9.9158}\right)^2$$

The entire compensator $G_c(s)$ for the system becomes

$$G_c(s) = \hat{G}_c(s)\frac{s + 4}{2s + 0.1} = K_c\frac{(s + 2)^2}{(s + 9.9158)^2}\frac{s + 4}{2s + 0.1}$$

The value of K_c can be determined from the magnitude condition. Since the open-loop transfer function is

$$G_c(s)G(s) = K_c\frac{(s + 2)^2(s + 4)}{(s + 9.9158)^2 s(s^2 + 0.1s + 4)}$$

the magnitude condition becomes

$$\left|K_c\frac{(s + 2)^2(s + 4)}{(s + 9.9158)^2 s(s^2 + 0.1s + 4)}\right|_{s=-2+j2\sqrt{3}} = 1$$

Hence,

$$\begin{aligned}K_c &= \left|\frac{(s + 9.9158)^2 s(s^2 + 0.1s + 4)}{(s + 2)^2(s + 4)}\right|_{s=-2+j2\sqrt{3}} \\ &= 88.0227\end{aligned}$$

Thus the compensator $G_c(s)$ becomes

$$G_c(s) = 88.0227 \frac{(s + 2)^2(s + 4)}{(s + 9.9158)^2(2s + 0.1)}$$

The open-loop transfer function is given by

$$G_c(s)G(s) = \frac{88.0227(s + 2)^2(s + 4)}{(s + 9.9158)^2 s(s^2 + 0.1s + 4)}$$

A root-locus plot for the compensated system is shown in Figure 7–45. The closed-loop poles for the compensated system are indicated in the plot. The closed-loop poles, the roots of the characteristic equation

$$(s + 9.9158)^2 s(s^2 + 0.1s + 4) + 88.0227(s + 2)^2(s + 4) = 0$$

are as follows:

$$s = -2.0000 \pm j3.4641$$
$$s = -7.5224 \pm j6.5326$$
$$s = -0.8868$$

Now that the compensator has been designed, we shall examine the transient response characteristics with MATLAB. The closed-loop transfer function is given by

$$\frac{C(s)}{R(s)} = \frac{88.0227(s + 2)^2(s + 4)}{(s + 9.9158)^2 s(s^2 + 0.1s + 4) + 88.0227(s + 2)^2(s + 4)}$$

Figures 7–46(a) and (b) show the plots of the unit-step response and unit-ramp response of the compensated system. These response curves show that the designed system is acceptable.

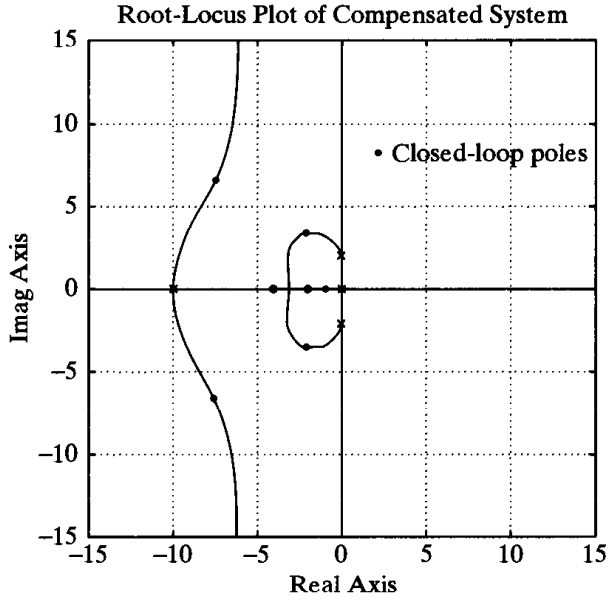

Figure 7–45
Root-locus plot of the compensated system.

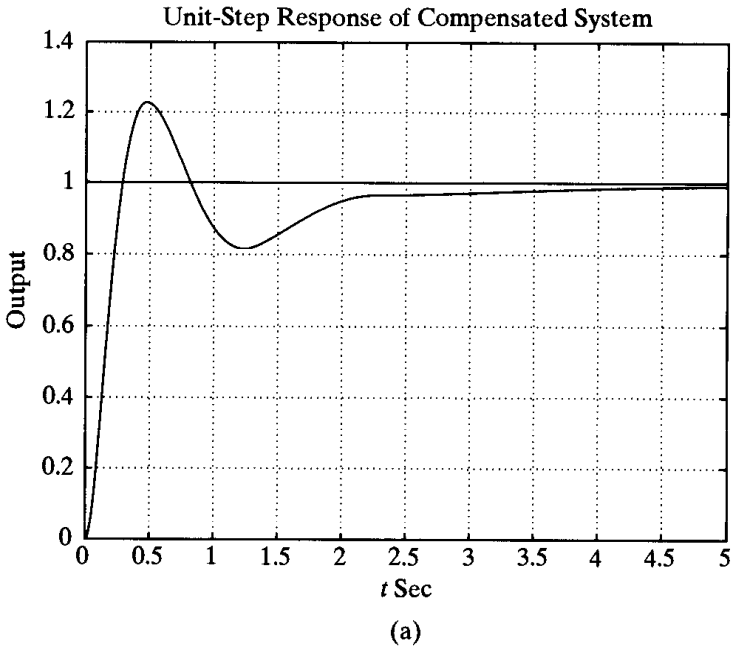

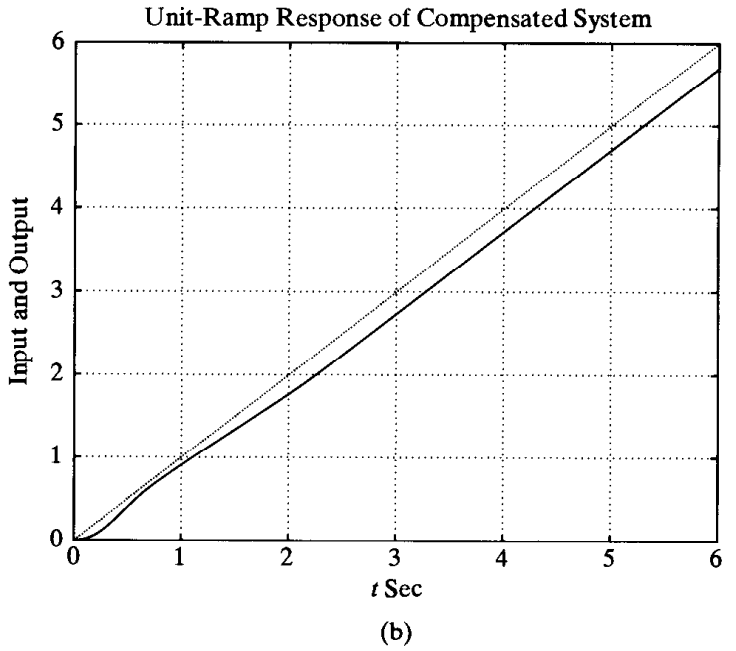

Figure 7–46
(a) Unit-step response of the compensated system; (b) unit-ramp response of the compensated system (Problem A-7-11).

A-7-12. Consider the model for a space vehicle control system shown in Figure 7–47. Design a lead compensator $G_c(s)$ such that the damping ratio ζ and the undamped natural frequency ω_n of the dominant closed-loop poles are 0.5 and 2 rad/sec, respectively.

Solution

First attempt: Assume the lead compensator $G_c(s)$ to be

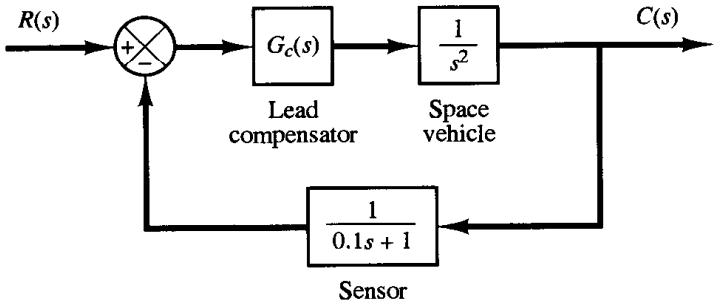

Figure 7–47
Space vehicle control system.

$$G_c(s) = K_c\left(\frac{s + \frac{1}{T}}{s + \frac{1}{\alpha T}}\right) \qquad (0 < \alpha < 1)$$

From the given specifications, $\zeta = 0.5$ and $\omega_n = 2$ rad/sec, the dominant closed-loop poles must be located at

$$s = -1 \pm j\sqrt{3}$$

We first calculate the angle deficiency at this closed-loop pole.

$$\begin{aligned}\text{Angle deficiency} &= -120° - 120° - 10.8934° + 180° \\ &= -70.8934°\end{aligned}$$

This angle deficiency must be compensated by the lead compensator. There are many ways to determine the locations of the pole and zero of the lead network. Let us choose the zero of the compensator at $s = -1$. Then, referring to Figure 7–48, we have the following equation:

$$\frac{1.73205}{x - 1} = \tan(90° - 70.8934°) = 0.34641$$

or

$$x = 1 + \frac{1.73205}{0.34641} = 6$$

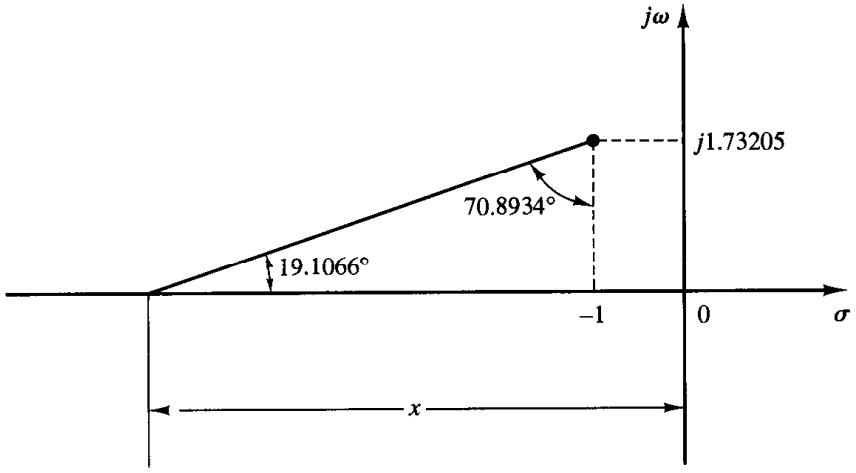

Figure 7–48
Determination of the pole of the lead network.

Hence,

$$G_c(s) = K_c \frac{s + 1}{s + 6}$$

The value of K_c can be determined from the magnitude condition

$$K_c \left| \frac{s + 1}{s + 6} \frac{1}{s^2} \frac{1}{0.1s + 1} \right|_{s=-1+j\sqrt{3}} = 1$$

as follows:

$$K_c = \left| \frac{(s + 6)s^2(0.1s + 1)}{s + 1} \right|_{s=-1+j\sqrt{3}} = 11.2000$$

Thus

$$G_c(s) = 11.2 \frac{s + 1}{s + 6}$$

Since the open-loop transfer function becomes

$$G_c(s)G(s)H(s) = 11.2 \frac{s + 1}{(s + 6)s^2(0.1s + 1)}$$

$$= \frac{11.2(s + 1)}{0.1s^4 + 1.6s^3 + 6s^2}$$

a root-locus plot of the compensated system can be obtained easily with MATLAB by entering num and den and using rlocus command. The result is shown in Figure 7–49.

The closed-loop transfer function for the compensated system becomes

$$\frac{C(s)}{R(s)} = \frac{11.2(s + 1)(0.1s + 1)}{(s + 6)s^2(0.1s + 1) + 11.2(s + 1)}$$

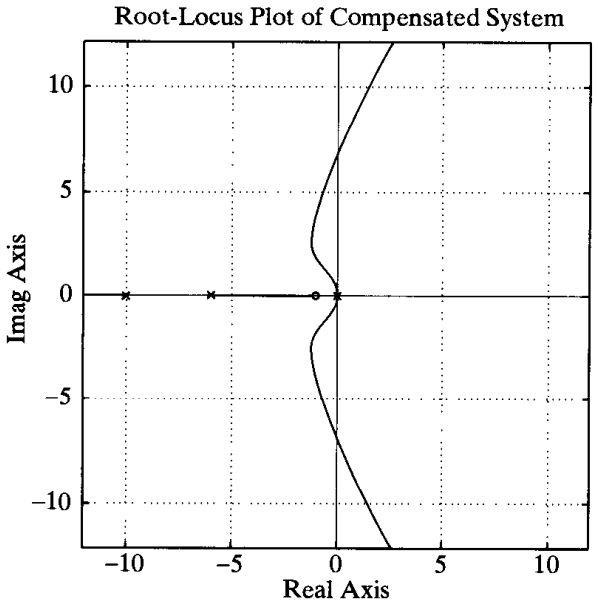

Figure 7–49
Root-locus plot of the compensated system.

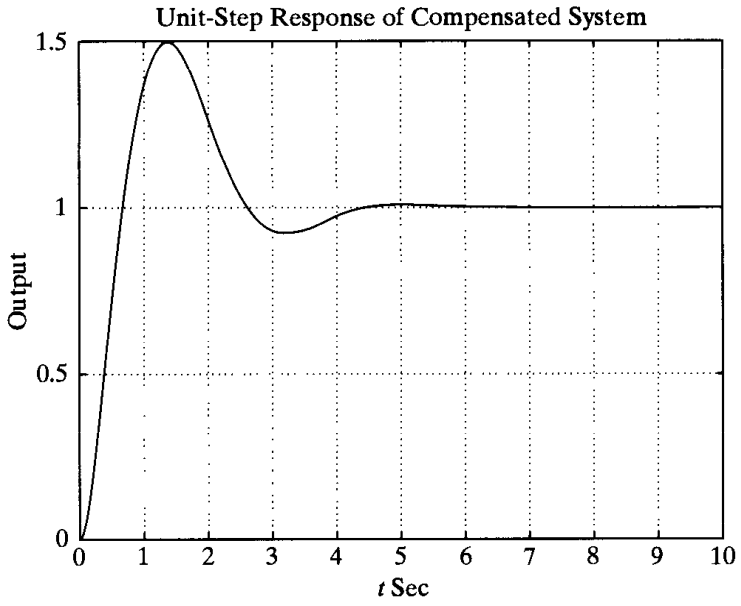

Figure 7–50
Unit-step response of the compensated system.

Figure 7–50 shows the unit-step response curve. It shows a fairly large overshoot (50% overshoot). It is desirable to modify the compensator and make the maximum overshoot smaller. A close look at the root-locus plot reveals that the presence of the zero at $s = -1$ is adding the amount of the maximum overshoot. One way to avoid this situation is to modify the lead compensator as presented in the following second attempt.

Second attempt: To modify the shape of the root loci, we may use two lead networks, each contributing half the necessary lead angle, which is 70.8934°/2 = 35.4467°. Let us choose the location of the zeros at $s = -3$. (This is an arbitrary choice. Other choices such as $s = -2.5$ and $s = -4$ may be made.)

Once we choose two zeros at $s = -3$, the necessary location of the poles can be determined as shown in Figure 7–51, or

$$\frac{1.73205}{y - 1} = \tan(40.89334° - 35.4467°)$$

$$= \tan 5.4466° = 0.09535$$

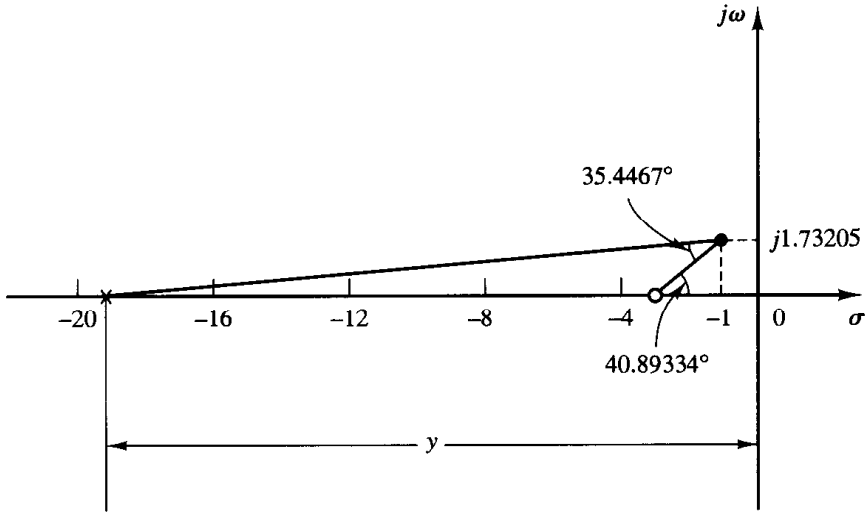

Figure 7–51
Determination of the pole of the lead network.

which yields

$$y = 1 + \frac{1.73205}{0.09535} = 19.1652$$

Hence, the lead compensator will have the following transfer function:

$$G_c(s) = K_c\left(\frac{s+3}{s+19.1652}\right)^2$$

The value of K_c can be determined from the magnitude condition as follows:

$$\left|K_c\left(\frac{s+3}{s+19.1652}\right)^2 \frac{1}{s^2}\frac{1}{0.1s+1}\right|_{s=-1+j\sqrt{3}} = 1$$

or

$$K_c = 174.3864$$

Then the lead compensator just designed is

$$G_c(s) = 174.3864\left(\frac{s+3}{s+19.1652}\right)^2$$

Then the open-loop transfer function becomes

$$G_c(s)G(s)H(s) = 174.3864\left(\frac{s+3}{s+19.1652}\right)^2 \frac{1}{s^2}\frac{1}{0.1s+1}$$

A root-locus plot for the compensated system is shown in Figure 7–52(a). Notice that there is no closed-loop zero near the origin. An expanded view of the root-locus plot near the origin is shown in Figure 7–52(b).

The closed-loop transfer function becomes

$$\frac{C(s)}{R(s)} = \frac{174.3864(s+3)^2(0.1s+1)}{(s+19.1652)^2s^2(0.1s+1) + 174.3864(s+3)^2}$$

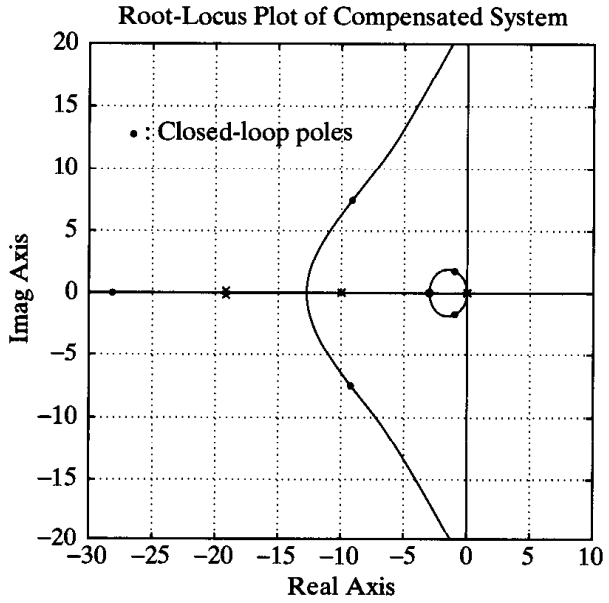

(a)

Figure 7–52
(a) Root-locus plot of compensated system; (b) root-locus plot near the origin.

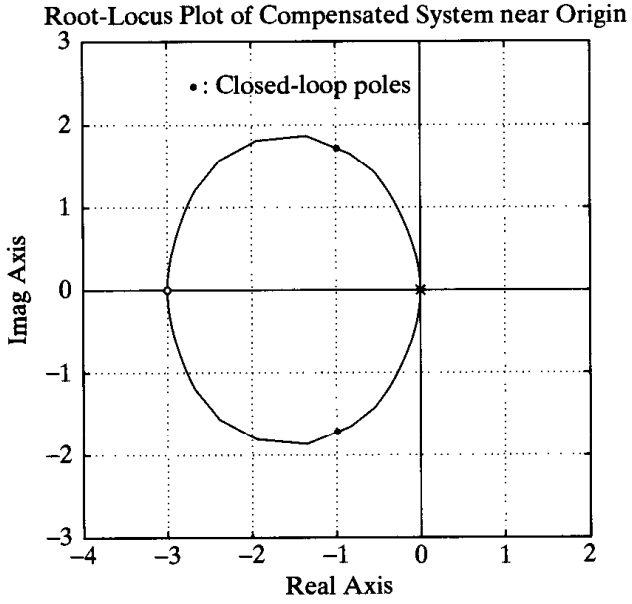

(b)

Figure 7–52
(Continued)

The closed-loop poles are found as follows:

$$s = -1 \pm j1.73205$$
$$s = -9.1847 \pm j7.4814$$
$$s = -27.9606$$

Figures 7–53(a) and (b) show the unit-step response and unit-ramp response of the compensated system. The unit-step response curve is reasonable and the unit-ramp response looks acceptable. Notice that in the unit-ramp response the output leads the input by a small amount. This is because the system has a feedback transfer function $1/(0.1s + 1)$. If the feedback signal versus t is plotted, together with the unit-ramp input, the former will not lead the input ramp at steady state. See Figure 7–53(c).

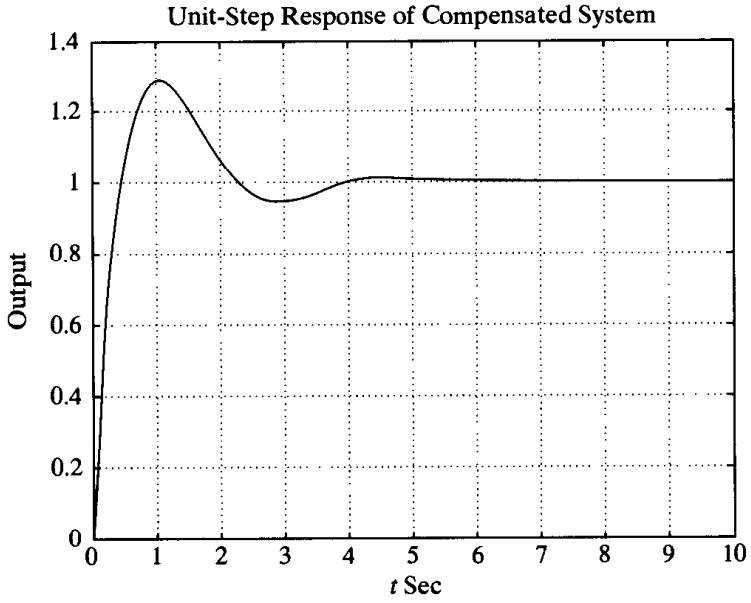

(a)

Figure 7–53
(a) Unit-step response of the compensated system; (b) unit-ramp response of the compensated system; (c) a plot of feedback signal versus t in the unit-ramp response.

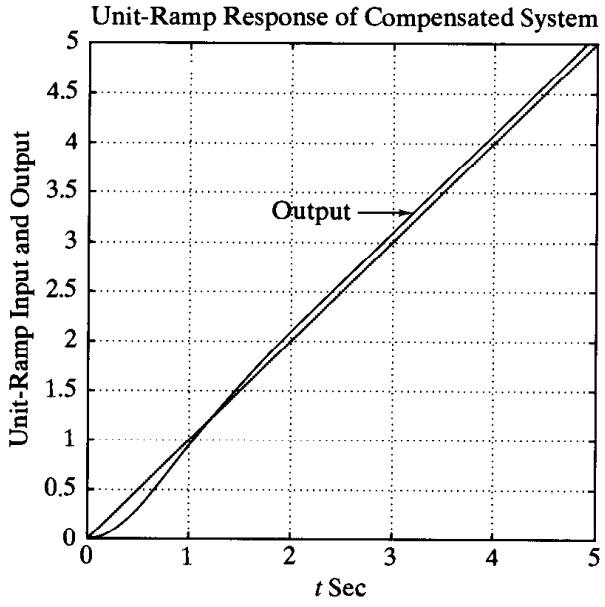

(b)

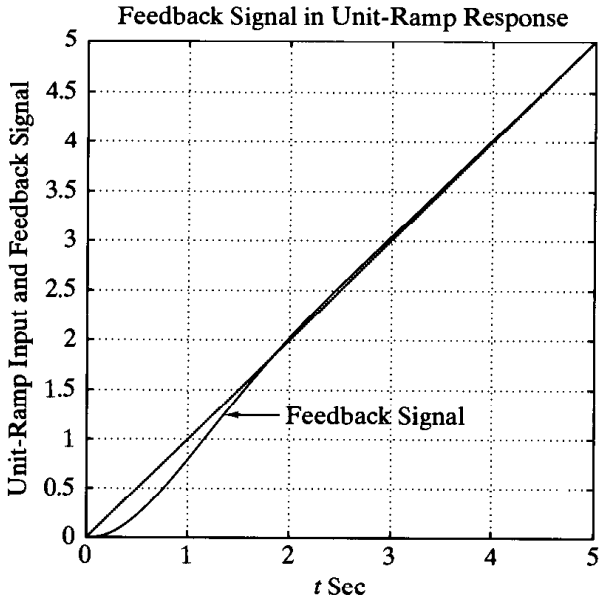

(c)

Figure 7–53
(Continued)

PROBLEMS

B-7-1. Consider the mechanical system shown in Figure 7–54. It consists of a spring and two dashpots. Obtain the transfer function of the system. The displacement x_i is the input and displacement x_o is the output. Is this system a mechanical lead network or lag network?

B-7-2. Obtain the transfer function of the electrical network shown in Figure 7–55. Show that it is a lag network.

B-7-3. Consider the system shown in Figure 7–56. Plot the root loci for the system. Determine the value of K such that the damping ratio ζ of the dominant closed-loop poles is 0.5. Then determine all closed-loop poles. Plot the unit-step response curve with MATLAB.

B-7-4. Determine the values of K, T_1, and T_2 of the system shown in Figure 7–57 so that the dominant closed-loop

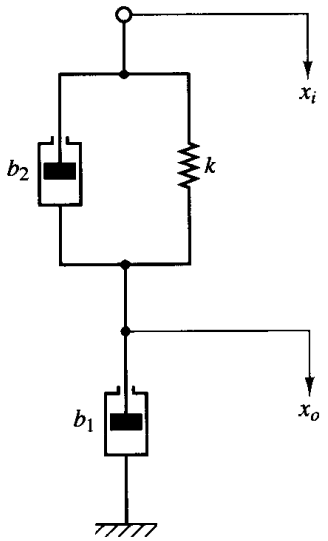

Figure 7–54
Mechanical system.

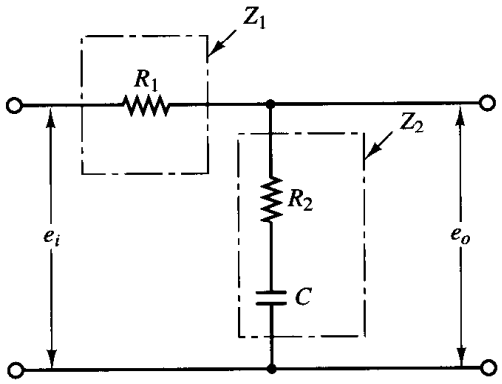

Figure 7–55
Electrical network.

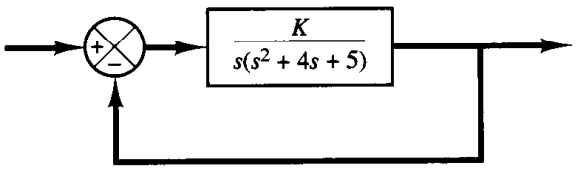

Figure 7–56
Control system.

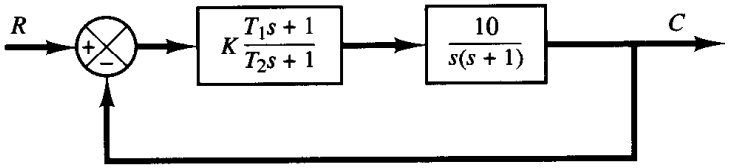

Figure 7–57
Control system.

poles have the damping ratio $\zeta = 0.5$ and the undamped natural frequency $\omega_n = 3$ rad/sec.

B-7-5. Consider the system shown in Figure 7–58, which involves velocity feedback. Determine the values of the amplifier gain K and the velocity feedback gain K_h so that the following specifications are satisfied:

1. Damping ratio of the closed-loop poles is 0.5
2. Settling time ≤ 2 sec
3. Static velocity error constant $K_v \geq 50\ \text{sec}^{-1}$
4. $0 < K_h < 1$

B-7-6. Consider the system shown in Figure 7–59. Design a lead compensator such that the dominant closed-loop poles

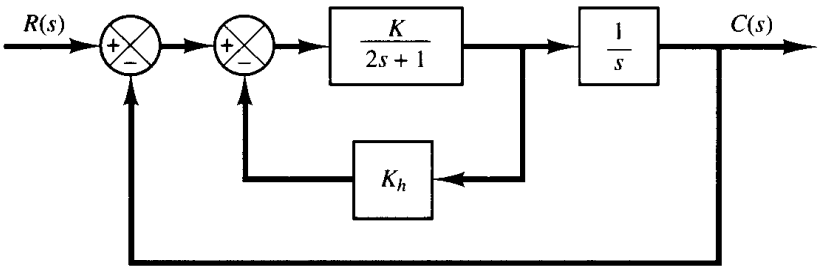

Figure 7–58
Control system.

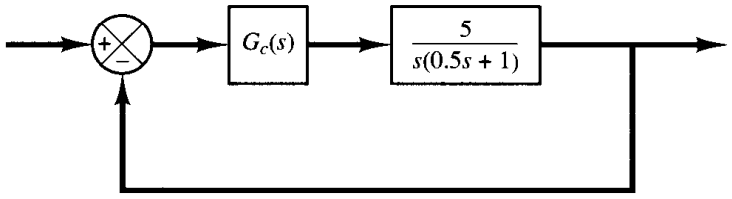

Figure 7–59
Control system.

are located at $s = -2 \pm j2\sqrt{3}$. Plot the unit-step response curve of the designed system with MATLAB.

B-7-7. Consider the system shown in Figure 7–60. Design a compensator such that the dominant closed-loop poles are located at $s = -1 \pm j1$.

B-7-8. Referring to the system shown in Figure 7–61, design a compensator such that the static velocity error constant K_v is 20 sec^{-1} without appreciably changing the original location ($s = -2 \pm j2\sqrt{3}$) of a pair of the complex-conjugate closed-loop poles.

B-7-9. Consider the angular-positional system shown in Figure 7–62. The dominant closed-loop poles are located at $s = -3.60 \pm j4.80$. The damping ratio ζ of the dominant closed-loop poles is 0.6. The static velocity error constant K_v is 4.1 sec^{-1}, which means that for a ramp input of 360°/sec the steady-state error in following the ramp input is

$$e_v = \frac{\theta_i}{K_v} = \frac{360°/\text{sec}}{4.1\ \text{sec}^{-1}} = 87.8°$$

It is desired to decrease e_v to one-tenth of the present value, or to increase the value of the static velocity error constant K_v to 41 sec^{-1}. It is also desired to keep the damping ratio ζ of the dominant closed-loop poles at 0.6. A small change in the undamped natural frequency ω_n of the dominant closed-loop poles is permissible. Design a suitable lag compensator to increase the static velocity error constant as desired.

B-7-10. Consider the control system shown in Figure 7–63. Design a compensator such that the dominant closed-loop poles are located at $s = -2 \pm j2\sqrt{3}$ and the static velocity error constant K_v is 50 sec^{-1}.

B-7-11. Consider the same system as considered in Problem A-7-10. It is desired to design a PID controller $G_c(s)$

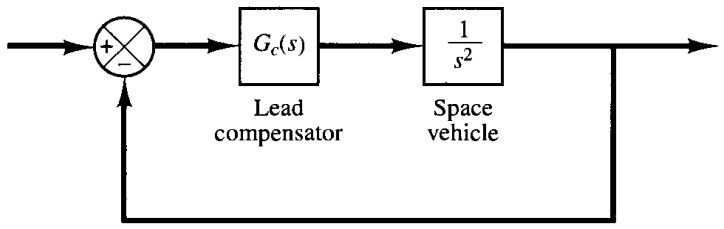

Figure 7–60
Control system.

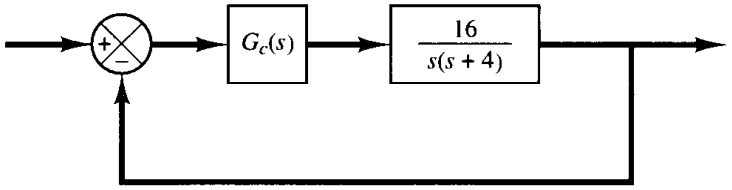

Figure 7–61
Control system.

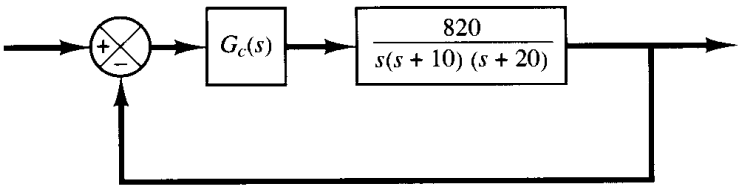

Figure 7–62
Angular-positional system.

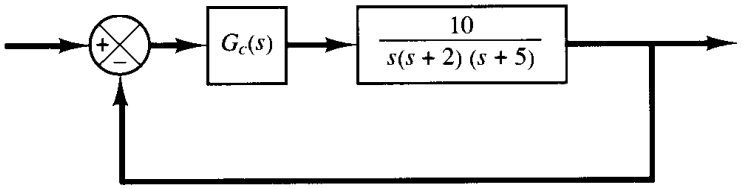

Figure 7–63
Control system.

such that the dominant closed-loop poles are located at $s = -1 \pm j\sqrt{3}$. For the PID controller, choose $a = 0.5$ (instead of $a = 1$ as discussed in Problem A-7-10) and then determine the values of K and b. Sketch the root-locus plot for the designed system. Also, obtain the unit-step response curve with MATLAB.

B-7-12. Consider the control system shown in Figure 7–64. The plant is critically stable in the sense that oscillations will continue indefinitely. Design a suitable compensator such that the unit-step response will exhibit maximum overshoot of less than 40% and settling time of 5 sec or less.

B-7-13. Consider the control system shown in Figure 7–65. Design a compensator such that the unit-step response curve will exhibit maximum overshoot of 30% or less and settling time of 3 sec or less.

B-7-14. Consider the control system shown in Figure 7–66. Design a compensator such that the unit-step response curve will exhibit maximum overshoot of 25% or less and settling time of 5 sec or less.

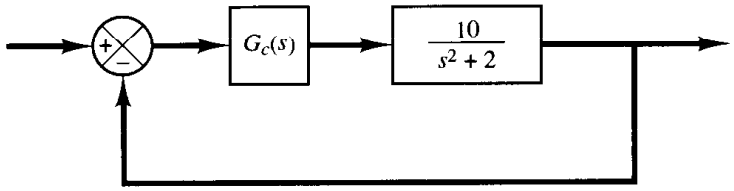

Figure 7–64
Control system.

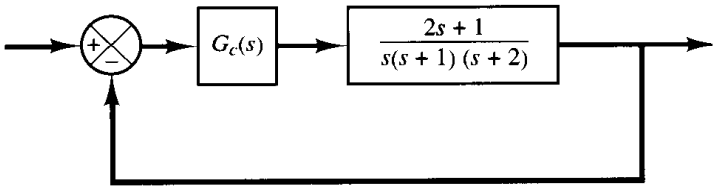

Figure 7–65
Control system.

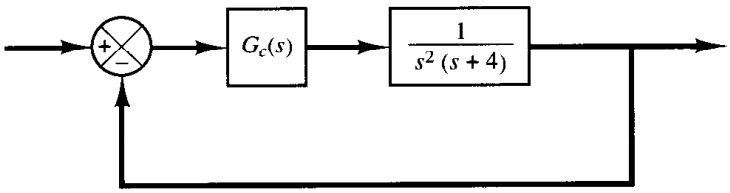

Figure 7–66
Control system.

8

Frequency-Response Analysis

8–1 INTRODUCTION

By the term *frequency response*, we mean the steady-state response of a system to a sinusoidal input. In frequency-response methods, we vary the frequency of the input signal over a certain range and study the resulting response.

The Nyquist stability criterion enables us to investigate both the absolute and relative stabilities of linear closed-loop systems from a knowledge of their open-loop frequency-response characteristics. An advantage of the frequency-response approach is that frequency-response tests are, in general, simple and can be made accurately by use of readily available sinusoidal signal generators and precise measurement equipment. Often the transfer functions of complicated components can be determined experimentally by frequency-response tests. In addition, the frequency-response approach has the advantages that a system may be designed so that the effects of undesirable noise are negligible and that such analysis and design can be extended to certain nonlinear control systems.

Although the frequency response of a control system presents a qualitative picture of the transient response, the correlation between frequency and transient responses is indirect, except for the case of second-order systems. In designing a closed-loop system, we adjust the frequency-response characteristic of the open-loop transfer function by using several design criteria in order to obtain acceptable transient-response characteristics for the system.

Steady-state output to sinusoidal input. Consider the linear time-invariant system shown in Figure 8–1. For this system

$$\frac{Y(s)}{X(s)} = G(s)$$

The input $x(t)$ is sinusoidal and is given by

$$x(t) = X \sin \omega t$$

As presented in Chapter 5, if the system is stable, then the output $y(t)$ can be given by

$$y(t) = Y \sin(\omega t + \phi)$$

where

$$Y = X|G(j\omega)|$$

and

$$\phi = \underline{/G(j\omega)} = \tan^{-1}\left[\frac{\text{imaginary part of } G(j\omega)}{\text{real part of } G(j\omega)}\right]$$

A stable linear time-invariant system subjected to a sinusoidal input will, at steady state, have a sinusoidal output of the same frequency as the input. But the amplitude and phase of the output will, in general, be different from those of the input. In fact, the amplitude of the output is given by the product of that of the input and $|G(j\omega)|$, while the phase angle differs from that of the input by the amount $\phi = \underline{/G(j\omega)}$. An example of input and output sinusoidal signals is shown in Figure 8–2.

Note that for sinusoidal inputs

$$|G(j\omega)| = \left|\frac{Y(j\omega)}{X(j\omega)}\right| = \text{amplitude ratio of the output sinusoid to the input sinusoid}$$

$$\underline{/G(j\omega)} = \underline{/\frac{Y(j\omega)}{X(j\omega)}} = \text{phase shift of the output sinusoid with respect to the input sinusoid}$$

Hence, the response characteristics of a system to a sinusoidal input can be obtained directly from

$$\frac{Y(j\omega)}{X(j\omega)} = G(j\omega)$$

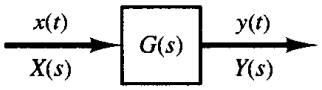

Figure 8–1
Linear time-invariant system.

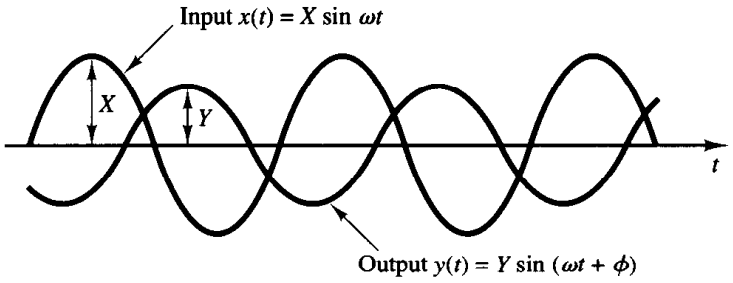

Figure 8–2
Input and output sinusoidal signals.

The sinusoidal transfer function $G(j\omega)$, the ratio of $Y(j\omega)$ to $X(j\omega)$, is a complex quantity and can be represented by the magnitude and phase angle with frequency as a parameter. (A negative phase angle is called *phase lag,* and a positive phase angle is called *phase lead.*) The sinusoidal transfer function of any linear system is obtained by substituting $j\omega$ for s in the transfer function of the system.

Presenting frequency-response characteristics in graphical forms. The sinusoidal transfer function, a complex function of the frequency ω, is characterized by its magnitude and phase angle, with frequency as the parameter. There are three commonly used representations of sinusoidal transfer functions:

1. Bode diagram or logarithmic plot
2. Nyquist plot or polar plot
3. Log-magnitude versus phase plot

We shall discuss these representations in detail in this chapter. We shall also discuss the MATLAB approach to obtain Bode diagrams and Nyquist plots.

Outline of the chapter. Section 8–1 has presented introductory material on the frequency response. Section 8–2 presents Bode diagrams of various transfer-function systems. Section 8–3 discusses a computational approach to obtain Bode diagrams with MATLAB, Section 8–4 treats polar plots of sinusoidal transfer functions, and Section 8–5 discusses drawing Nyquist plots with MATLAB. Section 8–6 briefly presents log-magnitude versus phase plots. Section 8–7 gives a detailed account of Nyquist stability criterion, Section 8–8 discusses the stability analysis of closed-loop systems using the Nyquist stability criterion, and Section 8–9 treats the relative stability analysis of closed-loop systems. Measures of relative stability such as phase margin and gain margin are introduced here. The correlation between the transient response and frequency response is also discussed. Section 8–10 presents a method for obtaining the closed-loop frequency response from the open-loop frequency response by use of the M and N circles. Use of the Nichols chart is also discussed for obtaining the closed-loop frequency response. Finally, Section 8–11 deals with the determination of the transfer function based on an experimental Bode diagram.

8–2 BODE DIAGRAMS

Bode diagrams or logarithmic plots. A sinusoidal transfer function may be represented by two separate plots, one giving the magnitude versus frequency and the other the phase angle (in degrees) versus frequency. A Bode diagram consists of two graphs: One is a plot of the logarithm of the magnitude of a sinusoidal transfer function; the other is a plot of the phase angle; both are plotted against the frequency in logarithmic scale.

The standard representation of the logarithmic magnitude of $G(j\omega)$ is $20 \log |G(j\omega)|$, where the base of the logarithm is 10. The unit used in this representation of the magnitude is the decibel, usually abbreviated dB. In the logarithmic representation, the curves are drawn on semilog paper, using the log scale for frequency and the linear scale

for either magnitude (but in decibels) or phase angle (in degrees). (The frequency range of interest determines the number of logarithmic cycles required on the abscissa.)

The main advantage of using the Bode diagram is that multiplication of magnitudes can be converted into addition. Furthermore, a simple method for sketching an approximate log-magnitude curve is available. It is based on asymptotic approximations. Such approximation by straight-line asymptotes is sufficient if only rough information on the frequency-response characteristics is needed. Should exact curve be desired, corrections can be made easily to these basic asymptotic ones. The phase-angle curves can be drawn easily if a template for the phase-angle curve of $1 + j\omega$ is available. Expanding the low-frequency range by use of a logarithmic scale for the frequency is very advantageous since characteristics at low frequencies are most important in practical systems. Although it is not possible to plot the curves right down to zero frequency because of the logarithmic frequency ($\log 0 = -\infty$), this does not create a serious problem.

Note that the experimental determination of a transfer function can be made simple if frequency-response data are presented in the form of a Bode diagram.

Basic factors of $G(j\omega)H(j\omega)$. As stated earlier, the main advantage in using the logarithmic plot is the relative ease of plotting frequency-response curves. The basic factors that very frequently occur in an arbitrary transfer function $G(j\omega)H(j\omega)$ are

1. Gain K
2. Integral and derivative factors $(j\omega)^{\mp 1}$
3. First-order factors $(1 + j\omega T)^{\mp 1}$
4. Quadratic factors $[1 + 2\zeta(j\omega/\omega_n) + (j\omega/\omega_n)^2]^{\mp 1}$

Once we become familiar with the logarithmic plots of these basic factors, it is possible to utilize them in constructing a composite logarithmic plot for any general form of $G(j\omega)H(j\omega)$ by sketching the curves for each factor and adding individual curves graphically, because adding the logarithms of the gains corresponds to multiplying them together.

The process of obtaining the logarithmic plot can be further simplified by using asymptotic approximations to the curves for each factor. (If necessary, corrections can be made easily to an approximate plot to obtain an accurate one.)

The gain K. A number greater than unity has a positive value in decibels, while a number smaller than unity has a negative value. The log-magnitude curve for a constant gain K is a horizontal straight line at the magnitude of $20 \log K$ decibels. The phase angle of the gain K is zero. The effect of varying the gain K in the transfer function is that it raises or lowers the log-magnitude curve of the transfer function by the corresponding constant amount, but it has no effect on the phase curve.

A number–decibel conversion line is given in Figure 8–3. The decibel value of any number can be obtained from this line. As a number increases by a factor of 10, the corresponding decibel value increases by a factor of 20. This may be seen from the following:

$$20 \log(K \times 10) = 20 \log K + 20$$

Similarly,

$$20 \log (K \times 10^n) = 20 \log K + 20n$$

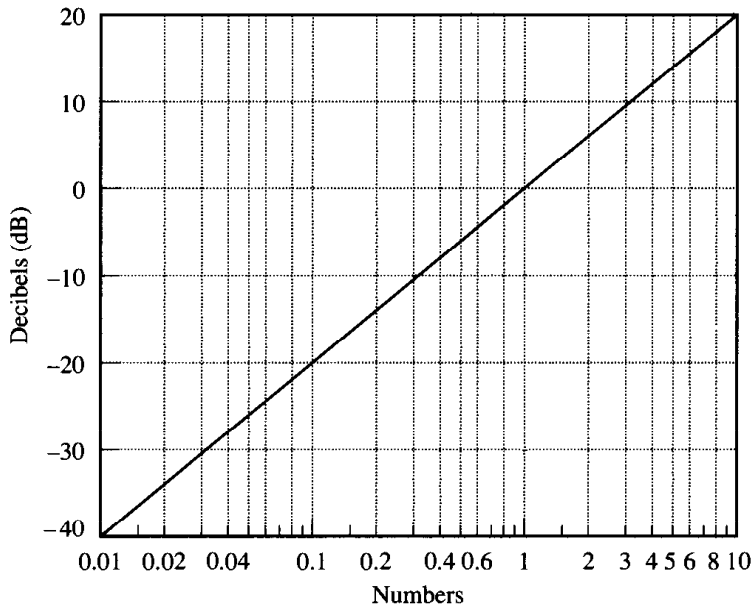

Figure 8–3
Number–decibel conversion line.

Note that, when expressed in decibels, the reciprocal of a number differs from its value only in sign; that is, for the number K,

$$20 \log K = -20 \log \frac{1}{K}$$

Integral and derivative factors $(j\omega)^{\mp 1}$. The logarithmic magnitude of $1/j\omega$ in decibels is

$$20 \log \left| \frac{1}{j\omega} \right| = -20 \log \omega \text{ dB}$$

The phase angle of $1/j\omega$ is constant and equal to $-90°$.

In Bode diagrams, frequency ratios are expressed in terms of octaves or decades. An octave is a frequency band from ω_1 to $2\omega_1$, where ω_1 is any frequency value. A decade is a frequency band from ω_1 to $10\omega_1$, where again ω_1 is any frequency. (On the logarithmic scale of semilog paper, any given frequency ratio can be represented by the same horizontal distance. For example, the horizontal distance from $\omega = 1$ to $\omega = 10$ is equal to that from $\omega = 3$ to $\omega = 30$.)

If the log magnitude $-20 \log \omega$ dB is plotted against ω on a logarithmic scale, it is a straight line. To draw this straight line, we need to locate one point (0 dB, $\omega = 1$) on it. Since

$$(-20 \log 10\omega) \text{ dB} = (-20 \log \omega - 20) \text{ dB}$$

the slope of the line is -20 dB/decade (or -6 dB/octave).

Similarly, the log magnitude of $j\omega$ in decibels is

$$20 \log |j\omega| = 20 \log \omega \text{ dB}$$

The phase angle of $j\omega$ is constant and equal to 90°. The log-magnitude curve is a straight line with a slope of 20 dB/decade. Figures 8–4 (a) and (b) show frequency-response

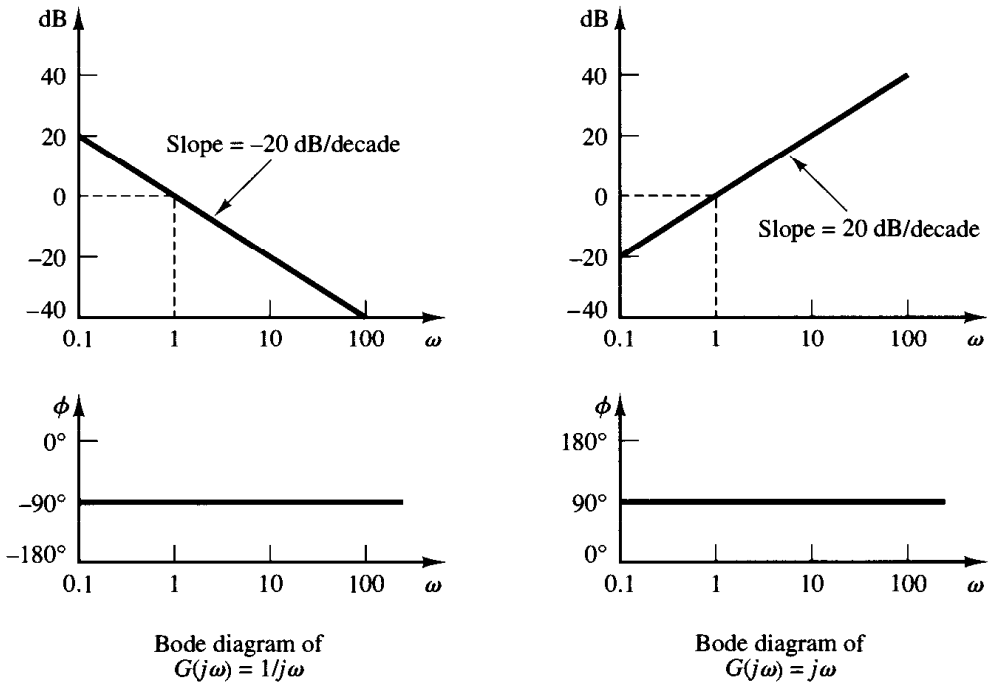

Bode diagram of $G(j\omega) = 1/j\omega$

(a)

Bode diagram of $G(j\omega) = j\omega$

(b)

Figure 8–4
(a) Bode diagram of $G(j\omega) = 1/j\omega$; (b) Bode diagram of $G(j\omega) = j\omega$.

curves for $1/j\omega$ and $j\omega$, respectively. We can clearly see that the differences in the frequency responses of the factors $1/j\omega$ and $j\omega$ lie in the signs of the slopes of the log-magnitude curves and in the signs of the phase angles. Both log magnitudes become equal to 0 dB at $\omega = 1$.

If the transfer function contains the factor $(1/j\omega)^n$ or $(j\omega)^n$, the log magnitude becomes, respectively,

$$20 \log \left| \frac{1}{(j\omega)^n} \right| = -n \times 20 \log |j\omega| = -20n \log \omega \text{ dB}$$

or

$$20 \log |(j\omega)^n| = n \times 20 \log |j\omega| = 20n \log \omega \text{ dB}$$

The slopes of the log-magnitude curves for the factors $(1/j\omega)^n$ and $(j\omega)^n$ are thus $-20n$ dB/decade and $20n$ dB/decade, respectively. The phase angle of $(1/j\omega)^n$ is equal to $-90° \times n$ over the entire frequency range, while that of $(j\omega)^n$ is equal to $90° \times n$ over the entire frequency range. The magnitude curves will pass through the point (0 dB, $\omega = 1$).

First-order factors $(1 + j\omega T)^{\mp 1}$. The log magnitude of the first-order factor $1/(1 + j\omega T)$ is

$$20 \log \left| \frac{1}{1 + j\omega T} \right| = -20 \log \sqrt{1 + \omega^2 T^2} \text{ dB}$$

For low frequencies, such that $\omega \ll 1/T$, the log magnitude may be approximated by

$$-20 \log \sqrt{1 + \omega^2 T^2} \doteq -20 \log 1 = 0 \text{ dB}$$

Thus, the log-magnitude curve at low frequencies is the constant 0-dB line. For high frequencies, such that $\omega \gg 1/T$,

$$-20 \log \sqrt{1 + \omega^2 T^2} \doteq -20 \log \omega T \text{ dB}$$

This is an approximate expression for the high-frequency range. At $\omega = 1/T$, the log magnitude equals 0 dB; at $\omega = 10/T$, the log magnitude is -20 dB. Thus, the value of $-20 \log \omega T$ dB decreases by 20 dB for every decade of ω. For $\omega \gg 1/T$, the log-magnitude curve is thus a straight line with a slope of -20 dB/decade (or -6 dB/octave).

Our analysis show that the logarithmic representation of the frequency-response curve of the factor $1/(1 + j\omega T)$ can be approximated by two straight-line asymptotes, one a straight line at 0 dB for the frequency range $0 < \omega < 1/T$ and the other a straight line with slope -20 dB/decade (or -6 dB/octave) for the frequency range $1/T < \omega < \infty$. The exact log-magnitude curve, the asymptotes, and the exact phase-angle curve are shown in Figure 8–5.

The frequency at which the two asymptotes meet is called the *corner* frequency or *break* frequency. For the factor $1/(1 + j\omega T)$, the frequency $\omega = 1/T$ is the corner frequency since at $\omega = 1/T$ the two asymptotes have the same value. (The low-frequency asymptotic expression at $\omega = 1/T$ is 20 log 1 dB = 0 dB, and the high-frequency asymptotic expression at $\omega = 1/T$ is also 20 log 1 dB = 0 dB.) The corner frequency divides the frequency-response curve into two regions, a curve for the low-frequency region and a curve for the high-frequency region. The corner frequency is very important in sketching logarithmic frequency-response curves.

The exact phase angle ϕ of the factor $1/(1 + j\omega T)$ is

$$\phi = -\tan^{-1} \omega T$$

At zero frequency, the phase angle is 0°. At the corner frequency, the phase angle is

$$\phi = -\tan^{-1} \frac{T}{T} = -\tan^{-1} 1 = -45°$$

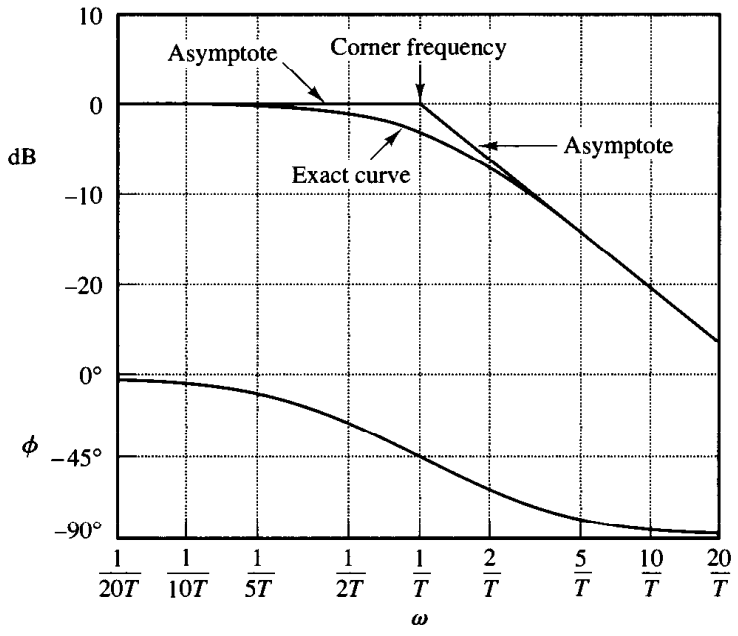

Figure 8–5
Log-magnitude curve together with the asymptotes and phase angle curve of $1/(1 + j\omega T)$.

At infinity, the phase angle becomes $-90°$. Since the phase angle is given by an inverse-tangent function, the phase angle is skew symmetric about the inflection point at $\phi = -45°$.

The error in the magnitude curve caused by the use of asymptotes can be calculated. The maximum error occurs at the corner frequency and is approximately equal to -3 dB since

$$-20 \log \sqrt{1 + 1} + 20 \log 1 = -10 \log 2 = -3.03 \text{ dB}$$

The error at the frequency one octave below the corner frequency, that is, at $\omega = 1/(2T)$, is

$$-20 \log \sqrt{\frac{1}{4} + 1} + 20 \log 1 = -20 \log \frac{\sqrt{5}}{2} = -0.97 \text{ dB}$$

The error at the frequency one octave above the corner frequency, that is, at $\omega = 2/T$, is

$$-20 \log \sqrt{2^2 + 1} + 20 \log 2 = -20 \log \frac{\sqrt{5}}{2} = -0.97 \text{ dB}$$

Thus, the error at one octave below or above the corner frequency is approximately equal to -1 dB. Similarly, the error at one decade below or above the corner frequency is approximately -0.04 dB. The error in decibels involved in using the asymptotic expression for the frequency-response curve of $1/(1 + j\omega T)$ is shown in Figure 8–6. The error is symmetric with respect to the corner frequency.

Since the asymptotes are quite easy to draw and are sufficiently close to the exact curve, the use of such approximations in drawing Bode diagrams is convenient in establishing the general nature of the frequency-response characteristics quickly with a minimum amount of calculation and may be used for most preliminary design work. If accurate frequency-response curves are desired, corrections may easily be made by referring to the curve given in Figure 8–6. In practice, an accurate frequency-response curve can be drawn by introducing a correction of 3 dB at the corner frequency and a correction of 1 dB at points one octave below and above the corner frequency and then connecting these points by a smooth curve.

Note that varying the time constant T shifts the corner frequency to the left or to the right, but the shapes of the log-magnitude and the phase-angle curves remain the same.

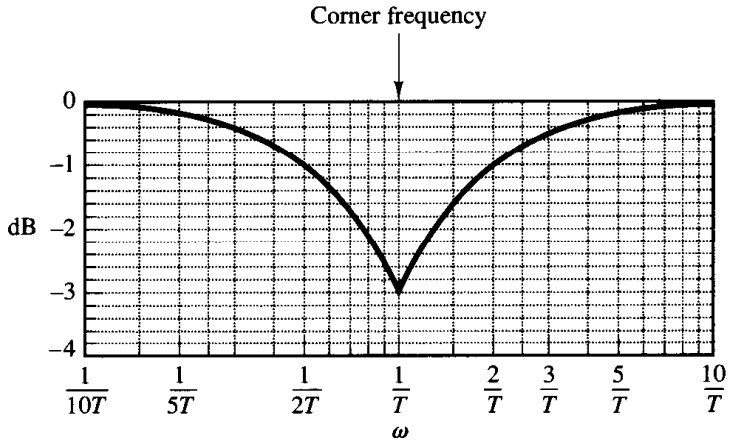

Figure 8–6
Log-magnitude error in the asymptotic expression of the frequency-response curve of $1/(1 + j\omega T)$.

The transfer function $1/(1 + j\omega T)$ has the characteristics of a low-pass filter. For frequencies above $\omega = 1/T$, the log magnitude falls off rapidly toward $-\infty$. This is essentially due to the presence of the time constant. In the low-pass filter, the output can follow a sinusoidal input faithfully at low frequencies. But as the input frequency is increased, the output cannot follow the input because a certain amount of time is required for the system to build up in magnitude. Thus, at high frequencies, the amplitude of the output approaches zero and the phase angle of the output approaches $-90°$. Therefore, if the input function contains many harmonics, then the low-frequency components are reproduced faithfully at the output, while the high-frequency components are attenuated in amplitude and shifted in phase. Thus, a first-order element yields exact, or almost exact, duplication only for constant or slowly varying phenomena.

An advantage of the Bode diagram is that for reciprocal factors, for example, the factor $1 + j\omega T$, the log-magnitude and the phase-angle curves need only be changed in sign. Since

$$20 \log |1 + j\omega T| = -20 \log \left| \frac{1}{1 + j\omega T} \right|$$

$$\underline{/1 + j\omega T} = \tan^{-1} \omega T = -\underline{/\frac{1}{1 + j\omega T}}$$

the corner frequency is the same for both cases. The slope of the high-frequency asymptote of $1 + j\omega T$ is 20 dB/decade, and the phase angle varies from 0° to 90° as the frequency ω is increased from zero to infinity. The log-magnitude curve together with the asymptotes and the phase-angle curve for the factor $1 + j\omega T$ are shown in Figure 8–7.

The shapes of phase-angle curves are the same for any factor of the form $(1 + j\omega T)^{\mp 1}$. Hence, it is convenient to have a template for the phase-angle curve on cardboard. Then such a template may be used repeatedly for constructing phase-angle

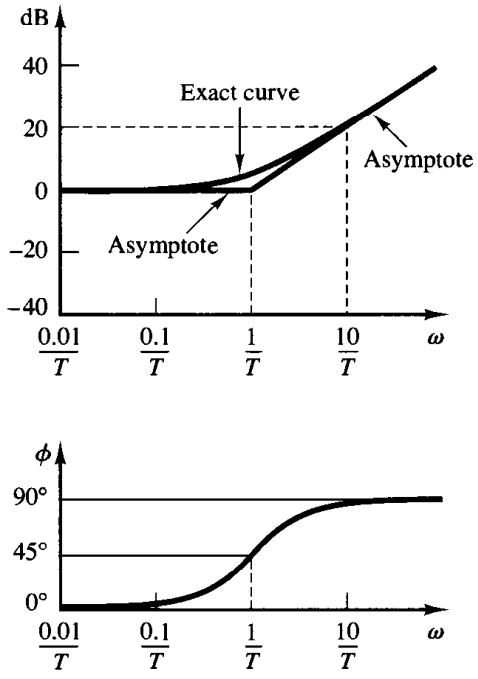

Figure 8–7
Log-magnitude curve together with the asymptotes and phase-angle curve for $1 + j\omega T$.

curves for any function of the form $(1 + j\omega T)^{\mp 1}$. If such a template is not available, we have to locate several points on the curve. The phase angles of $(1 + j\omega T)^{\mp 1}$ are

$$\mp 45° \quad \text{at} \quad \omega = \frac{1}{T}$$

$$\mp 26.6° \quad \text{at} \quad \omega = \frac{1}{2T}$$

$$\mp 5.7° \quad \text{at} \quad \omega = \frac{1}{10T}$$

$$\mp 63.4° \quad \text{at} \quad \omega = \frac{2}{T}$$

$$\mp 84.3° \quad \text{at} \quad \omega = \frac{10}{T}$$

For the case where a given transfer function involves terms like $(1 + j\omega T)^{\mp n}$, a similar asymptotic construction may be made. The corner frequency is still at $\omega = 1/T$, and the asymptotes are straight lines. The low-frequency asymptote is a horizontal straight line at 0 dB, while the high-frequency asymptote has the slope of $-20n$ dB/decade or $20n$ dB/decade. The error involved in the asymptotic expressions is n times that for $(1 + j\omega T)^{\mp 1}$. The phase angle is n times that of $(1 + j\omega T)^{\mp 1}$ at each frequency point.

Quadratic factors $[1 + 2\zeta(j\omega/\omega_n) + (j\omega/\omega_n)^2]^{\mp 1}$. Control systems often possess quadratic factors of the form

$$\frac{1}{1 + 2\zeta\left(j\frac{\omega}{\omega_n}\right) + \left(j\frac{\omega}{\omega_n}\right)^2} \tag{8-1}$$

If $\zeta > 1$, this quadratic factor can be expressed as a product of two first-order factors with real poles. If $0 < \zeta < 1$, this quadratic factor is the product of two complex-conjugate factors. Asymptotic approximations to the frequency-response curves are not accurate for a factor with low values of ζ. This is because the magnitude and phase of the quadratic factor depend on both the corner frequency and the damping ratio ζ.

The asymptotic frequency-response curve may be obtained as follows: Since

$$20 \log \left| \frac{1}{1 + 2\zeta\left(j\frac{\omega}{\omega_n}\right) + \left(j\frac{\omega}{\omega_n}\right)^2} \right| = -20 \log \sqrt{\left(1 - \frac{\omega^2}{\omega_n^2}\right)^2 + \left(2\zeta\frac{\omega}{\omega_n}\right)^2}$$

for low frequencies such that $\omega \ll \omega_n$, the log magnitude becomes

$$-20 \log 1 = 0 \text{ dB}$$

The low-frequency asymptote is thus a horizontal line at 0 dB. For high frequencies such that $\omega \gg \omega_n$, the log magnitude becomes

$$-20 \log \frac{\omega^2}{\omega_n^2} = -40 \log \frac{\omega}{\omega_n} \text{ dB}$$

The equation for the high-frequency asymptote is a straight line having the slope −40 dB/decade since

$$-40 \log \frac{10\omega}{\omega_n} = -40 - 40 \log \frac{\omega}{\omega_n}$$

The high-frequency asymptote intersects the low-frequency one at $\omega = \omega_n$ since at this frequency

$$-40 \log \frac{\omega_n}{\omega_n} = -40 \log 1 = 0 \text{ dB}$$

This frequency, ω_n, is the corner frequency for the quadratic factor considered.

The two asymptotes just derived are independent of the value of ζ. Near the frequency $\omega = \omega_n$, a resonant peak occurs, as may be expected from (8–1). The damping ratio ζ determines the magnitude of this resonant peak. Errors obviously exist in the approximation by straight-line asymptotes. The magnitude of the error depends on the value of ζ. It is large for small values of ζ. Figure 8–8 shows the exact log-magnitude curves together with the straight-line asymptotes and the exact phase-angle curves for the quadratic factor given by (8–1) with several values of ζ. If corrections are desired in the asymptotic curves, the necessary amounts of correction at a sufficient number of frequency points may be obtained from Figure 8–8.

The phase angle of the quadratic factor $[1 + 2\zeta(j\omega/\omega_n) + (j\omega/\omega_n)^2]^{-1}$ is

$$\phi = \angle \frac{1}{1 + 2\zeta\left(j\frac{\omega}{\omega_n}\right) + \left(j\frac{\omega}{\omega_n}\right)^2} = -\tan^{-1}\left[\frac{2\zeta\frac{\omega}{\omega_n}}{1 - \left(\frac{\omega}{\omega_n}\right)^2}\right] \tag{8–2}$$

The phase angle is a function of both ω and ζ. At $\omega = 0$, the phase angle equals 0°. At the corner frequency $\omega = \omega_n$, the phase angle is −90° regardless of ζ since

$$\phi = -\tan^{-1}\left(\frac{2\zeta}{0}\right) = -\tan^{-1}\infty = -90°$$

At $\omega = \infty$, the phase angle becomes −180°. The phase-angle curve is skew symmetric about the inflection point, the point where $\phi = -90°$. There are no simple ways to sketch such phase curves. We need to refer to the phase-angle curves shown in Figure 8–8.

The frequency-response curves for the factor

$$1 + 2\zeta\left(j\frac{\omega}{\omega_n}\right) + \left(j\frac{\omega}{\omega_n}\right)^2$$

can be obtained by merely reversing the sign of the log magnitude and that of the phase angle of the factor

$$\frac{1}{1 + 2\zeta\left(j\frac{\omega}{\omega_n}\right) + \left(j\frac{\omega}{\omega_n}\right)^2}$$

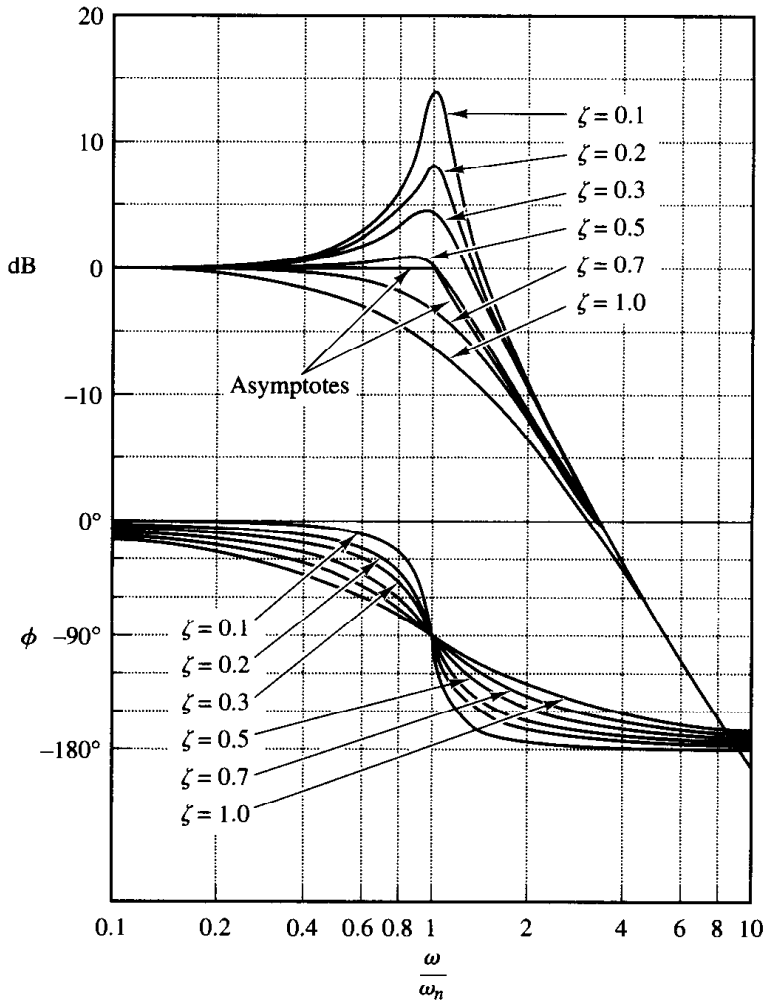

Figure 8–8
Log-magnitude curves together with the asymptotes and phase-angle curves of the quadratic transfer function given by (8–1).

To obtain the frequency-response curves of a given quadratic transfer function, we must first determine the value of the corner frequency ω_n and that of the damping ratio ζ. Then, by using the family of curves given in Figure 8–8, the frequency-response curves can be plotted.

The resonant frequency ω_r and the resonant peak value M_r. The magnitude of

$$G(j\omega) = \frac{1}{1 + 2\zeta\left(j\frac{\omega}{\omega_n}\right) + \left(j\frac{\omega}{\omega_n}\right)^2}$$

is

$$|G(j\omega)| = \frac{1}{\sqrt{\left(1 - \frac{\omega^2}{\omega_n^2}\right)^2 + \left(2\zeta\frac{\omega}{\omega_n}\right)^2}} \tag{8-3}$$

If $|G(j\omega)|$ has a peak value at some frequency, this frequency is called the *resonant* frequency. Since the numerator of $|G(j\omega)|$ is constant, a peak value of $|G(j\omega)|$ will occur when

$$g(\omega) = \left(1 - \frac{\omega^2}{\omega_n^2}\right)^2 + \left(2\zeta\frac{\omega}{\omega_n}\right)^2 \tag{8-4}$$

is a minimum. Since Equation (8–4) can be written

$$g(\omega) = \left[\frac{\omega^2 - \omega_n^2(1 - 2\zeta^2)}{\omega_n^2}\right]^2 + 4\zeta^2(1 - \zeta^2) \tag{8-5}$$

the minimum value of $g(\omega)$ occurs at $\omega = \omega_n\sqrt{1 - 2\zeta^2}$. Thus the resonant frequency ω_r is

$$\omega_r = \omega_n\sqrt{1 - 2\zeta^2}, \qquad \text{for } 0 \le \zeta \le 0.707 \tag{8-6}$$

As the damping ratio ζ approaches zero, the resonant frequency approaches ω_n. For $0 < \zeta \le 0.707$, the resonant frequency ω_r is less than the damped natural frequency $\omega_d = \omega_n\sqrt{1 - \zeta^2}$, which is exhibited in the transient response. From Equation (8–6) it can be seen that for $\zeta > 0.707$ there is no resonant peak. The magnitude $|G(j\omega)|$ decreases monotonically with increasing frequency ω. (The magnitude is less than 0 dB for all values of $\omega > 0$. Recall that, for $0.7 < \zeta < 1$, the step response is oscillatory, but the oscillations are well damped and are hardly perceptible.)

The magnitude of the resonant peak M_r can be found by substituting Equation (8–6) into Equation (8–3). For $0 \le \zeta \le 0.707$,

$$M_r = |G(j\omega)|_{\max} = |G(j\omega_r)| = \frac{1}{2\zeta\sqrt{1 - \zeta^2}} \tag{8-7}$$

For $\zeta > 0.707$,

$$M_r = 1 \tag{8-8}$$

As ζ approaches zero, M_r approaches infinity. This means that if the undamped system is excited at its natural frequency the magnitude of $G(j\omega)$becomes infinity. The relationship between M_r and ζ is shown in Figure 8–9.

The phase angle of $G(j\omega)$ at the frequency where the resonant peak occurs can be obtained by substituting Equation (8–6) into Equation (8–2). Thus, at the resonant frequency ω_r,

$$\angle G(j\omega_r) = -\tan^{-1}\frac{\sqrt{1 - 2\zeta^2}}{\zeta} = -90° + \sin^{-1}\frac{\zeta}{\sqrt{1 - \zeta^2}}$$

General procedure for plotting Bode diagrams. First rewrite the sinusoidal-transfer function $G(j\omega)H(j\omega)$ as a product of basic factors discussed above. Then

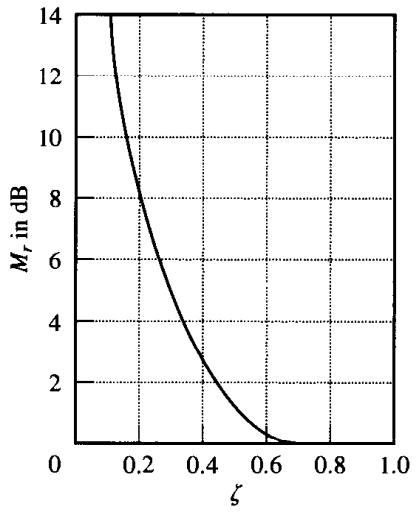

Figure 8–9
M_r versus ζ curve for the second-order system $1/[1 + 2\zeta(j\omega/\omega_n) + (j\omega/\omega_n)^2]$.

identify the corner frequencies associated with these basic factors. Finally, draw the asymptotic log-magnitude curves with proper slopes between the corner frequencies. The exact curve, which lies close to the asymptotic curve, can be obtained by adding proper corrections.

The phase-angle curve of $G(j\omega)H(j\omega)$ can be drawn by adding the phase-angle curves of individual factors.

The use of Bode diagrams employing asymptotic approximations requires much less time than other methods that may be used for computing the frequency response of a transfer function. The ease of plotting the frequency-response curves for a given transfer function and the ease of modification of the frequency-response curve as compensation is added are the main reasons why Bode diagrams are very frequently used in practice.

EXAMPLE 8–1 Draw the Bode diagram for the following transfer function:

$$G(j\omega) = \frac{10(j\omega + 3)}{(j\omega)(j\omega + 2)[(j\omega)^2 + j\omega + 2]}$$

Make corrections so that the log-magnitude curve is accurate.

To avoid any possible mistakes in drawing the log-magnitude curve, it is desirable to put $G(j\omega)$ in the following normalized form, where the low-frequency asymptotes for the first-order factors and the second-order factor are the 0-dB line.

$$G(j\omega) = \frac{7.5\left(\frac{j\omega}{3} + 1\right)}{(j\omega)\left(\frac{j\omega}{2} + 1\right)\left[\frac{(j\omega)^2}{2} + \frac{j\omega}{2} + 1\right]}$$

This function is composed of the following factors:

$$7.5, \quad (j\omega)^{-1}, \quad 1 + j\frac{\omega}{3}, \quad \left(1 + j\frac{\omega}{2}\right)^{-1}, \quad \left[1 + j\frac{\omega}{2} + \frac{(j\omega)^2}{2}\right]^{-1}$$

The corner frequencies of the third, fourth, and fifth terms are $\omega = 3$, $\omega = 2$, and $\omega = \sqrt{2}$, respectively. Note that the last term has the damping ratio of 0.3536.

To plot the Bode diagram, the separate asymptotic curves for each of the factors are shown in Figure 8–10. The composite curve is then obtained by adding algebraically the individual curves, also shown in Figure 8–10. Note that when the individual asymptotic curves are added at each frequency the slope of the composite curve is cumulative. Below $\omega = \sqrt{2}$, the plot has the slope of −20 dB/decade. At the first corner frequency $\omega = \sqrt{2}$, the slope changes to −60 dB/decade and continues to the next corner frequency $\omega = 2$, where the slope becomes −80 dB/decade. At the last corner frequency $\omega = 3$, the slope changes to −60 dB/decade.

Once such an approximate log-magnitude curve has been drawn, the actual curve can be obtained by adding corrections at each corner frequency and at frequencies one octave below and above the corner frequencies. For first-order factors $(1 + j\omega T)^{\mp 1}$, the corrections are ±3 dB at the corner frequency and ±1 dB at the frequencies one octave below and above the corner frequency. Corrections necessary for the quadratic factor are obtained from Figure 8–8. The exact log-magnitude curve for $G(j\omega)$ is shown by a dashed curve in Figure 8–10.

Note that any change in the slope of the magnitude curve is made only at the corner frequencies of the transfer function $G(j\omega)$. Therefore, instead of drawing individual magnitude curves and adding them up, as shown, we may sketch the magnitude curve without sketching individual curves. We may start drawing the lowest-frequency portion of the straight line (that is, the straight

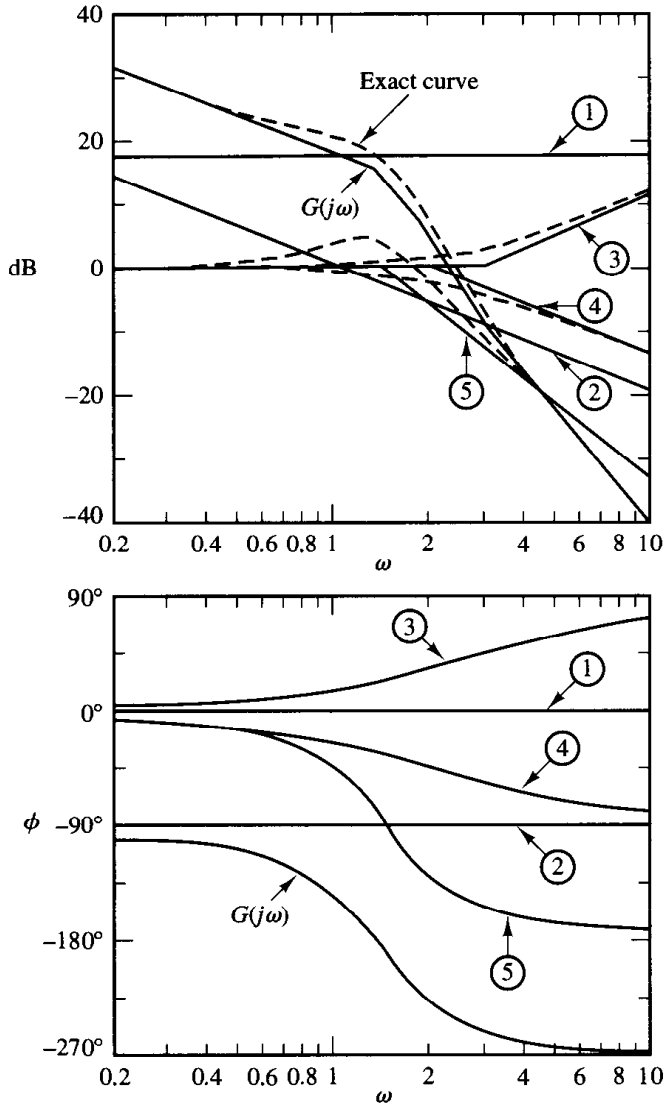

Figure 8–10
Bode diagram of the system considered in Example 8–1.

line with the slope −20 dB/decade for $\omega < \sqrt{2}$). As the frequency is increased, we get the effect of the complex-conjugate poles (quadratic term) at the corner frequency $\omega = \sqrt{2}$. The complex-conjugate poles cause the slopes of the magnitude curve to change from −20 to −60 dB/decade. At the next corner frequency, $\omega = 2$, the effect of the pole is to change the slope to −80 dB/decade. Finally, at the corner frequency $\omega = 3$, the effect of the zero is to change the slope from −80 to −60 dB/decade.

For plotting the complete phase-angle curve, the phase-angle curves for all factors have to be sketched. The algebraic sum of all phase-angle curves provides the complete phase-angle curve, as shown in Figure 8–10.

Minimum-phase systems and nonminimum-phase systems. Transfer functions having neither poles nor zeros in the right-half s plane are minimum-phase transfer functions, whereas those having poles and/or zeros in the right-half s plane are nonminimum-phase transfer functions. Systems with minimum-phase transfer functions are called *minimum-phase* systems, whereas those with nonminimum-phase transfer functions are called *nonminimum-phase* systems.

For systems with the same magnitude characteristic, the range in phase angle of the minimum-phase transfer function is minimum among all such systems, while the range in phase angle of any nonminimum-phase transfer function is greater than this minimum.

It is noted that for a minimum-phase system the transfer function can be uniquely determined from the magnitude curve alone. For a nonminimum-phase system, this is not the case. Multiplying any transfer function by all-pass filters does not alter the magnitude curve, but the phase curve is changed.

Consider as an example the two systems whose sinusoidal transfer functions are, respectively,

$$G_1(j\omega) = \frac{1 + j\omega T}{1 + j\omega T_1}, \qquad G_2(j\omega) = \frac{1 - j\omega T}{1 + j\omega T_1} \qquad 0 < T < T_1$$

The pole–zero configurations of these systems are shown in Figure 8–11. The two sinusoidal transfer functions have the same magnitude characteristics, but they have different phase-angle characteristics, as shown in Figure 8–12. These two systems differ from each other by the factor

$$G(j\omega) = \frac{1 - j\omega T}{1 + j\omega T}$$

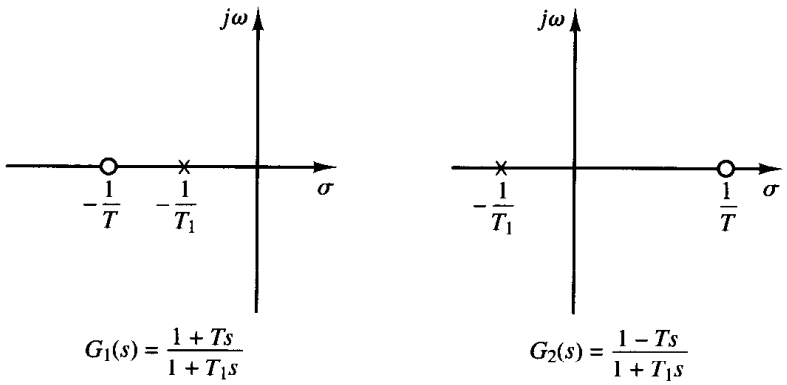

$G_1(s) = \frac{1 + Ts}{1 + T_1 s}$ $\qquad$ $G_2(s) = \frac{1 - Ts}{1 + T_1 s}$

Figure 8–11
Pole–zero configurations of a minimum-phase system $G_1(s)$ and nonminimum-phase system $G_2(s)$.

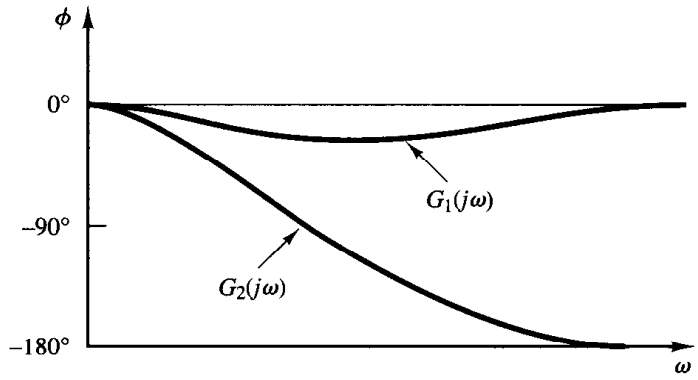

Figure 8–12
Phase-angle characteristics of the systems $G_1(s)$ and $G_2(s)$ shown in Figure 8–11.

The magnitude of the factor $(1 - j\omega T)/(1 + j\omega T)$ is always unity. But the phase angle equals $-2 \tan^{-1} \omega T$ and varies from 0° to −180° as ω is increased from zero to infinity.

As stated earlier, for a minimum-phase system, the magnitude and phase-angle characteristics are uniquely related. This means that if the magnitude curve of a system is specified over the entire frequency range from zero to infinity, then the phase-angle curve is uniquely determined, and vice versa. This, however, does not hold for a nonminimum-phase system.

Nonminimum-phase situations may arise in two different ways. One is simply when a system includes a nonminimum-phase element or elements. The other situation may arise in the case where a minor loop is unstable.

For a minimum-phase system, the phase angle at $\omega = \infty$ becomes $-90°(q - p)$, where p and q are the degrees of the numerator and denominator polynomials of the transfer function, respectively. For a nonminimum-phase system, the phase angle at $\omega = \infty$ differs from $-90°(q - p)$. In either system, the slope of the log-magnitude curve at $\omega = \infty$ is equal to $-20(q - p)$ dB/decade. It is therefore possible to detect whether the system is minimum phase by examining both the slope of the high-frequency asymptote of the log-magnitude curve and the phase angle at $\omega = \infty$. If the slope of the log-magnitude curve as ω approaches infinity is $-20(q - p)$ dB/decade and the phase angle at $\omega = \infty$ is equal to $-90°(q - p)$, then the system is minimum phase.

Nonminimum-phase systems are slow in response because of their faulty behavior at the start of response. In most practical control systems, excessive phase lag should be carefully avoided. In designing a system, if fast speed of response is of primary importance, we should not use nonminimum-phase components. (A common example of nonminimum-phase elements that may be present in control system is transport lag.)

It is noted that the techniques of frequency-response analysis and design to be presented in this and the next chapter are valid for both minimum-phase and nonminimum-phase systems.

Transport lag. Transport lag is of nonminimum-phase behavior and has an excessive phase lag with no attenuation at high frequencies. Such transport lags normally exist in thermal, hydraulic, and pneumatic systems.

Consider the transport lag given by

$$G(j\omega) = e^{-j\omega T}$$

The magnitude is always equal to unity since

$$|G(j\omega)| = |\cos \omega T - j \sin \omega T| = 1$$

Therefore, the log magnitude of the transport lag $e^{-j\omega T}$ is equal to 0 dB. The phase angle of the transport lag is

$$\underline{/G(j\omega)} = -\omega T \quad \text{(radians)}$$
$$= -57.3\,\omega T \quad \text{(degrees)}$$

The phase angle varies linearly with the frequency ω. The phase-angle characteristic of transport lag is shown in Figure 8–13.

EXAMPLE 8–2 Draw the Bode diagram of the following transfer function:

$$G(j\omega) = \frac{e^{-j\omega L}}{1 + j\omega T}$$

The log magnitude is

$$20 \log|G(j\omega)| = 20 \log|e^{-j\omega L}| + 20 \log\left|\frac{1}{1 + j\omega T}\right|$$
$$= 0 + 20 \log\left|\frac{1}{1 + j\omega T}\right|$$

The phase angle of $G(j\omega)$ is

$$\underline{/G(j\omega)} = \underline{/e^{-j\omega L}} + \underline{/\frac{1}{1 + j\omega T}}$$
$$= -\omega L - \tan^{-1} \omega T$$

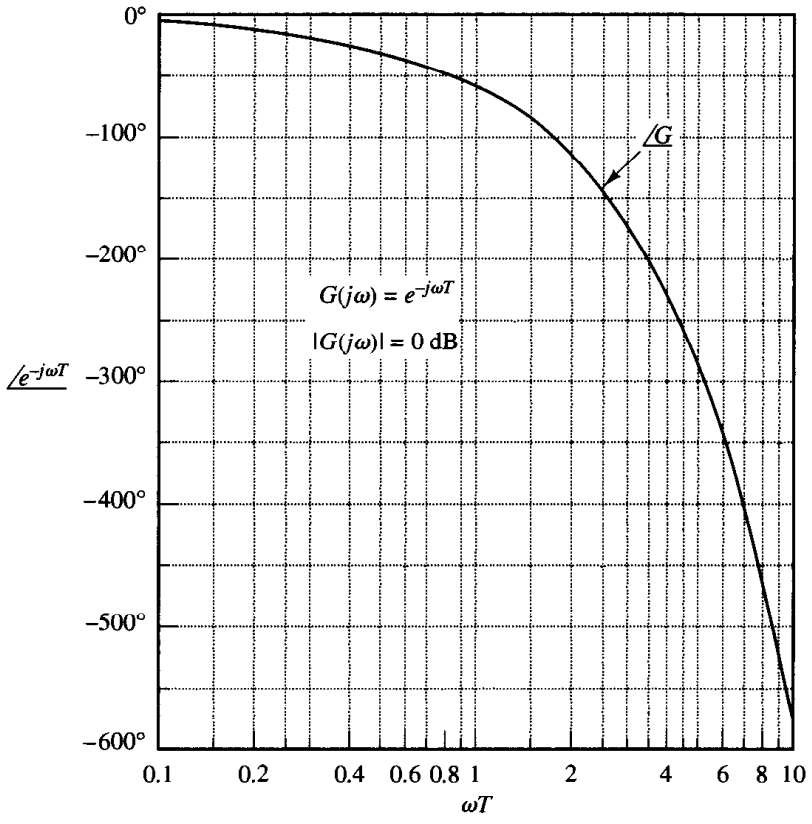

Figure 8–13 Phase-angle characteristic of transport lag.

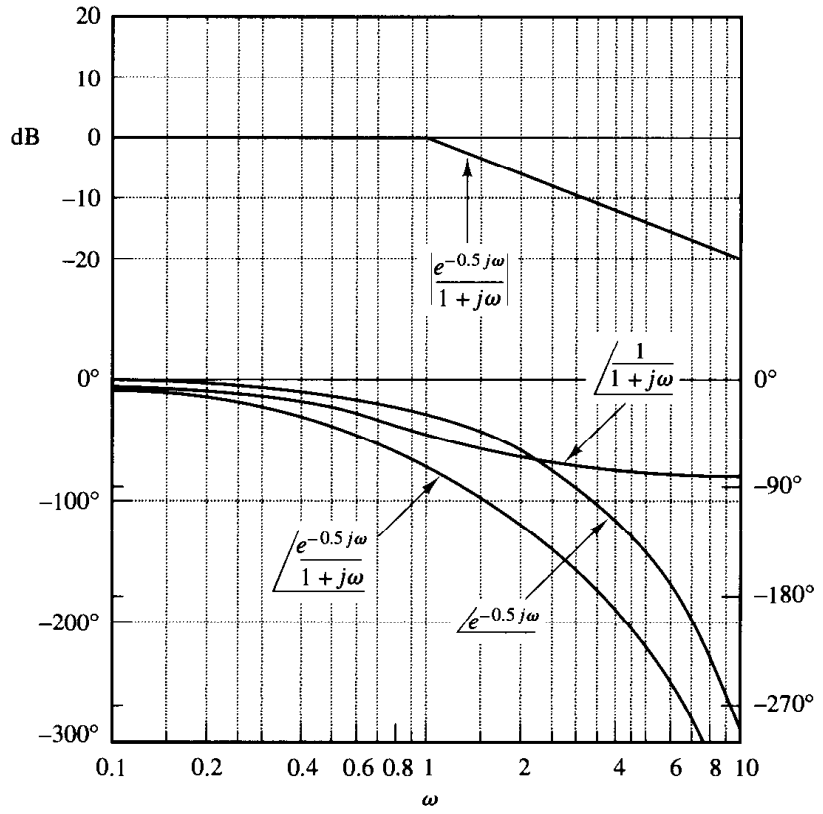

Figure 8–14
Bode diagram for the system $e^{-j\omega L}/(1 + j\omega T)$ with $L = 0.5$ and $T = 1$.

The log-magnitude and phase-angle curves for this transfer function with $L = 0.5$ and $T = 1$ are shown in Figure 8–14.

Relationship between system type and log-magnitude curve. Consider the unity-feedback control system. The static position, velocity, and acceleration error constants describe the low-frequency behavior of type 0, type 1, and type 2 systems, respectively. For a given system, only one of the static error constants is finite and significant. (The larger the value of the finite static error constant, the higher the loop gain is as ω approaches zero.)

The type of the system determines the slope of the log-magnitude curve at low frequencies. Thus, information concerning the existence and magnitude of the steady-state error of a control system to a given input can be determined from the observation of the low-frequency region of the log-magnitude curve.

Determination of static position error constants. Consider the unity-feedback control system shown in Figure 8–15. Assume that the open-loop transfer function is given by

$$G(s) = \frac{K(T_a s + 1)(T_b s + 1)\cdots(T_m s + 1)}{s^N(T_1 s + 1)(T_2 s + 1)\cdots(T_p s + 1)}$$

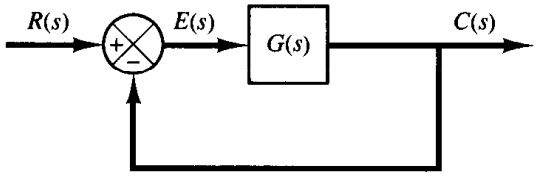

Figure 8–15
Unity-feedback control system.

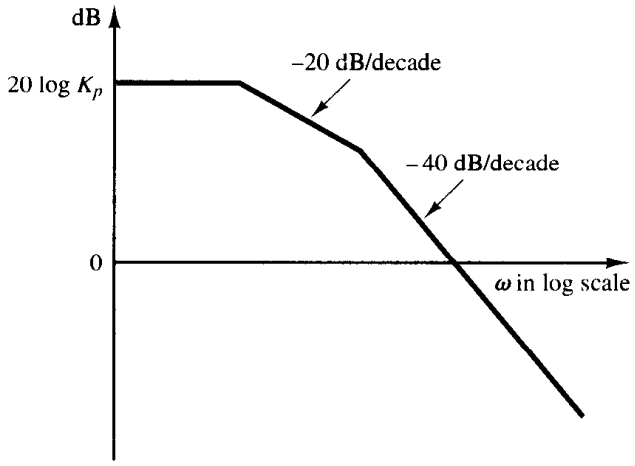

Figure 8–16
Log-magnitude curve of a type 0 system.

or

$$G(j\omega) = \frac{K(T_a j\omega + 1)(T_b j\omega + 1)\cdots(T_m j\omega + 1)}{(j\omega)^N(T_1 j\omega + 1)(T_2 j\omega + 1)\cdots(T_p j\omega + 1)}$$

Figure 8–16 shows an example of the log-magnitude plot of a type 0 system. In such a system, the magnitude of $G(j\omega)$ equals K_p at low frequencies, or

$$\lim_{\omega \to 0} G(j\omega) = K_p$$

It follows that the low-frequency asymptote is a horizontal line at 20 log K_p dB.

Determination of static velocity error constants. Consider the unity-feedback control system shown in Figure 8–15. Figure 8–17 shows an example of the log-magnitude plot of a type 1 system. The intersection of the initial −20 dB/decade segment (or its extension) with the line $\omega = 1$ has the magnitude 20 log K_v. This may be seen as follows: In a type 1 system

$$G(j\omega) = \frac{K_v}{j\omega}, \qquad \text{for } \omega \ll 1$$

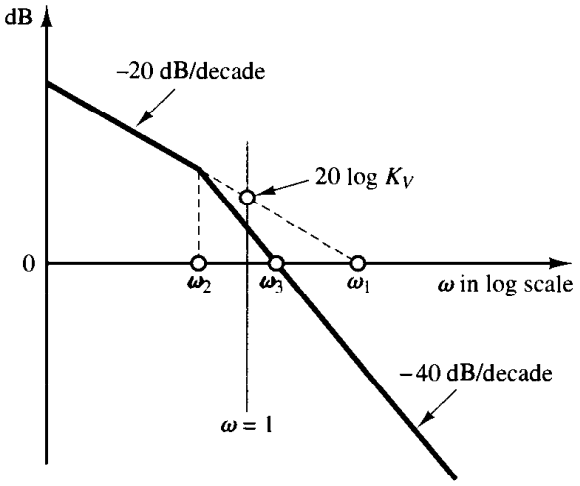

Figure 8–17
Log-magnitude curve of a type 1 system.

Thus,

$$20 \log \left| \frac{K_v}{j\omega} \right|_{\omega=1} = 20 \log K_v$$

The intersection of the initial -20-dB/decade segment (or its extension) with the 0-dB line has a frequency numerically equal to K_v. To see this, define the frequency at this intersection to be ω_1; then

$$\left| \frac{K_v}{j\omega_1} \right| = 1$$

or

$$K_v = \omega_1$$

As an example, consider the type 1 system with unity feedback whose open-loop transfer function is

$$G(s) = \frac{K}{s(Js + F)}$$

If we define the corner frequency to be ω_2 and the frequency at the intersection of the -40-dB/decade segment (or its extension) with 0-dB line to be ω_3, then

$$\omega_2 = \frac{F}{J}, \qquad \omega_3^2 = \frac{K}{J}$$

Since

$$\omega_1 = K_v = \frac{K}{F}$$

it follows that

$$\omega_1 \omega_2 = \omega_3^2$$

or

$$\frac{\omega_1}{\omega_3} = \frac{\omega_3}{\omega_2}$$

On the Bode diagram,

$$\log \omega_1 - \log \omega_3 = \log \omega_3 - \log \omega_2$$

Thus, the ω_3 point is just midway between the ω_2 and ω_1 points. The damping ratio ζ of the system is then

$$\zeta = \frac{F}{2\sqrt{KJ}} = \frac{\omega_2}{2\omega_3}$$

Determination of static acceleration error constants. Consider the unity-feedback control system shown in Figure 8–15. Figure 8–18 shows an example of the log-magnitude plot of a type 2 system. The intersection of the initial -40-dB/decade

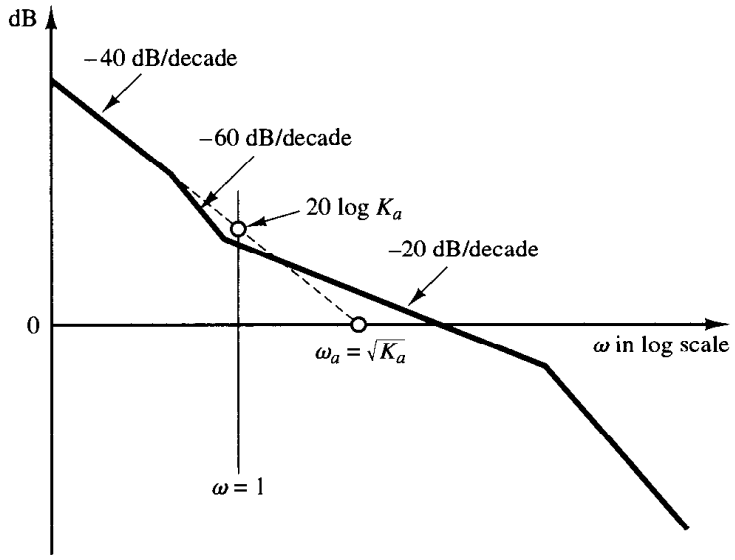

Figure 8–18
Log-magnitude curve of a type 2 system.

segment (or its extension) with the $\omega = 1$ line has the magnitude of 20 log K_a. Since at low frequencies

$$G(j\omega) = \frac{K_a}{(j\omega)^2}, \qquad \text{for } \omega \ll 1$$

it follows that

$$20 \log \left| \frac{K_a}{(j\omega)^2} \right|_{\omega=1} = 20 \log K_a$$

The frequency ω_a at the intersection of the initial −40-dB/decade segment (or its extension) with the 0-dB line gives the square root of K_a numerically. This can be seen from the following:

$$20 \log \left| \frac{K_a}{(j\omega_a)^2} \right| = 20 \log 1 = 0$$

which yields

$$\omega_a = \sqrt{K_a}$$

8–3 PLOTTING BODE DIAGRAMS WITH MATLAB

The command bode computes magnitudes and phase angles of the frequency response of continuous-time, linear, time-invariant systems.

When the command bode (without left-hand arguments) is entered in the computer, MATLAB produces a Bode plot on the screen.

When invoked with left-hand arguments,

```
[mag,phase,w] = bode(num,den,w)
```

bode returns the frequency response of the system in matrices mag, phase and w. No plot is drawn on the screen. The matrices mag and phase contain magnitudes and phase

angles of the frequency response of the system evaluated at user-specified frequency points. The phase angle is returned in degrees. The magnitude can be converted to decibels with the statement

```
magdB = 20*log10(mag)
```

To specify the frequency range, use the command logspace(d1,d2) or logspace (d1,d2,n). logspace(d1,d2) generates a vector of 50 points logarithmically equally spaced between decades 10^{d1} and 10^{d2}. That is, to generate 50 points between 0.1 rad/sec and 100 rad/sec, enter the command

```
w = logspace(-1,2)
```

logspace(d1,d2,n) generates n points logarithmically equally spaced between decades 10^{d1} and 10^{d2}. For example, to generate 100 points between 1 rad/sec and 1000 rad/sec, enter the following command:

```
w = logspace(0,3,100)
```

To incorporate these frequency points when plotting Bode diagrams, use the command bode(num,den,w) or bode(A,B,C,D,iu,w). These commands use the user-specified frequency vector w.

EXAMPLE 8–3 Consider the following transfer function:

$$G(s) = \frac{25}{s^2 + 4s + 25}$$

Plot a Bode diagram for this transfer function.

When the system is defined in the form

$$G(s) = \frac{\text{num}(s)}{\text{den}(s)}$$

use the command bode(num,den) to draw the Bode diagram. [When the numerator and denominator contain the polynomial coefficients in descending powers of s, bode(num,den) draws the Bode diagram.] MATLAB Program 8–1 shows a program to plot the Bode diagram for this system. The resulting Bode diagram is shown in Figure 8–19.

MATLAB Program 8–1

```
num = [0   0   25];
den = [1   4   25];
bode(num,den)
subplot(2,1,1);
title('Bode Diagram of G(s) = 25/(s^2 + 4s + 25)')
```

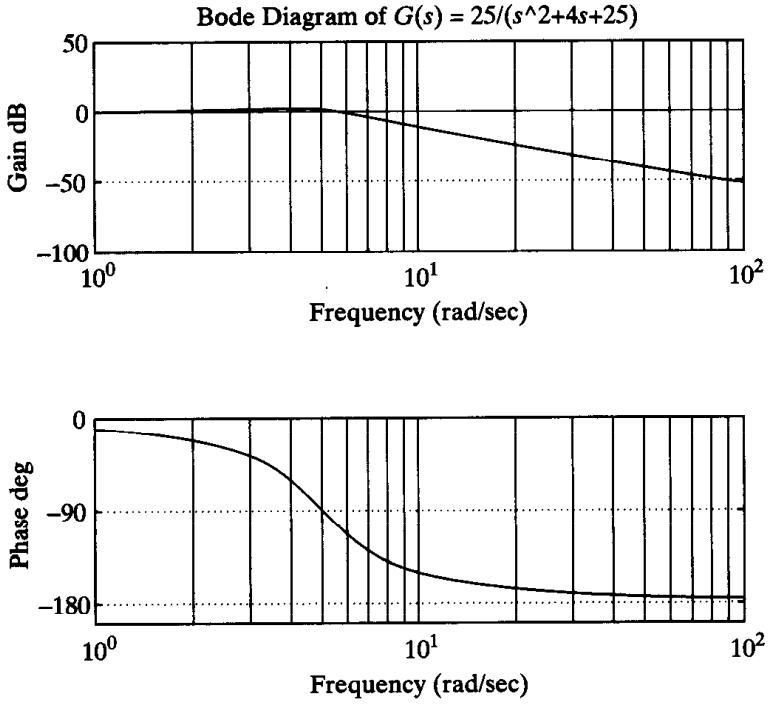

Figure 8–19
Bode diagram of $G(s) = \dfrac{25}{s^2 + 4s + 25}$.

EXAMPLE 8–4 Consider the system shown in Figure 8–20. The open-loop transfer function is

$$G(s) = \frac{9(s^2 + 0.2s + 1)}{s(s^2 + 1.2s + 9)}$$

Plot a bode diagram.

MATLAB Program 8–2 plots a Bode diagram for the system. The resulting plot is shown in Figure 8–21. The frequency range in this case is automatically determined to be from 0.1 to 10 rad/sec.

MATLAB Program 8–2

```
num = [0   9   1.8   9];
den = [1   1.2   9   0];
bode(num,den)
subplot(2,1,1);
title('Bode Diagram of G(s) = 9(s^2 + 0.2s + 1)/[s(s^2 + 1.2s + 9)]')
```

If it is desired to plot the Bode diagram from 0.01 to 1000 rad/sec, enter the following command:

```
w = logspace(-2,3,100)
```

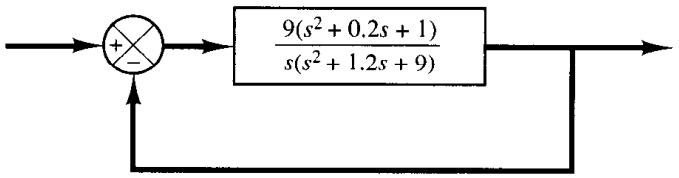

Figure 8–20
Control system.

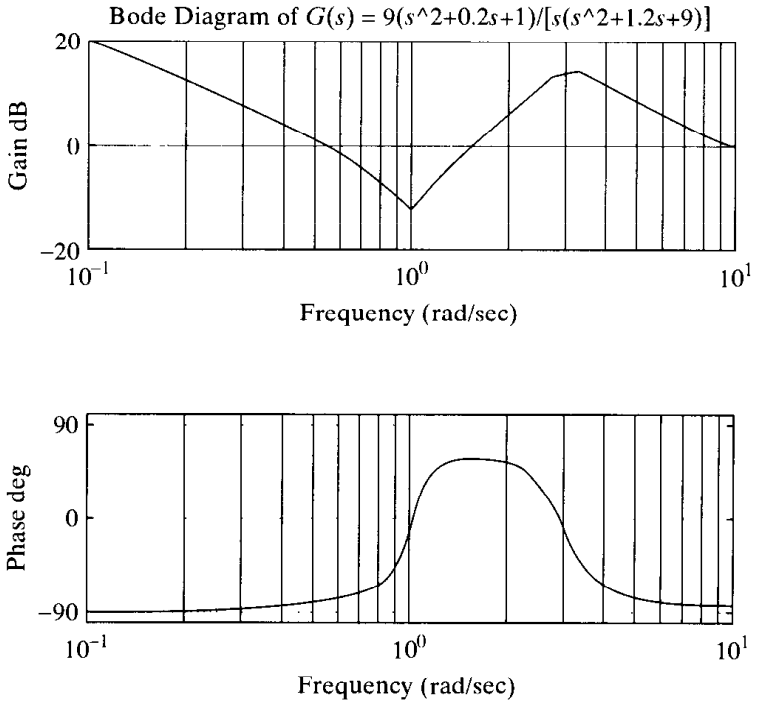

Figure 8–21
Bode diagram of $G(s) = \dfrac{9(s^2 + 0.2s + 1)}{s(s^2 + 1.2s + 9)}$.

This command generates 100 points logarithmically equally spaced between 0.01 and 1000 rad/sec. (Note that such a vector w specifies the frequencies in radians per second at which the frequency response will be calculated.)

If we use the command

```
bode(num,den,w)
```

then the frequency range is as user specified, but the magnitude range and phase-angle range will be automatically determined. See MATLAB Program 8–3 and the resulting plot in Figure 8–22.

To specify the magnitude range and phase-angle range, use the following command:

```
[mag,phase,w] = bode(num,den,w)
```

The matrices mag and phase contain the magnitudes and phase angles of the frequency response evaluated at the user-specified frequency points. The phase angle is returned in degrees. The magnitude can be converted to decibels with the statement

MATLAB Program 8–3

```
num = [0   9   1.8   9];
den = [1   1.2   9   0];
w = logspace(-2,3,100);
bode(num,den,w)
subplot(2,1,1);
title('Bode Diagram of G(s) = 9(s^2 + 0.2s + 1)/[s(s^2 + 1.2s + 9)]')
```

```
magdb = 20*log10(mag)
```

If we wish to specify the magnitude range to be, for example, at least between −45 dB and +45 dB, then enter invisible lines at −45 dB and +45 dB in the plot by specifying dBmax (maximum magnitude) and dBmin (minimum magnitude) as follows:

```
dBmax = 45*ones(1,100);
dBmin = -45*ones(1,100);
```

Then enter the following semilog plot command:

```
semilogx(w,magdB,'o',w,magdB,'-',w,dBmax,'--i',w,dBmin,':i')
```

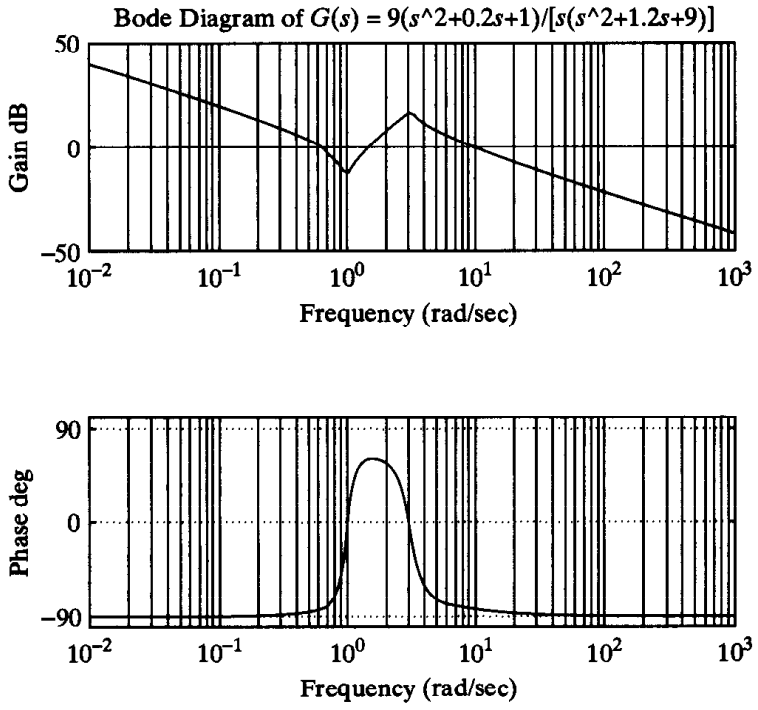

Figure 8–22
Bode diagram of $G(s) = \dfrac{9(s^2 + 0.2s + 1)}{s(s^2 + 1.2s + 9)}$.

(Note that the number of dBmax points and that of dBmin points must be equal to the number of frequency points in w. In this example, all numbers are 100.) Then the screen will show the magnitude curve magdB with 'o' marks. (Straight lines at +45 dB and −45 dB are invisible.)

Note that 'i' is an invisible color. For example, 'og' will show small circles in green color and 'oi' will show small circles in 'invisible' color: that is, you will not see small circles in the screen. By changing a portion of the preceding semilogx command from

```
w,dBmax,'--i',w,dBmin,':i'
```

to

```
w,dBmax,'--',w,dBmin,':'
```

the +45-dB line and −45-dB line will become visible on the screen.

The range for the magnitude is normally a multiple of 5, 10, 20, or 50 dB. (There are exceptions.) For the present case, the range for the magnitude will be from −50 dB to +50 dB.

For the phase angle, if we wish to specify the range to be, for example, at least between −145° and +115°, we enter invisible lines at −145° and +115° in the program by specifying pmax (maximum phase angle) and pmin (minimum phase angle) as follows:

```
pmax = 115*ones(1,100)
pmin = −145*ones(1,100)
```

Then enter the semilog plot command:

```
semilogx(w,phase,'o',w,phase,'-',w,pmax,'--i',w,pmin,':i')
```

(The number of pmax points and that of pmin points must be equal to the number of frequency points in w.) The screen will show the phase curve. Straight lines at +115° and −145° are invisible.

The range for the phase angle is normally a multiple of 5°, 10°, 50°, or 100°. (There are exceptions.) For the present case, the range for the phase angle will be from −150° to +150°.

MATLAB Program 8–4 produces the Bode diagram for the system such that the frequency range is from 0.01 to 1000 rad/sec, the magnitude range is from −50 to +50 dB (the magnitude range is a multiple of 50 dB), and the phase-angle range is from −150° to +150° (the phase-angle range is a multiple of 50°). Figure 8–23 shows the Bode diagram obtained by use of MATLAB Program 8–4.

What happens to the Bode diagram if the gain becomes infinite at a certain frequency point? If there is a system pole on the $j\omega$ axis and the w vector happens to contain this frequency point, the gain becomes infinite at this frequency. In such a case, MATLAB produces warning messages. Consider the following example.

MATLAB Program 8–4

```
% ---------- Bode diagram ----------

% ***** In this program we shall obtain Bode diagram of
% transfer-function system using user-specified frequency
% range *****

% ***** Enter the numerator and denominator of the transfer
% function *****

num = [0   9   1.8   9];
den = [1   1.2   9   0];

% ***** Specify the frequency range and enter the command
% [mag,phase,w] = bode(num,den,w) *****

w = logspace(-2,3,100);
[mag,phase,w] = bode(num,den,w);

% ***** Convert mag to decibels *****

magdB = 20*log10(mag);

% ***** Specify the range for magnitude. For the system
% considered, the magnitude range should include -45 dB
% and +45 dB. Enter dBmax and dBmin in the program and
% draw dBmax line and dBmin line in invisible color. To
% plot the magdB curve and invisible lines, enter the
% following dBmax, dBmin, and semilogx command *****

dBmax = 45*ones(1,100);
dBmin = -45*ones(1,100);
semilogx(w,magdB,'o',w,magdB,'-',w,dBmax,'--i',w,dBmin,':i')

% ***** Enter grid, title, xlabel, and ylabel *****

grid
title('Bode Diagram of G(s) = 9(s^2 + 0.2s + 1)/[s(s^2 + 1.2s + 9)]')
xlabel('Frequency (rad/sec)')
ylabel('Gain dB')

% ***** Next, we shall plot the phase-angle curve *****

% ***** Specify the range for phase angle. For the system
% considered, the phase-angle range should include -145 degrees
% and +115 degrees. Enter pmax and pmin in the program and
% draw pmax line and pmin line in invisible color. To plot
% the phase curve and invisible lines, enter the following
% pmax, pmin, and semilogx command *****
```

```
pmax = 115*ones(1,100);
pmin = -145*ones(1,100);
semilogx(w,phase,'o',w,phase,'-',w,pmax,'--i',w,pmin,':i')

% ***** Enter grid, xlabel, and ylabel *****

grid
xlabel('Frequency (rad/sec)')
ylabel('Phase deg')
```

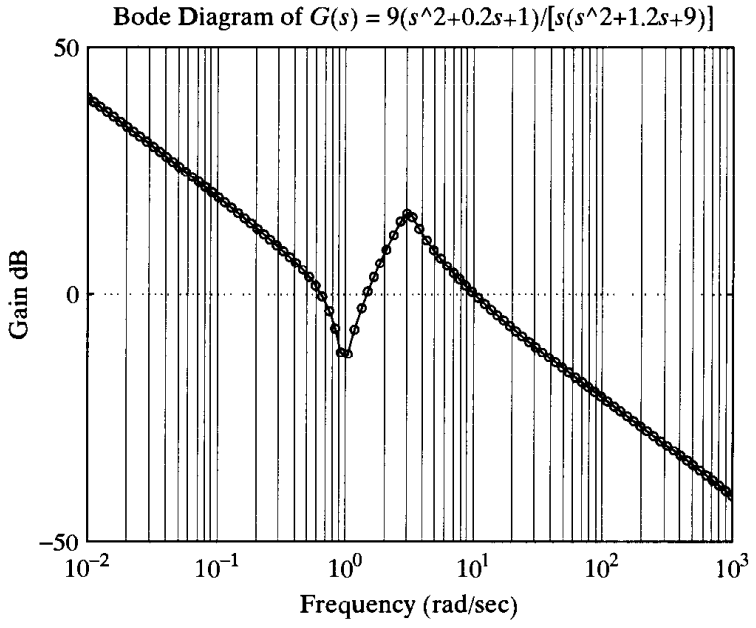

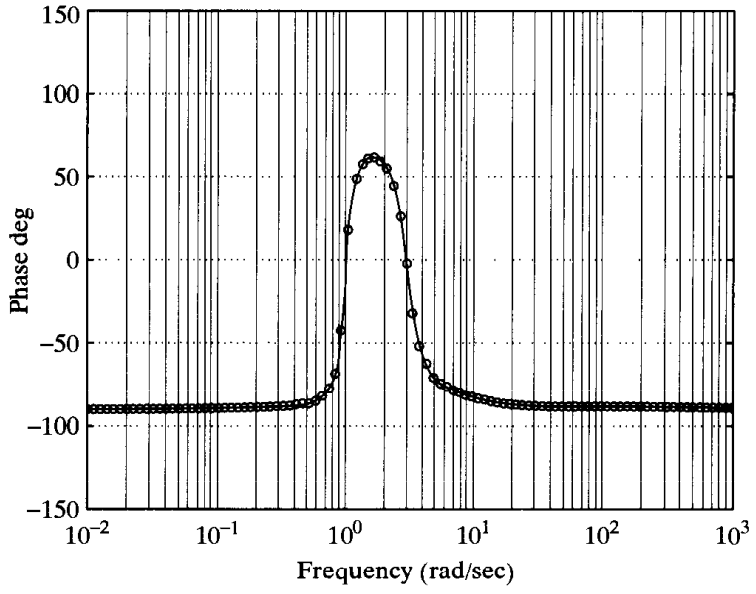

Figure 8–23
Bode diagram of $G(s) = \dfrac{9(s^2 + 0.2s + 1)}{s(s^2 + 1.2s + 9)}$.

EXAMPLE 8–5 Consider a system with the following open-loop transfer function:

$$G(s) = \frac{1}{s^2 + 1}$$

This open-loop transfer function has poles on the $j\omega$ axis at $\pm j$.

MATLAB Program 8–5 may be used to plot the Bode diagram for this system. The resulting plot is shown in Figure 8–24. Theoretically, the magnitude becomes infinite at a frequency point where $\omega = 1$ rad/sec. However, this frequency point is not among the computing frequency points. In the plot the peak magnitude is shown to be approximately 50 dB. This value is computed near, but not exactly at, $\omega = 1$ rad/sec.

MATLAB Program 8–5

```
num = [0   0   1];
den = [1   0   1];
bode(num,den)
subplot(2,1,1);
title('Bode Diagram of G(s) = 1/(s^2 + 1)')
```

If, however, one of the computing frequency points coincides with the pole at $\omega = 1$, then the magnitude becomes infinite at this point. MATLAB sends out warning messages. See MATLAB

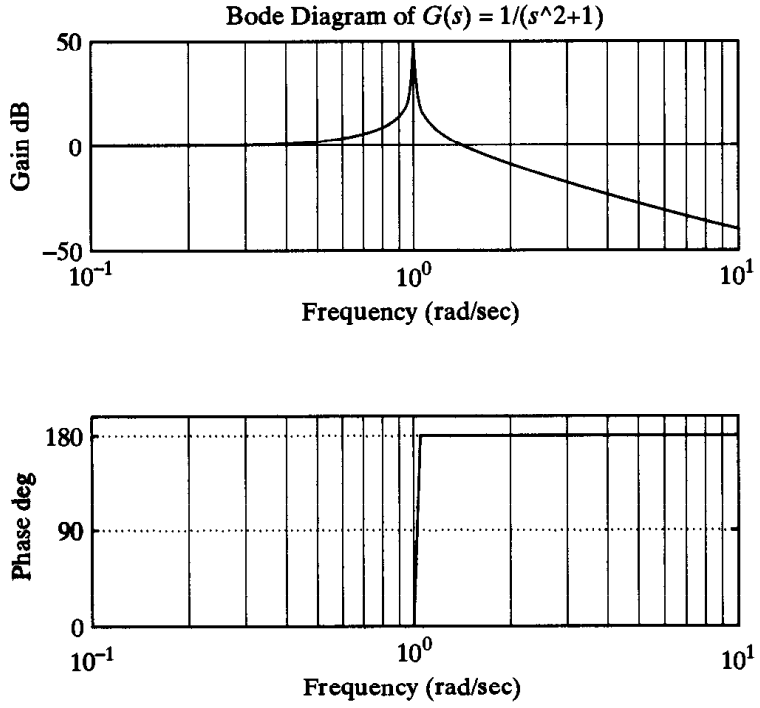

Figure 8–24
Bode diagram of $G(s) = \frac{1}{s^2 + 1}$.

Program 8–6 where computing points include the point at $\omega = 1$ rad/sec. (There are 101 computing points in this case. The computing points range from $\omega = 0.1$ to $\omega = 10$. The fifty-first point is at $\omega = 1$.) When MATLAB Program 8–6 is entered into the computer, warning messages appear, as shown. The resulting Bode diagram, shown in Figure 8–25, does not include the computed magnitude at $\omega = 1$. (Theoretically, this magnitude is infinite.) The magnitude curve shows the peak value at about 20 dB. The phase curve shows a gradual change in the phase angle from 0° to +180 ° near point $\omega = 1$. (Theoretically, the change in the phase angle from 0° to +180° should be abrupt at $\omega = 1$.) Obviously, the Bode diagram shown in Figure 8–25 is incorrect.

If the w vector contains such a frequency point, where the gain becomes infinite, change the number of frequency points, for example, from 101 to 100. Normally, a small change in the number of frequency points will avoid this kind of problem.

MATLAB Program 8–6

```
num = [0   0   1];
den = [1   0   1];
w = logspace(-1,1,101);
bode(num,den,w)

Warning: Divide by zero
subplot(2,1,1);
title('Incorrect Bode Diagram')
```

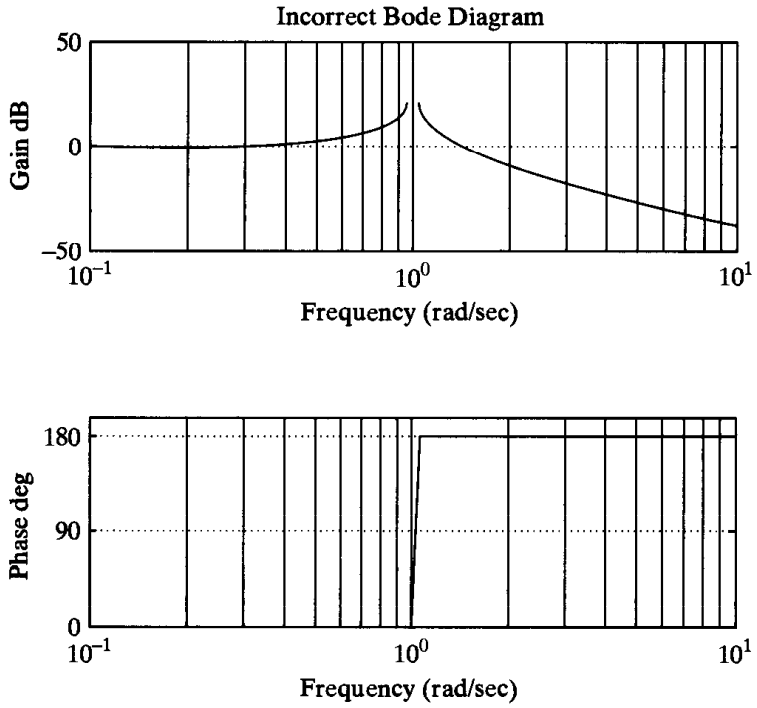

Figure 8–25
Incorrect Bode diagram of $G(s) = \dfrac{1}{s^2 + 1}$.

Obtaining Bode diagrams of systems defined in state space. Consider the system defined by

$$\dot{\mathbf{x}} = \mathbf{A}\mathbf{x} + \mathbf{B}\mathbf{u}$$

$$\mathbf{y} = \mathbf{C}\mathbf{x} + \mathbf{D}\mathbf{u}$$

where $\mathbf{x}$ = state vector (n-vector)
$\mathbf{y}$ = output vector (m-vector)
$\mathbf{u}$ = control vector (r-vector)
$\mathbf{A}$ = state matrix ($n \times n$ matrix)
$\mathbf{B}$ = control matrix ($n \times r$ matrix)
$\mathbf{C}$ = output matrix ($m \times n$ matrix)
$\mathbf{D}$ = direct transmission matrix ($m \times r$ matrix)

A Bode diagram for this system may be obtained by entering the command

```
bode(A,B,C,D)
```

or

```
bode(A,B,C,D,iu)
```

The command bode(A,B,C,D) produces a series of Bode plots, one for each input of the system, with the frequency range automatically determined. (More points are used when the response is changing rapidly.)

The command bode(A,B,C,D,iu) where iu is the ith input of the system, produces the Bode diagrams from the input iu to all the outputs ($y_1, y_2, \ldots, y_m$) of the system, with frequency range automatically determined. (The scalar iu is an index into the inputs of the system and specifies which input is to be used for plotting Bode diagrams). If the control vector $\mathbf{u}$ has three inputs such that

$$\mathbf{u} = \begin{bmatrix} u_1 \\ u_2 \\ u_3 \end{bmatrix}$$

then iu must be set to either 1, 2, or 3.

If the system has only one input u, then either of the following commands may be used:

```
bode(A,B,C,D)
```

or

```
bode(A,B,C,D,1)
```

EXAMPLE 8–6 Consider the following system:

$$\begin{bmatrix} \dot{x}_1 \\ \dot{x}_2 \end{bmatrix} = \begin{bmatrix} 0 & 1 \\ -25 & -4 \end{bmatrix} \begin{bmatrix} x_1 \\ x_2 \end{bmatrix} + \begin{bmatrix} 0 \\ 25 \end{bmatrix} u$$

$$y = \begin{bmatrix} 1 & 0 \end{bmatrix} \begin{bmatrix} x_1 \\ x_2 \end{bmatrix}$$

This system has one input u and one output y. By using the command

```
bode(A,B,C,D)
```

and entering MATLAB Program 8–7 into the computer, we obtain the Bode diagram shown in Figure 8–26.

MATLAB Program 8–7

```
A = [0   1;−25   −4];
B = [0;25];
C = [1   0];
D = [0];
bode(A,B,C,D)
subplot(2,1,1);
title('Bode Diagram')
```

If we replace the command bode(A,B,C,D) in MATLAB Program 8–7 with

```
bode(A,B,C,D,1)
```

then MATLAB will produce the Bode diagram identical to that shown in Figure 8–26.

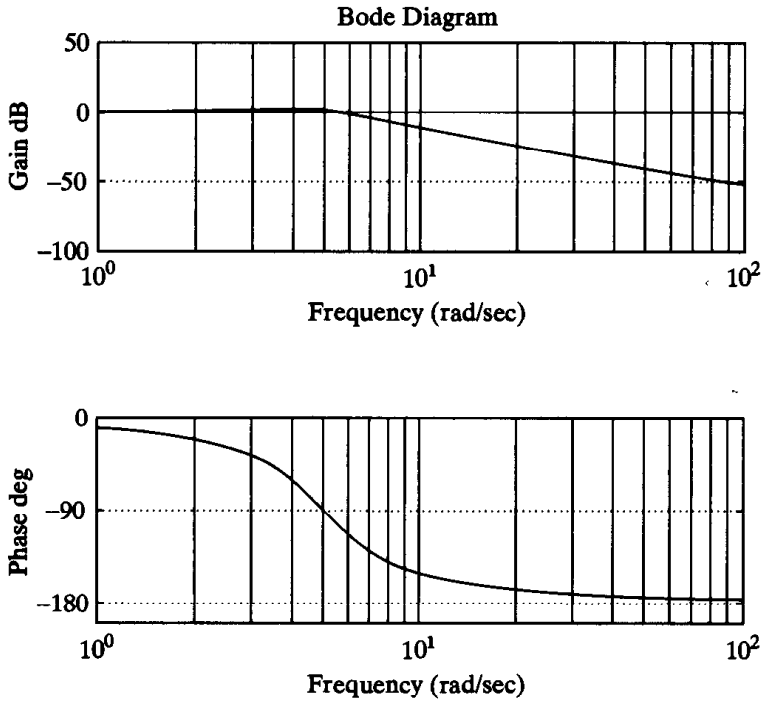

Figure 8–26
Bode diagram of the system considered in Example 8–6.

Note that if we use, by mistake, the command

```
bode(A,B,C,D,2)
```

MATLAB produces an error message, because the present system has only one input and iu should be set to '1', not '2' or any other number.

8–4 POLAR PLOTS

The polar plot of a sinusoidal transfer function $G(j\omega)$ is a plot of the magnitude of $G(j\omega)$ versus the phase angle of $G(j\omega)$ on polar coordinates as ω is varied from zero to infinity. Thus, the polar plot is the locus of vectors $|G(j\omega)|\underline{/G(j\omega)}$ as ω is varied from zero to infinity. Note that in polar plots a positive (negative) phase angle is measured counterclockwise (clockwise) from the positive real axis. The polar plot is often called the Nyquist plot. An example of such a plot is shown in Figure 8–27. Each point on the polar plot of $G(j\omega)$ represents the terminal point of a vector at a particular value of ω. In the polar plot, it is important to show the frequency graduation of the locus. The projections of $G(j\omega)$ on the real and imaginary axes are its real and imaginary components. Both the magnitude $|G(j\omega)|$ and phase angle $\underline{/G(j\omega)}$ must be calculated directly for each frequency ω in order to construct polar plots. Since the logarithmic plot is easy to construct, however, the data necessary for plotting the polar plot may be obtained directly from the logarithmic plot if the latter is drawn first and decibels are converted into ordinary magnitude. Or, of course, MATLAB may be used to obtain a polar plot $G(j\omega)$ or to obtain $|G(j\omega)|$ and $\underline{/G(j\omega)}$ accurately for various values of ω in the frequency range of interest. (See Section 8–5.)

An advantage in using a polar plot is that it depicts the frequency-response characteristics of a system over the entire frequency range in a single plot. One disadvantage is that the plot does not clearly indicate the contributions of each individual factor of the open-loop transfer function.

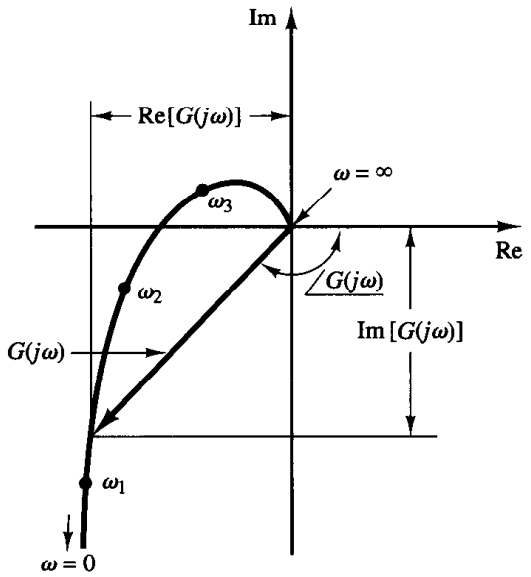

Figure 8–27
Polar plot.

Integral and derivative factors $(j\omega)^{\mp 1}$. The polar plot of $G(j\omega) = 1/j\omega$ is the negative imaginary axis since

$$G(j\omega) = \frac{1}{j\omega} = -j\frac{1}{\omega} = \frac{1}{\omega}\angle -90°$$

The polar plot of $G(j\omega) = j\omega$ is the positive imaginary axis.

First-order factors $(1 + j\omega T)^{\mp 1}$. For the sinusoidal transfer function

$$G(j\omega) = \frac{1}{1 + j\omega T} = \frac{1}{\sqrt{1 + \omega^2 T^2}}\angle -\tan^{-1}\omega T$$

the values of $G(j\omega)$ at $\omega = 0$ and $\omega = 1/T$ are, respectively,

$$G(j0) = 1\angle 0° \qquad \text{and} \qquad G\left(j\frac{1}{T}\right) = \frac{1}{\sqrt{2}}\angle -45°$$

If ω approaches infinity, the magnitude of $G(j\omega)$ approaches zero and the phase angle approaches $-90°$. The polar plot of this transfer function is a semicircle as the frequency ω is varied from zero to infinity, as shown in Figure 8–28(a). The center is located at 0.5 on the real axis, and the radius is equal to 0.5.

To prove that the polar plot is a semicircle, define

$$G(j\omega) = X + jY$$

where

$$X = \frac{1}{1 + \omega^2 T^2} = \text{real part of } G(j\omega)$$

$$Y = \frac{-\omega T}{1 + \omega^2 T^2} = \text{imaginary part of } G(j\omega)$$

Then we obtain

$$\left(X - \frac{1}{2}\right)^2 + Y^2 = \left(\frac{1}{2}\frac{1 - \omega^2 T^2}{1 + \omega^2 T^2}\right)^2 + \left(\frac{-\omega T}{1 + \omega^2 T^2}\right)^2 = \left(\frac{1}{2}\right)^2$$

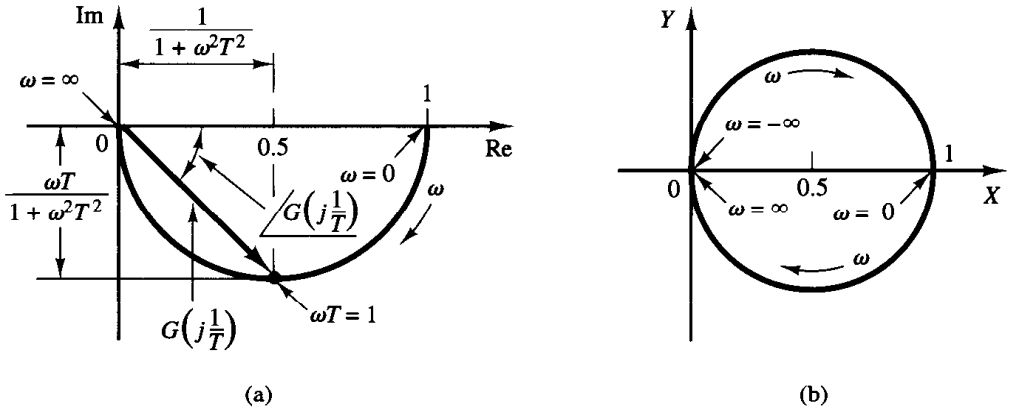

Figure 8–28
(a) Polar plot of $1/(1 + j\omega T)$; (b) plot of $G(j\omega)$ in X–Y plane.

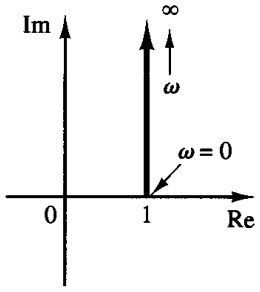

Figure 8–29
Polar plot of $1 + j\omega T$.

Thus, in the X–Y plane $G(j\omega)$ is a circle with center at $X = \frac{1}{2}$, $Y = 0$ and with radius $\frac{1}{2}$, as shown in Figure 8–28(b). The lower semicircle corresponds to $0 \le \omega \le \infty$, and the upper semicircle corresponds to $-\infty \le \omega \le 0$.

The polar plot of the transfer function $1 + j\omega T$ is simply the upper half of the straight line passing through point (1,0) in the complex plane and parallel to the imaginary axis, as shown in Figure 8–29. The polar plot of $1 + j\omega T$ has an appearance completely different from that of $1/(1 + j\omega T)$.

Quadratic factors $[1 + 2\zeta(j\omega/\omega_n) + (j\omega/\omega_n)^2]^{\mp 1}$. The low- and high-frequency portions of the polar lot of the following sinusoidal transfer function

$$G(j\omega) = \frac{1}{1 + 2\zeta\left(j\frac{\omega}{\omega_n}\right) + \left(j\frac{\omega}{\omega_n}\right)^2}, \qquad \text{for } \zeta > 0$$

are given, respectively, by

$$\lim_{\omega \to 0} G(j\omega) = 1\angle 0° \qquad \text{and} \qquad \lim_{\omega \to \infty} G(j\omega) = 0\angle -180°$$

The polar plot of this sinusoidal transfer function starts at $1\angle 0°$ and ends at $0\angle -180°$ as ω increases from zero to infinity. Thus, the high-frequency portion of $G(j\omega)$ is tangent to the negative real axis. The values of $G(j\omega)$ in the frequency range of interest can be calculated directly or by use of the Bode diagram or by use of MATLAB.

Examples of polar plots of the transfer function just considered are shown in Figure 8–30. The exact shape of a polar plot depends on the value of the damping ratio ζ, but the general shape of the plot is the same for both the underdamped case ($1 > \zeta > 0$) and overdamped case ($\zeta > 1$).

For the underdamped case at $\omega = \omega_n$, we have $G(j\omega_n) = 1/(j2\zeta)$, and the phase angle at $\omega = \omega_n$ is $-90°$. Therefore, it can be seen that the frequency at which the

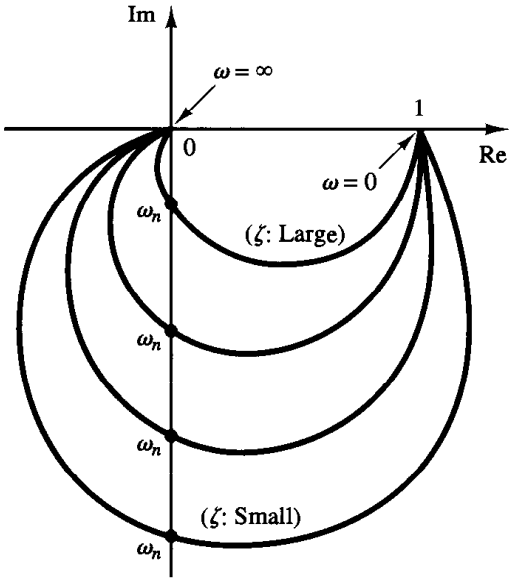

Figure 8–30
Polar plots of
$$\frac{1}{1 + 2\zeta\left(j\frac{\omega}{\omega_n}\right) + \left(j\frac{\omega}{\omega_n}\right)^2},$$
for $\zeta > 0$.

$G(j\omega)$ locus intersects the imaginary axis is the undamped natural frequency ω_n. In the polar plot, the frequency point whose distance from the origin is maximum corresponds to the resonant frequency ω_r. The peak value of $G(j\omega)$ is obtained as the ratio of the magnitude of the vector at the resonant frequency ω_r to the magnitude of the vector at $\omega = 0$. The resonant frequency ω_r is indicated in the polar plot shown in Figure 8–31.

For the overdamped case, as ζ increases well beyond unity, the $G(j\omega)$ locus approaches a semicircle. This may be seen from the fact that for a heavily damped system the characteristic roots are real and one is much smaller than the other. Since for sufficiently large ζ the effect of the larger root (larger in the absolute value) on the response becomes very small, the system behaves like a first-order one.

Next, consider the following sinusoidal transfer function:

$$G(j\omega) = 1 + 2\zeta\left(j\frac{\omega}{\omega_n}\right) + \left(j\frac{\omega}{\omega_n}\right)^2$$

$$= \left(1 - \frac{\omega^2}{\omega_n^2}\right) + j\left(\frac{2\zeta\omega}{\omega_n}\right)$$

The low-frequency portion of the curve is

$$\lim_{\omega \to 0} G(j\omega) = 1 \angle 0°$$

and the high frequency portion is

$$\lim_{\omega \to \infty} G(j\omega) = \infty \angle 180°$$

Since the imaginary part of $G(j\omega)$ is positive for $\omega > 0$ and is monotonically increasing and the real part of $G(j\omega)$ is monotonically decreasing from unity, the general shape of the polar plot of $G(j\omega)$ is as shown in Figure 8–32. The phase angle is between 0° and 180°.

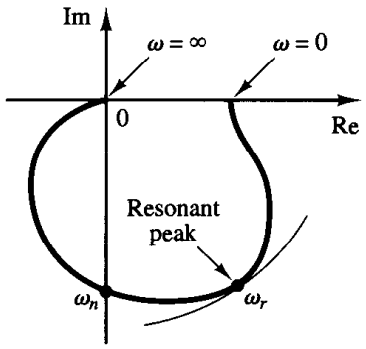

Figure 8–31
Polar plot showing the resonant peak and resonant frequency ω_r.

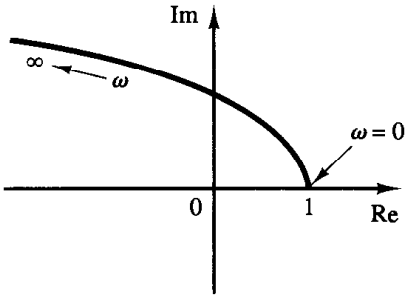

Figure 8–32
Polar plot of $1 + 2\zeta\left(j\frac{\omega}{\omega_n}\right) + \left(j\frac{\omega}{\omega_n}\right)^2$, for $\zeta > 0$.

EXAMPLE 8–7 Consider the following second-order transfer function:

$$G(s) = \frac{1}{s(Ts + 1)}$$

Sketch a polar plot of this transfer function.

Since the sinusoidal transfer function can be written

$$G(j\omega) = \frac{1}{j\omega(1 + j\omega T)} = -\frac{T}{1 + \omega^2 T^2} - j\frac{1}{\omega(1 + \omega^2 T^2)}$$

the low-frequency portion of the polar plot becomes

$$\lim_{\omega \to 0} G(j\omega) = -T - j\infty = \infty\angle -90°$$

and the high-frequency portion becomes

$$\lim_{\omega \to \infty} G(j\omega) = 0 - j0 = 0\angle -180°$$

The general shape of the polar plot of $G(j\omega)$ is shown in Figure 8–33. The $G(j\omega)$ plot is asymptotic to the vertical line passing through the point $(-T, 0)$. Since this transfer function involves an integrator $(1/s)$, the general shape of the polar plot differs substantially from those of second-order transfer functions that do not have an integrator.

Transport lag. The transport lag

$$G(j\omega) = e^{-j\omega T}$$

can be written

$$G(j\omega) = 1\angle \cos \omega T - j \sin \omega T$$

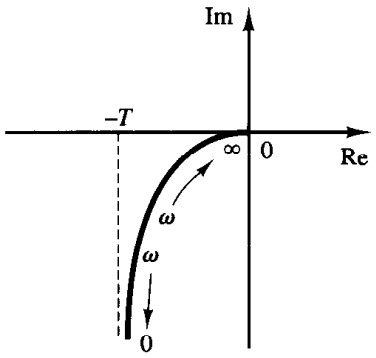

Figure 8–33
Polar plot of $1/[j\omega(1 + j\omega T)]$.

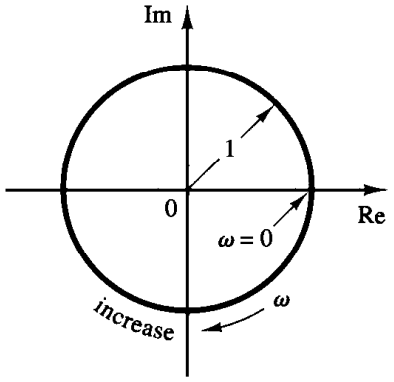

Figure 8–34
Polar plot of transport lag.

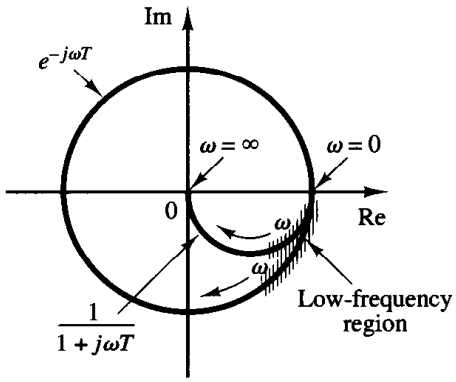

Figure 8–35
Polar plots of $e^{-j\omega T}$ and $1/(1 + j\omega T)$.

Since the magnitude of $G(j\omega)$ is always unity and the phase angle varies linearly with ω, the polar plot of the transport lag is a unit circle, as shown in Figure 8–34.

At low frequencies, the transport lag $e^{-j\omega T}$ and the first-order lag $1/(1 + j\omega T)$ behave similarly, as shown in Figure 8–35. The polar plots of $e^{-j\omega T}$ and $1/(1 + j\omega T)$ are tangent to each other at $\omega = 0$. This may be seen from the fact that, for $\omega \ll 1/T$,

$$e^{-j\omega T} \doteqdot 1 - j\omega T \qquad \text{and} \qquad \frac{1}{1 + j\omega T} \doteqdot 1 - j\omega T$$

For $\omega \gg 1/T$, however, an essential difference exists between $e^{-j\omega T}$ and $1/(1 + j\omega T)$, as may also be seen from Figure 8–35.

EXAMPLE 8–8 Obtain the polar plot of the following transfer function:

$$G(j\omega) = \frac{e^{-j\omega L}}{1 + j\omega T}$$

Since $G(j\omega)$ can be written

$$G(j\omega) = (e^{-j\omega L})\left(\frac{1}{1 + j\omega T}\right)$$

the magnitude and phase angle are, respectively,

$$|G(j\omega)| = |e^{-j\omega L}| \cdot \left|\frac{1}{1 + j\omega T}\right| = \frac{1}{\sqrt{1 + \omega^2 T^2}}$$

and

$$\angle G(j\omega) = \angle e^{-j\omega L} + \angle \frac{1}{1 + j\omega T} = -\omega L - \tan^{-1} \omega T$$

Since the magnitude decreases from unity monotonically and the phase angle also decreases monotonically and indefinitely, the polar plot of the given transfer function is a spiral, as shown in Figure 8–36.

General shapes of polar plots. The polar plots of a transfer function of the form

$$G(j\omega) = \frac{K(1 + j\omega T_a)(1 + j\omega T_b)\cdots}{(j\omega)^{\lambda}(1 + j\omega T_1)(1 + j\omega T_2)\cdots}$$
$$= \frac{b_0(j\omega)^m + b_1(j\omega)^{m-1} + \cdots}{a_0(j\omega)^n + a_1(j\omega)^{n-1} + \cdots}$$

where $n > m$ or the degree of the denominator polynomial is greater than that of the numerator, will have the following general shapes:

1. *For $\lambda = 0$ or type 0 systems:* The starting point of the polar plot (which corresponds to $\omega = 0$) is finite and is on the positive real axis. The tangent to the polar plot at $\omega = 0$ is perpendicular to the real axis. The terminal point, which corresponds to $\omega = \infty$, is at the origin, and the curve is tangent to one of the axes.

2. *For $\lambda = 1$ or type 1 systems:* the $j\omega$ term in the denominator contributes $-90°$ to the total phase angle of $G(j\omega)$ for $0 \leq \omega \leq \infty$. At $\omega = 0$, the magnitude of $G(j\omega)$ is infinity, and the phase angle becomes $-90°$. At low frequencies, the polar plot is asymptotic to a line parallel to the negative imaginary axis. At $\omega = \infty$, the magnitude becomes zero, and the curve converges to the origin and is tangent to one of the axes.

3. *For $\lambda = 2$ or type 2 systems:* The $(j\omega)^2$ term in the denominator contributes $-180°$ to the total phase angle of $G(j\omega)$ for $0 \leq \omega \leq \infty$. At $\omega = 0$, the magnitude of $G(j\omega)$ is infinity, and the phase angle is equal to $-180°$. At low frequencies, the polar plot is asymptotic to a line parallel to the negative real axis. At $\omega = \infty$, the magnitude becomes zero, and the curve is tangent to one of the axes.

The general shapes of the low-frequency portions of the polar plots of type 0, type 1, and type 2 systems are shown in Figure 8–37. It can be seen that, if the degree of the denominator polynomial of $G(j\omega)$ is greater than that of the numerator, then the $G(j\omega)$

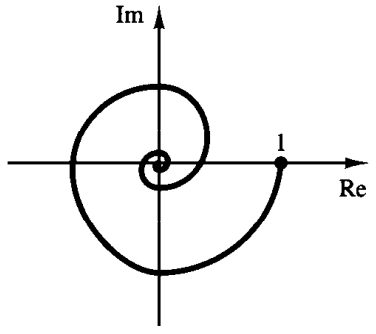

Figure 8–36
Polar plot of $e^{-j\omega L}/(1 + j\omega T)$.

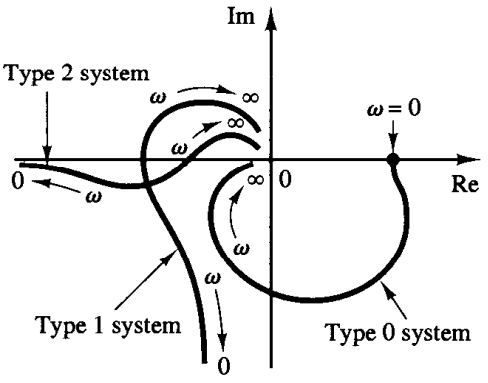

Figure 8–37
Polar plots of type 0, type 1, and type 2 systems.

loci converge to the origin clockwise. At $\omega = \infty$, the loci are tangent to one or the other axes, as shown in Figure 8–38.

Note that any complicated shapes in the polar plot curves are caused by the numerator dynamics, that is, by the time constants in the numerator of the transfer function. Figure 8–39 shows examples of polar plots of transfer functions with numerator dynamics. In analyzing control systems, the polar plot of $G(j\omega)$ in the frequency range of interest must be accurately determined.

Table 8–1 shows sketches of polar plots of several transfer functions.

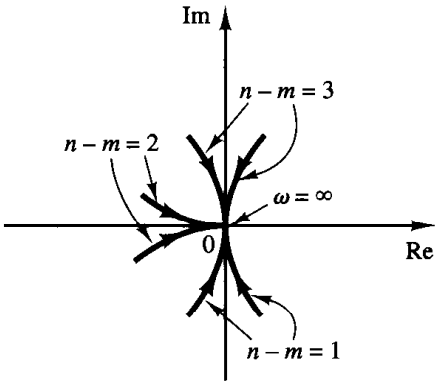

$$G(j\omega) = \frac{b_o(j\omega)^m + \cdots}{a_o(j\omega)^n + \cdots}$$

Figure 8–38
Polar plots in the high-frequency range.

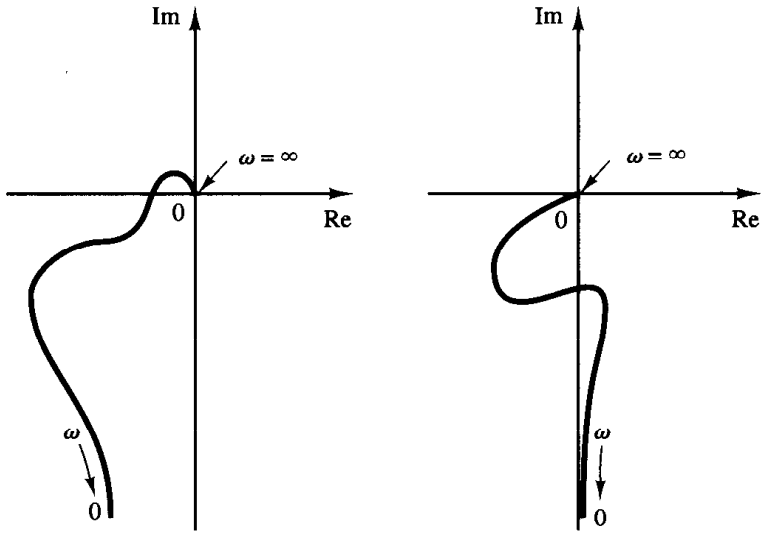

Figure 8–39
Polar plots of transfer functions with numerator dynamics.

Table 8–1 Polar Plots of Simple Transfer Functions

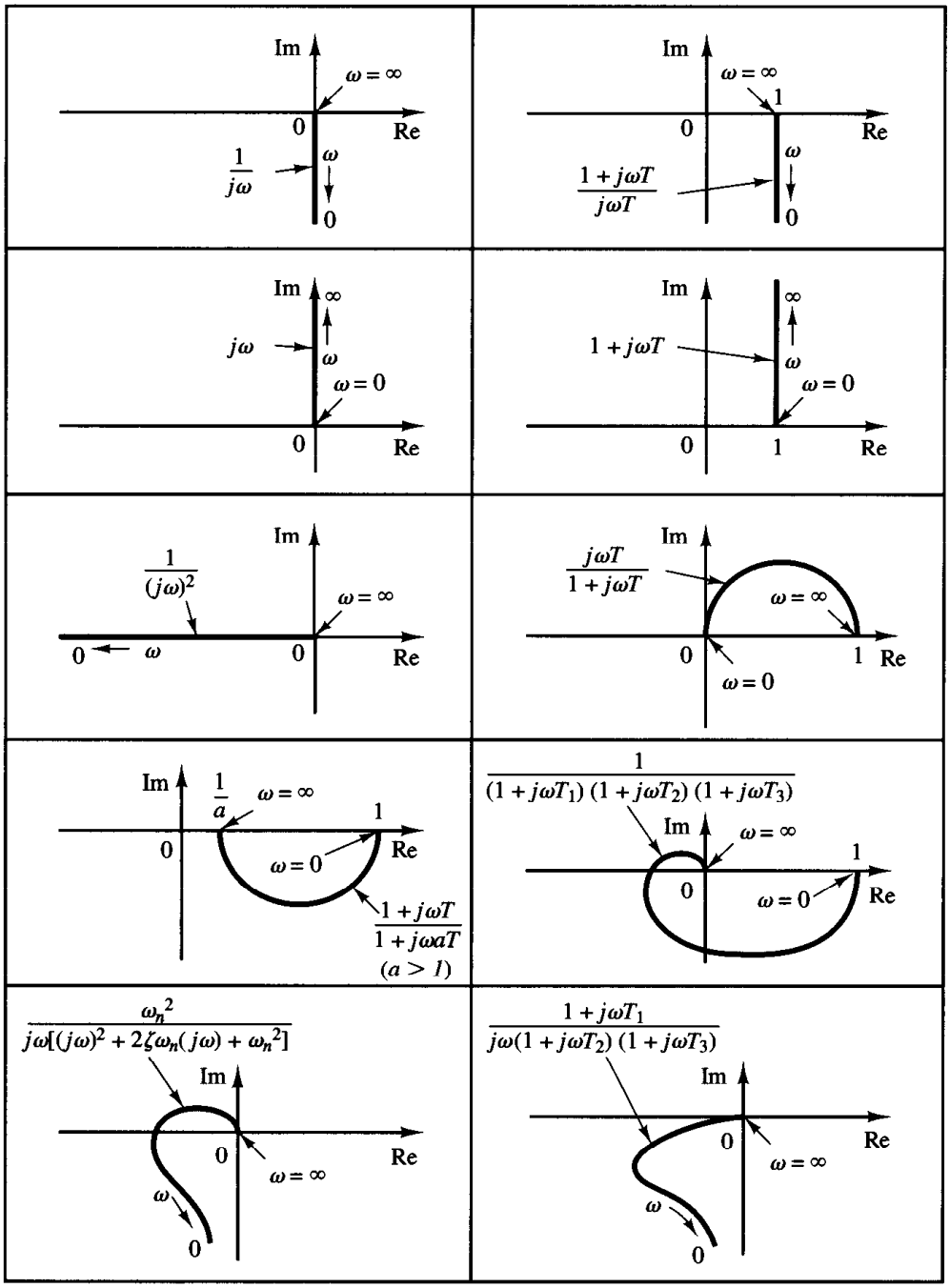

8–5 DRAWING NYQUIST PLOTS WITH MATLAB

Nyquist plots, just like Bode diagrams, are commonly used in the frequency-response representation of linear, time-invariant, feedback control systems. Nyquist plots are polar plots, while Bode diagrams are rectangular plots. One plot or the other may be more convenient for a particular operation, but a given operation can always be carried out in either plot.

The command nyquist computes the frequency response for continuous-time, linear, time-invariant systems. When invoked without left-hand arguments, nyquist produces a Nyquist plot on the screen.

The command

```
nyquist(num,den)
```

draws the Nyquist plot of the transfer function

$$G(s) = \frac{\text{num}(s)}{\text{den}(s)}$$

where num and den contain the polynomial coefficients in descending powers of s.

The command

```
nyquist(num,den,w)
```

uses the user-specified frequency vector w. The vector w specifies the frequency points in radians per second at which the frequency response will be calculated.

When invoked with the left-hand arguments

```
[re,im,w] = nyquist(num,den)
```

or

```
[re,im,w] = nyquist(num,den,w)
```

MATLAB returns the frequency response of the system in the matrices re, im and w. No plot is drawn on the screen. The matrices re and im contain the real and imaginary parts of the frequency response of the system evaluated at the frequency points specified in the vector w. Note that re and im have as many columns as outputs and one row for each element in w.

EXAMPLE 8–9 Consider the following open-loop transfer function:

$$G(s) = \frac{1}{s^2 + 0.8s + 1}$$

Draw a Nyquist plot with MATLAB.

Since the system is given in the form of the transfer function, the command

```
nyquist(num,den)
```

may be used to draw a Nyquist plot. MATLAB Program 8–8 produces the Nyquist plot shown in Figure 8–40. In this plot the ranges for the real axis and imaginary axis are automatically determined.

If we wish to draw the Nyquist plot using manually determined ranges, for example, from -2 to 2 on the real axis and from -2 to 2 on the imaginary axis, enter the following command into the computer:

```
MATLAB Program 8–8

num = [0   0   1];
den = [1   0.8   1];
nyquist(num,den)
grid
title('Nyquist Plot of G(s) = 1/(s^2+0.8s+1)')
```

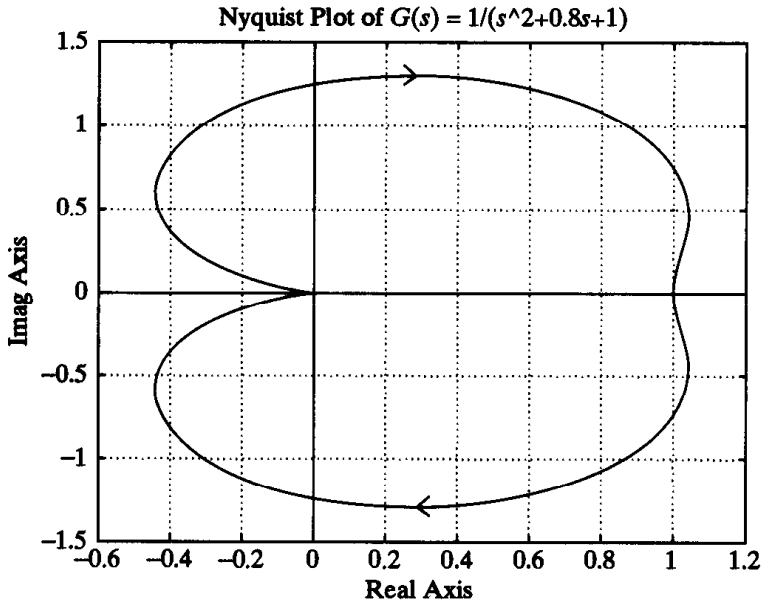

Figure 8–40
Nyquist plot of $G(s) = \dfrac{1}{s^2 + 0.8s + 1}$.

```
v = [−2   2   −2   2];
axis(v);
```

or, combining these two lines into one,

```
axis([−2   2   −2   2]);
```

See MATLAB Program 8–9 and the resulting Nyquist plot shown in Figure 8–41.

```
MATLAB Program 8–9

% ---------- Nyquist plot ----------

num = [0   0   1];
den = [1   0.8   1];
nyquist(num,den)
v = [−2   2   −2   2]; axis(v)
grid
title('Nyquist Plot of G(s) = 1/(s^2 + 0.8s + 1)')
```

Caution. In drawing a Nyquist plot, where MATLAB operation involves "Divide by zero," the resulting Nyquist plot may be erroneous. For example, if the transfer function $G(s)$ is given by

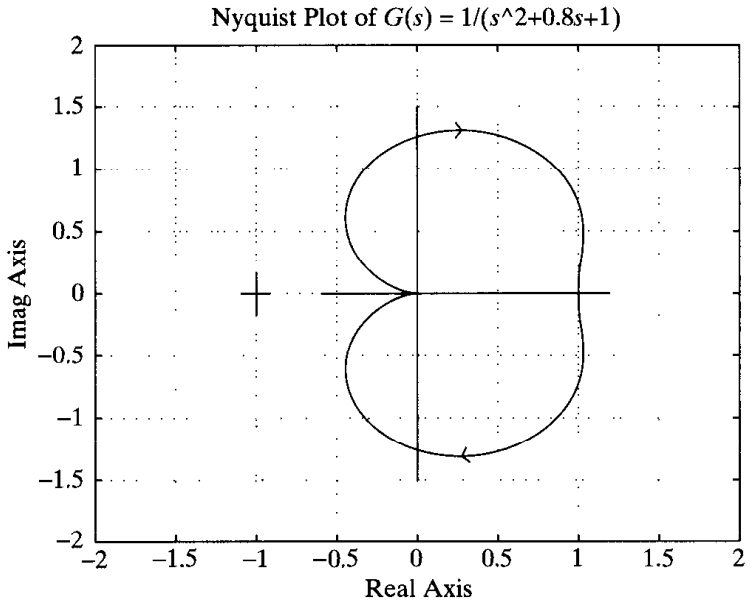

Figure 8–41
Nyquist plot of $G(s) = \dfrac{1}{s^2 + 0.8s + 1}$.

$$G(s) = \frac{1}{s(s + 1)}$$

then the MATLAB command

```
num = [0  0  1];
den = [1  1  0];
nyquist(num,den)
```

produces an erroneous Nyquist plot. An example of an erroneous Nyquist plot is shown in Figure 8–42. If such an erroneous Nyquist plot appears on the computer, then it can be corrected if we specify the axis(v). For example, if we enter the axis command

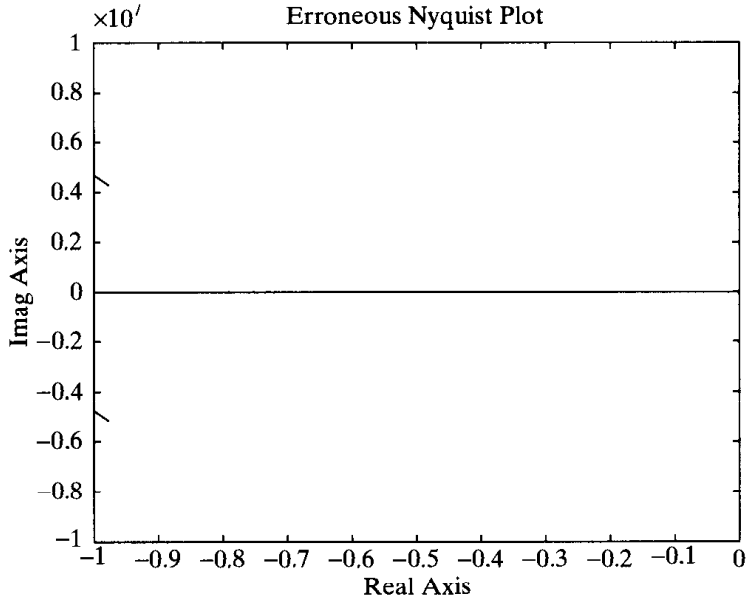

Figure 8–42
Erroneous Nyquist plot.

```
v = [−2   2   −5   5]; axis(v)
```

in the computer, then a correct Nyquist plot can be obtained. See Example 8–10.

EXAMPLE 8–10 Draw a Nyquist plot for the following $G(s)$:

$$G(s) = \frac{1}{s(s+1)}$$

MATLAB Program 8–10 will produce a correct Nyquist plot on the computer even though a warning message "Divide by zero" may appear on the screen. The resulting Nyquist plot is shown in Figure 8–43.

MATLAB Program 8–10

```
% ---------- Nyquist plot ----------

num = [0   0   1];
den = [1   1   0];
nyquist(num,den)
v = [−2   2   −5   5]; axis(v)
grid
title('Nyquist Plot of G(s) = 1/([s(s + 1)]')
```

Notice that the Nyquist plot shown in Figure 8–43 includes the loci for both $\omega > 0$ and $\omega < 0$. If we wish to draw the Nyquist plot for only the positive frequency region ($\omega > 0$), then we need to use the command

```
[re,im,w] = nyquist(num,den,w)
```

A MATLAB program using this nyquist command is shown in MATLAB Program 8–11. The resulting Nyquist plot is presented in Figure 8–44.

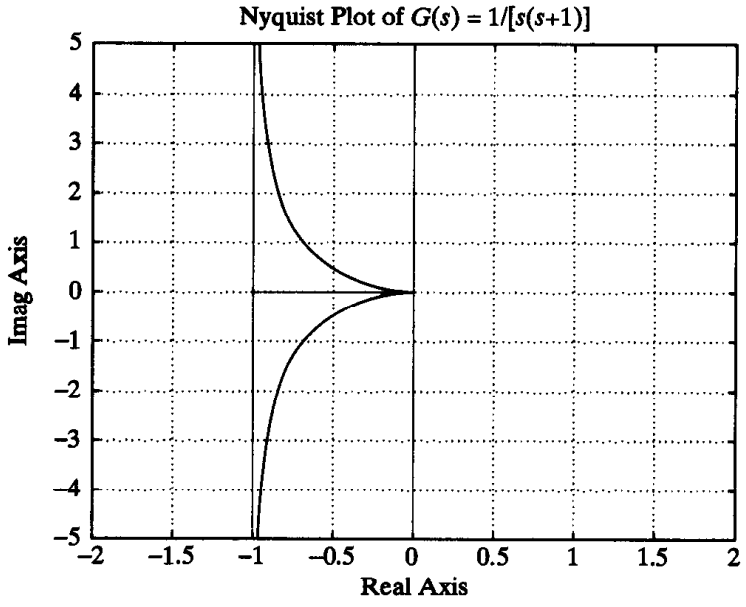

Figure 8–43
Nyquist plot of $G(s) = \dfrac{1}{s(s+1)}$.

MATLAB Program 8–11

```
% ---------- Nyquist plot ----------

num = [0   0   1];
den = [1   1   0];
w = 0.1:0.1:100;
[re,im,w] = nyquist(num,den,w);
plot(re,im)
v = [-2   2   -5   5]; axis(v)
grid
title('Nyquist Plot of G(s) = 1/[s(s + 1)]')
xlabel('Real Axis')
ylabel('Imag Axis')
```

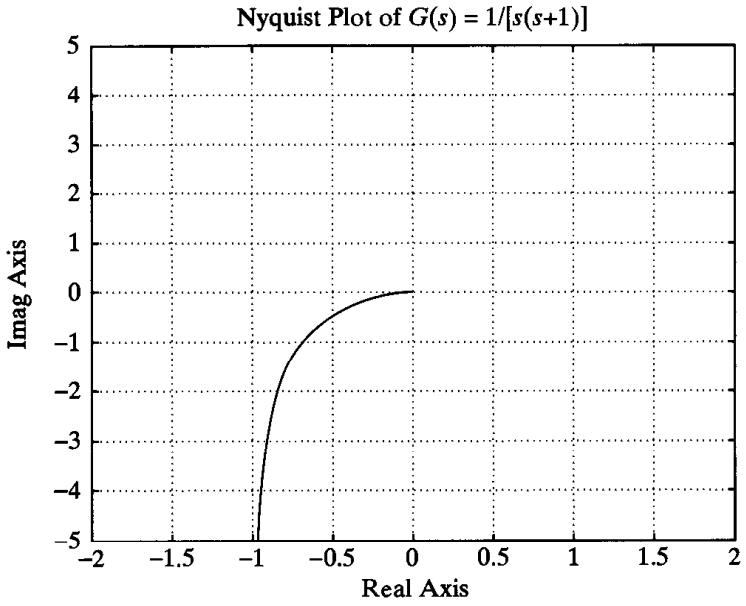

Figure 8–44
Nyquist plot of $G(s) = \dfrac{1}{s(s+1)}$.

Drawing Nyquist plots of a system defined in state space. Consider the system defined by

$$\dot{\mathbf{x}} = \mathbf{A}\mathbf{x} + \mathbf{B}\mathbf{u}$$

$$\mathbf{y} = \mathbf{C}\mathbf{x} + \mathbf{D}\mathbf{u}$$

where $\mathbf{x}$ = state vector (n-vector)
$\mathbf{y}$ = output vector (m-vector)
$\mathbf{u}$ = control vector (r-vector)
$\mathbf{A}$ = state matrix ($n \times n$ matrix)
$\mathbf{B}$ = control matrix ($n \times r$ matrix)
$\mathbf{C}$ = output matrix ($m \times n$ matrix)
$\mathbf{D}$ = direct transmission matrix ($m \times r$ matrix)

Nyquist plots for this system may be obtained by use of the command

```
nyquist(A,B,C,D)
```

This command produces a series of Nyquist plots, one for each input and output combination of the system. The frequency range is automatically determined.

The command

```
nyquist(A,B,C,D,iu)
```

produces Nyquist plots from the single input iu to all the outputs of the system, with the frequency range determined automatically. The scalar iu is an index into the inputs of the system and specifies which input to use for the frequency response.

The command

```
nyquist(A,B,C,D,iu,w)
```

uses the user-supplied frequency vector w. The vector w specifies the frequencies in radians per second at which the frequency response should be calculated.

EXAMPLE 8–11 Consider the system defined by

$$\begin{bmatrix} \dot{x}_1 \\ \dot{x}_2 \end{bmatrix} = \begin{bmatrix} 0 & 1 \\ -25 & -4 \end{bmatrix} \begin{bmatrix} x_1 \\ x_2 \end{bmatrix} + \begin{bmatrix} 0 \\ 25 \end{bmatrix} u$$

$$y = [1 \quad 0] \begin{bmatrix} x_1 \\ x_2 \end{bmatrix} + [0]u$$

Draw a Nyquist plot.

This system has a single input u and a single output y. A Nyquist plot may be obtained by entering the command

```
nyquist(A,B,C,D)
```

or

```
nyquist(A,B,C,D,1)
```

MATLAB Program 8–12 will provide the Nyquist plot. (Note that we obtain the identical result by using either of these two commands.) Figure 8–45 shows the Nyquist plot produced by MATLAB Program 8–12.

MATLAB Program 8–12

```
A = [0   1;−25   −4];
B = [0;25];
C = [1   0];
D = [0];
nyquist(A,B,C,D)
grid
title('Nyquist Plot')
```

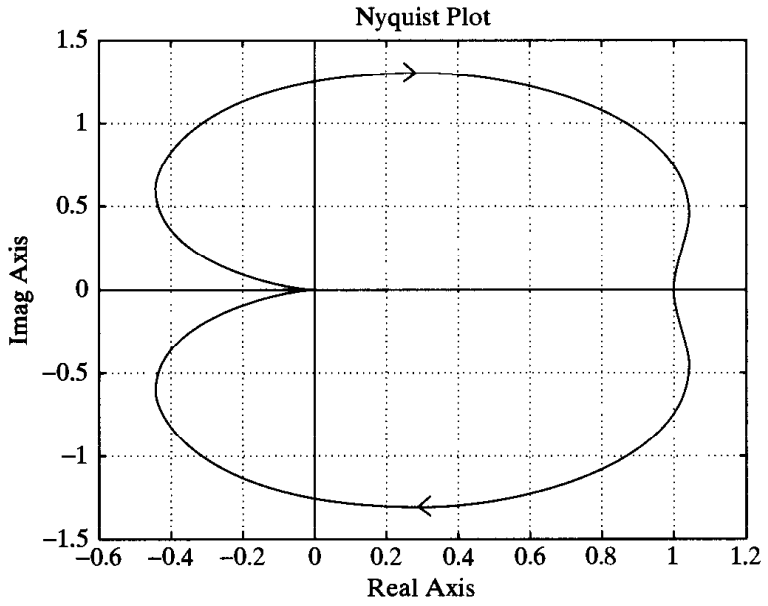

Figure 8–45
Nyquist plot of system considered in Example 8–11.

EXAMPLE 8–12 Consider the system defined by

$$\begin{bmatrix} \dot{x}_1 \\ \dot{x}_2 \end{bmatrix} = \begin{bmatrix} -1 & -1 \\ 6.5 & 0 \end{bmatrix} \begin{bmatrix} x_1 \\ x_2 \end{bmatrix} + \begin{bmatrix} 1 & 1 \\ 1 & 0 \end{bmatrix} \begin{bmatrix} u_1 \\ u_2 \end{bmatrix}$$

$$\begin{bmatrix} y_1 \\ y_2 \end{bmatrix} = \begin{bmatrix} 1 & 0 \\ 0 & 1 \end{bmatrix} \begin{bmatrix} x_1 \\ x_2 \end{bmatrix} + \begin{bmatrix} 0 & 0 \\ 0 & 0 \end{bmatrix} \begin{bmatrix} u_1 \\ u_2 \end{bmatrix}$$

This system involves two inputs and two outputs. There are four sinusoidal output–input relationships: $Y_1(j\omega)/U_1(j\omega)$, $Y_2(j\omega)/U_1(j\omega)$, $Y_1(j\omega)/U_2(j\omega)$, and $Y_2(j\omega)/U_2(j\omega)$. Draw Nyquist plots for the system. (When considering input u_1, we assume that input u_2 is zero, and vice versa.)

The four individual Nyquist plots can be obtained by use of the command

```
nyquist(A,B,C,D)
```

MATLAB Program 8–13 produces the four Nyquist plots. They are shown in Figure 8–46.

MATLAB Program 8–13

```
A = [−1   −1;6.5   0];
B = [1   1;1   0];
C = [1   0;0   1];
D = [0   0;0   0];
nyquist(A,B,C,D)
```

8–6 LOG-MAGNITUDE VERSUS PHASE PLOTS

Another approach to graphically portraying the frequency-response characteristics is to use the log-magnitude versus phase plot, which is a plot of the logarithmic magnitude in decibels versus the phase angle or phase margin for a frequency range of interest. [The phase margin is the difference between the actual phase angle ϕ and $-180°$; that

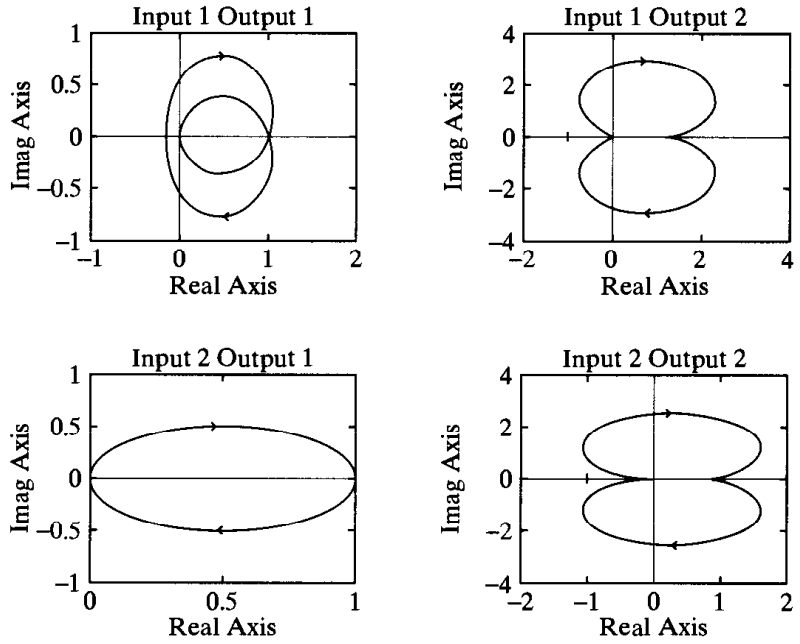

Figure 8–46
Nyquist plots of system considered in Example 8–12.

is, $\phi - (-180°) = 180° + \phi$.] The curve is graduated in terms of the frequency ω. Such log-magnitude versus phase plots are commonly called Nichols plots.

In the Bode diagram, the frequency-response characteristics of $G(j\omega)$ are shown on semilog paper by two separate curves, the log-magnitude curve and the phase-angle curve, while in the log-magnitude versus phase plot, the two curves in the Bode diagram are combined into one. The log-magnitude versus phase plot can easily be constructed by reading values of the log magnitude and phase angle from the Bode diagram. Notice that in the log-magnitude versus phase plot a change in the gain constant of $G(j\omega)$ merely shifts the curve up (for increasing gain) or down (for decreasing gain), but the shape of the curve remains the same.

Advantages of the log-magnitude versus phase plot are that the relative stability of the closed-loop system can be determined quickly and that compensation can be worked out easily.

The log-magnitude versus phase plots for the sinusoidal transfer function $G(j\omega)$ and $1/G(j\omega)$ are skew symmetrical about the origin since

$$\left|\frac{1}{G(j\omega)}\right| \text{ in dB} = -|G(j\omega)| \text{ in dB}$$

and

$$\angle\frac{1}{G(j\omega)} = -\angle G(j\omega)$$

Figure 8–47 compares frequency-response curves of

$$G(j\omega) = \frac{1}{1 + 2\xi\left(j\frac{\omega}{\omega_n}\right) + \left(j\frac{\omega}{\omega_n}\right)^2}$$

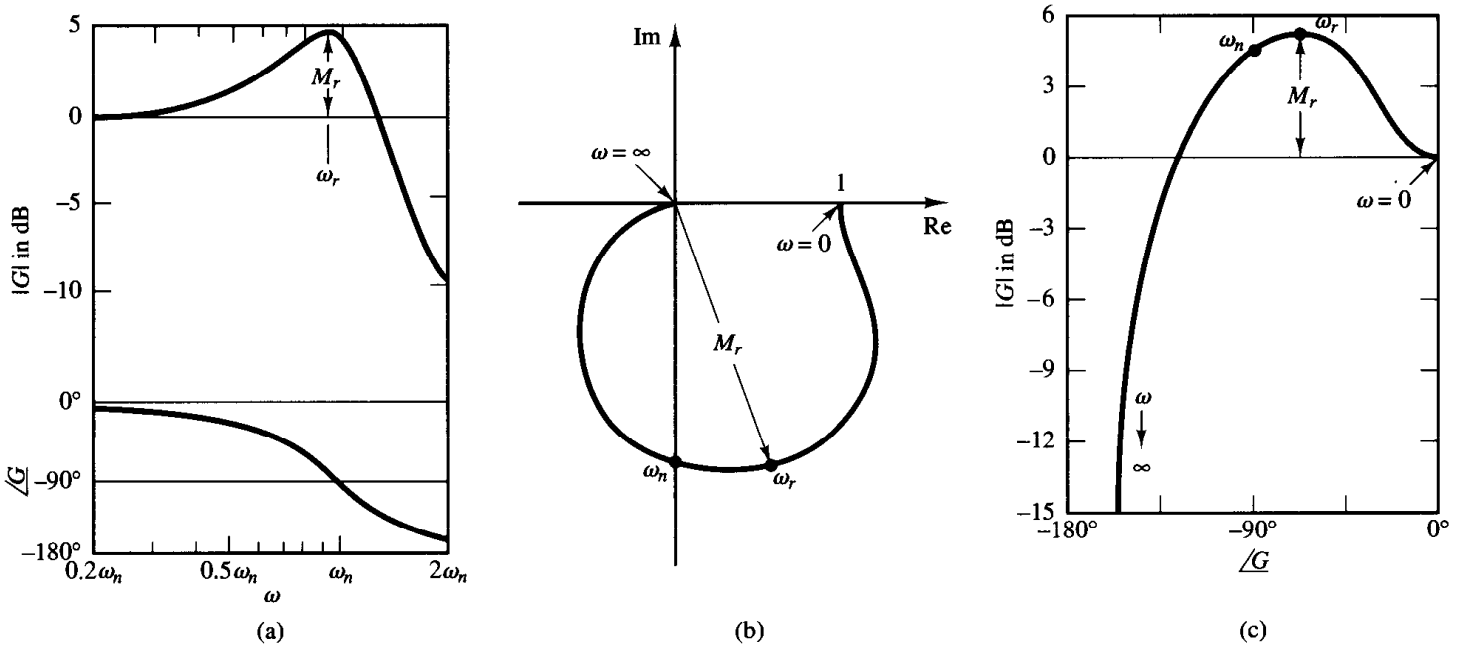

Figure 8–47
Three representations of the frequency response of $\dfrac{1}{1 + 2\zeta\left(j\dfrac{\omega}{\omega_n}\right) + \left(j\dfrac{\omega}{\omega_n}\right)^2}$, for $\zeta > 0$.

(a) Bode diagram; (b) polar plot; (c) log-magnitude versus phase plot.

in three different representations. In the log-magnitude versus phase plot, the vertical distance between the points $\omega = 0$ and $\omega = \omega_r$, where ω_r is the resonant frequency, is the peak value of $G(j\omega)$ in decibels.

Since log-magnitude and phase-angle characteristics of basic transfer functions have been discussed in detail in Sections 8–2 and 8–3, it will be sufficient here to give examples of some log-magnitude versus phase plots. Table 8–2 shows such examples.

8–7 NYQUIST STABILITY CRITERION

This section presents the Nyquist stability criterion and associated mathematical backgrounds. Consider the closed-loop system shown in Figure 8–48. The closed-loop transfer function is

$$\frac{C(s)}{R(s)} = \frac{G(s)}{1 + G(s)H(s)}$$

For stability, all roots of the characteristic equation

$$1 + G(s)H(s) = 0$$

Table 8–2 Log-Magnitude versus Phase Plots of Simple Transfer Functions

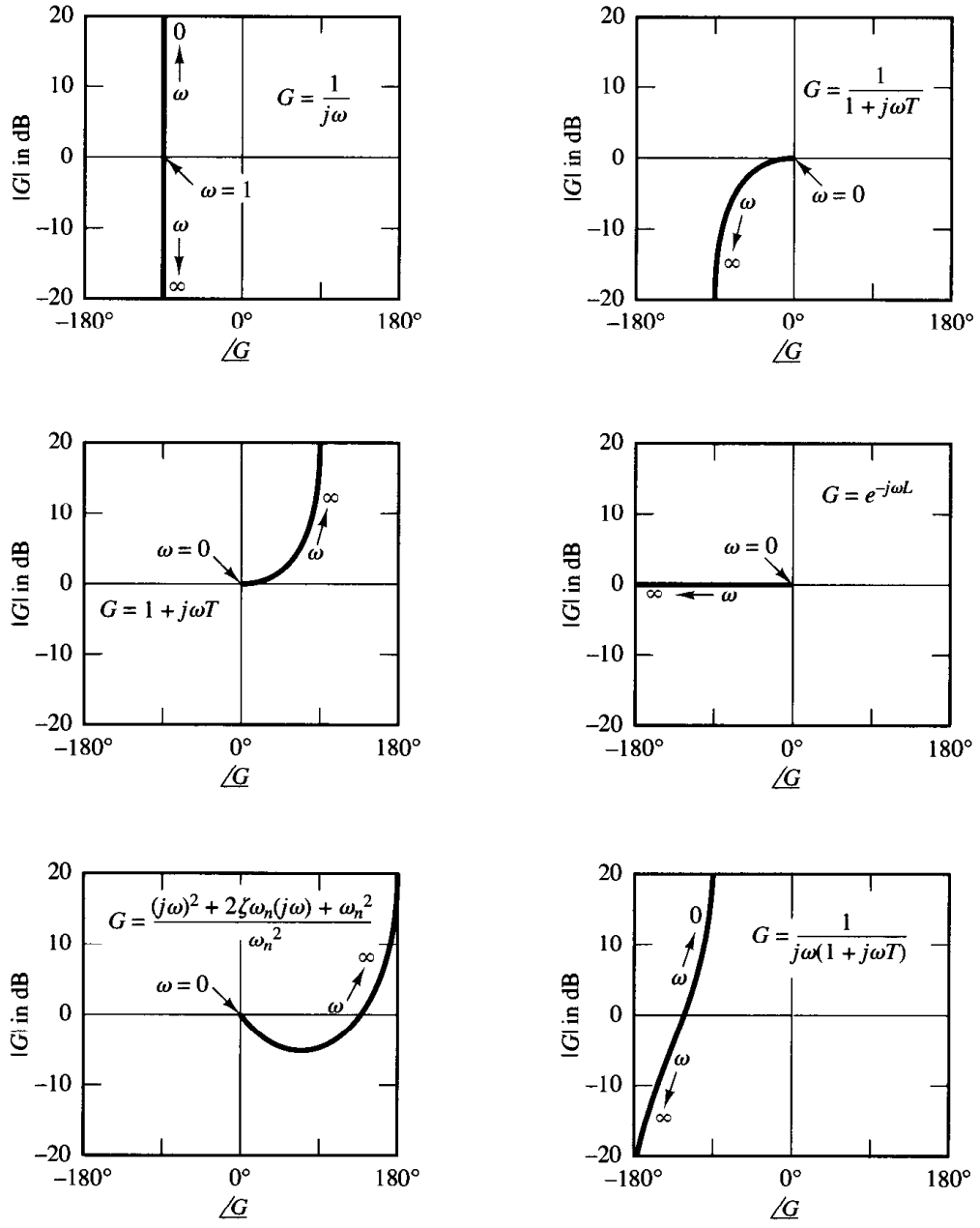

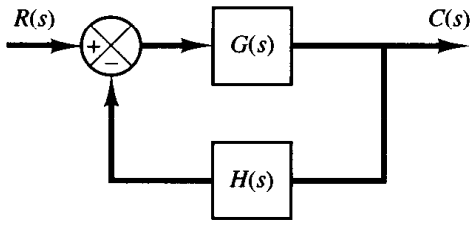

Figure 8–48
Closed-loop system.

must lie in the left-half s plane. [It is noted that, although poles and zeros of the open-loop transfer function $G(s)H(s)$ may be in the right-half s plane, the system is stable if all the poles of the closed-loop transfer function (that is, the roots of the characteristic equation) are in the left-half s plane.] The Nyquist stability criterion relates the open-loop frequency response $G(j\omega)H(j\omega)$ to the number of zeros and poles of $1 + G(s)H(s)$ that lie in the right-half s plane. This criterion, derived by H. Nyquist, is useful in control engineering because the absolute stability of the closed-loop system can be determined graphically from open-loop frequency-response curves, and there is no need for actually determining the closed-loop poles. Analytically obtained open-loop frequency-response curves, as well as those experimentally obtained, can be used for the stability analysis. This is convenient because, in designing a control system, it often happens that mathematical expressions for some of the components are not known; only their frequency-response data are available.

The Nyquist stability criterion is based on a theorem from the theory of complex variables. To understand the criterion, we shall first discuss mappings of contours in the complex plane.

We shall assume that the open-loop transfer function $G(s)H(s)$ is representable as a ratio of polynomials in s. For a physically realizable system, the degree of the denominator polynomial of the closed-loop transfer function must be greater than or equal to that of the numerator polynomial. This means that the limit of $G(s)H(s)$ as s approaches infinity is zero or a constant for any physically realizable system.

Preliminary study. The characteristic equation of the system shown in Figure 8–48 is

$$F(s) = 1 + G(s)H(s) = 0$$

We shall show that for a given continuous closed path in the s plane, which does not go through any singular points, there corresponds a closed curve in the $F(s)$ plane. The number and direction of encirclements of the origin of the $F(s)$ plane by the closed curve plays a particularly important role in what follows, for later we shall correlate the number and direction of encirclements with the stability of the system.

Consider, for example, the following open-loop transfer function:

$$G(s)H(s) = \frac{6}{(s + 1)(s + 2)}$$

The characteristic equation is

$$F(s) = 1 + G(s)H(s) = 1 + \frac{6}{(s + 1)(s + 2)}$$

$$= \frac{(s + 1.5 + j2.4)(s + 1.5 - j2.4)}{(s + 1)(s + 2)} = 0$$

The function $F(s)$ is analytic everywhere in the s plane except at its singular points. For each point of analyticity in the s plane, there corresponds a point in the $F(s)$ plane. For example, if $s = 1 + j2$, then $F(s)$ becomes

$$F(1 + j2) = 1 + \frac{6}{(2 + j2)(3 + j2)} = 1.115 - j0.577$$

Thus, the point $s = 1 + j2$ in the s plane maps into the point $1.115 - j0.577$ in the $F(s)$ plane.

Thus, as stated previously, for a given continuous closed path in the s plane, which does not go through any singular points, there corresponds a closed curve in the $F(s)$ plane. Figure 8–49 (a) shows conformal mappings of the lines $\omega = 0,1,2,3$ and the lines $\sigma = 1, 0, -1, -2, -3, -4$ in the upper-half s plane into the $F(s)$ plane. For example, the line $s = j\omega$ in the upper-half s plane ($\omega \geq 0$) maps into the curve denoted by $\sigma = 0$ in the $F(s)$ plane. Figure 8–49(b) shows conformal mappings of the lines $\omega = 0, -1, -2, -3$ and the lines $\sigma = 1, 0, -1, -2, -3, -4$ in the lower-half s plane into the $F(s)$ plane. Notice that for a given σ the curve for negative frequencies is symmetrical about the real axis with the curve for positive frequencies. Referring to Figures 8–49(a) and (b), we see that for the path $ABCD$ in the s plane traversed in the clockwise direction the corresponding curve in the $F(s)$ plane is $A'B'C'D'$. The arrows on the curves indicate directions of traversal. Similarly, the path $DEFA$ in the s plane maps into the curve $D'E'F'A'$ in the $F(s)$ plane. Because of the property of conformal mapping, the corresponding angles in the s plane and $F(s)$ plane are equal and have the same sense. [For example, since lines AB and BC intersect at right angles to each other in the s plane, curves $A'B'$ and $B'C'$ also intersect at right angles at point B' in the $F(s)$ plane.] Referring to Figure 8–49(c), we see that on the closed contour $ABCDEFA$ in the s plane the variable s starts at point A and assumes values on this path in a clockwise direction until it returns to the starting point A. The corresponding curve in the $F(s)$ plane is denoted $A'B'C'D'E'F'A'$. If we define the area to the right of the contour when a representative point s moves in the clockwise direction to be the inside of the contour and the area to the left to be the outside, then the shaded area in Figure 8–49(c) is enclosed by the contour $ABCDEFA$ and is inside it. From Figure 8–49(c), it can be seen that when the contour in the s plane encloses two poles of $F(s)$ the locus of $F(s)$ encircles the origin of the $F(s)$ plane twice in the counterclockwise direction.

The number of encirclements of the origin of the $F(s)$ plane depends on the closed contour in the s plane. If this contour encloses two zeros and two poles of $F(s)$, then the corresponding $F(s)$ locus does not encircle the origin, as shown in Figure 8–49(d). If this contour encloses only one zero, the corresponding locus of $F(s)$ encircles the origin once in the clockwise direction. This is shown in Figure 8–49(e). Finally, if the closed contour in the s plane encloses neither zeros nor poles, then the locus of $F(s)$ does not encircle the origin of the $F(s)$ plane at all. This is also shown in Figure 8–49(e).

Note that for each point in the s plane, except for the singular points, there is only one corresponding point in the $F(s)$ plane; that is, the mapping from the s plane into the $F(s)$ plane is one to one. The mapping from the $F(s)$ plane into the s plane may not be one to one, however, so that a given point in the $F(s)$ plane may correspond to more than one point in the s plane. For example, point B' in the $F(s)$ plane in Figure 8–49(d) corresponds to both point $(-3, 3)$ and point $(0, -3)$ in the s plane.

From the foregoing analysis, we can see that the direction of encirclement of the origin of the $F(s)$ plane depends on whether the contour in the s plane encloses a pole or a zero. Note that the location of a pole or zero in the s plane, whether in the right-half or left-half s plane, does not make any difference, but the enclosure of a pole or zero does. If the contour in the s plane encloses k zeros and k poles ($k = 0, 1, 2, \ldots$), that is, an equal number of each, then the corresponding closed curve in the $F(s)$ plane does not encircle the origin of the $F(s)$ plane. The foregoing discussion is a

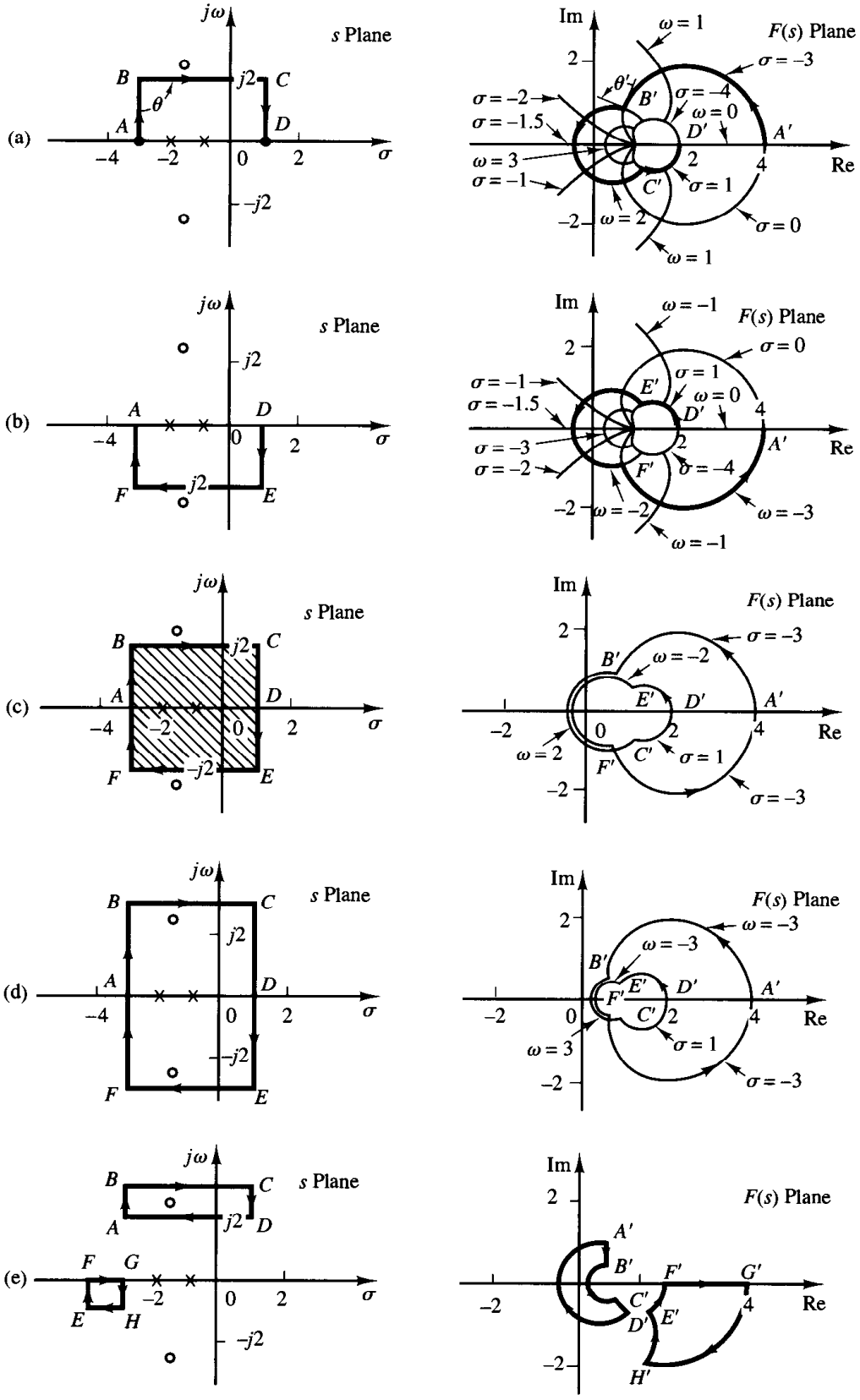

Figure 8–49
Conformal mapping of s plane grids into the $F(s)$ plane.

graphical explanation of the mapping theorem, which is the basis for the Nyquist stability criterion.

Mapping theorem. Let $F(s)$ be a ratio of two polynomials in s. Let P be the number of poles and Z be the number of zeros of $F(s)$ that lie inside some closed contour in the s plane, with multiplicity of poles and zeros accounted for. Let this contour be such that it does not pass through any poles or zeros of $F(s)$. This closed contour in the s plane is then mapped into the $F(s)$ plane as a closed curve. The total number N of clockwise encirclements of the origin of the $F(s)$ plane, as a representative point s traces out the entire contour in the clockwise direction, is equal to $Z - P$. (Note that by this mapping theorem the numbers of zeros and of poles cannot be found, only their difference.)

We shall not present a formal proof of this theorem here but leave the proof to Problem A-8-10. Note that a positive number N indicates an excess of zeros over poles of the function $F(s)$ and a negative N indicates an excess of poles over zeros. In control system applications, the number P can be readily determined for $F(s) = 1 + G(s)H(s)$ from the function $G(s)H(s)$. Therefore, if N is determined from the plot of $F(s)$, the number of zeros in the closed contour in the s plane can be determined readily. Note that the exact shapes of the s-plane contour and $F(s)$ locus are immaterial so far as encirclements of the origin are concerned, since encirclements depend only on the enclosure of poles and/or zeros of $F(s)$ by the s-plane contour.

Application of the mapping theorem to the stability analysis of closed-loop systems. For analyzing the stability of linear control systems, we let the closed contour in the s plane enclose the entire right-half s plane. The contour consists of the entire $j\omega$ axis from $\omega = -\infty$ to $+\infty$ and a semicircular path of infinite radius in the right-half s plane. Such a contour is called the Nyquist path. (The direction of the path is clockwise.) The Nyquist path encloses the entire right-half s plane and encloses all the zeros and poles of $1 + G(s)H(s)$ that have positive real parts. [If there are no zeros of $1 + G(s)H(s)$ in the right-half s plane, then there are no closed-loop poles there, and the system is stable.] It is necessary that the closed contour, or the Nyquist path, not pass through any zeros and poles of $1 + G(s)H(s)$. If $G(s)H(s)$ has a pole or poles at the origin of the s plane, mapping of the point $s = 0$ becomes indeterminate. In such cases, the origin is avoided by taking a detour around it. (A detailed discussion of this special case is given later.)

If the mapping theorem is applied to the special case in which $F(s)$ is equal to $1 + G(s)H(s)$, then we can make the following statement: If the closed contour in the s plane encloses the entire right-half s plane, as shown in Figure 8–50, then the number of right-half plane zeros of the function $F(s) = 1 + G(s)H(s)$ is equal to the number of poles of the function $F(s) = 1 + G(s)H(s)$ in the right-half s plane plus the number of clockwise encirclements of the origin of the $1 + G(s)H(s)$ plane by the corresponding closed curve in this latter plane.

Because of the assumed condition that

$$\lim_{s\to\infty} [1 + G(s)H(s)] = \text{constant}$$

the function of $1 + G(s)H(s)$ remains constant as s traverses the semicircle of infinite radius. Because of this, whether the locus of $1 + G(s)H(s)$ encircles the origin of the

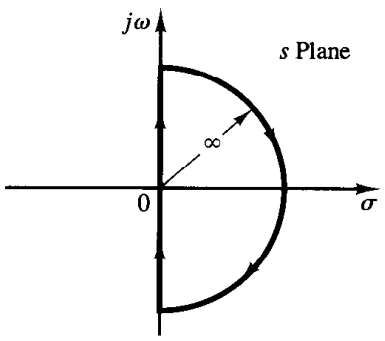

Figure 8–50
Closed contour in the s plane.

$1 + G(s)H(s)$ plane can be determined by considering only a part of the closed contour in the s plane, that is, the $j\omega$ axis. Encirclements of the origin, if there are any, occur only while a representative point moves from $-j\infty$ to $+j\infty$ along the $j\omega$ axis, provided that no zeros or poles lie on the $j\omega$ axis.

Note that the portion of the $1 + G(s)H(s)$ contour from $\omega = -\infty$ to $\omega = \infty$ is simply $1 + G(j\omega)H(j\omega)$. Since $1 + G(j\omega)H(j\omega)$ is the vector sum of the unit vector and the vector $G(j\omega)H(j\omega)$, $1 + G(j\omega)H(j\omega)$ is identical to the vector drawn from the $-1 + j0$ point to the terminal point of the vector $G(j\omega)H(j\omega)$, as shown in Figure 8–51. Encirclement of the origin by the graph of $1 + G(j\omega)H(j\omega)$ is equivalent to encirclement of the $-1 + j0$ point by just the $G(j\omega)H(j\omega)$ locus. Thus, stability of a closed-loop system can be investigated by examining encirclements of the $-1 + j0$ point by the locus of $G(j\omega)H(j\omega)$. The number of clockwise encirclements of the $-1 + j0$ point can be found by drawing a vector from the $-1 + j0$ point to the $G(j\omega)H(j\omega)$ locus, starting from $\omega = -\infty$, going through $\omega = 0$, and ending at $\omega = +\infty$, and by counting the number of clockwise rotations of the vector.

Plotting $G(j\omega)H(j\omega)$ for the Nyquist path is straightforward. The map of the negative $j\omega$ axis is the mirror image about the real axis of the map of the positive $j\omega$ axis. That is, the plot of $G(j\omega)H(j\omega)$ and the plot of $G(-j\omega)H(-j\omega)$ are symmetrical with each other about the real axis. The semicircle with infinite radius maps into either the origin of the GH plane or a point on the real axis of the GH plane.

In the preceding discussion, $G(s)H(s)$ has been assumed to be the ratio of two polynomials in s. Thus, the transport lag e^{-Ts} has been excluded from the discussion. Note, however, that a similar discussion applies to systems with transport lag, although a proof of this is not given here. The stability of a system with transport lag can be determined

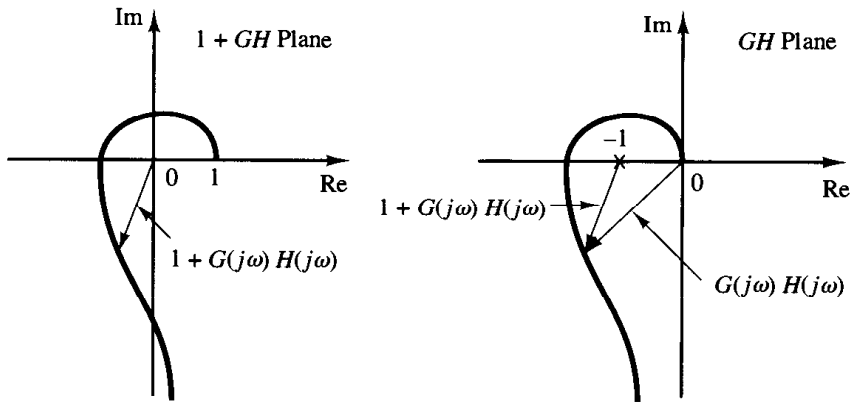

Figure 8–51
Plots of $1 + G(j\omega)H(j\omega)$ in the $1 + GH$ plane and GH plane.

from the open-loop frequency-response curves by examining the number of encirclements of the $-1 + j0$ point, just as in the case of a system whose open-loop transfer function is a ratio of two polynomials in s.

Nyquist stability criterion. The foregoing analysis, utilizing the encirclement of the $-1 + j0$ point by the $G(j\omega)H(j\omega)$ locus, is summarized in the following Nyquist stability criterion:

> *Nyquist stability criterion [for a special case when $G(s)H(s)$ has neither poles nor zeros on the $j\omega$ axis.]*: In the system shown in Figure 8–48, if the open-loop transfer function $G(s)H(s)$ has k poles in the right-half s plane and $\lim_{s\to\infty} G(s)H(s) =$ constant, then for stability the $G(j\omega)H(j\omega)$ locus, as ω varies from $-\infty$ to ∞, must encircle the $-1 + j0$ point k times in the counterclockwise direction.

Remarks on the Nyquist stability criterion

1. This criterion can be expressed as

$$Z = N + P$$

where Z = number of zeros of $1 + G(s)H(s)$ in the right-half s plane
N = number of clockwise encirclements of the $-1 + j0$ point
P = number of poles of $G(s)H(s)$ in the right-half s plane

If P is not zero, for a stable control system, we must have $Z = 0$, or $N = -P$, which means that we must have P counterclockwise encirclements of the $-1 + j0$ point.

If $G(s)H(s)$ does not have any poles in the right-half s plane, then $Z = N$. Thus, for stability there must be no encirclement of the $-1 + j0$ point by the $G(j\omega)H(j\omega)$ locus. In this case it is not necessary to consider the locus for the entire $j\omega$ axis, only for the positive-frequency portion. The stability of such a system can be determined by seeing if the $-1 + j0$ point is enclosed by the Nyquist plot of $G(j\omega)H(j\omega)$. The region enclosed by the Nyquist plot is shown in Figure 8–52. For stability, the $-1 + j0$ point must lie outside the shaded region.

2. We must be careful when testing the stability of multiple-loop systems since they may include poles in the right-half s plane. (Note that although an inner loop may be unstable the entire closed-loop system can be made stable by proper design.) Simple in-

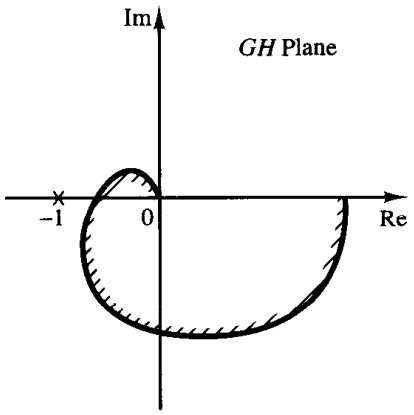

Figure 8–52
Region enclosed by a Nyquist plot.

spection of encirclements of the $-1 + j0$ point by the $G(j\omega)H(j\omega)$ locus is not sufficient to detect instability in multiple-loop systems. In such cases, however, whether any pole of $1 + G(s)H(s)$ is in the right-half s plane can be determined easily by applying the Routh stability criterion to the denominator of $G(s)H(s)$.

If transcendental functions, such as transport lag e^{-Ts}, are included in $G(s)H(s)$, they must be approximated by a series expansion before the Routh stability criterion can be applied. One form of a series expansion of e^{-Ts} was given in Chapter 5 and repeated here:

$$e^{-Ts} = \frac{1 - \frac{Ts}{2} + \frac{(Ts)^2}{8} - \frac{(Ts)^3}{48} + \cdots}{1 + \frac{Ts}{2} + \frac{(Ts)^2}{8} + \frac{(Ts)^3}{48} + \cdots}$$

As a first approximation, we may take only the first two terms in the numerator and denominator, respectively, or

$$e^{-Ts} \doteq \frac{1 - \frac{Ts}{2}}{1 + \frac{Ts}{2}} = \frac{2 - Ts}{2 + Ts}$$

This gives a good approximation to transport lag for the frequency range $0 \leq \omega \leq (0.5/T)$. [Note that the magnitude of $(2 - j\omega T)(2 + j\omega T)$ is always unity, and the phase lag of $(2 - j\omega T)/(2 + j\omega T)$ closely approximates that of transport lag within the stated frequency range.]

3. If the locus of $G(j\omega)H(j\omega)$ passes through the $-1 + j0$ point, then zeros of the characteristic equation, or closed-loop poles, are located on the $j\omega$ axis. This is not desirable for practical control systems. For a well-designed closed-loop system, none of the roots of the characteristic equation should lie on the $j\omega$ axis.

Special case when $G(s)H(s)$ involves poles and/or zeros on the $j\omega$ axis. In the previous discussion, we assumed that the open-loop transfer function $G(s)H(s)$ has neither poles nor zeros at the origin. We now consider the case where $G(s)H(s)$ involves poles and/or zeros on the $j\omega$ axis.

Since the Nyquist path must not pass through poles or zeros of $G(s)H(s)$, if the function $G(s)H(s)$ has poles or zeros at the origin (or on the $j\omega$ axis at points other than the origin), the contour in the s plane must be modified. The usual way of modifying the contour near the origin is to use a semicircle with the infinitesimal radius ϵ, as shown in Figure 8–53. A representative point s moves along the negative $j\omega$ axis from $-j\infty$ to $j0-$. From $s = j0-$ to $s = j0+$, the point moves along the semicircle of radius ϵ (where $\epsilon \ll 1$) and then moves along the positive $j\omega$ axis from $j0+$ to $j\infty$. From $s = j\infty$, the contour follows a semicircle with infinite radius, and the representative point moves back to the starting point. The area that the modified closed contour avoids is very small and approaches zero as the radius ϵ approaches zero. Therefore, all the poles and zeros, if any, in the right-half s plane are enclosed by this contour.

Consider, for example, a closed-loop system whose open-loop transfer function is given by

$$G(s)H(s) = \frac{K}{s(Ts + 1)}$$

The points corresponding to $s = j0+$ and $s = j0-$ on the locus of $G(s)H(s)$ in the $G(s)H(s)$ plane are $-j\infty$ and $j\infty$, respectively. On the semicircular path with radius ϵ (where $\epsilon \ll 1$), the complex variable s can be written

$$s = \epsilon e^{j\theta}$$

where θ varies from $-90°$ to $+90°$. Then $G(s)H(s)$ becomes

$$G(\epsilon e^{j\theta})H(\epsilon e^{j\theta}) = \frac{K}{\epsilon e^{j\theta}} = \frac{K}{\epsilon} e^{-j\theta}$$

The value K/ϵ approaches infinity as ϵ approaches zero, and $-\theta$ varies from $90°$ to $-90°$ as a representative point s moves along the semicircle. Thus, the points $G(j0-)H(j0-) = j\infty$ and $G(j0+)H(j0+) = -j\infty$ are joined by a semicircle of infinite radius in the right-half GH plane. The infinitesimal semicircular detour around the origin maps into the GH plane as a semicircle of infinite radius. Figure 8–54 shows the s-plane contour and the $G(s)H(s)$ locus in the GH plane. Points A, B, and C on the s-plane contour map into the respective points A', B', and C' on the $G(s)H(s)$ locus. As seen from Figure 8–54, points D, E, and F on the semicircle of infinite radius in the s plane map into the origin of the GH plane. Since there is no pole in the right-half s plane and the $G(s)H(s)$ locus does not encircle the $-1 + j0$ point, there are no zeros of the function $1 + G(s)H(s)$ in the right-half s plane. Therefore, the system is stable.

For an open-loop transfer function $G(s)H(s)$ involving a $1/s^n$ factor (where $n = 2, 3, \ldots$), the plot of $G(s)H(s)$ has n clockwise semicircles of infinite radius about the origin as a representative point s moves along the semicircle of radius ϵ (where $\epsilon \ll 1$). For example, consider the following open-loop transfer function:

$$G(s)H(s) = \frac{K}{s^2(Ts + 1)}$$

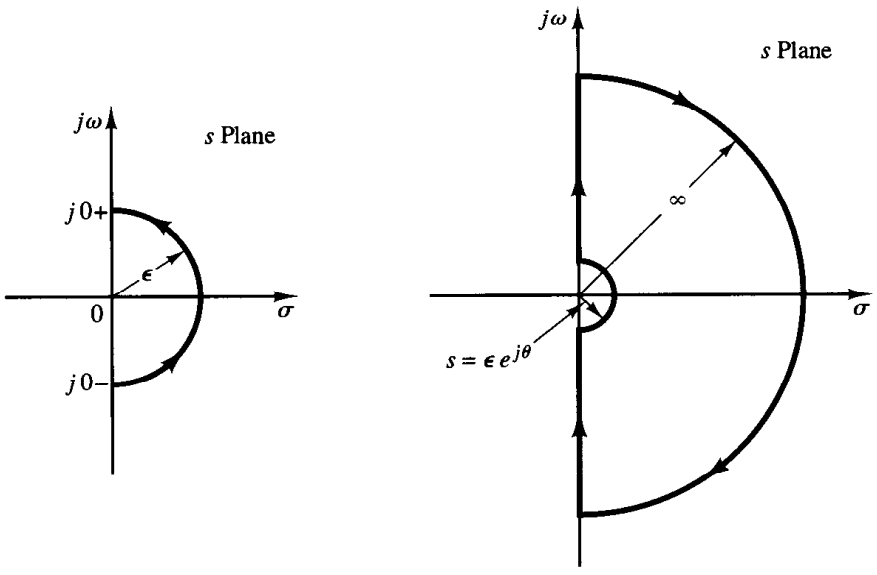

Figure 8–53
Closed contours in the s plane avoiding poles and zeros at the origin.

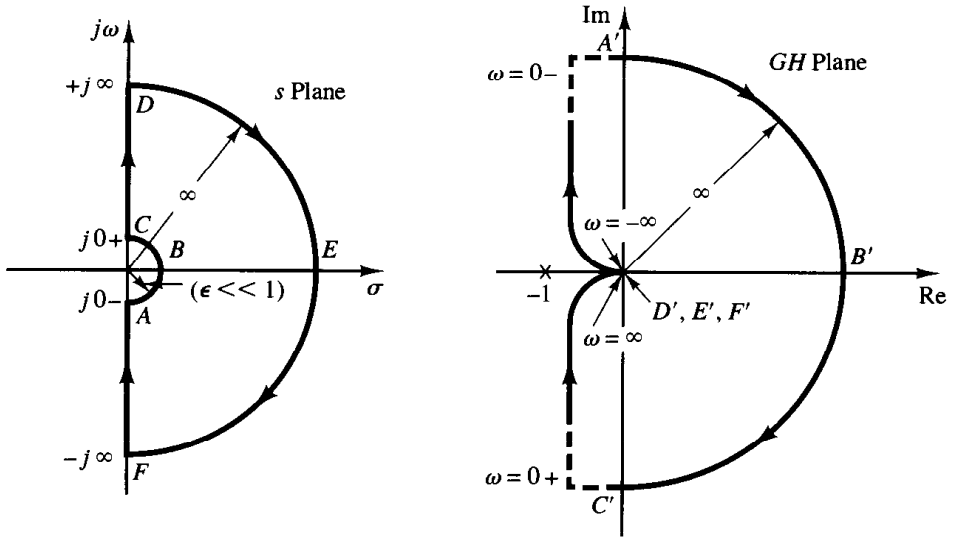

Figure 8–54
s-Plane contour and the $G(s)H(s)$ locus in the GH plane, where $G(s)H(s) = K/[s(Ts + 1)]$.

Then

$$\lim_{s \to \epsilon e^{j\theta}} G(s)H(s) = \frac{K}{\epsilon^2 e^{2j\theta}} = \frac{K}{\epsilon^2} e^{-2j\theta}$$

As θ varies from $-90°$ to $90°$ in the s plane, the angle of $G(s)H(s)$ varies from $180°$ to $-180°$, as shown in Figure 8–55. Since there is no pole in the right-half s plane and the locus encircles the $-1 + j0$ point twice clockwise for any positive value of K, there are two zeros of $1 + G(s)H(s)$ in the right-half s plane. Therefore, this system is always unstable.

Note that a similar analysis can be made if $G(s)H(s)$ involves poles and/or zeros on the $j\omega$ axis. The Nyquist stability criterion can now be generalized as follows:

Nyquist stability criterion [for a general case when $G(s)H(s)$ has poles and/or zeros on the $j\omega$ axis.]: In the system shown in Figure 8–48, if the open-loop transfer function $G(s)H(s)$ has k poles in the right-half s plane, then for stability the $G(s)H(s)$ locus, as a representative point s traces on the modified Nyquist path in the

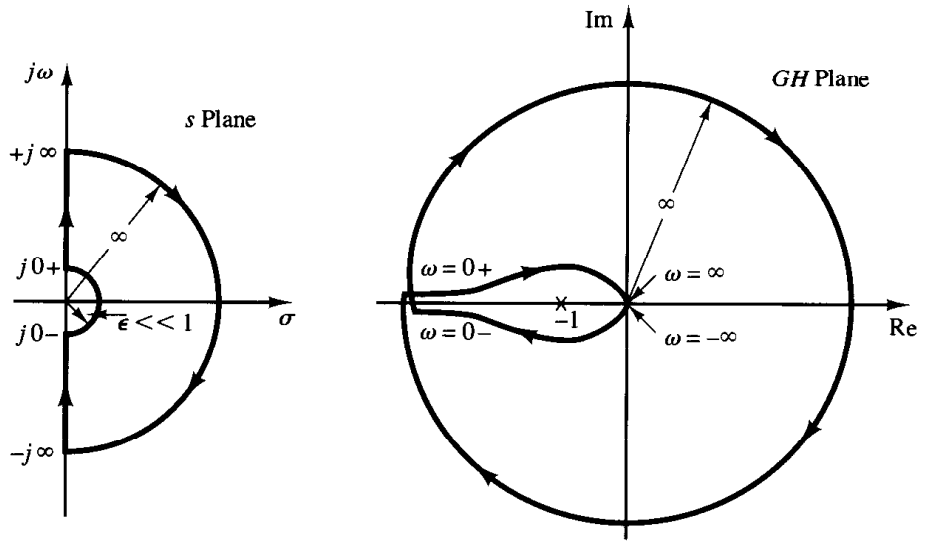

Figure 8–55
s-Plane contour and the $G(s)H(s)$ locus in the GH plane, where $G(s)H(s) = K/[s^2(Ts + 1)]$.

clockwise direction, must encircle the $-1 + j0$ point k times in the counterclockwise direction.

8–8 STABILITY ANALYSIS

In this section, we shall present several illustrative examples of the stability analysis of control systems using the Nyquist stability criterion.

If the Nyquist path in the s plane encircles Z zeros and P poles of $1 + G(s)H(s)$ and does not pass through any poles or zeros of $1 + G(s)H(s)$ as a representative point s moves in the clockwise direction along the Nyquist path, then the corresponding contour in the $G(s)H(s)$ plane encircles the $-1 + j0$ point $N = Z - P$ times in the clockwise direction. (Negative values of N imply counterclockwise encirclements.)

In examining the stability of linear control systems using the Nyquist stability criterion, we see that three possibilities can occur.

1. There is no encirclement of the $-1 + j0$ point. This implies that the system is stable if there are no poles of $G(s)H(s)$ in the right-half s plane; otherwise, the system is unstable.
2. There is a counterclockwise encirclement or encirclements of the $-1 + j0$ point. In this case the system is stable if the number of counterclockwise encirclements is the same as the number of poles $G(s)H(s)$ in the right-half s plane; otherwise, the system is unstable.
3. There is a clockwise encirclement or encirclements of the $-1 + j0$ point. In this case the system is unstable.

In the following examples, we assume that the values of the gain K and the time constants (such as T, T_1, and T_2) are all positive.

EXAMPLE 8–13 Consider a closed-loop system whose open-loop transfer function is given by

$$G(s)H(s) = \frac{K}{(T_1 s + 1)(T_2 s + 1)}$$

Examine the stability of the system.

A plot of $G(j\omega)H(j\omega)$ is shown in Figure 8–56. Since $G(s)H(s)$ does not have any poles in the right-half s plane and the $-1 + j0$ point is not encircled by the $G(j\omega)H(j\omega)$ locus, this system is stable for any positive values of K, T_1, and T_2.

EXAMPLE 8–14 Consider the system with the following open-loop transfer function:

$$G(s) = \frac{K}{s(T_1 s + 1)(T_2 s + 1)}$$

Determine the stability of the system for two cases: (1) the gain K is small and (2) K is large.

The Nyquist plots of the open-loop transfer function with a small value of K and a large value of K are shown in Figure 8–57. The number of poles of $G(s)H(s)$ in the right-half s plane is zero. Therefore, for this system to be stable, it is necessary that $N = Z = 0$ or that the $G(s)H(s)$ locus not encircle the $-1 + j0$ point.

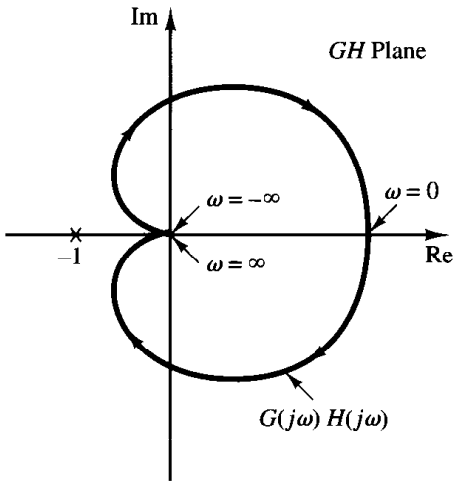

Figure 8–56
Polar plot of $G(j\omega)H(j\omega)$ considered in Example 8–13.

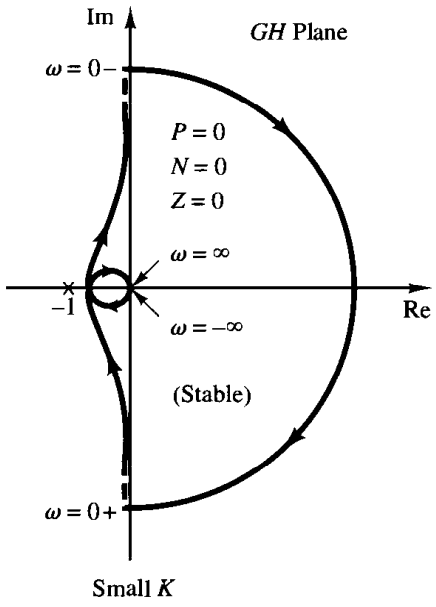

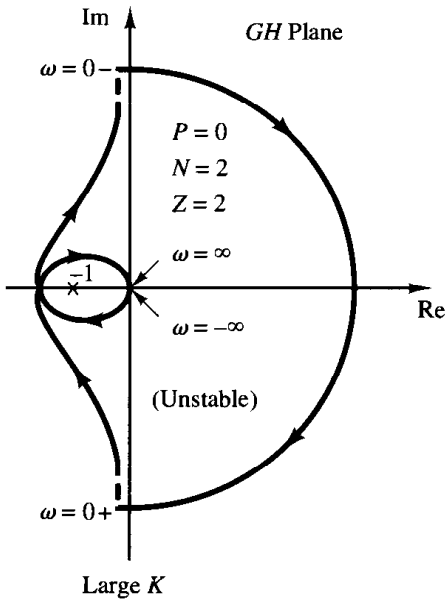

Figure 8–57
Polar plots of the system considered in Example 8–14.

For small values of K, there is no encirclement of the $-1 + j0$ point. Hence, the system is stable for small values of K. For large values of K, the locus of $G(s)H(s)$ encircles the $-1 + j0$ point twice in the clockwise direction, indicating two closed-loop poles in the right-half s plane, and the system is unstable. (For good accuracy, K should be large. From the stability viewpoint, however, a large value of K causes poor stability or even instability. To compromise between accuracy and stability, it is necessary to insert a compensation network into the system. Compensating techniques in the frequency domain are discussed in Chapter 9.)

EXAMPLE 8–15 The stability of a closed-loop system with the following open-loop transfer function

$$G(s)H(s) = \frac{K(T_2 s + 1)}{s^2(T_1 s + 1)}$$

depends on the relative magnitudes of T_1 and T_2. Draw Nyquist plots and determine the stability of the system.

Plots of the locus $G(s)H(s)$ for three cases, $T_1 < T_2$, $T_1 = T_2$, and $T_1 > T_2$, are shown in Figure 8–58. For $T_1 < T_2$, the locus of $G(s)H(s)$ does not encircle the $-1 + j0$ point, and the closed-loop system is stable. For $T_1 = T_2$ the $G(s)H(s)$ locus passes through the $-1 + j0$ point, which

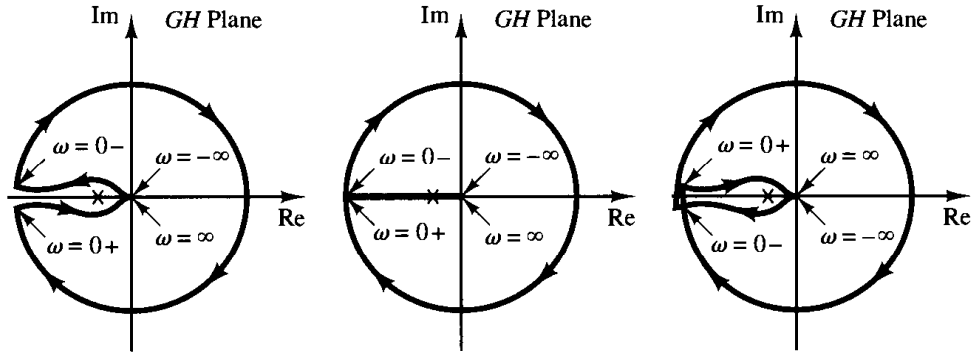

$T_1 < T_2$ (Stable)

$T_1 = T_2$ $G(j\omega)\,H(j\omega)$ locus passes through the $-1 + j0$ point

$T_1 > T_2$ (Unstable)

Figure 8–58
Polar plots of the system considered in Example 8–15.

indicates that the closed-loop poles are located on the $j\omega$ axis. For $T_1 > T_2$, the locus of $G(s)H(s)$ encircles the $-1 + j0$ point twice in the clockwise direction. Thus, the closed-loop system has two closed-loop poles in the right-half s plane, and the system is unstable.

EXAMPLE 8–16 Consider the closed-loop system having the following open-loop transfer function:

$$G(s)H(s) = \frac{K}{s(Ts - 1)}$$

Determine the stability of the system.

The function $G(s)H(s)$ has one pole ($s = 1/T$) in the right-half s plane. Therefore, $P = 1$. The Nyquist plot shown in Figure 8–59 indicates that the $G(s)H(s)$ plot encircles the $-1 + j0$ point once clockwise. Thus, $N = 1$. Since $Z = N + P$, we find that $Z = 2$. This means that the closed-loop system has two closed-loop poles in the right-half s plane and is unstable.

EXAMPLE 8–17 Investigate the stability of a closed-loop system with the following open-loop transfer function:

$$G(s)H(s) = \frac{K(s + 3)}{s(s - 1)} \qquad (K > 1)$$

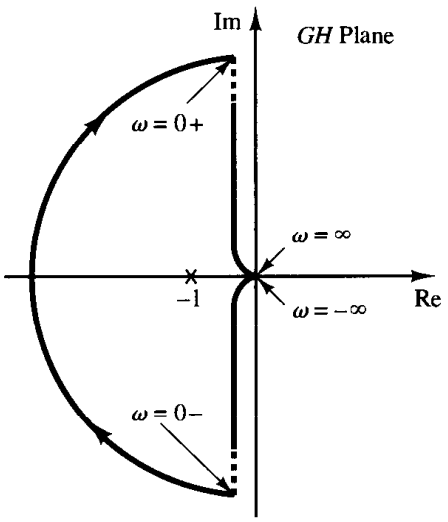

Figure 8–59
Polar plot of the system considered in Example 8–16.

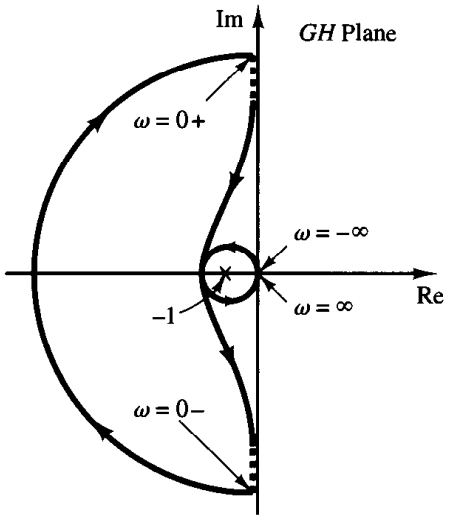

Figure 8–60
Polar plot of the system considered in Example 8–17.

The open-loop transfer function has one pole ($s = 1$) in the right-half s plane, or $P = 1$. The open-loop system is unstable. The Nyquist plot shown in Figure 8–60 indicates that the $-1 + j0$ point is encircled by the $G(s)H(s)$ locus once in the counterclockwise direction. Therefore, $N = -1$. Thus, Z is found from $Z = N + P$ to be zero, which indicates that there is no zero of $1 + G(s)H(s)$ in the right-half s plane, and the closed-loop system is stable. This is one of the examples for which an unstable open-loop system becomes stable when the loop is closed.

Conditionally stable systems. Figure 8–61 shows an example of a $G(j\omega)H(j\omega)$ locus for which the closed-loop system can be made unstable by varying the open-loop gain. If the open-loop gain is increased sufficiently, the $G(j\omega)H(j\omega)$ locus encloses the $-1 + j0$ point twice, and the system becomes unstable. If the open-loop gain is decreased sufficiently, again the $G(j\omega)H(j\omega)$ locus encloses the $-1 + j0$ point twice. For stable operation of the system considered here, the critical point $-1 + j0$ must not be located in the regions between OA and BC shown in Figure 8–61. Such a system that is stable only for limited ranges of values of the open-loop gain for which the $-1 + j0$ point is completely outside the $G(j\omega)H(j\omega)$ locus is a conditionally stable system.

A conditionally stable system is stable for the value of the open-loop gain lying between critical values, but it is unstable if the open-loop gain is either increased or decreased sufficiently. Such a system becomes unstable when large input signals are

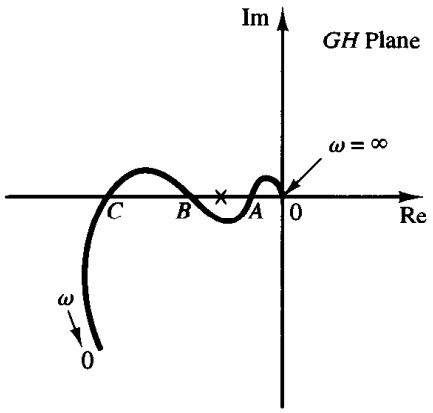

Figure 8–61
Polar plot of a conditionally stable system.

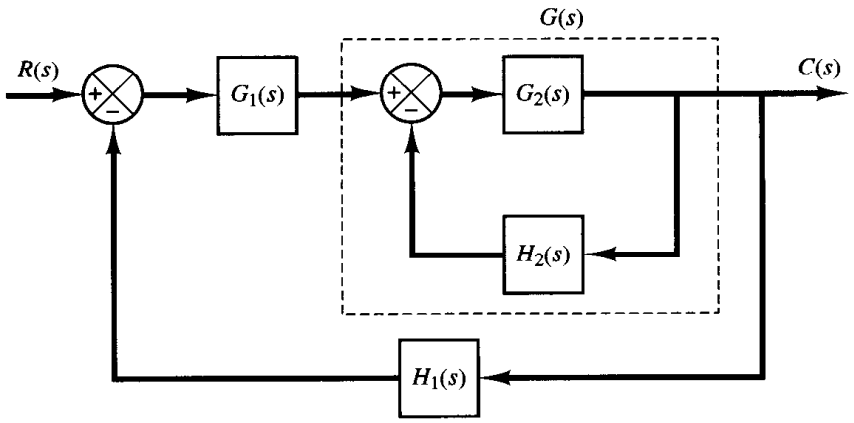

Figure 8–62
Multiple-loop system.

applied, since a large signal may cause saturation, which in turn reduces the open-loop gain of the system. It is advisable to avoid such a situation.

Multiple-loop system. Consider the system shown in Figure 8–62. This is a multiple-loop system. The inner loop has the transfer function

$$G(s) = \frac{G_2(s)}{1 + G_2(s)H_2(s)}$$

If $G(s)$ is unstable, the effects of instability are to produce a pole or poles in the right-half s plane. Then the characteristic equation of the inner loop, $1 + G_2(s)H_2(s) = 0$, has a zero or zeros in this portion of the plane. If $G_2(s)$ and $H_2(s)$ have P_1 poles here, then the number Z_1 of right-half plane zeros of $1 + G_2(s)H_2(s)$ can be found from $Z_1 = N_1 + P_1$, where N_1 is the number of clockwise encirclements of the $-1 + j0$ point by the $G_2(s)H_2(s)$ locus. Since the open-loop transfer function of the entire system is given by $G_1(s)G(s)H_1(s)$, the stability of this closed-loop system can be found from the Nyquist plot of $G_1(s)G(s)H_1(s)$ and knowledge of the right-half plane poles of $G_1(s)G(s)H_1(s)$.

Notice that if a feedback loop is eliminated by means of block diagram reductions there is a possibility that unstable poles are introduced; if the feedforward branch is eliminated by means of block diagram reductions, there is a possibility that right-half plane zeros are introduced. Therefore, we must note all right-half plane poles and zeros as they appear from subsidiary loop reductions. This knowledge is necessary in determining the stability of multiple-loop systems.

EXAMPLE 8–18 Consider the control system shown in Figure 8–63. The system involves two loops. Determine the range of gain K for stability of the system by use of the Nyquist stability criterion. (The gain K is positive).

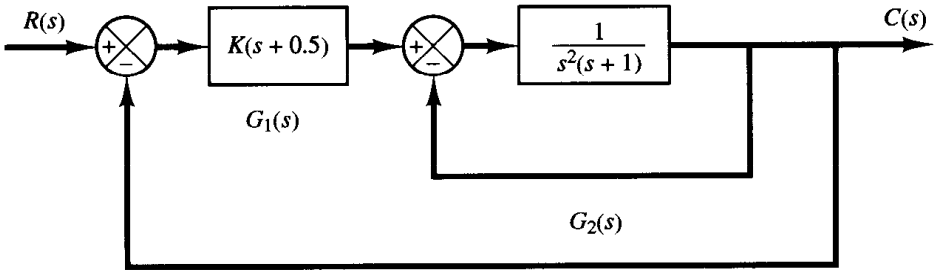

Figure 8–63
Control system.

To examine the stability of the control system, we need to sketch the Nyquist locus of $G(s)$, where

$$G(s) = G_1(s)G_2(s)$$

However, the poles of $G(s)$ are not known at this point. Therefore, we need to examine the minor loop if there are right-half s-plane poles. This can be done easily by use of the Routh stability criterion. Since

$$G_2(s) = \frac{1}{s^3 + s^2 + 1}$$

the Routh array becomes as follows:

s^3	1	0
s^2	1	1
s^1	−1	0
s^0	1	

Notice that there are two sign changes in the first column. Hence, there are two poles of $G_2(s)$ in the right-half s plane.

Once we find the number of right-half s plane poles of $G_2(s)$, we proceed to sketch the Nyquist locus of $G(s)$, where

$$G(s) = G_1(s)G_2(s) = \frac{K(s + 0.5)}{s^3 + s^2 + 1}$$

Our problem is to determine the range of gain K for stability. Hence, instead of plotting Nyquist loci of $G(j\omega)$ for various values of K, we plot the Nyquist locus of $G(j\omega)/K$. Figure 8–64 shows the Nyquist plot or polar plot of $G(j\omega)/K$.

Since $G(s)$ has two poles in the right-half s plane, we have $P_1 = 2$. Noting that

$$Z_1 = N_1 + P_1$$

for stability, we require $Z_1 = 0$ or $N_1 = -2$. That is, the Nyquist locus of $G(j\omega)$ must encircle the $-1 + j0$ point twice counterclockwise. From Figure 8–64, we see that, if the critical point lies between 0 and -0.5, then the $G(j\omega)/K$ locus encircles the critical point twice counterclockwise. Therefore, we require

$$-0.5K < -1$$

The range of gain K for stability is

$$2 < K$$

Nyquist stability criterion applied to inverse polar plots. In the previous analyses, the Nyquist stability criterion was applied to polar plots of the open-loop transfer function $G(s)H(s)$.

In analyzing multiple-loop systems, the inverse transfer function may sometimes be used in order to permit graphical analysis; this avoids much of the numerical calculation. (The Nyquist stability criterion can be applied equally well to inverse polar plots. The mathematical derivation of the Nyquist stability criterion for inverse polar plots is the same as that for direct polar plots.)

The inverse polar plot of $G(j\omega)H(j\omega)$ is a graph of $1/[G(j\omega)H(j\omega)]$ as a function of ω. For example, if $G(j\omega)H(j\omega)$ is

$$G(j\omega)H(j\omega) = \frac{j\omega T}{1 + j\omega T}$$

then

$$\frac{1}{G(j\omega)H(j\omega)} = \frac{1}{j\omega T} + 1$$

The inverse polar plot for $\omega \geq 0$ is the lower half of the vertical line starting at the point $(1, 0)$ on the real axis.

The Nyquist stability criterion applied to inverse plots may be stated as follows: For a closed-loop system to be stable, the encirclement, if any, of the $-1 + j0$ point by the $1/[G(s)H(s)]$ locus (as s moves along the Nyquist path) must be counterclockwise, and the number of such encirclements must be equal to the number of poles of $1/[G(s)H(s)]$ [that is, the zeros of $G(s)H(s)$] that lie in the right-half s plane. [The number of zeros of $G(s)H(s)$ in the right-half s plane may be determined by use of the Routh stability criterion.] If the open-loop transfer function $G(s)H(s)$ has no zeros in the right-half s

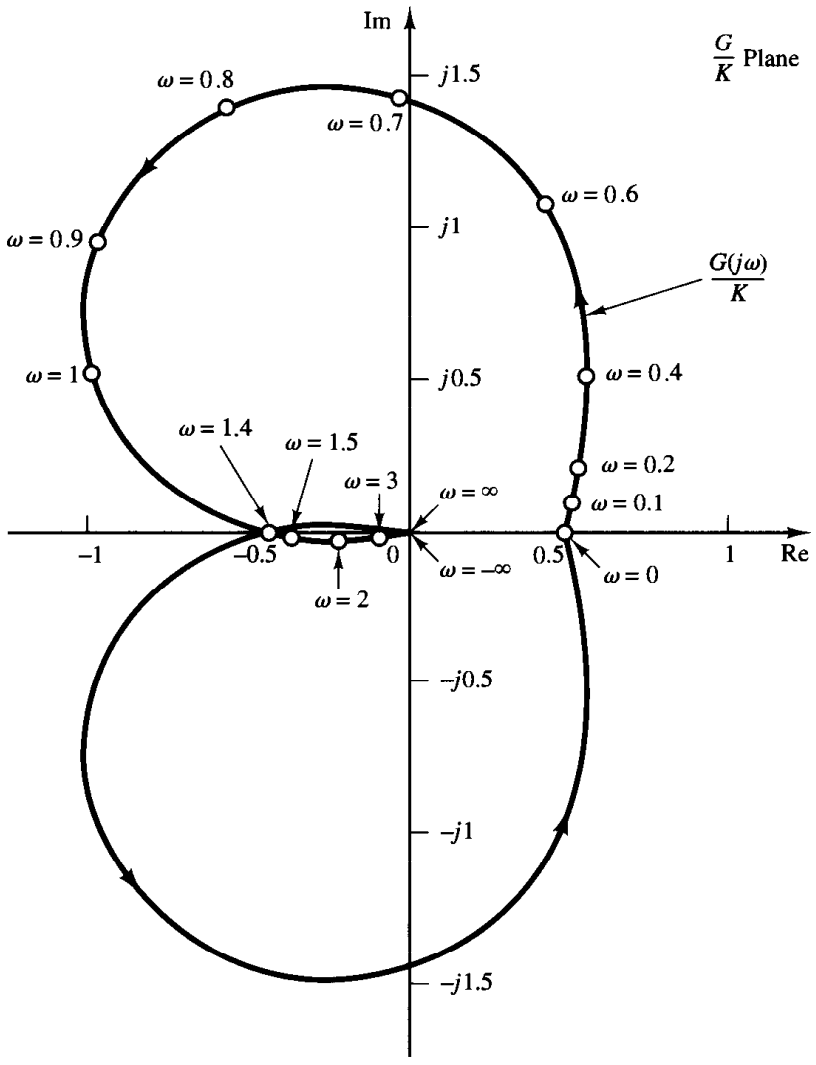

Figure 8–64
Polar plot of $G(j\omega)/K$.

plane, then for a closed-loop system to be stable the number of encirclements of the $-1 + j0$ point by the $1/[G(s)H(s)]$ locus must be zero.

Note that although the Nyquist stability criterion can be applied to inverse polar plots, if experimental frequency-response data are incorporated, counting the number of encirclements of the $1/[G(s)H(s)]$ locus may be difficult because the phase shift corresponding to the infinite semicircular path in the s plane is difficult to measure. For example, if the open-loop transfer function $G(s)H(s)$ involves transport lag such that

$$G(s)H(s) = \frac{Ke^{-j\omega L}}{s(Ts + 1)}$$

then the number of encirclements of the $-1 + j0$ point by the $1/[G(s)H(s)]$ locus becomes infinite, and the Nyquist stability criterion cannot be applied to the inverse polar plot of such an open-loop transfer function.

In general, if experimental frequency-response data cannot be put into analytical form, both the $G(j\omega)H(j\omega)$ and $1/[G(j\omega)H(j\omega)]$ loci must be plotted. In addition, the number of right-half plane zeros of $G(s)H(s)$ must be determined. It is more difficult to determine the right-half plane zeros of $G(s)H(s)$ (in other words, to determine whether a given component is minimum phase) than it is to determine the right-half plane poles of $G(s)H(s)$ (in other words, to determine whether the component is stable).

Depending on whether the data are graphical or analytical and whether nonminimum-phase components are included, an appropriate stability test must be used for multiple-loop systems. If the data are given in analytical form or if mathematical expressions for all the components are known, the application of the Nyquist stability criterion to inverse polar plots causes no difficulty, and multiple-loop systems may be analyzed and designed in the inverse GH plane.

EXAMPLE 8–19 Consider the control system shown in Figure 8–63. (Refer to Example 8–18.) Using the inverse polar plot, determine the range of gain K for stability.

Since

$$G_2(s) = \frac{1}{s^3 + s^2 + 1}$$

we have

$$G(s) = G_1(s)G_2(s) = \frac{K(s + 0.5)}{s^3 + s^2 + 1}$$

Hence

$$\frac{1}{G(s)} = \frac{s^3 + s^2 + 1}{K(s + 0.5)}$$

Notice that $1/G(s)$ has a pole at $s = -0.5$. It does not have any pole in the right-half s plane. Therefore, the Nyquist stability equation

$$Z = N + P$$

reduces to $Z = N$ since $P = 0$. The reduced equation states that the number Z of the zeros of $1 + [1/G(s)]$ in the right-half s plane is equal to N, the number of clockwise encirclements of the

$-1 + j0$ point. For stability, N must be equal to zero, or there should be no encirclement. Figure 8–65 shows the Nyquist plot or polar plot of $K/G(j\omega)$.

Notice that since

$$\frac{K}{G(j\omega)} = \left[\frac{(j\omega)^3 + (j\omega)^2 + 1}{j\omega + 0.5}\right]\left(\frac{0.5 - j\omega}{0.5 - j\omega}\right)$$
$$= \frac{0.5 - 0.5\omega^2 - \omega^4 + j\omega(-1 + 0.5\omega^2)}{0.25 + \omega^2}$$

the $K/G(j\omega)$ locus crosses the negative real axis at $\omega = \sqrt{2}$, and the crossing point at the negative real axis is -2.

From Figure 8–65 we see that if the critical point lies in the region between -2 and $-\infty$ then the critical point is not encircled. Hence, for stability we require

$$-1 < \frac{-2}{K}$$

Thus, the range of gain K for stability is

$$2 < K$$

which is the same result as we obtained in Example 8–18.

Relative stability analysis through modified Nyquist plots. The Nyquist path for stability tests can be modified in order that we may investigate the relative stability of closed-loop systems. For the following second-order characteristic equation,

$$s^2 + 2\zeta\omega_n s + \omega_n^2 = 0 \qquad (0 < \zeta < 1)$$

the roots are complex conjugates and are

$$s_1 = -\zeta\omega_n + j\omega_n\sqrt{1 - \zeta^2}, \qquad s_2 = -\zeta\omega_n - j\omega_n\sqrt{1 - \zeta^2}$$

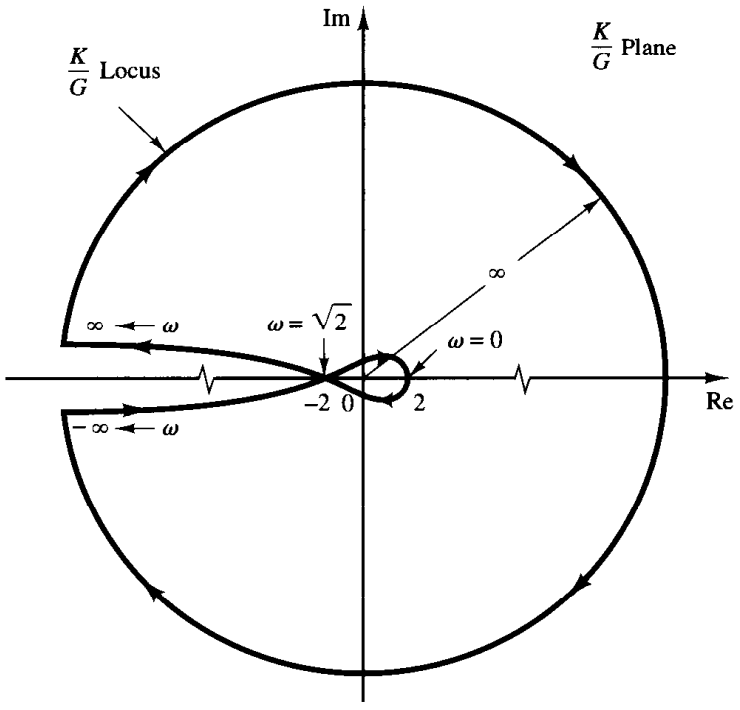

Figure 8–65
Polar plot of $K/G(j\omega)$.

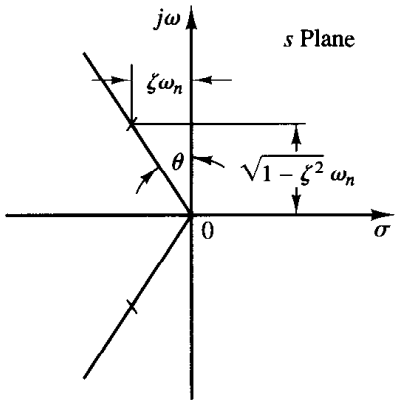

Figure 8–66
Plot of complex-conjugate roots in the s plane.

If these roots are plotted in the s plane, as shown in Figure 8–66, then we see that sin $\theta = \zeta$, or the angle θ is indicative of the damping ratio ζ. As θ becomes smaller, so does the value of ζ.

If we modify the Nyquist path and use radial lines with angle θ_x, instead of the $j\omega$ axis, as shown in Figure 8–67, then it can be said, following the same reasoning as in the case of the Nyquist stability criterion, that if the $G(s)H(s)$ locus corresponding to the modified s-plane contour does not encircle the $-1 + j0$ point and none of the poles of $G(s)H(s)$ lie within the closed s-plane contour then this contour does not enclose any zeros of $1 + G(s)H(s)$. The characteristic equation, $1 + G(s)H(s) = 0$, then does not have any roots within the modified s-plane contour. If no closed-loop poles of a higher-order system are enclosed by this contour, we can say that the damping ratio of each pair of complex-conjugate closed-loop poles of the system is greater than sin θ_x.

Suppose that the s-plane contour consists of a line to the left of and parallel to the $j\omega$ axis at a distance $-\sigma_o$ (or the line $s = -\sigma_o + j\omega$) and the semicircle of infinite radius enclosing the entire right-half s plane and that part of the left-half s plane between the lines $s = -\sigma_o + j\omega$ and $s = j\omega$, as shown in Figure 8–68(a). If the $G(s)H(s)$ locus corresponding to this s-plane contour does not encircle the $-1 + j0$ point and $G(s)H(s)$ has no poles within the enclosed s-plane contour, then the characteristic equation does not have any zeros in the region enclosed by the modified s-plane contour. All roots of the characteristic equation lie to the left of the line $s = -\sigma_o + j\omega$. An example of a $G(-\sigma_o + j\omega)H(-\sigma_o + j\omega)$ locus, together with a $G(j\omega)H(j\omega)$ locus, is shown in Figure 8–68(b). The magnitude $1/\sigma_o$ is indicative of the time constant of the dominant closed-loop poles. If all

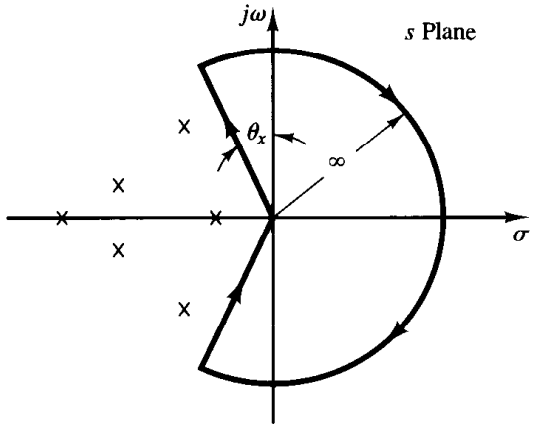

Figure 8–67
Modified Nyquist path.

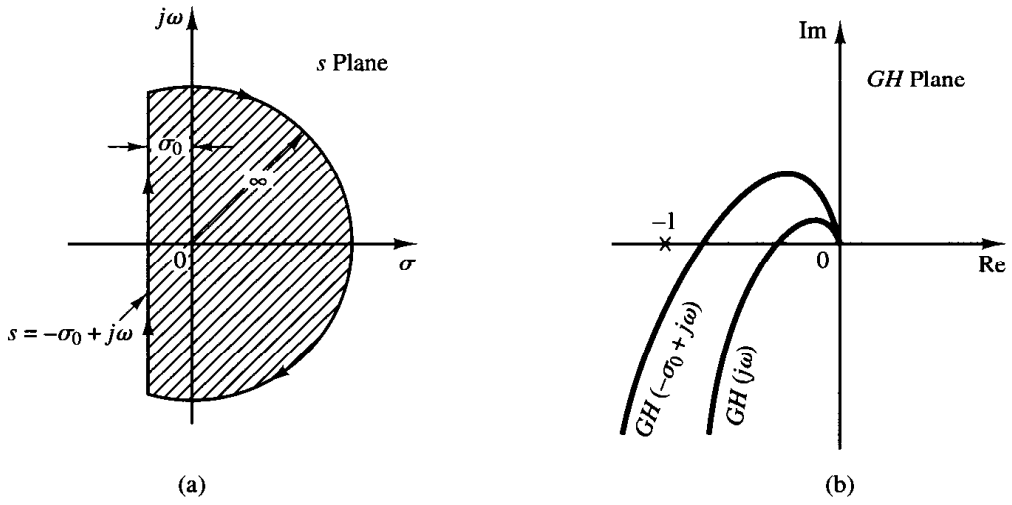

Figure 8–68
(a) Modified Nyquist path; (b) polar plots of $G(-\sigma_o + j\omega)H(-\sigma_o + j\omega)$ locus and $G(j\omega)H(j\omega)$ locus in the GH plane.

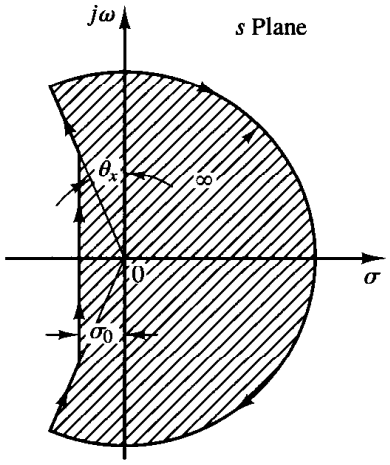

Figure 8–69
Modified Nyquist path.

roots lie outside the s-plane contour, all time constants of the closed-loop transfer function are less than $1/\sigma_o$. If the s-plane contour is chosen as shown in Figure 8–69, then the test of encirclements of the $-1 + j0$ point reveals the existence or nonexistence of the roots of the characteristic equation of the closed-loop system within this s-plane contour. If the test reveals that no roots lie in the s-plane contour, then it is clear that all the closed-loop poles have damping ratios greater than ζ_x and time constants less than $1/\sigma_o$. Thus, by taking an appropriate s-plane contour, we can investigate time constants and damping ratios of closed-loop poles from the open-loop transfer function.

8–9 RELATIVE STABILITY

In designing a control system, we require that the system be stable. Furthermore, it is necessary that the system have adequate relative stability.

In this section, we shall show that the Nyquist plot indicates not only whether a system is stable but also the degree of stability of a stable system. The Nyquist plot also gives information as to how stability may be improved, if this is necessary. (See Chapter 9.)

In the following discussion, we shall assume that the systems considered have unity feedback. Note that it is always possible to reduce a system with feedback elements to

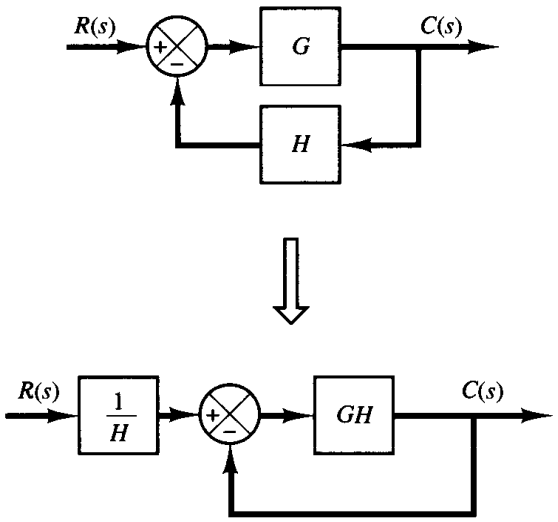

Figure 8–70
Modification of a system with feedback elements to a unity-feedback system.

a unity-feedback system, as shown in Figure 8–70. Hence, the extension of relative stability analysis for the unity-feedback system to nonunity-feedback systems is possible.

We shall also assume that, unless otherwise stated, the systems are minimum-phase systems; that is, the open-loop transfer function $G(s)$ has neither poles nor zeros in the right-half s plane.

Relative stability analysis by conformal mapping. One of the important problems in analyzing a control system is to find all closed-loop poles or at least those closest to the $j\omega$ axis (or the dominant pair of closed-loop poles). If the open-loop frequency-response characteristics of a system are known, it may be possible to estimate the closed-loop poles closest to the $j\omega$ axis. It is noted that the Nyquist locus $G(j\omega)$ need not be an analytically known function of ω. The entire Nyquist locus may be experimentally obtained. The technique to be presented here is essentially graphical and is based on a conformal mapping of the s plane into the $G(s)$ plane.

Consider the conformal mapping of constant-σ lines (lines $s = \sigma + j\omega$, where σ is constant and ω varies) and constant-ω lines (lines $s = \sigma + j\omega$, where ω is constant and σ varies) in the s plane. The $\sigma = 0$ line (the $j\omega$ axis) in the s plane maps into the Nyquist plot in the $G(s)$ plane. The constant-σ lines in the s plane map into curves that are similar to the Nyquist plot and are in a sense parallel to the Nyquist plot, as shown in Figure 8–71. The constant-ω lines in the s plane map into curves, also shown in Figure 8–71.

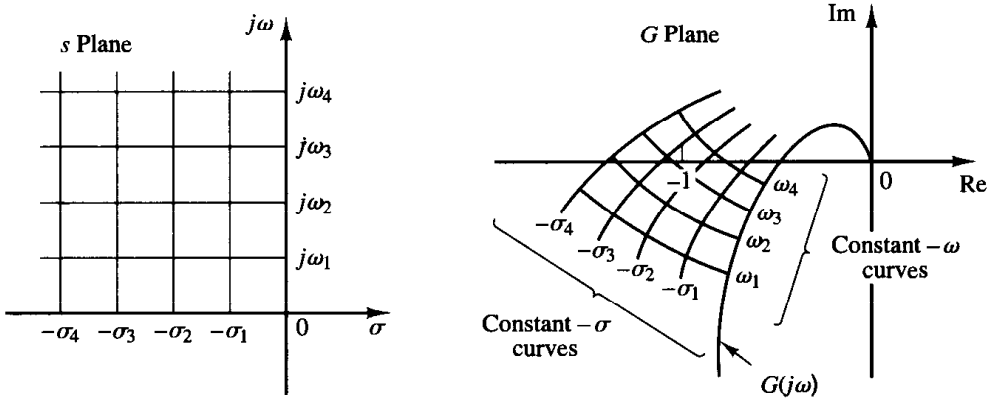

Figure 8–71
Conformal mapping of s-plane grids into the $G(s)$ plane.

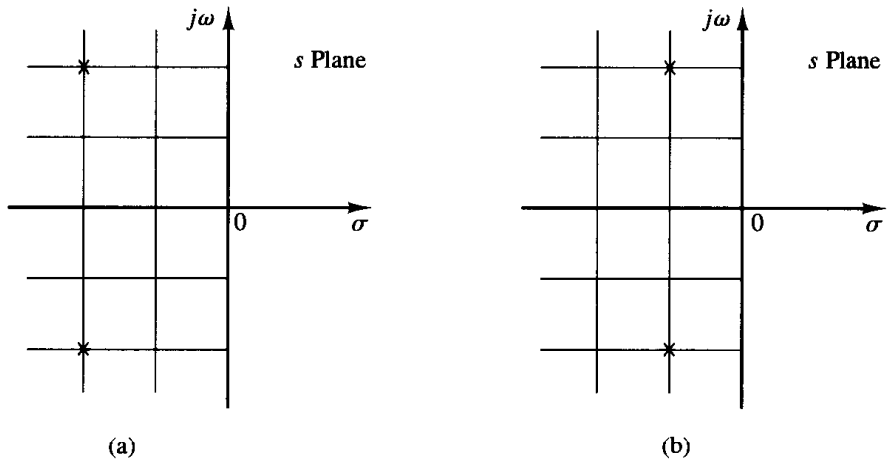

Figure 8–72
Two systems with two closed-loop poles.

Although the shapes of constant-σ and constant-ω loci in the $G(s)$ plane and the closeness of approach of the $G(j\omega)$ locus to the $-1 + j0$ point depend on a particular $G(s)$, the closeness of approach of the $G(j\omega)$ locus to the $-1 + j0$ point is an indication of the relative stability of a stable system. In general, we may expect that the closer the $G(j\omega)$ locus is to the $-1 + j0$ point, the larger the maximum overshoot is in the step transient response and the longer it takes to damp out.

Consider the two systems shown in Figure 8–72(a) and (b). (In Figure 8–72, the ×'s indicate closed-loop poles.) System (a) is obviously more stable than system (b) because the closed-loop poles of system (a) are located farther left than those of system (b). Figures 8–73(a) and (b) show the conformal mapping of s-plane grids into the $G(s)$ plane. The closer the closed-loop poles are located to the $j\omega$ axis, the closer the $G(j\omega)$ locus is to the $-1 + j0$ point.

Phase and gain margins. Figure 8–74 shows the polar plots of $G(j\omega)$ for three different values of the open-loop gain K. For a large value of the gain K, the system is unstable. As the gain is decreased to a certain value, the $G(j\omega)$ locus passes through the $-1 + j0$ point. This means that with this gain value the system is on the verge of instability, and the system will exhibit sustained oscillations. For a small value of the gain K, the system is stable.

In general, the closer the $G(j\omega)$ locus comes to encircling the $-1 + j0$ point, the more oscillatory is the system response. The closeness of the $G(j\omega)$ locus to the $-1 + j0$ point can be used as a measure of the margin of stability. (This does not apply, however,

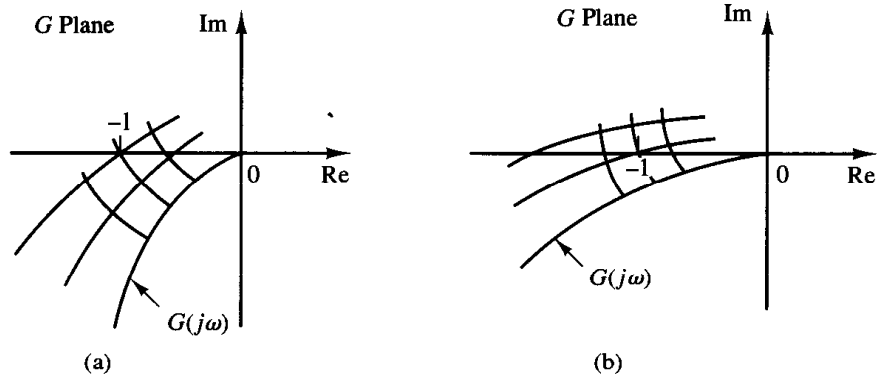

Figure 8–73
Conformal mappings of s-plane grids for the systems shown in Figure 8–72 into the $G(s)$ plane.

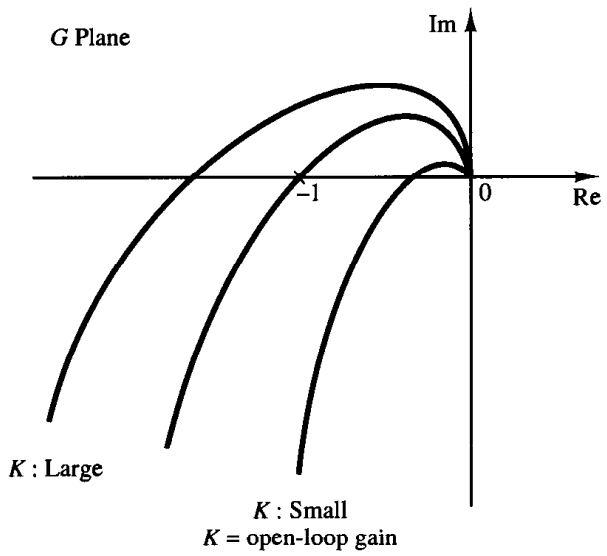

Figure 8–74
Polar plots of $\dfrac{K(1 + j\omega T_a)(1 + j\omega T_b)\cdots}{(j\omega)(1 + j\omega T_1)(1 + j\omega T_2)\cdots}$.

to conditionally stable systems.) It is common practice to represent the closeness in terms of phase margin and gain margin.

Phase margin: The phase margin is that amount of additional phase lag at the gain crossover frequency required to bring the system to the verge of instability. The gain crossover frequency is the frequency at which $|G(j\omega)|$, the magnitude of the open-loop transfer function, is unity. The phase margin γ is 180° plus the phase angle ϕ of the open-loop transfer function at the gain crossover frequency, or

$$\gamma = 180° + \phi$$

Figures 8–75(a), (b), and (c) illustrate the phase margin of both a stable system and an unstable system in Bode diagrams, polar plots, and log-magnitude versus phase plots. In the polar plot, a line may be drawn from the origin to the point at which the unit circle crosses the $G(j\omega)$ locus. The angle from the negative real axis to this line is the phase margin. The phase margin is positive for $\gamma > 0$ and negative for $\gamma < 0$. For a minimum-phase system to be stable, the phase margin must be positive. In the logarithmic plots, the critical point in the complex plane corresponds to the 0 dB and −180° lines.

Gain margin: The gain margin is the reciprocal of the magnitude $|G(j\omega)|$ at the frequency at which the phase angle is −180°. Defining the phase crossover frequency ω_1 to be the frequency at which the phase angle of the open-loop transfer function equals −180° gives the gain margin K_g:

$$K_g = \frac{1}{|G(j\omega_1)|}$$

In terms of decibels,

$$K_g \text{ dB} = 20 \log K_g = -20 \log |G(j\omega_1)|$$

The gain margin expressed in decibels is positive if K_g is greater than unity and negative if K_g is smaller than unity. Thus, a positive gain margin (in decibels) means that the

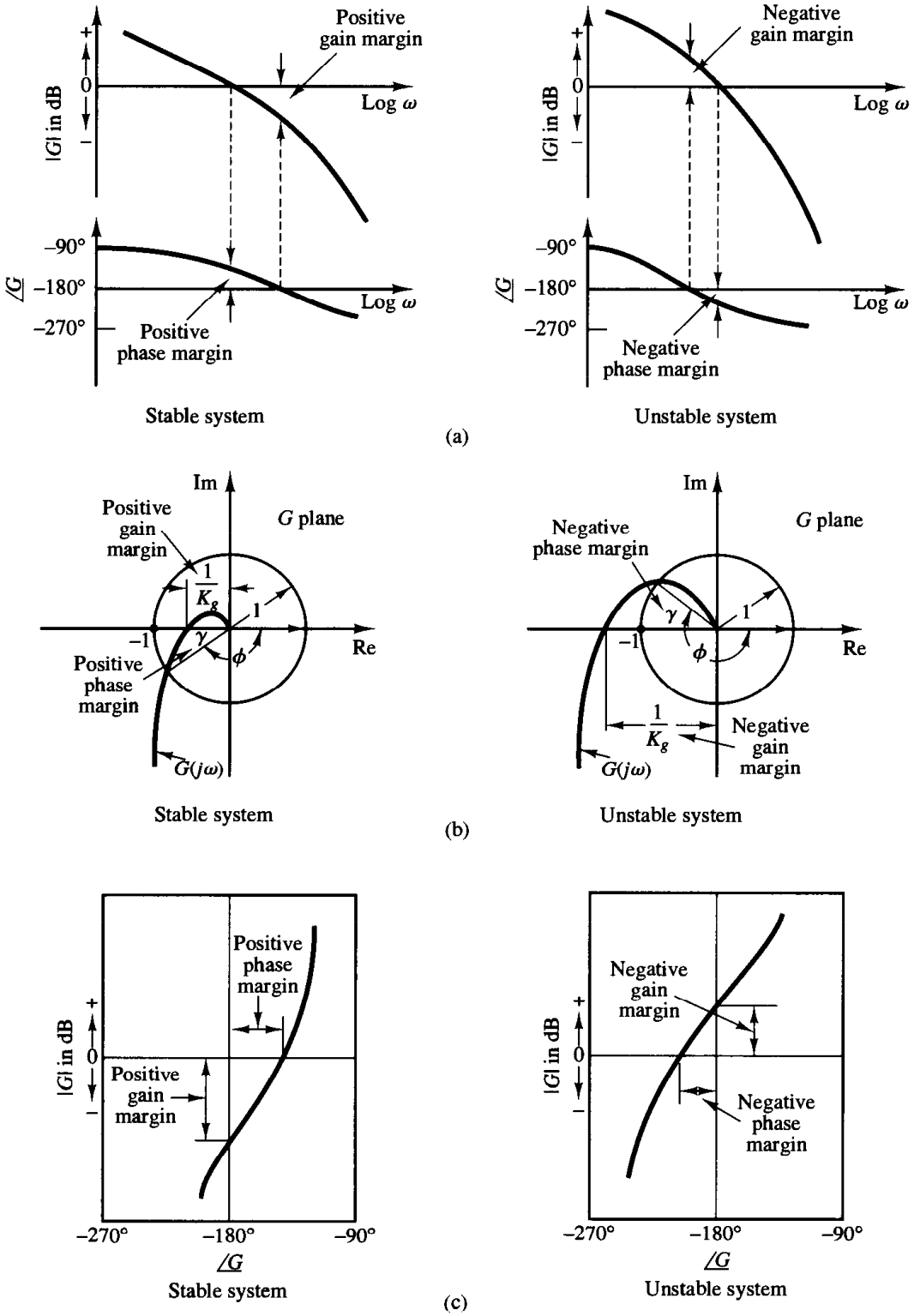

Figure 8–75
Phase and gain margins of stable and unstable systems. (a) Bode diagrams; (b) polar plots; (c) log-magnitude versus phase plots.

system is stable, and a negative gain margin (in decibels) means that the system is unstable. The gain margin is shown in Figures 8–75(a), (b), and (c).

For a stable minimum-phase system, the gain margin indicates how much the gain can be increased before the system becomes unstable. For an unstable system, the gain margin is indicative of how much the gain must be decreased to make the system stable.

The gain margin of a first- or second-order system is infinite since the polar plots for such systems do not cross the negative real axis. Thus, theoretically, first- or second-order systems cannot be unstable. (Note, however, that so-called first- or second-order systems are only approximations in the sense that small time lags are neglected in deriving the system equations and are thus not truly first- or second-order systems. If these small lags are accounted for, the so-called first- or second-order systems may become unstable.)

It is noted that for a nonminimum-phase system with unstable open loop the stability condition will not be satisfied unless the $G(j\omega)$ plot encircles the $-1 + j0$ point. Hence, such a stable nonminimum-phase system will have negative phase and gain margins.

It is also important to point out that conditionally stable systems will have two or more phase crossover frequencies, and some higher-order systems with complicated numerator dynamics may also have two or more gain crossover frequencies, as shown in Figure 8–76. For stable systems having two or more gain crossover frequencies, the phase margin is measured at the highest gain crossover frequency.

A few comments on phase and gain margins. The phase and gain margins of a control system are a measure of the closeness of the polar plot to the $-1 + j0$ point. Therefore, these margins may be used as design criteria.

It should be noted that either the gain margin alone or the phase margin alone does not give a sufficient indication of the relative stability. Both should be given in the determination of relative stability.

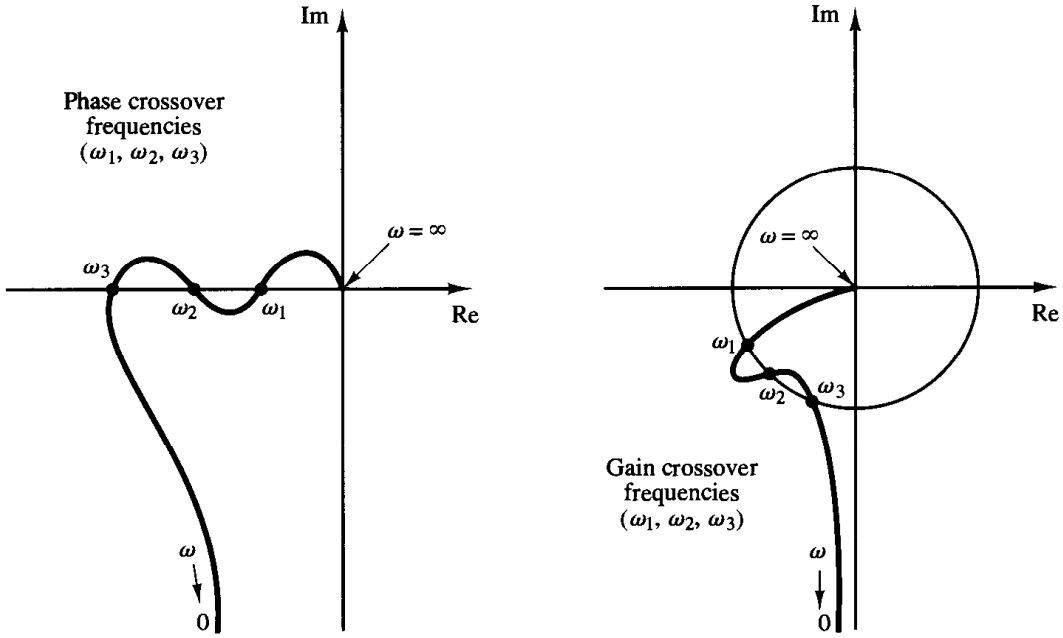

Figure 8–76
Polar plots showing more than two phase or gain crossover frequencies.

For a minimum-phase system, both the phase and gain margins must be positive for the system to be stable. Negative margins indicate instability.

Proper phase and gain margins ensure us against variations in the system components and are specified for definite values of frequency. The two values bound the behavior of the closed-loop system near the resonant frequency. For satisfactory performance, the phase margin should be between 30° and 60°, and the gain margin should be greater than 6 dB. With these values, a minimum-phase system has guaranteed stability, even if the open-loop gain and time constants of the components vary to a certain extent. Although the phase and gain margins give only rough estimates of the effective damping ratio of the closed-loop system, they do offer a convenient means for designing control systems or adjusting the gain constants of systems.

For minimum-phase systems, the magnitude and phase characteristics of the open-loop transfer function are definitely related. The requirement that the phase margin be between 30° and 60° means that in a Bode diagram the slope of the log-magnitude curve at the gain crossover frequency should be more gradual than −40 dB/ decade. In most practical cases, a slope of −20 dB/decade is desirable at the gain crossover frequency for stability. If it is −40 dB/decade, the system could be either stable or unstable. (Even if the system is stable, however, the phase margin is small.) If the slope at the gain crossover frequency is −60 dB/decade or steeper, the system is most likely unstable.

EXAMPLE 8–20 Obtain the phase and gain margins of the system shown in Figure 8–77 for the two cases where $K = 10$ and $K = 100$.

The phase and gain margins can easily be obtained from the Bode diagram. A Bode diagram of the given open-loop transfer function with $K = 10$ is shown in Figure 8–78(a). The phase and gain margins for $K = 10$ are

$$\text{Phase margin} = 21°, \qquad \text{Gain margin} = 8\ \text{dB}$$

Therefore, the system gain may be increased by 8 dB before the instability occurs.

Increasing the gain from $K = 10$ to $K = 100$ shifts the 0-dB axis down by 20 dB, as shown in Figure 8–78(b). The phase and gain margins are

$$\text{Phase margin} = -30°, \qquad \text{Gain margin} = -12\ \text{dB}$$

Thus, the system is stable for $K = 10$ but unstable for $K = 100$.

Notice that one of the very convenient aspects of the Bode diagram approach is the ease with which the effects of gain changes can be evaluated.

Note that to obtain satisfactory performance we must increase the phase margin to 30° ~ 60°. This can be done by decreasing the gain K. Decreasing K is not desirable, however, since a small value of K will yield a large error for the ramp input. This suggests that reshaping of the open-loop frequency-response curve by adding compensation may be necessary. Compensation techniques are discussed in detail in Chapter 9.

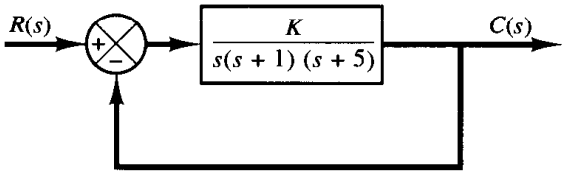

Figure 8–77
Control system.

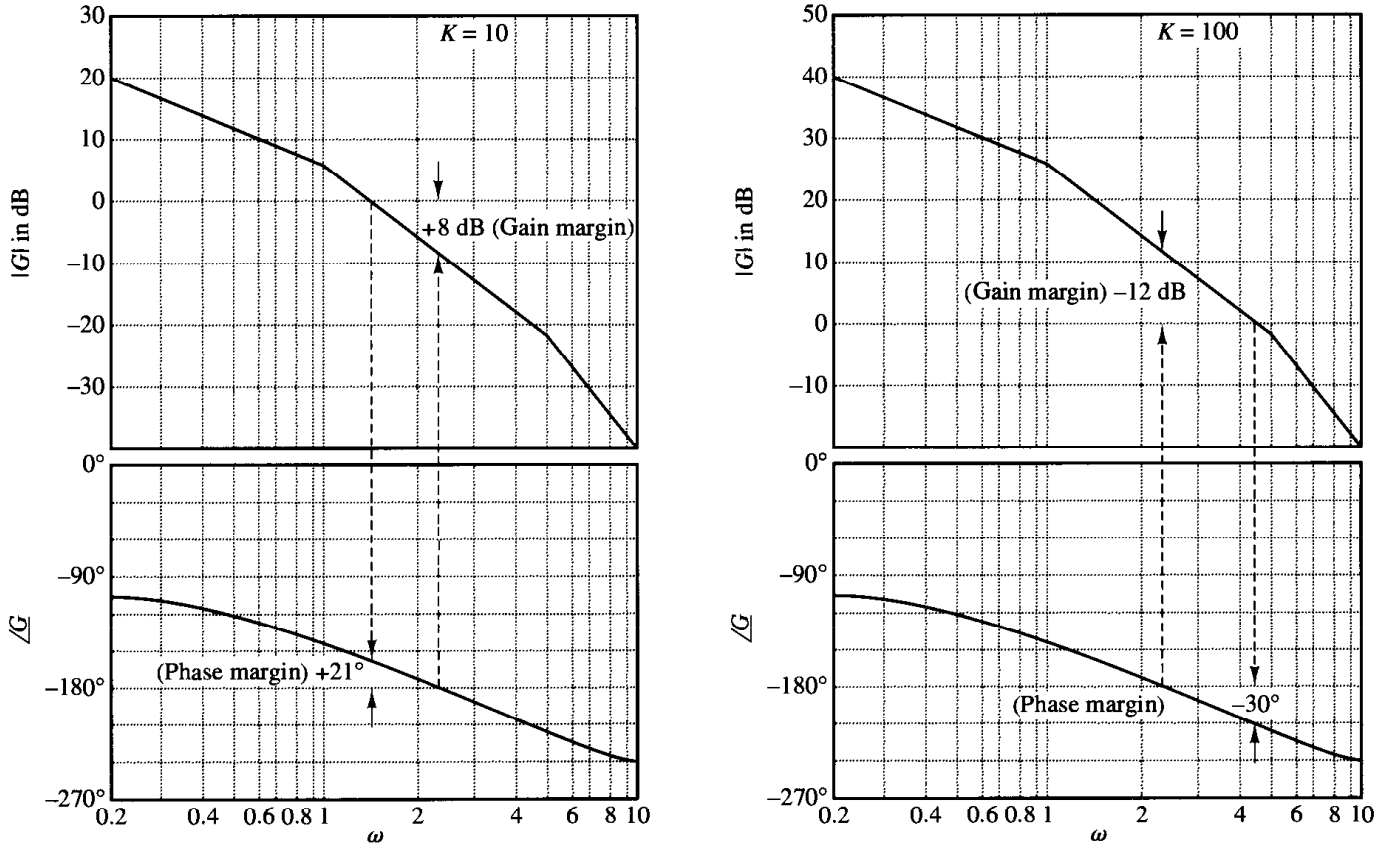

Figure 8–78
Bode diagrams of the system shown in Figure 8–77 (a) with $K = 10$ and (b) with $K = 100$.

Resonant peak magnitude M_r and resonant peak frequency ω_r. Consider the system shown in Figure 8–79. The closed-loop transfer function is

$$\frac{C(s)}{R(s)} = \frac{\omega_n^2}{s^2 + 2\zeta\omega_n s + \omega_n^2} \tag{8–9}$$

where ζ and ω_n are the damping ratio and the undamped natural frequency, respectively. The closed-loop frequency response is

$$\frac{C(j\omega)}{R(j\omega)} = \frac{1}{\left(1 - \dfrac{\omega^2}{\omega_n^2}\right) + j2\zeta\dfrac{\omega}{\omega_n}} = Me^{j\alpha}$$

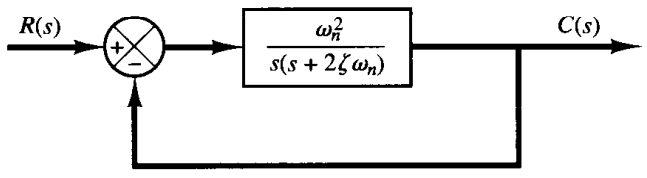

Figure 8–79
Control system.

where

$$M = \frac{1}{\sqrt{\left(1 - \frac{\omega^2}{\omega_n^2}\right)^2 + \left(2\zeta\frac{\omega}{\omega_n}\right)^2}}, \qquad \alpha = -\tan^{-1}\frac{2\zeta\frac{\omega}{\omega_n}}{1 - \frac{\omega^2}{\omega_n^2}}$$

As given by Equation (8–6), for $0 \leq \zeta \leq 0.707$ the maximum value of M occurs at the frequency ω_r, where

$$\omega_r = \omega_n\sqrt{1 - 2\zeta^2} = \omega_n\sqrt{\cos 2\theta} \tag{8–10}$$

The angle θ is defined in Figure 8–80. The frequency ω_r is the resonant frequency. At the resonant frequency, the value of M is maximum and is given by Equation (8–7), rewritten

$$M_r = \frac{1}{2\zeta\sqrt{1 - \zeta^2}} = \frac{1}{\sin 2\theta} \tag{8–11}$$

where M_r is defined as the *resonant peak magnitude.* The resonant peak magnitude is related to the damping of the system.

The magnitude of the resonant peak gives an indication of the relative stability of the system. A large resonant peak magnitude indicates the presence of a pair of dominant closed-loop poles with small damping ratio, which will yield an undesirable transient response. A smaller resonant peak magnitude, on the other hand, indicates the absence of a pair of dominant closed-loop poles with small damping ratio, meaning that the system is well damped.

Remember that ω_r is real only if $\zeta < 0.707$. Thus, there is no closed-loop resonance if $\zeta > 0.707$. [The value of M_r is unity only if $\zeta > 0.707$. See Equation (8–8).] Since the values of M_r and ω_r can be easily measured in a physical system, they are quite useful for checking agreement between theoretical and experimental analyses.

It is noted, however, that in practical design problems the phase margin and gain margin are more frequently specified than the resonant peak magnitude to indicate the degree of damping in a system.

Correlation between step transient response and frequency response in the standard second-order system. The maximum overshoot in the unit-step response of the standard second-order system, as shown in Figure 8–79, can be exactly correlated

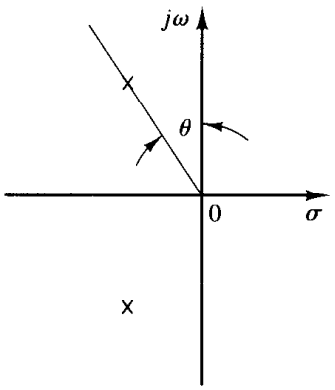

Figure 8–80
Definition of the angle θ.

to the resonant peak magnitude in the frequency response. Hence, essentially the same information of the system dynamics is contained in the frequency response as is in the transient response.

For a unit-step input, the output of the system shown in Figure 8–79 is given by Equation (4–21), or

$$c(t) = 1 - e^{-\zeta\omega_n t}\left(\cos\omega_d t + \frac{\zeta}{\sqrt{1-\zeta^2}}\sin\omega_d t\right), \qquad \text{for } t \geq 0$$

where

$$\omega_d = \omega_n\sqrt{1-\zeta^2} = \omega_n\cos\theta \tag{8–12}$$

On the other hand, the maximum overshoot M_p for the unit-step response is given by Equation (4–30), or

$$M_p = e^{-(\zeta/\sqrt{1-\zeta^2})\pi} \tag{8–13}$$

This maximum overshoot occurs in the transient response that has the damped natural frequency $\omega_d = \omega_n\sqrt{1-\zeta^2}$. The maximum overshoot becomes excessive for values of $\zeta < 0.4$.

Since the second-order system shown in Figure 8–79 has the open-loop transfer function

$$G(s) = \frac{\omega_n^2}{s(s+2\zeta\omega_n)}$$

for sinusoidal operation, the magnitude of $G(j\omega)$ becomes unity when

$$\omega = \omega_n\sqrt{\sqrt{1+4\zeta^4}-2\zeta^2}$$

which can be obtained by equating $|G(j\omega)|$ to unity and solving for ω. At this frequency, the phase angle of $G(j\omega)$ is

$$\angle G(j\omega) = -\angle j\omega - \angle j\omega + 2\zeta\omega_n = -90° - \tan^{-1}\frac{\sqrt{\sqrt{1+4\zeta^4}-2\zeta^2}}{2\zeta}$$

Thus, the phase margin γ is

$$\begin{aligned}\gamma &= 180° + \angle G(j\omega)\\ &= 90° - \tan^{-1}\frac{\sqrt{\sqrt{1+4\zeta^4}-2\zeta^2}}{2\zeta}\\ &= \tan^{-1}\frac{2\zeta}{\sqrt{\sqrt{1+4\zeta^4}-2\zeta^2}}\end{aligned} \tag{8–14}$$

Equation (8–14) gives the relationship between the damping ratio ζ and the phase margin γ. (Notice that the phase margin γ is a function only of the damping ratio ζ.)

In the following, we shall summarize the correlation between the step transient response and frequency response of the second-order system given by Equation (8–9):

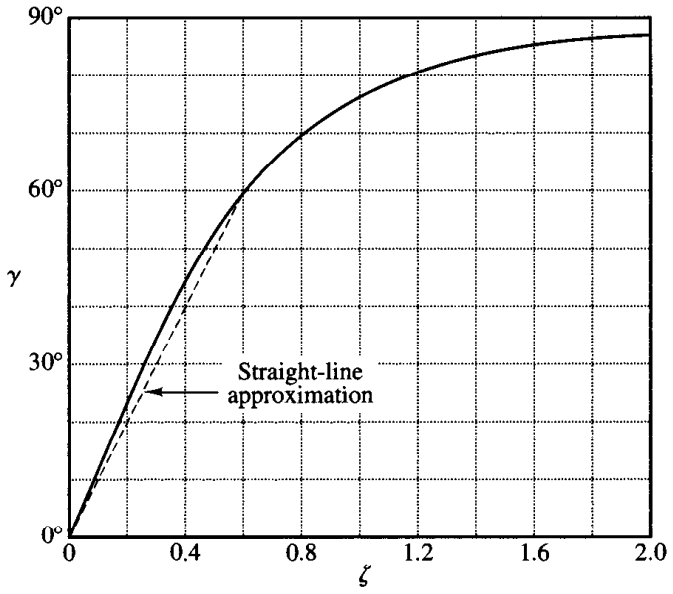

Figure 8–81
Curve γ (phase margin) versus ζ for the system shown in Figure 8–79.

1. The phase margin and the damping ratio are directly related. Figure 8–81 shows a plot of the phase margin γ as a function of the damping ratio ζ. It is noted that for the standard second-order system shown in Figure 8–79 the phase margin γ and the damping ratio ζ are related approximately by a straight line for $0 \leq \zeta \leq 0.6$, as follows:

$$\zeta = \frac{\gamma}{100}$$

Thus a phase margin of 60° corresponds to a damping ratio of 0.6. For higher-order systems having a dominant pair of closed-loop poles, this relationship may be used as a rule of thumb in estimating the relative stability in transient response (that is, the damping ratio) from the frequency response.

2. Referring to Equations (8–10) and (8–12), we see that the values of ω_r and ω_d are almost the same for small values of ζ. Thus, for small values of ζ, the value of ω_r is indicative of the speed of the transient response of the system.

3. From Equations (8–11) and (8–13), we note that the smaller the value of ζ is, the larger the values of M_r and M_p are. The correlation between M_r and M_p as a function of ζ is shown in Figure 8–82. A close relationship between M_r and M_p can be seen for $\zeta > 0.4$. For very small values of ζ, M_r becomes very large ($M_r \gg 1$), while the value of M_p does not exceed 1.

Correlation between step transient response and frequency response in general systems. The design of control systems is very often carried out on the basis of frequency response. The main reason for this is the relative simplicity of this approach as compared to others. Since in many applications it is the transient response of the

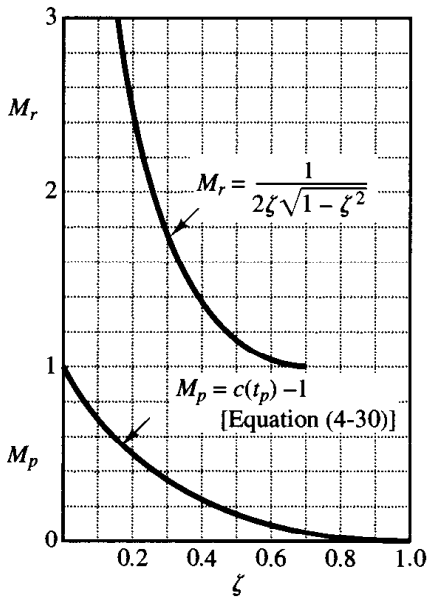

Figure 8–82
Curves M_r versus ζ and M_p versus ζ for the system shown in Figure 8–79.

system to aperiodic inputs rather than the steady-state response to sinusoidal inputs that is of primary concern, the question of correlation between transient response and frequency response arises.

For the second-order system shown in Figure 8–79, mathematical relationships correlating the step transient response and frequency response can be obtained easily. The time response of a second-order system can be exactly predicted from a knowledge of the M_r and ω_r of its closed-loop frequency response.

For higher-order systems, the correlation is more complex, and transient response may not be predicted easily from frequency response because additional poles may change the correlation between the step transient response and frequency response existing for a second-order system. Mathematical techniques for obtaining the exact correlation are available, but they are very laborious and of little practical value.

The applicability of the transient-response–frequency-response correlation existing for the second-order system shown in Figure 8–79 to higher-order systems depends on the presence of a dominant pair of complex-conjugate closed-loop poles in the latter systems. Clearly, if the frequency response of a higher-order system is dominated by a pair of complex-conjugate closed-loop poles, the transient-response–frequency-response correlation existing for the second-order system can be extended to the higher-order system.

For linear, time-invariant, higher-order systems having a dominant pair of complex-conjugate closed-loop poles, the following relationships generally exist between the step transient response and frequency response:

1. The value of M_r is indicative of the relative stability. Satisfactory transient performance is usually obtained if the value of M_r is in the range $1.0 < M_r < 1.4$ (0 dB <

$M_r < 3$ dB), which corresponds to an effective damping ratio of $0.4 < \zeta < 0.7$. For values of M_r greater than 1.5, the step transient response may exhibit several overshoots. (Note that in general a large value of M_r corresponds to a large overshoot in the step transient response. If the system is subjected to noise signals whose frequencies are near the resonant frequency ω_r, the noise will be amplified in the output and will present serious problems.)

2. The magnitude of the resonant frequency ω_r is indicative of the speed of the transient response. The larger the value of ω_r, the faster the time response is. In other words, the rise time varies inversely with ω_r. In terms of the open-loop frequency response, the damped natural frequency in the transient response is somewhere between the gain crossover frequency and phase crossover frequency.

3. The resonant peak frequency ω_r and the damped natural frequency ω_d for step transient response are very close to each other for lightly damped systems.

The three relationships just listed are useful for correlating the step transient response with the frequency response of higher-order systems, provided they can be approximated by a second-order system or a pair of complex-conjugate closed-loop poles. If a higher-order system satisfies this condition, a set of time-domain specifications may be translated into frequency-domain specifications. This simplifies greatly the design work or compensation work of higher-order systems.

In addition to the phase margin, gain margin, resonant peak M_r, and resonant peak frequency ω_r, there are other frequency-domain quantities commonly used in performance specifications. They are the cutoff frequency, bandwidth, and the cutoff rate. These will be defined in what follows.

Cutoff frequency and bandwidth. Referring to Figure 8–83, the frequency ω_b at which the magnitude of the closed-loop frequency response is 3 dB below its zero-frequency value is called the *cutoff frequency*. Thus

$$\left|\frac{C(j\omega)}{R(j\omega)}\right| < \left|\frac{C(j0)}{R(j0)}\right| - 3 \text{ dB}, \qquad \text{for } \omega > \omega_b$$

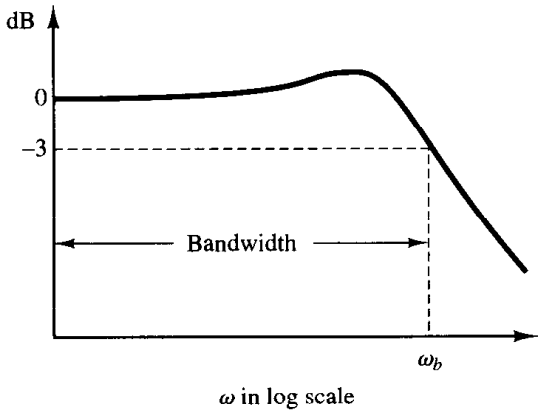

Figure 8–83
Plot of a closed-loop frequency response curve showing cutoff frequency ω_b and bandwidth.

For systems in which $|C(j0)/R(j0)| = 0$ dB,

$$\left|\frac{C(j\omega)}{R(j\omega)}\right| < -3 \text{ dB}, \qquad \text{for } \omega > \omega_b$$

The closed-loop system filters out the signal components whose frequencies are greater than the cutoff frequency and transmits those signal components with frequencies lower than the cutoff frequency.

The frequency range $0 \leq \omega \leq \omega_b$ in which the magnitude of the closed loop does not drop -3 dB is called the *bandwidth* of the system. The bandwidth indicates the frequency where the gain starts to fall off from its low-frequency value. Thus, the bandwidth indicates how well the system will track an input sinusoid. Note that for a given ω_n the rise time increases with increasing damping ratio ζ. On the other hand, the bandwidth decreases with the increase of ζ. Therefore, the rise time and the bandwidth are inversely proportional to each other.

The specification of the bandwidth may be determined by the following factors:

1. The ability to reproduce the input signal. A large bandwidth corresponds to a small rise time, or fast response. Roughly speaking, we can say that the bandwidth is proportional to the speed of response.
2. The necessary filtering characteristics for high-frequency noise.

For the system to follow arbitrary inputs accurately, it is necessary that the system have a large bandwidth. From the viewpoint of noise, however, the bandwidth should not be too large. Thus, there are conflicting requirements on the bandwidth, and a compromise is usually necessary for good design. Note that a system with large bandwidth requires high-performance components. So the cost of components usually increases with the bandwidth.

Cutoff rate. The cutoff rate is the slope of the log-magnitude curve near the cutoff frequency. The cutoff rate indicates the ability of a system to distinguish the signal from noise.

It is noted that a closed-loop frequency response curve with a steep cutoff characteristic may have a large resonant peak magnitude, which implies that the system has relatively small stability margin.

EXAMPLE 8–21 Consider the following two systems:

$$\text{System I: } \frac{C(s)}{R(s)} = \frac{1}{s+1}, \qquad \text{System II: } \frac{C(s)}{R(s)} = \frac{1}{3s+1}$$

Compare the bandwidths of these two systems. Show that the system with the larger bandwidth has a faster speed of response and can follow the input much better than the one with a smaller bandwidth.

Figure 8–84(a) shows the closed-loop frequency-response curves for the two systems. (Asymptotic curves are shown by dashed lines.) We find that the bandwidth of system I is $0 \leq \omega \leq 1$ rad/sec and that of system II is $0 \leq \omega \leq 0.33$ rad/sec. Figures 8–84(b) and (c) show, respectively, the unit-step response and unit-ramp response curves for the two systems. Clearly, system I, whose bandwidth is three times wider than that of system II, has a faster speed of response and can follow the input much better.

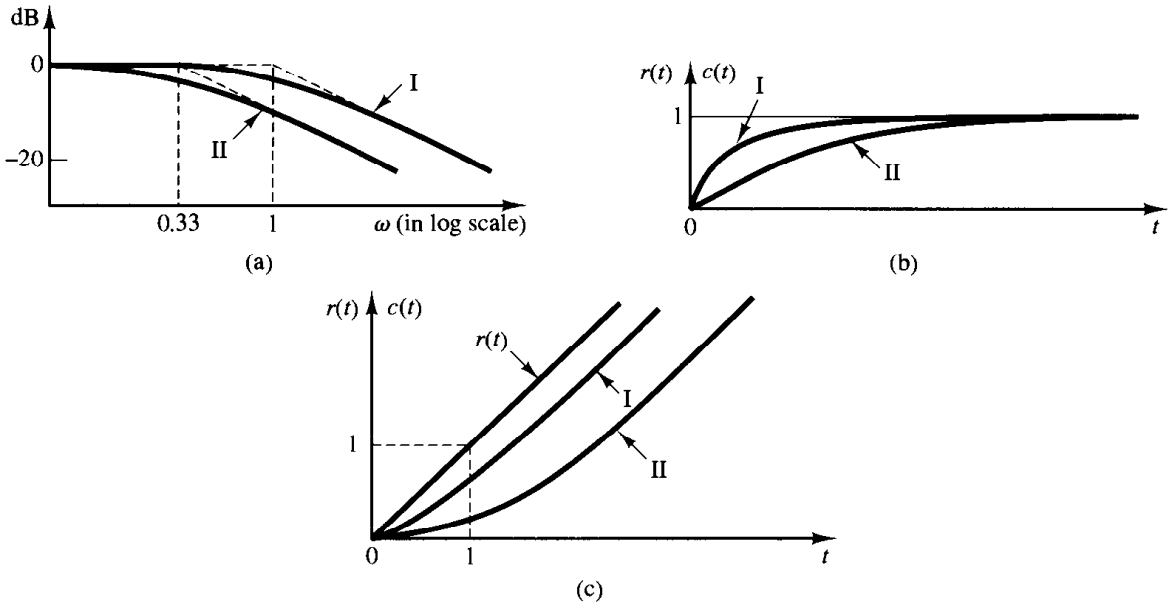

Figure 8–84
Comparison of dynamic characteristics of the two systems considered in Example 8–21. (a) Closed-loop frequency-response curves; (b) unit-step response curves; (c) unit-ramp response curves.

8–10 CLOSED-LOOP FREQUENCY RESPONSE

Closed-loop frequency response of unity-feedback systems. For a stable closed-loop system, the frequency response can be obtained easily from that of the open loop. Consider the unity-feedback system shown in Figure 8–85(a). The closed-loop transfer function is

$$\frac{C(s)}{R(s)} = \frac{G(s)}{1 + G(s)}$$

In the Nyquist or polar plot shown in Figure 8–85(b), the vector $\vec{OA}$ represents $G(j\omega_1)$, where ω_1 is the frequency at point A. The length of the vector $\vec{OA}$ is $|G(j\omega_1)|$ and the angle of the vector $\vec{OA}$ is $\angle G(j\omega_1)$. The vector $\vec{PA}$, the vector from the $-1 + j0$ point to the Nyquist locus, represents $1 + G(j\omega_1)$. Therefore, the ratio of $\vec{OA}$ to $\vec{PA}$ represents the closed-loop frequency response, or

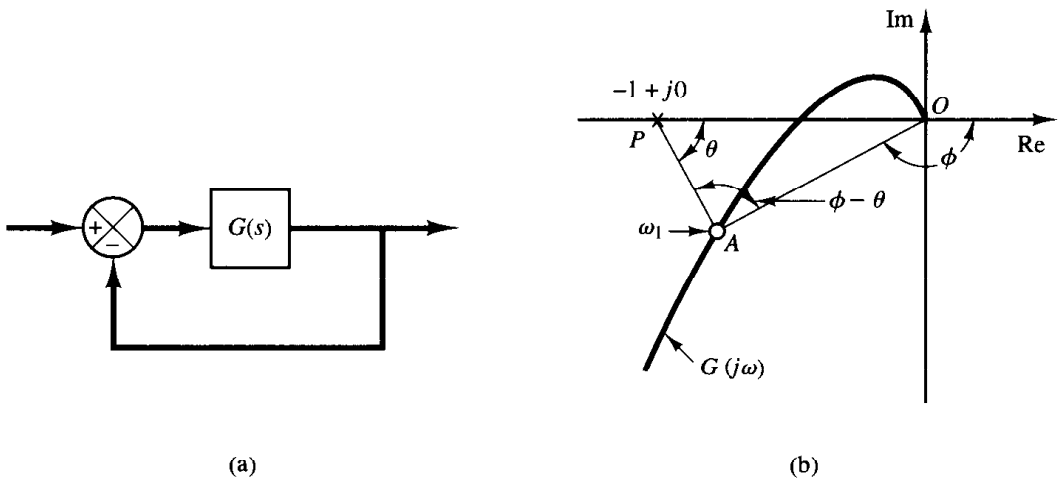

Figure 8–85
(a) Unity-feedback system; (b) determination of closed-loop frequency response from open-loop frequency response.

$$\frac{\vec{OA}}{\vec{PA}} = \frac{G(j\omega_1)}{1 + G(j\omega_1)} = \frac{C(j\omega_1)}{R(j\omega_1)}$$

The magnitude of the closed-loop transfer function at $\omega = \omega_1$ is the ratio of the magnitudes of $\vec{OA}$ to $\vec{PA}$. The phase angle of the closed-loop transfer function at $\omega = \omega_1$ is the angle formed by the vectors $\vec{OA}$ to $\vec{PA}$, that is $\phi - \theta$, shown in Figure 8–85(b). By measuring the magnitude and phase angle at different frequency points, the closed-loop frequency-response curve can be obtained.

Let us define the magnitude of the closed-loop frequency response as M and the phase angle as α, or

$$\frac{C(j\omega)}{R(j\omega)} = Me^{j\alpha}$$

In the following, we shall find the constant magnitude loci and constant phase-angle loci. Such loci are convenient in determining the closed-loop frequency response from the polar plot or Nyquist plot.

Constant-magnitude loci (M circles). To obtain the constant-magnitude loci, let us first note that $G(j\omega)$ is a complex quantity and can be written as follows:

$$G(j\omega) = X + jY$$

where X and Y are real quantities. Then M is given by

$$M = \frac{|X + jY|}{|1 + X + jY|}$$

and M^2 is

$$M^2 = \frac{X^2 + Y^2}{(1 + X)^2 + Y^2}$$

Hence

$$X^2(1 - M^2) - 2M^2X - M^2 + (1 - M^2)Y^2 = 0 \tag{8–15}$$

If $M = 1$, then from Equation (8–15) we obtain $X = -\frac{1}{2}$. This is the equation of a straight line parallel to the Y axis and passing through the point $(-\frac{1}{2}, 0)$.

If $M \neq 1$, Equation (8–15) can be written

$$X^2 + \frac{2M^2}{M^2 - 1}X + \frac{M^2}{M^2 - 1} + Y^2 = 0$$

If the term $M^2/(M^2 - 1)^2$ is added to both sides of this last equation, we obtain

$$\left(X + \frac{M^2}{M^2 - 1}\right)^2 + Y^2 = \frac{M^2}{(M^2 - 1)^2} \tag{8–16}$$

Equation (8–16) is the equation of a circle with center at $X = -M^2/(M^2 - 1)$, $Y = 0$ and with radius $|M/(M^2 - 1)|$.

The constant M loci on the $G(s)$ plane are thus a family of circles. The center and radius of the circle for a given value of M can be easily calculated. For example, for $M = 1.3$,

the center is at $(-2.45, 0)$ and the radius is 1.88. A family of constant M circles is shown in Figure 8–86. It is seen that as M becomes larger compared with 1, the M circles become smaller and converge to the $-1 + j0$ point. For $M > 1$, the centers of the M circles lie to the left of the $-1 + j0$ point. Similarly, as M becomes smaller compared with 1, the M circle becomes smaller and converges to the origin. For $0 < M < 1$, the centers of the M circles lie to the right of the origin. $M = 1$ corresponds to the locus of points equidistant from the origin and from the $-1 + j0$ point. As stated earlier, it is a straight line passing through the point $(-\frac{1}{2}, 0)$ and parallel to the imaginary axis. (The constant M circles corresponding to $M > 1$ lie to the left of the $M = 1$ line and those corresponding to $0 < M < 1$ lie to the right of the $M = 1$ line.) The M circles are symmetrical with respect to the straight line corresponding to $M = 1$ and with respect to the real axis.

Constant phase-angle loci (N circles). We shall obtain the phase angle α in terms of X and Y. Since

$$\angle e^{j\alpha} = \angle \frac{X + jY}{1 + X + jY}$$

the phase angle α is

$$\alpha = \tan^{-1}\left(\frac{Y}{X}\right) - \tan^{-1}\left(\frac{Y}{1 + X}\right)$$

If we define

$$\tan \alpha = N$$

then

$$N = \tan\left[\tan^{-1}\left(\frac{Y}{X}\right) - \tan^{-1}\left(\frac{Y}{1 + X}\right)\right]$$

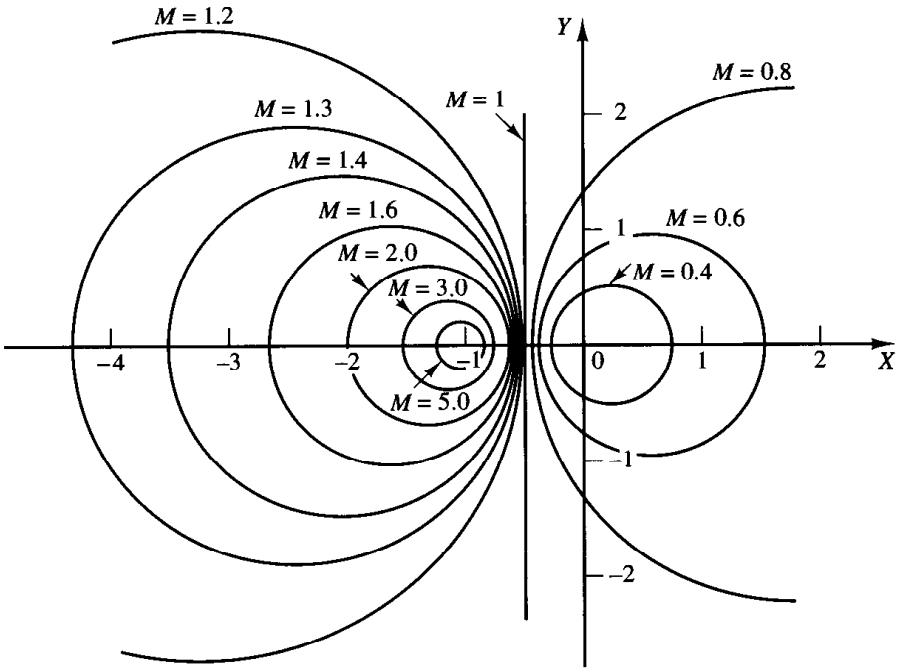

Figure 8–86
A family of constant M circles.

Since

$$\tan(A - B) = \frac{\tan A - \tan B}{1 + \tan A \tan B}$$

we obtain

$$N = \frac{\dfrac{Y}{X} - \dfrac{Y}{1+X}}{1 + \dfrac{Y}{X}\left(\dfrac{Y}{1+X}\right)} = \frac{Y}{X^2 + X + Y^2}$$

or

$$X^2 + X + Y^2 - \frac{1}{N}Y = 0$$

The addition of $(\frac{1}{4}) + 1/(2N)^2$ to both sides of this last equation yields

$$\left(X + \frac{1}{2}\right)^2 + \left(Y - \frac{1}{2N}\right)^2 = \frac{1}{4} + \left(\frac{1}{2N}\right)^2 \tag{8–17}$$

This is an equation of a circle with center at $X = -\frac{1}{2}$, $Y = 1/(2N)$ and with radius $\sqrt{(\frac{1}{4}) + 1/(2N)^2}$. For example, if $\alpha = 30°$, then $N = \tan \alpha = 0.577$, and the center and the radius of the circle corresponding to $\alpha = 30°$ are found to be $(-0.5, 0.866)$ and unity, respectively. Since Equation (8–17) is satisfied when $X = Y = 0$ and $X = -1, Y = 0$ regardless of the value of N, each circle passes through the origin and the $-1 + j0$ point. The constant α loci can be drawn easily once the value of N is given. A family of constant N circles is shown in Figure 8–87 with α as a parameter.

It should be noted that the constant N locus for a given value of α is actually not the entire circle but only an arc. In other words, the $\alpha = 30°$ and $\alpha = -150°$ arcs are parts of the same circle. This is so because the tangent of an angle remains the same if $\pm 180°$ (or multiplies thereof) is added to the angle.

The use of the M and N circles enables us to find the entire closed-loop frequency response from the open-loop frequency response $G(j\omega)$ without calculating the magnitude and phase of the closed-loop transfer function at each frequency. The intersections of the $G(j\omega)$ locus and the M circles and N circles gives the values of M and N at frequency points on the $G(j\omega)$ locus.

The N circles are multivalued in the sense that the circle for $\alpha = \alpha_1$ and that for $\alpha = \alpha_1 \pm 180°n$ $(n = 1, 2, \ldots)$ are the same. In using the N circles for the determination of the phase angle of closed-loop systems, we must interpret the proper value of α. To avoid any error, start at zero frequency, which corresponds to $\alpha = 0°$, and proceed to higher frequencies. The phase-angle curve must be continuous.

Graphically, the intersections of the $G(j\omega)$ locus and M circles give the values of M at the frequencies denoted on the $G(j\omega)$ locus. Thus, the constant M circle with the smallest radius that is tangent to the $G(j\omega)$ locus gives the value of the resonant peak magnitude M_r. If it is desired to keep the resonant peak value less than a certain value, then the system should not enclose the critical point $(-1 + j0$ point) and, at the same time, there should be no intersections with the particular M circle and the $G(j\omega)$ locus.

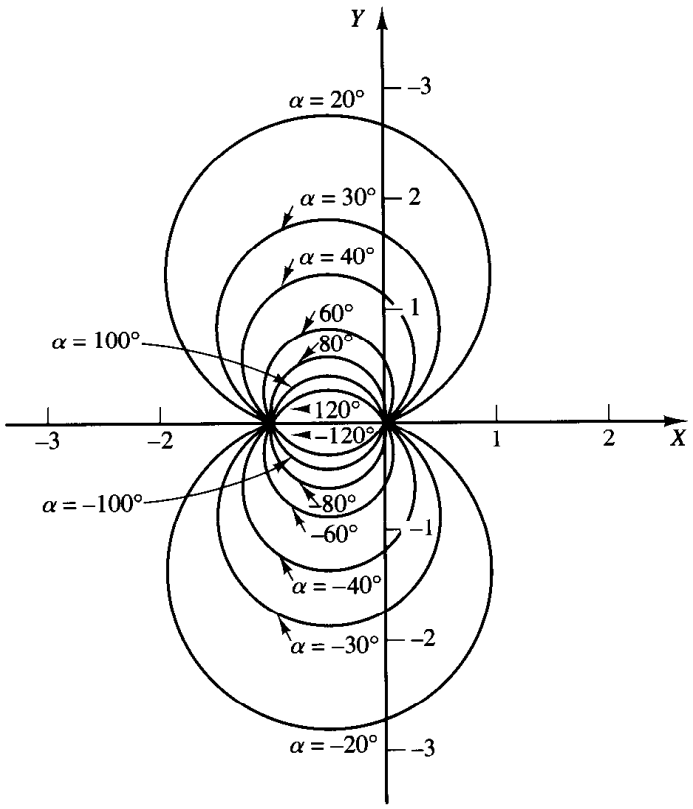

Figure 8–87
A family of constant N circles.

Figure 8–88(a) shows the $G(j\omega)$ locus superimposed on a family of M circles. Figure 8–88(b) shows the $G(j\omega)$ locus superimposed on a family of N circles. From these plots, it is possible to obtain the closed-loop frequency response by inspection. It is seen that the $M = 1.1$ circle intersects the $G(j\omega)$ locus at frequency point $\omega = \omega_1$. This means that at this frequency the magnitude of the closed-loop transfer function is 1.1. In Figure 8–88(a), the $M = 2$ circle is just tangent to the $G(j\omega)$ locus. Thus, there is only one point on the $G(j\omega)$ locus for which $|C(j\omega)/R(j\omega)|$ is equal to 2. Figure 8–88(c) shows the closed-loop frequency-response curve for the system. The upper curve is the M versus frequency ω curve, and the lower curve is the phase angle α versus frequency ω curve.

The resonant peak value is the value of M corresponding to the M circle of smallest radius that is tangent to the $G(j\omega)$ locus. Thus, in the Nyquist diagram, the resonant peak value M_r and the resonant frequency ω_r can be found from the M-circle tangency to the $G(j\omega)$ locus. (In the present example, $M_r = 2$ and $\omega_r = \omega_4$.)

Nichols chart. In dealing with design problems, we find it convenient to construct the M and N loci in the log-magnitude versus phase plane. The chart consisting of the M and N loci in the log-magnitude versus phase diagram is called the Nichols chart. This chart is shown in Figure 8–89, for phase angles between 0° and −240°.

Note that the critical point ($-1 + j0$ point) is mapped to the Nichols chart as the point (0 dB, −180°). The Nichols chart contains curves of constant closed-loop magnitude and phase angle. The designer can graphically determine the phase margin, gain margin, resonant peak magnitude, resonant peak frequency, and bandwidth of the closed-loop system from the plot of the open-loop locus, $G(j\omega)$.

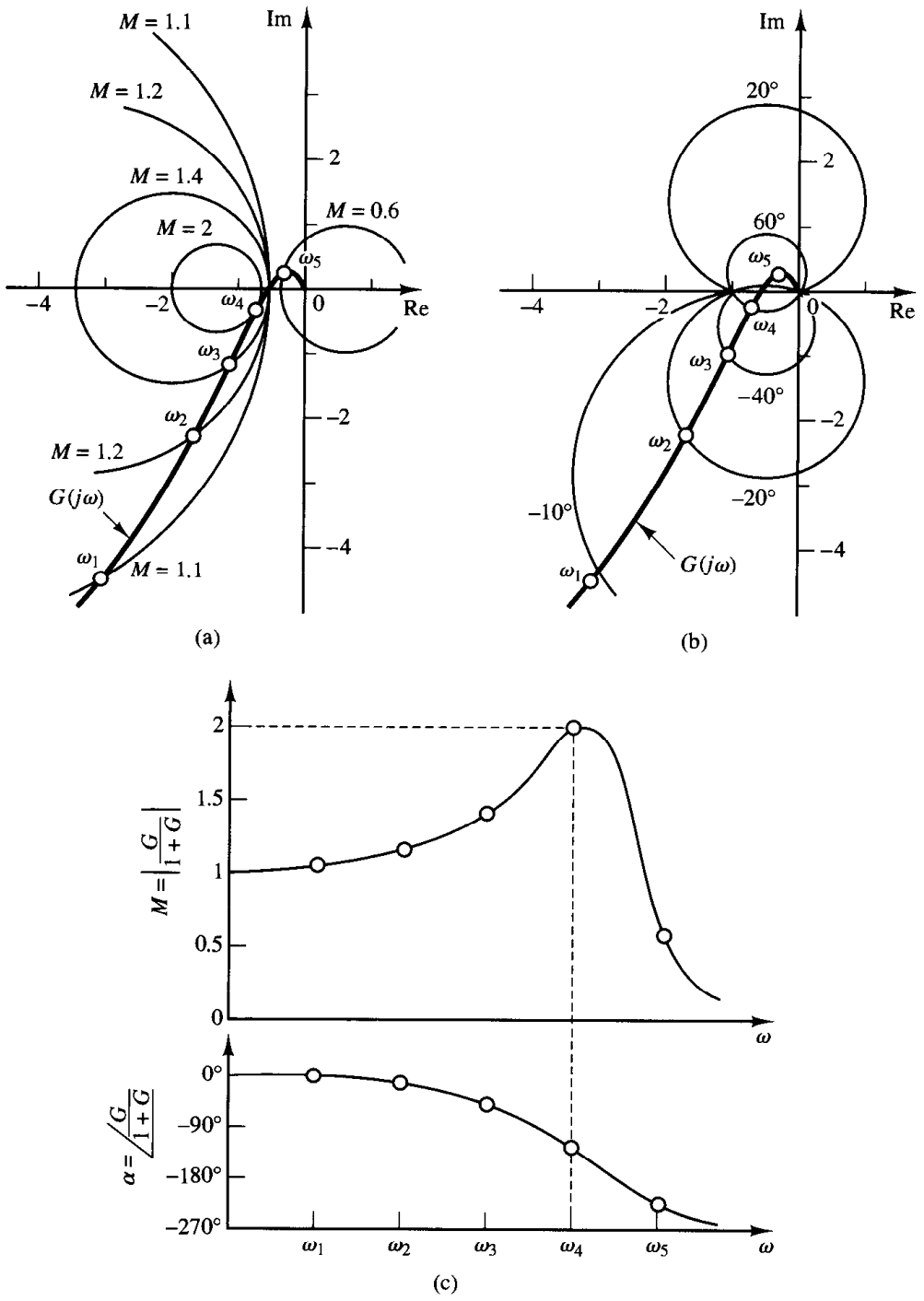

Figure 8–88
(a) $G(j\omega)$ locus superimposed on a family of M circles; (b) $G(j\omega)$ locus superimposed on a family of N circles; (c) closed-loop frequency-response curves.

The Nichols chart is symmetric about the $-180°$ axis. The M and N loci repeat for every 360°, and there is symmetry at every 180° interval. The M loci are centered about the critical point (0 dB, $-180°$). The Nichols chart is useful for determining the frequency response of the closed loop from that of the open loop. If the open-loop frequency-response curve is superimposed on the Nichols chart, the intersections of the open-loop frequency-response curve $G(j\omega)$ and the M and N loci give the values of the magnitude M and phase angle α of the closed-loop frequency response at each frequency point. If

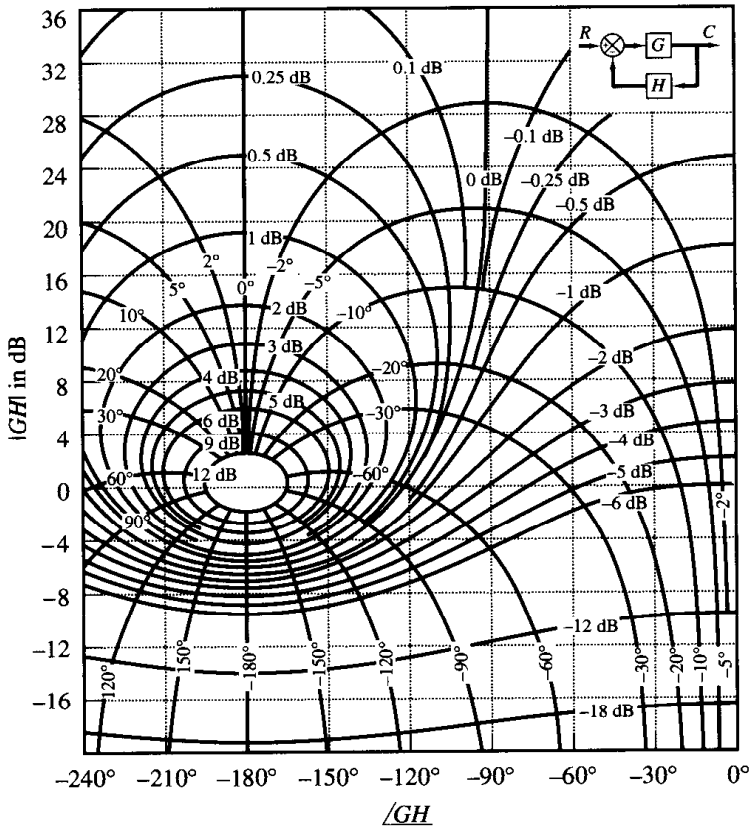

Figure 8–89
Nichols chart.

the $G(j\omega)$ locus does not intersect the $M = M_r$ locus but is tangent to it, then the resonant peak value of M of the closed-loop frequency response is given by M_r. The resonant peak frequency is given by the frequency at the point of tangency.

As an example, consider the unity-feedback system with the following open-loop transfer function:

$$G(j\omega) = \frac{K}{s(s + 1)(0.5s + 1)}, \qquad K = 1$$

To find the closed-loop frequency response by use of the Nichols chart, the $G(j\omega)$ locus is constructed in the log-magnitude versus phase plane from the Bode diagram. The use of the Bode diagram eliminates the lengthy numerical calculation of $G(j\omega)$. Figure 8–90(a) shows the $G(j\omega)$ locus together with the M and N loci. The closed-loop frequency-response curves may be constructed by reading the magnitudes and phase angles at various frequency points on the $G(j\omega)$ locus from the M and N loci, as shown in Figure 8–90(b). Since the largest magnitude contour touched by the $G(j\omega)$ locus is 5 dB, the resonant peak magnitude M_r is 5 dB. The corresponding resonant peak frequency is 0.8 rad/sec.

Notice that the phase crossover point is the point where the $G(j\omega)$ locus intersects the $-180°$ axis (for the present system, $\omega = 1.4$ rad/sec), and the gain crossover point is the point where the locus intersects the 0-dB axis (for the present system, $\omega = 0.76$

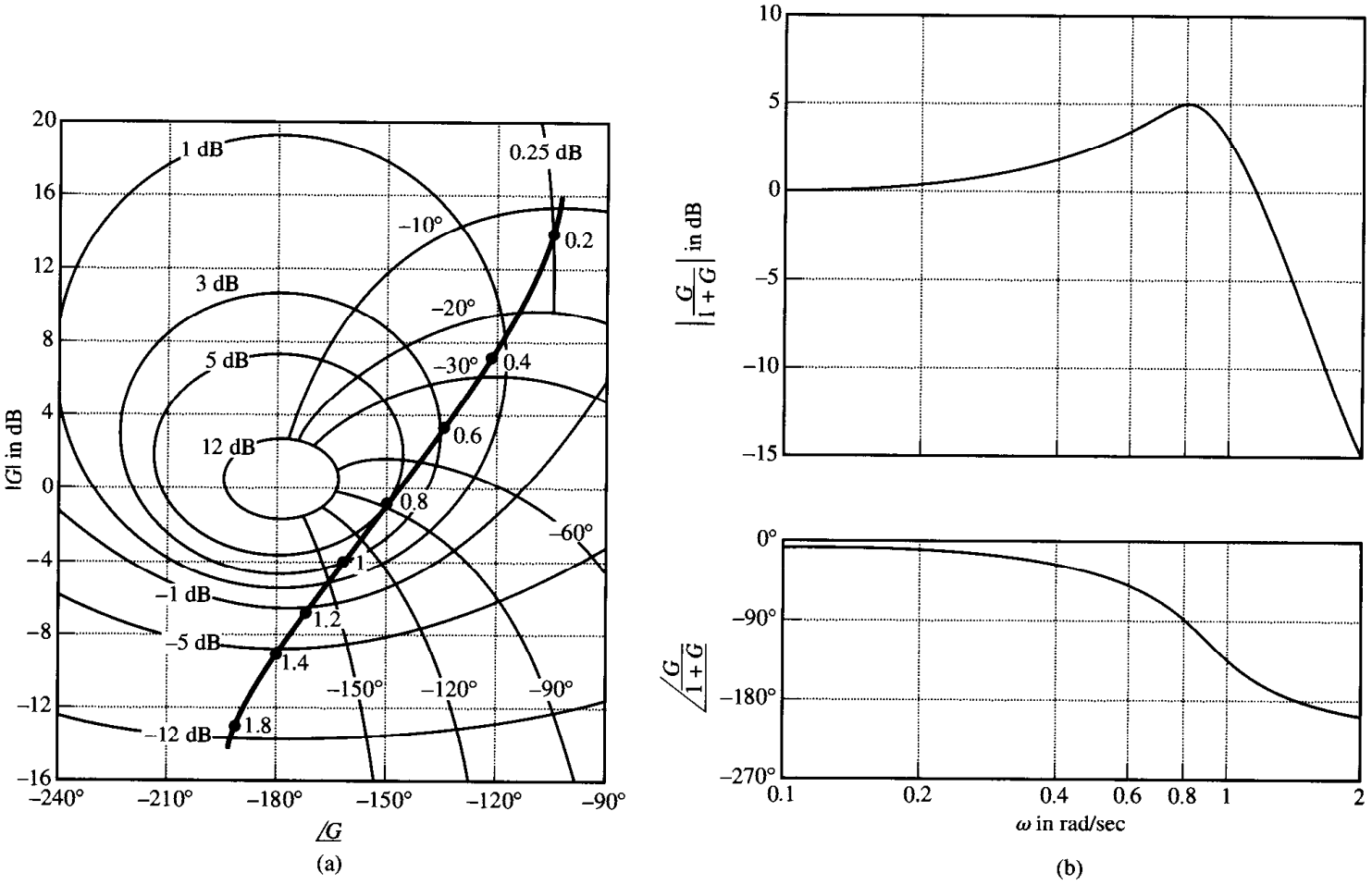

Figure 8–90
(a) Plot of $G(j\omega)$ superimposed on Nichols chart; (b) closed-loop frequency-response curves.

rad/sec). The phase margin is the horizontal distance (measured in degrees) between the gain crossover point and the critical point (0 dB, −180°). The gain margin is the distance (in decibels) between the phase crossover point and the critical point.

The bandwidth of the closed-loop system can easily be found from the $G(j\omega)$ locus in the Nichols diagram. The frequency at the intersection of the $G(j\omega)$ locus and the $M = -3$ dB locus gives the bandwidth.

If the open-loop gain K is varied, the shape of the $G(j\omega)$ locus in the log-magnitude versus phase diagram remains the same, but it is shifted up (for increasing K) or down (for decreasing K) along the vertical axis. Therefore, the $G(j\omega)$ locus intersects the M and N loci differently, resulting in a different closed-loop frequency-response curve. For a small value of the gain K, the $G(j\omega)$ locus will not be tangent to any of the M loci, which means that there is no resonance in the closed-loop frequency response.

Closed-loop frequency response for nonunity-feedback systems. In the preceding sections, our discussions were limited to closed-loop systems with unity

feedback. The constant M and N loci and the Nichols chart cannot be directly applied to control systems with nonunity feedback, but rather require a slight modification.

If the closed-loop system involves a nonunity-feedback transfer function, then the closed-loop transfer function may be written

$$\frac{C(s)}{R(s)} = \frac{G(s)}{1 + G(s)H(s)}$$

where $G(s)$ is the feedforward transfer function and $H(s)$ is the feedback transfer function. Then $C(j\omega)/R(j\omega)$ can be written

$$\frac{C(j\omega)}{R(j\omega)} = \frac{1}{H(j\omega)} \frac{G(j\omega)H(j\omega)}{1 + G(j\omega)H(j\omega)}$$

The magnitude and phase angle of

$$\frac{G_1(j\omega)}{1 + G_1(j\omega)}$$

where $G_1(j\omega) = G(j\omega)H(j\omega)$, may be obtained easily by plotting the $G_1(j\omega)$ locus on the Nichols chart and reading the values of M and N at various frequency points. The closed-loop frequency response $C(j\omega)/R(j\omega)$ may then be obtained by multiplying $G_1(j\omega)/[1 + G_1(j\omega)]$ by $1/H(j\omega)$. This multiplication can be made without difficulty if we draw Bode diagrams for $G_1(j\omega)/[1 + G_1(j\omega)]$ and $H(j\omega)$ and then graphically subtract the magnitude of $H(j\omega)$ from that of $G_1(j\omega)/[1 + G_1(j\omega)]$ and also graphically subtract the phase angle of $H(j\omega)$ from that of $G_1(j\omega)/[1 + G_1(j\omega)]$. Then the resulting log-magnitude curve and phase-angle curve give the closed-loop frequency response $C(j\omega)/R(j\omega)$.

To obtain acceptable values of M_r, ω_r, and ω_b for $|C(j\omega)/R(j\omega)|$, a trial-and-error process may be necessary. In each trial, the $G_1(j\omega)$ locus is varied in shape. Then Bode diagrams for $G_1(j\omega)/[1 + G_1(j\omega)]$ and $H(j\omega)$ are drawn, and the closed-loop frequency response $C(j\omega)R(j\omega)$ is obtained. The values of M_r, ω_r, and ω_b are checked until they are acceptable.

Gain adjustments. The concept of M circles will now be applied to the design of control systems. In obtaining suitable performance, the adjustment of gain is usually the first consideration. The adjustment may be based on a desirable value for the resonant peak.

In the following, we shall demonstrate a method for determining the gain K so that the system will have some maximum value M_r, not exceeded over the entire frequency range.

Referring to Figure 8–91, we see that the tangent line drawn from the origin to the desired M_r circle has an angle of ψ, as shown, if M_r is greater than unity. The value of $\sin\psi$ is

$$\sin\psi = \left| \frac{\dfrac{M_r}{M_r^2 - 1}}{\dfrac{M_r^2}{M_r^2 - 1}} \right| = \frac{1}{M_r} \tag{8–18}$$

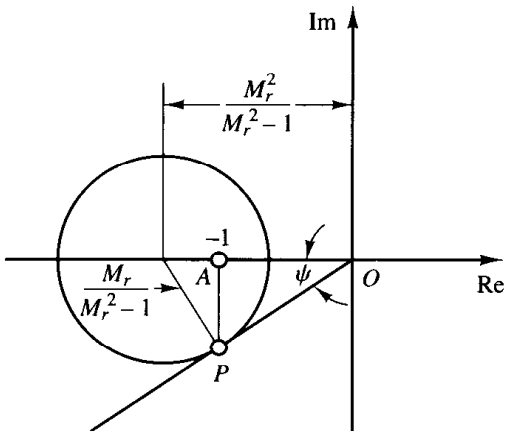

Figure 8–91
M circle.

Let us call the tangency point of the tangent line and the M_r circle as point P. It can easily be proved that the line drawn from point P, perpendicular to the negative real axis, intersects this axis at the $-1 + j0$ point.

Consider the system shown in Figure 8–92. The procedure for determining the gain K so that $G(j\omega) = KG_1(j\omega)$ will have a desired value of M_r (where $M_r > 1$) can be summarized as follows:

1. Draw the polar plot of the normalized open-loop transfer function $G_1(j\omega) = G(j\omega)/K$.
2. Draw from the origin the line that makes an angle of $\psi = \sin^{-1}(1/M_r)$ with the negative real axis.
3. Fit a circle with center on the negative real axis tangent to both the $G_1(j\omega)$ locus and the line PO.
4. Draw a perpendicular line to the negative real axis from point P, the point of tangency of this circle with the line PO. The perpendicular line PA intersects the negative real axis at point A.
5. For the circle just drawn to correspond to the desired M_r circle, point A should be the $-1 + j0$ point.
6. The desired value of the gain K is that value which changes the scale so that point A becomes the $-1 + j0$ point. Thus, $K = 1/\overline{OA}$.

Note that the resonant frequency ω_r is the frequency of the point at which the circle is tangent to the $G_1(j\omega)$ locus. The present procedure may not yield a satisfactory value for ω_r. If this is the case, the system must be compensated in order to increase the value

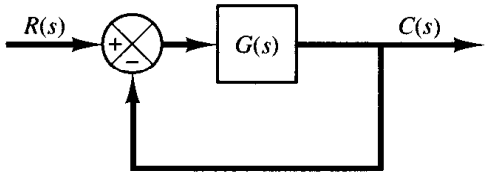

Figure 8–92
Control system.

of ω_r without changing the value of M_r. (For the compensation of control systems by frequency-response methods, see Chapter 9.)

Note also that if the system has nonunity feedback then the method requires some cut-and-try steps.

EXAMPLE 8–22 Consider the unity-feedback control system whose open-loop transfer function is

$$G(j\omega) = \frac{K}{j\omega(1 + j\omega)}$$

Determine the value of the gain K so that $M_r = 1.4$.

The first step in the determination of the gain K is to sketch the polar plot of

$$\frac{G(j\omega)}{K} = \frac{1}{j\omega(1 + j\omega)}$$

as shown in Figure 8–93. The value of ψ corresponding to $M_r = 1.4$ is obtained from

$$\psi = \sin^{-1}\frac{1}{M_r} = \sin^{-1}\frac{1}{1.4} = 45.6°$$

The next step is to draw the line OP that makes an angle $\psi = 45.6°$ with the negative real axis. Then draw the circle that is tangent to both the $G(j\omega)/K$ locus and the line OP. Define the point where the circle is tangent to the 45.6° line as point P. The perpendicular line drawn from point P intersects the negative real axis at $(-0.63, 0)$. Then the gain K of the system is determined as follows:

$$K = \frac{1}{0.63} = 1.59$$

It should be noted that such determination of the gain can also be done easily on the log-magnitude versus phase plot. In what follows, we shall demonstrate how the log-magnitude versus phase diagram can be used to determine the gain K so that the system will have a desired value of M_r.

Figure 8–94 shows the $M_r = 1.4$ locus and the $G(j\omega)/K$ locus. Changing the gain has no effect on the phase angle but merely moves the curve vertically up for $K > 1$ and down for $K < 1$.

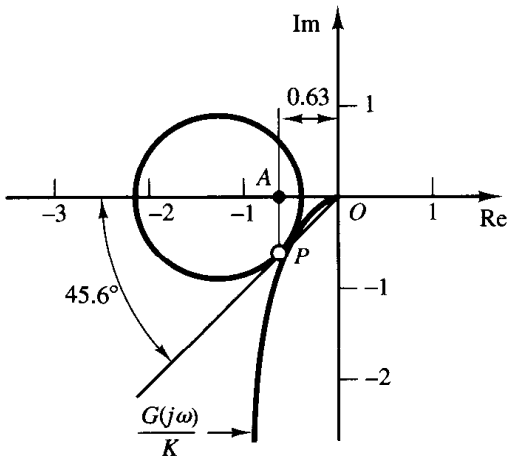

Figure 8–93
Determination of the gain K using an M circle.

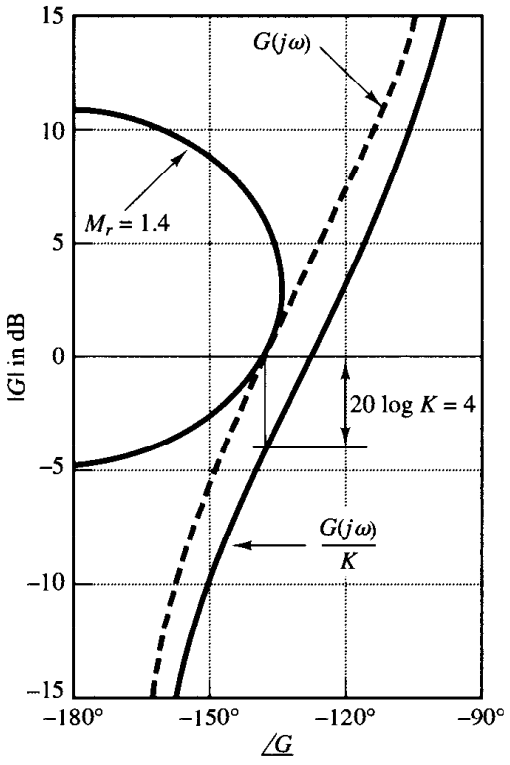

Figure 8–94
Determination of the gain K using the Nichols chart.

In Figure 8–94, the $G(j\omega)/K$ locus must be raised by 4 dB in order that it be tangent to the desired M_r locus and that the entire $G(j\omega)/K$ locus be outside the $M_r = 1.4$ locus. The amount of vertical shift of the $G(j\omega)/K$ locus determines the gain necessary to yield the desired value of M_r. Thus, by solving

$$20 \log K = 4$$

we obtain

$$K = 1.59$$

Thus, we have the same result as obtained earlier.

8–11 EXPERIMENTAL DETERMINATION OF TRANSFER FUNCTIONS

The first step in the analysis and design of a control system is to derive a mathematical model of the plant under consideration. Obtaining a model analytically may be quite difficult. We may have to obtain it by means of experimental analysis. The importance of the frequency-response methods is that the transfer function of the plant, or any other component of a system, may be determined by simple frequency-response measurements.

If the amplitude ratio and phase shift have been measured at a sufficient number of frequencies within the frequency range of interest, they may be plotted on the Bode diagram. Then the transfer function can be determined by asymptotic approximations. We build up asymptotic log-magnitude curves consisting of several segments. With some trial-and-error juggling of the corner frequencies, it is usually possible to find a very close fit to the curve. (Note that if the frequency is plotted in cycles per second rather

than radians per second the corner frequencies must be converted to radians per second before computing the time constants.)

Sinusoidal-signal generators. In performing a frequency-response test, suitable sinusoidal-signal generators must be available. The signal may have to be in mechanical, electrical, or pneumatic form. The frequency ranges needed for the test are approximately 0.001 to 10 Hz for large-time-constant systems and 0.1 to 1000 Hz for small-time-constant systems. The sinusoidal signal must be reasonably free from harmonics or distortion.

For very low frequency ranges (below 0.01 Hz) a mechanical signal generator (together with a suitable pneumatic or electrical transducer if necessary) may be used. For the frequency range from 0.01 to 1000 Hz, a suitable electrical-signal generator (together with a suitable transducer if necessary) may be used.

Determination of minimum-phase transfer functions from Bode diagrams. As stated previously, whether a system is minimum phase can be determined from the frequency-response curves by examining the high-frequency characteristics.

To determine the transfer function, we first draw asymptotes to the experimentally obtained log-magnitude curve. The asymptotes must have slopes of multiples of ±20 dB/decade. If the slope of the experimentally obtained log-magnitude curve changes from −20 to −40 dB/decade at $\omega = \omega_1$, it is clear that a factor $1/[1 + j(\omega/\omega_1)]$ exists in the transfer function. If the slope changes by −40 dB/decade at $\omega = \omega_2$, there must be a quadratic factor of the form

$$\frac{1}{1 + 2\zeta\left(j\frac{\omega}{\omega_2}\right) + \left(j\frac{\omega}{\omega_2}\right)^2}$$

in the transfer function. The undamped natural frequency of this quadratic factor is equal to the corner frequency ω_2. The damping ratio ζ can be determined from the experimentally obtained log-magnitude curve by measuring the amount of resonant peak near the corner frequency ω_2 and comparing this with the curves shown in Figure 8–8.

Once the factors of the transfer function $G(j\omega)$ have been determined, the gain can be determined from the low-frequency portion of the log-magnitude curve. Since such terms as $1 + j(\omega/\omega_1)$ and $1 + 2\zeta(j\omega/\omega_2 + (j\omega/\omega_2)^2$ become unity as ω approaches zero, at very low frequencies, the sinusoidal transfer function $G(j\omega)$ can be written

$$\lim_{\omega \to 0} G(j\omega) = \frac{K}{(j\omega)^\lambda}$$

In many practical systems, λ equals 0, 1, or 2.

1. For $\lambda = 0$, or type 0 systems,

$$G(j\omega) = K, \qquad \text{for } \omega \ll 1$$

or

$$20 \log |G(j\omega)| = 20 \log K, \qquad \text{for } \omega \ll 1$$

The low-frequency asymptote is a horizontal line at 20 log K dB. The value of K can thus be found from this horizontal asymptote.

2. For $\lambda = 1$, or type 1 systems,

$$G(j\omega) = \frac{K}{j\omega}, \qquad \text{for } \omega \ll 1$$

or

$$20 \log |G(j\omega)| = 20 \log K - 20 \log \omega, \qquad \text{for } \omega \ll 1$$

which indicates that the low-frequency asymptote has the slope −20 dB/decade. The frequency at which the low-frequency asymptote (or its extension) intersects the 0-dB line is numerically equal to K.

3. For $\lambda = 2$, or type 2 systems,

$$G(j\omega) = \frac{K}{(j\omega)^2}, \qquad \text{for } \omega \ll 1$$

or

$$20 \log |G(j\omega)| = 20 \log K - 40 \log \omega, \qquad \text{for } \omega \ll 1$$

The slope of the low-frequency asymptote is −40 dB/decade. The frequency at which this asymptote (or its extension) intersects the 0-dB line is numerically equal to $\sqrt{K}$.

Examples of log-magnitude curves for type 0, type 1, and type 2 systems are shown in Figure 8–95, together with the frequency to which the gain K is related.

The experimentally-obtained phase-angle curve provides a means of checking the transfer function obtained from the log-magnitude curve. For a minimum-phase system, the experimental phase-angle curve should agree reasonably well with the theoretical phase-angle curve obtained from the transfer function just determined. These two phase-angle curves should agree exactly in both the very low and very high frequency ranges. If the experimentally obtained phase angle at very high frequencies (compared with the corner frequencies) is not equal to $-90°(q - p)$, where p and q are the degrees of the numerator and denominator polynomials of the transfer function, respectively, then the transfer function must be a nonminimum-phase transfer function.

Nonminimum-phase transfer functions. If, at the high-frequency end, the computed phase lag is 180° less than the experimentally obtained phase lag, then one of the zeros of the transfer function should have been in the right-half s plane instead of the left-half s plane.

If the computed phase lag differed from the experimentally obtained phase lag by a constant rate of change of phase, then transport lag, or dead time, is present. If we assume the transfer function to be of the form

$$G(s)e^{-Ts}$$

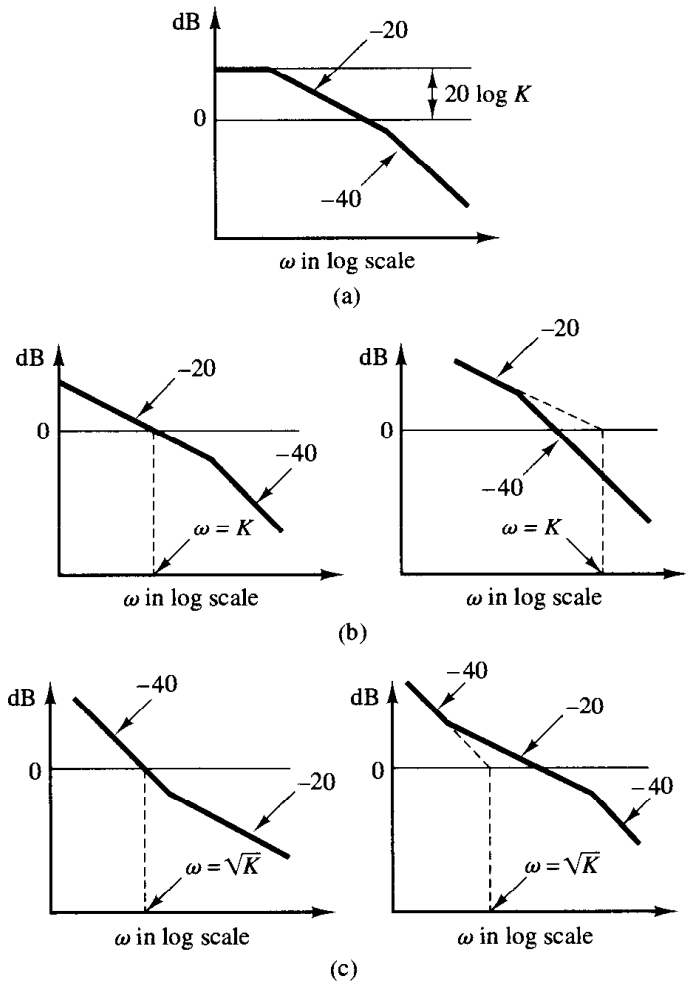

Figure 8–95
(a) Log-magnitude curve of a type 0 system; (b) log-magnitude curves of type 1 systems; (c) log-magnitude curves of type 2 systems. (The slopes shown are in dB/decade.)

where $G(s)$ is a ratio of two polynomials in s, then

$$\lim_{\omega\to\infty} \frac{d}{d\omega} \underline{/G(j\omega)e^{-j\omega T}} = \lim_{\omega\to\infty} \frac{d}{d\omega} \left[\underline{/G(j\omega)} + \underline{/e^{-j\omega T}} \right]$$
$$= \lim_{\omega\to\infty} \frac{d}{d\omega} \left[\underline{/G(j\omega)} - \omega T \right]$$
$$= 0 - T = -T$$

Thus, from this last equation, we can evaluate the magnitude of the transport lag T.

A few remarks on the experimental determination of transfer functions

1. It is usually easier to make accurate amplitude measurements than accurate phase-shift measurements. Phase-shift measurements may involve errors that may be caused by instrumentation or by misinterpretation of the experimental records.

2. The frequency response of measuring equipment used to measure the system output must have a nearly flat magnitude versus frequency curves. In addition, the phase angle must be nearly proportional to the frequency.

3. Physical systems may have several kinds of nonlinearities. Therefore, it is necessary to consider carefully the amplitude of input sinusoidal signals. If the amplitude of the input signal is too large, the system will saturate, and the frequency-response test will yield inaccurate results. On the other hand, a small signal will cause errors due to dead zone. Hence, a careful choice of the amplitude of the input sinusoidal signal must be made. It is necessary to sample the waveform of the system output to make sure that the waveform is sinusoidal and that the system is operating in the linear region during the test period. (The waveform of the system output is not sinusoidal when the system is operating in its nonlinear region.)

4. If the system under consideration is operating continuously for days and weeks, then normal operation need not be stopped for frequency-response tests. The sinusoidal test signal may be superimposed on the normal inputs. Then, for linear systems, the output due to the test signal is superimposed on the normal output. For the determination of the transfer function while the system is in normal operation, stochastic signals (white noise signals) also are often used. By use of correlation functions, the transfer function of the system can be determined without interrupting normal operation.

EXAMPLE 8–23 Determine the transfer function of the system whose experimental frequency-response curves are as shown in Figure 8–96.

The first step in determining the transfer function is to approximate the log-magnitude curve by asymptotes with slopes ±20 dB/decade and multiples thereof, as shown in Figure 8–96. We then estimate the corner frequencies. For the system shown in Figure 8–96, the following form of the transfer function is estimated.

$$G(j\omega) = \frac{K(1 + 0.5j\omega)}{j\omega(1 + j\omega)\left[1 + 2\zeta\left(j\frac{\omega}{8}\right) + \left(j\frac{\omega}{8}\right)^2\right]}$$

The value of the damping ratio ζ is estimated by examining the peak resonance near $\omega = 6$ rad/sec. Referring to Figure 8–8, ζ is determined to be 0.5. The gain K is numerically equal to the frequency at the intersection of the extension of the low-frequency asymptote and the 0-dB line. The value of K is thus found to be 10. Therefore, $G(j\omega)$ is tentatively determined as

$$G(j\omega) = \frac{10(1 + 0.5j\omega)}{j\omega(1 + j\omega)\left[1 + \left(j\frac{\omega}{8}\right) + \left(j\frac{\omega}{8}\right)^2\right]}$$

or

$$G(s) = \frac{320(s + 2)}{s(s + 1)(s^2 + 8s + 64)}$$

This transfer function is tentative because we have not examined the phase-angle curve yet.

Once the corner frequencies are noted on the log-magnitude curve, the corresponding phase-angle curve for each component factor of the transfer function can easily be drawn.

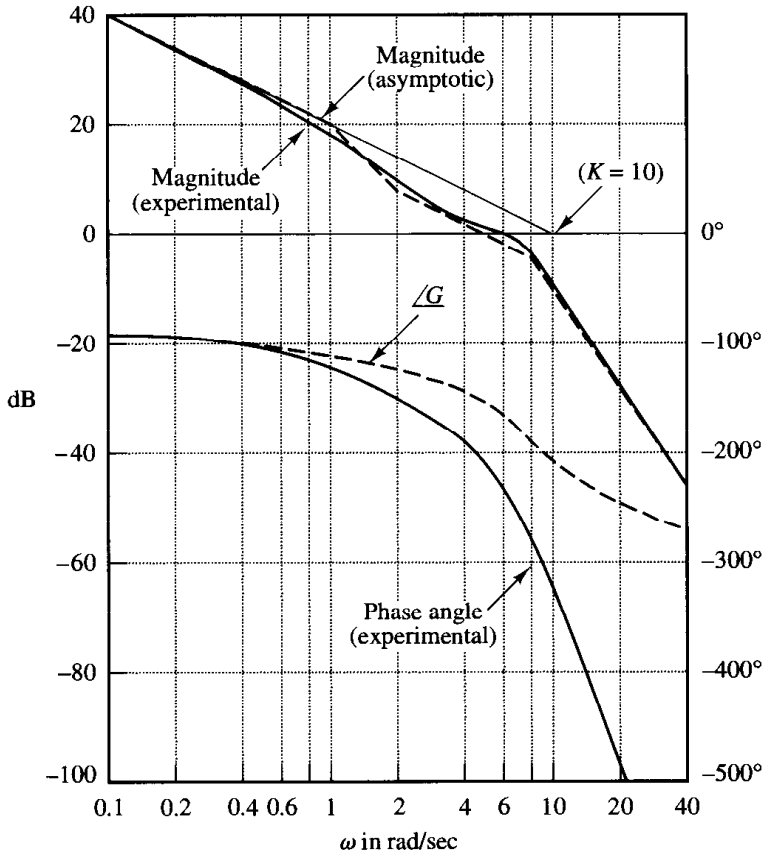

Figure 8–96
Bode diagram of a system. (Solid curves are experimentally obtained curves.)

The sum of these component phase-angle curves is that of the assumed transfer function. The phase-angle curve for $G(j\omega)$ is denoted by $\angle G$ in Figure 8–96. From Figure 8–96 we clearly notice a discrepancy between the computed phase-angle curve and the experimentally-obtained phase-angle curve. The difference between the two curves at very high frequencies appears to be a constant rate of change. Thus, the discrepancy in the phase-angle curves must be caused by transport lag.

Hence, we assume the complete transfer function to be $G(s)e^{-Ts}$. Since the discrepancy between the computed and experimental phase angles is -0.2ω rad for very high frequencies, we can determine the value of T as follows.

$$\lim_{\omega\to\infty} \frac{d}{d\omega} \underline{/G(j\omega)e^{-j\omega T}} = -T = -0.2$$

or

$$T = 0.2 \text{ sec}$$

The presence of transport lag can thus be determined, and the complete transfer function determined from the experimental curves is

$$G(s)e^{-Ts} = \frac{320(s+2)e^{-0.2s}}{s(s+1)(s^2+8s+64)}$$

EXAMPLE PROBLEMS AND SOLUTIONS

A-8-1. Consider a system whose closed-loop transfer function is

$$\frac{C(s)}{R(s)} = \frac{10(s + 1)}{(s + 2)(s + 5)}$$

(This is the same system considered in Problem A-6-9.) Clearly, the closed-loop poles are located at $s = -2$ and $s = -5$, and the system is not oscillatory. (The unit-step response, however, exhibits overshoot due to the presence of a zero at $s = -1$. See Figure 6–51.)

Show that the closed-loop frequency response of this system will exhibit a resonant peak, although the damping ratio of the closed-loop poles is greater then unity.

Solution. Figure 8–97 shows the Bode diagram for the system. The resonant peak value is approximately 3.5 dB. (Note that, in the absence of a zero, the second-order system with $\zeta > 0.7$ will not exhibit a resonant peak; however, the presence of a closed-loop zero will cause such a peak.)

A-8-2. Plot a Bode diagram for the following open-loop transfer function $G(s)$:

$$G(s) = \frac{20(s^2 + s + 0.5)}{s(s + 1)(s + 10)}$$

Solution. By substituting $s = j\omega$ into $G(s)$, we have

$$G(j\omega) = \frac{20[(j\omega)^2 + (j\omega) + 0.5]}{j\omega(j\omega + 1)(j\omega + 10)}$$

Notice that ω_n and ζ of the quadratic term in the numerator are

$$\omega_n = \sqrt{0.5} \qquad \text{and} \qquad \zeta = 0.707$$

This quadratic term can be written as

$$\omega_n^2\left[\left(j\frac{\omega}{\omega_n}\right)^2 + 2\zeta\left(j\frac{\omega}{\omega_n}\right) + 1\right] = (\sqrt{0.5})^2\left[\left(j\frac{\omega}{\sqrt{0.5}}\right)^2 + 2 \times 0.707\left(j\frac{\omega}{\sqrt{0.5}}\right) + 1\right]$$

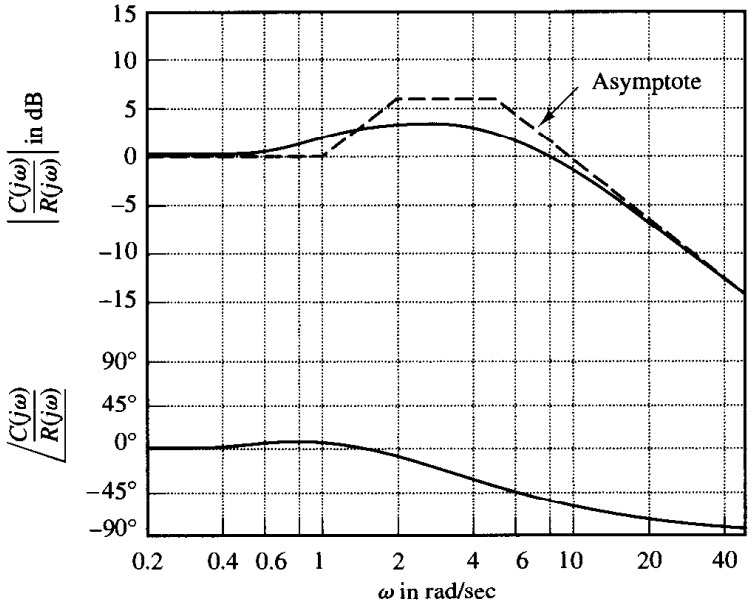

Figure 8–97
Bode diagram for $10(1 + j\omega)/[(2 + j\omega)(5 + j\omega)]$

Note that the corner frequency is at $\omega = \sqrt{0.5} = 0.707$ rad/sec. Now $G(j\omega)$ can be written as

$$G(j\omega) = \frac{\left(j\frac{\omega}{\sqrt{0.5}}\right)^2 + 1.414\left(j\frac{\omega}{\sqrt{0.5}}\right) + 1}{j\omega(j\omega + 1)(0.1j\omega + 1)}$$

The Bode diagram for $G(j\omega)$ is shown in Figure 8–98.

A-8-3. Draw the Bode diagram of the following nonminimum-phase system:

$$\frac{C(s)}{R(s)} = 1 - Ts$$

Obtain the unit-ramp response of the system and plot $c(t)$ versus t.

Solution. The Bode diagram of the system is shown in Figure 8–99. For a unit-ramp input, $R(s) = 1/s^2$, we have

$$C(s) = \frac{1 - Ts}{s^2} = \frac{1}{s^2} - \frac{T}{s}$$

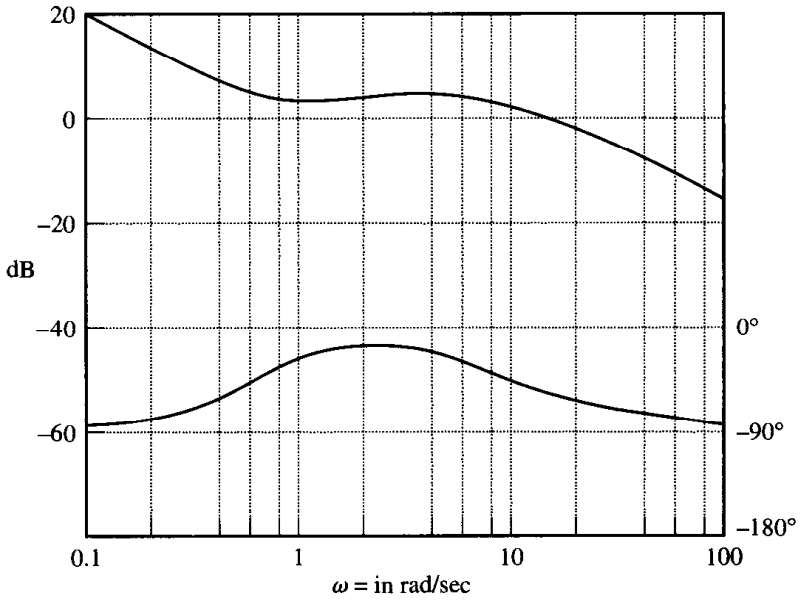

Figure 8–98
Bode diagram for $G(j\omega)$ of Problem A-8-2.

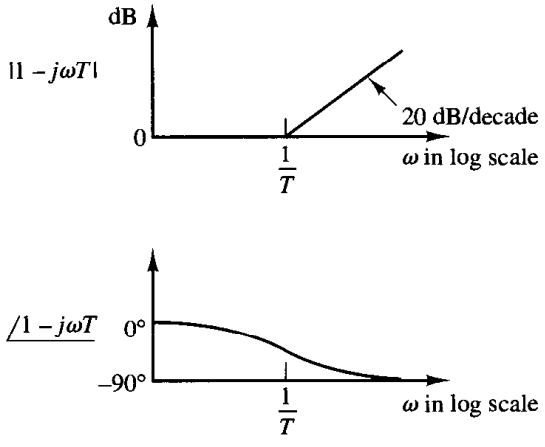

Figure 8–99
Bode diagram of $1 - j\omega T$.

The inverse Laplace transform of $C(s)$ gives

$$c(t) = t - T, \qquad \text{for } t \geq 0$$

Figure 8–100 shows the response curve $c(t)$ versus t. (Note the faulty behavior at the start of the response.) A characteristic property of such a nonminimum-phase system is that the transient response starts out in the opposite direction to the input but eventually comes back in the same direction.

A-8-4. Consider the system defined by

$$\begin{bmatrix} \dot{x}_1 \\ \dot{x}_2 \end{bmatrix} = \begin{bmatrix} 0 & 1 \\ -25 & -4 \end{bmatrix} \begin{bmatrix} x_1 \\ x_2 \end{bmatrix} + \begin{bmatrix} 1 & 1 \\ 0 & 1 \end{bmatrix} \begin{bmatrix} u_1 \\ u_2 \end{bmatrix}$$

$$\begin{bmatrix} y_1 \\ y_2 \end{bmatrix} = \begin{bmatrix} 1 & 0 \\ 0 & 1 \end{bmatrix} \begin{bmatrix} x_1 \\ x_2 \end{bmatrix}$$

Obtain the sinusoidal transfer functions $Y_1(j\omega)/U_1(j\omega)$, $Y_2(j\omega)/U_1(j\omega)$, $Y_1(j\omega)/U_2(j\omega)$, and $Y_2(j\omega)/U_2(j\omega)$. In deriving $Y_1(j\omega)/U_1(j\omega)$ and $Y_2(j\omega)/U_1(j\omega)$, we assume that $U_2(j\omega) = 0$. Similarly, in obtaining $Y_1(j\omega)/U_2(j\omega)$and $Y_2(j\omega)/U_2(j\omega)$, we assume that $U_1(j\omega) = 0$. Obtain also the Bode diagrams of these four transfer functions with MATLAB.

Solution. The transfer matrix expression for the system defined by

$$\dot{\mathbf{x}} = \mathbf{A}\mathbf{x} + \mathbf{B}\mathbf{u}$$

$$\dot{\mathbf{y}} = \mathbf{C}\mathbf{x} + \mathbf{D}\mathbf{u}$$

is given by

$$\mathbf{Y}(s) = \mathbf{G}(s)\mathbf{U}(s)$$

where $\mathbf{G}(s)$ is the transfer matrix and is given by

$$\mathbf{G}(s) = \mathbf{C}(s\mathbf{I} - \mathbf{A})^{-1}\mathbf{B} + \mathbf{D}$$

For the system considered here, the transfer matrix becomes

$$\begin{aligned} \mathbf{C}(s\mathbf{I} - \mathbf{A})^{-1}\mathbf{B} + \mathbf{D} &= \begin{bmatrix} 1 & 0 \\ 0 & 1 \end{bmatrix} \begin{bmatrix} s & -1 \\ 25 & s+4 \end{bmatrix}^{-1} \begin{bmatrix} 1 & 1 \\ 0 & 1 \end{bmatrix} \\ &= \frac{1}{s^2 + 4s + 25} \begin{bmatrix} s+4 & 1 \\ -25 & s \end{bmatrix} \begin{bmatrix} 1 & 1 \\ 0 & 1 \end{bmatrix} \\ &= \begin{bmatrix} \dfrac{s+4}{s^2+4s+25} & \dfrac{s+5}{s^2+4s+25} \\ \dfrac{-25}{s^2+4s+25} & \dfrac{s-25}{s^2+4s+25} \end{bmatrix} \end{aligned}$$

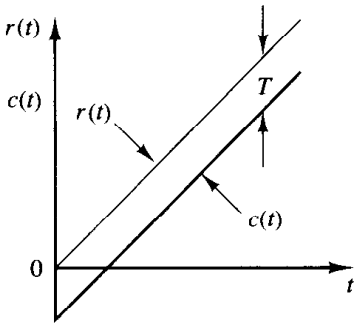

Figure 8–100
Unit-ramp response of the system considered in Problem A-8-3.

Hence

$$\begin{bmatrix} Y_1(s) \\ Y_2(s) \end{bmatrix} = \begin{bmatrix} \dfrac{s+4}{s^2+4s+25} & \dfrac{s+5}{s^2+4s+25} \\ \dfrac{-25}{s^2+4s+25} & \dfrac{s-25}{s^2+4s+25} \end{bmatrix} \begin{bmatrix} U_1(s) \\ U_2(s) \end{bmatrix}$$

Assuming that $U_2(j\omega) = 0$, we find $Y_1(j\omega)/U_1(j\omega)$ and $Y_2(j\omega)/U_1(j\omega)$ as follows:

$$\frac{Y_1(j\omega)}{U_1(j\omega)} = \frac{j\omega + 4}{(j\omega)^2 + 4j\omega + 25}$$

$$\frac{Y_2(j\omega)}{U_1(j\omega)} = \frac{-25}{(j\omega)^2 + 4j\omega + 25}$$

Similarly, assuming that $U_1(j\omega) = 0$, we find $Y_1(j\omega)/U_2(j\omega)$ and $Y_2(j\omega)/U_2(j\omega)$ as follows:

$$\frac{Y_1(j\omega)}{U_2(j\omega)} = \frac{j\omega + 5}{(j\omega)^2 + 4j\omega + 25}$$

$$\frac{Y_2(j\omega)}{U_2(j\omega)} = \frac{j\omega - 25}{(j\omega)^2 + 4j\omega + 25}$$

Notice that $Y_2(j\omega)/U_2(j\omega)$ is a nonminimum-phase transfer function.

To plot Bode diagrams for $Y_1(j\omega)/U_1(j\omega)$, $Y_2(j\omega)/U_1(j\omega)$, $Y_1(j\omega)/U_2(j\omega)$, and $Y_2(j\omega)/U_2(j\omega)$ with MATLAB, we may use the command

```
bode(A,B,C,D)
```

Then MATLAB produces Bode diagrams when u_1 is the input and u_2 is zero and when u_2 is the input and u_1 is zero. See MATLAB Program 8–14 and the resulting Bode diagrams shown in Figure 8–101. [Note that MATLAB produces two sets of figures (called Figure 1 and Figure 2) on the screen. Figure 8–101 consists of these two sets of Bode diagrams.]

MATLAB Program 8–14

```
A = [0   1;-25   -4];
B = [1   1;0   1];
C = [1   0;0   1];
D = [0   0;0   0];
bode(A,B,C,D)
```

A-8-5. Referring to Problem A-8-4, consider an alternative way to plot Bode diagrams of the system. One way to plot the Bode diagrams is to use the command

```
bode(A,B,C,D,1)
```

to obtain Bode diagrams for $Y_1(j\omega)/U_1(j\omega)$ and $Y_2(j\omega)/U_1(j\omega)$. To obtain Bode diagrams for $Y_1(j\omega)/U_2(j\omega)$ and $Y_2(j\omega)/U_2(j\omega)$, use the command

```
bode(A,B,C,D,2)
```

Write a MATLAB program to obtain Bode diagrams using these bode commands.

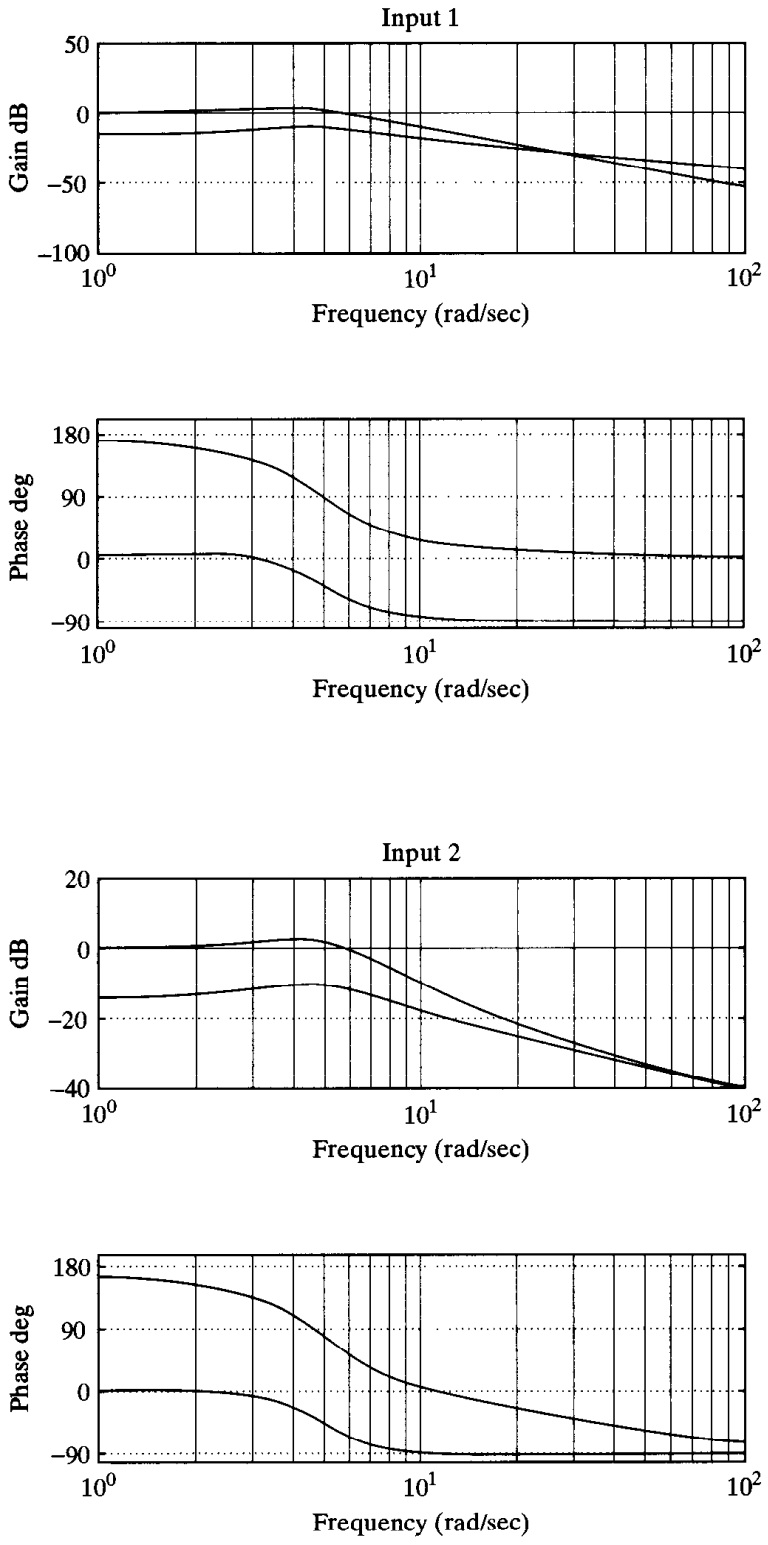

Figure 8–101
Bode diagrams of the system considered in Problem A-8-4.

MATLAB Program 8–15

```
A = [0   1;−25   −4];
B = [1   1;0   1];
C = [1   0;0   1];
D = [0   0;0   0];
bode(A,B,C,D,1)
subplot(2,1,1), title('Bode Diagrams; Input = u1 (u2 = 0)')
bode(A,B,C,D,2)
subplot(2,1,1), title ('Bode Diagrams; Input = u2 (u1 = 0)')
```

Solution. The program for this problem is given as MATLAB Program 8–15. The Bode diagrams produced by this program are shown in Figure 8–102. In these diagrams it may not be easy to identify which curves are for $Y_1(j\omega)$ or $Y_2(j\omega)$. Ordinarily the text command may be used to identify curves. However, the text command does not apply to the present bode commands. To use the text command, we may use the following command:

```
[mag,phase,w] = bode(A,B,C,D,iu,w)
```

See Problem A-8-6 for the details.

A-8-6. Referring to Problems A-8-4 and A-8-5, consider plotting Bode diagrams of the same system as discussed in these problems. Use the text command to distinguish curves in the diagrams. Write a possible MATLAB program for plotting Bode diagrams using the following command:

```
[mag,phase,w] = bode(A,B,C,D,iu,w)
```

Solution. In using the command specified, note that the matrices mag and phase contain the magnitudes of $Y_1(j\omega)$ and $Y_2(j\omega)$ and phase angles for $Y_1(j\omega)$ and $Y_2(j\omega)$ evaluated at each frequency point considered. To get the magnitude of $Y_1(j\omega)$, use the following command:

```
Y1 = mag*[1;0]
```

To convert the magnitude to decibels, use the statement

```
magdB = 20*log10(mag)
```

Hence, to convert Y1 to decibels, enter the statement

```
Y1dB = 20*log10(Y1)
```

Similarly, to plot the magnitude of Y2 in decibels, use the following command:

```
Y2 = mag*[0;1]
Y2dB = 20*log10(Y2)
```

Then enter the command

```
semilogx(w,Y1dB,'o',w,Y1dB,'-',w,Y2dB,'x',w,Y2dB,'-')
```

The text command can now be used to write text in the figure. See MATLAB Program 8–16.

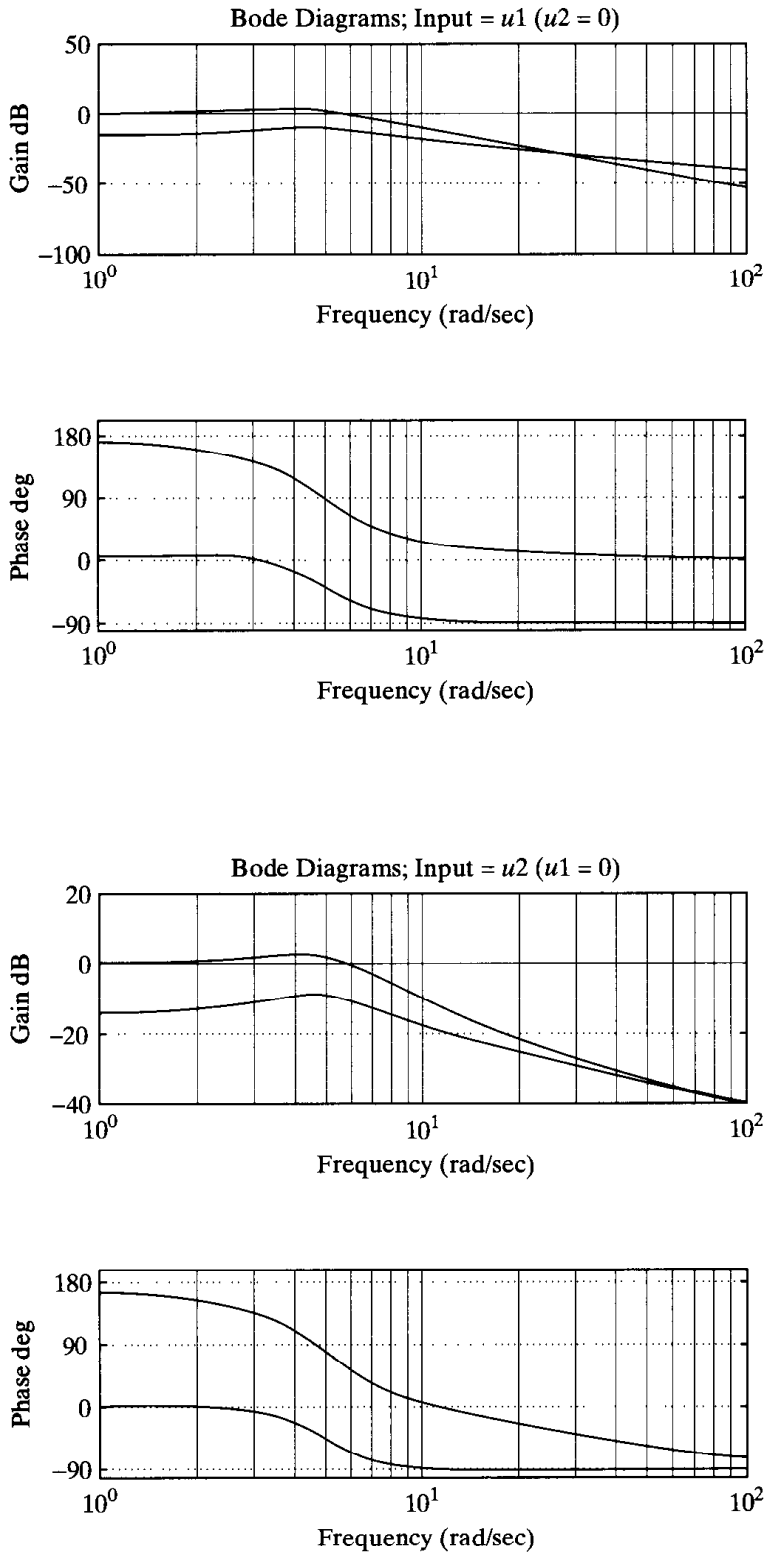

Figure 8–102
Bode diagrams.

MATLAB Program 8–16

```
% ***** We shall first obtain the frequency response when
% u2 = 0; that is, we obtain Y1(jw)/U1(jw) and Y2(jw)/U1(jw) *****

A = [0   1;−25   −4];
B = [1   1;0   1];
C = [1   0;0   1];
D = [0   0;0   0];
w = logspace(−1,3,100);
[mag1, phase1, w] = bode(A,B,C,D,1,w);
Y1 = mag1*[1;0]; Y1dB = 20*log10(Y1);
Y2 = mag1*[0;1]; Y2dB = 20*log10(Y2);
semilogx(w,Y1dB,'o',w,Y1dB,'-',w,Y2dB,'x',w,Y2dB,'-')
grid
subplot(2,1,1);
title('Bode Diagrams: Input = u1 (u2 = 0)')
xlabel('Frequency (rad/sec)')
ylabel('Gain dB')
text(1.2,−10,'Y1'); text(1.2,6,'Y2')

Y1p = phase1*[1;0];
Y2p = phase1*[0;1];
semilogx(w,Y1p,'o',w,Y1p,'-',w,Y2p,'x',w,Y2p,'-')
grid
xlabel('Frequency (rad/sec)')
ylabel('Phase deg')
text(1.2,25,'Y1');text(1.2,188,'Y2')

% ***** In the following, we shall obtain the frequency response
% when u1 = 0; that is, we obtain Y1(jw)/U2(jw) and Y2(jw)/U2(jw) *****

[mag2,phase2,w] = bode(A,B,C,D,2,w);
YY1 = mag2*[1;0]; YY1dB = 20*log10(YY1);
YY2 = mag2*[0;1]; YY2dB = 20*log10(YY2);
semilogx(w,YY1dB,'o',w,YY1dB,'-',w,YY2dB,'x',w,YY2dB,'-')
grid
subplot(2,1,1);
title('Bode Diagrams: Input = u2 (u1 = 0)')
xlabel('Frequency (rad/sec)')
ylabel('Gain dB')
text(1.2, −17,'Y1'); text(1.2,5,'Y2')

YY1p = phase2*[1;0];
YY2p = phase2*[0;1];
semilogx(w,YY1p,'o',w,YY1p,'-',w,YY2p,'x',w,YY2p,'-')
grid
xlabel('Frequency (rad/sec)')
ylabel('Phase deg')
text(1.2,20,'Y1'); text(1.2,182,'Y2')
```

Similarly, to plot the phase angles for $Y_1(j\omega)$ and $Y_2(j\omega)$, use the following commands:

```
Y1p = phase*[1;0];
Y2p = phase*[0;1];
semilogx(w,Y1p,'o',w,Y1p,'-',w,Y2p,'x',w,Y2p,'-')
```

Bode diagrams obtained by use of MATLAB Program 8–16 are shown in Figures 8–103 and 8–104.

A-8-7. Prove that the polar plot of the sinusoidal transfer function

$$G(j\omega) = \frac{j\omega T}{1 + j\omega T}, \qquad \text{for } 0 \le \omega \le \infty$$

is a semicircle. Find the center and radius of the circle.

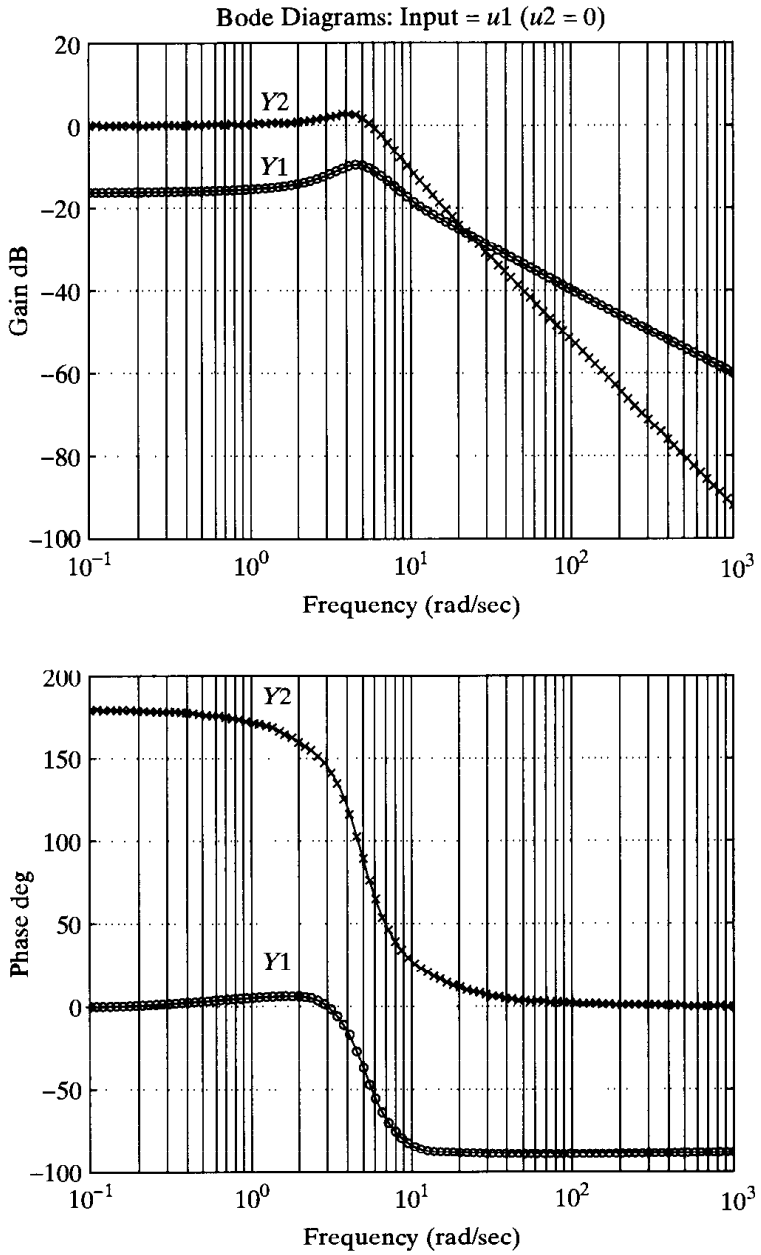

Figure 8–103
Bode diagrams.

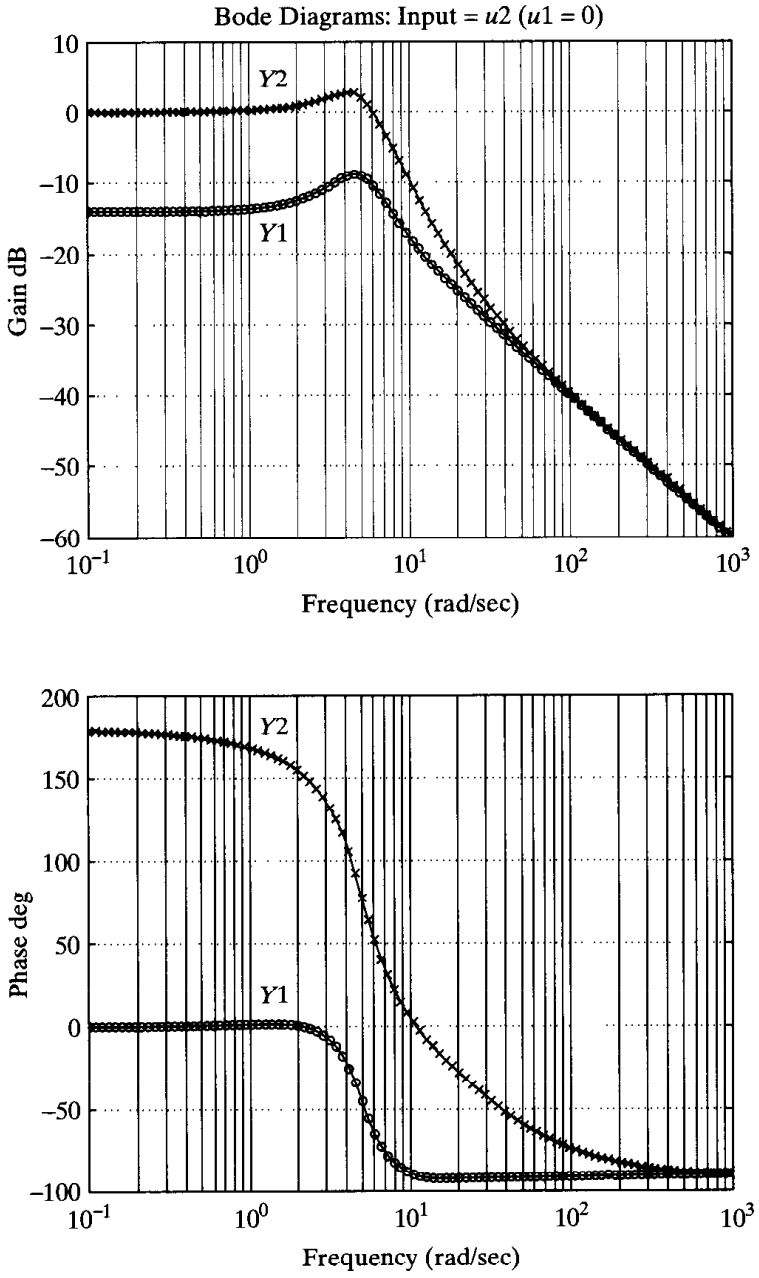

Figure 8–104
Bode diagrams.

Solution. The given sinusoidal transfer function $G(j\omega)$ can be written as follows:

$$G(j\omega) = X + jY$$

where

$$X = \frac{\omega^2 T^2}{1 + \omega^2 T^2}, \qquad Y = \frac{\omega T}{1 + \omega^2 T^2}$$

Then

$$\left(X - \frac{1}{2}\right)^2 + Y^2 = \frac{(\omega^2 T^2 - 1)^2}{4(1 + \omega^2 T^2)^2} + \frac{\omega^2 T^2}{(1 + \omega^2 T^2)^2} = \frac{1}{4}$$

Hence, we see that the plot of $G(j\omega)$ is a circle centered at (0.5,0) with radius equal to 0.5. The upper semicircle corresponds to $0 \leq \omega \leq \infty$, and the lower semicircle corresponds to $-\infty \leq \omega \leq 0$.

A-8-8. Referring to Problem A-8-2, plot the polar locus of $G(s)$ where

$$G(s) = \frac{20(s^2 + s + 0.5)}{s(s + 1)(s + 10)}$$

Locate on the polar locus frequency points where $\omega = 0.1, 0.2, 0.4, 0.6, 1.0, 2.0, 4.0, 6.0, 10.0, 20.0,$ and 40.0 rad/sec.

Solution. Noting that

$$G(j\omega) = \frac{2(-\omega^2 + j\omega + 0.5)}{j\omega(j\omega + 1)(0.1\,j\omega + 1)}$$

we have

$$|G(j\omega)| = \frac{2\sqrt{(0.5 - \omega^2)^2 + \omega^2}}{\omega\sqrt{1 + \omega^2}\sqrt{1 + 0.01\,\omega^2}}$$

$$\underline{/G(j\omega)} = \tan^{-1}\left(\frac{\omega}{0.5 - \omega^2}\right) - 90° - \tan^{-1}\omega - \tan^{-1}(0.1\omega)$$

The magnitude and phase angle may be obtained as shown in Table 8–3. (Note that the magnitude in decibels and phase angle in degrees can be easily read from Figure 8–98.) The magnitude in decibels can also be easily converted to a number. Figure 8–105 shows the polar plot. Notice the existence of a loop in the polar locus.

Table 8–3 Magnitude and Phase of $G(j\omega)$ Considered in Problem A-8-8

ω	$\lvert G(j\omega)\rvert$	$\underline{/G(j\omega)}$
0.1	9.952	−84.75°
0.2	4.918	−78.96°
0.4	2.435	−64.46°
0.6	1.758	−47.53°
1.0	1.573	−24.15°
2.0	1.768	−14.49°
4.0	1.801	−22.24°
6.0	1.692	−31.10°
10.0	1.407	−45.03°
20.0	0.893	−63.44°
40.0	0.485	−75.96°

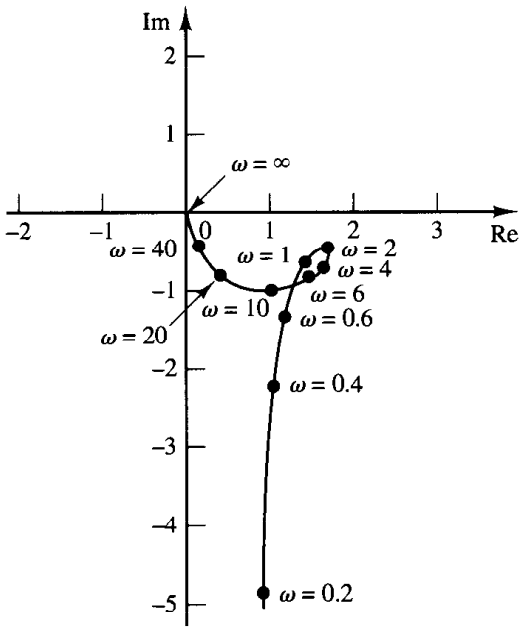

Figure 8–105
Polar plot of $G(j\omega)$ given in Problem A-8-8.

A-8-9. Consider the function

$$F(s) = \frac{s+1}{s-1}$$

The conformal mapping of the lines $\omega = 0, \pm 1, \pm 2$ and the lines $\sigma = 0, \pm 1, \pm 2$ yield circles in the $F(s)$ plane, as shown in Figure 8–106. Show that if the contour in the s plane encloses the pole of $F(s)$ there is one encirclement of the origin of the $F(s)$ plane in the counterclockwise direction. If the contour in the s plane encloses the zero of $F(s)$, there is one encirclement of the origin of the $F(s)$ plane in the clockwise direction. If the contour in the s plane encloses both the zero and pole or if the contour encloses neither the zero nor pole, then there is no encirclement of the origin of the $F(s)$ plane by the locus of $F(s)$. (Note that in the s plane a representative point s traces out a contour in the clockwise direction.)

Solution. A graphical solution is given in Figure 8–107; this shows closed contours in the s plane and their corresponding closed curves in the $F(s)$ plane.

A-8-10. Prove the following mapping theorem: Let $F(s)$ be a ratio of polynomials in s. Let P be the number of poles and Z be the number of zeros of $F(s)$ that lie inside a closed contour in the s plane, multiplicity accounted for. Let the closed contour be such that it does not pass through any poles or zeros of $F(s)$. The closed contour in the s plane then maps into the $F(s)$ plane as a closed curve. The number N of clockwise encirclements of the origin of the $F(s)$ plane, as a representative point s traces out the entire contour in the s plane in the clockwise direction, is equal to Z–P.

Solution. To prove this theorem, we use Cauchy's theorem and the residue theorem. Cauchy's theorem states that the integral of $F(s)$ around a closed contour in the s plane is zero if $F(s)$ is analytic within and on the closed contour, or

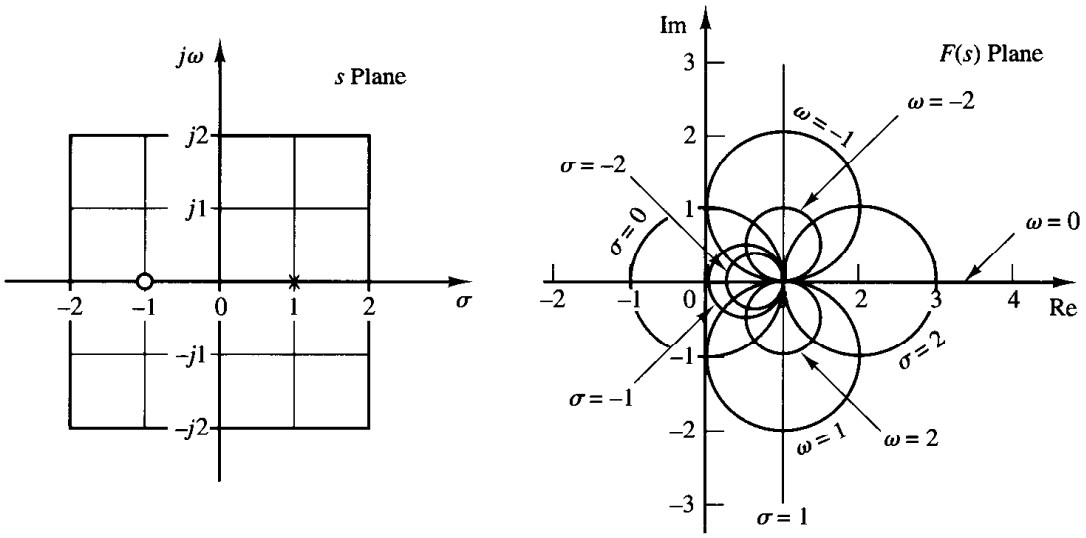

Figure 8–106
Conformal mapping of the s-plane grids into the $F(s)$ plane, where $F(s) = (s + 1)/(s - 1)$.

$$\oint F(s)\, ds = 0$$

Suppose that $F(s)$ is given by

$$F(s) = \frac{(s + z_1)^{k_1}(s + z_2)^{k_2} \cdots}{(s + p_1)^{m_1}(s + p_2)^{m_2} \cdots} X(s)$$

where $X(s)$ is analytic in the closed contour in the s plane and all the poles and zeros are located in the contour. Then the ratio $F'(s)/F(s)$ can be written

$$\frac{F'(s)}{F(s)} = \left(\frac{k_1}{s + z_1} + \frac{k_2}{s + z_2} + \cdots\right) - \left(\frac{m_1}{s + p_1} + \frac{m_2}{s + p_2} + \cdots\right) + \frac{X'(s)}{X(s)} \tag{8–19}$$

This may be seen from the following consideration: If $F(s)$ is given by

$$F(s) = (s + z_1)^k X(s)$$

then $F(s)$ has a zero of kth order at $s = -z_1$. Differentiating $F(s)$ with respect to s yields.

$$F'(s) = k(s + z_1)^{k-1} X(s) + (s + z_1)^k X'(s)$$

Hence,

$$\frac{F'(s)}{F(s)} = \frac{k}{s + z_1} + \frac{X'(s)}{X(s)} \tag{8–20}$$

We see that by taking the ratio $F'(s)/F(s)$ the kth-order zero of $F(s)$ becomes a simple pole of $F'(s)/F(s)$.

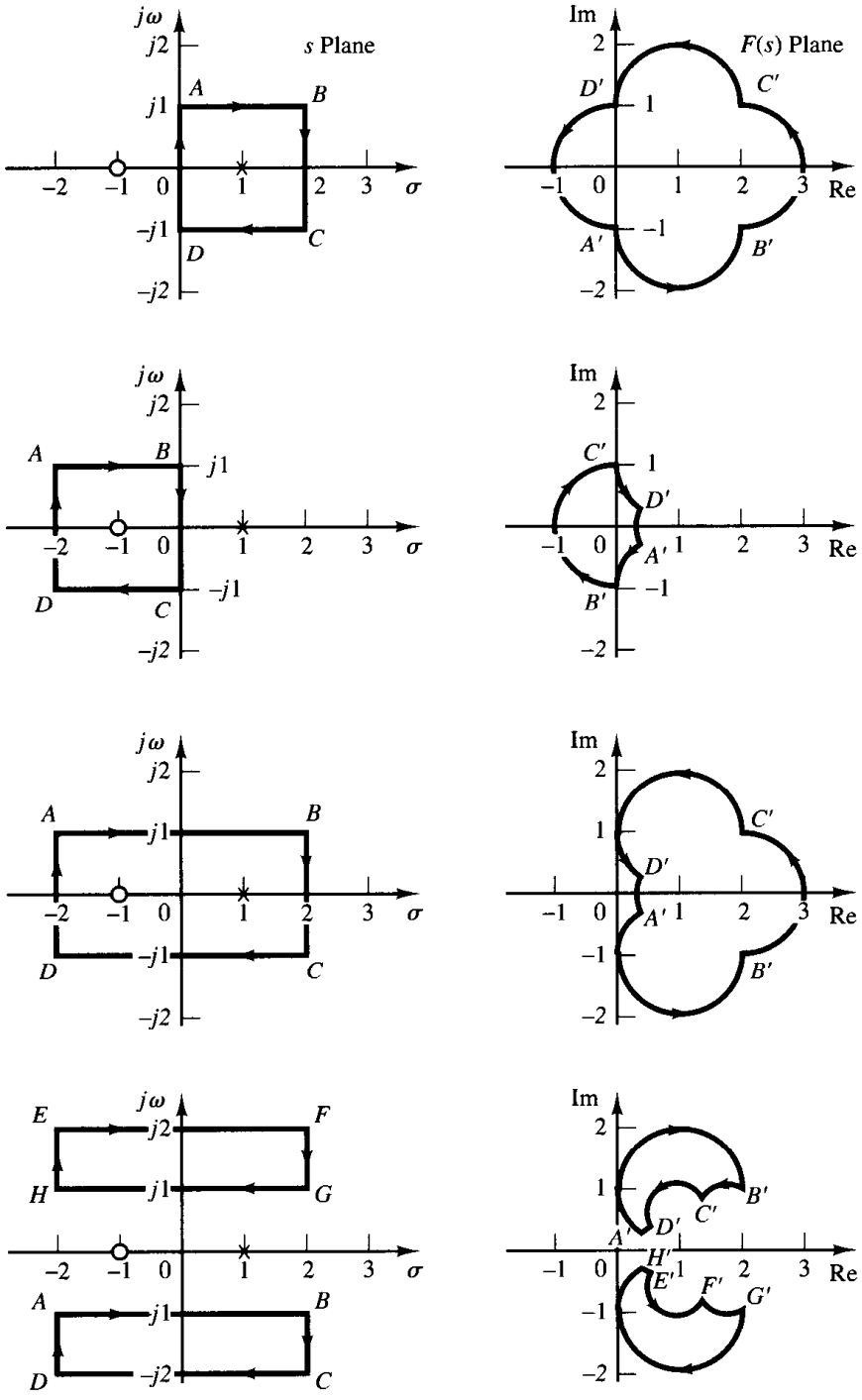

Figure 8–107
Conformal mapping of the s-plane contours into the $F(s)$ plane where $F(s) = (s + 1)/(s - 1)$.

If the last term on the right-hand side of Equation (8–20) does not contain any poles or zeros in the closed contour in the s plane, $F'(s)/F(s)$ is analytic in this contour except at the zero $s = -z_1$. Then, referring to Equation (8–19) and using the residue theorem, which states that the integral of $F'(s)/F(s)$ taken in the clockwise direction around a closed contour in the s plane is equal to $-2\pi j$ times the residues at the simple poles of $F'(s)/F(s)$, or

$$\oint \frac{F'(s)}{F(s)}\,ds = -2\pi j(\Sigma \text{ residues})$$

we have

$$\oint \frac{F'(s)}{F(s)}\,ds = -2\pi j[(k_1 + k_2 + \cdots) - (m_1 + m_2 + \cdots)] = -2\pi j(Z - P)$$

where $Z = k_1 + k_2 + \cdots$ = total number of zeros of $F(s)$ enclosed in the closed contour in the s plane

$P = m_1 + m_2 + \cdots$ = total number of poles of $F(s)$ enclosed in the closed contour in the s plane

[The k multiple zeros (or poles) are considered k zeros (or poles) located at the same point.] Since $F(s)$ is a complex quantity, $F(s)$ can be written

$$F(s) = |F|e^{j\theta}$$

and

$$\ln F(s) = \ln|F| + j\theta$$

Noting that $F'(s)/F(s)$ can be written

$$\frac{F'(s)}{F(s)} = \frac{d \ln F(s)}{ds}$$

we obtain

$$\frac{F'(s)}{F(s)} = \frac{d \ln |F|}{ds} + j\frac{d\theta}{ds}$$

If the closed contour in the s plane is mapped into the closed contour Γ in the $F(s)$ plane, then

$$\oint \frac{F'(s)}{F(s)}\,ds = \oint_\Gamma d \ln|F| + j\oint_\Gamma d\theta = j\int d\theta = 2\pi j(P - Z)$$

The integral $\oint_\Gamma d \ln|F|$ is zero since the magnitude $\ln|F|$ is the same at the initial point and the final point of the contour Γ. Thus we obtain

$$\frac{\theta_2 - \theta_1}{2\pi} = P - Z$$

The angular difference between the final and initial values of θ is equal to the total change in the phase angle of $F'(s)/F(s)$ as a representative point in the s plane moves along the closed contour. Noting that N is the number of clockwise encirclements of the origin of the $F(s)$ plane and $\theta_2 - \theta_1$ is zero or a multiple of 2π rad, we obtain

$$\frac{\theta_2 - \theta_1}{2\pi} = -N$$

Thus, we have the relationship

$$N = Z - P$$

This proves the theorem.

Note that by this mapping theorem the exact numbers of zeros and of poles cannot be found, only their difference. Note also that from Figures 8–108 (a) and (b) we see that, if θ does not change through 2π rad, then the origin of the $F(s)$ plane cannot be encircled.

A-8-11. The Nyquist plot (polar plot) of the open-loop frequency response of a unity-feedback control system is shown in Figure 8–109. Assuming that the Nyquist path in the s plane encloses the entire right-half s plane, draw a complete Nyquist plot in the G plane. Then answer the following questions:

(a) If the open-loop transfer function has no poles in the right-half s plane, is the closed-loop system stable?

(b) If the open-loop transfer function has one pole and no zeros in right-half s plane, is the closed-loop system stable?
(c) If the open-loop transfer function has one zero and no poles in the right-half s plane, is the closed-loop system stable?

Solution. Figure 8–110 shows a complete Nyquist plot in the G plane. The answers to the three questions are as follows:

(a) The closed-loop system is stable, because the critical point $(-1 + j0)$ is not encircled by the Nyquist plot. That is, since $P = 0$ and $N = 0$, we have $Z = N + P = 0$.
(b) The open-loop transfer function has one pole in the right-half s plane. Hence, $P = 1$. (The open-loop system is unstable.) For the closed-loop system to be stable, the Nyquist plot must encircle the critical point $(-1 + j0)$ once counterclockwise. However, the Nyquist plot does not encircle the critical point. Hence, $N = 0$. Therefore, $Z = N + P = 1$. The closed-loop system is unstable.
(c) Since the open-loop transfer function has one zero but no poles in the right-half s plane, we have $Z = N + P = 0$. Thus, the closed-loop system is stable. (Note that the zeros of the open-loop transfer function do not affect the stability of the closed-loop system.)

A-8-12. Is a closed-loop system with the following open-loop transfer function and with $K = 2$ stable?

$$G(s)H(s) = \frac{K}{s(s + 1)(2s + 1)}$$

Find the critical value of the gain K for stability.

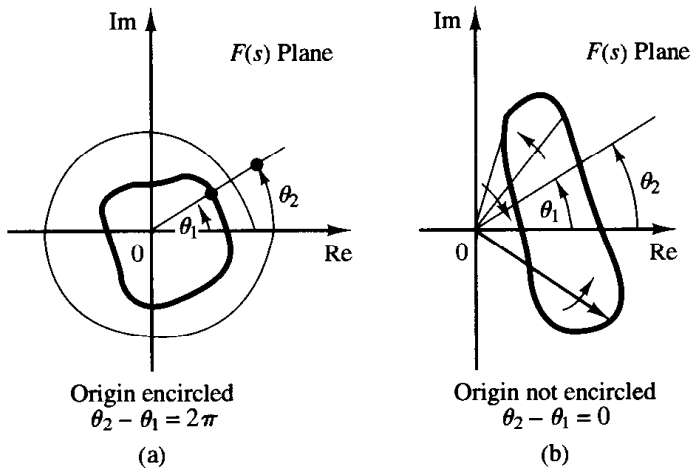

Figure 8–108
Determination of encirclement of the origin of $F(s)$ plane.

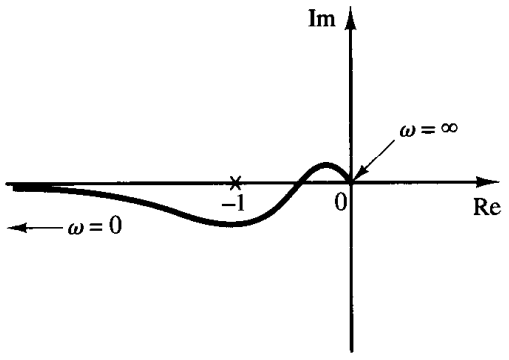

Figure 8–109
Nyquist plot.

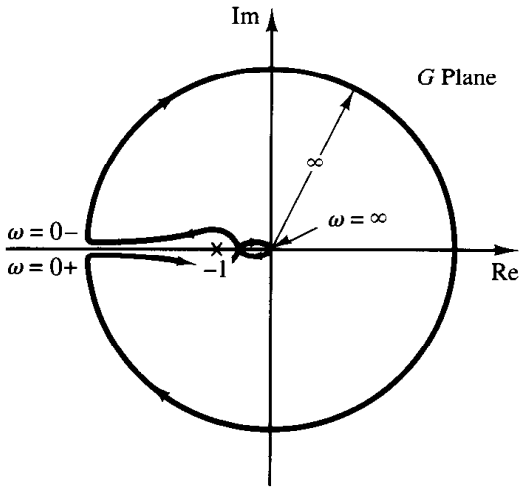

Figure 8–110
Complete Nyquist plot in the G plane.

Solution. The open-loop transfer function is

$$G(j\omega)H(j\omega) = \frac{K}{j\omega(j\omega + 1)(2j\omega + 1)}$$
$$= \frac{K}{-3\omega^2 + j\omega(1 - 2\omega^2)}$$

This open-loop transfer function has no poles in the right-half s plane. Thus, for stability the $-1 + j0$ point should not be encircled by the Nyquist plot. Let us find the point where the Nyquist plot crosses the negative real axis. Let the imaginary part of $G(j\omega)H(j\omega)$ be zero, or

$$1 - 2\omega^2 = 0$$

from which

$$\omega = \pm\frac{1}{\sqrt{2}}$$

Substituting $\omega = 1/\sqrt{2}$ into $G(j\omega)H(j\omega)$, we obtain

$$G\left(j\frac{1}{\sqrt{2}}\right)H\left(j\frac{1}{\sqrt{2}}\right) = -\frac{2K}{3}$$

The critical value of the gain K is obtained by equating $-2K/3$ to -1, or

$$-\frac{2}{3}K = -1$$

Hence,

$$K = \frac{3}{2}$$

The system is stable if $0 < K < \frac{3}{2}$. Hence, the system with $K = 2$ is unstable.

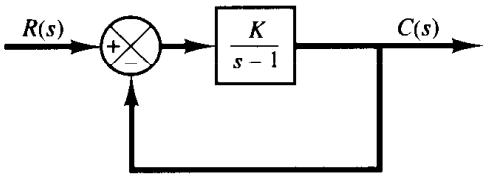

Figure 8–111
Closed-loop system.

A-8-13. Consider the closed-loop system shown in Figure 8–111. Determine the critical value of K for stability by use of the Nyquist stability criterion.

Solution. The polar plot of

$$G(j\omega) = \frac{K}{j\omega - 1}$$

is a circle with center at $-K/2$ on the negative real axis and radius $K/2$, as shown in Figure 8–112 (a). As ω is increased from $-\infty$ to ∞, the $G(j\omega)$ locus makes a counterclockwise rotation. In this system, $P = 1$ because there is one pole of $G(s)$ in the right-half s plane. For the closed-loop system to be stable, Z must be equal to zero. Therefore, $N = Z - P$ must be equal to -1, or there must be one counterclockwise encirclement of the $-1 + j0$ point for stability. (If there is no encirclement of the $-1 + j0$ point, the system is unstable.) Thus, for stability, K must be greater than unity, and $K = 1$ gives the stability limit. Figure 8–112(b) shows both stable and unstable cases of $G(j\omega)$ plots.

A-8-14. Consider a unity-feedback system whose open-loop transfer function is

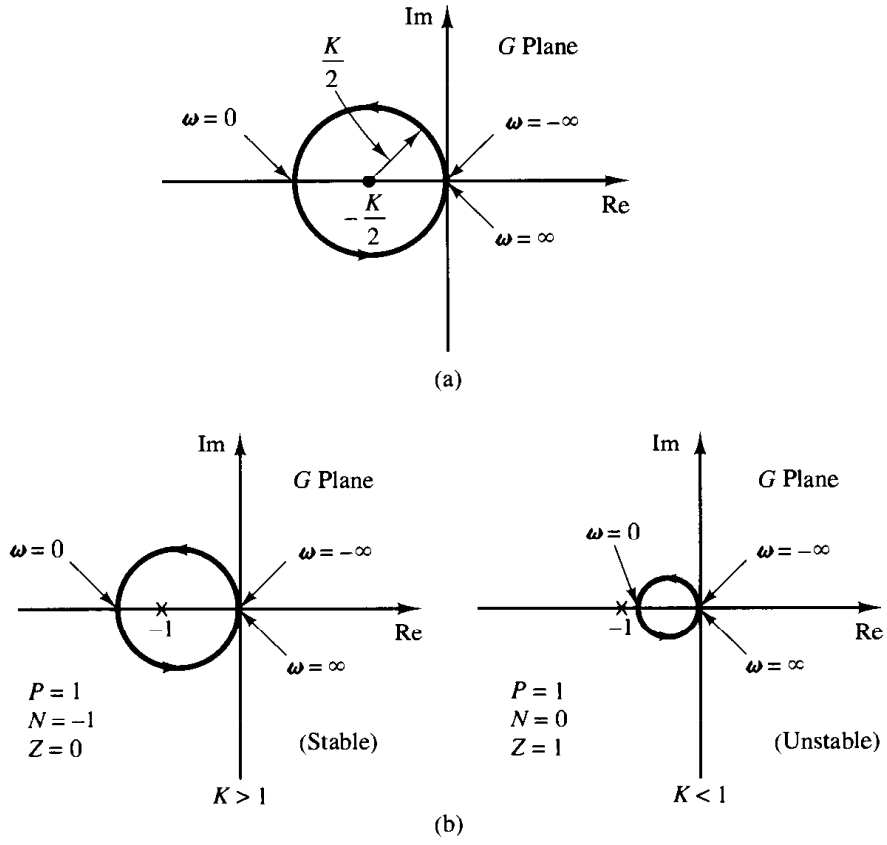

Figure 8–112
(a) Polar plot of $K/(j\omega - 1)$; (b) polar plots of $K/(j\omega - 1)$ for stable and unstable cases.

$$G(s) = \frac{Ke^{-0.8s}}{s + 1}$$

Using the Nyquist plot, determine the critical value of K for stability.

Solution. For this system,

$$G(j\omega) = \frac{Ke^{-0.8j\omega}}{j\omega + 1}$$

$$= \frac{K(\cos 0.8\omega - j \sin 0.8\omega)(1 - j\omega)}{1 + \omega^2}$$

$$= \frac{K}{1 + \omega^2}[(\cos 0.8\omega - \omega \sin 0.8\omega) - j(\sin 0.8\omega + \omega \cos 0.8\omega)]$$

The imaginary part of $G(j\omega)$ is equal to zero if

$$\sin 0.8\omega + \omega \cos 0.8\omega = 0$$

Hence,

$$\omega = -\tan 0.8\omega$$

Solving this equation for the smallest positive value of ω, we obtain

$$\omega = 2.4482$$

Substituting $\omega = 2.4482$ into $G(j\omega)$, we obtain

$$G(j2.4482) = \frac{K}{1 + 2.4482^2}(\cos 1.9586 - 2.4482 \sin 1.9586) = -0.378K$$

The critical value of K for stability is obtained by letting $G(j2.4482)$ equal -1. Hence,

$$0.378K = 1$$

or

$$K = 2.65$$

Figure 8–113 shows the Nyquist or polar plots of $2.65e^{-0.8j\omega}/(1 + j\omega)$ and $2.65/(1 + j\omega)$. The first-order system without transport lag is stable for all values of K, but the one with transport lag of 0.8 sec becomes unstable for $K > 2.65$.

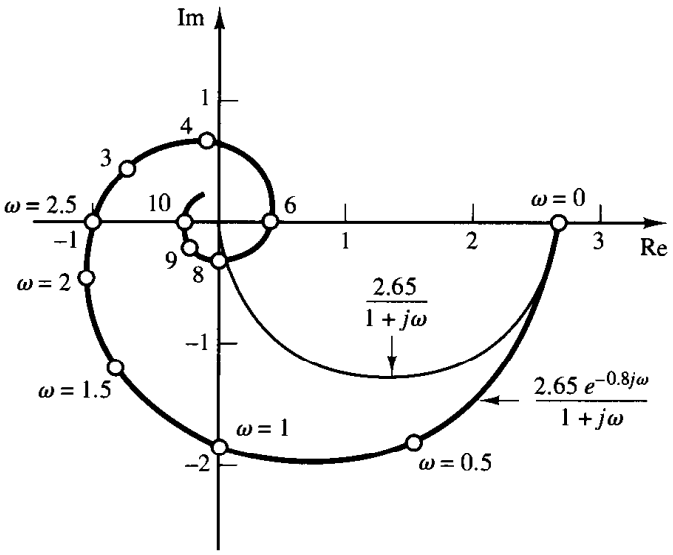

Figure 8–113
Polar plots of $2.65e^{-0.8j\omega}/(1 + j\omega)$ and $2.65/(1 + j\omega)$.

A-8-15. Consider a unity-feedback system with the following open-loop transfer function:

$$G(s) = \frac{20(s^2 + s + 0.5)}{s(s + 1)(s + 10)}$$

Draw a Nyquist plot with MATLAB and examine the stability of the closed-loop system.

Solution. We first enter MATLAB Program 8–17 into the computer. Because in this system MATLAB involves "Divide by zero" in the computation, the resulting Nyquist plot is erroneous, as shown in Figure 8–114.

MATLAB Program 8–17

```
num = [0   20   20   10];
den = [1   11   10   0];
nyquist(num,den)
```

This erroneous Nyquist plot can be corrected by entering the axis command, as shown in MATLAB Program 8–18. The resulting Nyquist plot is shown in Figure 8–115.

MATLAB Program 8–18

```
num = [0   20   20   10];
den = [1   11   10   0];
nyquist(num,d.en)
v = [−2   3   −3   3]; axis(v)
grid
title('Nyquist Plot of G(s) = 20(s^2 + s + 0.5)/[s(s + 1)(s + 10)]')
```

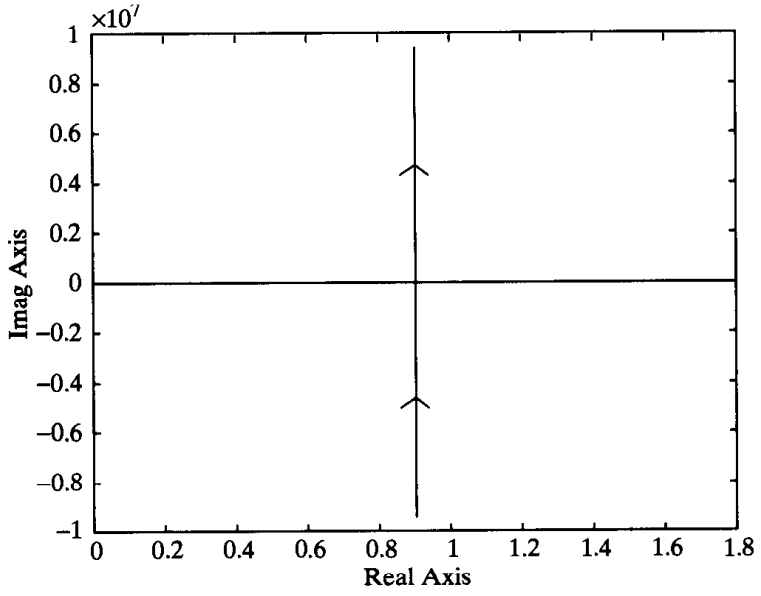

Figure 8–114
Erroneous Nyquist plot.

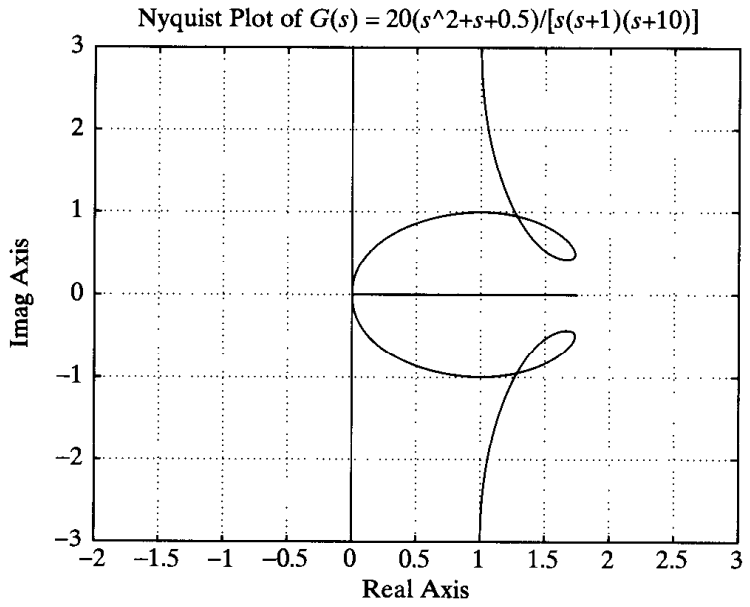

Figure 8–115
Nyquist plot of $G(s) = \dfrac{20(s^2 + s + 0.5)}{s(s + 1)(s + 10)}$.

Since no open-loop poles lie in the right-half s plane, $P = 0$ in the Nyquist stability criterion. From Figure 8–115 we see that the Nyquist plot does not encircle the $-1 + j0$ point. Hence, the closed-loop system is stable.

A-8-16. Consider the same system as discussed in Problem A-8-15. Draw the Nyquist plot for only the positive frequency region.

Solution. Drawing a Nyquist plot for only the positive frequency region can be done by use of the following command:

```
[re,im,w] = nyquist(num,den,w)
```

The frequency region may be divided into several subregions using different increments. For example, the frequency region of interest may be divided into three subregions as follows:

```
w1 = 0.1:0.1:10;
w2 = 10:2:100;
w3 = 100:10:500;
 w = [w1  w2  w3]
```

MATLAB Program 8–19 uses this frequency region. Using this program, we obtain the Nyquist plot shown in Figure 8–116.

A-8-17. Consider a unity-feedback, positive-feedback system with the following open-loop transfer function:

$$G(s) = \frac{s^2 + 4s + 6}{s^2 + 5s + 4}$$

Draw a Nyquist plot.

Solution. The Nyquist plot of the positive-feedback system can be obtained by defining num and den as

```
num = [−1   −4   −6]
den = [1   5   4]
```

MATLAB Program 8–19

```
% ---------- Nyquist plot ----------

num = [0   20   20   10];
den = [1   11   10   0];
w1 = 0.1:0.1:10; w2 = 10:2:100; w3 =100:10:500;
w = [w1   w2   w3];
[re,im,w] = nyquist(num,den,w);
plot(re,im)
v = [−3   3   −5   1]; axis(v)
grid
title('Nyquist Plot of G(s) = 20(s^2 + s + 0.5)/[s(s + 1)(s + 10)]')
xlabel('Real Axis')
ylabel('Imag Axis')
```

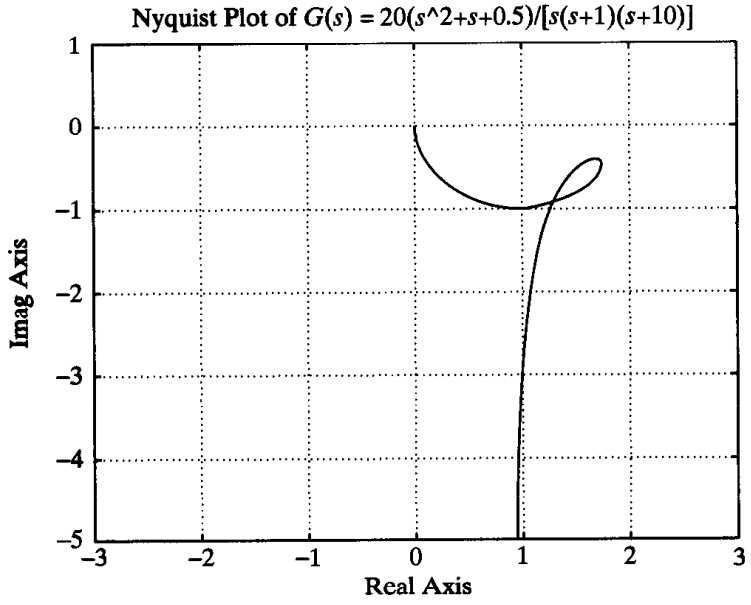

Figure 8–116
Nyquist plot for the positive frequency region.

and using the command nyquist(num,den). MATLAB Program 8–20 produces the Nyquist plot, as shown in Figure 8–117.

MATLAB Program 8–20

```
num = [−1   −4   −6];
den = [1   5   4];
nyquist(num,den);
grid
title('Nyquist Plot of G(s) = −(s^2 + 4s + 6)/(s^2 +5s + 4)')
```

This system is unstable because the $-1 + j0$ point is encircled once clockwise. Note that this is a special case where the Nyquist plot passes through $-1 + j0$ point and also encircles this point once clockwise. This means that the closed-loop system is degenerate; the system behaves as if it

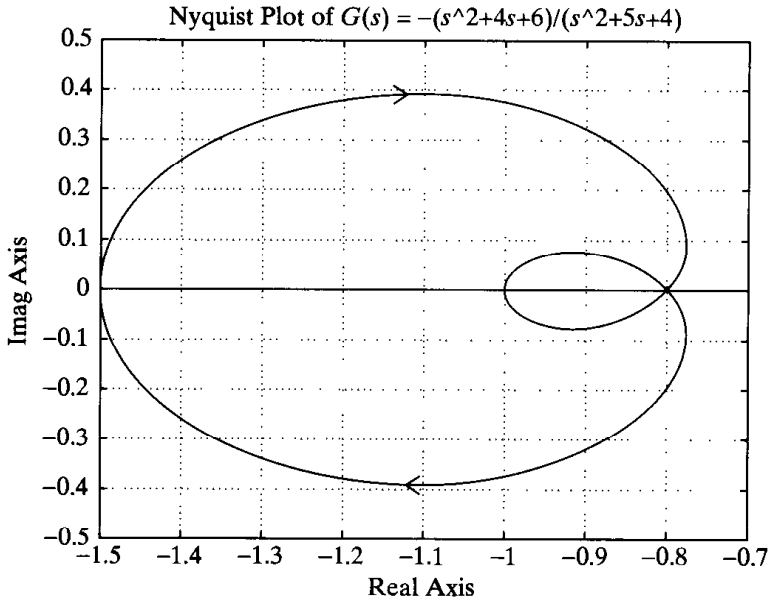

Figure 8–117
Nyquist plot for positive-feedback system.

is an unstable first-order system. See the following closed-loop transfer function of the positive-feedback system:

$$\frac{C(s)}{R(s)} = \frac{s^2 + 4s + 6}{s^2 + 5s + 4 - (s^2 + 4s + 6)}$$

$$= \frac{s^2 + 4s + 6}{s - 2}$$

Note that the Nyquist plot for the positive-feedback case is a mirror image about the imaginary axis of the Nyquist plot for the negative-feedback case. This may be seen from Figure 8–118, which was obtained by use of MATLAB Program 8–21.

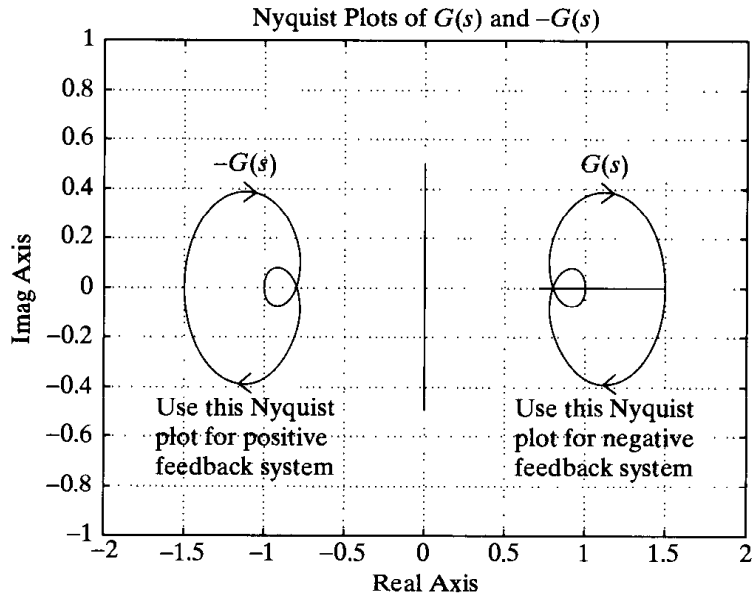

Figure 8–118
Nyquist plots for positive-feedback system and negative-feedback system.

MATLAB Program 8–21

```
num1 = [1   4   6];
den1 = [1   5   4];
num2 = [−1   −4   −6];
den2 = [1   5   4];
nyquist(num1,den1);
hold on
nyquist(num2,den2)
v = [−2   2   −1   1];
axis(v);
grid
title('Nyquist Plots of G(s) and −G(s)')
text(0.95,0.5,'G(s)')
text(0.57,−0.48,'Use this Nyquist')
text(0.57,−0.62,'plot for negative')
text(0.57,−0.73,'feedback system')
text(−1.3,0.5,'−G(s)')
text(−1.7,−0.48,'Use this Nyquist')
text(−1.7,−0.62,'plot for positive')
text(−1.7,−0.73,'feedback system')
```

A-8-18. Suppose that a system possesses at least one pair of complex-conjugate closed-loop poles. If the $-1 + j0$ point is found at the intersection of a constant-σ curve and a constant-ω curve in the $G(s)$ plane, then those particular values of σ and ω, which we define as $-\sigma_c$ and ω_c, respectively, characterize the closed-loop pole closest to the $j\omega$ axis in the upper-half s plane. (Note that $-\sigma_c$ represents the exponential decay and ω_c represents the damped natural frequency of the step transient-response term due to the pair of the closed-loop poles closest to the $j\omega$ axis.) Probable values of $-\sigma_c$ and ω_c may be estimated from the plot, as shown in Figure 8–119. Thus, the pair of complex-conjugate closed-loop poles that lies closest to the $j\omega$ axis can be determined graphically. It should be noted that all closed-loop poles are mapped into the $-1 + j0$ point in the $G(s)$ plane. Although the complex-conjugate closed-loop poles closest to the $j\omega$ axis can be found easily by this technique, finding other closed-loop poles, if any, by this technique is practically impossible.

If the data on $G(j\omega)$ are experimental, then a curvilinear square near the $-1 + j0$ point can be constructed by extrapolation. Referring to Figure 8–120, we can find the location of the dominant closed-loop poles in the s plane, or the damping ratio ζ and the damped natural frequency ω_d, by drawing the line AB that connects the $-1 + j0$ point (point A) and point B, the nearest approach to the $-1 + j0$ point, and then constructing a curvilinear square $CDEF$, as shown in

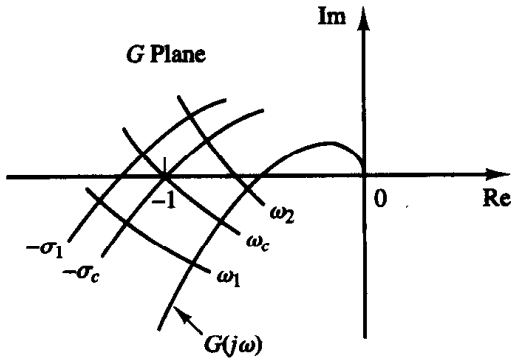

Figure 8–119
Estimation of $-\sigma_c$ and ω_c.

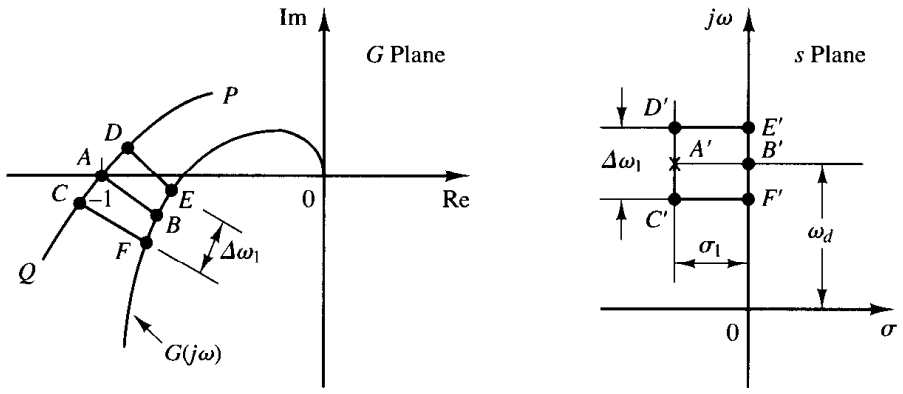

Figure 8–120
Conformal mapping of a curvilinear square near the $-1 + j0$ point in the $G(s)$ plane into the s plane.

Figure 8–120. This curvilinear square $CDEF$ may be constructed by drawing the most likely curve PQ (where PQ is the conformal mapping of a line parallel to the $j\omega$ axis in the s plane) passing through the $-1 + j0$ point and "parallel" to the $G(j\omega)$ locus, and adjusting the points C,D,E, and F such that $\widehat{FB} = \widehat{BE}$, $\widehat{CA} = \widehat{AD}$, and $\widehat{FE} + \widehat{CD} = \widehat{FC} + \widehat{ED}$. The corresponding s-plane contour $C'D'E'F'$, together with point A', the closed-loop pole closest to the $j\omega$ axis, is shown in Figure 8–120. The value of the frequency interval $\Delta\omega_1$ between points E and F is approximately equal to the value of σ_1 shown in Figure 8–120. The frequency at point B is approximately equal to the damped natural frequency ω_d. The closed-loop poles closest to the $j\omega$ axis are then estimated as

$$s = -\sigma_1 \pm j\omega_d$$

Then the damping ratio ζ of these closed-loop poles can be obtained from

$$\frac{\zeta}{\sqrt{1-\zeta^2}} = \frac{\sigma_1}{\omega_d} = \frac{\Delta\omega_1}{\omega_d}$$

It should be noted that the damped natural frequency ω_d of the step transient response actually is on the frequency contour that passes through the $-1 + j0$ point and is not necessarily the point of nearest approach to the $G(j\omega)$ locus. Therefore, the value ω_d obtained by the technique above is somewhat in error.

From our analysis, we may conclude that it is possible to estimate the closed-loop poles closest to the $j\omega$ axis from the closeness of approach of the $G(j\omega)$ locus to the $-1 + j0$ point, the frequency at the point of nearest approach, and the frequency graduation near this point.

Referring to the frequency-response plot of $G(j\omega)$ of a unity-feedback system, as shown in Figure 8–121, find the closed-loop poles closest to the $j\omega$ axis.

Solution. The line connecting the $-1 + j0$ point and the point of nearest approach of the $G(j\omega)$ locus to the $-1 + j0$ point is drawn first. Then the curvilinear square $ABCD$ is constructed. Since the frequency at the point of nearest approach is $\omega = 2.9$, the damped natural frequency is approximately 2.9, or $\omega_d = 2.9$. From the curvilinear square $ABCD$, it is found that

$$\Delta\omega = \omega_D - \omega_A = 3.4 - 2.4 = 1.0$$

The closed-loop poles closest to the $j\omega$ axis are then estimated as

$$s = -1 \pm j2.9$$

The $G(j\omega)$ locus shown in Figure 8–121 is actually a plot of the following open-loop transfer function:

$$G(s) = \frac{5(s + 20)}{s(s + 4.59)(s^2 + 3.41s + 16.35)}$$

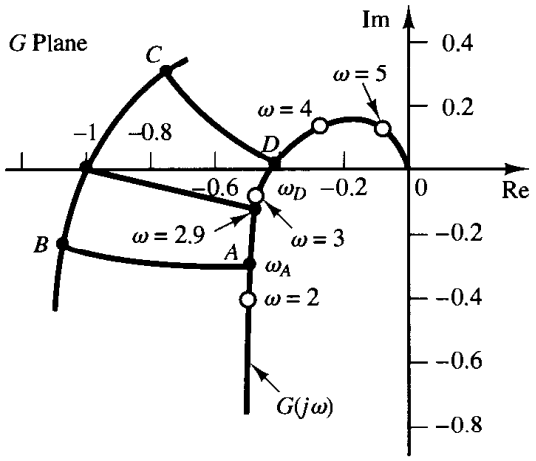

Figure 8–121
Polar plot and a curvilinear square.

The exact closed-loop poles of this system are $s = -1 \pm j3$ and $s = -3 \pm j1$. The closed loop poles closest to the $j\omega$ axis are $s = -1 \pm j3$. In this particular example, we see that the error involved is fairly small. In general, this error depends on a particular $G(j\omega)$ curve. The nearer the $G(j\omega)$ locus is to the $-1 + j0$ point, the smaller the error.

A-8-19. Figure 8–122 shows a block diagram of a space vehicle control system. Determine the gain K such that the phase margin is 50°. What is the gain margin in this case?

Solution. Since

$$G(j\omega) = \frac{K(j\omega + 2)}{(j\omega)^2}$$

we have

$$\underline{/G(j\omega)} = \underline{/j\omega + 2} - 2\underline{/j\omega} = \tan^{-1}\frac{\omega}{2} - 180°$$

The requirement that the phase margin be 50° means that $\underline{/G(j\omega_c)}$ must be equal to $-130°$, where ω_c is the gain crossover frequency, or

$$\underline{/G(j\omega_c)} = -130°$$

Hence, we set

$$\tan^{-1}\frac{\omega_c}{2} = 50°$$

from which we obtain

$$\omega_c = 2.3835 \text{ rad/sec}$$

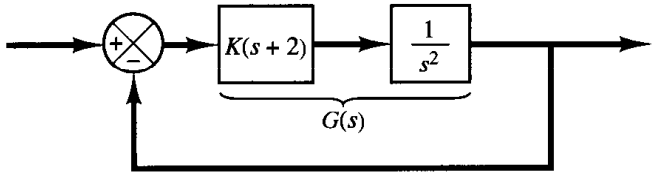

Figure 8–122
Space vehicle control system.

Since the phase curve never crosses the $-180°$ line, the gain margin is $+\infty$ dB. Noting that the magnitude of $G(j\omega)$ must be equal to 0 dB at $\omega = 2.3835$, we have

$$\left|\frac{K(j\omega + 2)}{(j\omega)^2}\right|_{\omega=2.3835} = 1$$

from which we get

$$K = \frac{2.3835^2}{\sqrt{2^2 + 2.3835^2}} = 1.8259$$

This K value will give the phase margin of 50°.

A-8-20. Draw a Bode diagram of the open-loop transfer function $G(s)$ of the closed-loop system shown in Figure 8–123. Determine the phase margin and gain margin.

Solution. Note that

$$G(j\omega) = \frac{20(j\omega + 1)}{j\omega(j\omega + 5)[(j\omega)^2 + 2j\omega + 10]}$$

$$= \frac{0.4(j\omega + 1)}{j\omega(0.2j\omega + 1)\left[\left(\frac{j\omega}{\sqrt{10}}\right)^2 + \frac{2}{10}j\omega + 1\right]}$$

The quadratic term in the denominator has the corner frequency of $\sqrt{10}$ rad/sec and the damping ratio ζ of 0.3162, or

$$\omega_n = \sqrt{10}, \qquad \zeta = 0.3162$$

The Bode diagram of $G(j\omega)$ is shown in Figure 8–124. From this diagram we find the phase margin to be 100° and the gain margin to be +13.3 dB.

A-8-21. For the standard second-order system

$$\frac{C(s)}{R(s)} = \frac{\omega_n^2}{s^2 + 2\zeta\omega_n s + \omega_n^2}$$

show that the bandwidth ω_b is given by

$$\omega_b = \omega_n(1 - 2\zeta^2 + \sqrt{4\zeta^4 - 4\zeta^2 + 2})^{1/2}$$

Note that ω_b/ω_n is a function only of ζ. Plot a curve ω_b/ω_n versus ζ.

Solution. The bandwidth ω_b is determined from $|C(j\omega_b)/R(j\omega_b)| = -3$ dB. Quite often, instead of -3 dB, we use -3.01 dB, which is equal to 0.707. Thus,

$$\left|\frac{C(j\omega_b)}{R(j\omega_b)}\right| = \left|\frac{\omega_n^2}{(j\omega_b)^2 + 2\zeta\omega_n(j\omega_b) + \omega_n^2}\right| = 0.707$$

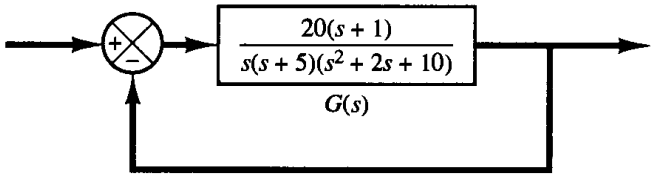

Figure 8–123
Closed-loop system.

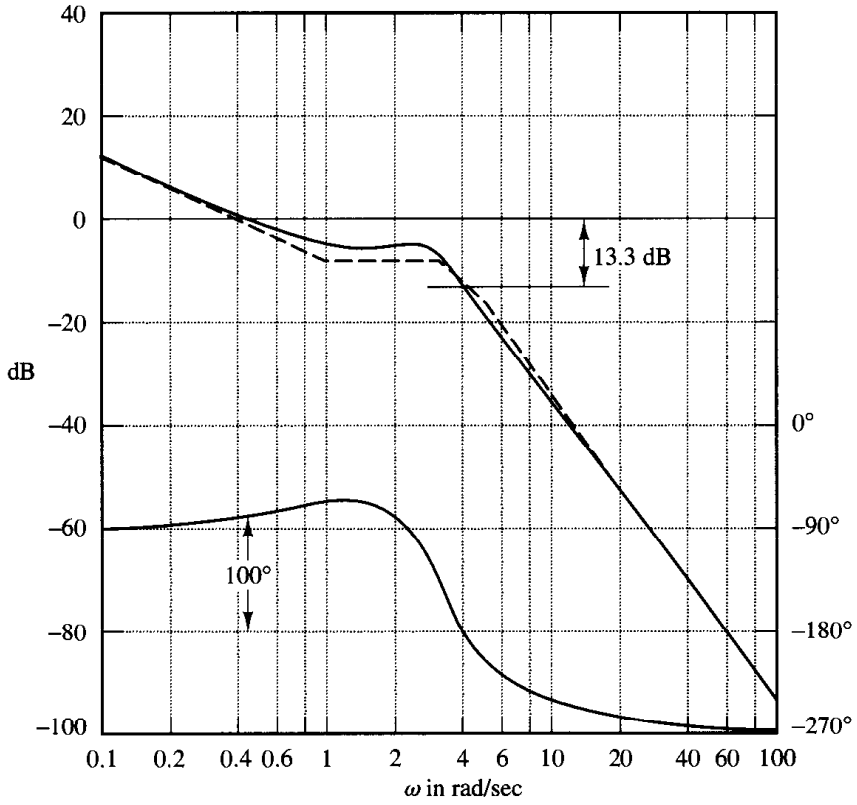

Figure 8–124
Bode diagram of $G(j\omega)$ of system shown in Figure 8–123.

Then

$$\frac{\omega_n^2}{\sqrt{(\omega_n^2 - \omega_b^2)^2 + (2\zeta\omega_n\omega_b)^2}} = 0.707$$

from which we get

$$\omega_n^4 = 0.5[(\omega_n^2 - \omega_b^2)^2 + 4\zeta^2\omega_n^2\omega_b^2]$$

By dividing both sides of this last equation by ω_n^4, we obtain

$$1 = 0.5\left\{\left[1 - \left(\frac{\omega_b}{\omega_n}\right)^2\right]^2 + 4\zeta^2\left(\frac{\omega_b}{\omega_n}\right)^2\right\}$$

Solving this last equation for $(\omega_b/\omega_n)^2$ yields

$$\left(\frac{\omega_b}{\omega_n}\right)^2 = -2\zeta^2 + 1 \pm \sqrt{4\zeta^4 - 4\zeta^2 + 2}$$

Since $(\omega_b/\omega_n)^2 > 0$, we take the plus sign in this last equation. Then

$$\omega_b^2 = \omega_n^2(1 - 2\zeta^2 + \sqrt{4\zeta^4 - 4\zeta^2 + 2})$$

or

$$\omega_b = \omega_n(1 - 2\zeta^2 + \sqrt{4\zeta^4 - 4\zeta^2 + 2})^{1/2}$$

Figure 8–125 shows a curve relating ω_b/ω_n versus ζ.

A-8-22. A unity-feedback control system has the following open-loop transfer function:

$$G(s) = \frac{K}{s(s + 1)(s + 2)}$$

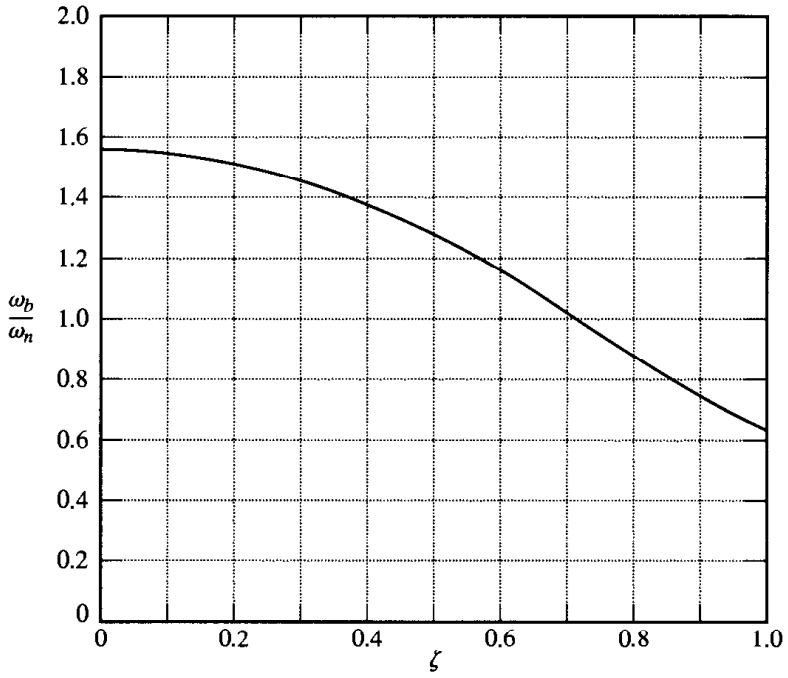

Figure 8–125
Curve ω_b/ω_n versus ζ, where ω_b is the bandwidth.

Consider the frequency response of this system. Plot a polar locus of $G(j\omega)/K$. Then determine the value of gain K such that the resonant peak magnitude M_r of the closed-loop frequency response is 2.

Solution. A plot of $G(j\omega)/K$ is shown in Figure 8–126. The value of angle ψ corresponding to $M_r = 2$ obtained from Equation (8–18) is

$$\psi = \sin^{-1}\frac{1}{2} = 30°$$

Hence, we draw the line $\overline{OP}$ that passes through the origin and makes an angle of 30° with the negative real axis as shown in Figure 8–126. We then draw the circle that is tangent to both the $G(j\omega)/K$ locus and line $\overline{OP}$. Define the point where the circle and line $\overline{OP}$ are tangent as point P. The perpendicular line drawn from point P intersects the negative real axis at $(-0.445,0)$. Then the gain K is determined as

$$K = \frac{1}{0.445} = 2.247$$

From Figure 8–126 we notice that the resonant frequency is approximately $\omega = 0.83$ rad/sec.

A-8-23. Figure 8–127 shows a block diagram of a chemical reactor system. Draw a Bode diagram of $G(j\omega)$. Also, draw the $G(j\omega)$ locus on the Nichols chart. From the Nichols diagram, read magnitudes and phase angles of the closed loop frequency response and then plot the Bode diagram of the closed-loop system, $G(j\omega)/[1 + G(j\omega)]$.

Solution. Noting that

$$G(s) = \frac{80e^{-0.1s}}{s(s + 4)(s + 10)} = \frac{2e^{-0.1s}}{s(0.25s + 1)(0.1s + 1)}$$

we have

$$G(j\omega) = \frac{2e^{-0.1j\omega}}{j\omega(0.25j\omega + 1)(0.1j\omega + 1)}$$

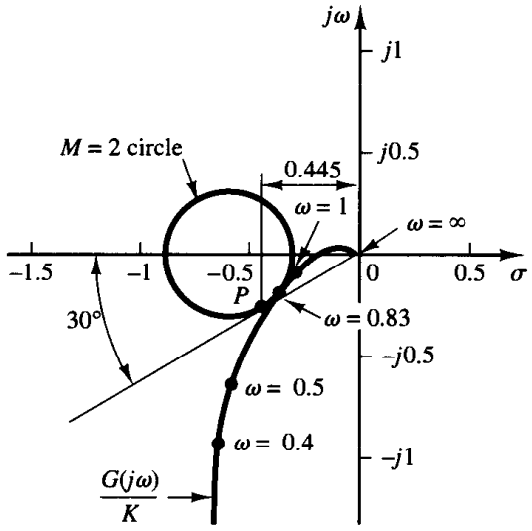

Figure 8–126
Plot of $G(j\omega)/K$ of the system considered in Problem A-8-22.

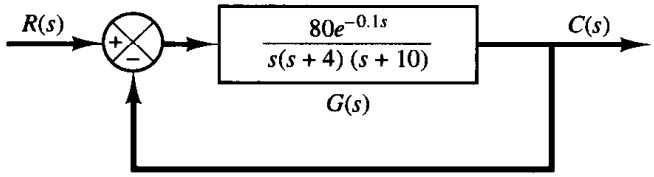

Figure 8–127
Block diagram of a chemical reactor system.

The phase angle of the transport lag $e^{-0.1j\omega}$ is

$$\angle e^{-0.1j\omega} = \angle \cos(0.1\omega) - j\sin(0.1\omega) = -0.1\omega \quad \text{(rad)}$$
$$= -5.73\omega \quad \text{(degrees)}$$

The Bode diagram of $G(j\omega)$ is shown in Figure 8–128.

Next, by reading magnitudes and phase angles of $G(j\omega)$ for various values of ω, it is possible to plot the gain versus phase plot on a Nichols chart. Figure 8–129 shows such a $G(j\omega)$ locus superimposed on the Nichols chart. From this diagram, magnitudes and phase angles of the closed-loop system at various frequency points can be read. Figure 8–130 depicts the Bode diagram of the closed-loop frequency response $G(j\omega)/[1 + G(j\omega)]$.

A-8-24. A Bode diagram of the open-loop transfer function $G(s)$ of a unity-feedback control system is shown in Figure 8–131. It is known that the open-loop transfer function is minimum phase. From the diagram it can be seen that there is a pair of complex-conjugate poles at $\omega = 2$ rad/sec. Determine the damping ratio of the quadratic term involving these complex-conjugate poles. Also, determine the transfer function $G(s)$.

Solution. Referring to Figure 8–8 and examining the Bode diagram of Figure 8–131, we find the damping ratio ζ and undamped natural frequency ω_n of the quadratic term to be

$$\zeta = 0.1, \qquad \omega_n = 2 \text{ rad/sec}$$

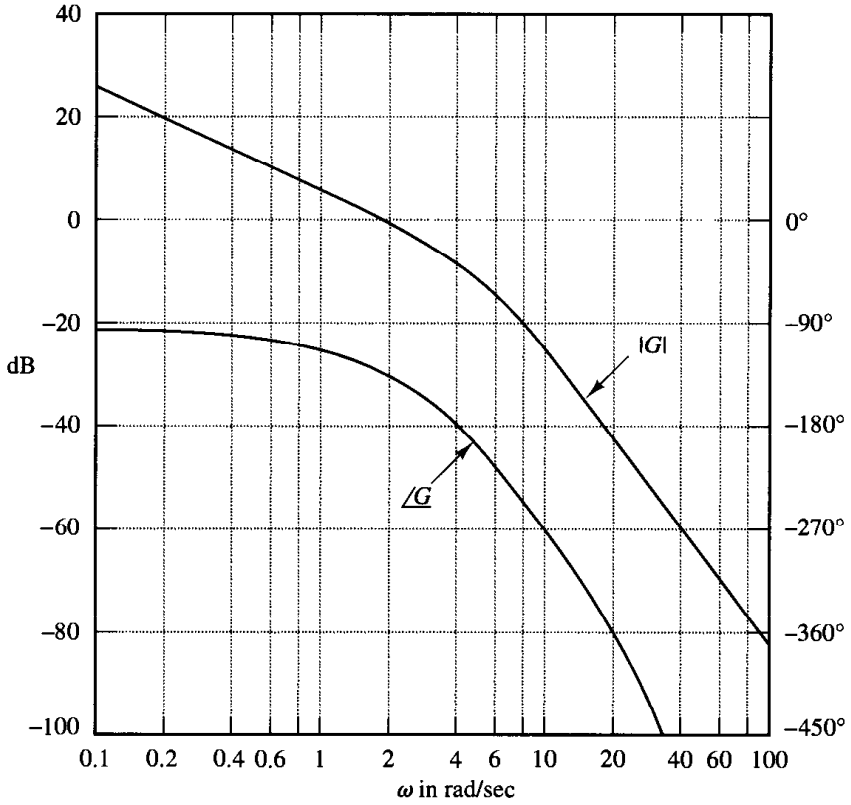

Figure 8–128
Bode diagram of $G(j\omega)$ of the system shown in Figure 8–127.

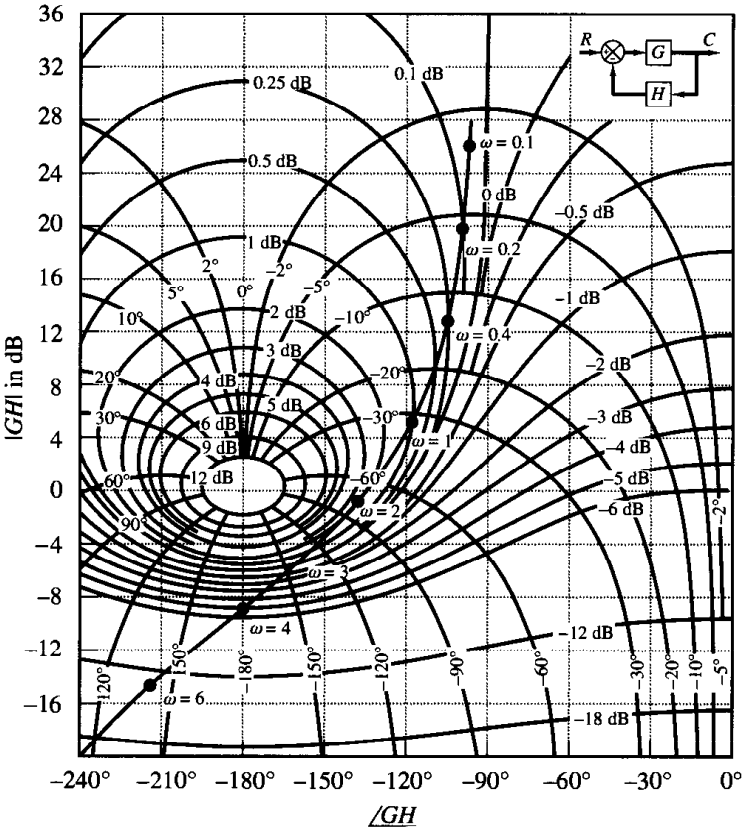

Figure 8–129
$G(j\omega)$ locus superimposed on Nichols chart (Problem A-8-23).

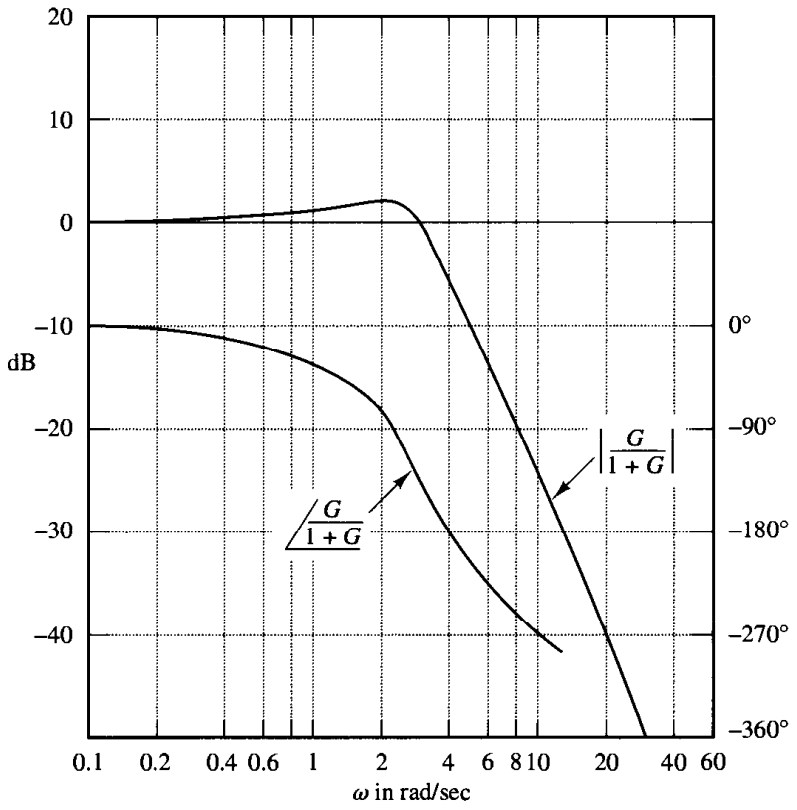

Figure 8–130
Bode diagram of the closed-loop frequency response (Problem A-8-23).

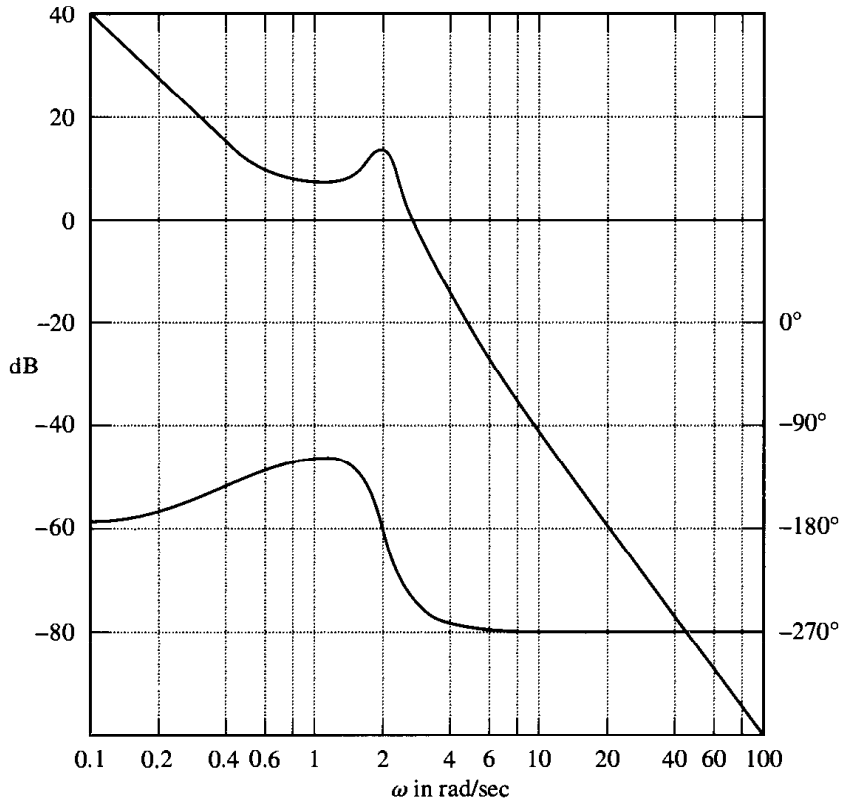

Figure 8–131
Bode diagram of the open-loop transfer function of a unity-feedback control system.

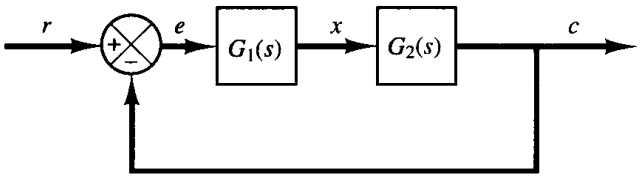

Figure 8–132
Control system.

Noting that there is another corner frequency at $\omega = 0.5$ rad/sec and the slope of the magnitude curve in the low-frequency region is -40 dB/decade, $G(j\omega)$ can be tentatively determined as follows:

$$G(j\omega) = \frac{K\left(\frac{j\omega}{0.5} + 1\right)}{(j\omega)^2\left[\left(\frac{j\omega}{2}\right)^2 + 0.1(j\omega) + 1\right]}$$

Since from Figure 8–131 we find $|G(j0.1)| = 40$ dB, the gain value K can be determined as unity. Also, the calculated phase curve, $\underline{/G(j\omega)}$ versus ω, agrees with the given phase curve. Hence, the transfer function $G(s)$ can be determined as

$$G(s) = \frac{4(2s + 1)}{s^2(s^2 + 0.4s + 4)}$$

A-8-25. A closed-loop control system may include an unstable element within the loop. When the Nyquist stability criterion is to be applied to such a system, the frequency-response curves for the unstable element must be obtained.

How can we obtain experimentally the frequency-response curves for such an unstable element? Suggest a possible approach to the experimental determination of the frequency response of an unstable linear element.

Solution. One possible approach is to measure the frequency-response characteristics of the unstable element by using it as a part of a stable system.

Consider the system shown in Figure 8–132. Suppose that the element $G_1(s)$ is unstable. The complete system may be made stable by choosing a suitable linear element $G_2(s)$. We apply a sinusoidal signal at the input. At steady state, all signals in the loop will be sinusoidal. We measure the signals $e(t)$, the input to the unstable element, and $x(t)$, the output of the unstable element. By changing the frequency [and possibly the amplitude for the convenience of measuring $e(t)$ and $x(t)$] of the input sinusoid and repeating this process, it is possible to obtain the frequency response of the unstable linear element.

PROBLEMS

B-8-1. Consider the unity-feedback system with the open-loop transfer functions.

$$G(s) = \frac{10}{s + 1}$$

Obtain the steady-state output of the system when it is subjected to each of the following inputs:

(a) $r(t) = \sin(t + 30°)$
(b) $r(t) = 2\cos(2t - 45°)$
(c) $r(t) = \sin(t + 30°) - 2\cos(2t - 45°)$

B-8-2. Consider the system whose closed-loop transfer function is

$$\frac{C(s)}{R(s)} = \frac{K(T_2s + 1)}{T_1s + 1}$$

Obtain the steady-state output of the system when it is subjected to the input $r(t) = R\sin\omega t$.

B-8-3. Sketch the Bode diagrams of the following three transfer functions:

(a) $G(s) = \dfrac{T_1 s + 1}{T_2 s + 1} \qquad (T_1 > T_2 > 0)$

(b) $G(s) = \dfrac{T_1 s - 1}{T_2 s + 1} \qquad (T_1 > T_2 > 0)$

(c) $G(s) = \dfrac{-T_1 s + 1}{T_2 s + 1} \qquad (T_1 > T_2 > 0)$

B-8-4. Plot the Bode diagram of

$$G(s) = \frac{10(s^2 + 0.4s + 1)}{s(s^2 + 0.8s + 9)}$$

B-8-5. Given

$$G(s) = \frac{\omega_n^2}{s^2 + 2\zeta\omega_n s + \omega_n^2}$$

show that

$$|G(j\omega_n)| = \frac{1}{2\zeta}$$

B-8-6. Consider a unity-feedback control system with the following open-loop transfer function:

$$G(s) = \frac{s + 0.5}{s^3 + s^2 + 1}$$

This is a nonminimum-phase system. Two of the three open-loop poles are located in the right-half s plane as follows:

Open-loop poles at $s = -1.4656$

$s = 0.2328 + j0.7926$

$s = 0.2328 - j0.7926$

Plot the Bode diagram of $G(s)$ with MATLAB. Explain why the phase-angle curve starts from 0° and approaches +180°.

B-8-7. Sketch the polar plots of the open-loop transfer function

$$G(s)H(s) = \frac{K(T_a s + 1)(T_b s + 1)}{s^2(Ts + 1)}$$

for the following two cases:

(a) $T_a > T > 0, \quad T_b > T > 0$
(b) $T > T_a > 0, \quad T > T_b > 0$

B-8-8. The pole–zero configurations of complex functions $F_1(s)$ and $F_2(s)$ are shown in Figures 8–133 (a) and (b), respectively. Assume that the closed contours in the s plane are those shown in Figures 8–133 (a) and (b). Sketch qualitatively the corresponding closed contours in the $F_1(s)$ plane and $F_2(s)$ plane.

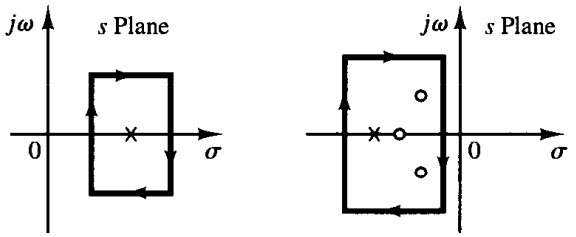

(a) (b)

Figure 8–133 (a) s-Plane representation of complex function $F_1(s)$ and a closed contour; (b) s-Plane representation of complex function $F_2(s)$ and a closed contour.

B-8-9. Draw a Nyquist locus for the unity feedback control system with the open loop transfer function

$$G(s) = \frac{K(1 - s)}{s + 1}$$

Using the Nyquist stability criterion, determine the stability of the closed loop system.

B-8-10. A system with the open-loop transfer function

$$G(s)H(s) = \frac{K}{s^2(T_1 s + 1)}$$

is inherently unstable. This system can be stabilized by adding derivative control. Sketch the polar plots for the open-loop transfer function with and without derivative control.

B-8-11. Consider the closed-loop system with the following open-loop transfer function:

$$G(s)H(s) = \frac{10K(s + 0.5)}{s^2(s + 2)(s + 10)}$$

Plot both the direct and inverse polar plots of $G(s)H(s)$ with $K = 1$ and $K = 10$. Apply the Nyquist stability criterion to the plots and determine the stability of the system with these values of K.

B-8-12. Consider the closed-loop system whose open-loop transfer function is

$$G(s)H(s) = \frac{Ke^{-2s}}{s}$$

Find the maximum value of K for which the system is stable.

B-8-13. Draw a Nyquist plot of the following $G(s)$:

$$G(s) = \frac{1}{s(s^2 + 0.8s + 1)}$$

B-8-14. Consider a unity-feedback control system with the following open-loop transfer function:

$$G(s) = \frac{1}{s^3 + 0.2s^2 + s + 1}$$

Draw a Nyquist plot of $G(s)$ and examine the stability of the system.

B-8-15. Consider a unity-feedback control system with the following open-loop transfer function:

$$G(s) = \frac{s^2 + 2s + 1}{s^3 + 0.2s^2 + s + 1}$$

Draw a Nyquist plot of $G(s)$ and examine the stability of the closed-loop system.

B-8-16. Consider the system defined by

$$\begin{bmatrix} \dot{x}_1 \\ \dot{x}_2 \end{bmatrix} = \begin{bmatrix} -1 & -1 \\ 6.5 & 0 \end{bmatrix} \begin{bmatrix} x_1 \\ x_2 \end{bmatrix} + \begin{bmatrix} 1 & 1 \\ 1 & 0 \end{bmatrix} \begin{bmatrix} u_1 \\ u_2 \end{bmatrix}$$

$$\begin{bmatrix} y_1 \\ y_2 \end{bmatrix} = \begin{bmatrix} 1 & 0 \\ 0 & 1 \end{bmatrix} \begin{bmatrix} x_1 \\ x_2 \end{bmatrix} + \begin{bmatrix} 0 & 0 \\ 0 & 0 \end{bmatrix} \begin{bmatrix} u_1 \\ u_2 \end{bmatrix}$$

There are four individual Nyquist plots involved in this system. Draw two Nyquist plots for the input u_1 in one diagram and two Nyquist plots for the input u_2 in another diagram. Write a MATLAB program to obtain these two diagrams.

B-8-17. Referring to Problem B-8-16, it is desired to plot only $Y_1(j\omega)/U_1(j\omega)$ for $\omega > 0$. Write a MATLAB program to produce such a plot.

If it is desired to plot $Y_1(j\omega)/U_1(j\omega)$ for $-\infty < \omega < \infty$, what changes must be made in the MATLAB program?

B-8-18. Consider the unity-feedback control system whose open-loop transfer function is

$$G(s) = \frac{as + 1}{s^2}$$

Determine the value of a so that the phase margin is 45°.

B-8-19. Consider the system shown in Figure 8–134. Draw a Bode diagram of the open-loop transfer function $G(s)$. Determine the phase margin and gain margin.

B-8-20. Consider the system shown in Figure 8–135. Draw a Bode diagram of the open-loop transfer function $G(s)$. Determine the phase margin and gain margin.

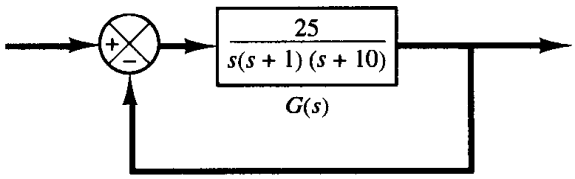

Figure 8–134 Control system.

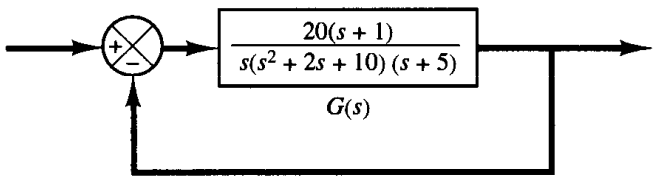

Figure 8–135 Control system.

B-8-21. Consider a unity-feedback control system with the open-loop transfer function

$$G(s) = \frac{K}{s(s^2 + s + 4)}$$

Determine the value of the gain K such that the phase margin is 50°. What is the gain margin with this gain K?

B-8-22. Consider the system shown in Figure 8–136. Draw a Bode diagram of the open-loop transfer function and determine the value of the gain K such that the phase margin is 50°. What is the gain margin of this system with this gain K?

B-8-23. Consider a unity-feedback control system whose open-loop transfer function is

$$G(s) = \frac{K}{s(s^2 + s + 0.5)}$$

Determine the value of the gain K such that the resonant peak magnitude in the frequency response is 2 dB, or $M_r = 2$ dB.

B-8-24. Figure 8–137 shows a block diagram of a process control system. Determine the range of gain K for stability.

B-8-25. Consider a closed-loop system whose open-loop transfer function is

$$G(s)H(s) = \frac{Ke^{-Ts}}{s(s + 1)}$$

Determine the maximum value of the gain K for stability as a function of dead time T.

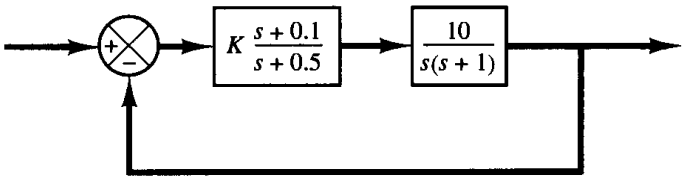

Figure 8–136 Control system.

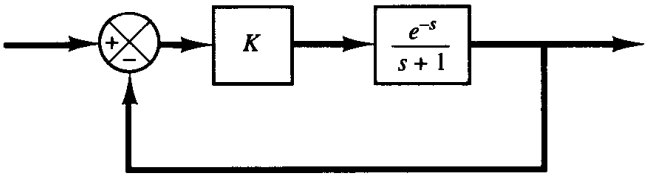

Figure 8–137 Process control system.

B-8-26. Sketch the polar plot of

$$G(s) = \frac{(Ts)^2 - 6(Ts) + 12}{(Ts)^2 + 6(Ts) + 12}$$

Show that, for the frequency range $0 < \omega T < 2\sqrt{3}$, this equation gives a good approximation to the transfer function of transport lag, e^{-Ts}.

B-8-27. Figure 8–138 shows a Bode diagram of a transfer function $G(s)$. Determine this transfer function.

B-8-28. The experimentally determined Bode diagram of a system $G(j\omega)$ is shown in Figure 8–139. Determine the transfer function $G(s)$.

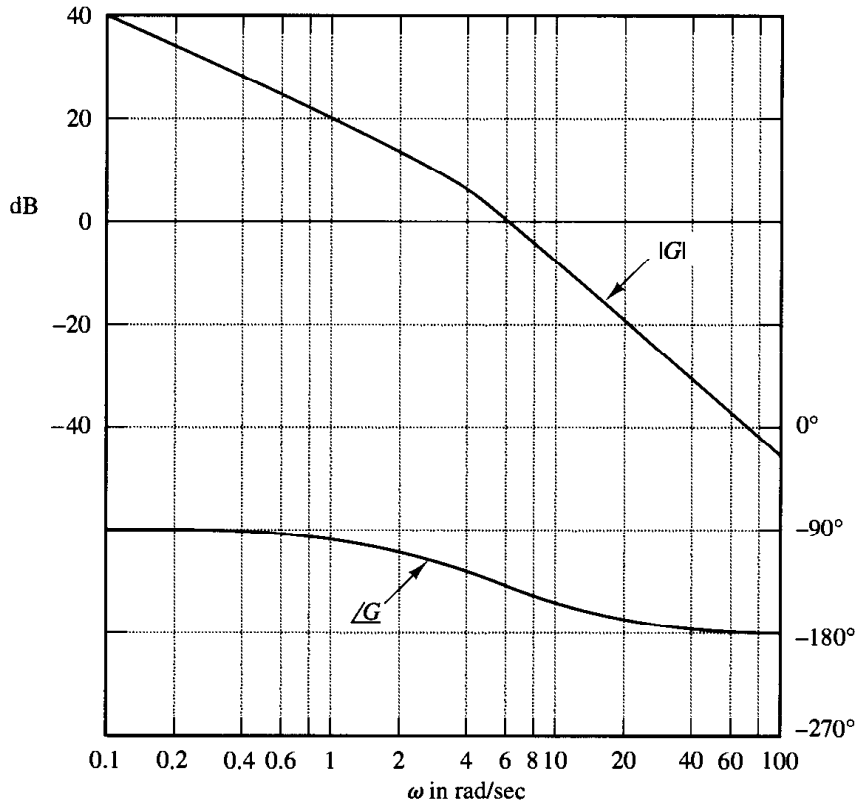

Figure 8–138 Bode diagram of a transfer function $G(s)$.

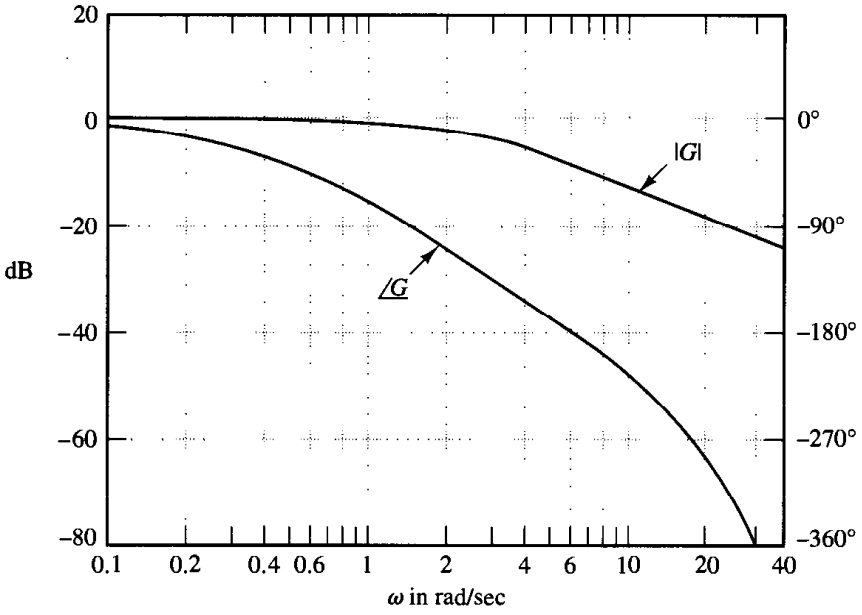

Figure 8–139 Experimentally determined Bode diagram of a system.

9

Control Systems Design by Frequency Response

9–1 INTRODUCTION

The primary objective of this chapter is to present procedures for the design and compensation of single-input–single-output, linear, time-invariant control systems by the frequency-response approach.

Frequency-response approach to control system design. It is important to note that in a control system design, transient-response performance is usually most important. In the frequency-response approach, we specify the transient-response performance in an indirect manner. That is, the transient-response performance is specified in terms of the phase margin, gain margin, resonant peak magnitude (they give a rough estimate of the system damping); the gain crossover frequency, resonant frequency, bandwidth (they give a rough estimate of the speed of transient response); and static error constants (they give the steady-state accuracy). Although the correlation between the transient response and frequency response is indirect, the frequency domain specifications can be conveniently met in the Bode diagram approach.

After the open loop has been designed by the frequency-response method, the closed-loop poles and zeros can be determined. The transient-response characteristics must be checked to see whether the designed system satisfies the requirements in the time domain. If it does not, then the compensator must be modified and the analysis repeated until a satisfactory result is obtained.

Design in the frequency domain is simple and straightforward. The frequency-response plot indicates clearly the manner in which the system should be modified,

although the exact quantitative prediction of the transient-response characteristics cannot be made. The frequency-response approach can be applied to systems or components whose dynamic characteristics are given in the form of frequency-response data. Note that because of difficulty in deriving the equations governing certain components, such as pneumatic and hydraulic components, the dynamic characteristics of such components are usually determined experimentally through frequency-response tests. The experimentally obtained frequency-response plots can be combined easily with other such plots when the Bode diagram approach is used. Note also that in dealing with high-frequency noises we find that the frequency-response approach is more convenient than other approaches.

There are basically two approaches in the frequency-domain design. One is the polar plot approach and the other is the Bode diagram approach. When a compensator is added, the polar plot does not retain the original shape, and, therefore, we need to draw a new polar plot, which will take time and is thus inconvenient. On the other hand, a Bode diagram of the compensator can be simply added to the original Bode diagram, and thus plotting the complete Bode diagram is a simple matter. Also, if the open-loop gain is varied, the magnitude curve is shifted up or down without changing the slope of the curve, and the phase curve remains the same. For design purposes, therefore, it is best to work with the Bode diagram.

A common approach to the Bode diagram is that we first adjust the open-loop gain so that the requirement on the steady-state accuracy is met. Then the magnitude and phase curves of the uncompensated open loop (with the open-loop gain just adjusted) is plotted. If the specifications on the phase margin and gain margin are not satisfied, then a suitable compensator that will reshape the open-loop transfer function is determined. Finally, if there are any other requirements to be met, we try to satisfy them, unless some of them are contradictory to each other.

Information obtainable from open-loop frequency response. The low-frequency region (the region far below the gain crossover frequency) of the locus indicates the steady-state behavior of the closed-loop system. The medium-frequency region (the region near the $-1 + j0$ point) of the locus indicates relative stability. The high-frequency region (the region far above the gain crossover frequency) indicates the complexity of the system.

Requirements on open-loop frequency response. We might say that, in many practical cases, compensation is essentially a compromise between steady-state accuracy and relative stability.

To have a high value of the velocity error constant and yet satisfactory relative stability, we find it necessary to reshape the open-loop frequency-response curve.

The gain in the low-frequency region should be large enough, and also, near the gain crossover frequency, the slope of the log-magnitude curve in the Bode diagram should be -20 dB/decade. This slope should extend over a sufficiently wide frequency band to assure a proper phase margin. For the high-frequency region, the gain should be attenuated as rapidly as possible to minimize the effects of noise.

Examples of generally desirable and undesirable open-loop and closed-loop frequency-response curves are shown in Figure 9–1.

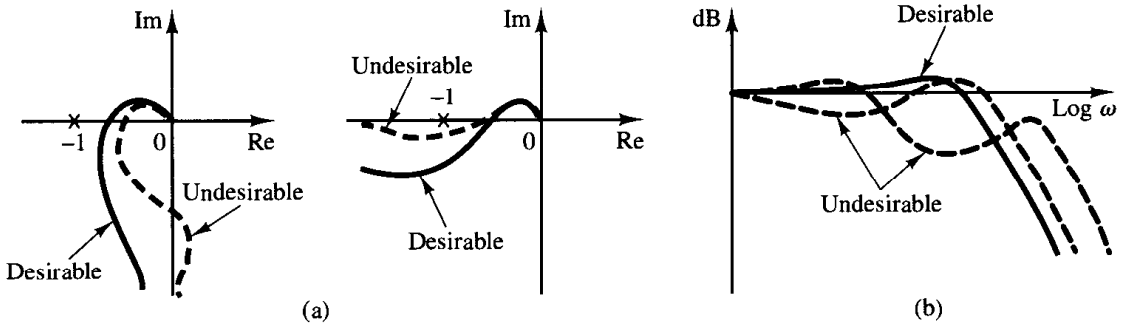

Figure 9–1
(a) Examples of desirable and undesirable open-loop frequency-response curves; (b) examples of desirable and undesirable closed-loop frequency-response curves.

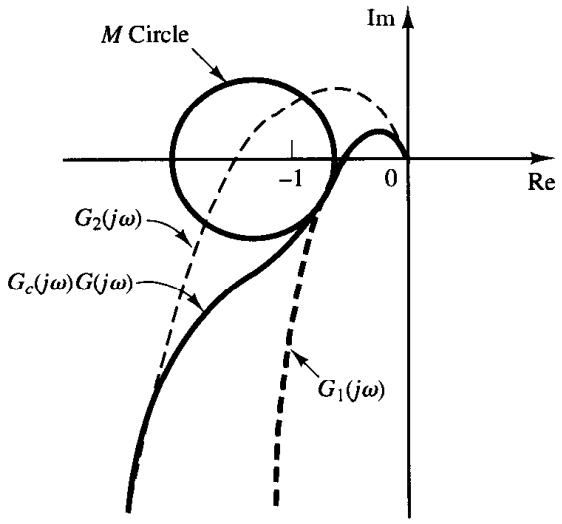

Figure 9–2
Reshaping of the open-loop frequency-response curve.

Referring to Figure 9–2, we see that the reshaping of the open-loop frequency-response curve may be done if the high-frequency portion of the locus follows the $G_1(j\omega)$ locus, while the low-frequency portion of the locus follows the $G_2(j\omega)$ locus. The reshaped locus $G_c(j\omega)G(j\omega)$ should have reasonable phase and gain margins or should be tangent to a proper M circle, as shown.

Basic characteristics of lead, lag, and lag–lead compensation. Lead compensation essentially yields an appreciable improvement in transient response and a small change in steady-state accuracy. It may accentuate high-frequency noise effects. Lag compensation, on the other hand, yields an appreciable improvement in steady-state accuracy at the expense of increasing the transient-response time. Lag compensation will suppress the effects of high-frequency noise signals. Lag–lead compensation combines the characteristics of both lead compensation and lag compensation. The use of a lead or lag compensator raises the order of the system by 1 (unless cancellation occurs between the zero of the compensator and a pole of the uncompensated open-loop transfer function). The use of a lag–lead compensator raises the order of the system by 2 [unless cancellation occurs between zero(s) of the lag–lead compensator and pole(s)

of the uncompensated open-loop transfer function], which means that the system becomes more complex and it is more difficult to control the transient response behavior. The particular situation determines the type of compensation to be used.

Outline of the chapter. Section 9–1 has presented introductory material. Section 9–2 discusses lead compensation by the Bode diagram approach and, Section 9–3 treats lag compensation by the Bode diagram approach. Section 9–4 discusses lag–lead compensation techniques based on the Bode diagram approach. Section 9–5 gives concluding comments on the frequency-response approach to the control systems design.

9–2 LEAD COMPENSATION

We shall first examine the frequency characteristics of the lead compensator. Then we present a design technique for the lead compensator by use of the Bode diagram.

Characteristics of lead compensators. Consider a lead compensator having the following transfer function:

$$K_c\alpha\frac{Ts+1}{\alpha Ts+1} = K_c\frac{s+\dfrac{1}{T}}{s+\dfrac{1}{\alpha T}} \qquad (0<\alpha<1)$$

It has a zero at $s = -1/T$ and a pole at $s = -1/(\alpha T)$. Since $0 < \alpha < 1$, we see that the zero is always located to the right of the pole in the complex plane. Note that for a small value of α the pole is located far to the left. The minimum value of α is limited by the physical construction of the lead compensator. The minimum value of α is usually taken to be about 0.05. (This means that the maximum phase lead that may be produced by a lead compensator is about 65°.)

Figure 9–3 shows the polar plot of

$$K_c\alpha\frac{j\omega T+1}{j\omega\alpha T+1} \qquad (0<\alpha<1)$$

with $K_c = 1$. For a given value of α, the angle between the positive real axis and the tangent line drawn from the origin to the semicircle gives the maximum phase lead angle,

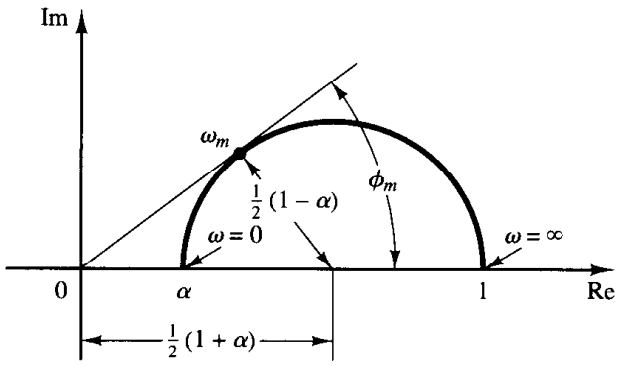

Figure 9–3
Polar plot of a lead compensator $\alpha(j\omega T + 1)/(j\omega\alpha T + 1)$, where $0 < \alpha < 1$.

ϕ_m. We shall call the frequency at the tangent point ω_m. From Figure 9–3 the phase angle at $\omega = \omega_m$ is ϕ_m, where

$$\sin \phi_m = \frac{\dfrac{1 - \alpha}{2}}{\dfrac{1 + \alpha}{2}} = \frac{1 - \alpha}{1 + \alpha} \tag{9–1}$$

Equation (9–1) relates the maximum phase lead angle and the value of α.

Figure 9–4 shows the Bode diagram of a lead compensator when $K_c = 1$ and $\alpha = 0.1$. The corner frequencies for the lead compensator are $\omega = 1/T$ and $\omega = 1/(\alpha T) = 10/T$. By examining Figure 9–4, we see that ω_m is the geometric mean of the two corner frequencies, or

$$\log \omega_m = \frac{1}{2}\left(\log \frac{1}{T} + \log \frac{1}{\alpha T}\right)$$

Hence,

$$\omega_m = \frac{1}{\sqrt{\alpha} T} \tag{9–2}$$

As seen from Figure 9–4, the lead compensator is basically a high-pass filter. (The high frequencies are passed, but low frequencies are attenuated.)

Lead compensation techniques based on the frequency-response approach. The primary function of the lead compensator is to reshape the frequency-response curve to provide sufficient phase-lead angle to offset the excessive phase lag associated with the components of the fixed system.

Consider the system shown in Figure 9–5. Assume that the performance specifications are given in terms of phase margin, gain margin, static velocity error constants, and so on. The procedure for designing a lead compensator by the frequency-response approach may be stated as follows:

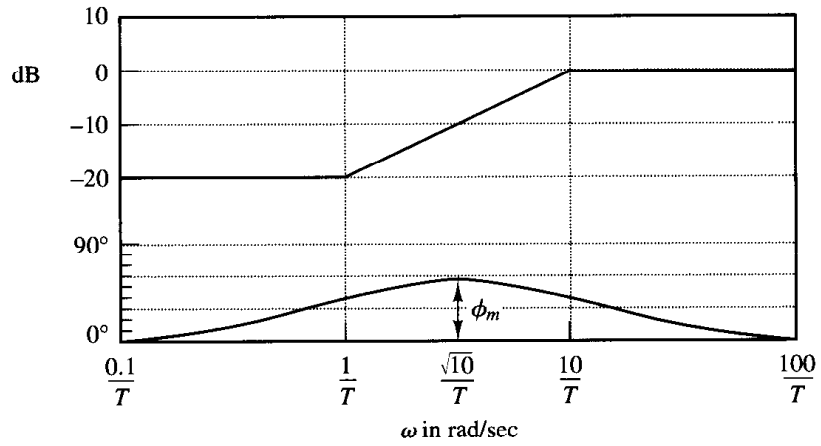

Figure 9–4
Bode diagram of a lead compensator $\alpha(j\omega T + 1)/(j\omega\alpha T + 1)$, where $\alpha = 0.1$.

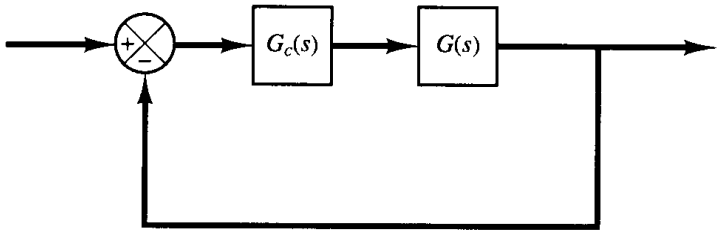

Figure 9–5
Control system.

1. Assume the following lead compensator:

$$G_c(s) = K_c\alpha\frac{Ts + 1}{\alpha Ts + 1} = K_c\frac{s + \dfrac{1}{T}}{s + \dfrac{1}{\alpha T}} \qquad (0 < \alpha < 1)$$

Define

$$K_c\alpha = K$$

Then

$$G_c(s) = K\frac{Ts + 1}{\alpha Ts + 1}$$

The open-loop transfer function of the compensated system is

$$G_c(s)G(s) = K\frac{Ts + 1}{\alpha Ts + 1}G(s) = \frac{Ts + 1}{\alpha Ts + 1}KG(s) = \frac{Ts + 1}{\alpha Ts + 1}G_1(s)$$

where

$$G_1(s) = KG(s)$$

Determine gain K to satisfy the requirement on the given static error constant.

2. Using the gain K thus determined, draw a Bode diagram of $G_1(j\omega)$, the gain-adjusted but uncompensated system. Evaluate the phase margin.

3. Determine the necessary phase lead angle ϕ to be added to the system.

4. Determine the attenuation factor α by use of Equation (9–1). Determine the frequency where the magnitude of the uncompensated system $G_1(j\omega)$ is equal to $-20 \log (1/\sqrt{\alpha})$. Select this frequency as the new gain crossover frequency. This frequency corresponds to $\omega_m = 1/(\sqrt{\alpha}T)$, and the maximum phase shift ϕ_m occurs at this frequency.

5. Determine the corner frequencies of the lead compensator as follows:

$$\text{Zero of lead compensator:} \qquad \omega = \frac{1}{T}$$

$$\text{Pole of lead compensator:} \qquad \omega = \frac{1}{\alpha T}$$

6. Using the value of K determined in step 1 and that of α determined in step 4, calculate constant K_c from

$$K_c = \frac{K}{\alpha}$$

7. Check the gain margin to be sure it is satisfactory. If not, repeat the design process by modifying the pole–zero location of the compensator until a satisfactory result is obtained.

EXAMPLE 9–1 Consider the system shown in Figure 9–6. The open-loop transfer function is

$$G(s) = \frac{4}{s(s + 2)}$$

It is desired to design a compensator for the system so that the static velocity error constant K_v is 20 $\sec^{-1}$, the phase margin is at least 50°, and the gain margin is at least 10 dB.

We shall use a lead compensator of the form

$$G_c(s) = K_c\alpha \frac{Ts + 1}{\alpha Ts + 1} = K_c \frac{s + \dfrac{1}{T}}{s + \dfrac{1}{\alpha T}}$$

The compensated system will have the open-loop transfer function $G_c(s)G(s)$.

Define

$$G_1(s) = KG(s) = \frac{4K}{s(s + 2)}$$

where $K = K_c\alpha$.

The first step in the design is to adjust the gain K to meet the steady-state performance specification or to provide the required static velocity error constant. Since this constant is given as 20 $\sec^{-1}$, we obtain

$$K_v = \lim_{s\to 0} sG_c(s)G(s) = \lim_{s\to 0} s \frac{Ts + 1}{\alpha Ts + 1} G_1(s) = \lim_{s\to 0} \frac{s4K}{s(s + 2)} = 2K = 20$$

or

$$K = 10$$

With $K = 10$, the compensated system will satisfy the steady-state requirement.

We shall next plot the Bode diagram of

$$G_1(j\omega) = \frac{40}{j\omega(j\omega + 2)} = \frac{20}{j\omega(0.5j\omega + 1)}$$

Figure 9–7 shows the magnitude and phase angle curves of $G_1(j\omega)$. From this plot, the phase and gain margins of the system are found to be 17° and $+\infty$ dB, respectively. (A phase margin of 17° implies that the system is quite oscillatory. Thus, satisfying the specification on the steady state

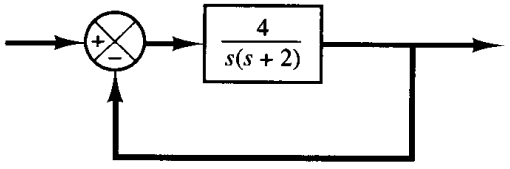

Figure 9–6
Control system.

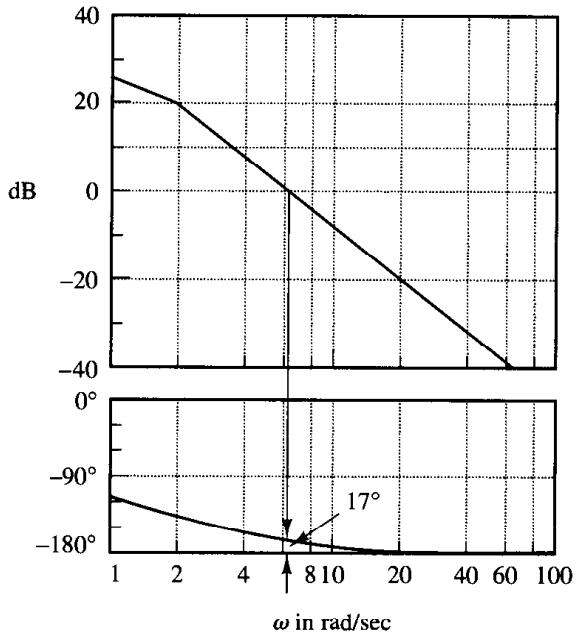

Figure 9–7
Bode diagram for $G_1(j\omega) = 10G(j\omega) = 40/[j\omega(j\omega + 2)]$

yields a poor transient-response performance.) The specification calls for a phase margin of at least 50°. We thus find the additional phase lead necessary to satisfy the relative stability requirement is 33°. To achieve a phase margin of 50° without decreasing the value of K, the lead compensator must contribute the required phase angle.

Noting that the addition of a lead compensator modifies the magnitude curve in the Bode diagram, we realize that the gain crossover frequency will be shifted to the right. We must offset the increased phase lag of $G_1(j\omega)$ due to this increase in the gain crossover frequency. Considering the shift of the gain crossover frequency, we may assume that ϕ_m, the maximum phase lead required, is approximately 38°. (This means that 5° has been added to compensate for the shift in the gain crossover frequency.)

Since

$$\sin \phi_m = \frac{1 - \alpha}{1 + \alpha}$$

$\phi_m = 38°$ corresponds to $\alpha = 0.24$. Once the attenuation factor α has been determined on the basis of the required phase lead angle, the next step is to determine the corner frequencies $\omega = 1/T$ and $\omega = 1/(\alpha T)$ of the lead compensator. To do so, we first note that the maximum phase lead angle ϕ_m occurs at the geometric mean of the two corner frequencies, or $\omega = 1/(\sqrt{\alpha}T)$. [See Equation (9–2).] The amount of the modification in the magnitude curve at $\omega = 1/(\sqrt{\alpha}T)$ due to the inclusion of the term $(Ts + 1)/(\alpha Ts + 1)$ is

$$\left|\frac{1 + j\omega T}{1 + j\omega\alpha T}\right|_{\omega = 1/(\sqrt{\alpha}T)} = \left|\frac{1 + j\dfrac{1}{\sqrt{\alpha}}}{1 + j\alpha\dfrac{1}{\sqrt{\alpha}}}\right| = \frac{1}{\sqrt{\alpha}}$$

Note that

$$\frac{1}{\sqrt{\alpha}} = \frac{1}{\sqrt{0.24}} = \frac{1}{0.49} = 6.2 \text{ dB}$$

and $|G_1(j\omega)| = -6.2$ dB corresponds to $\omega = 9$ rad/sec. We shall select this frequency to be the new gain crossover frequency ω_c. Noting that this frequency corresponds to $1/(\sqrt{\alpha}T)$, or $\omega_c = 1/(\sqrt{\alpha}T)$, we obtain

$$\frac{1}{T} = \sqrt{\alpha}\omega_c = 4.41$$

and

$$\frac{1}{\alpha T} = \frac{\omega_c}{\sqrt{\alpha}} = 18.4$$

The lead compensator thus determined is

$$G_c(s) = K_c \frac{s + 4.41}{s + 18.4} = K_c\alpha \frac{0.227s + 1}{0.054s + 1}$$

where the value of K_c is determined as

$$K_c = \frac{K}{\alpha} = \frac{10}{0.24} = 41.7$$

Thus, the transfer function of the compensator becomes

$$G_c(s) = 41.7 \frac{s + 4.41}{s + 18.4} = 10 \frac{0.227s + 1}{0.054s + 1}$$

Note that

$$\frac{G_c(s)}{K} G_1(s) = \frac{G_c(s)}{10} 10G(s) = G_c(s)G(s)$$

The magnitude curve and phase-angle curve for $G_c(j\omega)/10$ are shown in Figure 9–8. The compensated system has the following open-loop transfer function:

$$G_c(s)G(s) = 41.7 \frac{s + 4.41}{s + 18.4} \frac{4}{s(s + 2)}$$

The solid curves in Figure 9–8 show the magnitude curve and phase-angle curve for the compensated system. The lead compensator causes the gain crossover frequency to increase from 6.3 to 9 rad/sec. The increase in this frequency means an increase in bandwidth. This implies an increase in the speed of response. The phase and gain margins are seen to be approximately 50° and $+\infty$ dB, respectively. The compensated system shown in Figure 9–9 therefore meets both the steady-state and the relative-stability requirements.

Note that for type 1 systems, such as the system just considered, the value of the static velocity error constant K_v is merely the value of the frequency corresponding to the intersection of the extension of the initial -20-dB/decade slope line and the 0-dB line, as shown in Figure 9–8.

Figure 9–10 shows the polar plots of the uncompensated system $G_1(j\omega) = 10G(j\omega)$ and the compensated system $G_c(j\omega)G(j\omega)$. From Figure 9–10, we see that the resonant frequency of the uncompensated system is about 6 rad/sec and that of the compensated system is about 7 rad/sec. (This also indicates that the bandwidth has been increased.)

From Figure 9–10, we find that the value of the resonant peak M_r for the uncompensated system with $K = 10$ is 3. The value of M_r for the compensated system is found to be 1.29. This clearly shows that the compensated system has improved relative stability. (Note that

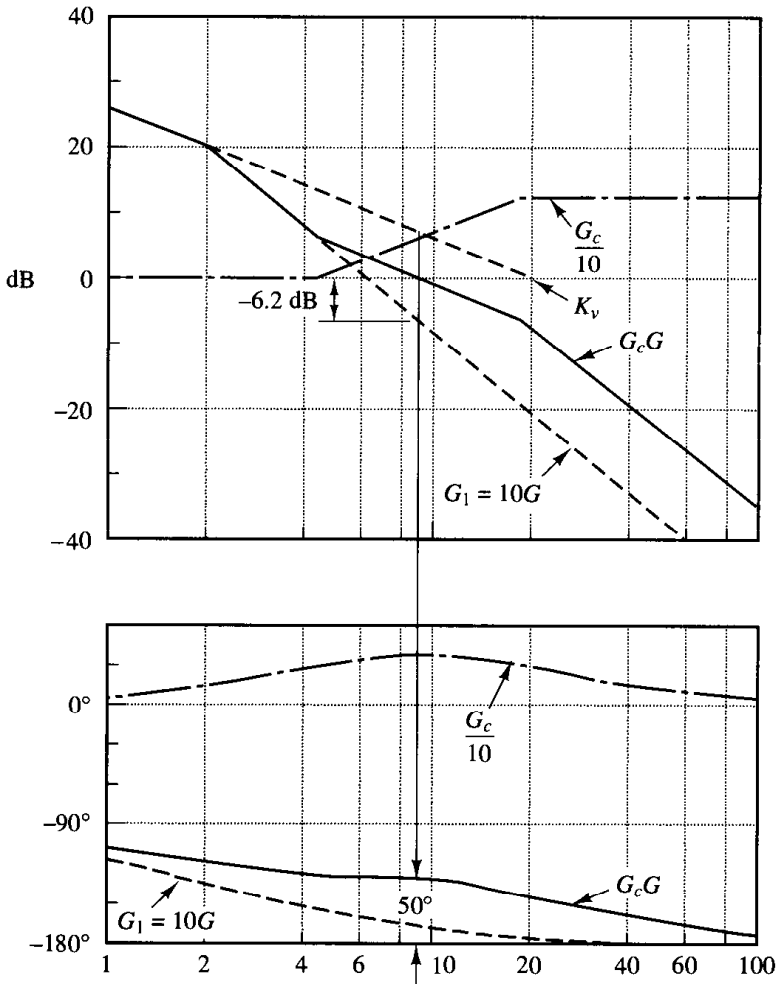

Figure 9–8
Bode diagram for the compensated system.

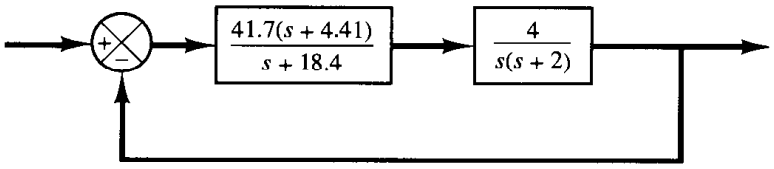

Figure 9–9
Compensated system.

the value of M_r may be obtained easily by transferring the data from the Bode diagram to the Nichol's chart.)

Note that, if the phase angle of $G_1(j\omega)$ decreases rapidly near the gain crossover frequency, lead compensation becomes ineffective because the shift in the gain crossover frequency to the right makes it difficult to provide enough phase lead at the new gain crossover frequency. This means that, to provide the desired phase margin, we must use a very small value for α. The value of α, however, should not be too small (smaller than 0.05) nor should the maximum phase lead ϕ_m be too large (larger than 65°), because such values will require an additional gain of excessive value. [If more than 65° is needed, two (or more) lead networks may be used in series with an isolating amplifier.]

Finally, we shall examine the transient-response characteristics of the designed system. We shall obtain the unit-step response and unit-ramp response curves of the compensated and un-

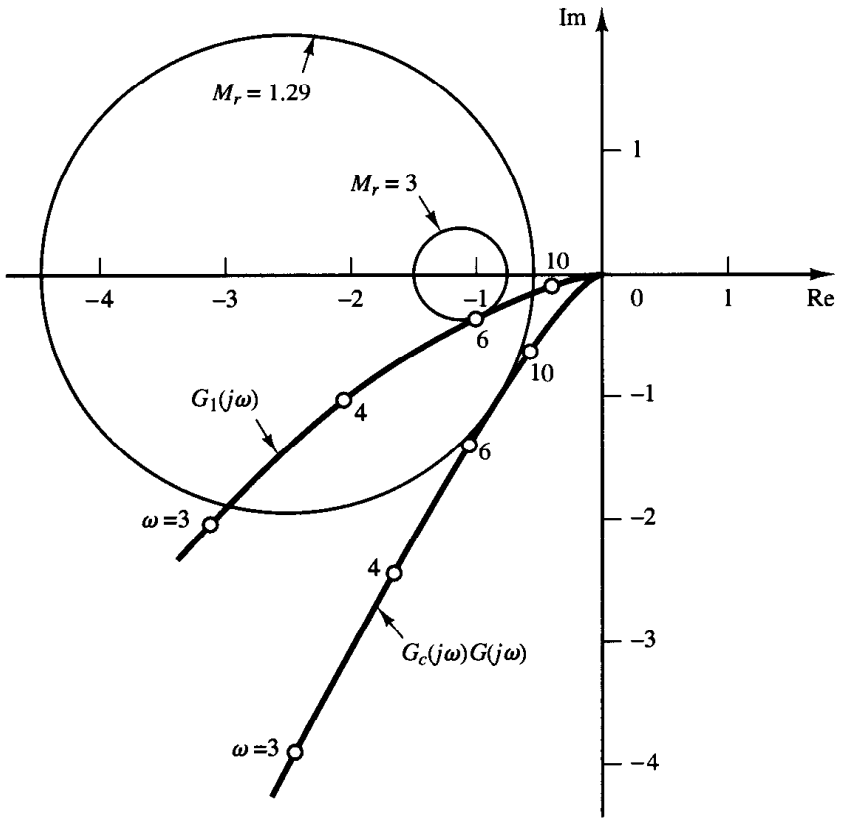

Figure 9–10
Polar plots of the uncompensated and compensated open-loop transfer function. (G_1: uncompensated system; G_cG: compensated system.)

compensated systems with MATLAB. Note that the closed-loop transfer functions of the uncompensated and compensated systems are given, respectively, by

$$\frac{C(s)}{R(s)} = \frac{4}{s^2 + 2s + 4}$$

and

$$\frac{C(s)}{R(s)} = \frac{166.8s + 735.588}{s^3 + 20.4s^2 + 203.6s + 735.588}$$

MATLAB programs for obtaining the unit-step response and unit-ramp response curves are given in MATLAB Program 9–1. Figure 9–11 shows the unit-step response curves and Figure 9–12 depicts the unit-ramp response curves. These response curves indicate that the designed system is satisfactory.

MATLAB Program 9–1

```
%*****Unit-step responses*****

num = [0   0   4];
den = [1   2   4];
numc = [0   0   166.8   735.588];
denc = [1   20.4   203.6   735.588];
t = 0:0.02:6;
```

```
[c1,x1,t] = step(num,den,t);
[c2,x2,t] = step(numc,denc,t);
plot [t,c1,'.',t,c2,'-')
grid
title('Unit-Step Responses of Compensated and Uncompensated Systems')
xlabel('t Sec')
ylabel('Outputs')
text(0.35,1.3,'Compensated system')
text(1.55,0.88,'Uncompensated system')

%*****Unit-ramp responses*****

num1 = [0   0   0   4];
den1 = [1   2   4   0];
num1c = [0   0   0   166.8   735.588];
den1c = [1   20.4   203.6   735.588   0];
t = 0:0.02:5;
[y1,z1,t] = step(num1,den1,t);
[y2,z2,t] = step(num1c,den1c,t);
plot(t,y1,'.',t,y2,'-',t,t,'--')
grid
title('Unit-Ramp Responses of Compensated and Uncompensated Systems')
xlabel('t Sec')
ylabel('Outputs')
text(0.89,3.7,'Compensated system')
text(2.25,1.1,'Uncompensated system')
```

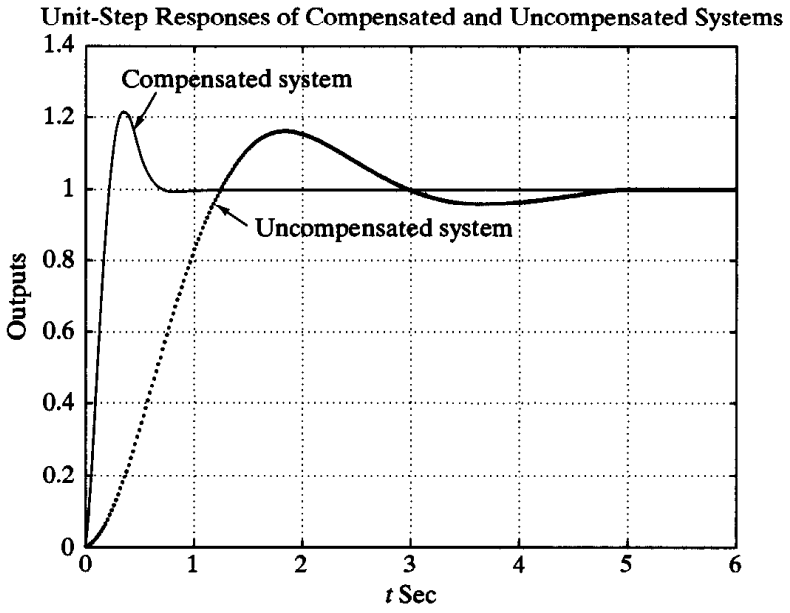

Figure 9–11
Unit-step response curves of the compensated and uncompensated systems.

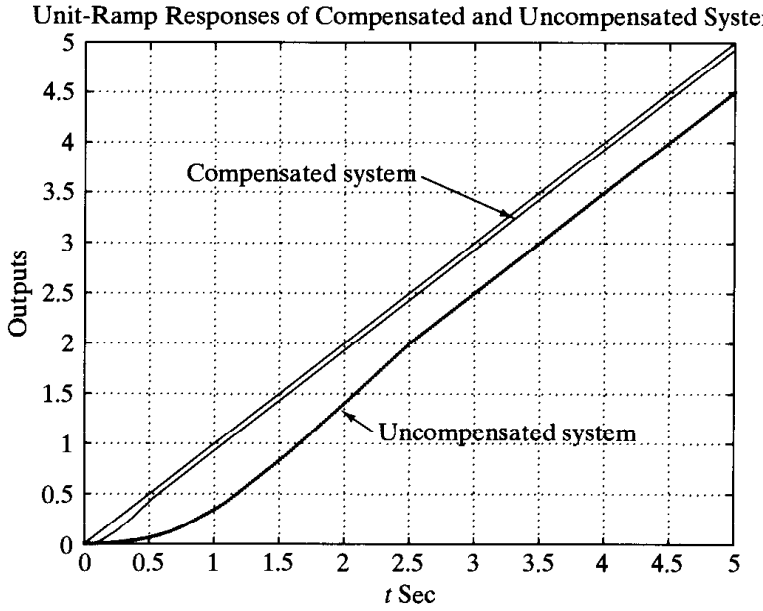

Figure 9–12
Unit-ramp response curves of the compensated and uncompensated systems.

It is noted that the closed-loop poles for the compensated system are located as follows:

$$s = -6.9541 \pm j8.0592$$

$$s = -6.4918$$

Because the dominant closed-loop poles are located far from the $j\omega$ axis, the response damps out quickly.

9–3 LAG COMPENSATION

In this section we first discuss the Nyquist plot and Bode diagram of the lag compensator. Then we present lag compensation techniques based on the frequency-response approach.

Characteristics of lag compensators. Consider a lag compensator having the following transfer function:

$$G_c(s) = K_c\beta\frac{Ts + 1}{\beta Ts + 1} = K_c\frac{s + \dfrac{1}{T}}{s + \dfrac{1}{\beta T}} \qquad (\beta > 1)$$

In the complex plane, a lag compensator has a zero at $s = -1/T$ and a pole at $s = -1/(\beta T)$. The pole is located to the right of the zero.

Figure 9–13 shows a polar plot of the lag compensator. Figure 9–14 shows a Bode diagram of the compensator, where $K_c = 1$ and $\beta = 10$. The corner frequencies of the lag compensator are at $\omega = 1/T$ and $\omega = 1/(\beta T)$. As seen from Figure 9–14, where the values of K_c and β are set equal to 1 and 10, respectively, the magnitude of the lag compensator becomes 10 (or 20 dB) at low frequencies and unity (or 0 dB) at high frequencies. Thus, the lag compensator is essentially a low-pass filter.

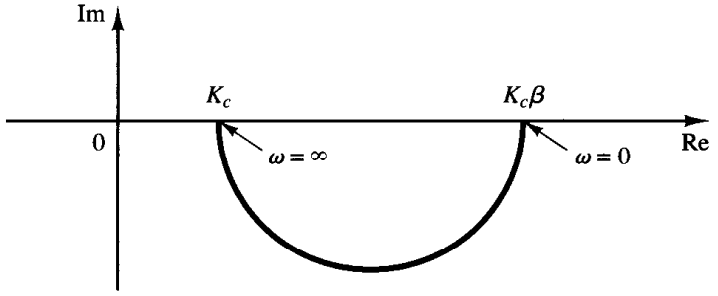

Figure 9–13
Polar plot of a lag compensator $K_c\beta(j\omega T + 1)/(j\omega\beta T + 1)$.

Lag compensation techniques based on the frequency-response approach. The primary function of a lag compensator is to provide attenuation in the high-frequency range to give a system sufficient phase margin. The phase lag characteristic is of no consequence in lag compensation.

The procedure for designing lag compensators for the system shown in Figure 9–5 by the frequency-response approach may be stated as follows:

1. Assume the following lag compensator:

$$G_c(s) = K_c\beta\frac{Ts + 1}{\beta Ts + 1} = K_c\frac{s + \dfrac{1}{T}}{s + \dfrac{1}{\beta T}} \qquad (\beta > 1)$$

Define

$$K_c\beta = K$$

Then

$$G_c(s) = K\frac{Ts + 1}{\beta Ts + 1}$$

The open-loop transfer function of the compensated system is

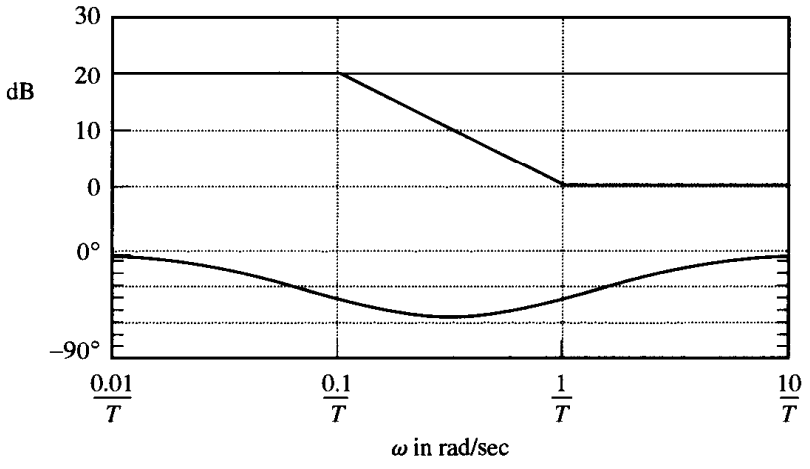

Figure 9–14
Bode diagram of a lag compensator $\beta(j\omega T + 1)/(j\omega\beta T + 1)$, with $\beta = 10$.

$$G_c(s)G(s) = K\frac{Ts+1}{\beta Ts+1}G(s) = \frac{Ts+1}{\beta Ts+1}KG(s) = \frac{Ts+1}{\beta Ts+1}G_1(s)$$

where

$$G_1(s) = KG(s)$$

Determine gain K to satisfy the requirement on the given static error constant.

2. If the uncompensated system $G_1(j\omega) = KG(j\omega)$ does not satisfy the specifications on the phase and gain margins, then find the frequency point where the phase angle of the open-loop transfer function is equal to $-180°$ plus the required phase margin. The required phase margin is the specified phase margin plus 5° to 12°. (The addition of 5° to 12° compensates for the phase lag of the lag compensator.) Choose this frequency as the new gain crossover frequency.

3. To prevent detrimental effects of phase lag due to the lag compensator, the pole and zero of the lag compensator must be located substantially lower than the new gain crossover frequency. Therefore, choose the corner frequency $\omega = 1/T$ (corresponding to the zero of the lag compensator) 1 octave to 1 decade below the new gain crossover frequency. (If the time constants of the lag compensator do not become too large, the corner frequency $\omega = 1/T$ may be chosen 1 decade below the new gain crossover frequency.)

4. Determine the attenuation necessary to bring the magnitude curve down to 0 dB at the new gain crossover frequency. Noting that this attenuation is $-20 \log \beta$, determine the value of β. Then the other corner frequency (corresponding to the pole of the lag compensator) is determined from $\omega = 1/(\beta T)$.

5. Using the value of K determined in step 1 and that of β determined in step 5, calculate constant K_c from

$$K_c = \frac{K}{\beta}$$

EXAMPLE 9–2 Consider the system shown in Figure 9–15. The open-loop transfer function is given by

$$G(s) = \frac{1}{s(s+1)(0.5s+1)}$$

It is desired to compensate the system so that the static velocity error constant K_v is 5 sec^{-1}, the phase margin is at least 40°, and the gain margin is at least 10 dB.

We shall use a lag compensator of the form

$$G_c(s) = K_c\beta\frac{Ts+1}{\beta Ts+1} = K_c\frac{s+\frac{1}{T}}{s+\frac{1}{\beta T}} \qquad (\beta > 1)$$

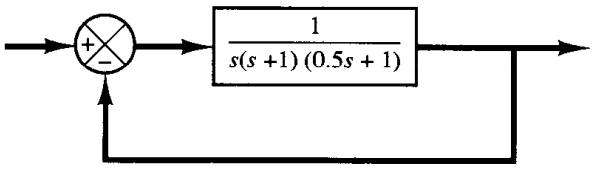

Figure 9–15
Control system.

Define

$$K_c\beta = K$$

Define also

$$G_1(s) = KG(s) = \frac{K}{s(s + 1)(0.5s + 1)}$$

The first step in the design is to adjust the gain K to meet the required static velocity error constant. Thus,

$$K_v = \lim_{s\to 0} sG_c(s)G(s) = \lim_{s\to 0} s\frac{Ts + 1}{\beta Ts + 1} G_1(s) = \lim_{s\to 0} sG_1(s)$$

$$= \lim_{s\to 0} \frac{sK}{s(s + 1)(0.5s + 1)} = K = 5$$

or

$$K = 5$$

With $K = 5$, the compensated system satisfies the steady-state performance requirement.

We shall next plot the Bode diagram of

$$G_1(j\omega) = \frac{5}{j\omega(j\omega + 1)(0.5j\omega + 1)}$$

The magnitude curve and phase-angle curve of $G_1(j\omega)$ are shown in Figure 9–16. From this plot, the phase margin is found to be $-20°$, which means that the system is unstable.

Noting that the addition of a lag compensator modifies the phase curve of the Bode diagram, we must allow 5° to 12° to the specified phase margin to compensate for the modification of the phase curve. Since the frequency corresponding to a phase margin of 40° is 0.7 rad/sec, the new gain crossover frequency (of the compensated system) must be chosen near this value. To avoid overly large time constants for the lag compensator, we shall choose the corner frequency $\omega = 1/T$ (which corresponds to the zero of the lag compensator) to be 0.1 rad/sec. Since this corner frequency is not too far below the new gain crossover frequency, the modification in the phase curve may not be small. Hence, we add about 12° to the given phase margin as an allowance to account for the lag angle introduced by the lag compensator. The required phase margin is now 52°. The phase angle of the uncompensated open-loop transfer function is $-128°$ at about $\omega = 0.5$ rad/sec. So we choose the new gain crossover frequency to be 0.5 rad/sec. To bring the magnitude curve down to 0 dB at this new gain crossover frequency, the lag compensator must give the necessary attenuation, which in this case is -20 dB. Hence,

$$20 \log \frac{1}{\beta} = -20$$

or,

$$\beta = 10$$

The other corner frequency $\omega = 1(\beta T)$, which corresponds to the pole of the lag compensator, is then determined as

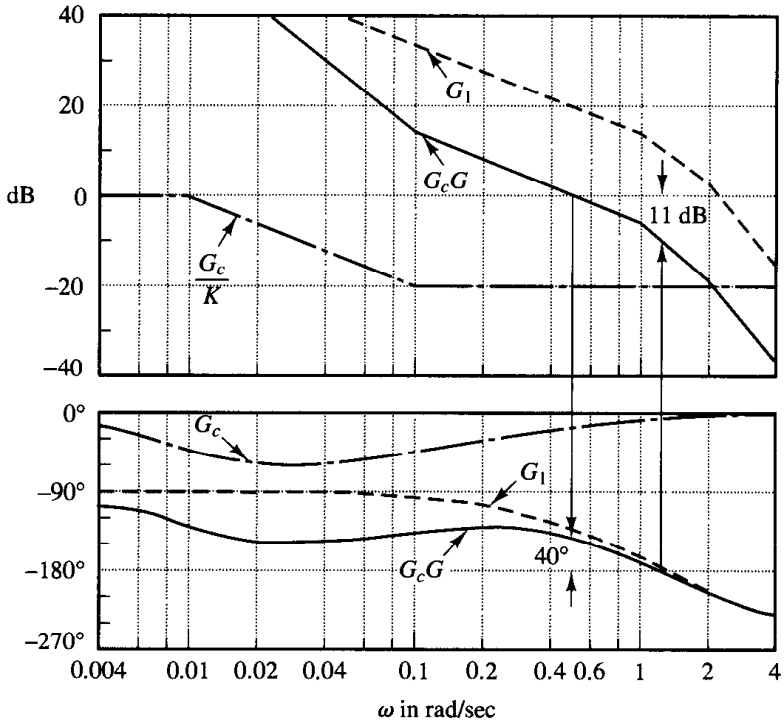

Figure 9–16
Bode diagrams for the uncompensated system, the compensator, and the compensated system. (G_1: uncompensated system, G_c: compensator, G_cG: compensated system.)

$$\frac{1}{\beta T} = 0.01 \text{ rad/sec}$$

Thus, the transfer function of the lag compensator is

$$G_c(s) = K_c(10)\frac{10s + 1}{100s + 1} = K_c\frac{s + \frac{1}{10}}{s + \frac{1}{100}}$$

Since the gain K was determined to be 5 and β was determined to be 10, we have

$$K_c = \frac{K}{\beta} = \frac{5}{10} = 0.5$$

The open-loop transfer function of the compensated system is

$$G_c(s)G(s) = \frac{5(10s + 1)}{s(100s + 1)(s + 1)(0.5s + 1)}$$

The magnitude and phase-angle curves of $G_c(j\omega)G(j\omega)$ are also shown in Figure 9–16.

The phase margin of the compensated system is about 40°, which is the required value. The gain margin is about 11 dB, which is quite acceptable. The static velocity error constant is 5 sec^{-1}, as required. The compensated system, therefore, satisfies the requirements on both the steady state and the relative stability.

Note that the new gain crossover frequency is decreased from approximately 1 to 0.5 rad/sec. This means that the bandwidth of the system is reduced.

To further show the effects of lag compensation, the log-magnitude versus phase plots of the gain-adjusted but uncompensated system $G_1(j\omega)$ and of the compensated system $G_c(j\omega)G(j\omega)$ are shown in Figure 9–17. The plot of $G_1(j\omega)$ clearly shows that the gain-adjusted but uncompensated system is unstable. The addition of the lag compensator stabilizes the system. The plot of $G_c(j\omega)G(j\omega)$ is tangent to the $M = 3$ dB locus. Thus, the resonant peak value is 3 dB, or 1.4, and this peak occurs at $\omega = 0.5$ rad/sec.

Compensators designed by different methods or by different designers (even using the same approach) may look sufficiently different. Any of the well-designed systems, however, will give similar transient and steady-state performance. The best among many alternatives may be chosen from the economic consideration that the time constants of the lag compensator should not be too large.

Finally, we shall examine the unit-step response and unit-ramp response of the compensated system and the original uncompensated system. The closed-loop transfer functions of the compensated and uncompensated systems are

$$\frac{C(s)}{R(s)} = \frac{50s + 5}{50s^4 + 150.5s^3 + 101.5s^2 + 51s + 5}$$

and

$$\frac{C(s)}{R(s)} = \frac{1}{0.5s^3 + 1.5s^2 + s + 1}$$

respectively. MATLAB Program 9–2 will produce the unit-step and unit-ramp responses of the compensated and uncompensated systems. The resulting unit-step response curves and unit-ramp response curves are shown in Figures 9–18 and 9–19, respectively. From the response curves we find that the designed system satisfies the given specifications and is satisfactory.

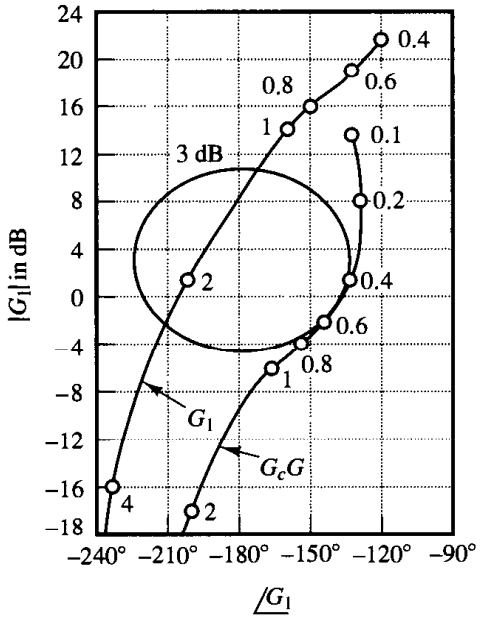

Figure 9–17
Log-magnitude versus phase plots of the uncompensated system and the compensated system. (G_1: uncompensated system, G_cG: compensated system.)

MATLAB Program 9–2

```
%*****Unit-step response*****

num = [0   0   0   1];
den = [0.5   1.5   1   1];
numc = [0   0   0   50   5];
denc = [50   150.5   101.5   51   5];
t = 0:0.1:40;
[c1,x1,t] = step(num,den,t);
[c2,x2,t] = step(numc,denc,t);
plot(t,c1,'.',t,c2,'-')
grid
title('Unit-Step Responses of Compensated and Uncompensated Systems')
xlabel('t Sec')
ylabel('Outputs')
text(12.2,1.27,'Compensated system')
text(12.2,0.7,'Uncompensated system')

%*****Unit-ramp response*****

num1 = [0   0   0   0   1];
den1 = [0.5   1.5   1   1   0];
num1c = [0   0   0   0   50   5];
den1c = [50   150.5   101.5   51   5   0];
t = 0:0.1:20;
[y1,z1,t] = step(num1,den1,t);
[y2,z2,t] = step(num1c,den1c,t);
plot(t,y1,'.',t,y2,'-',t,t,'--');
grid
title('Unit-Ramp Responses of Compensated and Uncompensated Systems')
xlabel('t Sec')
ylabel('Outputs')
text(8.4,3,'Compensated system')
text(8.4,5,'Uncompensated system')
```

Note that the zero and poles of the designed closed-loop systems are as follows:

$$\text{Zero at } s = -0.1$$

$$\text{Poles at } s = -0.2859 \pm j0.5196, \qquad s = -0.1228, \qquad s = -2.3155$$

The dominant closed-loop poles are very close to the $j\omega$ axis with the result that the response is slow. Also, a pair of the closed-loop pole at $s = -0.1228$ and the zero at $s = -0.1$ produces a slowly decreasing tail of small amplitude.

A few comments on lag compensation

1. Lag compensators are essentially low-pass filters. Therefore, lag compensation permits a high gain at low frequencies (which improves the steady-state performance)

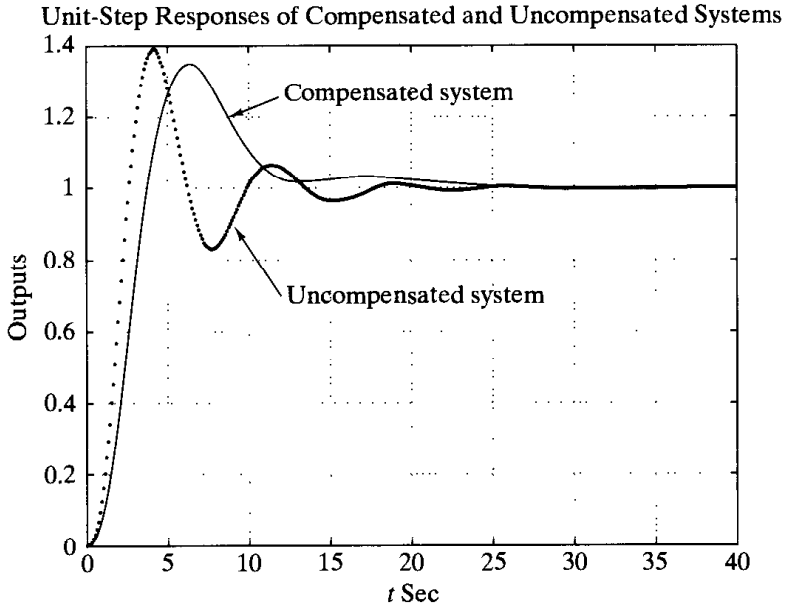

Figure 9–18
Unit-step response curves for the compensated and uncompensated systems (Example 9–2).

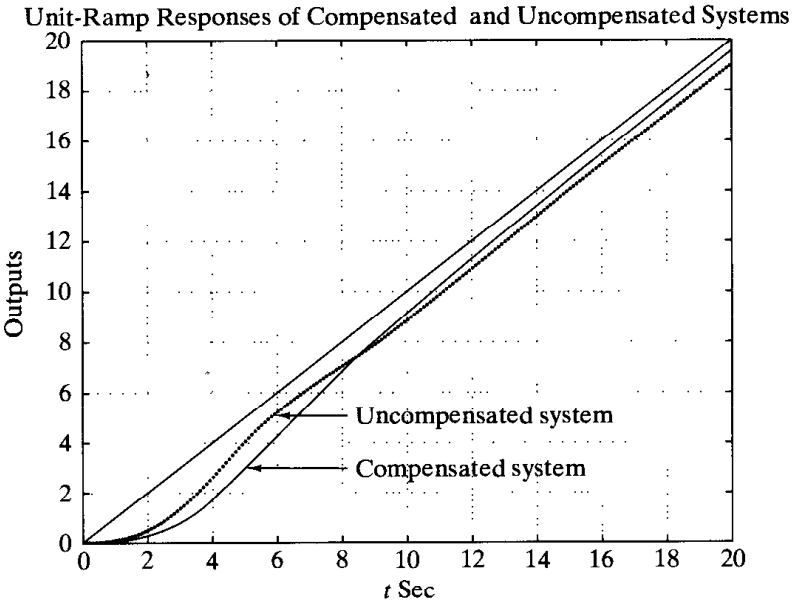

Figure 9–19
Unit-ramp response curves for the compensated and uncompensated systems (Example 9–2).

and reduces gain in the higher critical range of frequencies so as to improve the phase margin. Note that in lag compensation we utilize the attenuation characteristic of the lag compensator at high frequencies rather than the phase-lag characteristic. (The phase-lag characteristic is of no use for compensation purposes.)

2. Suppose that the zero and pole of a lag compensator are located at $s = -z$ and $s = -p$, respectively. Then the exact location of the zero and pole is not critical provided that they are close to the origin and the ratio z/p is equal to the required multiplication factor of the static velocity error constant.

It should be noted, however, that the zero and pole of the lag compensator should not be located unnecessarily close to the origin, because the lag compensator will create an additional closed-loop pole in the same region as the zero and pole of the lag compensator.

The closed-loop pole located near the origin gives a very slowly decaying transient response, although its magnitude will become very small because the zero of the lag compensator will almost cancel the effect of this pole. However, the transient response (decay) due to this pole is so slow that the settling time will be adversely affected.

It is also noted that in the system compensated by a lag compensator the transfer function between the plant disturbance and the system error may not involve a zero that is near this pole. Therefore, the transient response to the disturbance input may last very long.

3. The attenuation due to the lag compensator will shift the gain crossover frequency to a lower frequency point where the phase margin is acceptable. Thus, the lag compensator will reduce the bandwidth of the system and will result in slower transient response. [The phase angle curve of $G_c(j\omega)G(j\omega)$ is relatively unchanged near and above the new gain crossover frequency.]

4. Since the lag compensator tends to integrate the input signal, it acts approximately as a proportional-plus-integral controller. Because of this, a lag-compensated system tends to become less stable. To avoid this undesirable feature, the time constant T should be made sufficiently larger than the largest time constant of the system.

5. Conditional stability may occur when a system having saturation or limiting is compensated by use of a lag compensator. When the saturation or limiting takes place in the system, it reduces the effective loop gain. Then the system becomes less stable and unstable operation may even result, as shown in Figure 9–20. To avoid this, the system must be designed so that the effect of lag compensation becomes significant only when

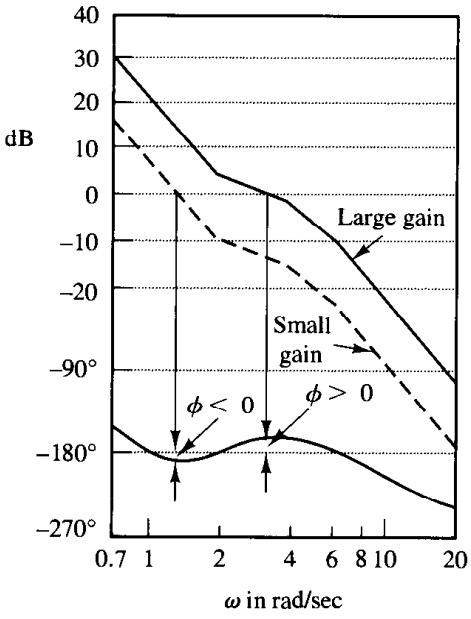

Figure 9–20
Bode diagram of a conditionally stable system.

the amplitude of the input to the saturating element is small. (This can be done by means of minor feedback-loop compensation.)

9–4 LAG–LEAD COMPENSATION

We shall first examine the frequency-response characteristics of the lag–lead compensator. Then we present the lag–lead compensation technique based on the frequency-response approach.

Characteristic of lag–lead compensator. Consider the lag–lead compensator given by

$$G_c(s) = K_c \left(\frac{s + \frac{1}{T_1}}{s + \frac{\gamma}{T_1}} \right) \left(\frac{s + \frac{1}{T_2}}{s + \frac{1}{\beta T_2}} \right) \tag{9–3}$$

where $\gamma > 1$ and $\beta > 1$. The term

$$\frac{s + \frac{1}{T_1}}{s + \frac{\gamma}{T_1}} = \frac{1}{\gamma} \left(\frac{T_1 s + 1}{\frac{T_1}{\gamma} s + 1} \right) \qquad (\gamma > 1)$$

produces the effect of the lead network, and the term

$$\frac{s + \frac{1}{T_2}}{s + \frac{1}{\beta T_2}} = \beta \left(\frac{T_2 s + 1}{\beta T_2 s + 1} \right) \qquad (\beta > 1)$$

produces the effect of the lag network.

In designing a lag–lead compensator, we frequently chose $\gamma = \beta$. (This is not necessary. We can, of course, choose $\gamma \neq \beta$.) In what follows, we shall consider the case where $\gamma = \beta$. The polar plot of the lag–lead compensator with $K_c = 1$ and $\gamma = \beta$ becomes as shown in Figure 9–21. It can be seen that, for $0 < \omega < \omega_1$, the compensator acts as a lag

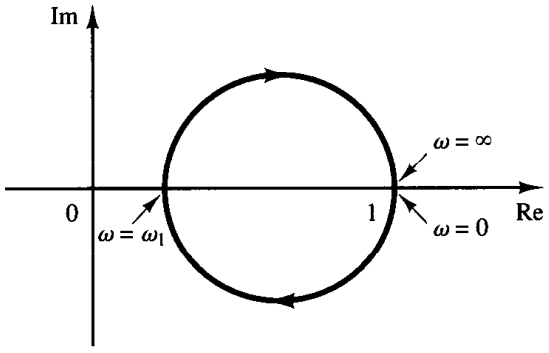

Figure 9–21
Polar plot of a lag–lead compensator given by Equation (9–3), with $K_c = 1$ and $\gamma = \beta$.

compensator, while for $\omega_1 < \omega < \infty$, it acts as a lead compensator. The frequency ω_1 is the frequency at which the phase angle is zero. It is given by

$$\omega_1 = \frac{1}{\sqrt{T_1 T_2}}$$

(To derive this equation, see Problem A–9–2.)

Figure 9–22 shows the Bode diagram of a lag–lead compensator when $K_c = 1$, $\gamma = \beta = 10$, and $T_2 = 10T_1$. Notice that the magnitude curve has the value 0 dB at the low- and high-frequency regions.

Lag–lead compensation based on the frequency-response approach. The design of a lag–lead compensator by the frequency-response approach is based on the combination of the design techniques discussed under lead compensation and lag compensation.

Let us assume that the lag–lead compensator is of the following form:

$$G_c(s) = K_c \frac{(T_1 s + 1)(T_2 s + 1)}{\left(\frac{T_1}{\beta} s + 1\right)(\beta T_2 s + 1)} = K_c \frac{\left(s + \frac{1}{T_1}\right)\left(s + \frac{1}{T_2}\right)}{\left(s + \frac{\beta}{T_1}\right)\left(s + \frac{1}{\beta T_2}\right)} \tag{9–4}$$

where $\beta > 1$. The phase lead portion of the lag–lead compensator (the portion involving T_1) alters the frequency-response curve by adding phase lead angle and increasing the phase margin at the gain crossover frequency. The phase lag portion (the portion involving T_2) provides attenuation near and above the gain crossover frequency and thereby allows an increase of gain at the low-frequency range to improve the steady-state performance.

We shall illustrate the details of the procedures for designing a lag–lead compensator by an example.

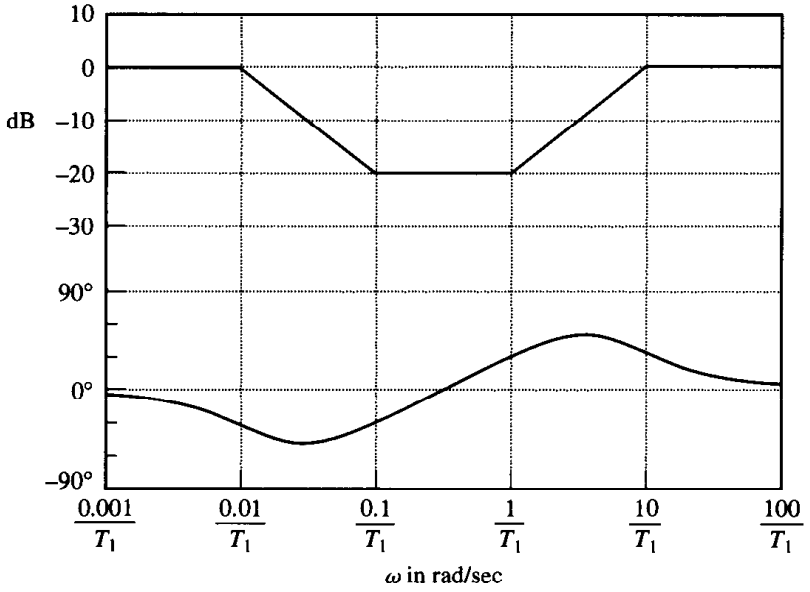

Figure 9–22
Bode diagram of a lag–lead compensator given by Equation (9–3) with $K_c = 1, \gamma = \beta = 10$, and $T_2 = 10T_1$.

EXAMPLE 9–3 Consider the unity-feedback system whose open-loop transfer function is

$$G(s) = \frac{K}{s(s + 1)(s + 2)}$$

It is desired that the static velocity error constant be 10 $\sec^{-1}$, the phase margin be 50°, and the gain margin be 10 dB or more.

Assume that we use the lag–lead compensator given by Equation (9–4). The open-loop transfer function of the compensated system is $G_c(s)G(s)$. Since the gain K of the plant is adjustable, let us assume that $K_c = 1$. Then, $\lim_{s\to 0} G_c(s) = 1$.

From the requirement on the static velocity error constant, we obtain

$$K_v = \lim_{s\to 0} sG_c(s)G(s) = \lim_{s\to 0} sG_c(s)\frac{K}{s(s + 1)(s + 2)} = \frac{K}{2} = 10$$

Hence,

$$K = 20$$

We shall next draw the Bode diagram of the uncompensated system with $K = 20$, as shown in Figure 9–23. The phase margin of the uncompensated system is found to be −32°, which indicates that the uncompensated system is unstable.

The next step in the design of a lag–lead compensator is to choose a new gain crossover frequency. From the phase angle curve for $G(j\omega)$, we notice that $\angle G(j\omega) = -180°$ at $\omega = 1.5$ rad/sec. It is convenient to choose the new gain crossover frequency to be 1.5 rad/sec so that the phase-lead angle required at $\omega = 1.5$ rad/sec is about 50°, which is quite possible by use of a single lag–lead network.

Once we choose the gain crossover frequency to be 1.5 rad/sec, we can determine the corner frequency of the phase lag portion of the lag–lead compensator. Let us choose the corner frequency $\omega = 1/T_2$ (which corresponds to the zero of the phase-lag portion of the compensator) to be 1 decade below the new gain crossover frequency, or at $\omega = 0.15$ rad/sec.

Recall that for the lead compensator the maximum phase lead angle ϕ_m is given by Equation (9–1), where α in Equation (9–1) is $1/\beta$ in the present case. By substituting $\alpha = 1/\beta$ in Equation (9–1), we have

$$\sin\phi_m = \frac{1 - \dfrac{1}{\beta}}{1 + \dfrac{1}{\beta}} = \frac{\beta - 1}{\beta + 1}$$

Notice that $\beta = 10$ corresponds to $\phi_m = 54.9°$. Since we need a 50° phase margin, we may choose $\beta = 10$. (Note that we will be using several degrees less than the maximum angle, 54.9°.) Thus,

$$\beta = 10$$

Then the corner frequency $\omega = 1/\beta T_2$ (which corresponds to the pole of the phase lag portion of the compensator) becomes $\omega = 0.015$ rad/sec. The transfer function of the phase lag portion of the lag–lead compensator then becomes

$$\frac{s + 0.15}{s + 0.015} = 10\left(\frac{6.67s + 1}{66.7s + 1}\right)$$

The phase lead portion can be determined as follows: Since the new gain crossover frequency is $\omega = 1.5$ rad/sec, from Figure 9–23, $G(j1.5)$ is found to be 13 dB. Hence, if the lag–lead compen-

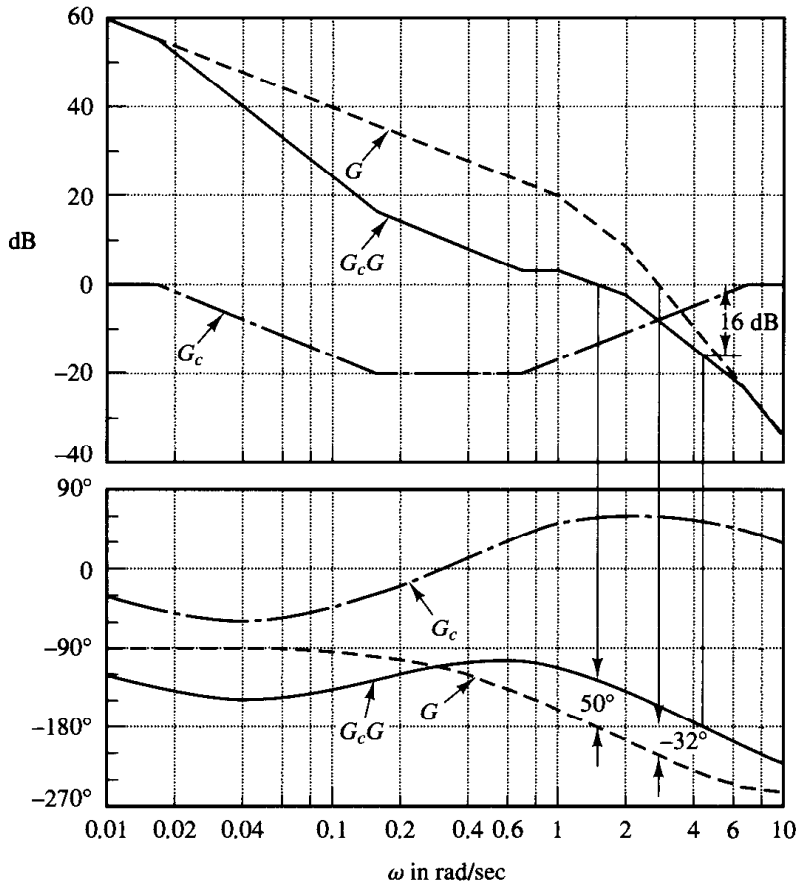

Figure 9–23
Bode diagrams for the uncompensated system, the compensator, and the compensated system. (*G:* uncompensated system, G_c: compensator, G_cG: compensated system.)

sator contributes −13 dB at $\omega = 1.5$ rad/sec, then the new gain crossover frequency is as desired. From this requirement, it is possible to draw a straight line of slope 20 dB/decade, passing through the point (−13 dB, 1.5 rad/sec). The intersections of this line and the 0-dB line and −20-dB line determine the corner frequencies. Thus, the corner frequencies for the lead portion are $\omega = 0.7$ rad/sec and $\omega = 7$ rad/sec. Thus, the transfer function of the lead portion of the lag–lead compensator becomes

$$\frac{s + 0.7}{s + 7} = \frac{1}{10}\left(\frac{1.43s + 1}{0.143s + 1}\right)$$

Combining the transfer functions of the lag and lead portions of the compensator, we obtain the transfer function of the lag–lead compensator. Since we chose $K_c = 1$, we have

$$G_c(s) = \left(\frac{s + 0.7}{s + 7}\right)\left(\frac{s + 0.15}{s + 0.015}\right) = \left(\frac{1.43s + 1}{0.143s + 1}\right)\left(\frac{6.67s + 1}{66.7s + 1}\right)$$

The magnitude and phase-angle curves of the lag–lead compensator just designed are shown in Figure 9–23. The open-loop transfer function of the compensated system is

$$G_c(s)G(s) = \frac{(s + 0.7)(s + 0.15)20}{(s + 7)(s + 0.015)s(s + 1)(s + 2)}$$

$$= \frac{10(1.43s + 1)(6.67s + 1)}{s(0.143s + 1)(66.7s + 1)(s + 1)(0.5s + 1)} \tag{9–5}$$

The magnitude and phase-angle curves of the system of Equation (9–5) are also shown in Figure 9–23. The phase margin of the compensated system is 50°, the gain margin is 16 dB, and the static velocity error constant is 10 $\sec^{-1}$. All the requirements are therefore met, and the design has been completed.

Figure 9–24 shows the polar plots of the uncompensated system and compensated system. The $G_c(j\omega)G(j\omega)$ locus is tangent to the $M = 1.2$ circle at about $\omega = 2$ rad/sec. Clearly, this indicates that the compensated system has satisfactory relative stability. The bandwidth of the compensated system is slightly larger than 2 rad/sec.

In the following we shall examine the transient-response characteristics of the compensated system. (The uncompensated system is unstable.) The closed-loop transfer function of the compensated system is

$$\frac{C(s)}{R(s)} = \frac{95.381s^2 + 81s + 10}{4.7691s^5 + 47.7287s^4 + 110.3026s^3 + 163.724s^2 + 82s + 10}$$

The unit-step and unit-ramp response curves obtained with MATLAB are shown in Figures 9–25 and 9–26, respectively.

Note that the designed closed-loop control system has the following closed-loop zeros and poles:

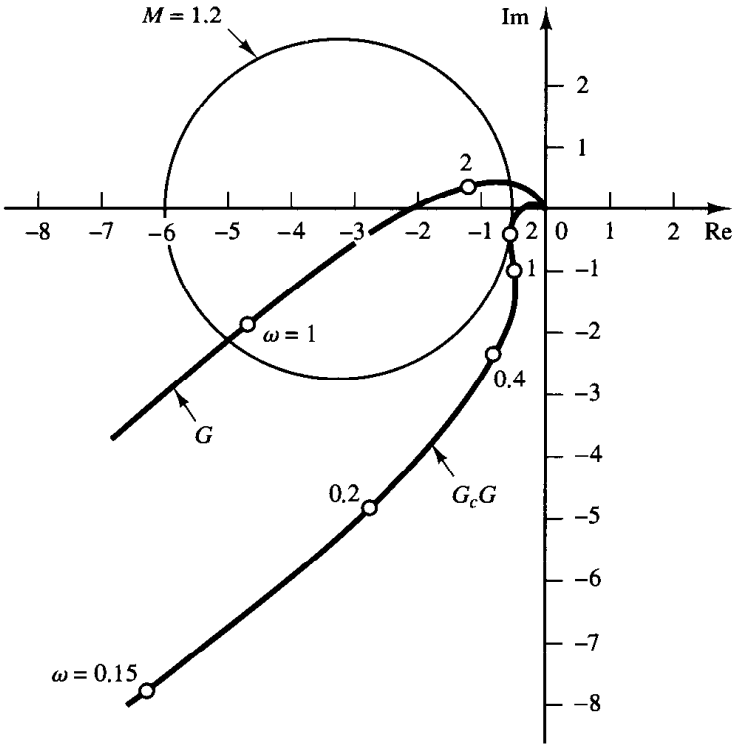

Figure 9–24
Polar plots of the uncompensated system and the compensated system. (*G:* uncompensated system, G_cG: compensated system.)

Zeros at $s = -0.1499$, $s = -0.6993$

Poles at $s = -0.8973 \pm j1.4439$

$s = -0.1785$, $s = -0.5425$, $s = -7.4923$

The pole at $s = -0.1785$ and zero at $s = -0.1499$ are located very close to each other. Such a pair of pole and zero produces a long tail of small amplitude in the step response, as seen in Figure 9–25. Also, the pole at $s = -0.5425$ and zero at $s = -0.6993$ are located fairly close to each other. This pair adds an amplitude to the long tail.

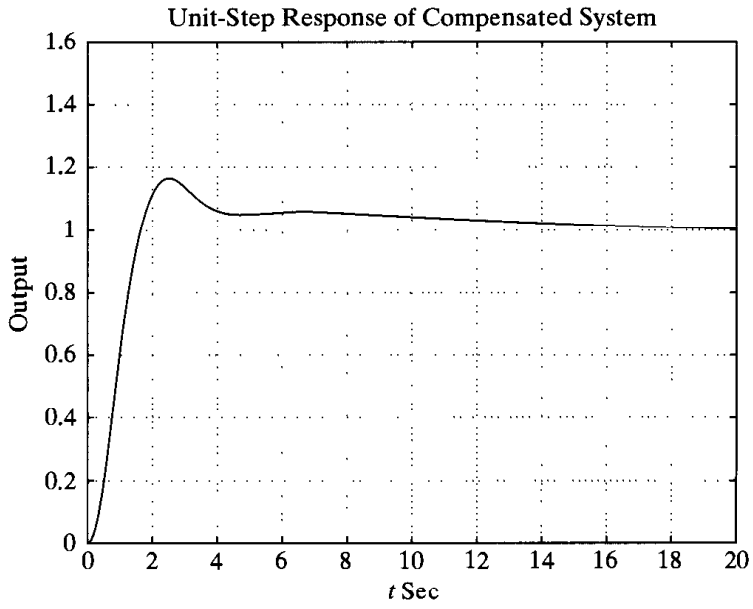

Figure 9–25
Unit-step response of the compensated system (Example 9–3).

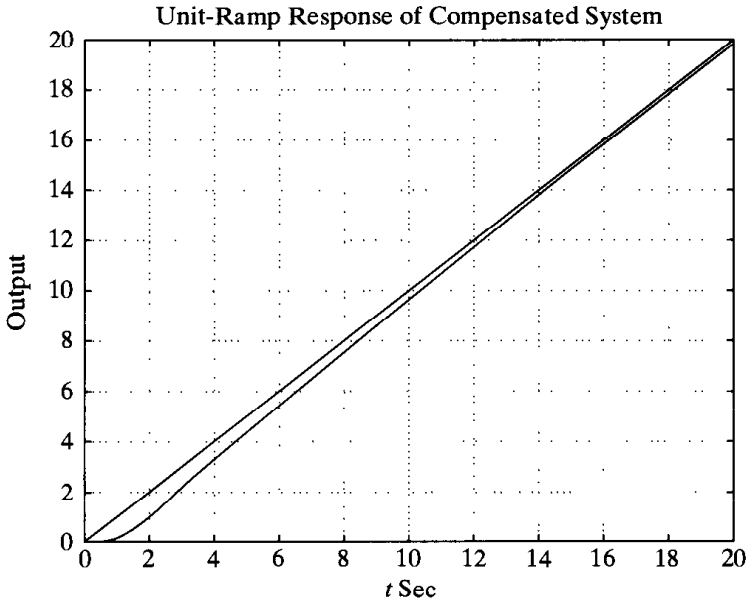

Figure 9–26
Unit-ramp response of the compensated system (Example 9–3).

9–5 CONCLUDING COMMENTS

This chapter has presented detailed procedures for designing lead, lag, and lag–lead compensators by the use of simple examples. We have shown that the design of a compensator to satisfy the given specifications (in terms of the phase margin and gain margin) can be carried out in the Bode diagram in a simple and straightforward manner. Note that a satisfactory design of a compensator for a complex system may require a creative application of these basic design principles.

Comparison of lead, lag and lag–lead compensation

1. Lead compensation achieves the desired result through the merits of its phase-lead contribution, whereas lag compensation accomplishes the result through the merits of its attenuation property at high frequencies. (In some design problems both lag compensation and lead compensation may satisfy the specifications.)

2. Lead compensation is commonly used for improving stability margins. Lead compensation yields a higher gain crossover frequency than is possible with lag compensation. The higher gain crossover frequency means larger bandwidth. A large bandwidth means reduction in the settling time. The bandwidth of a system with lead compensation is always greater than that with lag compensation. Therefore, if a large bandwidth or fast response is desired, lead compensation should be employed. If, however, noise signals are present, then a large bandwidth may not be desirable, since it makes the system more susceptible to noise signals because of increase in the high-frequency gain.

3. Lead compensation requires an additional increase in gain to offset the attenuation inherent in the lead network. This means that lead compensation will require a larger gain than that required by lag compensation. A larger gain, in most cases, implies larger space, greater weight, and higher cost.

4. Lag compensation reduces the system gain at higher frequencies without reducing the system gain at lower frequencies. Since the system bandwidth is reduced, the system has a slower speed to respond. Because of the reduced high-frequency gain, the total system gain can be increased, and thereby low-frequency gain can be increased and the steady-state accuracy can be improved. Also, any high-frequency noises involved in the system can be attenuated.

5. If both fast responses and good static accuracy are desired, a lag–lead compensator may be employed. By use of the lag–lead compensator, the low-frequency gain can be increased (which means an improvement in steady-state accuracy), while at the same time the system bandwidth and stability margins can be increased.

6. Although a large number of practical compensation tasks can be accomplished with lead, lag, or lag–lead compensators, for complicated systems, simple compensation by use of these compensators may not yield satisfactory results. Then, different compensators having different pole–zero configurations must be employed.

Graphical comparison. Figure 9–27(a) shows a unit-step response curve and unit-ramp response curve of an uncompensated system. Typical unit-step response and unit-ramp response curves for the compensated system using a lead, lag, and lag–lead network, respectively, are shown in Figures 9–27(b), (c), and (d). The system with a lead

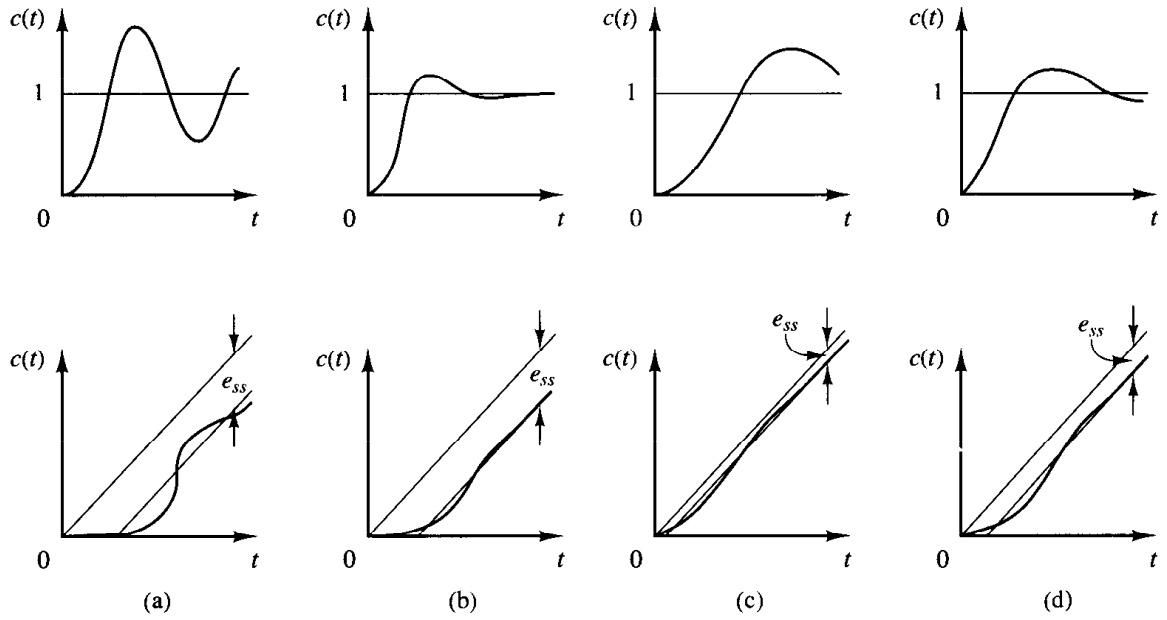

Figure 9–27
Unit-step response curves and unit-ramp response curves. (a) Uncompensated system; (b) lead compensated system; (c) lag compensated system; (d) lag–lead compensated system.

compensator exhibits the fastest response, while that with a lag compensator exhibits the slowest response, but with marked improvements in the unit-ramp response. The system with a lag–lead compensator will give a compromise; reasonable improvements in both the transient response and steady-state response can be expected. The response curves shown depict the nature of improvements that may be expected from using different types of compensators.

Feedback compensation. A tachometer is one of the rate feedback devices. Another common rate feedback device is the rate gyro. Rate gyros are commonly used in aircraft autopilot systems.

Velocity feedback using a tachometer is very commonly used in positional servo systems. It is noted that, if the system is subjected to noise signals, velocity feedback may generate some difficulty if a particular velocity feedback scheme performs differentiation of the output signal. (The result is the accentuation of the noise effects.)

Cancellation of undesirable poles. Since the transfer function of elements in cascade is the product of their individual transfer functions, it is possible to cancel some undesirable poles or zeros by placing a compensating element in cascade, with its poles and zeros being adjusted to cancel the undesirable poles or zeros of the original system. For example, a large time constant T_1 may be canceled by use of the lead network $(T_1 s + 1)/(T_2 s + 1)$ as follows:

$$\left(\frac{1}{T_1 s + 1}\right)\left(\frac{T_1 s + 1}{T_2 s + 1}\right) = \frac{1}{T_2 s + 1}$$

If T_2 is much smaller than T_1, we can effectively eliminate the large time constant T_1. Figure 9–28 shows the effect of canceling a large time constant in step transient response.

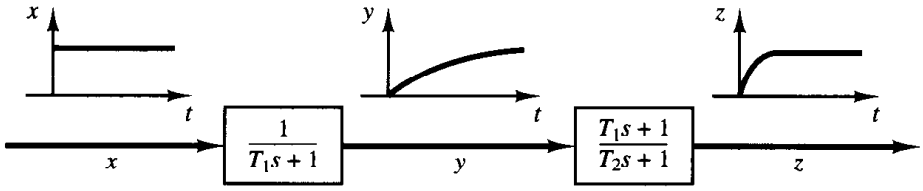

Figure 9–28
Step-response curves showing the effect of canceling a large time constant.

If an undesirable pole in the original system lies in the right-half s plane, this compensation scheme should not be used since, although mathematically it is possible to cancel the undesirable pole with an added zero, exact cancellation is physically impossible because of inaccuracies involved in the location of the poles and zeros. A pole in the right-half s plane not exactly canceled by the compensator zero will eventually lead to unstable operation, because the response will involve an exponential term that increases with time.

It is noted that if a left-half plane pole is almost canceled but not exactly canceled, as is almost always the case, the uncanceled pole-zero combination will cause the response to have a small amplitude but long-lasting transient-response component. If the cancellation is not exact but is reasonably good, then this component will be quite small.

It should be noted that the ideal control system is not the one that has a transfer function of unity. Physically, such a control system cannot be built since it cannot instantaneously transfer energy from the input to the output. In addition, since noise is almost always present in one form or another, a system with a unity transfer function is not desirable. A desired control system, in many practical cases, may have one set of dominant complex-conjugate closed-loop poles with a reasonable damping ratio and undamped natural frequency. The determination of the significant part of the closed-loop pole-zero configuration, such as the location of the dominant closed-loop poles, is based on the specifications that give the required system performance.

Cancellation of undesirable complex-conjugate poles. If the transfer function of a plant contains one or more pairs of complex-conjugate poles, then a lead, lag, or lag–lead compensator may not give satisfactory results. In such a case, a network that has two zeros and two poles may prove to be useful. If the zeros are chosen so as to cancel the undesirable complex-conjugate poles of the plant, then we can essentially replace the undesirable poles by acceptable poles. That is, if the undesirable complex-conjugate poles are in the left-half s plane and are in the form

$$\frac{1}{s^2 + 2\zeta_1\omega_1 s + \omega_1^2}$$

then the insertion of a compensating network having the transfer function

$$\frac{s^2 + 2\zeta_1\omega_1 s + \omega_1^2}{s^2 + 2\zeta_2\omega_2 s + \omega_2^2}$$

will result in an effective change of the undesirable complex-conjugate poles to acceptable poles. Note that even though the cancellation may not be exact the compensated system will exhibit better response characteristics. (As stated earlier, this approach cannot be used if the undesirable complex-conjugate poles are in the right-half s plane.)

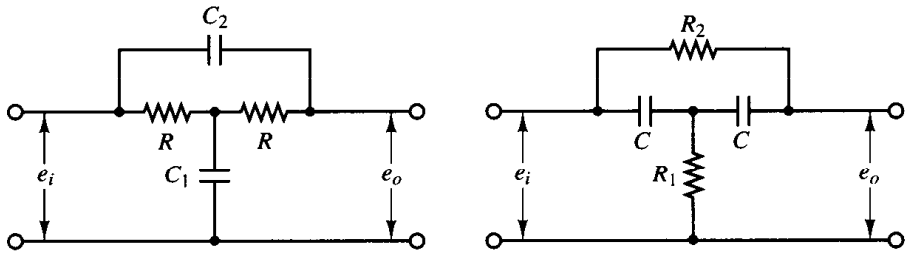

$$\frac{E_o(s)}{E_i(s)} = \frac{RC_1RC_2s^2 + 2RC_2s + 1}{RC_1RC_2s^2 + (RC_1 + 2RC_2)s + 1} \qquad \frac{E_o(s)}{E_i(s)} = \frac{R_1CR_2Cs^2 + 2R_1Cs + 1}{R_1CR_2Cs^2 + (R_2C + 2R_1C)s + 1}$$

(a) (b)

Figure 9–29
Bridged-T networks.

Familiar networks consisting only of RC components whose transfer functions possess two zeros and two poles are the bridged-T networks. Examples of bridged-T networks and their transfer functions are shown in Figure 9–29.

Concluding comments. In the design examples presented in this chapter, we have been primarily concerned only with the transfer functions of compensators. In actual design problems, we must choose the hardware. Thus, we must satisfy additional design constraints such as cost, size, weight, and reliability.

The system designed may meet the specifications under normal operating conditions but may deviate considerably from the specifications when environmental changes are considerable. Since the changes in the environment affect the gain and time constants of the system, it is necessary to provide automatic or manual means to adjust the gain to compensate for such environmental changes, for nonlinear effects that were not taken into account in the design, and also to compensate for manufacturing tolerances from unit to unit in the production of system components. (The effects of manufacturing tolerances are suppressed in a closed-loop system; therefore, the effects may not be critical in closed-loop operation but critical in open-loop operation.) In addition to this, the designer must remember that any system is subject to small variations due mainly to the normal deterioration of the system.

EXAMPLE PROBLEMS AND SOLUTIONS

A-9-1. Show that the lead network and lag network inserted in cascade in an open loop acts as proportional-plus-derivative control (in the region of small ω) and proportional-plus-integral control (in the region of large ω), respectively.

Solution. In the region of small ω, the polar plot of the lead network is approximately the same as that of the proportional-plus-derivative controller. This is shown in Figure 9–30(a).

Similarly, in the region of large ω, the polar plot of the lag network approximates the proportional-plus-integral controller, as shown in Figure 9–30(b).

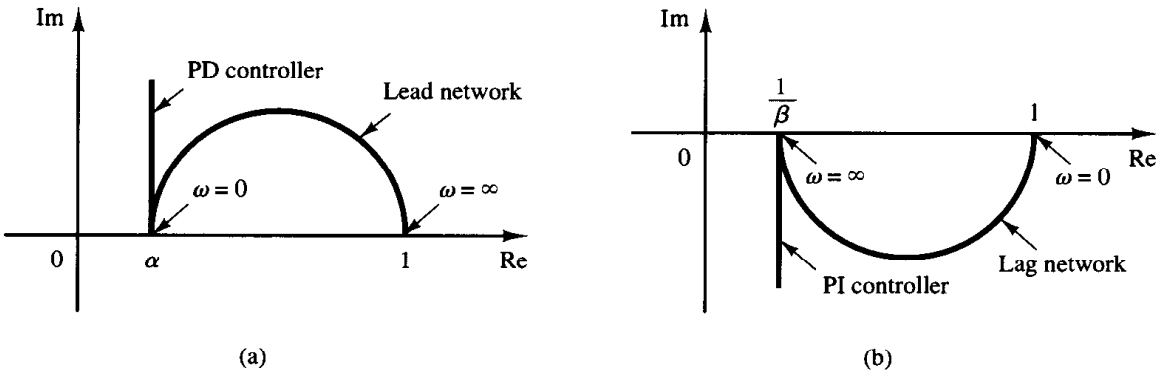

Figure 9–30
(a) Polar plots of a lead network and a proportional-plus-derivative controller; (b) polar plots of a lag network and a proportional-plus-integral controller.

A-9-2. Consider a lag–lead compensator $G_c(s)$ defined by

$$G_c(s) = K_c \frac{\left(s + \frac{1}{T_1}\right)\left(s + \frac{1}{T_2}\right)}{\left(s + \frac{\beta}{T_1}\right)\left(s + \frac{1}{\beta T_2}\right)}$$

Show that at frequency ω_1, where

$$\omega_1 = \frac{1}{\sqrt{T_1 T_2}}$$

the phase angle of $G_c(j\omega)$ becomes zero. (This compensator acts as a lag compensator for $0 < \omega < \omega_1$ and acts as a lead compensator for $\omega_1 < \omega < \infty$.)

Solution. The angle of $G_c(j\omega)$ is given by

$$\angle G_c(j\omega) = \angle j\omega + \frac{1}{T_1} + \angle j\omega + \frac{1}{T_2} - \angle j\omega + \frac{\beta}{T_1} - \angle j\omega + \frac{1}{\beta T_2}$$

$$= \tan^{-1}\omega T_1 + \tan^{-1}\omega T_2 - \tan^{-1}\omega T_1/\beta - \tan^{-1}\omega T_2\beta$$

At $\omega = \omega_1 = 1/\sqrt{T_1 T_2}$, we have

$$\angle G_c(j\omega_1) = \tan^{-1}\sqrt{\frac{T_1}{T_2}} + \tan^{-1}\sqrt{\frac{T_2}{T_1}} - \tan^{-1}\frac{1}{\beta}\sqrt{\frac{T_1}{T_2}} - \tan^{-1}\beta\sqrt{\frac{T_2}{T_1}}$$

Since

$$\tan\left(\tan^{-1}\sqrt{\frac{T_1}{T_2}} + \tan^{-1}\sqrt{\frac{T_2}{T_1}}\right) = \frac{\sqrt{\frac{T_1}{T_2}} + \sqrt{\frac{T_2}{T_1}}}{1 - \sqrt{\frac{T_1}{T_2}}\sqrt{\frac{T_2}{T_1}}} = \infty$$

or

$$\tan^{-1}\sqrt{\frac{T_1}{T_2}} + \tan^{-1}\sqrt{\frac{T_2}{T_1}} = 90°$$

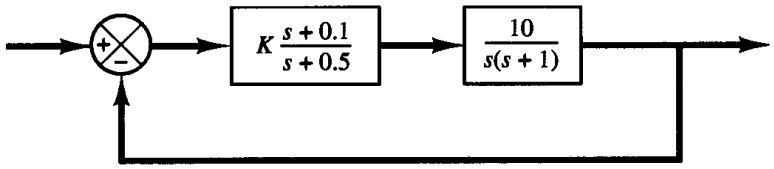

Figure 9–31
Control system.

and also

$$\tan^{-1}\frac{1}{\beta}\sqrt{\frac{T_1}{T_2}} + \tan^{-1}\beta\sqrt{\frac{T_2}{T_1}} = 90°$$

we have

$$\underline{/G_c(j\omega_1)} = 0°$$

Thus, the angle of $G_c(j\omega_1)$ becomes 0° at $\omega = \omega_1 = 1/\sqrt{T_1T_2}$.

A-9-3. Consider the control system shown in Figure 9–31. Determine the value of gain K such that the phase margin is 60°.

Solution. The open-loop transfer function is

$$G(s) = K\frac{s + 0.1}{s + 0.5}\frac{10}{s(s + 1)}$$

$$= \frac{K(10s + 1)}{s^3 + 1.5s^2 + 0.5s}$$

Let us plot the Bode diagram of $G(s)$ when $K = 1$. MATLAB Program 9–3 may be used for this purpose. Figure 9–32 shows the Bode diagram produced by this program. From this diagram the required phase margin of 60° occurs at the frequency $\omega = 1.15$ rad/sec. The magnitude of $G(j\omega)$ at this frequency is found to be 14.5 dB. Then gain K must satisfy the following equation:

$$20 \log K = -14.5 \text{ dB}$$

MATLAB Program 9–3

```
num = [0   0   10   1];
den = [1   1.5   0.5   0];
bode(num,den)
subplot(2,1,1);
title('Bode Diagram of G(s) = (10s + 1)/[s(s + 0.5)(s + 1)]')
```

or

$$K = 0.188$$

Thus, we have determined the value of gain K.

To verify the results, let us draw a Nyquist plot of G for the frequency range

$$w = 0.1{:}0.01{:}1.15$$

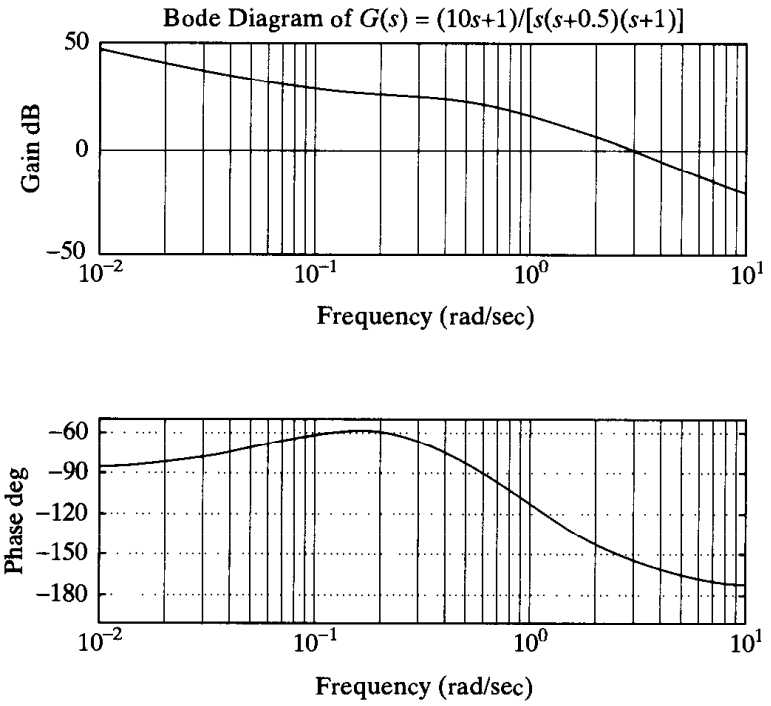

Figure 9–32

Bode diagram of $G(s) = \dfrac{10s + 1}{s(s + 0.5)(s + 1)}$.

The end point of the locus ($w = 1.15$ rad/sec) will be on a unit circle in the Nyquist plane. To check the phase margin, it is convenient to draw the Nyquist plot on a polar diagram, using polar grids.

To draw the Nyquist plot on a polar diagram, first define a complex vector z by

$$z = \text{re} + \text{i}*\text{im} = \text{re}^{\text{i}\theta}$$

where r and θ (theta) are given by

$$\text{r} = \text{abs}(z)$$
$$\text{theta} = \text{angle}(z)$$

The abs means the square root of the sum of the real part squared and imaginary part squared, angle means $\tan^{-1}$ (imaginary part/real part).

If we use the command

```
polar(theta,r)
```

MATLAB will produce a plot in the polar coordinates. Subsequent use of the *grid* command draws polar grid lines and grid circles.

MATLAB Program 9–4 produces the Nyquist plot of $G(j\omega)$, where ω is between 0.5 and 1.15 rad/sec. The resulting plot is shown in Figure 9–33. Notice that point $G(j1.15)$ lies on the unit circle, and the phase angle of this point is $-120°$. Hence, the phase margin is 60°. The fact that point $G(j1.15)$ is on the unit circle verifies that at $\omega = 1.15$ rad/sec the magnitude is equal to 1 or 0 dB.

MATLAB Program 9–4

```
%*****Nyquist plot in polar coordinates*****

num = [0   0   1.88   0.188];
den = [1   1.5   0.5   0];
w = 0.5:0.01:1.15;
[re,im,w] = nyquist(num,den,w);

%*****Convert rectangular coordinates into polar coordinates
% by defining z, r, theta as follows*****

z = re + i*im;
r = abs(z);
theta = angle(z);

%*****To draw polar plot, enter command 'polar(theta,r)'*****

polar(theta,r)
title('Check of Phase Margin')
text(0.1,-1.5,'Nyquist plot')
text(-2.25,-0.3,'Phase margin')
text(-2.25,-0.7,'is 60 degrees.')
```

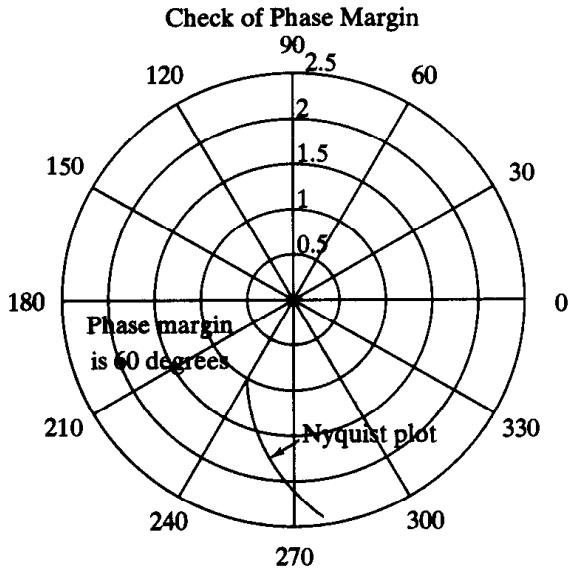

Figure 9–33
Nyquist plot of $G(j\omega)$ showing that the phase margin is 60°.

(Thus, $\omega = 1.15$ is the gain crossover frequency.) Thus, $K = 0.188$ gives the desired phase margin of 60°.

Note that in writing 'text' in the polar diagram we enter the *text* command as follows:

```
text(x,y,' ')
```

For example, to write 'Nyquist plot' starting at point (0.1, −1.5), enter the command

```
text(0.1, −1.5,'Nyquist plot')
```

The text is written horizontally on the screen.

A-9-4. If the open-loop transfer function $G(s)$ involves lightly damped complex-conjugant poles, then more than one M locus may be tangent to the $G(j\omega)$ locus.

Consider the unity-feedback system whose open-loop transfer function is

$$G(s) = \frac{9}{s(s + 0.5)(s^2 + 0.6s + 10)} \tag{9–6}$$

Draw the Bode diagram for this open-loop transfer function. Draw also the log-magnitude versus phase plot, and show that two M loci are tangent to the $G(j\omega)$ locus. Finally, plot the Bode diagram for the closed-loop transfer function.

Solution. Figure 9–34 shows the Bode diagram of $G(j\omega)$. Figure 9–35 shows the log-magnitude versus phase plot of $G(j\omega)$. It is seen that the $G(j\omega)$ locus is tangent to the $M = 8$-dB locus at $\omega = 0.97$ rad/sec, and it is tangent to the $M = -4$-dB locus at $\omega = 2.8$ rad/sec.

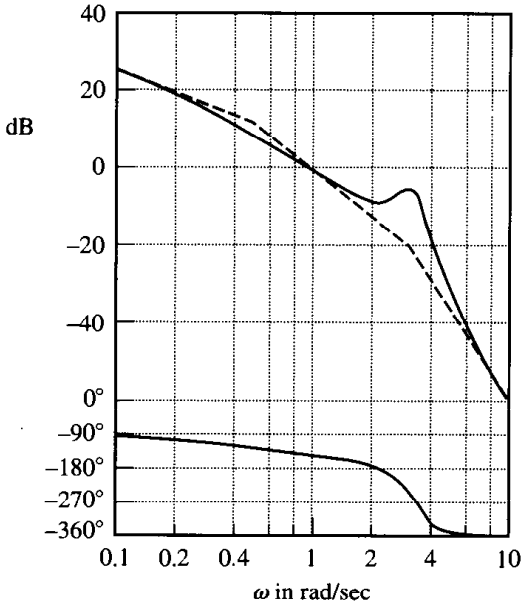

Figure 9–34
Bode diagram of $G(j\omega)$ given by Equation (9–6).

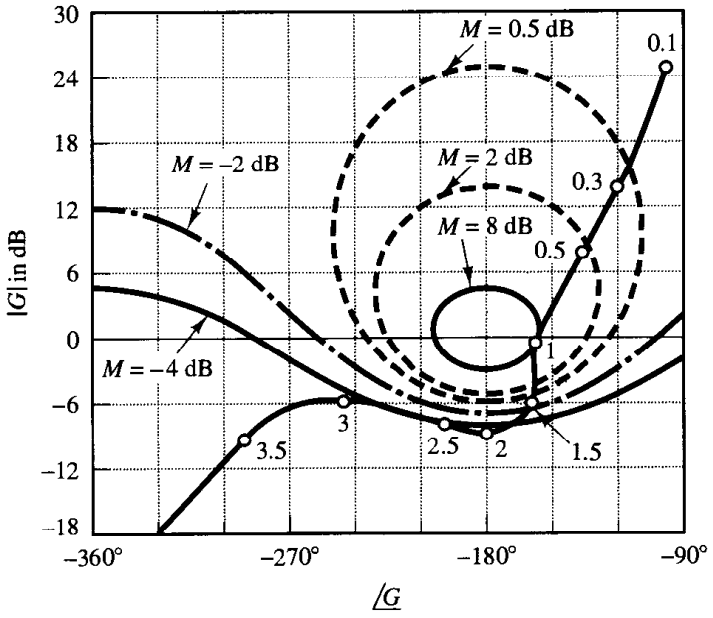

Figure 9–35
Log-magnitude versus phase plot of $G(j\omega)$ given by Equation (9–6).

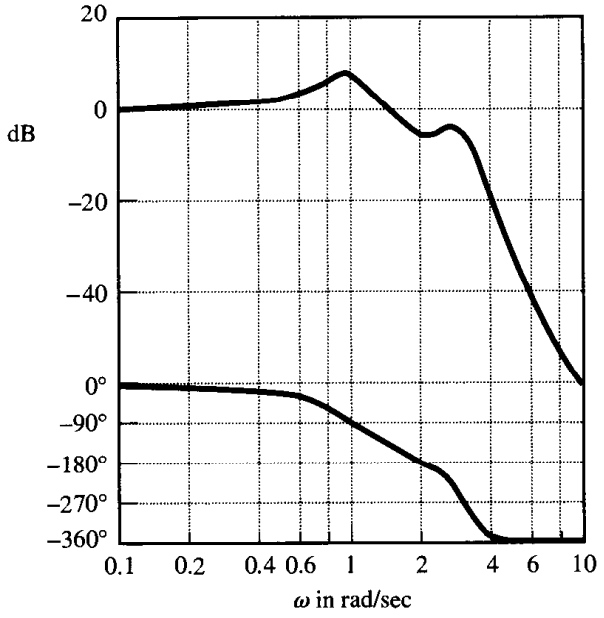

Figure 9–36
Bode diagram of $G(j\omega)/[1 + G(j\omega)]$, where $G(j\omega)$ is given by Equation (9–6).

Figure 9–36 shows the Bode diagram of the closed-loop transfer function. The magnitude curve of the closed-loop frequency response shows two resonant peaks. Note that such a case occurs when the closed-loop transfer function involves the product of two lightly damped second-order terms and the two corresponding resonant frequencies are sufficiently separated from each other. As a matter of fact, the closed-loop transfer function of this system can be written

$$\frac{C(s)}{R(s)} = \frac{G(s)}{1 + G(s)}$$

$$= \frac{9}{(s^2 + 0.487s + 1)(s^2 + 0.613s + 9)}$$

Clearly, the closed-loop transfer function is a product of two lightly damped second-order terms (the damping ratios are 0.243 and 0.102), and the two resonant frequencies are sufficiently separated.

A-9-5. Consider a unity-feedback system whose feedforward transfer function is given by

$$G(s) = \frac{1}{s^2}$$

It is desired to insert a series compensator so that the open-loop frequency-response curve is tangent to the M = 3-dB circle at ω = 3 rad/sec. The system is subjected to high-frequency noises and sharp cutoff is desired. Design an appropriate series compensator.

Solution. To stabilize the system, we may insert a proportional-plus-derivative type of compensator or a lead compensator. Since sharp cutoff is required, we choose a lead compensator. Consider the following lead compensator:

$$G_c(s) = K_c \frac{Ts + 1}{\alpha Ts + 1} \quad (\alpha < 1)$$

The compensated open-loop frequency-response curve must be tangent to the M = 3-dB locus. To minimize the additional gain K_c, we choose the tangent point to the 3-dB locus as shown in Figure 9–37. From Figure 9–37 we see that the lead compensator must provide about 45°. Then the necessary value of α is determined from

$$\sin 45° = \frac{1 - \alpha}{1 + \alpha}$$

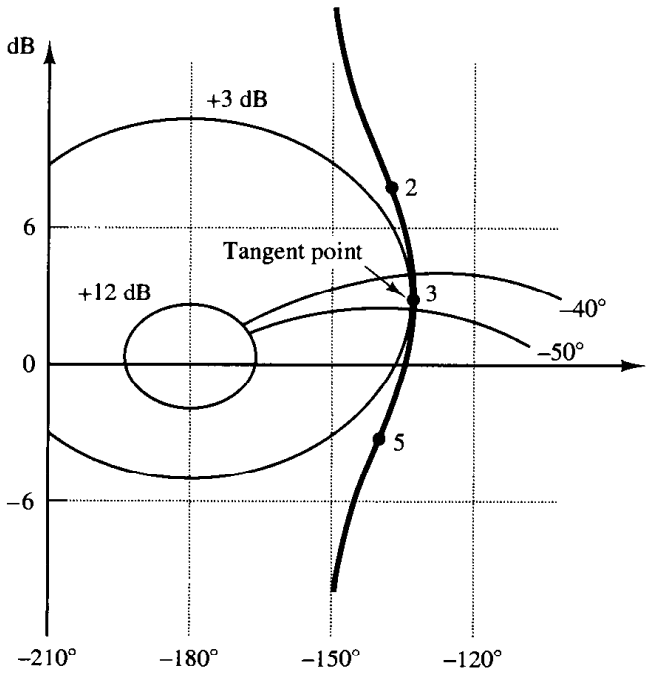

Figure 9–37
Nichols chart showing that the $G_c(j\omega)G(j\omega)$ locus is tangent to the M = 3-dB locus at ω = 3 rad/sec.

or $\alpha = 0.172 \doteq \frac{1}{6}$. Let us choose $\alpha = \frac{1}{6}$. Since it is required that the open-loop frequency-response curve $G_c(j\omega)G(j\omega)$ be tangent to the $M = 3$-dB locus at $\omega = 3$ rad/sec, we obtain

$$\begin{aligned} 20 \log |G_c(j\omega)G(j\omega)|_{\omega=3} &= 20 \log |G_c(j3)| + 20 \log |G(j3)| \\ &= 20 \log |G_c(j3)| + 20 \log \left|\frac{1}{9}\right| = 3 \text{ dB} \end{aligned}$$

or

$$20 \log |G_c(j3)| = 22.085 \text{ dB}$$

The two time constants T and αT of the lead compensator can be determined as follows: Noting that

$$\sqrt{\frac{1}{T} \cdot \frac{1}{\alpha T}} = 3$$

we have

$$\frac{1}{T} = \frac{3}{\sqrt{6}} = 1.225, \qquad \frac{1}{\alpha T} = 3\sqrt{6} = 7.348$$

From the Bode diagram as shown in Figure 9–38, we find the gain K_c to be 14.3 dB or 5.19. Thus, the designed compensator is given by

$$G_c(s) = 5.19 \frac{0.816s + 1}{0.136s + 1}$$

A-9-6. Consider the system shown in Figure 9–39. Design a lead compensator such that the closed-loop system will have the phase margin of 50° and gain margin of not less than 10 dB. Assume that

$$G_c(s) = K_c\alpha \left(\frac{Ts + 1}{\alpha Ts + 1}\right) \qquad (0 < \alpha < 1)$$

It is desired that the bandwidth of the closed-loop system be $1 \sim 2$ rad/sec. What are the values of M_r and ω_r of the compensated system?

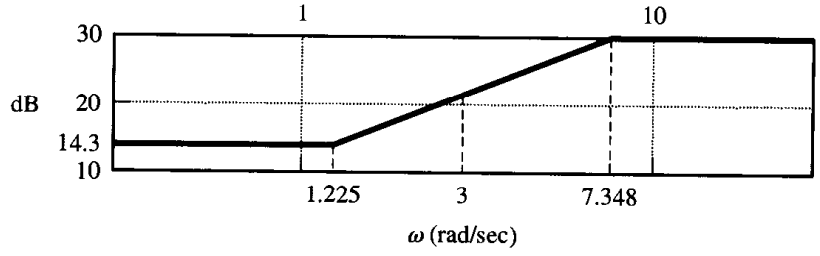

Figure 9–38
Bode diagram of the lead compensator designed in Problem A-9-5.

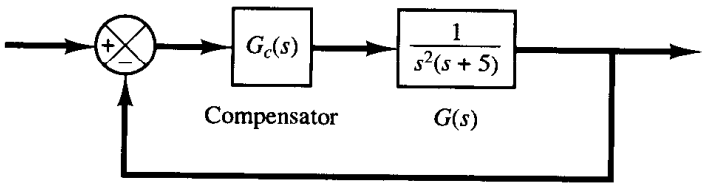

Figure 9–39
Closed-loop system.

Solution. Notice that

$$G_c(j\omega)G(j\omega) = K_c\alpha\left(\frac{Tj\omega + 1}{\alpha Tj\omega + 1}\right)\frac{0.2}{(j\omega)^2(0.2j\omega + 1)}$$

Since the bandwidth of the closed-loop system is close to the gain crossover frequency, we choose the gain crossover frequency to be 1 rad/sec. At $\omega = 1$, the phase angle of $G(j\omega)$ is 191.31°. Hence, the lead network needs to supply 50° + 11.31° = 61.31° at $\omega = 1$. Hence, α can be determined from

$$\sin\phi_m = \sin 61.31° = \frac{1 - \alpha}{1 + \alpha} = 0.8772$$

as follows:

$$\alpha = 0.06541$$

Noting that the maximum phase lead angle ϕ_m occurs at the geometric mean of the two corner frequencies, we have

$$\omega_m = \sqrt{\frac{1}{T}\frac{1}{\alpha T}} = \frac{1}{\sqrt{\alpha}T} = \frac{1}{\sqrt{0.06541}T} = \frac{3.910}{T} = 1$$

Thus,

$$\frac{1}{T} = \frac{1}{3.910} = 0.2558$$

and

$$\frac{1}{\alpha T} = \frac{0.2558}{0.06541} = 3.910$$

Hence,

$$G_c(j\omega)G(j\omega) = 0.06541K_c\frac{3.910j\omega + 1}{0.2558j\omega + 1}\frac{0.2}{(j\omega)^2(0.2j\omega + 1)}$$

or

$$\frac{G_c(j\omega)G(j\omega)}{0.06541K_c} = \frac{3.910j\omega + 1}{0.2558j\omega + 1}\frac{0.2}{(j\omega)^2(0.2j\omega + 1)}$$

A Bode diagram for $G_c(j\omega)G(j\omega)/(0.06541\ K_c)$ is shown in Figure 9–40. By simple calculations (or from the Bode diagram), we find that the magnitude curve must be raised by 2.306 dB so that the magnitude equals 0 dB at $\omega = 1$ rad/sec. Hence, we set

$$20\log 0.06541\ K_c = 2.306$$

or

$$0.06541\ K_c = 1.3041$$

which yields

$$K_c = 19.94$$

The magnitude and phase curves of the compensated system show that the system has the phase margin of 50° and gain margin of 16 dB. Hence, the design specifications are satisfied.

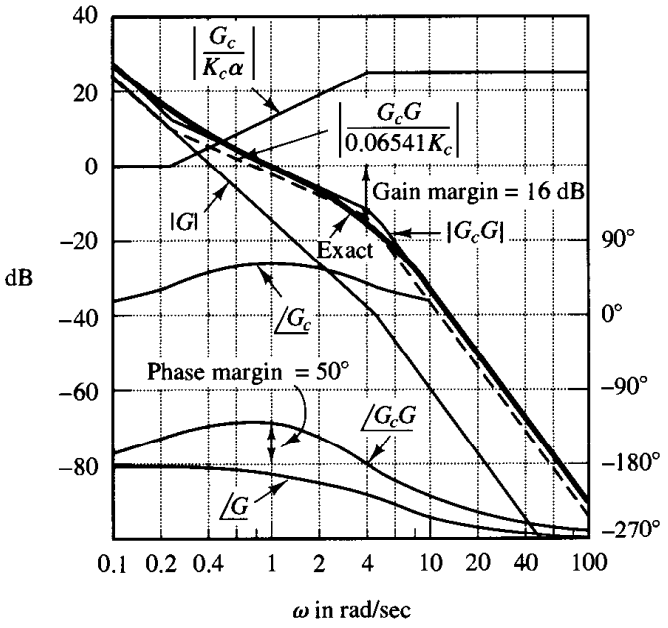

Figure 9–40
Bode diagram of the system shown in Figure 9–39.

Figure 9–41 shows the $G_c(j\omega)G(j\omega)$ locus superimposed on the Nichols chart. From this diagram, we find the bandwidth to be approximately 1.9 rad/sec. The values of M_r and ω_r are read from this diagram as follows:

$$M_r = 2.13 \text{ dB}, \qquad \omega_r = 0.58 \text{ rad/sec}$$

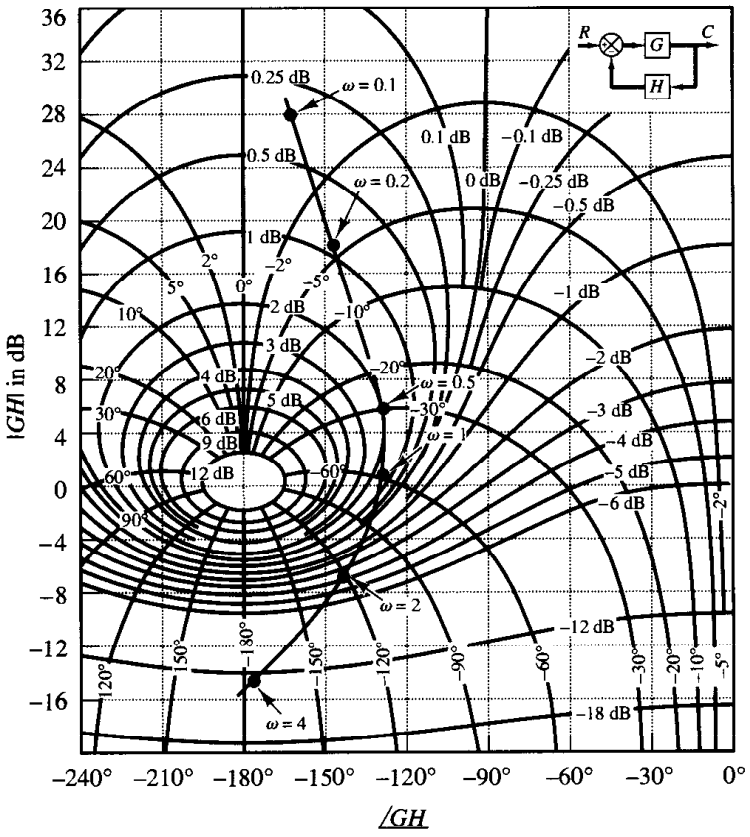

Figure 9–41
$G_c(j\omega)G(j\omega)$ locus superimposed on Nichols chart (Problem A-9-6).

A-9-7. Referring to Example 9–1, draw Nyquist plots of $G(j\omega)$, $G_1(j\omega)$, and $G_c(j\omega)G(j\omega)$ with MATLAB. (Compare the Nyquist plots obtained here with Figure 9–10.) Write a possible MATLAB program for drawing the Nyquist plots in one diagram. Note that $G(j\omega)$, $G_1(j\omega)$, and $G_c(j\omega)G(j\omega)$ are given by

$$G(j\omega) = \frac{4}{j\omega(j\omega + 2)}$$

$$G_1(j\omega) = \frac{40}{j\omega(j\omega + 2)}$$

$$G_c(j\omega)G(j\omega) = 41.7\frac{j\omega + 4.41}{j\omega + 18.4}\frac{4}{j\omega(j\omega + 2)}$$

Solution. A possible MATLAB program for this problem is given in MATLAB Program 9–5. The resulting Nyquist plots are shown in Figure 9–42.

MATLAB Program 9–5

```
%*****Nyquist plots in polar coordinates*****

num1 = [0   0   4];
den1 = [1   2   0];
num2 = [0   0   40];
den2 = [1   2   0];
num3 = [0   0   166.8   735.588];
den3 = [1   20.4   36.8   0];
w = 0.2:0.1:10;
ww = 1.5:0.1:10;
[re1,im1,w] = nyquist(num1,den1,w);
z1 = re1 + i*im1;
r1 = abs(z1);
theta1 = angle(z1);
polar(theta1,r1,'o')
hold on
[re2,im2,ww] = nyquist(num2,den2,ww);
z2 = re2 + i*im2;
r2 = abs(z2);
theta2 = angle(z2);
polar(theta2,r2,'o')
[re3,im3,ww] = nyquist(num3,den3,ww);
z3 = re3 + i*im3;
r3 = abs(z3);
theta3 = angle(z3);
polar(theta3,r3,'x')
title('Nyquist Plots of G(jw), G1(jw), and Gc(jw)G(jw)')
text(0.7,-8.8,'G(jw)')
text(-11.7,-8.7,'G1(jw)')
text(-6.6,-12.3,'Gc(jw)G(jw)')
```

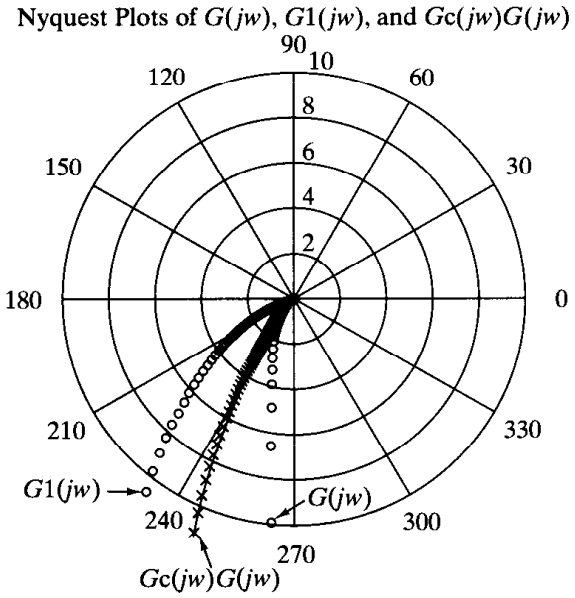

Figure 9–42
Nyquist plots of $G(j\omega)$, $G_1(j\omega)$, and $G_c(j\omega)G(j\omega)$.

A-9-8. Consider the system shown in Figure 9–43(a). Design a compensator such that the closed-loop system will satisfy the following requirements:

$$\text{Static velocity error constant} = 20\ \text{sec}^{-1}$$

$$\text{Phase margin} = 50°$$

$$\text{Gain margin} \geqq 10\ \text{dB}$$

Solution. To satisfy the requirements, we shall try a lead compensator $G_c(s)$ of the form

$$G_c(s) = K_c\alpha\frac{Ts + 1}{\alpha Ts + 1}$$

$$= K_c\frac{s + \dfrac{1}{T}}{s + \dfrac{1}{\alpha T}}$$

(If the lead compensator does not work, then we shall employ a compensator of different form.) The compensated system is shown in Figure 9–43(b).

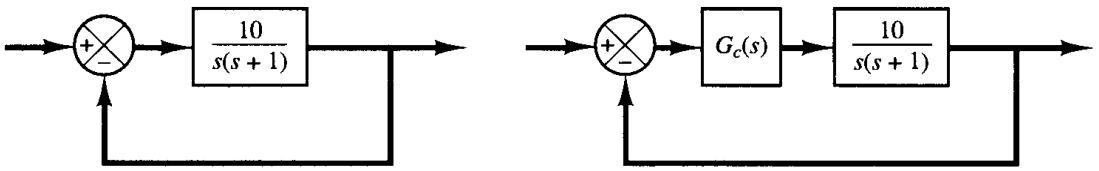

(a) (b)

Figure 9–43
(a) Control system; (b) compensated system.

Define

$$G_1(s) = KG(s) = \frac{10K}{s(s + 1)}$$

where $K = K_c\alpha$.

The first step in the design is to adjust the gain K to meet the steady-state performance specification or to provide the required static velocity error constant. Since the static velocity error constant K_v is given as 20 sec^{-1}, we have

$$\begin{aligned} K_v &= \lim_{s\to 0} sG_c(s)G(s) \\ &= \lim_{s\to 0} s\frac{Ts + 1}{\alpha Ts + 1} G_1(s) \\ &= \lim_{s\to 0} \frac{s10K}{s(s + 1)} \\ &= 10K = 20 \end{aligned}$$

or

$$K = 2$$

With $K = 2$, the compensated system will satisfy the steady-state requirement.

We shall next plot the Bode diagram of

$$G_1(s) = \frac{20}{s(s + 1)}$$

MATLAB Program 9–6 produces the Bode diagram shown in Figure 9–44. From this plot, the phase margin is found to be 14°. The gain margin is $+\infty$ dB.

MATLAB Program 9–6

```
num = [0   0   20];
den = [1   1   0];
w = logspace(-1,2,100);
bode(num,den,w)
subplot(2,1,1);
title('Bode Diagram of G1(s) = 20/[s(s + 1)]')
```

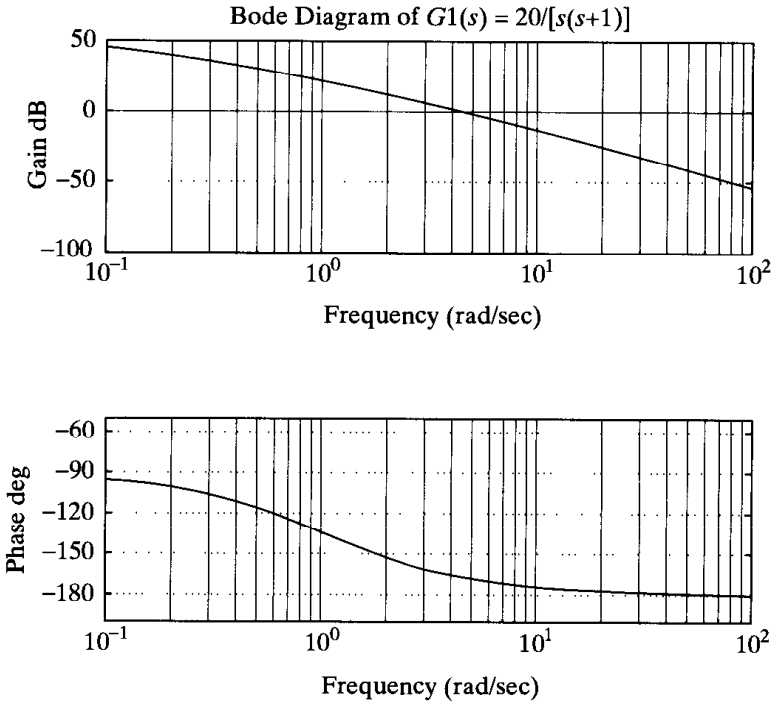

Figure 9–44
Bode diagram of $G_1(s)$.

Since the specification calls for a phase margin of 50°, the additional phase lead necessary to satisfy the phase-margin requirement is 36°. A lead compensator can contribute this amount.

Noting that the addition of a lead compensator modifies the magnitude curve in the Bode diagram, we realize that the gain crossover frequency will be shifted to the right. We must offset the increased phase lag of $G_1(j\omega)$ due to this increase in the gain crossover frequency. Taking the shift of the gain crossover frequency into consideration, we may assume that ϕ_m, the maximum phase lead required, is approximately 41°. (This means that approximately 5° has been added to compensate for the shift in the gain crossover frequency.) Since

$$\sin \phi_m = \frac{1 - \alpha}{1 + \alpha}$$

$\phi_m = 41°$ corresponds to $\alpha = 0.2077$. Note that $\alpha = 0.21$ corresponds to $\phi_m = 40.76°$. Whether we choose $\phi_m = 41°$ or $\phi_m = 40.76°$ does not make much difference in the final solution. Hence, let us choose $\alpha = 0.21$.

Once the attenuation factor α has been determined on the basis of the required phase-lead angle, the next step is to determine the corner frequencies $\omega = 1/T$ and $\omega = 1/(\alpha T)$ of the lead compensator. Notice that the maximum phase-lead angle ϕ_m occurs at the geometric mean of the two corner frequencies, or $\omega = 1/(\sqrt{\alpha}T)$.

The amount of the modification in the magnitude curve at $\omega = 1/(\sqrt{\alpha}T)$ due to the inclusion of the term $(Ts + 1)/(\alpha Ts + 1)$ is

$$\left|\frac{1 + j\omega T}{1 + j\omega\alpha T}\right|_{\omega = \frac{1}{\sqrt{\alpha}T}} = \left|\frac{1 + j\dfrac{1}{\sqrt{\alpha}}}{1 + j\alpha\dfrac{1}{\sqrt{\alpha}}}\right| = \frac{1}{\sqrt{\alpha}}$$

Note that

$$\frac{1}{\sqrt{\alpha}} = \frac{1}{\sqrt{0.21}} = 6.7778 \text{ dB}$$

We need to find the frequency point where, when the lead compensator is added, the total magnitude becomes 0 dB.

From Figure 9–44 we see that the frequency point where the magnitude of $G_1(j\omega)$ is -6.7778 dB occurs between $\omega = 1$ and 10 rad/sec. Hence, we plot a new Bode diagram of $G_1(j\omega)$ in the frequency range between $\omega = 1$ and 10 to locate the exact point where $G_1(j\omega) = -6.7778$ dB. MATLAB Program 9–7 produces the Bode diagram in this frequency range, which is shown in

MATLAB Program 9–7

```
num = [0   0   20];
den = [1   1   0];
w = logspace(0,1,100);
bode(num,den,w)
subplot(2,1,1);
title('Bode Diagram of G1(s) = 20/[s(s + 1)]')
```

Figure 9–45. From this diagram, we find the frequency point where $|G_1(j\omega)| = -6.7778$ dB occurs at $\omega = 6.5$ rad/sec. Let us select this frequency to be the new gain crossover frequency, or $\omega_c = 6.5$ rad/sec. Noting that this frequency corresponds to $1/(\sqrt{\alpha}T)$, or

$$\omega_c = \frac{1}{\sqrt{\alpha}T}$$

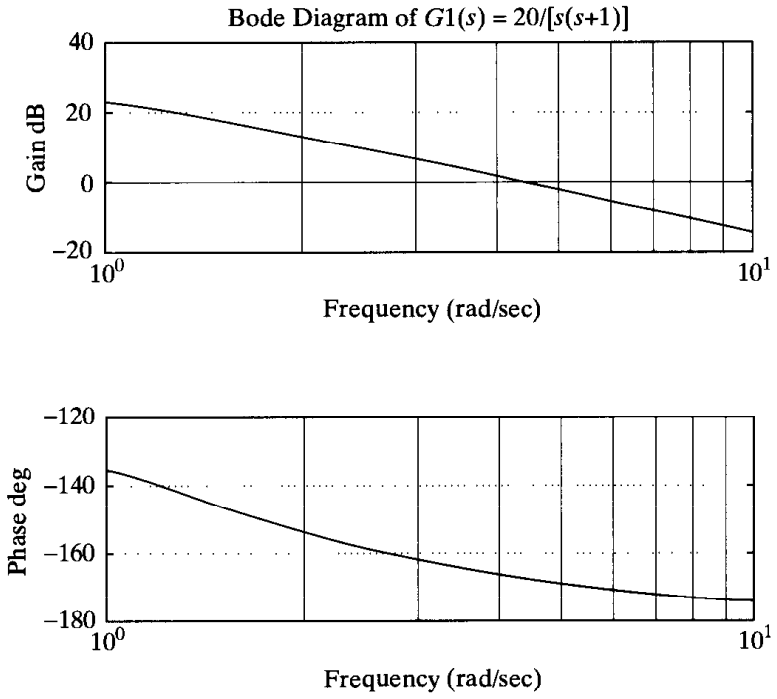

Figure 9–45
Bode diagram of $G_1(s)$.

we obtain

$$\frac{1}{T} = \omega_c\sqrt{\alpha} = 6.5\sqrt{0.21} = 2.9787$$

and

$$\frac{1}{\alpha T} = \frac{\omega_c}{\sqrt{\alpha}} = \frac{6.5}{\sqrt{0.21}} = 14.1842$$

The lead compensator thus determined is

$$G_c(s) = K_c\frac{s + 2.9787}{s + 14.1842} = K_c\alpha\frac{0.3357s + 1}{0.07050s + 1}$$

where K_c is determined as

$$K_c = \frac{K}{\alpha} = \frac{2}{0.21} = 9.5238$$

Thus, the transfer function of the compensator becomes

$$G_c(s) = 9.5238\frac{s + 2.9787}{s + 14.1842} = 2\frac{0.3357s + 1}{0.07050s + 1}$$

MATLAB Program 9–8 produces the Bode diagram of this lead compensator, which is shown in Figure 9–46.

MATLAB Program 9–8

```
numc = [9.5238   28.3685];
denc = [1   14.1842];
w = logspace(-1,3,100);
bode(numc,denc,w)
subplot(2,1,1);
title('Bode Diagram of Gc(s) = 9.5238(s + 2.9787)/(s + 14.1842)')
```

The open-loop transfer function of the designed system is

$$G_c(s)G(s) = 9.5238\frac{s + 2.9787}{s + 14.1842}\frac{10}{s(s + 1)}$$

$$= \frac{95.238s + 283.6854}{s^3 + 15.1842s^2 + 14.1842s}$$

MATLAB Program 9–9 will produce the Bode diagram of $G_c(s)G(s)$, which is shown in Figure 9–47.

From Figure 9–47 it is clearly seen that the phase margin is approximately 50° and the gain margin is $+\infty$ dB. Since the static velocity error constant K_v is 20 $\sec^{-1}$, all the specifications are met. Before we conclude this problem, we need to check the transient-response characteristics.

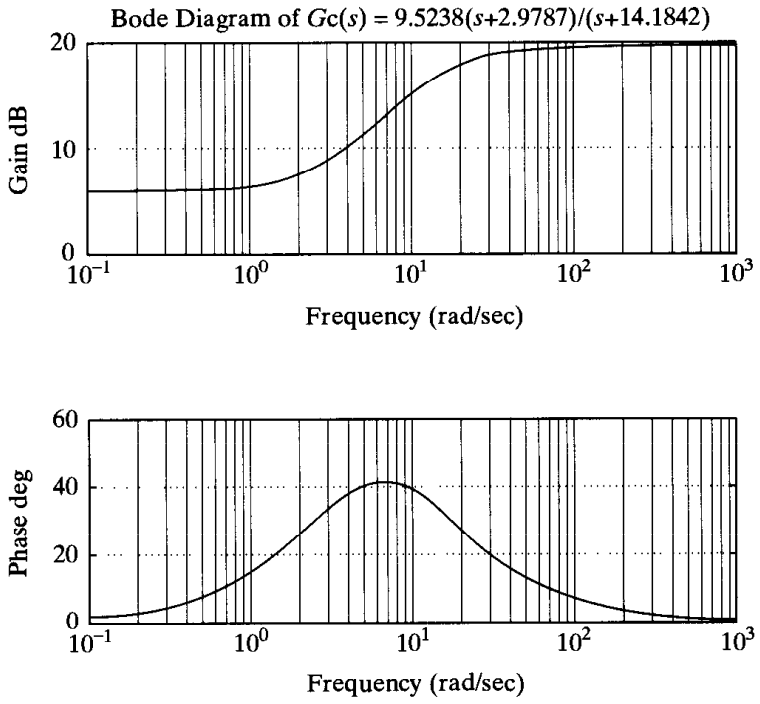

Figure 9–46
Bode diagram of $G_c(s)$.

Unit-step response: We shall compare the unit-step response of the compensated system and that of the original uncompensated system.

MATLAB Program 9–9

```
num = [0   0   95.238   283.6854];
den = [1   15.1842   14.1842   0];
w = logspace(-1,3,100);
bode(num,den,w)
subplot(2,1,1);
title('Bode Diagram of Gc(s)G(s)')
```

The closed-loop transfer function of the original uncompensated system is

$$\frac{C(s)}{R(s)} = \frac{10}{s^2 + s + 10}$$

The closed-loop transfer function of the compensated system is

$$\frac{C(s)}{R(s)} = \frac{95.238s + 283.6854}{s^3 + 15.1842s^2 + 109.4222s + 283.6854}$$

MATLAB Program 9–10 produces the unit-step responses of the uncompensated and compensated systems. The resulting response curves are shown in Figure 9–48. Clearly, the compensated system exhibits a satisfactory response. Note that the closed-loop zero and poles are located as follows:

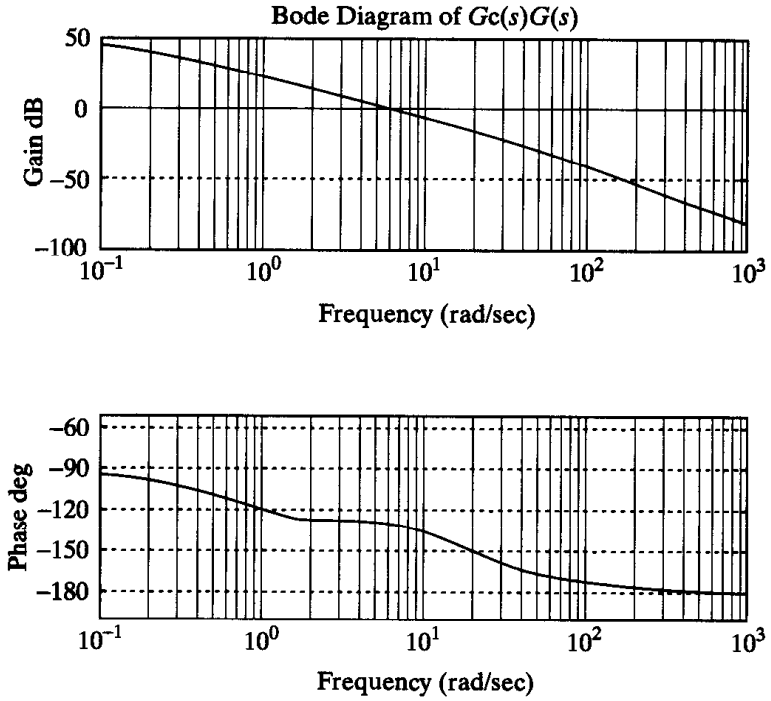

Figure 9–47
Bode diagram of $G_c(s)G(s)$.

MATLAB Program 9–10

```
%*****Unit-step responses*****

num1 = [0   0   10];
den1 = [1   1   10];
num2 = [0   0   95.238   283.6854];
den2 = [1   15.1842   109.4222   283.6854];
t = 0:0.01:6;
[c1,x1,t] = step(num1,den1,t);
[c2,x2,t] = step(num2,den2,t);
plot(t,c1,'.',t,c2,'-')
grid
title('Unit-Step Responses of Compensated and Uncompensated Systems')
xlabel('t Sec')
ylabel('Outputs')
text(1.1,0.5,'Compensated system')
text(1.7,1.46,'Uncompensated system')
```

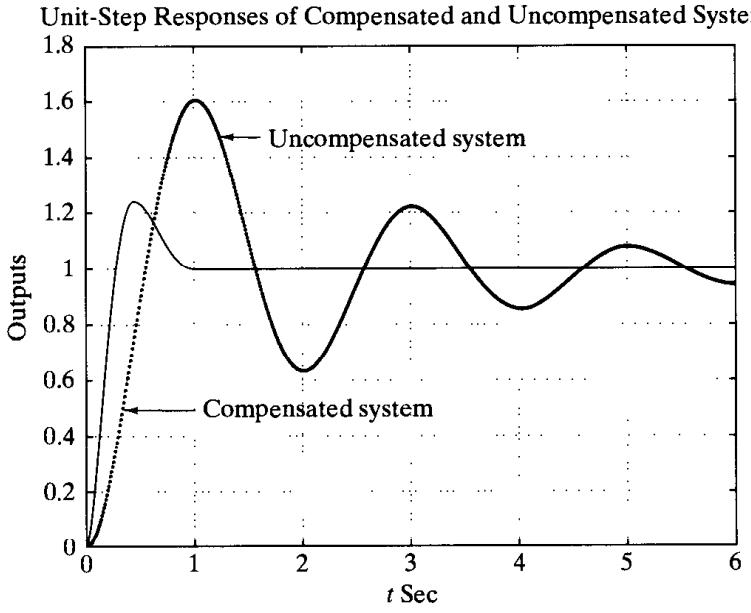

Figure 9–48
Unit-step responses of the compensated and uncompensated systems.

Zero at $s = -2.9787$

Poles at $s = -5.2270 \pm j5.7141$, $s = -4.7303$

Unit-ramp response: It is worthwhile to check the unit-ramp response of the compensated system. Since $K_v = 20\,\text{sec}^{-1}$, the steady-state error following the unit-ramp input will be $1/K_v = 0.05$. The static velocity error constant of the uncompensated system is $10\,\text{sec}^{-1}$. Hence, the original uncompensated system will have twice as large a steady-state error in following the unit-ramp input.

MATLAB Program 9–11 produces the unit-ramp response curves. [Note that the unit-ramp response is obtained as the unit-step response of $C(s)/sR(s)$.] The resulting curves are shown in Figure 9–49. The compensated system has a steady-state error equal to one-half that of the original uncompensated system.

A-9-9. Consider the unity feedback system whose open-loop transfer function is

$$G(s) = \frac{K}{s(s+1)(s+4)}$$

Design a compensator $G_c(s)$ such that the static velocity error constant is $10\,\text{sec}^{-1}$, the phase margin is 50°, and the gain margin is 10 dB or more.

Solution. We shall design a lag–lead compensator of the form

$$G_c(s) = K_c \frac{\left(s + \frac{1}{T_1}\right)\left(s + \frac{1}{T_2}\right)}{\left(s + \frac{\beta}{T_1}\right)\left(s + \frac{1}{\beta T_2}\right)}$$

MATLAB Program 9–11

```
%*****Unit-ramp responses*****

num1 = [0   0   0   10];
den1 = [1   1   10   0];
num2 = [0   0   0   95.238   283.6854];
den2 = [1   15.1842   109.4222   283.6854   0];
t = 0:0.01:3;
[c1,x1,t] = step(num1,den1,t);
[c2,x2,t] = step(num2,den2,t);
plot(t,c1,'.',t,c2,'-',t,t,'- -')
grid
title('Unit-Ramp Responses of Compensated and Uncompensated Systems')
xlabel('t Sec')
ylabel('Outputs')
text(0.07,1.3,'Compensated system')
text(1.2,0.65,'Uncompensated system')
```

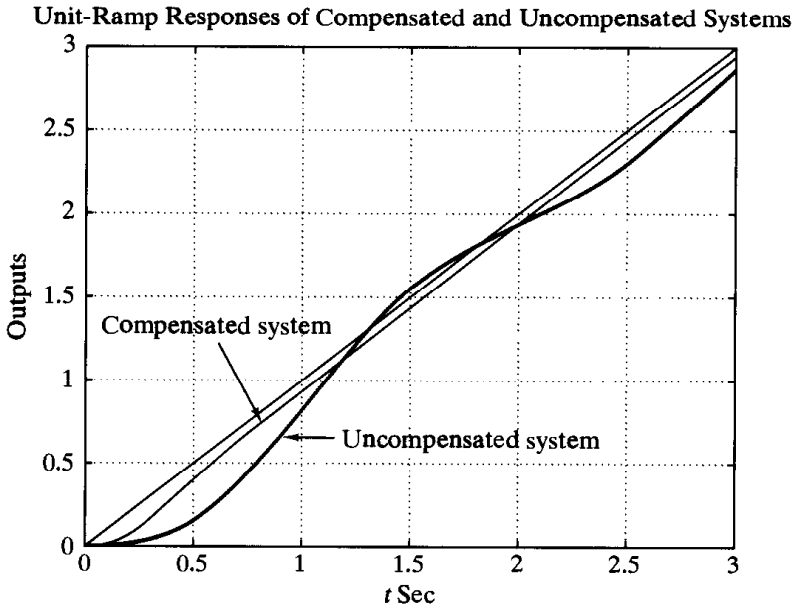

Figure 9–49
Unit-ramp responses of the compensated and uncompensated systems.

Then the open-loop transfer function of the compensated system is $G_c(s)G(s)$. Since the gain K of the plant is adjustable, let us assume that $K_c = 1$. Then $\lim_{s\to 0} G_c(s) = 1$. From the requirement on the static velocity error constant, we obtain

$$K_v = \lim_{s\to 0} sG_c(s)G(s) = \lim_{s\to 0} sG_c(s)\frac{K}{s(s+1)(s+4)}$$

$$= \frac{K}{4} = 10$$

Hence,

$$K = 40$$

We shall first plot a Bode diagram of the uncompensated system with $K = 40$. MATLAB Program 9–12 may be used to plot this Bode diagram. The diagram obtained is shown in Figure 9–50.

MATLAB Program 9–12

```
num = [0   0   0   40];
den = [1   5   4   0];
w = logspace(-1,1,100);
bode(num,den,w)
subpole(2,1,1);
title('Bode Diagram of G(s) = 40/[s(s + 1)(s + 4)]')
```

From Figure 9–50, the phase margin of the uncompensated system is found to be $-16°$, which indicates that the uncompensated system is unstable. The next step in the design of a lag–lead compensator is to choose a new gain crossover frequency. From the phase-angle curve for $G(j\omega)$, we notice that the phase crossover frequency is $\omega = 2$ rad/sec. We may choose the new gain crossover frequency to be 2 rad/sec so that the phase-lead angle required at $\omega = 2$ rad/sec is about 50°. A single lag–lead compensator can provide this amount of phase-lead angle quite easily.

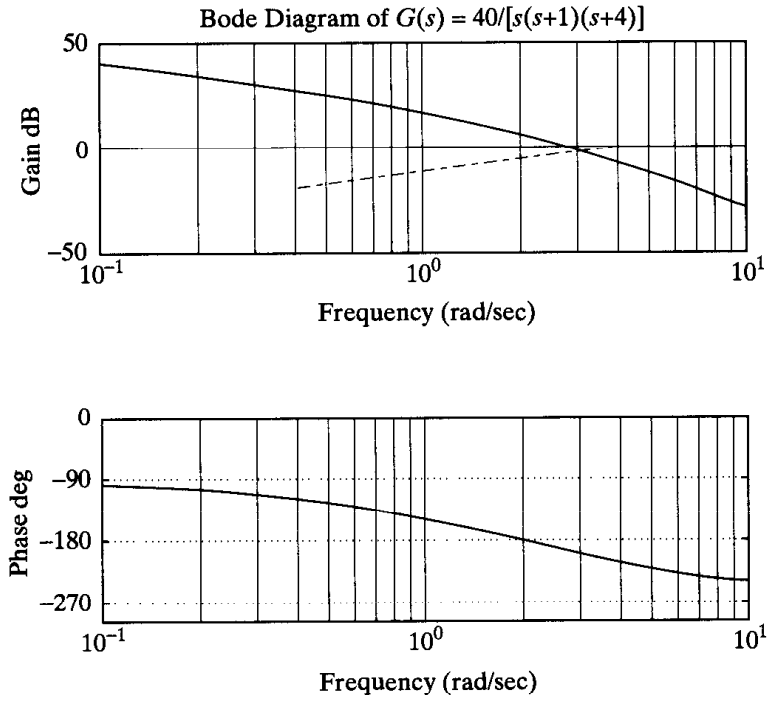

Figure 9–50
Bode diagram of $G(s) = 40/[s(s + 1)(s + 4)]$.

Once we choose the gain crossover frequency to be 2 rad/sec, we can determine the corner frequencies of the phase-lag portion of the lag–lead compensator. Let us choose the corner frequency $\omega = 1/T_2$ (which corresponds to the zero of the phase-lag portion of the compensator) to be 1 decade below the new gain crossover frequency, or at $\omega = 0.2$ rad/sec. For another corner frequency $\omega = 1/(\beta T_2)$, we need the value of β. The value of β can be determined from the consideration of the lead portion of the compensator, as shown next.

For the lead compensator, the maximum phase-lead angle ϕ_m is given by

$$\sin \phi_m = \frac{\beta - 1}{\beta + 1}$$

Notice that $\beta = 10$ corresponds to $\phi_m = 54.9°$. Since we need a 50° phase margin, we may choose $\beta = 10$. (Note that we will be using several degrees less than the maximum angle, 54.9°.) Thus,

$$\beta = 10$$

Then the corner frequency $\omega = 1/(\beta T_2)$ (which corresponds to the pole of the phase-lag portion of the compensator) becomes

$$\omega = 0.02$$

The transfer function of the phase-lag portion of the lag–lead compensator becomes

$$\frac{s + 0.2}{s + 0.02} = 10\left(\frac{5s + 1}{50s + 1}\right)$$

The phase-lead portion can be determined as follows: Since the new gain crossover frequency is $\omega = 2$ rad/sec, from Figure 9–50, $|G(j2)|$ is found to be 6 dB. Hence, if the lag–lead compensator contributes -6 dB at $\omega = 1$ rad/sec, then the new gain crossover frequency is as desired. From this requirement, it is possible to draw a straight line of slope 20 dB/decade passing through the point (-6 dB, 2 rad/sec). (Such a line has been manually drawn on Figure 9–50.) The intersections of this line and the 0-dB line and -20-dB line determine the corner frequencies. From this consideration, the corner frequencies for the lead portion can be determined as $\omega = 0.4$ rad/sec and $\omega = 4$ rad/sec. Thus, the transfer function of the lead portion of the lag–lead compensator becomes

$$\frac{s + 0.4}{s + 4} = \frac{1}{10}\left(\frac{2.5s + 1}{0.25s + 1}\right)$$

Combining the transfer functions of the lag and lead portions of the compensator, we can obtain the transfer function $G_c(s)$ of the lag–lead compensator. Since we chose $K_c = 1$, we have

$$G_c(s) = \frac{s + 0.4}{s + 4}\frac{s + 0.2}{s + 0.02} = \frac{(2.5s + 1)(5s + 1)}{(0.25s + 1)(50s + 1)}$$

The Bode diagram of the lag–lead compensator $G_c(s)$ can be obtained by entering MATLAB Program 9–13 into the computer. The resulting plot is shown in Figure 9–51.

MATLAB Program 9–13

```
numc = [1   0.6   0.08];
denc = [1   4.02   0.08];
bode(numc,denc)
subplot(2,1,1);
title('Bode Diagram of Lag–Lead Compensator')
```

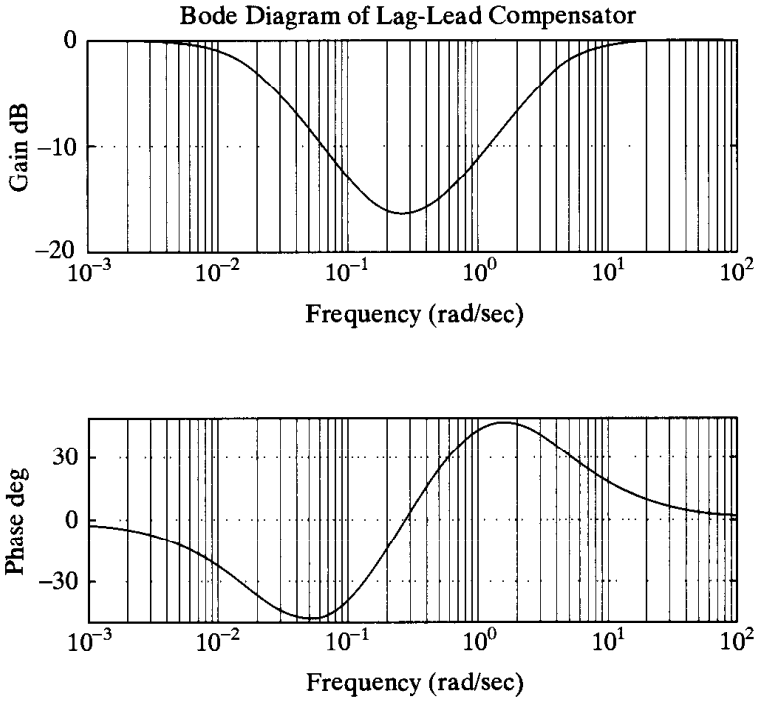

Figure 9–51
Bode diagram of the designed lag–lead compensator.

The open-loop transfer function of the compensated system is

$$G_c(s)G(s) = \frac{(s + 0.4)(s + 0.2)}{(s + 4)(s + 0.02)} \frac{40}{s(s + 1)(s + 4)}$$

$$= \frac{40s^2 + 24s + 3.2}{s^5 + 9.02s^4 + 24.18s^3 + 16.48s^2 + 0.32s}$$

Using MATLAB Program 9–14 the magnitude and phase-angle curves of the designed open-loop transfer function $G_c(s)G(s)$ can be obtained as shown in Figure 9–52. Note that the denominator polynomial den was obtained using the conv command, as follows:

```
a = [1   4.02   0.08];
b = [1   5   4   0];
conv(a,b)

ans =

    1.0000   9.0200   24.1800   16.4800   0.320000   0
```

From Figure 9–52, we see that the actual gain crossover frequency is slightly shifted from 2 rad/sec to a lower value. The actual gain crossover frequency can be found by plotting the Bode diagram in the region $1 \leq \omega \leq 10$. It is found to be $\omega = 1.86$ rad/sec. [Such a small shift of the gain crossover frequency from the assumed gain crossover frequency (2 rad/sec in this case) always occurs in the present method of design.]

```
MATLAB Program 9-14

num1 = [0   0   0   40   24   3.2];
den1 = [1   9.02   24.18   16.48   0.32   0];
bode(num1,den1)
subplot(2,1,1);
title('Bode Diagram of Gc(s)G(s)')
```

Since the phase margin of the compensated system is 50°, the gain margin is 12.5 dB, and the static velocity error constant is 10 sec^{-1}, all the requirements are met.

Figure 9–53 shows the Nyquist plots of $G(j\omega)$ (uncompensated case) and $G_c(j\omega)G(j\omega)$ (compensated case). MATLAB Program 9–15 was used to obtain Figure 9–53.

We shall next investigate the transient-response characteristics of the designed system.

Unit-step response: Noting that

$$G_c(s)G(s) = \frac{40(s + 0.4)(s + 0.2)}{(s + 4)(s + 0.02)s(s + 1)(s + 4)}$$

we have

$$\frac{C(s)}{R(s)} = \frac{G_c(s)G(s)}{1 + G_c(s)G(s)}$$

$$= \frac{40(s + 0.4)(s + 0.2)}{(s + 4)(s + 0.02)s(s + 1)(s + 4) + 40(s + 0.4)(s + 0.2)}$$

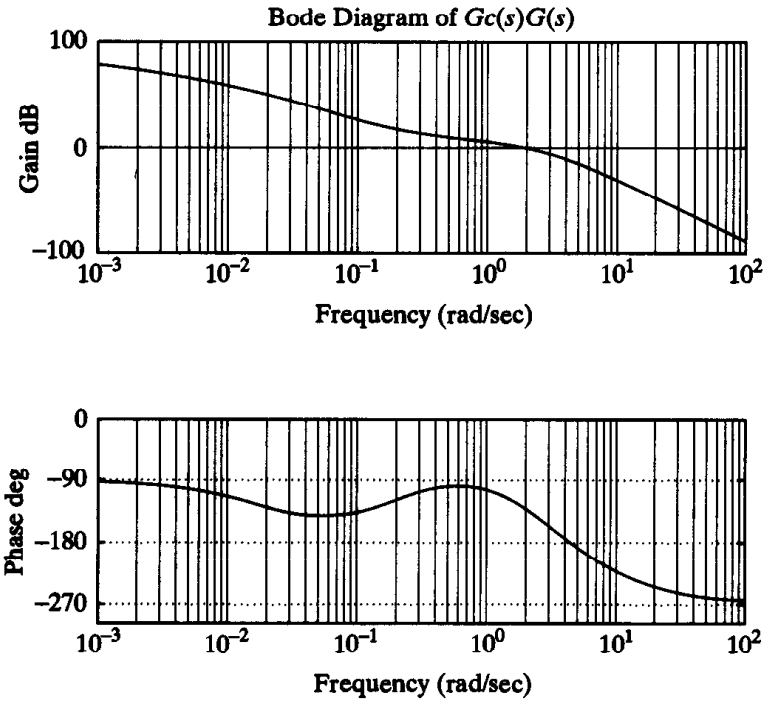

Figure 9–52
Bode diagram of the open-loop transfer function $G_c(s)G(s)$ of the compensated system.

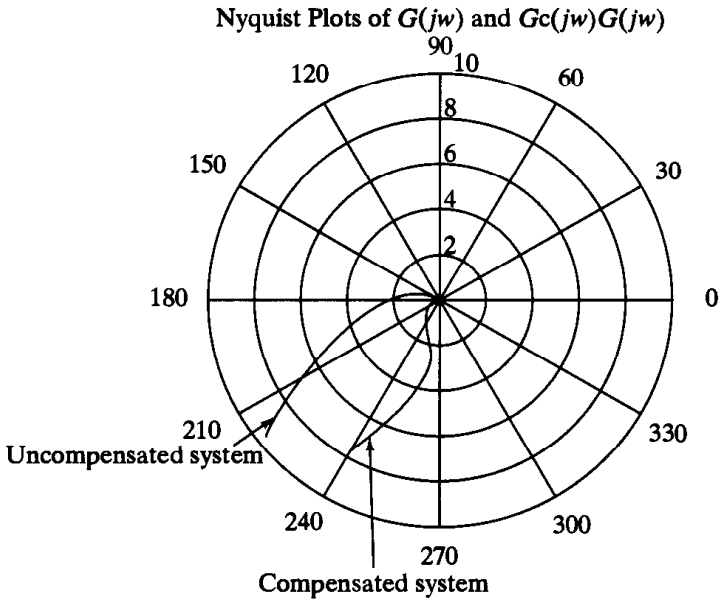

Figure 9–53
Nyquist plots of $G(j\omega)$ and $G_c(j\omega)G(j\omega)$.

MATLAB Program 9–15

```
%*****Nyquist plots*****

num0 = [0   0   0   40];
den0 = [1   5   4   0];
num1 = [0   0   0   40   24   3.2];
den1 = [1   9.02   24.18   16.48   0.32   0];
w = 0.8:0.02:10;
ww = 0.2:0.02:10;
[re0,im0,w] = nyquist(num0,den0,w);
z0 = re0 + i*im0;
r0 = abs(z0);
theta0 = angle(z0);
polar(theta0,r0)
hold on
[re1,im1,ww] = nyquist(num1,den1,ww);
z1 = re1 + i*im1;
r1 = abs(z1);
theta1 = angle(z1);
polar(theta1,r1)
text(-8, -12.7,'Compensated system')
text(-18.8, -7,'Uncompensated system')
title('Nyquist Plots of G(jw) and Gc(jw)G(jw)')
```

To determine the denominator polynomial with MATLAB, we may proceed as follows: Define

$$a(s) = (s + 4)(s + 0.02) = s^2 + 4.02s + 0.08$$

$$b(s) = s(s + 1)(s + 4) = s^3 + 5s^2 + 4s$$

$$c(s) = 40(s + 0.4)(s + 0.2) = 40s^2 + 24s + 3.2$$

Then we have

```
a = [1   4.02   0.08]
b = [1   5   4   0]
c = [40   24   3.2]
```

Using the following MATLAB program, we obtain the denominator polynomial.

```
a = [1   4.02   0.08];
b = [1   5   4   0];
c = [40   24   3.2];
p = [conv(a,b)] + [0   0   0   c]
p =
    1.0000   9.0200   24.1800   56.4800   24.3200   3.2000
```

MATLAB Program 9–16 is used to obtain the unit-step response of the compensated system. The resulting unit-step response curve is shown in Figure 9–54. (Note that the uncompensated system is unstable.)

MATLAB Program 9–16

```
%*****Unit-step response****

num = [0   0   0   40   24   3.2];
den = [1   9.02   24.18   56.48   24.32   3.2];
t = 0:0.2:40;
step(num,den,t)
grid
title('Unit-Step Response of Compensated System')
```

Unit-ramp response: The unit-ramp response of this system may be obtained by entering MATLAB Program 9–17 into the computer. Here we converted the unit-ramp response of $G_cG/(1 + G_cG)$ into the unit-step response of $G_cG/[s(1 + G_cG)]$. The unit-ramp response curve obtained using this program is shown in Figure 9–55.

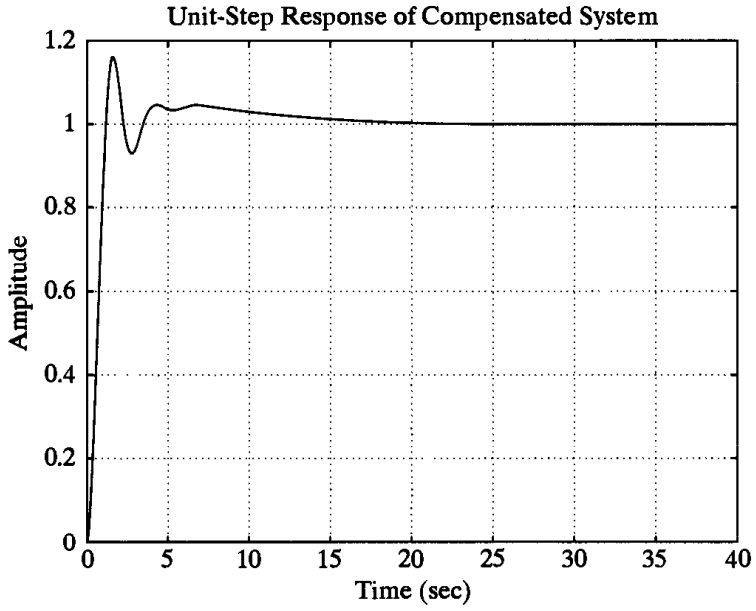

Figure 9–54
Unit-step response curve of the compensated system.

MATLAB Program 9–17

```
%*****Unit-ramp response*****

num = [0   0   0   0   40   24   3.2];
den = [1   9.02   24.18   56.48   24.32   3.2   0];
t = 0:0.05:20;
c = step(num,den,t);
plot(t,c,'-',t,t,'.')
grid
title('Unit-Ramp Response of Compensated System')
xlabel('Time (sec)')
ylabel('Amplitude')
```

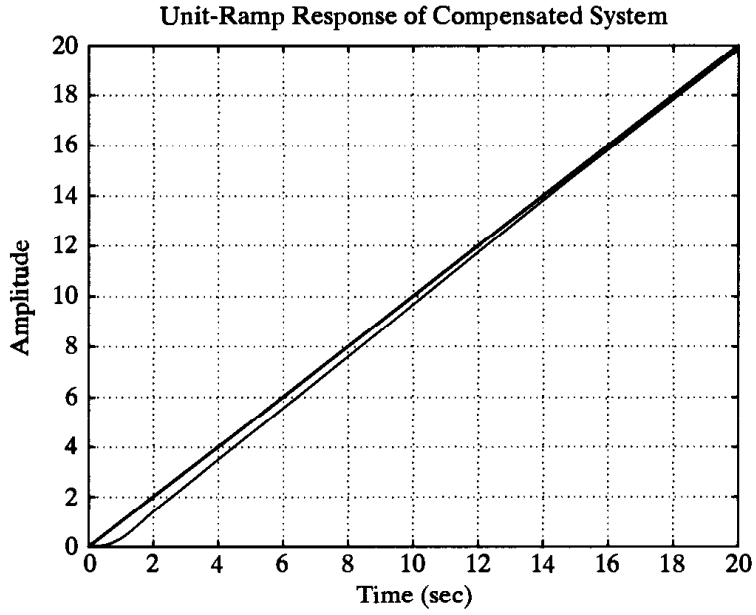

Figure 9–55
Unit-ramp response of the compensated system.

PROBLEMS

B-9-1. Draw Bode diagrams of the lead network and lag network shown in Figures 9–56 (a) and (b), respectively.

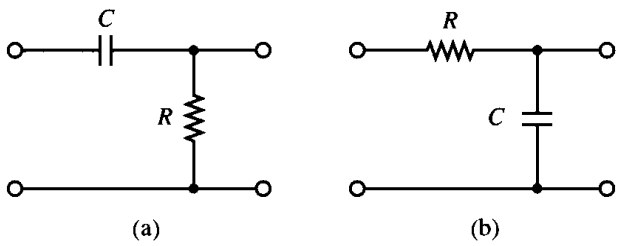

Figure 9–56 (a) Lead network; (b) lag network.

B-9-2. Draw Bode diagrams of the PI controller given by

$$G_c(s) = 5\left(1 + \frac{1}{2s}\right)$$

and the PD controller given by

$$G_c(s) = 5(1 + 0.5s)$$

B-9-3. Consider a PID controller given by

$$G_c(s) = 30.3215\frac{(s + 0.65)^2}{s}$$

Draw a Bode diagram of the controller.

B-9-4. Figure 9–57 shows a block diagram of a space vehicle attitude control system. Determine the proportional gain constant K_p and derivative time T_d such that the bandwidth of the closed-loop system is 0.4 to 0.5 rad/sec. (Note that the closed-loop bandwidth is close to the gain crossover frequency.) The system must have an adequate phase margin. Plot both the open-loop and closed-loop frequency response curves on Bode diagrams.

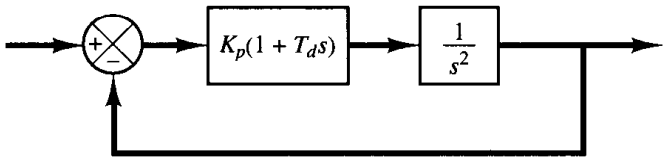

Figure 9–57 Block diagram of space vehicle attitude control system.

B-9-5. Referring to the closed-loop system shown in Figure 9–58, design a lead compensator $G_c(s)$ such that the phase margin is 45°, gain margin is not less than 8 dB, and the static velocity error constant K_v is 4.0 sec^{-1}. Plot unit-step and unit-ramp response curves of the compensated system with MATLAB.

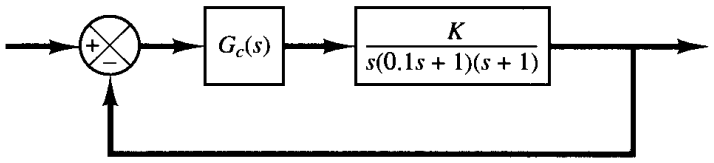

Figure 9–58 Closed-loop system

B-9-6. Consider the system shown in Figure 9–59. Design a compensator such that the static velocity error constant K_v is 50 sec^{-1}, phase margin is 50°, and gain margin not less than 8 dB. Plot unit-step and unit-ramp response curves of the compensated and uncompensated systems with MATLAB.

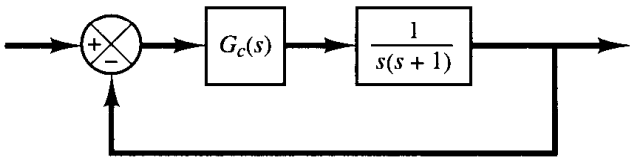

Figure 9–59 Control system.

B-9-7. Consider the system shown in Figure 9–60. Design a compensator such that the static velocity error constant is 4 sec^{-1}, phase margin is 50°, and gain margin is 10 dB or more. Plot unit-step and unit-ramp response curves of the compensated system with MATLAB. Also, draw a Nyquist plot of the compensated system with MATLAB.

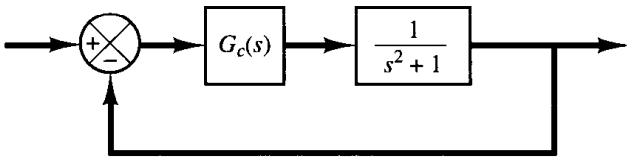

Figure 9–60 Control system.

B-9-8. Consider the system shown in Figure 9–61. It is desired to design a compensator such that the static velocity

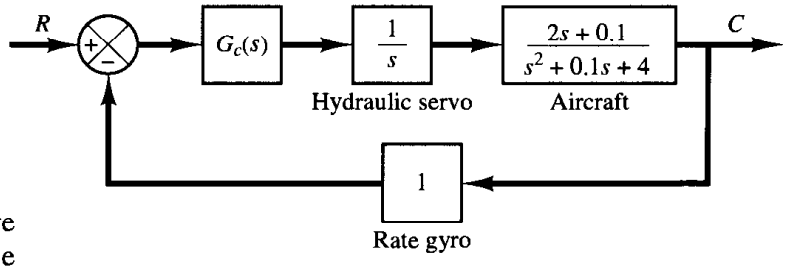

Figure 9–61 Control system.

error constant is 4 $\sec^{-1}$, phase margin is 50°, and gain margin is 8 dB or more. Plot the unit-step and unit-ramp response curves of the compensated system with MATLAB.

B-9-9. Consider the system shown in Figure 9–62. Design a lag–lead compensator such that the static velocity error constant K_v is 20 $\sec^{-1}$, phase margin is 60°, and gain margin is not less than 8 dB. Plot the unit-step and unit-ramp response curves of the compensated system with MATLAB.

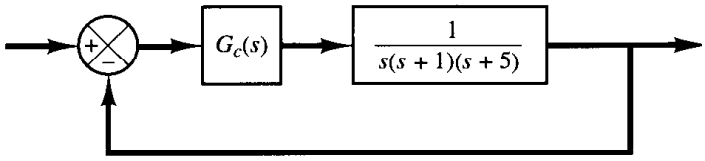

Figure 9–62 Control system.

10

PID Controls and Introduction to Robust Control

10–1 INTRODUCTION

In previous chapters we occasionally discussed the basic PID control schemes. For example, in Chapter 5 we presented hydraulic, pneumatic, and electronic PID controllers. In Chapters 7 and 9 we designed control systems where PID controllers were involved.

In this chapter we first present tuning rules for the basic PID controllers and then discuss modified forms of PID control schemes, including PI-D control, I-PD control, and two-degrees-of-freedom PID control. Finally, we introduce the concept of robust design.

It is interesting to note that more than half of the industrial controllers in use today utilize PID or modified PID control schemes. Analog PID controllers are mostly hydraulic, pneumatic, electric, and electronic types or their combinations. Currently, many of these are transformed into digital forms through the use of microprocessors.

Because most PID controllers are adjusted on site, many different types of tuning rules have been proposed in the literature. Using these tuning rules, delicate and fine tuning of PID controllers can be made on site. Also, automatic tuning methods have been developed and some of the PID controllers may possess on-line automatic tuning capabilities. Modified forms of PID control, such as I-PD control and two-degrees-of-freedom PID control, are currently in use in industry. Many practical methods for bumpless switching (from manual operation to automatic operation) and gain scheduling are commercially available.

The usefulness of PID controls lies in their general applicability to most control systems. In the field of process control systems, it is a well-known fact that the basic and

modified PID control schemes have proved their usefulness in providing satisfactory control, although they may not provide optimal control in many given situations.

Outline of the chapter. Section 10–1 has presented introductory material for the chapter. Section 10–2 deals with tuning methods for the basic PID control, commonly known as Ziegler–Nichols tuning rules. Section 10–3 discusses modified PID control schemes, such as PI-D control and I-PD control. Section 10–4 introduces two-degrees-of-freedom PID control schemes. Section 10–5 introduces the concept of robust control using a two-degrees-of-freedom control system as an example.

10–2 TUNING RULES FOR PID CONTROLLERS

PID control of plants. Figure 10–1 shows a PID control of a plant. If a mathematical model of the plant can be derived, then it is possible to apply various design techniques for determining parameters of the controller that will meet the transient and steady-state specifications of the closed-loop system. However, if the plant is so complicated that its mathematical model cannot be easily obtained, then analytical approach to the design of a PID controller is not possible. Then we must resort to experimental approaches to the tuning of PID controllers.

The process of selecting the controller parameters to meet given performance specifications is known as controller tuning. Ziegler and Nichols suggested rules for tuning PID controllers (meaning to set values K_p, T_i, and T_d) based on experimental step responses or based on the value of K_p that results in marginal stability when only the proportional control action is used. Ziegler–Nichols rules, which are presented in the following, are very convenient when mathematical models of plants are not known. (These rules can, of course, be applied to the design of systems with known mathematical models.)

Ziegler–Nichols rules for tuning PID controllers. Ziegler and Nichols proposed rules for determining values of the proportional gain K_p, integral time T_i, and derivative time T_d based on the transient response characteristics of a given plant. Such determination of the parameters of PID controllers or tuning of PID controllers can be made by engineers on site by experiments on the plant. (Numerous tuning rules for PID controllers have been proposed since the Ziegler–Nichols proposal. They are available in the literature. Here, however, we introduce only the Ziegler–Nichols tuning rules.)

There are two methods called Ziegler–Nichols tuning rules. In both methods, they aimed at obtaining 25% maximum overshoot in step response (see Figure 10–2).

First method. In the first method, we obtain experimentally the response of the plant to a unit-step input, as shown in Figure 10–3. If the plant involves neither inte-

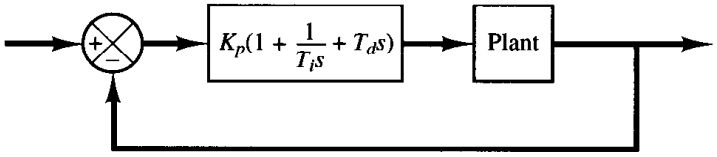

Figure 10–1
PID control of a plant.

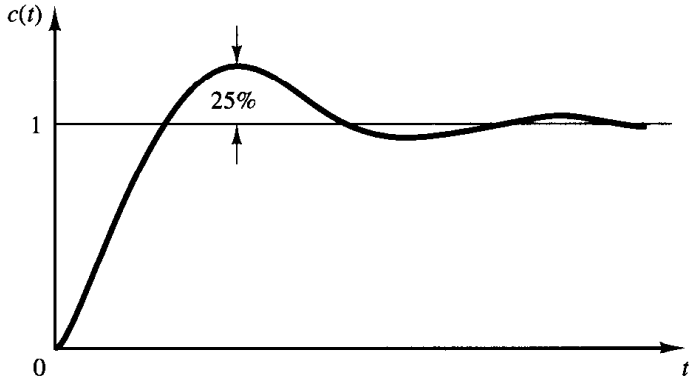

Figure 10–2
Unit-step response curve showing 25% maximum overshoot.

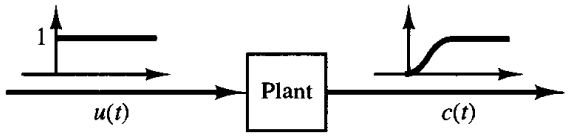

Figure 10–3
Unit-step response of a plant.

grator(s) nor dominant complex-conjugate poles, then such a unit-step response curve may look like an S-shaped curve, as shown in Figure 10–4. (If the response does not exhibit an S-shaped curve, this method does not apply.) Such step-response curves may be generated experimentally or from a dynamic simulation of the plant.

The S-shaped curve may be characterized by two constants, delay time L and time constant T. The delay time and time constant are determined by drawing a tangent line at the inflection point of the S-shaped curve and determining the intersections of the tangent line with the time axis and line $c(t) = K$, as shown in Figure 10–4. The transfer function $C(s)/U(s)$ may then be approximated by a first-order system with a transport lag as follows:

$$\frac{C(s)}{U(s)} = \frac{Ke^{-Ls}}{Ts + 1}$$

Ziegler and Nichols suggested to set the values of K_p, T_i, and T_d according to the formula shown in Table 10–1.

Notice that the PID controller tuned by the first method of Ziegler–Nichols rules gives

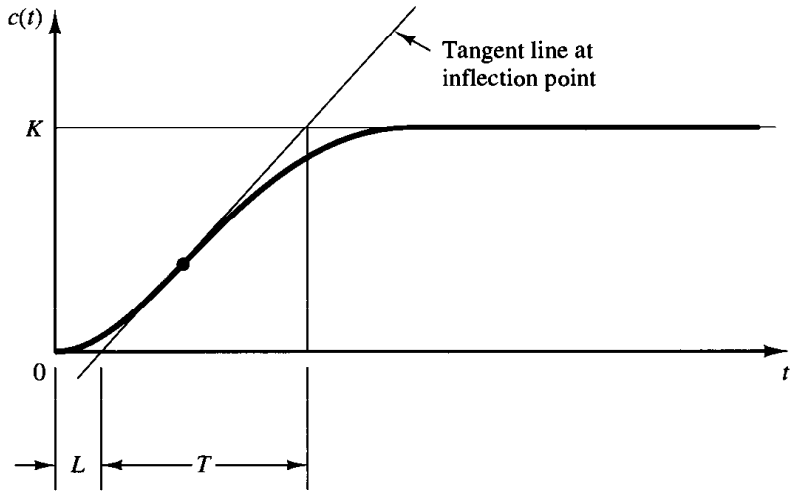

Figure 10–4
S-shaped response curve.

Table 10–1 Ziegler–Nichols Tuning Rule Based on Step Response of Plant (First Method)

Type of Controller	K_p	T_i	T_d
P	$\frac{T}{L}$	∞	0
PI	$0.9\frac{T}{L}$	$\frac{L}{0.3}$	0
PID	$1.2\frac{T}{L}$	$2L$	$0.5L$

$$G_c(s) = K_p\left(1 + \frac{1}{T_i s} + T_d s\right)$$

$$= 1.2\frac{T}{L}\left(1 + \frac{1}{2Ls} + 0.5Ls\right)$$

$$= 0.6T\frac{\left(s + \frac{1}{L}\right)^2}{s}$$

Thus, the PID controller has a pole at the origin and double zeros at $s = -1/L$.

Second method. In the second method, we first set $T_i = \infty$ and $T_d = 0$. Using the proportional control action only (see Figure 10–5), increase K_p from 0 to a critical value K_{cr} where the output first exhibits sustained oscillations. (If the output does not exhibit sustained oscillations for whatever value K_p may take, then this method does not apply.) Thus, the critical gain K_{cr} and the corresponding period P_{cr} are experimentally determined (see Figure 10–6). Ziegler and Nichols suggested that we set the values of the parameters K_p, T_i, and T_d according to the formula shown in Table 10–2.

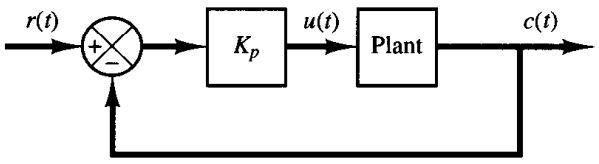

Figure 10–5
Closed-loop system with a proportional controller.

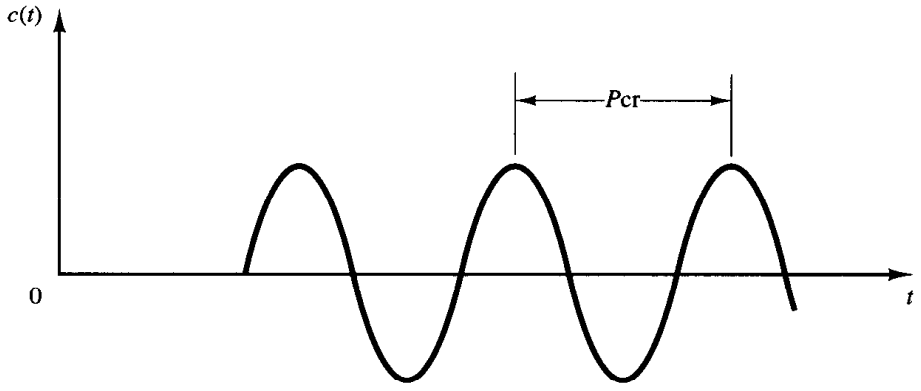

Figure 10–6
Sustained oscillation with period P_{cr}.

Table 10–2 Ziegler–Nichols Tuning Rule Based on Critical Gain K_{cr} and Critical Period P_{cr} (Second Method)

Type of Controller	K_p	T_i	T_d
P	$0.5K_{cr}$	∞	0
PI	$0.45K_{cr}$	$\frac{1}{1.2}P_{cr}$	0
PID	$0.6K_{cr}$	$0.5P_{cr}$	$0.125P_{cr}$

Notice that the PID controller tuned by the second method of Ziegler–Nichols rules gives

$$\begin{aligned} G_c(s) &= K_p\left(1 + \frac{1}{T_i s} + T_d s\right) \\ &= 0.6K_{cr}\left(1 + \frac{1}{0.5P_{cr}s} + 0.125\,P_{cr}s\right) \\ &= 0.075K_{cr}P_{cr}\frac{\left(s + \frac{4}{P_{cr}}\right)^2}{s} \end{aligned}$$

Thus, the PID controller has a pole at the origin and double zeros at $s = -4/P_{cr}$.

Comments. Ziegler–Nichols tuning rules (and other tuning rules presented in the literature) have been widely used to tune PID controllers in process control systems where the plant dynamics are not precisely known. Over many years, such tuning rules proved to be very useful. Ziegler–Nichols tuning rules can, of course, be applied to plants whose dynamics are known. (If plant dynamics are known, many analytical and graphical approaches to the design of PID controllers are available, in addition to Ziegler–Nichols tuning rules.)

If the transfer function of the plant is known, a unit-step response may be calculated or the critical gain K_{cr} and critical period P_{cr} may be calculated. Then, using those calculated values, it is possible to determine the parameters K_p, T_i, and T_d from Table 10–1 or 10–2. However, the real usefulness of Ziegler–Nichols tuning rules (and other tuning rules) becomes apparent when the plant dynamics are not known so that no analytical or graphical approaches to the design of controllers are available.

Generally, for plants with complicated dynamics but no integrators, Ziegler–Nichols tuning rules can be applied. However, if the plant has an integrator, these rules may not be applied in some cases. To illustrate such a case where Ziegler–Nichols rules do not apply, consider the following case: Suppose that a unity-feedback control system has a plant whose transfer function is

$$G(s) = \frac{(s + 2)(s + 3)}{s(s + 1)(s + 5)}$$

Because of the presence of an integrator, the first method does not apply. Referring to

Figure 10–3, the step response of this plant will not have an S-shaped response curve; rather, the response increases with time. Also, if the second method is attempted (see Figure 10–5), the closed-loop system with a proportional controller will not exhibit sustained oscillations whatever value the gain K_p may take. This can be seen from the following analysis. Since the characteristic equation is

$$s(s + 1)(s + 5) + K_p(s + 2)(s + 3) = 0$$

or

$$s^3 + (6 + K_p)s^2 + (5 + 5K_p)s + 6K_p = 0$$

the Routh array becomes

$$\begin{array}{lcc} s^3 & 1 & 5 + 5K_p \\ s^2 & 6 + K_p & 6K_p \\ s^1 & \dfrac{30 + 29K_p + 5K_p^2}{6 + K_p} & 0 \\ s^0 & 6K_p & \end{array}$$

The coefficients in the first column are positive for all values of positive K_p. Thus, in the present case the closed-loop system will not exhibit sustained oscillations and, therefore, the critical gain value K_{cr} does not exist. Hence, the second method does not apply.

If the plant is such that Ziegler–Nichols rules can be applied, then the plant with a PID controller tuned by Ziegler–Nichols rules will exhibit approximately 10% ~ 60% maximum overshoot in step response. On the average (experimented on many different plants), the maximum overshoot is approximately 25%. (This is quite understandable because the values suggested in Tables 10–1 and 10–2 are based on the average.) In a given case, if the maximum overshoot is excessive, it is always possible (experimentally or otherwise) to make fine tuning so that the closed-loop system will exhibit satisfactory transient responses. In fact, Ziegler–Nichols tuning rules give an educated guess for the parameter values and provide a starting point for fine tuning.

EXAMPLE 10–1 Consider the control system shown in Figure 10–7 in which a PID controller is used to control the system. The PID controller has the transfer function

$$G_c(s) = K_p\left(1 + \frac{1}{T_i s} + T_d s\right)$$

Although many analytical methods are available for the design of a PID controller for the present system, let us apply a Ziegler–Nichols tuning rule for the determination of the values of parameters K_p, T_i, and T_d. Then obtain a unit-step response curve and check to see if the designed system exhibits approximately 25% maximum overshoot. If the maximum overshoot is excessive (40% or more), make a fine tuning and reduce the amount of the maximum overshoot to approximately 25%.

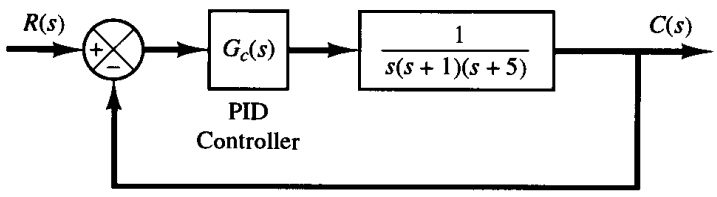

Figure 10–7 PID-controlled system.

Since the plant has an integrator, we use the second method of Ziegler–Nichols tuning rules. By setting $T_i = \infty$ and $T_d = 0$, we obtain the closed-loop transfer function as follows:

$$\frac{C(s)}{R(s)} = \frac{K_p}{s(s + 1)(s + 5) + K_p}$$

The value of K_p that makes the system marginally stable so that sustained oscillation occurs can be obtained by use of Routh's stability criterion. Since the characteristic equation for the closed-loop system is

$$s^3 + 6s^2 + 5s + K_p = 0$$

the Routh array becomes as follows:

$$\begin{array}{lll} s^3 & 1 & 5 \\ s^2 & 6 & K_p \\ s^1 & \dfrac{30 - K_p}{6} & \\ s^0 & K_p & \end{array}$$

Examining the coefficients of the first column of the Routh table, we find that sustained oscillation will occur if $K_p = 30$. Thus, the critical gain K_{cr} is

$$K_{cr} = 30$$

With gain K_p set equal to K_{cr} (= 30), the characteristic equation becomes

$$s^3 + 6s^2 + 5s + 30 = 0$$

To find the frequency of the sustained oscillation, we substitute $s = j\omega$ into this characteristic equation as follows:

$$(j\omega)^3 + 6(j\omega)^2 + 5(j\omega) + 30 = 0$$

or

$$6(5 - \omega^2) + j\omega(5 - \omega^2) = 0$$

from which we find the frequency of the sustained oscillation to be $\omega^2 = 5$ or $\omega = \sqrt{5}$. Hence, the period of sustained oscillation is

$$P_{cr} = \frac{2\pi}{\omega} = \frac{2\pi}{\sqrt{5}} = 2.8099$$

Referring to Table 10–2, we determine K_p, T_i, and T_d as follows:

$$K_p = 0.6K_{cr} = 18$$
$$T_i = 0.5P_{cr} = 1.405$$
$$T_d = 0.125P_{cr} = 0.35124$$

The transfer function of the PID controller is thus

$$\begin{aligned} G_c(s) &= K_p\left(1 + \frac{1}{T_i s} + T_d s\right) \\ &= 18\left(1 + \frac{1}{1.405s} + 0.35124s\right) \\ &= \frac{6.3223(s + 1.4235)^2}{s} \end{aligned}$$

Figure 10–8
Block diagram of the system with PID controller designed by use of Ziegler–Nichols tuning rule (second method).

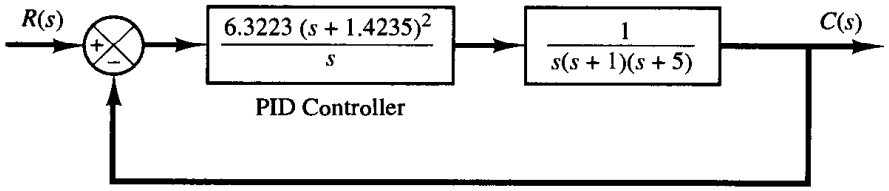

The PID controller has a pole at the origin and double zero at $s = -1.4235$. A block diagram of the control system with the designed PID controller is shown in Figure 10–8.

Next, let us examine the unit-step response of the system. The closed-loop transfer function $C(s)/R(s)$ is given by

$$\frac{C(s)}{R(s)} = \frac{6.3223s^2 + 18s + 12.811}{s^4 + 6s^3 + 11.3223s^2 + 18s + 12.811}$$

The unit-step response of this system can be obtained easily with MATLAB. See MATLAB Program 10–1. The resulting unit-step response curve is shown in Figure 10–9. The maximum overshoot in the unit-step response is approximately 62%. The amount of maximum overshoot is excessive. It can be reduced by fine tuning the controller parameters. Such fine tuning can be made on the computer. We find that by keeping $K_p = 18$ and by moving the double zero of the PID controller to $s = -0.65$, that is, using the PID controller

$$G_c(s) = 18\left(1 + \frac{1}{3.077s} + 0.7692s\right) = 13.846\,\frac{(s + 0.65)^2}{s} \tag{10–1}$$

the maximum overshoot in the unit-step response can be reduced to approximately 18% (see Figure 10–10). If the proportional gain K_p is increased to 39.42, without changing the location of the double zero ($s = -0.65$), that is, using the PID controller

$$G_c(s) = 39.42\left(1 + \frac{1}{3.077s} + 0.7692s\right) = 30.322\,\frac{(s + 0.65)^2}{s} \tag{10–2}$$

then the speed of response is increased, but the maximum overshoot is also increased to approximately 28%, as shown in Figure 10–11. Since the maximum overshoot in this case is fairly close to 25% and the response is faster than the system with $G_c(s)$ given by Equation (10–1), we may consider $G_c(s)$ as given by Equation (10–2) as acceptable. Then the tuned values of K_p, T_i, and T_d become

$$K_p = 39.42, \qquad T_i = 3.077, \qquad T_d = 0.7692$$

It is interesting to observe that these values respectively are approximately twice the values suggested by the second method of the Ziegler–Nichols tuning rule. The important thing to note here is that the Ziegler–Nichols tuning rule has provided a starting point for fine tuning.

It is instructive to note that, for the case where the double zero is located at $s = -1.4235$, increasing the value of K_p increases the speed of response, but as far as the percentage maximum

MATLAB Program 10–1

```
% ---------- Unit-step response ----------

num = [0   0   6.3223   18   12.811];
den = [1   6   11.3223   18   12.811];
step(num,den)
grid
title('Unit-Step Response')
```

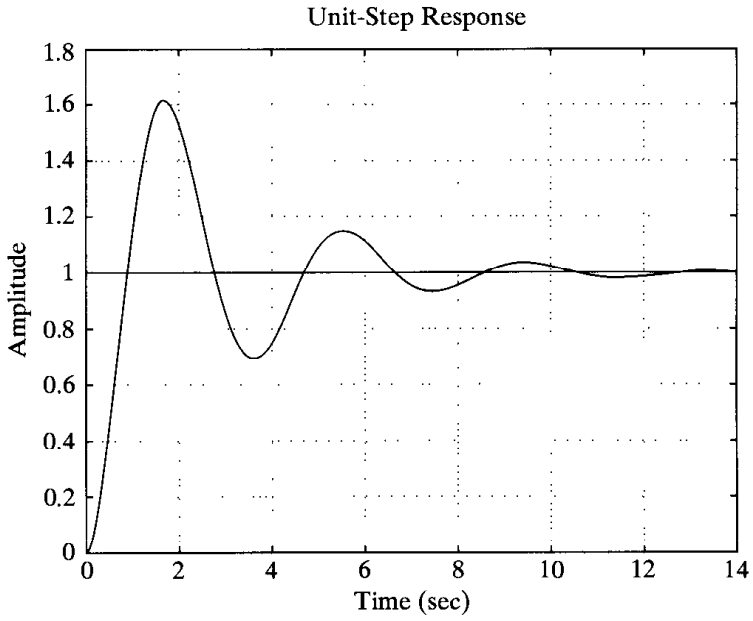

Figure 10–9
Unit-step response curve of PID-controlled system designed by use of Ziegler–Nichols tuning rule (second method).

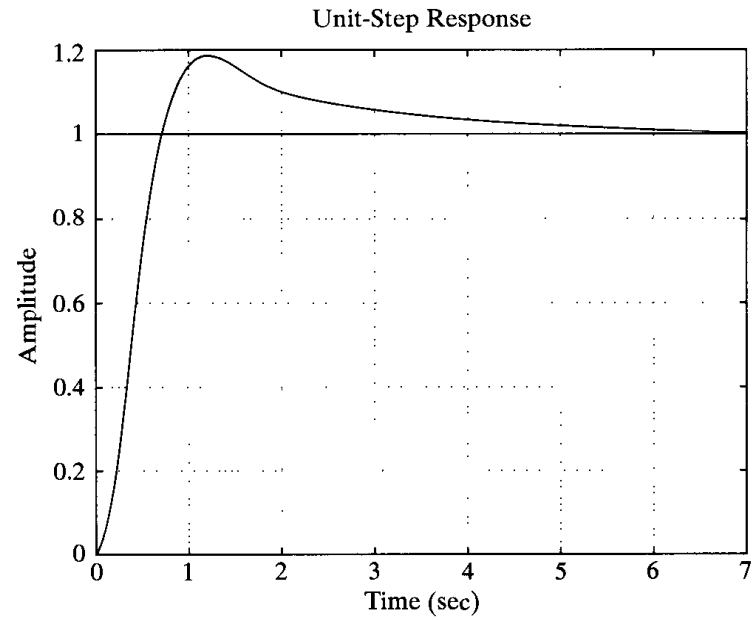

Figure 10–10
Unit-step response of the system shown in Figure 10–7 with PID controller having parameters $K_p = 18$, $T_i = 3.077$, and $T_d = 0.7692$.

overshoot is concerned, varying gain K_p has very little effect. The reason for this may be seen from the root-locus analysis. Figure 10–12 shows the root-locus diagram for the system designed by use of the second method of Ziegler–Nichols tuning rules. Since the dominant branches of root loci are along the $\zeta = 0.3$ lines for a considerable range of K, varying the value of K (from 6 to 30) will not change the damping ratio of the dominant closed-loop poles very much. However, varying the location of the double zero has a significant effect on the maximum overshoot, because the damping ratio of the dominant closed-loop poles can be changed significantly. This can also be seen from the root-locus analysis. Figure 10–13 shows the root-locus diagram for the system where the PID controller has the double zero at $s = -0.65$. Notice the change of the root-locus configuration. This change in the configuration makes it possible to change the damping ratio of the dominant closed-loop poles.